

Université de Montréal

Cyclopropanes to Spirocycles: A Study of Versatile B–N Motifs

By

Saher Hasan Siddiqui

Département de Chimie

Faculté des arts et des sciences

Thesis presented to the Faculté des études supérieures et postdoctorales to obtain

Doctor of Philosophy (Ph. D.) in Chemistry

September 2022

© Saher H. Siddiqui, 2022

Université de Montréal

Unité académique : Département de Chimie, Faculté des Arts et Sciences

This Thesis titled:

Cyclopropanes to Spirocycles: A Study of Versatile B–N Motifs

Presented by

Saher Hasan Siddiqui

Was evaluated by a Jury composed of:

James D. Wuest

President of the Jury

André B. Charette

Directeur de recherche

Shawn Collins

Jury Member

Dennis G. Hall

External Examiner

Résumé

Les dérivés cyclopropanoïques sont des composés importants dans plusieurs domaines tels que la synthèse organique, la chimie médicinale et la science des matériaux. La synthèse asymétrique des dérivés cyclopropanoïques s'est de plus en plus concentrée sur la synthèse stéréocontrôlée de cyclopropanes polysubstitués qui arborent toute une gamme de substituants distincts. Ces méthodes permettent d'accéder à des synthèses divergentes pour préparer des composés pharmaceutiques comportant cette sous-unité. De plus, l'ouverture facile de ce cycle très tendu en fait une bonne cible pour étudier l'activation de la liaison C–C. C'est pourquoi les cyclopropanes sont parmi les composés les plus attrayants et les plus diversifiés en synthèse organique.

La synthèse divergente de dérivés cyclopropanoïques repose sur l'utilisation de précurseurs stables mais réactifs. L'une des réactions pour former des liaisons C–C les plus couramment utilisées dans la fonctionnalisation à un stade avancé, est la réaction de couplage croisé de Suzuki-Miyaura. C'est l'une des raisons pour lesquelles les borocyclopropanes sont devenus des précurseurs synthétiques attrayants pour la fonctionnalisation et diversification des molécules complexes. L'accès à de telles molécules faciliterait la préparation de molécules cyclopropanoïques de structures diversifiées. Il est difficile de préparer des borocyclopropanes de manière énantiosélective. Dans cette thèse, une cyclopropanation énantiosélective d'acides boroniques protégés dérivés d'alcools allyliques a été réalisée via la réaction de cyclopropanation asymétrique en présence du ligand chiral de type dioxaborolane. Le développement de cette méthodologie a nécessité une modification de la décomplexation oxydative existante du dioxaborolane via son complexe dérivé de la diéthanolamine. Le protocole est maintenant applicable aux dérivés boronates qui incluent des groupements fonctionnels qui sont incompatibles avec les bases. Les borocyclopropanes tétracoordonnés obtenus permettent également la formation de liaisons C–C et ont démontré une stabilité améliorée par rapport à leurs dérivés tricoordonnés.

Une étude plus approfondie sur des complexes cyclopropylméthylamine-boranes (CAB) a démontré que ces derniers pouvaient conduire aux amine-boranes spirocycliques (SCAB). Ces

SCAB ont été obtenus grâce à une cascade d'activation des CABs en utilisant le bis(trifluorométhanesulfonimide) (Tf_2NH) comme initiateur. L'ouverture du cycle des CAB représente la première conversion des cyclopropanes en spirocycles contenant à la fois un *N*-spirocentre et un spiro amine-borane. Les amine-boranes ont démontré une activité pharmacologique telle que des propriétés anticancéreuses, anti-inflammatoires et anti-ostéoporotiques. L'incorporation de spirocycles dans un motif augmente le caractère sp^3 et la chiralité inhérente. Les SCAB rendent alors des candidats attrayants pour la conception de médicaments.

La réaction de SCAB avec de Tf_2NH en quantités stoechiométriques a donné un complexe $\text{SCAB}\cdot\text{NTf}_2$ qui est capable de réduire les fonctions cétone, aldéhyde, imine, nitrobenzène, nitrosobenzène, anthracène, indole et aryl méthyl éther. Le complexe $\text{SCAB}\cdot\text{NTf}_2$ est également capable de réduire le diphenylacétylène de manière *Z*-sélective en *cis*-stilbène. Des études spectroscopiques approfondies ont donné plus d'informations sur la structure de $\text{SCAB}\cdot\text{NTf}_2$ et nous ont permis de proposer un mécanisme de réduction des groupements fonctionnels ci-dessus. Les études spectroscopiques (RMN, IR et Raman) ont également révélé l'implication d'une liaison $\alpha\text{-C-H}$ au bore dans une liaison hydrogène hypsochromique « *improper hydrogen bond* » avec $[\text{Tf}_2\text{N}]^-$. L'hyperconjugaison avec l'atome de bore, un acide de Lewis, est proposée, ce qui rend la liaison C-H acide et donc suffisamment polarisée pour agir comme un donneur de pont hydrogène.

Mots-clés : Simmons-Smith cyclopropanation, borocyclopropane, cyclopropanes, amine-boranes, spirocycles, *N*-spirocentre, conception de médicament, agent réducteur, liaison hydrogène, liaison hydrogène hypsochromique « *improper hydrogen bond* »

Abstract

Cyclopropane derivatives are incredibly versatile building blocks used in organic synthesis, medicinal chemistry, and materials science. The asymmetric synthesis of cyclopropane derivatives has increasingly focused on achieving polysubstituted cyclopropanes with a range of distinct substituents and their use in divergent syntheses to access pharmaceutical compounds. Moreover, the ring-opening potential of the cyclopropane ring, due to its inherent strain, makes it a facile target for C–C bond activation and one of the most attractive and diverse cycloalkanes in organic synthesis.

Divergent synthesis of cyclopropanes relies on stable pre-installed handles on cyclopropanes that can be activated readily. One of the most common C–C bond formation approaches used in late-stage functionalization is the Suzuki-Miyaura cross-coupling reaction. As a result, borocyclopropanes have become attractive synthetic building blocks for their use in late-stage functionalization. Methods for the enantioselective synthesis of borocyclopropanes are scarce. In this thesis, the first enantioselective cyclopropanation of an allylic alcohol bearing a tetracoordinate boronate has been achieved via the Charette dioxaborolane-mediated enantioselective cyclopropanation reaction. The development of our method required modification of the existing oxidative decomplexation of dioxaborolane via diethanolamine. The protocol has now been expanded to include boronates and base-sensitive functionalities. The tetracoordinate borocyclopropane obtained was also shown to undergo C–C bond formation and demonstrated enhanced stability compared to its tricoordinate boronate derivative.

Further investigation of boron tethered cyclopropanes led to the discovery of the unique transformation of cyclopropane amine-boranes (CABs) to spirocyclic amine-boranes (SCABs). SCABs were obtained through a cascade activation of CAB via bis(trifluoromethane)sulfonimide (Tf_2NH). The ring-opening of CABs represents the first conversion of cyclopropanes to spirocycles containing an *N*-spirocenter and furthermore an amine-borane spirocore. Amine-boranes have shown pharmacological activity such as anti-cancer, anti-inflammatory, and anti-osteoporotic

properties. Incorporating spirocycles into a motif increases sp^3 character and inherent chirality, rendering SCABs as attractive candidates for drug design.

The reaction of SCAB with stoichiometric amounts of Tf_2NH resulted in a $SCAB \bullet NTf_2$ complex that was found to be able to reduce ketone, aldehyde, imine, nitrobenzene, nitrosobenzene, anthracene, and indole functionalities as well as demethylate aryl methyl ethers. The $SCAB \bullet NTf_2$ complex was also capable of reducing diphenylacetylene in a *Z*-selective manner to *cis*-stilbene. In-depth spectroscopic studies revealed the structure of $SCAB \bullet NTf_2$ and a mechanism for the reduction of the above functionalities is proposed. The spectroscopic studies (NMR, IR and Raman) revealed the involvement of an α -C–H bond to boron in improper hydrogen bonding with $[Tf_2N]^-$. Hyperconjugation to the Lewis acidic boron is proposed to make the C–H bond acidic and therefore polarized enough to act as a hydrogen bond donor.

Keywords: Simmons-Smith cyclopropanation, Borocyclopropane, Cyclopropanes, Amine-Boranes, Spirocycles, *N*-spirocenter, Drug Design, Reducing Agent, Hydrogen Bonding, Improper Hydrogen Bonding

Table of Contents

Résumé.....	3
Abstract.....	5
Table of Contents.....	7
List of Tables.....	12
List of Schemes.....	13
List of Figures.....	15
List of Abbreviations.....	19
Acknowledgements.....	24
Chapter 1 – Introduction.....	26
1.1 Boron.....	26
1.1.1 Organoboron Reagents.....	26
1.1.2 Boronate Esters.....	28
1.1.3 <i>N</i> -Coordinated Boronates.....	29
1.1.4 <i>N</i> -Coordinated Boranes: Amine-Boranes.....	32
1.2 Boron in Drug Design.....	35
1.3 Amine-Boranes in Drug Design.....	36
1.4 Spirocycles in Drug Design.....	38
1.5 Boron Hydrides as Proton Acceptors.....	41
1.5.1 Hydrogen Bonding.....	41
1.5.2 Reactivity of B–H Bonds.....	45
Chapter 2 – Enantioselective Synthesis of <i>cis</i> - and <i>trans</i> -Borocyclopropylmethanol: Simple Building Blocks to Access Heterocycle-Substituted Cyclopropylmethanols.....	47

Background.....	48
Context	50
Article 1	53
Enantioselective Synthesis of cis- and trans-Borocyclopropylmethanol: Simple Building Blocks to Access Heterocycle-Substituted Cyclopropylmethanols.....	54
Abstract	54
Introduction.....	55
Results and Discussion	58
Conclusion	64
Experimental Section	64
References.....	89
Chapter 3 – Unactivated Cyclopropanes to Spirocyclic Amine-Boranes with an <i>N</i> -Spiroatom.....	94
3.1 Introduction.....	95
3.2 Ring-Opening of Cyclopropanes.....	97
3.2.1 C–C Bond Activation of Unactivated Cyclopropanes	99
3.2.2 Borylative Ring-Opening of Cyclopropanes	101
3.2.2.1 Borylative Ring-Opening Using Transition-Metals	102
3.2.2.2 Transition Metal-Free Borylative Ring-Opening of Unactivated Cyclopropanes.....	103
3.3 Cyclopropanes to Spirocycles.....	105
3.3.1 Spirocycles in Drug Design	105
3.4 Research Goals	108
3.5 Results and Discussion	110
3.5.1 Cyclopropane Amine-Boranes (CABs) to Spirocyclic Amine-Boranes (SCABs).....	110
3.5.2 Optimization and Scope	112

3.5.2.1	Regioselectivity in the Transformation of CAB to SCAB.....	116
3.5.2.2	Scope of the Transformation of Various CABs to SCABs.....	117
3.5.3	Mechanisms for the Hydroboration of Cyclopropanes in the Literature	122
3.5.3.1	Mechanism of Brown Hydroboration	122
3.5.3.2	Shi and Co-Workers: Mechanism for the Hydroboration of Cyclopropanes	123
3.5.4	Activation of Boranes by Tf ₂ NH.....	124
3.5.4.1	NMR Study of Activated Species Between Amine-borane and Tf ₂ NH.....	124
3.5.4.2	Hydroboration of Alkenes Using NHC-Borane as Borenium Cation Equivalentents.	126
3.5.5	Mechanistic Studies for the Conversion of CAB to SCAB.....	128
3.5.5.1	Variable Temperature NMR Experiments of CAB with Tf ₂ NH	128
3.5.5.2	Determination of <i>Syn</i> vs. <i>Anti</i> -Hydroboration in CAB to SCAB Transformation ..	135
3.5.5.3	Deuterium Labelling Experiments.....	136
3.5.5.4	Remarks on Mechanism.....	140
3.6	Conclusion and Perspectives.....	140
Chapter 4 – Exploring the Reactivity of a Spirocyclic Alkyl Dihydrido Amine-Borane•NTf ₂ Complex in Functional Group Interconversion Reactions.....		
4.1	Introduction.....	149
4.1.1	Boron Hydrides as Proton Acceptors	150
4.1.2	Boron Hydrides in Dihydrogen Bonding.....	153
4.1.3	Proper vs. Improper Hydrogen Bonding	155
4.1.3.1	Proper Hydrogen Bonding.....	155
4.1.3.2	Improper Hydrogen Bonding	157
4.1.3.3	Proposed Theories to Explain Improper Hydrogen Bonding	158
(i)	A Tug of War Between Hyperconjugation and Rehybridization	158

(ii) Short-Range Repulsive Forces.....	159
(iii) Role of Electric Field.....	159
(iv) Redistribution of Electron Density.....	159
(v) Interplay of Contracting and Lengthening Forces.....	160
4.1.4 Research Goals.....	161
4.2 Understanding the Structure and Reactivity of a Spirocyclic Amine-Borane (SCAB) and Tf ₂ NH Complex: SCAB•NTf ₂ Complex (3).....	162
4.2.1 Introduction.....	162
4.2.2 Results and Discussion.....	164
4.2.2.1 Analysis of SCAB•NTf ₂ by NMR Spectroscopy.....	164
4.2.2.2 Effect of Lewis Acidic Boron Adjacent to C–H Bonds.....	169
4.2.2.3 Studies to determine potential acidity of the C–H bonds in SCAB NTf ₂	173
4.2.2.4 Analysis of SCAB•NTf ₂ by IR and Raman Spectroscopy.....	174
4.2.2.5 Variable Temperature NMR experiments of SCAB•NTf ₂	178
4.2.2.6 Reactivity of SCAB•NTf ₂ Complex 3.....	181
4.2.3 Interconversion of Functional Groups: Reaction Scope of SCAB•NTf ₂	183
4.2.4 Proposed Mechanism for the Reductions.....	186
4.2.4.1 Attempts to Regenerate SCAB 2a.....	187
4.2.4.2 Implication of “D ₂ O Shake” on Mechanism.....	188
4.3 Conclusion and Perspectives.....	189
Chapter 5 – Perspectives and Conclusion.....	192
5.1 Chiral <i>N</i> -coordinated Boronate Building Blocks.....	192
5.2 Combining C–H and C–C Bond Activation to Make Spirocyclic Amine-Boranes (SCABs) ..	193
5.3 The C–H Bond as a Hydrogen Bond Donor.....	194

5.4 Final Thoughts	195
References	196
Annexes	210
Annex 1: NMR Spectra for Chapter 2	211
Annex 2: Experimental Section and NMR Spectra for Chapter 3.....	259
Experimental Section for Chapter 3	260
Optimization of Reaction Conditions	263
Synthesis and Characterization of Compounds	266
Synthesis of Cyclopropane Amine-Boranes (CABs).....	266
Transformation of CABs to SCABs	301
Post-functionalization	332
Mechanistic Studies Using Deuterium Experiments	346
NMR Spectra for Chapter 3	361
NMR Spectra of Precursors	362
NMR Spectra of SCABs	485
NMR Spectra of Post-Functionalized Products	602
NMR Spectra of Deuterium Experiments.....	633
Annex 3.....	641
Experimental Section for Chapter 4	642
NMR Spectra for Chapter 4	660

List of Tables

Table 3.1 Optimization of Time and Temperature with Tf ₂ NH for CAB 1a	113
Table 3.2 Screening of Activating Reagent	114
Table 3.3 Effect of Substituent.....	115
Table 3.4 Scope of SCABs	117
Table 3.5 SCAB as a Potential Pharmacophore.....	146

List of Schemes

Chapter 1:

Scheme 1.1 Preparation of MIDA boronates	30
Scheme 1.2 Slow-release cross-coupling conditions for MIDA boronates	31
Scheme 1.3 Enantioselective dioxaborolane-mediated cyclopropanation of <i>N</i> -coordinate boronate allylic alcohols.....	32
Scheme 1.4 Amine-borane synthesis of substrates containing borane-incompatible functionalities.....	34

Chapter 2:

Scheme 2. 1 Charette enantioselective cyclopropanation reaction.....	51
Scheme 2. 2 Dioxaborolane-mediated enantioselective synthesis of borocyclopropanes.....	52

Chapter 3:

Scheme 3. 1 Metal-catalyzed borylative ring-opening of i. vinyl and ii. propargyl cyclopropanes	102
Scheme 3. 2 Iridium-catalyzed hydroboration of activated cyclopropanes	102
Scheme 3. 3 Brown hydroboration of an unactivated cyclopropane	103
Scheme 3. 4 Borylative ring-opening of unactivated cyclopropanes using an FLP system	103
Scheme 3. 5 Hydroboration of unactivated cyclopropanes	104
Scheme 3. 6 1,3-Difunctionalization of unactivated cyclopropanes	104
Scheme 3. 7 Borylative ring-opening of unactivated cyclopropane using sodium metal	105
Scheme 3. 8 Synthesis of CAB precursors.....	112
Scheme 3. 9 Species formed at rt and 100 °C post addition of Tf ₂ NH (5 mol%)	115
Scheme 3. 10 Regioselectivity observed in transformation of monosubstituted CAB 1a to 2a ..	116
Scheme 3. 11 Brown hydroboration of alkenes.....	123
Scheme 3. 12 Hydroboration of cyclopropane with diborane	123
Scheme 3. 13 1,3-Hydroboration of unactivated cyclopropanes using BBr ₃ and PhSiH ₃	123
Scheme 3. 14 C–H borylation via borenium cations.....	125
Scheme 3. 15 Study of activated species by Vedejs and co-workers	125

Scheme 3. 16 Variable temperature NMR experiment	128
Scheme 3. 17 Synthesis of deuterated CAB 4a	137
Scheme 3. 18 Hydroboration of CAB using a BD_3 moiety	138
Scheme 3. 19 Hydroboration of CAB with deuterium labeling at C3	139
Scheme 3. 20 Ring-opening of aziridine and epoxide analogues of CABs	141
Scheme 3. 21 Ring-opening of bicyclic CABs and proposed products	142
Scheme 3. 22 Modification of <i>N</i> -heterocycle	142
Scheme 3. 23 Phosphine-borane and oxyborane analogues of CABs	142
Scheme 3. 24 Proposed ring-opening of cyclobutane amine-borane	143
Scheme 3. 25 Transformation of CAB to SCAB using magic acid	144

Chapter 4:

Scheme 4. 1 Synthesis of NHC-boranes via BH_3 complexes	151
Scheme 4. 2 Reactivity of NHC-borane with strong acids	152
Scheme 4. 3 NHC-borane borenium cations for the hydroboration of alkenes	152
Scheme 4. 4 NMR tube sample of $SCAB \bullet NTf_2$	164
Scheme 4. 5 Analysis of CAB 1a : Tf_2NH (1:1) mixture	166
Scheme 4. 6 Expected products of reaction of SCAB (1 equivalent) with Tf_2NH (1 equivalent)	167
Scheme 4. 7 Reduction of 4-nitrobenzaldehyde using $SCAB \bullet NTf_2$ complex	182
Scheme 4. 8 Expected reaction between $SCAB \bullet NTf_2$ and $NaBH_4$	188
Scheme 4. 9 Enantioselective reduction via chiral SCAB	190
Scheme 4. 10 Deuterium experiment for mechanistic studies	191

List of Figures

Figure 1.1 Electron configuration of boron	26
Figure 1.2 Chemical transformations that use organoboron reagents	27
Figure 1.3 Classification of boron compounds	28
Figure 1.4 Examples of common boron reagents used in the Suzuki-Miyaura coupling reaction	29
Figure 1.5 <i>N</i> -Coordinated boronates used in Suzuki-Miyaura coupling reactions.....	30
Figure 1.6 Applications of amine-boranes	33
Figure 1.7 Synthesis of amine-boranes: 1. Displacement 2. Metathesis and 3. <i>Trans</i> -amination of ammonia-borane.....	34
Figure 1.8 Boron containing natural products.....	35
Figure 1.9 Boron containing drug molecules	36
Figure 1.10 Common borane functionalities in pharmacologically active compounds	37
Figure 1.11 Biologically active molecules containing spirocycles.....	38
Figure 1.12 Chemical transformations used in the synthesis of spirocycles	39
Figure 1.13 Ring-expansion of cyclopropane rings.....	40
Figure 1.14 Hydrogen and dihydrogen bonding	42
Figure 1.15 Structure of diborane (B ₂ H ₆).....	44
Figure 1.16 Structure of some common boranes	44
Figure 1.17 Structure of some common borohydrides.....	45
Figure 2.1 Cyclopropane-based natural products along with their biological property	48
Figure 2.2 Common methods for the synthesis of cyclopropanes	49
Figure 2.3 Examples of borocyclopropanation reactions	50
Figure 2.4 MIDA boronate allylic alcohol vs. CIDA boronate allylic alcohol	51
Figure 3.1 Metal-mediated C–H and C–C bond activation	95
Figure 3.2 Transformations of organoboron compounds	96
Figure 3.3 Ring-strain in cycloalkanes.....	98
Figure 3.4 Activated cyclopropanes: acceptor, donor, and donor-acceptor cyclopropanes	98
Figure 3.5 Methods to ring-open various substituted cyclopropanes	99

Figure 3.6 Ring-opening of unactivated cyclopropanes with metals	100
Figure 3.7 Metal-free ring-opening of unactivated cyclopropanes.....	101
Figure 3.8 i. Most common ring systems found in FDA approved drugs ii. Spirocyclic motifs in biologically active molecules.....	106
Figure 3.9 Growing interest in spirocyclic motifs	107
Figure 3.10 Reactions involved in the formation of spirocycles.....	108
Figure 3.11 a. Inspiration for C–H borylation of cyclopropanes using borenium cations b. Attempt to C–H borylate CAB	109
Figure 3.12 Isolated spirocyclic amine-boranes reported via C-H activation.....	110
Figure 3.13 Unactivated cyclopropanes to <i>N</i> -spiroatom heterocycles	111
Figure 3.15 Functionalization of C–B Bond in SCAB. a. Fluorinated analogues b. Boronic acid and boronate ester derivatives c. Suzuki-Miyaura cross-coupling d. Chan-Lam coupling e. Oxidation of SCAB	121
Figure 3.16 Proposed mechanism for the 1,3-hydroboration of cyclopropanes by Shi and co-workers.....	124
Figure 3.17 Comparison of C-H borylation and ring-opening reaction using activated amine-boranes.....	126
Figure 3.18 Hydroboration by NHC-borane mediated by Tf ₂ NH	127
As reported by Vedejs and co-workers we also found that without the presence of an activator such as Tf ₂ NH, CABs are not capable of intramolecular ring-opening via hydroboration (Figure 3.19).....	127
Figure 3.19 Activator-mediated hydroboration.....	128
Figure 3.20 ¹⁹ F NMR spectra at variable temperatures.....	130
Figure 3.21 ¹¹ B NMR spectra at variable temperatures.....	131
Figure 3.22 Regeneration of activated cationic species	132
Figure 3.23 ¹ H NMR spectra at variable temperatures.....	134
Figure 3.24 Hydroboration of a chiral CAB 1ab and single X-ray crystal structure of CAB 1ab and SCAB 2ab	135
Figure 3.25 Proposed reaction for deuterium labelling.....	136

Figure 3.26 Hydroboration of <i>gem</i> -C2 substituted CAB and lack of 1,2-migration observed in product from C2 to C1.....	138
Figure 3.27 SCAB precursors of biologically active compounds.....	145
Figure 4.1 a. Classification of boranes b. Hydroboration/oxidation reaction	149
Figure 4.2 Structures of some alkylborane reagents.....	150
Figure 4.3 Boron hydride as proton acceptors	150
Figure 4.4 Nomenclature for boron cation that is in current use.....	151
Figure 4.5 Borylation of aliphatic and aromatic C–H bonds using borenium cations	153
Figure 4.6 Aminoboron hydrides stabilized by C–H···H–B dihydrogen bonding	155
Figure 4.7 Intermolecular interactions of the C–H bonds of NHC-boranes.....	155
Figure 4.8 a. Depiction of hydrogen bond (HB) b. HBs in DNA.....	156
Figure 4.9 a. IR trends of HB and b. Summary of proper and pro-improper hydrogen bonds based on Jemmis and co-workers.....	161
Figure 4.10 Development of the theory of C–F bond activation via SCAB borenium cations.....	163
Figure 4.11 ¹ H NMR (toluene- <i>d</i> ₈) spectra of a. SCAB•NTf ₂ complex 3 vs. b. SCAB 2a	164
Figure 4.12 <i>N</i> -Directed aliphatic C–H borylation using borenium cation equivalents	165
Figure 4.13 Comparison of CAB•NTf ₂ (1:1) vs. SCAB•NTf ₂ (1:1).....	166
Figure 4.14 ¹ H NMR spectrum (Tol- <i>d</i> ₈) of SCAB•NTf ₂	167
Figure 4.15 ¹ H NMR (CD ₂ Cl ₂) spectra of acid screening.....	168
Figure 4.16 Unique C–B bond in SCAB	169
Figure 4.17 Hyperconjugation in the ethyl cation	169
Figure 4.18 Examples of hyperconjugation	170
Figure 4.19 Hyperconjugative interactions in SCAB•NTf ₂	171
Figure 4.20 i. ¹⁹ F NMR spectra of SCAB•NTf ₂ at rt ii. ¹ H NMR spectra of SCAB•NTf ₂ at rt.....	172
Figure 4.21 “D ₂ O shake” of SCAB•NTf ₂	174
Figure 4.22 IR spectra of SCAB 2a and SCAB•NTf ₂ 3	177
Figure 4.23 a. Formation and reactivity of imidazolium carbene b. IR and of C–H···NTf ₂ interaction of acidic imidazole C2–H and [Tf ₂ N] [–] c. Possible C–H···NTf ₂ interaction in SCAB•NTf ₂ 3 complex.....	177

Figure 4.24 Reduced C–H bands in Raman spectrum of SCAB•NTf ₂ (right) compared to SCAB 2a (left).....	178
Figure 4.25 ¹ H NMR (toluene- <i>d</i> ₈) spectra at variable temperature.....	179
Figure 4.26 ¹⁹ F NMR (toluene- <i>d</i> ₈) spectra of SCAB•NTf ₂ at variable temperatures.....	180
Figure 4.27 ¹¹ B NMR (toluene- <i>d</i> ₈) spectra at variable temperatures.....	180
Figure 4.28 Proposed structure of SCAB•NTf ₂ complex 3	181
Figure 4.29 Crude ¹ H NMR spectrum of reduction of 4-nitrobenzaldehyde with SCAB•NTf ₂ 3 ..	183
Figure 4.30 Potential mechanistic pathway for the reduction of 4-nitrobenzaldehyde	187
Figure 4.31 Proposed oligomerization byproduct of SCAB•NTf ₂ reduction reaction	190

List of Abbreviations

[α] _D	specific rotation
Å	angstrom
Ac	acetate
acac	acetoacetate
aq	aqueous
Ar	aryl
Atm	atmosphere
Boc	<i>t</i> -butyloxycarbonyl
Bn	benzyl
BNCT	boron neutron capture therapy
Bu	butyl
Bz	benzoyl
c	cyclo
CAB	cyclopropane amine-borane
CADD	computer-aided drug design
cat	catalyst
CIDA	cyclohexyliminodiacetic acid
CMD	concerted metalation deprotonation
Cy	cyclohexyl
DA	donor/acceptor
dba	dibenzylideneacetone
DBL	dioxaborolane
DBU	1,8-diazabicycloundec-7-ene
DCE	dichloroethane
DCM	dichloromethane
DEA	diethanolamine

DFT	density functional theory
DG	directing group
DIBAL	diisobutylaluminium hydride
DIPP	2,6-diisopropylphenyl
DME	1,2-dimethoxyethane
DMEDA	dimethylethyldiamine
DMF	<i>N,N</i> -dimethylformamide
DMSO	dimethylsulfoxide
dr	diastereomeric ratio
DTBB	4,4'-di-tert-butylbiphenyl
EDG	electron-donating group
ee	enantiomeric excess
Eq	equation
equiv	equivalent
Et	ethyl
EWG	electron-withdrawing group
FES	Faculté d'étude supérieure
FT-IR	Fourier-transform infrared spectroscopy
g	gram
GC	gas chromatography
<i>gem</i>	geminal
h	hour
HFIP	hexafluoro-2-propanol
HOMO	highest occupied molecular orbital
HPLC	high performance liquid chromatography
HRMS	high resolution mass spectroscopy
HTPS	high-throughput parallel synthesis
HTS	high-throughput screening
Hz	hertz

<i>i</i> Pr	<i>iso</i> -propyl
IR	infrared
<i>J</i>	coupling constant
kcal	kilocalorie
KIE	kinetic isotope effect
L	ligand
LA	Lewis acid
LAH	lithium aluminum hydride
LB	Lewis base
LC	liquid chromatography
LUMO	lowest unoccupied molecular orbital
LSF	late-stage functionalization
M	metal
<i>m</i>	meta
Me	methyl
MHz	megahertz
MIDA	methyliminodiacetic acid
min	minutes
mL	milliliter
mol	mole
mmol	millimole
mp	melting point
MS	molecular sieves
NMR	nuclear magnetic resonance
Nuc	nucleophile
<i>o</i>	ortho
<i>p</i>	para
Ph	phenyl
Piv	pivaloate

pKa	acid dissociation constant
ppm	parts per million
psi	pounds per square inch
pyr	pyridine
quant	quantitative
R	substituent
RCM	ring-closing metathesis
RCEM	ring-closing enyne metathesis
<i>R_f</i>	retention factor
ROCM	ring-opening cross metathesis
RRM	ring-rearrangement metathesis
rt	room temperature
SCAB	spirocyclic amine-borane
SFC	supercritical fluid chromatography
TBS	<i>tert</i> -butyldimethylsilyl
<i>t</i> Bu	<i>tert</i> -butyl
Temp	temperature
Tf	trifluoromethylsulfonyl
Tf ₂ NH	bis(trifluoromethane)sulfonimide
TFA	trifluoroacetic acid
THF	tetrahydrofuran
TLC	thin layer chromatography
TMS	trimethylsilyl
Tol	toluene

To my parents

“Education is a progressive discovery of our own ignorance”

-Will Durant

Acknowledgements

First and foremost, I would like to express my thanks to my research advisor, Professor André B. Charette who has supported me throughout my studies at the Université de Montréal. I thank you for your patience and for guiding me through my projects. Thank you for creating a productive environment for the research and discovery of my projects. Finally, thank you for your knowledge and for providing all the necessary resources over the years.

I would like to thank my thesis committee for their support since the beginning of my doctoral studies. Professor James D. Wuest and Professor Shawn Collins have always encouraged me to do my best and have always been available to discuss any concerns I may have had. I thank them sincerely for their understanding and support throughout my studies.

I would like to thank Barbara Bessis for all that she has done for the group. I thank her for her support and encouragement since the day I joined the group and for her help in facilitating administrative matters.

I would also like to thank Professor William D. Lubell for his support during my pre-doc exam and for his encouragement throughout my studies. I would like to thank Professor Hélène Lebel, Professor Davit Zargarian, Professor Christian Pellerin, Professor Christian Reber and Professor Joëlle Pelletier for their availability to discuss chemistry, share equipment and answer any questions I had.

I would like to thank both current and former Charette group members for their support over the years. I would like to give a special thanks Dr. Chandrasekhar Navuluri for his mentorship in my first year and for helping me get settled into the group. Thank you for your support and advice. It was a pleasure to work with you. I would also like to thank former group members Dr. Éric Lévesque, Dr. Guillaume Benoit and Dr. Laetitia Delion for their advice. I would like to thank current members Laurent Vinet, Kévin Saint-Jacques, Lauriane Peyrical, and Alex Raborg for their support, especially towards the end of my studies. I would like to thank some former and current members of the Lubell group, Zargarian group, Lebel group, Collins group, Hanessian group and

Pellerin group for sharing knowledge, lending chemicals and sharing equipment; a big thanks to Yousra Hamdane, Anh Minh Thao Nguyen, Dr. Julien Poupart, Dr. Loïc Mangin, Dr. Henri Piras, Dr. Clement Audubert, Dr. Éric Godin, Jean-Baptiste Garsi and Clarence Allen. I would like to give a special thanks to Dr. Loïc Mangin for teaching me how to apply computational chemistry to my methodology, run calculations, and interpret data. Thank you for your patience and sharing your expertise in the field. Thank you for answering all my questions whenever I needed help.

I would like to thank the NMR Regional Laboratory team: Dr. Pedro Aguiar, Dr. Cedric Malveau, Sylvie Bilodeau, Antoine Hamel and Natalie Baho for their time and effort that went into carrying out specific NMR experiments and for always being available to answer questions. I would also like to thank the Centre régional de spectrométrie de masse at l'Université de Montréal. Thank you to Dr. Alexandra Fürtös, Karine Gilbert, Marie-Christine Tang and Louiza Mahrouche for the analysis of the numerous compounds I have submitted over the years. I would also like to thank Thierry Maris, Francine Belanger-Gariepy and Daniel Chartrand for their expertise in X-ray analyses. I sincerely thank Thierry for his patience when training me and I thank him for sharing his knowledge.

Finally, I would like to thank my family and friends for their unconditional love and support over the years. I would like to thank my parents Abu and Shaheena, and my brothers Shaan and Asad. I would also like to thank Gursimranbir Singh for his unwavering support and constant motivation. You have stood by me at every turn, and for that I will be forever grateful. I thank your family for their support over the years.

Chapter 1 – Introduction

1.1 Boron

Boron is “arguably the most complex element in the periodic table”.¹ It was first isolated in 1808 by British chemist Sir Humphry Davy and by French chemists Joseph Louis Gay-Lussac and Louis-Jacques Thenard.^{2,3} It is the second most abundant group 13 element in the Earth’s crust and the 38th most abundant element overall.⁴ Boron sits right at the top of the metalloid line separating the metals and non-metals. It has three valence electrons with a ground state configuration of $1s^2 2s^2 2p^1$ (**Figure 1.1**). Boron’s peculiar position in the periodic table explains its unique electron deficient nature and allows it to have unusual electronic properties. The sp^2 hybridized boron atom has an empty p orbital and a trigonal planar geometry. When the p orbital is filled, it can form a negatively charged tetravalent compound and adopt a tetrahedral geometry. Organoboron chemistry has exploited the Lewis acidity of the boron atom to discover new reactivity of organoboron reagents. Boron brings to light novel chemistry unavailable to the ‘big four’ elements in drug design (H, C, N, and O).⁵

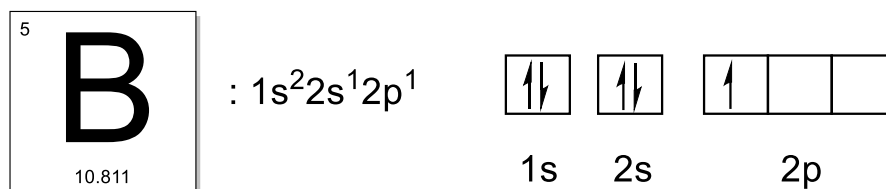


Figure 1.1 Electron configuration of boron

1.1.1 Organoboron Reagents

Organoboron reagents have been used for many years in synthetic organic and medicinal chemistry to enable numerous chemical transformations ranging from reductions,⁶ hydroboration reactions,⁷ Suzuki-Miyaura cross-coupling,^{8,9} allylboration,¹⁰ to the activation of hydrogen via frustrated Lewis-pairs (FLPs) (**Figure 1.2**).¹¹ Hydroboration and Suzuki-Miyaura cross-coupling are amongst the most widely used transformations in organic synthesis.¹²

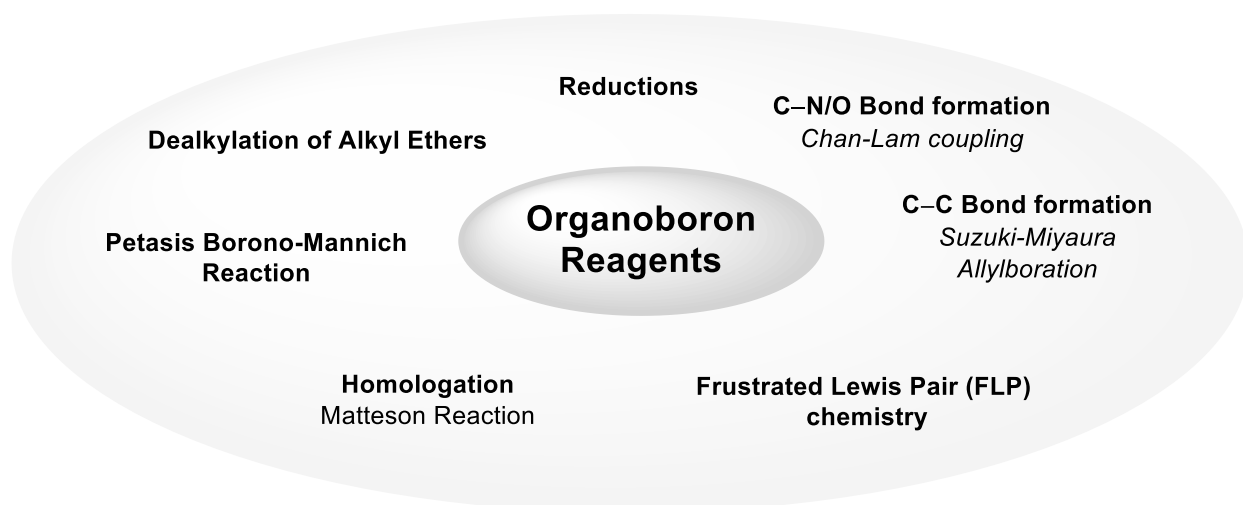


Figure 1.2 Chemical transformations that use organoboron reagents

The first boronic acid was isolated by Frankland in 1860 and the isolation and characterization of boron hydrides began in 1912 by German chemist, Alfred Stock. It was only in 1957 that the study and applications of organoboron reagents took off following the development of the hydroboration reaction by Herbert Charles Brown for which he was awarded the Nobel Prize for Chemistry in 1979.¹³ It was also in 1979 that the utility of organoboron reagents was highlighted by the discovery of the palladium catalyzed cross-coupling reaction by Suzuki and Miyaura.^{8, 9, 14}

Organoboron reagents consist of at least one B–C bond and many have B–O and B–N bonds. The B–C bond has a bond length of 1.55-1.59 Å in tricoordinate boron compounds. B–O bonds in trivalent organoboron compounds have a bond length of 1.31-1.38 Å, shorter than C–O bonds (1.43 Å).¹² The difference in bond length is because B–O bonds have a partial double bond character where the lone pair of oxygen is interacting with the empty *p* orbital on boron. The empty *p* orbital also leads to π -conjugation of the B–C bond in aryl- and alkenylboron compounds.¹²

Organoboron reagents can be categorized as boranes, borohydrides, boronic acids, borinic esters, boronic (boronate) esters, boronamides, boryl anions, and borate anions among others (**Figure 1.3**). The classification of organoboron compounds varies greatly in the literature. Boranes

are compounds that can be substituted with any combination of alkyl groups or hydrogen atoms and therefore they can be divided into two classes: boron hydrides which contain at least one hydrogen atom on boron and triorganoboranes which contain three organic group on boron. Boronic acids contain two hydroxyl groups and one organic group and boronic esters contain two alkoxy groups and one organic group. Together, boronic acids and esters and have been dubbed the most synthetically useful organoboron compounds.¹²

BR₃	BR₂(OH)	BR₂(OR)	BR(OH)₂
Boranes	Borinic acids	Borinic esters	Boronic acids
BR(OR)₂	B(OH)₃	B(OR)₃	RB(NR₂)₂
Boronic (boronate) esters	Boric acid	Borate (boric) esters	Boronoamides
BX₃	[: BR₂]⁻	[RBH₃]⁻	[RBF₃]⁻
Boron trihalides	Boryl anions	Borohydrides	Trifluoroborates

Figure 1.3 Classification of boron compounds

1.1.2 Boronate Esters

Boronic acids and boronate esters have been extensively studied since the discovery of the Suzuki-Miyaura cross-coupling reaction in 1979.⁸ The Suzuki-Miyaura reaction has undergone major improvements in terms of scope expansion,^{15, 16} optimization for lower reaction temperatures,^{17, 18} catalyst loading,^{19, 20} and for the development of boron reagents as boronic acid precursors (**Figure 1.4**).²¹ Despite boronic acids being tremendously useful building blocks in organic synthesis, 2-heterocyclic, vinyl, and cyclopropyl derivatives are inherently unstable.²² As an alternative, a variety of boronate ester derivatives have been synthesized and studied.

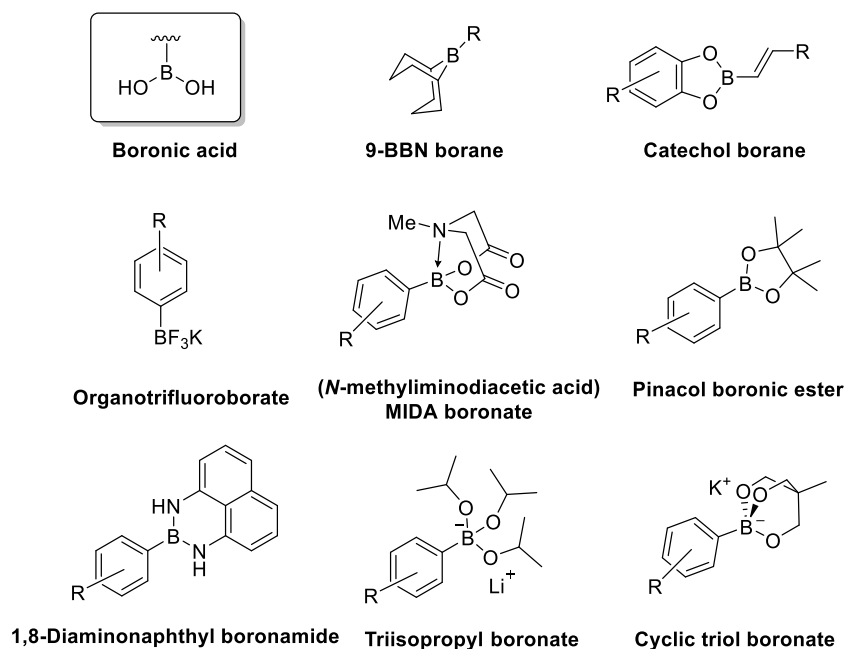


Figure 1.4 Examples of common boron reagents used in the Suzuki-Miyaura coupling reaction

1.1.3 *N*-Coordinated Boronates

In 1986, Wrackmeyer and co-workers synthesized air-stable bicyclic boronic esters derived from iminodiacetic acids.²³ The study was inspired by the high degree of hydrolytic stability of boron amino acid derivatives and their potential use in biological studies.²⁴ The B–N bond has also been appreciated in advancements for the preparation of boron reagents for the Suzuki-Miyaura cross-coupling reaction.²⁵ The cyclic backbone of *N*-coordinated boronates consist of two B–O covalent bonds plus a dative B–N bond that forms from the donation of the Lewis base lone pair on the nitrogen atom, forcing the boron into a tetrahedral geometry. *N*-Coordinated boronates are typically free-flowing, crystalline solids and are stable to air, moisture, and silica-gel chromatography. Examples of *N*-coordinating ligands include but are not limited to diethanolamine, *N*-methyldiethanolamine, *N*-phenyldiethanolamine and *N*-methyliminodiacetic acid (MIDA) (**Figure 1.5**).²⁵

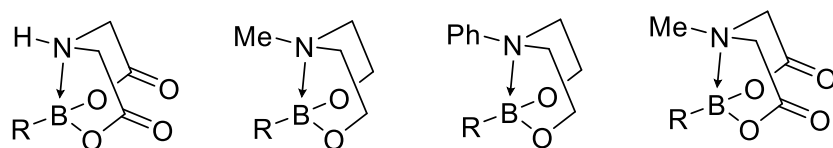
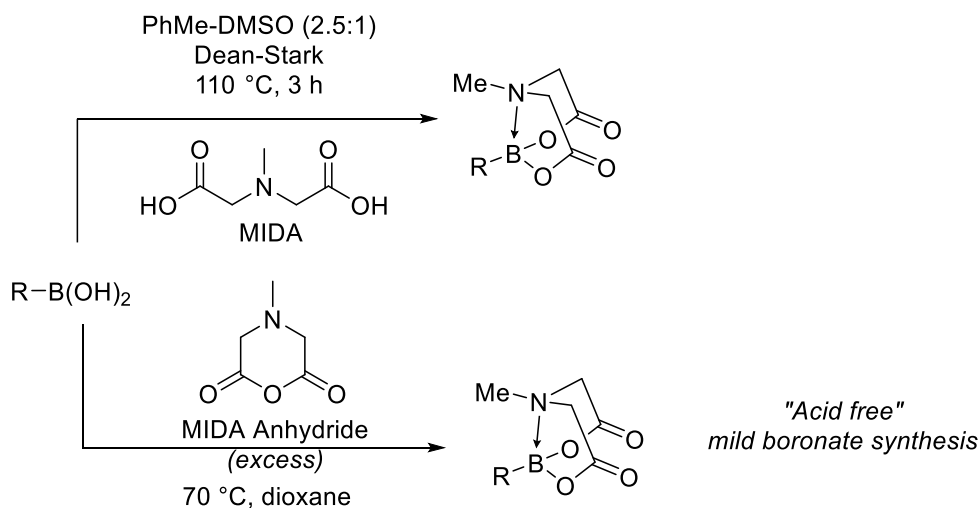


Figure 1.5 *N*-Coordinated boronates used in Suzuki-Miyaura coupling reactions

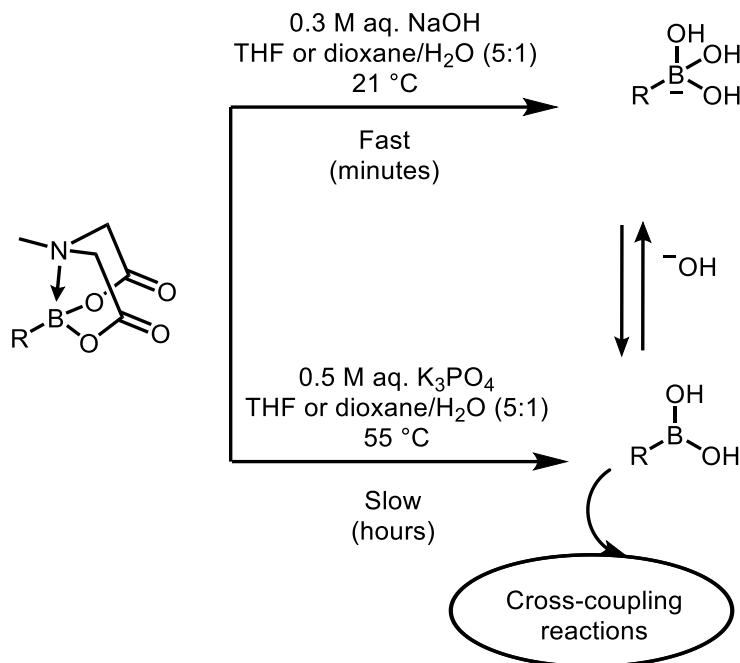
N-Coordinated boronates can be synthesized from their corresponding boronic acid via condensation with diethanolamine or iminodiacetic acid based ligands (**Scheme 1.1**).^{26, 27} The stability of MIDA boronates makes them attractive handles to introduce on biologically relevant motifs that are bench stable and can be used on demand. Burke and co-workers have studied the compatibility of MIDA boronates with a variety of common reagents.^{28, 29} MIDA boronates were found to be stable under Evans aldol, Horner-Wadsworth-Emmons olefination and Takai olefination reaction conditions.²⁹ They have also been shown to tolerate a variety of workup/extraction solutions such as water, pH 7 buffer, brine, aq. HCl, aq. NH₄Cl, aq. Na₂S₂O₃ and aq. hydrogen peroxide at pH 6.²⁹



Scheme 1.1 Preparation of MIDA boronates

Burke and co-workers developed a protocol for the controlled release of boronic acids from MIDA boronates to prevent the accumulation of boronic acid during cross-coupling reactions which has facilitated iterative cross-coupling (**Scheme 1.2**).^{21, 22} Since then, MIDA boronates have taken off as a general platform for small-molecule construction based on MIDA-

bearing building blocks and a range of MIDA boronates have become commercially available.²⁵ Although the MIDA ligand is expensive, the increase in demand for stable boron precursors has resulted in the availability of well-priced MIDA complexed boronates.

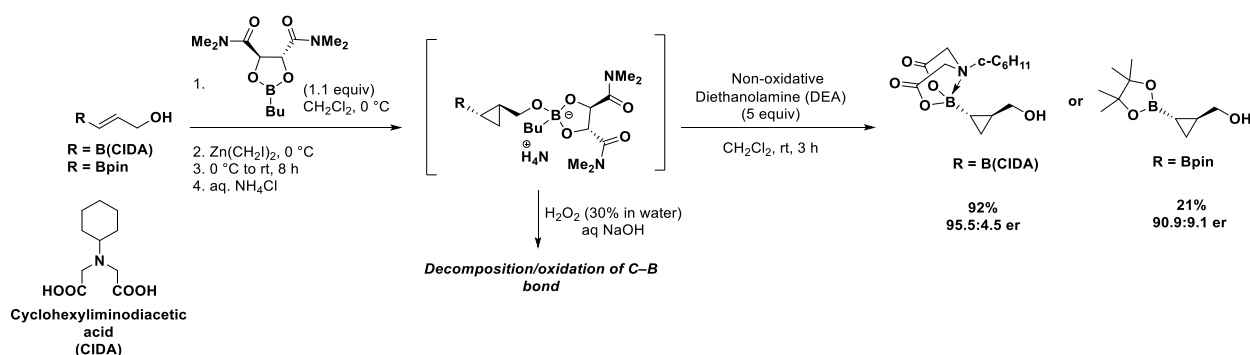


Scheme 1.2 Slow-release cross-coupling conditions for MIDA boronates

The development of stable tetracoordinate boronates expands the scope for the application of organoboronates to include: small-molecule synthesis,³⁰ synthesis of natural products³¹ as well as the synthesis of drug candidates.³² Moreover, tetracoordinate boronates can be used as stable handles on small chiral building blocks that can be readily converted to their corresponding boronic acid upon demand. They have also shown significant progress in the asymmetric synthesis of organoboronates which has allowed for the development of a library of chiral building blocks that can be used in late-stage functionalization (LSF).^{33, 34}

Chapter 2 addresses challenges associated with the synthesis of enantioselective borocyclopropanation reactions using the Charett dioxaborolane-mediated cyclopropanation reaction.³⁵ To overcome these challenges, the exceptional stability of tetracoordinate boronates is explored. MIDA boronates have been established to exhibit exceptional stability in synthesis and we proposed that MIDA borocyclopropanes could be synthesized in an enantioenriched

manner from their corresponding allylic alcohols and provide robust building blocks. However, the cyclopropanation reaction conditions could not accommodate the allylic alcohol bearing a MIDA boronate as it exhibited solubility issues. A soluble and robust alternative allylic alcohol bearing an *N*-cyclohexyliminodiacetic acid (CIDA) boronate was synthesized to overcome the challenge. With an ideal precursor in hand, we moved to develop an alternative to the traditional oxidative work up used to decomplex the chiral dioxaborolane ligand that is bound to the cyclopropyl intermediate. The development of a non-oxidative work-up using diethanolamine allowed for the selective cleavage of the dioxaborolane in the presence of boronates (**Scheme 1.3**). The enantioselective borocyclopropanation reaction is a significant addition to the highly versatile and robust enantioselective zinc carbenoid-mediated cyclopropanation reactions, which can now be extended to base-sensitive substrates.



Scheme 1.3 Enantioselective dioxaborolane-mediated cyclopropanation of *N*-coordinate boronate allylic alcohols

1.1.4 *N*-Coordinated Boranes: Amine-Boranes

Gay-Lussac³⁶ reported the first boron-nitrogen ($\text{H}_3\text{N}-\text{BF}_3$) dative bond in 1809 which was followed by the first report of an amine-borane by Burg and Schlesinger in 1937.³⁷ Burg and Schlesinger synthesized trimethylamine-borane from trimethylamine and diborane and from carbon monoxide displacement by trimethylamine from a borane-carbon monoxide adduct.³⁷ Amine-boranes and their derivatives have a diverse set of applications ranging from reagents in organic synthesis³⁸ to hydrogen storage materials^{39, 40} to pharmacologically active compounds (**Figure 1.6**).⁴¹

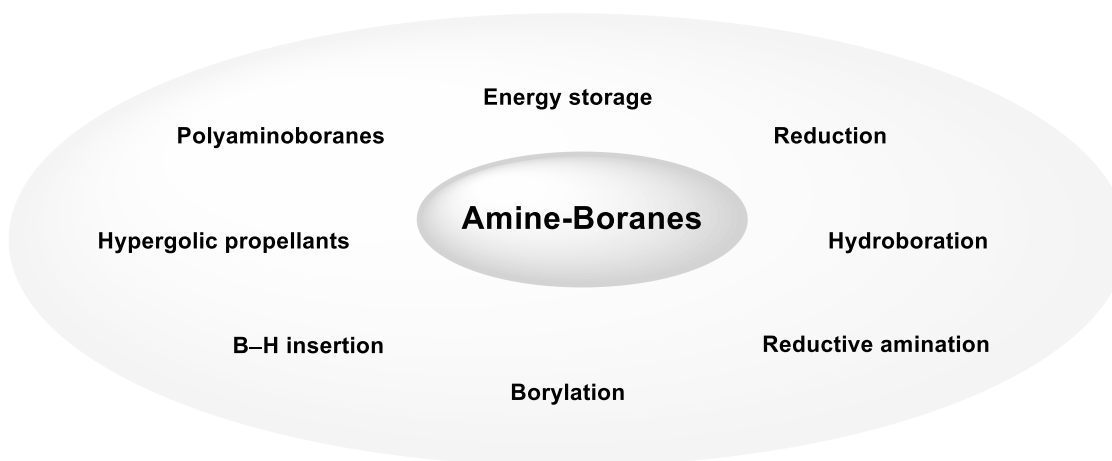
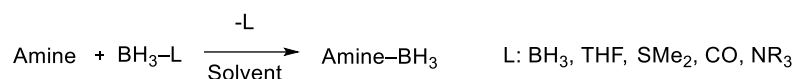


Figure 1.6 Applications of amine-boranes

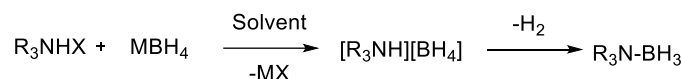
Amine-boranes are typically stable white crystalline solids apart from *sec*-butylamine-borane and diethylborane which are liquid at room temperature. The hydridic nature of the hydrogen atoms on the borane functionality is what enables the diverse and unique chemistry of amine-boranes.⁴² The borane functionality can also bear mono or dialkyl ligands. Alkyl boranes bonded to a nitrogen bearing a protic hydrogen will readily undergo dehydrogenation reactions.⁴³ Increasing the steric bulk on both the B- and N-atoms is known to reduce stability of the amine borane due to a poor orbital overlap.⁴²

Amine-boranes are highly sought after synthetic targets due to the similarity in atomic radii and characteristic equivalence of the B–N unit to C–C bonds.⁴⁴ The B–N bond is isoelectronic to the C–C bond. The C–C bond length in ethane is 1.533 Å compared to that of ammonia-borane 1.658 Å; however, they vary significantly in terms of bond strength: 89 kcal/mol and 31 kcal/mol, respectively. The synthesis of amine-boranes can be classified into three categories including but not limited to Lewis acid displacement, metathesis, and *trans*-amination of ammonia-borane (**Figure 1.7**). The Lewis acid displacement-based protocol has been used to synthesize various amine-borane derivatives using precursors such as borane-tetrahydrofuran (BH₃·THF) and borane-dimethylsulfide (BH₃·DMS).⁴² Alternatively, amine-boranes can be synthesized from metal borohydrides in the presence of alkyl ammonium salts proceeding via salt metathesis followed by dehydrogenation.⁴⁵ Amine-boranes can also be synthesized via the *trans*-amination of ammonia-borane which is an alternative to BH₃·THF and BH₃·DMS in terms of stability.⁴⁶

1. Displacement of Lewis-base:



2. Metathesis:



3. *Trans*-Amination of Ammonia-Borane:

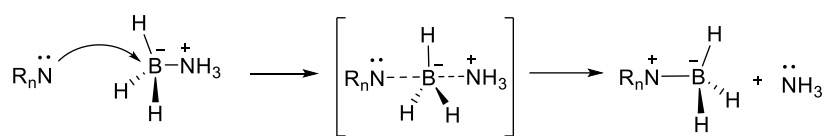
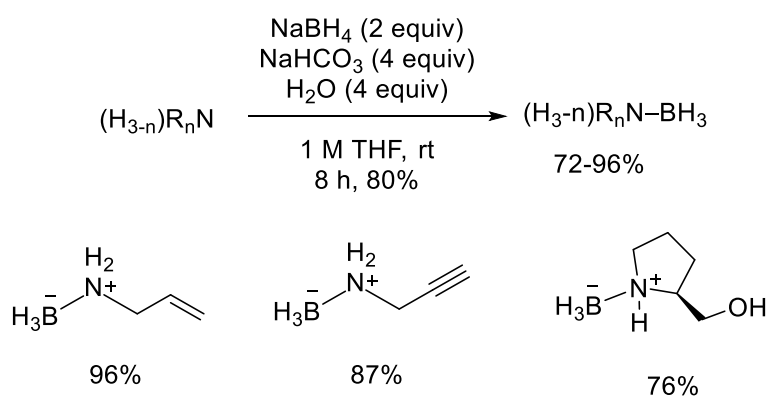


Figure 1.7 Synthesis of amine-boranes: 1. Displacement 2. Metathesis and 3. *Trans*-amination of ammonia-borane

The synthesis of amine-borane reagents is limited by functional group tolerance to borane-adducts. Ramachandran and co-workers developed a convenient and scalable protocol for the synthesis of a variety of amine-boranes bearing borane-reactive functionalities such as alkenes, alkynes, hydroxyl, thiol, ester, amide, nitrile and nitro substituents (**Scheme 1.4**).⁴⁷ The method has been recognized to enhance the design and development of amine-boranes.



Scheme 1.4 Amine-borane synthesis of substrates containing borane-incompatible functionalities

1.2 Boron in Drug Design

The ability of boron to undergo reversible covalent interactions by switching between sp^2 and sp^3 hybridization upon protein binding has made it a fascinating element in drug design.^{5, 48} Boron sits in the same period as carbon and nitrogen that form the backbone of life, yet its potential in medicinal chemistry has been overlooked for quite some time.⁴⁹ Although a small number of boron-containing natural products have been isolated, the design of potential drugs containing boron is of increasing interest (**Figure 1.8**).⁴⁹ Boromycin was isolated from *Streptomyces antibioticus* and was the first identified natural product that contained boron. Boromycin is a polyether-macrolide antibiotic with selective activity against most gram-positive bacteria and has shown to have anti-HIV activity.^{50, 51}

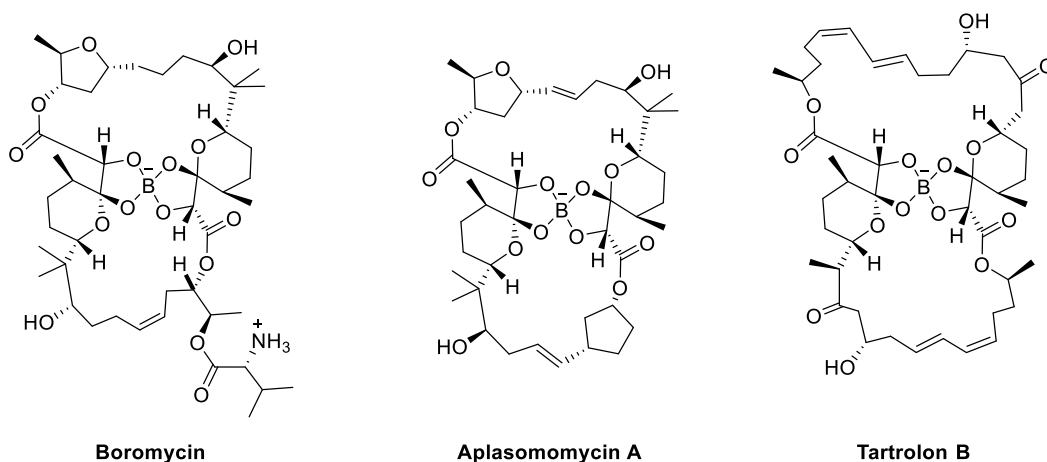


Figure 1.8 Boron containing natural products

The therapeutic activity of boron is relatively new to medicinal chemists as compared to carbon, hydrogen, nitrogen, and oxygen. The lack of identified natural products containing boron that can serve as leads for medicinal chemists has led them to shy away from using boron in drug design.⁵² Apprehensions resulting from the perceived toxicity of boron in drug molecules resulted in boron being undermined in the medicinal chemistry community. A study in 2009 found that the belief that boron is toxic arose from boric acid ($B(OH)_3$) being an ingredient in ant poisons but boric acid has an LD_{50} of 2660 mg/kg (rat, oral) which is similar to that of table salt (3000 mg/kg (rat, oral)).⁵² Furthermore, toxicity concerns were also considered to have risen from the boron-based therapeutic used to treat multiple myeloma, Velcade®. However, a recent study found that

the toxicity was due to the mechanism of action and not because of the boron element itself.⁵² The boronic acid in Velcade is metabolized to boric acid and can be excreted by the body.⁵³ Skepticism of the use of boron in drug design has decreased from the overwhelming data stating the safety of the use of boron as well as showing that the human body is quite familiar with boron.^{52, 54} Understanding that there is no inherent toxicity associated with boron has inspired its use in medicinal chemistry. Advances in the field of boron chemistry have led to the approval of several boron containing drugs by FDA as of 2003 such as bortezomib (Velcade[®]), tavaborole (Kerydin[®]) and crisaborole (Eucrisa[®]) (**Figure 1.9**).

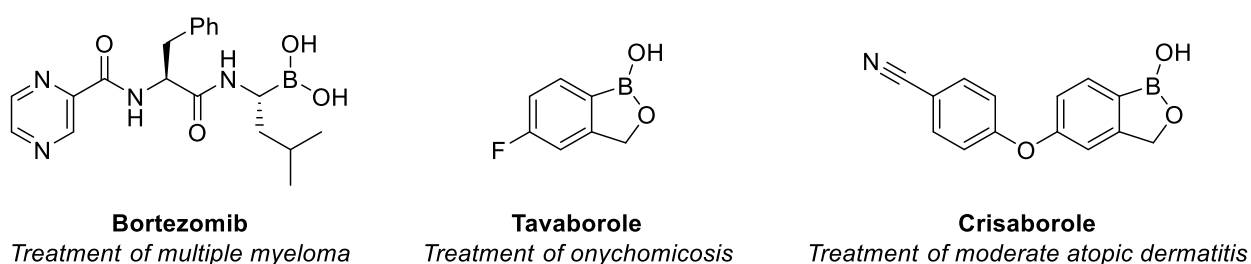


Figure 1.9 Boron containing drug molecules

Boron containing compounds are effective isosteres of their carbon counterparts and several boron-containing heterocycles such as diazaborines, oxadiazaboroles, oxazaborolidines, azaborines, and benzoxaboroles have shown potent biological activity and are at various stages of FDA approval as drug candidates.⁵⁵ The recent renaissance of boron in medicinal chemistry is expected to continue as scientists discover the previous overlooked role of boron in drug design and therefore any methodology providing access to new motifs containing boron could be of interest to synthetic as well as medicinal chemists.

1.3 Amine-Boranes in Drug Design

Tetrahedral borane complexes are isosteres of tetrahedral carbons but have more lipophilic pharmacological properties thus enhancing lipid solubility and facilitating their crossing through biological membranes.⁵⁶ Under certain physiological conditions, boron can convert from a neutral trigonal planar sp^2 to tetrahedral sp^3 hybridization.⁴⁸ In addition to boronic acid and benzoxaborole derivatives in approved FDA drug molecules, amine-boranes and related derivatives also possess a wide range of biological activities.⁴¹ Aliphatic, heterocyclic amines and

nucleic acids have been shown to possess potent anti-cancer, anti-inflammatory, and anti-osteoporotic properties which can lead to potentially exciting new drug candidates.⁴¹ A large number of aliphatic and heterocyclic amine-boranes have been prepared, some of which are analogues of biologically important molecules.⁴¹ Common borane functionalities in pharmacologically active compounds include BH₃, cyanoborane (BH₂CN), carboxyborane (BH₂COOH), carbomethoxyborane (BH₂COOCH₃) and *N*-ethyl carbamoylborane (BH₂CONHCH₂CH₃) (**Figure 1.10**).⁵⁶

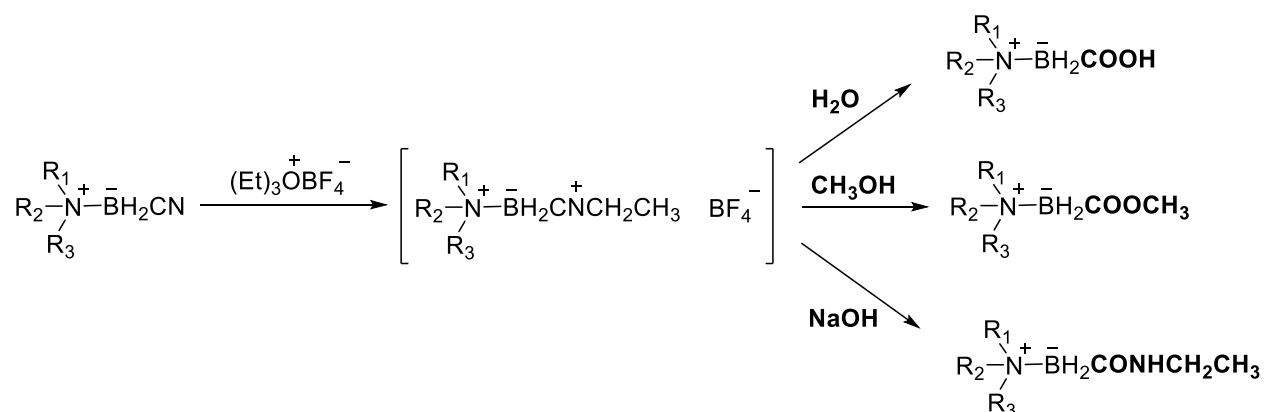


Figure 1.10 Common borane functionalities in pharmacologically active compounds

Amine-borane adducts of simple heterocyclic amines (i.e.: morpholine, piperidine, piperazine, and imidazole) have also been synthesized and evaluated for their pharmacological activity and have shown to have potent cytotoxic activity *in vitro* and *in vivo* against murine and human tumor models.⁴¹ Amine-boranes have also been incorporated into di- and tripeptides via the *N*-terminus and have shown hypolipidemic activity.⁵⁷ In addition, they have been investigated as therapeutic agents in boron neutron capture therapy (BNCT) used in treatment for inoperable tumors.⁵⁸ Despite a wide range of biological activity, the lack of methodologies to integrate amine-boranes into motifs of interest has slowed down the development of amine-borane containing clinically approved drug molecules.⁴²

1.4 Spirocycles in Drug Design

The advent of combinatorial chemistry to synthesize new drugs coupled with drug profiling techniques such as high throughput screening (HTS) has revolutionized the field of drug discovery. Despite tremendous scientific advancements, the drug efficiency measured in the number of new drugs approved by the FDA versus dollars spent on R&D shows a declining trend for the past few decades.⁵⁹ Lovering and co-workers⁶⁰ identified the presence of a high number of planar aromatic and achiral molecules in potential drug libraries as a key criterion for the lack of successful drug candidates. Increase in sp^3 character and three-dimensionality along with conformational restriction resulting from rigidity have shown to improve the potency, selectivity, physicochemical properties, and pharmacokinetic profile of drug molecules thus increasing the chances of finding a biologically active hit.⁶¹⁻⁶³ One way Nature accomplishes the task of having more saturated molecules with enhanced 3D character is by the presence of spirocycles in their structure.⁶⁴ Spirocycles are found to be prevalent in biologically active drug-like compounds and have become privileged motifs in drug design (**Figure 1.11**).⁶⁴

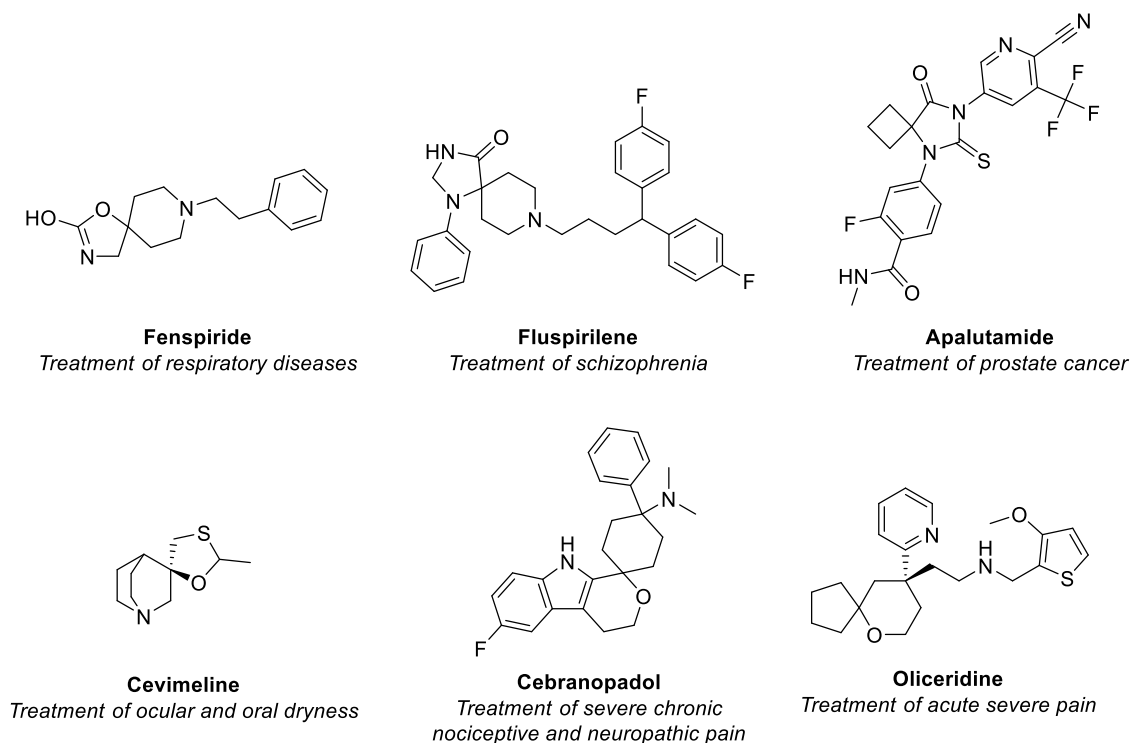


Figure 1.11 Biologically active molecules containing spirocycles

Over the last couple of decades, the use of the key word “spiro” has increased in medicinal chemistry journals.^{63, 65} Spirocycles were first synthesized by Baeyer in 1900.⁶⁶ The construction of spirocycles requires the creation of a quaternary center which is in itself a challenging task in synthetic organic chemistry.⁶⁷ Spirocycles can be synthesized through metathesis, cycloaddition and rearrangement reactions. Some popular named reactions that are often used in spirocyclization protocols include Fischer indolization, Suzuki-Miyaura cross-coupling and retro-Diels Alder (rDA) reaction (**Figure 1.12**).⁶⁸

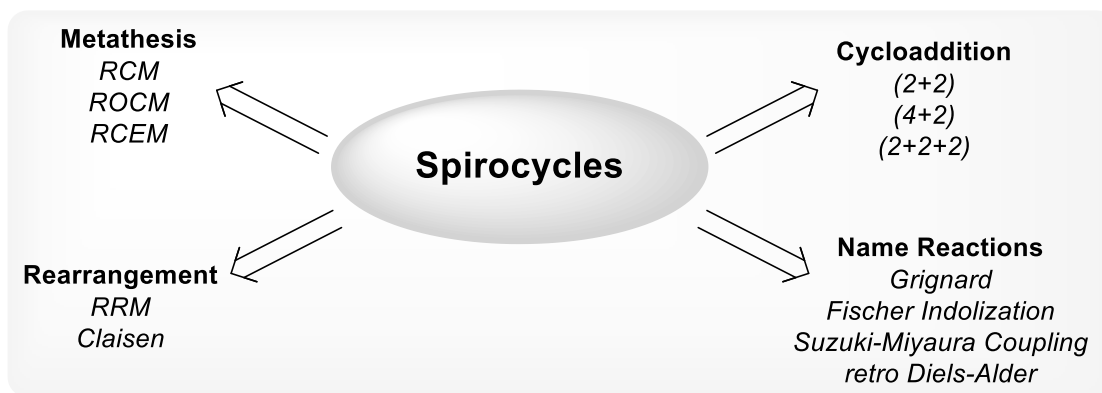


Figure 1.12 Chemical transformations used in the synthesis of spirocycles

The enhanced pharmaceutical activity seen in the spirocyclic derivatization of parent drug molecules has led medicinal chemists to continue in the pursuit of drug targets containing spirocycles despite multi-step, time consuming and expensive protocols.⁶⁸

Currently there are no approaches that allow access to a class of spirocyclic amine-boranes. As mentioned above, the synthesis of amine-boranes typically involves the use of reactive borane adducts that are incompatible with many functional groups. The lack of amine-boranes in drug molecules despite having potent anti-cancer, anti-inflammatory, and anti-osteoporotic properties can be partly attributed to the challenges associated with incorporating them into parent drug molecules that contain borane incompatible functional groups.⁴²

One way of developing complex heterocyclic molecules is via ring expansion of smaller cyclic systems such as cyclopropane. The cyclopropane ring possesses a ring strain energy of 27.5 kcal/mol making it an ideal target for ring opening as well as ring expansion reactions. The release

of ring strain gives scalable and controlled access to complex target molecules with high step economy. Cyclopropanes have been extensively studied as a building block in organic chemistry and a substantial number of reactions to manipulate cyclopropanes have been reported.⁶⁹⁻⁷³ Cyclopropanes have olefinic character due to the bent nature of the orbitals involved in the C–C bond formation and therefore cyclopropanes are known to show extensive reactivity towards nucleophiles, electrophiles and radical species.⁷² The main techniques used for the ring expansion of cyclopropanes involve ring opening of a bicyclic system via functional group promoted C–C bond cleavage followed by a carbon insertion, C–C bond migration to an exocyclic group or through electrocyclic and sigmatropic reactions (**Figure 1.13**).⁷¹

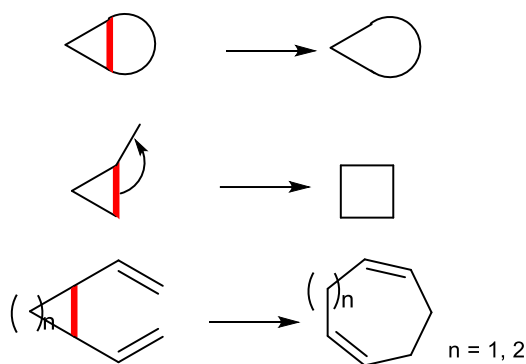


Figure 1.13 Ring-expansion of cyclopropane rings

Cyclopropanes are classified as activated if they are decorated by substituents which can result in an electronic bias in the strained C–C bond. Unactivated cyclopropanes, on the other hand, lack any substituents which can generate electronic bias in the C–C bond. There is a wide body of literature which describes ways to ring open activated cyclopropanes but the ring opening of unactivated cyclopropanes has proven to be challenging.^{74, 75} Unactivated cyclopropanes and their use as a building block in synthetic chemistry is very attractive since they are ubiquitous in nature and do not encumber the target molecule with unnecessary functionalities as is the case with activated cyclopropanes.

As discussed above, the synthesis of a spirocycle is challenging and often results in low step economy which has prevented spirocycles from realizing their full potential. A methodology

involving the conversion of unactivated cyclopropanes to spirocycles would result in high step economy and therefore could be potentially attractive to chemists.

Chapter 3 presents the development of a single-step, atom-efficient and regioselective methodology to synthesize spirocyclic amine-boranes (SCABs) via ring opening of unactivated cyclopropanes. Unactivated cyclopropanes in presence of an amine-borane tether were found to ring open upon activation by a catalytic amount of Tf_2NH . The conversion of a 1,2,2-substituted CAB to the corresponding SCAB was obtained as a single diastereomer and the product was found to be net anti-hydroborated. The proposed mechanism involves the breaking of both a C–C and C–H bond resulting in a high step economy. The SCABs were obtained with various degrees of substitution and are highly stable motifs. They also represent a new class of amine-boranes with potentially unexplored reactivity. Spirocyclic analogues are well known to modulate physiochemical properties of their parent compounds by enhancing the sp^3 character of the molecule without significantly increasing the molecular weight.⁷⁶ The single step transformation of unactivated cyclopropanes to spirocycles is the first reported in literature and could be of utility to synthetic as well as medicinal chemists.

1.5 Boron Hydrides as Proton Acceptors

1.5.1 Hydrogen Bonding

Hydrogen bonding is described as an interaction ($\text{X-H}\cdots\text{Y}$) between a hydrogen atom covalently bonded to an electronegative atom (X) such as (N, O and F) and the lone pair of electrons of a hydrogen bond acceptor (Y). The ability of a hydrogen atom to generate attractive electrostatic interactions with another electron rich and electronegative atom has intrigued scientists ever since its discovery in the early 1900s.⁷⁷ What is now widely known as hydrogen bonding (HB), plays a decisive role in determining the chemical and physical properties of a substance.⁷⁸ Latimer and Rodebush have been credited with being the first to mention hydrogen bonding in 1920, yet citations of their report remained scarce for decades until it was discovered that base pairs in DNA are bound by hydrogen bonds.⁷⁹ Hydrogen bonds are understood to be stronger than non-covalent interactions such as van der Waals forces but weaker than a

conventional covalent or ionic bond.⁸⁰ The exact nature of a hydrogen bond has always been a matter of debate and hydrogen bonding is understood to lie at the intersection of weak non-covalent bonding interactions and a strong covalent bond (**Figure 1.14, i**). In fact, recent research done by Tokmakoff and co-workers show that in the case of hydrogen fluoride (HF) the F–H–F hydrogen bond can even undergo transformation to a covalent bond.⁸¹

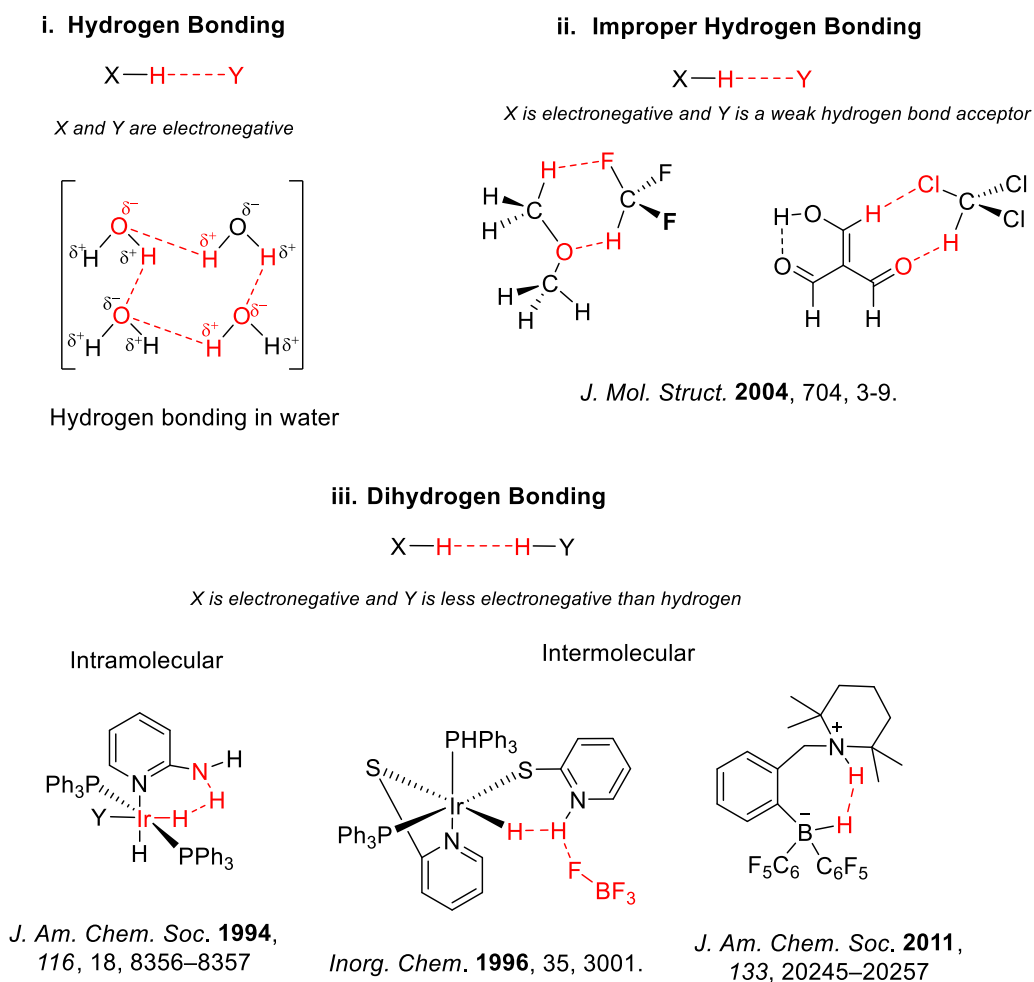


Figure 1.14 Hydrogen and dihydrogen bonding

As predicted by Linus Pauling in 1931, hydrogen bonding has been shown to lie at the heart of several life sustaining systems which has led to hydrogen bonding being extensively studied in physics, chemistry and biology.^{82, 83} Due to the presence of a covalent character in a hydrogen bond, it is reasoned that a hydrogen bond acceptor populates the σ^* orbital of the X–H bond leading to the lengthening of the X–H bond. The lengthening and consequent weakening

of the X–H bond is studied by a characteristic red shift in the stretching frequency (FTIR) of the X–H band. Hydrogen bonded interactions are classified as strong, moderate or weak with the bond strength of the hydrogen bond ranging from 15-40 kcal/mol, 4-15 kcal/mol, and 1-4 kcal/mol respectively.⁸⁴

C–H bonds are expected to be fairly inert despite carbon being slightly more electronegative than hydrogen. Therefore, when C–H bonds were found to participate in hydrogen bonding like interactions, scientists were rightly left puzzled (**Figure 1.14, ii**).⁸⁵⁻⁸⁸ Initial work done showing C–H···O interactions via crystallography was met with much skepticism by the scientific community.⁸⁷ Since then several experimental studies have convincingly established the presence of such C–H···Y interactions and are now considered to be integral parts of several biological systems.^{89, 90} Even though such interactions are classified as a category of hydrogen bonding, they have their own unusual characteristics that warranted deeper investigations. Hydrogen bonds are typically characterized by a red shift and enhanced intensity of the band in the IR spectrum accompanied by a weakening of the X–H bond. On the other hand, some of the C–H···Y interactions lead to a blue shift and a reduced intensity of the C–H band in the IR spectrum which is referred to as an 'improper hydrogen bond'. In most cases where an improper hydrogen bond is observed, the carbon atom is bonded to highly electronegative atoms such as CHF₃ which aids in the polarizability of the C–H bond which can then bond with a hydrogen bond acceptor 'Y' leading to an X–H···Y improper hydrogen bond. The activation of a C–H bond is of high importance to chemists and therefore any sort of interaction that involves a C–H bond becomes a matter of interest.

Borane chemistry involves the use of organoboron reagents that have a boron and hydrogen bond. Alfred Stock investigated borane compounds with the general formula B_xH_y in the beginning of the 19th century.⁹¹ He developed methods for purification of extremely reactive and flammable boron hydrides using high-vacuum manifolds. Boron hydrides exist as dimers when there are no steric restrictions and only exist as monomers when they form adducts with a Lewis base or if the dimers are heated to high temperatures.¹² The formation of boron hydride dimers is driven by the need to have a complete octet of valence shell electrons. For example, borane (BH₃) prefers to exist as B₂H₆.

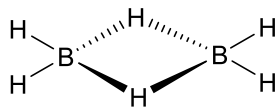


Figure 1.15 Structure of diborane (B_2H_6)

Boranes have been used to synthesize precursors for the Suzuki-Miyaura reaction, regioselective and stereoselective hydroborations and asymmetric hydroboration. Boranes have been used to synthesize allylboranes which have been used to transfer an allyl group to aldehydes and ketones via an allylic rearrangement. Below are some of the common boranes that are used in organic chemistry.

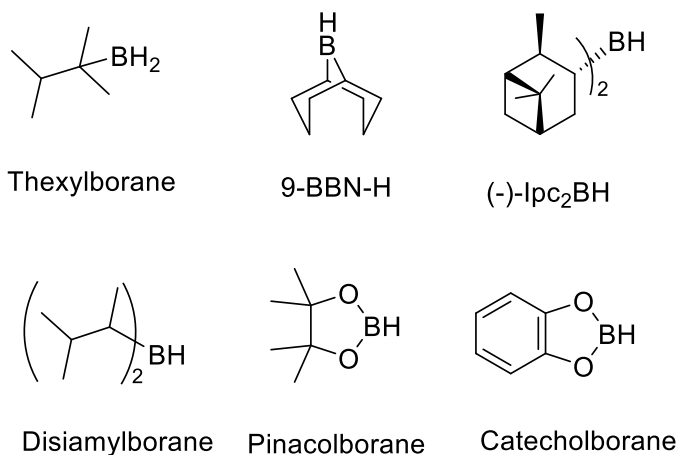


Figure 1.16 Structure of some common boranes

While boranes are strong Lewis acids, borohydrides are nucleophilic and have been used as a source of hydrides. In 1940, Hermann Irving Schlesinger and Herbert Charles Brown synthesized the first alkali metal borohydride, lithium borohydride.⁹² Since then a variety of metal borohydrides have been synthesized. The most common borohydride is sodium borohydride which has been used to reduce aldehydes, ketones, enones, acid chlorides, and other functional groups.^{93, 94} In addition to lithium and sodium borohydride, common borohydrides include sodium cyanoborohydride, and lithium triethylborohydride (superhydride).

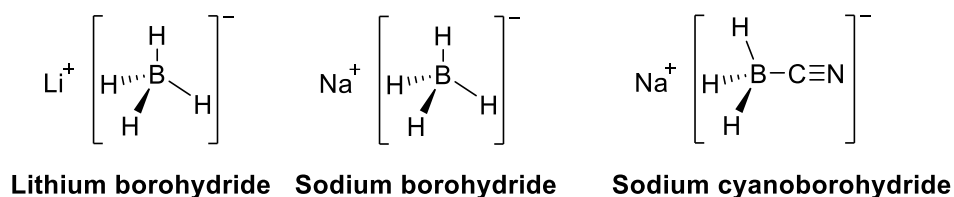


Figure 1.17 Structure of some common borohydrides

1.5.2 Reactivity of B–H Bonds

Borohydrides were believed to be incompatible with a highly acidic medium due to their hydride donor properties.⁹⁵ Borohydrides are proton acceptors and react with acids to evolve hydrogen gas. Borohydrides have since then been reported to be able to modulate their reactivity based on the proton donor. Sodium borohydride in acidic media has shown to reduce aldehydes, ketones and dienamines.⁹⁵ Proton acceptor behaviour can also be observed in the unique class of NHC-boranes. NHC-boranes consist of Lewis acidic borane, BH_3 , complexed to an *N*-heterocyclic carbene.⁹⁶ While NHC-boranes do not exhibit the same reactivity as other boranes, NHC-boranes upon reaction with strong acids were found to hydroborate alkenes.⁹⁷

Boron hydrides are interesting motifs with respect to hydrogen bonding since the hydride atom has a partial negative charge in the B–H bond on account of being a slightly more electronegative element than boron. Therefore, under certain circumstances, B–H bonds can act as hydrogen bond acceptors and have been extensively studied for their hydrogen bonding behaviour.⁹⁸ Dihydrogen bonds in which a hydrogen atom bonded to a less electronegative atom such as metal or boron can act as the electron donor, have a good combination of strength and directionality, potentially allowing rapid self-organization of molecular building blocks into extended regular structures and defining the physical properties of materials (**Figure 1.14**, iii).⁹⁹

Chapter 4 discusses the reactivity of the spirocyclic amine boranes (SCAB) with stoichiometric amounts of Tf_2NH . SCAB upon reacting with Tf_2NH liberated H_2 gas and led to formation of a $SCAB \cdot NTf_2$ complex. The 1H NMR spectrum of the $SCAB \cdot NTf_2$ was comprised of broad signals and the IR spectrum of the complex had blue shifted C–H bands with significantly reduced intensity. Further spectroscopic studies confirmed the formation of an ‘improper’

hydrogen bond with the C–H bond acting as hydrogen bond donor and $[\text{Tf}_2\text{N}]^-$ acting as hydrogen bond acceptors. Preliminary studies from the previous chapter suggested the potential of such species to activate C–F bonds. When further explored, we were able to use a $\text{SCAB}\cdot\text{NTf}_2$ complex as a mild reducing agent for aldehydes, ketones, imines, nitro-, nitrosobenzene, anthracene, indole and the Z-selective reduction of diphenylacetylene as well as a reagent to demethylate aryl methyl ethers.

**Chapter 2 – Enantioselective Synthesis of cis- and trans-
Borocyclopropylmethanol: Simple Building Blocks to Access
Heterocycle-Substituted Cyclopropylmethanols**

Background

Cyclopropane, a colorless, flammable and sweet smelling gas, was first synthesized in 1882 by August Freund.¹⁰⁰ Its anesthetic properties were first reported at the University of Toronto by Valyien E. Henderson and George H. W. Lucas in 1929.¹⁰¹ It was introduced in medicine as a general anesthetic by American anaesthetist Ralph Water in 1934 and was used until the mid 1980s.¹⁰² Cyclopropanes are ubiquitous in Nature and are found in various naturally occurring compounds including terpenes, pheromones and fatty acid metabolites.¹⁰³ Cyclopropanes can be isolated from plants, fungi, or microorganisms.⁷⁰ They have been incorporated in drug molecules and have been shown to enhance potency, reduce off-target effects, increase metabolic stability, increase brain permeability, decrease plasma clearance, and contribute to an entropically favorable binding to the receptor.⁶¹ Considering its medicinal value, the cyclopropyl scaffold has been increasingly incorporated into drug molecules with the goal of achieving enhanced therapeutic activity. Since the 1960s, the cyclopropane ring has begun to appear more frequently in the U.S. FDA approved drugs (**Figure 2.1**).⁶¹ As a result it is amongst

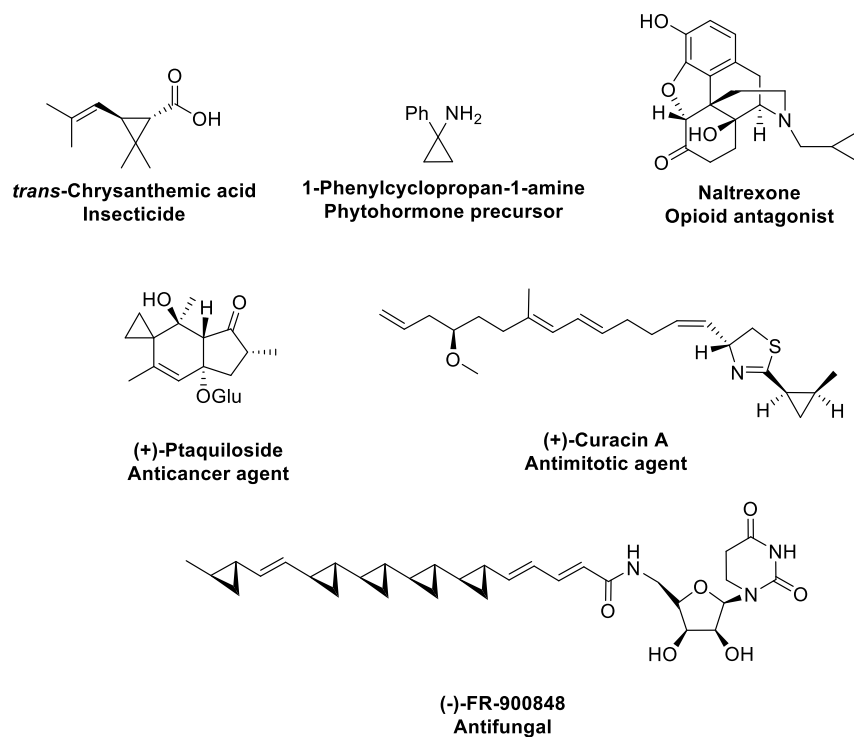


Figure 2.1 Cyclopropane-based natural products along with their biological property

the top 10 common cycloalkane rings found in drug molecules.¹⁰⁴ It also contributes to the insecticidal properties in pyrethrin (*trans*-chrysanthemic acid) from pyrethrum flowers.⁶¹ The incorporation of the “cyclopropyl fragment” into drug molecules can be traced back to two major classes of drugs: phenylcyclopropylamine-based, monoamine oxidase (MAO) and opioid antagonists (naltrexone).

The “cyclopropyl fragment” has aided in the transitioning of preclinical drug candidates to the clinical stage encouraging the development of elegant methodologies to synthesize a wide array of functionalized chiral cyclopropanes.¹⁰⁵ Chiral cyclopropanes are key pharmacophores and play a vital role in the discovery of new bioactive molecules.^{61, 106} Several methods, including metal-mediated or metal-catalyzed cyclopropanation, base-promoted formation of cyclopropanes, and Lewis-acid promoted formation of cyclopropanes, have been developed to incorporate chiral cyclopropanes in organic synthesis and medicinal chemistry. The Simmons-Smith cyclopropanation,¹⁰⁷ diazo-derived carbenoids,¹⁰⁸ Kulinkovich reaction¹⁰⁹ and nucleophilic displacement reactions,¹¹⁰ have been increasingly used to synthesize polysubstituted cyclopropanes as synthetic intermediates (**Figure 2.2**).

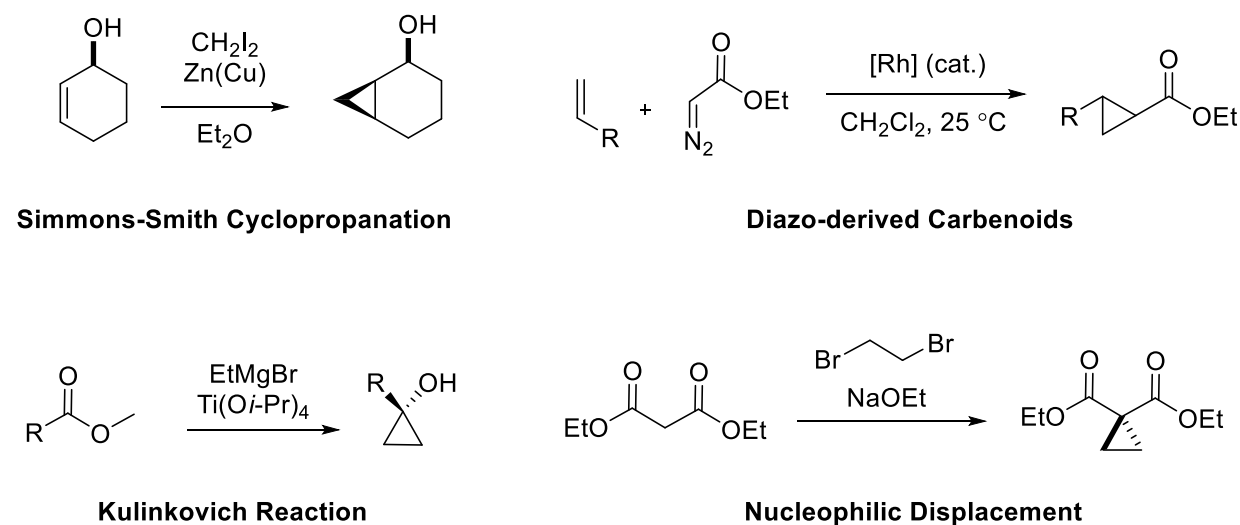


Figure 2.2 Common methods for the synthesis of cyclopropanes

Context

Late-stage functionalization (LSF) is frequently used to introduce greater complexity and functionality without affecting preinstalled functional groups.¹¹¹ Thus, the synthesis of stable chiral cyclopropanes with coupling handles allows for useful building blocks that can introduce enhanced therapeutic value to drug motifs via LSF.

The most common method to integrate key motifs into larger and more complex frameworks has been the use of Suzuki-Miyaura cross-coupling.¹¹² Suzuki-Miyaura cross-coupling has become a valuable synthetic tool and is one of the most reliable and widely applied palladium-catalyzed reactions in total synthesis.¹¹³ As a result, methods to synthesize chiral boron-bearing building blocks have become of increasing interest.¹¹⁴ Cyclopropyl boronic acids can be accessed through a variety of methods including: lithium/halogen exchange followed by electrophilic trapping with a borate ester (*e.g.* B(Oi-Pr)₃ or B(OMe)₃),¹¹⁵ cyclopropanation of alkenylboronates,¹¹⁶⁻¹¹⁹ Rh-catalyzed enantioselective hydroboration of cyclopropenes,¹²⁰ C–H borylation of cyclopropanes,¹²¹ and direct borocyclopropanation of olefins using a boronate-substituted zinc carbenoid (**Figure 2.3**).¹²² While access to diastereoselective borocyclopropanes in a diastereoselective manner is available, methods for enantioselective borocyclopropanation are limited.

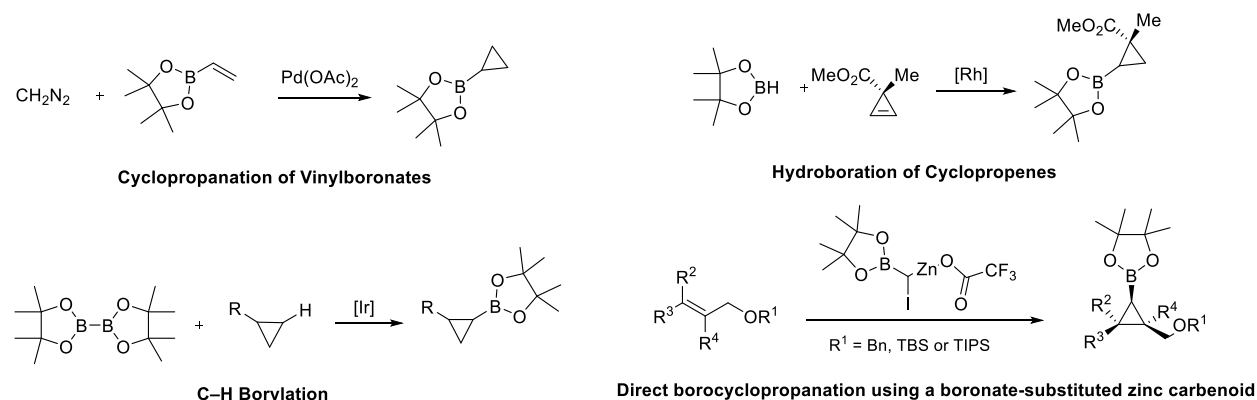
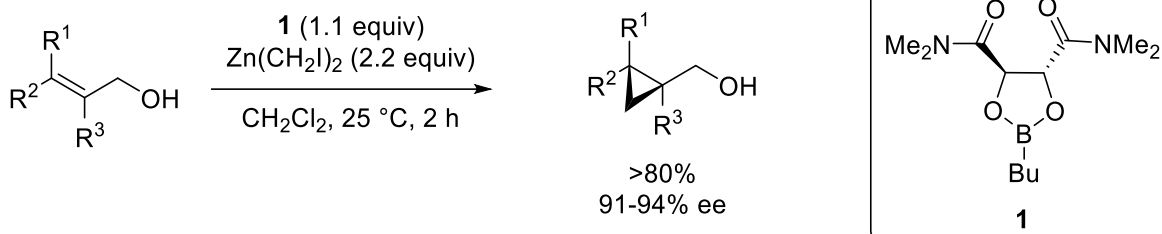


Figure 2.3 Examples of borocyclopropanation reactions

Chapter 2 reveals the first enantioselective Simmons-Smith cyclopropanation of an allylic alcohol bearing a tetracoordinate boronate. The dioxaborolane-mediated enantioselective

cyclopropanation reaction allows for direct access to enantiopure cyclopropanes from their corresponding allylic alcohols (**Scheme 2.1**).³⁵ However, the reaction requires a highly oxidative work-up ($\text{H}_2\text{O}_2/\text{aq. NaOH}$) in order to cleave the chiral dioxaborolane ligand and the work-up would simultaneously decompose sensitive substituents on the cyclopropane.



Scheme 2.1 Charette enantioselective cyclopropanation reaction

Borocyclopropanation methodologies have often used pinacolate analogues.^{116, 123-126} In 2008, Burke and co-workers²⁹ demonstrated tetracoordinate amine-boronates, termed *N*-methyliminodiacetic acid (MIDA) boronates, as highly air-stable and crystalline handles to have utility in multistep synthesis.²⁸ Albeit stable, MIDA boronates were not readily soluble in the optimized enantioselective Simmons-Smith reaction conditions. Soluble tetracoordinate boronates could have significant utility for the development of an enantioselective Simmons-Smith cyclopropanation. A dichloromethane (CH_2Cl_2) soluble tetracoordinate boronate bearing allylic alcohol was synthesized, *N*-cyclohexyliminodiacetic acid (CIDA), to substitute the insoluble MIDA boronate bearing allylic alcohol (**Figure 2.4**). The solubility of the MIDA boronate analogue was not the sole limitation of the enantioselective borocyclopropanation reaction. The traditional oxidative work-up would lead to the simultaneous oxidation and loss of the boron moiety during dioxaborolane decomplexation.

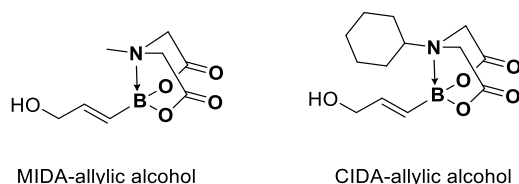
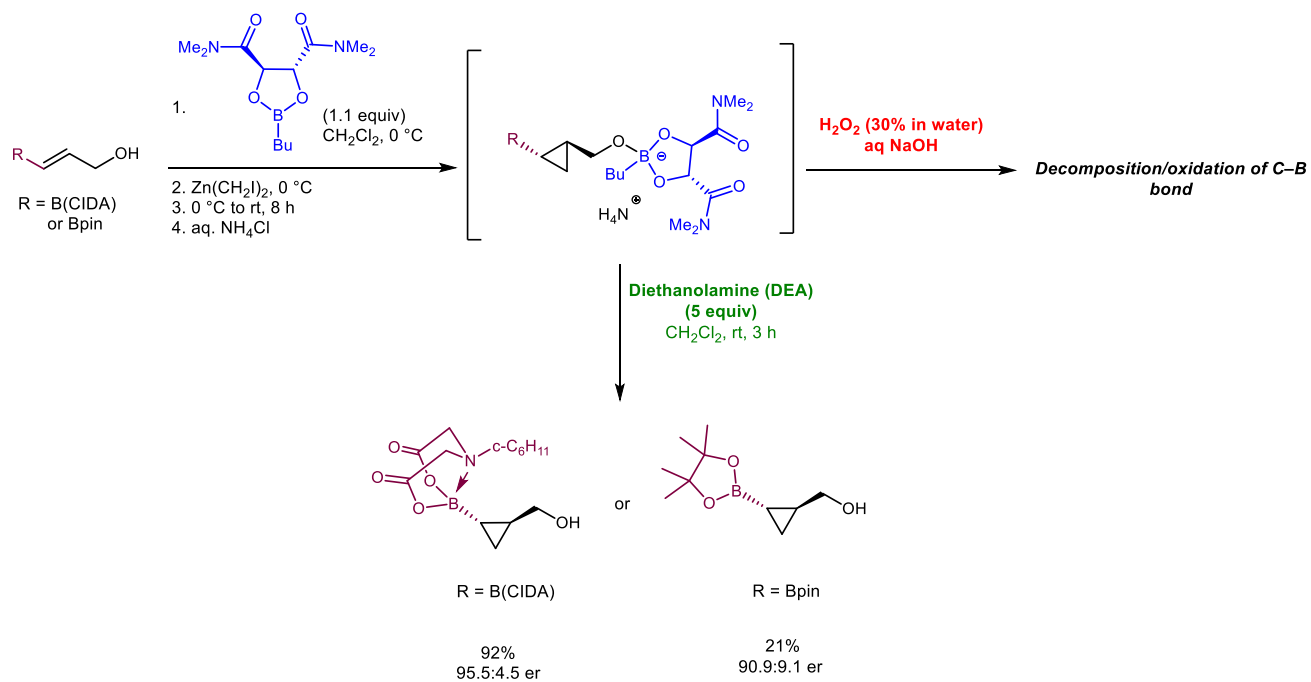


Figure 2.4 MIDA boronate allylic alcohol vs. CIDA boronate allylic alcohol

The paper focuses on development of a non-oxidative work up using diethanolamine to decomplex the dioxaborolane ligand in the presence of a boronate (**Scheme 2.2**). Our method not only enhances the scope of the dioxaborolane-mediated enantioselective cyclopropanation reaction towards boronate bearing allylic alcohols and other base-sensitive functional groups, but also introduces a CIDA-boronate ligand as a soluble alternative to MIDA boronates.



Scheme 2. 2 Dioxaborolane-mediated enantioselective synthesis of borocyclopropanes

Article 1

Siddiqui, S. H.; Navuluri, C.; Charette, A. B., Enantioselective Synthesis of Cis- and Trans-Borocyclopropylmethanol: Simple Building Blocks to Access Heterocycle-Substituted Cyclopropylmethanols. *Synthesis* **2019**, *51*, 3834-3846.

DOI: 10.1055/s-0037-1611896

Author contributions:

Chandrasekhar Navuluri, a former post-doc in our group, synthesized a batch of the CIDA ligand and worked on the initial optimization of the cyclopropanation reaction.

All other synthetic work and optimization was done by me.

The manuscript was written by myself and edited by Professor André Charette.

Enantioselective Synthesis of *cis*- and *trans*-Borocyclopropylmethanol: Simple Building Blocks to Access Heterocycle-Substituted Cyclopropylmethanols

Saher H. Siddiqui, Chandrasekhar Navuluri, André B. Charette*

FRQNT Centre in Green Chemistry and Catalysis, Department of Chemistry, Université de Montréal, P.O. Box 6128, Station Downtown, Québec, Canada, H3C 3J7.

Keywords

borocyclopropanes, heterocycles, Simmons-Smith reaction, zinc-cyclopropanation, cross-coupling

Abstract

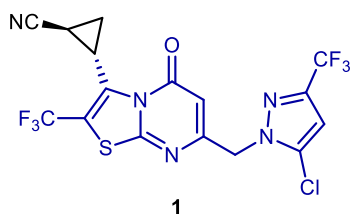
An enantioselective and non-oxidative methodology was developed to obtain enantioenriched cyclopropylboronates using a diethanolamine-promoted selective decomplexation of dioxaborolane. The non-oxidative decomplexation of the dioxaborolane ligand from the cyclopropylmethoxide species formed in the dioxaborolane-mediated Simmons-Smith cyclopropanation reaction provided the enantioenriched CIDA-based (CIDA = *N*-cyclohexyliminodiacetic acid) borocyclopropane in 92% yield and 95.6:4.4 er. A robustness screen has shown diethanolamine to be compatible with esters, carbamates, and *N*-heterocycles, providing a tool to access enantioenriched cyclopropanes carrying not only base-sensitive but oxidizable functional groups as well. Diethanolamine was found to be compatible with the modified zinc-cyclopropanation reaction of allyl alcohol to remove residual dioxaborolane from the corresponding *cis-N*-heterocycle cyclopropylmethanol, thereby leading to improved yields.

Introduction

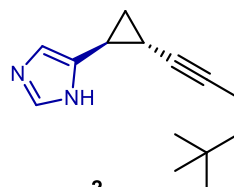
Cyclopropane motifs are ubiquitous in Nature¹ and are widely employed in pharmaceutically and agrochemically relevant compounds.² Cyclopropylboronic acids and derivatives are excellent synthons for the rapid introduction of the cyclopropyl motif into complex molecules.³ Suzuki-Miyaura cross-coupling of cyclopropylboronic acids with heteroaryls provides heteroaryl substituted cyclopropanes, which serve as chiral cores in many natural products and biologically active drug candidates.⁴ For example, thiazolopyrimidinones comprising the cyclopropane group (Figure 1, 1) serve as *N*-methyl-D-aspartate (NMDA) receptor activity modulators and rely on racemic borocyclopropylmethanols as optimal synthons for the introduction of cyclopropane groups in a racemic fashion.⁵ Similarly, borocyclopropane building blocks have been employed in the synthesis of cyclopropane-containing drug candidates (Figure 1, 2–4), where the products are delivered as racemates requiring chiral HPLC separation.⁶ Although an array of methodologies to access substituted borocyclopropane subunits in a diastereoselective manner are available,⁷ access to optically active borocyclopropane subunits is often limited. Thus far, asymmetric cyclopropanation methodologies to access enantioenriched borocyclopropanes include palladium-catalyzed cyclopropanation of chiral vinylboronates via diazo decomposition,⁸ and copper-catalyzed carbene transfer of ethyldiazoacetate to alkenylboronates for the preparation of chiral 1,2,3-trisubstituted cyclopropanes (Scheme 1, part i).⁹ The in situ preparation of enantioenriched borocyclopropanes via the zinc-cyclopropanation of substituted allylic alcohols is an alternative to the use of stoichiometric quantities of diazo compounds (Scheme 1, part ii).¹⁰ The Simmons-Smith reaction has also been employed for the synthesis of chiral vinylpinacolboronates as separable racemic diastereomeric mixtures.^{8b}

The Simmons-Smith cyclopropanation mediated by dioxaborolane **11** is a versatile methodology for the conversion of allylic alcohols and allylic ethers into an array of diversely substituted cyclopropane motifs in high enantioselectivities.¹¹ We report herein the first enantioselective Simmons-Smith cyclopropanation of boronate-bearing allylic alcohols for the preparation of enantioenriched borocyclopropane building blocks.¹² Pinacolate analogs have often been used in borocyclopropanation methodologies.^{4-6, 13} Many of these derivatives are oils and are prone to decomposition through protodeboronation, and are hence recurrently deemed

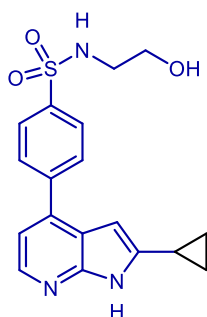
'unstable' boronic acids.¹⁴ In contrast, cyclopropyltrifluoroborates are solids and display reduced propensity to undergo protodeboronation but have limited solubility in moderately polar solvents.^{15, 16}



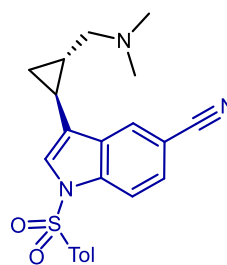
1
Genentech (GNE-0723)
GluN2A-Selective NMDA receptor



2
Merck (GT-2331)
histamine H3-antagonist



3
IκB Kinase (IKK2) inhibitor

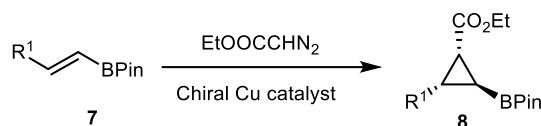
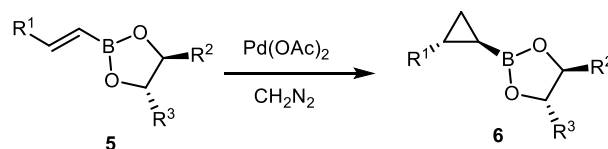


4
Bristol-Myers Squibb (BMS-505130)
serotonin transport inhibitor

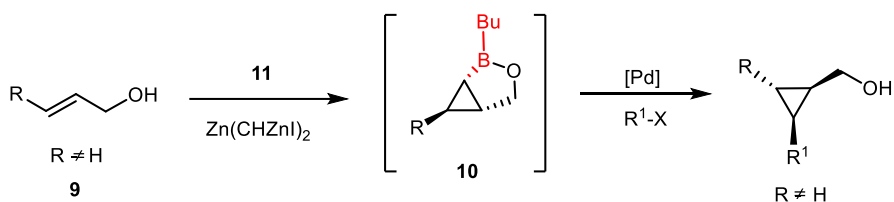
Figure 1 Selected cyclopropane-containing biologically active drug candidates

Previous work:

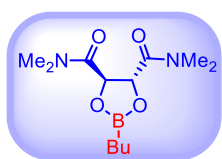
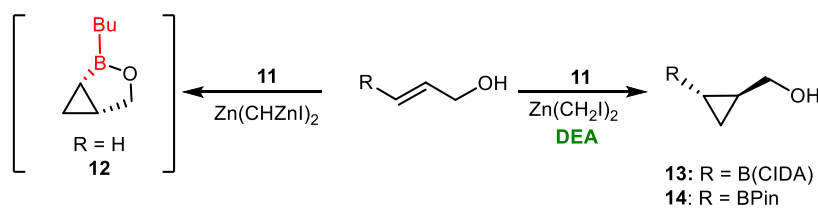
i. Diazo-mediated borocyclopropanation



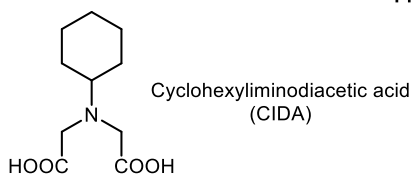
ii. Zinco-cyclopropanation of substituted allylic alcohols



This work:



11



Scheme 1 Synthesis of enantioenriched cyclopropylboronates

N-Methyliminodiacetic acid (MIDA) boronates have emerged as efficient building blocks due to their air stability, crystallinity, monomeric constitution, and compatibility with silica gel chromatography. The most attractive property of MIDA boronates is their reversibly attenuated reactivity towards anhydrous cross-coupling conditions and compatibility with a wide range of reagents, which make them ideal coupling candidates for late-stage functionalization.³ For these reasons, we envisioned the enantioselective Simmons-Smith cyclopropanation of MIDA boronate bearing allylic alcohol to prepare the corresponding cyclopropylmethanol, which could serve as a robust building block for diversification reactions and the synthesis of cyclopropane-containing chiral cores in complex molecules discussed previously (Figure 1). Our initial Simmons-Smith

cyclopropanation attempt was thwarted by two aspects of the reaction: (a) the insolubility of the vinyl MIDA boronate bearing the (*E*)-allylic alcohol in the solvents typically used for dioxaborolane-mediated cyclopropanations, such as dichloromethane, chloroform, and chlorobenzene and (b) decomposition of the boronate under the oxidative conditions used for the removal of dioxaborolane.¹¹

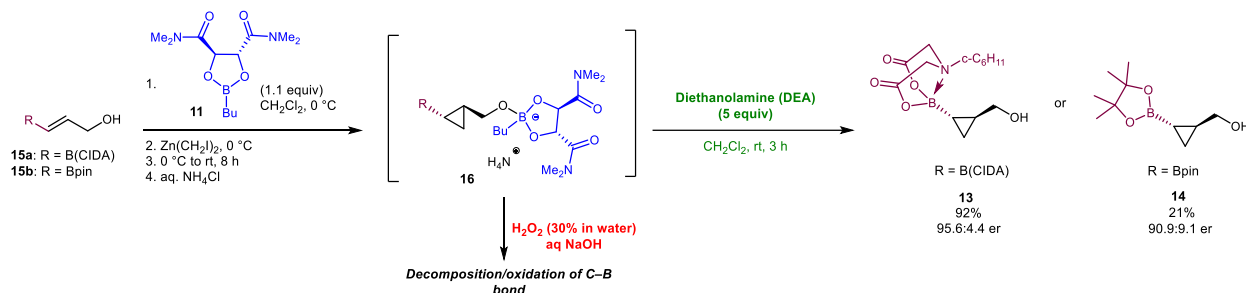
To improve solubility, we proposed the replacement of the *N*-methyl substituent in MIDA boronates with a cyclohexyl group to prepare *N*-cyclohexyliminodiacetic acid (CIDA) protected boronates. The CIDA-bearing boronate allylic alcohol **15a** (Scheme 2) can be synthesized on a multigram scale in three steps starting from TBS-protected vinyl-Bpin-bearing (*E*)-allylic alcohol in 80% overall yield. During the synthesis of the free allylic alcohol **15a**, we were pleased to find orthogonal deprotection conditions for boronate substrates bearing silyl protecting groups. The in situ deprotection of the TBS group was a result of a mixture of DMSO, used as a cosolvent, and minimal amounts of water, generated during the CIDA protection, which provided the CIDA boronate allylic alcohol in 20% yield and the TBS-protected allylic alcohol in 60% yield. Heating the crude reaction mixture in DMSO/water (5:1) enhanced the overall yield to 80%.¹⁷ Once obtained, we were pleased to find that the CIDA allylic alcohol **15a** was readily soluble in dichloromethane.

Results and Discussion

The cyclopropanation reaction with **15a** using $\text{Zn}(\text{CH}_2\text{I})_2$ (2.2 equiv) and dioxaborolane **11** (1.1 equiv) proceeded smoothly with full conversion of the starting material. However, isolation of the cyclopropylmethanol by decomplexation of the chiral dioxaborolane ligand using hydrogen peroxide and sodium hydroxide led to the complete hydrolysis of the product (Scheme 2). Attempts to use less equivalents of peroxide did not prevent the hydrolysis of the product. The traditional workup conditions for the dioxaborolane-mediated cyclopropanation involve the use of 30% hydrogen peroxide and 2 M sodium hydroxide²⁹ or the use of highly basic 5 M aqueous potassium hydroxide to decomplex the dioxaborolane from the cyclopropyl methoxide species **16** formed in the reaction. Indeed, the hydrolysis of alkyltriorborates is known to involve harsh

oxidative conditions,¹⁸ resulting in narrow functional group compatibility and challenging purifications.¹⁹

Considering MIDA boronates are highly labile to aqueous basic conditions and the presence of strong oxidants, we investigated a non-oxidative process for selective decomplexation of the tartaramide-boronate complex in the presence of the CIDA group in intermediate **16**. Diethanolamine (DEA) and ethanolamine have been used for the transesterification of certain pinacolboronate esters bearing electron-withdrawing groups.²⁰



Scheme 2 Enantioselective borocyclopropanation of borosubstituted allylic alcohols **15a** and **15b**

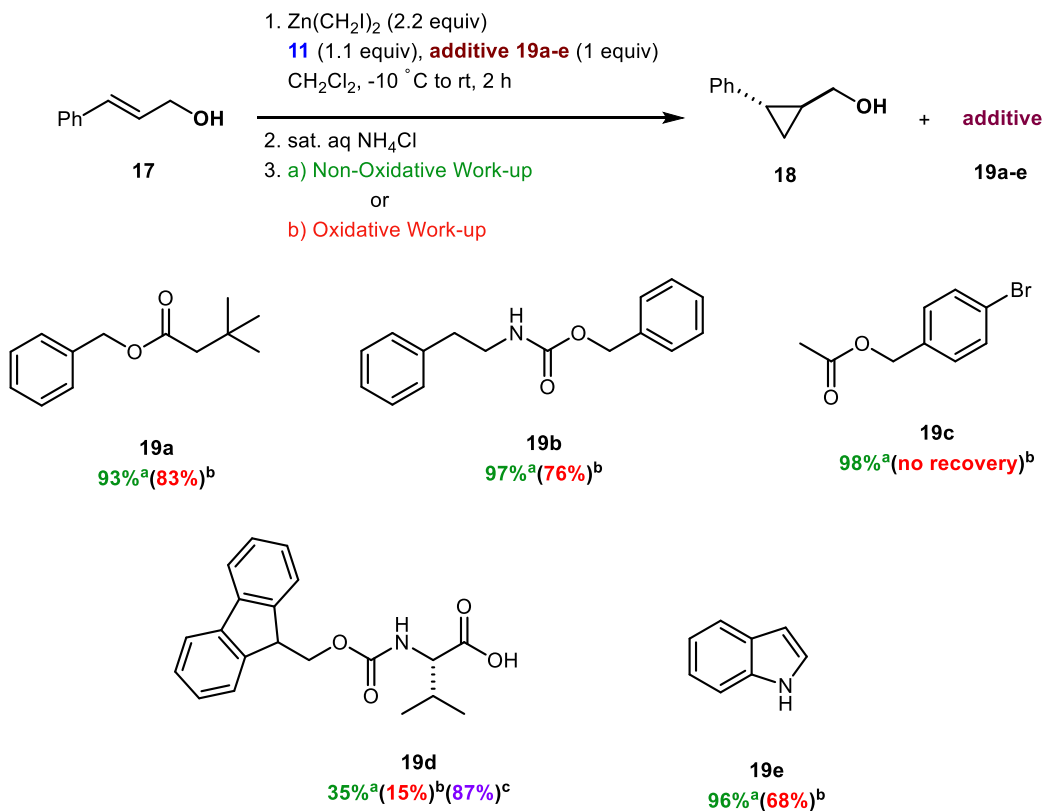
However, Szabò recently observed that the diethanolamine cyclic boronate deprotection protocol is unsuccessful for transesterification of some electron-deficient vinylpinacolate analogs.²¹ To the best of our knowledge, DEA has not been used for the transesterification of alkyltrialborates. We investigated the use of DEA for the transesterification of the (cyclopropylmethanol)boronate complexes. After extensive screening for isolation conditions, the decomplexation of the boron-ligated intermediate **16** was achieved by direct addition of DEA (5 equiv) to the reaction mixture and stirring for 3 hours at room temperature. Purification of the decomplexed crude product by silica gel chromatography afforded **13** in 92% yield and 95.6:4.4 er (Scheme 2).

For comparative purposes, BPin-substituted allylic alcohol **15b** was subjected to the Simmons-Smith cyclopropanation conditions. After optimization, the pinacol-protected borocyclopropane **14** was obtained in 21% yield with a reproducible 90.9:9.1 er (Scheme 2). The low yield of the pinacol derivative is likely due to the transesterification of the pinacol ligand with

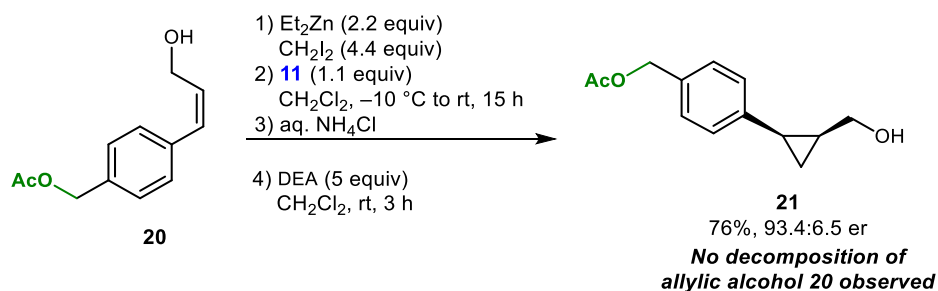
excess DEA or due to decomposition by flash chromatography of pinacolboronates. We evaluated the robustness of the DEA decomplexation process using Glorius's intermolecular screening tool²² for the cyclopropanation of allylic alcohol **17**¹¹ with five substrates containing base-sensitive functionalities, such as esters and carbamates, as well as an indole, to study an example of an oxidizable group (Scheme 3).

The recovery of the additives is consistently higher with the use of the non-oxidative conditions. The superiority is striking in the case of the substrate **19c** (Scheme 3) bearing the acetate functionality, where the non-oxidative decomplexation allows isolation in 98% yield in comparison to no recovery using the traditional procedure. The base sensitive Fmoc-group-containing compound **19d** was found to be labile using both oxidative and non-oxidative protocols, allowing only 35% isolated yield. We investigated the use of a more hindered DEA such as *N*-methyl DEA, and were pleased to find an improved recovery of 87% in comparison to the 15% yield isolated using the oxidative conditions. For highly base-sensitive groups, the *N*-methyl DEA work-up is recommended for better yields. Indole was recovered in 96% yield when using the DEA decomplexation, in comparison to the 68% recovered using the traditional decomplexation procedure, demonstrating the use of DEA-promoted cleavage of dioxaborolane to obtain oxidation-sensitive *N*-heterocycle-substituted cyclopropanes which are typically incompatible with the traditional conditions.²³

Based on the robustness screen of DEA, cyclopropanation of substrate **20** bearing the sensitive *O*-acetyl group was attempted (Scheme 4). The cyclopropylmethanol **21** bearing the acetate group was obtained in 76% isolated yield. During analysis of the byproducts, it was determined that the moderate yield was not a result of the decomposition of the acetyl allylic alcohol, but due to the lower reactivity of the substrate, evidenced by the recovery of the starting material in 24% isolated yield. Thus, the DEA-promoted decomplexation procedure proved to be quite versatile, and functional groups such as esters, carbamates, and others were shown to be compatible under the new non-oxidative conditions for the decomplexation of **11**.



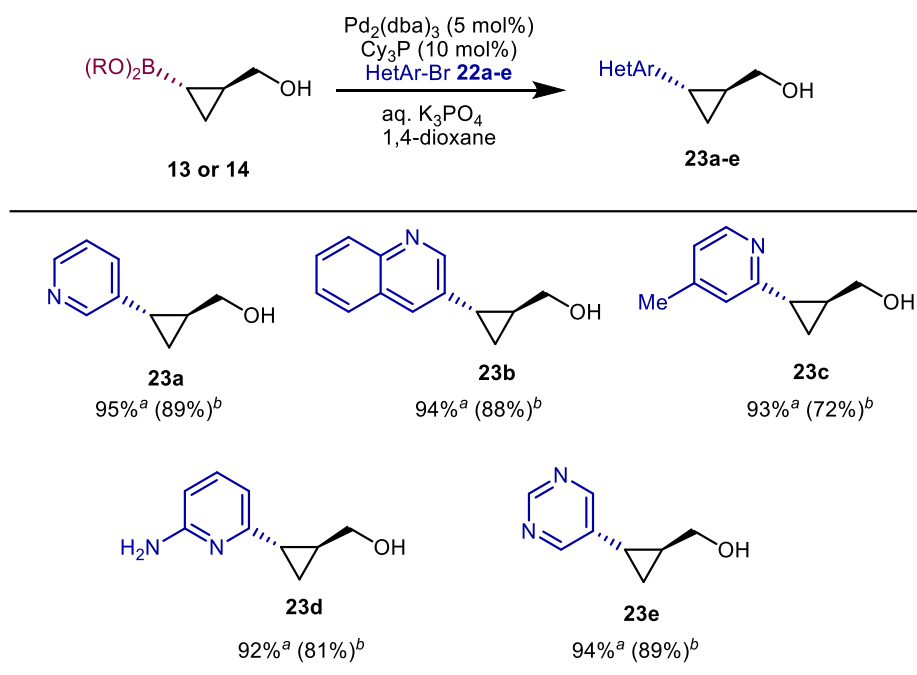
Scheme 3 Cyclopropanation of allylic alcohol **17**. ^a Diethanolamine (5 equiv), rt, 3 h; ^b H_2O_2 (30% in water), 2 M aq NaOH, rt, 10 min; ^c *N*-Methyldiethanolamine (5 equiv), rt, 3 h.



Scheme 4 Cyclopropanation of highly base-sensitive substrate

With the two borocyclopropane derivatives in hand, we turned our attention to the cross-coupling conditions for the Suzuki-Miyaura reaction, which is arguably the most effective method to integrate the cyclopropyl moiety into aromatic or heteroaromatic systems.²⁴ Heterocycles are the most widely used motifs in medicinal chemistry, and to aid introduction of the cyclopropane

motif into heterocycles, we evaluated a series of cross-couplings of heteroaryl halides with **13** and **14** to obtain enantioenriched heteroaryl substituted cyclopropanes. Methods for the cross-coupling of cyclopropyl boronic acids and their pinacol analogs have been previously exploited.^{3, 25} Cross-coupling of cyclopropyl MIDA boronates has been achieved using SPhos and Pd(OAc)₂ to afford excellent yields of the coupled products while the cross-coupling of racemic *trans*-2-(trifluoromethyl)cyclopropyl MIDA boronates in the presence of Pd(OAc)₂ and PCy₃ provides the cyclopropyl adducts in only 17-32% yields.²⁶ After screening various cross-coupling conditions, we found the use of PCy₃ and Pd₂(dba)₃ as a suitable combination for the cross-coupling of the CIDA-boronate-bearing cyclopropylmethanol **13** (Scheme 5). It should be noted that cyclopropylboronic acids prepared immediately prior to the reaction can be as effective as the MIDA boronates.

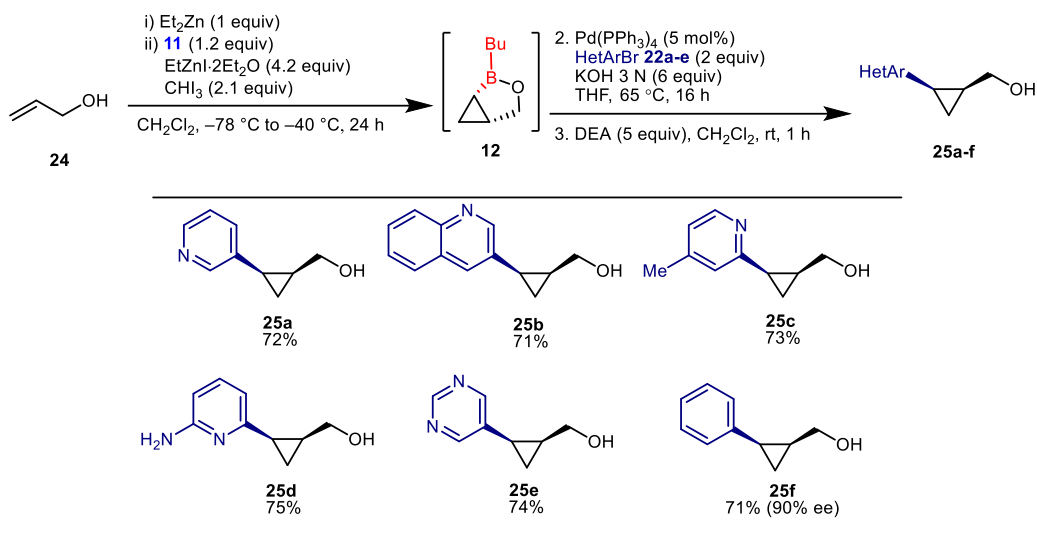


Scheme 5 Suzuki cross-coupling of borocyclopropanes. ^a Yields obtained when using borocyclopropane **13**. ^b Yields obtained when using borocyclopropane **14**.

The cross coupling of **13** (95.6:4.4 er) with five heteroaryl bromides in the presence of Pd₂(dba)₃ (5 mol%), PCy₃ (10 mol%) and aqueous potassium triphosphate afforded the cross-coupled cyclopropylmethanols **23a-e** in excellent yields (Scheme 5). When the same coupling reactions were performed with the Bpin-substituted cyclopropane **14** (90.9:9.1 er), lower yields

were obtained even though cyclopropane **14** was freshly prepared. The higher cross-coupling efficiency of the CIDA borocyclopropane compared to that of the Bpin-borocyclopropanes can be attributed to stability and controlled hydrolytic character of tetracoordinate boronates in cross-coupling reactions.¹⁹ Moreover, enantioenriched cyclopropane **13** exhibited benchtop air-stability even after 5 months, while borocyclopropane **14** partially decomposed (by about 20%) over 3 weeks.

Having evaluated an approach to access *trans-N*-heterocycle-substituted cyclopropanes, we turned our attention to the *cis* analogues. Attempts to synthesize the CIDA-bearing *cis*-boronate allylic alcohols failed due to lack of stability. To overcome these challenges, we took to an in situ approach to obtain the disubstituted borocyclopropylmethanol via the enantioselective zinc-cyclopropanation reaction of allyl alcohol followed by cross-coupling with *N*-heterocycles to prepare *cis-N*-heterocycle-substituted cyclopropanes (Scheme 6). A modified procedure was employed to enhance the yield of the zinc-cyclopropanation of the non-substituted allylic alcohol substrate. Treatment of allyl alcohol **24** with the *gem*-dizinc carbenoid in the presence of the chiral ligand **11** led to the cyclic boronate **12**, which was subjected to Suzuki-Miyaura cross-coupling. In the case of allyl alcohol, the product often contained residual dioxaborolane or complexed dioxaborolane affecting the yield of the reaction. To overcome the lower yield arising from the residual complexed dioxaborolane, the non-oxidative DEA-promoted decomplexation was applied to the crude reaction mixture to obtain the completely decomplexed *cis*-isomer. Purification of the crude reaction mixture provided the desired *N*-heterocycle-substituted cyclopropanes in good yields and excellent enantioselectivity (Scheme 6).



Scheme 6 Synthesis of *cis*-heteroaryl-substituted cyclopropanes

Conclusion

In conclusion, a non-oxidative and enantioselective methodology has been developed that not only allows for the preparation of enantiopure borocyclopropane building blocks, but also provides a tool for the decomplexation of boron-ligated intermediates in the zinc-cyclopropanation reaction. Using our methodology, a novel air-stable enantioenriched CIDA borocyclopropane **13** building block was obtained in 92% yield and 95.6:4.4 er compared to the pinacol borocyclopropane **14** obtained in 21% yield and 90.9:9.1 er. Efficient cross-coupling conditions for the CIDA borocyclopropane allowed access to enantioenriched *trans-N*-heterocycle-substituted cyclopropanes in excellent yields. The non-oxidative DEA decomplexation was also applied in the zinc-cyclopropanation reaction to allow access to the fully decomplexed *cis-N*-heterocycle substituted cyclopropanes, resulting in higher yields. The work demonstrates a robust and mild alternative for dioxaborolane-mediated cyclopropanations, broadening compatibility with highly base-sensitive and oxidizable substrates.

Experimental Section

Unless otherwise stated, all glassware was oven-dried and/or was flame-dried prior to use and all reactions were set up and carried out under an argon atmosphere²⁷ with the exclusion of

moisture. Anhydrous solvents were obtained either by filtration through drying columns on a GlassContour system (Irvine, CA) (benzene and THF) or by distillation over calcium hydride (Et₃N, pyridine, CH₂Cl₂) or sodium (THF). Absolute EtOH, glacial acetic acid, and Ac₂O were used as is from commercial bottles. Unless otherwise noted, all solutions are aqueous solutions. Analytical TLC was performed on pre-coated, glass-backed silica gel (Merck 60 F254). Visualization of the developed chromatogram was aided by UV absorbance (254 nm), UV fluorescence (350 nm), or by using aq potassium permanganate (KMnO₄), *p*-anisaldehyde, and ninhydrin. Flash column chromatography was performed on silica gel (pore size 60 Å, 230–400 mesh particle size, 40–63 µm particle size) in glass columns for the separation of products. Melting points were obtained on a Buchi melting point B-540 apparatus and are uncorrected. Specific rotations, [α]_D values, were calculated from optical rotations measured at 25 °C in MeOH at the specified concentrations (c in g/100 mL) using a 0.5-dm cell length (l) on a Perkin-Elmer Polarimeter 241 at 589 nm, using the general formula: $[\alpha]_D^{25} = (100 \times \alpha)/(l \times c)$. ¹H and ¹³C NMR spectra were recorded on Bruker AV400, AV500, and AV700 MHz spectrometers. The corresponding chemical shifts for ¹H NMR and ¹³C NMR spectra are recorded in CDCl₃ or acetone-*d*₆, and reported in ppm relative to the chemical shift of tetramethylsilane or the residual CHCl₃ (¹H: δ = 7.26, ¹³C: δ = 77.2), residual (CD₃)₂CO (¹H: δ = 2.09, ¹³C: δ = 205.9), or residual (CD₃)₂SO (¹H: δ = 2.54, ¹³C: δ = 40.5) as reference. All ¹³C NMR spectra were obtained with complete proton decoupling. IR spectra were obtained on a Bruker Vertex Series FTIR (neat). High resolution mass spectra were recorded on an LC-MSD instrument from Agilent technologies 1200 series in positive electrospray ionization (ESI) and atmospheric-pressure chemical ionization (APCI) modes and analytical Supercritical Fluid Chromatography (SFC) were performed by the Centre régional de spectroscopie de masse de l'Université de Montréal. SFC data are reported as follows: (column type, eluent, flow rate, pressure: retention time (t_R)). All organic extracts were dried over sodium

sulfate and concentrated under vacuum. Et₂Zn was purchased neat from AkzoNobel and used without further purification. Diethanolamine and *N*-methyldiethanolamine were purchased from Aldrich and were used without further purification. Fmoc-Val-OH was purchased from AAPPTec

and used without further purification. Unless specified otherwise, all reagents for Suzuki cross-coupling reactions were used without further purification and catalysts were handled in the glovebox. All reagents used were purified using standardized protocols.

Procedures

(E)-6-Cyclohexyl-2-(3-hydroxyprop-1-en-1-yl)-1,3,6,2-dioxaborocane-4,8-dione (15a)

To a dry microwave vial, (*E*)-2-(3-[(*tert*-butyldimethylsilyl)oxy]prop-1-en-1-yl)-6-cyclohexyl-1,3,6,2-dioxaborocane-4,8-dione **15aa** (see below for preparation of **15aa**) (440 mg, 1.10 mmol) was added, followed by DMSO (14 mL) and H₂O (2.8 mL). The vial was sealed and placed under microwave irradiation for 1 h at 130 °C. The reaction mixture was cooled, transferred into a 40 mL flask, diluted with H₂O (10 mL) and lyophilized until dryness; this gave **15a**.

Yield: 313 mg (99%); white solid; *R_f* = 0.3 (CH₂Cl₂/MeCN, 1:1); mp 117-118 °C.

IR (neat): 2939, 2860, 1740, 1644, 1448, 1326, 1290, 1244 cm⁻¹.

¹H NMR (400 MHz, acetone-*d*₆) δ = 6.22 (dt, *J* = 17.7, 4.2 Hz, 1 H), 5.78 (dt, *J* = 17.7, 1.9 Hz, 1 H), 4.20 – 4.13 (m, 4 H), 3.92 – 3.87 (m, 2 H), 3.74 (br, 1 H), 3.21 (tt, *J* = 12.1, 3.4 Hz, 1 H), 2.81 (m, 2 H), 1.87 – 1.81 (m, 2 H), 1.65 – 1.59 (m, 1 H), 1.71 – 1.49 (m, 2 H), 1.44 – 1.25 (m, 3 H).

¹³C NMR (126 MHz, CDCl₃) δ = 169.5 (2 C), 146.3 (2 C), 123.9, 67.0, 64.5, 56.5 (2 C), 27.4 (2 C), 25.51, 25.46.

¹¹B NMR (128 MHz, acetone-*d*₆) δ = 10.7.

HRMS (ESI): *m/z* [M + H]⁺ calcd for C₁₃H₂₀BNO₅: 282.1507; found 282.1509.

(E)-3-(4,4,5,5-Tetramethyl-1,3,2-dioxaborolan-2-yl)prop-2-en-1-ol (15b):

To a stirred solution of (*E*)-*tert*-butyldimethyl([3-(4,4,5,5-tetramethyl-1,3,2-dioxaborolan-2-yl)allyl]oxy)silane²⁸ (12.0 g, 40.2 mmol) in EtOH (201 mL) was added dropwise a solution of trichloroacetic acid in EtOH (46.9 mL, 3 M). The reaction mixture was stirred for 12 h. The reaction

mixture was concentrated, and the residue was diluted with EtOAc (20 mL) and washed with sat. NaHCO₃ (2 x 15 mL). The organic layer was dried with Na₂SO₄ and concentrated under reduced pressure to provide a crude brown oil which was purified by flash chromatography (silica gel, EtOAc/hexanes, 3:7).

Yield: 4.20 g (57%); yellow oil; R_f = 0.4 (3:7 EtOAc:Hexanes, 3:7).

IR (neat): 3420, 2977, 2929, 1643, 1358, 1317, 1411, 1004, 970 cm⁻¹.

¹H NMR (400 MHz, CDCl₃) δ = 6.74 (dt, *J* = 18.2, 4.2 Hz, 1 H), 5.70 (dt, *J* = 18.2, 4.2 Hz, 1 H), 4.24 (dd, *J* = 4.2, 1.9 Hz, 2 H), 1.79 (br, 1 H), 1.27 (s, 12 H).

¹³C NMR (101 MHz, CDCl₃) δ = 151.9, 117.3, 83.5, 64.8 (2 C), 25.0 (4 C).

HRMS (ESI): *m/z* [M + H]⁺ calcd for C₉H₁₇BO₃: 185.1343; found: 185.1344.

6-Cyclohexyl-2-[(1*R*,2*R*)-2-(hydroxymethyl)cyclopropyl]-1,3,6,2-dioxaborocane-4,8-dione (13)

A 10 mL flame-dried flask was charged with **15a** (48.3 mg, 0.17 mmol), **11** (51.1 mg, 0.19 mmol), and CH₂Cl₂ (2 mL). The mixture was sonicated for 1 min to provide a homogeneous solution. In another flame-dried flask, neat Et₂Zn (40.3 μL, 0.4 mmol) was added to CH₂Cl₂ (2 mL) at 0 °C; dropwise addition of diiodomethane (63.6 μL, 0.8 mmol) followed. The mixture was stirred at 0 °C for 10 min. The mixture of dioxaborolane **11** and **15a** was cannulated slowly into the reaction flask. After complete addition, the reaction mixture was allowed to stir for 8 h. The mixture remained homogeneous throughout. Upon completion of the reaction, the mixture was quenched with NH₄Cl (2 mL), and diluted with EtOAc (5 mL) and brine (5 mL). The organic layer was separated, and the aqueous layer was washed with EtOAc (2 x 5 mL). The organic layers were combined, dried with Na₂SO₄, and concentrated under reduced pressure. To the resulting residue was added a solution of diethanolamine (93.5 mg, 0.9 mmol) in CH₂Cl₂ (750 μL) and the mixture was allowed to stir for 3 h. After this, the mixture was saturated with silica gel, dried, and directly

loaded for flash chromatography (silica gel, EtOAc/hexanes (1:1) then MeCN); this gave product **13**.

Yield: 48.3 mg (92%); 95.6:4.4 er; SFC (Chiralpak OD-H 25cm, 30 °C, 150 bar, 10% MeOH, 3 mL/min): $t_{R(\text{major})}$: 9.76 min; $t_{R(\text{minor})}$: 8.63 min; white solid; mp 132–133 °C; R_f = 0.3 (MeCN); $[\alpha]_D^{25}$ +10.8 (c 0.83, MeOH).

IR (neat): 2936, 2861, 1741, 1449, 1292, 1247, 1000, 898 cm^{-1} .

^1H NMR (500 MHz, acetone- d_6) δ = 4.18 – 4.08 (m, 2 H), 3.92 – 3.83 (m, 3 H), 3.67 (dd, J = 11.1, 5.9 Hz, 1H), 3.22 (dd, J = 10.6, 7.6 Hz, 1 H), 2.83 (br, 1 H), 2.16 – 2.08 (m, 2 H), 1.89 – 1.82 (m, 2 H), 1.67 – 1.63 (m, 1 H), 1.60 – 1.56 (m, 1 H), 1.56 – 1.40 (m, 3 H), 1.32 – 1.23 (m, 1 H), 0.91 – 0.84 (m, 1 H), 0.42 – 0.36 (m, 2 H), -0.26 – -0.30 (m, 1 H).

^{13}C NMR (126 MHz, acetone- d_6) δ 168.8, 168.0, 72.3, 66.4, 65.4, 57.0, 55.2, 27.1, 26.6, 24.7(2 C), 24.5, 17.3, 5.9.

HRMS (ESI): m/z $[\text{M} + \text{H}]^+$ calcd for $\text{C}_{14}\text{H}_{22}\text{BNO}_5$: 296.1664; found: 296.1672.

Larger-Scale Preparation of **13** (5.6 mmol)

In a 250 mL flame-dried flask, **15a** (1.56 g, 5.6 mmol) and **11** (51.7 g, 6.10 mmol) were dissolved in CH_2Cl_2 (25 mL). Sonication for 1 min allowed **15a** to dissolve in the CH_2Cl_2 . In another flame-dried flask, Et_2Zn (1.26 mL, 12.2 mmol) was added to CH_2Cl_2 (50 mL) and DME (1 mL) at 0 °C; dropwise addition of diiodomethane (1.9 mL, 24.2 mmol) followed. The mixture was stirred at 0 °C for 10 min. The mixture of dioxaborolane **11** and **15a** was cannulated slowly into the cooled reaction flask. After complete addition, the reaction mixture was allowed to stir for 12 h. The reaction remained homogeneous throughout. Upon completion, the mixture was quenched with NH_4Cl (5 mL) and diluted with EtOAc (20 mL) and brine (10 mL). The organic layer was separated, and the aqueous layer was washed with EtOAc (2 × 20 mL). The organic layers were combined, dried with Na_2SO_4 , and concentrated under reduced pressure. To the resulting residue was added a solution of diethanolamine (2.92 g, 27.8 mmol) in CH_2Cl_2 (21 mL), and the mixture was allowed to stir for 3 h. The crude reaction mixture was loaded directly for flash chromatography (silica gel,

EtOAc/hexanes (1:1) then MeCN). This gave product **13** as a white solid spectroscopically identical to **13** obtained at a 0.2 mmol scale.

Yield: 1.52 g (93%); 92.9:7.3 er; SFC (Chiralpak OD-H 25cm, 30 °C, 150 bar, 10% MeOH, 3 mL/min): $t_{R(\text{major})}$: 10.11 min, $t_{R(\text{minor})}$: 8.41 min; $[\alpha]_D^{25} +9.3$ (c 1.0, MeOH).

[(1*R*,2*R*)-2-(4,4,5,5-Tetramethyl-1,3,2-dioxaborolan-2-yl)cyclopropyl]methanol (14**)**

Neat Et₂Zn (169 μL, 1.64 mmol) was added to stirred CH₂Cl₂ (3 mL) in a flame-dried flask at rt. The solution was cooled to 0 °C and diiodomethane (264 μL, 3.28 mmol) was added dropwise over 5 min while maintaining the temperature at -5 to 0 °C. Once the addition was complete, the mixture was allowed to stir for 10 min, after which a solution of premixed **15b** (137 mg, 0.74 mmol) and **11** (221 mg, 0.82 mmol) in CH₂Cl₂ (2 mL) was added dropwise over 1 min. The resulting mixture was stirred for 6 h at rt. The reaction mixture was diluted with NH₄Cl (1 mL) and EtOAc (3 mL). The organic layer was separated and washed with brine (2 mL). The aqueous layer was extracted with EtOAc (2 × 3 mL) and the organic layers were combined, dried with Na₂SO₄, and concentrated under reduced pressure. To the residue was added diethanolamine (2.85 g, 27.1 mmol) in CH₂Cl₂ (21 mL) and the mixture was allowed to stir for 3 h. The crude reaction mixture was loaded directly onto a column for chromatography (silica gel, EtOAc/hexanes, 1:3). After purification the pure product was obtained as a yellow oil.

Yield: 31 mg (21%); 90.9:9.1 er; TOF (6224) (Chiralpak OJ-RH, 13% MeCN, 0.4 mL/min): $t_{R(\text{major})}$: 20.19 min, $t_{R(\text{minor})}$: 17.74 min; $R_f = 0.3$ (EtOAc/hexane, 1:3); $[\alpha]_D^{25} +7.4$ (c 0.83, MeOH).

IR (neat): 2977, 2932, 1644, 1425, 1371, 1314, 1141, 1042, 854 cm⁻¹.

¹H NMR (400 MHz, CDCl₃) δ = 3.45 (d, J = 6.8 Hz, 2 H), 1.65 (br, 1 H), 1.30 – 1.34 (m, 1 H), 1.21 (s, 12 H), 0.76 – 0.73 (m, 1 H), 0.56 – 0.54 (m, 1 H), -0.21 – -0.28 (m, 1 H).

¹³C NMR (101 MHz, CDCl₃) δ = 83.2, 68.0, 24.8 (2C), 20.5 (4C), 9.3, -1.6.

^{11}B NMR (128 MHz, CDCl_3) δ 33.1.

HRMS (ESI): m/z $[\text{M} + \text{H} - \text{H}_2\text{O}]^+$ calcd for $\text{C}_{10}\text{H}_{19}\text{BO}_3$: 180.1431; found: 180.1423.

Larger-Scale Preparation of **14 (5.4 mmol)**

Neat Et_2Zn (1.23 mL, 12.0 mmol) was added to a flame-dried flask containing a stir bar, CH_2Cl_2 (25.0 mL), and DME (1.13 mL). The solution was cooled to 0 °C, after which diiodomethane (1.93 mL, 23.9 mmol) was added dropwise over 5 min, while maintaining the temperature at –5 to 0 °C. Once the addition was complete, the mixture was allowed to stir for 10 min, after which a solution of premixed **15b** (1.00 g, 5.43 mmol) and **11** (1.61 g, 5.98 mmol) in CH_2Cl_2 (25 mL) was added dropwise over 1 min. The resulting mixture was stirred for 15 h at rt. The reaction mixture was diluted with NH_4Cl (10 mL) and EtOAc (20 mL). The organic layer was separated and washed with brine (10 mL). The aqueous layer was extracted with EtOAc (2 × 10 mL). The organic layers were combined, dried with Na_2SO_4 and concentrated under reduced pressure. To the residue was added warm diethanolamine (2.85 g, 27.1 mmol) in CH_2Cl_2 (21 mL) and the mixture was allowed to stir for 3 h. Once the reaction was complete, the crude reaction mixture was loaded directly for chromatography (silica gel, EtOAc/hexanes, 1:3). After purification the pure product was obtained as a yellow oil spectroscopically identical to **14** at the 1.64 mmol scale.

Yield: 452 mg (42%); 89.6:10.3 er; TOF (6224) (Chiralpak OJ-RH, 9% MeCN, 0.4 mL/min): $t_{\text{R}(\text{major})}$: 25.24 min; $t_{\text{R}(\text{minor})}$: 21.86; $[\alpha]_{\text{D}}^{25} +7.6$ (c 1.0, MeOH).

Products **19a–e by Rapid Assessment of Functional Groups: Intermolecular Screening Protocol for Non-oxidative Workup; General Procedure D**

To a solution of Et_2Zn (113 μL , 1.10 mmol) in CH_2Cl_2 (2.5 mL) at 0 °C was added diiodomethane (177 μL , 2.20 mmol). The mixture was stirred at 0 °C for 10 min to give a white precipitate, to which was added a solution of alcohol **17** (67.1 mg, 0.50 mmol), additive **19** (0.50 mmol), and dioxaborolane **11** (149 mg, 1.1 mmol) in CH_2Cl_2 (2.5 mL) via a cannula. The resulting mixture was stirred for 2 h at rt and was quenched by the addition of sat. aq NH_4Cl (5 mL). The mixture was

transferred into a separatory funnel and the reaction flask was rinsed with Et₂O (5 mL). The two layers were separated, and the aqueous layer was extracted with Et₂O (3 × 5 mL). The combined organic layers were dried and concentrated to afford a colorless residue. Warm diethanolamine (263 mg, 2.50 mmol) was dissolved in CH₂Cl₂ (2.5 mL) and transferred to the flask containing the reaction mixture. Additional CH₂Cl₂ (2.5 mL) was used to rinse the diethanolamine and transferred to the flask containing the reaction mixture. The mixture was stirred at rt for 3 h. Silica gel was added to the reaction mixture, which was concentrated, resulting in dry silica gel saturated with the crude reaction mixture. Purification by column chromatography afforded cyclopropane **18** as a colorless oil, which was identical in all aspects to the reported compound,²⁹ and additives **19a–e**.

Products 18 and 19a–e by Rapid Assessment of Functional Groups: Intermolecular Screening Protocol for Oxidative Workup; General Procedure E

To a solution of Et₂Zn (113 μL, 1.10 mmol) in CH₂Cl₂ (2.5 mL) at 0 °C was added diiodomethane (177 μL, 2.20 mmol). The mixture was stirred at 0 °C for 10 min to give a white precipitate, to which was added a solution of alcohol **17** (67.1 mg, 0.50 mmol), additive (0.50 mmol), and dioxaborolane **11** (149 mg, 1.1 mmol) in CH₂Cl₂ (2.5 mL) via a cannula. The resulting mixture was stirred for 2 h at rt and was quenched by the addition of sat. aq NH₄Cl (5 mL). The mixture was transferred into a separatory funnel and the reaction flask was rinsed with Et₂O (5 mL). The two layers were separated, and the aqueous layer was extracted with Et₂O (3 × 5 mL). The combined organic layers were transferred into an Erlenmeyer flask, and a solution containing 2 N aq NaOH (8.7 mL) and 30% aq H₂O₂ (1.5 mL) was added in one portion. The resulting biphasic solution was vigorously stirred for 10 min, after which the two layers were separated. The aqueous layer was extracted with Et₂O (3 × 5 mL) and the combined organic layers were washed with 10% aq HCl (10 mL). The aqueous layer was extracted with Et₂O (3 × 5 mL) and the combined organic layers were successively washed with sat. aq Na₂SO₃ (10 mL), sat. aq NaHCO₃ (10 mL), and brine (10 mL), dried over Na₂SO₄, filtered, and concentrated under reduced pressure. Purification by column chromatography afforded cyclopropane **18** and additive **19a–e**.

Benzyl 3,3-Dimethylbutanoate (19a)

General Procedure D: Purification by column chromatography (silica gel, EtOAc/hexanes, 1:9) resulted in the recovered additive **19a** (95.9 mg, 93%) and the desired cyclopropane **18** (70.4 mg, 95%).

General Procedure E: Recovered additive **19a** (85.6 mg, 83%) and the desired cyclopropane **18** (67.4 mg, 91%).

Benzyl Phenethylcarbamate (19b)

General Procedure D: Purification by column chromatography (silica gel, EtOAc/hexanes, 1:9) resulted in the recovered additive **19b** (125 mg, 97%) and the desired cyclopropane **18** (69.7 mg, 94%).

General Procedure E: Recovered additive **19b** (97.0 mg, 76%) and the desired cyclopropane **18** (70.4 mg, 95%).

4-Bromobenzyl Acetate (19c)

General Procedure D: Purification by column chromatography (silicagel, EtOAc/hexanes, 1:3) resulted in the recovered additive **19c** (83.7 mg, 98%) and the desired cyclopropane **18** (51.9 mg, 94%).

General Procedure E: No recovery of **19c** and the desired cyclopropane **18** (51.9 mg, 94%).

(((9H-Fluoren-9-yl)methoxy)carbonyl)-L-valine (19d)

General Procedure D: Purification by column chromatography (silica gel, MeOH/CH₂Cl₂, 1:9) resulted in the recovered additive **19d** (59.4 mg, 35%) and the desired cyclopropane **18** (68.9 mg, 93%).

General Procedure E: Recovered additive **19d** (25.5 mg, 15%) and the desired cyclopropane **18** (69.7 mg, 94%).

1H-Indole (19e)

General Procedure D: Purification by column chromatography (silica gel, MeOH/CH₂Cl₂, 1:9) resulted in the recovered additive **19e** (58.0 mg, 99%) and the desired cyclopropane **18** (68.9 mg, 93%).

General Procedure E: Recovered additive **19e** (39.8 mg, 68%) and the desired cyclopropane **18** (69.7 mg, 94%).

N-Methyldiethanolamine Workup for Fmoc-Containing Additive (19d)

To a solution of Et₂Zn (113 μL, 1.1 mmol) in CH₂Cl₂ (2.5 mL) at 0 °C was added diiodomethane (179 μL, 2.2 mmol). The mixture was stirred at 0 °C for 10 min to give a white precipitate, to which was added a solution of alcohol **17** (67 mg, 0.5 mmol), **19d** (0.5 mmol), and dioxaborolane **11** (162 mg, 0.6 mmol) in CH₂Cl₂ (2.5 mL) via a cannula. The resulting mixture was stirred for 2 h at rt and was quenched by the addition of sat. aq NH₄Cl (5 mL). The mixture was transferred into a separatory funnel and the reaction flask was rinsed with Et₂O (5 mL). The two layers were separated, and the aqueous layer was extracted with Et₂O (3 × 5 mL). The combined organic layers were dried and concentrated to afford a colorless residue. *N*-Methyldiethanolamine (298 mg, 2.5 mmol) was weighed into a vial, dissolved in CH₂Cl₂ (2.5 mL), and transferred to the flask containing the reaction mixture. Additional CH₂Cl₂ (2.5 mL) was used to rinse the diethanolamine and transferred to the flask containing the reaction mixture. The mixture was stirred at rt for 3 h and was then adsorbed onto silica gel. Purification by column chromatography (silica gel, MeOH/CH₂Cl₂, 1:9) resulted in the recovered additive **19d** (148 mg, 87%) and the desired cyclopropane **18** (68.9 mg, 93%).

4-[(1*R*,2*S*)-2-(Hydroxymethyl)cyclopropyl]benzyl acetate (**21**)

To a solution of Et₂Zn (233 μL, 2.26 mmol) in CH₂Cl₂ (3.7 mL) at 0 °C was added diiodomethane (365 μL, 4.52 mmol). The mixture was stirred at 0 °C for 10 min to give a white precipitate, to which was added a solution of allylic alcohol **20** (212 mg, 1.03 mmol) and dioxaborolane **11** (306 mg, 1.13 mmol) in CH₂Cl₂ (5.5 mL) via a cannula. The resulting mixture was stirred for 15 h at rt and was quenched by the addition of sat. aq NH₄Cl (15 mL). The mixture was transferred into a separatory funnel and the reaction flask was rinsed with Et₂O (15 mL). The two layers were separated, and the aqueous layer was extracted with Et₂O (3 × 4 mL). The combined organic layers were dried and concentrated to afford a colorless residue. Warm diethanolamine (541 mg, 5.15 mmol), weighed into a vial and dissolved in CH₂Cl₂ (4 mL), was transferred to the flask containing the reaction mixture. Additional CH₂Cl₂ (4 mL) was used to rinse the diethanolamine and transferred to the flask containing the reaction mixture. The mixture was stirred at rt for 3 h. The mixture was stirred at rt for 3 h. Silica gel was added to the reaction mixture, which was concentrated, resulting in dry silica gel saturated with the crude reaction mixture. Purification of the saturated silica by column chromatography (silica gel, EtOAc/hexanes, 1:4) afforded **21**.

Yield: 172 mg (76%); 93.4:6.6 er; SFC (Chiralpak AD-H 25 cm, 30 °C, 150 bar, 10% MeOH, 3 mL/min): *t*_{R(major)}: 5.65 min; *t*_{R(minor)}: 9.73 min; colorless oil; [α]_D²⁵ -20.0 (*c* 0.20, MeOH).

IR (neat): 3389, 2931, 2871, 1734, 1376, 1226, 1026, 1016 cm⁻¹.

¹H NMR (500 MHz, CDCl₃): δ = 7.28 – 7.24 (m, 4 H), 5.07 (s, 2 H), 3.47 (dd, *J* = 11.8, 6.2 Hz, 1 H), 3.26 (dd, *J* = 11.6, 8.5 Hz, 1 H), 2.36 – 2.28 (m, 1 H), 2.09 (s, 3 H), 1.54–1.47 (m, 1 H), 1.13 – 1.06 (m, 1 H), 0.89 – 0.85 (m, 1 H).

¹³C NMR (126 MHz, CDCl₃): δ = 171.1, 138.7, 134.0, 129.3 (2 C), 128.6 (2 C), 66.3, 63.9, 21.23, 21.22, 20.7, 8.0.

HRMS (ESI): *m/z* [M + Na]⁺ calcd for C₁₃H₁₆O₃: 243.0991; found: 243.0987.

(2-Heterylcyclopropyl)methanol Compounds 23a–e by Suzuki-Miyaura Cross-Coupling of 13; General Procedure A

To a dried round-bottom flask equipped with a stir bar was added HetArBr **22a–e** (0.28 mmol), **13** (0.14 mmol), Pd₂(dba)₃ (6.4 mg, 5 mol%), and Cy₃P (3.9 mg, 10 mol%). The vial was sealed with a septum and flushed with argon. To the vial was added dioxane (500 μL), and the resulting mixture was stirred at 23 °C for 20 min. To the mixture was then added 3.0 M aq K₃PO₄ (280 μL), and the mixture was degassed by sparging with argon for 20 min. The vial was placed in an oil bath and heated at 110 °C while stirring for 20 h. After completion, the reaction mixture was cooled and diluted with EtOAc (4 mL) and brine (2 mL) and the organic layer was separated. The aqueous layer was washed with EtOAc (2 × 2 mL), dried, and concentrated. Purification by column chromatography provided the coupled products **23a–e**.

(2-Heterylcyclopropyl)methanol Compounds 23a–e by Suzuki-Miyaura Cross-Coupling of 14; General Procedure B

To a dried flask equipped with a stir bar was added HetArBr **22a–e** (0.28 mmol), **14** (0.14 mmol), Pd₂(dba)₃ (6.4 mg, 5 mol %), and Cy₃P (3.93 mg, 10 mol%). The vial was sealed with a septum and flushed with argon. To the vial was added dioxane (500 μL) and the resulting mixture was stirred at 23 °C for 20 min. To the mixture was then added 3.0 M aq K₃PO₄ (280 μL, degassed with argon for 20 min). The vial was placed in an oil bath and heated at 110 °C while stirring for 20 h. After completion, the reaction mixture was cooled and diluted with EtOAc (4 mL) and brine (2 mL) and the organic layer was separated. The aqueous layer was washed with EtOAc (2 × 2 mL), dried, and concentrated. Purification by column chromatography provided the coupled products **23a–e**.

[(1S,2S)-2-(Pyridin-3-yl)cyclopropyl]methanol (23a)

General Procedure A: 3-Bromopyridine (47.1 mg, 0.29 mmol) and **13** (41.3 mg, 0.14 mmol) were used.

Yield: 19.8 mg (95%); pale yellow oil; *R*_f = 0.3 (MeOH/CH₂Cl₂, 1:9); [α]_D²⁵ +25.6 (c 0.83, MeOH).

General Procedure B: 3-Bromopyridine (47.1 mg, 0.29 mmol) and **14** (27.7 mg, 0.14 mmol) were used.

Yield: 18.6 mg (89%); pale yellow oil.

IR (neat): 3352, 3269, 3002, 2926, 2853, 11642, 1472, 1426, 1109 cm^{-1} .

^1H NMR (500 MHz, CDCl_3): δ = 8.43 – 8.39 (m, 2 H), 7.30 (dt, J = 7.8, 2.0 Hz, 1 H), 7.17 (dd, J = 7.8, 5.0 Hz, 1 H), 3.71 (dd, J = 11.5, 6.4 Hz, 1 H), , 3.64 (dd, J = 11.3, 6.6 Hz, 1 H), 2.03 (br, 1 H), 1.88 – 1.82 (m, 1 H), 1.53 – 1.46 (m, 1 H), 1.03–0.97 (m, 2 H).

^{13}C NMR (126 MHz, CDCl_3): δ = 148.5, 147.2, 138.2, 132.9, 123.4, 66.2, 25.4, 19.0, 13.8.

HRMS (ESI): m/z [$\text{M} + \text{H}$] $^+$ calcd for $\text{C}_9\text{H}_{11}\text{NO}$: 150.0913; found:150.0910.

[(1*S*,2*S*)-2-(Quinolin-3-yl)cyclopropyl]methanol (23b)

General Procedure A: 5-Bromoquinoline, 98% (58.3 mg, 0.28 mmol) and **13** (41.3 mg, 0.14 mmol) were used.

Yield: 26.2 mg (94%); pale yellow oil; R_f = 0.3 (MeOH/ CH_2Cl_2 , 1:9); $[\alpha]_{\text{D}}^{25}$ +36.3 (c 0.87, MeOH).

General Procedure B: 5-Bromoquinoline, 98% (58.3 mg, 0.28 mmol) and **14** (27.7 mg, 0.14 mmol) were used.

Yield: 24.5 mg (88%); pale yellow oil.

IR (neat): 3352, 3303, 3001, 2922, 2854, 1706, 1495, 1332, 1028 cm^{-1} .

^1H NMR (500 MHz, CDCl_3): δ = 8.72 (d, J = 2.2 Hz, 1 H), 8.05 (d, J = 8.4 Hz, 1 H), 7.70 (s, 2 H), 7.64–7.62 (m, 1 H), 7.52–7.50 (m, 1 H), 3.77 (dd, J = 11.3, 6.3 Hz, 1 H), 3.68 (dd, J = 11.3, 6.9 Hz, 1 H), 2.02–1.99 (m, 1 H), 1.62–1.58 (m, 1 H), 1.13–1.08 (m, 2 H).

^{13}C NMR (126 MHz, CDCl_3): δ = 150.6, 146.9, 135.5, 131.3, 129.3, 128.7, 128.2, 127.4, 126.9, 66.3, 25.6, 19.3, 13.9.

HRMS (ESI): m/z [$\text{M} + \text{H}$] $^+$ calcd for $\text{C}_{13}\text{H}_{13}\text{NO}$: 200.1069; found: 200.1067.

[(1S,2S)-2-(4-Methylpyridin-2-yl)cyclopropyl]methanol (23c)

General Procedure A: 2-Bromo-4-methylpyridine, 98% (48.2 mg, 0.28 mmol) and **13** (41.3 mg, 0.14 mmol) were used.

Yield: 21.3 mg (93%); clear oil; $R_f = 0.4$ (MeOH/CH₂Cl₂, 1:9); $[\alpha]_D^{25} +44.0$ (c 0.56, MeOH).

General Procedure B: 2-Bromo-4-methylpyridine, 98% (48.2 mg, 0.28 mmol) and **14** (27.7 mg, 0.14 mmol) were used.

Yield: 16.5 mg (72%); clear oil.

IR (neat): 3350, 2923, 2850, 1608, 1447, 1376, 1024, 848 cm⁻¹.

¹H NMR (500 MHz, CDCl₃): $\delta = 8.28$ (d, $J = 5.1$ Hz, 1 H), 6.95 (d, $J = 11.8$ Hz, 1 H), 6.86 (d, 1 H), 3.70 (dd, $J = 11.3, 6.4$ Hz, 1 H), 3.58 (dd, $J = 11.3, 7.1$ Hz, 1 H), 2.30 (s, 3 H), 1.95–1.91 (m, 1 H), 1.74 (tdd, $J = 10.6, 5.3, 3.2$ Hz, 1 H), 1.64 (s, 1 H), 1.27–1.24 (m, 1 H), 0.94 (ddd, $J = 8.6, 5.7, 4.4$ Hz, 1 H).

¹³C NMR (126 MHz, CDCl₃): $\delta = 161.3, 149.1, 147.2, 122.4, 121.9, 66.4, 25.7, 23.0, 21.1, 14.0$.

HRMS (ESI): m/z [M + H]⁺ calcd for C₁₃H₁₃NO: 164.1069; found: 164.1069.

[(1S,2S)-2-(6-Aminopyridin-2-yl)cyclopropyl]methanol (23d)

General Procedure A: 2-Amino-6-bromopyridine, 98% (48.4 mg, 0.28 mmol) and **13** (41.3 mg, 0.14 mmol) were used.

Yield: 21.1 mg (92%); yellow oil; $R_f = 0.3$ (MeOH/CH₂Cl₂, 1:9); $[\alpha]_D^{25} +37.5$ (c 0.85, MeOH).

General Procedure B: 2-Amino-6-bromopyridine, 98% (27.7 mg, 0.14 mmol) and **14** (41.3 mg, 0.14 mmol) were used.

Yield: 18.6 mg (81%); yellow oil.

IR (neat): 3337, 3206, 2927, 2851, 1574, 1464, 1025, 791 cm⁻¹.

^1H NMR (500 MHz, CDCl_3): δ = 7.29 (t, J = 7.8 Hz, 1 H), 6.43 (d, J = 7.4 Hz, 1 H), 6.27 (d, J = 8.1 Hz, 1 H), 3.67 (dd, J = 11.3, 6.3 Hz, 1 H), 3.52 (dd, J = 11.2, 7.3 Hz, 1 H), 1.85 – 1.82 (m, 1 H), 1.64 (d, J = 6.0 Hz, 1 H), 1.18–1.15 (m, 1 H), 0.88 – 0.85 (m, 1 H).

^{13}C NMR (126 MHz, CDCl_3): δ = 148.5, 147.2, 138.2, 132.9, 123.4, 66.2, 25.4, 19.0, 13.8.

HRMS (ESI): m/z $[\text{M} + \text{H}]^+$ calcd for $\text{C}_9\text{H}_{11}\text{NO}$: 165.1027; found: 165.1022.

[(1S,2S)-2-(Pyrimidin-5-yl)cyclopropyl]methanol (23e)

General Procedure A: 5-Bromopyrimidine, 97% (44.5 mg, 0.28 mmol) and **13** (41.3 mg, 0.14 mmol) were used.

Yield: 19.8 mg (94%); yellow oil; R_f = 0.3 (MeOH/ CH_2Cl_2 , 1:9); $[\alpha]_{\text{D}}^{25}$ +38.9 (c 0.87, MeOH).

General Procedure B: 5-Bromopyrimidine, 97% (44.5 mg, 0.28 mmol) and **14** (27.7 mg, 0.14 mmol) were used.

Yield: 18.7 mg (89%); pale yellow oil.

IR (neat): 3335, 3003, 2925, 2853, 1721, 1559, 1416, 1076, 1025 cm^{-1} .

^1H NMR (500 MHz, CDCl_3): δ = 9.01 (s, 1 H), 8.46 (s, 2 H), 3.74 (dd, J = 11.3, 6.1 Hz, 1 H), 3.63 (dd, J = 11.3, 6.7 Hz, 1 H), 2.01 (br, 1 H), 1.83–1.79 (m, 1 H), 1.54–1.50 (m, 1 H), 1.11 – 1.01 (m, 2 H).

^{13}C NMR (126 MHz, CDCl_3): δ = 156.4 (2 C), 154.8, 136.0, 65.6, 25.2, 16.6, 13.5.

HRMS (ESI): m/z $[\text{M} + \text{H}]^+$ calcd for $\text{C}_8\text{H}_{10}\text{N}_2\text{O}$: 151.0865; found: 151.0859.

cis-Cyclopropylmethanol Derivatives 25a–f; General Procedure C

A solution of **24** (66.5 μL , 1.1 mmol) in CH_2Cl_2 (4.6 mL) was added to Et_2Zn (115 μL , 1.1 mmol) in a 50 mL round-bottom flask at 0 °C. Gas evolution was observed. After 5 min, a solution of dioxaborolane **11** (371 mg, 1.37 mmol) in CH_2Cl_2 (7 mL) was added. The reaction mixture was stirred for 10 min at 0 °C.

In a 50 mL round-bottom flask at $-40\text{ }^{\circ}\text{C}$, neat Et_2Zn (507 μL , 4.92 mmol) was added dropwise to a mixture of I_2 (1.22 g, 4.81 mmol), Et_2O (0.98 mL, 9.33 mmol), and CH_2Cl_2 (4.7 mL). Once the I_2 was completely consumed, the reaction mixture was cooled to $-78\text{ }^{\circ}\text{C}$ and a solution of CHI_3 (951 mg, 2.42 mmol) in CH_2Cl_2 (14 mL) was slowly added to the IZnEt solution. The mixture was stirred at $-78\text{ }^{\circ}\text{C}$ for 10 min.

The alkoxide solution was quickly cannulated over the carbenoid solution and the reaction mixture was allowed to reach $-40\text{ }^{\circ}\text{C}$ (cryostat bath). The reaction mixture was stirred 24 h at this temperature. The reaction mixture was quenched with sat. aq NH_4Cl . The aqueous layer was extracted with Et_2O (3×10 mL). The organic layers were gathered and dried over MgSO_4 and the solvents were removed until 500 μL under reduced pressure. The intermediate is unstable and highly volatile, and care must be taken to avoid loss of the volatile boronate. The residue was taken up in degassed THF (4.4 mL) and added to a sealed tube containing $\text{Pd}(\text{PPh}_3)_4$ (68.7 mg, 5 mol%) in THF (2.2 mL). Then 3 N aq degassed KOH (2.2 mL) was added followed by the desired coupling partner **22a–e** (2.2 mmol). The reaction mixture was heated at $65\text{ }^{\circ}\text{C}$ overnight (16 h). After the mixture had cooled down, H_2O was added to it. The aqueous layer was extracted with Et_2O (3×7 mL). The combined organic layers were dried over MgSO_4 . The solvents were removed under reduced pressure. The residue was stirred in diethanolamine (602 mg, 5.72 mmol) in CH_2Cl_2 (3 mL) for 1 h to remove any dioxaborolane bound to the cyclopropane. The residue was taken up in CH_2Cl_2 and purified by flash chromatography (silica gel, $\text{MeOH}/\text{CH}_2\text{Cl}_2$, 5:95, unless stated otherwise) to provide the desired coupled products **25a–f**.

[(1*R*,2*S*)-2-(Pyridin-3-yl)cyclopropyl]methanol (25a)

The product was prepared according to general procedure C using 3-bromopyridine (217 μL , 2.28 mmol).

Yield: 92 mg (72%); light yellow oil; $R_f = 0.23$ ($\text{MeOH}/\text{CH}_2\text{Cl}_2$, 1:9); $[\alpha]_{\text{D}}^{25} -45.2$ (c 1.00, MeOH).

IR (neat): 3264, 3005, 2866, 1573, 1573, 1480, 1418, 1167, 1025 cm^{-1} .

^1H NMR (400 MHz, CDCl_3): δ = 8.53 (s, 1 H), 8.42 (d, J = 4.5 Hz, 1 H), 7.60 – 7.56 (m, 1 H), 7.21 (dd, J = 7.8, 4.8 Hz, 1 H), 3.47 (dd, J = 11.5, 6.4 Hz, 1 H), 3.25 (dd, J = 11.5, 8.3 Hz, 1 H), 2.30 – 2.25 (m, 1 H), 1.93 (br, 1 H), 1.62 – 1.54 (m, 1 H), 1.13 (td, J = 8.4, 5.4 Hz, 1 H), 0.87 (q, J = 5.7 Hz, 1 H).

^{13}C NMR (126 MHz, CDCl_3): δ = 151.0, 147.7, 137.0, 134.6, 123.5, 62.9, 21.2, 18.7, 8.0.

HRMS (ESI): m/z [$\text{M} + \text{H}$] $^+$ calcd for $\text{C}_9\text{H}_{11}\text{NO}$: 150.0913; found: 150.0912.

[(1*R*,2*S*)-2-(Quinolin-3-yl)cyclopropyl]methanol (25b)

The product was prepared according to general procedure C using 3-bromoquinoline (308 μL , 2.28 mmol).

Yield: 162 mg (71%); light yellow oil; R_f = 0.26 (MeOH/ CH_2Cl_2 , 1:9); $[\alpha]_{\text{D}}^{25}$ +38.6 (c 1.00, MeOH).

IR (neat): 3262, 3064, 3005, 2872, 1571, 1493, 1464, 1417 cm^{-1} .

^1H NMR (500 MHz, CDCl_3): δ = 8.86 (d, J = 2.1 Hz, 1 H), 8.01 (d, J = 8.6 Hz, 1 H), 7.88 (s, 1 H), 7.71 (d, J = 8.1 Hz, 1 H), 7.61 (ddd, J = 8.4, 5.1, 1.4 Hz, 1 H), 7.50–7.46 (m, 1 H), 3.49 (dd, J = 11.5, 6.3 Hz, 1 H), 3.26 (dd, J = 11.5, 8.4 Hz, 1 H), 2.39 (dd, J = 14.7, 8.3 Hz, 1 H), 1.89 (br, 1 H), 1.62 (qt, J = 8.5, 6.0 Hz, 1 H), 1.19 (td, J = 8.4, 5.5 Hz, 1 H), 0.97 (q, J = 5.7 Hz, 1 H).

^{13}C NMR (126 MHz, CDCl_3): δ = 152.7, 146.7, 134.7, 131.6, 129.0, 128.9, 127.8, 127.4, 126.8, 62.3, 21.2, 18.6, 7.7.

HRMS (ESI): m/z [$\text{M} + \text{H}$] $^+$ calcd for $\text{C}_{13}\text{H}_{13}\text{NO}$: 200.1069; found: 200.1066.

[(1*R*,2*S*)-2-(4-Methylpyridin-2-yl)cyclopropyl]methanol (25c)

The product was prepared according to general procedure C using 2-bromo-4-methylpyridine (252 μL , 2.28 mmol).

Yield: 136 mg (73%); light yellow oil; R_f = 0.32 (MeOH/ CH_2Cl_2 , 1:9); $[\alpha]_{\text{D}}^{25}$ +31.1 (c 1.00, MeOH).

IR (neat): 3350, 3053, 3003, 2849, 1606, 1543, 1480, 1032 cm^{-1} .

^1H NMR (500 MHz, CDCl_3): δ = 8.23 (d, J = 5.1 Hz, 1 H), 7.20 – 7.17 (m, 1 H), 6.96 – 6.93 (d, J = 5.1 Hz, 1 H), 3.93 (dd, J = 12.1, 3.6 Hz, 1 H), 3.34 (dd, J = 12.1, 8.6 Hz, 1 H), 2.31 (s, 3 H), 2.22 – 2.15 (m, 1 H), 1.67 – 1.59 (m, 1 H), 1.06 – 1.01 (m, 1 H).

^{13}C NMR (126 MHz, CDCl_3): δ = 160.3, 148.0, 147.9, 126.1, 122.2, 61.3, 22.5, 22.4, 21.0, 10.5.

HRMS (ESI): m/z [$\text{M} + \text{H}$] $^+$ calcd for $\text{C}_{10}\text{H}_{13}\text{NO}$: 164.1069; found: 164.1071.

[(1*R*,2*S*)-2-(6-Aminopyridin-2-yl)cyclopropyl]methanol (25d)

The product was prepared according to general procedure C using 2-amino-6-bromopyridine (392 mg, 2.28 mmol).

Yield: 141 mg (75%); bright yellow oil; R_f = 0.22 (MeOH/ CH_2Cl_2 , 1:9); $[\alpha]_{\text{D}}^{25}$ –57.7 (c 1.00, MeOH).

IR (neat): 3332, 3202, 3002, 2860, 1616, 1594, 1324, 1020 cm^{-1} .

^1H NMR (500 MHz, CDCl_3): δ = 7.35 (m, 1 H), 6.67 (d, J = 7.4 Hz, 1 H), 6.31 (d, J = 8.2 Hz, 1 H), 4.41 (br, 2 H), 3.93 (dd, J = 12.0, 3.8 Hz, 1 H), 3.33 (dd, J = 12.0, 8.8 Hz, 1 H), 2.10 (td, J = 8.6, 6.0 Hz, 1 H), 1.59–1.51 (m, 1 H), 1.13 – 1.08 (m, 1 H), 0.98–0.95 (m, 1 H).

^{13}C NMR (126 MHz, CDCl_3): δ = 158.4, 157.1, 138.3, 114.8, 105.9, 61.5, 22.3, 21.8, 9.8.

HRMS (ESI): m/z [$\text{M} + \text{H}$] $^+$ calcd for $\text{C}_9\text{H}_{12}\text{N}_2\text{O}$: 165.1022; found: 165.1022

[(1*R*,2*S*)-2-(Pyrimidin-5-yl)cyclopropyl]methanol (25e)

The product was prepared according to general procedure C using 5-bromopyrimidine (360 mg, 2.28 mmol).

Yield: 127 mg (74%); light yellow oil; R_f = 0.27 (MeOH/ CH_2Cl_2 , 1:9); $[\alpha]_{\text{D}}^{25}$ –11.2 (c 1.00, MeOH).

IR (neat): 3329, 3009, 2872, 1556, 1415, 1239, 1168, 1026 cm^{-1} .

^1H NMR (500 MHz, CDCl_3): δ = 9.03 (s, 1 H), 8.65 (s, 2 H), 3.57 (dd, J = 11.4, 6.0 Hz, 1 H), 3.17 (dd, J = 11.4, 8.6 Hz, 1 H), 2.24 – 2.17 (m, 1 H), 1.78 (s, 1 H), 1.67 – 1.59 (m, 1 H), 1.18 (dt, J = 8.4, 5.5 Hz, 1 H), 0.87 (q, J = 5.8 Hz, 1 H).

^{13}C NMR (126 MHz, CDCl_3): $\delta = 157.6$ (2 C), 156.6, 132.3, 62.0, 20.5, 16.0, 7.4 cm^{-1} .

HRMS (ESI): m/z $[\text{M} + \text{H}]^+$ calcd for $\text{C}_8\text{H}_{10}\text{N}_2\text{O}$: 151.0866; found: 151.0860.

[(1*R*,2*S*)-2-Phenylcyclopropyl]methanol (25f)

The product was prepared according to general procedure C using bromobenzene (238 μL , 2.28 mmol).

Yield: 120 mg (71%); 95.2:4.7 er; SFC (Chiralpak AD-H 25cm, 30 $^\circ\text{C}$, 150 bar, 10% MeOH, 3 mL/min): $t_{\text{R}(\text{major})}$: 6.76 min, $t_{\text{R}(\text{minor})}$: 4.25 min; light yellow oil; $R_f = 0.45$ (EtOAc/hexanes, 1:4); $[\alpha]_{\text{D}}^{25} -22.4$ (c 1.00, MeOH).

IR (neat): 3330, 2962, 2865, 1638, 1603, 1496, 1451, 1019 cm^{-1} .

^1H NMR (500 MHz, CDCl_3): $\delta = 7.32$ – 7.23 (m, 4 H), 7.23– 7.17 (m, 1 H), 3.48 (dd, $J = 11.7, 6.3$ Hz, 1 H), 3.27 (dd, $J = 11.7, 8.5$ Hz, 1 H), 2.30 (td, $J = 8.5, 6.2$ Hz, 1 H), 1.54– 1.47 (m, 1 H), 1.13 (br, 1 H), 1.05 (td, $J = 8.4, 5.3$ Hz, 1 H), 0.89 (dd, $J = 11.4, 5.6$ Hz, 1 H).

^{13}C NMR (126 MHz, CDCl_3): $\delta = 138.4, 129.0$ (2 C), 128.5 (2 C), 126.4, 63.1, 21.1, 20.9, 7.8.

HRMS (ESI): m/z $[\text{M} + \text{NH}_4]^+$ calcd for $\text{C}_{10}\text{H}_{12}\text{O}$: 166.1226; found: 166.1219.

Synthesis of Starting Materials

2,2'-(Cyclohexylazanediyl)diacetic Acid (CIDA)

To a stirred solution of chloroacetic acid (6.94 mL, 116 mmol) and H_2O (9 mL) was added dropwise aq NaOH (9.28 g, 232 mmol in 30 mL of H_2O) maintaining the temperature below 30 $^\circ\text{C}$ by using an ice bath. The mixture was stirred for 5 min after the addition, and the ice bath was removed. Cyclohexylamine was added dropwise, keeping the temperature below 50 $^\circ\text{C}$. After addition was complete, the reaction mixture was heated at 80 $^\circ\text{C}$ for 3 h. A solution of barium chloride dihydrate (12.9 g, 52.9 mmol), dissolved in hot H_2O (24 mL), was added in one portion and the mixture was heated for 30 min. A heavy precipitate of the barium salt of the amino acid separated

at once. The stirring was continued, keeping the heating bath at 100 °C, and then the mixture was cooled down and kept in an ice bath. The precipitate was then filtered off. The dry barium salt was placed in a flask into which boiling H₂O (24 mL) was added and heated to boiling; 5 M sulfuric acid (9 mL) was added gradually over 30 min. Once the addition was complete, the mixture was stirred for 10 min and then concentrated under reduced pressure to 5 mL. The solution was filtered on Celite and concentrated.

Yield: 7.38 g (68%); yellow crystalline solid; mp 198–199 °C.

IR (neat): 3012, 2979, 2941, 2856, 1716 1584, 1400, 1240 cm⁻¹.

¹H NMR (500 MHz, DMSO-*d*₆): δ = 3.44 (s, 4 H), 2.58 (d, *J* = 7.6 Hz, 1 H), 1.75–1.65 (m, 4 H), 1.52 (d, *J* = 12.2 Hz, 1 H), 1.21–1.10 (m, 4 H), 1.10–1.00 (m, 1 H).

¹³C NMR (126 MHz, DMSO-*d*₆): δ = 173.9, 62.4, 54.1, 29.9, 26.2, 26.0.

HRMS (ESI): *m/z* [M + H]⁺ calcd for C₁₀H₁₇NO₄: 216.1230; found: 216.1227.

(*E*)-2-(3-[(*tert*-Butyldimethylsilyl)oxy]prop-1-en-1-yl)-6-cyclohexyl-1,3,6,2-dioxaborocane-4,8-dione (15aa)

To a stirred solution of (*E*)-*tert*-butyldimethyl([3-(4,4,5,5-tetramethyl-1,3,2-dioxaborolan-2-yl)allyl]oxy)silane²⁸ (4.18 g, 14 mmol) in a mixture of acetone/H₂O (1:1; 94 mL) was added in one portion, sodium periodate (15.0 g, 70.1 mmol) and ammonium acetate (5.57 g, 70.1 mmol). The mixture was stirred at rt for 24 h. The flask was fitted with a short-path distillation setup and at rt the acetone and H₂O were removed to dryness. The resulting white solid was suspended in acetone and stirred for 15 min and then filtered. The filtrate was then concentrated to almost dryness. The crude boronic acid was used immediately for the next step. The crude boronic acid (3.03 g, 14.0 mmol) and 2,2'-(cyclohexylazanediyl)diacetic acid (6.00 g, 27.9 mmol) were dissolved in a mixture of DMSO (14 mL) and benzene (85 mL), and the mixture was refluxed using a Dean–Stark condenser for 6 h at 95 °C (internal temperature). The reaction mixture was cooled and concentrated to remove benzene. The residue was diluted with EtOAc (20 mL) and brine (10 mL). The organic layer was washed with H₂O (3 × 10 mL), dried with Na₂SO₄, and concentrated

under reduced pressure to afford a light brown solid. Following column chromatography (silica gel, CH₂Cl₂/MeCN, 1:1), the protected allylic alcohol **15aa** was isolated.

Yield: 3.33 g (60%); white solid; *R_f* = 0.5 (CH₂Cl₂/MeCN, 1:1); mp 132–133 °C.

IR (neat): 2931, 2856, 1747, 1648, 1449, 1252, 1104, 956 cm⁻¹.

¹H NMR (400 MHz, acetone-*d*₆): δ = 6.21 (dt, *J* = 17.5, 3.8 Hz, 1 H), 5.87 (dt, *J* = 17.9, 1.9 Hz, 1 H), 4.28 (dd, *J* = 3.8, 2.0 Hz, 2 H), 4.15 (d, *J* = 16.8 Hz, 2 H), 3.93 (d, *J* = 16.8 Hz, 2 H), 3.22 (t, *J* = 11.9 Hz, 1 H), 1.89 (m, 2 H), 1.71–1.49 (m, 4 H), 1.44–1.24 (m, 4 H), 0.95 (s, 9 H), 0.11 (s, 6 H).

¹³C NMR (126 MHz, acetone-*d*₆): δ = 169.1 (2 C), 146.3 (2 C), 67.2, 62.6, 56.6 (2 C), 27.4, 26.3 (2 C), 25.5 (2 C), 25.4 (3 C), 18.7, –5.0 (2 C).

HRMS (ESI): *m/z* [M + H]⁺ calcd for C₁₉H₃₄BNO₅Si: 395.2408; found: 395.2416.

Base-Sensitive Allylic Alcohol (Z)-4-(3-Hydroxyprop-1-en-1-yl)benzyl Acetate (20)

(4-(3-[(*tert*-Butyldimethylsilyl)oxy]prop-1-yn-1-yl)phenyl)- methanol (20a)

To a dry sealed tube was added [Pd(PPh₃)₂Cl₂] (304 mg, 0.433 mmol) and copper iodide (82.3 mg, 0.433 mmol). Et₃N (10.5 mL) was added to the sealed tube and the mixture was flushed with argon while stirring for 5 min. To this was added 4-bromobenzyl alcohol (540 mg, 2.89 mmol), followed by the immediate addition of the TBS-protected propargyl alcohol³⁰ (1.96 g, 11.5 mmol). The reaction mixture was then stirred for 15 h at 77 °C under an argon atmosphere. The reaction mixture was diluted with EtOAc and washed with 10% HCl solution (2 × 15 mL) and brine (2 × 15 mL). The layers were separated, and the aqueous layer was extracted with EtOAc (3 × 15 mL). The organic layers were combined, dried with Na₂SO₄, and concentrated. Purification by column chromatography (silica gel, MeOH/CH₂Cl₂, 1:9) afforded the coupled product **20a**.

Yield: 670.4 mg (84%); yellow oil. *R_f* = 0.5 (MeOH/CH₂Cl₂, 1:9).

IR (neat): 3369, 2923, 2857, 1736, 1720, 1231, 1045, 1033, 1017 cm⁻¹.

^1H NMR (500 MHz, CDCl_3): δ = 7.42 (d, J = 8.2 Hz, 2 H), 7.28 (d, J = 8.2 Hz, 2 H), 4.68 (s, 2 H), 4.54 (s, 2 H), 0.94 (s, 9 H), 0.17 (s, 6 H).

^{13}C NMR (126 MHz, CDCl_3): δ = 141.2, 132.0 (2 C), 127.0 (2 C), 122.4, 88.2, 85.0, 65.1, 52.5, 26.1 (3 C), 18.6, -5.0 (2 C).

HRMS (ESI): m/z [$\text{M} + \text{H}$] $^+$ calcd for $\text{C}_{16}\text{H}_{24}\text{O}_2\text{Si}$: 277.2; found: 277.7.

(Z)-(4-(3-((*tert*-Butyldimethylsilyl)oxy)prop-1-en-1-yl)phenyl)- methanol (20b)

To a stirred solution of nickel(II) acetate tetrahydrate (883 mg, 3.55 mmol) in EtOH (19.7 mL) under an argon atmosphere was added sodium borohydride (134 mg, 3.55 mmol), resulting in a black amorphous precipitate. After 5 min of stirring, ethylenediamine was added (237 mg, 3.94 mmol). The mixture was then allowed to stir for 30 min under an argon atmosphere. The flask was purged with hydrogen, and alkyne **20a** (1.09 g, 3.94 mmol) was rapidly added to the reaction mixture. The reaction was monitored by NMR. Upon completion, the reaction mixture was filtered over Celite, and the Celite was washed with Et₂O. The filtrate was washed with brine and extracted with Et₂O (3 × 10 mL). The filtrate was dried with Na₂SO₄ and concentrated under reduced pressure to provide the desired pure product **20b**. The solids along with the Celite were quenched in a 10% HCl solution.

Yield: 1.07 g (97%); R_f = 0.5 (EtOAc/hexane, 1:4).

IR (neat): 2952, 2927, 2855, 1737, 1378, 1227, 1028, 835 cm^{-1} .

^1H NMR (500 MHz, CDCl_3): δ = 7.34 (d, J = 8.1 Hz, 2 H), 7.19 (d, J = 8.1 Hz, 2 H), 6.48 (d, J = 11.8 Hz, 1 H), 5.83 (dt, J = 12.0, 6.1 Hz, 1 H), 4.69 (s, 2 H), 4.44 (dd, J = 6.1, 1.8 Hz, 2 H), 0.90 (s, 9 H), 0.06 (s, 6 H).

^{13}C NMR (126 MHz, CDCl_3): δ = 139.8, 136.5, 133.0, 129.4, 129.2 (2 C), 127.0 (2 C), 65.3, 60.6, 25.1 (3 C), 18.5, -5.0 (2 C).

HRMS (ESI): m/z [$\text{M} + \text{NH}_4$] $^+$ calcd for $\text{C}^{16}\text{H}^{26}\text{O}^2\text{Si}$: 296.2; found: 296.2.

(Z)-4-(3-[(*tert*-Butyldimethylsilyl)oxy]prop-1-en-1-yl)benzyl Acetate (20c)

Anhydrous pyridine (12 mL) was added to **20b** (1.19 g, 4.27 mmol) in a dried flask. The mixture was allowed to stir for 10 min and cooled to 0 °C. Upon cooling, acetic anhydride (12 mL) was added dropwise to the mixture. The mixture was allowed to stir for 12 h. Upon completion of the reaction, the mixture was diluted with Et₂O and washed with 10% HCl (2 × 20 mL), brine (2 × 20 mL), and NaHCO₃ (2 × 20 mL). The aqueous layer was extracted with EtOAc (2 × 20 mL), dried with Na₂SO₄, and concentrated. Purification by column chromatography (silica gel, EtOAc/hexanes, 1:4) afforded product **20c**.

Yield: 985 mg (72%); yellow oil; *R_f* = 0.6 (EtOAc/hexanes, 1:4).

IR (neat): 3022, 2953, 2928, 2888, 2855, 2070, 2040, 2031 cm⁻¹.

¹H NMR (500 MHz, CDCl₃): δ = 7.33 (d, *J* = 8.1 Hz, 2 H), 7.20 (d, *J* = 8.1 Hz, 2 H), 6.48 (d, *J* = 11.8 Hz, 1 H), 5.85 (dt, *J* = 12.0, 6.1 Hz, 1 H), 5.10 (s, 2 H), 4.44 (dd, *J* = 6.1, 1.8 Hz, 2 H), 2.11 (s, 3 H), 0.90 (s, 9 H), 0.06 (s, 6 H).

¹³C NMR (126 MHz, CDCl₃): δ = 171.0, 137.0, 134.8, 133.2, 129.2, 129.1 (2 C), 128.3 (2 C), 66.2, 60.4, 26.1 (3 C), 21.2, 18.4, -5.0 (2 C).

HRMS (ESI): *m/z* [M + NH₄]⁺ calcd for C₁₈H₂₈O₃Si: 338.2; found: 338.2.

(Z)-4-(3-Hydroxyprop-1-en-1-yl)benzyl Acetate (20)

Acetate **20c** (330 mg, 1.03 mmol) was loaded into a dried flask containing THF (4.20 mL). The mixture was cooled to 0 °C and TBAF (1.13 mL, 1.13 mmol) was added dropwise. The cooling bath was removed, and the mixture was stirred and monitored by TLC until completion. Upon completion, the reaction mixture was quenched with NH₄Cl (5 mL) and diluted with EtOAc (8 mL). The aqueous layer was extracted with EtOAc (3 × 8 mL), dried with Na₂SO₄, and concentrated. Purification by column chromatography (silica gel, EtOAc/hexanes, 1:1) afforded the desired product **20**.

Yield: 210 mg (99%); yellow oil; *R_f* = 0.4 (EtOAc/hexanes, 1:1).

IR (neat): 3389, 3021, 2931, 2871, 1734, 1226, 1026, 1016 cm^{-1} .

^1H NMR (500 MHz, CDCl_3): δ = 7.33 (d, J = 8.1 Hz, 2 H), 7.21 (d, J = 8.1 Hz, 2 H), 6.56 (d, J = 11.8 Hz, 1 H), 5.92–5.87 (m, 1 H), 5.10 (s, 2 H), 4.43 (dd, J = 6.5, 1.6 Hz, 2 H), 2.11 (s, 3 H), 1.86 (s, 1 H).

^{13}C NMR (126 MHz, CDCl_3): δ = 171.1, 136.7, 135.2, 131.8, 130.8, 129.2 (2 C), 128.4 (2 C), 66.2, 59.8, 21.2.

HRMS (ESI): m/z [$\text{M} + \text{NH}_4$] $^+$ calcd for $\text{C}_{12}\text{H}_{14}\text{O}_3$: 224.1; found: 224.1.

Base-Sensitive Additives

Benzyl 3,3-Dimethylbutanoate (19a)

To a suspension of NaH (88.8 mg, 3.70 mmol) in THF (13 mL) at 0 °C was added a solution of benzyl alcohol (385 μL , 3.70 mmol) in THF (5.3 mL). The reaction mixture was stirred at rt for 30 min. The mixture was then cooled to 0 °C and *tert*-butylacetyl chloride (488 μL , 3.51 mmol) was added dropwise. The reaction mixture was allowed to stir at rt for 6 h. The mixture was quenched with sat. aq NH_4Cl (13 mL) and H_2O (7 mL) and diluted with EtOAc (13 mL). The layers were separated and the aqueous layer was washed with EtOAc (3 \times 13 mL). The organic layers were combined, dried with Na_2SO_4 , and concentrated. Purification by flash chromatography (silica gel, hexanes/ CH_2Cl_2 , 8:2 to 6:4) resulted in the desired product **19a**. The NMR spectra matched those in the literature.³¹

Yield: 650 mg (85%).

Benzyl Phenethylcarbamate (19b)

To a reaction flask containing anhydrous THF (16.5 mL) was added 2-phenethylamine (400 mg, 3.30 mmol) and 4-dimethylaminopyridine (20.2 mg, 5 mol%). Benzyl chloroformate was added dropwise to the solution and the reaction mixture was allowed to stir for 6 h. The mixture was quenched with H_2O (10 mL) and diluted with Et_2O (13 mL). The aqueous layer was washed with Et_2O (3 \times 20 mL). The organic layers were combined, dried with Na_2SO_4 , and concentrated under

reduced pressure and the white solid was washed with hexanes to result in the desired product **19b**. The spectra matched those reported in the literature.³²

Yield: 758 mg (90%)

4-Bromobenzyl Acetate (19c)

Additive **19c** was synthesized according to the literature.⁸ In a dried flask, 4-bromobenzyl alcohol (600 mg, 3.21 mmol) was dissolved in anhydrous pyridine (9 mL). The mixture was allowed to stir for 10 min and cooled down to 0 °C. Upon cooling, acetic anhydride (9.10 mL, 96.2 mmol) was added dropwise to the mixture. The mixture was allowed to stir for 12 h. Upon completion of the reaction, the mixture was diluted with Et₂O and washed with 10% HCl (2 × 20 mL), brine (2 × 20 mL), and NaHCO₃ (2 × 20 mL). The aqueous layer was extracted with EtOAc (2 × 20 mL), dried with Na₂SO₄, and concentrated under reduced pressure. Purification by column chromatography (silica gel, EtOAc/hexanes, 1:20) afforded product **19c**. The spectra matched those reported in the literature.³³

Yield: 640 mg (87%); yellow oil.

Funding Information

This work was supported by the Natural Sciences and Engineering Research Council of Canada (NSERC) (Discovery Grant DG-06438), the Canada Research Chairs program (227346), the Canada Foundation for Innovation (Leaders Opportunity Funds 227346), the Fonds de Recherche du Québec - Nature et Technologies (FRQNT Centre in Green Chemistry and Catalysis; RS-171310), and the Université de Montréal.

Supporting Information

Supporting information for this article is available online at <https://doi.org/10.1055/s-0037-1611896>.

References

- [1]. Wessjohann, L. A.; Brandt, W.; Thiemann, T. *Chem. Rev.* **2003**, *103*, 1625-1648.
- [2]. Talele, T. T. *J. Med. Chem.* **2016**, *59*, 8712-8756.
- [3]. Knapp, D. M.; Gillis, E. P.; Burke, M. D. *J. Am. Chem. Soc.* **2009**, *131*, 6961-6963.
- [4]. Ebner, C.; Carreira, E. M. *Chem. Rev.* **2017**, *117*, 11651-11679.
- [5]. Volgraf, M.; Sellers, B. D.; Jiang, Y.; Wu, G.; Ly, C. Q.; Villemure, E.; Pastor, R. M.; Yuen, P.-w.; Lu, A.; Luo, X.; Liu, M.; Zhang, S.; Sun, L.; Fu, Y.; Lupardus, P. J.; Wallweber, H. J. A.; Liederer, B. M.; Deshmukh, G.; Plise, E.; Tay, S.; Reynen, P.; Herrington, J.; Gustafson, A.; Liu, Y.; Dirksen, A.; Dietz, M. G. A.; Liu, Y.; Wang, T.-M.; Hanson, J. E.; Hackos, D.; Scarce-Levie, K.; Schwarz, J. B. *J. Med. Chem.* **2016**, *59*, 2760-2779.
- [6]. (a) Tedford, C. E.; Phillips, J. G.; Gregory, R.; Panlowski, G. P.; Fadnis, L.; Khan, M. A.; Ali, S. M.; Handley, M. K.; Yates, S. L. *J. Pharmacol. Exp. Ther.* **1999**, *289*, 1160-1168. (b) Liddle, J.; Bamborough, P.; Barker, M. D.; Campos, S.; Chung, C. W.; Cousins, R. P. C.; Faulder, P.; Heathcote, M. L.; Hobbs, H.; Holmes, D. S.; Ioannou, C.; Ramirez-Molina, C.; Morse, M. A.; Osborn, R.; Payne, J. J.; Pritchard, J. M.; Rumsey, W. L.; Tape, D. T.; Vicentini, G.; Whitworth, C.; Williamson, R. A. *Bioorg. Med. Chem. Lett.* **2012**, *22*, 5222-5226. (c) Raheem, I. T.; Schreier, J. D.; Fuerst, J.; Gantert, L.; Hostetler, E. D.; Huszar, S.; Joshi, A.; Kandebo, M.; Kim, S. H.; Li, J.; Ma, B.; McGaughey, G.; Sharma, S.; Shipe, W. D.; Uslaner, J.; Vandever, G. H.; Yan, Y.; Renger, J. J.; Smith, S. M.; Coleman, P. J.; Cox, C. D. *Bioorg. Med. Chem. Lett.* **2016**, *26*, 126-132.
- [7]. Sayes, M.; Charette, A. B. *Angew. Chem. Int. Ed.* **2018**, *57*, 13514-13518. (b) Benoit, G.; Charette, A. B. *J. Am. Chem. Soc.* **2017**, *139*, 1364-1367. (c) Spencer, J. A.; Jamieson, C.; Talbot, E.

P. A. *Org. Lett.* **2017**, *19*, 3891-3894. (d) de Meijere, A.; Khlebnikov, A. F.; Sünnemann, H. W.; Frank, D.; Rauch, K.; Yufit, D. S. *Eur J. Org. Chem.* **2010**, *2010*, 3295-3301. (e) Fontani, P.; Carboni, B.; Vaultier, M.; Carrie, R. *Tetrahedron Lett.* **1989**, *30*, 4815-4818. (f) Fontani, P.; Carboni, B.; Vaultier, M.; Maas, G. *Synthesis* **1991**, *1991*, 605-609. (g) Fujioka, Y.; Amii, H., *Org. Lett.* **2008**, *10*, 769-772. (h) He, J.; Jiang, H.; Takise, R.; Zhu, R. Y.; Chen, G.; Dai, H. X.; Dhar, T.; Shi, J.; Zhang, H.; Cheng, P. T. *Angew. Chem. Int. Ed.* **2016**, *55*, 785-789. (i) Hussain, M. M.; Li, H.; Hussain, N.; Ureña, M.; Carroll, P. J.; Walsh, P. J. *J. Am. Chem. Soc.* **2009**, *131*, 6516-6524. (j) Liskey, C. W.; Hartwig, J. F. *J. Am. Chem. Soc.* **2013**, *135*, 3375-3378. (k) Markó, I. E.; Giard, T.; Sumida, S.; Gies, A.-E. *Tetrahedron letters* **2002**, *43*, 2317-2320. (l) Markó, I. E.; Kumamoto, T.; Giard, T. *Adv. Synth. Catal.* **2002**, *344*, 1063-1067. (m) Miyamura, S.; Araki, M.; Suzuki, T.; Yamaguchi, J.; Itami, K. *Angew. Chem. Int. Ed.* **2015**, *54*, 846-851.

[8]. Imai, T.; Mineta, H.; Nishida, S. *J. Org. Chem.* **1990**, *55*, 4986-4988. (b) Luithle, J. E. A.; Pietruszka, J. *J. Org. Chem.* **1999**, *64*, 8287-8297.

[9]. Carreras, J.; Caballero, A.; Pérez, P. J. *Angew. Chem. Int. Ed.* **2018**, *57*, 2334-2338.

[10]. Zimmer, L. E.; Charette, A. B. *J. Am. Chem. Soc.* **2009**, *131*, 15624-15626.

[11]. (a) Charette, A. B.; Beauchemin, A. *Org. React. (Hoboken, NJ, U. S.)* **2001**, *58*, 1-415. (b) Charette, A. B.; Juteau, H. *J. Am. Chem. Soc.* **1994**, *116*, 2651-2652.

[12]. For a related preparation of cyclopropane building blocks, see: (a) Chawner, S. J.; Cases-Thomas, M. J.; Bull, J. A. *Eur. J. Org. Chem.* **2017**, 5015-5024. (b) Bajaj, P.; Sreenilayam, G.; Tyagi, V.; Fasan, R. *Angew. Chem., Int. Ed.* **2016**, *55*, 16110-16114

[13]. Hohn, E.; Paleček, J.; Pietruszka, J.; Frey, W., *Eur. J. Org. Chem.* **2009**, *2009*, 3765-3782.

- [14]. (a) Uno, B. E.; Gillis, E. P.; Burke, M. D. *Tetrahedron* **2009**, *65*, 3130-3138. (b) Morrill, C.; Grubbs, R. H, *J. Org. Chem.* **2003**, *68*, 6031-6034.
- [15]. (a) Molander, G. A.; Biolatto, B. *J. Org. Chem.* **2003**, *68*, 4302-4314. (b) Molander, G. A.; Canturk, B.; Kennedy, L. E. *J. Org. Chem.* **2008**, *74*, 973-980. (c) Molander, G. A.; Gormisky, P. E. *J. Org. Chem.* **2008**, *73*, 7481-7485.
- [16]. (a) Lennox, A. J., Organotrifluoroborate Preparation. In *Organotrifluoroborate Preparation, Coupling and Hydrolysis*, Springer2013; pp 11-36.
- [17]. Maiti, G.; Roy, S. C. *Tetrahedron Lett.* **1997**, *38*, 495-498.
- [18]. (a) Coutts, S. J.; Adams, J.; Krolikowski, D.; Snow, R. J. *Tetrahedron Lett.* **1994**, *35*, 5109-5112. (b) Snow, R. J.; Bachovchin, W. W.; Barton, R. W.; Campbell, S. J.; Coutts, S. J.; Freeman, D. M.; Gutheil, W. G.; Kelly, T. A.; Kennedy, C. A. *J. Am. Chem. Soc.* **1994**, *116*, 10860-10869. (c) Coutts, S. J.; Kelly, T. A.; Snow, R. J.; Kennedy, C. A.; Barton, R. W.; Adams, J.; Krolikowski, D. A.; Freeman, D. M.; Campbell, S. J.; Ksiazek, J. F. *J. Med. Chem.* **1996**, *39*, 2087-2094. (d) Kinder, D. H.; Katzenellenbogen, J. A. *J. Med. Chem.* **1985**, *28*, 1917-1925. (e) Matteson, D. S.; Jesthi, P. K.; Sadhu, K. M. *Organometallics* **1984**, *3*, 1284-1288. (f) Martichonok, V.; Jones, J. B. *J. Am. Chem. Soc.* **1996**, *118*, 950-958. (g) Martin, R.; Jones, J. B. *Tetrahedron Lett.* **1995**, *36*, 8399-8402.
- [19]. Gonzalez, J. A.; Ogba, O. M.; Morehouse, G. F.; Rosson, N.; Houk, K. N.; Leach, A. G.; Cheong, P. H. Y.; Burke, M. D.; Lloyd-Jones, G. C. *Nat. Chem.* **2016**, *8*, 1067-1075.
- [20]. (a) Kettner, C. A.; Shenvi, A. B. *J. Biol. Chem.* **1984**, *259*, 15106-15114. (b) Tripathy, P. B.; Matteson, D. S. *Synthesis* **1990**, *1990*, 200-206. (c) Sun, J.; Perfetti, M. T.; Santos, W. L. *J. Org. Chem.* **2011**, *76*, 3571-3575. (d) Rettig, S. J.; Trotter, J. *Can. J. Chem.* **1975**, *53*, 1393-1401.

- [21]. Zhao, J.; Jonker, S. J. T.; Meyer, D. N.; Schulz, G.; Tran, C. D.; Eriksson, L.; Szabò, K. J. *Chem. Sci.* **2018**.
- [22]. Collins, K. D.; Glorius, F. *Nat. Chem.* **2013**, *5*, 597.
- [23]. (a) Bobbitt, J., Periodate oxidation of carbohydrates. In *Advances in carbohydrate chemistry*, Elsevier 1956; Vol. 11, pp 1-41; (b) Copéret, C.; Adolffsson, H.; Khuong, T.-A. V.; Yudin, A. K.; Sharpless, K. B. *J. Org. Chem.* 1998, *63*, 1740-1741.
- [24]. (a) Chemler, S. R.; Trauner, D.; Danishefsky, S. J. *Angew. Chem. Int. Ed.* **2001**, *40*, 4544-4568. (b) Miyaura, N.; Suzuki, A. *Chem. Rev.* **1995**, *95*, 2457-2483. (c) Molander, G. A.; Jean-Gérard, L. *Org. React.* **2013**, *79*, 1-316.
- [25]. Gillis, E. P.; Burke, M. D. *Aldrichimica Acta* **2009**, *42*, 17-27.
- [26]. Duncton, M. A. J.; Singh, R. *Org. Lett.* **2013**, *15*, 4284-4287.
- [27]. Shriver, D. F. & Drezzdon, M. A. *The Manipulation of Air-Sensitive Compounds*; 2nd Edition; Wiley: New York, 1986.
- [28]. Wang, K.; Bates, R. W. *Synthesis* **2017**, *49*, 2749-2752.
- [29]. Charette, A. B.; Juteau, H.; Lebel, H.; Molinaro, C. *J. Am. Chem. Soc.* **1998**, *120*, 11943-11952.
- [30]. Nicolaou, K. C.; Rhoades, D.; Lamani, M.; Pattanayak, M. R.; Kumar, S. M. *J. Am. Chem. Soc.* **2016**, *138*, 7532-7535.
- [31]. Joliton, A.; Plancher, J. M.; Carreira, E. M. *Angew. Chem., Int. Ed.* **2016**, *55*, 2113-2117.

[32]. Ohtsuka, N.; Okuno, M.; Hoshino, Y.; Honda, K. *Org. Bio. Chem.* **2016**, *14*, 9046-9054.

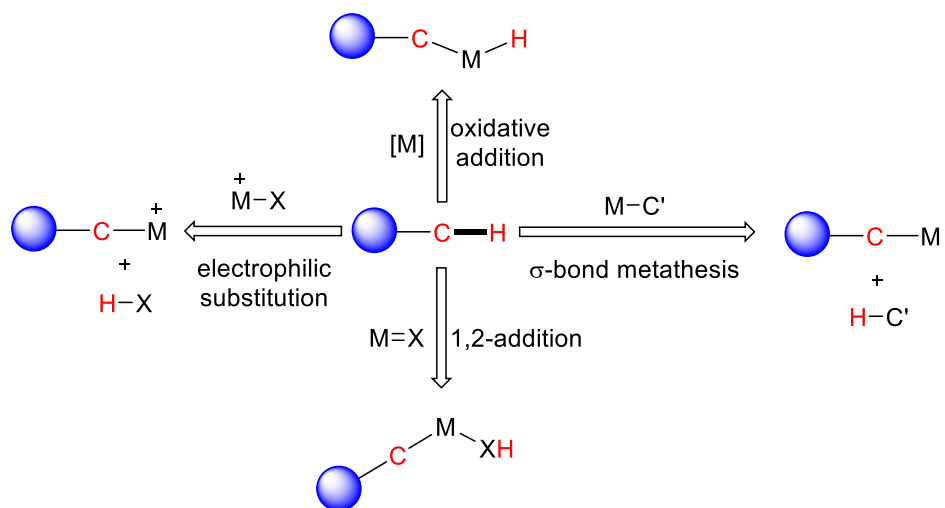
[33]. Kumpulainen, E. T. T.; Pohjakallio, A. *Adv. Synth. Catal.* **2014**, *356*, 1555-1561.

Chapter 3 – Unactivated Cyclopropanes to Spirocyclic Amine- Boranes with an *N*-Spiroatom

3.1 Introduction

In pursuit of ideal chemical synthesis, organic chemists have been driven by several core principles such as maximizing atom efficiency, incorporating regio-, diastereo- and enantiocontrol, minimizing the number of synthetic steps and limiting the formation of side products.¹²⁷ Owing to the pervasiveness of C–H and C–C bonds in organic molecules, an extremely challenging yet incredibly attractive way to achieve molecular diversity and complexity is by the activation of the highly inert C–H and C–C bonds.¹²⁸⁻¹³¹ Over the years, metal-mediated activation of C–H and C–C bonds has been explored extensively (**Figure 3.1**).¹³¹

Transition metal C–H bond activation pathways



Transition metal C–C bond activation pathways

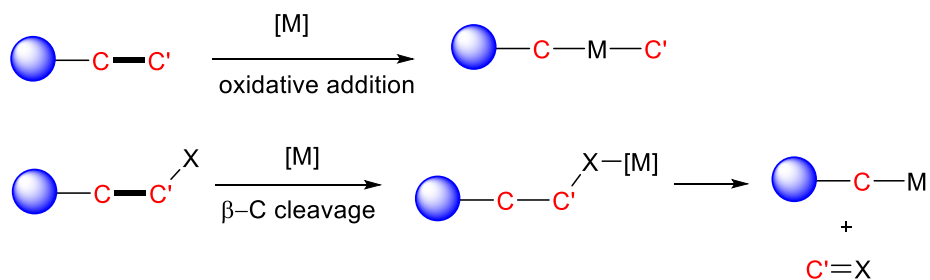


Figure 3.1 Metal-mediated C–H and C–C bond activation

While C–H activation has made significant progress in the last decade, C–C bond activation is underexplored due to C–C bonds being sterically less accessible and having unfavourable orbital

directionality to be able to interact with transition metal complexes as compared to C–H bonds.¹³² One of the most coveted transformations of a C–C bond is the conversion of a C–C bond to a C–B bond as the C–B bond can readily undergo a wide range of synthetic transformations (**Figure 3.2**).^{12, 133-139} Hence, the borylation of C–C bonds is a powerful technique to access an incredibly diverse library of compounds without preinstallation of unnecessary functional groups; however, the conversion of inert C–C bonds to C–B bonds is challenging due to their high thermodynamic stability. Due to the polar nature of C–B bonds relative to the non-polar C–C bonds and the Lewis acidic nature of boron, C–B bonds can be easily functionalized (**Figure 3.2**). The stereocontrolled conversion of C–B bonds to C–X (X = C, N, and O) bonds is highly valued in medicinal chemistry, agrochemistry, and natural products chemistry as well as materials science.¹³⁴

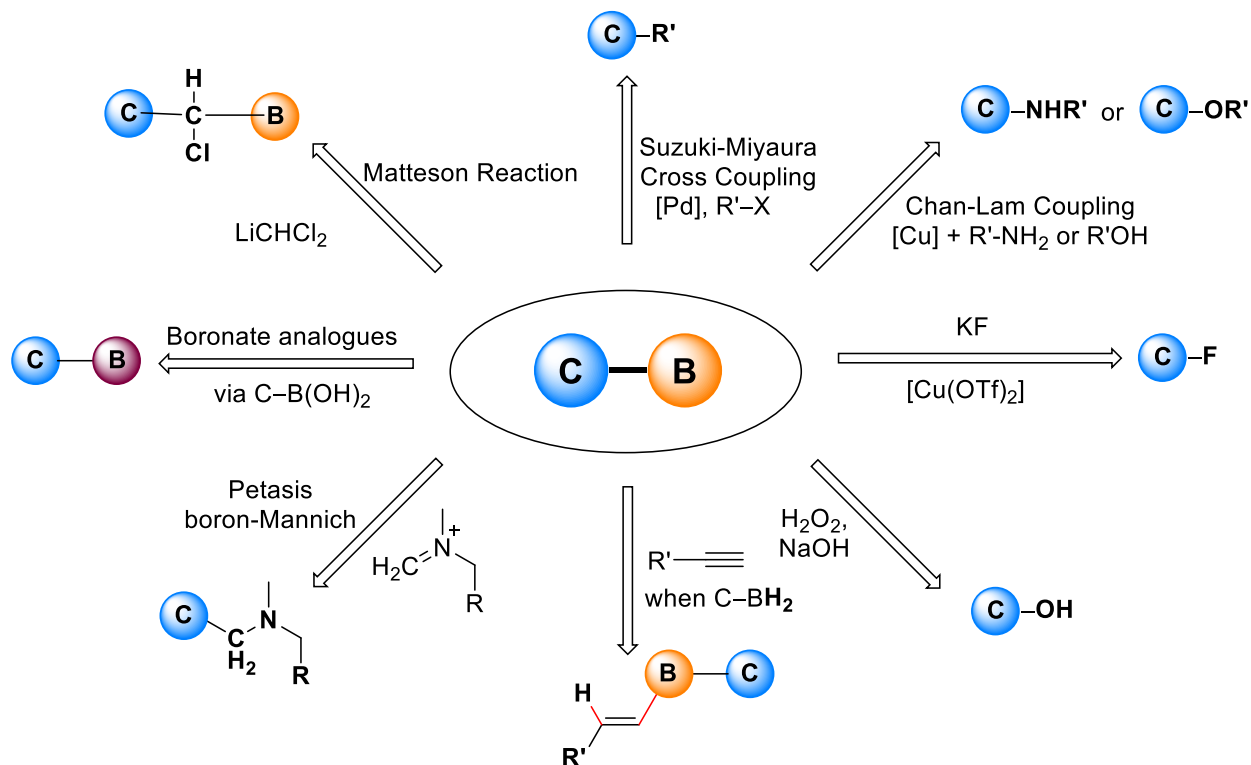


Figure 3.2 Transformations of organoboron compounds

To activate a C–C bond, transition metals rely on the release of ring-strain of three or four membered cycloalkanes to compensate for the unfavorable energetics of C–C bond cleavage.¹⁴⁰ Transition metals activate C–C bonds via oxidative addition or chelation to a directing group to activate the bond by enforcing a “proximity effect”.¹⁴⁰ Transition metals can undergo oxidative

addition with C–C bonds of strained cycloalkanes to generate more stable ring expanded metallacycles.¹⁴¹ In the absence of ring strain, C–C bond cleavage can still be achieved if the product is lower in energy such as in systems where C–C bond cleavage can lead to aromatization.¹⁴² C–C bond cleavage of unstrained systems has proven to be challenging and often relies on the use of transition metals and directing groups.

3.2 Ring-Opening of Cyclopropanes

Cyclopropanes are useful building blocks due to their inherent torsional and angle strain and therefore a plethora of research has been dedicated to functionalizing its C–C bonds.^{143, 144} Cyclopropanes possess bond angles of 60° between the sp^3 hybridized carbon atoms as opposed to the typical bond angles of 109.5° observed for sp^3 carbons. The angular strain within the ring in addition to the torsional strain resulting from the coplanar arrangement of the carbon atoms forces the C–H bonds into an eclipsed conformation.¹⁴⁵ The cyclopropane C–C bond is often compared to alkenes and owing to their π -character can act like alkenes in certain cases. The π -character of the cyclopropane C–C bonds consequently enhances the 's' character of its C–H bonds making them shorter and stronger (106 kcal/mol) than those found in ethane (101 kcal/mol).¹⁴⁶ The C–C bonds of cyclopropanes are significantly weaker (65 kcal/mol) than typical alkane C–C bonds (80–85 kcal/mol). Such characteristics make cyclopropane rings facile targets for C–C bond cleavage relative to other cycloalkanes (**Figure 3.3**).¹⁴⁷ In fact, the C–C bond cleavage of cyclopropanes has become a powerful approach to reveal sp^3 centers in acyclic systems and has been extensively illustrated in the total synthesis of many natural products as well.⁶⁹


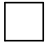
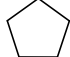
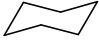
				
Cycloalkane	cyclopropane	cyclobutane	cyclopentane	cyclohexane
Ring-strain	28 kcal/mol	27 kcal/mol	7 kcal/mol	-
Bond angle	60°	90°	108°	109.5°
Type of strain	<i>angle strain torsional strain</i>	<i>angle strain torsional strain</i>	<i>mostly torsional strain</i>	-

Figure 3.3 Ring-strain in cycloalkanes

The ring-opening reactivity of cyclopropanes was first explored by Bone and Perkin in 1885 in which they reported the C–C bond cleavage of cyclopropane with ethyl malonate.¹⁴⁸ Cyclopropanes can be classified into activated and unactivated analogues based on their substituents. Activated cyclopropanes can be substituted with an electron acceptor group, electron donor group or both (DA cyclopropanes), whereas unactivated cyclopropanes do not have substituents that bias their electronic structure (**Figure 3.4**).

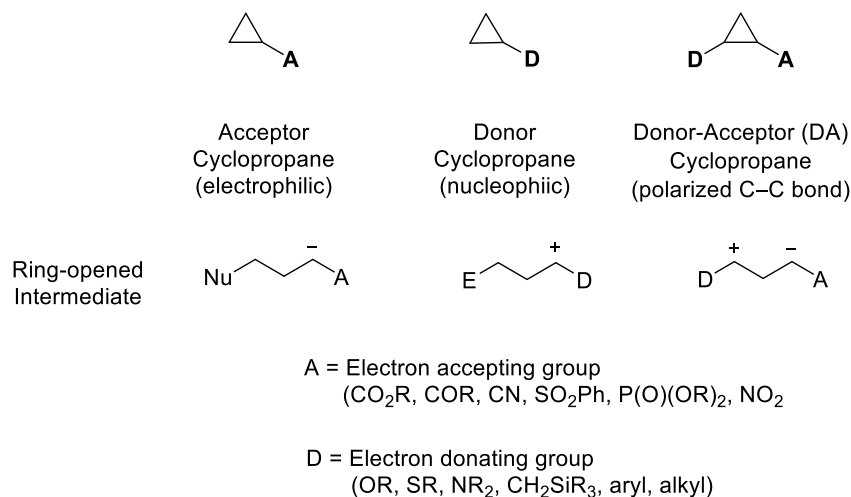


Figure 3.4 Activated cyclopropanes: acceptor, donor, and donor-acceptor cyclopropanes

A cyclopropane substituted with an acceptor group will be more electrophilic, whereas one with a donor group will have enhanced nucleophilicity. In the case of acceptor substituted cyclopropanes, the nucleophile can attack the cyclopropane leading to the formation of an anion that is stabilized by the acceptor group. A cyclopropane with a donor group can react with an electrophile and will form a carbocation that is stabilized by the donor group. Among activated and unactivated cyclopropane rings, direct oxidative addition into the σ -bond is the most classic approach to ring-open the cyclopropane.⁶⁹ Activated cyclopropanes can undergo Lewis acid-mediated ring-opening, β -carbon elimination, nucleophilic substitution, electrophilic activation, and rearrangement reactions (**Figure 3.5**).

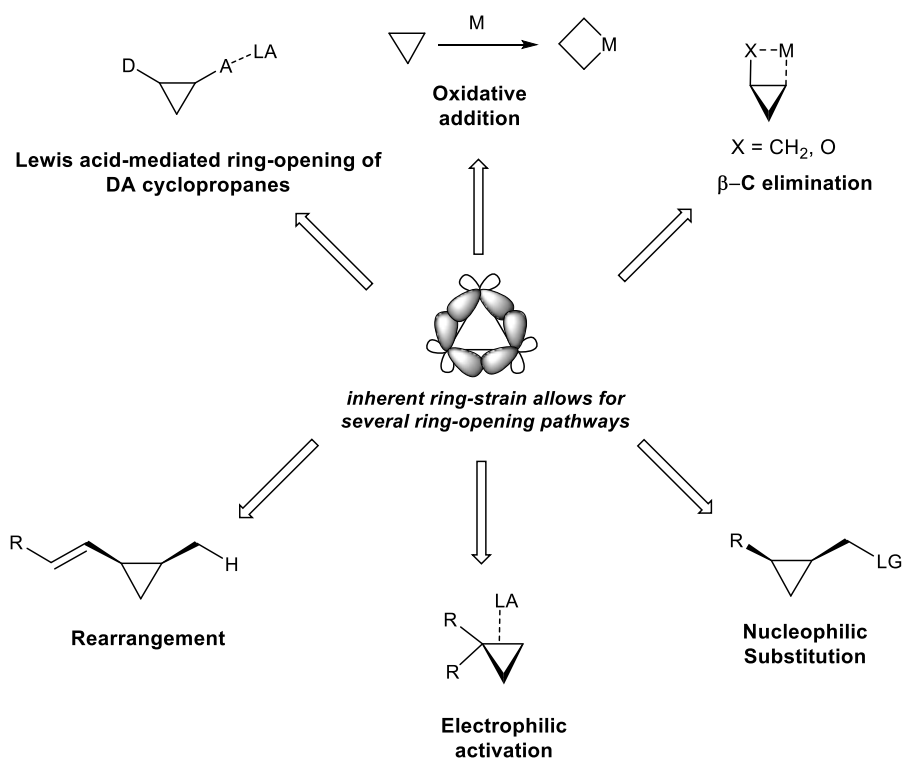


Figure 3.5 Methods to ring-open various substituted cyclopropanes

3.2.1 C–C Bond Activation of Unactivated Cyclopropanes

While the activation of C–C bonds has been widely reported for DA cyclopropanes, the ring-opening of the far more naturally ubiquitous unactivated cyclopropanes with regio- and stereocontrol has proved to be a lot more challenging.¹⁴⁹ Usually, a cyclopropane is substituted with DA groups across one of its C–C bonds to generate an electronic bias that enables C–C bond activation; however, an unactivated cyclopropane lacks any such electronic bias in its structure and is therefore more challenging to functionalize especially with regiocontrol. Unactivated cyclopropanes are substituted with alkyl or aryl groups and do not have a preinstalled functional group that can chelate to a transition metal or a Lewis acid to direct it to one of its C–C bonds and facilitate the ring opening process. Ring-opening methodologies to cleave unactivated cyclopropanes are very attractive as they avoid encumbrance of the ring-opened product with unnecessary reactive functionalities used to mediate the ring-opening process such as DA groups.

The ring-opening of unactivated cyclopropanes can be classified into metal and metal-free approaches. Current strategies to ring-open unactivated cyclopropanes using transition metals include platinum catalyzed hydrogenolysis,¹⁵⁰ mercury-mediated ring-opening,^{151, 152} and copper-catalyzed ring-opening of arylcyclopropanes to obtain aminotrifluoromethylated analogues (**Figure 3.6**).¹⁵³

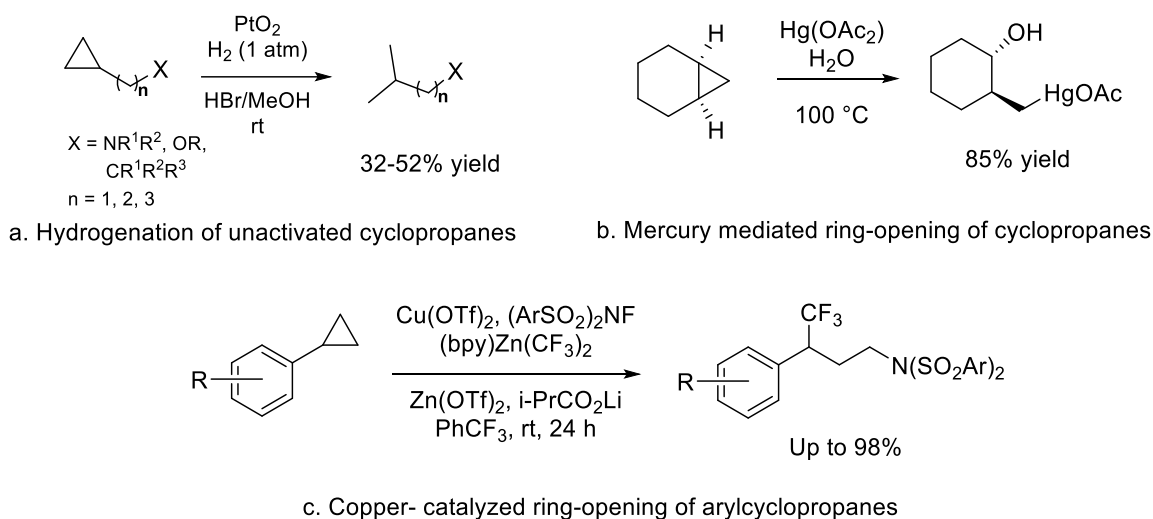


Figure 3.6 Ring-opening of unactivated cyclopropanes with metals

Some metal-free methods to cleave cyclopropane C–C bonds include bromination of unactivated cyclopropanes,¹⁵⁴ Lewis base-promoted ring-opening using hypervalent iodine reagents,¹⁵⁵ intermolecular electrophilic bromoesterification,¹⁵⁶ 1,3-bifunctionalization via electrolysis,¹⁵⁷ HFIP mediated hydroarylation,¹⁵⁸ 1,3-hydrosilylation using weakly coordinating anions,¹⁵⁹ and C–C bond activation by a Lewis acid (**Figure 3.7**).¹⁶⁰

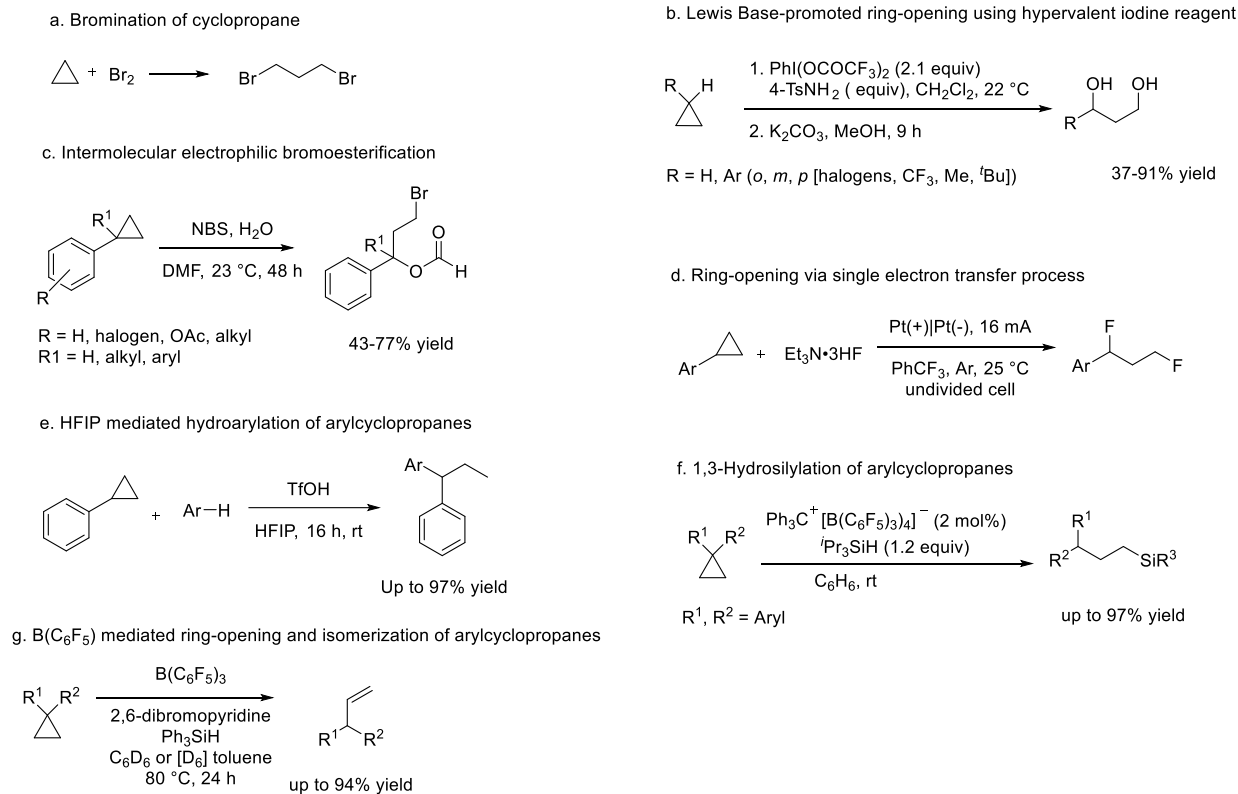


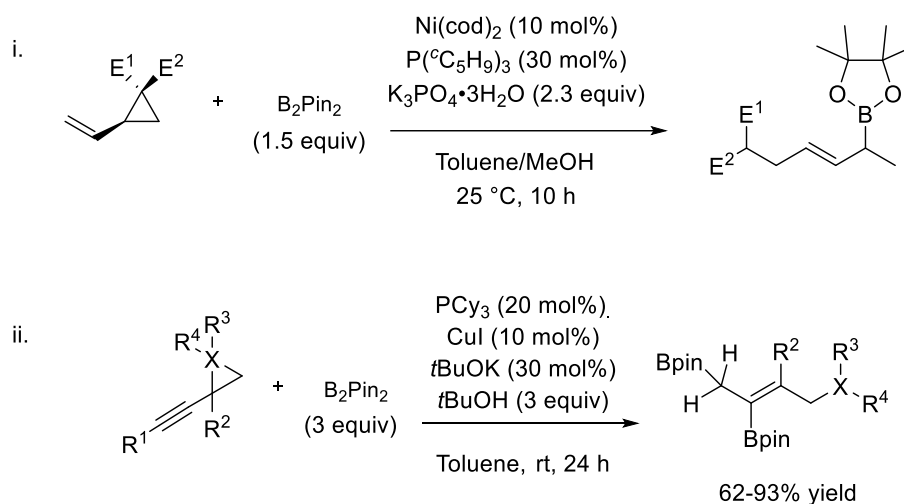
Figure 3.7 Metal-free ring-opening of unactivated cyclopropanes

3.2.2 Borylative Ring-Opening of Cyclopropanes

Enantioselective and diastereoselective syntheses of cyclopropanes have been extensively explored over the past few decades allowing access to variety of polysubstituted cyclopropanes.^{161, 162} The ring-opening of polysubstituted cyclopropanes allows for direct access to acyclic systems enriched with stereocenters.⁶⁹ While cyclopropanes can be ring-opened with various nucleophiles and electrophiles, the electrophilic borylative ring-opening of cyclopropanes provides access to cyclic and acyclic building blocks that can be used in late-stage functionalization via C–B bond transformations.

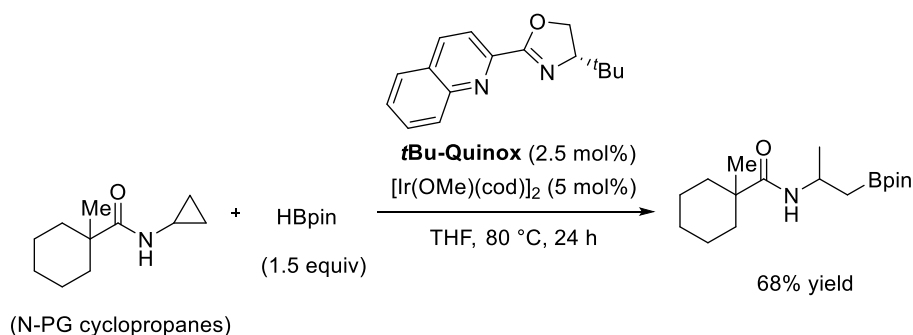
3.2.2.1 Borylative Ring-Opening Using Transition-Metals

Catalytic borylative ring-opening has been achieved for activated cyclopropanes such as vinyl and propargyl cyclopropanes. Examples of borylative ring-opening of activated cyclopropanes include the nickel-catalyzed ring-opening of vinylcyclopropanes in the presence of bis(pinacolato)diboron (B_2Pin_2) to provide allylic boronates (**Scheme 3.1**, i).¹⁶³ In addition to vinyl cyclopropanes, propargyl cyclopropanes have also been shown to undergo a copper-catalyzed borylative ring-opening in the presence of B_2Pin_2 (**Scheme 3.1**, ii).¹⁶⁴



Scheme 3. 1 Metal-catalyzed borylative ring-opening of i. vinyl and ii. propargyl cyclopropanes

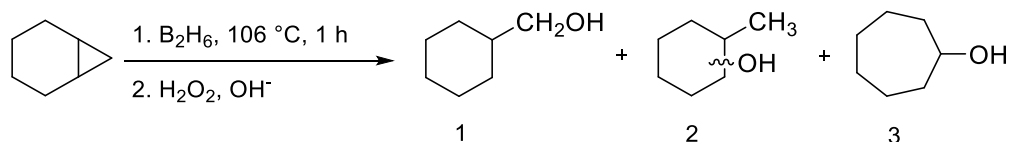
Yamaguchi and co-workers have reported an iridium catalyzed hydroboration of electron rich cyclopropanes substituted with acylamines that used pinacolborane as the borylating source instead of B_2Pin_2 (**Scheme 3.2**).¹⁶⁵



Scheme 3. 2 Iridium-catalyzed hydroboration of activated cyclopropanes

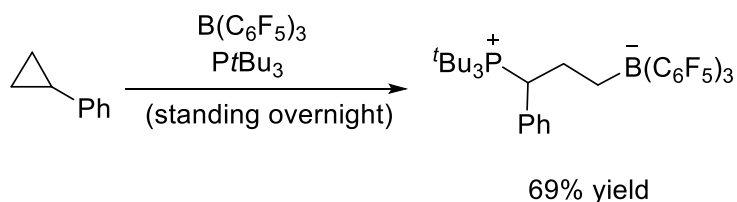
3.2.2.2 Transition Metal-Free Borylative Ring-Opening of Unactivated Cyclopropanes

The π -character of the C–C bonds in cyclopropanes allows them to mimic the reactivity of alkenes for certain types of reactions. Hydroboration of alkenes is the most common reaction to introduce C–B bonds to form organoboron reagents. The hydroboration of the relatively weak σ -bonds of cyclopropanes was explored as early as 1957 by Graham and Stones.¹⁶⁶ They were the first to report the ring-opening of cyclopropane in the presence of diborane in the vapor phase to provide tri-*n*-propylborane.¹⁶⁶ Brown's hydroboration was used as a mean to cleave the cyclopropane C–C bond of bicyclo[4.1.0]heptane, but the reaction proved to be very “sluggish” in terms of yield and regioselectivity (**Scheme 3.3**).^{133, 166, 167} While the direct hydroboration of bicyclo[4.1.0]heptane with diborane was challenging,¹⁶⁶ it attracted significant attention to the reactivity of unactivated cyclopropanes towards borylative ring-opening and hydroboration chemistry, which led to the careful design of systems for the regioselective borylative ring-opening of unactivated cyclopropanes.



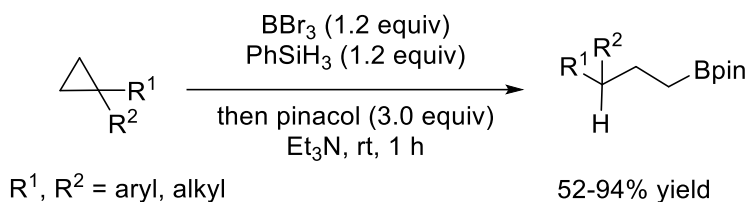
Scheme 3. 3 Brown hydroboration of an unactivated cyclopropane

Stephan and co-workers applied their work in the field of frustrated Lewis pair (FLP) systems towards the borylative ring-opening of unactivated cyclopropanes.¹⁶⁸ In 2010, Stephan and co-workers developed an FLP system consisting of a $B(C_6F_5)_3$ and $PtBu_3$ which was capable of cleaving the C–C bond of unactivated cyclopropanes in a regioselective manner.¹⁶⁸ The FLP system allows for the heterolytic cleavage of an unactivated cyclopropane resulting in the formation of the ring-opening zwitterionic product (**Scheme 3.4**).



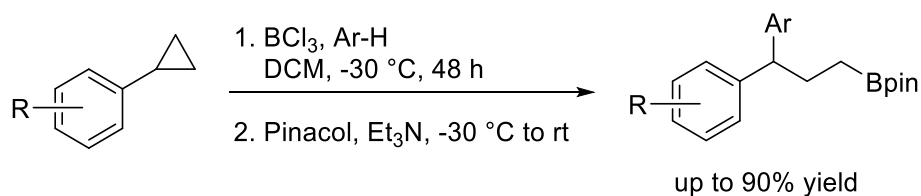
Scheme 3. 4 Borylative ring-opening of unactivated cyclopropanes using an FLP system

While Stephan had not expanded on the scope of the ring-opening of unactivated cyclopropanes, Shi and co-workers made a significant advance in the field of metal-free borylative ring-opening of unactivated cyclopropanes. They were able to achieve a 1,3-hydroboration of unactivated cyclopropanes using stoichiometric amounts of BBr_3 coupled with PhSiH_3 and an excess of pinacol to form acyclic organoboron compounds (**Scheme 3.5**).⁷⁵



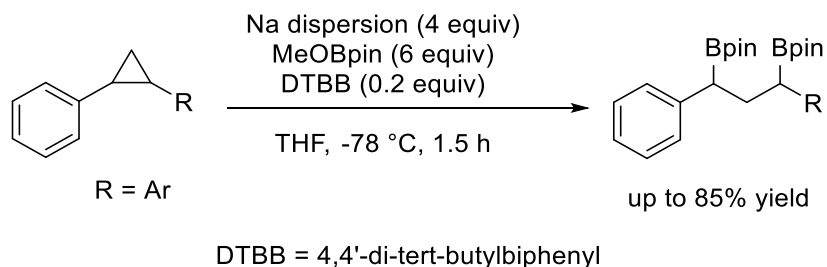
Scheme 3. 5 Hydroboration of unactivated cyclopropanes

Following Shi's work, in 2020 Murai and co-workers developed a system for the 1,3-arylborylation of unactivated cyclopropanes using BCl_3 and arene nucleophiles (**Scheme 3.6**).¹⁶⁹ Their method for the borylative ring-opening of unactivated cyclopropanes allowed for the introduction of a second functional group in the form of an arene as opposed to only a hydrogen atom as was the case in the hydroboration reported by Shi and co-workers. The driving force of these reactions appeared to be the formation of very stable cations (tertiary or benzylic that are trapped by an arene or silane nucleophile in a Friedel-Crafts or reduction reaction).



Scheme 3. 6 1,3-Difunctionalization of unactivated cyclopropanes

An example of the 1,3-diborylative ring-opening of unactivated cyclopropanes was reported by Yorimitsu and co-workers.¹⁷⁰ A sodium dispersion mediated the ring-opening of various arene substituted cyclopropanes in a *syn*-selective manner (**Scheme 3.7**).



Scheme 3. 7 Borylative ring-opening of unactivated cyclopropane using sodium metal

3.3 Cyclopropanes to Spirocycles

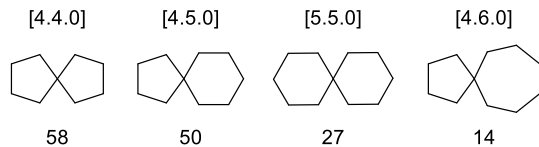
Spirocycles are challenging to synthesize due to the presence of a quaternary atom. Cyclopropanes can be transformed into acyclic or cyclic products resulting from ring-opening or ring-expansion, respectively. To the best of our knowledge, a transformation of an unactivated cyclopropane ring to a spirocycle has not been reported in literature but a methodology involving the use of readily available cyclopropane building blocks to make spirocycles could be very useful to the scientific community.

3.3.1 Spirocycles in Drug Design

Spirocycles are abundant in natural products and have found increasing relevance in medicinal chemistry and drug design (**Figure 3.8**).¹⁷¹ The success rate of a new drug molecule getting approved by the FDA has stayed constant for the past 50 years despite significant advancements in drug probing techniques via computer-aided drug design (CADD) and high-throughput screening (HTS).⁵⁹ The rigid application of Lipinski's 'rule of five' and tractability of planar molecules towards high-throughput parallel synthesis (HTPS) has steered chemists towards the development of mostly planar, achiral, and aromatic candidates in drug discovery, which has contributed to the lowering of R&D efficiency in drug design, forcing chemists to consider factors that were previously overlooked.^{59, 172} Lovering and co-workers in their landmark paper 'escape from flatland' have demonstrated that molecules possessing higher sp^3 character and chiral atoms have a better chance of achieving clinical success as compared to their achiral and flat aromatic counterparts.⁶⁰ Spirocycles bring three-dimensionality to a molecule by virtue

of two ring systems fused at a shared tetrahedral spiroatom. The attributes of high three-

i. Occurance of top four spiro ring-systems found in natural products:⁶⁴



ii. Examples of approved drugs containing a spirocycle

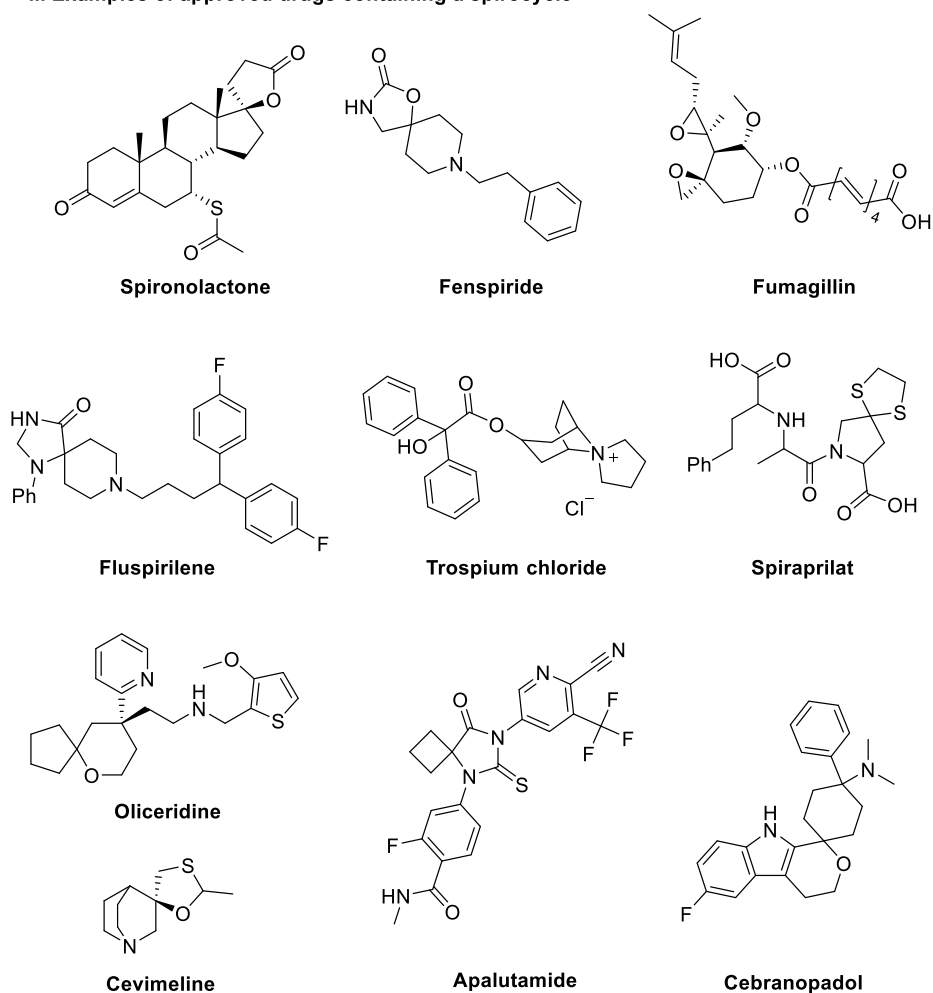


Figure 3.8 i. Most common ring systems found in FDA approved drugs ii. Spirocyclic motifs in biologically active molecules

dimensionality and conformational rigidity combined with their ability to display axial and central chirality makes spirocycles ‘privileged’ motifs in drug design.^{171, 173} The ever-growing interest in spirocycles can be gauged by the remarkable increase in the use of the key word “spiro” in

medicinal chemistry journals as well as an exponential rise as a key term in the SciFinder database over the last few decades (**Figure 3.9**).^{174, 175} Examples of a non-carbon spirocenter are scarce but having a non-carbon spirocenter has shown to enhance the potency of the drug molecule compared to its carbon spirocenter analogue.¹⁷⁶ In addition to their use as drugs,^{175, 177, 178} *N*-heterocycles

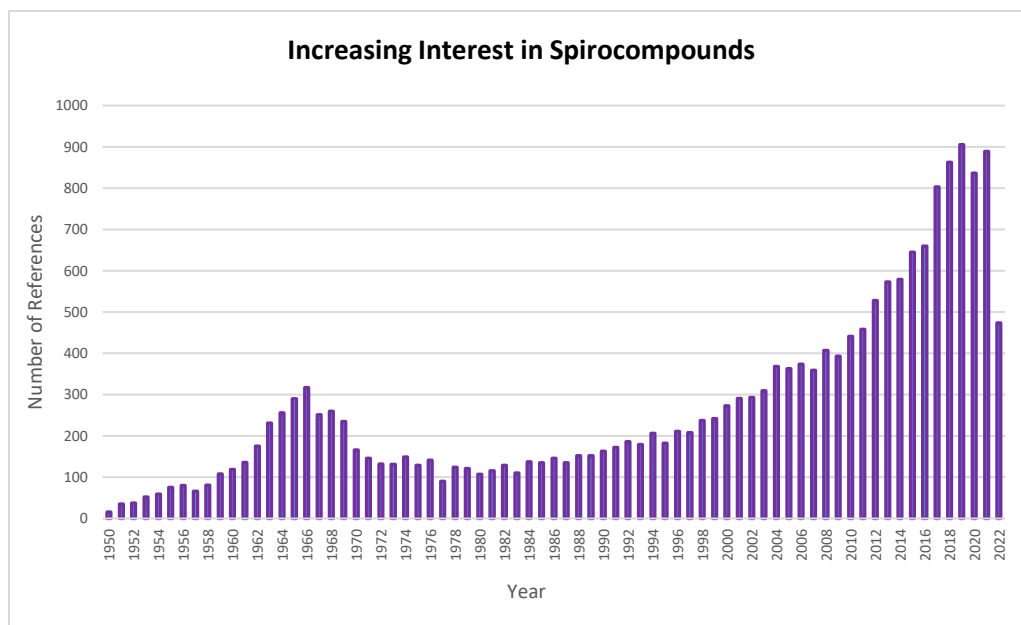


Figure 3.9 Growing interest in spirocyclic motifs

containing an *N*-spirocenter, have also been applied as phase transfer catalysts,¹⁷⁹ and as materials for anion-exchange membranes.¹⁸⁰

Strategies to construct heterospirocycles include cycloaddition,^{181, 182} metathesis,¹⁸³ and rearrangement reactions,¹⁸⁴ all of which rely on directing groups and burden the core spirocycle with potentially unnecessary functionalities.^{185, 186} These approaches adversely increase the molecular weight of the target drug molecule (**Figure 3.10**).¹⁸⁷

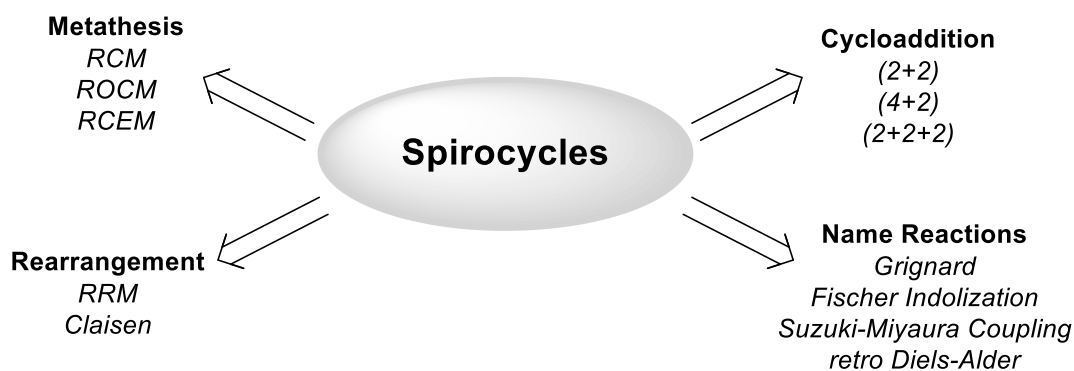


Figure 3.10 Reactions involved in the formation of spirocycles

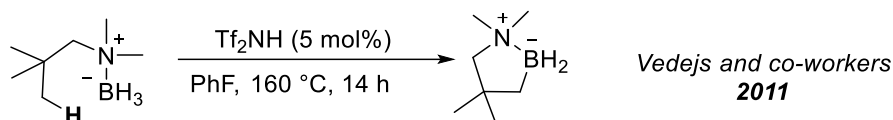
Heterospirocycles are often made by forming a carbocycle onto a heterocycle and vice-versa, both of which result in the heteroatom being adjacent to the usual carbon spiroatom. Moreover, the ability to introduce spirocycles with multiple stereocenters in a controlled manner has proven to be challenging which has prevented spirocycles from realizing their full potential in drug design since tackling chemistry with multiple stereocenters is a significant challenge in commercial drug discovery with short timelines.⁶³ Spirocycles require multistep syntheses but are pursued regardless by medicinal chemists due to expected improvements in potency, selectivity, and physicochemical properties over their parent drug molecules.¹⁷⁵ Ideally, a versatile and intramolecular approach imparting regioselectivity and stereospecificity without an increase in molecular weight to provide spirocycles would be of interest to synthetic and medicinal chemists.

3.4 Research Goals

As described above, the concept of activating highly inert and stable C–C bonds offers an important tool for organic chemists to streamline syntheses without having to prefunctionalize the substrate with reactive functional groups.¹⁸⁸ Unactivated cyclopropanes are ubiquitous in Nature; however, their utility as synthetic building blocks is limited by the lack of methods to activate their C–C bonds and transform them into molecules with a higher degree of complexity and functionality. The following sections describe the first ever reported transformation of unactivated cyclopropanes to spirocyclic motifs.

As is true for many scientific advances, our goal was different from what we achieved. Our intent was not to convert unactivated cyclopropanes to spirocyclic motifs. Instead, we wanted to C–H borylate an unactivated cyclopropane due to the growing interest in boron substituted cyclopropanes being used as highly versatile building blocks to integrate cyclopropanes into larger and more complex motifs.¹⁸⁹⁻¹⁹² Vedejs and co-workers have shown that amine-boranes, upon reacting with Tf₂NH, generate electrophilic borenium cations capable of borylating aliphatic and aromatic C–H bonds (**Figure 3.11**, a).¹⁹³⁻¹⁹⁵ Inspired by Vedejs’s work, we hypothesized that we can use amine-borane handles to borylate C–H bonds of unactivated cyclopropanes which led us to synthesize cyclopropane amine-boranes (CABs). However, to our surprise, the addition of a catalytic amount of Tf₂NH to CABs resulted in the ring-opened spirocyclic amine-borane (SCAB) products and no C–H borylation product was observed (**Figure 3.11**, b).

a. C–H borylation of alkyl amine-boranes



b. Attempt to C–H borylated unactivated cyclopropane

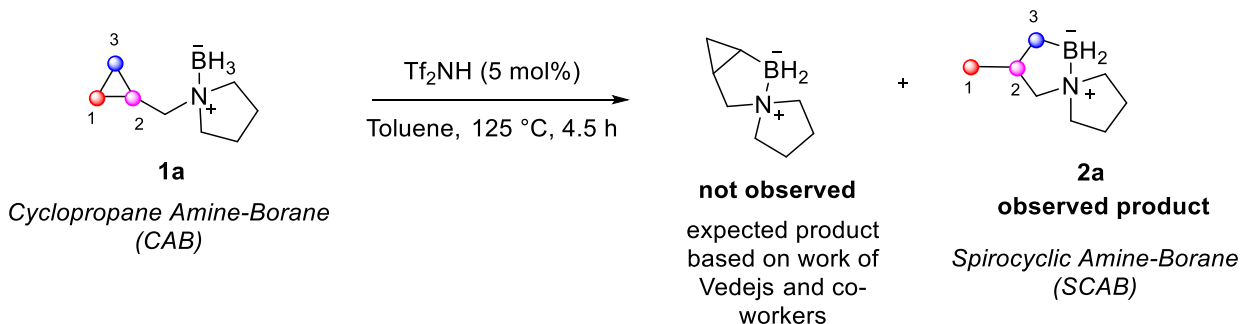


Figure 3.11 a. Inspiration for C–H borylation of cyclopropanes using borenium cations b.

Attempt to C–H borylate CAB

Our methodology uses a catalytic amount of Tf₂NH that permits unactivated CABs to undergo a cascade intramolecular ring-opening to form SCABs possessing a unique C–B–N bond with an *N*-spiroatom. The unique SCAB motifs were readily functionalized to provide structural diversity in the form of spirocyclic amine-boronic acids (SCABAc), fluorinated spirocyclic amine-

boranes (SCAB-F₂), boronate derivatives (SCABo) and analogues of the potent antifungal drug, fenpropidin, through C–B bond transformations. In the following sections, the scope of our methodology and the experimental studies done to understand the mechanism for the transformation of a CAB to a SCAB motif are described.

3.5 Results and Discussion

3.5.1 Cyclopropane Amine-Boranes (CABs) to Spirocyclic Amine-Boranes (SCABs)

To the best of our knowledge, no methodologies to access a library of SCAB analogues have been reported in the literature. Isolated examples of substrate dependent SCABs are reported by Vedejs and co-workers via C–H borylation (**Figure 3.12, a and b**)^{195, 196} while selected examples of unsaturated SCABs were obtained through alkenylcarbene insertion into B–H bonds by Zhou and co-workers (**Figure 3.12, c**).¹⁹⁷

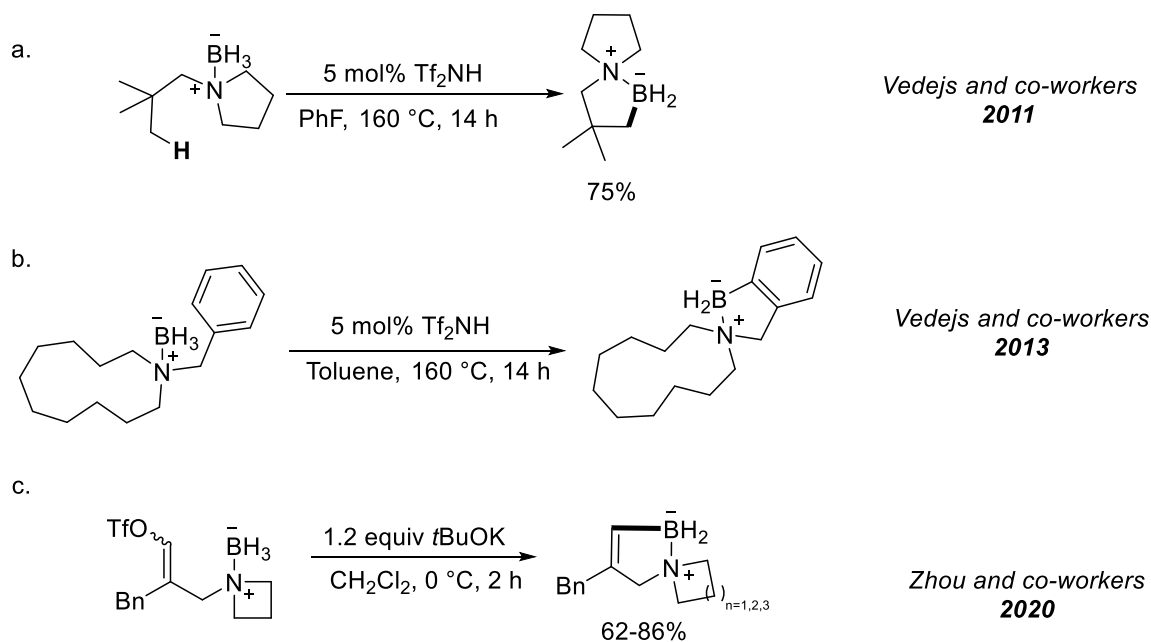


Figure 3.12 Isolated spirocyclic amine-boranes reported via C–H activation

Herein, I report a methodology for the intramolecular ring-opening of unactivated cyclopropanes with a cyclic amine-borane tether (CABs) activated by a catalytic amount of Tf_2NH to form spirocyclic amine-boranes (SCABs) possessing an *N*-spiroatom (**Figure 3.13**, a).

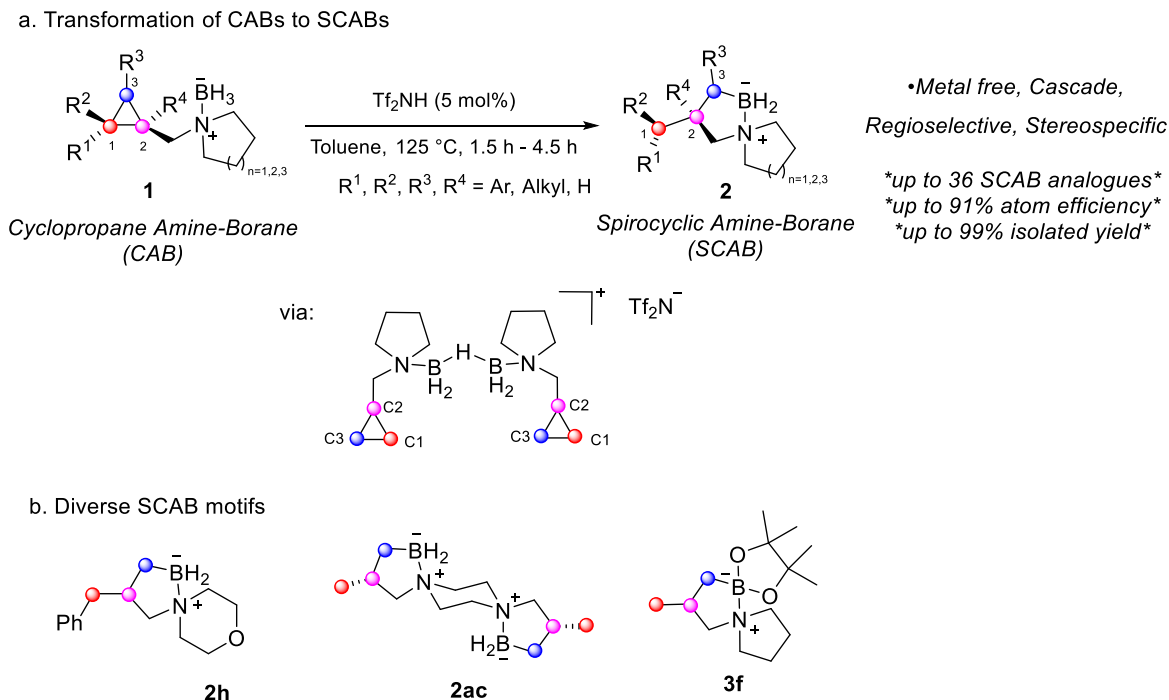


Figure 3.13 Unactivated cyclopropanes to *N*-spiroatom heterocycles

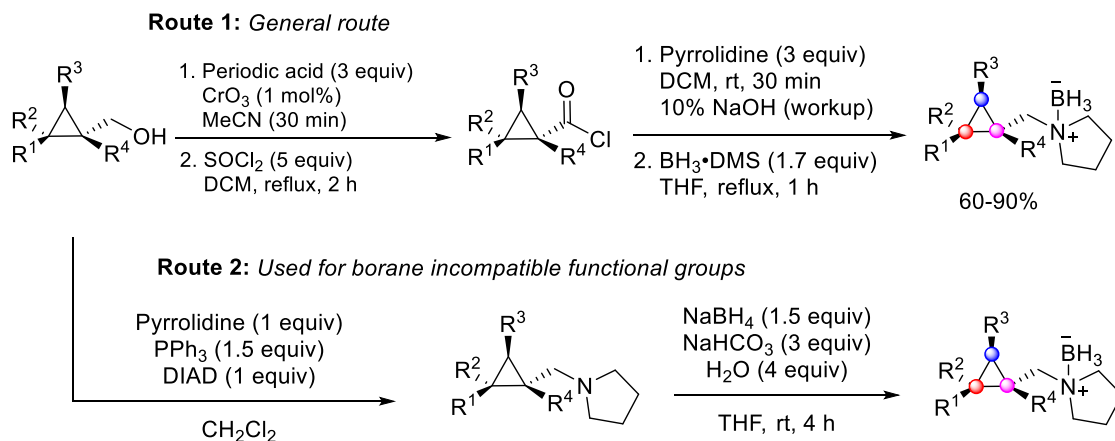
A methodology which brings intramolecularity to the borylative ring-opening of electronically unactivated cyclopropane building blocks coupled with regio- and stereocontrol can be utilized in organic synthesis for the efficient design of complex molecules. An intramolecular approach typically requires shorter reaction times due to a high effective concentration and can carry forward reactions that may not occur in an intermolecular reaction.¹⁴⁴ The B–H bond in CAB, upon reacting with Tf_2NH , evolves hydrogen gas leading to the formation of a borenium cation species capable of a regioselective C–C bond activation of the distal cyclopropane bond accompanied by a selective hydride transfer from an sp^3 carbon. The conversion of a 1,2,2-substituted CAB to its corresponding SCAB was stereospecific and resulted in a single diastereomer. An X-ray crystal structure of the product showed that the corresponding SCAB was net *anti*-hydroborated wherein the methyl and amine-borane are anti to each other. Further, the methodology demonstrates stereocontrol wherein the ring-opening of an enantioenriched 1,2,2-

substituted CAB results in a single diastereomer and provides an enantioenriched SCAB. All these findings are discussed in detail later in the chapter (Section 3.5.2). It is also important to note that when the cyclopropane was replaced by a cyclobutane and the ring-opening of a cyclobutane amine-borane was attempted with Tf_2NH (5 mol% or 1 equivalent), no ring-opened product was observed which implies that the significantly higher angle strain in cyclopropanes might play a fundamental role in the conversion of CAB to SCAB.

I was also able to apply our methodology to synthesize a SCAB containing two *N*-spiroatoms, which offers a template for synthesizing complex spirocyclic motifs containing more than one spirocenter (**Figure 3.13**, b). A unique motif containing two different spiroatoms in the form of boron and nitrogen was also obtained (**Figure 3.13**, b). The SCABs are bench stable and can be stored under ambient conditions for extended times (~10 months) without decomposition.

3.5.2 Optimization and Scope

The precursor CAB was synthesized via two routes depending on functional group tolerance via the reduction of the corresponding amide with $\text{BH}_3 \cdot \text{DMS}$ or amination of the corresponding cyclopropylmethanol (**Scheme 3.8**).

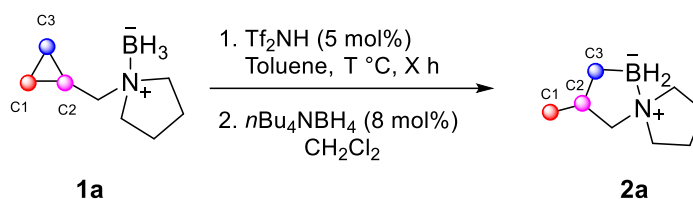


Scheme 3. 8 Synthesis of CAB precursors

CAB **1a** was added to the reaction vessel followed by the addition of Tf_2NH (5 mol%) and toluene (0.4 M) (**Table 3.1**). The reaction conditions were optimized to provide the 5-5-SCAB **2a** with complete conversion at 125 °C in 4.5 h (**Table 3.1**). A hydride quench with 8 mol% *n*- Bu_4NBH_4 was done to convert the borenium equivalent derived from the 5 mol% Tf_2NH to the amine-

borane.¹⁹⁵ The mixture was then filtered over a short pad of silica gel to retain polar bistriflimide-containing byproducts.¹⁹⁵ The solvent was evaporated and the product was isolated without further purification. It is important to note that when the reaction mixture was not quenched with $n\text{Bu}_4\text{NBH}_4$, product **2a** was observed in slightly lower yields. A maximum of 25% conversion to SCAB **2a** was achieved when the reaction was run for 60 h at 80 °C. A stoichiometric amount of Tf_2NH led to the formation of the product **2a** in 1 h at 125 °C quantitatively.

Table 3.1 Optimization of Time and Temperature with Tf_2NH for CAB **1a**

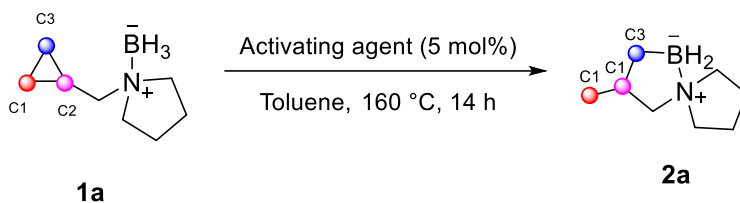


Entry	Temperature (°C)	Tf_2NH (mol%)	Time (h)	2a Yield (%)
1	160	5	14	99
2	140	5	4	99
3	125	5	4.5	99
4	125	5	3	69
5	125	5	1.5	20
6	125	100	1	99
7	100	5	16	47
8	100	5	4	15
9	80	5	60	25
10	rt	5	16	No conversion

We expected the reaction to work with any acid strong enough to protonate the B–H bond in CAB, evolving hydrogen gas, thereby forming the borenium cation species. However, we were surprised to find that the reaction does not proceed upon the addition of triflic acid (TfOH) (catalytic or stoichiometric amounts) to CAB **1a**, which also evolved hydrogen gas upon reaction

with CAB **1a**. We hypothesize that since the conjugate base $[\text{TfO}]^-$ is stronger relative to $[\text{Tf}_2\text{N}]^-$, it binds to the Lewis acidic boron much more effectively thereby quenching the reactive Lewis acidic species and preventing the formation of SCAB **2a**. An acid screening using weaker acids such as acetic acid, formic acid, and benzoic acid also resulted in no conversion to SCAB **2a** (**Table 3.2**)

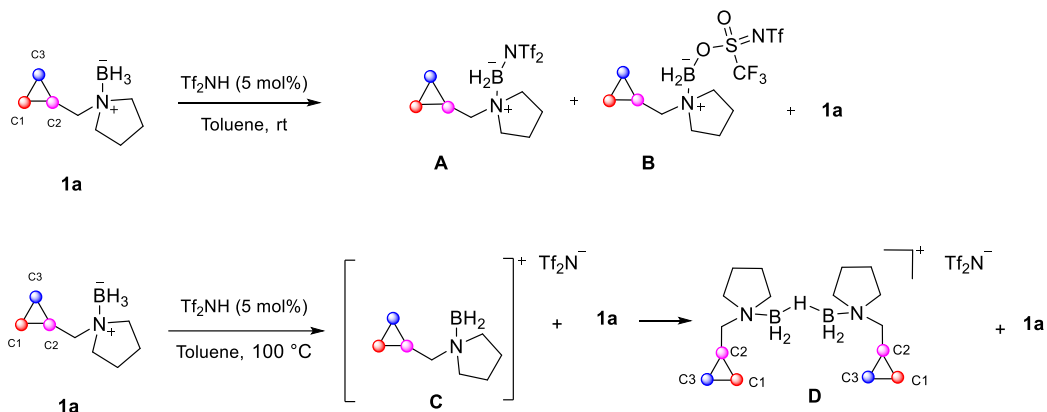
Table 3.2 Screening of Activating Reagent



Entry	Activating Reagent	pKa (MeCN)	Result
1	None	N/A	SM
2	Tf ₂ NH	0.3	2a (99% conversion)
3	4-Nitrobenzenesulfonamide	24.9	SM
4	TfOH	0.7	SM
5	Acetic Acid	23.5	SM
6	Formic acid	21.5	SM
7	Benzoic acid	20.5	SM

The distinctive reactivity of Tf₂NH can be attributed to the weakly-coordinating nature of the conjugate base, $[\text{Tf}_2\text{N}]^-$. The unique transoid orientation of $[\text{Tf}_2\text{N}]^-$ allows the negative charge to be delocalized in an efficient manner thereby making it a poor nucleophile.¹⁹⁸ Upon reaction of Tf₂NH with CAB, hydrogen gas is evolved and a $[\text{Tf}_2\text{N}]^-$ anion is generated. The poor nucleophilicity of $[\text{Tf}_2\text{N}]^-$ prevents it from binding to the Lewis acidic boron in an effective manner and upon heating the reaction mixture to temperatures >100 °C, completely dissociates from boron,¹⁶⁸ generating a highly Lewis acidic boron species capable of activating the C–C bond of CABs. At room temperature, the Lewis acidic boron, post evolution of hydrogen gas, forms

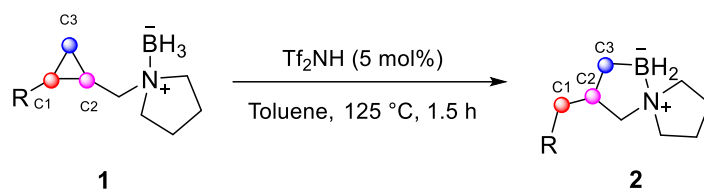
isomers **A** (B–N) and **B** (B–O) with $[\text{Tf}_2\text{N}]^-$. Upon heating, the isomers dissociate to form a B–H–B bridged dimer **D** at temperatures greater than 100 °C (**Scheme 3.9**). The formation of isomers **A**, **B** and the formation of a B–H–B bridged dimer **D** is supported by NMR spectroscopy and is discussed in detail along with other mechanistic studies in section 3.5.5.



Scheme 3. 9 Species formed at rt and 100 °C post addition of Tf_2NH (5 mol%)

The reaction time was optimized to 1.5 h for aromatic substituted CABs whereas the alkyl substituted CABs required 4.5 h to go to completion (**Table 3.3**).

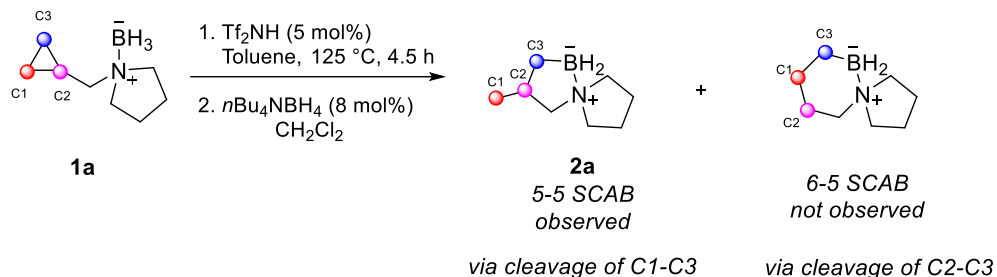
Table 3.3 Effect of Substituent



Entry	R	Yield (%)
1	Pr	15
2	H	20
3	Ph	99
4	<i>p</i> -Fluorobenzene	99

3.5.2.1 Regioselectivity in the Transformation of CAB to SCAB

Mono-substituted CAB **1a** underwent a regioselective C–C bond activation to form the 5–5 SCAB **2a** and no evidence of the 6–5–SCAB regioisomer was observed (**Scheme 3.10**).



Scheme 3.10 Regioselectivity observed in transformation of monosubstituted CAB **1a** to **2a**

To determine the regioselectivity of substituted CABs, we sought the use of CAB **1e** with a phenyl substitution on C1 to differentiate between the three cyclopropane C–C bonds. A substitution at C1 would allow differentiation of C1–C2, C1–C3 or C2–C3 bond cleavage (**Figure 3.14**). Absolute selectivity for the *anti*-Markovnikov product from the activation of the distal C1–C3 bond was observed providing **2e** and no Markovnikov product was observed (**Figure 3.14**, i). No activation of the C2–C3 carbon leading to either the *anti*-Markovnikov 6–5 ring system (**Figure 3.14**, ii) or the highly strained Markovnikov product (**Figure 3.14**, iii) was observed. There was also no experimental evidence that would allude to the cleavage of the C1–C2 bond (**Figure 3.14**, iv and v).

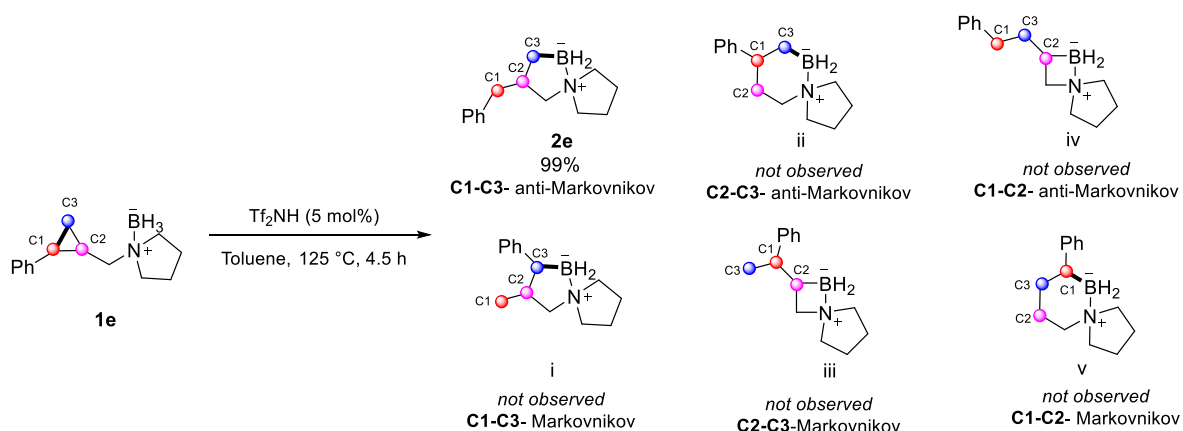


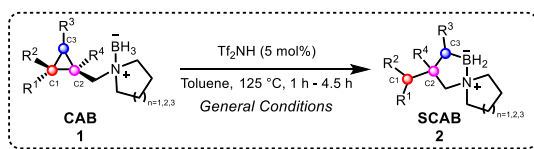
Figure 3.14 Possible regioisomers of disubstituted CAB **1e**

3.5.2.2 Scope of the Transformation of Various CABs to SCABs

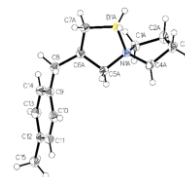
Having optimized reactions conditions, we carried forward a substrate scope. We were pleased to obtain amine-borane analogues of **2a** in the form of azapane **2b**, diethylamine **2c** and piperidine **2d** (Table 3.4). In addition to the regioselective conversion to the 5–5-SCAB **2e**, amine analogues of **1e**, **1f** (diethylamine), **1g** (piperidine) and **1h** (morpholine) also provided their corresponding C1–C3 cleaved regioselective SCAB analogues, **2f–2h**, in excellent yields (Table 3.4).

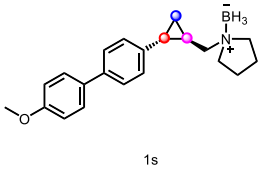
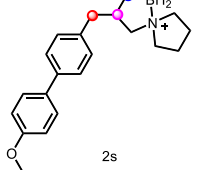
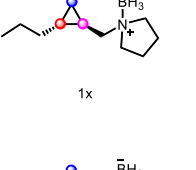
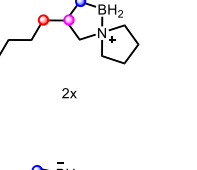
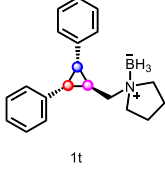
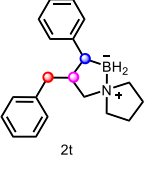
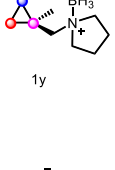
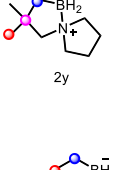
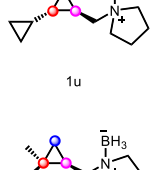
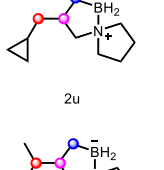
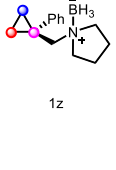
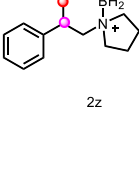
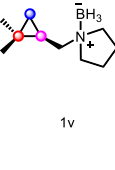
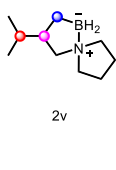
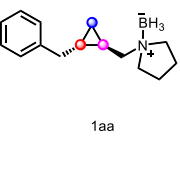
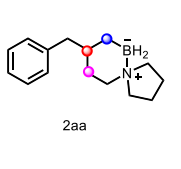
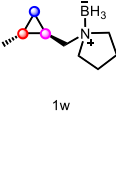
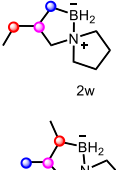
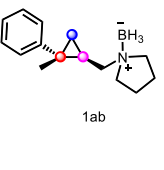
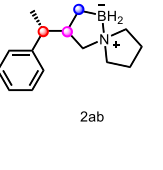
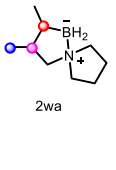
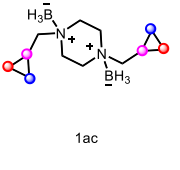
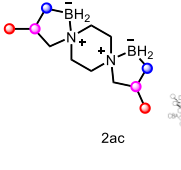
Increasing the steric bulk by introducing a naphthalene group at C1 did not affect the regioselectivity and provided **2i** in 88% yield. We were also able to successfully synthesize various aromatic substituted halide derivatives of SCAB (**2j–2m**) in >97% yield. *Tert*-butyl, mesityl and *o*-, *m*-, and *p*-methyl substituted aromatic SCABs (**2n–2r**) were also obtained in excellent yields. In the case of a *p*-OMe substituent, no *O*-demethylation was observed and the corresponding SCAB **2s** was obtained in quantitative yield and it represents the only instance of a borylative ring-opening of a cyclopropane bearing a methoxy group to proceed smoothly.⁷⁵ While disubstituted cyclopropanes provided absolute regioselectivity, a trisubstituted CAB was also investigated. The corresponding SCAB **2t** was obtained regioselectively in 95% yield.

Table 3.4 Scope of SCABs



Entry	Substrate	Product	Yield (%)	Entry	Substrate	Product	Yield (%)
1.			99 ^a	10.			97 ^b
2.			99 ^a	11.			97 ^b
3.			99 ^a	12.			99 ^b
4.			98 ^a	13.			97 ^b
5.			99 ^b	14.			96 ^b
6.			97 ^b	15.			96 ^b
7.			98 ^b	16.			98 ^b
8.			96 ^b	17.			99 ^b
9.			88 ^b	18.			97 ^b



Entry	Substrate	Product	Yield (%)	Entry	Substrate	Product	Yield (%)
20.			98 ^b	25.			96% ^d
21.			95 ^{b,c}	26.			92 ^f
22.			98 ^a	27.			93 ^f
23.			99 ^a	28.			95 ^b
24.			2w: 76% ^d 2wa: 24% ^d	29.			99 ^b
				30.			95 ^g

Conditions: a. Reaction time: 4.5 h. b. Reaction time: 1.5 h. c. T = 150 °C. d. Reaction time: 1 h, Tf₂NH: 50 mol% e. Reaction time: 8 h. f. Reaction time: 1 h, Tf₂NH: 1 equivalent. g. Reaction time: 2 h, Tf₂NH: 2 equivalents.

We introduced a second cyclopropyl fragment on CAB (R¹ = cyclopropyl) to deduce whether a regio- and chemoselective ring-opening of the proximate cyclopropane would occur. The ring-opening via the borenium cation tether was selective for the proximate cyclopropane and **2u** was obtained in 98% yield, ruling out an intermolecular mechanism.

We sought to explore the regioselectivity of a C1 *gem*-dimethyl CAB (where R¹ and R² = Me). The *gem*-dimethyl substituted CAB underwent ring-opening at the C2–C3 bond and we obtained a single 5–5 SCAB species **2v** in quantitative yield. We compared these results to CABs where only one alkyl group was present on C2 such as methyl substituted CAB (R¹ = Me) which provided **2w** and **2wa** (R¹ = Me) in a 3.2:1 ratio. A propyl substituted CAB (R¹ = Pr) provided SCAB **2x** in 96% yield. It is important to note that the conditions were further optimized to obtain these SCABs and 50 mol% of Tf₂NH was used with a reaction time of 1 h.

A CAB with a methyl substituent (R⁴ = Me) provided the expected 5–5 spirocyclic product **2y** in 92% yield. However, when modified to a phenyl group (R⁴ = Ph), the resulting SCAB showed a ¹¹B NMR signal as a triplet at -5.5 ppm, shifted from the regular signal of the 5–5–SCAB at ~3.7 ppm. A thorough NMR correlation analysis established the formation of a new 6–5 spirocyclic structure resulting from the cleavage of the C1–C3 bond. The 6–5–SCAB **2z** was obtained in 93% yield and a single crystal X-ray structure was obtained (**Table 3.4**). When compared to a benzyl substituted CAB (R¹ = Bn), we observed the formation of a product with a similar ¹¹B NMR shift as **2z** (triplet at -5.6 ppm). An NMR correlation study confirmed the formation of a 6–5 spirocyclic product **2aa** which was obtained in 95% yield.

When subjected to the optimized reaction conditions, an enantioenriched chiral CAB **1ab** provided the desired SCAB **2ab** in quantitative yield and provided a single diastereomer implying stereospecificity. A racemic mixture of SCAB **2ab** was synthesized in parallel and a single crystal structure was obtained confirming a net *anti*-hydroborated product. Replacing the pyrrolidine moiety with piperazine allowed two tethers of amine-borane to be attached (**1ac**) and provided a unique SCAB **2ac** with two spirocenters in 95% yield. It should be noted that 2 equivalents of Tf₂NH were used to obtain a 95% yield and a significantly lower yield (<55% conversion) was obtained when 5 mol% of Tf₂NH was used.

In addition to modifying the amine group we sought to transform the boron center to target a diverse library of SCAB analogues containing fluorine, boronic acids, and boronates. The ability of fluorine to significantly enhance metabolic stability and lipophilicity has led chemists to explore the use of fluorine in potential drug candidates via substitution of the hydrogen atom

with its bioisostere, fluorine.¹⁹⁹ Increasing the Lewis acidity of boron by conversion to a more electron withdrawing BF₂ could further enhance the strength of the B–N bond making the spirocycle less susceptible to degradation. Selected SCABs were functionalized to their fluorine derivatives by replacing the boron hydrogen atoms with fluorine to obtain SCAB-F₂ **3a–3d** in >70% yield (**Figure 3.15**, a). The structures of the products were confirmed by ¹⁹F NMR analysis and proton decoupled ¹¹B NMR analysis which showed the BF₂ signal as a triplet.

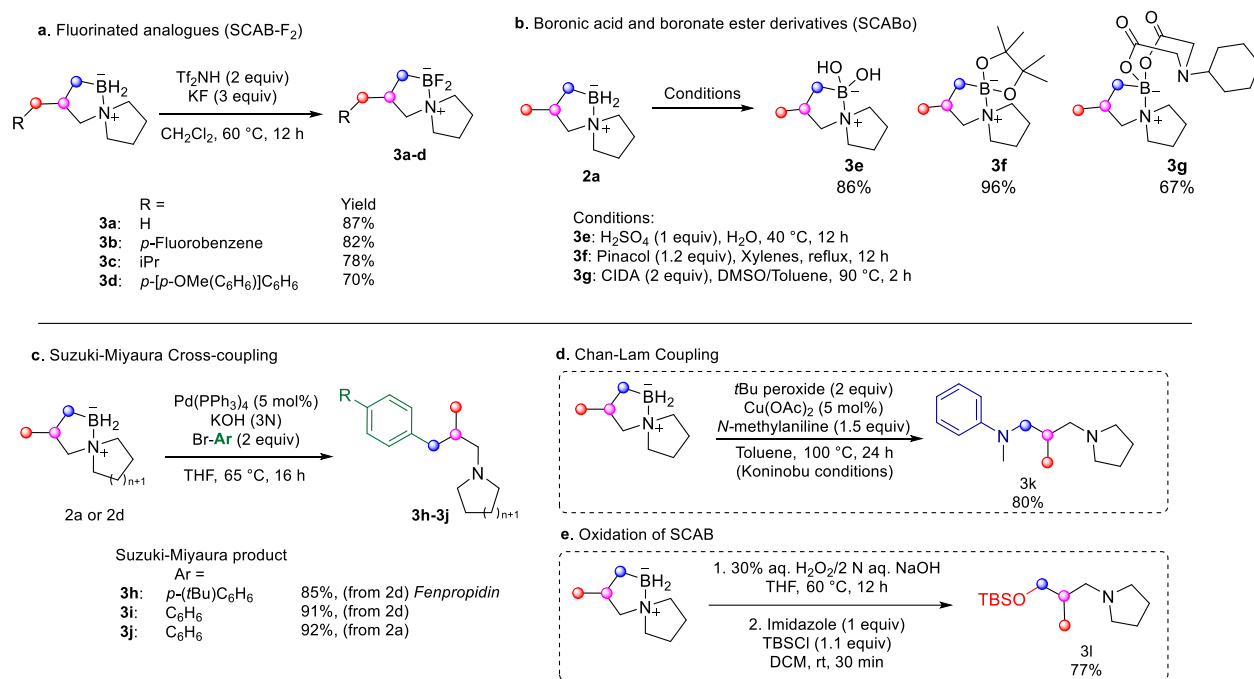


Figure 3.15 Functionalization of C–B Bond in SCAB. **a.** Fluorinated analogues **b.** Boronic acid and boronate ester derivatives **c.** Suzuki-Miyaura cross-coupling **d.** Chan-Lam coupling **e.**

Oxidation of SCAB

Aminoboronic acids are highly sought-after synthetic targets that represent isoelectronic and isostructural analogues of many biologically active compounds with the ability to interact covalently and reversibly with proteins and carbohydrates.²⁰⁰ The approval of the first boronic acid-containing drug, Bortezomib, has sparked a renewed interest in the study of boronic acids. Its success against multiple myeloma and defeating concerns over toxicity has brought boron to prominence in drug design.^{52, 201, 202} SCAB **2a** can readily convert to its corresponding boronic acid derivative (SCABAc) to provide **3e** in 86% yield (**Figure 3.15**, b). Moreover, SCABs can be converted

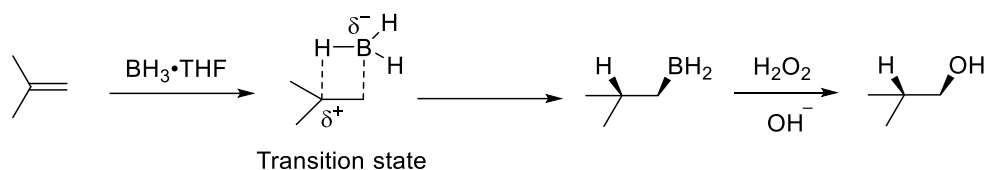
to their pinacol and *N*-cyclohexyliminodiacetic acid (CIDA) boronate derivatives **3f** and **3g** in excellent yields (**Figure 3.15**, b).¹⁹² The spirocyclic boronate **3f** represents a motif with two different spiroatoms in the form of boron and nitrogen. For SCABs **3e-3f**, the products can exist in equilibrium with the B–N bond dissociated product. Further diversification of the SCAB C–B bond to *N*-heterocyclic containing motifs can be achieved through Suzuki–Miyaura cross-coupling to provide analogues of fenpropidin (**3h-3j**), an antifungal used to treat Dutch elm disease (DED), in excellent yields (**Figure 3.15**, c).^{203, 204} Chan–Lam coupling of **2a** with *N*-methylaniline provided **3k** in 80% yield (**Figure 3.15**, d). Finally, the robust air- and moisture stable SCABs can be oxidized to their corresponding alcohol in-situ to access **3l** in 77% yield (**Figure 3.15**, e).

The ability to diversify SCAB demonstrates the well-understood versatility of a C–B bond and lays the groundwork for further transformations involving SCAB. The scope highlights the efficiency of our methodology to access a range of various substituted analogues of SCAB.

3.5.3 Mechanisms for the Hydroboration of Cyclopropanes in the Literature

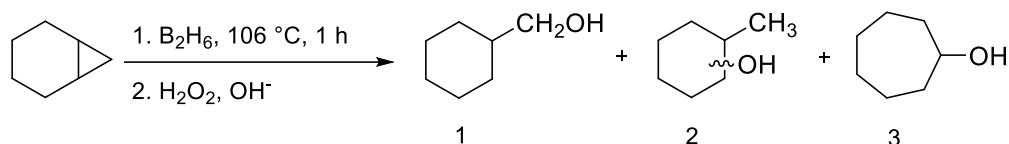
3.5.3.1 Mechanism of Brown Hydroboration

The Brown hydroboration is the most prominent hydroboration mechanism to consider when attempting to postulate a mechanism for a reaction that involves the addition of a boron and hydrogen atom across a C–C bond (**Scheme 3.11**). Since it was first reported in 1957, the Brown hydroboration-oxidation reaction has been used extensively in synthetic organic chemistry.²⁰⁵ The Brown hydroboration reaction is regioselective and a *syn*-stereospecific process. The reaction proceeds in an *anti*-Markovnikov manner where the hydrogen from the BH₃ attaches to the more substituted carbon atom and the boron attaches to the least substituted carbon atom from the same face (**Scheme 3.11**). It has been established that the mechanism occurs in concerted manner and proceeds through a four-membered transition state between the B–H and C–C bond. It is understood that the formation of the C–B bond proceeds slightly faster than the formation of the C–H bond, which results in a partial negative charge on the boron atom and a partial positive charge on the more substituted carbon atom in the transition state.



Scheme 3.11 Brown hydroboration of alkenes

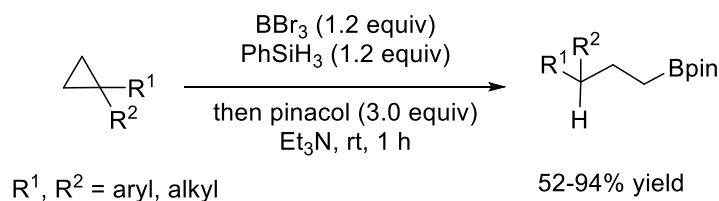
In 1971, Wood and co-workers used the analogy between olefins and cyclopropanes to propose the hydroboration of cyclopropanes using diborane. However, the hydroboration of unactivated cyclopropane, bicyclo[4.1.0]heptane, proved to be “sluggish” in terms of yield and regioselectivity (**Scheme 3.12**).¹⁶⁶



Scheme 3.12 Hydroboration of cyclopropane with diborane

3.5.3.2 Shi and Co-Workers: Mechanism for the Hydroboration of Cyclopropanes

Shi and co-workers reported an advance in the hydroboration of unactivated cyclopropanes using BBr_3 and an external hydride source in the form of PhSiH_3 (**Scheme 3.13**).²⁰⁶



Scheme 3.13 1,3-Hydroboration of unactivated cyclopropanes using BBr_3 and PhSiH_3

DFT calculations suggest that the ring-opening of the cyclopropane is promoted by Lewis acidic BBr_3 which leads to the formation of a benzylic carbocation followed by a hydride abstraction from PhSiH_3 . The transition state for the hydride abstraction was found to have an energy barrier of $9.1 \text{ kcal mol}^{-1}$ relative to the benzylic carbocation. They also found that a 1,2-H migration of the benzylic carbocation had an energy barrier of only $6.3 \text{ kcal mol}^{-1}$ and was likely

to occur. Indeed, when the ring-opening of an enantioenriched cyclopropane was attempted, they observed racemization due to a 1,2-H migration. The intermediates based on DFT calculations are presented below (**Figure 3.16**).

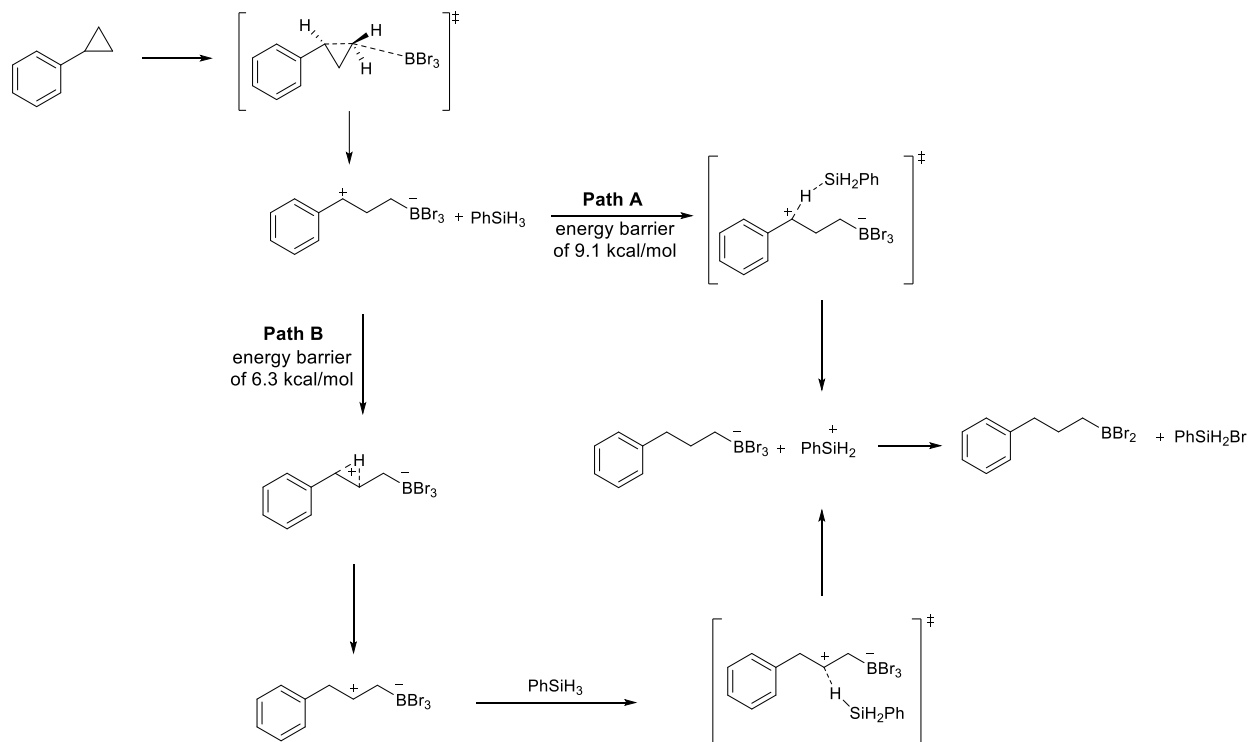
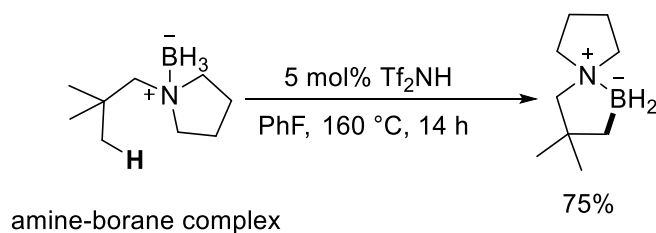


Figure 3.16 Proposed mechanism for the 1,3-hydroboration of cyclopropanes by Shi and co-workers

3.5.4 Activation of Boranes by Tf_2NH

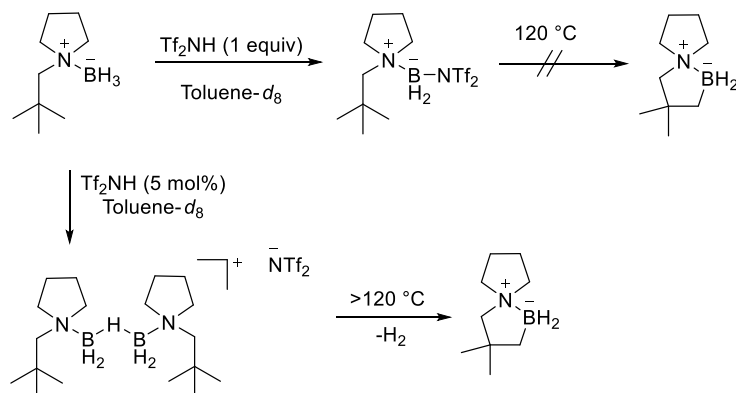
3.5.4.1 NMR Study of Activated Species Between Amine-borane and Tf_2NH

In 2011, Vedejs and co-workers reported a metal-free aliphatic and aromatic C–H borylation using an amine-borane tether activated by a catalytic amount of Tf_2NH . Their report is one of the first instances of an sp^3 C–H bond interacting with a borenium cation to form C–B bonds (**Scheme 3.14**).¹⁹⁵



Scheme 3. 14 C–H borylation via borenium cations

The authors conducted multiple NMR experiments from which they were able to deduce that the reactive species was in the form of a B–H–B bridged dimer that was characterized as a broad signal in the ^{11}B NMR spectrum (~ 1.1 ppm) (**Scheme 3.15**). NMR experiments to study the mechanism were conducted where a stoichiometric amount of Tf_2NH was added to the amine-borane complex. The addition of Tf_2NH (1 equivalent) to their amine-borane complex resulted in the evolution of hydrogen gas and formation of B–N and B–O isomers of the trivalent Lewis acidic boron with $[\text{Tf}_2\text{N}]^-$; however, there was no evidence for the formation of a B–H–B bridged dimer (**Scheme 3.15**). The B–O isomer was observed as an unresolved triplet at 0.6 ppm in the ^{11}B NMR spectrum and as two singlets in the ^{19}F NMR spectrum at -76.7 ppm and at -78.8 ppm. The B–N isomer was observed as an unresolved triplet at -4.6 ppm in the ^{11}B NMR spectrum and as a singlet in the ^{19}F NMR spectrum at -69.2 ppm. The authors found that if a stoichiometric amount of Tf_2NH is added then the C–H borylation does not proceed despite heating. When the reaction was studied with 5 mol% Tf_2NH they observed the formation of B–N and B–O isomers as well as the B–H–B bridged dimer and therefore concluded that the B–H–B bridged dimer was necessary for the C–H borylation reaction to proceed (**Scheme 3.15**).



Scheme 3. 15 Study of activated species by Vedejs and co-workers

The only difference between the amine-borane complexes used by Vedejs and co-workers in the C–H borylation reaction and the CAB motifs synthesized by us is the presence of a cyclopropane ring (**Figure 3.17**). Therefore, a logical approach to postulate a mechanism for the conversion of CAB to SCAB should involve the consideration of the work done by Vedejs and co-workers and is likely to proceed through a similar B–H–B bridged dimer intermediate (**Figure 3.17**).

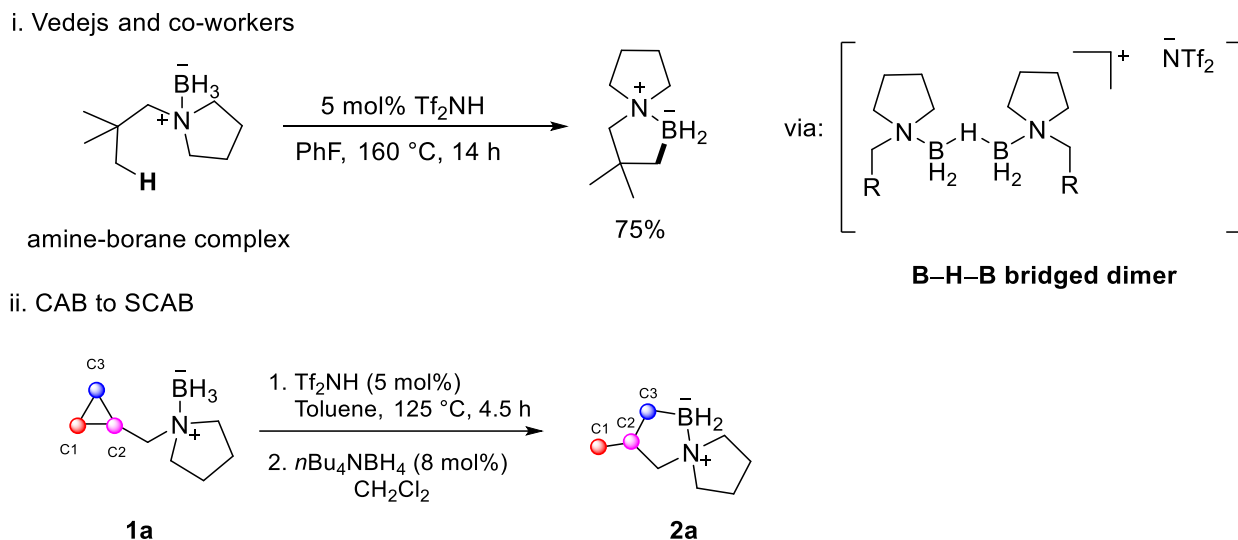


Figure 3.17 Comparison of C–H borylation and ring-opening reaction using activated amine-boranes

3.5.4.2 Hydroboration of Alkenes Using NHC-Borane as Borenium Cation Equivalents

In 2012, Vedejs and co-workers reported the hydroboration of alkenes using NHC-boranes (**Figure 3.18**).²⁰⁷ Their work was based on the hydroboration of alkenes using Lewis base (LB) complexes of borane. Lewis bases of these complexes, such as an ether or sulfide can exchange with alkenes to form a short-lived-alkene-borane complex that quickly undergoes hydroboration to provide an alkylborane.²⁰⁷ In contrast, NHC-boranes do not undergo decomplexation and are therefore inert to hydroboration reactions. Vedejs and co-workers hypothesized that NHC-borane can be used to hydroborate alkenes if instead of forcing a carbene of an NHC-borane to leave, they vacated a coordination site on boron by the removal of a hydride to generate a cationic NHC-borenium species. To do so, NHC-borane was reacted with Tf_2NH resulting in the evolution of

hydrogen gas and formation of a cationic NHC-borenum ion isoelectronic to free borane and capable of hydroborating alkenes (**Figure 3.18**).

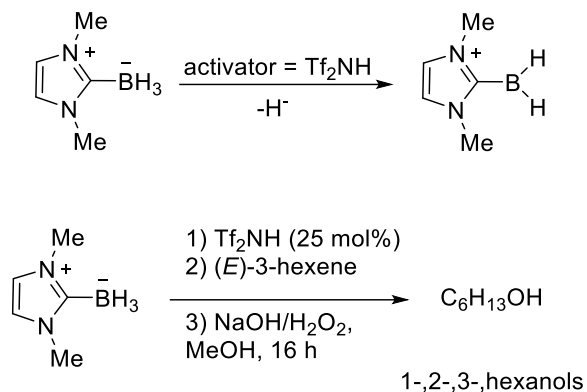
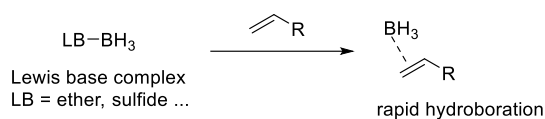


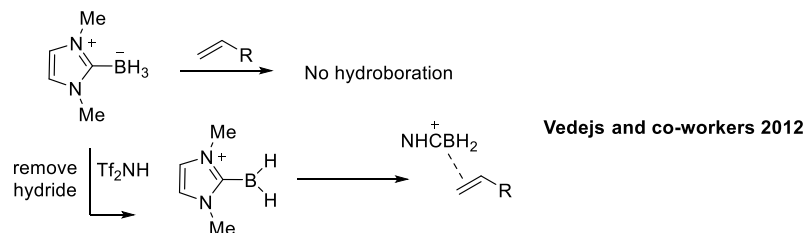
Figure 3.18 Hydroboration by NHC-borane mediated by Tf₂NH

As reported by Vedejs and co-workers we also found that without the presence of an activator such as Tf₂NH, CABs are not capable of intramolecular ring-opening via hydroboration (**Figure 3.19**).

i. Classic Lewis base-borane chemistry



ii. NHC-borane chemistry: BH₃ parallel with [NHCBH₂]⁺



iii. This work: Parallel of [NHCBH₂]⁺ hydroboration chemistry with CABs

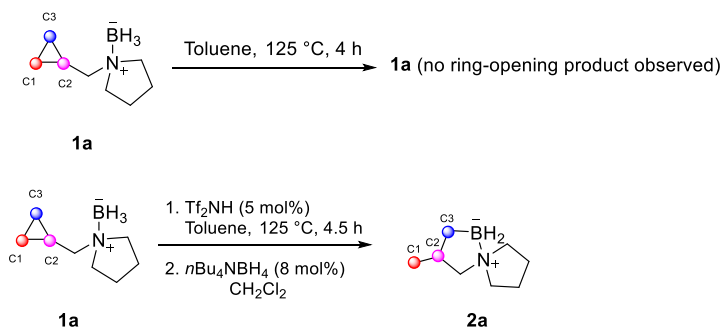
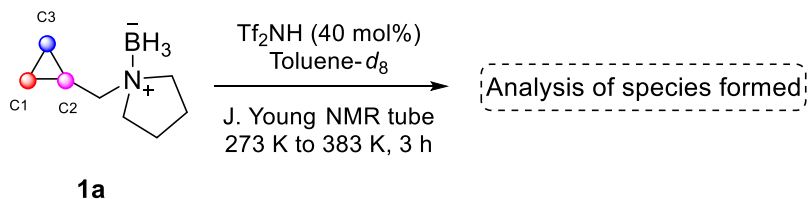


Figure 3.19 Activator-mediated hydroboration

3.5.5 Mechanistic Studies for the Conversion of CAB to SCAB

3.5.5.1 Variable Temperature NMR Experiments of CAB with Tf₂NH

To gain insight into the activated species forming in our reaction we conducted a variable temperature NMR experiment using 40% mol of Tf₂NH (**Scheme 3.16**). A ¹⁹F, ¹¹B, ¹¹B [H] (boron NMR decoupled from proton), and a ¹H NMR spectrum was collected at five different temperatures between 298 K and 383 K.



Scheme 3. 16 Variable temperature NMR experiment

The reaction of CAB **1a** with Tf₂NH (40 mol%) evolved hydrogen gas and resulted in the formation of B–N and B–O isomers (**A** and **B**) (**Figure 3.20**). The B–N and B–O isomers between CAB and [Tf₂N]⁻ at room temperature were confirmed by ¹⁹F, ¹H and ¹¹B NMR analysis. The ¹⁹F NMR spectrum collected at room temperature showed signals for the B–N isomer of [Tf₂N]⁻ bound to the Lewis acidic boron of the protonated CAB **1a**, which appeared at -69.2 ppm. The ¹⁹F NMR spectrum also showed two singlets for the B–O isomer at -76.5 ppm and -78.8 ppm.¹⁹⁵ As the temperature increases, [Tf₂N]⁻ dissociates and a single ¹⁹F NMR signal is observed at -77.3 ppm for [Tf₂N]⁻ (**Figure 3.20**).

It is also important to note that the conversion of CAB to SCAB does not occur at room temperature and only occurs efficiently at temperatures above 383 K, thereby confirming that the dissociation of the B–N and B–O isomers is necessary for the ring-opening process to proceed. The tetracoordinated boron species in the form of **A** and **B** is incapable of the reactivity required to convert CAB to SCAB but upon heating the reaction mixture to temperatures above 100 °C, [Tf₂N]⁻ dissociates from boron to generate a trivalent Lewis acidic boron species that could be capable of ring-opening.

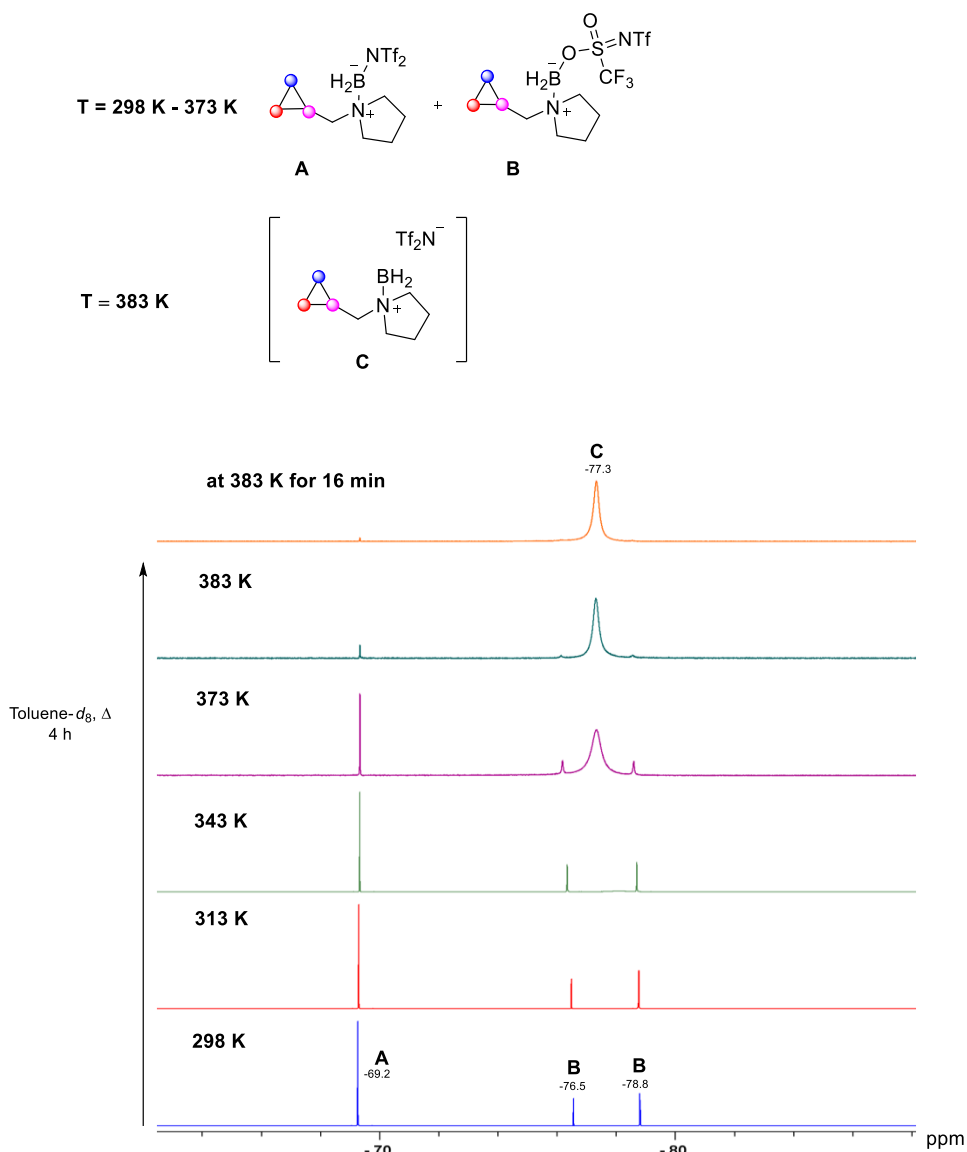


Figure 3.20 ^{19}F NMR spectra at variable temperatures

The ^{11}B NMR spectra obtained at varying temperatures are stacked below (**Figure 21**). Having added only 40 mol%, it was reasonable to expect a quartet at -10.6 ppm for the unreacted CAB **1a**. As the reaction was heated there was evidence of the dissociation of the B–N and B–O isomers as their corresponding peaks at -5.3 ppm and 1.9 ppm disappeared. According to Vedejs and co-workers, a broad signal at \sim -1.1 ppm is an indication of the presence of a B–H–B bridged dimer.¹⁹⁵ The ^{11}B NMR spectrum at T = 373 K for our reaction showed a broad signal at -1.7 ppm which can be attributed to the B–H–B bridged dimer. The dissociation of the B–N and B–O isomers would result in a trivalent super Lewis acidic boron species in the presence of many

tetracoordinate CAB **1a** species. The remaining starting material CAB **1a** and the activated trivalent dihydrido species could react to form a B–H–B bridged dimer species, **D** (Figure 3.21).

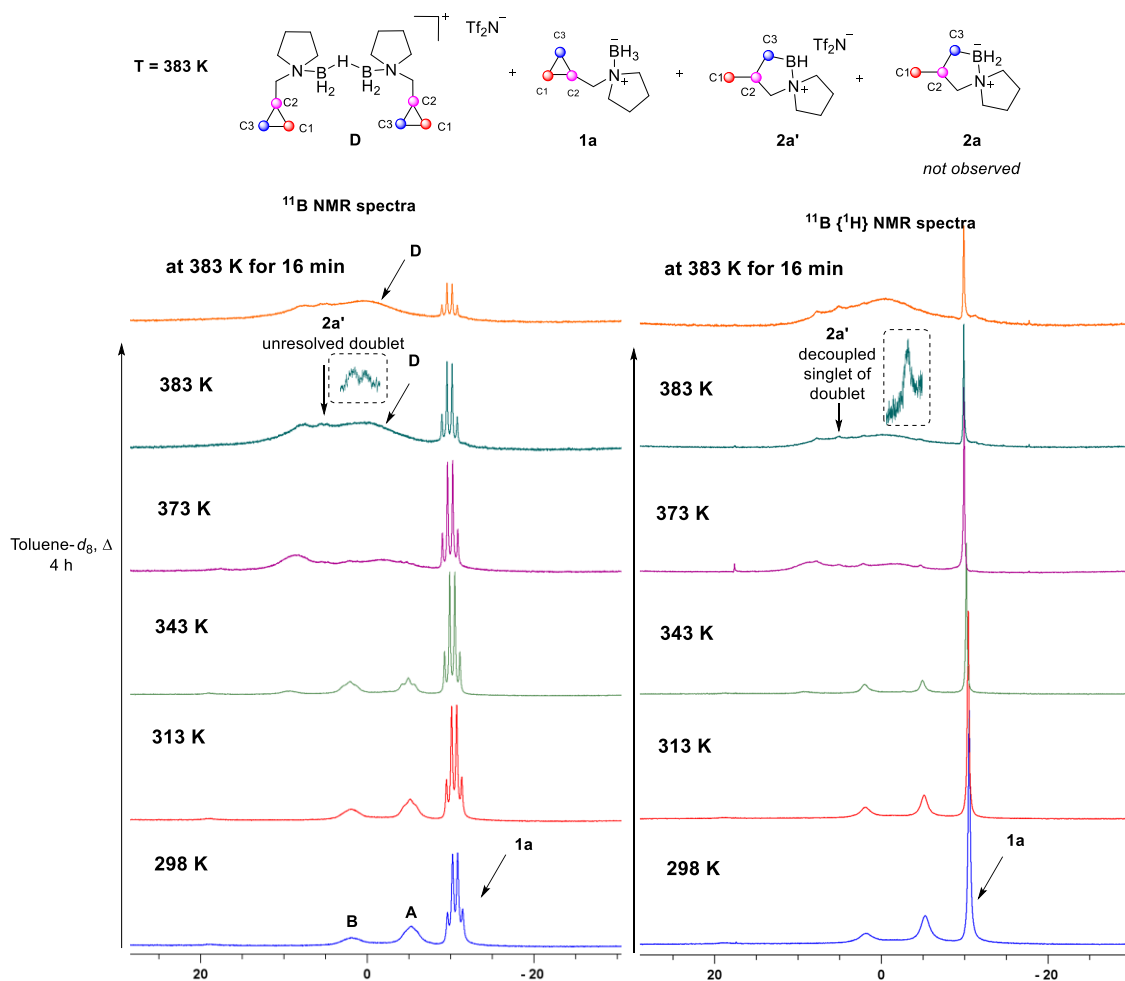
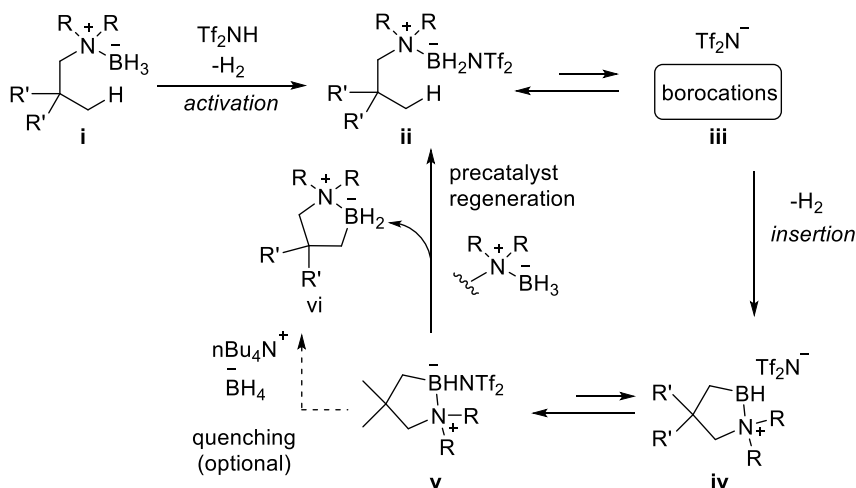


Figure 3.21 ¹¹B NMR spectra at variable temperatures

As the temperature increases to 383 K, there is an unresolved doublet that appears at 5.28 ppm (Figure 3.21). The ¹¹B [H] spectrum presented to the right of the ¹¹B NMR spectrum at 383 K shows that the unresolved doublet decouples to form a singlet which means the doublet signal was due to the presence of one single hydrogen atom on the boron (Figure 3.21). We propose that the monohydrido (B–H) species observed could be in the form of **2a'**. It is reasonable to expect that **2a'** should not be stable enough to be observed by NMR. However, as reported by Vedejs and co-workers such species can be observed by NMR.¹⁹⁵ There is no formation of SCAB **2a** which would appear as a characteristic triplet at -3.8 ppm in the ¹¹B NMR spectra. Vedejs and

co-workers reported a mechanism for the C–H borylation via borenium cation species generated by Tf₂NH activation (**Figure 3.22, a**).¹⁹⁵ The quench of nBu₄NBH₄ is reported to be optional as they observed the desired product even when the reaction was not quenched by nBu₄NBH₄. They postulated that the remaining starting material can serve as a hydride source for the borylated monohydride intermediate **v**. SCAB **2a** was also formed with 5 mol% of Tf₂NH when the reaction was not quenched with nBu₄NBH₄ albeit with slightly lower yields; therefore, it is likely that a species in the form of **2a'** would abstract a hydride from unreacted CAB **1a** to generate **2a** and regenerate **C** to continue the catalytic process (**Figure 3.22, b**). A similar cascade initiation step was also proposed by Vedejs and co-workers in their report on C–H borylation initiated by Tf₂NH (**Figure 3.16, a**).¹⁹⁵ Considering the analysis above, the species present at T ≥ 373 K are **2a'**, the B–H–B bridged dimer species **D** as well as unreacted CAB **1a**.

a. Proposed mechanism for C–H borylation: regeneration of precatalyst



b. Use of remaining starting material to form SCAB **2a** and regenerate reactive intermediate **C**

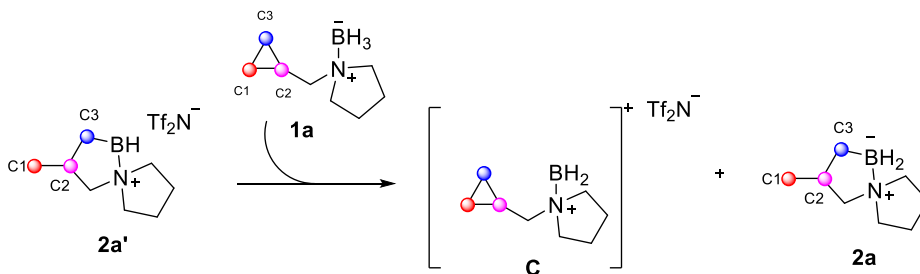
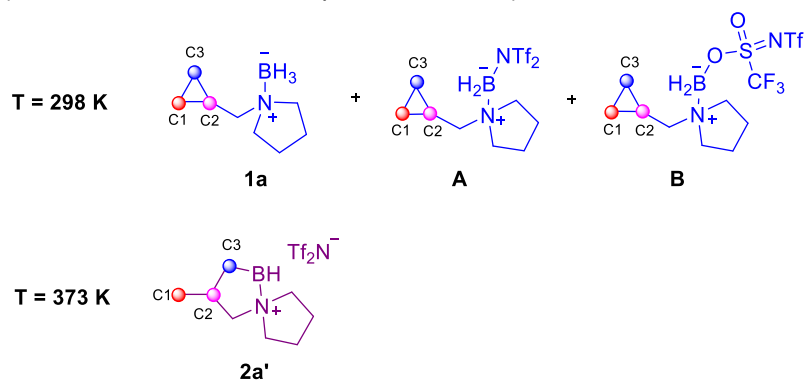


Figure 3.22 Regeneration of activated cationic species

The ^1H NMR spectra collected between 298 K to 383 K are stacked below (**Figure 23**). In the ^1H NMR spectrum at room temperature the peaks for B–N/O isomers are visible along with unreacted CAB **1a**. In the ^1H NMR spectrum taken at 298 K there are three species that can be observed. Having added only 40 mol% of Tf_2NH , starting material CAB **1a** can be observed as well as the expected B–N (**A**) and B–O (**B**) isomers (**Figure 23**). Species **A**, **B** and CAB **1a** are labeled by the diastereotopic protons on C1 and C3 that appear between -0.24 ppm - 0.38 ppm (**Figure 23**). Once the temperature is increased to 373 K, the ring-opening of CAB **1a** can be observed and was identified by a characteristic doublet at 0.94 ppm for the methyl group expected in SCAB **2a**. In the ring-opened product the doublet integrates for three protons relative to one hydrogen atom per diastereotopic signal (-0.24 ppm and 0.38 ppm) for the C3–H protons in **2a**. However, the peaks for the ring-opened product in the ^1H NMR spectra at temperatures $> 373\text{K}$ do not align with the proton signals of SCAB **2a**. Based on the observation made in the ^{11}B NMR analysis discussed above combined with the ^1H NMR analysis, we propose that the ring-opened product is in the form of **2a'** instead of **2a**. As mentioned above **2a'** eventually converts to **2a** by abstracting a hydride from unreacted CAB **1a** (**Figure 3.22, b**).

Moreover, upon increasing the temperature, we observed a slight downfield shift (0.1 ppm) of the proton signals corresponding to the C–Hs of the C1 and C3 carbon of CAB **1a**. The fact that the proton signals were shifted downfield upon heating implies that the trivalent Lewis acidic boron could be interacting with the C1 and C3–H atoms and withdrawing electron density without cleaving it, leading to its deshielding. Trivalent boron species are classified as super Lewis acids in the literature and have been shown to be capable of activating sp^2 and sp^3 C–H bonds.²⁰⁸⁻²¹¹ As discussed above, the C–H borylation reported by Vedejs and co-workers also demonstrates the ability of a Lewis acidic boron to activate an sp^3 C–H bond leading to a transition metal-free C–H borylation.¹⁹⁵

i. Structure of species observed in ^1H NMR analysis at different temperature



ii. Variable temperature experiment (^1H NMR spectra)

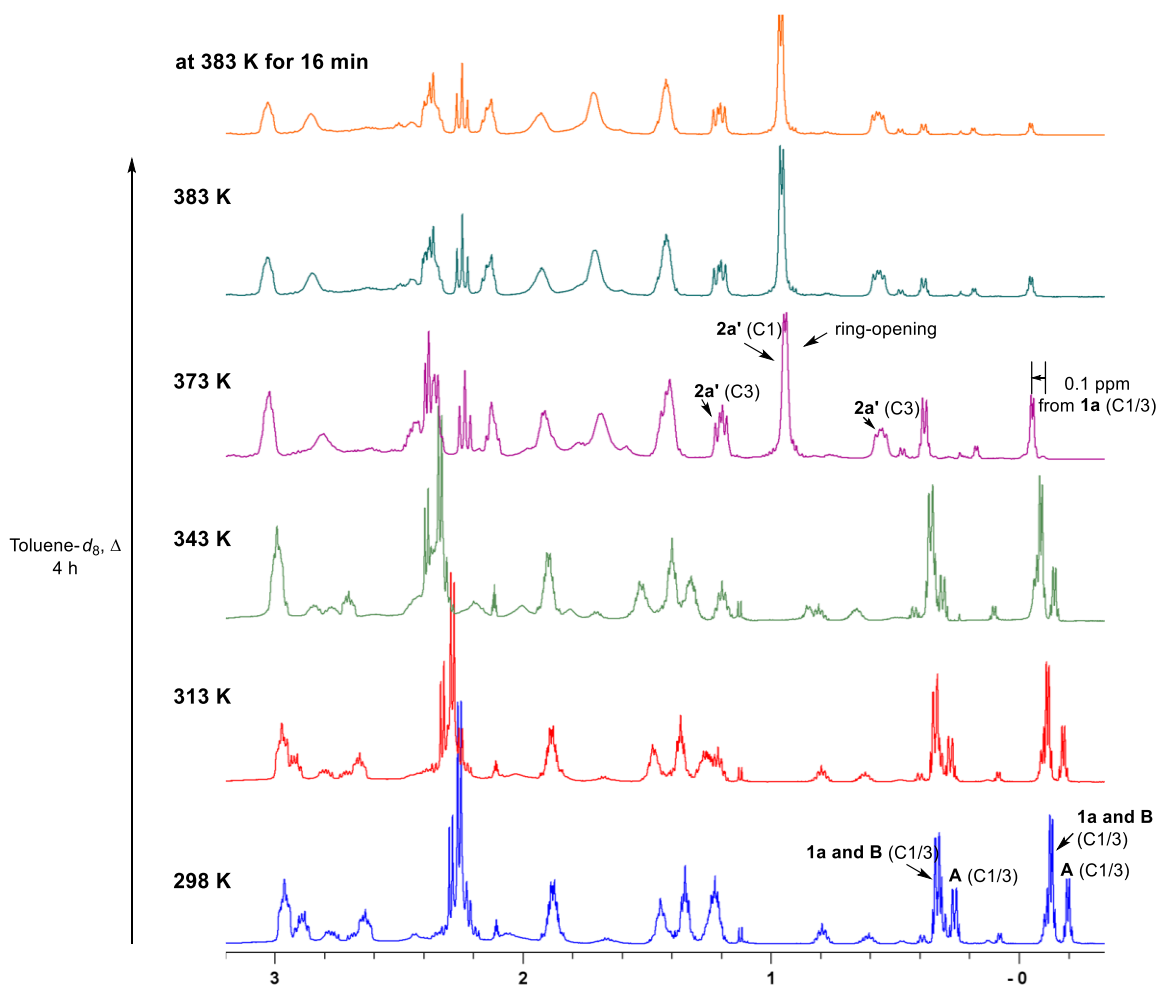


Figure 3.23 ^1H NMR spectra at variable temperatures

3.5.5.2 Determination of *Syn* vs. *Anti*-Hydroboration in CAB to SCAB Transformation

The hydroboration of chiral CAB **1ab** presented in the scope table (Table 3.4, entry 29) was used to examine the stereospecificity of the ring-opening process (Figure 3.24). We expected the hydroboration of CAB to proceed via a mechanism similar to that of the Brown hydroboration reaction and provide a *syn*-hydroborated product (Scheme 3.11). CAB **1ab** was subjected to 5 mol% of Tf₂NH and heated to 125 °C for 1.5 h (Figure 3.24). Once the reaction time was complete, the mixture was quenched with 5 mol% of *n*Bu₄NBH₄, diluted with CH₂Cl₂ and filtered over a short pad of silica gel. The solvent was removed, and the compound was fully characterized.

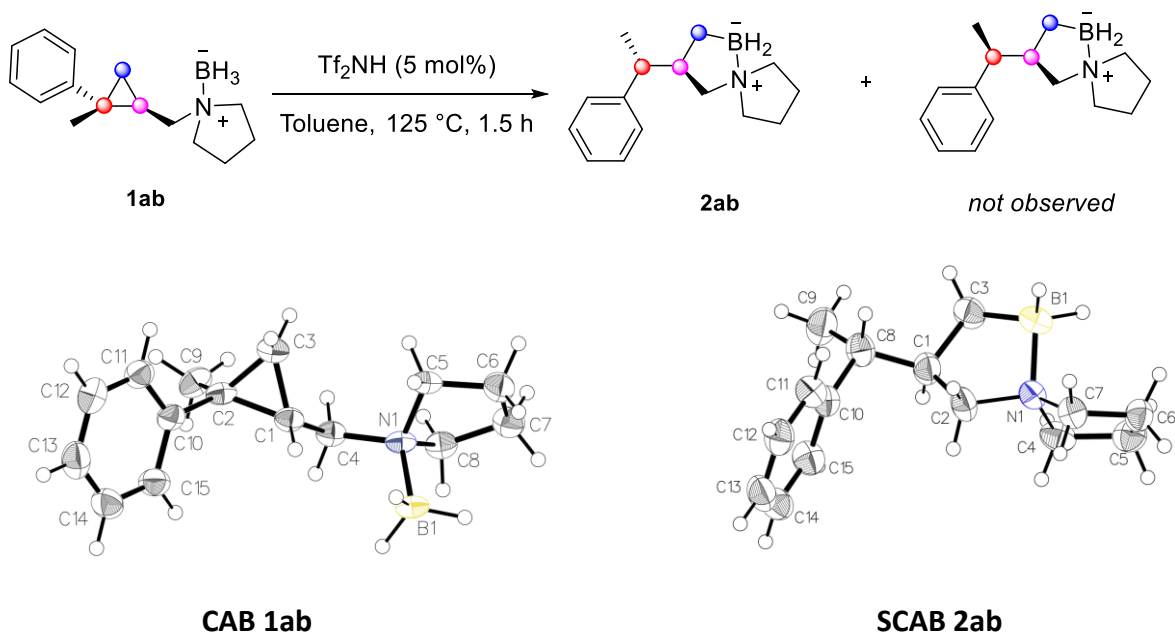


Figure 3.24 Hydroboration of a chiral CAB **1ab** and single X-ray crystal structure of CAB **1ab** and SCAB **2ab**

To determine the stereochemistry of the SCAB **2ab** we sought to obtain a single crystal X-ray structure. CAB **1ab** was a solid and therefore a crystal structure of the starting material was readily obtained through a slow diffusion of hexanes and CH₂Cl₂. However, SCAB **2ab** was obtained as a viscous oil. The crystal of SCAB **2ab** was obtained via lyophilization (48 h). The X-ray crystal structure of the hydroborated product revealed that the hydroboration of CAB **1ab** resulted in a net *anti*-hydroborated product SCAB **2ab**. The ¹H NMR spectrum showed a single set of peaks which meant that the ring-opening process provided one single diastereomer.

Theoretically it is possible that the ^1H NMR shifts of the two potential diastereomers can overlap perfectly in the ^1H NMR spectrum (CDCl_3). Consequently, a ^1H NMR spectrum was also collected in deuterated benzene, C_6D_6 . The ^1H NMR spectrum collected in C_6D_6 did not show any evidence of a second diastereomer and a single set of peaks were observed for SCAB **2ab**. Another method to differentiate between two diastereomers is by ^{13}C NMR analysis.^{212, 213} The ^{13}C spectrum collected in CDCl_3 for SCAB **2ab** showed the presence of a single diastereomer. Similarly, the ^{13}C NMR spectrum collected in C_6D_6 showed the presence of a single diastereomer.

NMR spectroscopy combined with the single X-ray crystal structure of SCAB **2ab** suggests that the ring-opening process results in a single diastereomer which is net *anti*-hydroborated.

3.5.5.3 Deuterium Labelling Experiments

We thought of doing labelling experiments in which the BH_3 moiety on CAB would be replaced with a BD_3 moiety (**Figure 3.25**). If the reaction were to proceed through a Brown hydroboration mechanism, we should expect the B–D bond to add across the C1–C3 bond which would result in a SCAB with a C1–D bond and a C3–B bond (**Figure 3.25**, compound **5a'**).

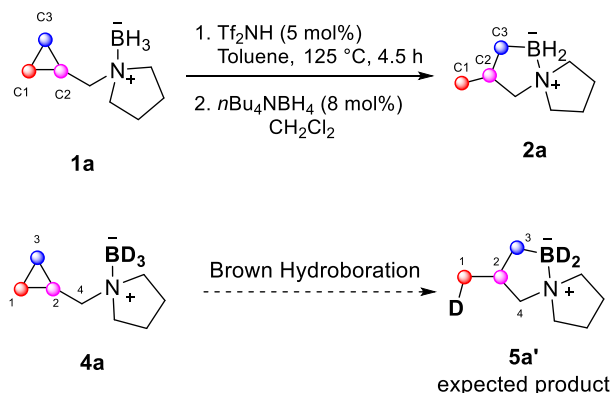
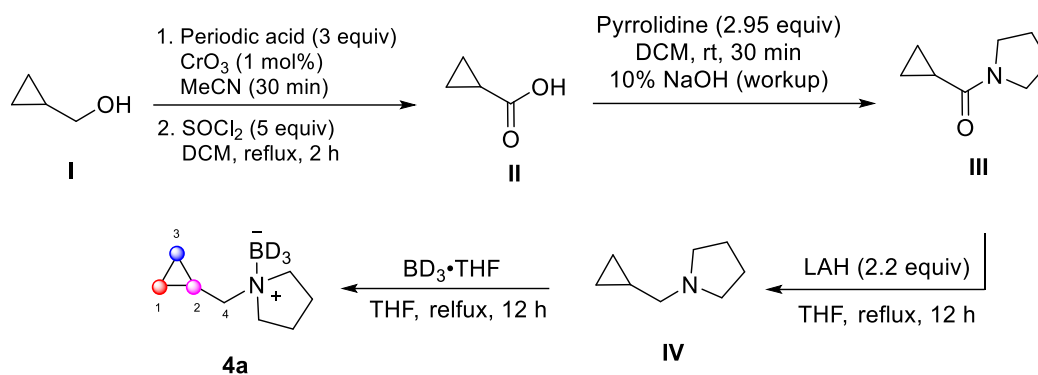


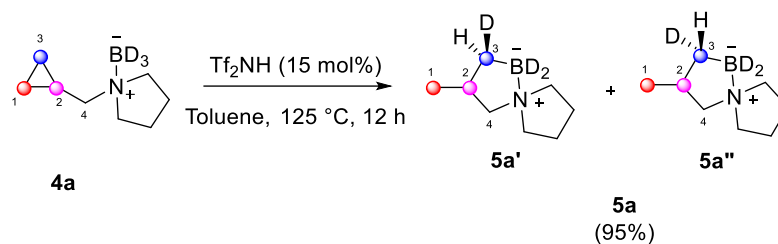
Figure 3.25 Proposed reaction for deuterium labelling

The first mechanistic study involved the preparation of CAB **4a** (**Scheme 3.17**). Cyclopropanemethanol **I** was transformed to its amide analogue **III** in three steps (**Scheme 3.17**). The amide was then reduced with LAH (2.2 equiv) to obtain the cyclopropyl amine that was then reacted with $\text{BD}_3 \cdot \text{THF}$ to obtain the deuterated CAB **4a**.



Scheme 3.17 Synthesis of deuterated CAB **4a**

CABs **4a** was subjected to a 15 mol% of Tf₂NH and heated at 125 °C for 12 h in toluene. The reaction time was increased to account for the deuterium isotope effect that could slow down the reaction rate. Once the reaction was complete, the mixture was quenched with 15 mol% of *n*Bu₄NBD₄, diluted with CH₂Cl₂ and filtered over a short pad of silica. The solvent was removed and the resulting SCAB **5a** was characterized by NMR spectroscopy. The ¹H and ²H NMR analysis revealed that SCAB **5a** exists as **5a'** and **5a''** in a 1.8:1 ratio (**Scheme 3.18**). SCAB **5a** was not consistent with the Brown hydroboration hypothesis. A product consistent with a Brown hydroboration would mean a B–D bond would add across the distal C1–C3 bond to form a C3–B bond and a C1–D bond; however, no deuterium was observed on C1. We were also curious to see whether we could observe the activation of the sp³ C1–H or C3–H bond of CAB since the variable temperature ¹H NMR studies discussed above hinted towards the involvement of the C1–H and C3–H bonds of CAB **1a**, which was observed by a downfield shift of its ¹H NMR signals (**Figure 3.23**). Vedejs and co-workers showed that a B–H–B bridged dimer could do C–H borylation via the activation of a C–H bond and we wondered if the B–H–B bridged dimer **D** (**Figure 3.21**) forming in our reaction could also activate the C–H bonds of CAB. The involvement of the C3–H bond in the ring-opening of **4a** is evident from the deuterium observed on C3 in SCAB **5a** (**Scheme 3.18**).



Scheme 3.18 Hydroboration of CAB using a BD_3 moiety

The labelling experiment discussed above helped us rule out the possibility of a hydride transfer from boron to C1, but we were still interested in determining whether the C2–H can undergo a hydride transfer to C1. The results obtained for SCAB **2y** and **2z** show that the substituents on C2, in the form of a methyl and phenyl group, do not undergo a 1,2–shift to C1, helping us rule out the participation of the C2 substituents in the ring-opening mechanism (**Figure 3.26**)

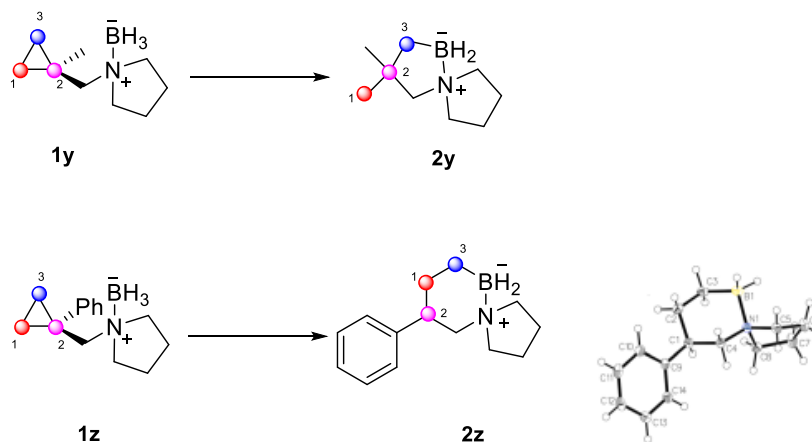
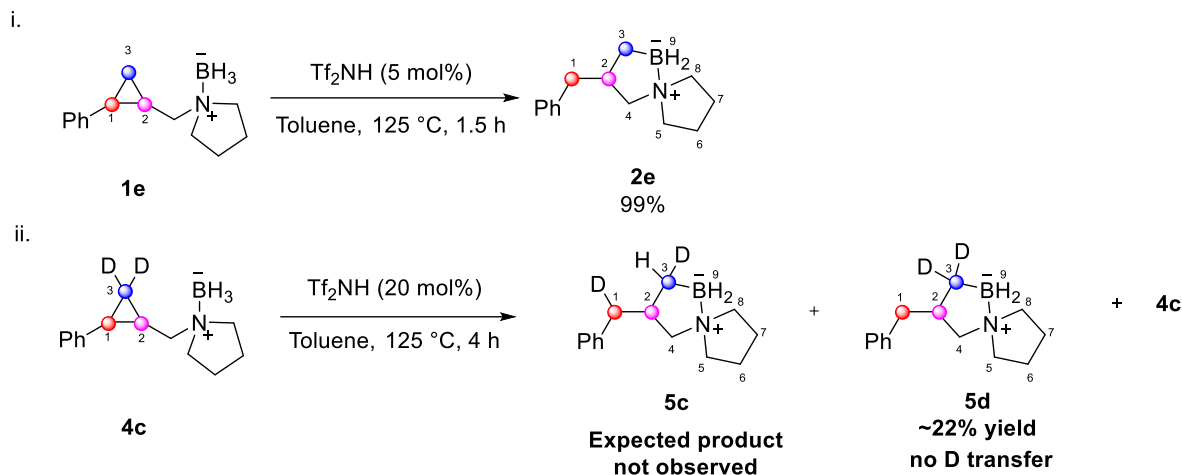


Figure 3.26 Hydroboration of *gem*-C2 substituted CAB and lack of 1,2-migration observed in product from C2 to C1

Based on the labelling experiments above and the potential stereospecificity observed for the chiral SCAB **2ab**, we questioned if a selective hydride transfer is occurring from C3 to C1 in the ring-opening mechanism. We wanted to extend our labelling experiments to substituted CABs to help rule out any bias involved in the deuterium experiment using unsubstituted CAB **1a**. To observe the hydride transfer from C3 to C1, a second labelling experiment was done. A deuterated analogue of CAB **1e** was synthesized as CAB **4c** in which the hydrogen atoms on C3 were replaced

with deuterium atoms. CAB **4c** was reacted with 20 mol% of Tf₂NH and heated at 125 °C for 4 h. We proposed that CAB **4c** would convert to **5c** based on the results obtained for CAB **4a** which provided a SCAB with a H–C3–D α to boron (**Scheme 3.19**).



Scheme 3. 19 Hydroboration of CAB with deuterium labeling at C3

However, to our surprise, no evidence of the formation of **5c** was observed. Instead, SCAB **5d** was obtained in 22% isolated yield. As presented in the scope, CAB **1e** is converted to SCAB **2e** in 1.5 h in quantitative yields using only 5 mol% of Tf₂NH; however, replacing the C3 carbon with two deuterium atoms only provided SCAB **5d** in 22% yield after 4 h despite the use of 20 mol% Tf₂NH. In the optimization of the CAB to SCAB transformation, we have established a direct correlation of the reaction rate with the equivalents of Tf₂NH used (up to 1 equivalent). To account for an expected KIE (kinetic isotope effect), we used 20 mol% of Tf₂NH to ensure good conversion to the expected SCAB product **5c**. SCAB **5d** was the only product observed in the ¹H NMR spectrum and a ²H NMR analysis confirmed that SCAB **5d** contained a C3 carbon that had two deuterium atoms on it. The fact that the yield is significantly lower suggests that the alternative pathway that does not involve the C3–H is less favored.

As per classical models, a KIE as high as 8 can be expected when a hydrogen is replaced by a deuterium, but the complete suppression of a reaction pathway is very puzzling and cannot be explained by classical models.²¹⁴⁻²¹⁶ If the hydrogen atom on C3 was not participating in the reaction, then the reaction rate should not be affected. The results obtained for CAB **4c** suggest that SCAB **5d** was obtained by an alternative pathway. We postulate that the C3–H could be

activated by the Lewis acidic B–H–B bridged dimer **D**. A replacement of the hydrogen atoms on C3 with deuterium resulting in the complete suppression of the reaction pathway would mean the hydride transfer from C3-H could involve quantum tunneling.^{215, 216}

3.5.5.4 Remarks on Mechanism

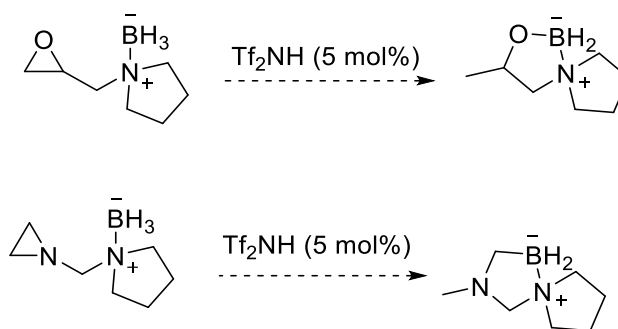
The labelling experiments hint towards the activation of the sp^3 C3–H bond by a Lewis acidic boron species, generated upon heating the reaction mixture above 100 °C, and subsequent hydride transfer from the activated C3–H bond. The conversion of CAB **1ab** to SCAB **2ab** resulting in a single diastereomer indicates that the hydride transfer is selective. Additional experimental work and computational studies can be done to gain a higher degree of understanding of the mechanism for the transformation of CABs to SCABs.

3.6 Conclusion and Perspectives

The activation of C–H and C–C bonds presents one of the most effective ways of building complex molecules. C–H and C–C bonds are ubiquitous in Nature; however, they are difficult to functionalize or involve in any sort of reactivity as they are fairly inert. Since C–H bonds are more abundant than C–C bonds and sterically more accessible, a few methodologies do exist to activate the C–H bonds using transition metal catalysts. Fontaine and co-workers have recently demonstrated a metal free C–H activation using a frustrated Lewis pair (FLP) system.²¹⁰ C–C bonds are more challenging to activate as compared to C–H bonds due to the unfavorable directionality of the C–C bond orbitals making them more difficult to access. Any methodology that can involve the breaking of either a C–H or C–C bond is pioneering in itself but a methodology that includes simultaneous control of a C–H and C–C bond can be an even more powerful tool to access new complex molecules previously thought to be inaccessible. The conversion of a CAB to SCAB discussed above involves the functionalization of a strained C–C bond coupled with a hydride transfer from an sp^3 carbon. The merging of C–H and C–C bond reactivity in the method makes it highly atom efficient and could prove to be a valuable tool for synthetic chemists. The formation of SCABs proceeds via a cascade mechanism upon activation of the CAB precursors by a catalytic amount of Tf_2NH . SCABs are formed mostly in quantitative yields and the methodology is shown to possess functional group tolerance to a good degree. The conversion of 1,2,2-substituted CAB

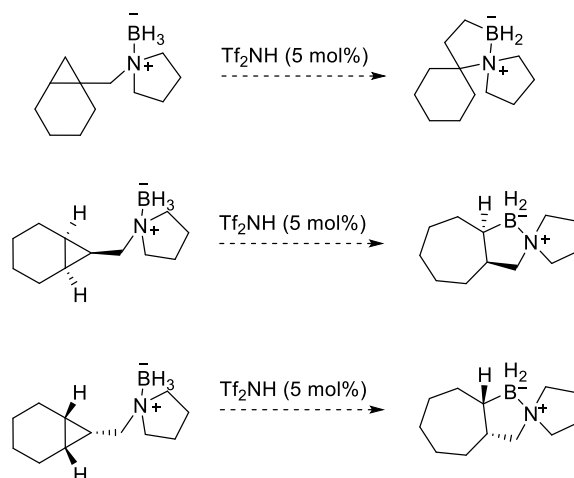
1ab to the corresponding SCAB **2ab** was obtained in a potentially stereospecific manner and was net *anti*-hydroborated. The versatility of the method to access complex motifs containing multiple spirocenters was demonstrated by the conversion of **1ac** to **2ac** (Table 3.4). Owing to the presence of a C–B and B–H bond, SCABs were shown to readily undergo functionalization to access a diverse range of substrates (Figure 3.15). Upon reaction of SCAB **2a** with pinacol, a unique spirocyclic motif containing two different spiroatoms (**3f**) was obtained (Figure 3.15, b).

The conversion of a CAB to SCAB involves the ring opening of a strained system which means our methodology could be employed to ring open other useful three membered ring systems in which one of the carbon atoms in the cyclopropane ring is replaced with a heteroatom such as nitrogen or oxygen (Scheme 3.20). Aziridines are known to be valuable synthons and the ring opening reactions of aziridine could provide a highly diverse and useful class of organic compounds.²¹⁷



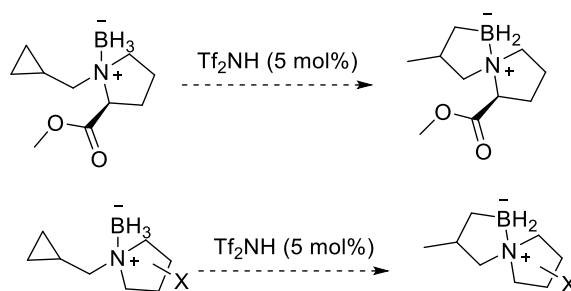
Scheme 3. 20 Ring-opening of aziridine and epoxide analogues of CABs

The method could also access complex motifs containing multiple ring systems via the ring opening of bicyclic CAB motifs (Scheme 3.21).



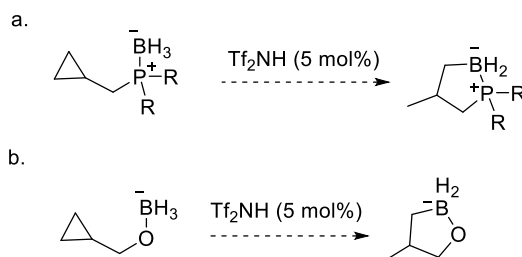
Scheme 3. 21 Ring-opening of bicyclic CABs and proposed products

Similarly, the *N*-pyrrolidone ring in CAB can be diversified to generate diverse *N*-heterocycles containing an *N*-spiroatom (**Scheme 3.22**).



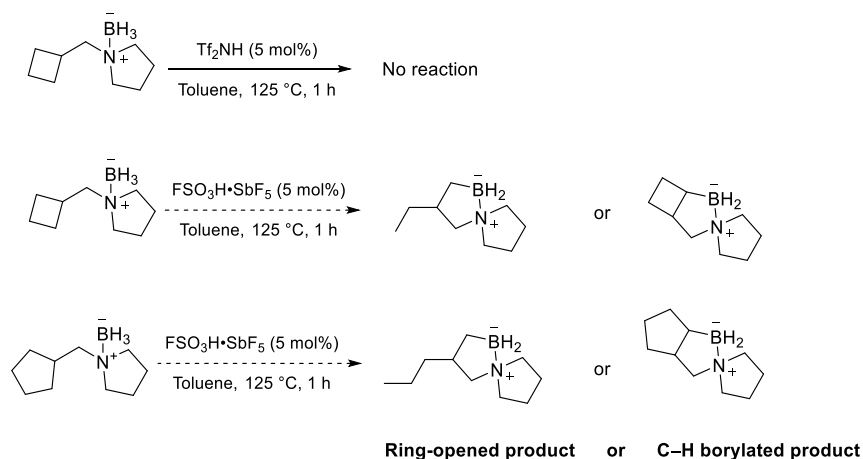
Scheme 3. 22 Modification of *N*-heterocycle

Furthermore, the amine-borane moiety can be replaced by a phosphine-borane or oxyborane moiety giving access to P or O containing rings or spirocycles (**Scheme 3.23**).



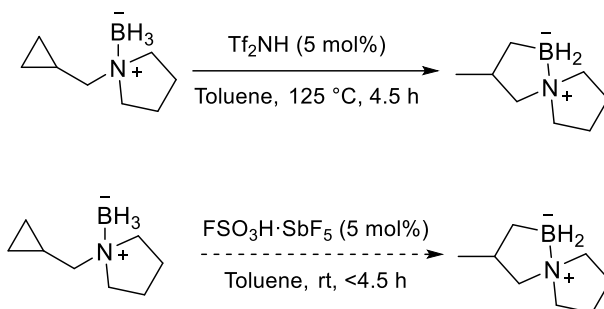
Scheme 3. 23 Phosphine-borane and oxyborane analogues of CABs

As mentioned in the chapter, the optimized conditions for the conversion of CAB to SCAB could not be extended to the ring-opening of the cyclobutane amine-borane analogue of CAB **1a**. Cyclobutane rings have a lower propensity to ring-open compared to cyclopropane rings, therefore this result was not surprising. Since we are only using catalytic amounts of strong acids such as Tf_2NH , it would be interesting to attempt the ring-opening of cyclobutane amine-borane in the presence of even stronger acids such as magic acid ($\text{FSO}_3\text{H}\cdot\text{SbF}_5$) etc. George A. Olah discovered the use of superacids, such as $\text{FSO}_3\text{H}\cdot\text{SbF}_5$, to prepare stable carbocations.^{218, 219} $\text{FSO}_3\text{H}\cdot\text{SbF}_5$ has been used to observe stable carbocations due to the extremely weak nucleophilicity of superacids. We speculate that Olah's work could be used to generate Lewis acidic boron cations to further explore and expand our method. We propose that the Lewis acidity of the boron might be further enhanced in the presence of a conjugate base weaker than $[\text{Tf}_2\text{N}]^-$ and the resulting Lewis acidic boron might be able to cleave the C–H bond of the cyclobutane to generate a cyclobutane carbocation which can then undergo ring-opening (**Scheme 3.24**). If the Lewis acidic boron of the amine-borane moiety can activate the C–H bond of a cyclobutane ring, we may be able to ring-open other cycloalkanes such as a cyclopentane ring. It is also important to consider that if the ring-strain of cyclobutane and cyclopentane ring is not enough for the ring-opening to proceed then a C–H borylation could also occur.



Scheme 3. 24 Proposed ring-opening of cyclobutane amine-borane

In the reported methodology for the conversion of a CAB to SCAB, the reaction requires heating to temperatures >100 °C to generate a Lewis acidic boron species capable of activating the C–H bond. We speculate that the use of a super acid such as $\text{FSO}_3\text{H}\cdot\text{SbF}_5$ could generate the Lewis acidic boron species at room temperature due to the weak nucleophilicity of the conjugate base and therefore the transformation of CAB to SCAB may proceed without heating (**Scheme 3.25**).



Scheme 3. 25 Transformation of CAB to SCAB using magic acid

SCABs contain a spirocyclic ring system with an uncommon *N*-spiroatom. The three dimensionality of a spirocycle lends itself well to the rise in the use of non-planar molecules in drug discovery. Incorporation of spirocycles has been shown to positively affect the potency, selectivity, pharmacokinetics, and physiochemical properties of drug molecules.^{220, 221} Therefore, despite the significant challenges faced in making spirocyclic motifs, medicinal chemists have actively pursued them. Our method provides access to spirocyclic motifs via borylative ring opening of a cyclopropane. The use of a catalytic amount of Tf_2NH and the cascade nature of the mechanism makes access to spirocycles highly atom efficient which could be potentially valuable to medicinal chemists. The similarity in atomic radii and ability to replace C–C bonds with isoelectronic B–N units present chemists with an incredible opportunity to develop an isosteric class of new molecules and explore their reactivities making the SCAB motif an excellent addition to the *N*-heterocycle library.²²²⁻²²⁵ Boron has found increasing prominence in drug design which has led to organoboranes finding utility in medicinal chemistry.¹³³ Amine-boranes possess potent anti-cancer, anti-inflammatory, and anti-osteoporotic properties.⁴¹ Boron-based heterocycles, including B–N heterocycles, have shown promise as potential drug candidates and several of these motifs are in line for FDA approval (**Figure 3.27**).⁵⁵

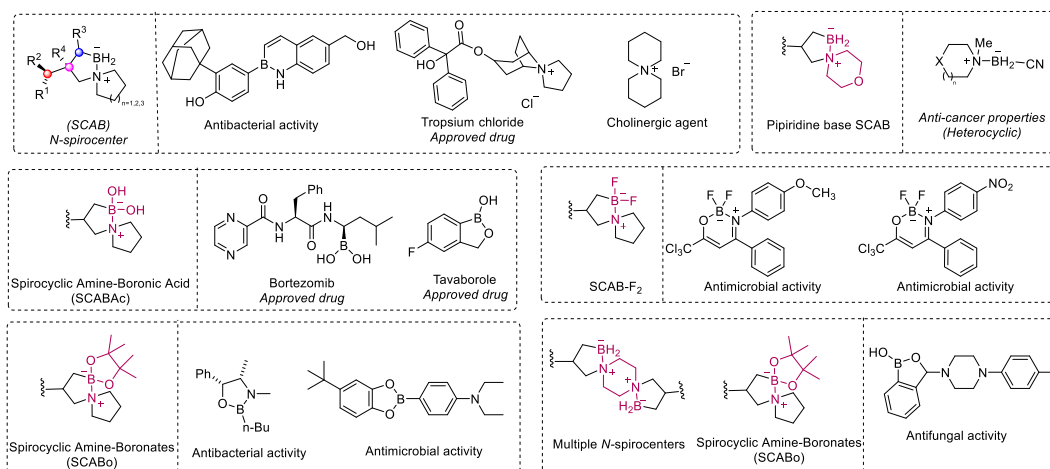
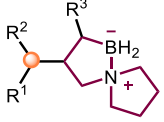
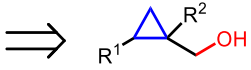
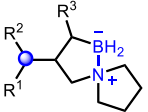
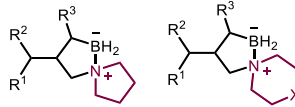
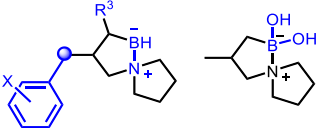
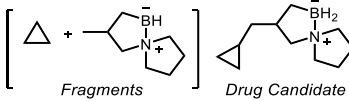
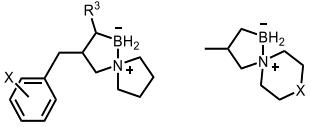
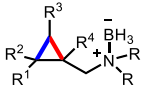
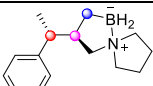


Figure 3.27 SCAB precursors of biologically active compounds

While aliphatic and heterocyclic amine-boranes exist, an approach to access structurally diverse and three-dimensional spirocyclic libraries has been absent so far. The scope presented for the methodology developed in the chapter could help in bridging this gap.

Boron neutron capture therapy (BNCT) is a radiotherapeutic modality for treating locally invasive malignant tumors that do not respond to standard radiation therapy.⁷ Studies have shown that fluorinated borono-phenylalanine (¹⁹F-BPA) can also have a potential future application in boron neutron capture therapy (BNCT) clinical trials and SCAB-F₂ derivatives could serve as interesting motifs to study.²²⁶ Furthermore, the potential of the SCAB analogues as promising pharmacophores is highlighted in **Table 3.5**.

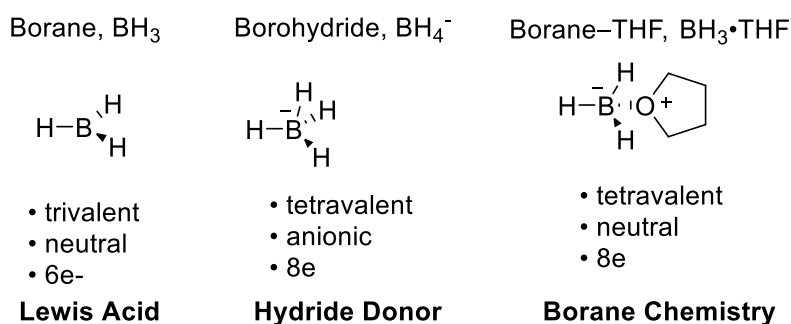
Table 3.5 SCAB as a Potential Pharmacophore

Properties	Description	This work	
Molecular recognition	<ul style="list-style-type: none"> • Polar groups • Chemotypes 	<ul style="list-style-type: none"> • B-H, B-N, B-OH, B-F 	✓
Physiochemical properties	<ul style="list-style-type: none"> • MW: 140-230 • Non-H atoms: 10-16 • Solubility ≥ 5 nM in 5% DMSO • Stability (>24 h) • log P (partition coefficient) ~ 1.35-1.8 	<ul style="list-style-type: none"> • Within range • 10-16 • Soluble • Bench stable • Average Log P = 1.8²²⁷ 	✓
Shape	<ul style="list-style-type: none"> • Spirocyclic amine-boranes • 3D sp³ character • Rings • Number of freely rotatable bonds: 0-1 		✓
Synthetic tractability	<ul style="list-style-type: none"> • Typically, 50-100 mg • ≤ 4 steps (commercially available reagents) 		✓
Chirality	<ul style="list-style-type: none"> • Number of stereogenic center 0-1 maybe 2 		✓
Heterocycles	<ul style="list-style-type: none"> • 60% of small-molecule drugs contain a N-based heterocycle²²⁸ 		✓
Synthetic vectors	<ul style="list-style-type: none"> • Synthetic vectors for fragment growth 		✓
FBDD	<ul style="list-style-type: none"> • Fragment based drug design 		✓
DOS	<ul style="list-style-type: none"> • Diversity oriented structure 		✓
Regiocontrol	<ul style="list-style-type: none"> • Efficient access to desired motif 		✓
Stereospecific	<ul style="list-style-type: none"> • Aid in selective protein binding 		✓

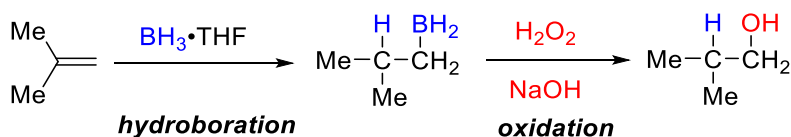
**Chapter 4 – Exploring the Reactivity of a Spirocyclic Alkyl
Dihydrido Amine-Borane•NTf₂ Complex in Functional Group
Interconversion Reactions**

4.1 Introduction

Boron hydrides were first synthesized and characterized by German chemist Alfred Stock and his collaborators between the years 1912-1937.⁹¹ The term boranes was assigned to boron hydrides (B–H bonds) as an analogy to alkanes (C–H bonds). Stock and co-workers prepared boranes with the general formula B_nH_{n+4} and B_nH_{n+6} , amongst which B_2H_6 was the most extensively studied. Many boranes and their derivatives can be synthesized from B_2H_6 . While free BH_3 is unstable, it can be isolated as a stable adducts with Lewis bases. Herbert Charles Brown shared the Nobel prize for chemistry in 1979 for the development of the hydroboration reaction.¹³ The hydroboration reaction has been used extensively in organic synthesis to generate useful synthetic intermediates containing C–B bonds and has been applied as a common synthetic pathway to generate alcohols through the hydroboration/oxidation reaction (**Figure 4.1**).



a. Classification of B–H Borane Compounds



b. H. C. Brown Hydroboration and Oxidation

Figure 4.1 a. Classification of boranes b. Hydroboration/oxidation reaction

The alkylboranes obtained from the hydroboration of alkenes are seldom isolated due to their lack of stability.²²⁹ Thexylborane, 9-BBN-H and diisopinocampheylborane are examples of

monoalkyl- and dialkylboranes that have been used as reagents in hydroboration reactions (**Figure 4.2**). While 9-BBN-H can be stored as a solution or in its crystalline form indefinitely, thexylborane is not stable for prolonged storage and is recommended to be freshly prepared for use.²³⁰

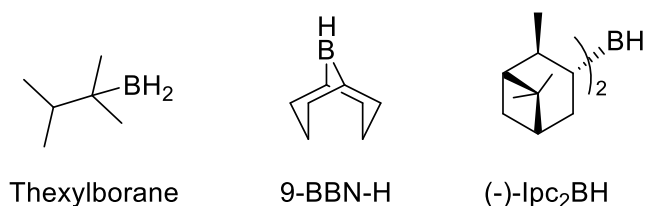


Figure 4.2 Structures of some alkylborane reagents

4.1.1 Boron Hydrides as Proton Acceptors

The ability of borohydrides to react with acidic protons has contributed to the rising interest in borohydrides as potential hydrogen storage materials over the last decades.²³¹ Sodium borohydride can be hydrolyzed in the presence of water to generate hydrogen gas and it serves as an alternative to the more expensive metal-hydride-based hydrogen storage systems. The reactivity of borohydrides with proton donors can be tuned based on the strength of the proton donor (**Figure 4.3**).

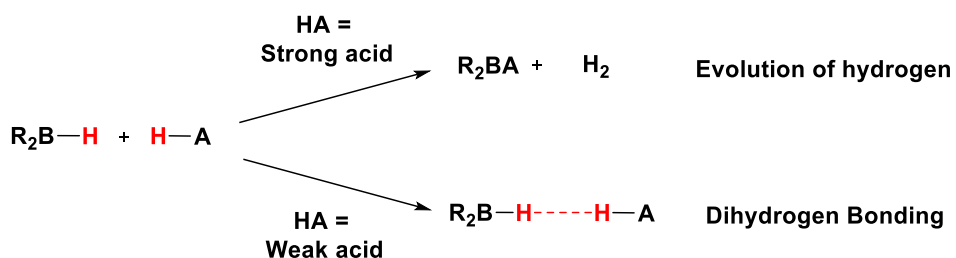


Figure 4.3 Boron hydride as proton acceptors

Borohydrides can act as proton acceptors to generate reactive borenium species in the presence of strong acids or can undergo dihydrogen bonding when weak acids are used as proton donors. The reaction of boranes with strong acids leads to the formation of reactive borenium cations capable of the hydroboration of alkenes and performing C–H borylation of aromatic and

aliphatic bonds.^{97, 195} Boron cations are generally classified as borinium, borenium, and boronium cations depending on the number of coordinating ligands (**Figure 4.4**).

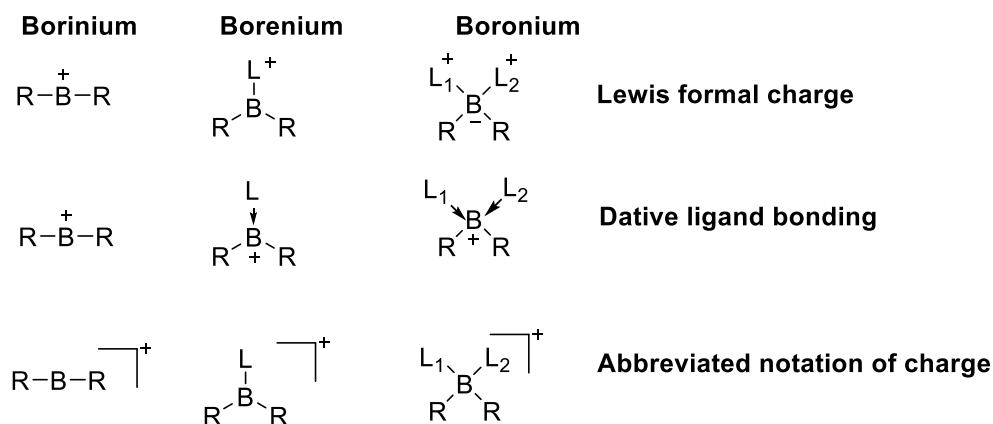
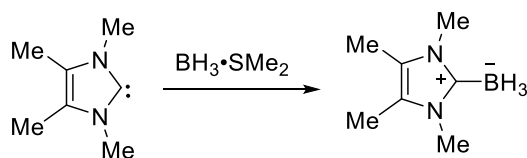


Figure 4.4 Nomenclature for boron cation that is in current use

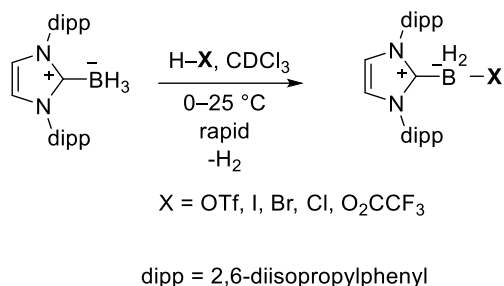
N-Heterocyclic carbene boranes (NHC-boranes) are another class of boron hydrides containing C–B bonds where the boron is complexed to an *N*-heterocyclic carbene. NHC-Borane adducts are stable to air and water and can be purified by column chromatography. They can be synthesized via the complexation of isolated NHCs with $BH_3 \cdot THF$ and $BH_3 \cdot SMe_2$.²³² NHC-boranes can also be obtained from readily available reactants such as heterocyclic salts, and amine- or phosphine-boranes (**Scheme 4.1**).²³²



Scheme 4. 1 Synthesis of NHC-boranes via BH_3 complexes

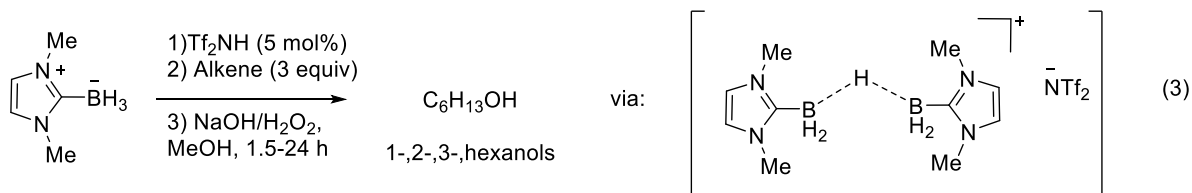
Formally analogous to Lewis-acid and Lewis-base complexes, NHC-boranes were thought to exhibit reactivity similar to other borane complexes; however, it was found that they exhibit their own chemistry resulting from their exceptional stability.⁹⁶ In contrast to typical borane chemistry, NHC-boranes are inert to hydroboration reactions.²⁰⁷ NHC-borane chemistry has been known since 1967 but it was only after 2008 that NHC-boranes became popular due to

developments in their synthesis and efficient isolation techniques.⁹⁶ NHC-boranes can be used as catalysts and as frustrated Lewis pair (FLP) systems.²³³ They can form reactive intermediates such as boronium cations, boryl anions and radicals in-situ.²³⁴ Such versatility allows NHC-boranes to react with electrophiles and metal complexes, undergo nucleophilic substitution on boron, form boryl anions through reductive metalation, participate in elimination reactions, and act as ionic reducing reagents.⁹⁶ Curran and co-workers²³⁵ and Lindsay and co-workers²³⁶ observed acid/base reactions of NHC-boranes with very strong acids (pKa values ≤ 2) to make NHC-borane reactive intermediates. NHC-boryl triflates can be obtained from reacting dipp-Imd-BH₃ with triflic acid (**Scheme 4.2**).



Scheme 4. 2 Reactivity of NHC-borane with strong acids

Vedejs and co-workers reported that reacting NHC-boranes with strong acids such as Tf₂NH and TfOH generates boronium cations in the form of [NHC-BH₂-LB]⁺ that are capable of doing hydroboration.⁹⁷ In the presence of an extremely weak conjugate base, boronium cations could behave as boronium cations which are known to be super Lewis acids. For example, neutral carbene-boranes, such as NHC-BH₂-LG (where LG = bistriflimidate or triflate, etc.) are regarded as boronium equivalents. Vedejs and coworkers were able to hydroborate 3-hexene, 3-octene, and 1-cyclohexyl-1-butene with an NHC-borane derivative in the presence of a catalytic amount of Tf₂NH (**Scheme 4.3**).⁹⁷



Scheme 4. 3 NHC-borane boronium cations for the hydroboration of alkenes

In 2011, Vedejs and co-workers reported the intramolecular aliphatic C–H borylation of amine-boranes via borenium cation equivalents from the reaction of the amine-borane moiety with a very strong acid such as Tf₂NH.¹⁹⁵ Tf₂NH reacts with amine-boranes to generate borenium cations in the form of B–H–B bridged dimers which proved to be essential for C–H borylation reactivity. Addition of 1 equivalent of Tf₂NH resulted in the formation of B–N/O isomers and quenched the reactivity (**Figure 4.5**). Vedejs and co-workers further analyzed the reactivity

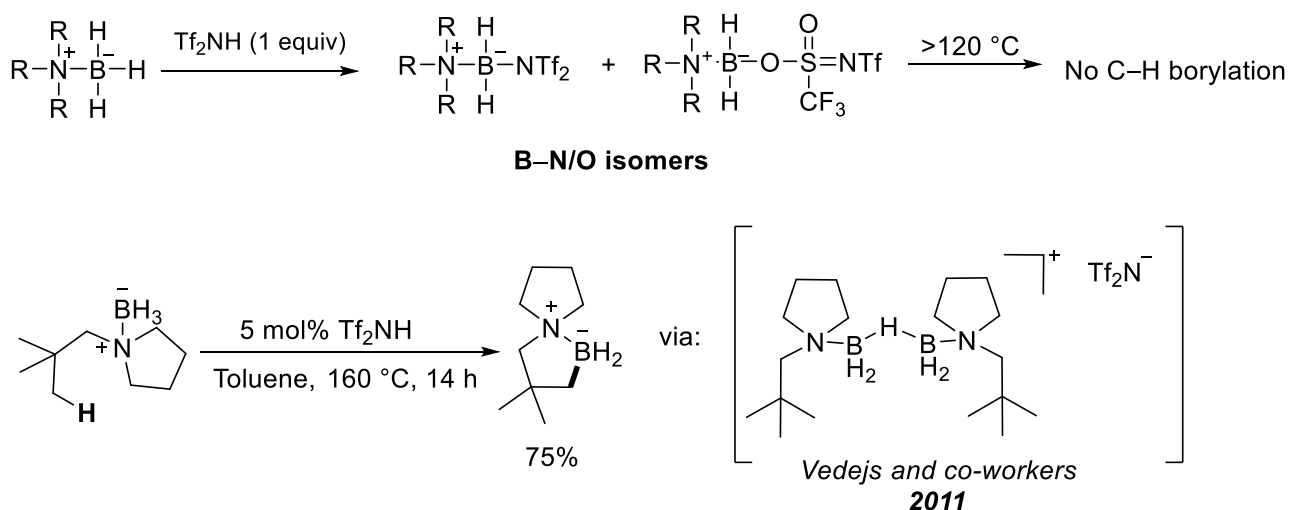


Figure 4.5 Borylation of aliphatic and aromatic C–H bonds using borenium cations

observed in the catalytic C–H borylation of aromatic C–H bonds.²³⁷ The reaction of the amine-borane with Tf₂NH generates a key intermediate R₃N–BH₂–NTf₂, which exists in equilibrium with the B–H–B bridged dimer responsible for C–H borylation. It is important to note that the use of TfOH did not result in the formation of the B–H–B bridged dimer and instead resulted in the formation of a tetracoordinate analogue of the reactive intermediate, preventing the borylation reaction.^{237, 238} The difference in reactivity between Tf₂NH and TfOH can be explained by the unique transoid structure of [Tf₂N][–] which makes it a significantly weaker coordinating anion relative to TfO[–].²³⁸

4.1.2 Boron Hydrides in Dihydrogen Bonding

Dihydrogen bonding is classified as a type of inter- or intramolecular interaction in which a hydrogen atom bonded to a relatively less electronegative atom can act as a proton acceptor.

In the 1960s, Burg reported close contacts between B–H and N–H bonds in $(\text{CH}_3)_2\text{NH}\cdot\text{BH}_3$ (liquid) and suggested N–H \cdots H–B hydrogen bonding type intermolecular interactions based on the N–H and B–H bands in the IR spectrum.²³⁹ Kozlovski and co-workers attributed the chemical reactivity of amine-boranes towards H_2 loss to the “close spatial arrangement of the oppositely charged hydrogen atoms”.²⁴⁰ While these reports suggested intermolecular interactions between the positively and negatively charged hydrogen atoms, it was in the late 1960s that M. P. Brown and co-workers proposed the formation of a novel type of hydrogen bond in which the BH_3 and BH_2 groups acted as proton acceptors despite their lack of lone pairs or π electrons.^{241, 242} Such interactions were observed in the IR spectrum of boron coordinated compounds such as $\text{BH}_3\cdot\text{L}$ (L = Me_3N , Et_3N , Py, Et_3P) and of $\text{BH}_2\text{X}\cdot\text{NMe}_2$ (X = Cl, Br, I) in the presence of proton donors such as methanol and phenol.⁹⁹

Stankevich and co-workers also showed that B–H bonds can act as proton acceptors and form dihydrogen bonds.²⁴³⁻²⁴⁵ Their work showed that the unconventional dihydrogen bonding interactions between O–H \cdots H–B behave in a manner similar to classical hydrogen bonds and that the strength of the dihydrogen bonded interactions was found to be directly proportional to the proton donor acidity.

Intramolecular dihydrogen bonding can also exist as C–H \cdots H–B in amine-boranes with an adjacent C–H bond.²⁴⁶ Dihydrogen bonding interactions were found to be responsible for the stabilization of aminoboron-hydrides (**Figure 4.6**). The relatively small H–C–N exocyclic angles that were found adjacent to the B–H bonds in the complexes encouraged attractive forces between the α -carbon C–H and the hydridic atoms of the B–H bonds. C–H \cdots H–B interaction also played an important role in controlling and stabilizing the conformation of azacyclohexane-borane adducts.²⁴⁷ It was found that the BH_3 groups were always in an equatorial position which was a result of favorable attractive forces between the hydrides on boron and the positively charged H atoms on the α -carbon (**Figure 4.6**).

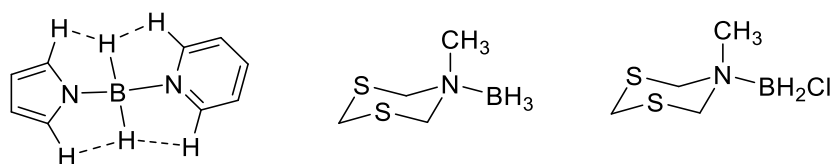


Figure 4.6 Aminoboron hydrides stabilized by C–H···H–B dihydrogen bonding

An interesting observation about intermolecular interactions of NHCs was made by Clyburne and co-workers.²⁴⁸ Clyburne reported an X-ray structure of an NHC borane where he observed a close intermolecular contact between hydrides of the B–H bond and the partially positive H of the C–H bond of a neighbouring imidazolylidene ring (**Figure 4.7**).

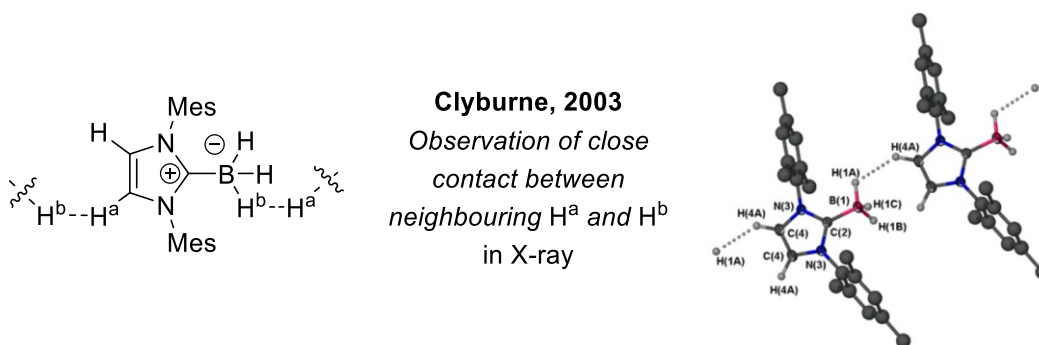


Figure 4.7 Intermolecular interactions of the C–H bonds of NHC-boranes

4.1.3 Proper vs. Improper Hydrogen Bonding

4.1.3.1 Proper Hydrogen Bonding

The ability of a hydrogen atom to generate attractive electrostatic interactions with another electron rich and electronegative atom has intrigued scientists ever since its discovery in the early 1900s.⁷⁷ Intermolecular interactions play an important role in determining the physical and chemical properties of matter. Hydrogen bonds (HBs) are considered the most important and strongest intermolecular interaction that is fundamental to life as it has evolved on Earth. They play an integral role in biological structures, conformational dynamics and are crucial in the life-sustaining properties of water.⁷⁸ Our genetic code is held together by hydrogen bonds which are responsible for the double helix structure of DNA (**Figure 4.8**).²⁴⁹ The hydrogen bonds holding the nucleotide base pairs together are strong yet weak enough to be disrupted and separate for the replication of DNA.

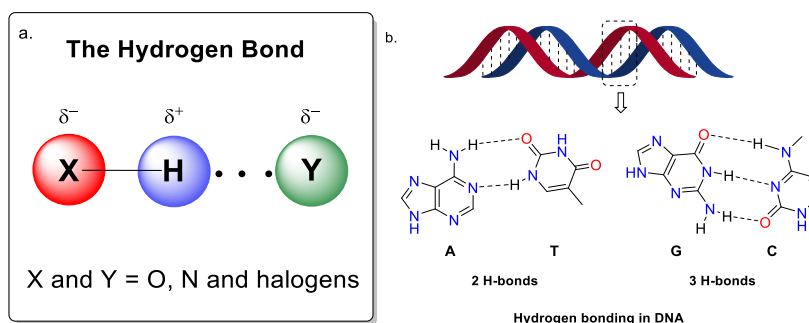


Figure 4.8 a. Depiction of hydrogen bond (HB) b. HBs in DNA

HBs are understood to be stronger than non-covalent interactions such as van der Waals forces yet weaker than a conventional covalent or ionic bond.⁸⁰ The concept of H-bonding dates back to 1912 when Moore and Winmill explained the weaker basic properties of trimethylammonium hydroxide in comparison to the basic properties of tetramethylammonium hydroxide.²⁵⁰ In 1920, Latimer and Rodebush suggested that the formation of binary complexes such as $\text{H}_2\text{O}-\text{H}_2\text{O}$ or $\text{H}_2\text{O}-\text{NH}_3$ was due to the fact that ‘the hydrogen nucleus held between two octets constitutes a weak bond’.⁷⁹ In both reports, the interactions were not referred to as hydrogen bonding interactions. It was only in 1931 that Linus Pauling credited Latimer and Rodebush’s work as the first report of hydrogen bonding in his famous book ‘The Nature of the Chemical Bond’.^{79, 82} Citations of their report remained scarce for decades until it was discovered that base pairs in DNA are bound by hydrogen bonds.²⁴⁹ While thousands of papers have since been published discussing hydrogen bonds, it has been difficult to propose generalities and principles about them until recent years.⁷⁸ Fortunately, computational studies combined with experimental data have stimulated discussions and debates that have led to a simple depiction of the structure of hydrogen bonds. A hydrogen bond can be represented as $\text{X}-\text{H}\cdots\text{Y}$, where the three dots indicate the HB. In a conventional HB, the X and Y atoms are electronegative atoms such as O, N, and halogens.⁹⁹ The X–H bond is a covalent bond in which the X atom, also known as a ‘hydrogen bond donor’ (HBD), has a high affinity for electron density causing the H atom to take on a slight positive charge. The electronegative Y atom is known as a hydrogen bond acceptor (HBA) and typically has a lone pair that can attract the positively charged H atom. The attraction between H and Y leads to the lengthening of the X–H bond and the high affinity of both X and Y for electron density leads to a hydrogen-bonded bridge between X and Y forming the classic

hydrogen bond structure X–H···Y. Infrared (IR) spectroscopy has become the norm for studying hydrogen bonding. HBs lead to significant changes in the IR spectrum causing a substantial red shift in the order of magnitude of hundreds of cm^{-1} as well as an increase in the IR intensity of the bands related to the vibrational modes of functional groups directly involved in the hydrogen-bonded bridges.²⁵¹

4.1.3.2 Improper Hydrogen Bonding

For a conventional hydrogen bond, the lengthening of the X–H bond can be explained by the population of the empty σ^* orbital of the X–H bond by the electronegative atom Y. As expected, an increase in the electronegativity of X leads to a better interaction between H and Y and an increase in the red shift. It was reasoned that a decrease in the electronegativity of X would lead to a less polarized X–H bond and a smaller red shift. Therefore, scientists were left puzzled when a blue-shift was observed for a $\text{F}_3\text{C–H}$ bond in the presence of an electron donor Y (where $\text{Y} = \text{H}_2\text{O}$).²⁵² While carbon is not an electronegative atom, C–H···Y–H bonding has received significant attention due to its contribution in chemistry and biology. The concept of C–H···Y dates back to 1935 when Kumlar explained that HCN is a liquid due to the weak association of the HCN molecules via C–H···N interactions.⁸⁸ In a span of two years, Glasstone and Pauling reported the existence of C–H···Y interactions to explain atypical physical properties of some liquids.⁸⁸ They used X-ray crystallography to study C–H···Y bonding in which the shortening of the C–H bond was observed. An initial study of such C–H···Y interactions was published in 1962 by Sutor where she reported frequent short distances between the C atom of the C–H bond and the O atom of the neighbouring molecule.^{253, 254} Her analysis was widely criticized by the scientific community who questioned the accuracy of her crystallography experiments in deducing the distance between the C–H bond and the O atom. Such apprehensions were put to rest in 1982 when Taylor and Kennard used high resolution neutron diffraction data to firmly establish the presence of C–H···Y interactions and since then many other chemists have reported such interactions.²⁵⁵ It was found that this HB is weaker than the conventional HB yet capable of providing structural rigidity or secondary stabilization in a system.²⁵⁶ C–H···Y bonds are known to play a critical role in determining the structure of several important biological molecules and in providing 3D structure to many organic and inorganic supramolecular complexes, as well as in molecular recognition and

enzymatic catalysis.²⁵⁶⁻²⁶¹ Moreover, Lai and co-workers calculated that an average of 17% of the total stabilization across 469 protein-protein complexes was contributed by C–H...O HB interactions and in some instances the contribution was found to be as high as 40-50%.²⁶²

4.1.3.3 Proposed Theories to Explain Improper Hydrogen Bonding

Typically, the C–H that participates in C–H...Y interactions is activated due to the presence of an electron withdrawing group (C=O, –NH–) adjacent to it.²⁵⁶ As mentioned above, the formation of a hydrogen bond between X–H and Y results in the lengthening of the X–H bond which shows up in the IR spectra as a red shift and an increase in the intensity of the IR stretch (**Figure 4.9**, a). It is well established now that apart from the conventional HB, a different category of weak bond interactions exists between H and Y which leads to X–H bond shortening. The X–H bands in such interactions are observed in the IR spectra with reduced intensity and are blue shifted. Initially classified as 'anti' hydrogen bonds, C–H...Y interactions were later termed as 'improper hydrogen bonds' since the use of the word 'anti' incorrectly implied that the interaction was destabilising. Since the role of C–H...Y interactions has been widely established in several biological systems, it is important to understand the nature of improper hydrogen bonds and develop a comprehensive understanding of the factors contributing to the shortening of C–H bonds in C–H...Y interactions. Several computational chemists have proposed explanations for improper HBs but five theories have gained the most traction albeit with limitations of their own.⁸⁹

(i) A Tug of War Between Hyperconjugation and Rehybridization

Weinhold and co-workers proposed rehybridization at X of the X–H...Y bond as a theory to explain the shortening of the X–H bond.²⁵² Bent's rule states that an atom will have an enhanced 's' character if its orbital is directed towards a more electropositive substituent.²⁶³ In the hydrogen bond, X–H...Y, the hydrogen atom tends to become electropositive as it is attached to a significantly more electronegative element. Based on Bent's rule, it follows that an increase in electropositivity of hydrogen in X–H will lead to an increase in the 's' character and the rehybridization of the X hybrid orbitals of the bond. An increase in 's' character of X–H will result in the shortening of the X–H bond. However, the hyperconjugative transfer of the electron density

from Y to the σ^* orbital of X–H can lead to the lengthening of the X–H bond. In a proper hydrogen bond the hyperconjugative interaction dominates leading to the lengthening of the bond and a red shift in the IR spectrum. For an improper hydrogen bond, rehybridization dominates over the hyperconjugative interaction leading to the shortening of the X–H bond and resulting in the reduced intensity and blue shift of the corresponding bands in the IR spectrum.

(ii) Short-Range Repulsive Forces

Schlegel and co-workers proposed that the X–H bond contraction in improper hydrogen bonds is a result of the domination of short-range Pauli repulsion forces over the attractive electrostatic interactions between positively charged H and hydrogen bond acceptor, Y.²⁶⁴ The attractive electrostatic force between H and Y will lead to an increase in the bond length of X–H but at the equilibrium geometry of a complex the repulsive forces can also come into play which can shorten the X–H bond and lead to a blue shift. Hobza et al. have published many reports that have also reasoned that to increase the stabilizing dispersion interaction, the H atom can come too close in contact with Y causing the short-range repulsive force to come into play leading to the shortening of the X–H bond.^{265, 266}

(iii) Role of Electric Field

Under the presence of a weak negative electric field, molecules that have a negative dipole derivative along the X–H bond undergo bond shortening as well as a blue shift in the IR spectrum. Therefore, chemists have proposed models where the electron donor Y exhibiting a negative electric field can result in X–H bond shortening in certain complexes such as F_3C-H and H_3C-H .

267-269

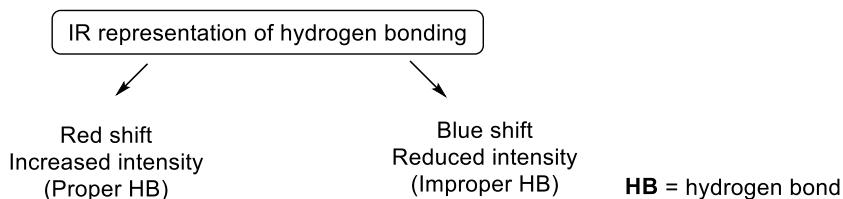
(iv) Redistribution of Electron Density

Hobza reported, on the basis of natural bond orbital (NBO) analysis, that for some improper HBs the electron density in the σ^* orbital of the X–H bond increases only slightly or can even decrease.^{85, 270-272} The analysis indicated that a substantial amount of electron density was transferred from Y to the orbitals of other atoms bonded to X and not to σ^* orbital of X–H. It was reasoned that the redistribution of electron density of the system will lead to an internal rearrangement resulting in a geometrical change and X–H bond contraction.

(v) Interplay of Contracting and Lengthening Forces

Jemmis and co-workers proposed that hydrogen bonds could be classified as proper or pro-improper bonds depending on the electronegativity of X in X–H...Y interactions (**Figure 4.9, b**).⁸⁹ They theorized that both types of hydrogen bonds (proper and improper) can be explained based on the interplay of bond contracting and lengthening forces. The high electron affinity of X in an X–H bond causes a shift of electron density towards X. When Y approaches, the X–H bond is further polarized due to the interaction of electropositive H with Y. The polarization of the X–H bond leads to a contraction of the bond length and a blue shift in the IR spectrum. However, there is a counteracting lengthening force at play due to the interaction between electropositive H and Y. Potential energy scans showed that when X is a highly electronegative element such as F, O, N etc. the lengthening force dominates the contracting force and a bond lengthening, or a red shift is observed as is the case for proper HBs. However, if the X–H bond is less polar, as is the case in C–H bonds, the nature of the electron donor Y becomes the deciding factor. If Y is a weak HBA then the contraction force will dominate leading to a bond shortening whereas if Y is a strong HBA then the lengthening force will dominate.

a. IR trends of HB



b. Proposed theory of Jemmis and co-workers to explain proper and improper HBs

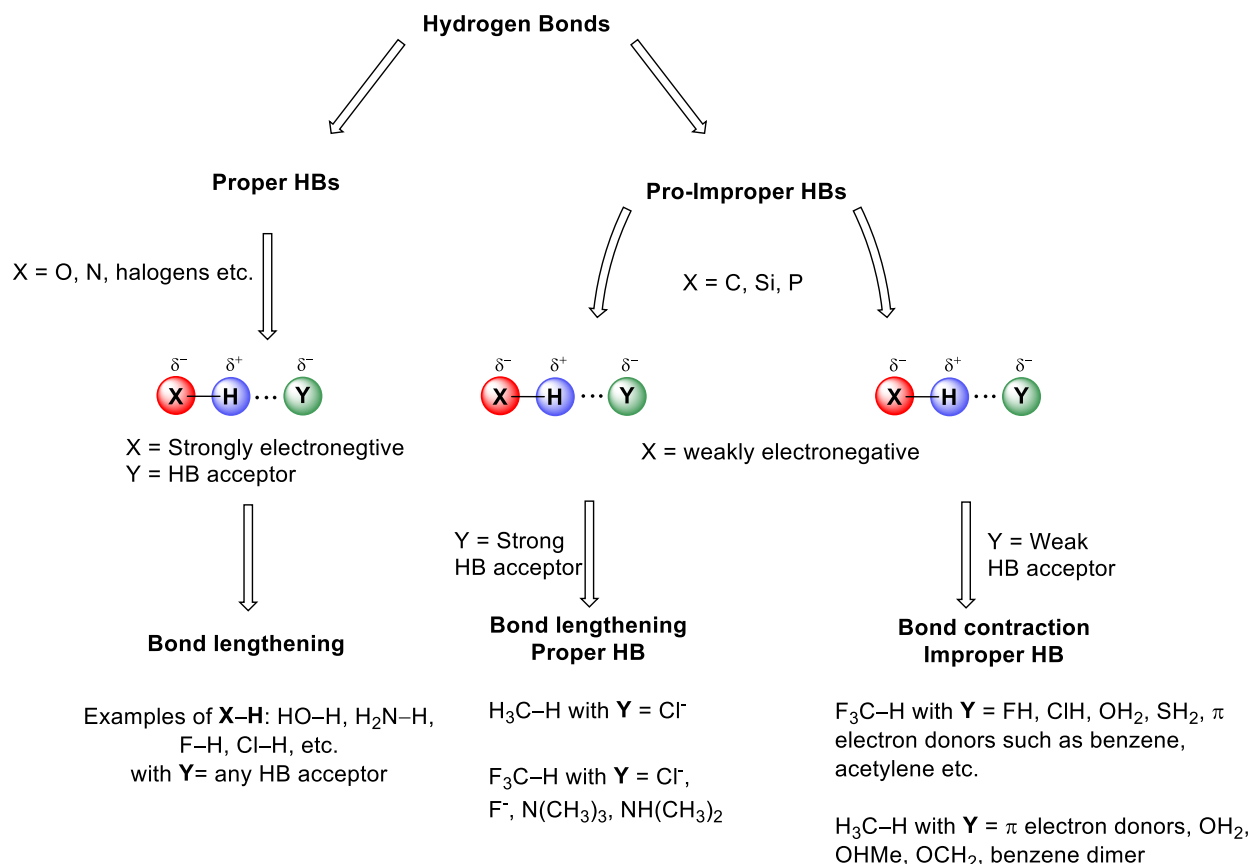


Figure 4.9 a. IR trends of HB and b. Summary of proper and pro-improper hydrogen bonds based on Jemmis and co-workers

4.1.4 Research Goals

As discussed above, strong acids can react with amine-boranes to form transient intermediates as well as stable borenium salts. The spirocyclic amine-boranes (SCABs) presented in the previous chapter represent a new class of amine-boranes wherein a boron hydride is present adjacent to a nitrogen spiroatom. One of the most studied reactions of Lewis base

complexes of boranes is the hydroboration reaction. NHC-boranes can undergo a variety of reactions but are inert to hydroboration reactions. Vedejs and co-workers showed that NHC-borane upon reaction with a strong acid such as Tf₂NH generates a NHC-borenium ion, which is isoelectronic with free borane and a 'super Lewis acid', capable of hydroborating alkenes.²⁰⁷ Given the reactivity of NHC-boranes in the presence of strong acids and their potential to function as reagents for hydroboration and C–H borylation reactions, we were interested in exploring the reactivity of SCABs with strong acids such as Tf₂NH. The reaction of SCAB and diphenylacetylene did not yield the hydroborated product. We wondered if we could react SCAB with Tf₂NH to generate a borenium cation species that would be capable of activating unsaturated C–C bonds as well as other functional groups.

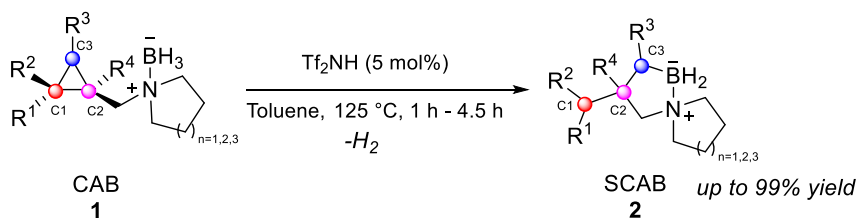
4.2 Understanding the Structure and Reactivity of a Spirocyclic Amine-Borane (SCAB) and Tf₂NH Complex: SCAB•NTf₂ Complex (3)

4.2.1 Introduction

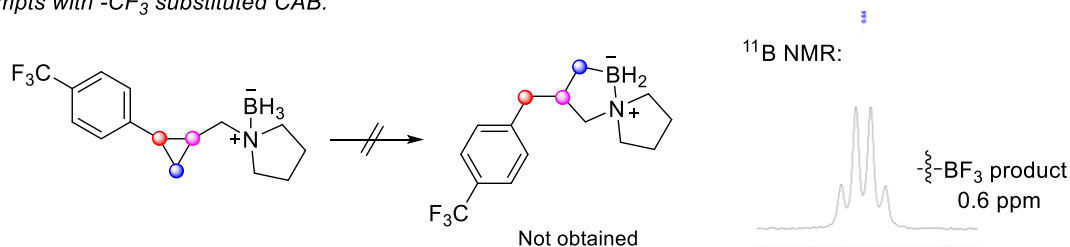
In the previous chapter, I reported the ring-opening of cyclopropane amine-boranes **1** (CABs) in the presence of a catalytic amount of Tf₂NH to generate novel spirocyclic amine-borane **2** (SCABs) motifs (**Figure 4.10**, i). The formation of SCAB was a result of an intramolecular C–C bond activation by a borenium cation formed by reacting CAB with Tf₂NH. The method tolerates a wide range of functional groups, and most of the SCAB motifs were obtained in quantitative yields. However, when exploring the scope of the reaction we realized that the method was not compatible with CF₃ substituted CAB motifs. When the reaction was attempted with a CF₃ substituted CAB, the ¹¹B NMR spectrum indicated the formation of SCAB as well as products containing B–F bonds (**Figure 4.10**, ii). Typically, the reaction of CABs with Tf₂NH provides a clean conversion to SCABs and therefore when a mixture of products was obtained for one specific substrate it led us to presume the ability of borenium cations to activate C–F bonds. Since SCAB itself does not have any strained C–C bonds that could be activated, we theorized that SCAB **2a** could react with Tf₂NH to form a reactive borenium cation capable of activating C–F bonds. To test our theory, we mixed Tf₂NH and SCAB **2a** in a stoichiometric ratio in benzene followed by the

addition of 1 equivalent of trifluorotoluene and heated the reaction mixture at 65 °C for 1 h. The reaction of Tf₂NH and SCAB **2a** resulted in the rapid evolution of hydrogen gas. NMR analysis of the crude reaction mixture showed the formation of a SCAB-F₂ motif (**Figure 4.10**, iii). We were interested in understanding the structure and reactivity of the SCAB•NTf₂ complex and therefore we conducted several spectroscopic studies in the form of variable temperature NMR experiments, as well as infrared and Raman spectroscopy.

i. Previous work: Unactivated CABs to Spirocyclic Amine-boranes



ii. Attempts with -CF₃ substituted CAB:



iii. Initial attempts to activate C–F bonds using SCAB

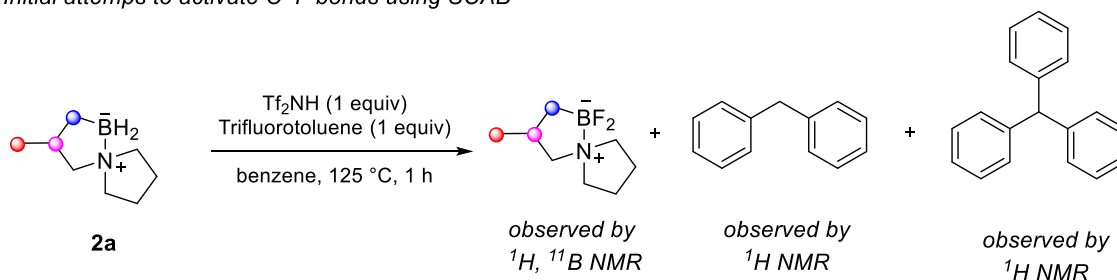
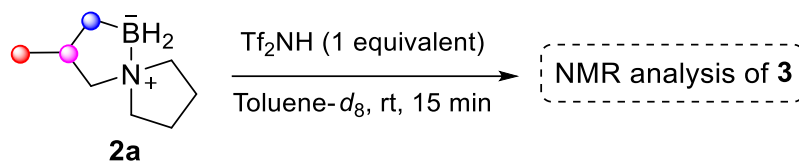


Figure 4.10 Development of the theory of C–F bond activation via SCAB borenium cations

4.2.2 Results and Discussion

4.2.2.1 Analysis of SCAB•NTf₂ by NMR Spectroscopy

A sample of SCAB•NTf₂ complex **3** was prepared by adding SCAB **2a** to a vial followed by the addition of Tf₂NH (1 equivalent). To the vial was added toluene-*d*₈ and the mixture was stirred for 15 minutes at room temperature (Scheme 4.4).



Scheme 4. 4 NMR tube sample of SCAB•NTf₂

After 15 minutes the mixture was transferred to an NMR tube and the sample was characterized by NMR spectroscopy. The ¹H NMR spectrum of the SCAB•NTf₂ complex **3** resulted in very broad signals compared to the well-resolved ¹H NMR spectrum of SCAB **2a** (Figure 4.11).

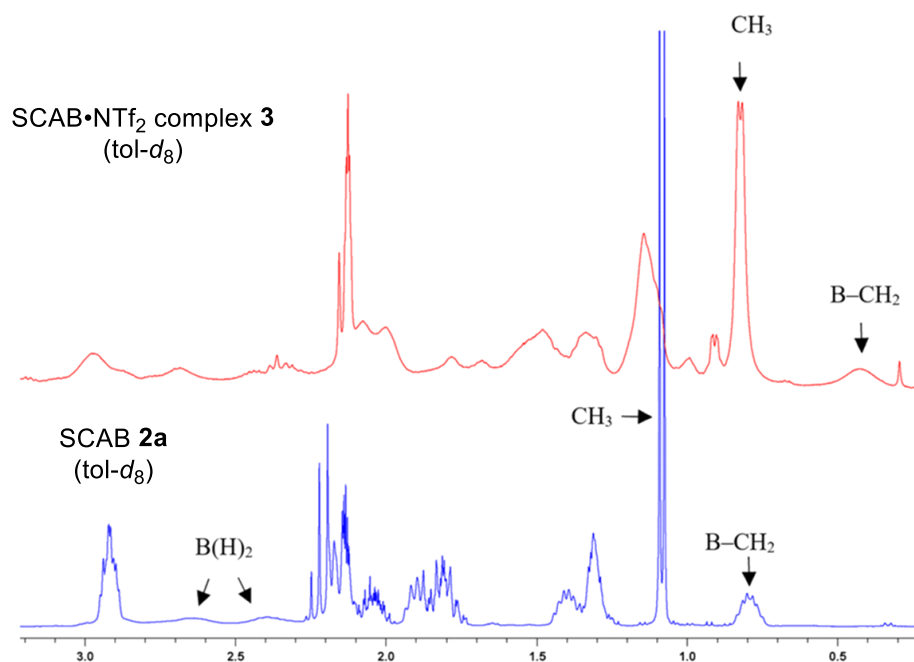


Figure 4.11 ¹H NMR (toluene-*d*₈) spectra of a. SCAB•NTf₂ complex **3** vs. b. SCAB **2a**

The reaction of Tf₂NH with boranes has been extensively studied in literature and the reaction typically leads to the evolution of hydrogen gas accompanied by the formation of

borenium cation species capable of hydroboration and C–H borylation reactions.^{97, 195, 211, 237} Vedejs and co-workers conducted NMR experiments to study the species formed after mixing an aliphatic amine-borane with catalytic and stoichiometric amounts of Tf₂NH (**Figure 4.12, a**).¹⁹⁵ In both cases, they observed the evolution of hydrogen gas. When a catalytic amount of Tf₂NH was used they observed the formation a B–H–B bridged dimer as well as B–N and B–O isomers that formed with [Tf₂N]⁻; however, when a stoichiometric amount of Tf₂NH was added, they observed the formation of the B–N and B–O isomers but no B–H–B bridged dimer was observed (**Figure 4.12, b**). It is to be noted that the C–H borylation reaction did not work when a stoichiometric of Tf₂NH was used.

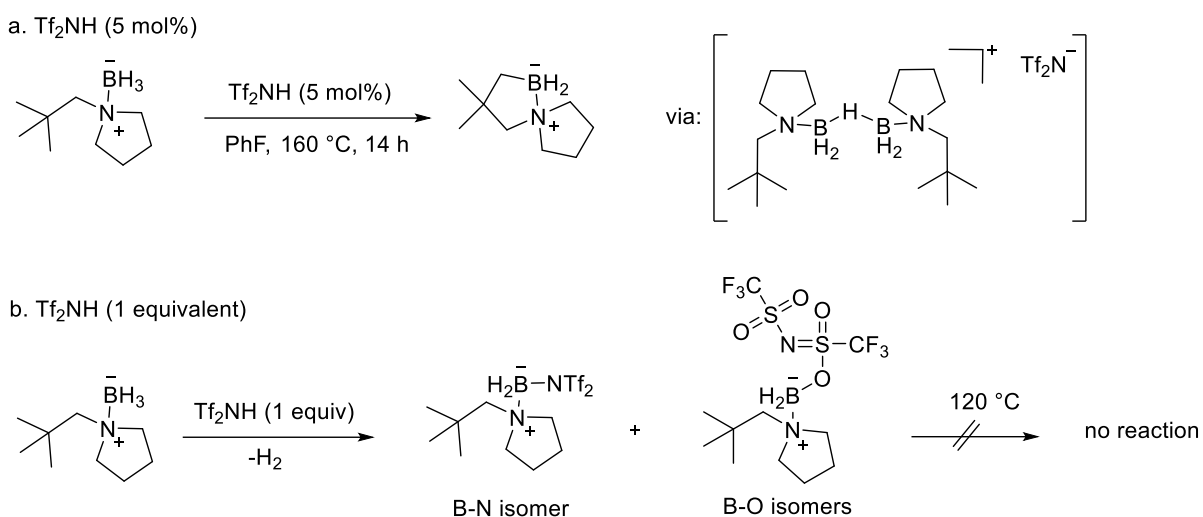
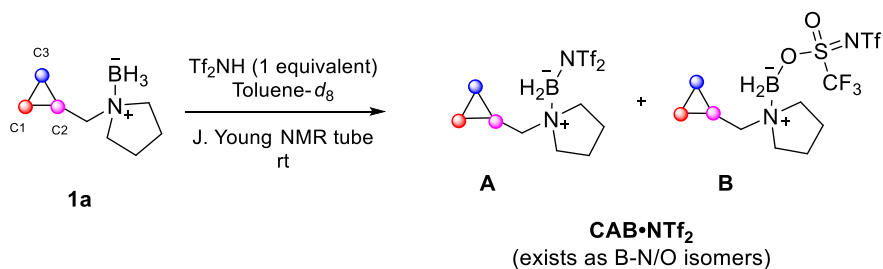


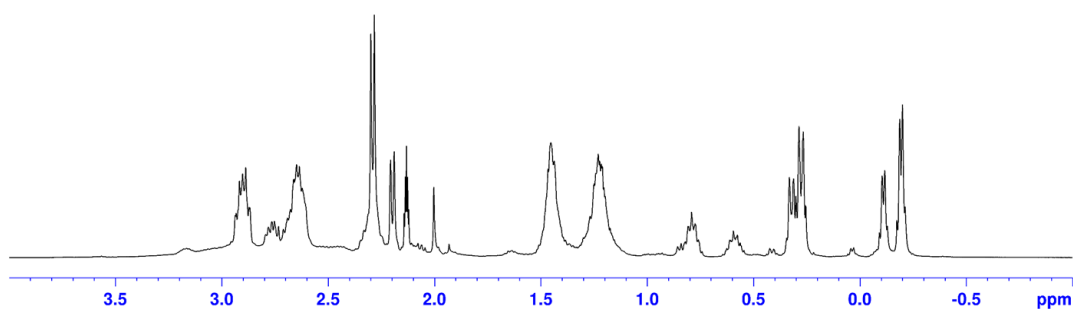
Figure 4.12 *N*-Directed aliphatic C–H borylation using borenium cation equivalents

The results reported by Vedejs and co-workers are to be expected since the reaction between Tf₂NH and a B–H bond will lead to a highly Lewis acidic boron (post the formation of hydrogen gas) which will have a high affinity for [Tf₂N]⁻. We conducted a similar experiment with an amine-borane **1a** prepared in the previous chapter (**Scheme 4.5**). When Tf₂NH (1 equivalent) was added to CAB **1a**, we also observed the formation of hydrogen gas and the expected B–N and B–O isomers (**Figure 4.13**).



Scheme 4. 5 Analysis of CAB **1a**:Tf₂NH (1:1) mixture

CAB•NTf₂ (1:1)



SCAB•NTf₂ (1:1) complex
3

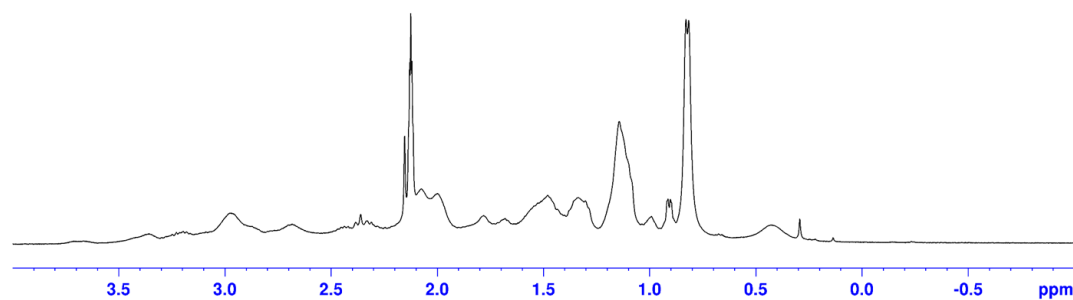
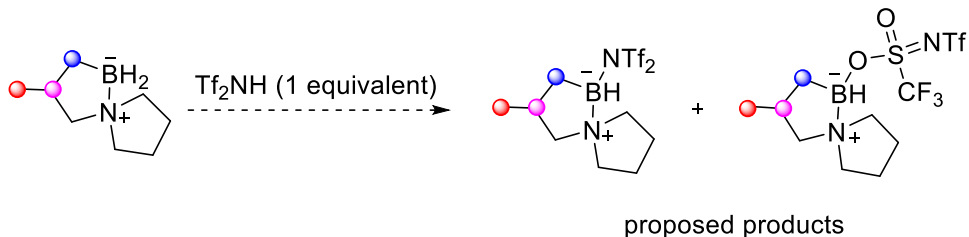


Figure 4.13 Comparison of CAB•NTf₂ (1:1) vs. SCAB•NTf₂ (1:1)

Since we added 1 equivalent of Tf₂NH to SCAB **2a** we expected to see the formation of the two isomers resulting from Tf₂N-bound SCAB in the form of B–N and B–O isomers (**Scheme 4.6**).



Scheme 4. 6 Expected products of reaction of SCAB (1 equivalent) with Tf_2NH (1 equivalent)

Indeed, the ^{11}B NMR and ^{19}F NMR spectra show the presence of B–N and B–O isomers among other unexpected signals. Also, the broad ^1H NMR spectrum obtained for $\text{SCAB}\cdot\text{NTf}_2$ does not match with the NMR spectra reported in literature for B–N/O isomers nor that of the B–H–B bridged dimer and therefore the possibility of a different reactive intermediate was explored.

Typically, broad signals in a ^1H NMR spectrum are attributed to an exchange of protons due to inter- or intramolecular interactions such as hydrogen bonding.²⁷³ However, we were surprised by the broad peaks in the ^1H NMR spectrum of $\text{SCAB}\cdot\text{NTf}_2$ since there are no obvious sites for hydrogen bonding. Most of the peaks in the ^1H NMR spectrum of $\text{SCAB}\cdot\text{NTf}_2$ can be assigned to a C–H proton but C–H protons do not usually undergo hydrogen bonding (**Figure 4.14**).

SCAB•NTf₂ (1:1) complex
3

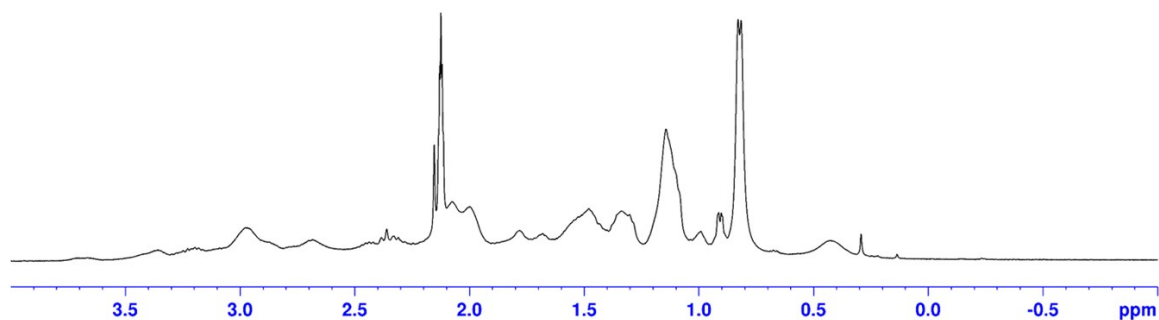


Figure 4.14 ^1H NMR spectrum ($\text{Tol}-d_8$) of $\text{SCAB}\cdot\text{NTf}_2$

The diastereotopic CH_2 α to the boron shows up as two broad signals at 0.43 ppm and 1.14 ppm in toluene- d_8 and were confirmed by NMR correlation analysis via ^1H - ^1H -COSY and ^1H - ^{13}C

HSQC. $[\text{Tf}_2\text{N}]^-$ is a very weak LB and its unique weakly-coordinating nature has been exploited for a wide range of chemical transformations.²³⁸ Despite $[\text{Tf}_2\text{N}]^-$ being a very weak conjugate base, as discussed above, we should still expect it to bind to a highly Lewis acidic boron and form B–N and B–O isomers at room temperature which would be observed in the ^1H NMR spectrum as sharp signals. When SCAB (1 equivalent) was reacted with TfOH (1 equivalent), we observed sharp signals in the ^1H NMR spectrum along with the evolution of hydrogen gas (**Figure 4.15**). Therefore, the unusual ^1H NMR spectra obtained for the SCAB• NTf_2 complex is puzzling. An acid screening was done to study whether a SCAB•X complex can be formed with mild and more commonly used organic acids such as acetic acid, formic acid, TFA and TfOH (**Figure 4.15**). In the case of acetic acid, benzoic acid and formic acid, the ^1H NMR spectrum shows that the SCAB **2a** remained intact. When SCAB **2a** was reacted with TFA/TfOH, the ^1H NMR spectrum showed a mixture of SCAB **2a** and a product with sharp signals which can be assigned to the dehydrogenated product in which boron is bound to the conjugate base of the acids. The lack of any broad signal in these ^1H NMR spectra rule out the possibility of polarized C–H bonds undergoing hydrogen bonding as is the case for SCAB• NTf_2 (**Figure 4.15**).

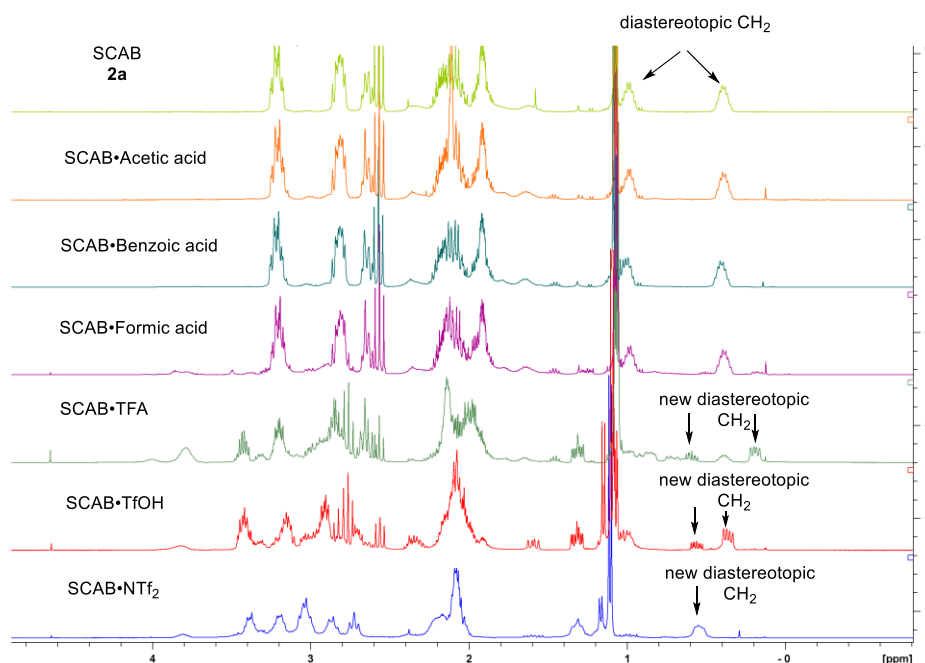


Figure 4.15 ^1H NMR (CD_2Cl_2) spectra of acid screening

4.2.2.2 Effect of Lewis Acidic Boron Adjacent to C–H Bonds

A significant difference between CAB **1a** and the aliphatic amine-borane used by Vedejs and co-workers versus SCAB **2a** is the presence of a C–B bond (**Figure 4.16**).

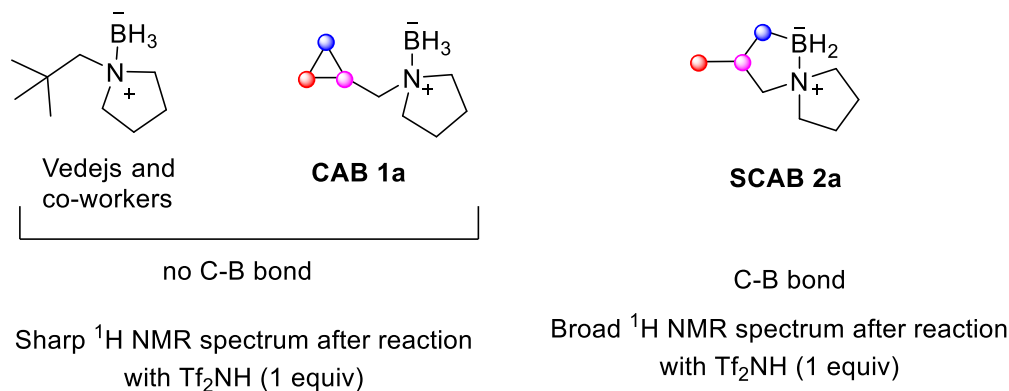


Figure 4.16 Unique C–B bond in SCAB

σ -C–H bonds adjacent to an atom that has a vacant p -orbital are well understood to undergo hyperconjugation.²⁷⁴ The participation of σ -C–H bonds in hyperconjugation is used to explain the enhanced stability of tertiary carbocations as compared to secondary carbocations. Tertiary carbocations have significantly more σ -C–H bonds available for hyperconjugation with the empty p -orbital of carbon as compared to secondary carbocations, making tertiary carbocations more stable (**Figure 4.17**).

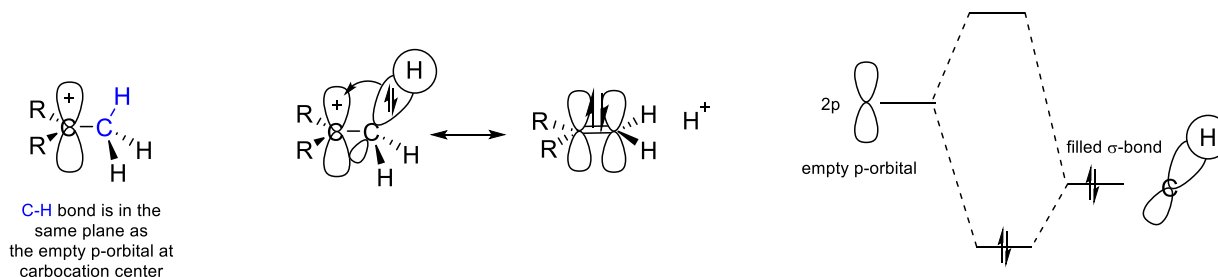
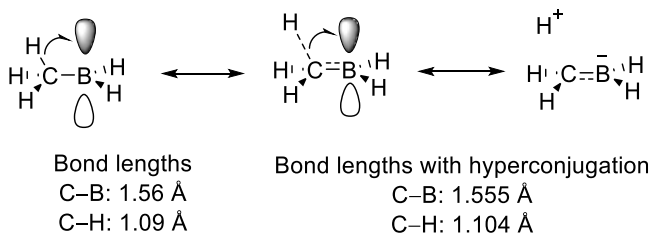


Figure 4.17 Hyperconjugation in the ethyl cation

Methyl boranes are isosteres of the ethyl carbocation and have attracted significant attention as candidates for studying hyperconjugation.²⁷⁴⁻²⁷⁹ In methyl boranes, the Lewis acidic boron contains an empty p -orbital which has been shown to interact with a σ -C–H bond of the adjacent carbon atom (**Figure 4.18**, i). Although the hyperconjugative interaction observed in

methyl boranes is less than that in carbocations, it is still presumed to play an important role in the structure of methyl boranes.²⁷⁵ Hyperconjugation in methyl boranes leads to the lengthening of the σ -C-H bond due to the delocalization of the σ -C-H electrons and shortening of the C-B bond due to a partial double bond character (**Figure 4.18, i**).²⁷⁴ Such hyperconjugation of C-H bonds can also be observed in σ -C-H bonds adjacent to phosphine and sulfur (**Figure 4.18, ii**).

i. Hyperconjugation in methyl boranes



ii. Hyperconjugation in phosphorous and sulfur containing systems

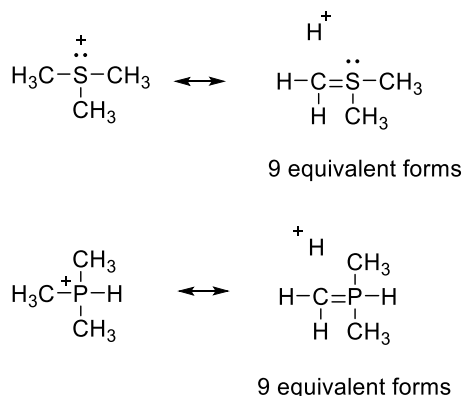


Figure 4.18 Examples of hyperconjugation

The reaction of SCAB (1 equivalent) with Tf_2NH (1 equivalent) will result in a Lewis acidic boron adjacent to a CH_2 group. Therefore, it is reasonable to propose that the C-H bond α to the Lewis acidic boron could participate in hyperconjugation with the empty p -orbital of the Lewis acidic boron. Invoking hyperconjugation in the C-H bonds of the CH_2 α to the Lewis acidic boron would explain the broad ^1H NMR spectrum observed for the $\text{SCAB}\cdot\text{NTf}_2$ complex since hyperconjugation of the σ C-H bond (α to boron) would lend them an acidic character. Due to the acidic nature of the C-H bond, an exchange of protons can occur within the system leading to broad ^1H NMR signals. The hyperconjugative interaction of the sigma C-H bond with the empty p -orbital of boron can potentially quench the Lewis acidity of boron. Despite the Lewis acidity of

boron having been quenched to a certain extent by the C–H bond, $[\text{Tf}_2\text{N}]^-$ can still potentially bind to boron since the hyperconjugative interactions in methyl boranes are known to be weak.²⁷⁵ Therefore, it is safe to conclude that the Lewis acidity of boron has been quenched by hyperconjugative interactions as well as $[\text{Tf}_2\text{N}]^-$.

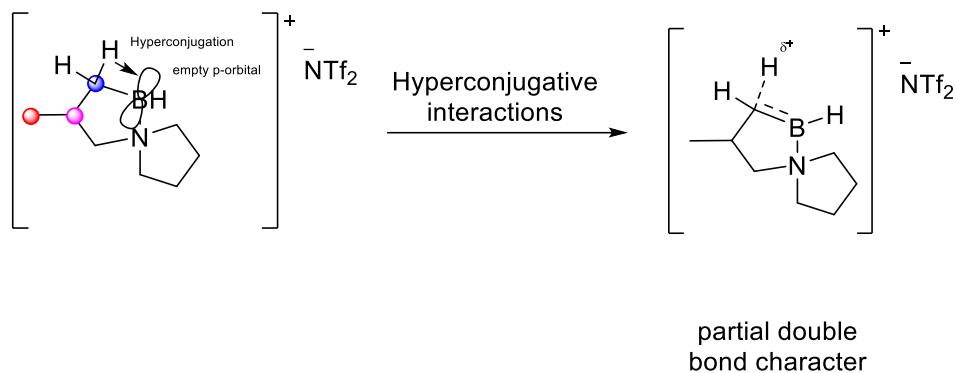


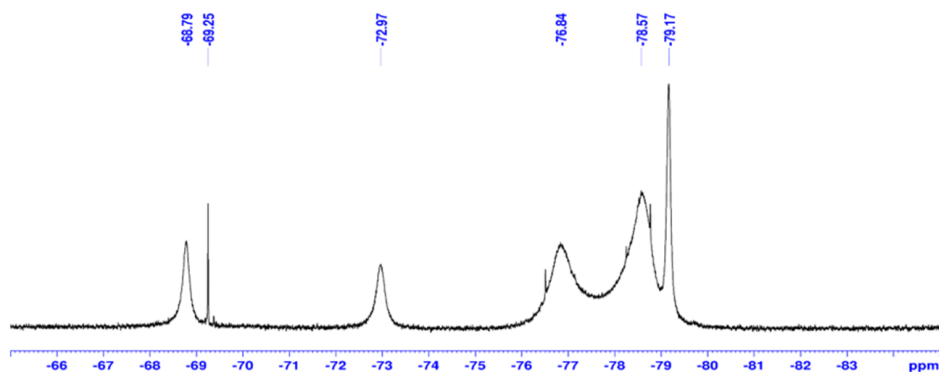
Figure 4.19 Hyperconjugative interactions in $\text{SCAB}\cdot\text{NTf}_2$

It is also important to note here that the reaction of **SCAB 2a** with Tf_2NH would lead to a stereogenic center at boron resulting in the formation of a set of diastereomers for both B–N and B–O isomers (**Scheme 4.6**). Moreover, the B–N/O bond in the $\text{SCAB}\cdot\text{NTf}_2$ complex **3** could be fluxional as well. The set of diastereomers and the fluxional B–N/O bond in the $\text{SCAB}\cdot\text{NTf}_2$ complex **3** could explain the broadness of its ^1H NMR spectrum. However, variable temperature NMR experiments discussed later in Section 4.2.2.5, where heating the $\text{SCAB}\cdot\text{NTf}_2$ complex **3** at temperatures >383 K results in the dissociation of $[\text{Tf}_2\text{N}]^-$ wherein boron is no longer a stereogenic center, yet the ^1H NMR spectrum obtained at 383 K is still broad, helped rule out the assertion that the formation of the diastereomers was leading to the broadness of the signals in the ^1H NMR spectrum of **3**.

Further evidence for weaker than expected interactions between $[\text{Tf}_2\text{N}]^-$ and the Lewis acidic boron in the $\text{SCAB}\cdot\text{NTf}_2$ **3** was provided by ^{19}F NMR analysis. If $[\text{Tf}_2\text{N}]^-$ preferred to bind strongly to the Lewis acidic boron then the ^{19}F NMR spectrum should have sharp signal for the corresponding isomer that form upon binding with $[\text{Tf}_2\text{N}]^-$. We expected the ^{19}F NMR spectrum to have a set of sharp signals corresponding to the B–N and B–O isomers and their corresponding diastereomers. For each diastereomer we expected to see one signal for the B–N isomer and two

signals for the B–O isomer accounting for the two inequivalent CF₃ groups.¹⁹⁵ However, we were surprised to see multiple broad signals in the ¹⁹F NMR spectrum at room temperature (**Figure 4.20, i**). We expected to see a doublet in the ¹¹B NMR spectrum for the B–H bond in the SCAB•NTf₂ complex **3**; however, the ¹¹B NMR spectrum showed two broad signals at 4.1 ppm and 9.9 ppm which can be attributed to the interaction between the Lewis acidic boron and [Tf₂N]⁻ (**Figure 4.20, ii**).

i. ¹⁹F NMR spectrum of SCAB•NTf₂ at rt



ii. ¹¹B NMR spectrum of SCAB•NTf₂ at rt

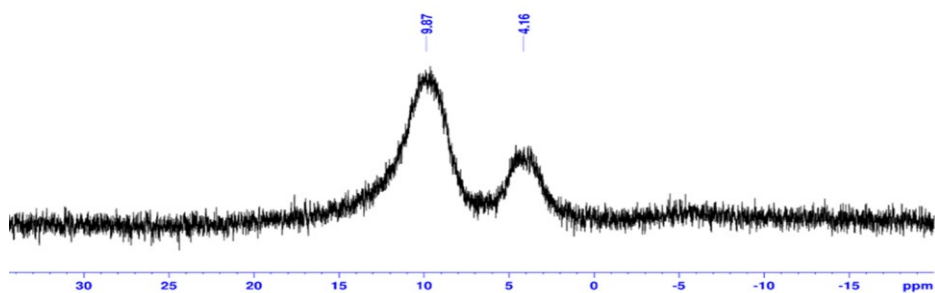


Figure 4.20 i. ¹⁹F NMR spectra of SCAB•NTf₂ at rt ii. ¹¹B NMR spectra of SCAB•NTf₂ at rt

[Tf₂N]⁻ itself is known to be a very weak conjugate base which results in its unique weak coordinating nature relative to other weak conjugate bases such as [TfO]⁻. In the case of SCAB:TfOH (1:1), [TfO]⁻ will bind to the Lewis acidic boron formed post the evolution of hydrogen gas and quench the Lewis acidity of boron. As mentioned above, the ¹H NMR spectrum of SCAB:TfOH (1:1) shows sharp signals as a result of the quenched Lewis acidity of boron due to the efficient binding of [TfO]⁻ to boron.²⁸⁰ The quenched Lewis acidity of boron would prevent

hyperconjugative interactions between the CH₂ adjacent to boron which would prevent the CH₂ adjacent to boron from developing an acidic character.

4.2.2.3 Studies to determine potential acidity of the C–H bonds in SCAB NTf₂

One way of determining whether an acidic proton is present on a compound is by doing H/D exchange experiments using D₂O. Known as a “D₂O shake”, a single drop of D₂O is added to an NMR tube containing the compound to be tested and an ¹H NMR spectrum is obtained. The deuterium present in D₂O rapidly exchanges with the acidic protons on the compound and their corresponding NMR signals disappear from the ¹H NMR spectrum. A ²H NMR experiment can also be done to observe the deuterium signals resulting from the H/D exchange.

We were curious to see what would happen if we added D₂O to the SCAB•NTf₂ complex. To a vial was added SCAB **2a** and Tf₂NH in a 1:1 ratio followed by toluene-*d*₈ and stirred for 15 minutes. After 15 minutes, an NMR was acquired to ensure the formation of the SCAB•NTf₂ complex **3**. To the NMR tube was then added a drop of D₂O and vigorous bubbling was observed. Once the bubbling stopped the sample was analyzed by NMR spectroscopy. We hoped to see an H/D exchange with the acidic proton in the substrate. However, we were surprised to see new signals in the ¹H NMR spectrum which showed that instead of just exchanging with the acidic proton, D₂O reacted with the SCAB•NTf₂ complex (**Figure 4.21**). The most obvious reaction pathway to consider upon the addition of D₂O to SCAB•NTf₂ complex **3** is the quenching of the Lewis acidic boron to form a B–O bond, however such an interaction would not lead to new signals in the ¹H NMR spectrum (**Figure 4.21**). The ¹H NMR spectrum of the SCAB•NTf₂ complex **3** after the D₂O shake had a new signal at 5.4 ppm (**Figure 4.21**). Signals appearing between 5-6 ppm are typically characteristic of vinylic protons. A potential reaction pathway for the formation of an alkene could be the abstraction of the C–H proton α to boron by D₂O leading to the transfer of electron density to the Lewis acidic boron followed by the formation of a carbon boron double bond and [D₂OH]⁺ as the byproduct. The signal at 5.4 ppm appears as a broad multiplet. A C–H proton adjacent to a boron atom typically appears as a broad signal due to the quadrupole nature of the boron nuclei. A ¹H–¹H COSY NMR analysis showed a correlation of the signal appearing at

5.4 ppm with a signal at 2.4 ppm which is where the C2-H proton typically appears. The signal at 2.4 ppm was confirmed to be a C–H proton by blue signal in the edited HSQC (which provides multiplicity information similar to that of a ^{13}C DEPT-135 sequence: blue = CH_3 or CH and green = CH_2) and to be a C2–H proton by ^1H – ^1H COSY NMR correlation which showed a signal for the correlation between itself and the C1– H_3 , which appears as a doublet at 1.37 ppm (^1H NMR). We also observed the formation of HD gas from a characteristic triplet (1:1:1) that appears at 4.5 ppm (**Figure 4.21**). HD gas can be a byproduct of the reaction between D_2O^+ and the B–H bond which can then be quenched with Tf_2N^- .

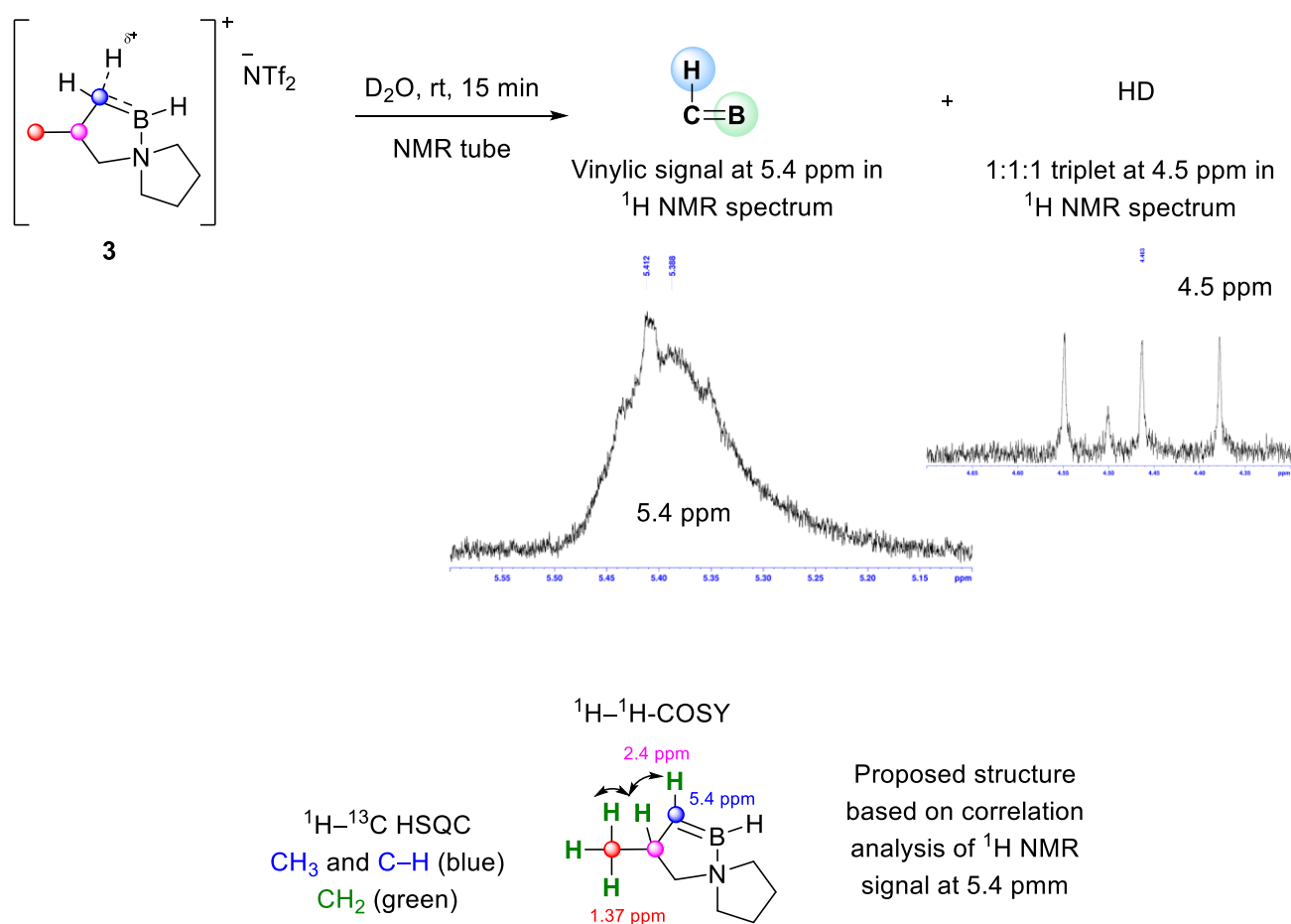


Figure 4.21 “ D_2O shake” of $\text{SCAB}\cdot\text{NTf}_2$

4.2.2.4 Analysis of $\text{SCAB}\cdot\text{NTf}_2$ by IR and Raman Spectroscopy

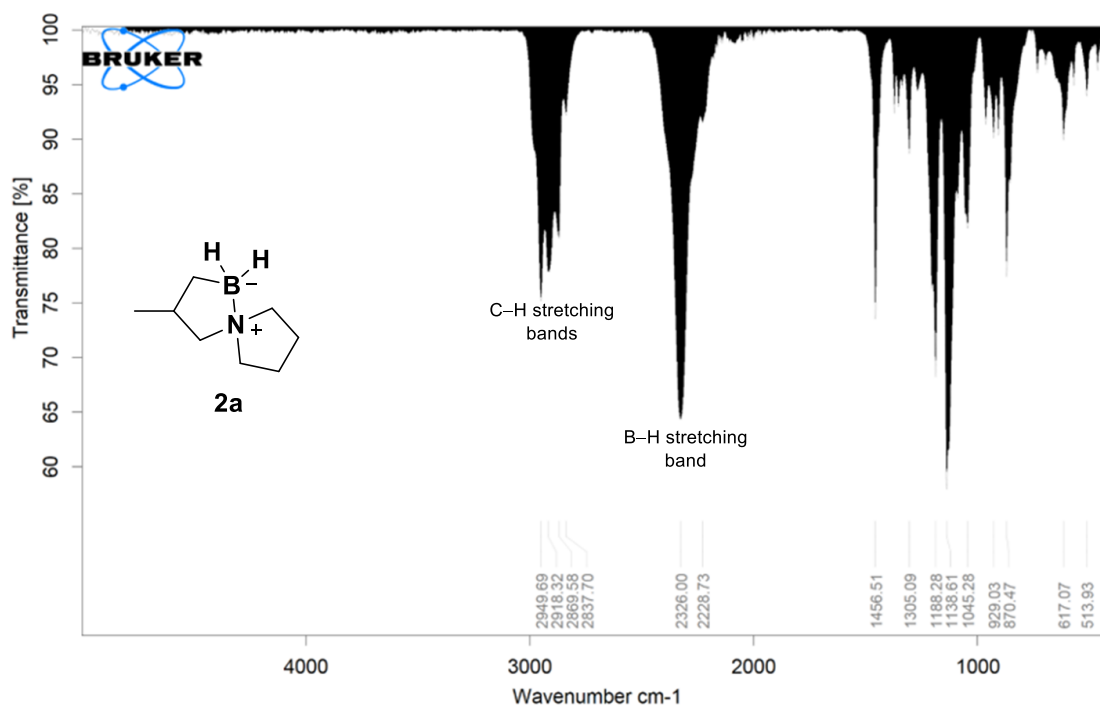
The IR spectrum of $\text{SCAB}\cdot\text{NTf}_2$ **3** was expected to be very similar to the IR spectrum of SCAB **2a** with respect to the C–H and B–H bands. In the IR spectrum of SCAB **2a**, the B–H stretching

bands can be seen at 2326 cm^{-1} , and we expected a B–H band to appear in the same region for the SCAB•NTf₂ complex as well (**Figure 4.22**, a) Therefore, we were surprised to see the absence of a B–H stretch between 2200 to 2500 cm^{-1} (**Figure 4.22**, b). Monoborohydride such as 9-BBN exist as dimers and the IR band of the B–H–B bridged dimer appears at 1567 cm^{-1} .²⁸¹ Therefore, it is likely that the B–H bond in the SCAB•NTf₂ complex exists as a B–H–B dimer as well and therefore the B–H band shifts to a significantly lower frequency.

In the IR spectrum of SCAB **2a**, several stretching bands for the multiple C–Hs on the SCAB **2a** motif at 2837 cm^{-1} , 2869 cm^{-1} , 2918 cm^{-1} , and 2949 cm^{-1} were observed (**Figure 4.22**, a). However, we were surprised to find that in the IR spectrum of SCAB•NTf₂, the intensity of the C–H bands was significantly reduced and that these bands were blue shifted to 2895 cm^{-1} , 2919 cm^{-1} , 2971 cm^{-1} , and 3170 cm^{-1} (**Figure 4.22**, b). The C–H bands mostly blue-shifted by a maximum of 20 cm^{-1} except the band at 3170 cm^{-1} which shifted by more than 200 cm^{-1} which implies that the C–H bonds in SCAB•NTf₂ might be undergoing varying degrees of improper hydrogen bonding depending on the polarization of the C–H bond. The reduced intensity and the blue shifting of the C–H bands implicates the hydrogen atom of the C–H bond in hydrogen bonding.⁸⁹ Typically, hydrogen bonding leads to a red shift in the IR spectra but in some cases hydrogen bonding in the form of X₃C–H...Y (X = F, or H and Y = Cl, F, O etc.) interactions can lead to a reduction in the intensity and cause a blue shift of the C–H bands.

Such an unusual interaction between a hydrogen atom of a polarized C–H bond and an electron donor is termed as an improper hydrogen bond.²⁵² In the case of SCAB•NTf₂, the carbon α to boron is not attached to any electronegative element but does have a highly Lewis acidic boron adjacent to it generated due to the reaction between the B–H bond of SCAB and Tf₂NH resulting in the evolution of hydrogen gas. As discussed above, the Lewis acidic boron can polarize the C–H bond via hyperconjugative interactions leading to a partial positive charge on the hydrogen atom which can then accept electron density from the bidentate [Tf₂N][−] leading to an improper hydrogen bond. Since the C–H bond α to boron would be undergoing hyperconjugative interactions as discussed above, we propose that it would undergo the maximum polarization and could be the most blue-shifted C–H band in the IR spectrum. Therefore, the band at 3170 cm^{-1} is attributed to the C–H α to boron (**Figure 4.22**, b).

a. IR spectrum of SCAB (2a)



b. IR Spectrum of SCAB•NTf₂ (3)

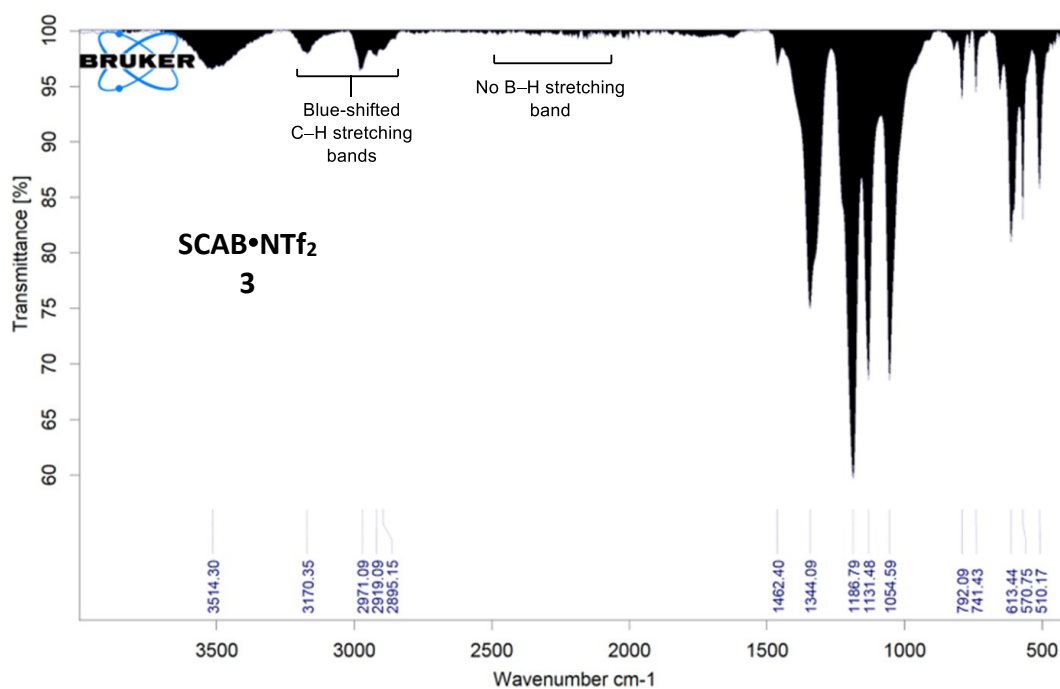


Figure 4.22 IR spectra of SCAB **2a** and SCAB•NTf₂ **3**

In the literature, a band appearing at $\sim 3170\text{ cm}^{-1}$ is attributed to an intermolecular hydrogen bond between an acidic C–H and [Tf₂N][−] in imidazolium-based ionic liquids.^{282, 283} The presence of acidic C–H bonds in imidazolium-based ionic liquids has led to a wide body of research to understand their reactivity towards proton abstraction from their C–H bond using a base followed by the addition of a electrophile (**Figure 4.23**, a).^{284, 285} Imidazolium-based ionic liquids are known to possess acidic C–H bonds at several different carbon positions on the imidazolium ring.^{284, 285} Such ionic liquids have been thoroughly studied via IR spectroscopy and a signal at 3170 cm^{-1} is well understood to be evidence of an intermolecular hydrogen bond in the form of C–H⋯X interactions between the most acidic C–H bond (C–H on C2) and anions such as [Tf₂N][−] (in the form of C–H⋯NTf₂) and [TfO][−] (in the form of C–H⋯OTf) (**Figure 4.23**, b).^{282, 283} Therefore, the emergence of a new band at 3170 cm^{-1} in the SCAB•NTf₂ complex is an indication of the acidity of its C–H bonds and the presence of a (C–H⋯NTf₂) interaction (**Figure 4.23**, c).

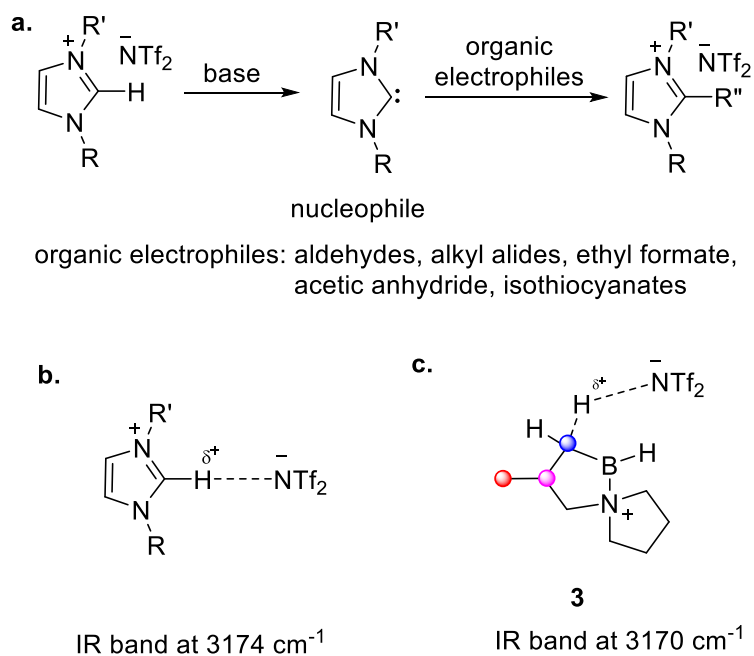


Figure 4.23 a. Formation and reactivity of imidazolium carbene b. IR and of C–H⋯NTf₂ interaction of acidic imidazole C2–H and [Tf₂N][−] c. Possible C–H⋯NTf₂ interaction in SCAB•NTf₂ **3** complex

Raman spectroscopy experiments for SCAB•NTf₂ also corroborated the results obtained from IR spectroscopy and showed reduced C–H bands in SCAB•NTf₂ as compared to the Raman spectrum obtained for SCAB **2a**. There were also no bands observed for the B–H bond in the expected region of 2200-2500 cm⁻¹ (**Figure 4.24**).

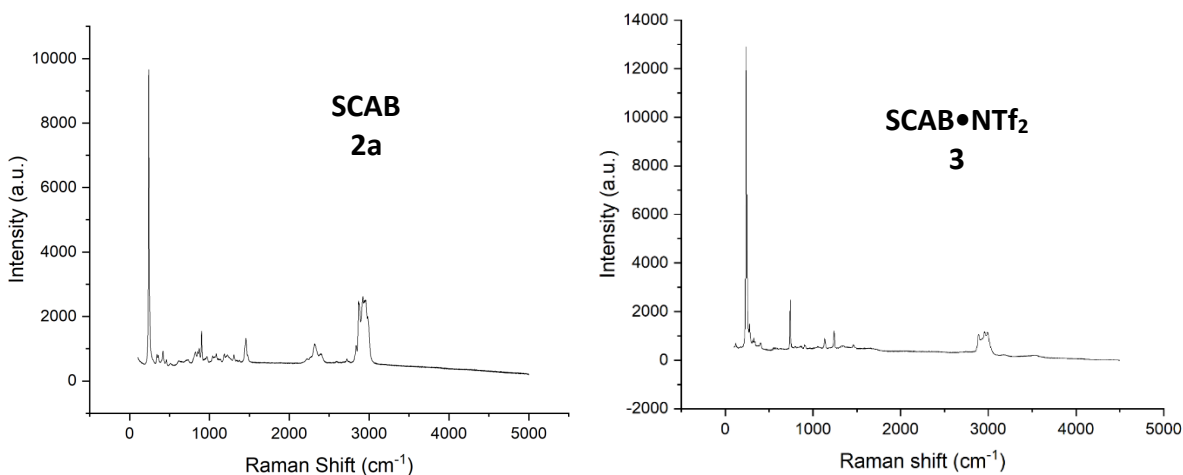


Figure 4.24 Reduced C–H bands in Raman spectrum of SCAB•NTf₂ (right) compared to SCAB **2a** (left)

4.2.2.5 Variable Temperature NMR experiments of SCAB•NTf₂

To enhance our understanding of the structure of SCAB•NTf₂ we carried out variable temperature NMR experiments. A low temperature NMR experiment was conducted and ¹H and ¹⁹F NMR spectra were collected. We theorized that lowering the temperature could decrease the rate of exchange of the protons and also enhance the intermolecular bonding of [Tf₂N]⁻ to boron in SCAB•NTf₂, both of which will result in better resolved peaks. Expectedly, a ¹H NMR spectrum collected at 198 K shows some resolution of the diastereotopic CH₂ peak that was observed at 0.43 ppm at room temperature, into a set of well resolved quartets at 0.35 ppm and 0.51 ppm at 198 K; however, there remains other broad peaks in the same region (**Figure 4.25**). The decrease in the exchange rate of protons and strengthening of the intermolecular bonding of [Tf₂N]⁻ and boron can also be seen by the sharpening of the signals appearing in the low temperature ¹⁹F NMR spectrum (**Figure 4.26**). Similarly, a high temperature NMR experiment of SCAB•NTf₂ was conducted and ¹H, ¹¹B, and ¹⁹F NMR spectra were collected. The broad signals observed at room temperature in the ¹¹B NMR spectrum resolved into a doublet at 9.2 ppm at 383 K confirming the

presence of a single hydrogen atom on boron (**Figure 4.27**). The fact that the ^{11}B NMR spectrum only shows a doublet at 383 K implies that B–H–B interactions are prevalent at room temperature and that the interactions only break at temperatures significantly higher than room temperature.

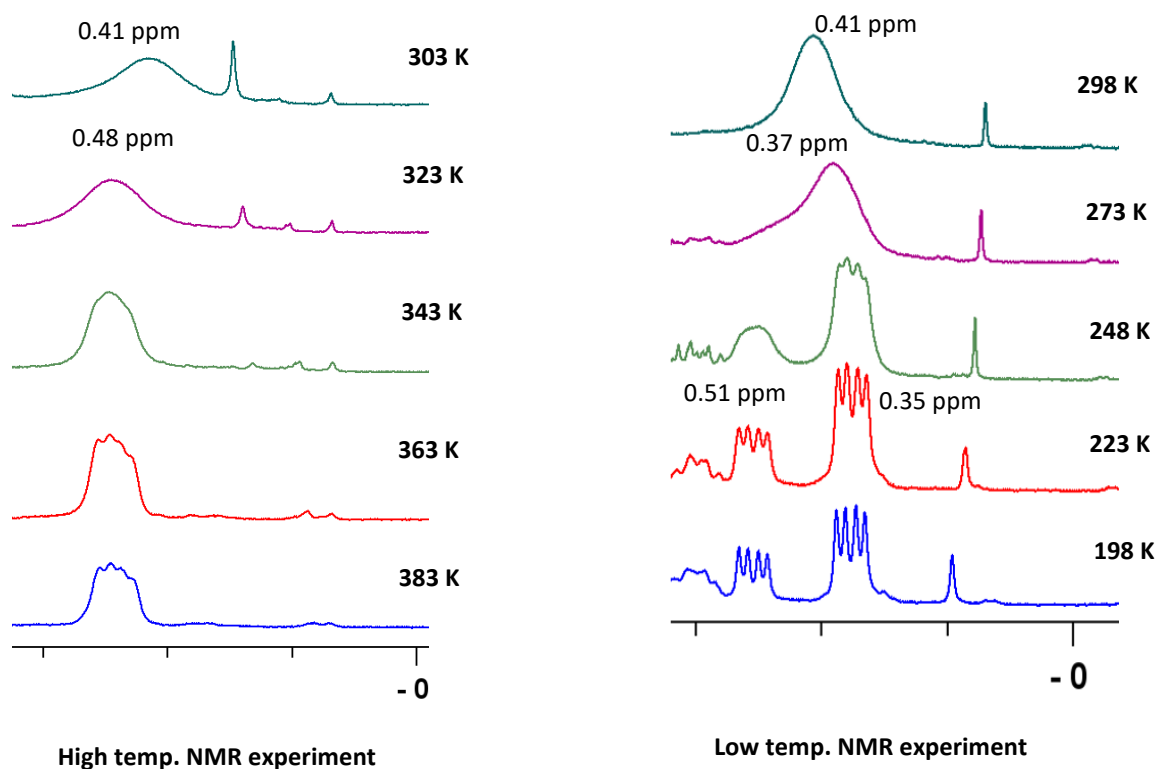


Figure 4.25 ^1H NMR (toluene- d_8) spectra at variable temperature

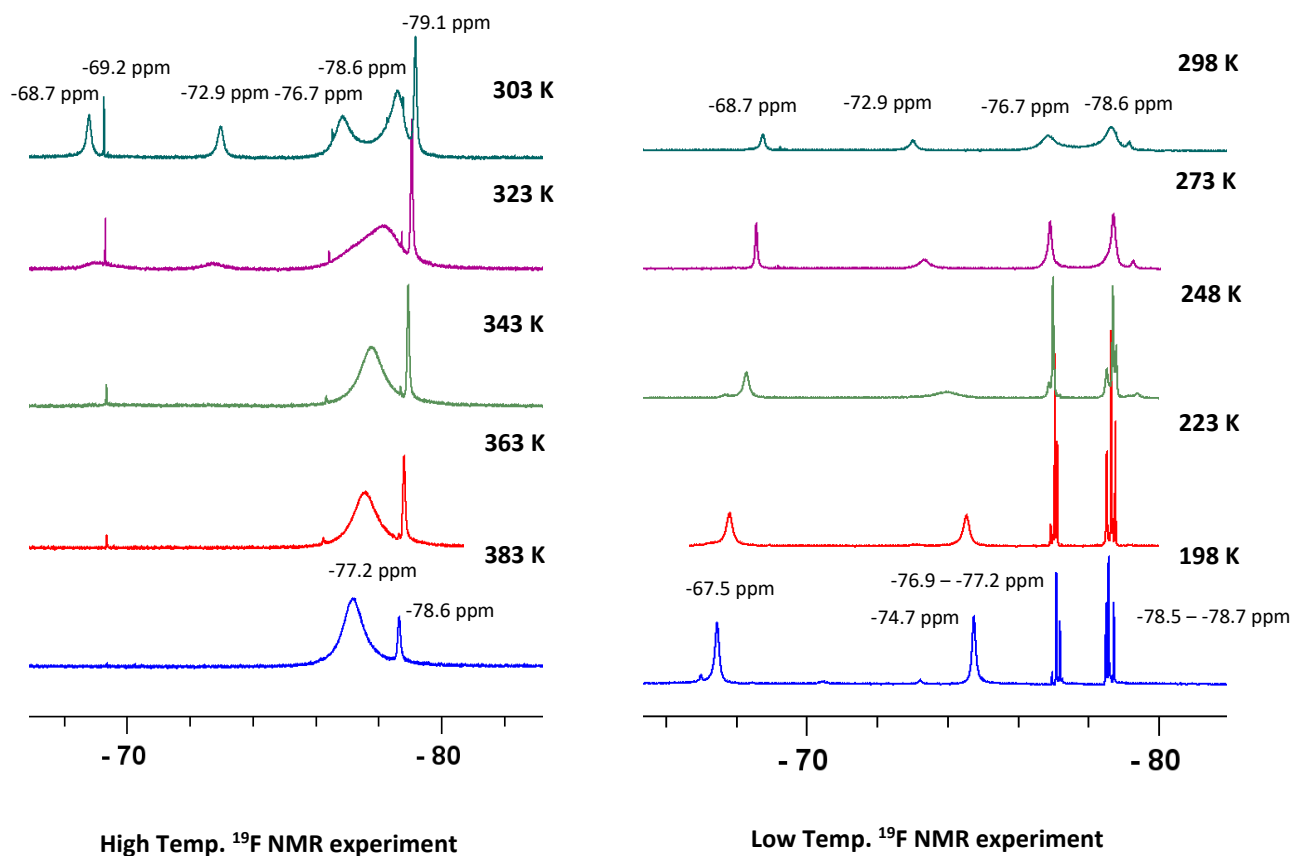


Figure 4.26 ^{19}F NMR (toluene- d_8) spectra of SCAB•NTf₂ at variable temperatures

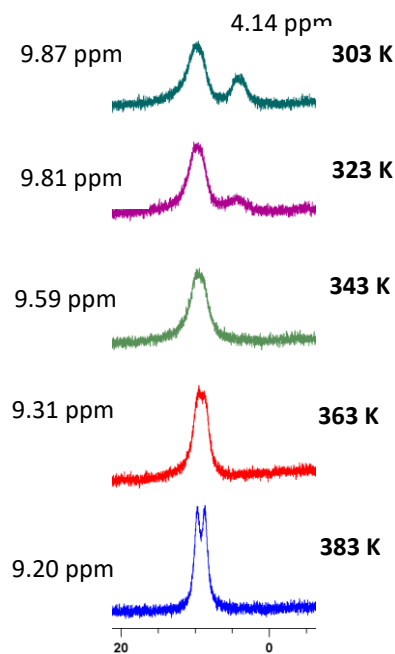


Figure 4.27 ^{11}B NMR (toluene- d_8) spectra at variable temperatures

As reported by Vedejs and co-workers, upon reaction of an alkyl amine-borane with 1 equivalent of Tf_2NH , the ^{19}F NMR spectrum shows the B–N bound isomer at -69.2 ppm and the B–O bound isomer at -76.7 ppm and -78.8 ppm (**Figure 4.12**).¹⁹⁵ The ^{19}F NMR at 303 K shows signals at -68.7 ppm, -69.2 ppm, -72.9 ppm, -76.7 ppm, -78.6, and -79.1 ppm. Based on literature, the peak at -69.2 ppm and the peaks at -76.7 ppm and -78.6 ppm can be attributed to the B–N and B–O isomers, respectively.¹⁹⁵ Therefore, the peaks at -68.7 ppm and -72.9 ppm would be consistent with a $\text{C–H}\cdots\text{NTf}_2$ hydrogen bonded complex. The interaction between the C–H and $[\text{Tf}_2\text{N}]^-$ could occur via the nitrogen or either of the oxygen atoms on $[\text{Tf}_2\text{N}]^-$. Further evidence for the attribution of these peaks was provided by the high temperature ^{19}F NMR experiments. Upon heating, the signals at -68.7 ppm and -72.9 ppm disappear rapidly. We expected the $\text{C–H}\cdots\text{NTf}_2$ interactions to be reasonably weak since $[\text{Tf}_2\text{N}]^-$ is a poor electron donor so it is no surprise that the interactions disappear upon heating. The peak at -79.1 ppm at room temperature can be attributed to unbound $[\text{Tf}_2\text{N}]^-$.

We expected that upon reaction of SCAB with Tf_2NH , hydrogen gas would evolve and the weak conjugate base $[\text{Tf}_2\text{N}]^-$ will bind to the Lewis acidic boron. However, the ^1H NMR spectrum of the $\text{SCAB}\cdot\text{NTf}_2$ complex suggests that the C–H bonds of the complex are polarized enough to act as hydrogen bond donors and the ^{19}F NMR at 303 K shows some unbound $[\text{Tf}_2\text{N}]^-$. A structure for the $\text{SCAB}\cdot\text{NTf}_2$ complex **3** is proposed based on the spectroscopic analysis presented above (**Figure 4.28**).

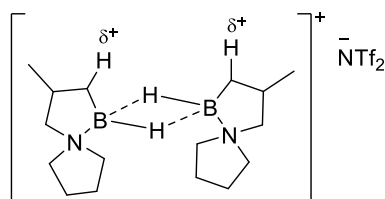
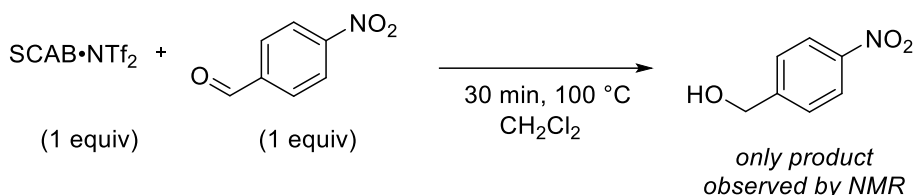


Figure 4.28 Proposed structure of $\text{SCAB}\cdot\text{NTf}_2$ complex **3**

4.2.2.6 Reactivity of $\text{SCAB}\cdot\text{NTf}_2$ Complex **3**

The spectroscopic analysis presented above led us to suspect that the C–H proton α to the boron in $\text{SCAB}\cdot\text{NTf}_2$ **3** could be acidic enough to act as a proton source and coupled with the hydride on boron could make the $\text{SCAB}\cdot\text{NTf}_2$ complex a possible reducing reagent. As a control

experiment, we attempted the reduction of 4-nitrobenzaldehyde with SCAB **2a**. The NMR spectrum of the reaction showed SCAB **2a** and 4-nitrobenzaldehyde intact. We proceeded by adding 1 equivalent of SCAB **2a** and 1 equivalent of Tf₂NH to a flask followed by the addition of CH₂Cl₂. A rapid evolution of hydrogen gas was observed, and the mixture was stirred for 15 minutes to allow for the formation of the SCAB•NTf₂ complex. After 15 minutes, 4-nitrobenzaldehyde (1 equivalent) was added and the reaction mixture was sealed and heated at 100 °C for 20 minutes. The reaction mixture was cooled, diluted with CH₂Cl₂, and filtered over a short pad of silica. Once the solvent was removed an NMR spectrum of the residue was acquired. We were pleased to observe the conversion of 4-nitrobenzaldehyde to (4-nitrophenyl)methanol (**Scheme 4.7**).



Scheme 4. 7 Reduction of 4-nitrobenzaldehyde using SCAB•NTf₂ complex

The results obtained from the reaction of SCAB•NTf₂ with 4-nitrobenzaldehyde led us to question the mechanism for the reduction of the aldehyde group. The reduced product required a proton source as well as a hydride source. The reduced product could obtain a hydride from the B–H bond of SCAB•NTf₂, however the proton could come from the work-up conditions. The work-up of the reaction involved a filtration over a short pad of silica gel. Curran and co-workers have reported reductions of aldehydes and ketones using silica gel as a source of protons.²⁸⁶ When control experiments were conducted where the mixture was not filtered over silica gel, the reduced product was still observed thus confirming that the proton consumed in the reduced product was indeed coming from SCAB•NTf₂ complex. The crude ¹H NMR spectrum was analyzed, and NMR correlation analysis obtained did not show the presence of a diastereotopic CH₂ α to boron (**Figure 4.29**). The disappearance of the diastereotopic peaks suggest that the proton consumed in the reduction reaction could come from the diastereotopic CH₂ α to boron. Such protonation would leave behind a C–H adjacent to boron. A ¹H-¹³C 2D-HSQC correlation analysis

showed that indeed there was now a C–H at 1.06 ppm in the ^1H NMR spectrum. The C–H corresponds to a broad signal in the carbon NMR, characteristic of a carbon adjacent to boron.

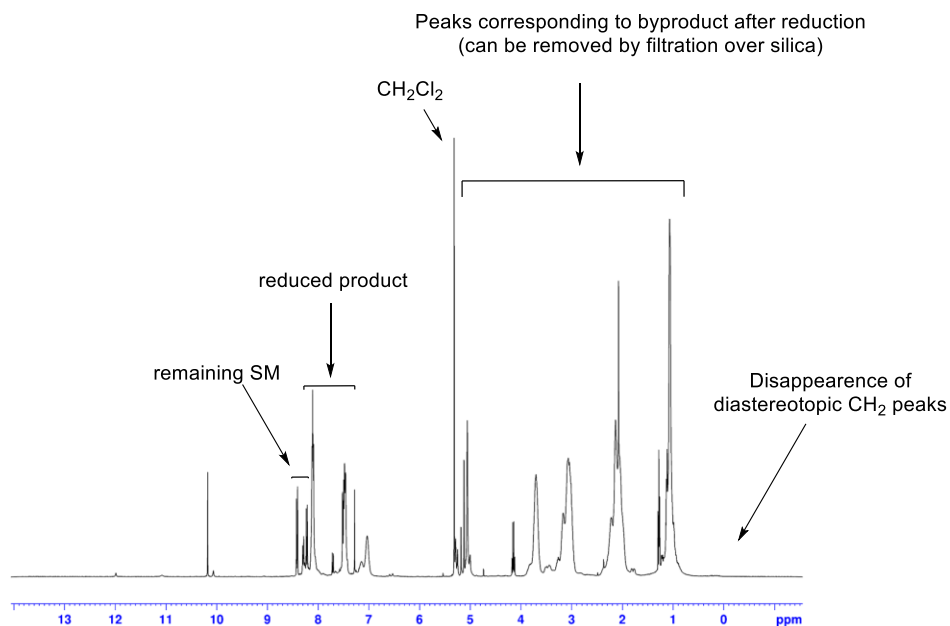


Figure 4.29 Crude ^1H NMR spectrum of reduction of 4-nitrobenzaldehyde with SCAB•NTf₂ **3**

4.2.3 Interconversion of Functional Groups: Reaction Scope of SCAB•NTf₂

The SCAB•NTf₂ complex **3** could be manipulated under air and stoichiometric amounts proved to be capable of reducing ketones, aldehydes, imines, nitrosobenzene, nitrobenzene, anthracene, indole, and reducing diphenylacetylene in a Z-selective manner. SCAB•NTf₂ was also found to be capable of demethylating aryl methyl ethers and activating C–F bonds (**Table 4.1**). All the reactions shown in **Table 4.1** were first attempted with one or two equivalents of the SCAB•NTf₂ complex depending on the substrate, (for example, acetophenone to 1-phenylethan-1-ol requires one equivalent of proton and hydride), and conversion to the reduced product was observed albeit with lower yields in some substrates than the optimized conditions. During the development of the scope and optimization of the reaction conditions per functional group, we observed that an excess of SCAB **2a** was required. For example, the reduction of a benzophenone (entry 5) requires 3 equivalents of SCAB•NTf₂ and one additional equivalent of SCAB **2a** was added to account for byproducts such as water that may deactivate the SCAB•NTf₂ complex.

Table 4.1 Scope of reactions between SCAB•Tf₂N and various functional groups

SCAB•Tf ₂ N + Substrate		CH ₂ Cl ₂ or Toluene		Product			
3		4		5			
entry	substrate	product	Yield (%) ^a	entry	substrate	product	Yield (%) ^a
1			92 ^{b, g}	7			53 ⁱ
	4a	5a			4g	5g	
2			89 ^c	8			92 ^j
	4b	5b			4h	5h	
3			86 ^{d, h}	9			42 ^{d, k}
	4c	5c			4i	5i	
4			91 ^e	10			90 ^l
	4d	5d			4j	5j	
5			94 ^f	11			86 ^f
	4e	5e			4k	5k	
6			87 ^e	12			93 ^d
	4f	5f			4l	5l	

Reactions were run with SCAB•NTf₂ (1 equiv) for 12 h at 100 °C in CH₂Cl₂ unless specified otherwise^a. Yields of isolated product.

^b. SCAB•NTf₂ (2 equiv), **2a** (1 equiv) ^c. SCAB•NTf₂ (3.5 equiv) ^d. SCAB•NTf₂ (4 equiv), **2a** (1 equiv) ^e. SCAB•NTf₂ (2 equiv), **2a** (2 equiv) ^f. SCAB•NTf₂ (3 equiv), **2a** (1 equiv) ^g. 70 °C ^h. 160 °C ⁱ. 1 h ^j. 20 min ^k. 72 h ^l. Toluene **2a** = SCAB

Demethylation of anisole and subsequent conversion to phenol has been extensively studied due to the utility of phenol in the synthesis of rubber, pesticides, and medicines with global annual demand of phenol reaching as high as 8 million tons.^{287, 288} Currently to achieve a >90% yield, a metallic catalyst and temperatures >150 °C are required.²⁸⁹ Alternative methods for converting aryl ethers such as anisole to phenol involve the use of very strong and unstable acids such as HBr and HI or strong Lewis acids such as BBr₃ that are moisture sensitive.²⁹⁰ SCAB•NTf₂

was able to demethylate anisole and provide phenol in 92% isolated yield (**Table 4.1**, entry 1). We were also able to obtain the mono-demethylated product to obtain 3-methoxyphenol in 89% isolated yield (entry 2). The complete demethylation of 1,3-dimethoxybenzene was also achieved and resorcinol was isolated in 86% yield (entry 3). The reduction of an imine and ketone was demonstrated using benzophenone imine and benzophenone. Both the C=NH and C=O groups were reduced to obtain diphenylmethane in >91% (entry 4 and 5). SCAB•NTf₂ was also able to reduce indole to obtain indoline in 87% yield (entry 6).

We also subjected diphenylacetylene to SCAB•NTf₂ to examine the reactivity of SCAB•NTf₂ towards alkynes. We were pleased to observe a Z-selective reduction of diphenylacetylene which resulted in the formation of *cis*-stilbene in 53% yield when the reaction was stopped after 30 minutes (entry 7).

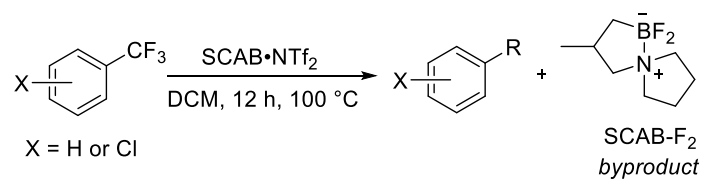
The chemo-selective reduction of 4-nitrobenzaldehyde to 4-(nitrophenyl)methanol was achieved in 92% yield (entry 8). To test the stability of SCAB•NTf₂, a solution of SCAB•NTf₂ in CH₂Cl₂ was stirred at room temperature without an inert atmosphere for 10 days following which a reduction of 4-nitrobenzaldehyde was attempted. The reduced alcohol was obtained with no effect on the reaction yield. SCAB•NTf₂ also successfully reduced anthracene to the 4H-hydrogenated product in 42% yield (entry 9). Acetophenone was reduced selectively to 1-phenylethan-1-ol in 90% yield (entry 10). It should be noted that the reduction of aldehydes and ketones did proceed at room temperature albeit with prolonged reaction times (>16 h vs 20 min).

Furthermore, aniline, an important precursor of various pharmaceuticals, agrochemicals and dyes is typically made by reducing nitrobenzene with a strong acid in the presence of a metal or using sulfur reagents.²⁹¹ The process generates a lot of metallic and acidic waste which makes it expensive and environmentally unfriendly. Herein, we report a non-metallic reduction of nitrobenzene and nitrosobenzene to aniline in >85% yield (entry 11 and 12). Other methods to reduce nitrobenzene to aniline involve the use of highly unstable hydroiodic acid or reduction using hydrazine in the presence of a metal catalyst.²⁹²

C–F bonds are fairly inert despite being polarized and are not readily activated. Increasing the number of fluorine atoms on a single carbon atom increases the strength of the C–F bonds

thus making trifluoromethyl groups even more difficult to activate. Boron has a very high affinity for fluorine as is evident from the fact that B–F bonds are amongst the strongest bonds in organic chemistry.²⁹³ SCAB•NTf₂ was successfully used for the defluorination of trifluorotoluene and 4-chlorobenzotrifluoride. The crude NMR showed >95% conversion of 4-chlorobenzotrifluoride to 4-chlorotoluene. In the presence of 3 equivalents of benzene in CH₂Cl₂, SCAB•NTf₂ was also able to convert trifluorotoluene into diphenylmethane in 72% yield. In both reactions the fluorinated SCAB was obtained as a byproduct (**Table 4.2**).

Table 4.2. Defluorination of trifluorotoluene and defluorination of 4-chlorobenzotrifluoride in the presence of benzene



entry	substrate	product	Yield (%)
1			(>95%) ^a
	4m	5m^c	
2			72% ^b
	4n	5n^d	

^a. NMR yield ^b. isolated yield ^c. SCAB•NTf₂ (2 equiv), **2a** (2 equiv)

^d. SCAB•NTf₂ (1 equiv), benzene (3 equiv)

4.2.4 Proposed Mechanism for the Reductions

We have proposed a potential pathway for the reduction reactions presented in the scope table (**Table 4.1**) in Figure 4.30. Based on the literature, it is reasonable to expect that the addition of nucleophile to SCAB•NTf₂ will result in the formation of an adduct with the Lewis acidic boron accompanied by the transfer of the hydride from the B–H bond in SCAB•NTf₂ to the electrophilic site. The resulting B–O bond can undergo hydrolysis in the presence of moisture to provide the

reduced product. It is important to mention here that a crude NMR of the reduction of 4-nitrobenzaldehyde proceeding by the mechanism below (**Figure 4.30**) should result in the formation of a B–O bond which would show up as an intense signal in the ^{11}B NMR spectrum between 25-35 ppm. However, we do not see any such signal in the ^{11}B NMR spectrum that would appear for **III** or for the intermediate **I** and **II**. Also, we should see clear diastereotopic signals for the carbon α to boron in **III** but we do not observe diastereotopic signals. One explanation for the lack of diastereotopic signals for the carbon α to boron could be the cleavage of the C–B bond however, the ^{13}C NMR spectrum shows a broad signal at 19 ppm for a carbon adjacent to boron.

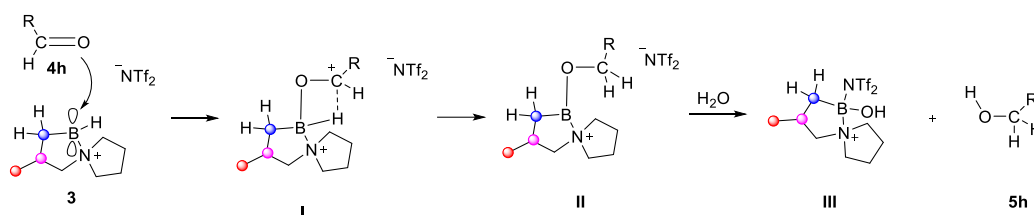
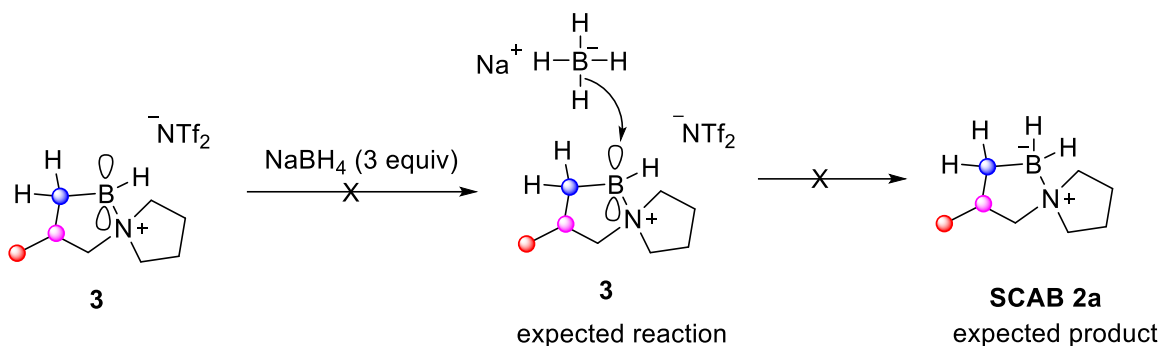


Figure 4.30 Potential mechanistic pathway for the reduction of 4-nitrobenzaldehyde

4.2.4.1 Attempts to Regenerate SCAB 2a

Based on the mechanism discussed above we expected that the addition of NaBH_4 would regenerate SCAB **2a** (**Scheme 4.8**). In attempts to regenerate SCAB **2a** from the $\text{SCAB}\cdot\text{NTf}_2$ complex **3**, we thought of adding a hydride source such as NaBH_4 . We proposed that the Lewis acidic boron in $\text{SCAB}\cdot\text{NTf}_2$ would readily take up a hydride from NaBH_4 and regenerate SCAB **2a**. To a vial containing $\text{SCAB}\cdot\text{NTf}_2$ in CD_2Cl_2 was added NaBH_4 (3 equivalents). Immediately after the addition of NaBH_4 vigorous bubbling was observed. The solution was stirred for 15 minutes, and an NMR was acquired. The ^1H NMR spectrum showed a characteristic sharp singlet at 4.6 ppm which implied that the reaction of $\text{SCAB}\cdot\text{NTf}_2$ and NaBH_4 resulted in the evolution of hydrogen gas. The hydrogen gas formation could be a result of the reaction of NaBH_4 and the acidic proton α to boron. The ^1H and ^{11}B NMR spectrum did not show the formation of SCAB **2a**.



Scheme 4. 8 Expected reaction between SCAB•NTf₂ and NaBH₄

4.2.4.2 Implication of “D₂O Shake” on Mechanism

The results obtained in the “D₂O shake” experiment (section 4.2.2.3) where D₂O was added to SCAB•NTf₂ and a signal for a vinylic proton was observed further indicates that the Lewis acidity of boron might be quenched by the hyperconjugative interactions between the C–H α to the boron and the empty *p*-orbital of boron as well as the interaction between boron and [Tf₂N][−]. Therefore, the addition of D₂O could lead to a deprotonation of the acidic C–H α to boron. The experiments between SCAB•NTf₂ complex with NaBH₄ and D₂O suggest that there might be a different reaction pathway for the reduction reactions that involves the acidic protons adjacent to boron.

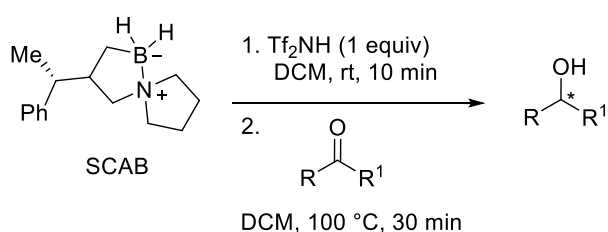
4.3 Conclusion and Perspectives

C–H bonds are ubiquitous in nature and therefore any new reactivity involving these bonds becomes a matter of interest. Although carbon is more electronegative than hydrogen, C–H bonds are fairly inert, and the selective activation of C–H bonds has proven to be challenging. The notion that a C–H bond can act as a proton donor is not new. HCN has been known to act as a strong acid in the presence of a suitable acceptor. Imidazolium-based ionic liquids possess acidic C–H bonds that can be deprotonated readily by a mild base.²⁸⁵ The C–H bonds of acetylene can also undergo interactions which resemble hydrogen bonds.²⁹⁴ However, these interactions have been primarily observed in sp or sp^2 hybridized carbons. sp^3 hybridized carbons typically require highly electronegative substituents to undergo hydrogen bonding type interactions. The role of C–H...O/N interactions is firmly established in lending stability to several biological systems and therefore we should try to enhance our understanding of such systems.²⁵⁶⁻²⁶¹

Although C–H...Y interactions clearly demonstrate that C–H bonds can act as proton donors in hydrogen bonding-like interactions, the ability of a C–H bond to act as a proton source has only been shown in very few instances, for example in the case of HCN. The IR spectrum of SCAB•NTf₂ showed the presence of blue-shifted C–H bands with reduced intensity around the 3000 cm⁻¹ which implied that various C–H bonds in the SCAB•NTf₂ complex are undergoing improper hydrogen bonding. The NMR experiments for the SCAB•NTf₂ complex corroborated the IR results and established the participation of the C–H bonds in hydrogen bonding. The role of [Tf₂N]⁻ as a weakly coordinating ligand in lending stability to the SCAB•NTf₂ complex via formation of bonds between itself and the Lewis acidic boron as well as the presence of C–H...NTf₂ interactions was also demonstrated. It was found that the formation of a SCAB•NTf₂ complex is unique to Tf₂NH since other strong acids such as TFA and TfOH could not form a similar complex with SCAB **2a**. The presence of an acidic hydrogen (C–H) and a hydride in the B–H bond lent the SCAB•NTf₂ complex the ability to reduce a wide range of functional groups. SCAB•NTf₂ was also found to be capable of activating the C–F bonds and the defluorination of Ar–CF₃ motifs was demonstrated.

The reactivity of the SCAB•NTf₂ complex opens a wide range of exciting possibilities. Future work could involve studying the formation of SCAB•NTf₂ complex via computational methods

such as DFT in order to gain a better understanding of the bonding patterns in the complex. We were not successful in obtaining a crystal structure for the SCAB•NTf₂ complex but a crystal structure will certainly help to provide further evidence of the proposed bonding interactions. We have developed an entire library of SCABs in chapter 3 and the effect of various substituted SCABs on the formation and reactivity of SCAB•NTf₂ complexes can be explored. In chapter 3, we synthesized an enantiopure SCAB to demonstrate the potential stereospecificity of the ring-opening of cyclopropane amine-boranes. The resulting SCAB has a stereogenic center that could induce enantioselectivity in the reduction of ketones (**Scheme 4.9**).



Scheme 4. 9 Enantioselective reduction via chiral SCAB

A potential improvement to the reduction reactions discussed in this chapter is to find a way to use catalytic amounts of Tf₂NH instead of stoichiometric amounts and also find a method to regenerate SCAB. We have not discussed the structure of the oligomer formed post the reduction reaction, but we speculate that it could involve the formation of intermolecular bonds between an anionic carbon after the loss of a proton and a Lewis acidic boron in an intermolecular manner (**Figure 4.31**).

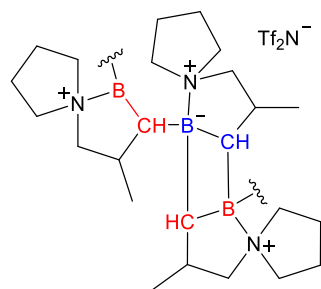
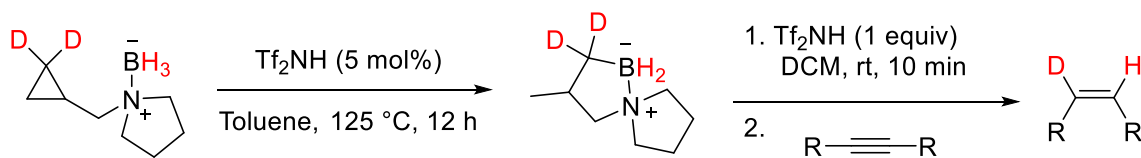


Figure 4.31 Proposed oligomerization byproduct of SCAB•NTf₂ reduction reaction

Further studies can be done to gain insight into the mechanism of the reaction and potentially confirm the proposed mechanism. A deuterated-C3 SCAB can be obtained from its

corresponding CAB (**Scheme 4.10**). A reduction of an alkyne can be done to observe the transfer of a deuterium from C3 across the triple bond which would demonstrate that the C3–H is indeed acting as a proton source.



Scheme 4. 10 Deuterium experiment for mechanistic studies

Since this is the first instance where the reactivity of a spirocyclic amine-borane with Tf_2NH is being explored, more experimental and computational work needs to be done to understand the role of the spirocyclic motif in the formation of $\text{SCAB}\cdot\text{NTf}_2$.

Chapter 5 – Perspectives and Conclusion

5.1 Chiral *N*-coordinated Boronate Building Blocks

The work presented in the thesis highlights the complexity of the boron element and its diverse applications in organic synthesis. Organoboron reagents have been extensively studied especially for their application in the Suzuki-Miyaura reaction, the most popular palladium catalyzed C–C bond formation methods. Due to its mild reaction conditions, it has become one of the go-to reactions, and the development of libraries containing biologically relevant organoboron building blocks is of great interest. Thus, we were interested in developing biologically relevant chiral building blocks that can be integrated into larger and more complex frameworks in late-stage functionalization. The Charette enantioselective dioxaborolane-mediated cyclopropanation reaction was an excellent starting point to access borocyclopropane motifs from boronate-bearing allylic alcohols.³⁵ Our non-oxidative work-up using diethanolamine allowed for the selective decomplexation of the chiral dioxaborolane ligand in the presence of these boronate handles. Moreover, the use of tetracoordinate boronates not only provided highly stable borocyclopropane but also underwent efficient C–C bond formation to access *N*-heterocyclic substituted cyclopropanes in very good yields with excellent diastereo- and enantiocontrol. The non-oxidative work-up allowed to expand the scope of the Charette enantioselective cyclopropanation reaction towards other base-sensitive functionalities as shown via a robustness screen. While the robustness screen showed tolerance of several base-sensitive functionalities, cyclopropanation of allylic alcohols bearing base-sensitive functional groups could also be done. Moreover, organoboron compounds are a growing area of research and therefore expanding the reaction scope to other boronate-bearing allylic alcohols would allow for a universal approach to access a library of borocyclopropanes bearing a variety of boronates that can be functionalized.

5.2 Combining C–H and C–C Bond Activation to Make Spirocyclic Amine-Boranes (SCABs)

Step economy is one of the most crucial factors that determines the practicality of a synthetic methodology. The synthesis of spirocycles involves multiple steps and therefore generally suffers from low step economy which has contributed to spirocycles not realizing their full potential in synthetic as well as medicinal chemistry. C–H and C–C bonds are two of the most common bonds found in organic chemistry and the transformation of these bonds is actively pursued due to the obvious advantages it offers to the synthetic chemists. Cyclopropanes are useful building blocks owing to their ring strain and therefore offer atom economical approaches for many reactions involving the ring opening of cyclopropanes. The methodology developed in chapter 3, where a transformation of a CAB to SCAB is demonstrated, gives access to spirocyclic motifs in a single step procedure using catalytic amounts of Tf_2NH . The high step economy access to spirocyclic motifs could help ring scalable synthesis to spirocyclic amine-boranes. The proposed mechanism involves the breaking of a C–H and a C–C bond of an unactivated cyclopropane and a net anti-hydroborated product as a single diastereomer is obtained when a 1,2,2 substituted CAB is used.

With the approval of boron containing drugs such as bortezomib, tavorole and crisaborole, boron is emerging as a new frontier in drug design. Lipinski's rule of 5 highlights the importance of factors such as molecular mass, lipophilicity, polar surface area, hydrogen bonding and charge of the molecules in drug design but the rigid application of Lipinski's rules steered medicinal chemists mostly towards planar, aromatic, and achiral molecules.²⁹⁵ Lovering and co-workers in his seminal paper brought to the forefront the importance of molecular complexity for a successful drug candidate, a factor which had previously been overlooked.⁶⁰ Lovering co-workers reported that increasing the saturation of a molecule resulted in more three dimensionality and a higher number of chiral centres and both these factors had an important role to play in drug design. Increasing three dimensionality of a molecule can lead to better interactions with target protein and thereby enhance potency of a drug molecule. Spirocycles enhance the three dimensionality of the molecule without significantly increasing the molecular

mass and are privileged motifs in drug design.⁶⁵ Spirocycles, although highly sought after, are difficult to synthesize due to the presence of a quaternary atom. The work presented in chapter 3 provides a single step, cascade and regioselective methodology to access a diverse library of spirocyclic amine-boranes (SCAB) via the ring-opening of unactivated cyclopropanes. The methodology was also used to make a new class of SCABs containing more than one spirocenter and can be tailored to include even more than two *N*-spirocenters and further diversify the SCAB library. Modification of the *N*-heterocycle to have substituents of various functionalities could also provide a diverse scope and provide a coupling handle to introduce SCAB motifs into parent drug molecules.

As mentioned in chapter 3, boronic acids are bioisosteres of carboxylic acids and are finding increasing acceptance in FDA approved drugs. Our unsubstituted SCAB was further functionalized to obtain spirocyclic boronic acids. The boronic acid derivative of SCAB could have enhanced biological activity due to the presence of a spirocyclic system.²⁹⁶ A selected number of SCAB compounds were converted to their fluorinated derivatives. The integration of fluorine into motifs has shown to have a major bearing on the bioactive properties of molecules. Amine-boranes are already known to be biologically active and having access to a diverse set of SCABs can lead to attractive drug candidates. Absorption, distribution, metabolism, and excretion (ADME) studies are designed to investigate how a drug compound is processed by a living organism and conducting these studies on our unique SCAB scaffolds would give insight to their pharmacological activity.

5.3 The C–H Bond as a Hydrogen Bond Donor

In chapter 4, we studied the protonation of SCAB via Tf₂NH (1 equivalent). The studies came about from unusual trends observed during the synthesis of the SCAB in chapter 3. The ring-opening of CABs bearing CF₃ showed the formation of species containing B–F bonds and some formation of SCAB product. We proposed that a system containing SCAB **2a** in the presence of Tf₂NH could activate C–F bonds in good yields as there would not be byproducts resulting from C–C bond activation as was the case when CAB was used. Spectroscopic studies showed that SCAB, upon reaction with a stoichiometric amount of Tf₂NH, generated a Lewis acid boron which

could polarize the C–H bond adjacent to it via hyperconjugative interactions. The polarized C–H bonds can act as hydrogen bond donors with the $[\text{Tf}_2\text{N}]^-$ resulting in an ‘improper’ hydrogen bond. SCAB•NTf₂ complex was capable of reducing aldehyde, ketone, imine, nitro, and nitroso functionalities while also being able to reduce diphenylacetylene to *cis*-stilbene. Ideally, a crystal structure for the SCAB•NTf₂ complex can provide further insight into the bonding patterns prevalent in the complex. C–H···Y interactions (Y = O, N etc.) have been reported in several biological systems which implies that the interactions might be more important than previously understood. Over the past couple of decades computational studies have been done to understand the ‘improper’ hydrogen bond but a comprehensive theory is still lacking. Typically, when the C–H bond undergoes improper hydrogen bonding, the carbon atom is substituted by a highly electronegative element (for example CHF₃). Our discovery where an improper hydrogen bond is observed in presence of a Lewis acidic boron could give a new template for computational chemists to gain insights into improper hydrogen bonding.

5.4 Final Thoughts

Scientific discovery does not happen in isolation. We rely on the work done by scientists before us and hope that we can add a chapter of our own. The work done by Professor André Charette served as a starting point for us to develop an enantioselective borocyclopropanation by adding a non-oxidative work-up to the dioxaborolane-mediated cyclopropanation reaction. We took inspiration from the work published by Professor Edwin Vedejs involving C–H borylation and stumbled upon a methodology to ring-open cyclopropanes which led to the development of an efficient synthesis of spirocyclic amine-boranes. We are grateful for the work done by Dr. June Sutor who despite the initial rejection of her ideas by the scientific community, persevered and helped lay the corner stone of improper hydrogen bonding. Without her work and that of several chemists that followed her, we may not have been able to make sense of our own experimental results in which we propose that a C–H bond can act as a source of proton through improper hydrogen bonding. We hope that the work presented in the thesis can serve as a starting point for other chemists and help advance our collective understanding of the world of chemistry.

References

1. Oganov, A.; Solozhenko, V., *J. Superhard Mater.* **2009**, *31*, 285-291.
2. Gay-Lussac, J. L.; Thénard, L. J., *J Ann. Chim. Phys.* **1808**, *68*, 169-174.
3. Davy, H., *An Account of Some New Analytical Researches on the Nature of Certain Bodies, Particularly the Alkalies, Phosphorus, Sulphur, Carbonaceous Matter, and the Acids Hitherto Undecomposed; with Some General Observations on Chemical Theory... From the Philosophical Transactions.* W. Bulmer & Company: 1809.
4. Krebs, R. E., *The History and Use of Our Earth's Chemical Elements: A Reference Guide.* Greenwood Publishing Group: 2006.
5. Kahlert, J.; Austin, C. J. D.; Kassiou, M.; Rendina, L. M., *Aust. J. Chem.* **2013**, *66*, 1118-1123.
6. Corey, E. J.; Bakshi, R. K.; Shibata, S., *J. Am. Chem. Soc.* **1987**, *109*, 5551-5553.
7. Brown, H.; Rao, B. C., *J. Org. Chem.* **1957**, *22*, 1137-1138.
8. Miyaura, N.; Suzuki, A., *J. Chem. Soc., Chem. Commun.* **1979**, 866-867.
9. Miyaura, N.; Yamada, K.; Suzuki, A., *Tetrahedron Lett.* **1979**, *20*, 3437-3440.
10. Kennedy, J. W. J.; Hall, D. G., *J. Org. Chem.* **2004**, *69*, 4412-4428.
11. Welch, G. C.; Juan, R. R. S.; Masuda, J. D.; Stephan, D. W., *Science* **2006**, *314*, 1124-1126.
12. DeFrancesco, H.; Dudley, J.; Coca, A., *Synthesis* **2016**, 1-25.
13. Brown, H.; Rao, B., *J. Org. Chem.* **1957**, *22*, 1136-1137.
14. Hall, D. G., Structure, Properties, and Preparation of Boronic Acid Derivatives. Overview of Their Reactions and Applications. Hall, D. G., Ed. Wiley-VCH: Weinheim, 2005; Vol. 1, pp 1-99.
15. Littke, A. F.; Fu, G. C., *Angew. Chem. Int. Ed.* **2002**, *41*, 4176-4211.
16. Altenhoff, G.; Goddard, R.; Lehmann, C. W.; Glorius, F., *J. Am. Chem. Soc.* **2004**, *126*, 15195-15201.
17. Littke, A. F.; Dai, C.; Fu, G. C., *J. Am. Chem. Soc.* **2000**, *122*, 4020-4028.
18. Zim, D.; Gruber, A. S.; Ebeling, G.; Dupont, J.; Monteiro, A. L., *Org. Lett.* **2000**, *2*, 2881-2884.

19. Wolfe, J. P.; Singer, R. A.; Yang, B. H.; Buchwald, S. L., *J. Am. Chem. Soc.* **1999**, *121*, 9550-9561.
20. Alimardanov, A.; Schmieder-van de Vondervoort, L.; de Vries, A. H. M.; de Vries, J. G., *Adv. Synth. Catal.* **2004**, *346*, 1812-1817.
21. Gonzalez, J. A.; Ogba, O. M.; Morehouse, G. F.; Rosson, N.; Houk, K. N.; Leach, A. G.; Cheong, P. H. Y.; Burke, M. D.; Lloyd-Jones, G. C., *Nat. Chem.* **2016**, *8*, 1067-1075.
22. Knapp, D. M.; Gillis, E. P.; Burke, M. D., *J. Am. Chem. Soc.* **2009**, *131*, 6961-6963.
23. Mancilla, T.; Contreras, R.; Wrackmeyer, B., *J. Organomet. Chem.* **1986**, *307*, 1-6.
24. Mikhailov, B. M., *Pure Appl. Chem.* **1977**, *49*, 749-764.
25. Lennox, A. J. J.; Lloyd-Jones, G. C., *Chem. Soc. Rev.* **2014**, *43*, 412-443.
26. Kelly, A. M.; Chen, P.-J.; Klubnick, J.; Blair, D. J.; Burke, M. D., *Org. Lett.* **2020**, *22*, 9408-9414.
27. Mancilla, T.; Contreras, R.; Wrackmeyer, B., *J. Organomet. Chem.* **1986**, *307*, 1-6.
28. Gillis, E. P.; Burke, M. D., *Aldrichimica Acta.* **2009**, *42*, 17-27.
29. Gillis, E. P.; Burke, M. D., *J. Am. Chem. Soc.* **2008**, *130*, 14084-14085.
30. Li, J.; Ballmer, S. G.; Gillis, E. P.; Fujii, S.; Schmidt, M. J.; Palazzolo, A. M.; Lehmann, J. W.; Morehouse, G. F.; Burke, M. D., *Science* **2015**, *347*, 1221-1226.
31. Haley, H. M. S.; Hill, A. G.; Greenwood, A. I.; Woerly, E. M.; Rienstra, C. M.; Burke, M. D., *J. Am. Chem. Soc.* **2018**, *140*, 15227-15240.
32. Tan, J.; Grouleff, J. J.; Jitkova, Y.; Diaz, D. B.; Griffith, E. C.; Shao, W.; Bogdanchikova, A. F.; Poda, G.; Schimmer, A. D.; Lee, R. E., *J. Med. Chem.* **2019**, *62*, 6377-6390.
33. Matteson, D. S., *Tetrahedron* **1998**, *54*, 10555-10607.
34. Lee, J. C. H.; Hall, D. G., *J. Am. Chem. Soc.* **2010**, *132*, 5544-5545.
35. Charette, A. B.; Juteau, H., *J. Am. Chem. Soc.* **1994**, *116*, 2651-2652.
36. Gay-Lussac, J.; Thenard, J., *J. Mem. Phys. Chim. Soc.* **1809**, *2*, 210-211.
37. Burg, A. B.; Schlesinger, H. I., *J. Am. Chem. Soc.* **1937**, *59*, 780-787.
38. Couturier, M.; Andresen, B. M.; Tucker, J. L.; Dubé, P.; Brenek, S. J.; Negri, J. T., *Tetrahedron Lett.* **2001**, *42*, 2763-2766.

39. Carre-Burritt, A. E.; Davis, B. L.; Rekken, B. D.; Mack, N.; Semelsberger, T. A., *Energy Environ. Sci.* **2014**, *7*, 1653-1656.
40. Dietrich, B. L.; Goldberg, K. I.; Heinekey, D. M.; Autrey, T.; Linehan, J. C., *J. Inorg. Chem.* **2008**, *47*, 8583-8585.
41. Burnham, B. S., *Curr. Med. Chem.* **2005**, *12*, 1995-2010.
42. Reddy, D. O., *Chem. Rev. Lett.* **2020**, *3*, 184-191.
43. Alcaraz, G.; Sabo-Etienne, S., *Angew. Chem. Int. Ed.* **2010**, *49*, 7170-7179.
44. Colebatch, A. L.; Weller, A. S., *Chemistry* **2019**, *25*, 1379.
45. Schaeffer, G. W.; Anderson, E. R., *J. Am. Chem. Soc.* **1949**, *71*, 2143-2145.
46. Veeraraghavan Ramachandran, P.; Kulkarni, A. S., *RSC Adv.* **2014**, *4*, 26207-26210.
47. Veeraraghavan Ramachandran, P.; Kulkarni, A. S.; Zhao, Y.; Mei, J., *Chem. Comm.* **2016**, *52*, 11885-11888.
48. Diaz, D. B.; Yudin, A. K., *Nat. Chem.* **2017**, *9*, 731-742.
49. Fernandes, G. F. S.; Denny, W. A.; Dos Santos, J. L., *Eur. J. Med. Chem.* **2019**, *179*, 791-804.
50. Moreira, W.; Aziz, D. B.; Dick, T., *Front. Microbiol.* **2016**, *7*, 199-199.
51. Kohno, J.; Kawahata, T.; Otake, T.; Morimoto, M.; Mori, H.; Ueba, N.; Nishio, M.; Kinumaki, A.; Komatsubara, S.; Kawashima, K., *Biosci., Biotechnol., Biochem* **1996**, *60*, 1036-1037.
52. Baker, S. J.; Ding, C. Z.; Akama, T.; Zhang, Y.-K.; Hernandez, V.; Xia, Y., *Future Med. Chem.* **2009**, *1*, 1275-1288.
53. Pekol, T.; Daniels, J. S.; Labutti, J.; Parsons, I.; Nix, D.; Baronas, E.; Hsieh, F.; Gan, L.-S.; Miwa, G., *Drug Met. Disp.* **2005**, *33*, 771-777.
54. Rainey, C. J.; Nyquist, L. A.; Christensen, R. E.; Strong, P. L.; Culver, D.; Coughlin, J. R., *J. Am. Diet Assoc.* **1999**, *99*, 335-340.
55. Das, B. C.; Shareef, M. A.; Das, S.; Nandwana, N. K.; Das, Y.; Saito, M.; Weiss, L. M., *Bioorg. Med. Chem.* **2022**, 116748.
56. Burnham, B. S., Amine-Boranes. In *Encyclopedia of Metalloproteins*, Kretsinger, R. H.; Uversky, V. N.; Permyakov, E. A., Eds. Springer New York: New York, NY, 2013; pp 58-62.
57. Sood, A.; Sood, C. K.; Spielvogel, B. F.; Hall, I. H., *Eur. J. Med. Chem.* **1990**, *25*, 301-308.

58. Győri, B.; Lázár, I.; Berente, Z.; Király, R.; Bényei, A., *J. Organomet. Chem.* **2004**, *689*, 3567-3581.
59. Scannell, J. W.; Blanckley, A.; Boldon, H.; Warrington, B., *Nat. Rev. Drug Discov.* **2012**, *11*, 191-200.
60. Lovering, F.; Bikker, J.; Humblet, C., *J. Med. Chem.* **2009**, *52*, 6752-6756.
61. Talele, T. T., *J. Med. Chem.* **2016**, *59*, 8712-8756.
62. Zheng, Y.; Tice, C. M.; Singh, S. B., *Bioorg. Med. Chem. Lett.* **2014**, *24*, 3673-3682.
63. Zheng, Y.-J.; Tice, C. M., *Expert Opin. Drug Discovery* **2016**, *11*, 831-834.
64. Chupakhin, E.; Babich, O.; Prosekov, A.; Asyakina, L.; Krasavin, M., *Molecules* **2019**, *24*, 4165.
65. Hiesinger, K.; Dar'ın, D.; Proschak, E.; Krasavin, M., *J. Med. Chem.* **2021**, *64*, 150-183.
66. Baeyer, A., *Berichte der deutschen chemischen Gesellschaft* **1900**, *33*, 3771-3775.
67. Hudlický, T. š.; Reed, J. W., *The Way of Synthesis*. Wiley-VCH: Weinheim, 2007.
68. Kotha, S.; Panguluri, N. R.; Ali, R., *Eur. J. Org. Chem.* **2017**, *2017*, 5316-5342.
69. Cohen, Y.; Cohen, A.; Marek, I., *Chem. Rev.* **2021**, *121*, 140-161.
70. Wessjohann, L. A.; Brandt, W.; Thiemann, T., *Chem. Rev.* **2003**, *103*, 1625-1648.
71. Biletskyi, B.; Colonna, P.; Masson, K.; Parrain, J.-L.; Commeiras, L.; Chouraqui, G., *Chem. Soc. Rev.* **2021**, *50*, 7513-7538.
72. Carson, C. A.; Kerr, M. A., *Chem. Soc. Rev.* **2009**, *38*, 3051-3060.
73. Schneider, T. F.; Kaschel, J.; Werz, D. B., *Angew. Chem. Int. Ed.* **2014**, *53*, 5504-5523.
74. Taily, I. M.; Saha, D.; Banerjee, P., *Org. Biomol. Chem.* **2021**, *19*, 8627-8645.
75. Wang, D.; Xue, X.-S.; Houk, K. N.; Shi, Z., *Angew. Chem. Int. Ed.* **2018**, *57*, 16861-16865.
76. Lipinski, C. A.; Lombardo, F.; Dominy, B. W.; Feeney, P. J., *Adv. Drug Delivery* **1997**, *23*, 3-25.
77. Karas, L. J.; Wu, C.-H.; Das, R.; Wu, J. I. C., *Wiley Interdiscip. Rev. Comput. Mol. Sci.* **2020**, *10*, e1477.
78. Herschlag, D.; Pinney, M. M., *Biochemistry* **2018**, *57*, 3338-3352.
79. Latimer, W. M.; Rodebush, W. H., *J. Am. Chem. Soc.* **1920**, *42*, 1419-1433.
80. Van der Lubbe, S. C. C.; Fonseca Guerra, C., *Chem. Asian J.* **2019**, *14*, 2760-2769.

81. Dereka, B.; Yu, Q.; Lewis, N. H. C.; Carpenter, W. B.; Bowman, J. M.; Tokmakoff, A., *Science* **2021**, *371*, 160-164.
82. Pauling, L., *J. Am. Chem. Soc.* **1931**, *53*, 1367-1400.
83. Jeffrey, G. A., *An Introduction to Hydrogen Bonding*. Oxford university press New York: 1997; Vol. 12.
84. Grabowski, S. J., *Hydrogen Bonding: New Insights*. Springer: 2006; Vol. 3.
85. Hobza, P.; Havlas, Z., *Theor. Chem. Acc.* **2002**, *108*, 325-334.
86. Arunan, E., *J. Indian Inst. Sci.* **2020**, *100*, 249-255.
87. Schwalbe, C. H., *Crystallogr. Rev.* **2012**, *18*, 191-206.
88. Desiraju, G. R.; Steiner, T., *The Weak Hydrogen Bond: In Structural Chemistry and Biology*. International Union of Crystal: 2001; Vol. 9.
89. Joseph, J.; Jemmis, E. D., *J. Am. Chem. Soc.* **2007**, *129*, 4620-4632.
90. Jiang, L.; Lai, L., *J. Biol. Chem.* **2002**, *277*, 37732-40.
91. Stock, A., *J. Phys. Chem.* **1934**, *38*, 714-715.
92. Schlesinger, H. I.; Brown, H. C., *J. Am. Chem. Soc.* **1940**, *62*, 3429-3435.
93. Johnson, M. R.; Rickborn, B., *J. Org. Chem.* **1970**, *35*, 1041-1045.
94. Chaikin, S. W.; Brown, W. G., *J. Am. Chem. Soc.* **1949**, *71*, 122-125.
95. Nutaitis, C. F., *J. Chem. Educ.* **1989**, *66*, 673.
96. Curran, D. P.; Solovyev, A.; Makhlouf Brahmī, M.; Fensterbank, L.; Malacria, M.; Lacôte, E., *Angew. Chem. Int. Ed.* **2011**, *50*, 10294-10317.
97. Prokofjevs, A.; Boussonnière, A.; Li, L.; Bonin, H. I. n.; Lacôte, E.; Curran, D. P.; Vedejs, E., *J. Am. Chem. Soc.* **2012**, *134*, 12281-12288.
98. Filippov, O. A.; Belkova, N. V.; Epstein, L. M.; Shubina, E. S., *J. Organomet. Chem.* **2013**, *747*, 30-42.
99. Custelcean, R.; Jackson, J. E., *Chem. Rev.* **2001**, *101*, 1963-1980.
100. Freund, A., *J. Prakt. Chem.* **1882**, *26*, 367-377.
101. Henderson, V.; Lucas, G., *Anesth. Analg.* **1930**, *9*, 1-6.
102. Gavrus, D., *Scientia Canadensis.* **2010**, *33*, 3-28.
103. Donaldson, W. A., *Tetrahedron* **2001**, *57*, 8589-8627.

104. Taylor, R. D.; MacCoss, M.; Lawson, A. D. G., *J. Med. Chem.* **2014**, *57*, 5845-5859.
105. Lebel, H.; Marcoux, J.-F.; Molinaro, C.; Charette, A. B., *Chem. Rev.* **2003**, *103*, 977-1050.
106. Nam, D.; Steck, V.; Potenzino, R. J.; Fasan, R., *J. Am. Chem. Soc.* **2021**, *143*, 2221-2231.
107. Simmons, H. E.; Smith, R. D., *J. Am. Chem. Soc.* **1958**, *80*, 5323-5324.
108. Davies, H. M. L.; Panaro, S. A., *Tetrahedron* **2000**, *56*, 4871-4880.
109. Kulinkovich, O. G.; Sviridov, S. V.; Vasilevskii, D. A.; Pritytskaya, T. S., *Zh. Neorg. Khim.* **1989**, *25*, 2244-2245.
110. Schubert, H.; Rack, M.; Muehlstoedt, M., *J. Prakt. Chem.* **1990**, *332*, 812-14.
111. Kadu, B. S., *Catal. Sci. Technol.* **2021**, *11*, 1186-1221.
112. L. Budarin, V.; S. Shuttleworth, P.; H. Clark, J.; Luque, R., *Curr. Org. Synth.* **2010**, *7*, 614-627.
113. Taheri Kal Koshvandi, A.; Heravi, M. M.; Momeni, T., *Appl. Organometal. Chem.* **2018**, *32*, e4210.
114. Uno, B. E.; Gillis, E. P.; Burke, M. D., *Tetrahedron.* **2009**, *65*, 3130-3138.
115. de Meijere, A.; Khlebnikov, A. F.; Sünnemann, H. W.; Frank, D.; Rauch, K.; Yufit, D. S., *Eur. J. Org. Chem.* **2010**, *2010*, 3295-3301.
116. Hohn, E.; Paleček, J.; Pietruszka, J.; Frey, W., *Eur. J. Org. Chem.* **2009**, *2009*, 3765-3782.
117. Luthle, J. E. A.; Pietruszka, J., *J. Org. Chem.* **1999**, *64*, 8287-8297.
118. Bassan, E. M.; Baxter, C. A.; Beutner, G. L.; Emerson, K. M.; Fleitz, F. J.; Johnson, S.; Keen, S.; Kim, M. M.; Kuethe, J. T.; Leonard, W. R.; Mullens, P. R.; Muzzio, D. J.; Roberge, C.; Yasuda, N., *Org. Process Res. Dev.* **2012**, *16*, 87-95.
119. Markó, I. E.; Kumamoto, T.; Giard, T., *Adv. Synth. Catal.* **2002**, *344*, 1063-1067.
120. Rubina, M.; Rubin, M.; Gevorgyan, V., *J. Am. Chem. Soc.* **2003**, *125*, 7198-7199.
121. Liskey, C. W.; Hartwig, J. F., *J. Am. Chem. Soc.* **2013**, *135*, 3375-3378.
122. Benoit, G.; Charette, A. B., *J. Am. Chem. Soc.* **2017**, *139*, 1364-1367.
123. Ebner, C.; Carreira, E. M., *Chem. Rev.* **2017**, *117*, 11651-11679.
124. Tedford, C. E.; Phillips, J. G.; Gregory, R.; Pawlowski, G. P.; Fadnis, L.; Khan, M. A.; Ali, S. M.; Handley, M. K.; Yates, S. L., *J. Pharmacol. Exp. Ther.* **1999**, *289*, 1160-1168.

125. Liddle, J.; Bamborough, P.; Barker, M. D.; Campos, S.; Chung, C.-W.; Cousins, R. P.; Faulder, P.; Heathcote, M. L.; Hobbs, H.; Holmes, D. S., *Bioorg. Med. Chem. Lett.* **2012**, *22*, 5222-5226.
126. Raheem, I. T.; Schreier, J. D.; Fuerst, J.; Gantert, L.; Hostetler, E. D.; Huszar, S.; Joshi, A.; Kandebo, M.; Kim, S. H.; Li, J., *Bioorg. Med. Chem. Lett.* **2016**, *26*, 126-132.
127. Gaich, T.; Baran, P. S., *J. Org. Chem.* **2010**, *75*, 4657-4673.
128. Park, Y. J.; Park, J. W.; Jun, C. H., *Acc. Chem. Res.* **2008**, *41*, 222-34.
129. Narayan, R.; Matcha, K.; Antonchick, A. P., *Chemistry* **2015**, *21*, 14678-93.
130. Song, F.; Gou, T.; Wang, B.-Q.; Shi, Z.-J., *Chem. Soc. Rev.* **2018**, *47*, 7078-7115.
131. Balcells, D.; Clot, E.; Eisenstein, O., *Chem. Rev.* **2010**, *110*, 749-823.
132. Nairoukh, Z.; Cormier, M.; Marek, I., *Nat. Rev. Chem.* **2017**, *1*, 0035.
133. Wang, M.; Shi, Z., *Chem. Rev.* **2020**, *120*, 7348-7398.
134. Bose, S. K.; Mao, L.; Kuehn, L.; Radius, U.; Nekvinda, J.; Santos, W. L.; Westcott, S. A.; Steel, P. G.; Marder, T. B., *Chem. Rev.* **2021**, *121*, 13238-13341.
135. Yang, W.; Gao, X.; Wang, B., *Med. Res. Rev.* **2003**, *23*, 346-368.
136. Frisch, A. C.; Beller, M., *Angew. Chem. Int. Ed.* **2005**, *44*, 674-688.
137. Entwistle, C. D.; Marder, T. B., *J. Chem. Mater.* **2004**, *16*, 4574-4585.
138. Crudden, C. M.; Glasspoole, B. W.; Lata, C. J., *Chem. Commun.* **2009**, 6704-6716.
139. Pattison, G., *Org. Biomol. Chem.* **2019**, *17*, 5651-5660.
140. Xia, Y.; Dong, G., *Nat. Chem. Rev.* **2020**, *4*, 600-614.
141. Crabtree, R. H., *Chem. Rev.* **1985**, *85*, 245-269.
142. Crabtree, R. H.; Dion, R. P.; Gibboni, D. J.; McGrath, D. V.; Holt, E. M., *J. AM. Chem. Soc.* **1986**, *108*, 7222-7227.
143. Pirenne, V.; Muriel, B.; Waser, J., *Chem. Rev.* **2021**, *121*, 227-263.
144. Cavitt, M. A.; Phun, L. H.; France, S., *Chem. Soc. Rev.* **2014**, *43*, 804-818.
145. Meijere, A. d., *Angew. Chem. Int. Ed.* **1979**, *18*, 809-826.
146. Gagnon, A.; Duplessis, M.; Fader, L., *Org. Prep. Proced. Int.* **2010**, *42*, 1-69.
147. Wang, T.; Wang, Y.-N.; Wang, R.; Zhang, B.-C.; Yang, C.; Li, Y.-L.; Wang, X.-S., *Nat. Commun.* **2019**, *10*, 5373.

148. Bone, W. A.; Perkin, W. H., *J. Chem. Soc., Trans.* **1895**, *67*, 108-119.
149. Ge, L.; Wang, D.-X.; Xing, R.; Ma, D.; Walsh, P. J.; Feng, C., *Nat. Commun.* **2019**, *10*, 4367.
150. Fujii, H.; Okada, K.; Ishihara, M.; Hanamura, S.; Osa, Y.; Nemoto, T.; Nagase, H., *Tetrahedron* **2009**, *65*, 10623-10630.
151. Levina, R. Y.; Gladshtein, B. In *Reaction of Cyclopropane Hydrocarbons with Mercuric Salts*, Dokl. Akad. Nauk. SSSR, 1950; pp 65-68.
152. Collum, D. B.; Mohamadi, F.; Hallock, J. S., *J. Am. Chem. Soc.* **1983**, *105*, 6882-6889.
153. Zhang, H.; Xiao, H.; Jiang, F.; Fang, Y.; Zhu, L.; Li, C., *Org. Lett.* **2021**, *23*, 2268-2272.
154. Ogg, R. A., Jr.; Priest, W. J., *J. Am. Chem. Soc.* **1938**, *60*, 217-18.
155. Gieuw, M. H.; Ke, Z.; Yeung, Y.-Y., *Angew. Chem. Int. Ed.* **2018**, *57*, 3782-3786.
156. Leung, V. M.-Y.; Gieuw, M. H.; Ke, Z.; Yeung, Y.-Y., *Adv. Synth. Catal.* **2020**, *362*, 2039-2044.
157. Peng, P.; Yan, X.; Zhang, K.; Liu, Z.; Zeng, L.; Chen, Y.; Zhang, H.; Lei, A., *Nat. Commun.* **2021**, *12*, 3075.
158. Richmond, E.; Yi, J.; Vuković, V. D.; Sajadi, F.; Rowley, C. N.; Moran, J., *Chem. Sci.* **2018**, *9*, 6411-6416.
159. Roy, A.; Bonetti, V.; Wang, G.; Wu, Q.; Klare, H. F. T.; Oestreich, M., *Org. Lett.* **2020**, *22*, 1213-1216.
160. Zhang, Z.-Y.; Liu, Z.-Y.; Guo, R.-T.; Zhao, Y.-Q.; Li, X.; Wang, X.-C., *Angew. Chem. Int. Ed.* **2017**, *56*, 4028-4032.
161. Kim, H. Y.; Walsh, P. J., *Acc. Chem. Res.* **2012**, *45*, 1533-1547.
162. Wu, W.; Lin, Z.; Jiang, H., *Org. Biomol. Chem.* **2018**, *16*, 7315-7329.
163. Sumida, Y.; Yorimitsu, H.; Oshima, K., *Org. Lett.* **2008**, *10*, 4677-4679.
164. Zhao, J.; Szabó, K. J., *Angew. Chem. Int. Ed.* **2016**, *55*, 1502-1506.
165. Kondo, H.; Miyamura, S.; Matsushita, K.; Kato, H.; Kobayashi, C.; Arifin; Itami, K.; Yokogawa, D.; Yamaguchi, J., *J. Am. Chem. Soc.* **2020**, *142*, 11306-11313.
166. Rickborn, B.; Wood, S. E., *J. Am. Chem. Soc.* **1971**, *93*, 3940-3946.
167. Hurd, D. T., *J. Am. Chem. Soc.* **1948**, *70*, 2053-5.
168. Morton, J. G.; Dureen, M. A.; Stephan, D. W., *Chem. Commun.* **2010**, *46*, 8947-8949.
169. Kuboki, Y.; Arisawa, M.; Murai, K., *RSC Adv.* **2020**, *10*, 37797-37799.

170. Wang, S.; Kaga, A.; Yorimitsu, H., *Synlett* **2020**, 32, 219-223.
171. Chupakhin, E.; Babich, O.; Prosekov, A.; Asyakina, L.; Krasavin, M., *Molecules* **2019**, 24, 4165.
172. Kingwell, K., *Nat. Rev. Drug Discov.* **2009**, 8, 931-931.
173. Gober, C. M.; Carroll, P. J.; Joullié, M. M., *Mini-Rev. Org. Chem.* **2016**, 13, 126-142.
174. Hiesinger, K.; Dar'in, D.; Proschak, E.; Krasavin, M., *J. Med. Chem.* **2020**.
175. Torres, R. R., *Spiro Compounds: Synthesis and Applications*. John Wiley & Sons: 2022.
176. Wang, J.; Ma, C.; Wu, Y.; Lamb, R. A.; Pinto, L. H.; DeGrado, W. F., *J. Am. Chem. Soc.* **2011**, 133, 13844-13847.
177. Krebs, A.; Schäfer, B.; Kochner, A. Method for Producing Azoniaspironortropine Esters and Nortropan-3-One Compounds. 2010.
178. Blicke, F.; Hotelling, E. B., *J. Am. Chem. Soc.* **1954**, 76, 5099-5103.
179. Ooi, T.; Kameda, M.; Maruoka, K., *J. Am. Chem. Soc.* **2003**, 125, 5139-5151.
180. Pham, T. H.; Olsson, J. S.; Jannasch, P., *J. Am. Chem. Soc.* **2017**, 139, 2888-2891.
181. Voituriez, A.; Marinetti, A.; Gicquel, M., *Synlett* **2015**, 26, 142-166.
182. Jørgensen, K. A., *Cycloaddition Reactions in Organic Synthesis*. John Wiley & Sons: 2002.
183. Kotha, S.; Aswar, V. R.; Tangella, Y., Design and Synthesis of Spirocycles Via Olefin Metathesis. In *Spiro Compounds*, 2022; pp 65-101.
184. Miyamoto, H.; Hirano, T.; Okawa, Y.; Nakazaki, A.; Kobayashi, S., *Tetrahedron* **2013**, 69, 9481-9493.
185. Shennan, B. D. A.; Smith, P. W.; Ogura, Y.; Dixon, D. J., *Chem. Sci.* **2020**, 11, 10354-10360.
186. Dake, G., *Tetrahedron* **2006**, 62, 3467-3492.
187. Lipinski, C. A.; Lombardo, F.; Dominy, B. W.; Feeney, P. J., *Adv. Drug Delivery Rev.* **1997**, 23, 3-25.
188. Trost, B., *Science* **1991**, 254, 1471-1477.
189. Benoit, G.; Charette, A. B., *J. Am. Chem. Soc.* **2017**, 139, 1364-1367.
190. Sayes, M.; Benoit, G.; Charette, A. B., *Angew. Chem. Int. Ed.* **2018**, 57, 13514-13518.
191. Liskey, C. W.; Hartwig, J. F., *J. Am. Chem. Soc.* **2013**, 135, 3375-3378.
192. Siddiqui, S. H.; Navuluri, C.; Charette, A. B., *Synthesis* **2019**, 51, 3834-3846.

193. Scheideman, M.; Wang, G.; Vedejs, E., *J. Am. Chem. Soc.* **2008**, *130*, 8669-8676.
194. Scheideman, M.; Shapland, P.; Vedejs, E., *J. Am. Chem. Soc.* **2003**, *125*, 10502-10503.
195. Prokofjevs, A.; Vedejs, E., *J. Am. Chem. Soc.* **2011**, *133*, 20056-20059.
196. Prokofjevs, A.; Jermaks, J.; Borovika, A.; Kampf, J. W.; Vedejs, E., *Organometallics* **2013**, *32*, 6701-6711.
197. Yang, J.-M.; Guo, F.-K.; Zhao, Y.-T.; Zhang, Q.; Huang, M.-Y.; Li, M.-L.; Zhu, S.-F.; Zhou, Q.-L., *J. Am. Chem. Soc.* **2020**, *142*, 20924-20929.
198. Zhao, W.; Sun, J., *Chem. Rev.* **2018**, *118*, 10349-10392.
199. Meanwell, N. A., *J. Med. Chem.* **2018**, *61*, 5822-5880.
200. Srebnik, M. T., K.; Shalom, E. Novel Amine-Borane Compounds and Uses Thereof. WO 2007/032005, March 22, 2007.
201. Li, X.; Hall, D. G., *Adv. Synth. Catal.* **2021**, *363*, 2209-2223.
202. Das, B. C.; Thapa, P.; Karki, R.; Schinke, C.; Das, S.; Kambhampati, S.; Banerjee, S. K.; Van Veldhuizen, P.; Verma, A.; Weiss, L. M., *Future Med. Chem.* **2013**, *5*, 653-676.
203. Jachak, G. R.; Ramesh, R.; Sant, D. G.; Jorwekar, S. U.; Jadhav, M. R.; Tupe, S. G.; Deshpande, M. V.; Reddy, D. S., *ACS Med. Chem. Lett.* **2015**, *6*, 1111-1116.
204. Majerić, M.; Avdagić, A.; Hameršak, Z.; Šunjić, V., *J. Biotechnol. Lett.* **1995**, *17*, 1189-1194.
205. Brown, H.; Rao, B. C., *J. Org. Chem.* **1957**, *22*, 1137-1138.
206. Wang, D.; Xue, X.-S.; Houk, K. N.; Shi, Z., *Angew. Chem. Int. Ed.* **2018**, *57*, 16861-16865.
207. Prokofjevs, A.; Boussonniere, A.; Li, L.; Bonin, H.; Lacote, E.; Curran, D. P.; Vedejs, E., *J. Am. Chem. Soc.* **2012**, *134*, 12281-12288.
208. Osi, A.; Mahaut, D.; Tumanov, N.; Fusaro, L.; Wouters, J.; Champagne, B.; Chardon, A.; Berionni, G., *Angew. Chem. Int. Ed.* **2022**, *61*, e202112342.
209. Rochette, É.; Courtemanche, M. A.; Fontaine, F. G., *Chem. - Eur. J.* **2017**, *23*, 3567-3571.
210. Légaré, M.-A.; Courtemanche, M.-A.; Rochette, É.; Fontaine, F.-G., *Science* **2015**, *349*, 513-516.
211. De Vries, T. S.; Prokofjevs, A.; Vedejs, E., *Chem. Rev.* **2012**, *112*, 4246-4282.
212. Bremser, W.; Vogel, F. G. M., *Org. Magn. Reson.* **1980**, *14*, 155-156.
213. Lankhorst, P. P.; van Rijn, J. H. J.; Duchateau, A. L. L., *Molecules* **2018**, *23*.

214. Cook, P., *Isot. Environ. Health Stud.* **1998**, *34*, 3-17.
215. Schreiner, P. R., *Trends Chem.* **2020**, *2*, 980-989.
216. Ley, D.; Gerbig, D.; Schreiner, P. R., *Org. Biomol. Chem.* **2012**, *10*, 3781-3790.
217. Sabir, S.; Kumar, G.; Verma, V. P.; Jat, J. L., *ChemistrySelect* **2018**, *3*, 3702-3711.
218. Mathew, T., *Nature* **2017**, *544*, 162-162.
219. Olah, G. A., *Angew. Chem. Int. Ed.* **1973**, *12*, 173-212.
220. Lukin, A.; Chudinov, M.; Vedekhina, T.; Rogacheva, E.; Kraeva, L.; Bakulina, O.; Krasavin, M., *Molecules* **2022**, *27*, 4864.
221. Zheng, Y.; Tice, C. M.; Singh, S. B., *Bioorganic & Medicinal Chemistry Letters* **2014**, *24*, 3673-3682.
222. Bosdet, M. J.; Piers, W. E., *Can. J. Chem.* **2009**, *87*, 8-29.
223. Ma, K.; Scheibitz, M.; Scholz, S.; Wagner, M., *J. Organomet. Chem.* **2002**, *652*, 11-19.
224. Brand, J.; Braunschweig, H.; Sen, S. S., *Acc. Chem. Res.* **2014**, *47*, 180-191.
225. Colebatch, A. L.; Weller, A. S., *Chemistry* **2019**, *25*, 1379-1390.
226. Porcari, P.; Capuani, S.; D'Amore, E.; Lecce, M.; La Bella, A.; Fasano, F.; Migneco, L.; Campanella, R.; Maraviglia, B.; Pastore, F., *Appl. Radiat. Isot.* **2009**, *67*, S365-S368.
227. Daina, A.; Michielin, O.; Zoete, V., *Sci. Rep.* **2017**, *7*, 42717.
228. Heravi, M. M.; Zadsirjan, V., *RSC Adv.* **2020**, *10*, 44247-44311.
229. Matteson, D., Preparation and Use of Organoboranes in Organic Synthesis. In *The Metal—Carbon Bond*, Hartley, F., Ed. John Wiley & Sons Ltd.: 1987; Vol. 4, pp 307-409.
230. Mungall, W. S., Thexylborane. In *Encyclopedia of Reagents for Organic Synthesis*.
231. Muir, S. S.; Yao, X., *Int. J. Hydrogen Energy* **2011**, *36*, 5983-5997.
232. Brahmi, M. M.; Monot, J.; Desage-El Murr, M.; Curran, D. P.; Fensterbank, L.; Lacôte, E.; Malacria, M., *J. Org. Chem.* **2010**, *75*, 6983-6985.
233. Holschumacher, D.; Bannenberg, T.; Hrib, C. G.; Jones, P. G.; Tamm, M., *Angew. Chem. Int. Ed.* **2008**, *47*, 7428-7432.
234. Ueng, S.-H.; Makhlouf Brahmi, M.; Derat, É.; Fensterbank, L.; Lacôte, E.; Malacria, M.; Curran, D. P., *J. Am. Chem. Soc.* **2008**, *130*, 10082-10083.

235. Solovyev, A.; Chu, Q.; Geib, S. J.; Fensterbank, L.; Malacria, M.; Lacôte, E.; Curran, D. P., *J. Am. Chem. Soc.* **2010**, *132*, 15072-15080.
236. McArthur, D.; Butts, C. P.; Lindsay, D. M., *Chem. Commun.* **2011**, *47*, 6650-6652.
237. Prokofjevs, A.; Jermaks, J.; Borovika, A.; Kampf, J. W.; Vedejs, E., *Organometallics* **2013**, *32*, 6701-6711.
238. Zhao, W.; Sun, J., *Chem. Rev.* **2018**, *118*, 10349-10392.
239. Burg, A. B. J. I. C., *Inorg. Chem.* **1964**, *3*, 1325-1327.
240. Titov, L.; Makarova, M.; Y., R. V., *Dokl. Akad. Nauk* **1968**, *180*, 381-&.
241. Brown, M.; Heseltine, R., *Chem. Commun.* **1968**, 1551-1552.
242. Brown, M.; Heseltine, R.; Smith, P. A.; Walker, P., *J. Chem. Soc. A* **1970**, 410-414.
243. Epstein, L. M.; Shubina, E. S.; Bakhmutova, E. V.; Saitkulova, L. N.; Bakhmutov, V. I.; Chistyakov, A. L.; Stankevich, I. V., *Inorg. Chem.* **1998**, *37*, 3013-3017.
244. Shubina, E. S.; Belkova, N. V.; Epstein, L. M., *J. Organomet. Chem.* **1997**, *536-537*, 17-29.
245. Shubina, E. S.; Bakhmutova, E. V.; Saitkulova, L. N.; Epstein, L. M., *Mendeleev Commun.* **1997**, *7*, 83-84.
246. Padilla-Martínez, I. I.; Rosalez-Hoz, M. D. J.; Tlahuext, H.; Camacho-Camacho, C.; Ariza-Castolo, A.; Contreras, R., *Chem. Ber.* **1996**, *129*, 441-449.
247. Flores-Parra, A.; Sánchez-Ruiz, S. A.; Guadarrama, C.; Nöth, H.; Contreras, R., *Eur. J. Inorg. Chem.* **1999**, *1999*, 2069-2073.
248. Ramnial, T.; Jong, H.; McKenzie, I. D.; Jennings, M.; Clyburne, J. A., *Chem. Commun.* **2003**, 1722-1723.
249. Watson, J. D.; Crick, F. H., *Nature* **1953**, *171*, 737-738.
250. Moore, T. S.; Winmill, T. F., *J. Chem. Soc., Trans.* **1912**, *101*, 1635-1676.
251. Fornaro, T.; Burini, D.; Biczysko, M.; Barone, V., *J. Phys. Chem. A* **2015**, *119*, 4224-4236.
252. Alabugin, I. V.; Manoharan, M.; Peabody, S.; Weinhold, F., *J. Am. Chem. Soc.* **2003**, *125*, 5973-5987.
253. Sutor, D. J., *Nature* **1962**, *195*, 68-69.
254. Sutor, D. J., *J. Chem. Soc., Trans.* **1963**, 1105-1110.
255. Taylor, R.; Kennard, O., *J. Am. Chem. Soc.* **1982**, *104*, 5063-5070.

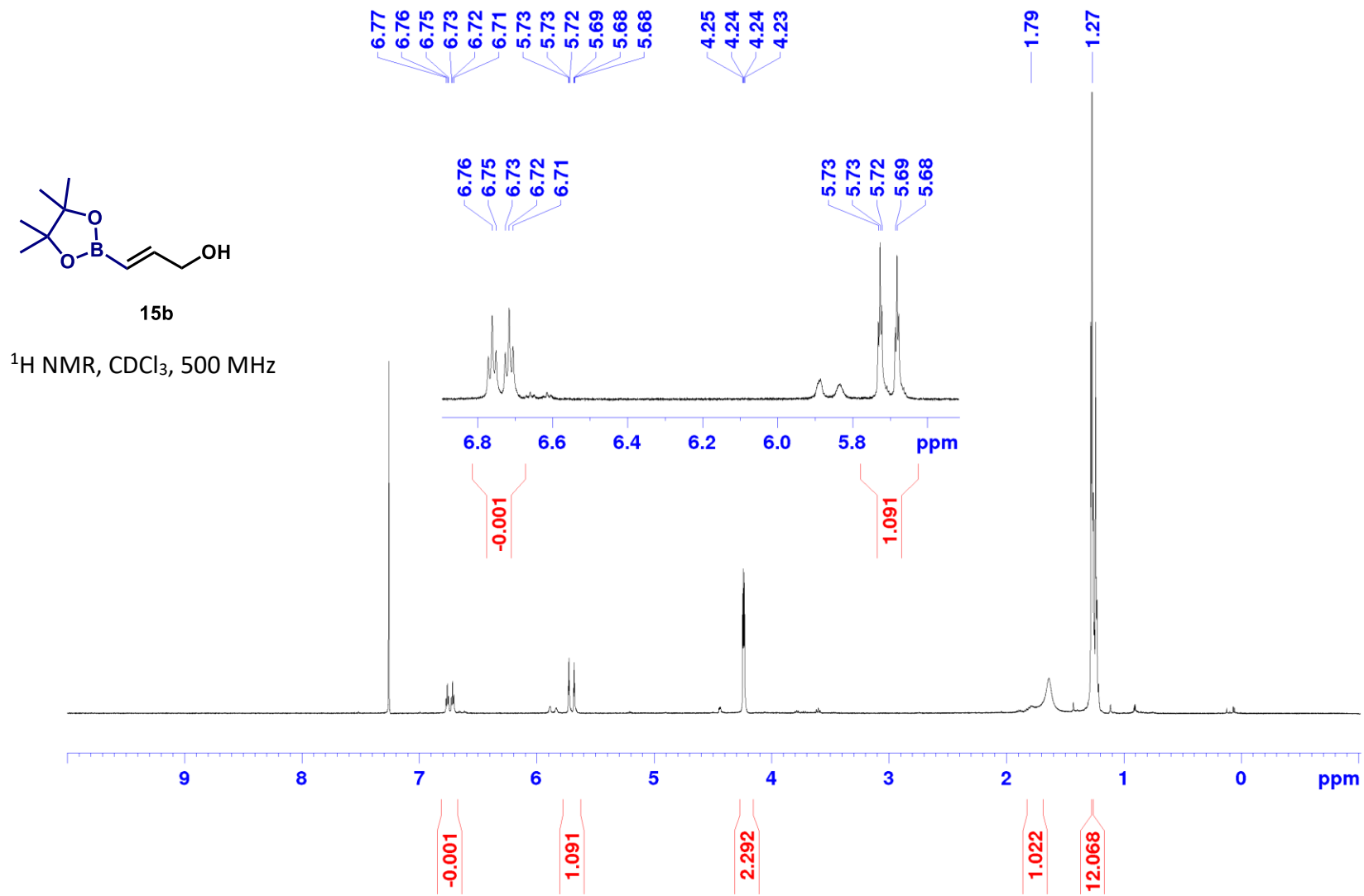
256. Ghosh, S.; Wategaonkar, S., *J. Indian Inst. Sci.* **2020**, *100*, 101-125.
257. Thakur, T. S.; Kirchner, M. T.; Bläser, D.; Boese, R.; Desiraju, G. R., *CrystEngComm* **2010**, *12*, 2079-2085.
258. Chatterjee, J.; Mierke, D. F.; Kessler, H., *Chem. - Eur. J.* **2008**, *14*, 1508-1517.
259. Erez, E.; Fass, D.; Bibi, E., *Nature* **2009**, *459*, 371-378.
260. Horowitz, S.; Trievel, R. C., *J. Biol. Chem.* **2012**, *287*, 41576-41582.
261. Brovarets', O. h. O.; Yurenko, Y. P.; Hovorun, D. M. J. J. o. B. S., *J. Biomol. Struct. Dyn.* **2014**, *32*, 993-1022.
262. Jiang, L.; Lai, L., *J. Biol. Chem.* **2002**, *277*, 37732-37740.
263. Bent, H. A., *Chem. Rev.* **1961**, *61*, 275-311.
264. Li, X.; Liu, L.; Schlegel, H. B., *J. Am. Chem. Soc.* **2002**, *124*, 9639-9647.
265. Hobza, P.; Špirko, V.; Selzle, H. L.; Schlag, E. W., *J. Phys. Chem.* **1998**, *102*, 2501-2504.
266. Hobza, P.; Havlas, Z., *Chem. Rev.* **2000**, *100*, 4253-4264.
267. Hobza, P.; Havlas, Z., *Chem. Phys. Lett.* **1999**, *303*, 447-452.
268. Delanoye, S. N.; Herrebout, W. A.; Van der Veken, B. J., *J. Am. Chem. Soc.* **2002**, *124*, 7490-7498.
269. Qian, W.; Krimm, S., *J. Phys. Chem.* **2002**, *106*, 6628-6636.
270. van der Veken, B. J.; Herrebout, W. A.; Szostak, R.; Shchepkin, D. N.; Havlas, Z.; Hobza, P., *J. Am. Chem. Soc.* **2001**, *123*, 12290-12293.
271. Hobza, P., *J. Phys. Chem.* **2001**, *3*, 2555-2556.
272. Zierkiewicz, W.; Michalska, D.; Havlas, Z.; Hobza, P., *ChemPhysChem* **2002**, *3*, 511-518.
273. Charisiadis, P.; Kontogianni, V. G.; Tsiafoulis, C. G.; Tzakos, A. G.; Siskos, M.; Gerothanassis, I. P., *Molecules* **2014**, *19*, 13643-82.
274. Alabugin, I. V.; dos Passos Gomes, G.; Abdo, M. A., *WIREs Comput. Mol. Sci.* **2019**, *9*, e1389.
275. Mo, Y.; Jiao, H.; Schleyer, P. v. R., *J. Org. Chem.* **2004**, *69*, 3493-3499.
276. Dill, J. D.; Schleyer, P. v. R.; Pople, J. A., *J. Am. Chem. Soc.* **1975**, *97*, 3402-3409.
277. Apeloig, Y.; Schleyer, P. v. R.; Pople, J. A., *J. Am. Chem. Soc.* **1977**, *99*, 5901-5909.
278. Boese, R.; Bläser, D.; Niederprüm, N.; Nüsse, M.; Brett, W. A.; von Ragué Schleyer, P.; Bühl, M.; van Eikema Hommes, N. J. R., *Angew. Chem. Int. Ed.* **1992**, *31*, 314-316.

279. McDaniel, D. H., *Science* **1957**, *125*, 545-546.
280. Zhao, W.; Sun, J., *Chem. Rev.* **2018**, *118*, 10349-10392.
281. Dhillon, R. S., *Hydroboration and Organic Synthesis: 9-Borabicyclo [3.3. 1] Nonane (9-Bbn)*. Springer Science & Business Media: 2007.
282. Paschoal, V. H.; Faria, L. F.; Ribeiro, M. C., *Chem. Rev.* **2017**, *117*, 7053-7112.
283. Katsyuba, S. A.; Vener, M. V.; Zvereva, E. E.; Fei, Z.; Scopelliti, R.; Laurencyzy, G.; Yan, N.; Paunescu, E.; Dyson, P. J. J. T. J. o. P. C. B., *J. Phys. Chem.* **2013**, *117*, 9094-9105.
284. Sowmiah, S.; Srinivasadesikan, V.; Tseng, M.-C.; Chu, Y.-H., *Molecules* **2009**, *14*, 3780-3813.
285. Wang, B.; Qin, L.; Mu, T.; Xue, Z.; Gao, G. J. C. r., *Chem. Rev.* **2017**, *117*, 7113-7131.
286. Taniguchi, T.; Curran, D. P., *Org. Lett.* **2012**, *14*, 4540-4543.
287. Wong, S. S.; Shu, R.; Zhang, J.; Liu, H.; Yan, N., *Chem. Soc. Rev.* **2020**, *49*, 5510-5560.
288. Ji, N.; Wang, Z.; Diao, X.; Jia, Z.; Li, T.; Zhao, Y.; Liu, Q.; Lu, X.; Ma, D.; Song, C., *Catal. Sci. Technol.* **2021**, *11*, 800-809.
289. Bomon, J.; Bal, M.; Achar, T. K.; Sergeyevev, S.; Wu, X.; Wambacq, B.; Lemièere, F.; Sels, B. F.; Maes, B. U. W., *Green Chem.* **2021**, *23*, 1995-2009.
290. McOmie, J. F. W.; Watts, M. L.; West, D. E., *Tetrahedron.* **1968**, *24*, 2289-2292.
291. Huber, D.; Andermann, G.; Leclerc, G., *Tetrahedron Lett.* **1988**, *29*, 635-638.
292. Kadam, H. K.; Tilve, S. G., *RSC Adv.* **2015**, *5*, 83391-83407.
293. Kameo, H.; Sakaki, S., *Chem. Eur. J.* **2015**, *21*, 13588-13597.
294. Hartmann, M.; Wetmore, S. D.; Radom, L., *J. Phys. Chem. A* **2001**, *105*, 4470-4479.
295. Lipinski, C. A., *Drug Discovery Today: Technol.* **2004**, *1*, 337-341.
296. Plescica, J.; Moitessier, N., *Eur. J. Med. Chem.* **2020**, *195*, 112270.

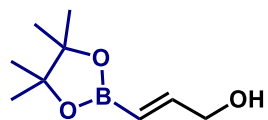
Annexes

Annex 1: NMR Spectra for Chapter 2

(E)-3-(4,4,5,5-Tetramethyl-1,3,2-dioxaborolan-2-yl)prop-2-en-1-ol (15b):

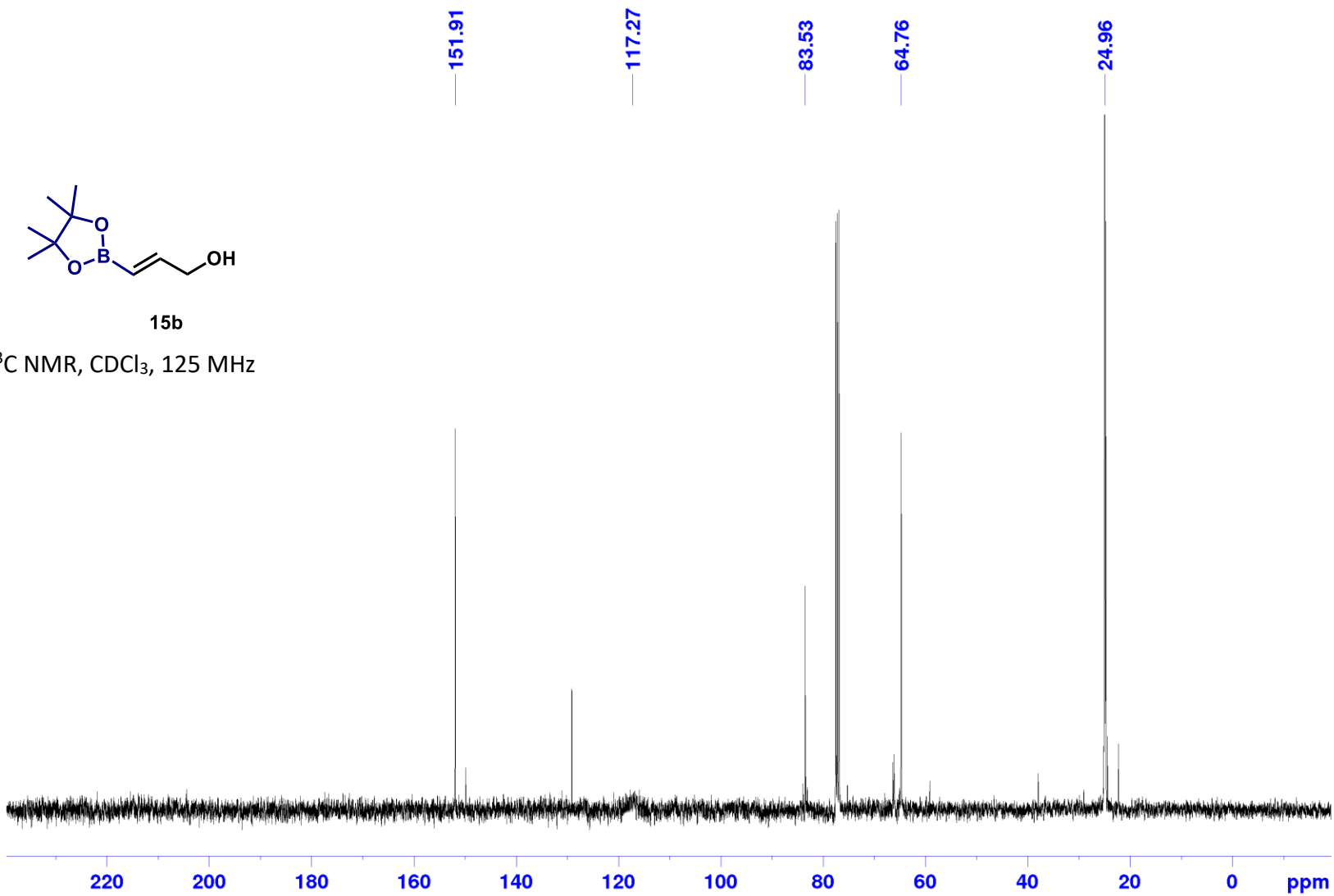


¹³C

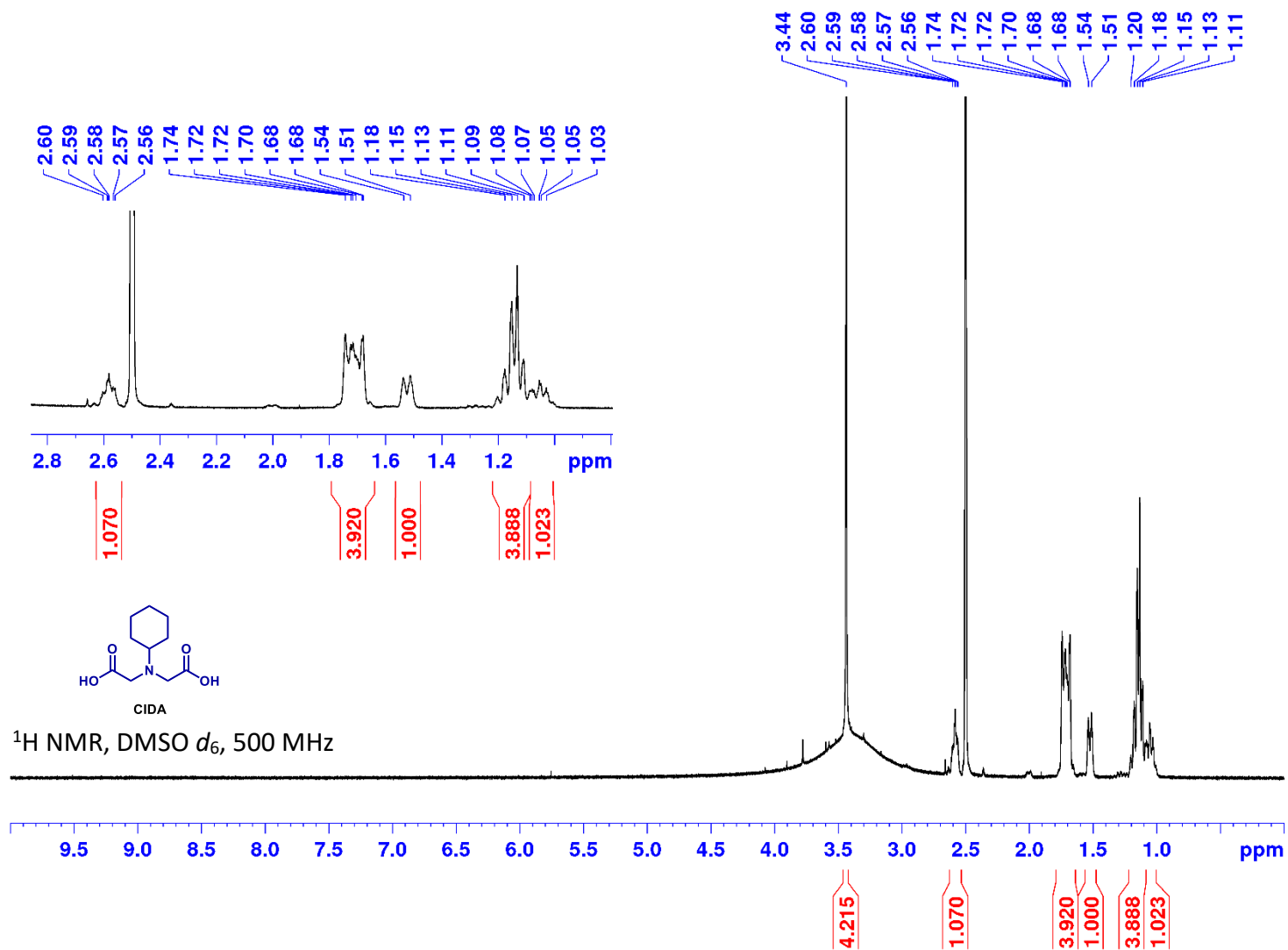


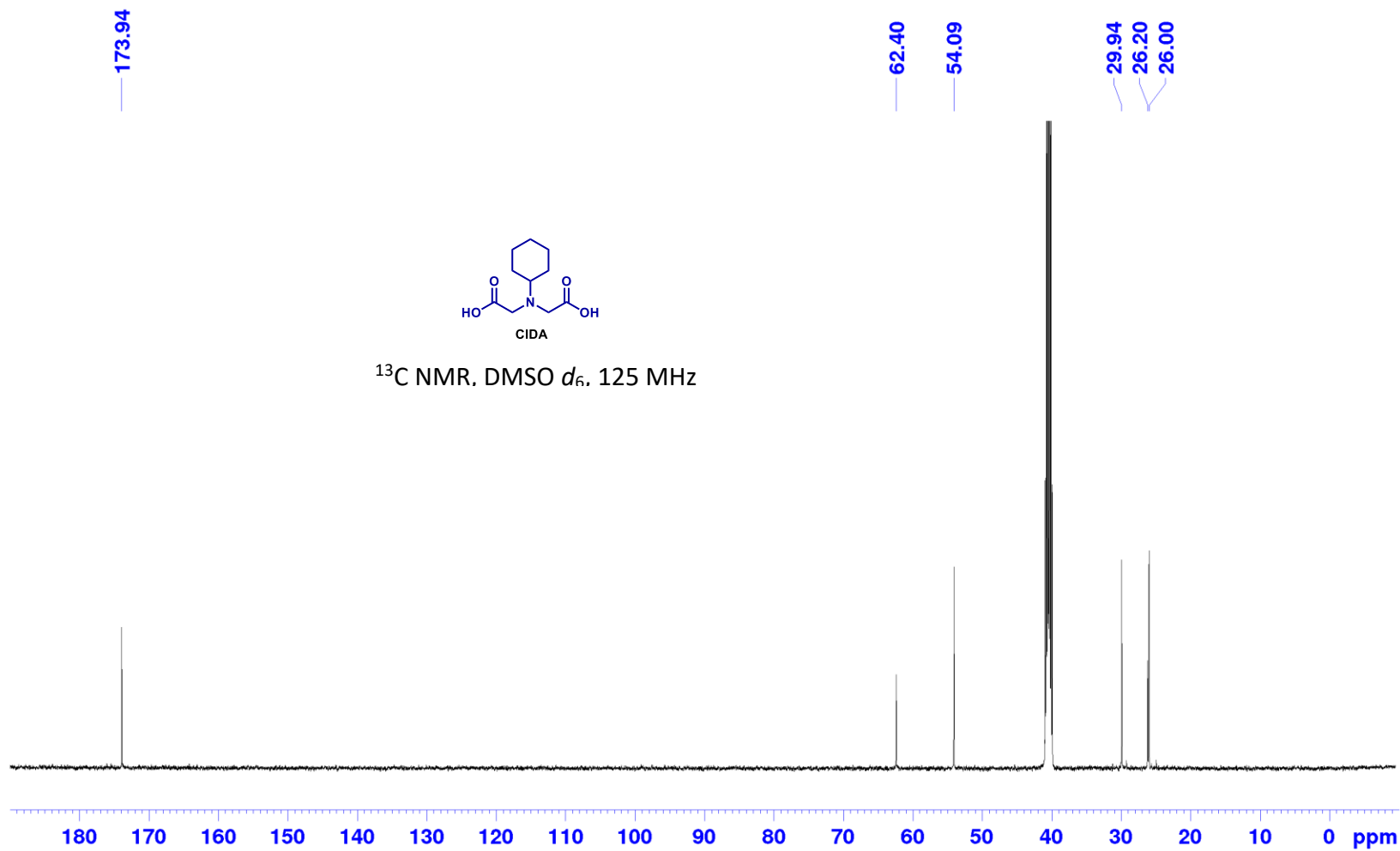
15b

¹³C NMR, CDCl₃, 125 MHz

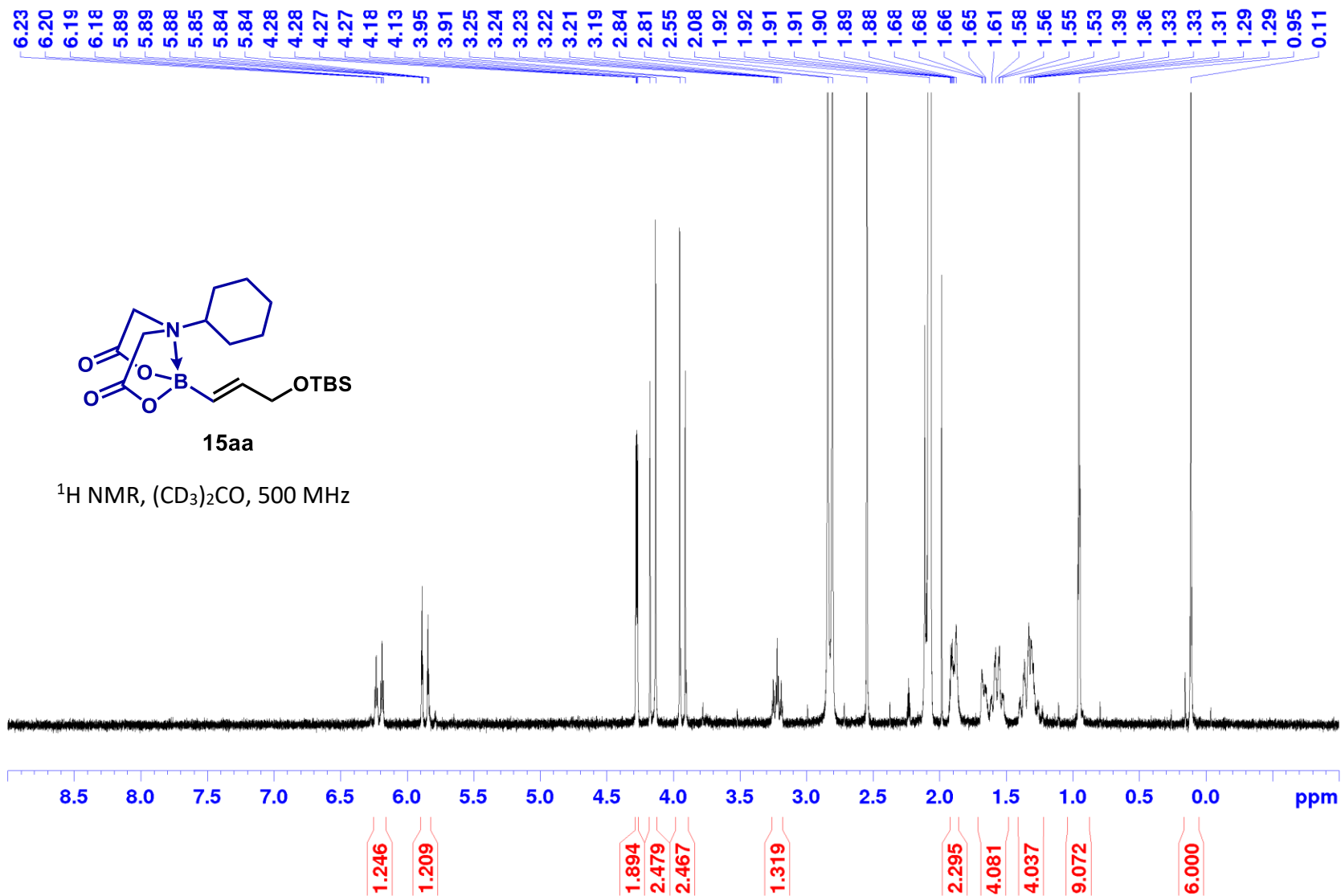


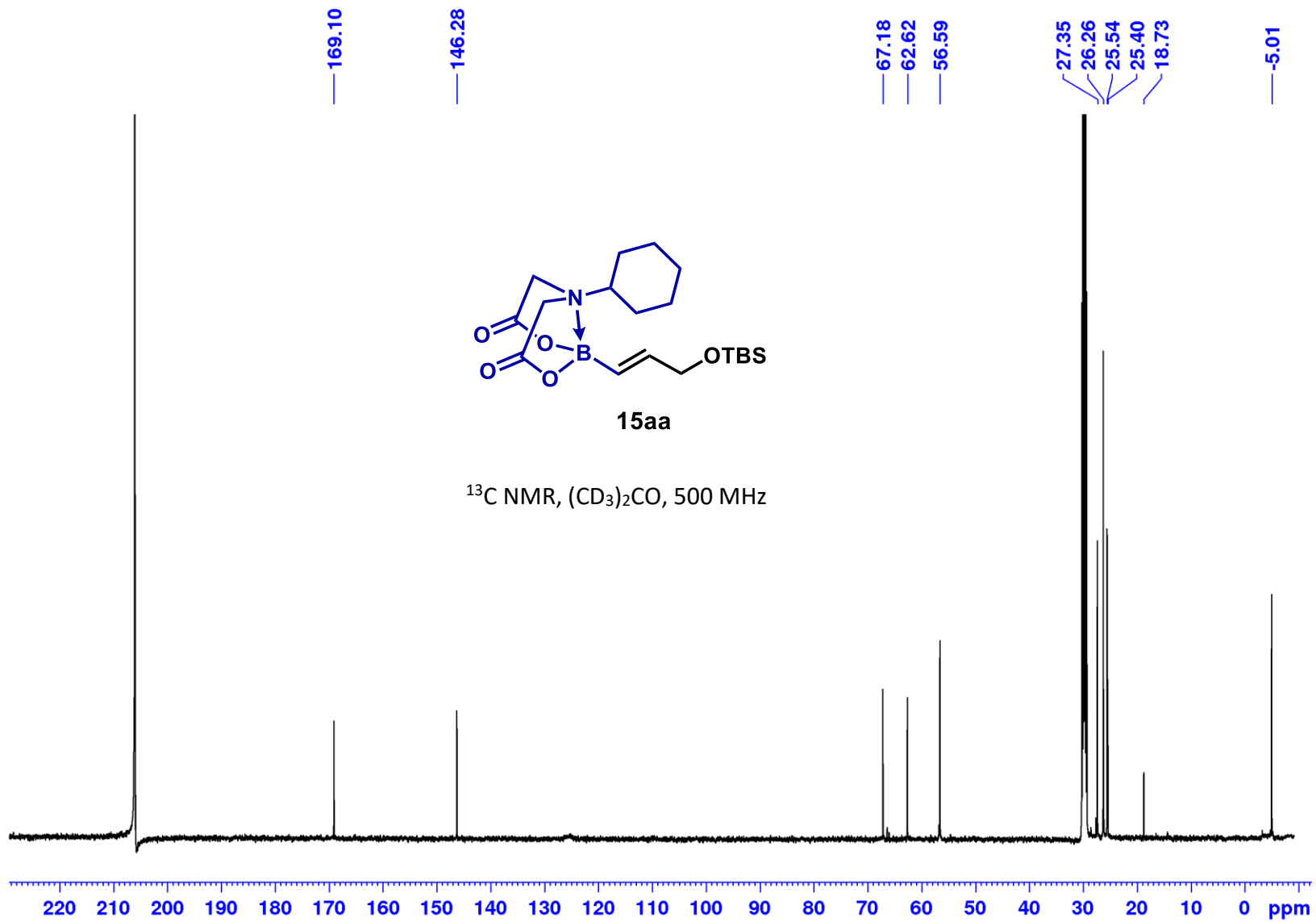
2,2'-(Cyclohexylazanediy)diacetic acid (CIDA):



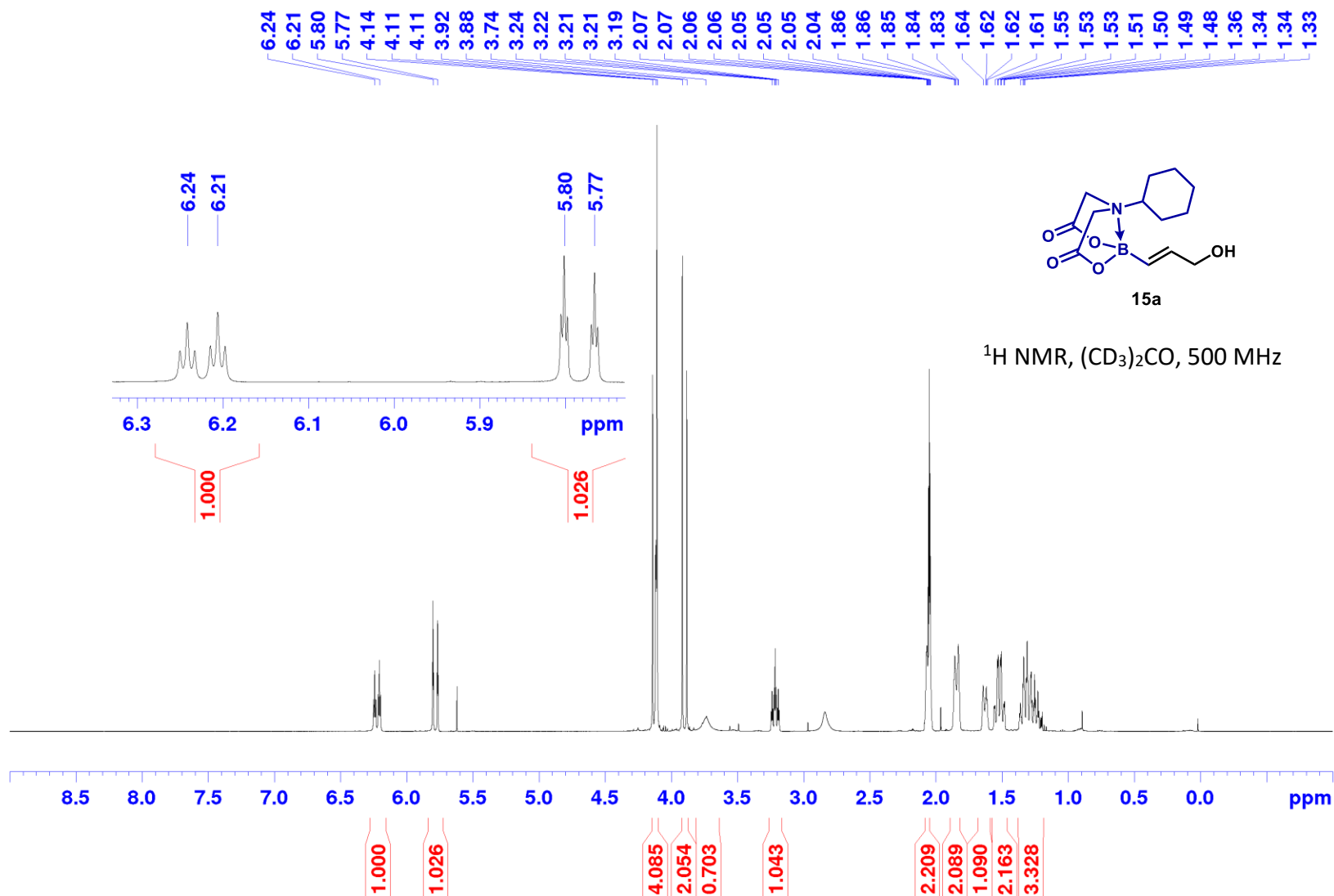


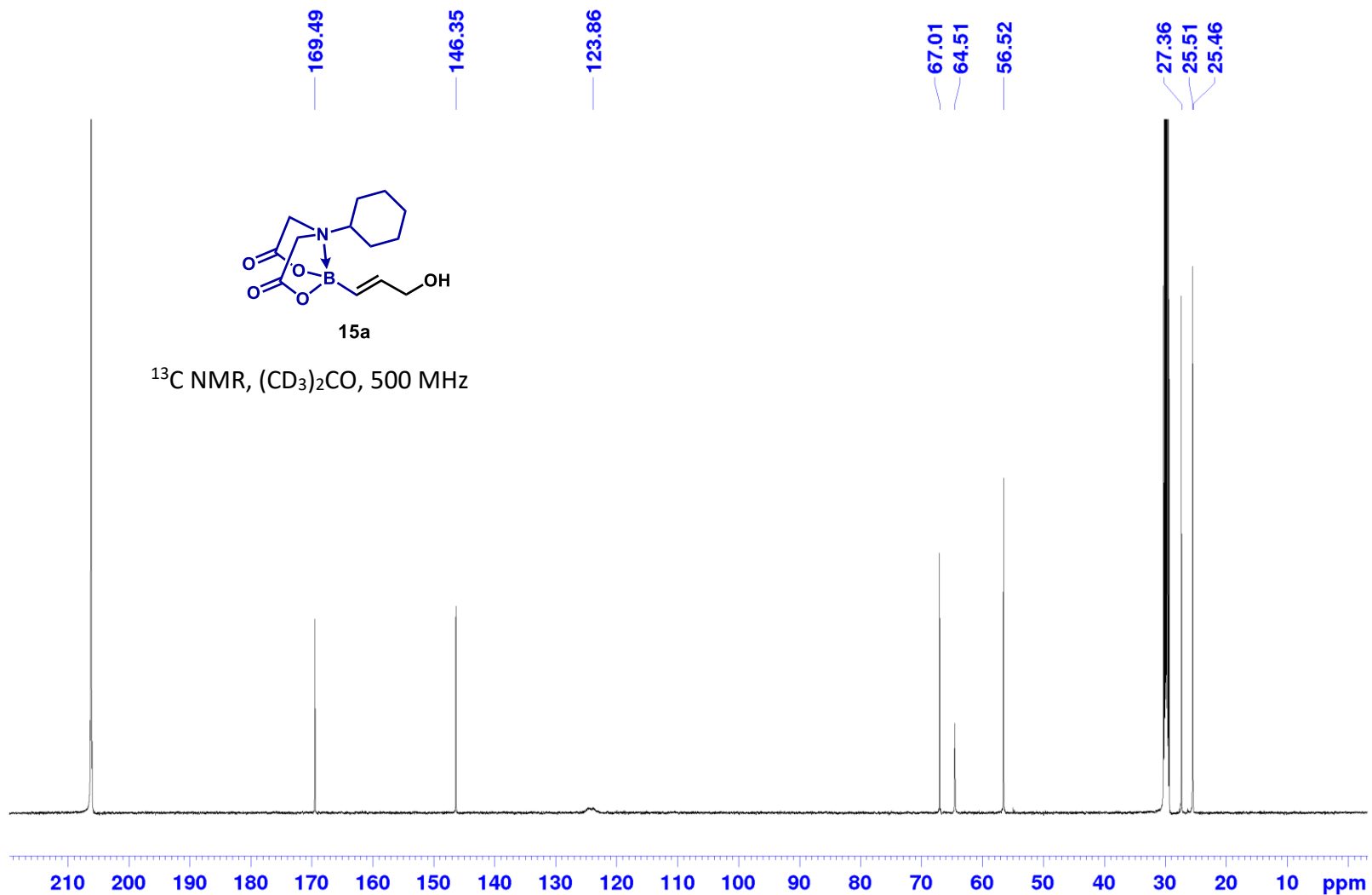
(E)-2-(3-((tert-Butyldimethylsilyl)oxy)prop-1-en-1-yl)-6-cyclohexyl-1,3,6,2-dioxazaborocane-4,8-dione (15aa):

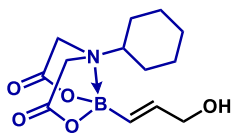




(E)-6-Cyclohexyl-2-(3-hydroxyprop-1-en-1-yl)-1,3,6,2-dioxazaborocane-4,8-dione (15a):

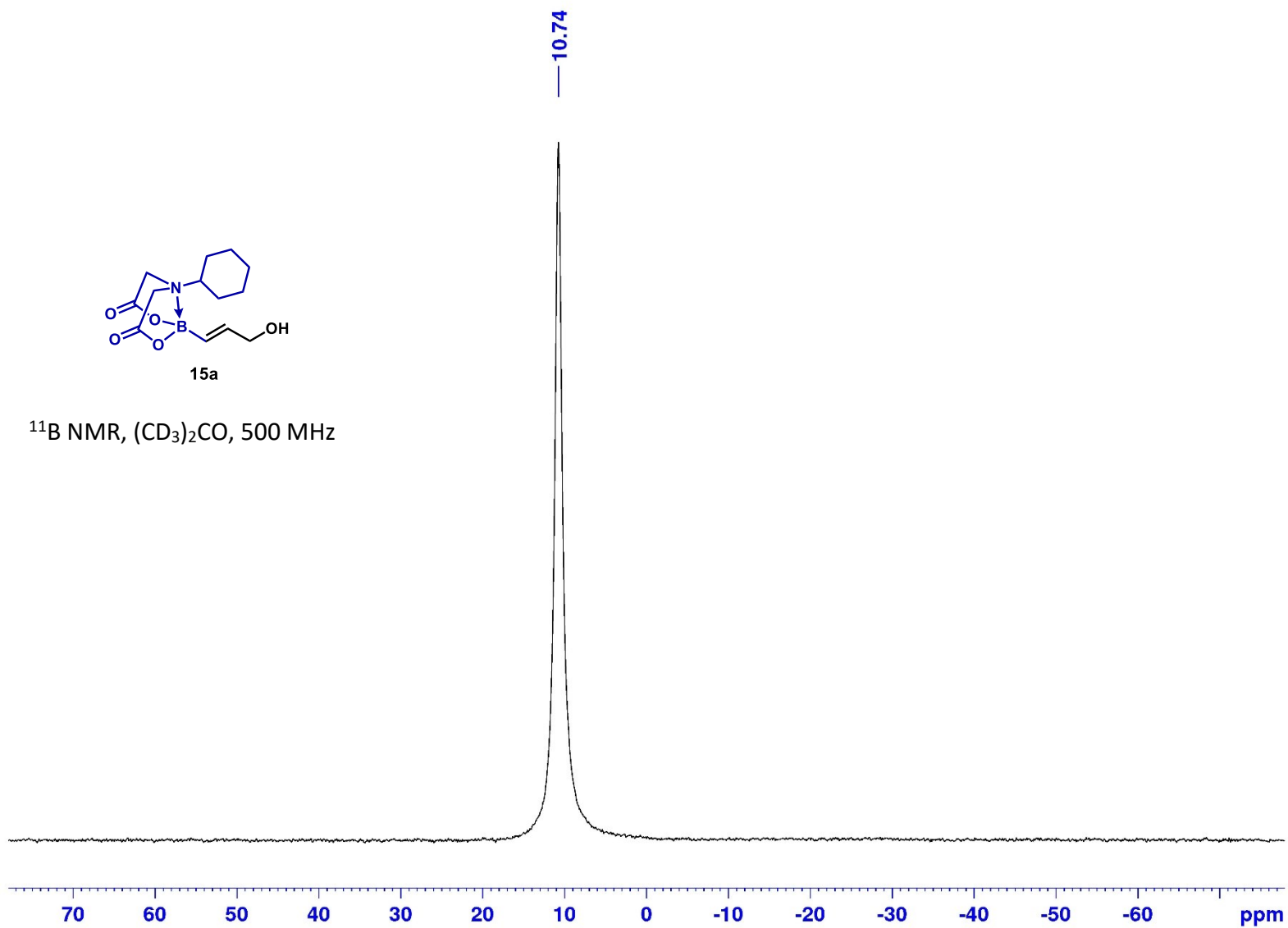




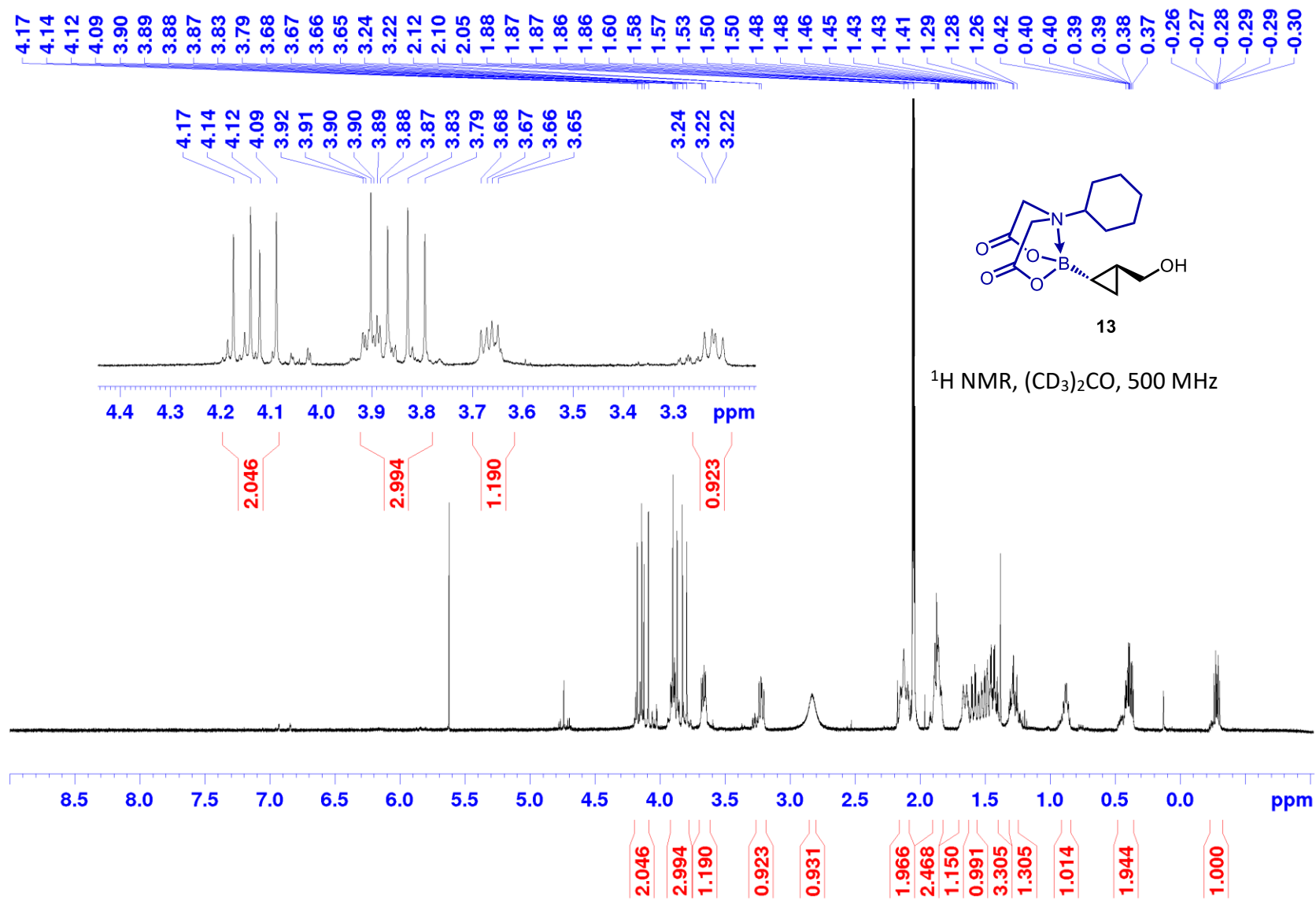


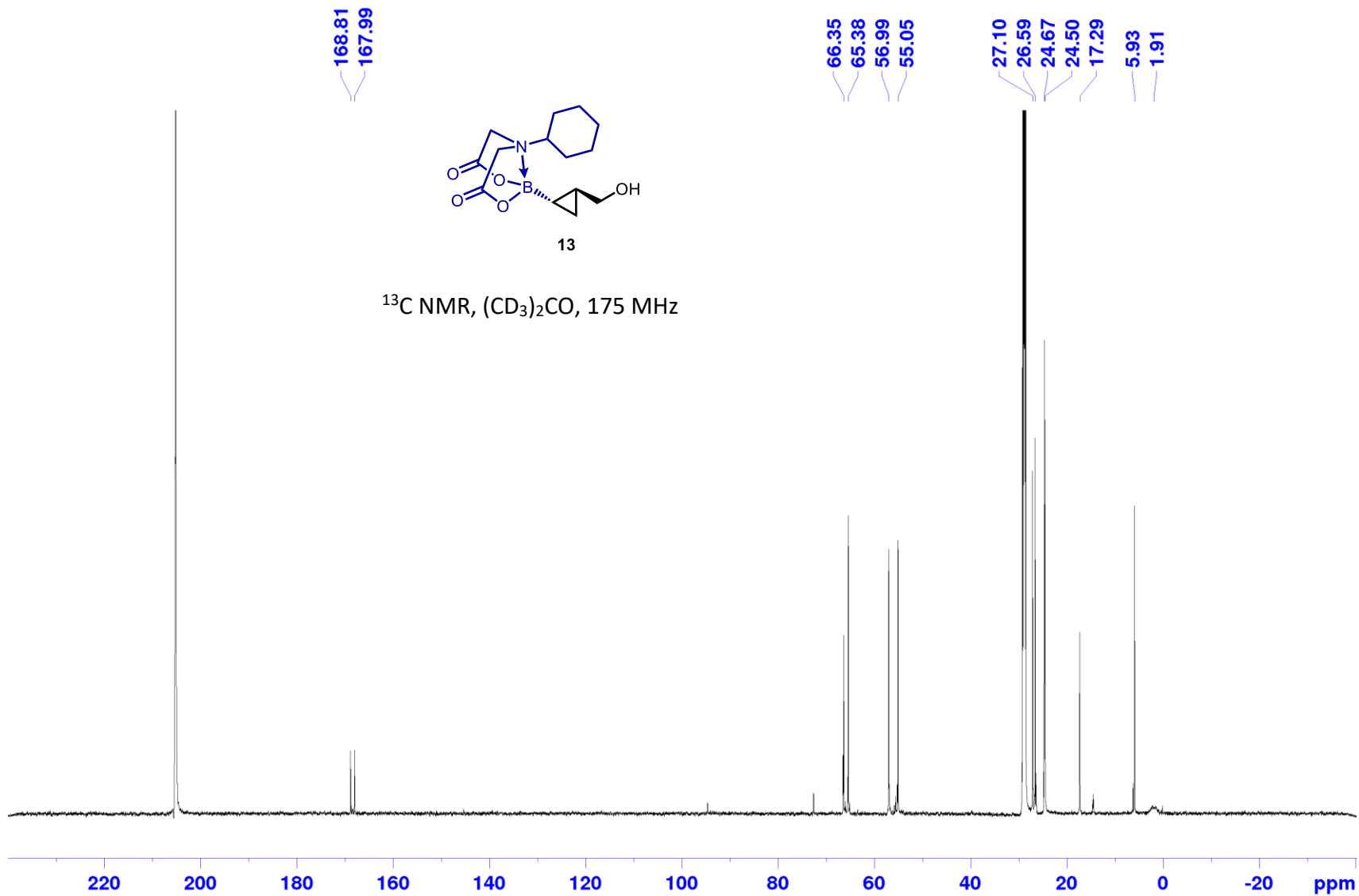
15a

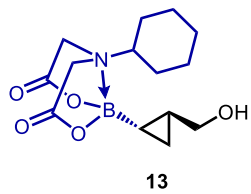
^{11}B NMR, $(\text{CD}_3)_2\text{CO}$, 500 MHz



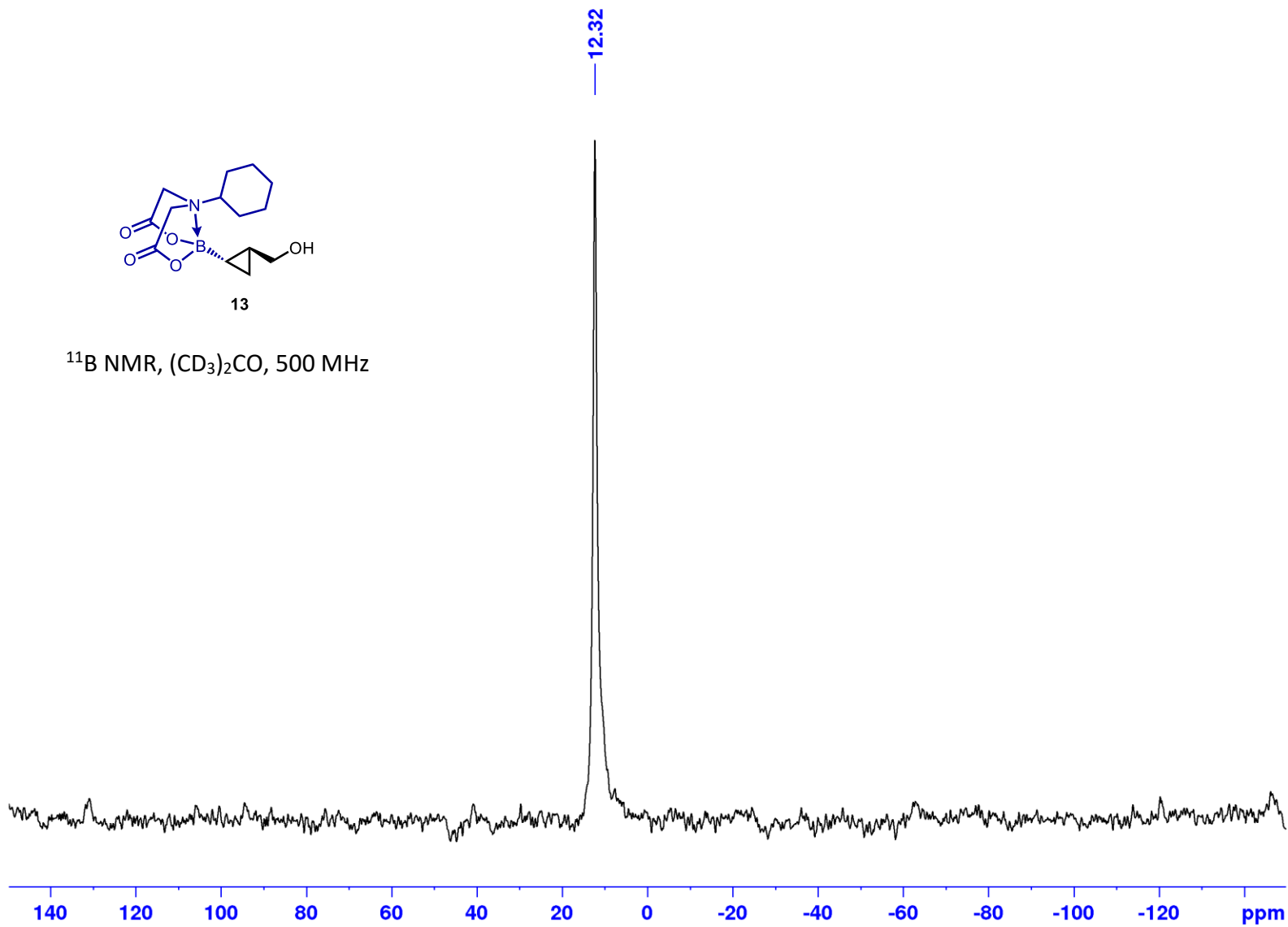
6-Cyclohexyl-2-((1R,2R)-2-(hydroxymethyl)cyclopropyl)-1,3,6,2-dioxazaborocane-4,8-dione (13):



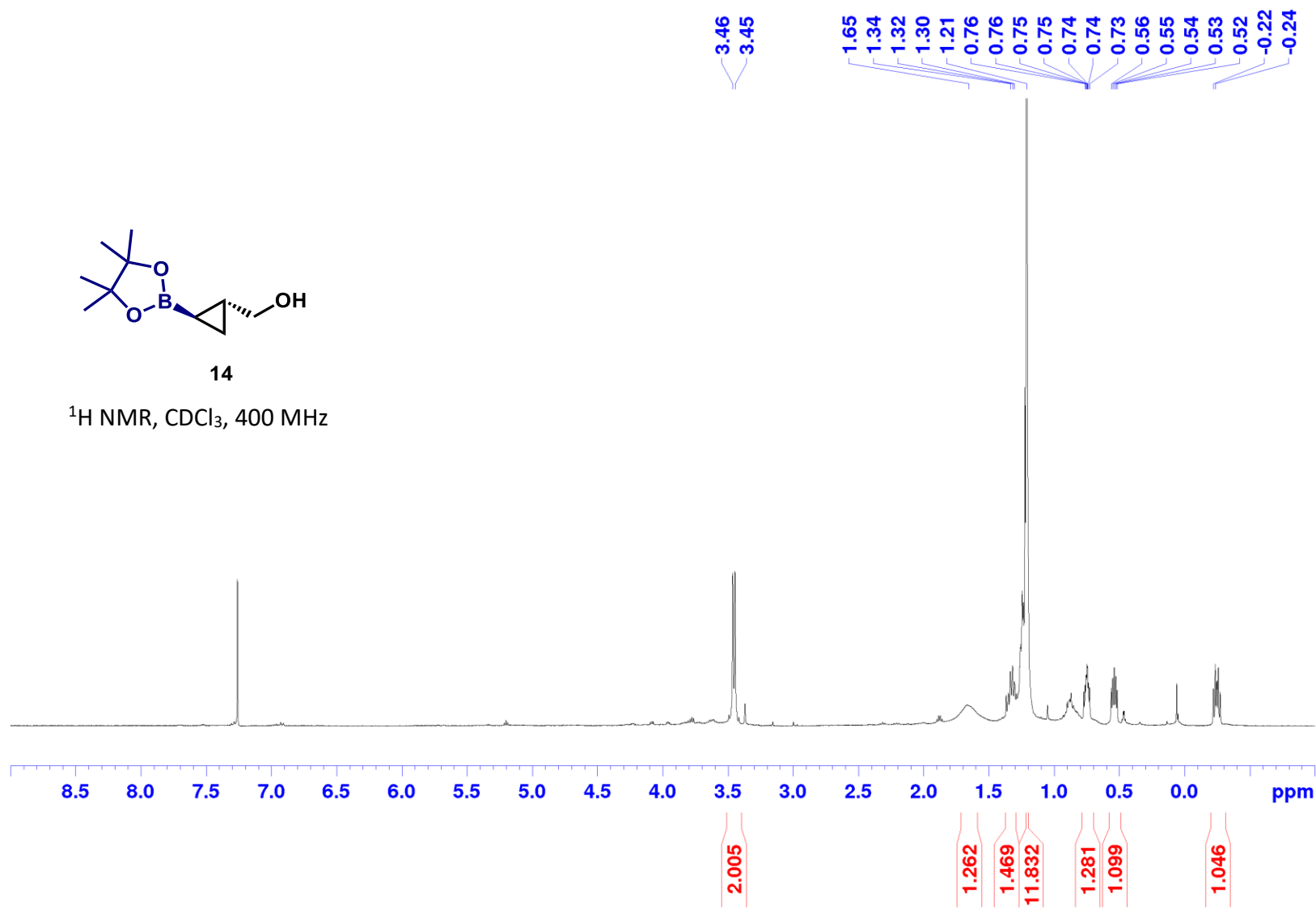


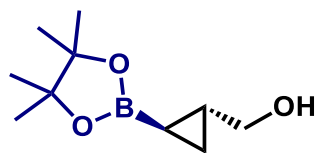


^{11}B NMR, $(\text{CD}_3)_2\text{CO}$, 500 MHz



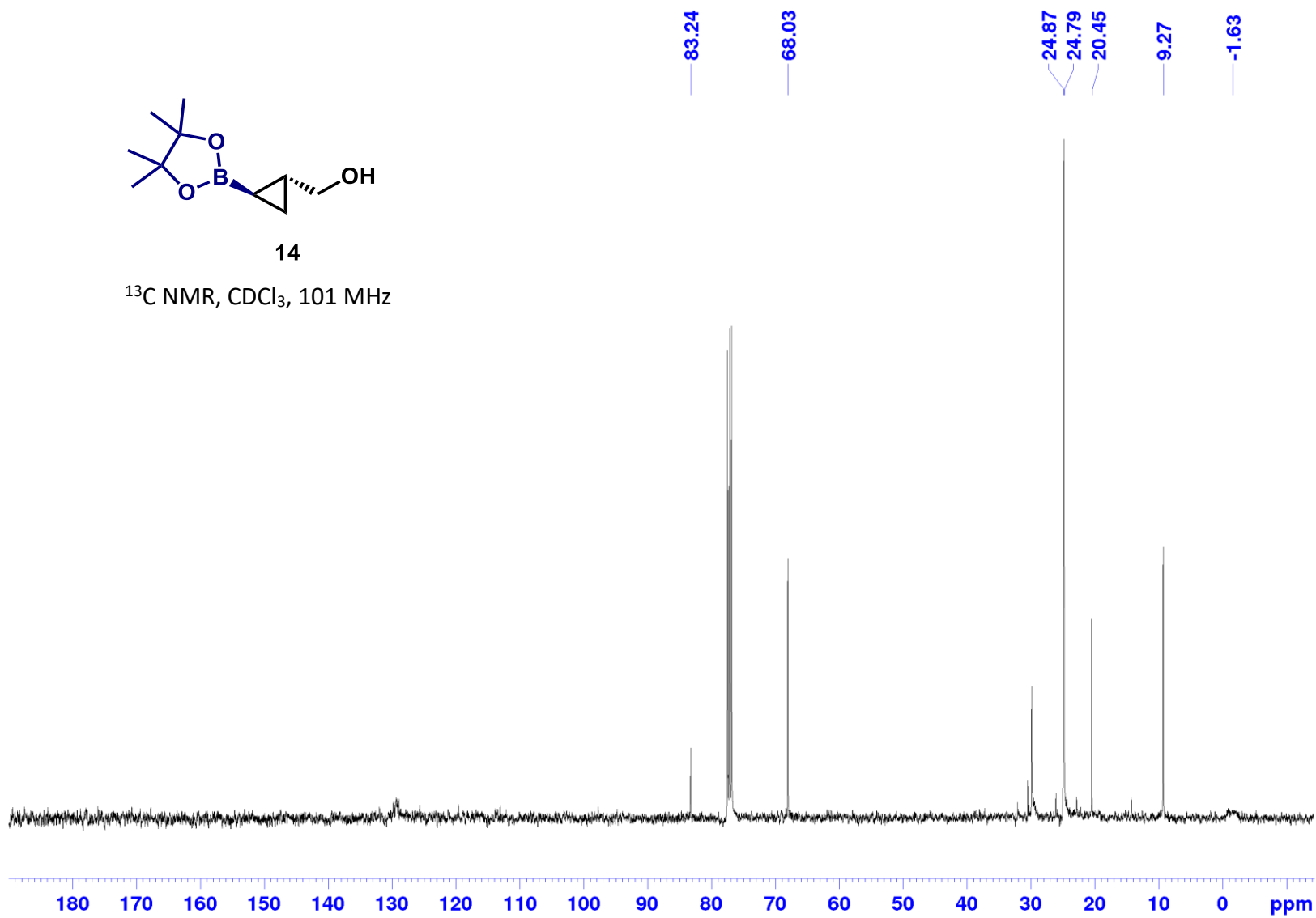
((1*R*,2*R*)-2-(4,4,5,5-Tetramethyl-1,3,2-dioxaborolan-2-yl)cyclopropyl)methanol (14):

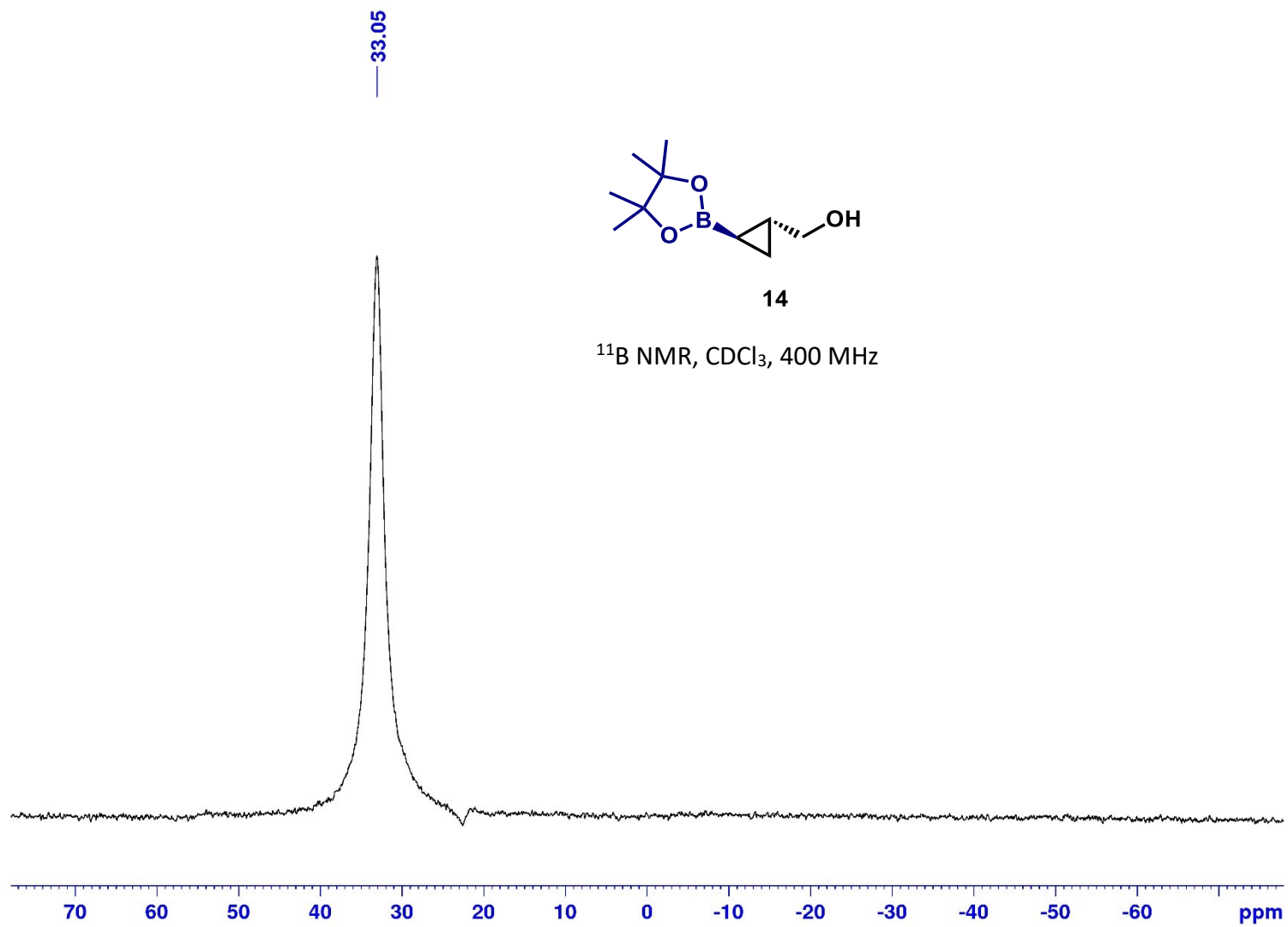




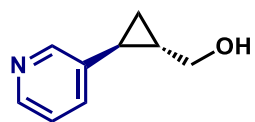
14

^{13}C NMR, CDCl_3 , 101 MHz



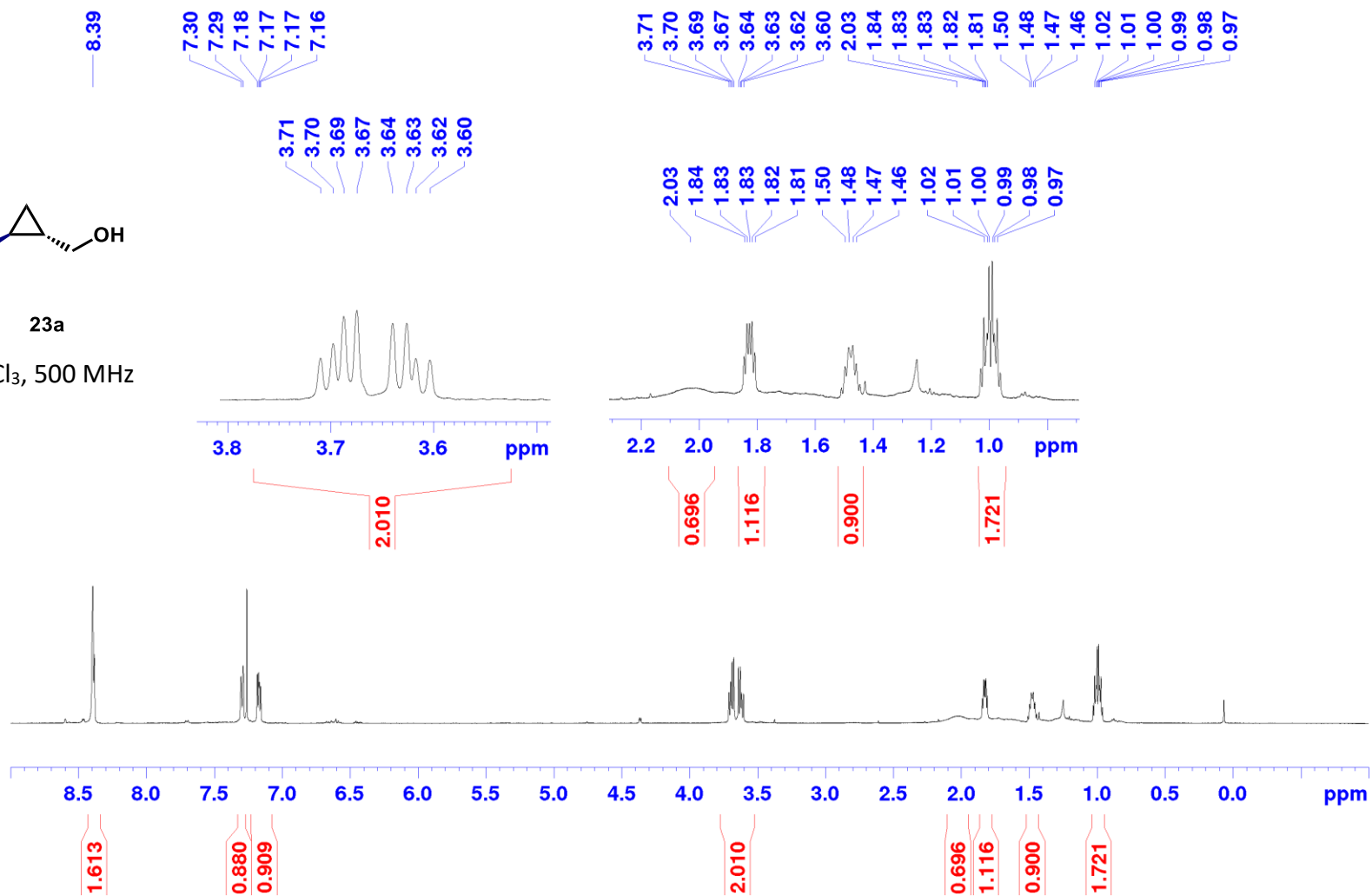


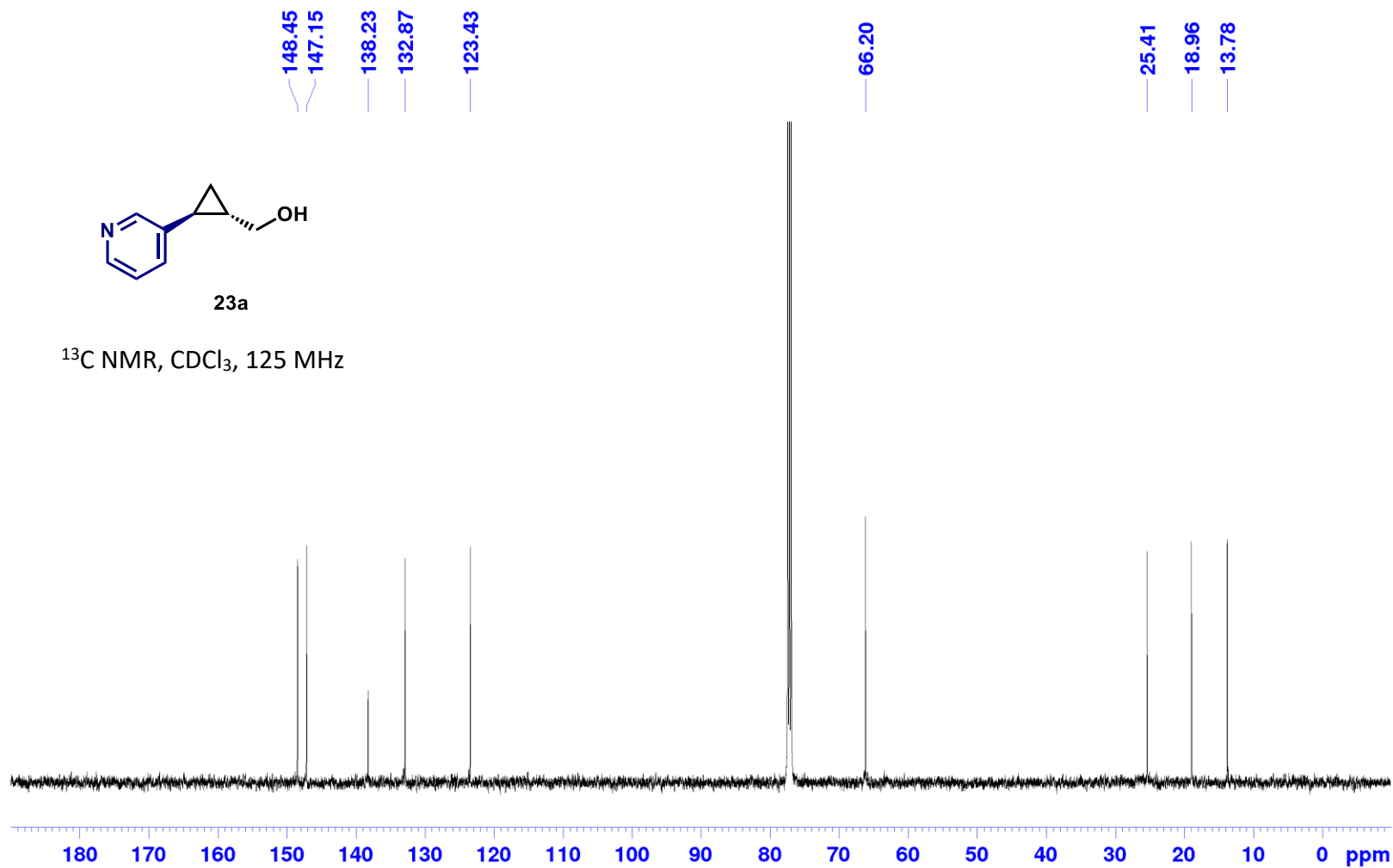
((1S,2S)-2-(Pyridin-3-yl)cyclopropyl)methanol (23a):



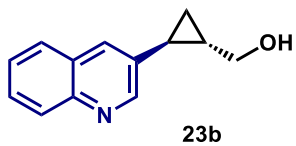
23a

$^1\text{H NMR}$, CDCl_3 , 500 MHz

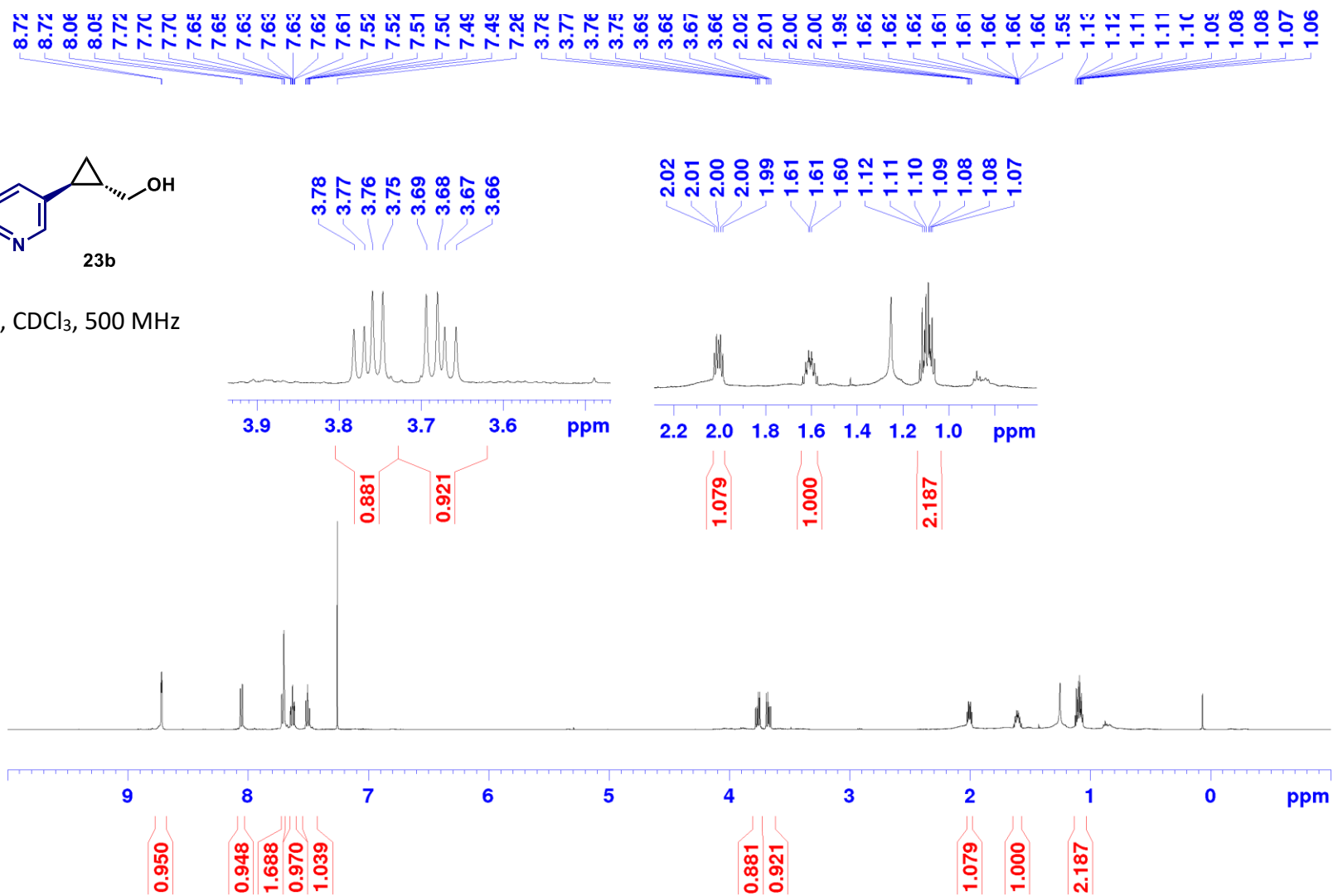


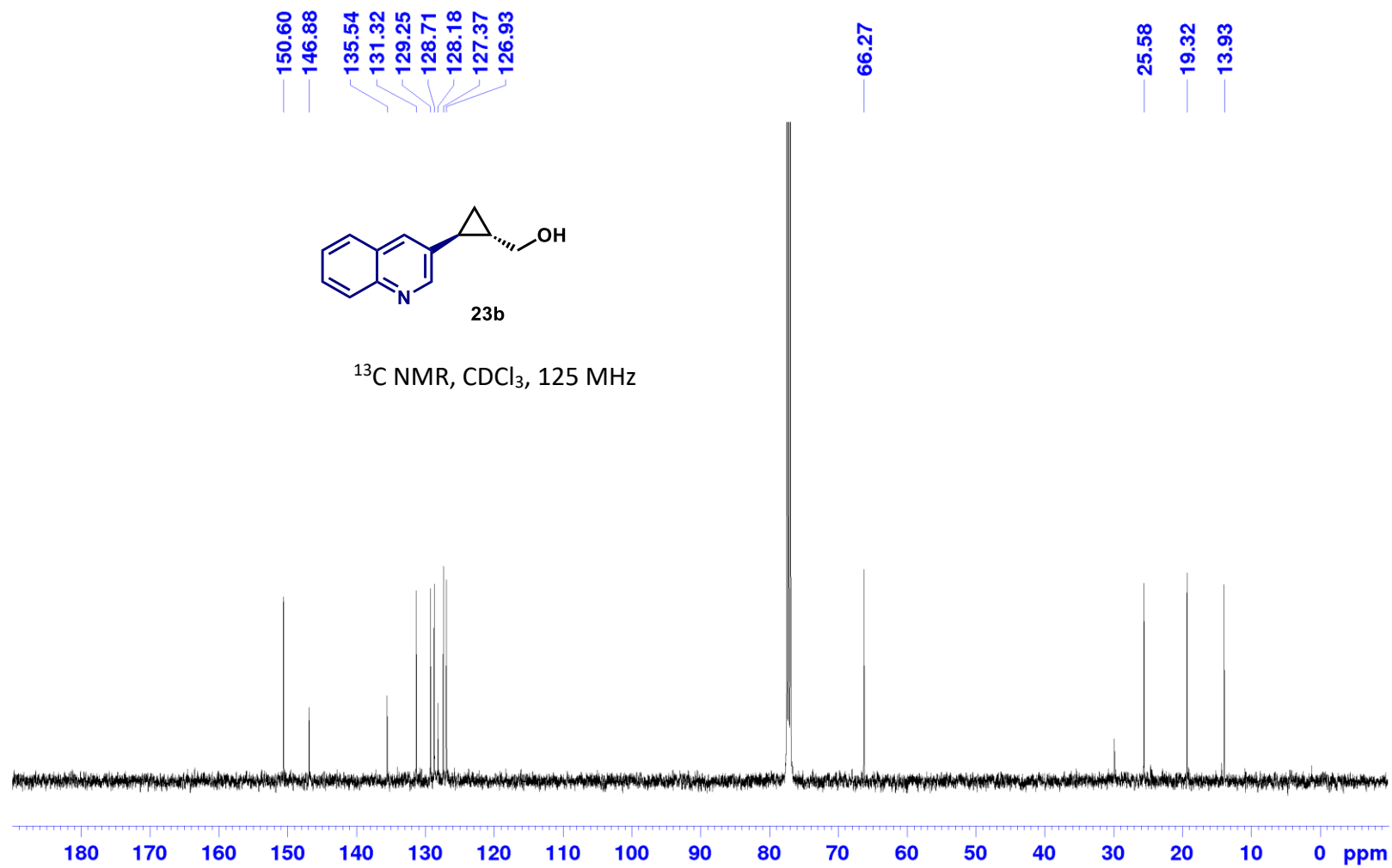


((1S,2S)-2-(Quinolin-3-yl)cyclopropyl)methanol (23b):

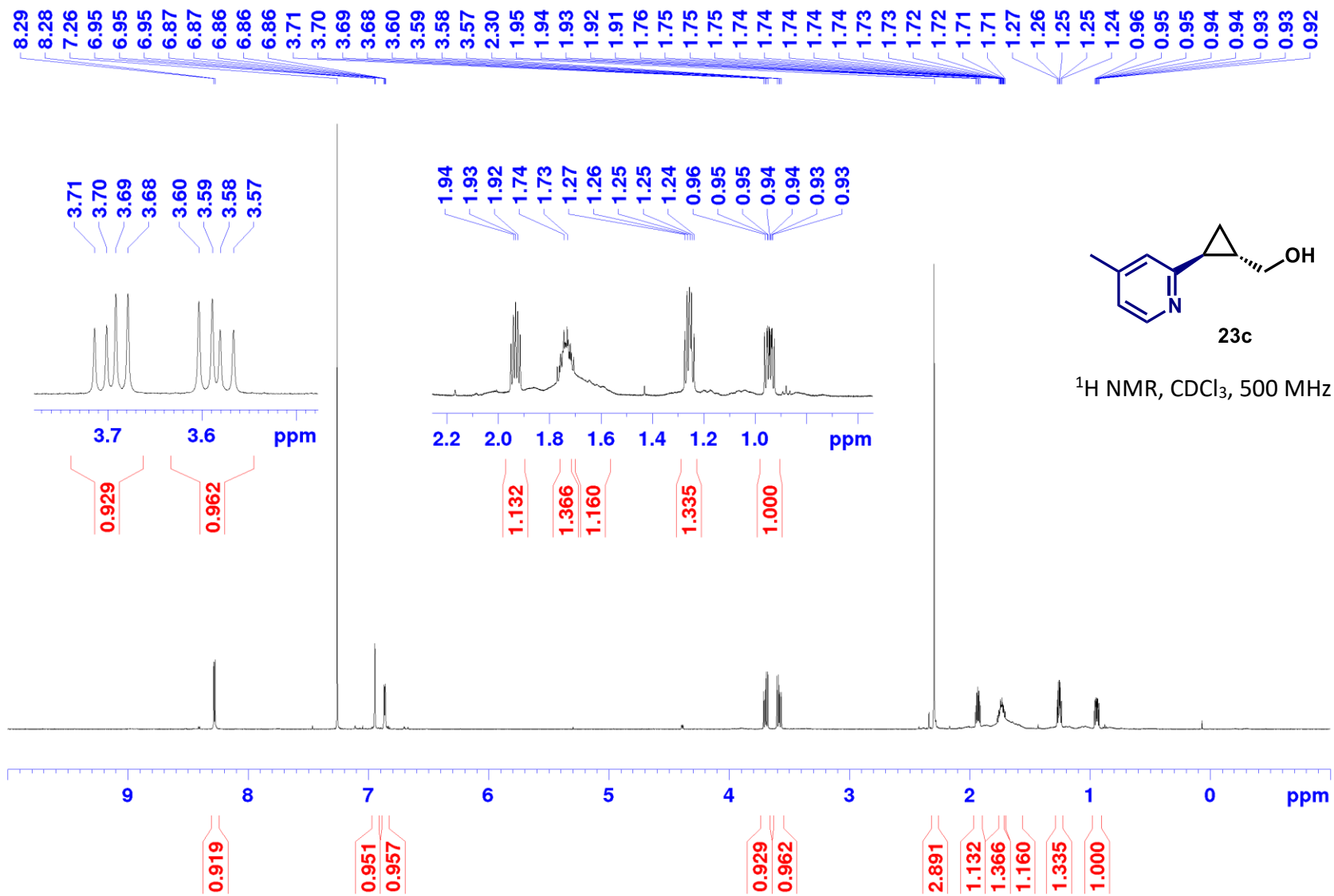


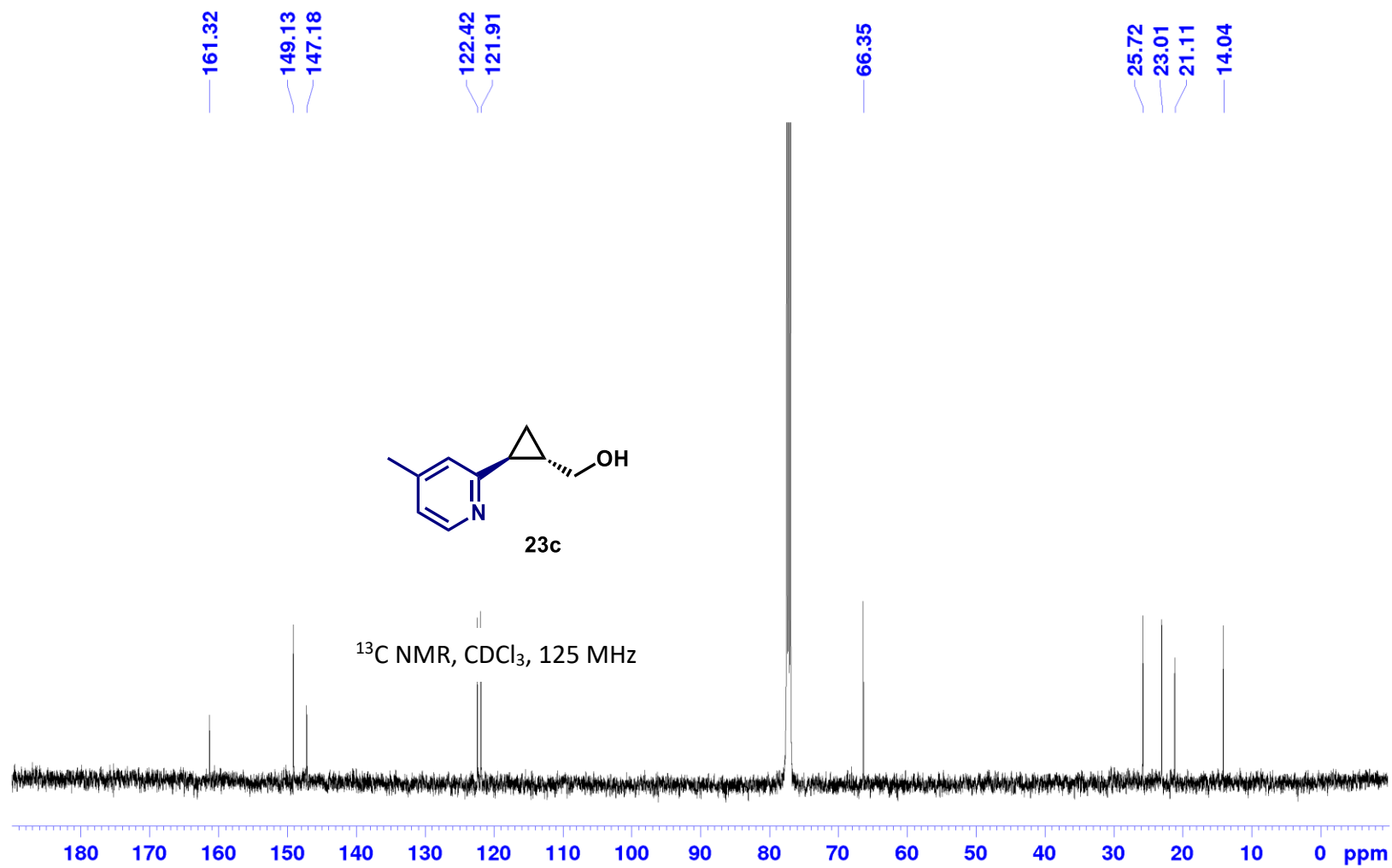
¹H NMR, CDCl₃, 500 MHz



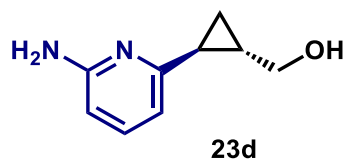


((1S,2S)-2-(4-Methylpyridin-2-yl)cyclopropyl)methanol (23c):





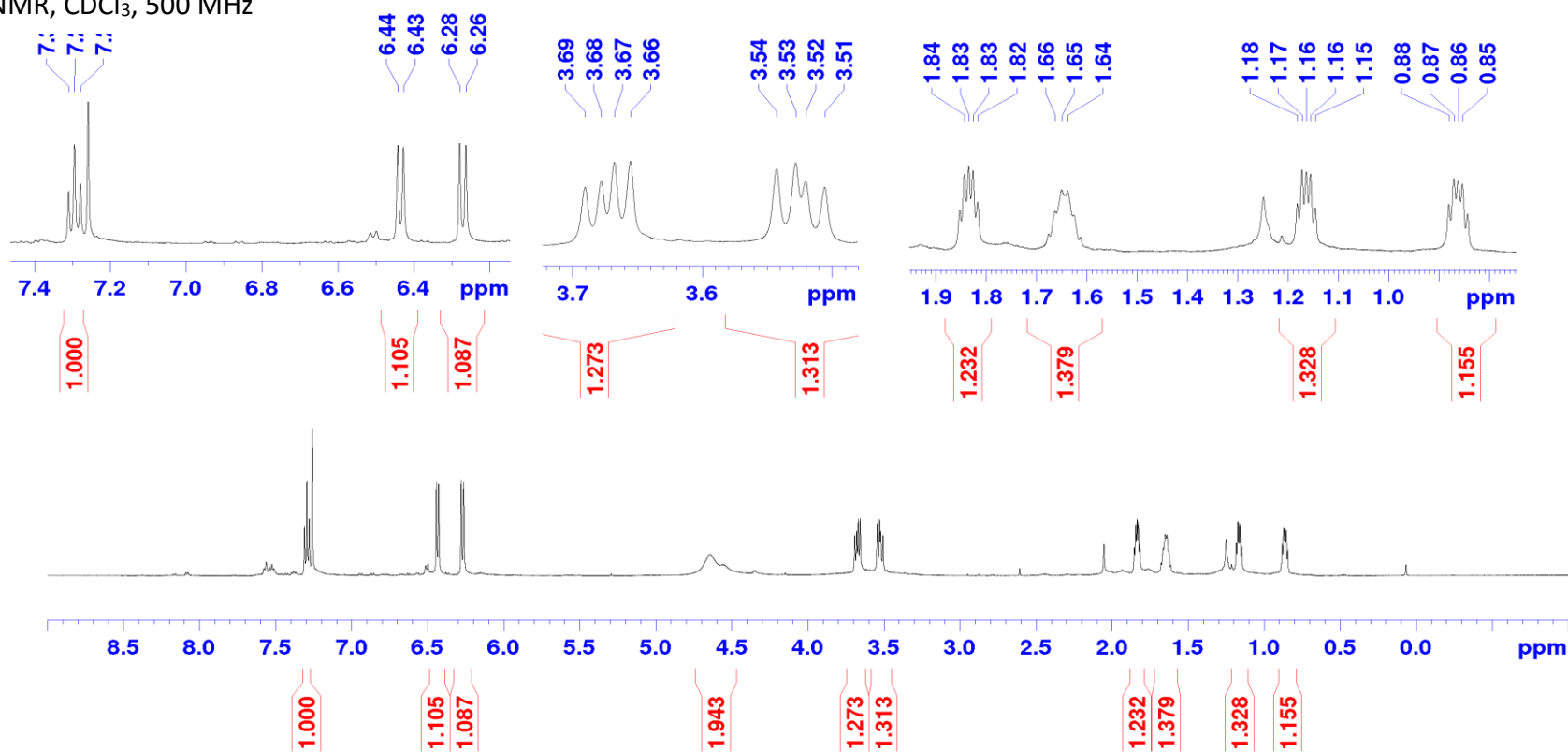
((1S,2S)-2-(6-Aminopyridin-2-yl)cyclopropyl)methanol (23d)

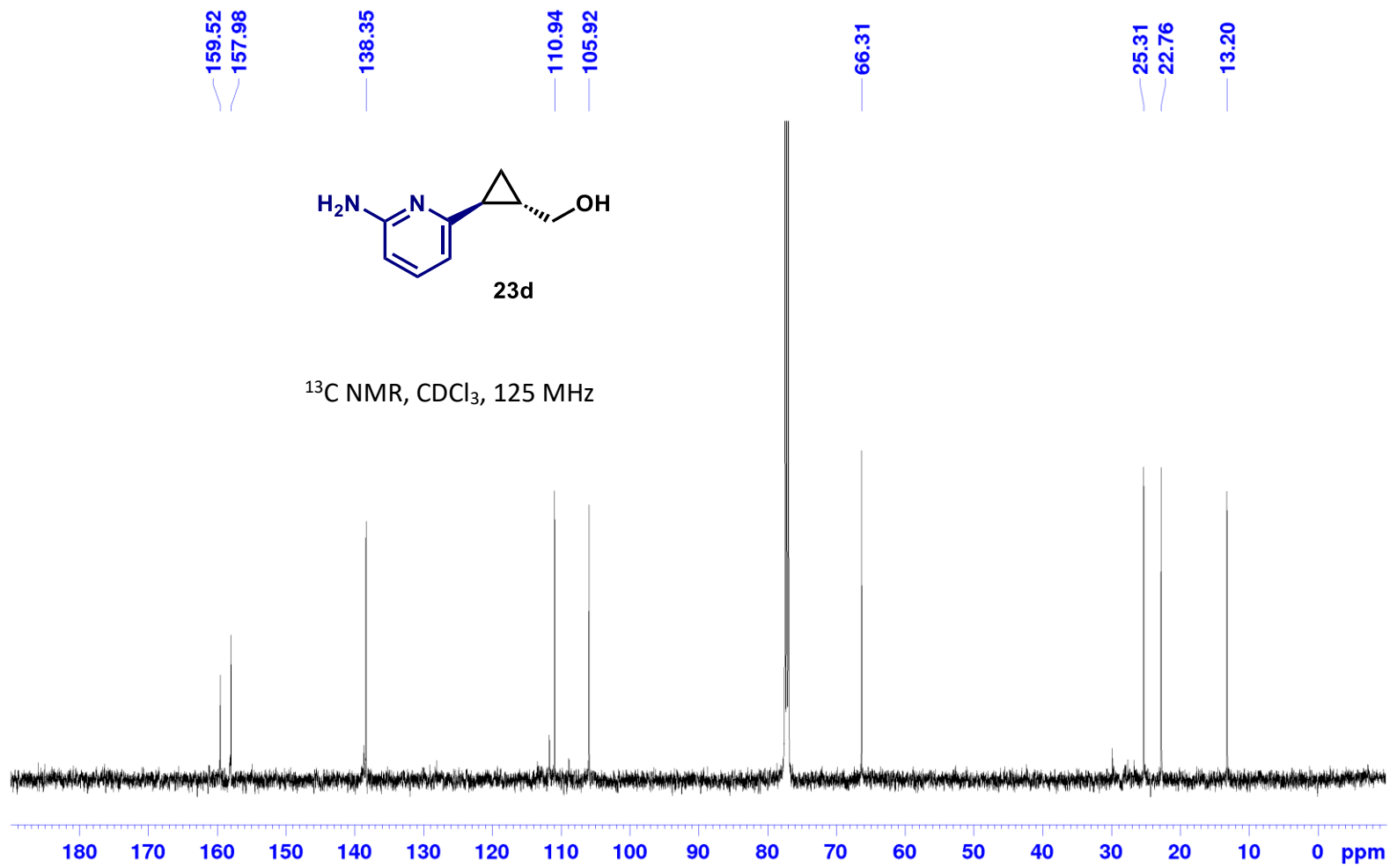


7.31
7.29
7.28
6.44
6.43
6.28
6.26

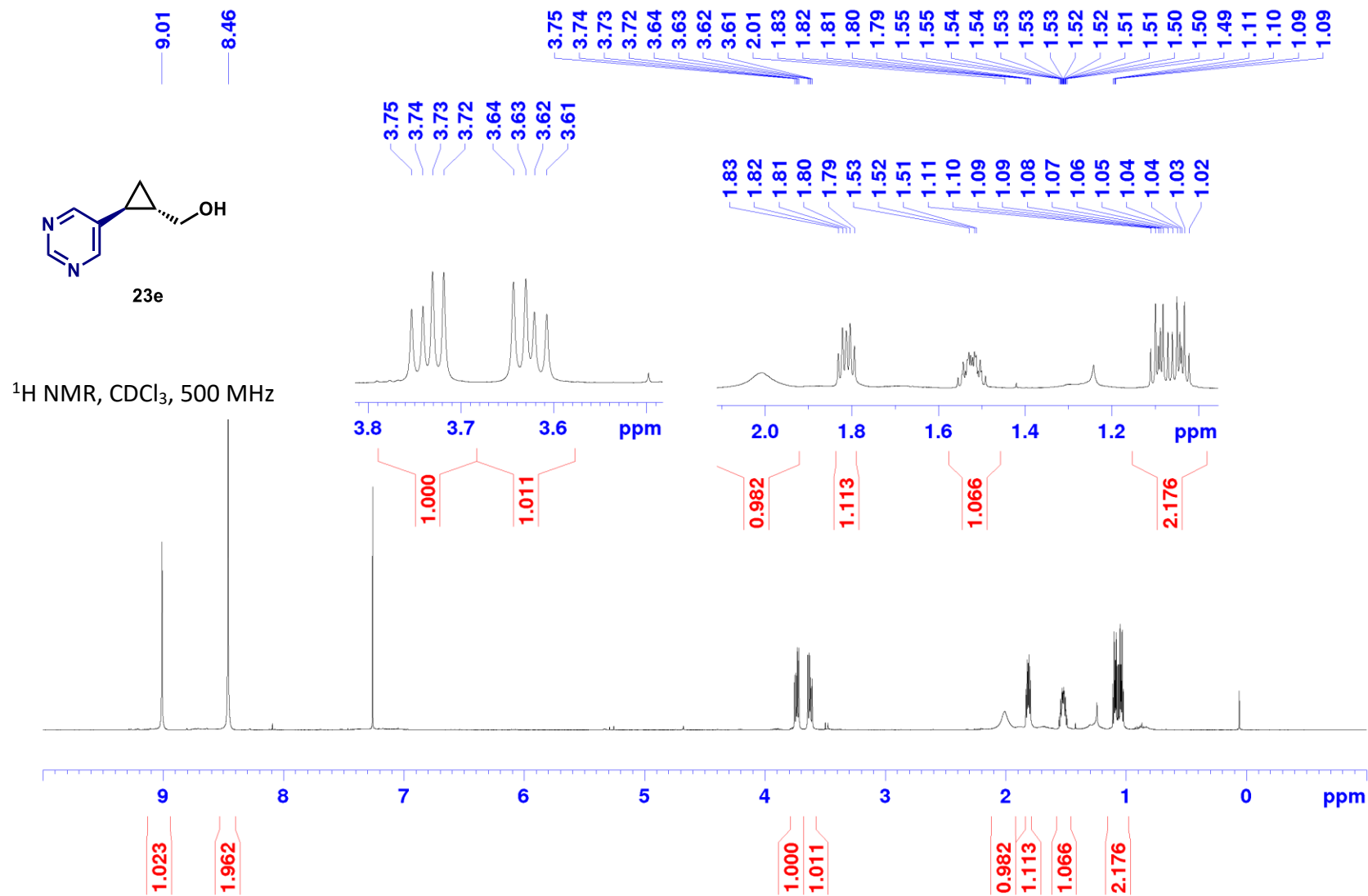
3.69
3.68
3.67
3.66
3.54
3.53
3.52
3.51
1.85
1.84
1.83
1.83
1.82
1.66
1.65
1.64
1.18
1.17
1.16
1.16
1.15
0.88
0.87
0.86
0.85
0.84

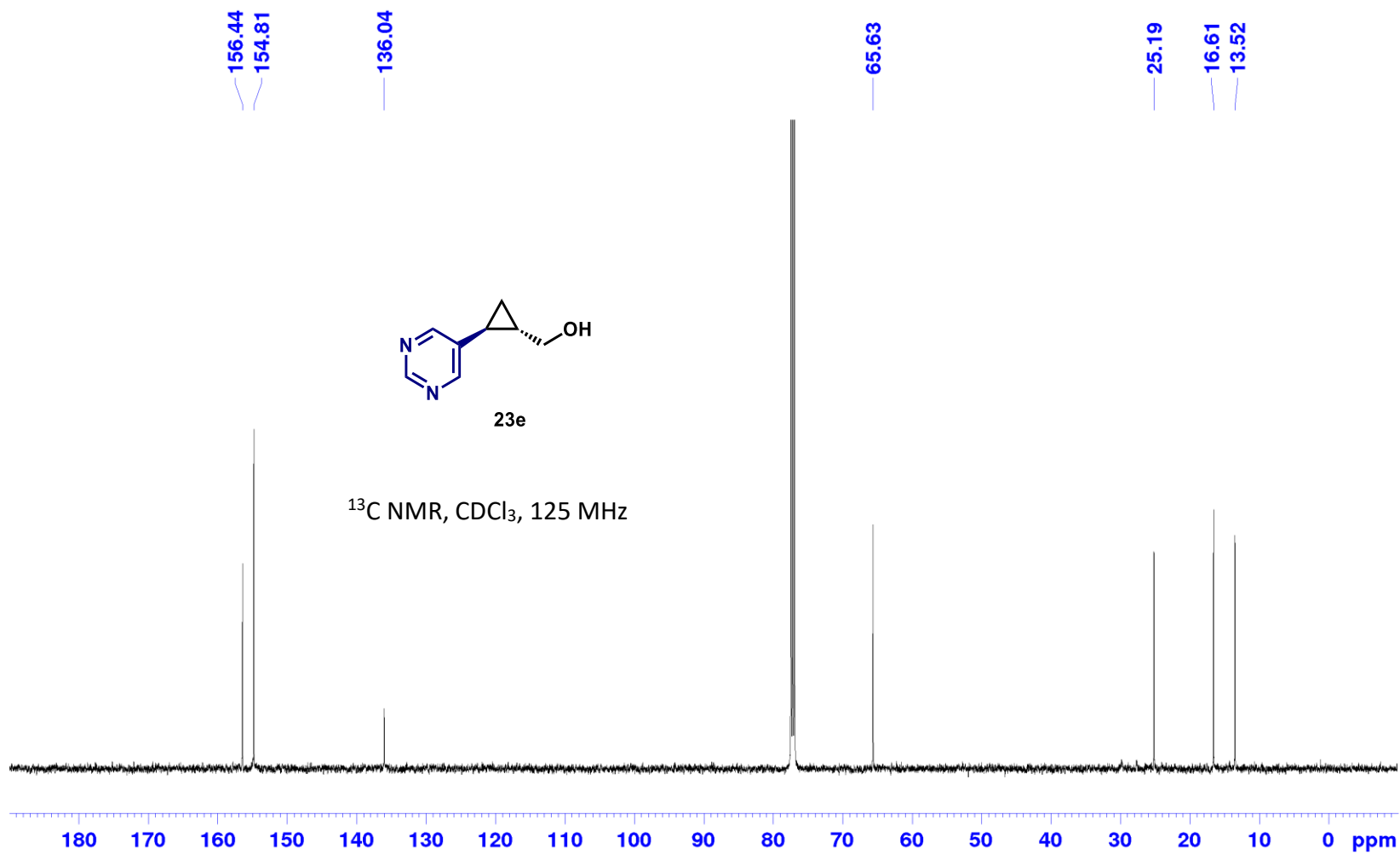
¹H NMR, CDCl₃, 500 MHz



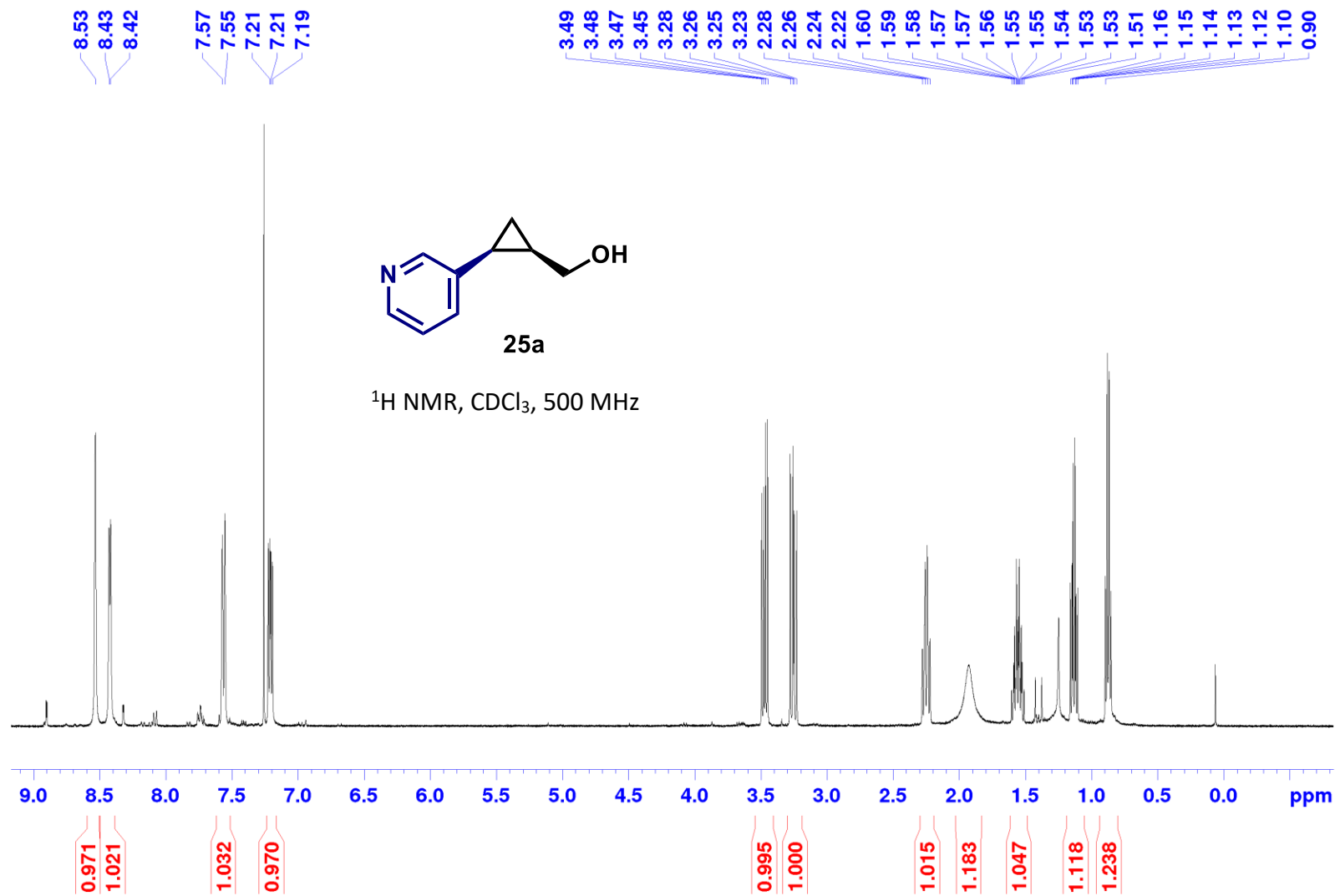


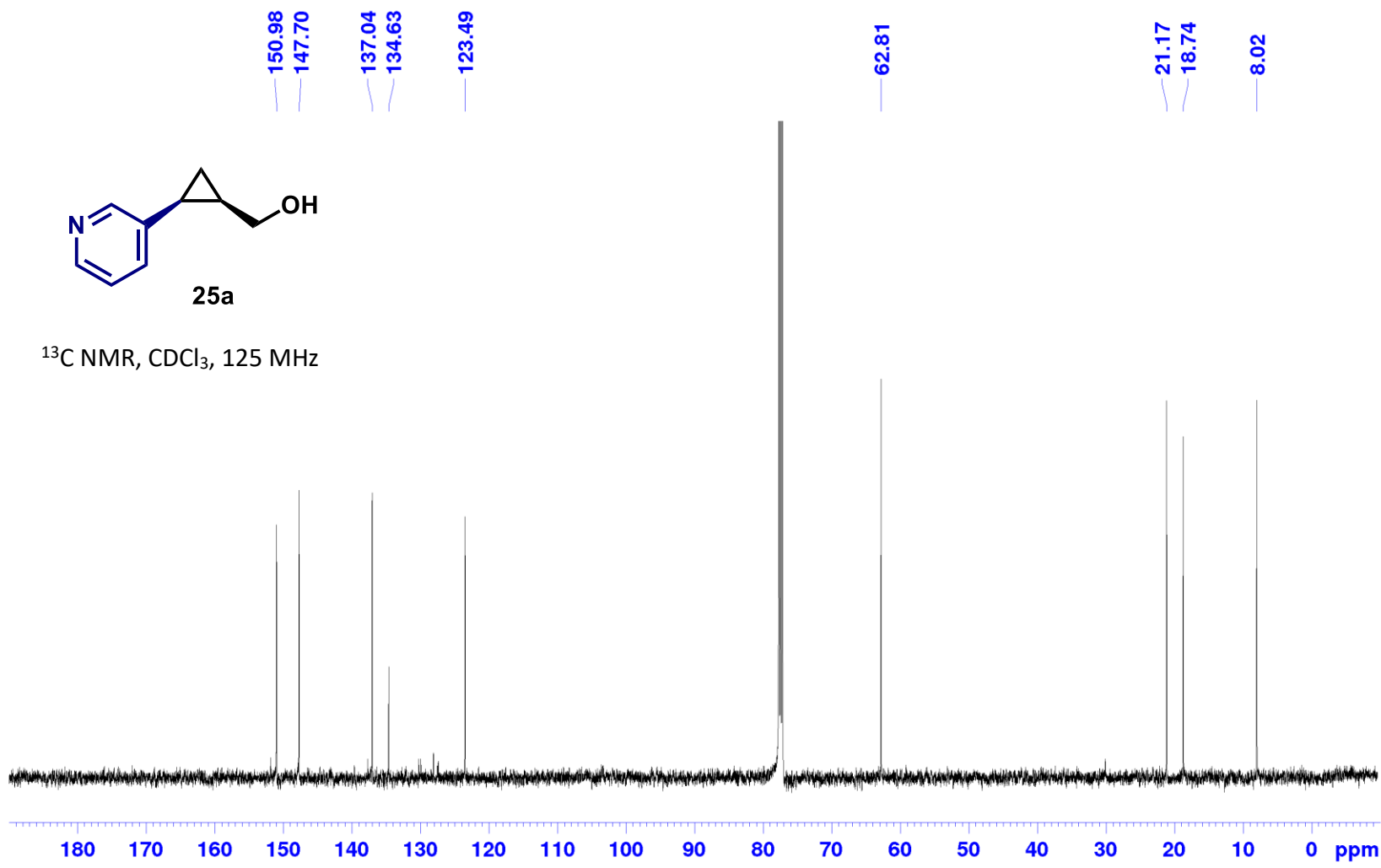
((1S,2S)-2-(Pyrimidin-5-yl)cyclopropyl)methanol (23e):



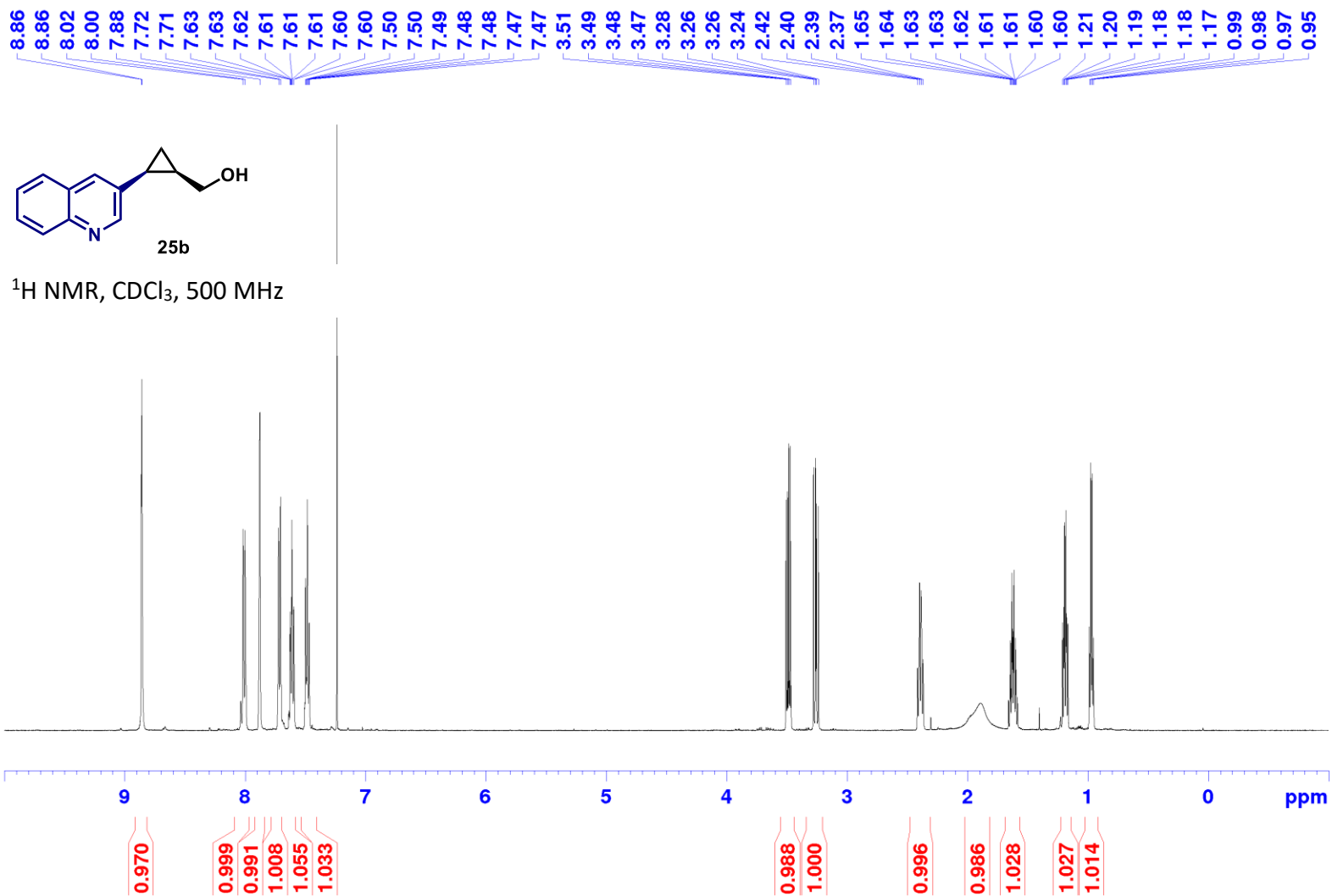


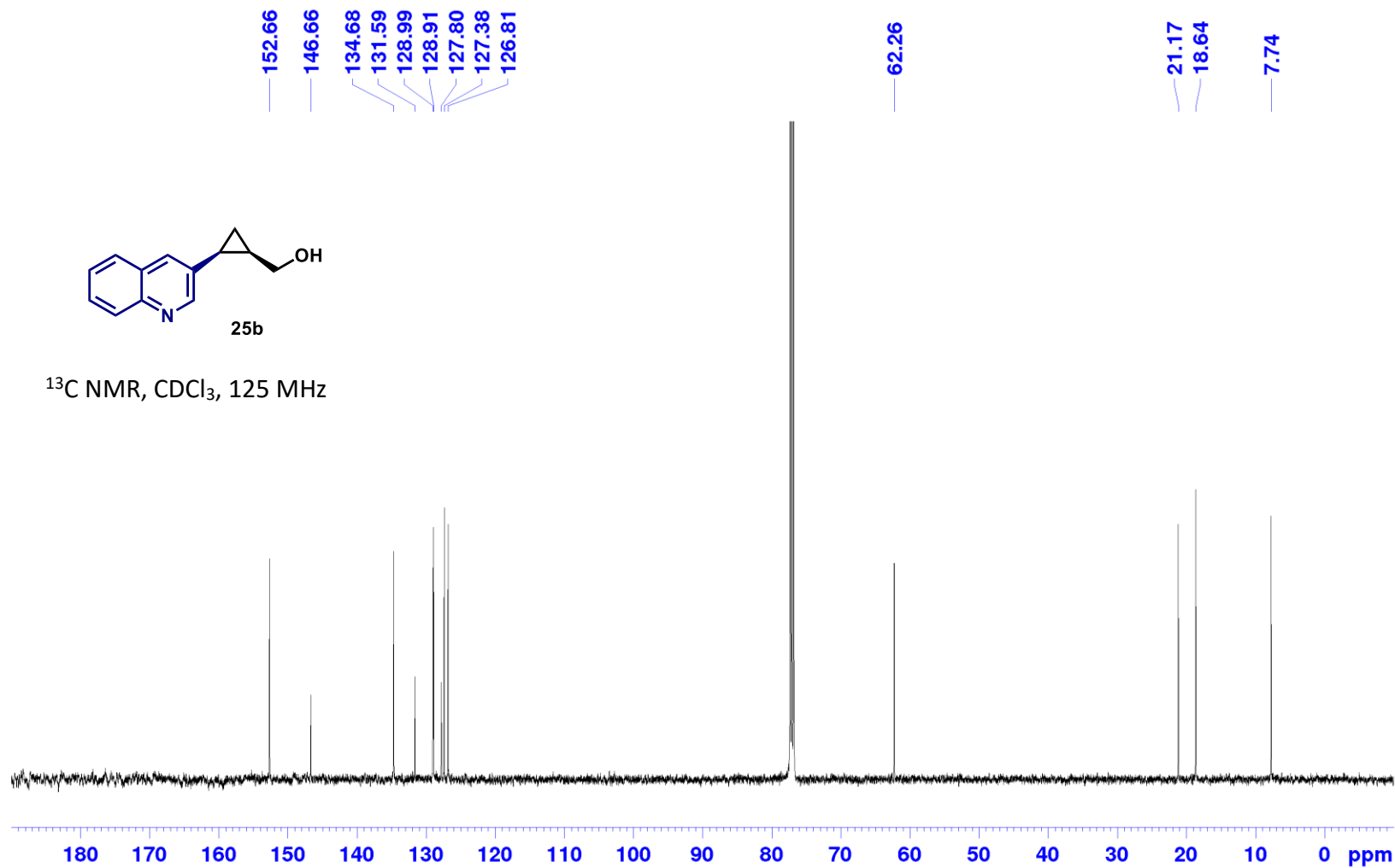
((1*R*,2*S*)-2-(Pyridin-3-yl)cyclopropyl)methanol (25a):



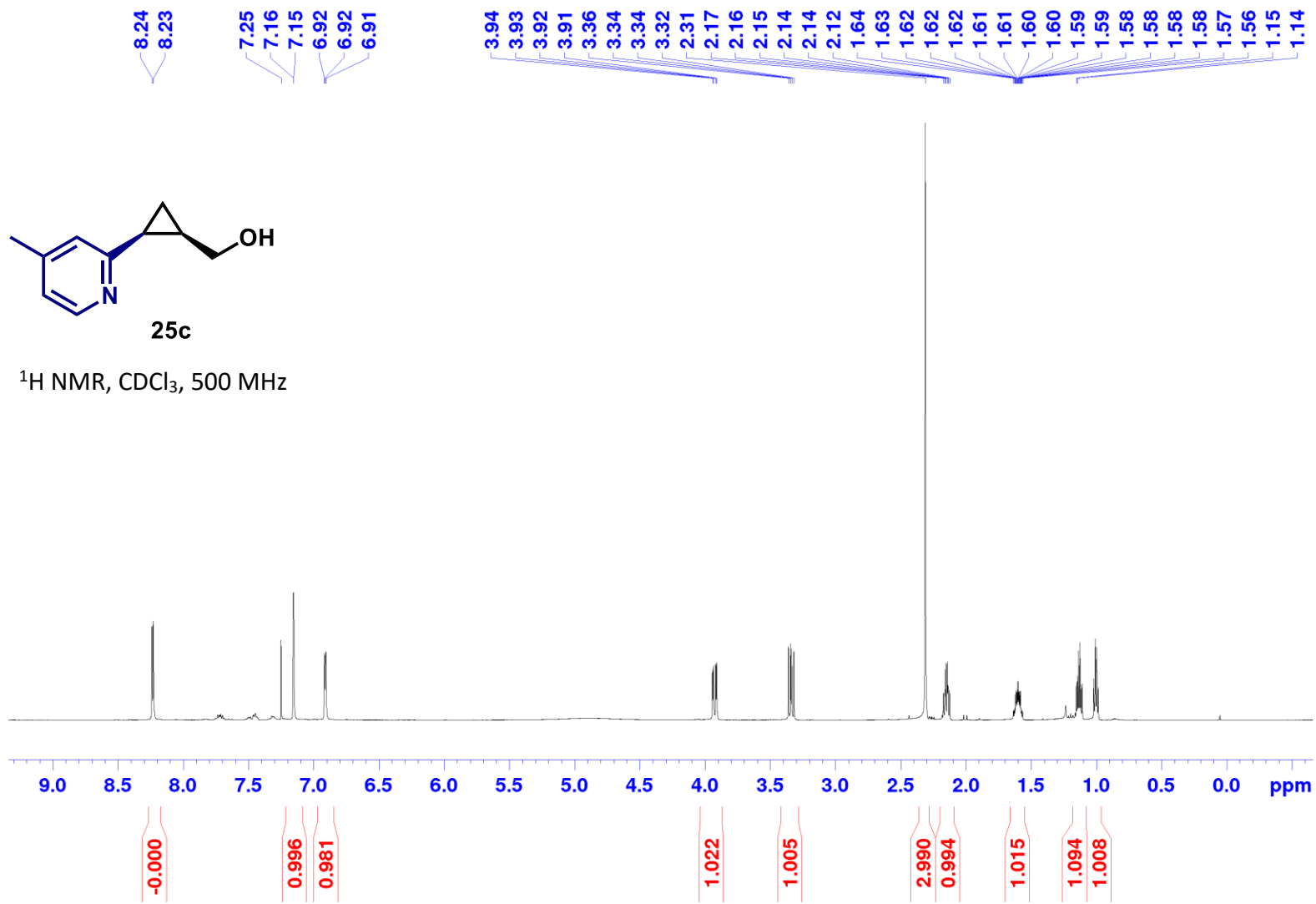


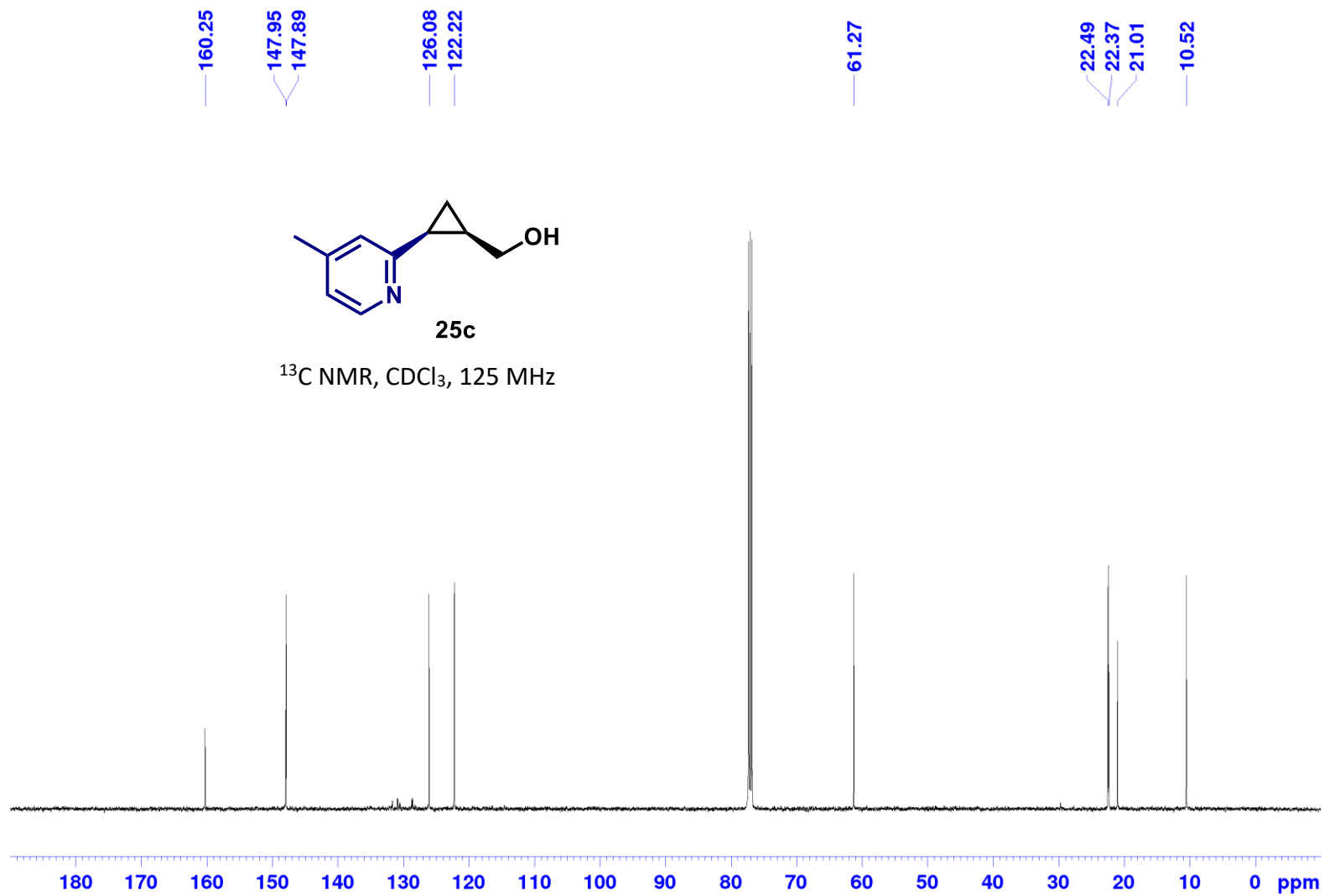
((1*R*,2*S*)-2-(Quinolin-3-yl)cyclopropyl)methanol (25b);



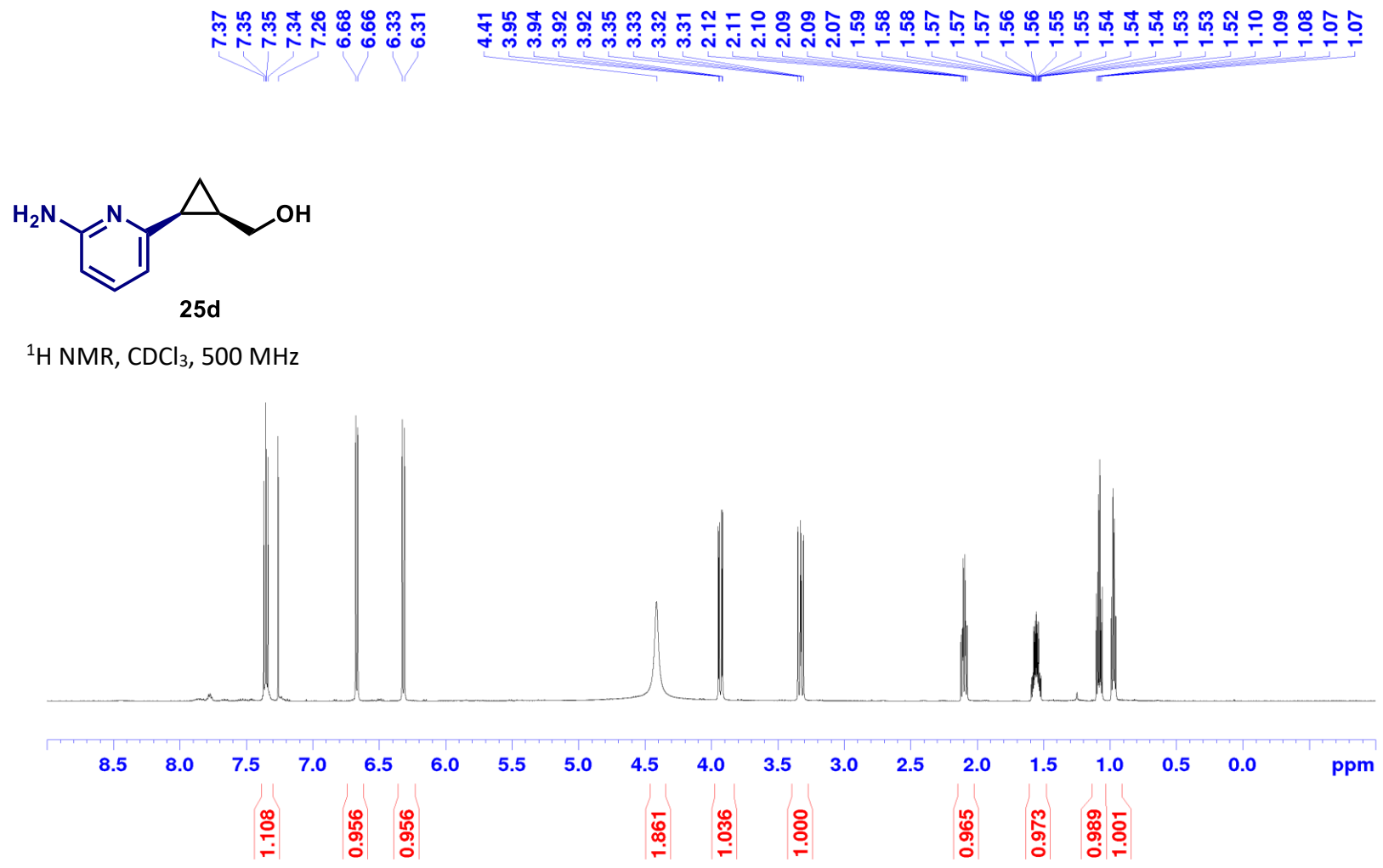


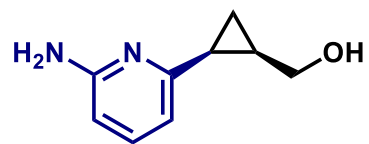
((1*R*,2*S*)-2-(4-Methylpyridin-2-yl)cyclopropyl)methanol (25c):





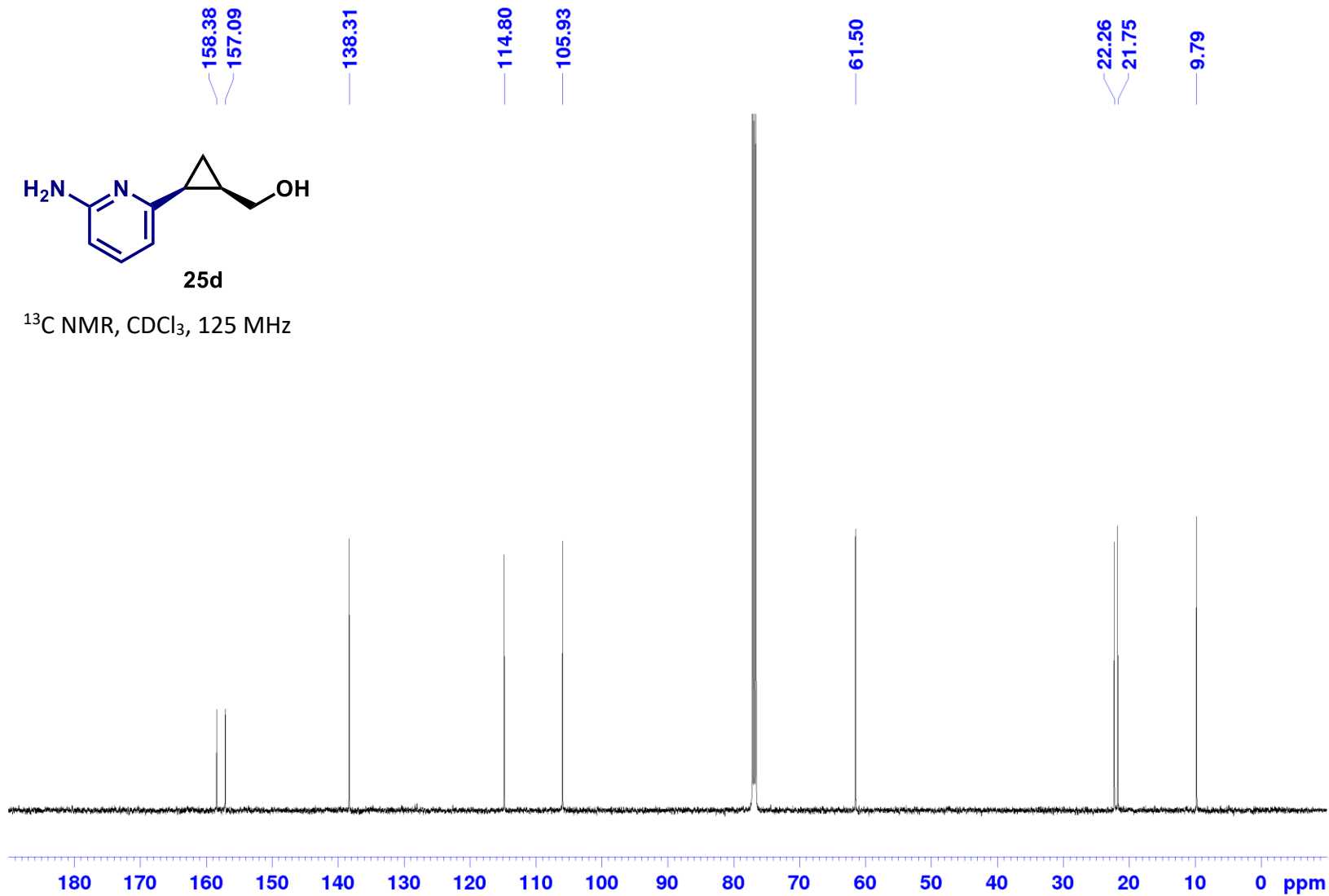
((1*R*,2*S*)-2-(6-Aminopyridin-2-yl)cyclopropyl)methanol (25d):



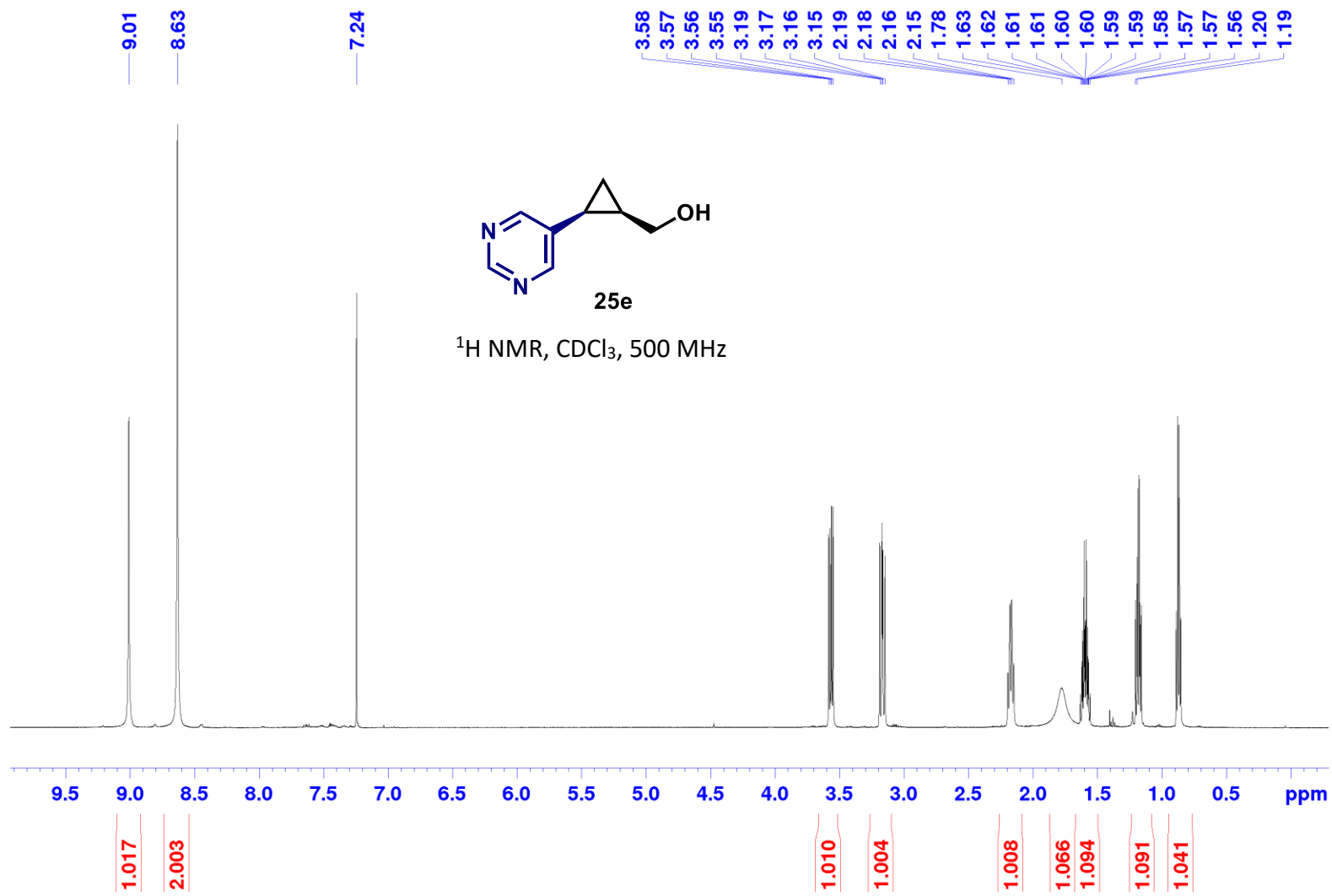


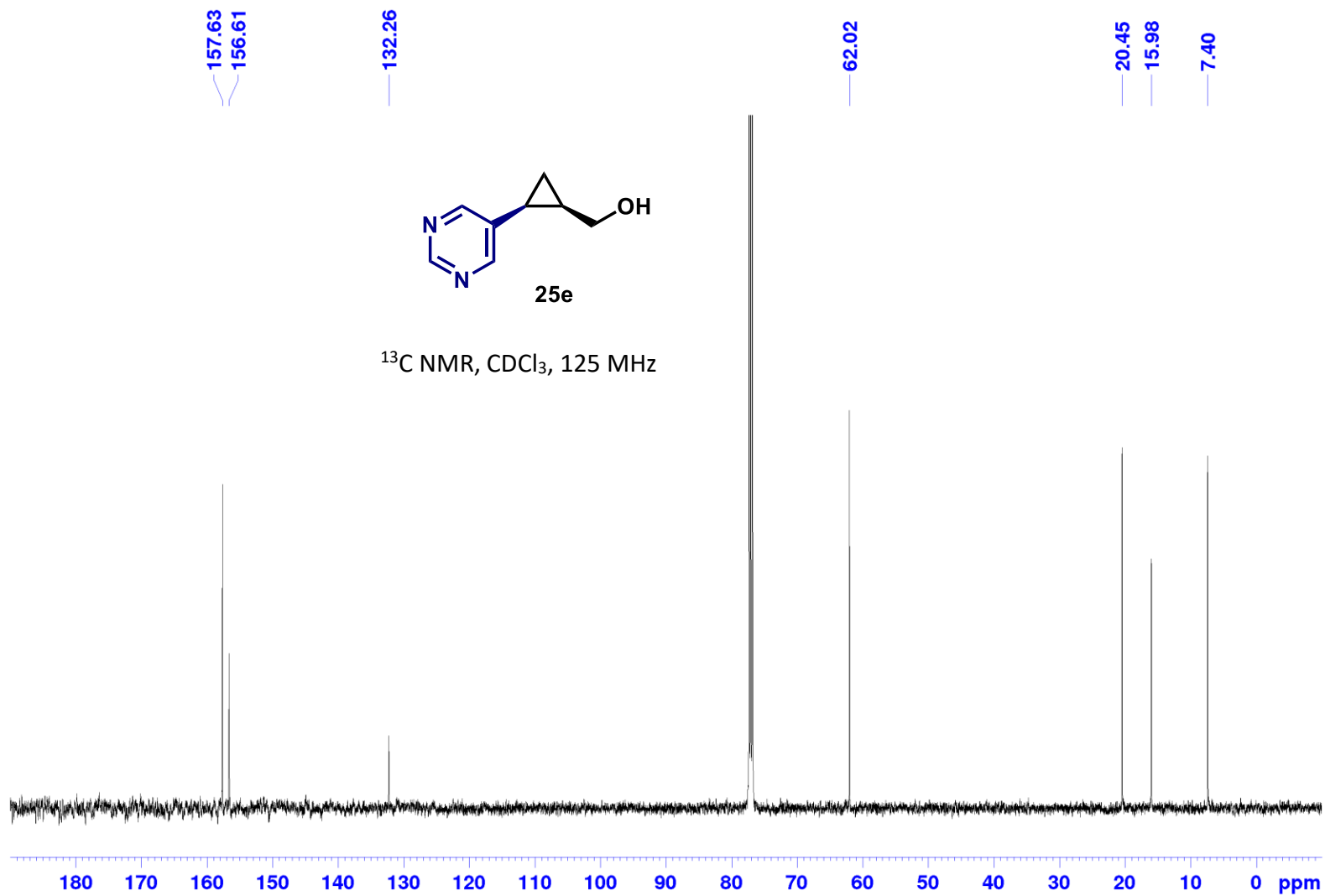
25d

^{13}C NMR, CDCl_3 , 125 MHz

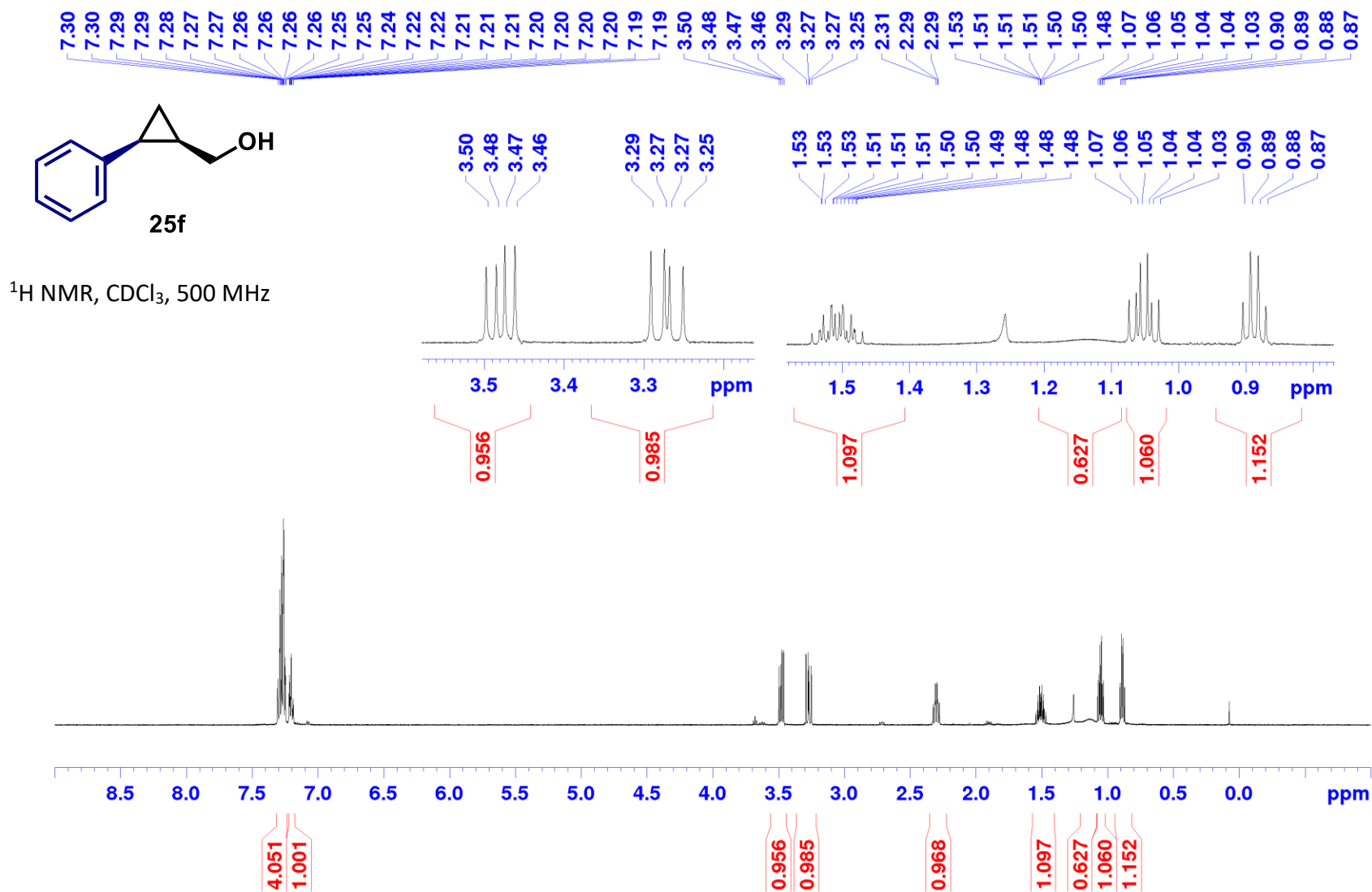


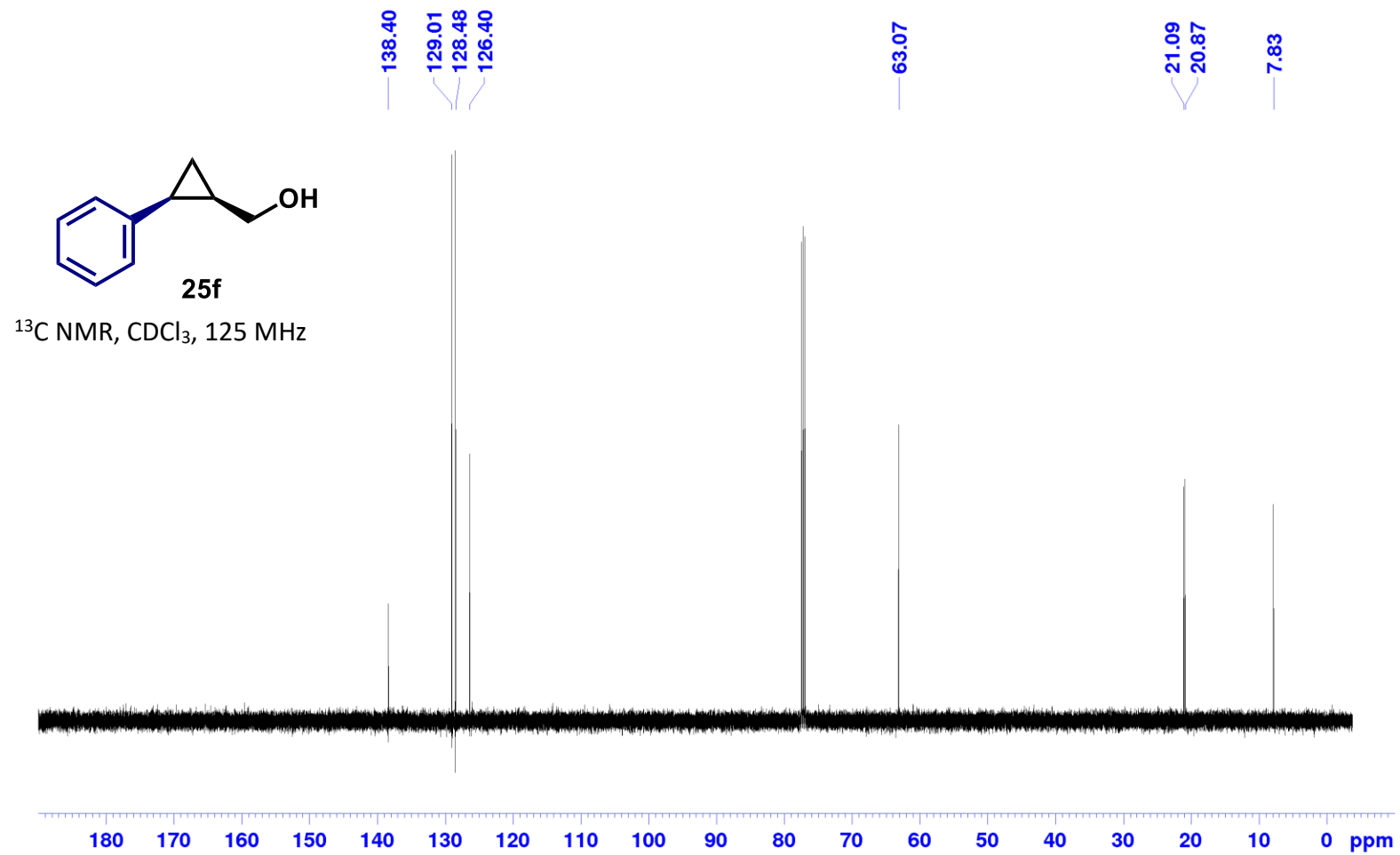
((1*R*,2*S*)-2-(Pyrimidin-5-yl)cyclopropyl)methanol (25e):



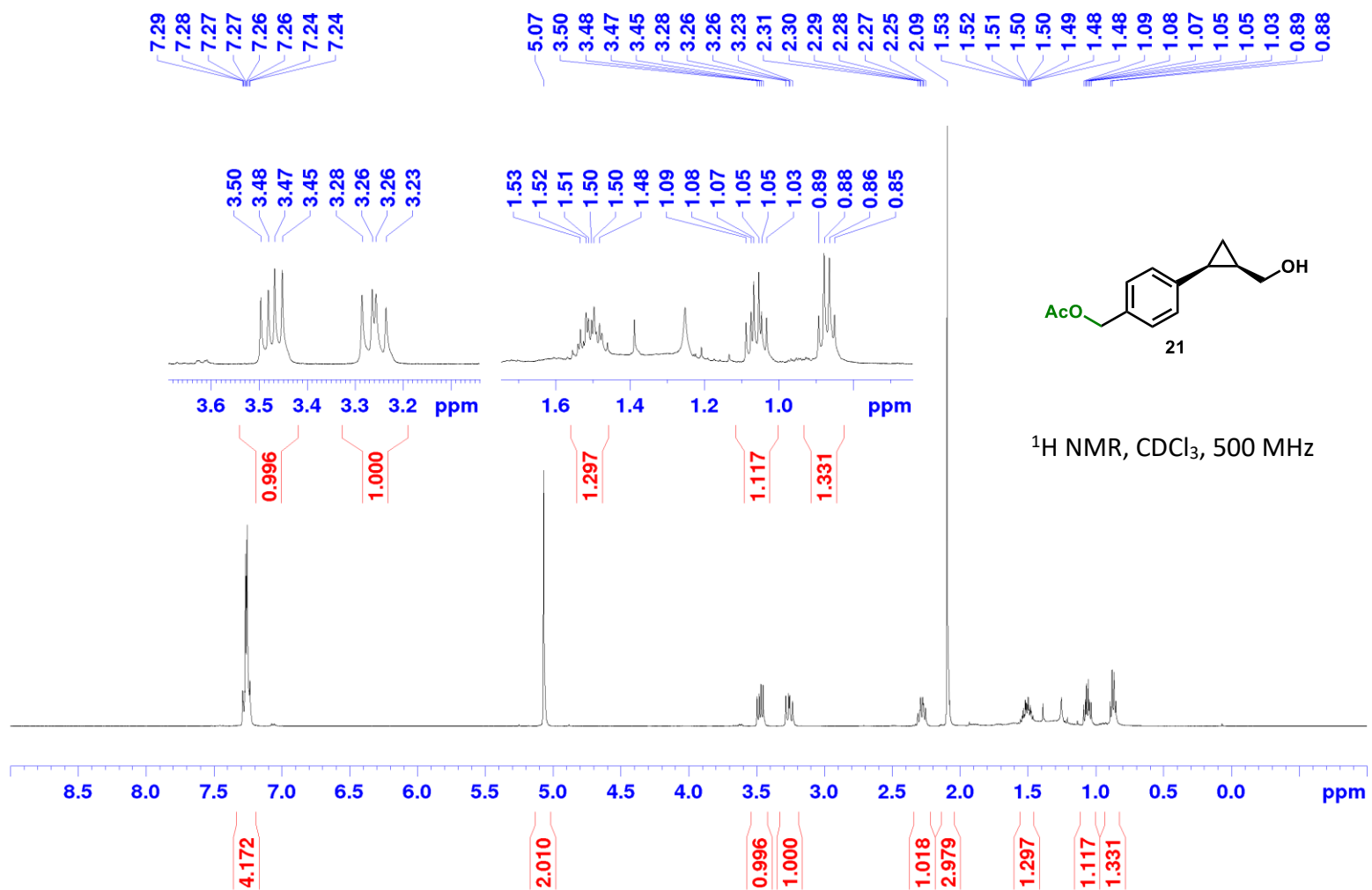


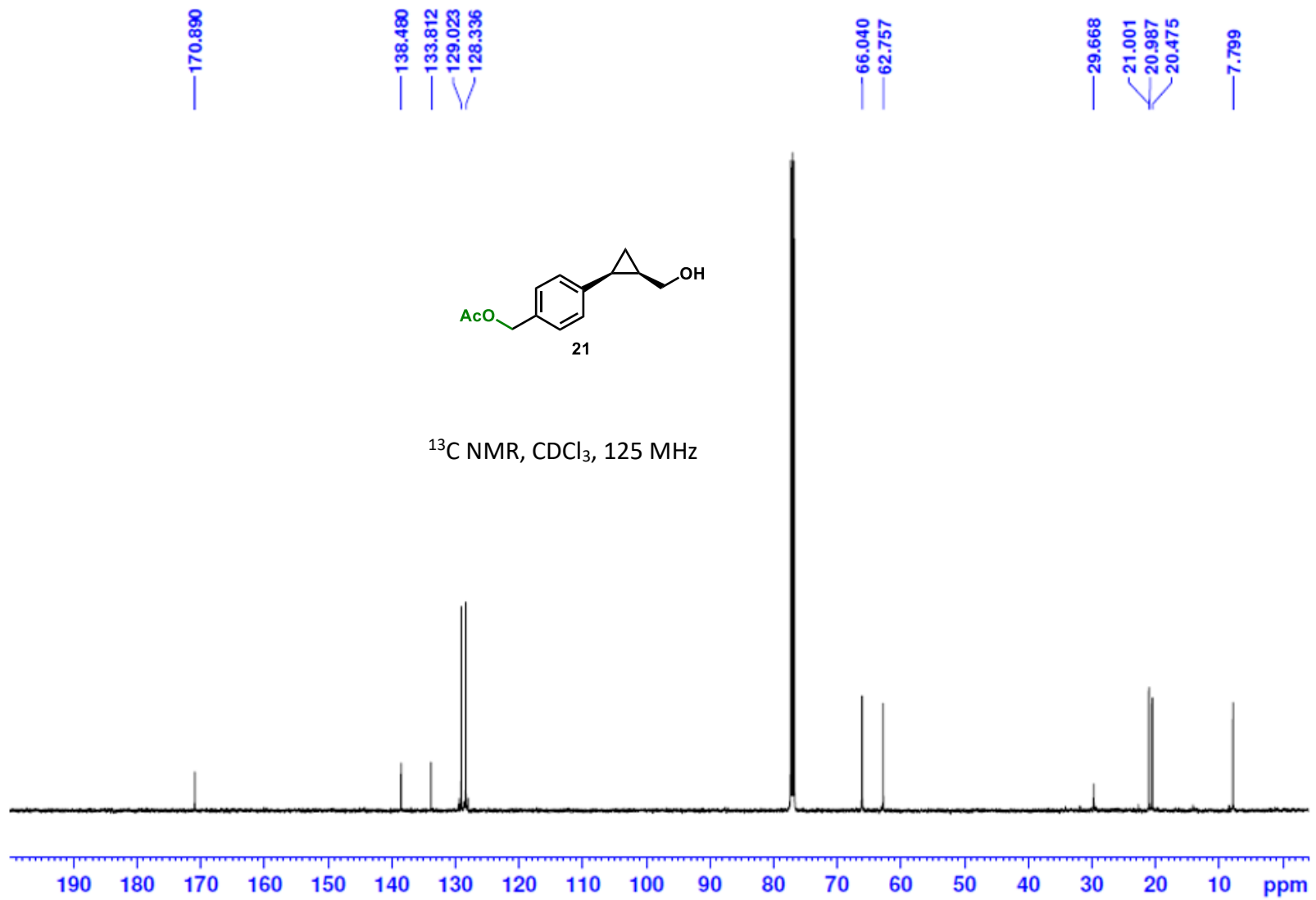
((1*R*,2*S*)-2-Phenylcyclopropyl)methanol (25f):



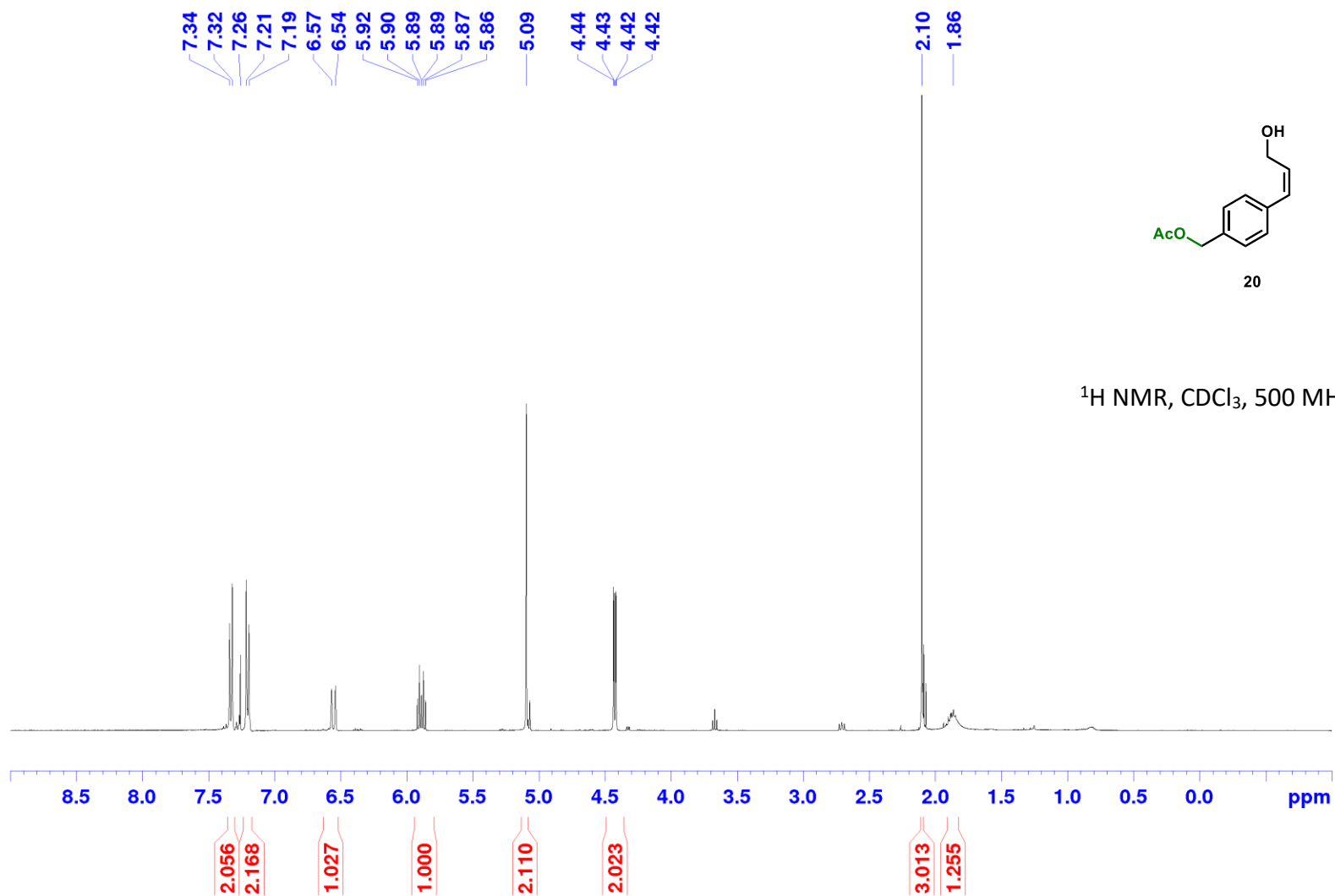


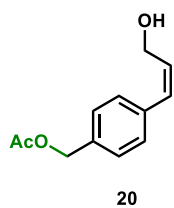
4-((1R,2S)-2-(Hydroxymethyl)cyclopropyl)benzyl acetate (21):



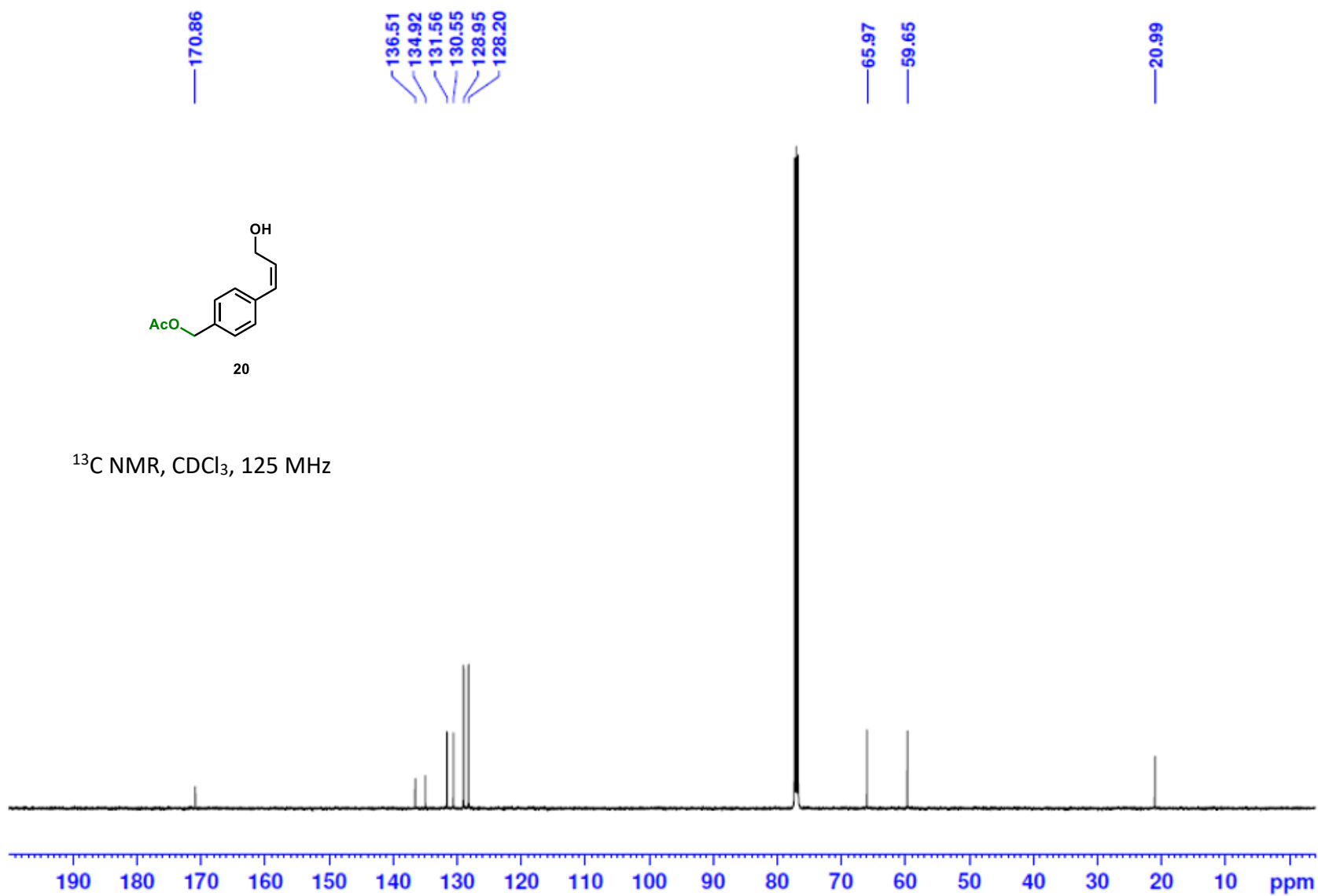


(Z)-4-(3-Hydroxyprop-1-en-1-yl)benzyl acetate (20):

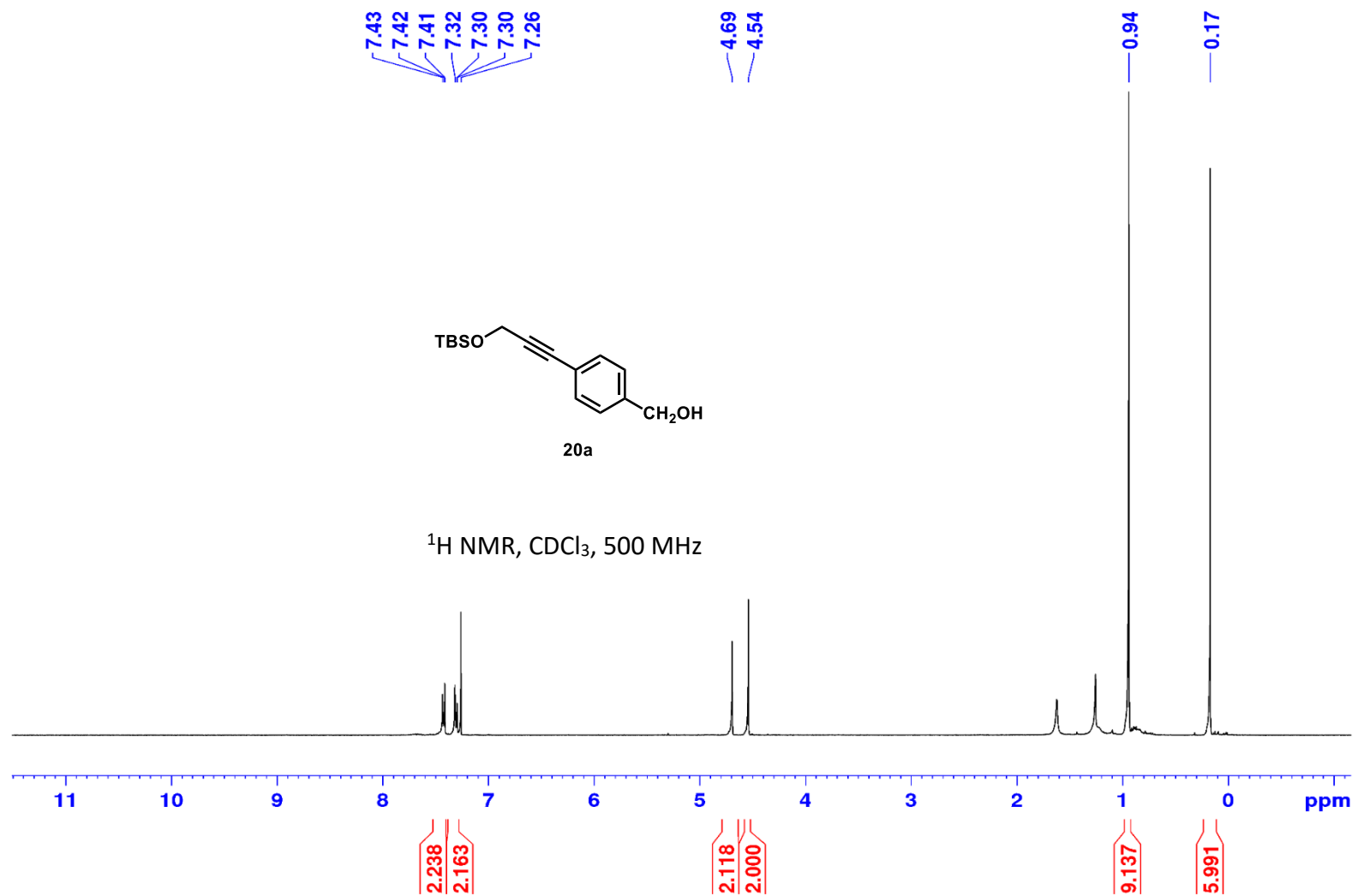


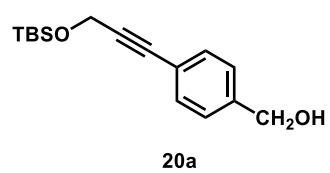


^{13}C NMR, CDCl_3 , 125 MHz

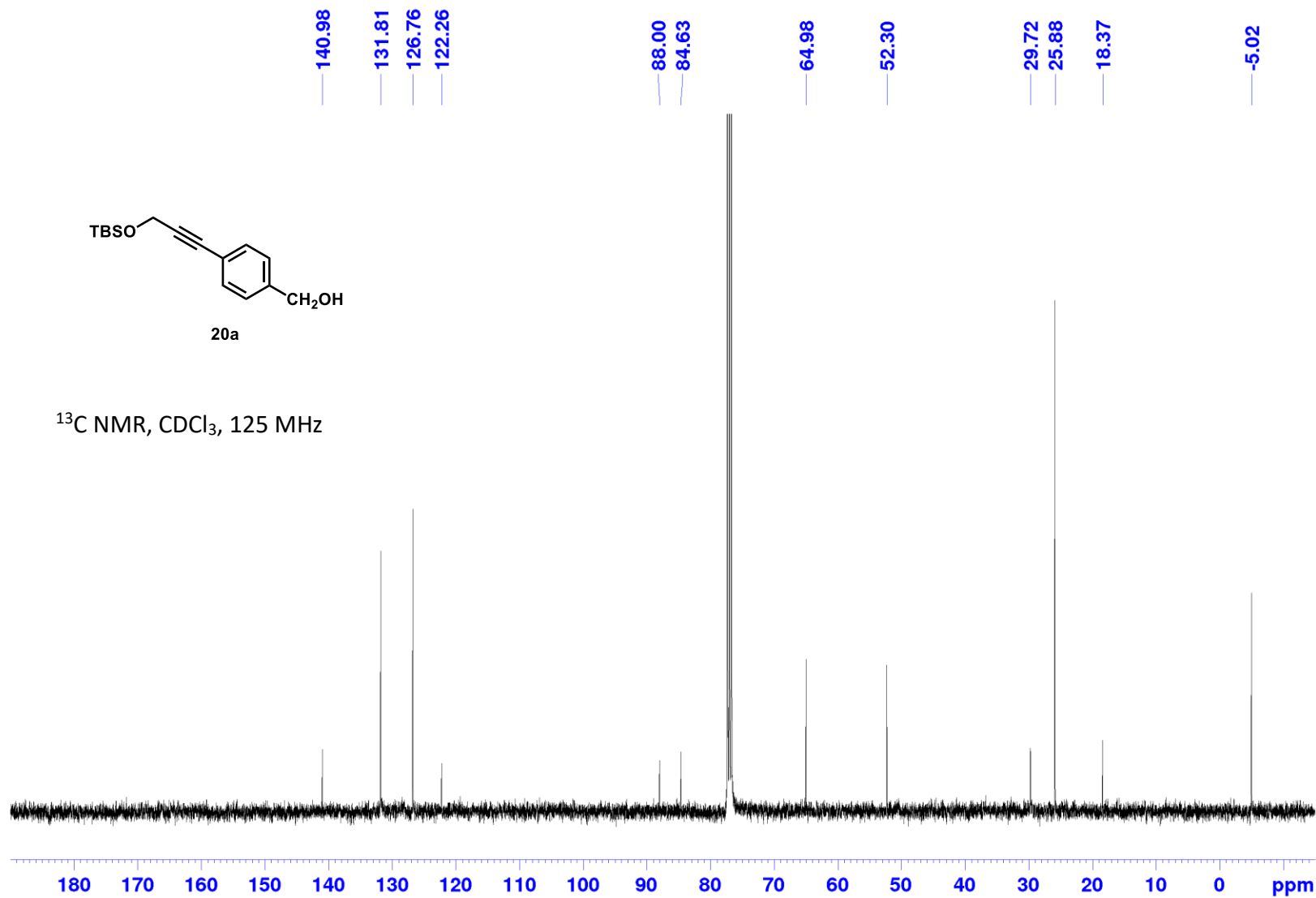


(4-(3-((*tert*-Butyldimethylsilyl)oxy)prop-1-yn-1-yl)phenyl)methanol (20a):

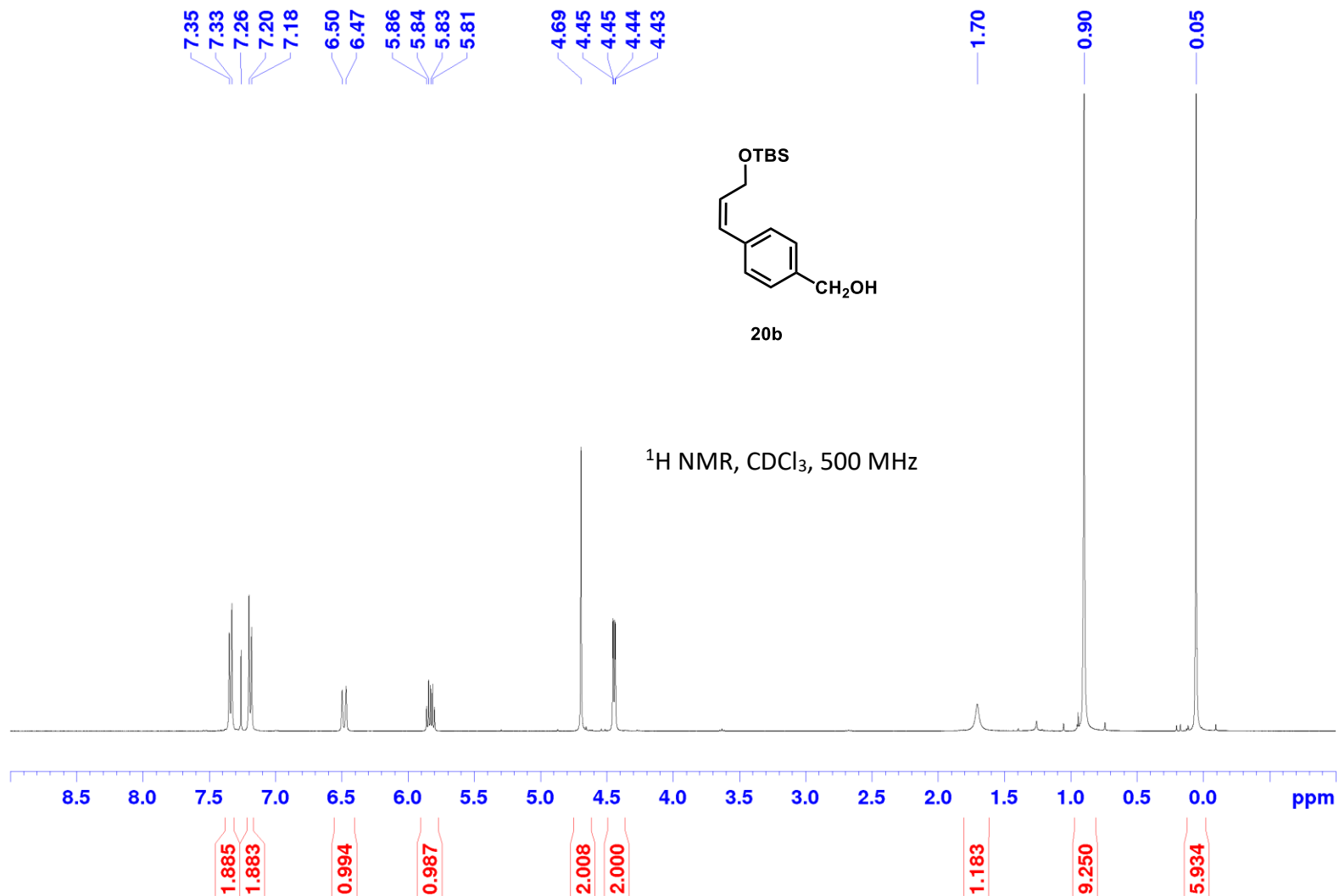


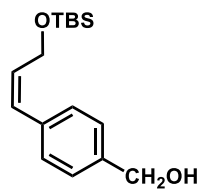


^{13}C NMR, CDCl_3 , 125 MHz



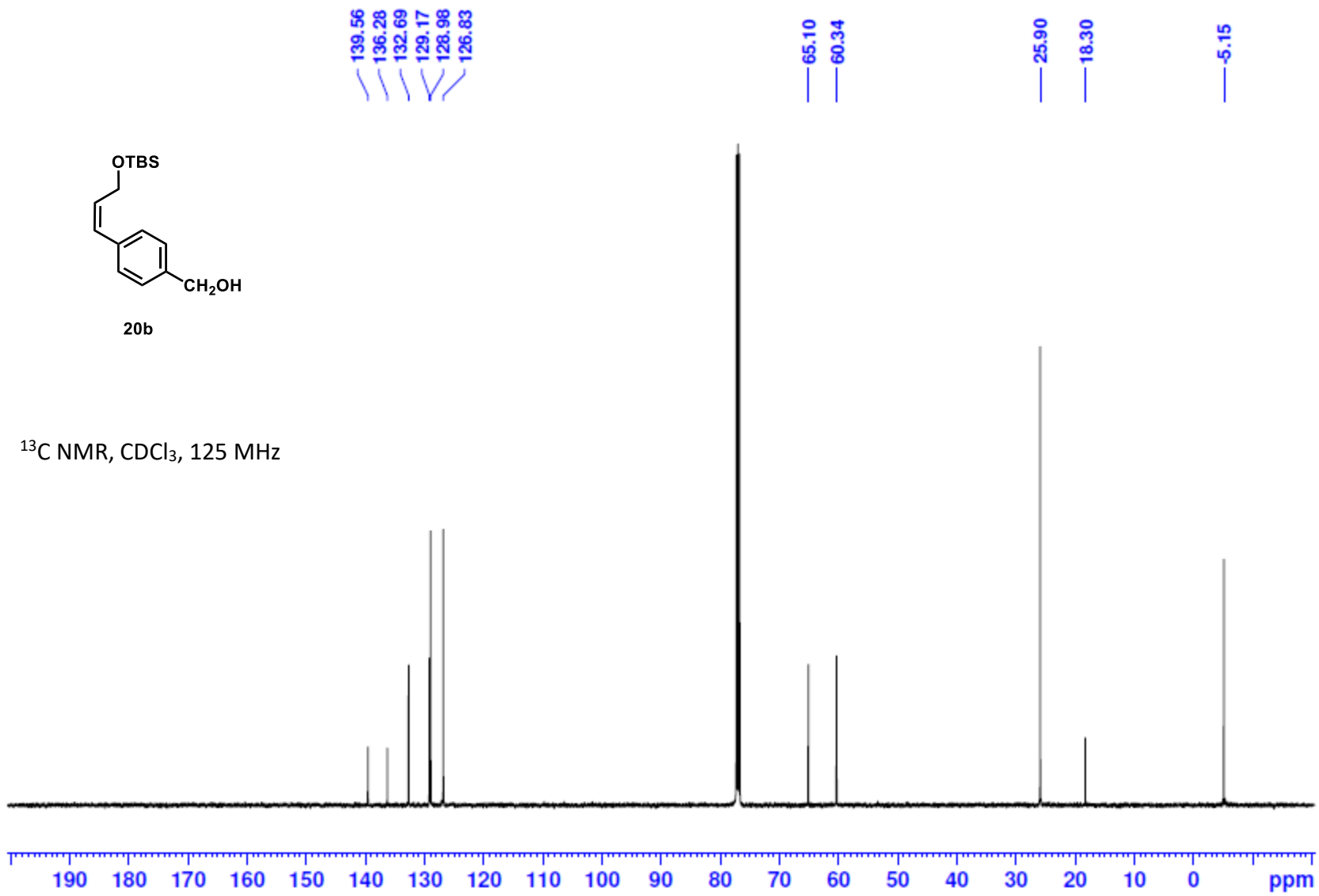
(Z)-4-(3-((*tert*-Butyldimethylsilyl)oxy)prop-1-en-1-yl)phenyl)methanol (20b):



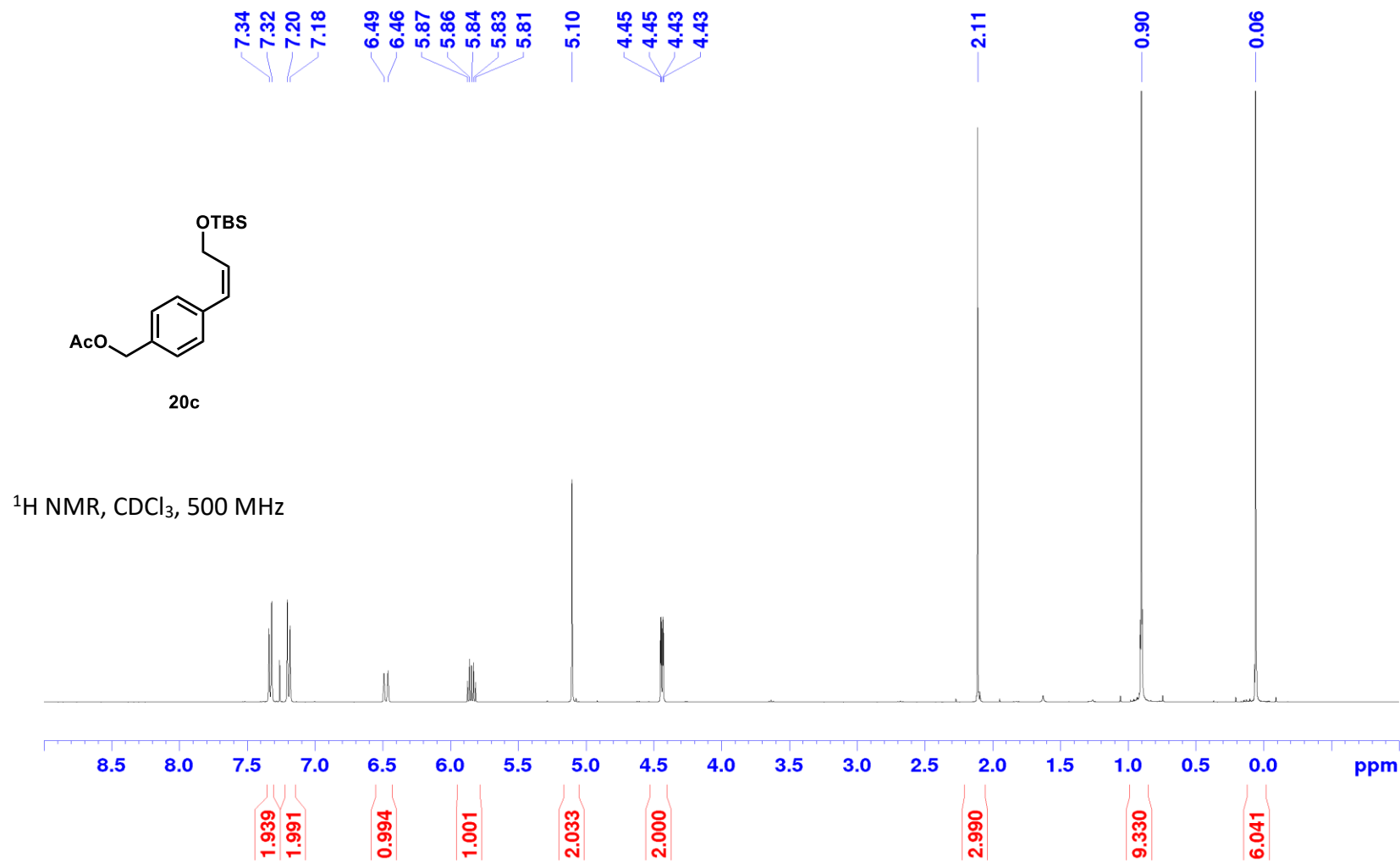


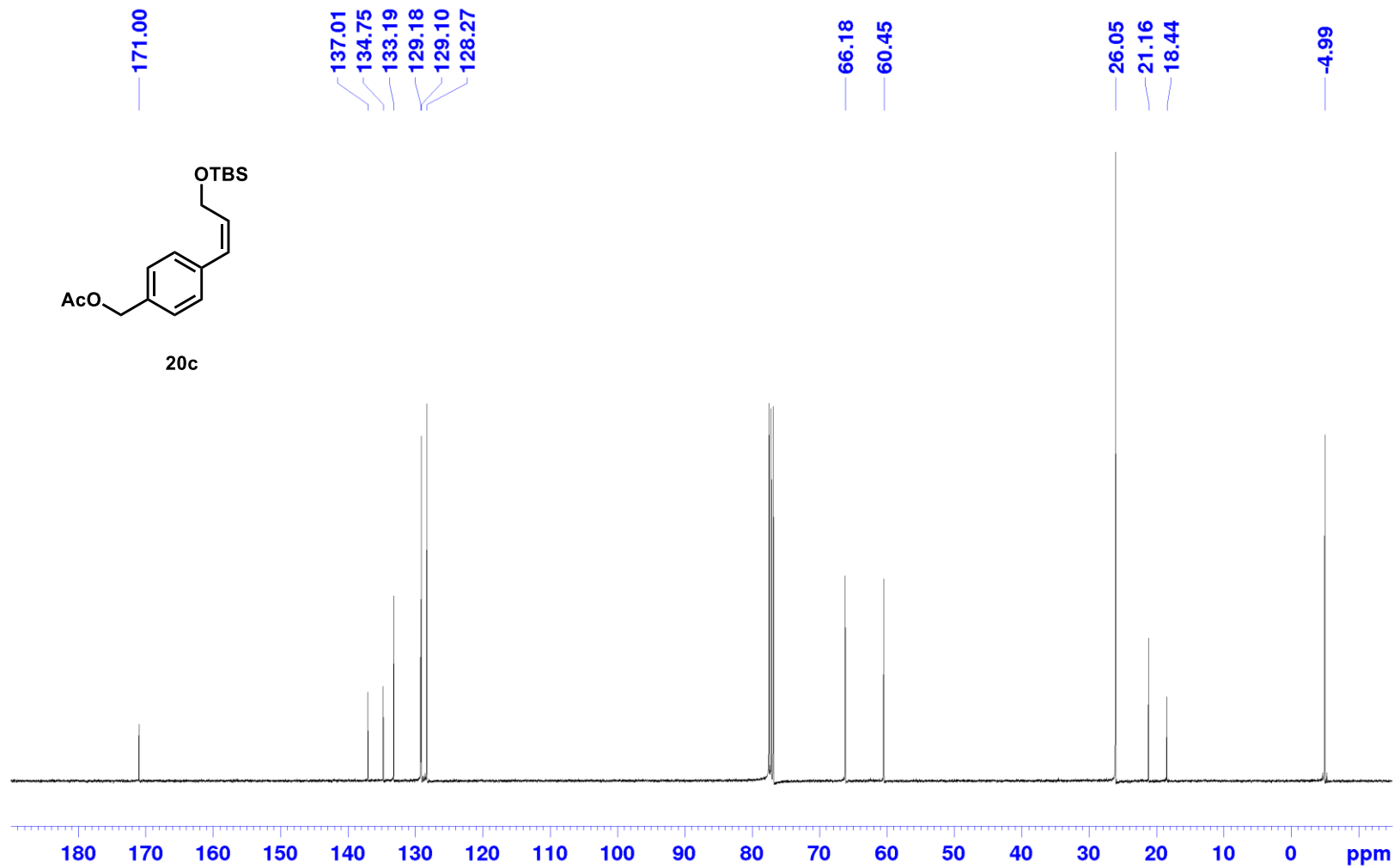
20b

¹³C NMR, CDCl₃, 125 MHz



(Z)-4-(3-((*tert*-Butyldimethylsilyl)oxy)prop-1-en-1-yl)benzyl acetate (20c):





Annex 2: Experimental Section and NMR Spectra for Chapter 3

Experimental Section for Chapter 3

General Methods

Unless otherwise stated, all glassware was oven dried and/or was flame-dried prior to use. All reactions were set up and carried out under an argon atmosphere.¹ Anhydrous solvents (benzene, acetonitrile, and THF) were obtained either by filtration through drying columns on a GlassContour system (Irvine, CA) or by distillation over calcium hydride (triethylamine, pyridine and dichloromethane) or sodium (THF). Methanol, glacial acetic acid, formic acid, and benzoic acid were used as is from commercial bottles. Unless otherwise noted, all solutions are aq. solutions. Analytical thin-layer chromatography (TLC) was performed on precoated, glass-backed silica gel (Merck 60 F254). Visualization of the developed chromatogram was performed by UV absorbance (254 nm), UV fluorescence (350 nm) or by staining with aq. potassium permanganate (KMnO₄), *p*-Anisaldehyde, or ninhydrin. Flash column chromatography was performed using silica gel (pore size 60 Å, 230-400 mesh particle size, 40-63 µm particle size) in glass columns for the separation of products. Melting points were obtained on a Buchi melting point B-540 apparatus and are uncorrected. Specific rotations, $[\alpha]_D$ values, were calculated from optical rotations measured at 25 °C in MeOH at the specified concentrations (*c* in g/100 ml) using a 0.5-dm cell length (*l*) on a Perkin-Elmer Polarimeter 241 at 589 nm, using the general formula: $[\alpha]^{25}_D = (100 \times \alpha)/(l \times c)$. Nuclear magnetic resonance spectra (¹H NMR, ¹³C NMR) were recorded on Bruker AV400, AV500, and AV700 MHz spectrometers and ¹¹B and ¹⁹F NMR spectra were recorded on AV400 and AV500. The corresponding chemical shifts for ¹H NMR, ¹³C NMR spectra are reported in parts per million relative to the chemical shift of tetramethylsilane and recorded in CDCl₃, using the residual CHCl₃ as a reference (¹H: δ 7.26 ppm, ¹³C: δ 77.2 ppm), (CD₃)₂CO using the residual solvent as a reference (¹H: δ 2.09 ppm, ¹³C: δ 205.9 ppm) and (CD₃)₂SO using the residual solvent as a reference (¹H: δ 2.54 ppm, ¹³C: δ 40.5 ppm). All ¹³C NMR spectra were obtained with complete proton decoupling. Data is reported as follows: chemical shift, multiplicity (s = singlet, d = doublet, t = triplet, q = quartet, qn = quintet, sx = sextet, h = heptet, m = multiplet and br = broad), coupling constant in Hz and integration. Infrared spectra were taken on a Bruker Vertex Series FTIR (neat) and are reported in reciprocal centimeters (cm⁻¹). High resolution mass spectra (HRMS) were performed on an LC-MSD instrument from Agilent technologies 1200 series in positive electrospray ionization (ESI Pos) and atmospheric-pressure chemical ionization (APCI). Analytical SFC were performed by the Centre de Spectroscopie de Masse de l'Université de Montréal. SFC data are reported as follows: (column type, eluent, flow rate, pressure: retention time (tr)).

Reagents used: All organic extracts were dried over sodium sulfate, filtered, and concentrated under vacuum. Diethylzinc was purchased neat from AkzoNobel and used without further purification. Bis(trifluoromethanesulfonamide), thionyl chloride, pyrrolidine, BH₃-DMS were purchased from Sigma-Aldrich and were used without further purification. Unless specified all

¹Shriver, D. F. & Drezdson, M. A. The Manipulation of Air-Sensitive Compounds; 2nd Edition; Wiley: New York, 1986.

reagents for Suzuki cross-coupling reactions were used without further purification and palladium catalysts were handled in the glovebox. All reagents used were purified using standardized protocols.

Optimization of Reaction Conditions

Optimization of Activating Reagent, Time, and Temperature

Cyclopropane **1a** was added to the reaction vessel under a positive argon pressure followed by the addition of the activating agent (5 mol%) and solvent (0.4 M). The vial was sealed and the solution was heated at the temperatures described below (see Table S1 and S2). Once the reaction time was complete, (*n*Bu₄)NBH₄ (x mol%) (where x= mol% of activating reagent) was added directly to the mixture and diluted with CH₂Cl₂. The mixture was then filtered over short pad of silica, washed with CH₂Cl₂ and concentrated under reduced pressure to obtain **2a**.

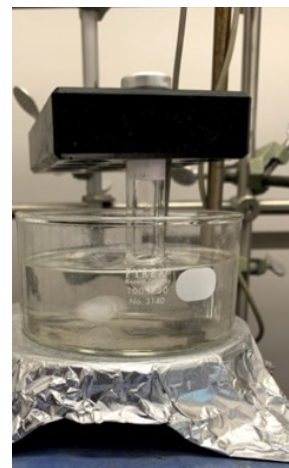
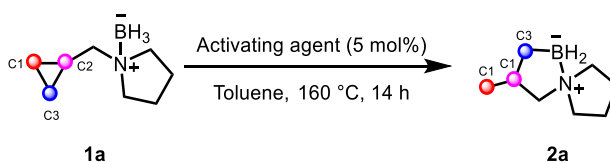
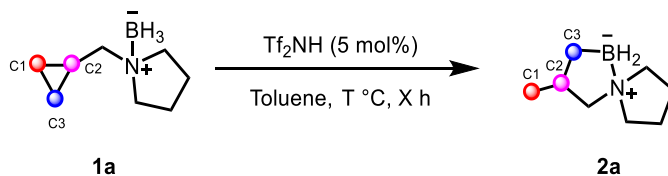


Table A1: Screening of Activating Reagent



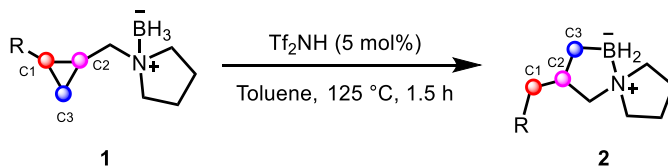
Entry	Activating Reagent	pKa (MeCN)	Result
1	None	N/A	SM
2	Tf ₂ NH	0.3	2a (99% conversion)
3	4-Nitrobenzenesulfonamide	24.9	SM
4	TfOH	0.7	SM
5	Acetic Acid	23.5	SM
6	Formic acid	21.5	SM
7	Benzoic acid	20.5	SM

Table A2: Optimization of Time and Temperature Using Tf₂NH



Entry	Temperature (°C)	Tf ₂ NH (mol%)	Time (h)	2a Yield (%)
1	160	5	14	99
2	140	5	4	99
3	125	5	4.5	99
4	125	5	3	69
5	125	5	1.5	20
6	125	100	1	99
7	100	5	16	47
8	100	5	4	15
9	80	5	60	25
10	rt	5	16	No conversion

Table A1: Type of Substituent vs. Reaction Time



Entry	R	Yield (%)
1	Pr	15
2	H	20
3	Ph	99
4	<i>p</i> -Fluorobenzene	99

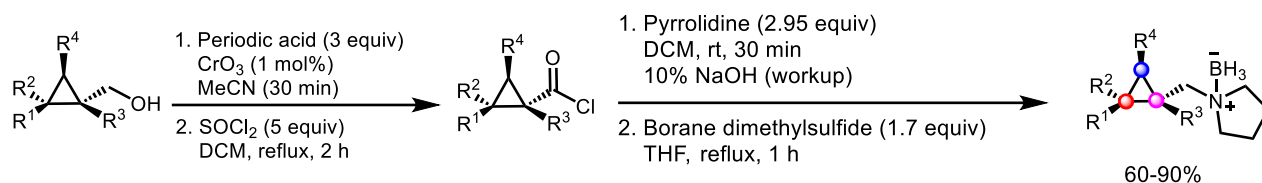
A general trend of the effect of substituents on the reaction time was observed. CABs substituted with electron withdrawing substituents underwent ring-opening faster than electron donating substituents. For entries 1 and 2, the reactions did not go to completion and starting material was present in the crude ^1H NMR spectrum.

Summary of Optimization Results

The reaction was optimized to provide quantitative yield at 125 °C in 4.5 h using Tf_2NH (5 mol%) as the activating agent and toluene as the solvent (Table S2). During optimization it was found that heating the mixture to 160 °C for 16 h provided the 5–5 spirocyclic amine–borane motif resulting from the cleavage of C2–C3 distal carbon bond. A doublet was observed in the ^1H NMR spectrum at 1.07 ppm and NMR correlation studies revealed the presence of a methyl group arising from the ring–opening of CAB **1a**. Further analysis of a broad signal in the ^{13}C NMR spectrum at 21.9 ppm and a well-resolved triplet in the ^{11}B NMR spectrum at –3.6 ppm supported the formation of a C–B bond where the boron was bearing two hydrogen atoms thus indicating the presence of a C–BH₂ species in SCAB **2a**. During the optimization, it was also established that no conversion to **2a** occurred at room temperature in the presence of Tf_2NH or while heating in the absence of Tf_2NH . No ring-opening product was observed when replacing Tf_2NH with other activating agents (Table S1). At 100 °C and 16 h, the yield decreased to 47% conversion while only 15% yield was obtained after 4 h at this temperature (Table S2). Temperatures below 100 °C required longer reaction times. A maximum of 25% conversion to **2a** was achieved when the reaction was run for 60 h at 80 °C. Generally, an increase in temperature and reaction time provided a linear correlation with respect to conversion. A stoichiometric amount of Tf_2NH led to the formation of the product **2a** in 1 h at 125 °C quantitatively.

Synthesis and Characterization of Compounds

Synthesis of Cyclopropane Amine-Boranes (CABs)



General Procedure A – Synthesis of Cyclopropyl Methanols

Cyclopropanemethanol derivatives were synthesized according to literature procedures.¹ To a round bottom flask was added CH₂Cl₂ (30 mL) and DME (1 equiv) followed by Et₂Zn (1 equiv). The reaction mixture was cooled to -12 °C and diiodomethane (1 equiv) was added dropwise over a period of 5 min while maintaining the internal temperature between -12 °C to -8 °C. The reaction mixture was stirred for 10 min and a solution of the corresponding allylic alcohol (7 mmol) in CH₂Cl₂ (6 mL) was added over a period of 5 min while maintaining an internal temperature of -5 °C. The mixture was warmed to room temperature and stirred for 12 h. The reaction mixture was quenched with a dropwise addition of aq. NH₄Cl (3 mL) and the mixture was transferred to a separatory funnel. The organic layer was separated, and the aqueous layer was extracted with EtOAc (3 x 25 mL). The combined organic layers were dried over anhydrous Na₂SO₄, filtered, and concentrated under reduced pressure. The residue was purified by silica gel chromatography (1:4 EtOAc/hexanes) to provide the corresponding cyclopropylmethanols in 50% to 85% yield.

Synthesis of Allylic Alcohols: A mixture of the corresponding aldehyde (~10 mmol) and (carbethoxymethylene)triphenylphosphorane (2 equiv) in toluene (0.1 M) was refluxed for 16 h. The solvent was removed *under reduced pressure* and the residue was purified by silica gel chromatography (1:4 EtOAc/hexanes) to provide the corresponding ester. The product was

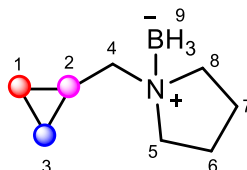
added to a dried round bottom flask and diluted with toluene (22 mL). The mixture was cooled to 0 °C and DIBAL-H (1.0 M in hexanes, 2 equiv) was added. The reaction mixture was stirred at 0 °C for 2 h and then quenched with a dropwise addition of 1 N HCl (10 mL). The mixture was then diluted with H₂O (10 mL) and EtOAc (20 mL) and transferred into a separatory funnel. The organic layer was separated, and the aqueous layer was extracted with EtOAc (3 x 20 mL). The combined organic layers were dried over anhydrous Na₂SO₄, filtered, and concentrated under reduced pressure. The residue was purified by silica gel chromatography (1:4 EtOAc/hexanes) to provide the pure corresponding allylic alcohol.

General Procedure B – Synthesis of Cyclopropyl Carboxylic Acids

Periodic acid (2 equiv) and CrO₃ (1 mol%) were added to a flask containing MeCN (0.2 M). The reaction mixture was allowed to stir for 10 min at rt. The flask was cooled to 0 °C and a solution of the cyclopropanemethanol (1 equiv) (synthesized according to general procedure A) dissolved in MeCN (1.5M) was added dropwise to the flask while stirring vigorously. Once the addition was complete the mixture was stirred for 10 min and the flask was concentrated to dryness under reduced pressure. The residue was suspended in H₂O (~3 mL/mmol) and the mixture was extracted with EtOAc (3 x 20 mL). The combined organic layers were washed with H₂O, dried over anhydrous Na₂SO₄, filtered, and concentrated under reduced pressure to provide a residue typically in the form of an orange oil/solid depending on the substrate. The residue was used as is for the next step without further purification.

General Procedure C – Synthesis of Cyclopropane Amine–Boranes

1-(Cyclopropylmethyl)pyrrolidine borane: Scaled to ~14 g (1a)



Cyclopropanecarboxylic acid (12.0 g, 120 mmol) was added to a 250 mL round bottom flask followed by the addition of CH₂Cl₂ (100 mL). The flask was cooled to –10 °C and SOCl₂ (26.1 mL, 360 mmol) was added in one portion. The resulting mixture was refluxed for 2 h. After 2 h, the excess SOCl₂ and CH₂Cl₂ was distilled off. The residue was dissolved in CH₂Cl₂ (40 mL) and the solution was added dropwise to a stirring solution of pyrrolidine (32.9 mL, 401 mmol) in CH₂Cl₂ (15 mL) at 0 °C over a period of 10 min (exothermic!). The resulting mixture was stirred at room temperature for 20 min, and then washed with 150 mL 10% aq. NaOH solution. The organic layer was separated and the aqueous layer was extracted with CH₂Cl₂ (2 x 100 mL). The combined organic layers were dried over anhydrous Na₂SO₄, filtered, and concentrated under reduced pressure to provide the corresponding amide as a viscous oil. The oil was then dissolved in anhydrous THF (110 mL) and the solution was cooled to 0 °C to which BH₃•SMe₂ (21.5 mL, 227 mmol, 1.7 equiv) was added dropwise over 10 min. (exothermic!). After the exothermic reaction had ceased (~30 sec to 1 min), the reaction mixture was refluxed for 2 h. The mixture was poured slowly over a short pad of silica gel to decompose residual BH₃•SMe₂ and eluted with CH₂Cl₂ (3 x 5 mL). The filtrate was concentrated under reduced pressure to provide the product as a clear oil in 75% yield (13.8 g, 136 mmol).

¹H NMR (500 MHz, CDCl₃) δ 3.26 – 3.15 (m, 2H, **H**_{5,8}), 2.95 – 2.87 (m, 2H, **H**_{5,8}), 2.69 (d, *J* = 6.7 Hz, 2H, **H**₄), 2.21 – 2.11 (m, 2H, **H**_{6,7}), 1.95 (br, 1H, **BH**₉), 1.91 – 1.80 (m, 2H, **H**_{6,7}), 1.77 (br, 1H, **BH**₉), 1.58 (br, 1H, **BH**₉), 1.41 – 1.28 (m, 1H, **H**₂), 0.68 – 0.58 (m, 2H, **H**_{1,3}), 0.22 – 0.14 (m, 2H, **H**_{1,3}).

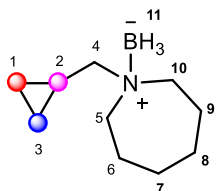
¹³C NMR (126 MHz, CDCl₃) δ 67.7, 60.5 (2C), 23.0 (2C), 6.9, 4.4 (2C).

¹¹B NMR δ –11.7 ppm.

IR (film) ν_{max} : 2996, 2368, 2275, 1458, 1166, 1026, 935, 830 cm^{-1} .

HRMS (ESI, m/z): calculated for $[\text{M} + \text{Na}]^+$ $\text{C}_8\text{H}_{18}\text{BN}$ requires m/z 162.1424, found m/z 162.1431.

1-(Cyclopropylmethyl)azepane borane (**1b**)



Cyclopropanecarboxylic acid (300 mg, 2.9 mmol) was transformed into **1b** using general procedure C modified using azepane (647 μL , 5.7 mmol). The desired product was obtained in 71% yield (340 mg, 2.0 mmol).

^1H NMR (400 MHz, CDCl_3) δ 3.10 (dd, $J = 13.6, 8.4$ Hz, 2H, $\text{H}_{5,10}$), 2.99 (dd, $J = 13.7, 8.8$ Hz, 2H, $\text{H}_{5,10}$), 2.63 (d, $J = 6.7$ Hz, 2H, H_4), 2.06 – 1.77 (m, 2H, $\text{H}_{6,9}$), 1.68 – 1.45 (m, 8H, $\text{H}_{6,9}$, $\text{H}_{7,8}$, H_{11}), 1.45 – 1.28 (m, 2H, H_2 , H_{11}), 0.72 – 0.56 (m, 2H, $\text{H}_{1,3}$), 0.21 – 0.15 (m, 2H, $\text{H}_{1,3}$).

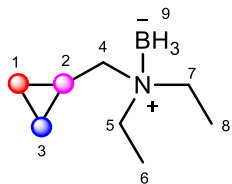
^{13}C NMR (101 MHz, CDCl_3) δ 68.5, 60.6 (2C), 29.5 (2C), 22.7 (2C), 6.4, 4.7 (2C).

^{11}B NMR δ -10.9 ppm.

IR (film) ν_{max} 2962, 2857, 2364, 2322, 2277, 1342, 1165, 1048, 1014, 880 cm^{-1} .

HRMS (ESI, m/z): calculated for $[\text{M} - 2\text{H}]^+$ $\text{C}_{10}\text{H}_{20}\text{BN}$ requires m/z 166.1762, found m/z 166.1760.

***N*-(Cyclopropylmethyl)-*N*-ethylethanamine borane (**1c**)**



Cyclopropanecarboxylic acid (103 mg, 1.2 mmol) was transformed into **1c** using general procedure C modified using diethylamine (247 μ L, 2.4 mmol). The desired product was obtained in 87% yield (147 mg, 1.0 mmol).

^1H NMR (500 MHz, CDCl_3) δ 3.00 – 2.81 (m, 4H, $\text{H}_{5,7}$), 2.62 (d, $J = 6.7$ Hz, 2H, H_4), 1.73 (br, 1H, H_9), 1.42 (br, 1H, H_9), 1.30 (br, 1H, H_9), 1.21 (t, $J = 7.3$ Hz, 6H, $\text{H}_{6,8}$), 1.19 – 1.11 (m, 1H, H_2), 0.70 – 0.54 (m, 2H, $\text{H}_{1,3}$), 0.25 – 0.20 (m, 2H, $\text{H}_{1,3}$).

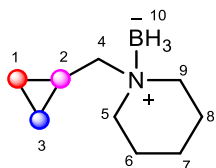
^{13}C NMR (126 MHz, CDCl_3) δ 63.0, 53.2 (2C), 9.1 (2C), 5.48, 4.5 (2C).

^{11}B NMR δ –13.1 ppm.

IR (film) ν_{max} : 3081, 3001, 2980, 2380, 2326, 2278, 1468, 1388, 1168, 1021, 828 cm^{-1} .

HRMS (ESI, m/z): calculated for $[\text{M} - 2\text{H}]^+ \text{C}_8\text{H}_{18}\text{BN}$ requires m/z 140.1605, found m/z 140.1605.

1-(Cyclopropylmethyl)piperidine borane (1d**)**



Cyclopropanecarboxylic acid was transformed into **1d** using general procedure C modified using piperidine (4.0 g, 47.5 mmol). The desired product was obtained in 76% yield (1.9 g, 12.2 mmol).

^1H NMR (400 MHz, CDCl_3) δ 3.01 – 2.94 (m, 2H, $\text{H}_{5,9}$), 2.88 – 2.71 (m, 2H, $\text{H}_{5,9}$), 2.63 (d, $J = 6.7$ Hz, 2H, H_4), 2.01 – 1.90 (m, 2H, $\text{H}_{6,8}$), 1.74 (br, 1H, H_{10}), 1.62 – 1.45 (m, 4H, $\text{H}_{6,8}$, H_7 , H_{10}), 1.44 – 1.28 (m, 3H, H_2 , H_7 , H_{10}), 0.68 – 0.50 (m, 2H, $\text{H}_{1,3}$), 0.18 – 0.14 (m, 2H, $\text{H}_{1,3}$).

^{13}C NMR (101 MHz, CDCl_3) δ 68.6, 58.1 (2C), 23.0, 20.7 (2C), 5.5, 4.4 (2C).

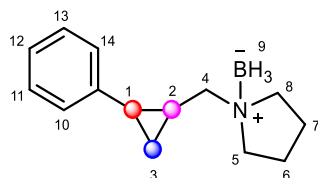
^{11}B NMR δ –12.1 ppm.

IR (film) ν_{max} : 2954, 2863, 2365, 2274, 1449, 1172, 1088, 1038 cm^{-1} .

HRMS (ESI, m/z): calculated for $[\text{M} - 2\text{H}]^+$ $\text{C}_9\text{H}_{18}\text{BN}$ requires m/z 152.1605, found m/z 152.1601.

*Compounds **1e-1h** were synthesized starting from Phenylcyclopropane-1-carbonyl chloride (200 mg, 1.1 mmol) and according to general procedure C (modified with respective amines)*

1-((2-Phenylcyclopropyl)methyl)pyrrolidine borane (**1e**)



Phenylcyclopropane-1-carbonyl chloride was converted into **1e** according to general procedure C. Modification: (Beginning with commercially available acid chloride derivative) 2-Phenylcyclopropane-1-carbonyl chloride (200 mg, 1.1 mmol) was dissolved in CH_2Cl_2 (529 μL), and the solution was added slowly to pyrrolidine (100 μL , 1.2 mmol) in CH_2Cl_2 (794 μL) at 0 $^\circ\text{C}$ (exothermic reaction!). The title compound **1e** was obtained as a white solid in 86% yield (205 mg, 1.0 mmol).

^1H NMR (500 MHz, CDCl_3) δ 7.27 (t, $J = 7.5$ Hz, 2H, ArH), 7.20 (tt, $J = 7.4$, 1.3 Hz, 1H, ArH), 7.12 (dd, $J = 8.8$, 0.9 Hz, 2H, ArH), 3.31 – 3.13 (m, 2H, $\text{H}_{5,8}$), 2.98 (dd, 1H, $J = 12.9$, 6.3 Hz, 1H, H_4), 2.92

– 2.82 (m, 2H, **H**_{5,8}), 2.78 (dd, *J* = 12.8, 7.2 Hz, 1H, **H**₄), 2.25 – 2.18 (m, 2H, **H**_{6,7}), 1.96 – 1.82 (m, 3H, **H**_{6,7}, **H**₉), 1.82 – 1.76 (m, 1H, **H**₁), 1.76 – 1.68 (m, 1H, **H**₂), 1.58 (br, 1H, **H**₉), 1.50 – 1.36 (br, 1H, **H**₉), 1.08 (dt, *J* = 8.6, 5.3 Hz, 1H, **H**₃), 0.93 – 0.84 (dt, *J* = 8.8, 5.3 Hz 1H, **H**₃).

¹³C NMR (126 MHz, CDCl₃) δ 141.6, 128.6 (2C), 126.1, 126.0 (2C), 67.1, 60.9, 60.5, 23.3, 22.9 (2C), 18.6, 14.8.

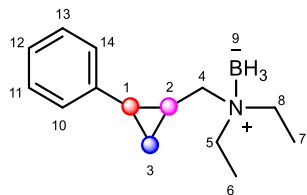
¹¹B NMR δ –11.6 ppm.

IR (film) ν_{max}: 2367, 2273, 1603, 1497, 1458, 1164, 1095, 756, 697 cm⁻¹.

HRMS (ESI, *m/z*): calculated for [M + Na]⁺ C₁₄H₂₂BN requires *m/z* 238.1738, found *m/z* 238.1730.

mp 44–46 °C.

N-Ethyl-*N*-((2-phenylcyclopropyl)methyl)ethanamine borane (**1f**)



The title compound was prepared according to the procedure described for **1e** where the amine was replaced with Et₂NH. The title compound **1f** was obtained as a clear oil in 86% yield (207 mg, 1.0 mmol).

¹H NMR (500 MHz, CDCl₃) δ 7.30 – 7.24 (m, 2H, ArH), 7.21 (tt, *J* = 7.3, 1.3 Hz, 1H, ArH), 7.11 – 7.05 (m, 2H, ArH), 2.95 – 2.83 (m, 5H, **H**_{5,8}, **H**₄), 2.72 (dd, *J* = 13.5, 7.4 Hz, 1H, **H**₄), 1.83 – 1.75 (m, 1H, **H**₁), 1.53 – 1.45 (m, 1H, **H**₂), 1.88 – 1.39 (br, 3H, **H**₉), 1.23 (td, *J* = 7.3, 4.9 Hz, 6H, **H**_{6,7}), 1.08 (dt, *J* = 8.7, 5.3 Hz, 1H₃), 0.89 (dt, *J* = 8.9, 5.5 Hz, 1H₃).

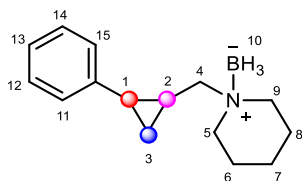
^{13}C NMR (126 MHz, CDCl_3) δ 141.7, 128.6 9 (2C), 126.1, 125.9 (2C), 62.7, 53.4, 53.1, 23.3, 17.4, 14.7, 9.1 (2C).

^{11}B NMR δ -12.9 ppm.

IR (film) ν_{max} : 2379, 2328, 2278, 1603, 1461, 1389, 1167, 1029, 758, 697 cm^{-1} ;

HRMS (ESI, m/z): calculated for $[\text{M} + \text{Na}]^+$ $\text{C}_{14}\text{H}_{24}\text{BN}$ requires m/z 240.1894, found m/z 240.1896.

1-((2-Phenylcyclopropyl)methyl)piperidine borane (**1g**)



The title compound was prepared according to the procedure described for **1e** on a 1.9 mmol scale where the amine was replaced with piperidine. The title compound **1g** was obtained as a clear oil in 87% yield (370 mg, 1.6 mmol).

^1H NMR (500 MHz, CDCl_3) δ 7.30 – 7.22 (m, 2H, ArH), 7.20 (tt, J = 7.3, 1.2 Hz 1H, ArH), 7.13 – 7.10 (m, 2H, ArH), 3.08 – 2.95 (m, 2H, $\text{H}_{5,9}$), 2.91 (dd, J = 12.9, 5.7 Hz, 1H, H_4), 2.85 (dd, J = 13.3, 7.8 Hz, 2H, $\text{H}_{5,9}$), 2.79 (dd, J = 13.0, 6.8 Hz, 1H, H_4), 1.97 – 1.89 (m, 2H, $\text{H}_{6,8}$), 1.83 – 1.70 (m, 3H, H_2 , $\text{H}_{6,8}$), 1.65 – 1.53 (m, 4H, H_7 , 3H_{10}), 1.53 – 1.40 (m, 2H, H_1 , H_7), 1.08 (dt, J = 8.5, 5.3 Hz, 1H, H_3), 0.89 (dt, J = 8.8, 5.5 Hz, 1H, H_3).

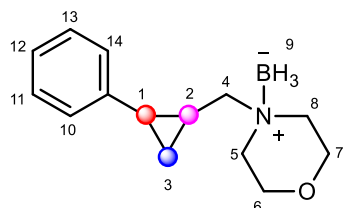
^{13}C NMR (126 MHz, CDCl_3) δ 141.6, 128.5 (2C), 126.03, 126.0 (2C), 65.9, 58.6, 58.0, 23.3, 23.0, 20.9, 20.8, 17.3, 14.8.

^{11}B NMR δ -11.9 ppm.

IR (film) ν_{\max} : 2954, 2939, 2861, 2361, 2341, 1457, 1173, 757 cm^{-1} .

HRMS (ESI, m/z): calculated for $[\text{M} + \text{Na}]^+$ $\text{C}_{15}\text{H}_{24}\text{BN}$ requires m/z 252.1894, found m/z 252.1902.

4-((2-Phenylcyclopropyl)methyl)morpholine borane (**1h**)



The title compound was prepared according to the procedure described for **1e** on a 1.4 mmol scale where the amine was replaced with morpholine. The title compound **1h** was obtained as a clear oil in 84% yield (270 mg, 1.2 mmol).

^1H NMR (500 MHz, CDCl_3) δ 7.32 – 7.28 (m, 2H, ArH), 7.21 (tt, $J = 7.4, 1.2$ Hz, 1H, ArH), 7.15 – 7.07 (m, 2H, ArH), 4.39 – 4.18 (m, 2H, $\text{H}_{5,8}$), 3.73 (dq, $J = 6.1, 2.8$ Hz, 2H, $\text{H}_{5,8}$), 3.13 – 2.96 (m, 3H, $\text{H}_4, \text{H}_{6,7}$), 2.94 – 2.87 (m, 2H, $\text{H}_{6,7}$), 2.84 (dd, $J = 13.5, 7.4$ Hz, 1H, H_4), 1.97 (br, 1H, H_9), 1.87 – 1.72 (m, 3H, $\text{H}_1, \text{H}_2, \text{H}_9$), 1.64 (br, 1H, H_9), 1.15 (dt, $J = 8.6, 5.4$ Hz, 1H, H_3), 0.94 (dt, $J = 8.8, 5.5$ Hz, 1H, H_3).

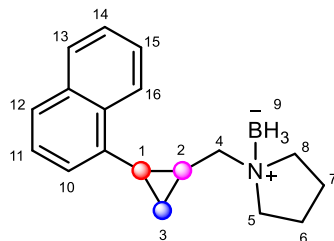
^{13}C NMR (126 MHz, CDCl_3) δ 141.2, 128.7 (2C), 126.2, 126.0 (2C), 70.4, 62.2, 62.1, 57.8, 57.4, 23.5, 16.6, 15.0.

^{11}B NMR δ –13.3 ppm.

IR (film) ν_{\max} : 2954, 2939, 2861, 2361, 2341, 1457, 1173, 757 cm^{-1} .

HRMS (ESI, m/z): calculated for $[\text{M} + \text{Na}]^+$ $\text{C}_{14}\text{H}_{22}\text{BNO}$ requires m/z 254.1687, found m/z 254.1678.

1-((2-(Naphthalen-1-yl)cyclopropyl)methyl)pyrrolidine borane (**1i**)



2-(Naphthalen-1-yl)cyclopropane-1-carboxylic acid (332 mg, 1.6 mmol) was transformed to amine borane **1i** according to general procedure C. The desired product was obtained in 56% yield (274 mg, 1.0 mmol).

¹H NMR (500 MHz, CDCl₃) δ 7.78 (d, J = 8.6 Hz, 1H, ArH), 7.76 (d, J = 8.8 Hz, 2H, ArH), 7.55 (s, 1H, ArH), 7.49 – 7.37 (m, 2H, ArH), 7.21 (dd, J = 8.5, 1.6 Hz, 1H, ArH), 3.32 – 3.15 (m, 2H, H_{5,8}), 3.02 (dd, J = 12.8, 6.0 Hz, 1H, H₄), 2.95 – 2.86 (m, 2H, H_{5,8}), 2.82 (dd, J = 12.8, 7.4 Hz, 1H, H₄), 2.23 – 2.13 (m, 2H, H_{6,7}), 2.00 – 1.92 (m, 1H, H₁), 1.91 – 1.79 (m, 4H, H_{6,7}, H₂, H₉), 1.65 (br, 2H, H₉), 1.20 (dt, J = 8.7, 5.3 Hz, 1H, H₃), 0.97 (dt, J = 8.9, 5.5 Hz, 1H, H₃).

¹³C NMR (126 MHz, CDCl₃) δ 139.1, 133.6, 132.2, 128.3, 127.7, 127.5, 126.3, 125.3, 124.7, 124.2, 67.1, 61.0, 60.5, 23.6, 23.0, 22.96, 18.6, 14.8.

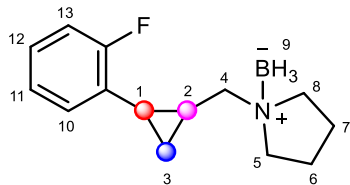
¹¹B NMR δ –11.6 ppm.

IR (film) ν_{max} : 2980, 2925, 2850, 2359, 2338, 2274, 2177, 1631, 1599, 1457, 1170, 1094 cm⁻¹

HRMS (ESI, m/z): calculated for [M + Na]⁺ C₁₈H₂₄BN requires m/z 288.18940, found m/z 288.18941.

mp 116–117 °C.

1-((2-(2-Fluorophenyl)cyclopropyl)methyl)pyrrolidine borane (**1j**)



2-(2-Fluorophenyl)cyclopropane-1-carboxylic acid (1.13 g, 6.2 mmol) was transformed to the title compound **1j** according to general procedure C. The desired product was obtained as a white solid in 96% yield (1.39 g, 5.94 mmol).

¹H NMR (400 MHz, CDCl₃) δ 7.21 – 7.15 (m, 1H, ArH), 7.09 – 6.89 (m, 3H, ArH), 3.32 – 3.14 (m, 2H, H_{5,8}), 2.99 (dd, *J* = 12.8, 6.0 Hz, 1H, H₄), 2.96 – 2.84 (m, 2H, H_{5,8}), 2.76 (dd, *J* = 12.8, 7.3 Hz, 1H, H₄), 2.26 – 2.11 (m, 2H, H_{6,7}), 2.03 – 1.93 (m, 1H, H₁), 1.94 – 1.84 (m, 2H, H_{6,7}), 1.86 – 1.79 (m, 2H, H₂, H₉), 1.63 (br, 1H, H₉), 1.43 (br, 1H, H₉), 1.11 (dt, *J* = 8.7, 5.3 Hz, 1H, H₃), 0.96 – 0.85 (dt, *J* = 8.9, 5.4 Hz, 1H, H₃).

¹³C NMR (101 MHz, CDCl₃) δ 161.8, 128.4, 127.4, 126.3, 124.3, 115.2, 67.0, 61.4, 60.4, 23.0, 22.8, 17.6, 16.4, 13.4.

¹¹B NMR δ –11.8 ppm.

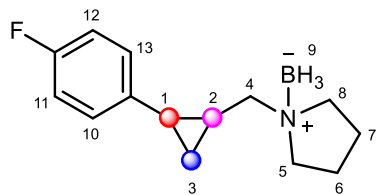
¹⁹F NMR δ –120.1 ppm.

IR (film) *v*_{max}: 2958, 2369, 2273, 1495, 1455, 1237, 1164, 1101, 754 cm⁻¹.

HRMS (ESI, *m/z*): calculated for [M + Na]⁺ C₁₄H₂₁BFN requires *m/z* 256.1643, found *m/z* 256.1644.

mp 51–52 °C.

1-((2-(4-Fluorophenyl)cyclopropyl)methyl)pyrrolidine borane (1k)



2-(4-Fluorophenyl)cyclopropane-1-carboxylic acid (457 mg, 2.5 mmol) was transformed to amine borane **1k** according to general procedure C. The desired product was obtained as a white solid in 89% yield (527 mg, 2.3 mmol).

¹H NMR (500 MHz, CDCl₃) δ 7.11 – 7.00 (m, 2H, ArH), 7.00 – 6.90 (m, 2H, ArH), 3.29 – 3.21 (m, 2H, H_{5,8}), 2.94 (dd, *J* = 12.8, 6.0 Hz, 1H, H₄), 2.90 – 2.79 (m, 2H, H_{5,8}), 2.74 (dd, *J* = 12.8, 7.4 Hz, 1H, H₄), 2.24 – 2.10 (m, 2H, H_{6,7}), 1.92 – 1.82 (m, 2H, H_{6,7}), 1.82 – 1.75 (m, 1H, H₁), 1.73 – 1.63 (m, 2H, H₂, H₉), 1.41 (br, 2H, H₉), 1.02 (dt, *J* = 8.7, 5.3 Hz, 1H, H₃), 0.86 (dt, *J* = 8.9, 5.5 Hz, 1H, H₃).

¹³C NMR (126 MHz, CDCl₃) δ 161.5, 137.2, 127.6 (2C), 115.3 (2C), 67.1, 60.9 (2C), 22.9 (2C), 22.8, 18.5, 14.5.

¹¹B NMR δ –11.7 ppm.

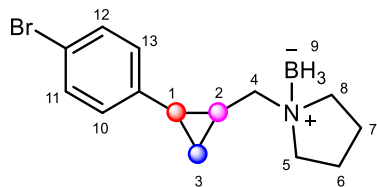
¹⁹F NMR δ –117.3 ppm.

IR (film) ν_{max}: 2960, 2371, 2274, 1603, 1510, 1215, 1162, 830, 540 cm⁻¹.

HRMS (ESI, *m/z*): calculated for [M + Na]⁺ C₁₄H₂₁BFN requires *m/z* 256.1643, found *m/z* 256.1641.

mp 59–60 °C.

1-((2-(4-Bromophenyl)cyclopropyl)methyl)pyrrolidine borane (1l)



2-(4-Bromophenyl)cyclopropane-1-carboxylic acid (384 mg, 1.7 mmol) was transformed to amine borane **11** according to general procedure C. The desired product was obtained as a white solid in 82% yield (408 mg, 1.4 mmol).

¹H NMR (500 MHz, CDCl₃) δ 7.38 (d, *J* = 8.4 Hz, 2H, ArH), 6.97 (d, *J* = 8.4 Hz, 2H, ArH), 3.30 – 3.19 (m, 2H, H_{5,8}), 2.94 (dd, *J* = 12.8, 5.9 Hz, 1H, H₄), 2.91 – 2.83 (m, 2H, H_{5,8}), 2.74 (dd, *J* = 12.8, 7.4 Hz, 1H, H₄), 2.25 – 2.16 (m, 2H, H_{6,7}), 1.97 – 1.83 (m, 2H, H_{6,7}), 1.81 – 1.73 (m, 1H, H₁), 1.70 (dd, *J* = 13.3, 7.3 Hz, 1H, H₂), 1.96 – 1.36 (br, 3H, H₉) 1.05 (dt, *J* = 8.8, 5.3 Hz, 1H, H₃), 0.90 (dt, *J* = 8.8, 5.5 Hz, 1H, H₃).

¹³C NMR (126 MHz, CDCl₃) δ 140.7, 131.6 (2C), 127.8 (2C), 119.7, 67.1, 60.9 (2C), 22.96 (2C), 22.9, 18.9, 14.8.

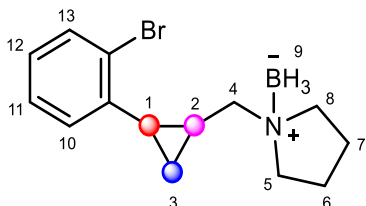
¹¹B NMR δ –11.7 ppm.

IR (film) ν_{max}: 2990, 2966, 2369, 2329, 2274, 1634, 1457, 1165, 1007cm⁻¹.

HRMS (ESI, *m/z*): calculated for [M + Na]⁺ C₁₄H₂₁BBrN requires *m/z* 316.08426, found *m/z* 316.08420.

mp 100–101 °C.

1-((2-(2-Bromophenyl)cyclopropyl)methyl)pyrrolidine borane (**1m**)



2-(2-Bromophenyl)cyclopropane-1-carboxylic acid (486 mg, 2.1 mmol) was transformed to amine borane **1m** according to general procedure C. The desired product was obtained as a white solid in 52% yield (324 mg, 1.1 mmol).

¹H NMR (500 MHz, CDCl₃) δ 7.53 (dd, J = 7.9, 1.2 Hz, 1H, ArH), 7.22 (td, J = 7.5, 0.9 Hz, 1H, ArH), 7.10 – 7.05 (m, 2H, ArH), 3.29 – 3.16 (m, 2H, H_{5,8}), 2.96 (dd, J = 12.7, 6.5 Hz, 1H, H₄), 2.95 – 2.86 (m, 3H, H_{5,8}, H₄), 2.23 – 2.12 (m, 2H, H_{6,7}), 2.08 – 1.99 (m, 1H, H₁), 1.94 – 1.83 (m, 3H, H_{6,7}, H₉), 1.87 – 1.79 (m, 2H, H₂, H₉), 1.64 – 1.42 (br, 1H, H₉), 1.04 (dt, J = 8.6, 5.4 Hz, 1H, H₃), 0.97 (dt, J = 8.9, 5.5 Hz, 1H, H₃).

¹³C NMR (126 MHz, CDCl₃) δ 140.5, 132.5, 127.68, 127.67, 127.01, 125.8, 66.9, 61.3, 60.5, 23.17, 22.9, 22.8, 17.84, 14.54.

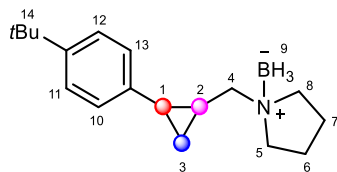
¹¹B NMR δ –11.8 ppm.

IR (film) ν_{max} : 3056, 2956, 2879, 2368, 2272, 1477, 1455, 1163, 1022, 747 cm⁻¹.

HRMS (ESI, m/z): calculated for [M + Na]⁺ C₁₄H₂₁BBrN requires m/z 316.0843, found m/z 316.0847.

mp 88–89 °C.

1-((2-(4-(*tert*-Butyl)phenyl)cyclopropyl)methyl)pyrrolidine borane (**1n**)



2-(4-(*tert*-Butyl)phenyl)cyclopropane-1-carboxylic acid (1.1 g, 5.1 mmol) was transformed to **1n** according to general procedure C. The desired product was obtained as a white solid in 87% yield (1.2 g, 4.4 mmol).

¹H NMR (400 MHz, CDCl₃) δ 7.29 (d, *J* = 8.3 Hz, 2H, ArH), 7.03 (d, *J* = 8.3 Hz, 2H, ArH), 3.28 – 3.19 (m, 2H, H_{5,8}), 2.99 – 2.82 (m, 3H, H_{5,8}, H₄), 2.77 (dd, *J* = 12.8, 7.1 Hz, 1H, H₄), 2.26 – 2.07 (m, 2H, H_{6,7}), 1.93 – 1.80 (m, 3H, H_{6,7}, H₉), 1.79 – 1.62 (m, 3H, H₁, H₂, H₉), 1.50 (br, 1H, H₉), 1.30 (s, 9H, H₁₄), 1.06 (dt, *J* = 8.6, 5.3 Hz, 1H, H₃), 0.86 (dt, *J* = 8.9, 5.4 Hz, 1H, H₃).

¹³C NMR (101 MHz, CDCl₃) δ 140.0, 138.5, 125.8 (2C), 125.5 (2C), 67.0, 60.9, 60.4, 34.5, 31.5 (3C), 23.0 (2C), 22.8, 18.3, 14.7.

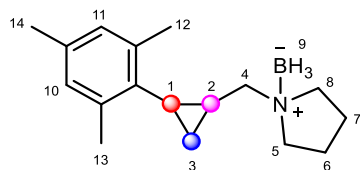
¹¹B NMR δ –11.6 ppm.

IR (film) ν_{max}: 2959, 2871, 2367, 2325, 2273, 1458, 1164, 826, 568 cm⁻¹.

HRMS (ESI, *m/z*): calculated for [M + Na]⁺ C₁₈H₃₀BN requires *m/z* 294.2364, found *m/z* 294.2375.

mp 57–58 °C.

1-((2-Mesitylcyclopropyl)methyl)pyrrolidine borane (**1o**)



2-Mesitylcyclopropane-1-carboxylic acid (850 mg, 4.2 mmol) was transformed to amine borane **1o** according to general procedure C. The desired product was obtained as a white solid in 51% yield (540 mg, 2.1 mmol).

¹H NMR (400 MHz, CDCl₃) δ 6.86 (s, 2H, ArH), 3.79 (d, J = 12.7 Hz, 1H, H₄), 3.38 – 3.14 (m, 2H, H_{5,8}), 3.05 – 2.83 (m, 2H, H_{5,8}), 2.38 (s, 6H, H_{12,13}), 2.28 (s, 3H, H₁₄), 2.26 – 2.18 (m, 4H, H_{5,7}, H₄, H₉), 1.93 (d, J = 3.3 Hz, 3H, H_{6,7}, H₉), 1.67 – 1.55 (m, 2H, H₁, H₉), 1.49 (dd, J = 13.9, 5.9 Hz, 1H, H₂), 1.16 – 1.05 (dt, J = 8.9, 5.0 Hz, 1H, H₃), 1.04 – 0.95 (m, 1H, H₃).

¹³C NMR (101 MHz, CDCl₃) δ 138.6 (2C), 136.1, 134.4, 128.9 (2C), 67.1, 61.9, 59.5, 23.3, 22.8, 20.9 (3C), 17.7, 17.1, 16.7.

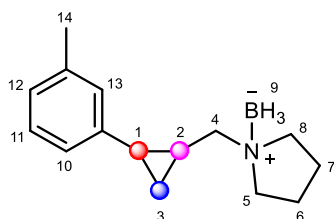
¹¹B NMR δ –11.6 ppm.

IR (film) ν_{max} : 2950, 2887, 2366, 2328, 1635, 1452, 1402, 1069, 579 cm⁻¹.

HRMS (ESI, m/z): calculated for [M + Na]⁺ C₁₇H₂₈BN requires m/z 280.2207, found m/z 280.2210.

mp 74–76 °C.

1-((2-(*m*-Tolyl)cyclopropyl)methyl)pyrrolidine borane (**1p**)



2-(*m*-Tolyl)cyclopropane-1-carboxylic acid (875 mg, 5.0 mmol) was transformed to amine borane **1p** according to general procedure C. The desired product was obtained as a pale-yellow viscous paste in 77% yield (877 mg, 3.8 mmol).

¹H NMR (500 MHz, CDCl₃) δ 7.16 (t, *J* = 7.8 Hz, 1H, ArH), 6.99 (d, *J* = 7.5 Hz, 1H, ArH), 6.93 – 6.86 (m, 2H, ArH), 3.33 – 3.12 (m, 2H, H_{5,8}), 2.98 – 2.82 (m, 3H, H_{5,8}, H₄), 2.78 (dd, *J* = 12.8, 7.0 Hz, 1H, H₄), 2.32 (s, 3H, H₁₄), 2.24 – 2.15 (m, 2H, H_{6,7}), 1.95 – 1.86 (m, 3H, H_{6,7}, H₉), 1.80 – 1.67 (m, 3H, H₁, H₂, H₉), 1.49 (br, 1H, H₉), 1.07 (dt, *J* = 8.6, 5.3 Hz, 1H, H₃), 0.88 (dt, *J* = 8.8, 5.5 Hz, 1H, H₃).

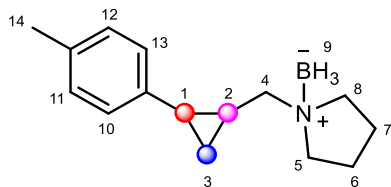
¹³C NMR (126 MHz, CDCl₃) δ 141.5, 138.1, 128.4, 126.8, 126.6, 123.0, 67.0, 60.8, 60.4, 23.1, 22.9 (2C), 21.5, 18.4, 14.8.

¹¹B NMR δ –11.6 ppm.

IR (film) ν_{max}: 2992, 2956, 2920, 2367, 2324, 2273, 1607, 1457, 1165, 776, 698 cm⁻¹

HRMS (ESI, *m/z*): calculated for [M + Na]⁺ C₁₅H₂₄BN requires *m/z* 252.1894, found *m/z* 252.1906.

1-((2-(*p*-Tolyl)cyclopropyl)methyl)pyrrolidine borane (**1q**)



2-(*p*-Tolyl)cyclopropane-1-carboxylic acid (1.31 g, 7.4 mmol) was transformed to amine borane **1q** according to general procedure C. The desired product was obtained as a white solid in 82% yield (1.6 g, 6.9 mmol).

¹H NMR (500 MHz, CDCl₃) δ 7.08 (d, *J* = 8.0 Hz, 2H, ArH), 7.00 (d, *J* = 8.1 Hz, 2H, ArH), 3.26 – 3.15 (m, 2H, H_{5,8}), 2.96 (dd, *J* = 12.9, 6.0 Hz, 1H, H₄), 2.92 – 2.83 (m, 2H, H_{5,8}), 2.76 (dd, *J* = 12.8, 7.3 Hz, 1H, H₄), 2.31 (s, 3H, H₁₄), 2.22 – 2.10 (m, 2H, H_{6,7}), 1.92 – 1.81 (m, 3H, H_{6,7}, H₉), 1.78 – 1.73 (m, 2H, H₁, H₉), 1.70 – 1.61 (m, 1H, H₂), 1.52 (br, 1H, H₉), 1.04 (dt, *J* = 8.6, 5.3 Hz, 1H, H₃), 0.86 (dt, *J* = 8.9, 5.4 Hz, 1H, H₃).

¹³C NMR (126 MHz, CDCl₃) δ 138.5, 135.6, 129.2 (2C), 125.9 (2C), 67.0, 60.9, 60.4, 23.0, 22.9 (2C), 21.1, 18.3, 14.5.

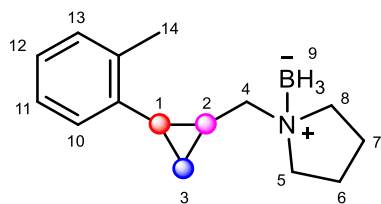
¹¹B NMR δ –11.6 ppm.

IR (film) ν_{max}: 2948, 2326, 2271, 1516, 1457, 1175, 1163, 815, 780 cm⁻¹.

HRMS (ESI, *m/z*): calculated for [M + Na]⁺ C₁₅H₂₄BN requires *m/z* 252.1894, found *m/z* 252.1899.

mp 75–76 °C.

1-((2-(*o*-Tolyl)cyclopropyl)methyl)pyrrolidine borane (**1r**)



2-(*o*-Tolyl)cyclopropane-1-carboxylic acid (576 mg, 3.3 mmol) to amine borane **1r** according to general procedure C. The desired product was obtained as a white solid in 95% yield (1.4 g, 6.2 mmol).

¹H NMR (400 MHz, CDCl₃) δ 7.17 – 7.03 (m, 4H, ArH), 3.32 – 3.16 (m, 2H, H_{5,8}), 3.04 – 2.81 (m, 4H, H₄, H_{5,8}), 2.39 (s, 3H, H₁₄), 2.27 – 2.10 (m, 3H, H_{6,7}, H₉), 1.98 – 1.71 (m, 5H, H₁, H₂, H_{6,7}, H₉), 1.60 (br, 1H, H₉) 1.06 – 0.81 (m, 2H, H₃).

¹³C NMR (101MHz, CDCl₃) δ 139.3, 137.6, 129.9, 126.3, 126.2, 125.9, 67.2, 61.0, 60.6, 23.0, 22.9, 20.7, 19.4, 16.0, 14.1.

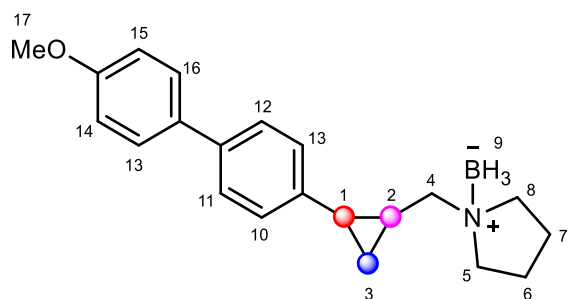
¹¹B NMR δ –11.6 ppm.

IR (film) ν_{max}: 2955, 2368, 2325, 2274, 1493, 1458, 1165, 1109, 757, 732 cm⁻¹.

HRMS (ESI, m/z): calculated for [M + Na]⁺ C₁₅H₂₄BN requires m/z 252.1894, found m/z 252.1903.

mp 56–57 °C.

1-((2-(4'-Methoxy-[1,1'-biphenyl]-4-yl)cyclopropyl)methyl)pyrrolidine borane (1s)



The title compound was prepared in a 3-step procedure from (2-(4-bromophenyl)cyclopropyl)methanol.

Step 1. A solution of Pd(OAc)₂ (15.0 mg, 0.07 mmol) and PPh₃ (88.1 mg, 0.33 mmol) in EtOH (5 mL) and toluene (5 mL) was stirred at room temperature for 10 min under a nitrogen atmosphere. After 10 min, (2-(4-Bromophenyl)cyclopropyl)methanol (500 mg, 2.2 mmol) was added followed by a sequential addition of a 2 M aq. solution of sodium carbonate (5 mL, 9.78 mmol), and commercially available 4-methoxyphenylboronic acid (535 mg, 3.52 mmol). The resulting mixture was heated at 100 °C in a sealed vial for 16 h. The reaction mixture was then cooled to room temperature and diluted with water. The organic layer was separated, and the aqueous layer was extracted with EtOAc (3 x 5 mL). The combined organic layers were washed with brine (10 mL), dried over anhydrous Na₂SO₄, filtered and concentrated under reduced pressure. Purification by silica gel chromatography (1:4 EtOAc/hexanes) provided (2-(4'-methoxy-[1,1'-biphenyl]-4-yl)cyclopropyl)methanol in 80% yield (448 mg, 1.8 mmol).

Step 2. The cyclopropanemethanol was converted to the pyrrolidine derivative by a Mitsunobu reaction.² Procedure: To a flame dried 10 mL flask equipped with a stir bar and a septum was added pyrrolidine (147 μL, 1.76 mmol) and CH₂Cl₂ (1.80 mL) followed by the addition of triphenylphosphine (700 mg, 2.64 mmol) and (2-(4'-methoxy-[1,1'-biphenyl]-4-yl)cyclopropyl)methanol (448 mg, 1.8 mmol). The mixture was stirred and DIAD (347 μL, 1.76

mmol) was added slowly at 0 °C. Once the addition was complete, the mixture was stirred for 18 h at room temperature. The solvent was evaporated and the residue was subjected to flash chromatography (4:6 EtOAc/hexanes) to obtain 1-((2-(4'-methoxy-[1,1'-biphenyl]-4-yl)cyclopropyl)methyl)pyrrolidine in 80% yield (433 mg, 1.41 mmol).

Step 3. 1-((2-(4'-methoxy-[1,1'-biphenyl]-4-yl)cyclopropyl)methyl)pyrrolidine was transformed to amine-borane **1s** according to a literature protocol by Ramachandran and co-workers.³ Procedure: NaBH₄ (107 mg, 2.82 mmol) and NaHCO₃ (473 mg, 5.63 mmol) were transferred to a microwave vial containing a stir bar. The previously obtained 1-((2-(4'-methoxy-[1,1'-biphenyl]-4-yl)cyclopropyl)methyl)pyrrolidine (433 mg, 1.41 mmol) was added to the reaction flask followed by the addition of THF (2.1 mL). A 14.4% v/v solution of water in THF (704 μL) was added dropwise to prevent excessive frothing. The mixture was stirred for 4 h at room temperature. The reaction contents were then filtered through a short pad of sodium sulfate and celite and the solid residue was washed with THF. The filtrate was evaporated, and the residue was purified by flash chromatography (1:4 EtOAc/hexanes) to obtain the pure product **1s** in 16% yield (72.4 mg, 0.23 mmol).

¹H NMR (400 MHz, CDCl₃) δ 7.51 (d, *J* = 8.7 Hz, 2H, ArH), 7.47 (d, *J* = 8.2 Hz, 2H, ArH), 7.15 (d, *J* = 8.2 Hz, 2H, ArH), 6.98 (d, *J* = 8.7 Hz, 2H, ArH), 3.85 (s, 3H, H₁₇), 3.23 (dd, *J* = 6.3, 3.5 Hz, 2H, H_{5,8}), 2.97 (dd, *J* = 12.8, 6.2 Hz, 1H, H₄), 2.95 – 2.83 (m, 2H, H_{5,8}), 2.78 (dd, *J* = 12.8, 7.2 Hz, 1H, H₄), 2.24 – 2.12 (m, 2H, H_{6,7}), 1.93 – 1.80 (m, 4H, H_{6,7}, H₉, H₁), 1.79 – 1.71 (m, 2H, H₂, H₉), 1.56 (br, 1H, H₉), 1.11 (dt, *J* = 8.7, 5.3 Hz, 1H, H₃), 0.92 (dt, *J* = 8.9, 5.4 Hz, 1H, H₃).

¹³C NMR (101 MHz, CDCl₃) δ 159.1, 140.1, 138.6, 133.5, 128.0 (2C), 126.8 (2C), 126.4 (2C), 114.3 (2C), 67.0, 60.9, 60.5, 55.4, 22.9 (2C), 22.8, 18.6, 14.7

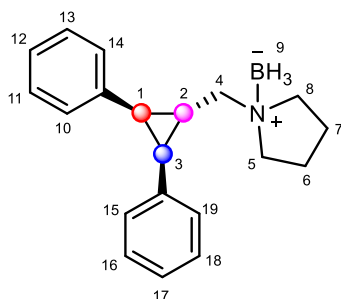
¹¹B NMR δ –11.6 ppm.

IR (film) ν_{max} : 3269, 2917, 2838, 1495, 1431, 1242, 1171, 1016, 806 cm^{-1} .

HRMS (ESI, m/z): calculated for $[\text{M} - 2\text{H}]^+ \text{C}_{21}\text{H}_{26}\text{BNO}$ requires m/z 320.2189, found m/z 320.2180.

mp 151 $^{\circ}\text{C}$.

1-(((1*R*,2*R*,3*S*)-2,3-diphenylcyclopropyl)methyl)pyrrolidine borane (1t**)**



(((1*R*,2*R*,3*S*)-2,3-Diphenylcyclopropyl)methanol (383 mg, 1.6 mmol) was transformed to the amine borane **1t** according to general procedure C. The title compound was obtained as a colorless white solid in 67% yield (314 mg, 1.1 mmol).

^1H NMR (400 MHz, CDCl_3) δ 7.18 – 7.04 (m, 6H, ArH), 7.03 – 6.99 (m, 4H, ArH), 3.37 – 3.27 (m, 2H, $\text{H}_{5,8}$), 3.04 (d, $J = 6.5$ Hz, 2H, H_4), 2.90 (dd, $J = 10.6, 6.1$ Hz, 2H, $\text{H}_{5,8}$), 2.65 – 2.57 (m, 1H, H_2), 2.36 (d, $J = 5.7$ Hz, 2H, $\text{H}_{1,3}$), 2.28 – 2.14 (m, 2H, $\text{H}_{6,7}$), 2.04 (br, 1H, H_9), 1.95 – 1.85 (m, 3H, $\text{H}_{6,7, \text{H}_9}$), 1.78 (br, 1H, H_9).

^{13}C NMR (101 MHz, CDCl_3) δ 136.7 (2C), 129.0 (4C), 128.2 (4C), 126.2 (2C), 67.3, 61.3 (2C), 31.0 (2C), 22.8 (2C), 20.8.

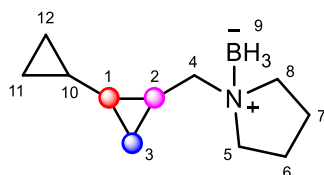
^{11}B NMR δ –12.0 ppm.

IR (film) ν_{max} : 2957, 2379, 2327, 2275, 1601, 1455, 1185, 751, 730 cm^{-1} .

HRMS (ESI, m/z): calculated for $[M - 3H]^+ C_{20}H_{23}N$ requires m/z 278.1912, found m/z 278.1903.

mp 155.3–156.0 °C.

1-([1,1'-Bi(cyclopropan)]-2-ylmethyl)pyrrolidine borane (**1u**)



[1,1'-Bi(cyclopropane)]-2-carboxylic acid (316 mg, 2.5 mmol) was transformed to amine borane **1u** according to general procedure C. The desired product was obtained as a clear oil in 78% yield (347 mg, 1.9 mmol).

1H NMR (500 MHz, $CDCl_3$) δ 3.20 – 3.10 (m, 2H, $H_{5,8}$), 2.86 (dd, $J = 11.3, 5.4$ Hz, 2H, $H_{5,8}$), 2.77 (dd, $J = 12.8, 6.1$ Hz, 1H, H_4), 2.55 (dd, $J = 12.8, 7.5$ Hz, 1H, H_4), 2.22 – 2.09 (m, 2H, $H_{6,7}$), 1.92 – 1.79 (m, 3H, $H_{6,7}, H_9$), 1.72 (br, 1H, H_9), 1.51 (br, 1H, H_9), 1.18 – 1.08 (m, 1H, H_2), 0.85 – 0.78 (m, 1H, H_{10}), 0.71 – 0.65 (m, 1H, H_1), 0.43 – 0.38 (m, 2H, $H_{11,12}$), 0.38 – 0.31 (m, 1H, H_3), 0.23 (dt, $J = 8.7, 5.1$ Hz, 1H, H_3), 0.07 (q, $J = 4.7$ Hz, 2H, $H_{11,12}$).

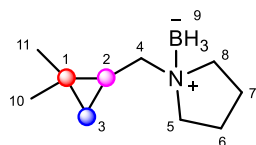
^{13}C NMR (126 MHz, $CDCl_3$) δ 67.0, 60.7, 60.3, 22.9 (2C), 20.6, 12.9, 11.8, 9.0, 3.3, 2.7.

^{11}B NMR δ –11.8 ppm.

IR (film) ν_{max} : 2995, 2957, 2880, 2364, 2325, 2273, 1475, 1165, 1017 cm^{-1} .

HRMS (ESI, m/z): calculated for $[M + Na]^+ C_{11}H_{22}BN$ requires m/z 202.1738, found m/z 202.1738.

1-((2,2-Dimethylcyclopropyl)methyl)pyrrolidine borane (**1v**)



2,2-Dimethylcyclopropane-1-carboxylic acid (1.3 g, 11.3 mmol) was transformed to amine borane **1v** according to general procedure C. The desired product was obtained as a clear oil in 81% yield (1.5 g, 9.2 mmol).

¹H NMR (500 MHz, CDCl₃) δ 3.17 – 3.11 (m, 2H, **H_{5,8}**), 2.96 (dd, $J = 13.0, 6.3$ Hz, 1H, **H₄**), 2.92 – 2.75 (m, 2H, **H_{5,8}**), 2.69 (dd, $J = 13.0, 7.0$ Hz, 1H, **H₄**), 2.24 – 2.06 (m, 2H, **H_{6,7}**), 1.94 – 1.77 (m, 3H, **H_{6,7, H₉}**), 1.74 (br, 1H, **H₉**), 1.44 (br, 1H, **H₉**), 1.11 – 1.05 (m, 1H, **H₂**), 1.07 (s, 3H, **H₁₁**), 1.03 (s, 3H, **H₁₀**), 0.60 (dd, $J = 8.7, 4.5$ Hz, 1H, **H₃**), 0.07 (t, $J = 5.1$ Hz, 1H, **H₃**).

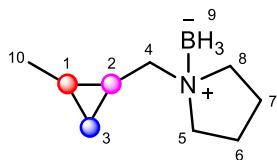
¹³C NMR (126 MHz, CDCl₃) δ 63.3, 60.6, 59.7, 27.0, 23.2 (2C), 20.3, 19.6, 19.5, 16.0.

¹¹B NMR δ –11.5 ppm.

IR (film) ν_{max} : 2947, 2882, 2366, 2325, 2275, 1457, 1168, 1095, 875 cm⁻¹.

HRMS (ESI, m/z): calculated for $[M + \text{Na}]^+$ C₁₀H₂₂BN requires m/z 190.1738, found m/z 190.1737.

1-((2-Methylcyclopropyl)methyl)pyrrolidine borane (**1w**)



2-Methylcyclopropane-1-carboxylic acid (1.4 g, 14.0 mmol) was transformed to amine borane **1w** according to general procedure C. The desired product was obtained as a clear oil in 78% yield (1.7 g, 10.8 mmol).

¹H NMR (500 MHz, CDCl₃) δ 3.26 – 3.09 (m, 2H, **H**_{5,8}), 2.91 – 2.86 (m, 2H, **H**_{5,8}), 2.80 (dd, *J* = 12.8, 6.0 Hz, 1H, **H**₄), 2.57 (dd, *J* = 12.8, 7.6 Hz, 1H, **H**₄), 2.17 (ddd, *J* = 7.5, 4.7, 2.3 Hz, 2H, **H**_{6,7}), 1.95 – 1.80 (m, 3H, **H**_{6,7}, **H**₉), 1.80 – 1.67 (br, 1H, **H**₉), 1.49 (br, H, **H**₉), 1.08 (d, *J* = 6.0 Hz, 3H, **H**₁₀), 1.05 – 0.95 (m, 1H, **H**₂), 0.60 (dd, *J* = 8.1, 5.5 Hz, 1H, **H**₁), 0.41– 0.33 (m, 2H, **H**₃).

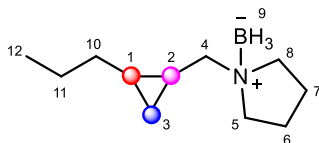
¹³C NMR (126 MHz, CDCl₃) δ 67.3, 60.5 (2C), 23.1 (2C), 18.3, 15.3, 13.2, 12.2.

¹¹B NMR δ –11.7 ppm.

IR (film) *v*_{max}: 2953, 2366, 2273, 1456, 1165, 1079, 1037, 882 cm⁻¹.

HRMS (ESI, *m/z*): calculated for [M + Na]⁺ C₉H₂₀BN requires *m/z* 176.1581, found *m/z* 176.1575.

1-((2-Propylcyclopropyl)methyl)pyrrolidine borane (**1x**)



(1*S*,2*S*)-2-Ethylcyclopropane-1-carboxylic acid (1.3 g, 11.3 mmol) was transformed to amine borane **1x** according to general procedure C. The desired product was obtained as a clear oil in 93% yield (1.9 g, 11.3 mmol).

¹H NMR (500 MHz, CDCl₃) δ 3.18 – 3.07 (m, 2H, **H**_{5,8}), 2.91 – 2.78 (m, 2H, **H**_{5,8}), 2.70 (dd, *J* = 12.8, 6.5 Hz, 1H, **H**₄), 2.61 (dd, *J* = 12.8, 7.0 Hz, 1H, **H**₄), 2.19 – 2.12 (m, 2H, **H**_{6,7}), 2.03 – 1.77 (m, 3H, **H**_{6,7}, **H**₉), 1.62 (br, 1H, **H**₉), 1.43 – 1.32 (m, 3H, **H**₉, **H**₁₁), 1.30 (dd, *J* = 9.2, 6.9 Hz, 1H, **H**₁₀), 1.20 – 1.12 (m, 1H, **H**₁₀), 1.08 (dd, *J* = 14.9, 11.1 Hz, 1H, **H**₂), 0.87 (t, *J* = 7.2 Hz, 3H, **H**₁₂), 0.61 – 0.55 (m, 1H, **H**₁), 0.37 (dt, *J* = 8.3, 5.0 Hz, 1H, **H**₃), 0.34 – 0.25 (dt, *J* = 8.3, 5.0 Hz, 1H, **H**₃).

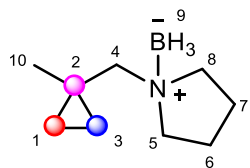
¹³C NMR (126 MHz, CDCl₃) δ 67.2, 60.5, 60.3, 35.7, 22.9 (2C), 22.5, 18.4, 14.1, 14.0, 11.2.

¹¹B NMR δ –11.8 ppm.

IR (film) ν_{max} : 2956, 2922, 2872, 2369, 2325, 2273, 1458, 1166, 1094, 1030, 875 cm⁻¹.

HRMS (ESI, *m/z*): calculated for [M – 2H]⁺ C₁₁H₂₂BN requires *m/z* 180.1918, found *m/z* 180.1920.

1-((1-Methylcyclopropyl)methyl)pyrrolidine borane (1y)



1-Methylcyclopropane-1-carboxylic acid (680 mg, 6.8 mmol) was transformed to amine borane **1aa** according to general procedure C. The desired product was obtained as a white solid in 64% yield (666 mg, 4.4 mmol).

¹H NMR (500 MHz, CDCl₃) δ 3.27 – 3.10 (m, 2H, **H_{5,8}**), 2.95 – 2.84 (m, 2H, **H_{5,8}**), 2.78 (s, 2H, **H₄**), 2.27 – 2.21 (m, 2H, **H_{6,7}**), 1.94 – 1.81 (m, 3H, **H_{6,7}**, **H₉**), 1.81 – 1.64 (br, 1H, **H₉**), 1.57 – 1.40 (br, 1H, **H₉**), 1.23 (s, 3H, **H₁₀**), 0.57 (t, *J* = 5.3 Hz, 2H, **H_{1,3}**), 0.42 (t, *J* = 5.4 Hz, 2H, **H_{1,3}**).

¹³C NMR (126 MHz, CDCl₃) δ 72.3, 61.2 (2C), 24.1, 23.1 (2C), 14.6 (2C), 13.9.

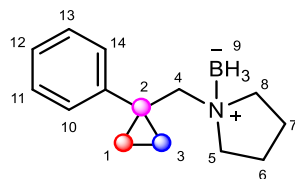
¹¹B NMR δ –11.1 ppm.

IR (film) ν_{max} : 2958, 2928, 2879, 2363, 2330, 2280, 1062, 1166, 1104, 1042, 513 cm⁻¹.

HRMS (ESI, *m/z*): calculated for [M + Na]⁺ C₉H₂₀BN requires *m/z* 176.1581, found *m/z* 176.1587.

mp 45–46 °C.

1-((1-Phenylcyclopropyl)methyl)pyrrolidine borane (**1z**)



1-Phenylcyclopropane-1-carboxylic acid was prepared according to literature.⁴ 1-Phenylcyclopropane-1-carboxylic acid (575 mg, 3.5 mmol) was transformed to amine borane **1z** according to general procedure C. The desired product was obtained as a white solid in 88% yield (671 mg, 3.1 mmol).

¹H NMR (500 MHz, CDCl₃) δ 7.46 (dd, J = 8.2, 1.2 Hz, 2H, ArH), 7.29 (t, J = 7.6 Hz, 2H, ArH), 7.23 – 7.17 (tt, J = 7.5, 1.3 Hz, 1H, ArH), 3.18 (s, 2H, H₄), 2.88 – 2.78 (m, 2H, H_{5,8}), 2.59 – 2.43 (m, 2H, H_{5,8}), 2.11 – 1.98 (m, 2H, H_{6,7}), 1.80 (br, 1H, H₉), 1.69 – 1.58 (m, 3H, H_{6,7}, H₉), 1.41 (br, 1H, H₉), 1.08 – 0.99 (m, 4H, H_{1,3}).

¹³C NMR (126 MHz, CDCl₃) δ 143.5, 129.9 (2C), 128.6 (2C), 127.0, 72.1, 60.6 (2C), 23.3, 22.7 (2C), 14.2 (2C).

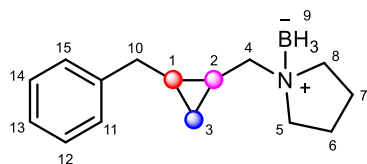
¹¹B NMR δ –11.2 ppm.

IR (film) ν_{max} : 2956, 2879, 2372, 2327, 2276, 1601, 1457, 1163, 1095, 1025, 701 cm⁻¹.

HRMS (ESI, m/z): calculated for [M + Na]⁺ C₁₄H₂₂BN requires m/z 238.1738, found m/z 238.1731;

mp 67–68 °C.

1-((2-Benzylcyclopropyl)methyl)pyrrolidine borane (**1aa**)



2-Benzylcyclopropane-1-carboxylic acid (760 mg, 4.3 mmol) was transformed to amine borane **1y** according to general procedure C. The desired product was obtained as a viscous oil in 63% yield (616 mg, 2.7 mmol).

¹H NMR (400 MHz, CDCl₃) δ 7.28 – 7.22 (m, 2H, ArH), 7.19 (tt, J = 7.1, 1.3 Hz, 1H, ArH), 7.07 (d, J = 7.3 Hz, 2H, ArH), 3.23 (dd, J = 8.9, 3.9 Hz, 2H, H_{5,8}), 2.99 – 2.88 (m, 2H, H₁₀), 2.83 – 2.62 (m, 2H, H_{5,8}), 2.21– 2.15 (m, 2H, H_{6,7}), 1.96 – 1.85 (m, 5H, H₁, H_{6,7}, H₄), 1.83 – 1.70 (m, 2H, H₂, H₉), 1.50 (br, 2H, H₉), 0.97 – 0.92 (m, 1H, H₃), 0.87 – 0.82 (m, 1H, H₃).

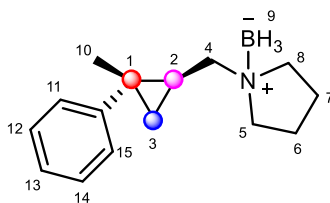
¹³C NMR (126 MHz, CDCl₃) δ 143.2, 128.5 (2C), 125.7 (2C), 125.6, 63.9, 61.6, 61.5, 30.3, 23.2, 22.9 (2C), 21.3, 16.0.

¹¹B NMR δ –12.4 ppm.

IR (film) ν_{max} : 3025, 2368, 2324, 2272, 1603, 1496, 1458, 1166, 1109, 754, 698 cm⁻¹.

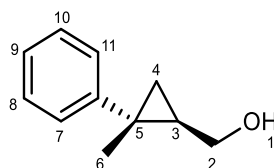
HRMS (ESI, m/z): calculated for [M + Na]⁺ C₁₅H₂₄BN requires m/z 252.1894, found m/z 252.1897.

1-(((1*S*,2*S*)-2-Methyl-2-phenylcyclopropyl)methyl)pyrrolidine borane (**1ab**)



Synthesis of Enantioenriched Cyclopropylmethanol Derivative

(((1*S*,2*S*)-2-Methyl-2-phenylcyclopropyl)methanol (**S1**))



S1 was synthesized using the enantioselective Charette cyclopropanation method from (*E*)-3-phenylbut-2-en-1-ol.¹ To a round bottom flask was added CH₂Cl₂ (22.6 mL) and DME (1.6 mL) followed by the addition of Et₂Zn (1.7 mL, 16.7 mmol). The reaction mixture was cooled to –12 °C and diiodomethane (1.4 mL, 16.7 mmol) was added dropwise over a period of 5 min while maintaining the internal temperature between –12 °C to –8 °C. The reaction mixture was stirred for 10 min and dioxaborolane (2.5 g, 9.2 mmol) in CH₂Cl₂ (11.3 mL) was cannulated into the reaction flask followed by the addition of (*E*)-3-phenylbut-2-en-1-ol (1.13 g, 7.6 mmol) in CH₂Cl₂ (11.3 mL) with an internal temperature of –5 °C over a period of 5 min. The mixture was allowed to warm to room temperature and stirred for 12 h. The reaction mixture was quenched with a dropwise addition of NH₄Cl (5 mL), transferred to a separatory funnel, and the organic layer was separated. The aqueous layer was extracted with EtOAc (3 x 25 mL) and the organic layers were combined. The combined organic layers were transferred into an Erlenmeyer flask, and a solution containing 2 N aq. NaOH (32 mL) and 30% aq. H₂O₂ (6 mL) was added in one portion. The resulting biphasic solution was stirred vigorously for 10 min, after which the mixture was transferred into a separatory funnel and the organic layer was separated. The aqueous layer was extracted with

EtOAc (3 × 10 mL) and the combined organic layers were washed with 10% aq. HCl (10 mL) and successively washed with sat. aq. Na₂SO₃ (10 mL), sat. aq. NaHCO₃ (10 mL), and brine (10 mL), dried over anhydrous Na₂SO₄, filtered, and concentrated under reduced pressure. The residue was purified by silica gel chromatography (1:4 EtOAc/hexanes) to give the title compound **S1** as a white solid in 42% yield (520 mg, 3.2 mmol, 89% ee) and was identical to reported literature data.⁵ A chiral prep purification provided the enantioenriched **S1** with 99% ee.

¹H NMR (500 MHz, CDCl₃) δ 7.31 – 7.25 (m, 4H, **H_{Ar}**), 7.24 – 7.12 (m, 1H, **H₉**), 3.91 (dd, *J* = 11.5, 6.4 Hz, 1H, **H₂**), 3.71 (dd, *J* = 11.5, 8.6 Hz, 1H, **H₂**), 1.49 (br, 1H, **H₁**), 1.46 (s, 3H, **H₆**), 1.45 – 1.39 (m, 1H, **H₃**), 1.14 (dd, *J* = 8.9, 4.8 Hz, 1H, **H₄**), 0.60 (t, *J* = 5.3, Hz, 1H, **H₄**).

¹³C NMR (126 MHz, CDCl₃) δ 147.7, 128.5 (2C), 127.4 (2C), 126.0, 63.7, 27.9, 25.0, 20.6, 18.8.

IR (film) ν_{max} : 3339, 3060, 2954, 2865, 1496, 1025, 762, 698, 578 cm⁻¹.

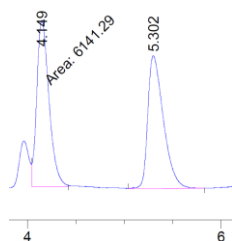
HRMS (ESI, *m/z*): calculated for [M + Na]⁺ : C₁₁H₁₄O requires *m/z* 185.0937, found *m/z* 185.0939.

mp 45–46 °C.

[α]_D²⁵ = +38 (c 0.20, MeOH).

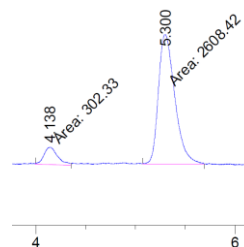
SFC (Chiralpak OJ-H 21 x 250 mm, 5 μ m, 30 °C, 150 bar, 6% of co-solvent of 20% IPA/hexanes, 60 g/min) *t_R* major: 5.30 min. *t_R* minor: 4.15 min.

Racemic mixture



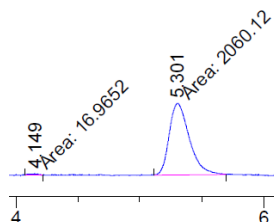
Peak #	RetTime [min]	Type	Width [min]	Area [mAU*s]	Height [mAU]	Area %
1	4.149	MM	0.1459	6141.29297	701.72998	49.6074
2	5.302	BB	0.1722	6238.50879	558.86127	50.3926

S1, 90% ee



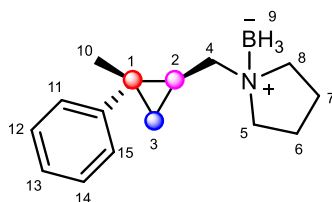
Peak #	RetTime [min]	Type	Width [min]	Area [mAU*s]	Height [mAU]	Area %
1	4.138	MM	0.1604	302.32965	31.41856	10.3866
2	5.300	MM	0.1895	2608.42432	229.37376	89.6134

S1 (after chiral purification), 99% ee



Peak #	RetTime [min]	Type	Width [min]	Area [mAU*s]	Height [mAU]	Area %
1	4.149	MM	0.0785	16.96516	3.60287	0.8168
2	5.301	MM	0.1879	2060.11670	182.74319	99.1832

1-(((1*S*,2*S*)-2-Methyl-2-phenylcyclopropyl)methyl)pyrrolidine borane (1ab**):**



Enantiopure **S1** was converted to the corresponding carboxylic acid using general procedure B. Crude (1*S*,2*S*)-2-methyl-2-phenylcyclopropane-1-carboxylic acid (520 mg, 3.2 mmol) was then converted to obtain **1ab** as described in general procedure C. Purification by column chromatography provided the product as a white solid in 50% yield (175 mg, 1.54 mmol).

¹H NMR (500 MHz, CDCl₃) δ 7.33 – 7.30 (m, 2H, ArH), 7.29 (d, *J* = 1.1 Hz, 2H, ArH), 7.20 – 7.16 (m, 1H, ArH), 3.28 – 3.21 (m, 2H, H_{5,8}), 3.19 (dd, *J* = 13.0, 6.0 Hz, 1H, H₄), 2.93 – 2.91 (m, 3H, H_{5,8}, H₄), 2.24 – 2.11 (m, 2H, H_{6,7}), 1.95 – 1.78 (m, 4H, H_{6,7}, H₉), 1.68 – 1.58 (m, 2H, H₂, H₉), 1.46 – 1.35 (s, 3H, H₁₀), 1.27 (dd, *J* = 9.0, 4.9 Hz, 1H, H₃), 0.62 – 0.44 (t, *J* = 5.5 Hz 1H, H₃).

¹³C NMR (126 MHz, CDCl₃) δ 141.1, 128.6 (2C), 127.2 (2C), 126.2, 63.3, 60.8, 60.3, 24.6, 23.3, 23.2, 21.1, 20.9, 20.4.

¹¹B NMR δ –11.4 ppm.

IR (film) ν_{max}: 3359, 2961, 2387, 1981, 1604, 1493, 1460, 1165, 760, 698 cm⁻¹.

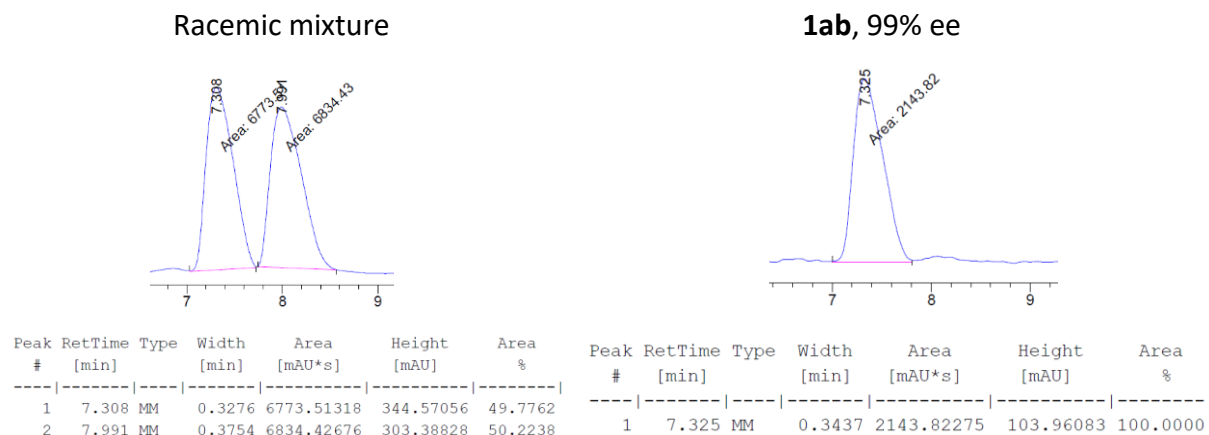
HRMS (ESI, *m/z*): calculated for [M + H]⁺ C₁₅H₂₄BN requires *m/z* 228.1918, found *m/z* 228.1918.

mp 45–46 °C.

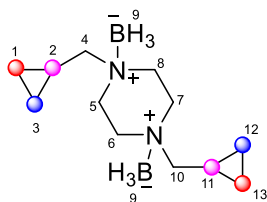
$[\alpha]_D^{25} = +12$ (c 0.20, MeOH).

SFC (Chiralpak OJ-H 21mm x 250 mm, 5 μ m, 30 $^{\circ}$ C, 150 bar, 95% CO₂; 5% Modifier (IPA), 60 g/min)

trmajor: 7.31 min. trminor: 7.9 min.



1,4-Bis(cyclopropylmethyl)piperazine borane (**1ac**)



A solution of cyclopropanecarbonyl chloride (1.04 mL, 11.5 mmol) in CH₂Cl₂ (2.75 mL) was added dropwise to a solution of piperazine (494 mg, 5.74 mmol) in CH₂Cl₂ (4 mL) at 0 $^{\circ}$ C over 10 min (exothermic reaction!). After stirring for 20 min, 10 mL of 10% aq. NaOH solution was added, and the organic layer was separated. The aqueous layer was extracted with CH₂Cl₂ (2 x 10 mL), and the combined organic layers were dried over anhydrous Na₂SO₄, filtered, and concentrated under reduced pressure. The crude amide was converted to **1ac** using general procedure C to obtain the title compound as a viscous oil in 76% yield (968 mg, 4.4 mmol).

¹H NMR (500 MHz, CDCl₃) δ 3.77 – 3.59 (m, 4H, H_{5,6,7,8}), 2.96 – 2.86 (m, 4H, H_{5,6,7,8}), 2.81 (d, *J* = 6.9 Hz, 4H, H_{4,10}), 2.04 – 1.47 (m, 5H, H₉), 1.48 – 1.38 (m, 3H, H₂, H₉, H₁₁), 0.75 – 0.67 (m, 4H, H_{1,3}, H_{12,13}), 0.34 – 0.23 (m, 4H, H_{1,3}, H_{12,13}).

¹³C NMR (126 MHz, CDCl₃) δ 72.04 (2C), 52.42 (4C), 4.81 (2C), 4.60 (4C).

¹¹B NMR δ -14.0 ppm

IR: 3001, 2357, 2333, 2280, 1347, 1416, 1155, 1124, 1027, 976, 889 cm⁻¹.

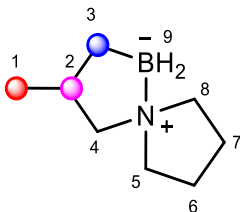
HRMS (ESI, m/z): calculated for [M - 6H]⁺ C₁₂H₂₂N₂ requires *m/z* 195.1856, found *m/z* 195.1861.

Transformation of CABs to SCABs

General Procedure D: (2a–2ac): Into a microwave vial was added amine-borane (~0.2 mmol) followed by bis(trifluoromethanesulfonimide) (5 mol%). Toluene (0.4 M) was added and the formation of H₂ was observed. The reaction mixture was stirred for 10 min until no bubbles were observed. The vial was then sealed and heated at 125 °C (oil bath) for the indicated time. The reaction mixture was quenched by adding (nBu)₄NBH₄ (5 mol%) under an argon atmosphere. The mixture was diluted with CH₂Cl₂, and filtered through a short plug of silica, eluting with CH₂Cl₂. The products were isolated by concentrating the solution.



3-Methyl-5-aza-1-borasp[iro[4.4]nonane (2a)



The title compound was obtained in 99% yield (2.0 g, 14.4 mmol) as a clear oil. Reaction time: 4.5 h.

¹H NMR (400 MHz, CDCl₃) δ 3.26 – 3.17 (m, 2H, **H_{5,8}**), 2.83 – 2.72 (m, 2H, **H_{5,8}**), 2.64 – 2.52 (m, 2H, **H₄**), 2.25 – 2.00 (m, 4H, **H₂, H_{6,7}, H₉**), 1.99 – 1.78 (m, 3H, **H_{6,7}, H₉**), 1.04 (d, *J* = 6.7 Hz, 3H, **H₁**) 1.11 – 0.96 (m, 1H, **H₃**), 0.48 – 0.37 (m, 1H, **H₃**).

¹³C NMR (126 MHz, CDCl₃) δ 70.0, 61.6, 60.4, 53.6, 33.0, 22.9, 22.6, 21.2.

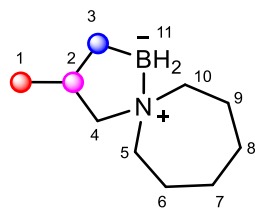
¹¹B NMR δ –3.6 ppm.

IR (film) ν_{max} : 2952, 2868, 2780, 1456, 1361, 1208, 1153, 835, 607 cm⁻¹.

HRMS (ESI, *m/z*): calculated for [M + H]⁺ C₈H₁₈BNO₂ requires *m/z* 172.1503, found *m/z* 172.1498.

Note: The mass of the spirocycles is often reported as the corresponding boronic acid derivative due to mass spectrometer conditions

3-Methyl-5-aza-1-borasp[iro[4.6]undecane (2b)



The title compound was obtained in 99% yield (30 mg, 0.18 mmol) a clear oil. Reaction time: 4.5 h.

¹H NMR (500 MHz, CDCl₃) δ 3.19 – 3.09 (m, 2H, **H_{5,10}**), 2.98 – 2.92 (m, 1H, **H₄**), 2.90 – 2.84 (m, 1H, **H₅**), 2.82 – 2.75 (m, 1H, **H₁₀**), 2.24 (t, *J* = 11.0 Hz, 1H, **H₄**), 2.21 – 2.02 (m, 1H, **H₂**), 1.93 – 1.73 (m, 3H, **H_{6,8, H₁₁}**), 1.73 – 1.49 (m, 7H, **H_{6,8,7, H₁₁}**), 1.03 (d, *J* = 6.5 Hz, 3H, **H₁**), 1.03 – 0.95 (m, 1H, **H₃**), 0.43 – 0.33 (m, 1H, **H₃**).

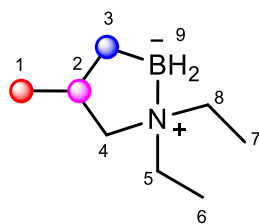
¹³C NMR (126 MHz, CDCl₃) δ 70.4, 63.2, 60.2, 31.8, 28.6, 28.3, 24.2, 23.1, 21.3, 21.0.

¹¹B NMR δ –2.6 ppm.

IR (film) *v*_{max}: 2922, 2861, 2334, 2246, 1454, 1188, 1129, 999, 806, 745 cm⁻¹.

HRMS (ESI, *m/z*): calculated for [M + H]⁺ C₁₀H₂₂BNO₂ requires *m/z* 200.1816, found *m/z* 200.1810.

1,1-Diethyl-4-methyl-1,2-azaborolidine (2c)



The title compound was obtained in 99% yield (28 mg, 0.19 mmol) as clear oil. Reaction time: 4.5 h.

$^1\text{H NMR}$ (500 MHz, CDCl_3) δ 2.99 – 2.68 (m, 5H, $\text{H}_{5,8}$, H_4), 2.28 – 2.23 (m, 1H, H_4), 2.22 – 2.14 (m, 1H, H_2), 1.81 (br, 2H, H_9), 1.15 (t, $J = 7.2$ Hz, 3H, H_7), 1.10 (t, $J = 7.2$ Hz, 3H, H_6), 1.02 (d, $J = 6.4$ Hz, 3H, H_1), 0.98 – 0.89 (m, 1H, H_3), 0.38 – 0.29 (m, 1H, H_3).

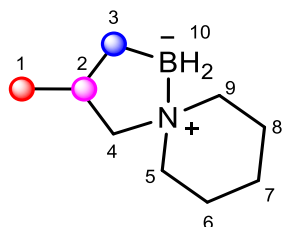
$^{13}\text{C NMR}$ (126 MHz, CDCl_3) δ 67.2, 52.9, 49.4, 31.7, 21.7, 21.2, 9.6, 8.6.

$^{11}\text{B NMR}$ δ –3.9 ppm

IR (film) ν_{max} : 2948, 2922, 2868, 2345, 1456, 1385, 1265, 1128, 1026, 829, 770 cm^{-1} .

HRMS (ESI, m/z): calculated for $[\text{M} - 2\text{H}]^+$ $\text{C}_8\text{H}_{18}\text{BN}$ requires m/z 140.1605, found m/z 140.1607.

3-Methyl-5-aza-1-borasp[iro[4.5]decane (2d)



The title compound was obtained in 98% yield (30 mg, 0.19 mmol) as a clear oil. Reaction time: 4.5 h.

$^1\text{H NMR}$ (500 MHz, CDCl_3) δ 3.03 – 2.88 (m, 2H, $\text{H}_{5,9}$), 2.87 – 2.80 (m, 1H, H_4), 2.74 – 2.59 (m, 1H, H_5), 2.56 – 2.47 (m, 1H, H_9), 2.24 (t, $J = 11.2$ Hz, 1H, H_4), 2.19 – 2.00 (m, 2H, $\text{H}_{6,8}$), 1.99 – 1.77 (m, 3H, $\text{H}_{6,8,10}$), 1.65 – 1.49 (m, 3H, $\text{H}_7, \text{H}_{10}$), 1.45 – 1.35 (m, 1H, H_2), 0.99 (d, $J = 6.5$ Hz, 3H, H_1), 0.94 – 0.83 (m, 1H, H_3), 0.36 – 0.24 (m, 1H, H_3).

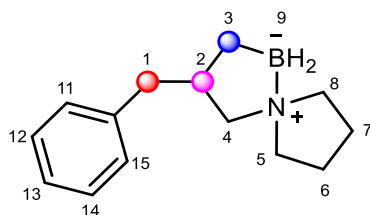
$^{13}\text{C NMR}$ (126 MHz, CDCl_3) δ 70.5, 61.0, 58.1, 31.2, 23.1, 22.8, 21.8, 21.7, 21.0.

$^{11}\text{B NMR}$ δ –4.5 ppm.

IR (film) ν_{max} : 2837, 2863, 2350, 1372, 1272, 1228, 1119, 997, 859, 781 cm^{-1} .

HRMS (ESI, m/z): calculated for $[\text{M} + \text{H}]^+$ $\text{C}_9\text{H}_{20}\text{BNO}_2$ requires m/z 186.1660, found m/z 186.1669.

3-Benzyl-5-aza-1-borasp[iro[4.4]nonane (2e)



The title compound was obtained in 99% yield (43 mg, 0.19 mmol) as a white solid. Reaction time: 1.5 h.

^1H NMR (500 MHz, CDCl_3) δ 7.29 – 7.25 (m, 2H, ArH), 7.20 – 7.16 (m, 3H, ArH), 3.30 – 3.11 (m, 2H, $\text{H}_{5,8}$), 2.85 (dd, $J = 13.5, 6.5$ Hz, 1H, H_4), 2.80 – 2.73 (m, 1H, H_5), 2.73 – 2.64 (m, 2H, H_1), 2.64 – 2.56 (m, 1H, H_4), 2.63 – 2.49 (m, 1H, H_8), 2.45 – 2.31 (m, 1H, H_2), 2.18 – 2.02 (m, 3H, $\text{H}_{6,7,9}$), 1.97 – 1.70 (m, 3H, $\text{H}_{6,7,9}$), 1.07 – 0.98 (m, 1H, H_3), 0.63 – 0.55 (m, 1H, H_3).

^{13}C NMR (126 MHz, CDCl_3) δ 141.9, 128.8 (2C), 128.4 (2C), 125.9, 68.1, 61.6, 60.4, 43.1, 40.3, 22.9, 22.6, 20.3.

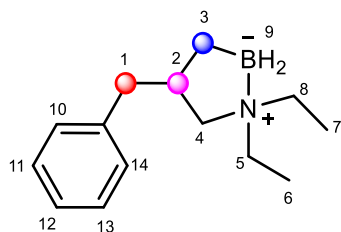
^{11}B NMR δ –3.9 ppm.

IR (film) ν_{max} : 3023, 2958, 2922, 2358, 2330, 1452, 1365, 1214, 1133, 700 cm^{-1} .

HRMS (ESI, m/z): calculated for $[\text{M} + \text{H}]^+$ $\text{C}_{14}\text{H}_{22}\text{BNO}_2$ requires m/z 248.1816, found m/z 248.1823.

mp 62–63 $^\circ\text{C}$.

4-Benzyl-1,1-diethyl-1,2-azaborolidine (2f)



The title compound was obtained in 97% yield (44 mg, 0.19 mmol) as a pale-yellow viscous oil.

Reaction time: 1.5 h.

¹H NMR (500 MHz, CDCl₃) δ 7.34 – 7.23 (m, 2H, ArH), 7.22 – 7.19 (m, 3H, ArH), 2.93 – 2.62 (m, 6H, H_{5,8}, H₁), 2.56 (dd, J = 13.5, 7.5 Hz, 1H, H₄), 2.45 – 2.26 (m, 2H, H₂, H₄), 2.23 – 1.98 (br, 1H, H₉), 1.14 (t, J = 7.2 Hz, 3H, H₇), 1.06 (t, J = 7.2 Hz, 4H, H₆, H₉), 0.98 – 0.89 (m, 1H, H₃), 0.54 – 0.45 (m, 1H, H₃).

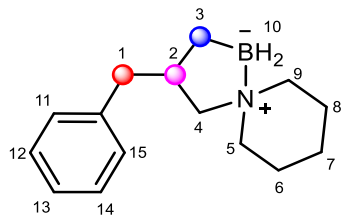
¹³C NMR (126 MHz, CDCl₃) δ 141.8, 128.8 (2C), 128.4 (2C), 125.9, 65.5, 53.0, 49.6, 43.1, 39.1, 19.5, 9.6, 8.7.

¹¹B NMR δ –4.1 ppm.

IR (film) ν_{max} : 2965, 2926, 1495, 1452, 1395, 1268, 1213, 742, 700 cm⁻¹.

HRMS (ESI, m/z): calculated for [M + H]⁺ C₁₄H₂₄BNO₂ requires m/z 250.1973, found m/z 250.1982.

3-Benzyl-5-aza-1-borasp[iro[4.5]decane (2g)



The title compound was obtained in 98% yield (49 mg, 0.21 mmol) as a pale-yellow viscous oil.
Reaction time: 1.5 h.

¹H NMR (500 MHz, CDCl₃) δ 7.32 – 7.27 (m, 2H, ArH), 7.18 – 7.23 (m, 3H, ArH), 3.04 – 2.95 (m, 2H, H_{5,9}), 2.91 – 2.77 (m, 2H, H₁, H₄), 2.77 – 2.65 (m, 1H, H₅), 2.62 – 2.55 (m, 1H, H₄), 2.56 – 2.47 (m, 1H, H₉), 2.47 – 2.35 (m, 2H, H₂, H₁), 2.32 – 2.10 (br, 1H, H₁₀), 2.08 – 1.80 (m, 3H, H_{6,8}, H₁₀), 1.75 – 1.48 (m, 3H, H_{6,8}, H₇), 1.49 – 1.35 (m, 1H, H₇), 1.11 – 0.91 (m, 1H, H₃), 0.63 – 0.44 (m, 1H, H₃).

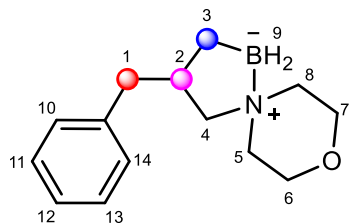
¹³C NMR (126 MHz, CDCl₃) δ 141.8, 128.8 (2C), 128.4 (2C), 125.9, 68.9, 61.1, 58.2, 43.1, 38.7, 23.2, 22.9, 21.8, 19.5.

¹¹B NMR δ –4.8 ppm.

IR (film) ν_{max}: 3023, 2958, 2922, 2782, 2358, 2330, 1365, 1214, 1133, 700 cm⁻¹.

HRMS (ESI, m/z): calculated for [M + H]⁺ C₁₅H₂₄BNO₂ requires m/z 262.1973, found m/z 262.1966.

3-Benzyl-8-oxa-5-aza-1-borasp[iro[4.5]decane (2h)



The title compound was obtained in 96% yield (44 mg, 0.19 mmol) pale-yellow viscous oil.
Reaction time: 1.5 h.

¹H NMR (500 MHz, CDCl₃) δ 7.32 – 7.27 (m, 2H, ArH), 7.23 – 7.17 (m, 3H, ArH), 4.22 – 4.09 (m, 1H, H₆), 4.06 – 3.99 (m, 1H, H₇), 3.76 (tt, *J* = 12.5, 2.9 Hz, 2H, H_{6,7}), 3.14 – 2.92 (m, 1H, H₁), 2.98 – 2.81 (m, 3H, H_{5,8}, H₄), 2.78 (dd, *J* = 11.0, 6.0 Hz, 1H, H₁), 2.73 – 2.50 (m, 3H, H₄, H_{5,8}), 2.46 – 2.24 (m, 1H, H₂), 1.94 (br, 2H, H₉), 1.09 – 0.92 (m, 1H, H₃), 0.63 – 0.53 (m, 1H, H₃).

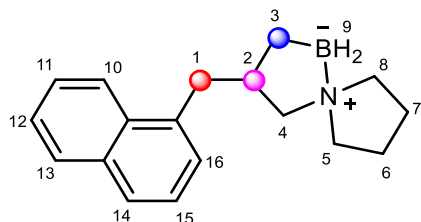
¹³C NMR (126 MHz, CDCl₃) δ 141.5, 129.8 (2C), 128.5 (2C), 126.0, 71.7, 64.2, 63.2, 59.9, 58.1, 42.8, 38.4, 19.7.

¹¹B NMR δ –5.3 ppm.

IR (film) ν_{max}: 3024, 2960, 2353, 1494, 1451, 1276, 1200, 1119, 866, 700 cm⁻¹.

HRMS (ESI, *m/z*): calculated for [M + H]⁺ C₁₄H₂₂BNO₃ requires *m/z* 264.1766, found *m/z* 262.1762.

3-(Naphthalen-1-ylmethyl)-5-aza-1-borasp[4.4]nonane (2i)



The title compound was obtained in 88% yield (46 mg, 0.17 mmol) as a pale-yellow solid. Reaction time: 1.5 h.

¹H NMR (400 MHz, CDCl₃) δ 7.86 – 7.70 (m, 3H, ArH), 7.63 (s, 1H, ArH), 7.46 (dq, *J* = 6.8, 5.4 Hz, 2H, ArH), 7.36 (dd, *J* = 8.4, 1.6 Hz, 1H, ArH), 3.26 – 3.17 (m, 2H, H_{5,8}), 3.05 (dd, *J* = 13.5, 6.3 Hz, 1H, H₁), 2.87 – 2.63 (m, 4H, H₁, H₄, H₉), 2.62 – 2.38 (m, 2H, H_{5,8}), 2.27 – 1.96 (m, 3H, H₂, H_{6,7}), 1.95 – 1.68 (m, 3H, H_{6,7}, H₉), 1.12 – 1.02 (m, 1H, H₃), 0.71 – 0.59 (m, *J* = 13.3, 8.1 Hz, 1H, H₃).

¹³C NMR (126 MHz, CDCl₃) δ 139.4, 133.7, 132.1, 128.0, 127.73, 127.68, 127.6, 126.0, 125.2, 68.1, 61.6, 60.4, 43.2, 40.3, 29.8, 22.8, 22.6, 20.4.

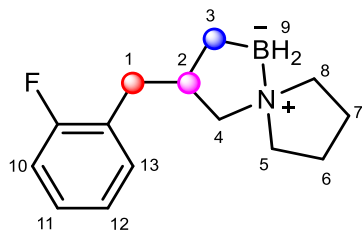
¹¹B NMR δ –3.8 ppm.

IR (film) ν_{max}: 2955, 2920, 2848, 2321, 2264, 1459, 1379, 1138, 857, 748, 475 cm⁻¹.

HRMS (ESI, *m/z*): calculated for [M – 2H]⁺ C₁₈H₂₂BN requires *m/z* 264.1918, found *m/z* 264.1918.

mp: 127–128 °C.

3-(2-Fluorobenzyl)-5-aza-1-borasp[4.4]nonane (2j)



The title compound was obtained in 97% yield (45 mg, 0.19 mmol) as a white solid. Reaction time: 1.5 h.

¹H NMR (500 MHz, CDCl₃) δ 7.21 – 7.13 (m, 2H, ArH), 7.05 (t, J = 7.3 Hz, 1H, ArH), 6.99 (t, J = 9.2 Hz, 1H, ArH), 3.22 (q, J = 8.8 Hz, 2H, H_{5,8}), 2.84 – 2.75 (m, 2H, H₄, H₅), 2.75 – 2.63 (m, 3H, H₁, H₄), 2.56 – 2.49 (m, 1H, H₈), 2.48 – 2.32 (m, 1H, H₂), 2.16 – 2.02 (m, 3H, H_{6,7}, H₉), 1.90 – 1.81 (m, 2H, H_{6,7}), 1.75 – 1.54 (m, 1H, H₉), 1.05 – 0.96 (m, 1H, H₃), 0.64 – 0.55 (m, 1H, H₃).

¹³C NMR (126 MHz, CDCl₃) δ 161.2, 160.2, 131.2, 127.5, 123.97, 115.3, 67.9, 61.6, 60.4, 39.2, 35.6, 22.7, 22.4, 20.1.

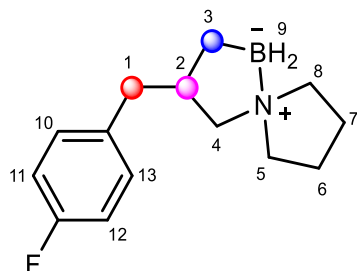
¹¹B NMR δ –3.8 ppm.

IR (film) ν_{max} : 2951, 2922, 2862, 2360, 2330, 1490, 1455, 1365, 1226, 754 cm⁻¹.

HRMS (ESI, m/z): calculated for [M + H]⁺ C₁₄H₂₁BFNO₂ requires m/z 266.1722, found m/z 266.1710.

mp: 61–62 °C.

3-(4-Fluorobenzyl)-5-aza-1-borasp[iro[4.4]nonane (2k)



The title compound was obtained in 97% yield (46 mg, 0.19 mmol) as a white solid. Reaction time: 1.5 h.

^1H NMR (500 MHz, CDCl_3) δ 7.15 – 7.09 (m, 2H, ArH), 6.98 – 6.91 (m, 2H, ArH), 3.26 – 3.18 (m, 2H, $\text{H}_{5,8}$), 2.87 – 2.71 (m, 2H, H_5 , H_4), 2.66 (d, $J = 8.8$ Hz, 2H, H_1), 2.62 – 2.47 (m, 2H, H_4 , H_8), 2.37 – 2.27 (m, 1H, H_2), 2.16 – 2.01 (m, 3H, $\text{H}_{6,7}$, H_9), 1.91 – 1.80 (m, 3H, $\text{H}_{6,7}$, H_9), 1.04 – 0.94 (m, 1H, H_3), 0.62 – 0.51 (m, 1H, H_3).

^{13}C NMR (126 MHz, CDCl_3) δ 162.3, 160.4, 137.4, 130.1, 115.2, 115.2, 68.0, 61.6, 60.4, 42.0, 40.4, 22.7, 22.4, 19.8.

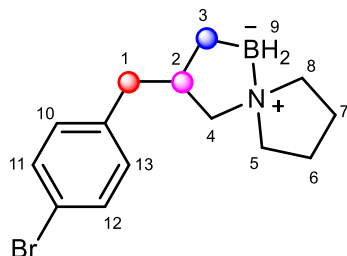
^{11}B NMR δ –3.8 ppm.

IR (film) ν_{max} : 2964, 2916, 2852, 2358, 2341, 1508, 1364, 1218 cm^{-1} .

HRMS (ESI, m/z): calculated for $[\text{M} + \text{H}]^+$ $\text{C}_{14}\text{H}_{21}\text{BFNO}_2$ requires m/z 266.1722, found m/z 226.1717.

mp: 64–65 $^\circ\text{C}$.

3-(4-Bromobenzyl)-5-aza-1-borasp[iro[4.4]nonane (2l)



The title compound was obtained in 99% yield (58 mg, 0.19 mmol) as a white solid. Reaction time: 1.5 h.

^1H NMR (500 MHz, CDCl_3) δ 7.38 (d, $J = 8.3$ Hz, 2H, ArH), 7.05 (d, $J = 8.3$ Hz, 2H, ArH), 3.35 – 3.11 (m, 2H, $\text{H}_{5,8}$), 2.88 – 2.69 (m, 2H, H_4 , H_5), 2.65 (d, $J = 8.9$ Hz, 2H, H_1), 2.61 – 2.46 (m, 2H, H_4 , H_8), 2.43 – 2.24 (m, 1H, H_2), 2.22 – 1.98 (m, 3H, $\text{H}_{6,7}$, H_9), 1.95 – 1.70 (m, 3H, $\text{H}_{6,7}$, H_9), 1.03 – 0.94 (m, 1H, H_3), 0.59 – 0.51 (m, 1H, H_3).

^{13}C NMR (126 MHz, CDCl_3) δ 140.8, 131.4 (2C), 130.6 (2C), 119.6, 68.0, 61.7, 60.4, 42.3, 40.2, 22.82, 22.6, 20.0.

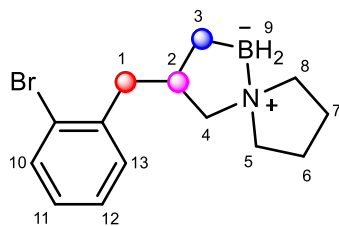
^{11}B NMR δ –3.4 ppm.

IR (film) ν_{max} : 2955, 2880, 2359, 1486, 1365, 1212, 1072, 1011 cm^{-1} .

HRMS (ESI, m/z): calculated for $[\text{M} + \text{H}]^+$ $\text{C}_{14}\text{H}_{21}\text{BBrNO}_2$ requires m/z 326.0922, found m/z 326.0937.

mp: 101–102 $^\circ\text{C}$.

3-(2-Bromobenzyl)-5-aza-1-borasp[iro[4.4]nonane (2m)



The title compound was obtained in 97% yield (49 mg, 0.16 mmol) as a white solid. Reaction time: 1.5 h.

¹H NMR (500 MHz, CDCl₃) δ 7.55 (d, *J* = 8.1 Hz, 1H, ArH), 7.37 – 7.16 (m, 2H, ArH), 7.16 – 7.01 (m, 1H, ArH), 3.37 – 3.17 (m, 2H, H_{5,8}), 2.99 – 2.79 (m, 4H, H₁, H₄, H₅), 2.79 – 2.64 (m, 1H, H₄), 2.64 – 2.53 (m, 1H, H₈), 2.53 – 2.44 (m, 1H, H₂), 2.19 – 2.05 (m, 3H, H_{6,7}, H₉), 1.98 – 1.69 (m, 3H, H_{6,7}, H₉), 1.07 – 0.98 (m, 1H, H₃), 0.68 – 0.59 (m, 1H, H₃).

¹³C NMR (126 MHz, CDCl₃) δ 141.0, 132.9, 131.1, 127.6, 127.4, 124.6, 67.9, 61.7, 60.5, 42.6, 38.7, 22.9, 22.6, 19.9.

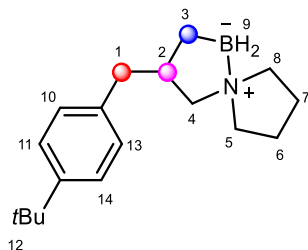
¹¹B NMR δ –3.8 ppm.

IR (film) ν_{max}: 2922, 2852, 2331, 1467, 1200, 1135, 1024, 750 cm⁻¹.

HRMS (ESI, *m/z*): calculated for [M + H]⁺ C₁₄H₂₁BBrNO₂ requires *m/z* 326.0921, found *m/z* 326.0927.

mp: 98–99 °C.

3-(4-(*tert*-Butyl)benzyl)-5-aza-1-borasp[4.4]nonane (2n)



The title compound was obtained in 96% yield (55 mg, 0.20 mmol) as a viscous oil. Reaction time: 1.5 h.

^1H NMR (500 MHz, CDCl_3) δ 7.30 (d, J = 8.3 Hz, 2H, ArH), 7.11 (d, J = 8.2 Hz, 2H, ArH), 3.26 – 3.19 (m, 2H, $\text{H}_{5,8}$), 2.89 – 2.75 (m, 2H, H_4 , H_5), 2.70 (d, J = 9.4 Hz, 2H, H_1), 2.60 – 2.51 (m, 2H, H_4 , H_8), 2.48 – 2.26 (m, 1H, H_2), 2.22 – 1.98 (m, 3H, $\text{H}_{6,7}$, H_9), 1.96 – 1.72 (m, 3H, $\text{H}_{6,7}$, H_9), 1.32 (s, 9H, H_{12}), 1.09 – 1.00 (m, 1H, H_3), 0.63 – 0.55 (m, 1H, H_3).

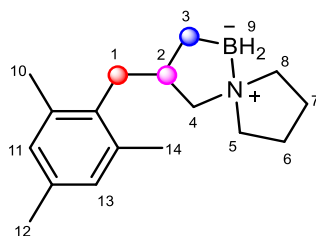
^{13}C NMR (126 MHz, CDCl_3) δ 148.6, 138.7 (2C), 128.4 (2C), 125.2, 68.2, 61.6, 60.3, 42.5, 40.2, 34.5, 31.5 (3C), 22.8, 22.6, 20.0.

^{11}B NMR δ –3.8 ppm.

IR (film) ν_{max} : 2960, 2925, 2870, 2355, 1511, 1363, 1209, 1133, 829 cm^{-1} .

HRMS (ESI, m/z): calculated for $[\text{M} + \text{H}]^+$ $\text{C}_{18}\text{H}_{30}\text{BNO}_2$ requires m/z 304.2442, found m/z 304.2457.

3-(2,4,6-Trimethylbenzyl)-5-aza-1-borasp[iro[4.4]nonane (2o)



The title compound was obtained in 96% yield (49 mg, 0.19 mmol) as a pale-yellow solid. Reaction time: 1.5 h.

¹H NMR (500 MHz, CDCl₃) δ 6.83 (s, 2H, ArH), 3.28 – 3.16 (m, 2H, H_{5,8}), 2.86 – 2.74 (m, 3H, H₁, H₄, H₅), 2.73 – 2.59 (m, 2H, H₁, H₄), 2.56 – 2.43 (m, 1H, H₈), 2.35 – 2.27 (m, 7H, H₂, H₁₀, H₁₄), 2.25 (s, 3H, H₁₂), 2.20 – 1.97 (m, 3H, H_{6,7}, H₉), 1.93 – 1.65 (m, 3H, H_{6,7}, H₉), 1.09 – 1.01 (m, 1H, H₃), 0.71 – 0.62 (m, 1H, H₃).

¹³C NMR (126 MHz, CDCl₃) δ 136.2, 135.8, 134.9, 129.1 (2C), 68.2, 62.0 (2C), 60.6, 38.6, 35.5, 22.7, 22.5, 21.2, 20.9, 20.6 (2C).

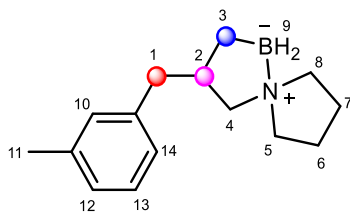
¹¹B NMR δ –3.6 ppm.

IR (film) ν_{max}: 2984, 2946, 2879, 2360, 2237, 2208, 2036, 1458, 1364, 1216 cm⁻¹.

HRMS (ESI, m/z): calculated for [M + H]⁺ C₁₇H₂₈BNO₂ requires m/z 290.2286, found m/z 290.2302.

mp: 74–75 °C.

3-(3-Methylbenzyl)-5-aza-1-borasp[iro[4.4]nonane (2p)



The title compound was obtained in 98% yield (47 mg, 0.21 mmol) as a viscous clear oil. Reaction time: 1.5 h.

¹H NMR (500 MHz, CDCl₃) δ 7.16 (t, *J* = 7.8 Hz, 1H, ArH), 7.01 – 6.95 (m, 3H, ArH), 3.31 – 3.09 (m, 2H, H_{5,8}), 2.84 – 2.74 (m, 2H, H₄, H₅), 2.68 (d, *J* = 9.7 Hz, 2H, H₁), 2.57 – 2.49 (m, 2H, H₄, H₈), 2.41 – 2.33 (m, 1H, H₂), 2.33 (s, 3H, H₁₁), 2.20 – 1.98 (m, 3H, H_{6,7}, H₉), 1.90 – 1.79 (m, 3H, H_{6,7}, H₉), 1.09 – 0.97 (m, 1H, H₃), 0.63 – 0.54 (m, 1H, H₃).

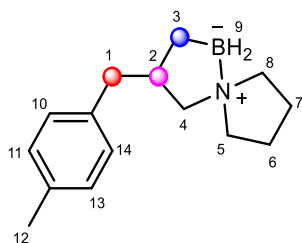
¹³C NMR (126 MHz, CDCl₃) δ 141.8, 137.9, 129.7, 128.3, 126.6, 125.8, 68.2, 61.6, 60.3, 43.0, 40.3, 22.9, 22.6, 21.6, 20.4.

¹¹B NMR δ –3.8 ppm.

IR (film) ν_{max} : 2952, 2920, 2874, 2357, 2334, 1458, 1364, 1211, 1135, 781 cm⁻¹.

HRMS (ESI, *m/z*): calculated for [M + H]⁺ C₁₅H₂₄BNO₂ requires *m/z* 262.1973, found *m/z* 262.1961.

3-(4-Methylbenzyl)-5-aza-1-borasp[iro[4.4]nonane (2q)



The title compound was obtained in 99% yield (45 mg, 0.19 mmol) as a viscous oil. Reaction time: 1.5 h.

¹H NMR (500 MHz, CDCl₃) δ 7.11 – 7.04 (m, 4H, ArH), 3.28 – 3.12 (m, 2H, H_{5,8}), 2.85 – 2.74 (m, 2H, H₄, H₅), 2.67 (d, *J* = 9.1 Hz, 2H, H₁), 2.58 – 2.49 (m, 2H, H₄, H₈), 2.43 – 2.35 (m, 1H, H₂), 2.32 (s, 3H, H₁₂), 2.21 – 1.98 (m, 3H, H_{6,7}, H₉), 1.89 – 1.80 (m, 3H, H_{6,7}, H₉), 1.08 – 0.98 (m, 1H, H₃), 0.63 – 0.54 (m, 1H, H₃).

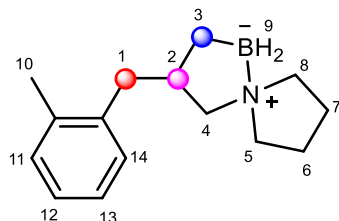
¹³C NMR (126 MHz, CDCl₃) δ 138.8, 135.3, 129.1 (2C), 128.7 (2C), 68.1, 61.6, 60.3, 42.6, 40.3, 22.8, 22.6, 21.2, 20.2.

¹¹B NMR δ –3.8 ppm.

IR (film) ν_{max}: 2824, 2356, 2331, 2250, 2156, 2031, 1977, 807 cm⁻¹.

HRMS (ESI, *m/z*): calculated for [M + H]⁺ C₁₅H₂₄BNO₂ requires *m/z* 262.1972, found *m/z* 262.1983.

3-(2-Methylbenzyl)-5-aza-1-borasp[iro[4.4]nonane (2r)



The title compound was obtained in 97% yield (49 mg, 0.21 mmol) as a viscous clear oil. Reaction time: 1.5 h.

¹H NMR (500 MHz, CDCl₃) δ 7.17 – 7.08 (m, 4H, ArH), 3.36 – 3.12 (m, 2H, H_{5,8}), 2.88 (dd, *J* = 13.9, 6.2 Hz, 1H, H₄), 2.79 – 2.71 (m, 1H, H₅), 2.75 – 2.63 (m, 2H, H₁), 2.60 (dd, *J* = 13.9, 8.3 Hz, 1H, H₄), 2.56 – 2.49 (m, 1H, H₈), 2.43 – 2.35 (m, 1H, H₂), 2.35 (s, 3H, H₁₀), 2.21 – 1.98 (m, 3H, H_{6,7}, H₉), 1.98 – 1.76 (m, 3H, H_{6,7}, H₉), 1.11 – 1.01 (m, 1H, H₃), 0.67 – 0.57 (m, 1H, H₃).

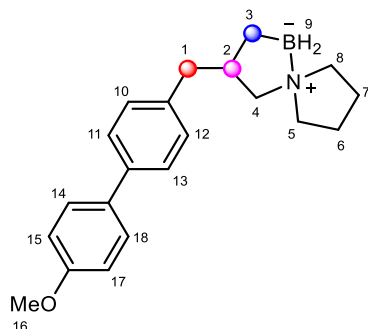
¹³C NMR (126 MHz, CDCl₃) δ 140.0, 136.0, 130.3, 129.3, 126.0, 125.8, 68.2, 61.7, 60.4, 40.2, 38.8, 22.8, 22.6, 20.8, 19.7.

¹¹B NMR δ –3.8 ppm.

IR (film) ν_{max}: 2918, 2874, 2327, 2492, 1458, 1377, 1198, 1134, 740 cm⁻¹.

HRMS (ESI, *m/z*): calculated for [M + H]⁺ C₁₅H₂₄BNO₂ requires *m/z* 262.1973, found *m/z* 262.1980.

3-((4'-Methoxy-[1,1'-biphenyl]-4-yl)methyl)-5-aza-1-borasp[4.4]nonane (2s)



The title compound was obtained in 98% yield (59 mg, 0.18 mmol) as a white solid. Reaction time: 1.5 h.

¹H NMR (500 MHz, CDCl₃) δ 7.55 (d, *J* = 8.7 Hz, 2H, ArH), 7.49 (d, *J* = 8.1 Hz, 2H, ArH), 7.25 (d, *J* = 8.0 Hz, 2H, ArH), 7.00 (d, *J* = 8.7 Hz, 2H, ArH), 3.88 (s, 3H, H₁₆), 3.33 – 3.15 (m, 2H, H_{5,8}), 2.90 (dd, *J* = 13.5, 6.5 Hz, 1H, H₄), 2.81 – 2.75 (m, 1H, H₅), 2.74 (d, *J* = 8.8 Hz, 2H, H₁), 2.64 (dd, *J* = 13.5, 8.3 Hz, 1H, H₄), 2.59 – 2.48 (m, 1H, H₈), 2.49 – 2.33 (m, 1H, H₂), 2.25 – 2.00 (m, 3H, H_{6,7}, H₉), 1.98 – 1.76 (m, 3H, H_{6,7}, H₉), 1.10 – 1.03 (m, 1H, H₃), 0.68 – 0.59 (m, 1H, H₃).

¹³C NMR (126 MHz, CDCl₃) δ 159.1, 140.3, 138.4, 133.8, 129.2 (2C), 128.1 (2C), 126.7 (2C), 114.3 (2C), 68.1, 61.6, 60.3, 55.5, 42.6, 40.3, 29.8, 22.6, 20.3.

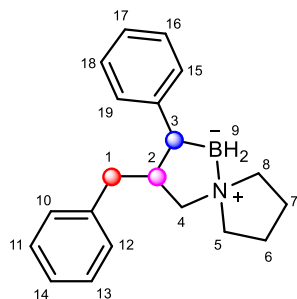
¹¹B NMR δ –3.7 ppm.

IR (film) ν_{max}: 2918, 2850, 2323, 1608, 1497, 1457, 1244, 1175, 1037, 806, 515 cm⁻¹.

HRMS (ESI, *m/z*): calculated for [M – 2H]⁺ C₂₁H₂₆BNO requires *m/z* 320.2180, found *m/z* 320.2180.

mp: 171–172 °C.

3-Benzyl-2-phenyl-5-aza-1-boraspino[4.4]nonane (2t)



The reaction mixture was heated to 150 °C. The title compound was obtained as a white solid in 95% yield (57 mg, 0.19 mmol). Reaction time: 1.5 h.

¹H NMR (300 MHz, CDCl₃) δ 7.35 – 7.28 (m, 7H, ArH), 7.26 – 7.20 (m, *J* = 7.1 Hz, 1H, ArH), 7.17 – 7.12 (m, *J* = 7.3 Hz, 2H, ArH), 3.43 (t, *J* = 8.6 Hz, 1H, H₅), 3.32 (t, *J* = 8.7 Hz, 1H, H₈), 3.08 (dd, *J* = 13.7, 3.5 Hz, 1H, H₄), 2.97 – 2.77 (m, 3H, H₁, H₄), 2.76 – 2.61 (m, 3H, H₂, H_{5,8}), 2.45 – 2.30 (m, 2H, H_{6,7}), 2.27 – 1.99 (m, 3H, H_{6,7}, H₉), 1.99 – 1.84 (m, 2H, H₃, H₉).

¹³C NMR (126 MHz, CDCl₃) δ 148.9, 141.5, 128.8, 128.1 (4C), 127.8 (4C), 126.0, 123.7, 67.2, 62.9, 62.7, 47.4, 44.2, 40.1, 22.5, 22.4.

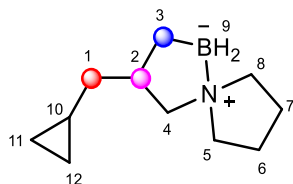
¹¹B NMR δ –0.1 ppm.

IR (film) ν_{max}: 3379, 2935, 2356, 2310, 1599, 1491, 1454, 11188, 1129, 757, 703 cm⁻¹.

HRMS (ESI, *m/z*): calculated for [M – 2H]⁺ C₂₀H₂₄BN requires *m/z* 290.2075, found *m/z* 290.2079.

mp: 162–163 °C.

3-(Cyclopropylmethyl)-5-aza-1-borasp[4.4]nonane (2u)



The title compound was obtained as a clear oil in 98% yield (35 mg, 0.19 mmol). Reaction time: 4.5 h.

¹H NMR (500 MHz, CDCl₃) δ 3.28 – 3.17 (m, 2H, **H_{5,8}**), 2.91 – 2.72 (m, 2H, **H₄, H₅**), 2.67 – 2.58 (m, 2H, **H₄, H₈**), 2.25 – 2.02 (m, 4H, **H₂, H_{6,7}, H₉**), 1.99 – 1.77 (m, 3H, **H_{6,7}, H₉**), 1.43 (dt, *J* = 13.3, 6.6 Hz, 1H, **H₁**), 1.19 – 1.08 (m, 1H, **H₁**), 1.02 (dd, *J* = 13.7, 6.0 Hz, 1H, **H₃**), 0.73 – 0.60 (m, 1H, **H₁₀**), 0.56 – 0.42 (m, 1H, **H₃**), 0.42 – 0.31 (m, 2H, **H_{11,12}**), 0.07 – 0.001 (m, 1H, **H₁₁**), -0.006 – -0.07 (m, 1H, **H₁₂**).

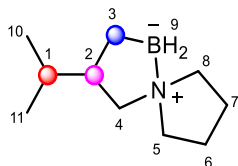
¹³C NMR (126 MHz, CDCl₃) δ 68.5, 61.6, 60.3, 41.7, 39.1, 22.9, 22.6, 20.5, 9.9, 4.8, 4.5.

¹¹B NMR δ -3.9 ppm.

IR (film) ν_{max} : 3073, 2995, 2916, 2840, 2330, 1459, 1363, 1207, 1139, 1013, 823 cm⁻¹.

HRMS (ESI, *m/z*): calculated for [M + H]⁺ C₁₁H₂₂BNO₂ requires *m/z* 212.1816, found *m/z* 212.1820.

3-Isopropyl-5-aza-1-borasp[iro[4.4]nonane (2v)



The title compound was obtained in 99% yield (33 mg, 0.19 mmol) as a clear oil. Reaction time: 4.5 h.

^1H NMR (500 MHz, CDCl_3) δ 3.26 – 3.16 (m, 2H, **H_{5,8}**), 2.83 – 2.73 (m, 2H, **H₄**, **H₅**), 2.68 (t, $J = 11.1$ Hz, 1H, **H₄**), 2.59 – 2.52 (m, 1H, **H₈**), 2.23 – 1.96 (m, 3H, **H_{6,7}**, **H₉**), 1.96 – 1.79 (m, 3H, **H_{6,7}**, **H₉**), 1.79 – 1.60 (m, 1H, **H₂**), 1.48 – 1.39 (m, 1H, **H₁**), 0.96 – 0.87 (m, 4H, **H₃**, **H₁₁**), 0.85 (d, $J = 6.6$ Hz, 3H, **H₁₀**), 0.56 – 0.37 (m, 1H, **H₃**).

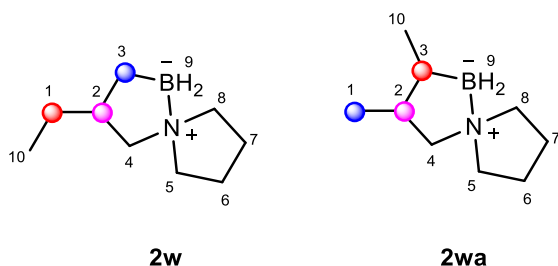
^{13}C NMR (126 MHz, CDCl_3) δ 67.2, 61.6, 60.2, 45.9, 33.9, 22.8, 22.6, 21.6, 21.2, 17.6.

^{11}B NMR δ –3.9 ppm.

IR (film) ν_{max} : 2953, 2925, 2871, 2334, 1459, 1365, 1205, 1130, 873 cm^{-1} .

HRMS (ESI, m/z): calculated for $[\text{M} + \text{H}]^+$ $\text{C}_{10}\text{H}_{22}\text{BNO}_2$ requires m/z 200.1816, found m/z 200.1812.

3-Ethyl-5-aza-1-borasp[4.4]nonane (2w) and 2,3-Dimethyl-5-aza-1-borasp[4.4]nonane (2wa)



The mixture of products was obtained in 76% yield (26 mg, 0.17 mmol) of **2w** and 24% yield (8.2 mg, 0.05 mmol) of **2wa** as a pale-yellow oil. Reaction time: 1 h (50 mol% Tf₂NH). Major isomer **2w**:

¹H NMR (500 MHz, CDCl₃) δ 3.31 – 3.15 (m, 2H, **H**_{5,8}), 2.86 – 2.76 (m, 3H, **H**_{5,8}, **H**₄), 2.68 – 2.60 (m, 2H, **H**₄, **H**₁), 2.18 – 2.06 (m, 1H, **H**₄), 1.98 – 1.85 (m, 3H, **H**₂, **H**_{6,7}), 1.48 – 1.39 (m, 1H, **H**₉), 1.37 – 1.27 (m, 3H, **H**_{6,7}, **H**₉), 1.01 – 0.97 (m, 1H, **H**₃), 0.96 – 0.90 (m, 3H, **H**₁₀), 0.47 – 0.40 (m, 1H, **H**₃).

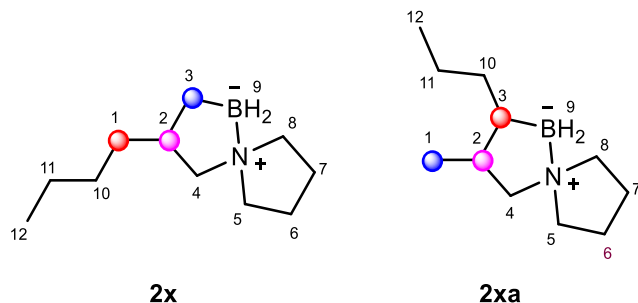
¹³C NMR (126 MHz, CDCl₃) δ 68.5, 61.5, 60.3, 40.2, 29.2, 22.9, 22.6, 19.5, 12.6.

¹¹B NMR δ –3.7 ppm, –0.03 ppm.

IR (film) ν_{max}: 2953, 2366, 2273, 1456, 1165, 1079, 1037, 882 cm⁻¹.

HRMS (ESI, m/z): calculated for [M + H]⁺ C₉H₂₀BNO₂ requires m/z 186.1660, found m/z 186.1667.

3-Propyl-5-aza-1-borasp[4.4]nonane (2x), 2-ethyl-3-methyl-5-aza-1-borasp[4.4]nonane (2xa)



The title compound **2x** was obtained in 96% yield (35.6 mg, 0.21 mmol) as a pale-yellow oil. Reaction time: 1 h (50 mol% Tf₂NH).

¹H NMR (500 MHz, CDCl₃) δ 3.39 – 3.01 (m, 2H, **H_{5,8}**), 2.85 – 2.74 (m, 2H, **H_{5,8}**), 2.64 – 2.58 (m, 1H, **H₄**), 2.17 – 2.04 (m, 3H, **H₄**, **H_{6,7}**), 2.04 – 1.99 (m, 1H, **H₂**), 1.93 – 1.76 (m, 3H, **H_{6,7}**, **H₉**), 1.76 – 1.62 (m, 1H, **H₉**), 1.40 – 1.16 (m, 6H, **H₁**, **H₁₀**, **H₁₁**), 0.89 – 0.78 (m, 4H, **H₃**, **H₁₂**), 0.45 – 0.26 (m, 1H, **H₃**).

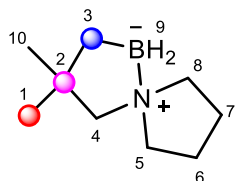
¹³C NMR (126 MHz, CDCl₃) δ 68.7, 61.5, 60.3, 38.4, 36.4, 30.7, 23.1, 22.9, 22.6, 19.8, 14.2.

¹¹B NMR δ –3.9 ppm, –0.7 ppm.

IR (film) ν_{max}: 2953, 2921, 2870, 2333, 1457, 1363, 1215, 1137, 854 cm⁻¹.

HRMS (ESI, *m/z*): calculated for [M + H]⁺ C₁₁H₂₄BNO₂ requires *m/z* 214.1973, found *m/z* 214.1963.

3,3-Dimethyl-5-aza-1-borasp[iro[4.4]nonane (2y)



The title compound was obtained in 92% yield (27 mg, 0.18 mmol) as a clear oil. Reaction time: 1.5 h.

$^1\text{H NMR}$ (500 MHz, CDCl_3) δ 3.31 – 3.20 (m, 2H, $\text{H}_{5,8}$), 2.77 – 2.66 (m, 4H, $\text{H}_{5,8}$, H_4), 2.17 – 2.02 (m, 2H, $\text{H}_{6,7}$), 1.99 – 1.76 (m, 4H, $\text{H}_{6,7}$, H_9), 1.11 (s, 6H, H_1 , H_{10}), 0.74 (t, $J = 5.6$ Hz, 2H, H_3).

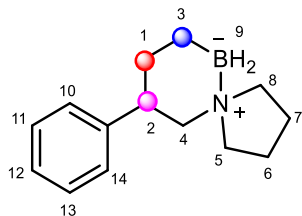
$^{13}\text{C NMR}$ (126 MHz, CDCl_3) δ 75.8, 61.8 (2C), 37.8, 32.0, 30.6 (2C), 22.8 (2C).

$^{11}\text{B NMR}$ δ -4.2 ppm.

IR (film) ν_{max} : 2952, 2870, 2336, 2196, 1457, 1351, 1239, 1191, 1143, 869 cm^{-1} .

HRMS (ESI, m/z): calculated for $[\text{M} + \text{H}]^+$ $\text{C}_9\text{H}_{20}\text{BNO}_2$ requires m/z 186.1660, found m/z 186.1661.

9-Phenyl-5-aza-6-borasp[iro[4.5]decane (2z)



The title compound was obtained in 93% yield (43 mg, 0.19 mmol) as a clear crystalline solid.
Reaction time: 1.5 h.

¹H NMR (500 MHz, CDCl₃) δ 7.38 – 7.30 (m, 2H, ArH), 7.30 – 7.14 (m, 3H, ArH), 3.53 – 3.46 (m, 1H, H₅), 3.44 – 3.28 (m, 1H, H₈), 3.10 (dd, *J* = 12.5, 11.6 Hz, 1H, H₄), 2.87 – 2.76 (m, 2H, H₂, H₅), 2.76 – 2.65 (m, 2H, H₄, H₈), 2.24 – 2.12 (m, 2H, H_{6,7}), 2.12 – 2.02 (m, 1H, H₁), 2.01 – 1.82 (m, 3H, H_{6,7}, H₉), 1.73 (ddd, *J* = 25.2, 12.6, 3.9 Hz, 2H, H₁), 0.78 – 0.72 (m, 1H, H₃), 0.72 – 0.60 (m, 1H, H₃).

¹³C NMR (126 MHz, CDCl₃) δ 144.2, 128.7 (2C), 127.4 (2C), 126.8, 67.4, 65.0, 56.3, 43.7, 34.4, 23.2, 22.1, 14.9.

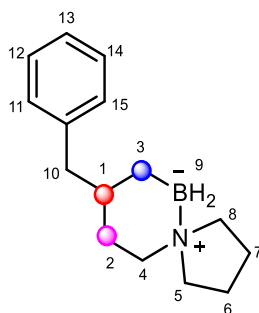
¹¹B NMR δ –5.5 ppm.

IR (film) ν_{max}: 2907, 2357, 2329, 2220, 1454, 1139, 700 cm⁻¹.

HRMS (ESI, *m/z*): calculated for [M + H]⁺ C₁₄H₂₂BNO₂ requires *m/z* 248.1816, found *m/z* 248.1822.

mp: 85–87 °C.

8-Benzyl-5-aza-6-borasp[iro[4.5]decane (2aa)



The title compound was obtained in 95% yield (45 mg, 0.19 mmol) as a viscous oil. Reaction time: 1.5 h.

¹H NMR (300 MHz, CDCl₃) δ 7.25 (d, *J* = 7.1 Hz, 2H, ArH), 7.16 (dd, *J* = 7.4, 1.7 Hz, 3H, ArH), 3.40 – 3.07 (m, 2H, H_{5,8}), 2.91 (ddd, *J* = 13.1, 11.8, 3.0 Hz, 1H, H₄), 2.78 – 2.52 (m, 4H, H_{5,8}, H₁₀), 2.43 (dd, *J* = 13.2, 8.2 Hz, 1H, H₄), 2.25 – 1.97 (m, 3H, H_{6,7}, H₉), 1.97 – 1.69 (m, 4H, H_{6,7}, H₉, H₁), 1.68 – 1.46 (m, 1H, H₂), 1.37 – 1.10 (m, 1H, H₂), 0.66 (d, *J* = 14.1 Hz, 1H, H₃), 0.27 (td, *J* = 14.0, 3.3 Hz, 1H, H₃).

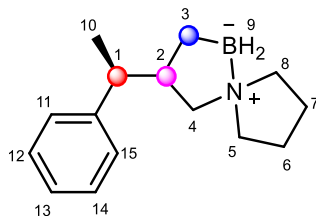
¹³C NMR (126 MHz, CDCl₃) δ 142.1, 129.4 (2C), 128.1 (2C), 125.5, 64.0, 61.3, 55.9, 46.7, 40.1, 31.5, 23.0, 22.7, 22.3.

¹¹B NMR δ –5.6 ppm.

IR (film) ν_{max} : 3023, 2909, 2804, 2320, 2238, 1494, 1451, 1158, 730, 698 cm⁻¹.

HRMS (ESI, *m/z*): calculated for [M – 2H]⁺ C₁₅H₂₂BN requires *m/z* 228.1918, found *m/z* 228.1917.

3-((S)-1-Phenylethyl)-5-aza-1-borasp[iro[4.4]nonane (2ab)



The title compound was obtained in 99% yield (45 mg, 0.19 mmol) as clear viscous oil. Reaction time: 1.5 h.

¹H NMR (500 MHz, CDCl₃) δ 7.35 – 7.25 (m, 2H, ArH), 7.25 – 7.08 (m, 3H, ArH), 3.28 – 3.09 (m, 2H, H_{5,8}), 2.72 – 2.64 (m, 1H, H₅), 2.59 (t, *J* = 11.1 Hz, 1H, H₄), 2.53 – 2.40 (m, 2H, H₁, H₈), 2.36 – 2.30 (m, 1H, H₄), 2.29 – 2.19 (m, 1H, H₂), 2.19 – 1.99 (m, 3H, H_{6,7}, H₉), 1.92 – 1.73 (m, 3H, H_{6,7}, H₉), 1.35 (d, *J* = 6.9 Hz, 3H, H₁₀), 1.21 – 1.11 (m, 1H, H₃), 0.67 – 0.57 (m, 1H, H₃).

¹³C NMR (126 MHz, CDCl₃) δ 147.9, 128.6 (2C), 127.1 (2C), 126.1, 67.9, 61.5, 60.3, 47.3, 45.7, 22.8, 22.6, 21.5, 19.1.

¹¹B NMR δ –3.8 ppm.

IR (film) ν_{max} : 3060, 2996, 2954, 2922, 2865, 1601, 1444, 1025, 762, 698, 578 cm⁻¹.

HRMS (ESI, *m/z*): calculated for [M + H]⁺ C₁₅H₂₄BNO₂ requires *m/z* 262.1973, found *m/z* 262.1968.

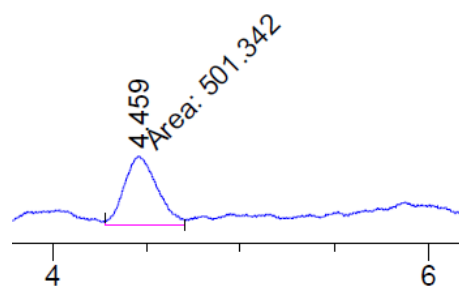
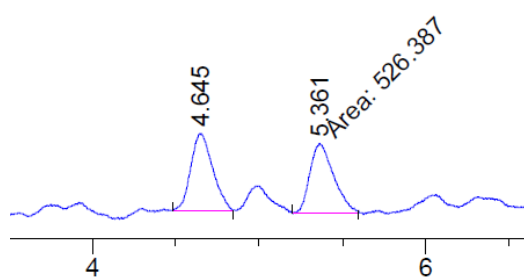
[α]_D²⁵ = +40 (c 0.20, MeOH).

SFC (Chiralpak OJ-H 21mm x 250 mm, 5 μ m, 30 $^{\circ}$ C, 150 bar, 95% CO₂; 5% Modifier (IPA), 60 g/min).

t_R major: 4.46 min.

Racemic mixture

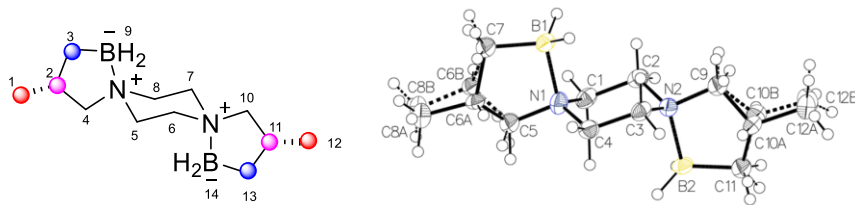
1ab, 99% ee



Peak #	RetTime [min]	Type	Width [min]	Area [mAU*s]	Height [mAU]	Area %
1	4.645	BV	0.1091	533.67633	58.42089	50.3438
2	5.361	MM	0.1667	526.38684	52.64318	49.6562

Peak #	RetTime [min]	Type	Width [min]	Area [mAU*s]	Height [mAU]	Area %
1	4.459	MM	0.2004	501.34171	41.69611	100.0000

3,11-Dimethyl-5,8-diaza-1,9-diboradispiro[4.2.4]tetradecane (**2ac**)



The title compound was synthesized using general procedure D. *Two equivalents of Tf₂NH were used and the reaction mixture was heated for 1 h.*

Compound **2ac** was obtained as a viscous oil in 95% (47.5 mg, 0.21 mmol).

¹H NMR (500 MHz, CDCl₃) δ 3.61 – 3.49 (m, 1H, **H₅**), 3.42 (d, *J* = 8.5 Hz, 1H, **H₄**), 3.28 (d, *J* = 8.9 Hz, 1H, **H₁₀**), 3.19 – 3.12 (m, 1H, **H₈**), 3.04 – 2.98 (m, 2H, **H_{5,8}**), 2.91 – 2.77 (m, 4H, **H_{6,7}**, **H_{4,10}**), 2.52 – 2.47 (m, 2H, **H_{6,7}**), 2.39 – 2.22 (m, 2H, **H_{9,14}**), 2.22 – 2.07 (m, 3H, **H₂**, **H₁₁**, **H₉**), 1.98 (br, 1H, **H₁₄**), 1.07 – 1.01 (d(two doublets), *J* = 6.5 Hz(each), 6H, **H₁**, **H₁₂**), 0.99 – 0.90 (m, 2H, **H₃**, **H₁₃**), 0.39 (tt, *J* = 8.3, 4.3 Hz, 2H, **H₃**, **H₁₃**).

¹³C NMR (176 MHz, CDCl₃) δ 73.9, 57.0 (2C), 56.1, 55.1, 54.1, 31.2, 31.1, 29.9, 22.1, 20.6 (2C).

¹¹B NMR δ –5.6 ppm.

IR (film) ν_{max}: 2923, 2419, 2389, 2238, 2003, 1456, 1349, 1189, 1109 cm⁻¹.

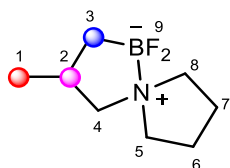
HRMS (ESI, *m/z*): calculated for [M + H]⁺ C₁₂H₂₈BN₂O₄ requires *m/z* 287.23079, found *m/z* 287.2314.

Post-functionalization

General Procedure E: Fluorinated spirocycle

SCAB (0.2 mmol) was added to a microwave vial followed by the addition of Tf₂NH (115 mg, 410 μmol) and KF (35.7 mg, 615 μmol). CH₂Cl₂ (683 μL) was added and the vial was sealed. The mixture was heated to 60 °C and stirred for 12 h at this temperature. The vial was cooled, and the mixture was filtered over a short pad of silica, washed with CH₂Cl₂ and concentrated under reduced pressure. The products were obtained as pale-yellow viscous oils.

1,1-Difluoro-3-methyl-5-aza-1-borasp[iro[4.4]nonane (3a)



The title compound was obtained in 87% yield (31 mg, 0.17 mmol).

¹H NMR (500 MHz, CDCl₃) δ 3.53 – 3.40 (m, 2H, **H**_{5,8}), 2.77 – 2.71 (m, 1H, **H**₅), 2.71 – 2.65 (m, 1H, **H**₄), 2.61 – 2.46 (m, 2H, **H**₄, **H**₈), 2.12 – 2.01 (m, 3H, **H**_{6,7}, **H**₂), 2.00 – 1.81 (m, 2H, **H**_{6,7}), 1.01 (d, *J* = 6.6 Hz, 3H, **H**₁), 0.96 – 0.88 (m, 1H, **H**₃), 0.27 – 0.15 (m, 1H, **H**₃).

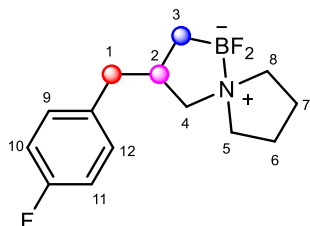
¹³C NMR (126 MHz, CDCl₃) δ 67.2, 54.7 (2C), 28.8, 23.1, 22.8, 22.0, 20.8.

¹¹B NMR δ 9.5 ppm.

IR (film) ν_{max}: 2954, 2930, 2902, 1459, 1232, 1190, 1150, 1099, 1063, 930, 812 cm⁻¹.

HRMS (ESI, *m/z*): calculated for [M + H]⁺ C₈H₁₆BF₂N requires *m/z* 176.14166, found *m/z* 176.14245.

1,1-Difluoro-3-(4-fluorobenzyl)-5-aza-1-borasp[4.4]nonane (3b)



The title compound was obtained in 82% yield (44 mg, 0.16 mmol).

¹H NMR (500 MHz, CDCl₃) δ 7.21 – 7.06 (m, 2H, ArH), 7.06 – 6.94 (m, 2H, ArH), 3.48 – 3.42 (m, 2H, H_{5,8}), 2.76 – 2.69 (m, 1H, H₄), 2.56 – 2.47 (m, 3H, H₁, H₅), 2.47 – 2.38 (m, 2H, H₄, H₈), 2.28 – 2.15 (m, 1H, H₂), 2.13 – 1.99 (m, 2H, H_{6,7}), 1.96 – 1.84 (m, 2H, H_{6,7}), 0.92 – 0.83 (m, 1H, H₃), 0.32 – 0.29 (m, 1H, H₃).

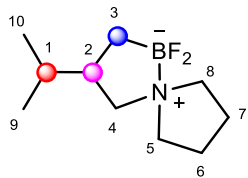
¹³C NMR (126 MHz, CDCl₃) δ 135.5, 130.5, 115.5, 115.2, 65.4, 56.2, 54.9, 54.8, 41.7, 36.1, 23.3, 23.0, 22.9, 20.6.

¹¹B NMR δ 9.4 ppm.

IR (film) ν_{max}: 2951, 1349, 1181, 1135, 1054, 823, 652, 508 cm⁻¹.

HRMS (ESI, m/z): calculated for [M + H]⁺ C₁₄H₂₁BFNO₂ requires *m/z* 266.1724, found *m/z* 266.1738.

1,1-Difluoro-3-isopropyl-5-aza-1-borasp[4.4]nonane (3c)



The title compound was obtained in 78% yield (31 mg, 0.15 mmol).

¹H NMR (500 MHz, CDCl₃) δ 3.49 – 3.43 (m, 2H, **H**_{5,8}), 2.82 – 2.75 (m, 1H, **H**₅), 2.73 – 2.63 (m, 1H, **H**₄), 2.53 (d, *J* = 9.0 Hz, 1H, **H**₈), 2.19 – 2.13 (m, 1H, **H**₄), 2.12 – 2.01 (m, 1H, **H**₆), 1.99 – 1.86 (m, 2H, **H**_{6,7}), 1.67 – 1.67 (m, 2H, **H**₇, **H**₂), 1.45 – 1.33 (m, 1H, **H**₁), 0.93 (d, *J* = 6.6 Hz, 3H, **H**₁₀), 0.89 – 0.86 (m, 1H, **H**₃), 0.86 (d, *J* = 6.6 Hz, 3H, **H**₉), 0.37 – 0.24 (m, 1H, **H**₃).

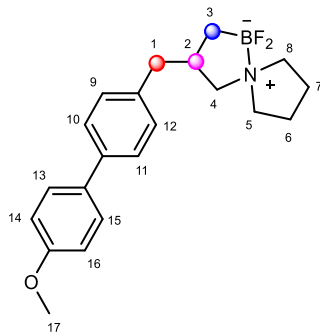
¹³C NMR (126 MHz, CDCl₃) δ 64.6, 54.8 (2C), 41.4, 33.6, 23.24, 23.4, 20.8 (2C), 17.1.

¹¹B NMR δ 9.4 ppm.

IR (film) ν_{max} : 2959, 2876, 1464, 1351, 1228, 1057, 787, 653, 614, 511 cm⁻¹.

HRMS (ESI, *m/z*): calculated for [M + H]⁺ C₁₀H₂₂BNO₂ requires *m/z* 200.18183, found *m/z* 200.18258.

1,1-Difluoro-3-((4'-methoxy-[1,1'-biphenyl]-4-yl)methyl)-5-aza-1-borasp[iro][4.4]nonane (3d)



The title compound was obtained in 70% yield (45 mg, 0.13 mmol).

^1H NMR (500 MHz, CDCl_3) δ 7.51 (dd, $J = 6.6, 2.0$ Hz, 2H, ArH), 7.47 (dd, $J = 8.1, 2.8$ Hz, 2H, ArH), 7.21 (d, $J = 8.1$ Hz, 2H, ArH), 7.00 – 6.93 (m, 2H, ArH), 3.85 (s, 3H, H_{17}), 3.53 – 3.40 (m, 2H, $\text{H}_{5,8}$), 2.90 – 2.76 (dd, $J = 13.2, 5.5$ Hz, 1H, H_4), 2.77 – 2.62 (m, 3H, H_1, H_5), 2.55 (dd, $J = 13.2, 8.3$ Hz, 1H, H_4), 2.52 – 2.40 (m, 1H, H_8), 2.33 – 2.22 (m, 1H, H_2), 2.08 – 1.93 (m, 2H, $\text{H}_{6,7}$), 1.94 – 1.80 (m, 2H, $\text{H}_{6,7}$), 0.89 – 0.76 (m, 1H, H_3), 0.47 – 0.35 (m, 1H, H_3).

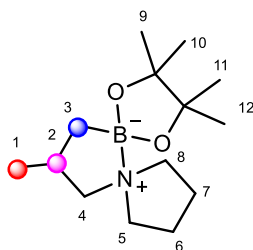
^{13}C NMR (126 MHz, CDCl_3) δ 159.2, 139.1, 138.6, 133.6, 129.2 (2C), 128.1 (2C), 126.8 (2C), 114.3 (2C), 65.5, 55.4, 54.8, 54.7, 42.3, 36.0, 23.3, 23.1, 20.0.

^{11}B NMR δ 9.5 ppm.

IR (film) ν_{max} : 2923, 2853, 1609, 1498, 1349, 1189, 1139, 1057, 816, 597, 514 cm^{-1} .

HRMS (ESI, m/z): calculated for $[\text{M} + \text{H}]^+$ $\text{C}_{21}\text{H}_{28}\text{BNO}_3$ requires m/z 354.22388, found m/z 354.22475.

1-(2-Methyl-3-(4,4,5,5-tetramethyl-1,3,2-dioxaborolan-2-yl)propyl)pyrrolidine (**3f**)



The title compound **3f** was prepared by adding **2a** (450 mg, 3.24 mmol), pinacol (459 mg, 3.88 mmol) and xylenes (16 mL) into a flask equipped with a stir bar. The reaction mixture was refluxed for 16 h. Once completed, the solvent was removed under reduced pressure and the title compound **3f** was obtained as pale-yellow oil in 96% yield (787 mg, 3.11 mmol).

¹H NMR (500 MHz, CDCl₃) δ 2.62 – 2.57 (m, 4H, **H**_{5,8}), 2.39 – 2.32 (m, 1H, **H**₄), 2.16 (dd, *J* = 11.4, 8.0 Hz, 1H, **H**₄), 1.93 – 1.83 (m, 1H, **H**₂), 1.82 – 1.76 (m, 4H, **H**_{6,7}), 1.21 (s, 12H, **H**_{9,10,11,12}), 0.97 (d, *J* = 6.6 Hz, 3H, **H**₁), 0.78 – 0.65 (m, 2H, **H**₃).

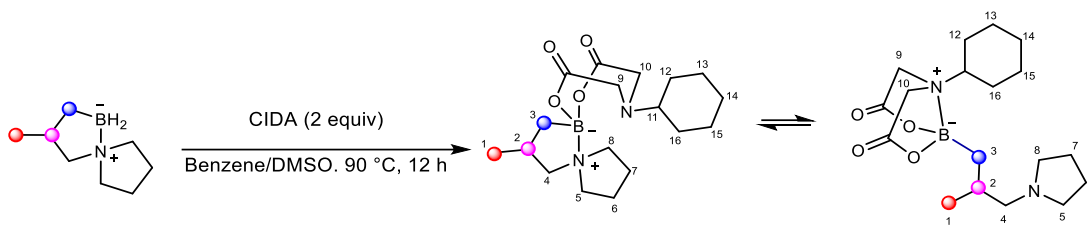
¹³C NMR (126 MHz, CDCl₃) δ 82.2 (2C), 66.7, 54.8, 29.4, 25.24 (2C), 25.20 (2C), 24.9, 24.6, 23.6, 21.2, 20.3.

¹¹B NMR δ 29.8 ppm.

IR (film) ν_{max} : 2974, 2873, 2782, 1476, 1368, 1313, 1211, 1144, 970, 886, 847 cm⁻¹.

HRMS (ESI, *m/z*): calculated for [M + H]⁺ C₁₄H₂₈BNO₂ requires *m/z* 254.2289, found *m/z* 254.2291.

6-Cyclohexyl-2-(2-methyl-3-(pyrrolidin-1-yl)propyl)-1,3,6,2-dioxazaborocane-4,8-dione (3g)



The Cyclohexyliminodiacetic acid (CIDA) derivative was prepared according to literature procedure.⁶

SCAB **2a** (100 mg, 719 μmol) was added to a dried round bottom flask containing benzene (5 mL), DMSO (2.5 mL) and the CIDA ligand (310 mg, 1.44 mmol). The reaction mixture was refluxed at 95 °C for 12 h. The reaction mixture was then diluted with brine (10 mL) and was extracted with EtOAc (3 X 10 mL). The organic layers were separated, dried with anhydrous Na_2SO_4 , filtered, and concentrated under reduced pressure. The residue was transferred into a 20 mL vial and prepared for lyophilization. Lyophilization procedure: 10 drops of H_2O were added to the vial and the solution was allowed to freeze in an ice bath (ice bath = acetone/dry ice). Lyophilization provided **3g** as a white solid in 67% yield (176 mg, 0.48 mmol).

^1H NMR (500 MHz, Acetone) δ 4.13 (dd, $J = 16.8, 11.8$ Hz, 2H, **H₉**), 3.84 (dd, $J = 30.2, 16.8$ Hz, 2H, **H₁₀**), 3.46 – 3.30 (m, 1H, **H₁₁**), 2.43 – 2.34 (m, 1H, **H₄**), 2.33 – 2.25 (m, 1H, **H₄**), 2.10 – 2.01 (m, 1H, **H₅**), 1.92 – 1.83 (m, 4H, **H₂**, **H₆**, **H_{C-hexyl}**), 1.82 – 1.70 (m, 5H, **H₅**, **H_{C-hexyl}**), 1.67 – 1.63 (m, 1H, **H₈**), 1.63 – 1.53 (m, 1H, **H_{C-hexyl}**), 1.53 – 1.45 (m, 1H, **H_{C-hexyl}**), 1.42 – 1.32 (m, 2H, **H_{6,7}**), 1.32 – 1.21 (m, 3H, **H₆**, **H_{C-hexyl}**), 1.13 – 1.05 (m, 1H, **H₇**), 0.99 (d, $J = 6.6$ Hz, 3H, **H₁**), 0.91 – 0.82 (m, 1H, **H₃**), 0.38 (dd, $J = 14.3, 9.2$ Hz, 1H, **H₃**).

^{13}C NMR (126 MHz, CDCl_3) δ 169.7, 169.0, 66.1, 63.3, 57.4, 57.2, 55.9, 54.7 (2C), 30.0, 29.9, 25.5, 26.4, 25.6, 25.5, 24.1, 21.7, 21.0.

^{11}B NMR δ 13.1 ppm.

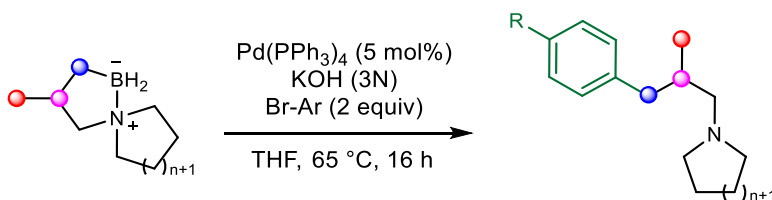
IR (film) ν_{max} : 3307, 2941, 2856, 1717, 1588, 1366, 1305, 1241, 1103, 975, 869, 720, 516, 424 cm^{-1} .

HRMS (ESI, m/z): calculated for $[\text{M} + \text{H}]^+$ $\text{C}_{18}\text{H}_{31}\text{BN}_2\text{O}_4$ requires m/z 351.2450, found m/z 351.2443.

mp: 67–68 °C.

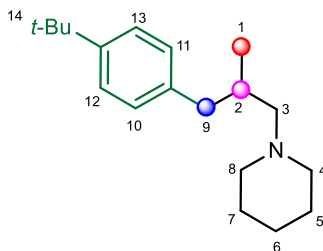
C–C bond formation

Suzuki-Miyaura Cross-Coupling



Tetrakis(triphenylphosphine)palladium(0) (5 mol%) was added to a microwave reaction vial followed by addition of degassed THF (654 μL). The reaction mixture was degassed and purged with nitrogen for 5 min. The required **CAB** (~ 0.3 mmol) was taken up in degassed THF (1.3 mL) and added to the vial while purging. To the vial was then added 720 μL of 3 N KOH followed by 1-bromo-4-*tert*-butylbenzene or bromobenzene (2 equiv). The vial was sealed, and the reaction mixture was heated at 65 °C for 16 h. After cooling down, water was added to the reaction mixture and the mixture was transferred into a separatory funnel. The organic layer was separated, and the aqueous layer was extracted with EtOAc (3 x 5 mL). The combined organic layers were dried over anhydrous Na_2SO_4 , filtered and concentrated under reduced pressure. The excess bromobenzene was distilled off and the residue was filtered over silica in a solution of 1% Et_3N /hexanes providing the title compound.

1-(3-(4-(*tert*-Butyl)phenyl)-2-methylpropyl)piperidine (**3h**):



The title compound was obtained as a pale-yellow oil in 85% yield (76 mg, 0.28 mmol).

$^1\text{H NMR}$ (500 MHz, CDCl_3) δ 7.28 (d, $J = 8.3$ Hz, 2H, ArH), 7.08 (d, $J = 8.2$ Hz, 2H, ArH), 2.78 (dd, $J = 13.1, 5.6$ Hz, 1H, H_9), 2.56 – 2.38 (br, 3H, $\text{H}_{4,8}$, H_3), 2.37 – 2.27 (m, 3H, H_9 , H_4 , H_3), 2.25 (br, 1H,

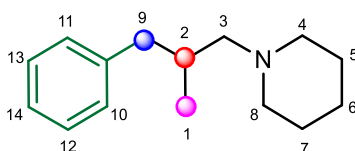
H_8), 2.12 – 1.96 (m, 1H, H_2), 1.72 – 1.58 (br, 4H, $\text{H}_{5,7}$), 1.49 – 1.40 (m, 2H, H_6), 1.31 (s, 9H, H_{14}), 0.99 – 0.83 (m, 3H, H_1).

^{13}C NMR (126 MHz, CDCl_3) δ 148.7, 129.4, 129.0 (2C), 125.2 (2C), 65.3, 54.8, 41.1 (2C), 34.5, 32.2, 31.6 (3C), 25.4 (2C), 24.2, 18.7.

IR (film) ν_{max} : 2933, 2867, 2523, 1456, 1363, 1269, 1108, 856, 734, 572 cm^{-1} .

HRMS (ESI, m/z): calculated for $[\text{M} + \text{H}]^+$ $\text{C}_{19}\text{H}_{31}\text{N}$ requires m/z 274.2529, found m/z 274.2522.

1-(2-Methyl-3-phenylpropyl)piperidine (3i)



The title compound was obtained in 91% isolate yield (65 mg, 0.29 mmol) as a pale-yellow oil.

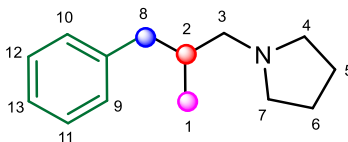
^1H NMR (400 MHz, CDCl_3) δ 7.26 – 7.33 (m, 2H, ArH), 7.24 – 7.15 (m, 3H, ArH), 3.01 – 2.89 2.85 (dd, $J = 13.4, 4.9$ Hz, 1H, H_9), 2.51 – 2.39 (m, 3H, $\text{H}_{4,8}, \text{H}_9$), 2.37 – 2.29 (m, 2H, H_3), 2.27 – 2.12 (m, 2H, $\text{H}_{4,8}$), 2.11 – 1.98 (m, 1H, H_2), 1.71 – 1.58 (m, 4H, $\text{H}_{5,7}$), 1.53 – 1.41 (m, 2H, H_6), 0.91 (d, $J = 6.3$ Hz, 3H, H_1).

^{13}C NMR (126 MHz, CDCl_3) δ 132.3, 129.4 (2C), 128.3 (2C), 64.9, 54.8 (2C), 41.7 (2C), 32.3, 29.4, 24.2, 24.0, 18.7.

IR (film) ν_{max} : 2930, 2852, 1376, 1301, 1119, 1058, 974, 740, 698 cm^{-1} .

HRMS (ESI, m/z): calculated for $[\text{M} + \text{H}]^+$ $\text{C}_{15}\text{H}_{23}\text{N}$ requires m/z 218.1903, found m/z 274.1894.

1-(2-Methyl-3-phenylpropyl)pyrrolidine (3j)



The title compound was obtained in 92% isolate yield (67 mg, 0.33 mmol) as a pale-yellow oil.

¹H NMR (400 MHz, CDCl₃) δ 7.32 – 7.27 (m, 2H, ArH), 7.25 – 7.09 (m, 3H, ArH), 2.84 (dd, *J* = 13.5, 5.8 Hz, 1H, **H₃**), 2.81 – 2.69 (m, 4H, **H_{4,7}**), 2.61 – 2.49 (m, 2H, **H₈**), 2.45 (dd, *J* = 13.5, 8.3 Hz, 1H, **H₃**), 2.13 – 2.00 (m, 1H, **H₂**), 1.98 – 1.86 (m, 4H, **H_{5,6}**), 1.03 (d, *J* = 6.6 Hz, 3H, **H₁**).

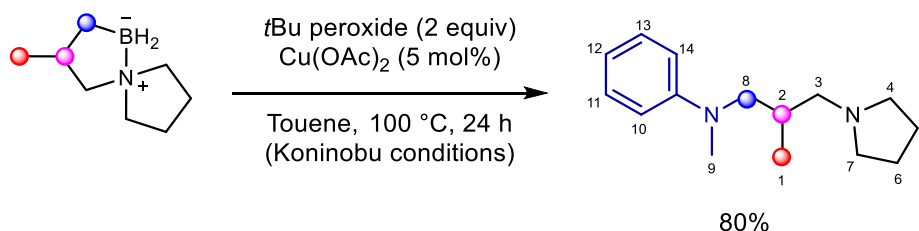
¹³C NMR (126 MHz, CDCl₃) δ 141.0, 129.4 (2C), 128.5 (2C), 125.9, 63.2, 54.6 (2C), 41.7, 34.4, 23.6 (2C), 18.5.

IR (film) ν_{max} : 2956, 2924, 2784, 1602, 1453, 1082, 740, 699 cm⁻¹.

HRMS (ESI, *m/z*): calculated for [M + H]⁺ C₁₄H₂₁N requires *m/z* 204.1747, found *m/z* 204.1741.

Chan-Lam Coupling

N-Methyl-*N*-(2-methyl-3-(pyrrolidin-1-yl)propyl)aniline (**3k**)



A mixture of *N*-methylaniline (58.4 μL , 539 μmol), copper (II) acetate, anhydrous (32.7 mg, 180 μmol), **2a** (50.0 mg, 360 μmol), di-*t*-butyl peroxide, 98% (131 μL , 716 μmol), and toluene (719 μL) was stirred at 100 °C for 24 h in a sealed tube. Once the reaction was completed, the solvent was removed under reduced pressure. The product was isolated by column chromatography on silica gel (1% Et_3N in 1:9 EtOAc :Hexanes). The title compound **3k** was obtained as a dark yellow oil in 80% yield (67 mg, 0.29 mmol).

$^1\text{H NMR}$ (400 MHz, CDCl_3) δ 7.26 – 7.16 (m, 2H, ArH), 6.73 – 6.62 (m, 3H, ArH), 3.43 (dd, $J = 14.6$, 5.8 Hz, 1H, H_8), 3.03 (dd, $J = 14.6$, 8.1 Hz, 1H, H_8), 2.96 (s, 3H, H_9), 2.57 – 2.42 (m, 4H, $\text{H}_{4,7}$), 2.44 – 2.26 (m, 2H, H_3), 2.18 – 2.08 (m, 1H, H_2), 1.87 – 1.74 (m, 4H, $\text{H}_{5,6}$), 0.99 (d, $J = 6.6$ Hz, 3H, H_1).

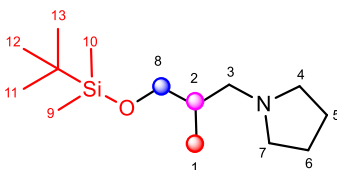
$^{13}\text{C NMR}$ (126 MHz, CDCl_3) δ 149.8, 129.2 (2C), 115.9, 112.1 (2C), 61.5, 58.2, 54.8 (2C), 39.7, 32.1, 23.7 (2C), 17.5.

IR (film) ν_{max} : 2957, 2904, 2785, 1597, 1505, 1370, 1032, 744, 690 cm^{-1} .

HRMS (ESI, m/z): calculated for $[\text{M} + \text{H}]^+$ $\text{C}_{15}\text{H}_{24}\text{N}_2$ requires m/z 233.2012, found m/z 233.2016.

Oxidation

1-(3-((*tert*-Butyldimethylsilyloxy)-2-methylpropyl)pyrrolidine (3l)



Into a dry microwave vial was added **2a** (50 mg, 0.36 mmol), 2 N aq. NaOH (2.2 mL), and aq. 35% H₂O₂ (1.27 mL) in THF (1.8 mL). The mixture was stirred for 12 h at 60 °C. The mixture was then filtered over a short pad of silica and washed with 1% Et₃N/CH₂Cl₂ (4 x 5 mL). The solvent was evaporated, and the residue was taken up in CH₂Cl₂ (816 μL) and transferred in a microwave vial. Imidazole, 99% (22.2 mg, 0.33 mmol) was added to a flask and stirred for 10 min after which *tert*-butyldimethylchlorosilane (54 mg, 0.36 mmol) and a white slurry was formed. The mixture was allowed to stir for 30 min. The solvent was then removed under reduced pressure. The product was obtained in 77% yield (69 mg, 0.25 mmol) as a clear oil.

¹H NMR (500 MHz, CDCl₃) δ 3.56 (dd, *J* = 9.9, 5.1 Hz, 1H, **H₈**), 3.51 – 3.41 (dd, *J* = 9.5, 5.3 Hz, 1H, **H₈**), 3.04 – 2.88 (m, 3H, **H_{4,7}**, **H₃**), 2.86 – 2.76 (m, 2H, **H₃**, **H₄**), 2.67 – 2.55 (m, 1H, **H₇**), 1.98 – 1.94 (m, 4H, **H_{5,6}**, **H₂**), 1.65 – 1.50 (m, 1H, **H₆**), 1.09 (d, *J* = 6.5 Hz, 3H, **H₁**), 0.88 (s, 9H, **H_{11,12,13}**), 0.08 – 0.05 (s, 6H, **H_{9,10}**).

¹³C NMR (126 MHz, CDCl₃) δ 66.4 (2C), 59.8 (2C), 54.7, 29.8, 25.0, 23.6 (3C), 18.4, 16.1, -5.3 (2C).

IR (film) ν_{max} : 2954, 2926, 2854, 1462, 1255, 1088, 1036, 835, 775 cm⁻¹.

HRMS (ESI, *m/z*): calculated for [M + H]⁺ C₁₄H₃₁NOSi requires *m/z* 258.2240, found *m/z* 258.2247.

Structural Assignments of New Compounds

To determine the regioselectivity, we sought the use of **1e** with a phenyl substitution on C1 to differentiate between the three cyclopropane C–C bonds. A substitution at C1 would allow differentiation of C1–C2, C1–C3 or C2–C3 bond cleavage (**Fig. 2**).

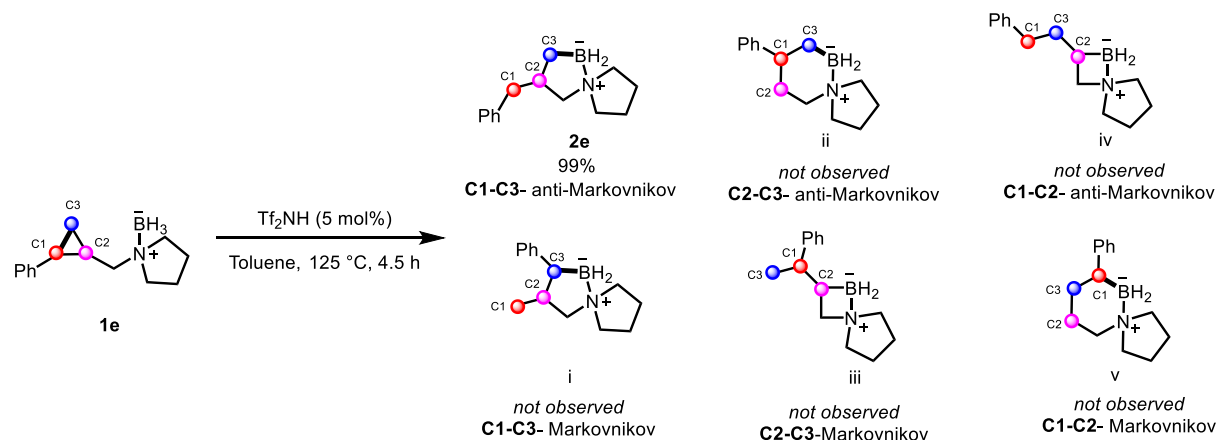


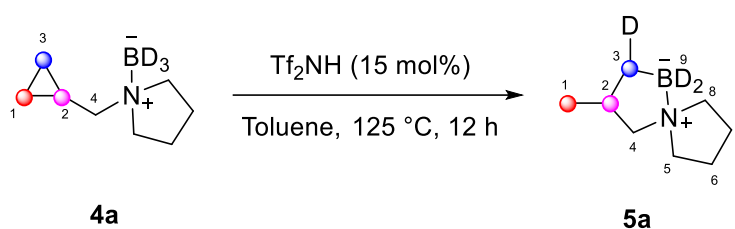
Figure A1: Possible regioisomers of disubstituted CABs

Absolute selectivity for the anti-Markovnikov product from the activation of the distal C1–C3 bond was observed providing **2e** and no Markovnikov product was observed (**Fig. S1, i**). No activation of the C2–C3 carbon leading to either the anti-Markovnikov 6–5 ring system (**Fig. S1, ii**) or the highly strained Markovnikov product (**Fig. S1, iii**) was observed. There was also no experimental evidence that would allude to the cleavage of the C1–C2 bond (**Fig. S1, iv and v**).

Mechanistic Studies Using Deuterium Experiments

Deuterium experiments were designed to gain mechanistic insight of the CAB to SCAB transformation. A deuterated derivative of CAB **1a** was synthesized with its BH₃ moiety replaced with BD₃. A second experiment was designed where C₄ (CH₂) of **1a** was replaced with a CD₂ moiety.

Deuterium experiment with a BD₃ moiety (**4a**)

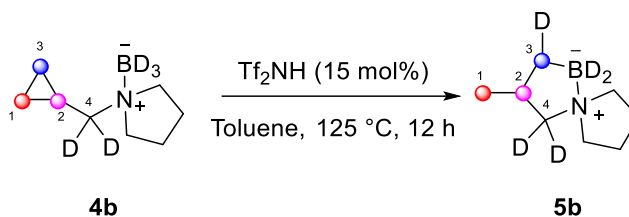


Scheme A1: Transformation to SCAB **5a**

The deuterated CAB **4a** was prepared according to general procedure A-C. In general procedure C, the amide was first reduced to the amine using LAH using the following procedure. LAH (240 mg, 6.3 mmol) was added to a flame dried flask followed by the addition of THF (14 mL). The slurry was allowed to stir for 10 minutes and then cooled to -5 °C. The cyclopropyl(pyrrolidin-1-yl)methanone (400 mg, 2.9 mmol) was dissolved in THF (4 mL) and was added in a dropwise manner to the stirring slurry at -5 °C over 5 minutes. The mixture was brought to room temperature and allowed to reflux overnight. The mixture was cooled to 0 °C and 2 g of sodium sulfate decahydrate was added in small portions until no hydrogen evolution was observed. The mixture was stirred for 15 minutes and decanted with ether (50 mL). The filtrate was evaporated under reduced pressure to obtain the amine as a brown oil. The oil was then dissolved in THF (5 mL) and transferred to a 20 mL microwave vial. BD₃•THF (1.5 equiv) was added dropwise to the stirring solution and refluxed for 12 h. CAB **4a** was obtained in 59% isolated yield. Synthesis of **5a**: CAB **4a** (52.0 mg, 0.363 mmol) was added to a microwave vial followed by the addition of Tf₂NH (15.0 mg, 0.055 mmol) and Toluene (825 μ L). The vial was sealed, and the reaction was heated

for 12 h after which the reaction mixture was cooled, and the solvent was evaporated. An NMR of the crude reaction mixture was taken and full conversion to SCAB **5a** was obtained.

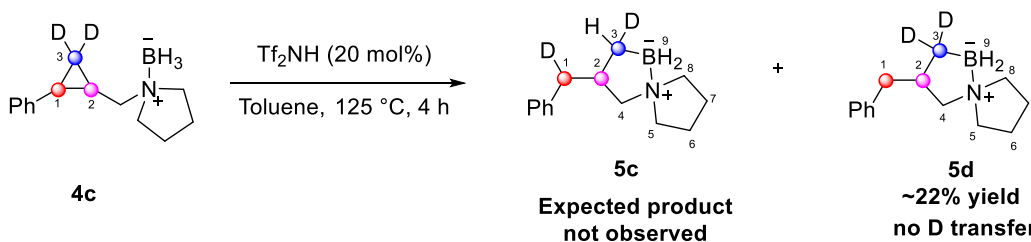
Deuterium experiment with a D₂ on C4 and BD₃ moiety (**4b**)



Scheme A2: Transformation to SCAB **5b**

The deuterated CAB **4b** was prepared according to general procedure A-C. In general procedure C, BH₃•THF was replaced with BD₃•THF. Synthesis of **5b**: CAB **4b** (51.0 mg, 0.354 mmol) was added to a microwave vial followed by the addition of Tf₂NH (15.0 mg, 0.053 mmol) and Toluene (804 μ L). The vial was sealed, and the reaction was heated for 12 h after which the reaction mixture was cooled, and the solvent was evaporated. An NMR of the crude reaction mixture was taken and full conversion to SCAB **5b** was obtained.

Deuterium experiment with D₂ on C3 (**4c**)



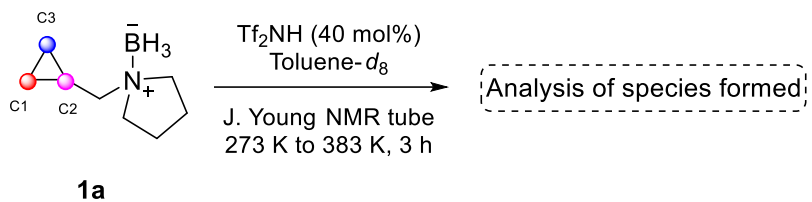
Scheme A3: Transformation to SCAB **5d**

The deuterated CAB **4c** was synthesized according to General procedure A-C. In general procedure A, CH₂I₂ was replaced with CD₂I₂ and no dioxaborolane ligand was used. The reaction was done on a 4.5 mmol scale. Synthesis of **5d**: CAB **4c** (30.0 mg, 0.14 mmol) was added to a microwave vial followed by the addition of Tf₂NH (7.8 mg, 0.03 mmol) and Toluene (314 μ L). The vial was sealed, and the reaction was heated for 4 h after which the reaction mixture was cooled,

and the solvent was evaporated. An NMR of the crude reaction mixture was taken and the presence of CAB **4c** and CAB **5b** was observed. Purification by silica gel chromatography resulted in the pure SCAB **5b** in 22% yield (6.5 mg, 0.03 mmol)

Variable Temperature NMR Experiment

To gain insight into the activated species forming in our reaction we conducted a variable temperature NMR experiment. To a J. Young NMR tube was added CAB **1a** (32.4 mg, 0.23 mmol) and Tf₂NH (26.2 mg, 0.093 mmol) (Scheme A4). Toluene-*d*₈ was added to the NMR tube and the sample was shaken for 5 minutes. A ¹⁹F, ¹¹B, ¹¹B [H] (boron NMR decoupled from proton), and ¹H NMR spectrum was collected at five different temperatures between 298 K and 383 K over 3 h.



Scheme A4: Variable temperature NMR experiment

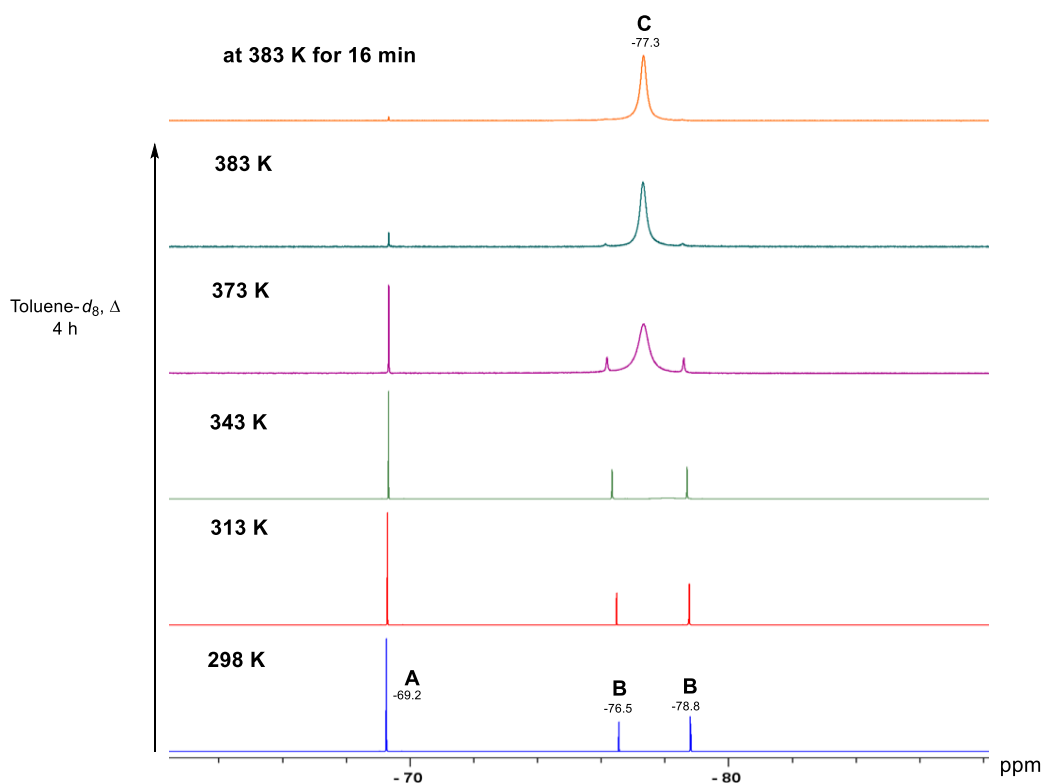
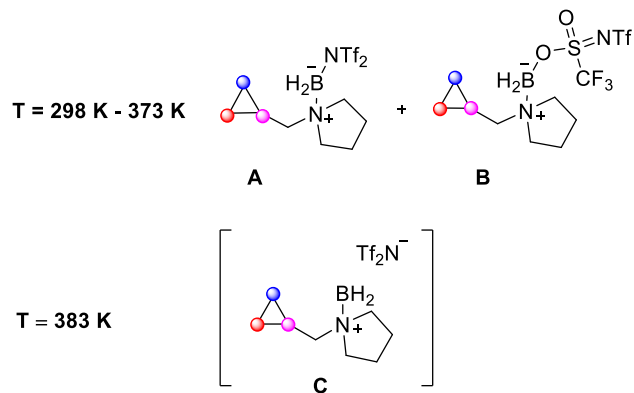


Figure A2: ^{19}F NMR spectra at varying temperatures

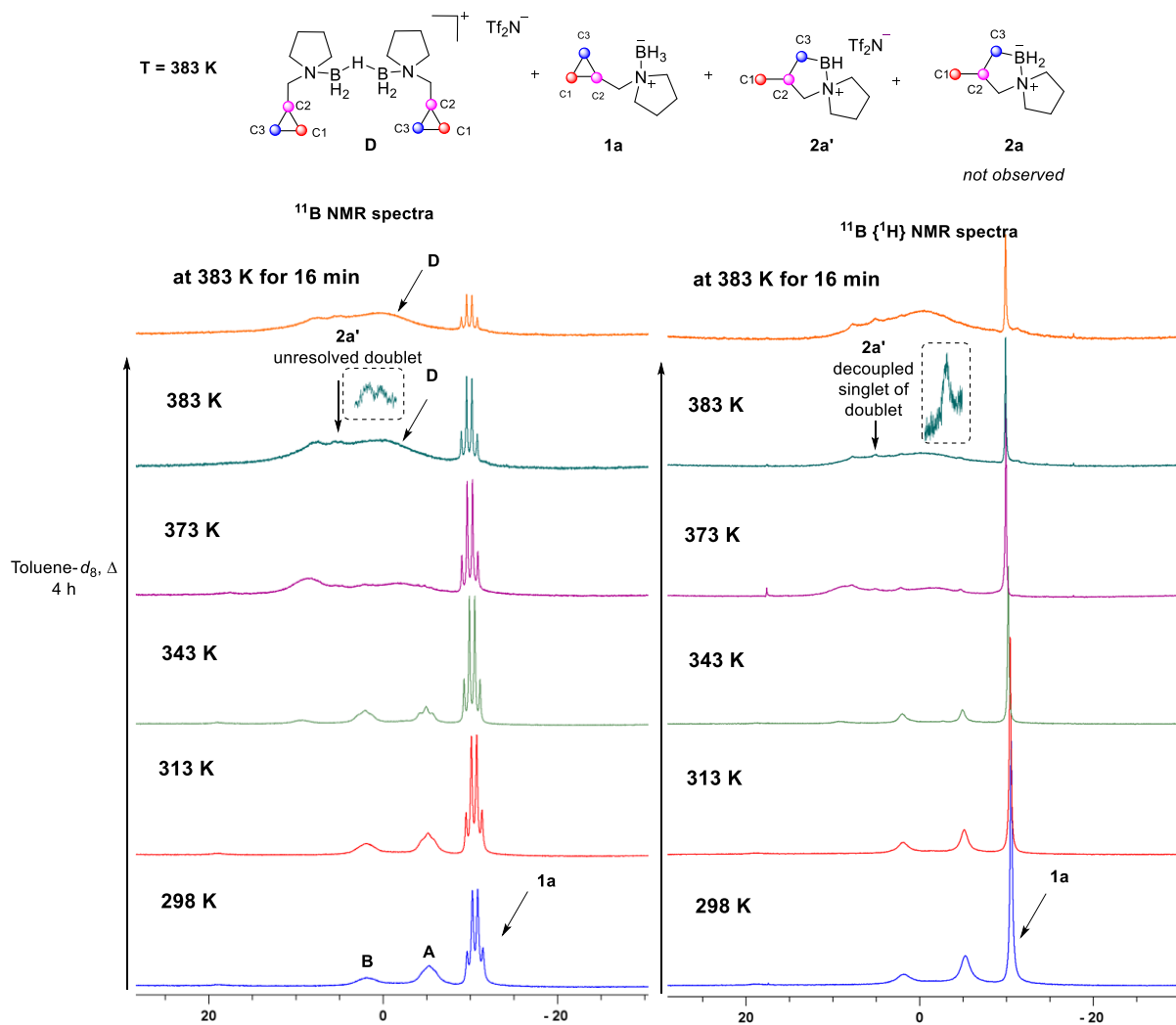
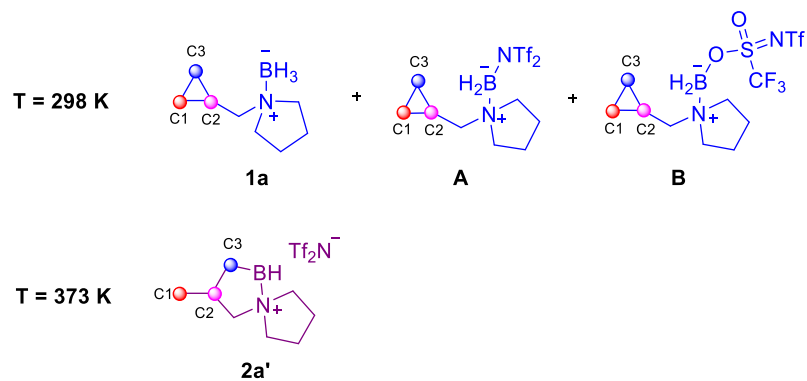


Figure A3: ^{11}B NMR spectra at varying temperatures

i. Structure of species observed in ^1H NMR analysis at different temperature



ii. Variable temperature experiment (^1H NMR spectra)

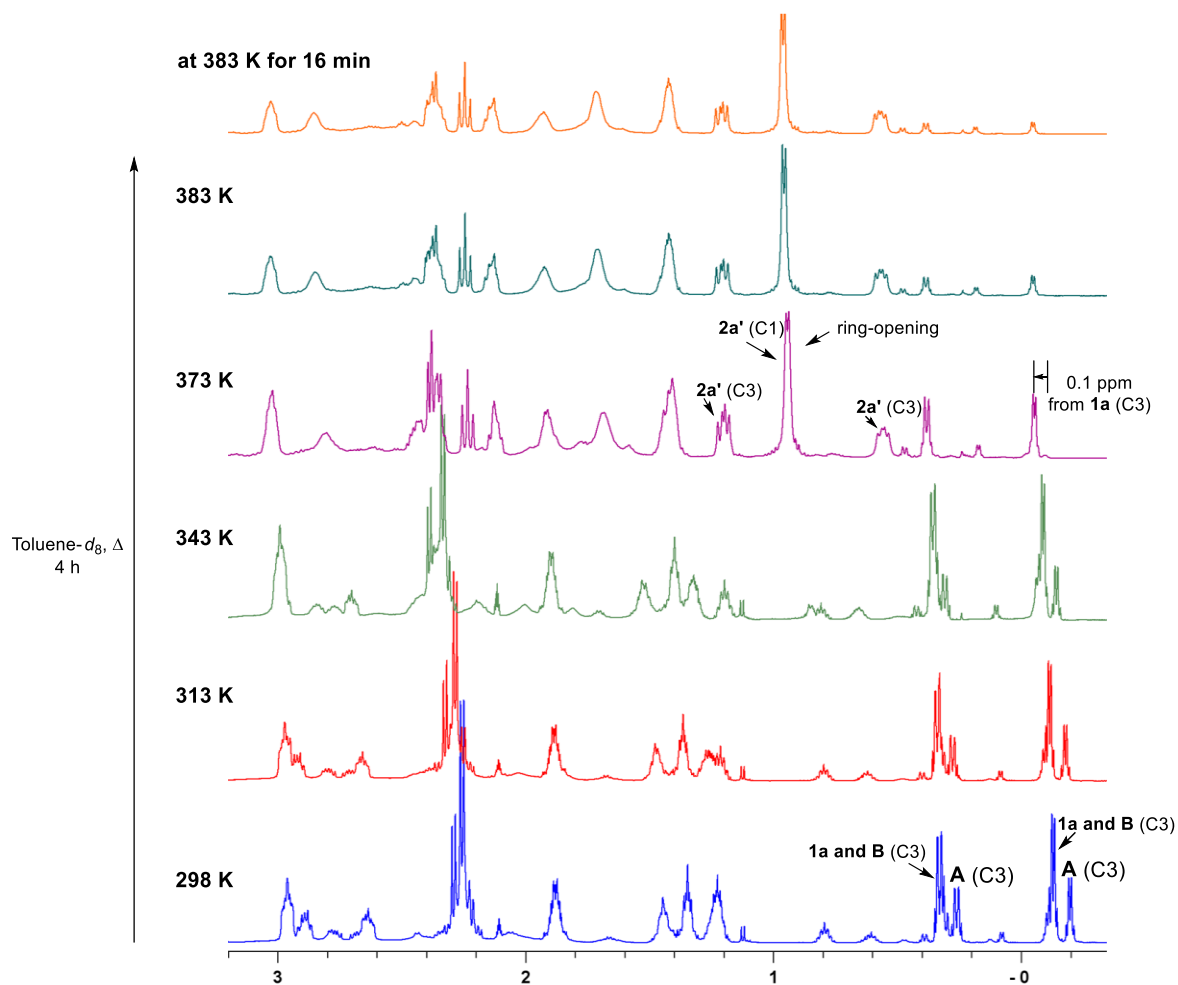


Figure A4: ^1H NMR spectra at varying temperatures

X-ray Crystallography Data

1-((2-(*p*-Tolyl)cyclopropyl)methyl)pyrrolidine borane (1q):

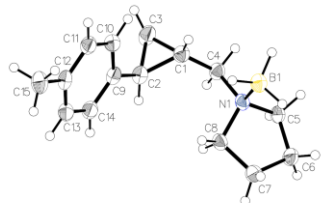


Table 1 Crystal data and structure refinement for saher10.

Identification code	saher10
Empirical formula	C ₁₅ H ₂₄ BN
Formula weight	229.16
Temperature/K	100
Crystal system	monoclinic
Space group	P2 ₁ /n
a/Å	5.7339(2)
b/Å	11.6824(4)
c/Å	20.5876(7)
α/°	90
β/°	92.341(2)
γ/°	90
Volume/Å ³	1377.92(8)
Z	4
ρ _{calc} /cm ³	1.105
μ/mm ⁻¹	0.458
F(000)	504.0
Crystal size/mm ³	0.15 × 0.04 × 0.02
Radiation	CuKα (λ = 1.54178)
2θ range for data collection/°	8.596 to 140.12
Index ranges	-6 ≤ h ≤ 6, -14 ≤ k ≤ 14, -25 ≤ l ≤ 25
Reflections collected	18518
Independent reflections	2597 [R _{int} = 0.0567, R _{sigma} = 0.0362]
Data/restraints/parameters	2597/0/167
Goodness-of-fit on F ²	1.058
Final R indexes [I ≥ 2σ (I)]	R ₁ = 0.0563, wR ₂ = 0.1495
Final R indexes [all data]	R ₁ = 0.0624, wR ₂ = 0.1583
Largest diff. peak/hole / e Å ⁻³	0.40/-0.24

3-(4-Methylbenzyl)-5-aza-1-borasp[4.4]nonane (2q):

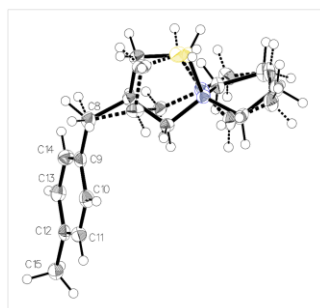


Table 1 Crystal data and structure refinement for saher92.

Identification code	saher92
Empirical formula	C ₁₅ H ₂₄ BN
Formula weight	229.16
Temperature/K	100
Crystal system	monoclinic
Space group	P2 ₁ /n
a/Å	11.3630(5)
b/Å	6.1934(3)
c/Å	19.5336(9)
α/°	90
β/°	96.729(2)
γ/°	90
Volume/Å ³	1365.22(11)
Z	4
ρ _{calc} /g/cm ³	1.115
μ/mm ⁻¹	0.463
F(000)	504.0
Crystal size/mm ³	0.39 × 0.18 × 0.1
Radiation	CuKα (λ = 1.54178)
2θ range for data collection/°	8.59 to 140.172
Index ranges	-13 ≤ h ≤ 13, -7 ≤ k ≤ 6, -23 ≤ l ≤ 23
Reflections collected	25123
Independent reflections	2548 [R _{int} = 0.0240, R _{sigma} = 0.0116]
Data/restraints/parameters	2548/295/237
Goodness-of-fit on F ²	1.037
Final R indexes [I >= 2σ(I)]	R ₁ = 0.0427, wR ₂ = 0.1138
Final R indexes [all data]	R ₁ = 0.0437, wR ₂ = 0.1171
Largest diff. peak/hole / e Å ⁻³	0.24/-0.26

9-Phenyl-5-aza-6-borasp[iro[4.5]decane (2z):

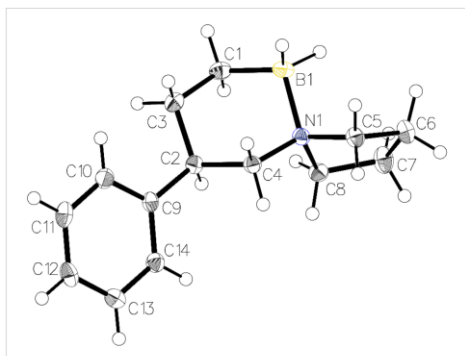


Table 1 Crystal data and structure refinement for saher12.

Identification code	saher12
Empirical formula	C ₁₄ H ₂₂ BN
Formula weight	215.13
Temperature/K	100
Crystal system	monoclinic
Space group	P2 ₁ /c
a/Å	9.2915(4)
b/Å	12.2620(5)
c/Å	11.2292(5)
α/°	90
β/°	102.9850(10)
γ/°	90
Volume/Å ³	1246.65(9)
Z	4
ρ _{calc} /cm ³	1.146
μ/mm ⁻¹	0.477
F(000)	472.0
Crystal size/mm ³	0.34 × 0.34 × 0.17
Radiation	CuKα (λ = 1.54178)
2θ range for data collection/°	9.768 to 140.276
Index ranges	-11 ≤ h ≤ 10, -14 ≤ k ≤ 14, -13 ≤ l ≤ 13
Reflections collected	24226
Independent reflections	2360 [R _{int} = 0.0273, R _{sigma} = 0.0153]
Data/restraints/parameters	2360/0/153
Goodness-of-fit on F ²	1.026
Final R indexes [I >= 2σ (I)]	R ₁ = 0.0420, wR ₂ = 0.1097
Final R indexes [all data]	R ₁ = 0.0422, wR ₂ = 0.1100
Largest diff. peak/hole / e Å ⁻³	0.31/-0.21

1-(((1*S*,2*S*)-2-Methyl-2-phenylcyclopropyl)methyl)pyrrolidine borane (1ab):

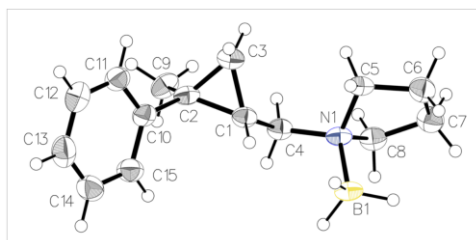


Table 1 Crystal data and structure refinement for saher11(2).

Identification code	saher11(2)
Empirical formula	C ₁₅ H ₂₄ BN
Formula weight	229.16
Temperature/K	100
Crystal system	monoclinic
Space group	P2 ₁
a/Å	6.0342(4)
b/Å	9.9763(6)
c/Å	11.9260(7)
α/°	90
β/°	96.777(3)
γ/°	90
Volume/Å ³	712.92(8)
Z	2
ρ _{calc} /cm ³	1.068
μ/mm ⁻¹	0.443
F(000)	252.0
Crystal size/mm ³	0.16 × 0.14 × 0.01
Radiation	CuKα (λ = 1.54178)
2θ range for data collection/°	7.464 to 144.276
Index ranges	-7 ≤ h ≤ 6, -12 ≤ k ≤ 12, -14 ≤ l ≤ 14
Reflections collected	18267
Independent reflections	2726 [R _{int} = 0.0355, R _{sigma} = 0.0177]
Data/restraints/parameters	2726/4/165
Goodness-of-fit on F ²	1.028
Final R indexes [I >= 2σ (I)]	R ₁ = 0.0491, wR ₂ = 0.1309
Final R indexes [all data]	R ₁ = 0.0499, wR ₂ = 0.1322
Largest diff. peak/hole / e Å ⁻³	0.28/-0.19
Flack parameter	-0.2(7)

3-((S)-1-Phenylethyl)-5-aza-1-borasp[4.4]nonane (2ab):

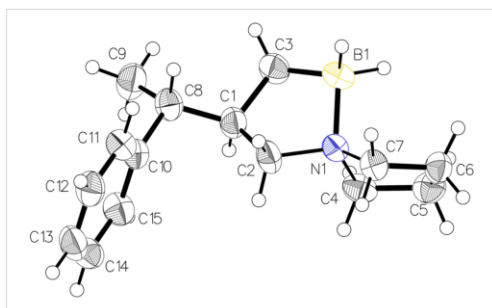


Table 1 Crystal data and structure refinement for ABC-SHS-2671 / SAHER40(2).

Identification code	ABC-SHS-2671 / SAHER40(2)
Empirical formula	C ₁₅ H ₂₄ BN
Formula weight	229.16
Temperature/K	150
Crystal system	monoclinic
Space group	P2 ₁
a/Å	6.1145(5)
b/Å	11.6448(10)
c/Å	9.8210(8)
α/°	90
β/°	91.035(6)
γ/°	90
Volume/Å ³	699.16(10)
Z	2
ρ _{calc} /cm ³	1.089
μ/mm ⁻¹	0.288
F(000)	252.0
Crystal size/mm ³	0.13 × 0.06 × 0.03
Radiation	Ga Kα (λ = 1.34139)
2θ range for data collection/°	7.834 to 109.886
Index ranges	-7 ≤ h ≤ 7, -12 ≤ k ≤ 13, -11 ≤ l ≤ 11
Reflections collected	5187
Independent reflections	2336 [R _{int} = 0.0818, R _{sigma} = 0.1100]
Data/restraints/parameters	2336/2/164
Goodness-of-fit on F ²	1.076
Final R indexes [I ≥ 2σ (I)]	R ₁ = 0.0651, wR ₂ = 0.1351
Final R indexes [all data]	R ₁ = 0.1170, wR ₂ = 0.1548
Largest diff. peak/hole / e Å ⁻³	0.24/-0.21
Flack parameter	-1.2(19)

1,4-Bis(cyclopropylmethyl)piperazine borane (1ac):

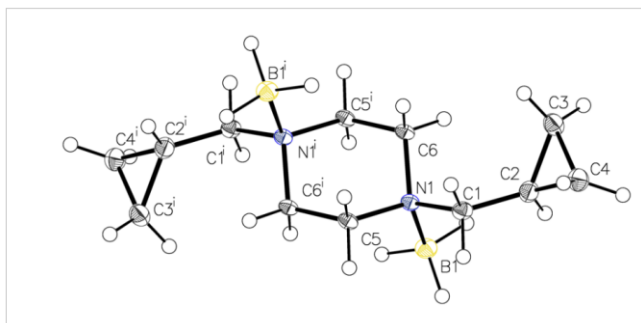


Table 1 Crystal data and structure refinement for saher161.

Identification code	saher161
Empirical formula	C ₁₂ H ₂₈ B ₂ N ₂
Formula weight	221.98
Temperature/K	100
Crystal system	monoclinic
Space group	P2 ₁ /c
a/Å	11.2826(5)
b/Å	6.0833(2)
c/Å	10.5290(4)
α/°	90
β/°	107.856(2)
γ/°	90
Volume/Å ³	687.85(5)
Z	2
ρ _{calc} /cm ³	1.072
μ/mm ⁻¹	0.444
F(000)	248.0
Crystal size/mm ³	0.24 × 0.06 × 0.03
Radiation	Cu Kα (λ = 1.54178)
2θ range for data collection/°	8.232 to 144.094
Index ranges	-13 ≤ h ≤ 13, -6 ≤ k ≤ 7, -12 ≤ l ≤ 12
Reflections collected	9296
Independent reflections	1348 [R _{int} = 0.0396, R _{sigma} = 0.0243]
Data/restraints/parameters	1348/0/85
Goodness-of-fit on F ²	1.028
Final R indexes [I ≥ 2σ (I)]	R ₁ = 0.0370, wR ₂ = 0.0959
Final R indexes [all data]	R ₁ = 0.0394, wR ₂ = 0.0983
Largest diff. peak/hole / e Å ⁻³	0.22/-0.22

3,11-Dimethyl-5,8-diaza-1,9-diboradisp[4.2.4]tetradecane (2ac):

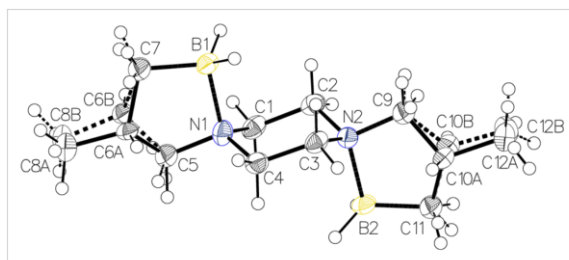


Table 1 Crystal data and structure refinement for saher177.

Identification code	saher177
Empirical formula	C ₁₂ H ₂₈ B ₂ N ₂
Formula weight	221.98
Temperature/K	100
Crystal system	monoclinic
Space group	C2/m
a/Å	23.0668(12)
b/Å	5.9251(3)
c/Å	10.9279(6)
α/°	90
β/°	109.254(3)
γ/°	90
Volume/Å ³	1410.01(13)
Z	4
ρ _{calc} /cm ³	1.046
μ/mm ⁻¹	0.433
F(000)	496.0
Crystal size/mm ³	0.3 × 0.075 × 0.045
Radiation	Cu Kα (λ = 1.54178)
2θ range for data collection/°	8.12 to 143.858
Index ranges	-28 ≤ h ≤ 26, 0 ≤ k ≤ 7, 0 ≤ l ≤ 13
Reflections collected	1507
Independent reflections	1507 [R _{int} = ?, R _{sigma} = 0.0211]
Data/restraints/parameters	1507/37/180
Goodness-of-fit on F ²	1.086
Final R indexes [I ≥ 2σ (I)]	R ₁ = 0.0690, wR ₂ = 0.1831
Final R indexes [all data]	R ₁ = 0.0765, wR ₂ = 0.1896
Largest diff. peak/hole / e Å ⁻³	0.32/-0.23

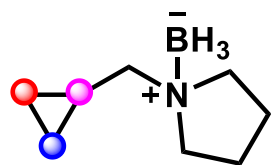
References

1. Charette, A. B.; Juteau, H., *J. Am. Chem. Soc.* **1994**, *116*, 2651-2652.
2. Luo, G.; Xiang, M.; Krische, M. J., *Org. Lett.* **2019**, *21*, 2493-2497.
3. Veeraraghavan Ramachandran, P.; Kulkarni, A. S.; Zhao, Y.; Mei, J., *Chem. Commun.* **2016**, *52*, 11885-11888.
4. Gieuw, M. H.; Leung, V. M. Y.; Ke, Z.; Yeung, Y. Y. J. A. S.; *Catalysis, Adv. Synth. Catal.* **2018**, *360*, 4306-4311.
5. Denmark, S. E.; O'Connor, S. P., *J. Org. Chem.* **1997**, *62*, 584-594.
6. Siddiqui, S. H.; Navuluri, C.; Charette, A. B., *Synthesis* **2019**, *51*, 3834-3846.

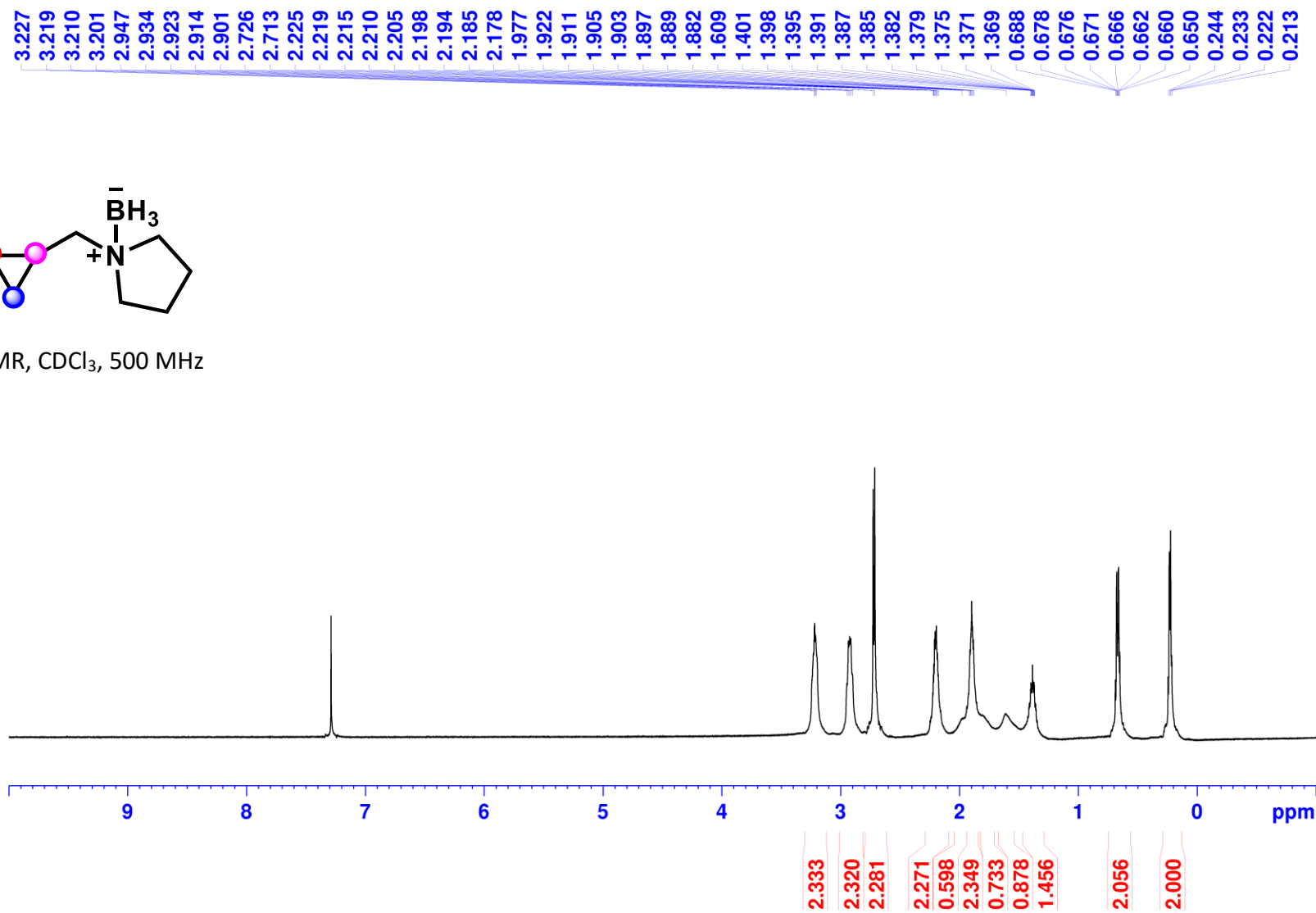
NMR Spectra for Chapter 3

NMR Spectra of Precursors

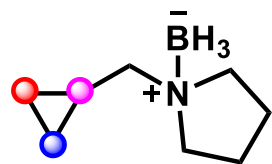
1-(Cyclopropylmethyl)pyrrolidine Borane (**1a**):



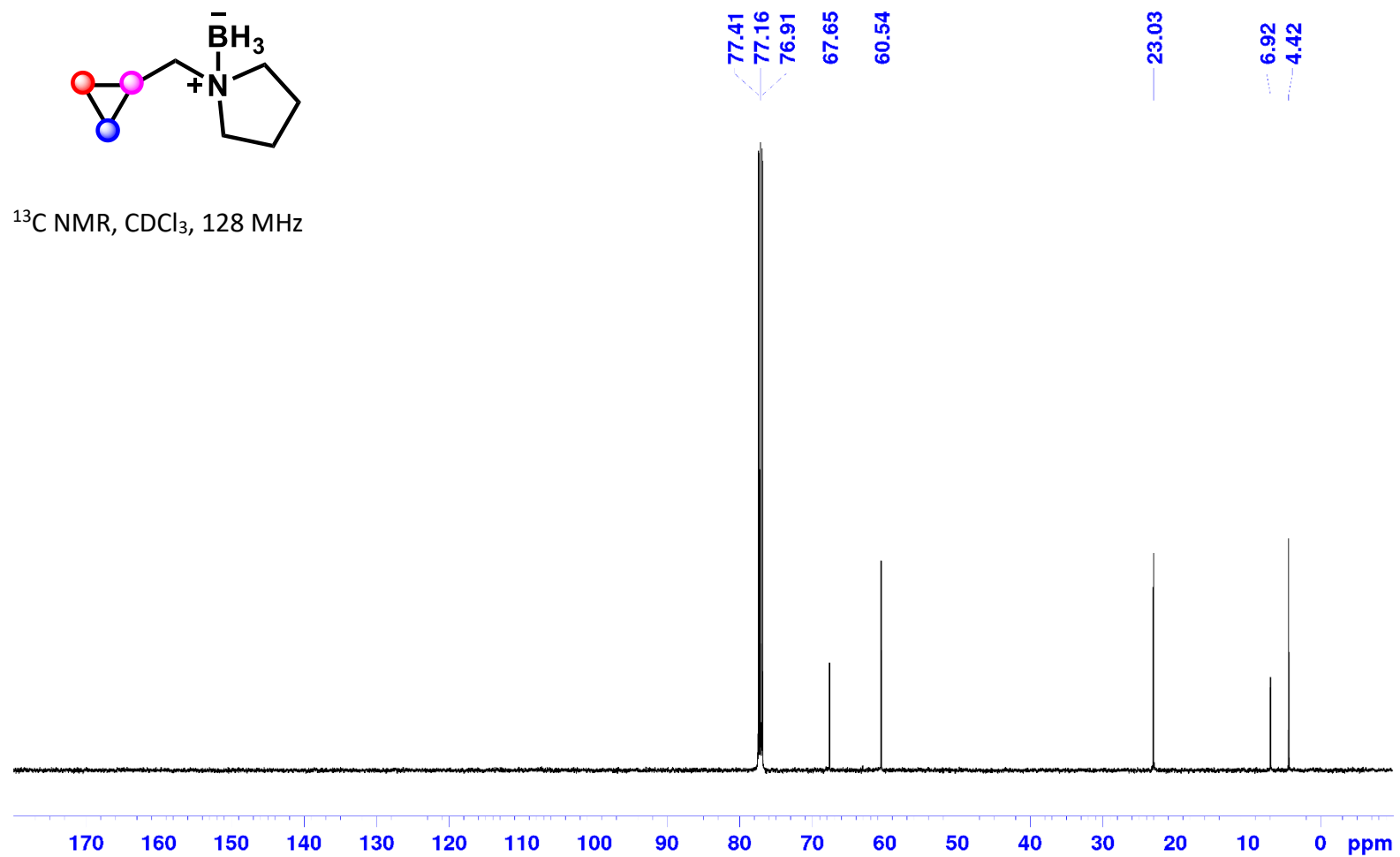
¹H NMR, CDCl₃, 500 MHz



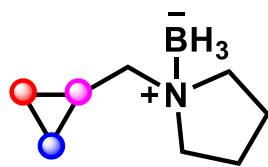
1-(Cyclopropylmethyl)pyrrolidine Borane (1a):



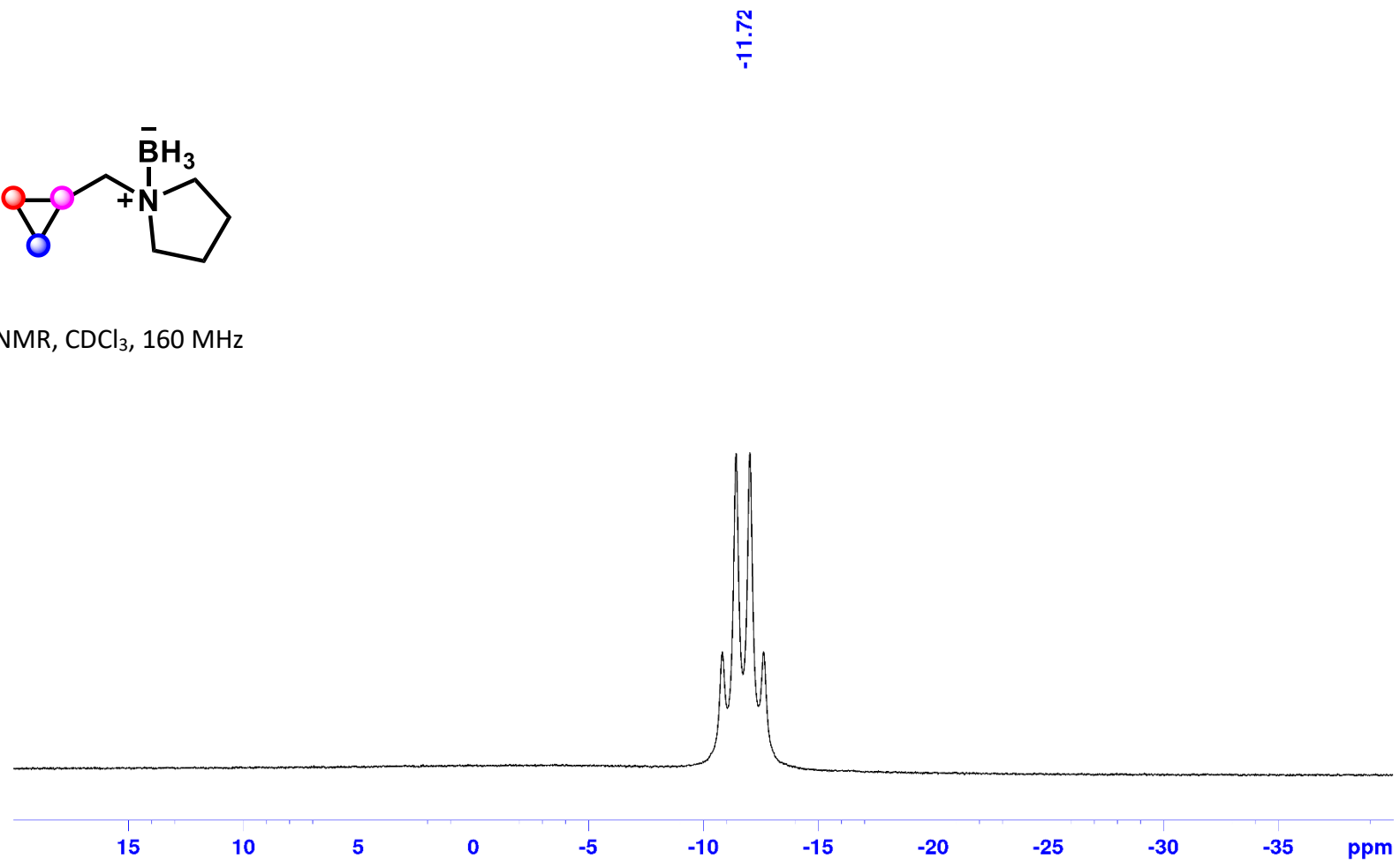
^{13}C NMR, CDCl_3 , 128 MHz



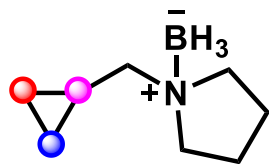
1-(Cyclopropylmethyl)pyrrolidine Borane (1a):



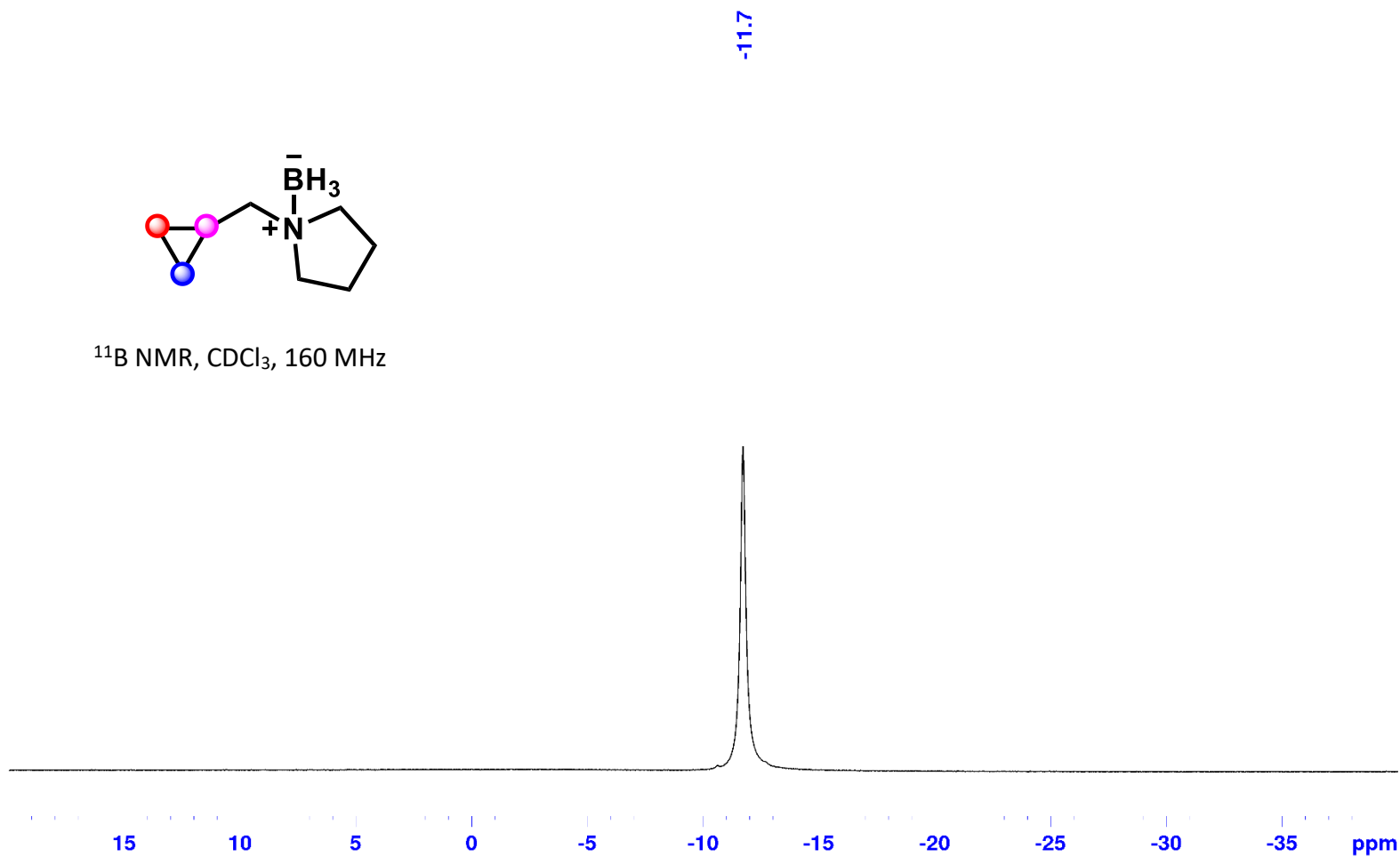
^{11}B NMR, CDCl_3 , 160 MHz



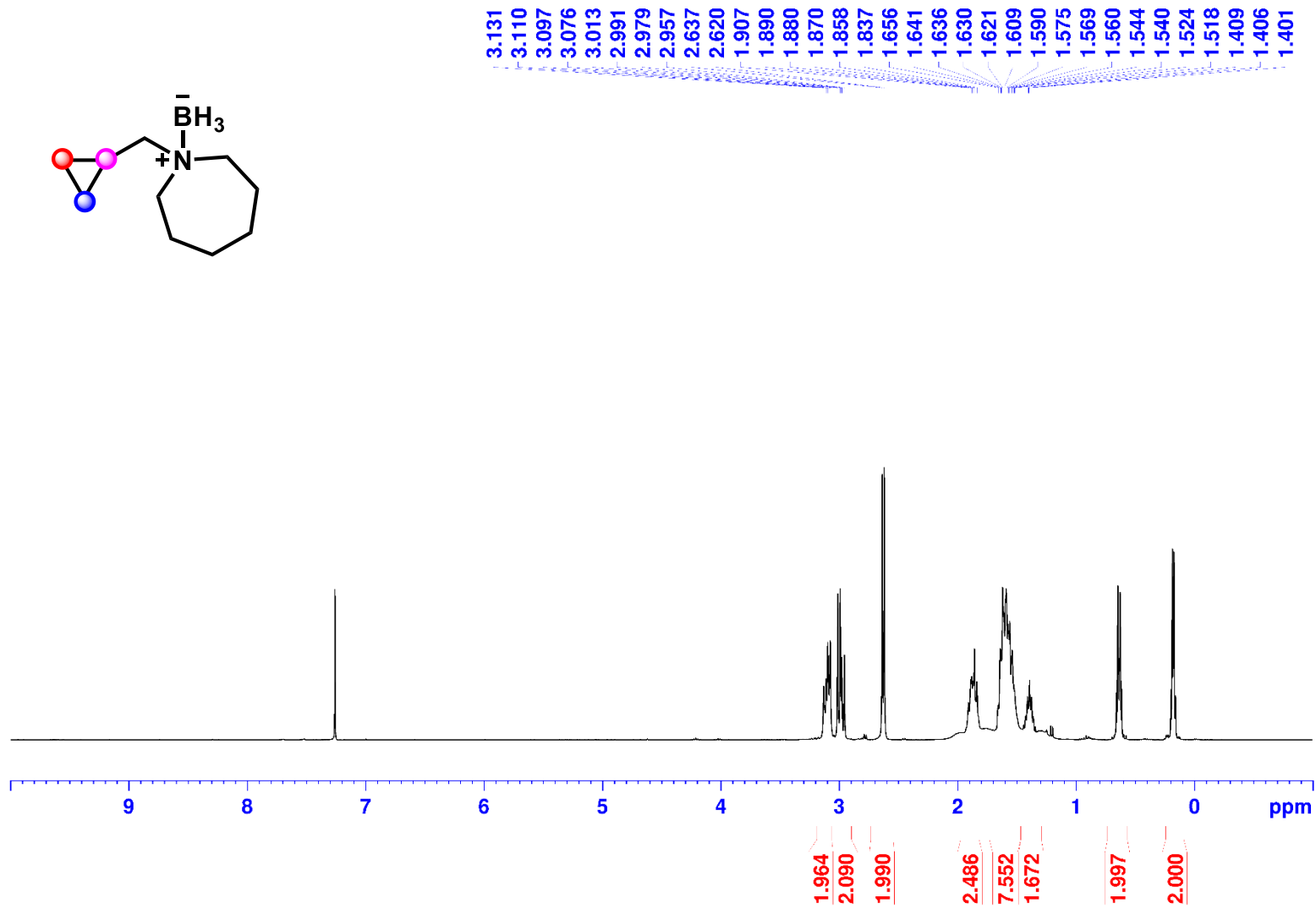
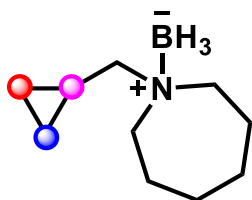
1-(Cyclopropylmethyl)pyrrolidine Borane (1a):



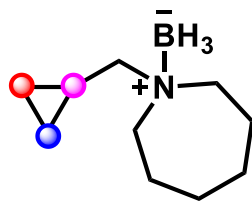
^{11}B NMR, CDCl_3 , 160 MHz



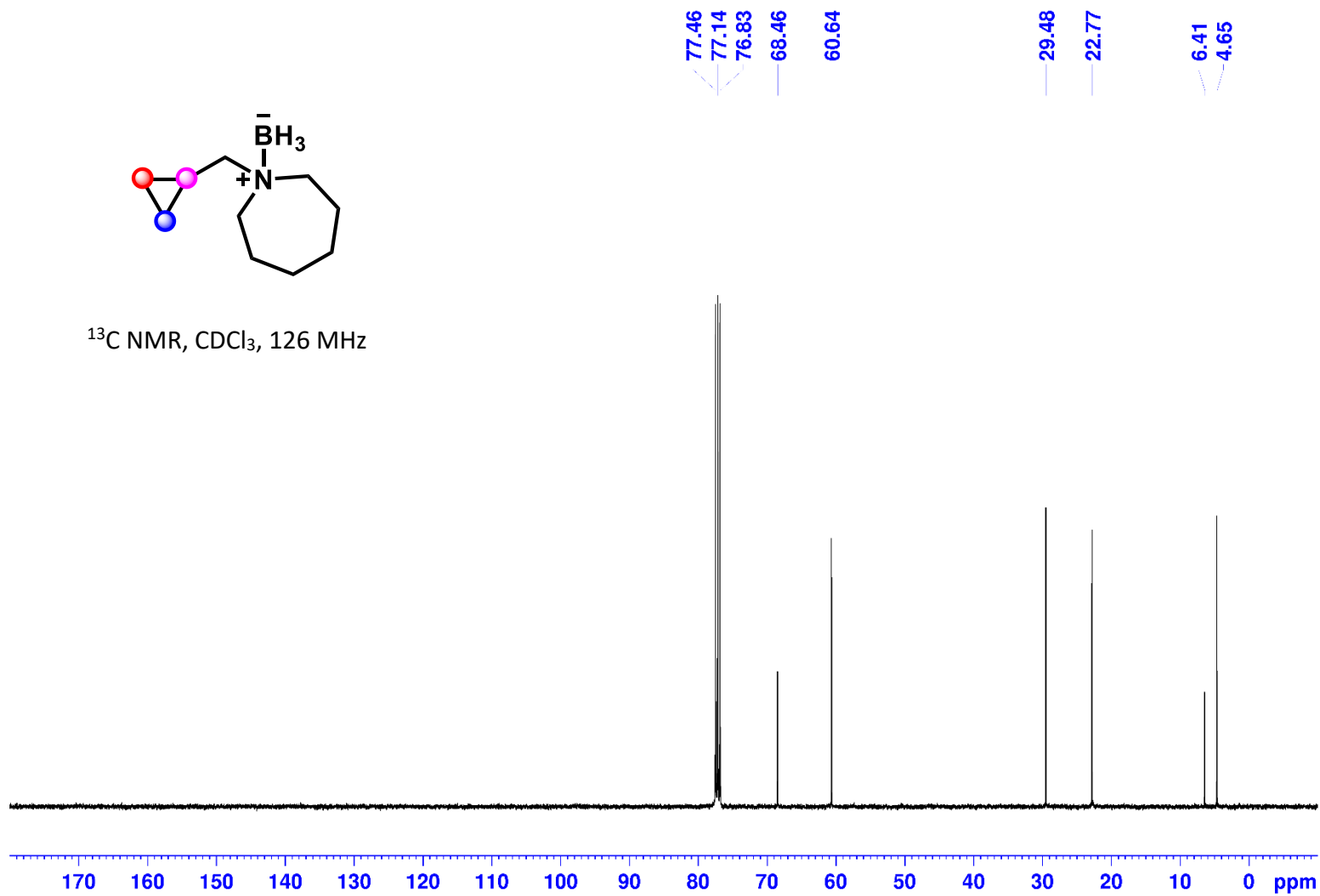
1-(Cyclopropylmethyl)azepane Borane (1b):



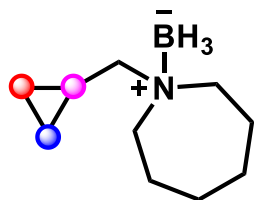
1-(Cyclopropylmethyl)azepane Borane (1b):



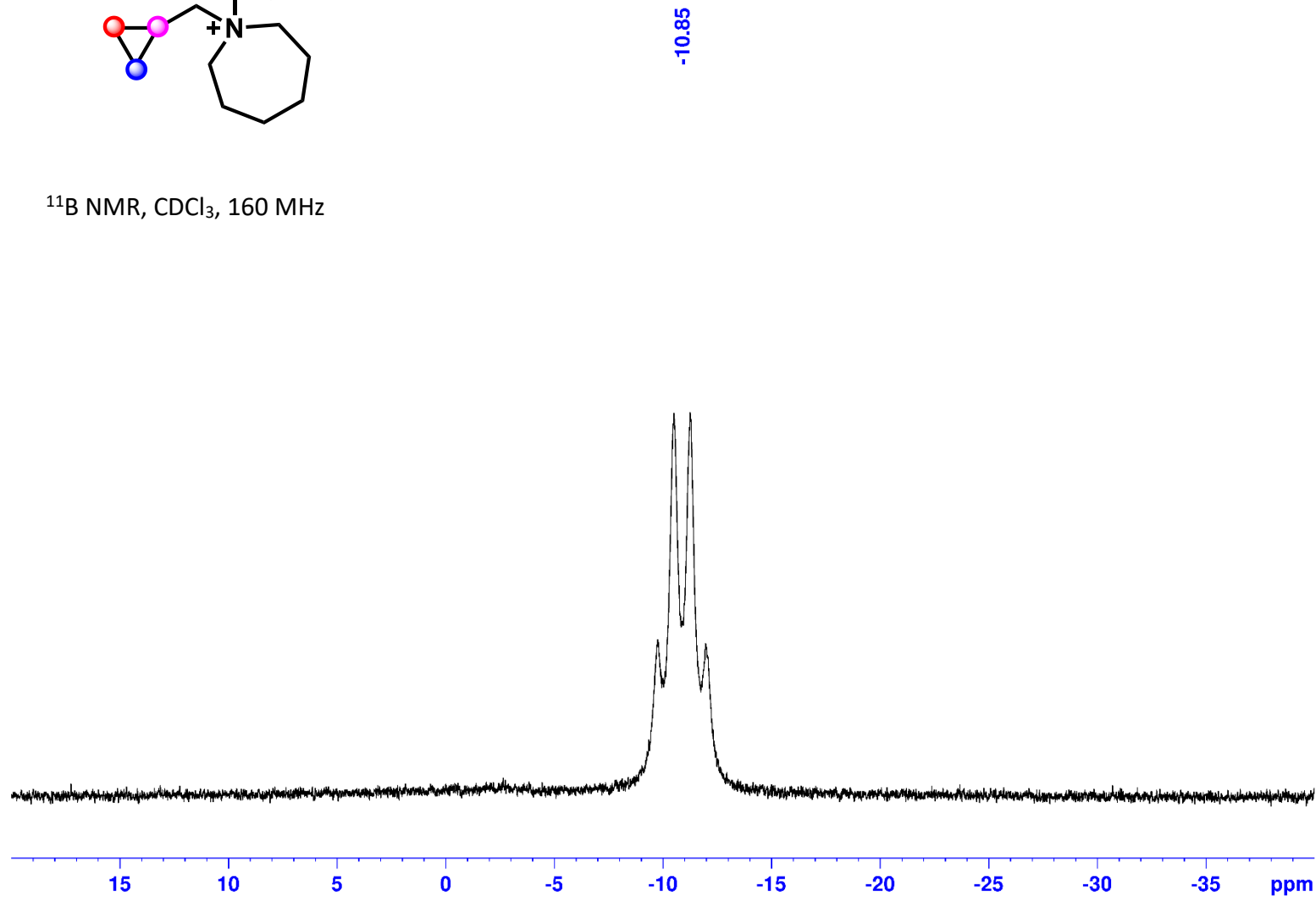
^{13}C NMR, CDCl_3 , 126 MHz



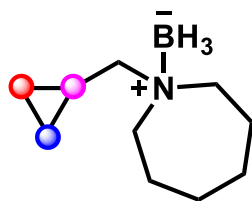
1-(Cyclopropylmethyl)azepane Borane (1b):



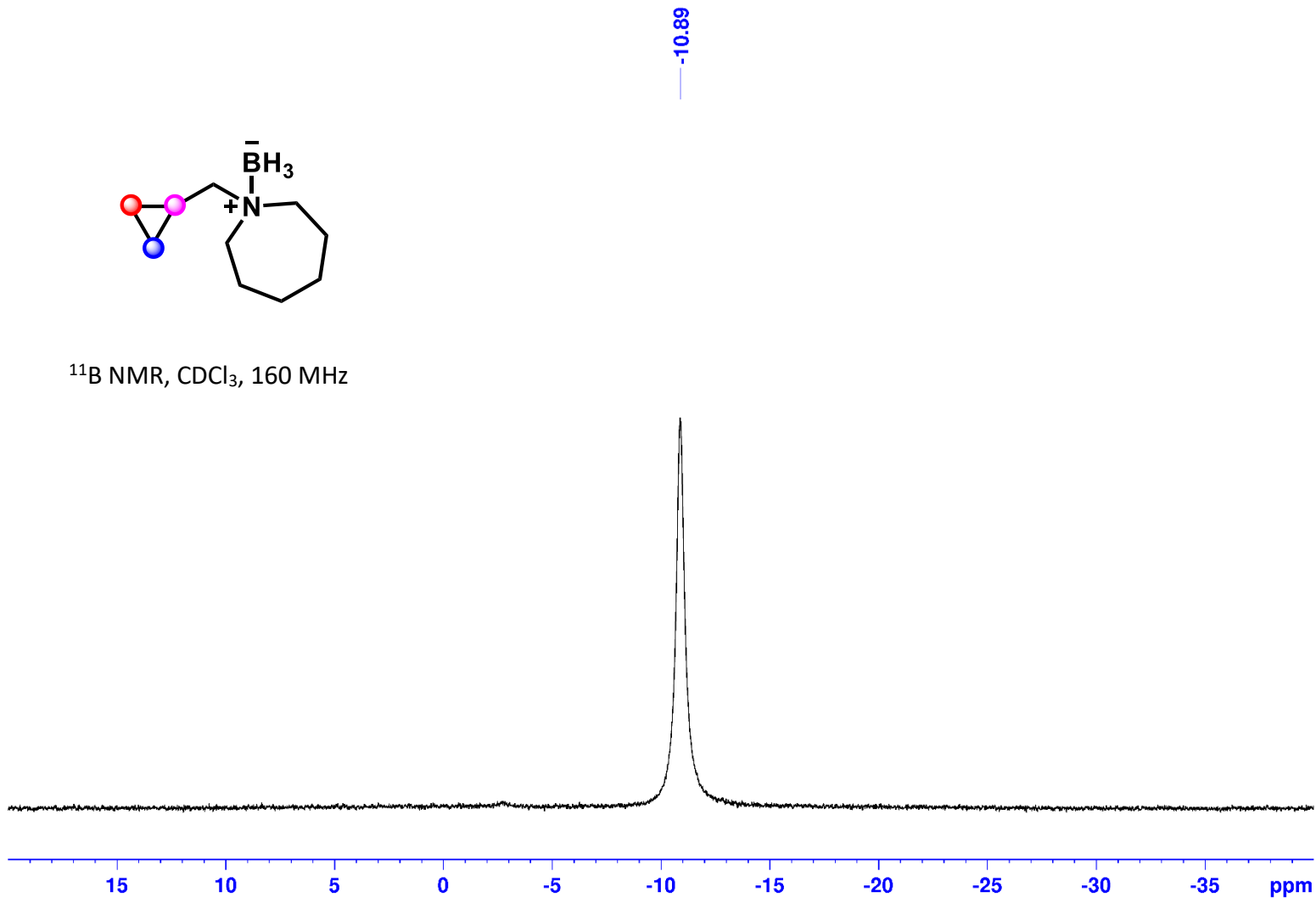
^{11}B NMR, CDCl_3 , 160 MHz



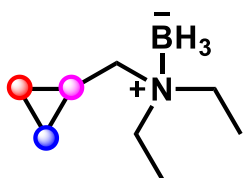
(1-(Cyclopropylmethyl)azepane Borane (1b):



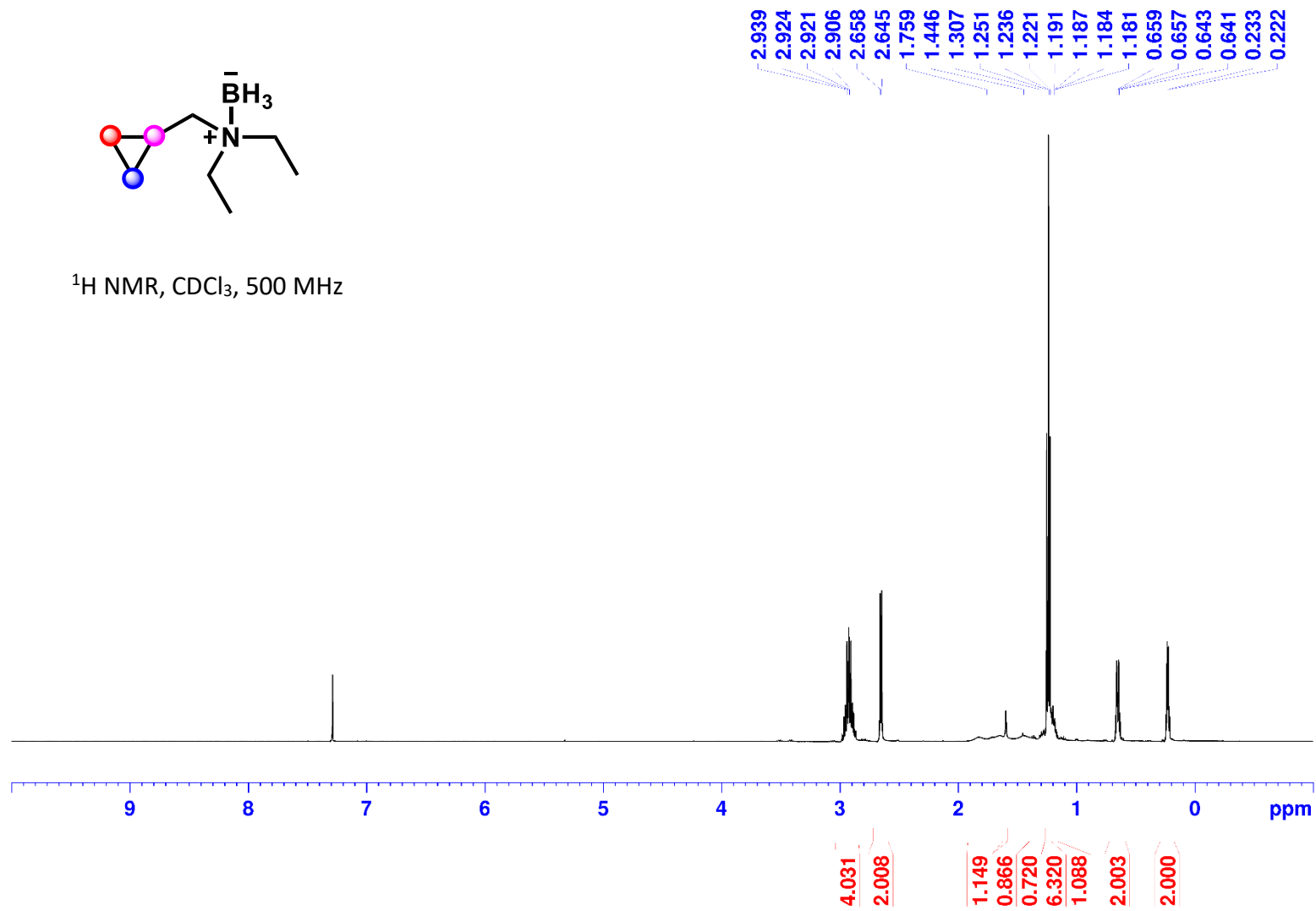
^{11}B NMR, CDCl_3 , 160 MHz



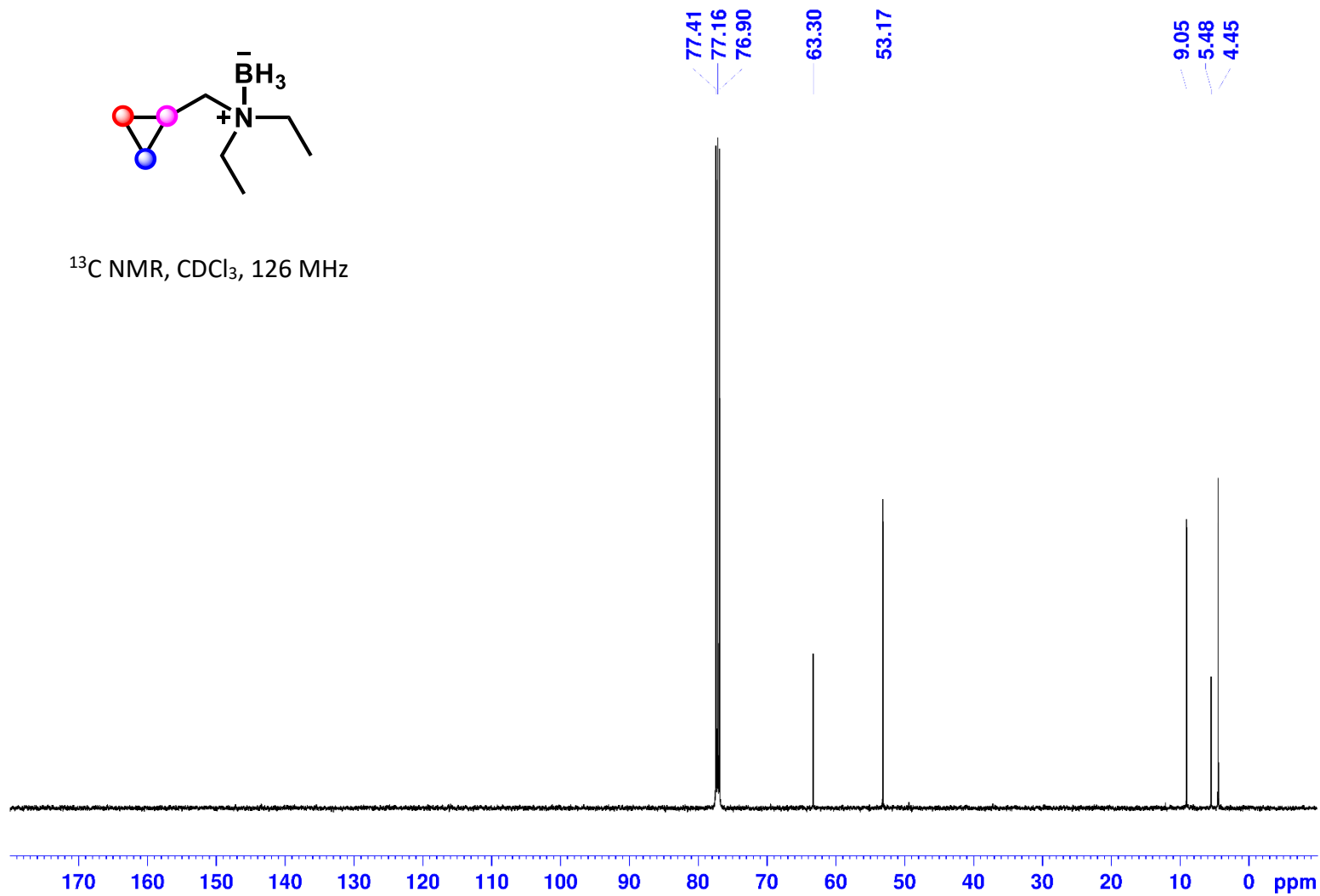
N-(Cyclopropylmethyl)-*N*-ethylethanamine Borane (1c):



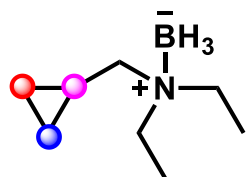
^1H NMR, CDCl_3 , 500 MHz



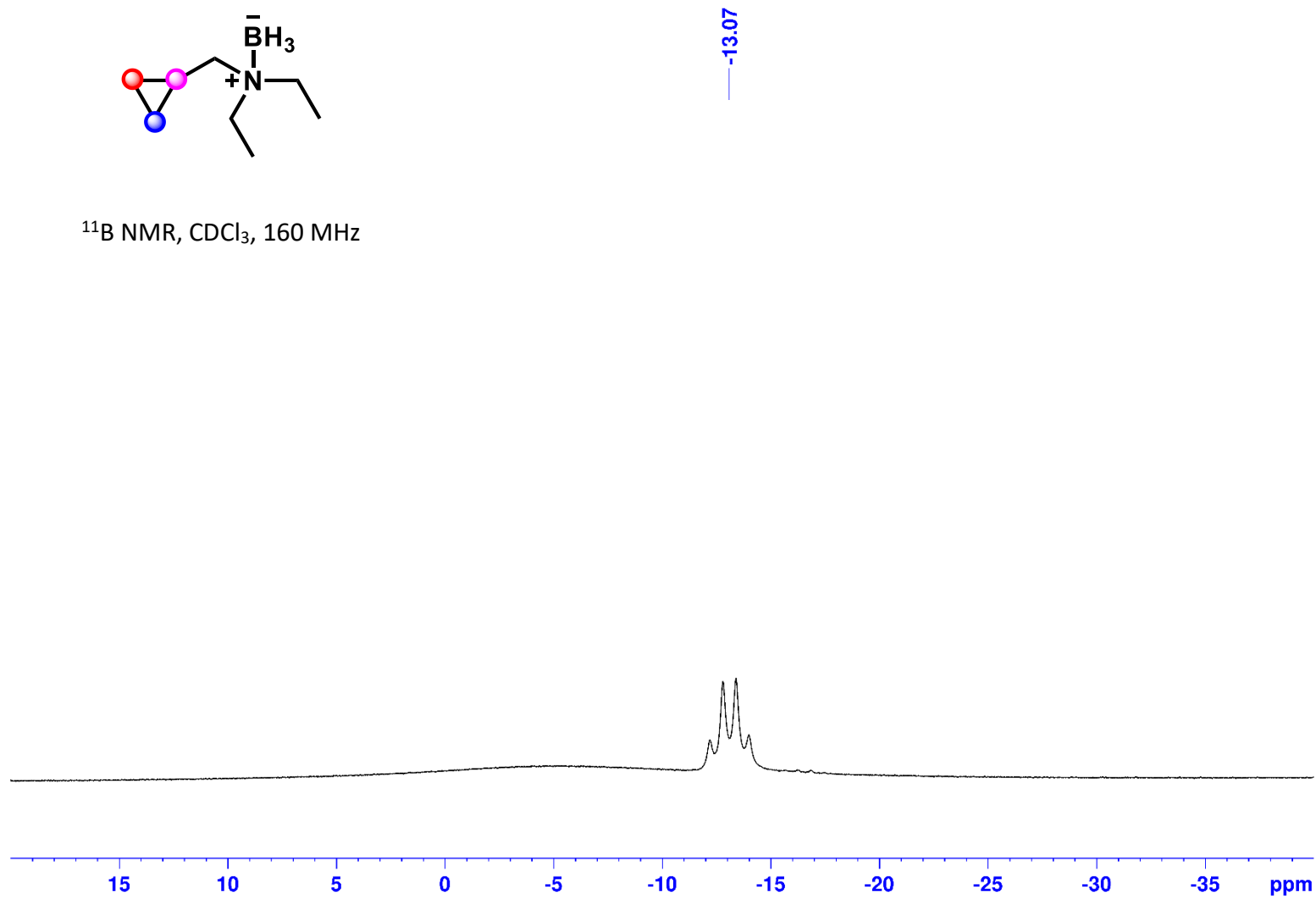
N-(Cyclopropylmethyl)-*N*-ethylethanamine Borane (1c):



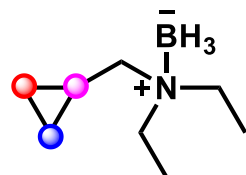
***N*-(Cyclopropylmethyl)-*N*-ethylethanamine Borane (1c):**



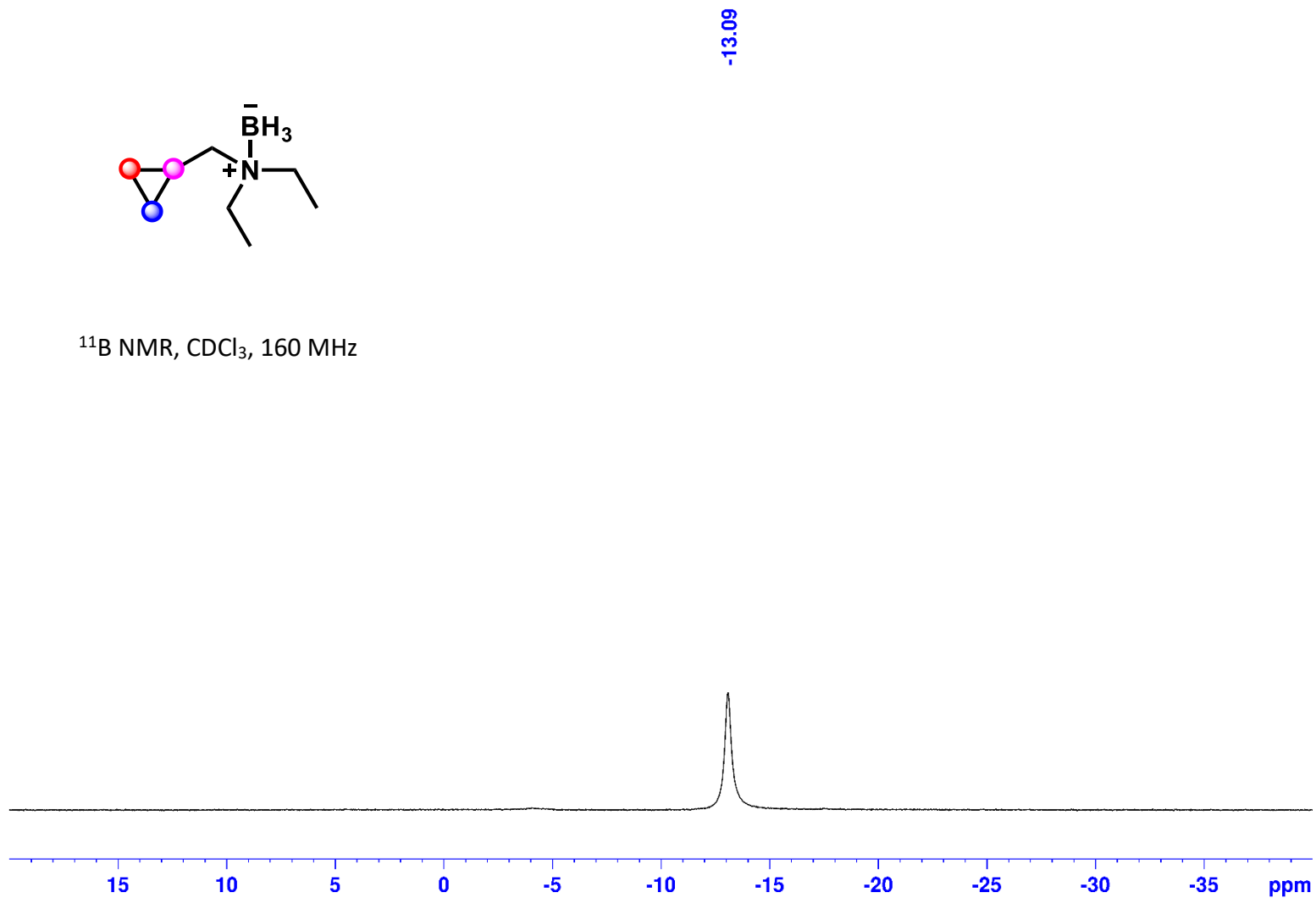
¹¹B NMR, CDCl₃, 160 MHz



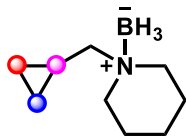
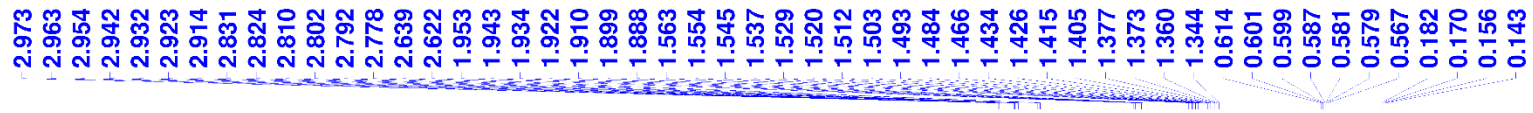
N-(Cyclopropylmethyl)-*N*-ethylethanamine Borane (1c):



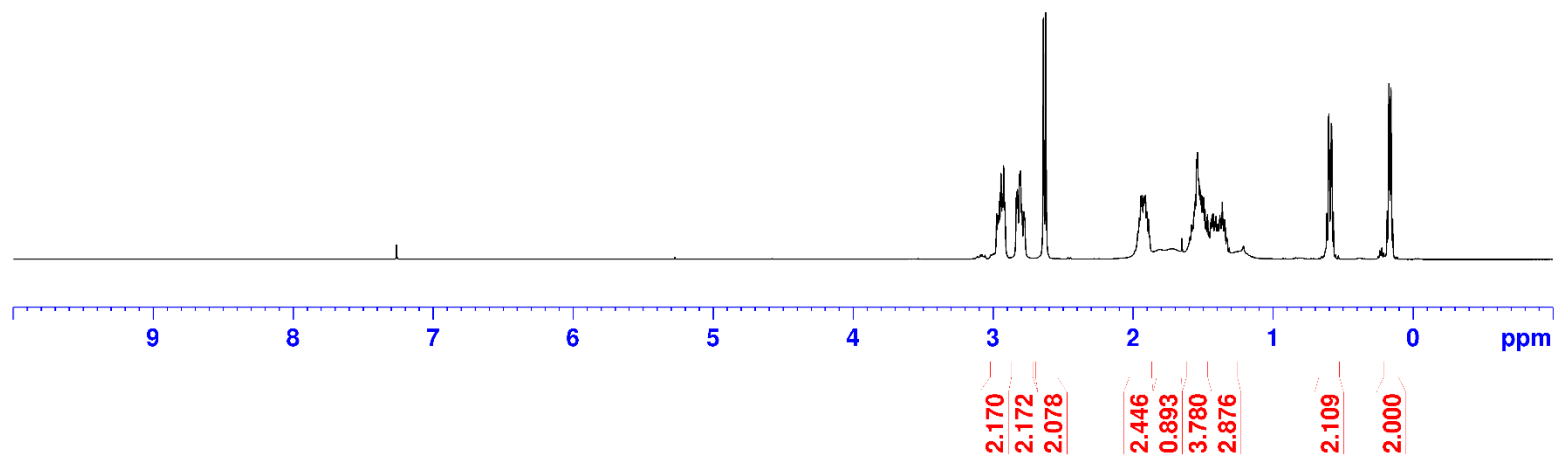
^{11}B NMR, CDCl_3 , 160 MHz



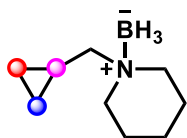
1-(Cyclopropylmethyl)piperidine Borane (1d) :



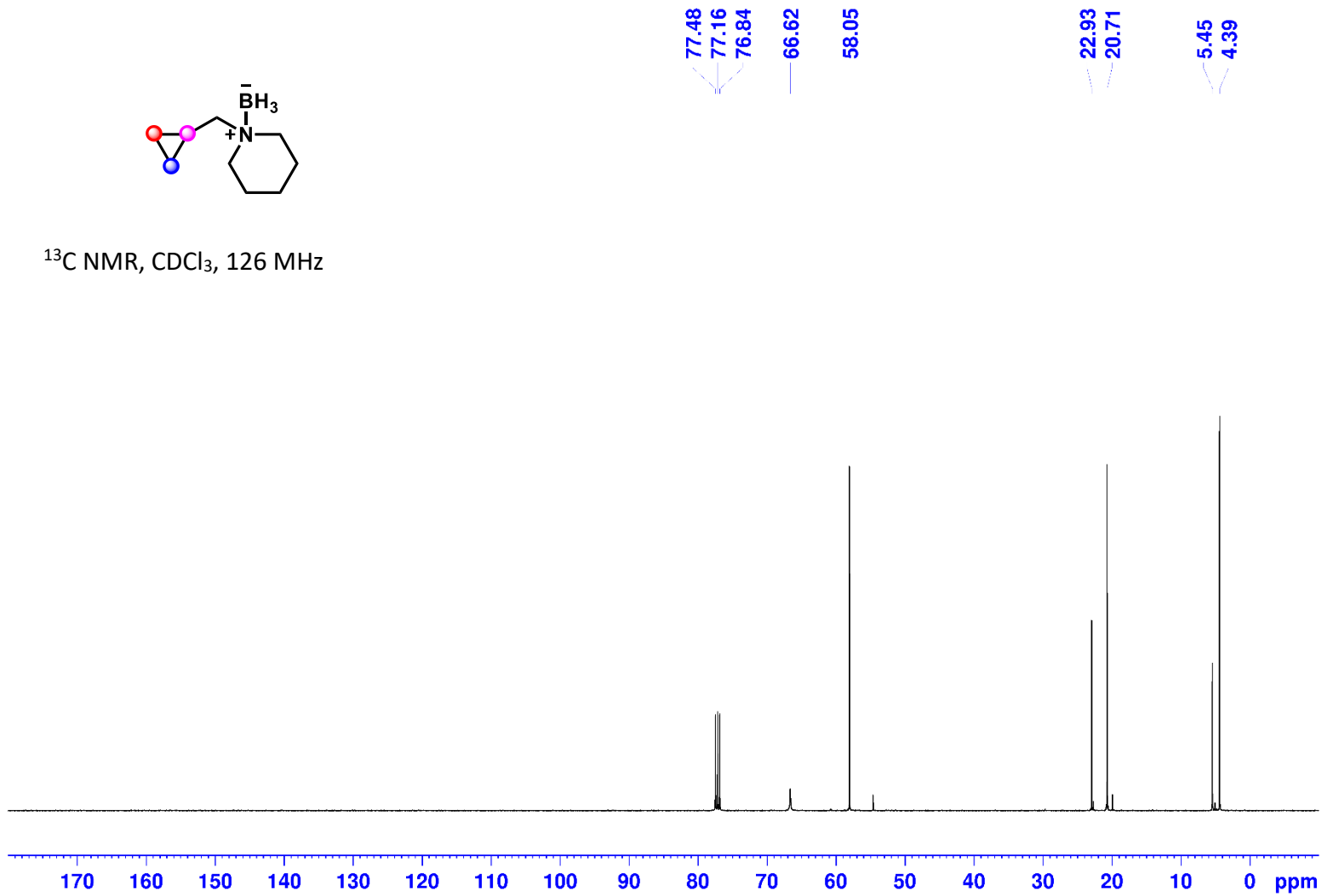
^1H NMR, CDCl_3 , 500 MHz



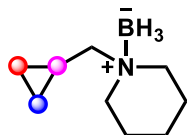
1-(Cyclopropylmethyl)piperidine Borane (1d) :



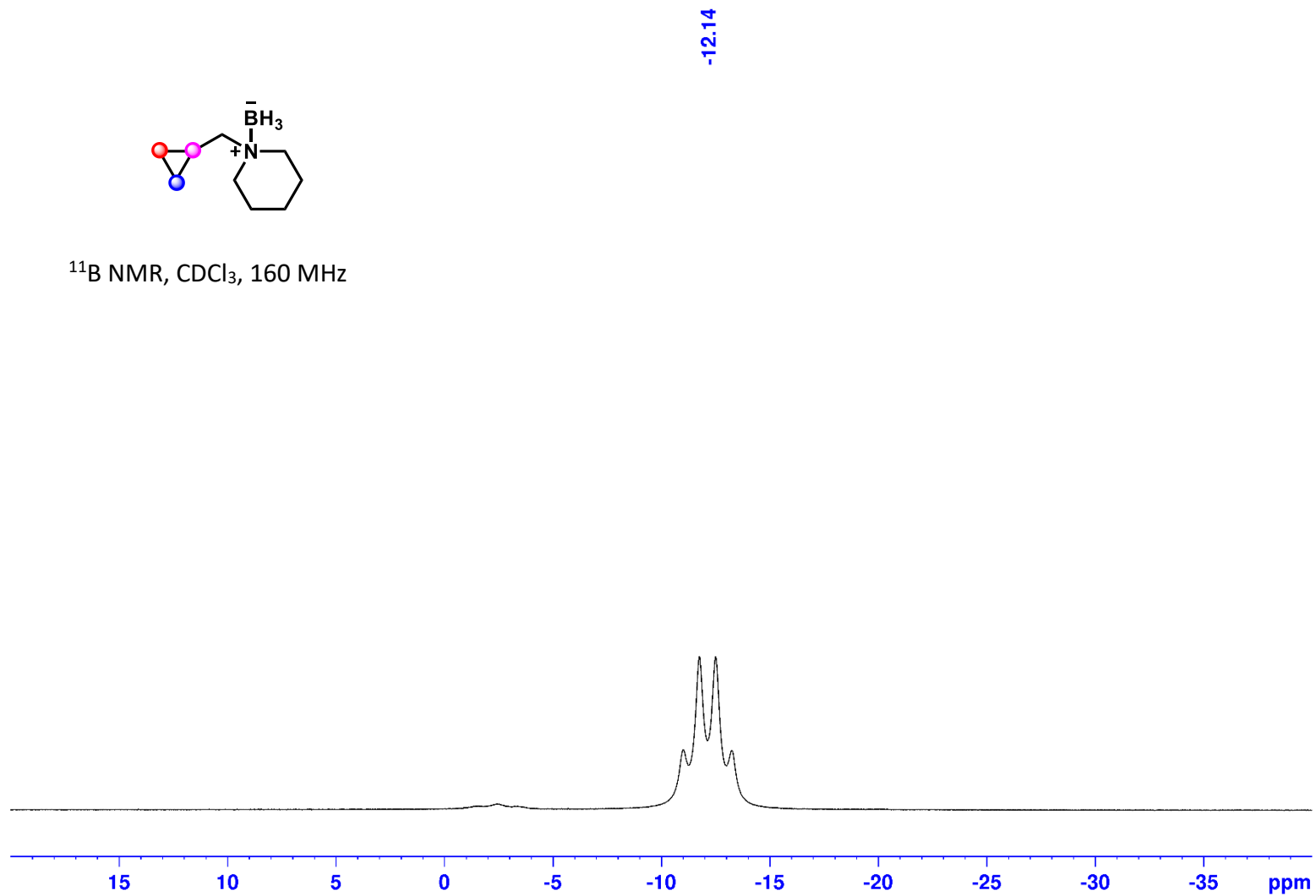
^{13}C NMR, CDCl_3 , 126 MHz



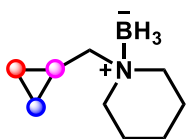
1-(Cyclopropylmethyl)piperidine Borane (1d) :



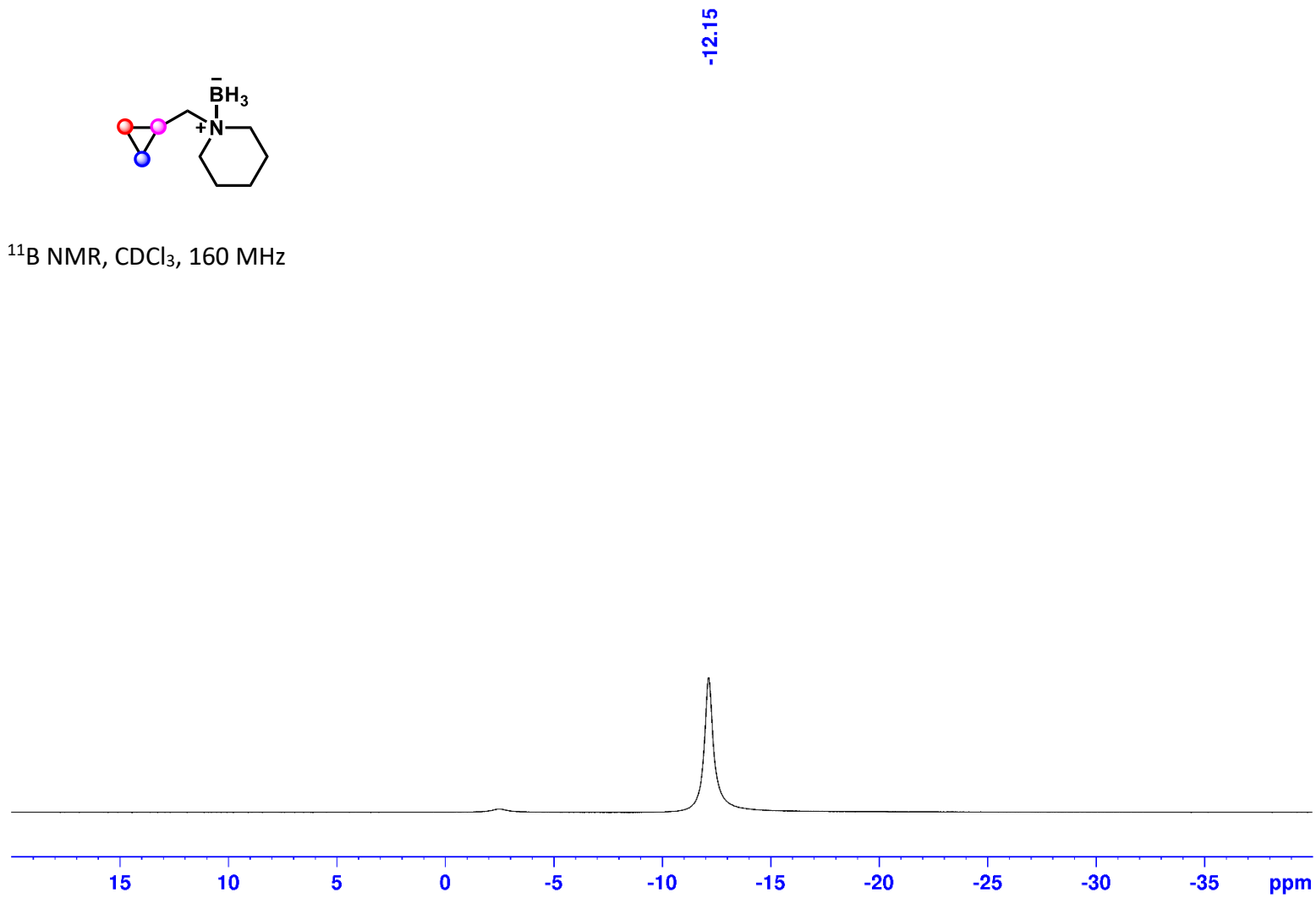
^{11}B NMR, CDCl_3 , 160 MHz



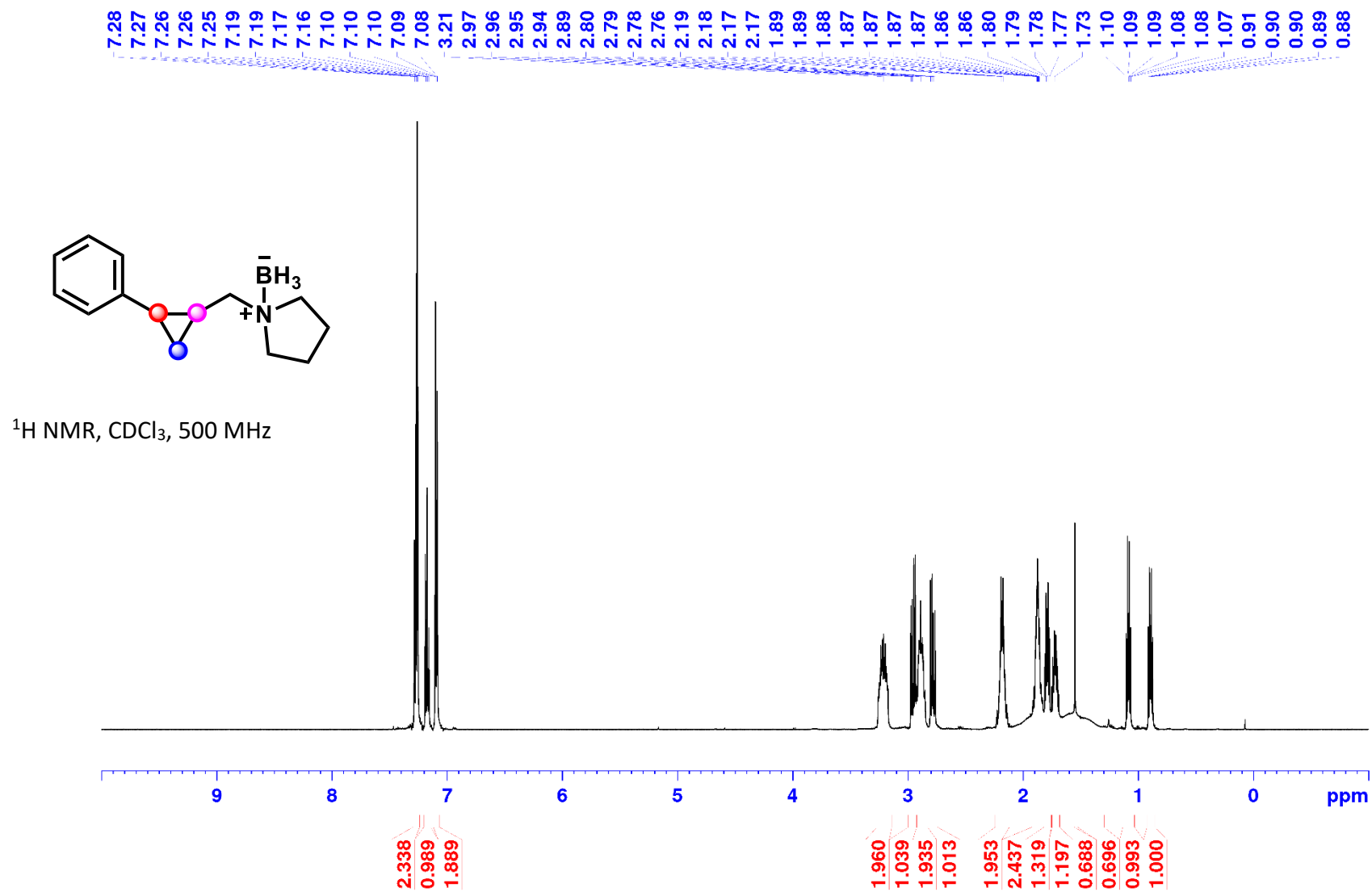
1-(Cyclopropylmethyl)piperidine Borane (1d) :



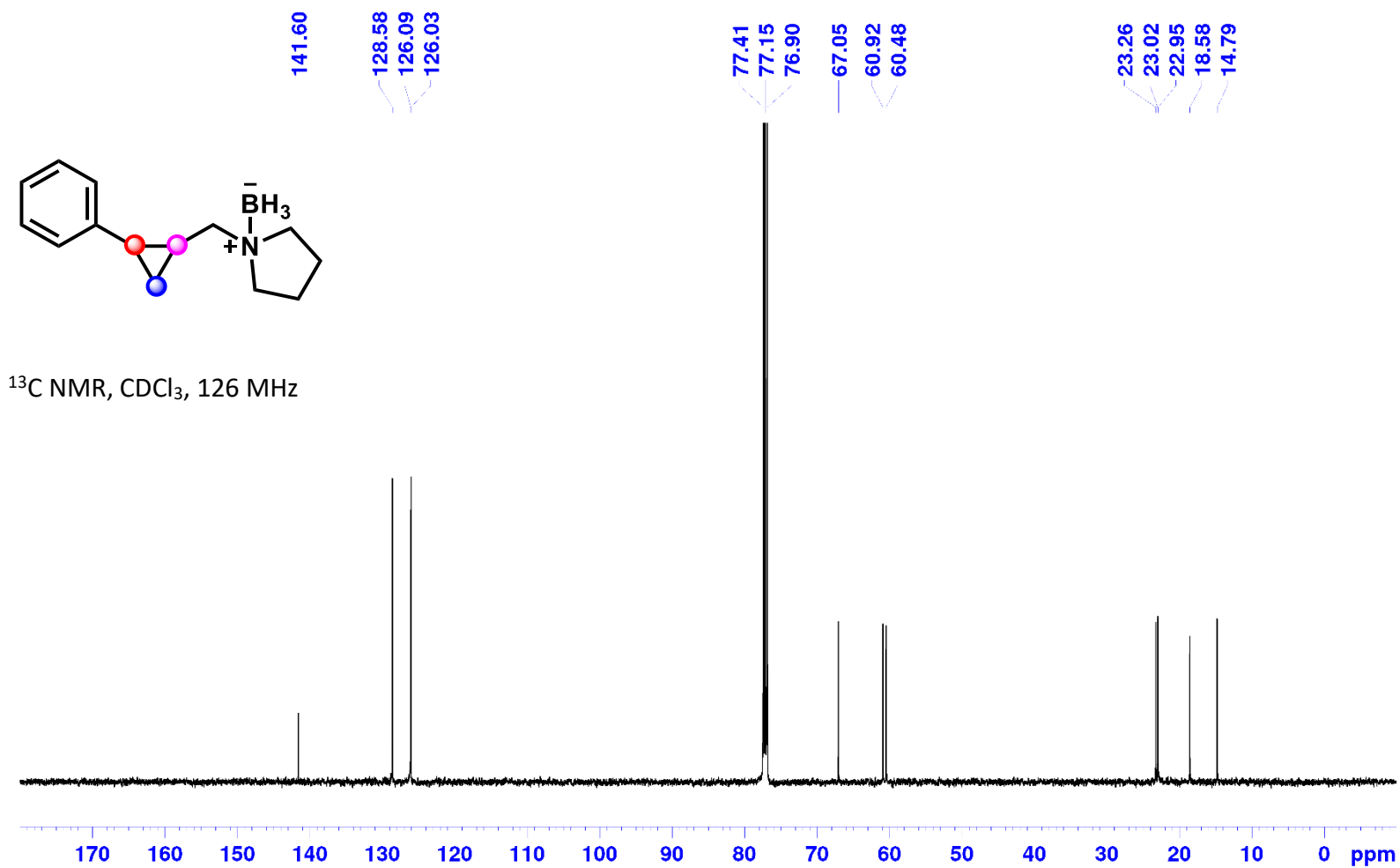
^{11}B NMR, CDCl_3 , 160 MHz



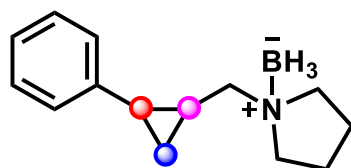
1-((2-Phenylcyclopropyl)methyl)pyrrolidine Borane (1e):



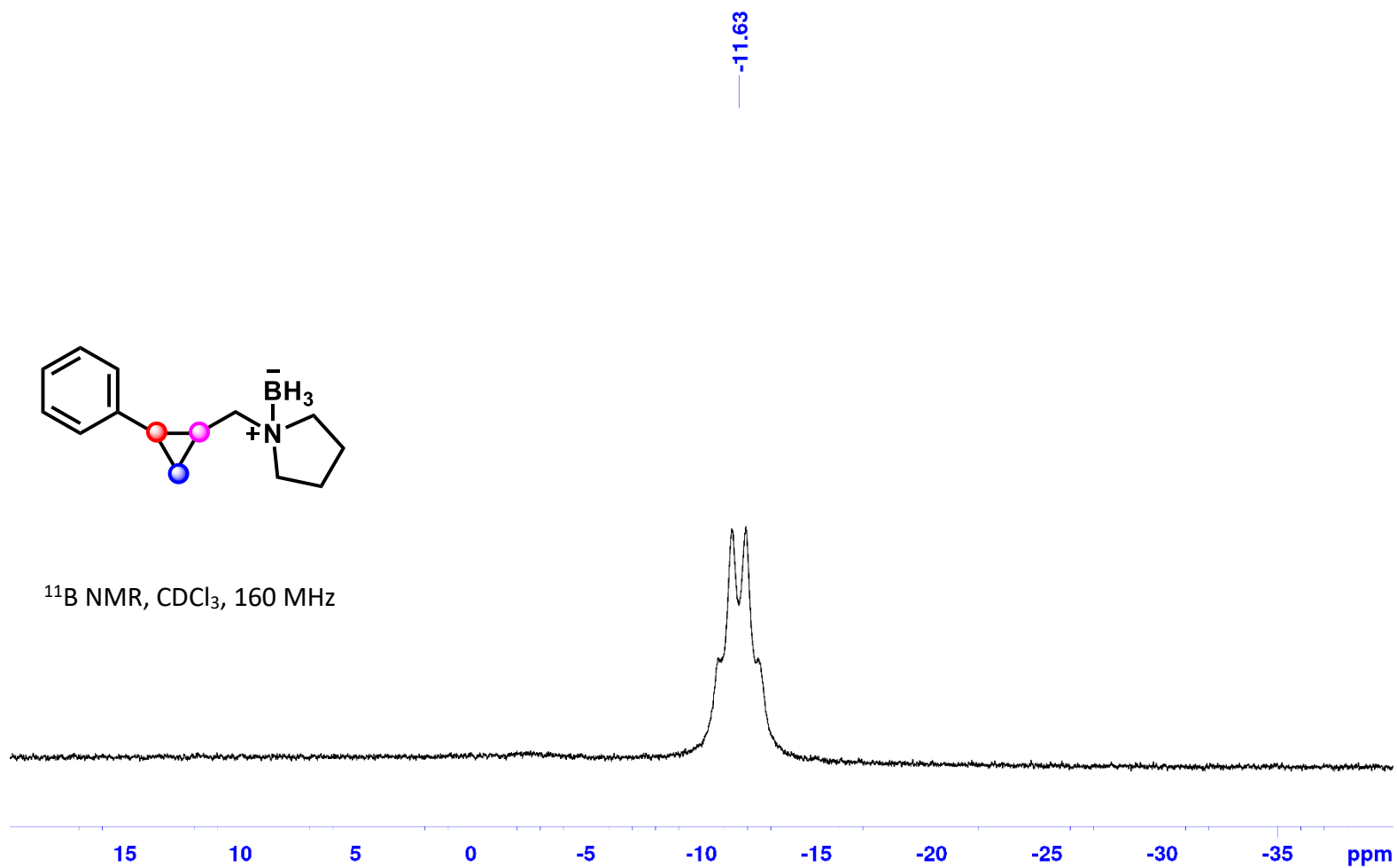
1-((2-Phenylcyclopropyl)methyl)pyrrolidine Borane (1e):



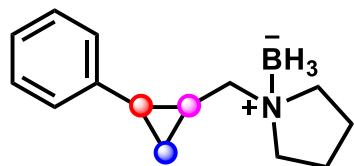
1-((2-Phenylcyclopropyl)methyl)pyrrolidine Borane (1e):



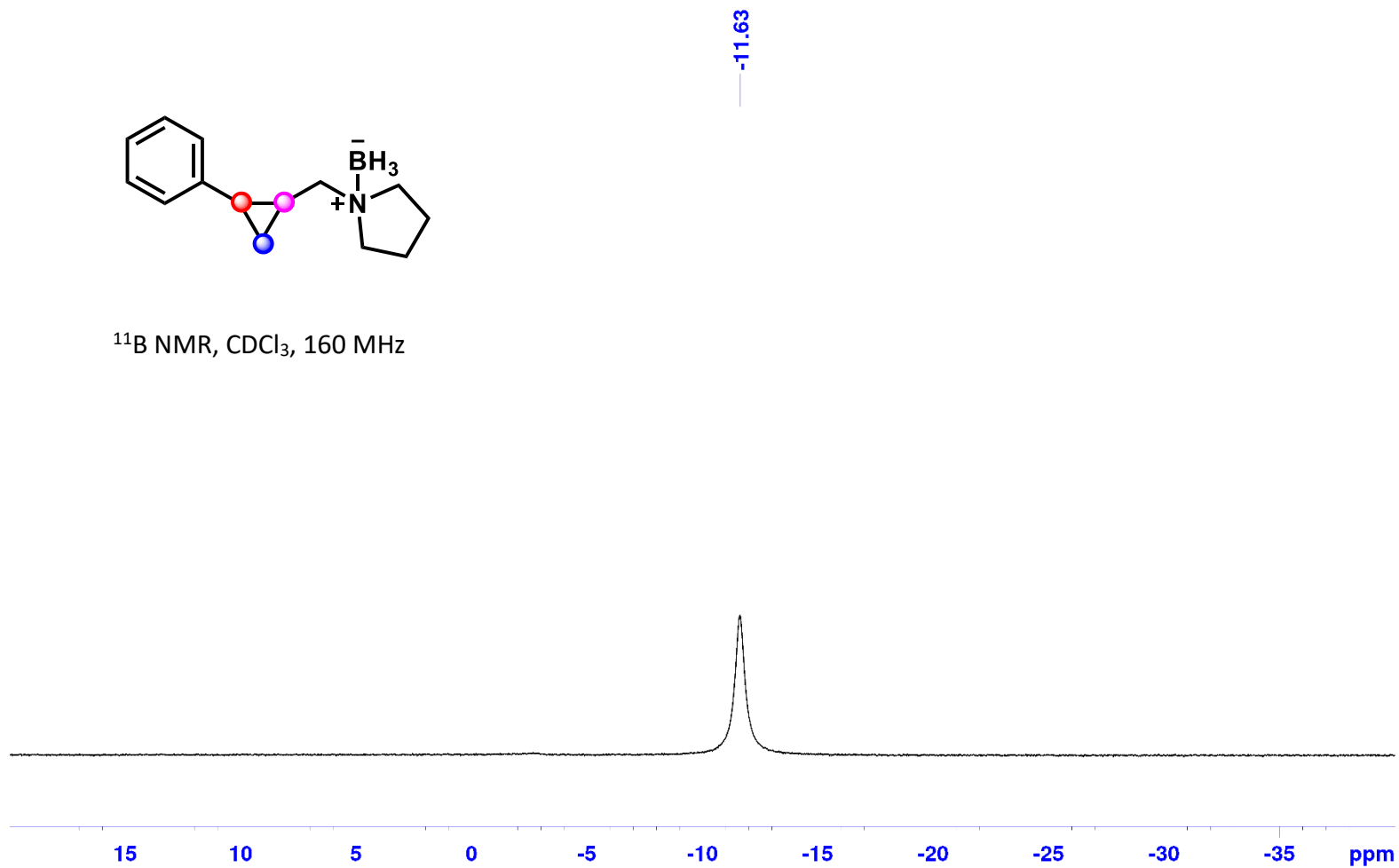
^{11}B NMR, CDCl_3 , 160 MHz



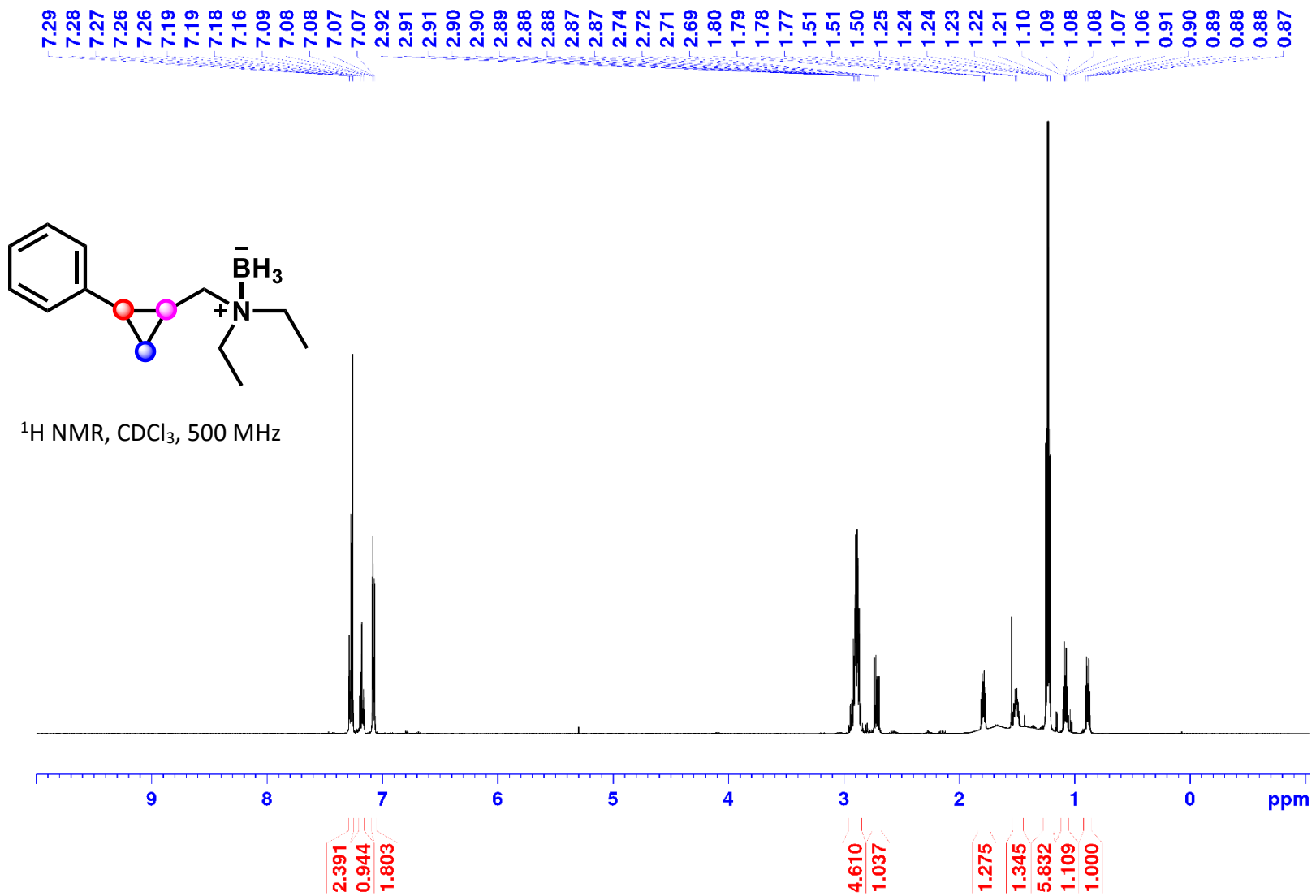
1-((2-Phenylcyclopropyl)methyl)pyrrolidine Borane (1e):



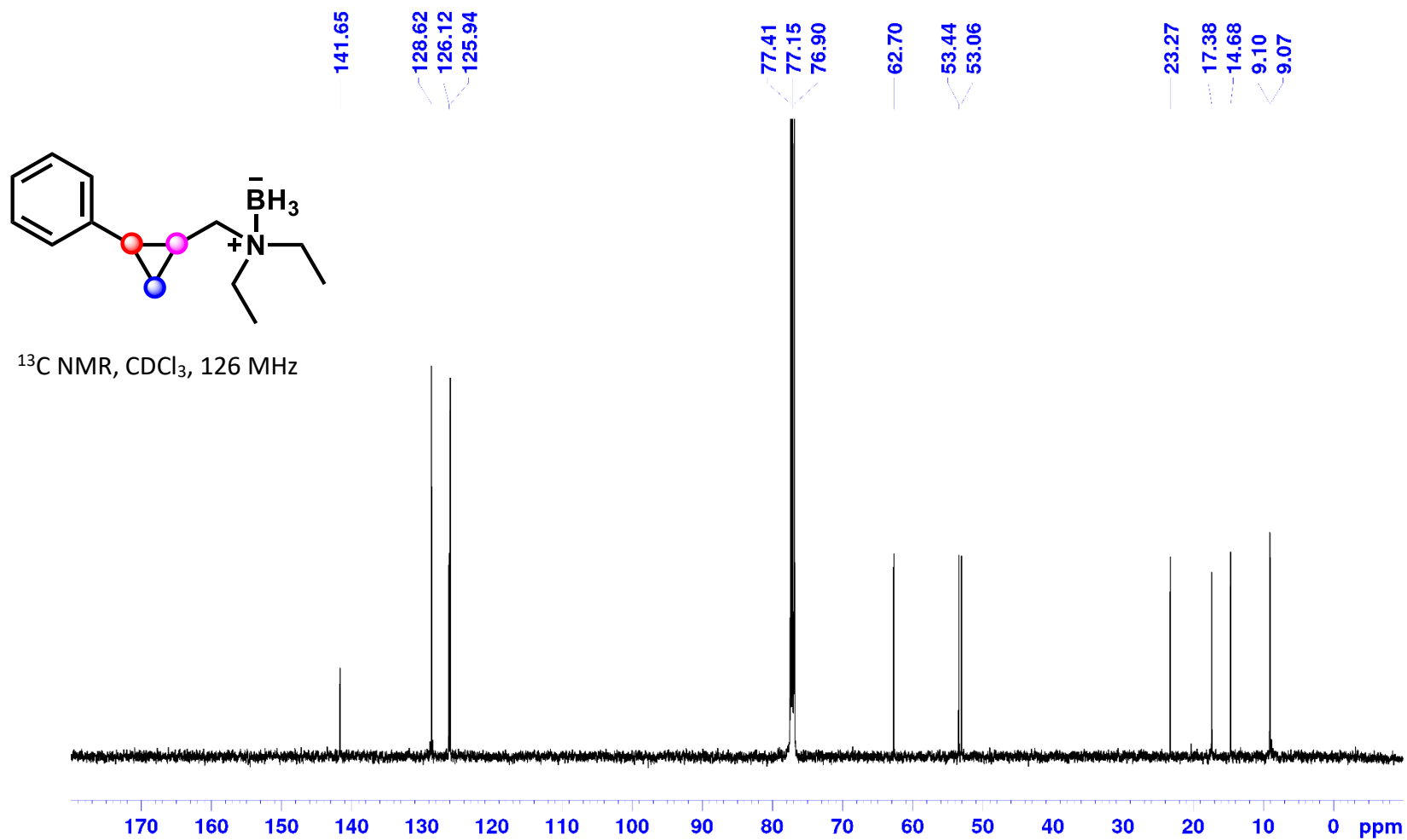
^{11}B NMR, CDCl_3 , 160 MHz



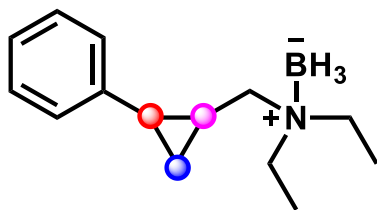
***N*-Ethyl-*N*-((2-phenylcyclopropyl)methyl)ethanamine Borane (1f):**



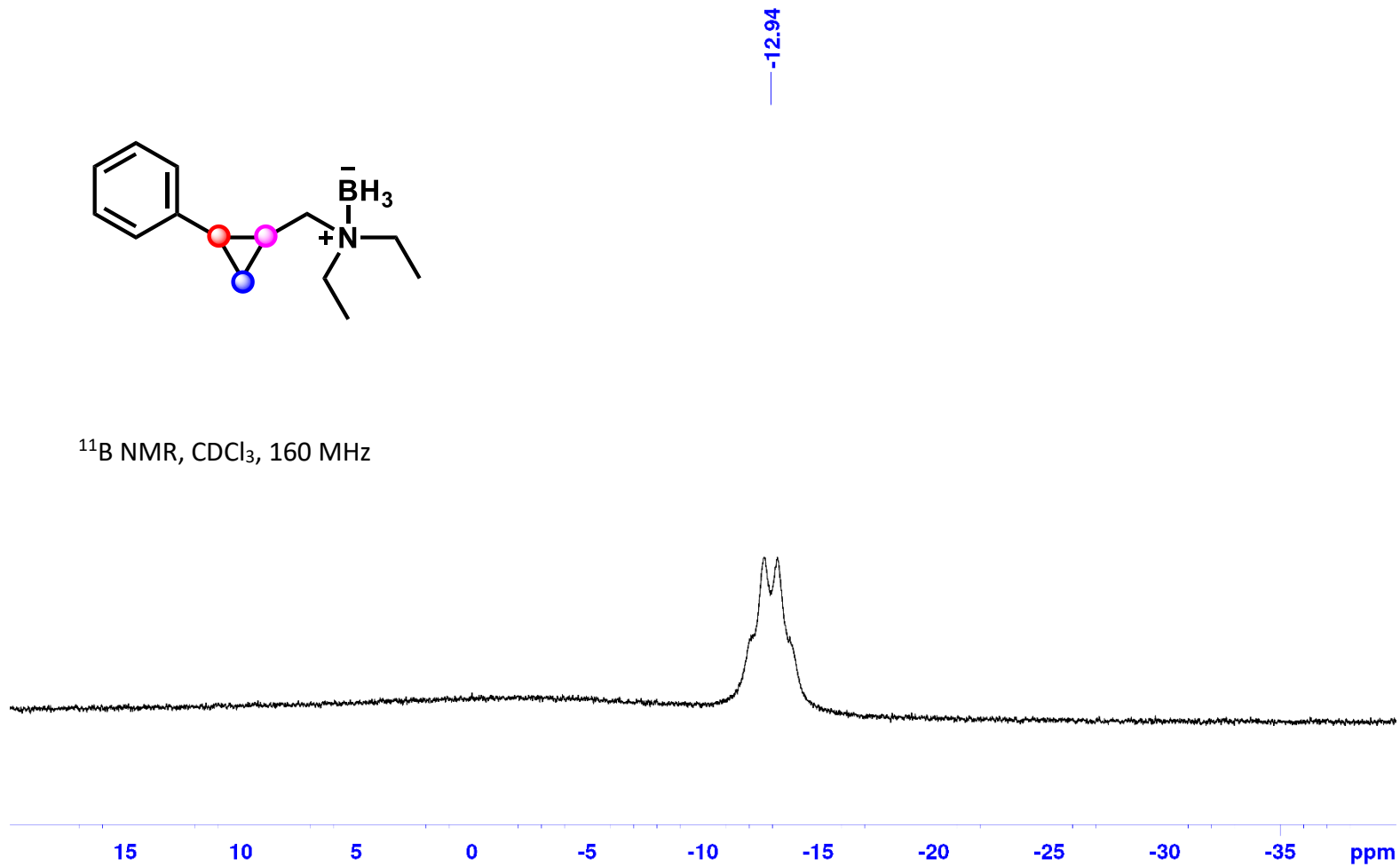
N-Ethyl-*N*-((2-phenylcyclopropyl)methyl)ethanamine Borane (1f):



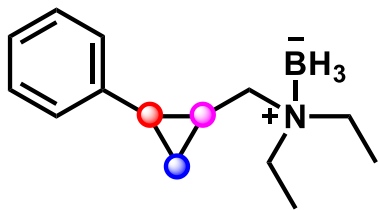
N-Ethyl-*N*-((2-phenylcyclopropyl)methyl)ethanamine Borane (1f):



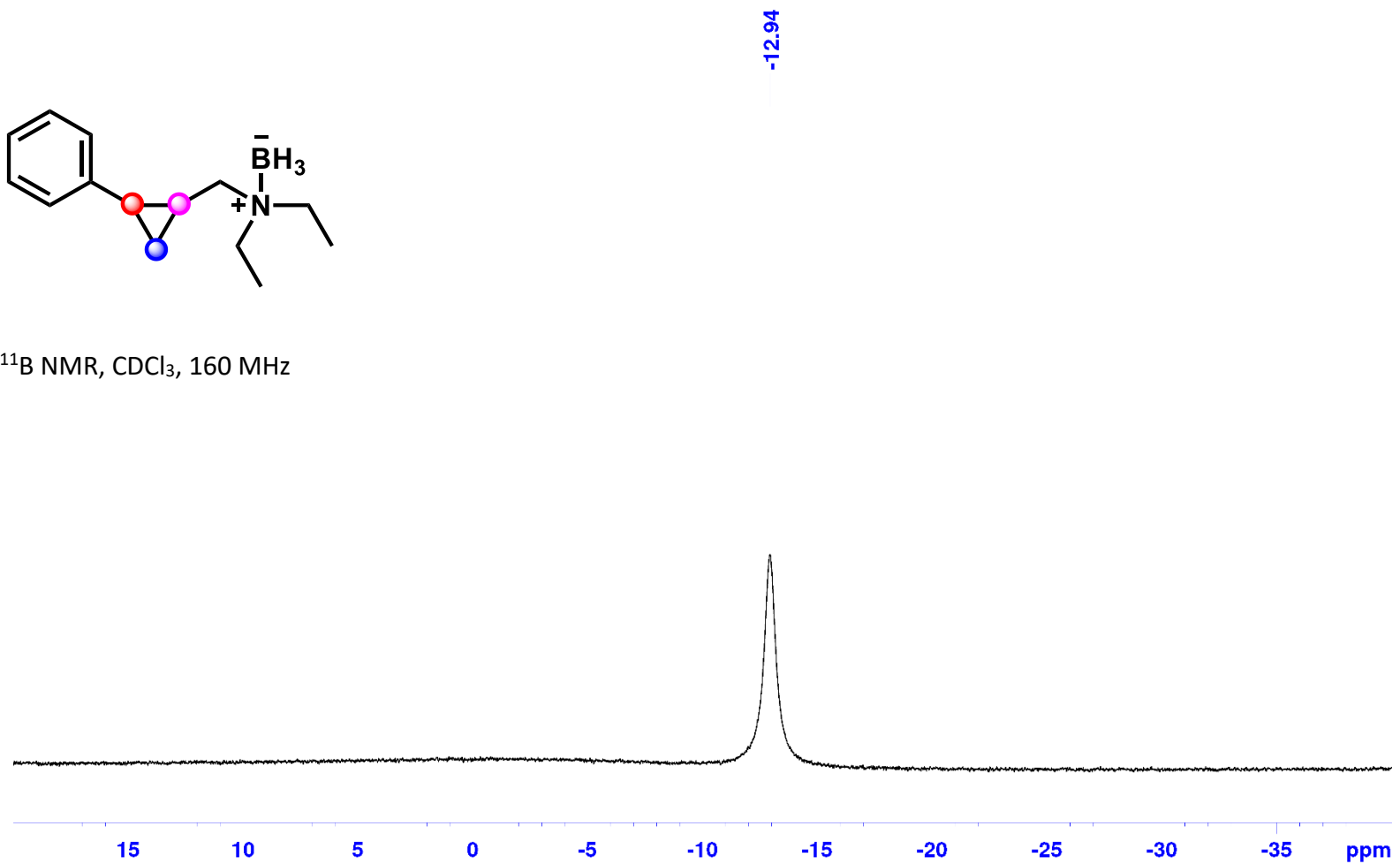
^{11}B NMR, CDCl_3 , 160 MHz



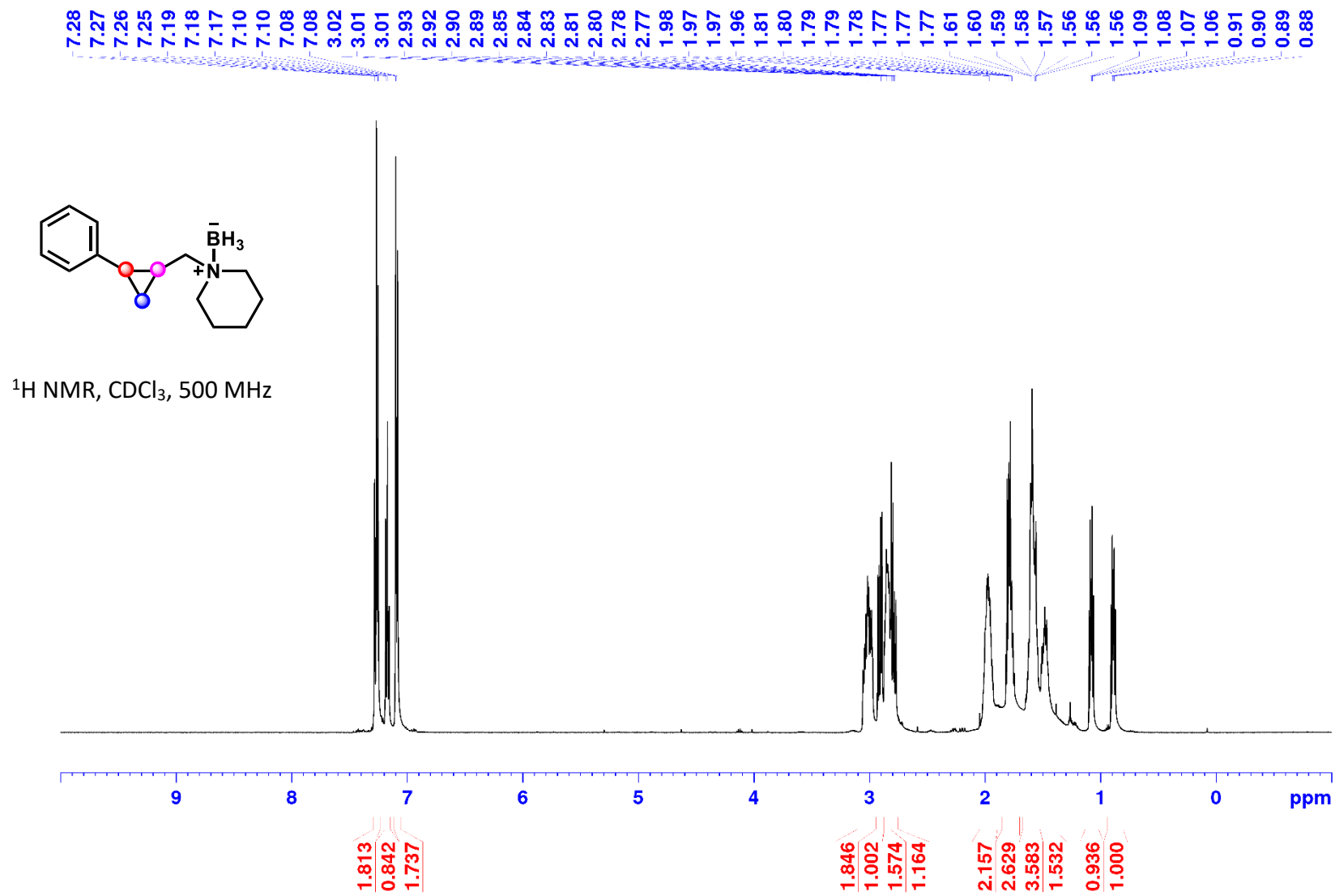
N-Ethyl-*N*-((2-phenylcyclopropyl)methyl)ethanamine Borane (1f):



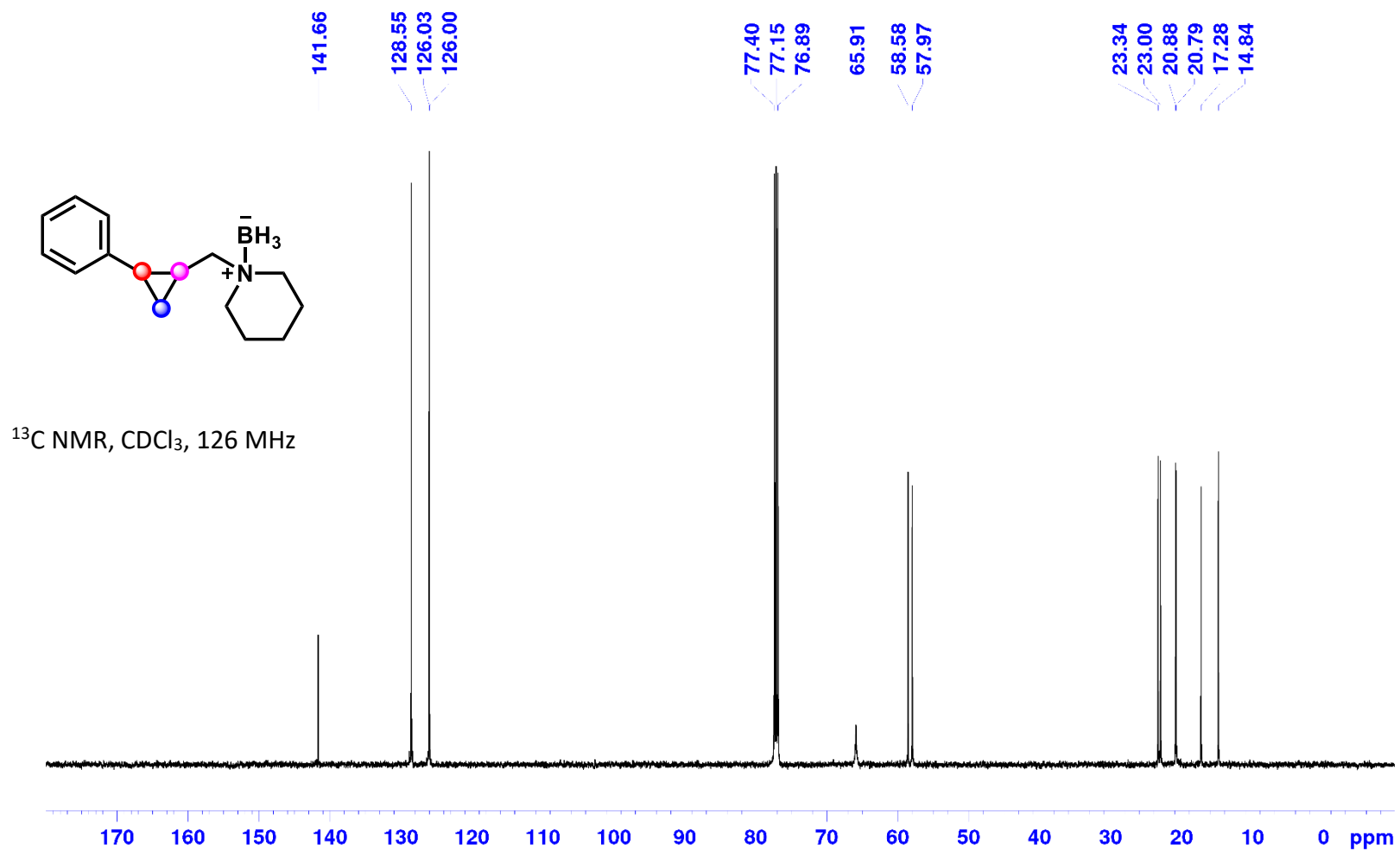
^{11}B NMR, CDCl_3 , 160 MHz



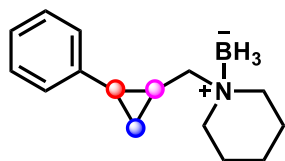
1-((2-Phenylcyclopropyl)methyl)piperidine Borane (1g):



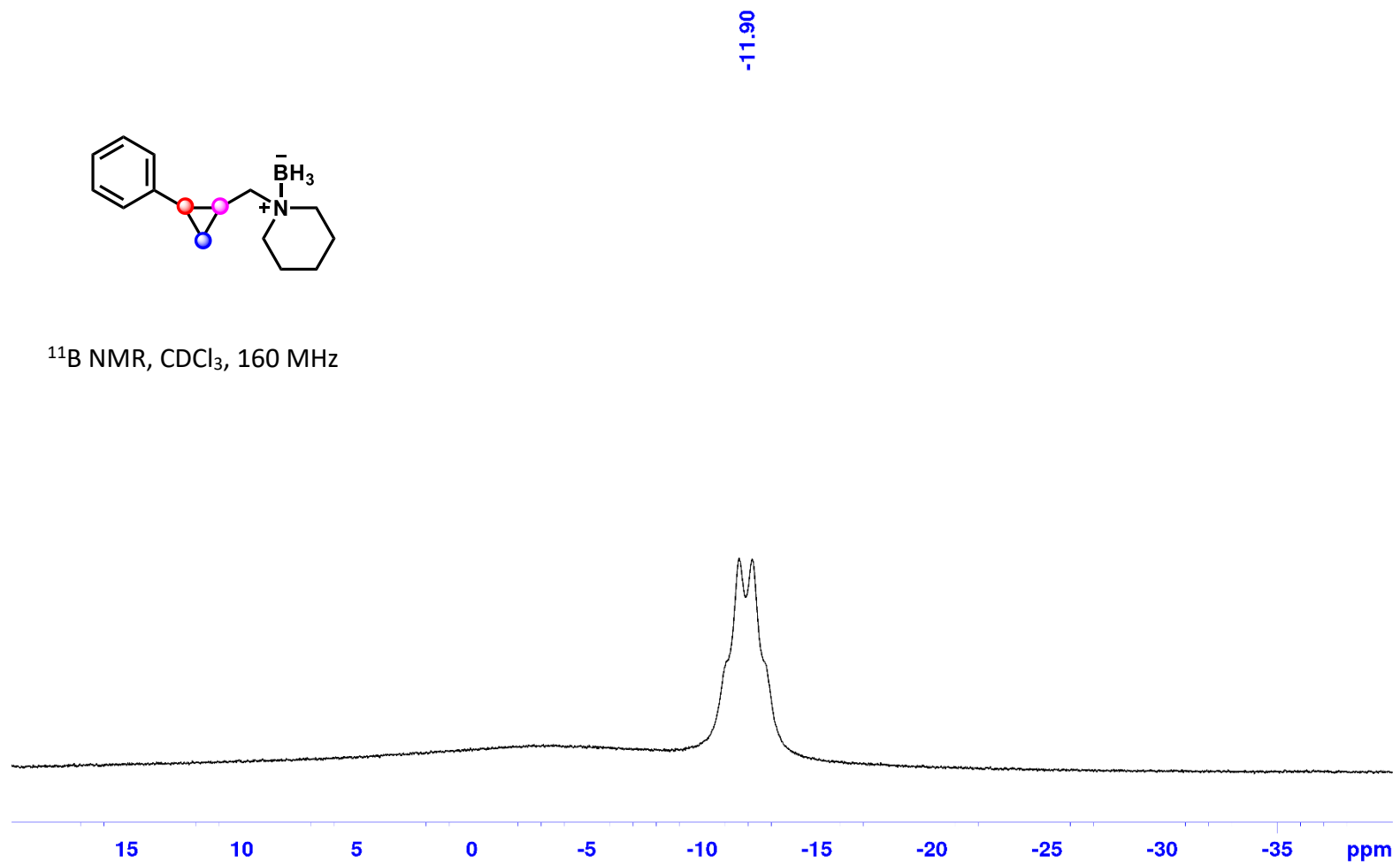
1-((2-Phenylcyclopropyl)methyl)piperidine Borane (1g):



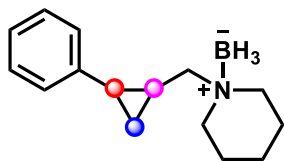
1-((2-Phenylcyclopropyl)methyl)piperidine Borane (1g):



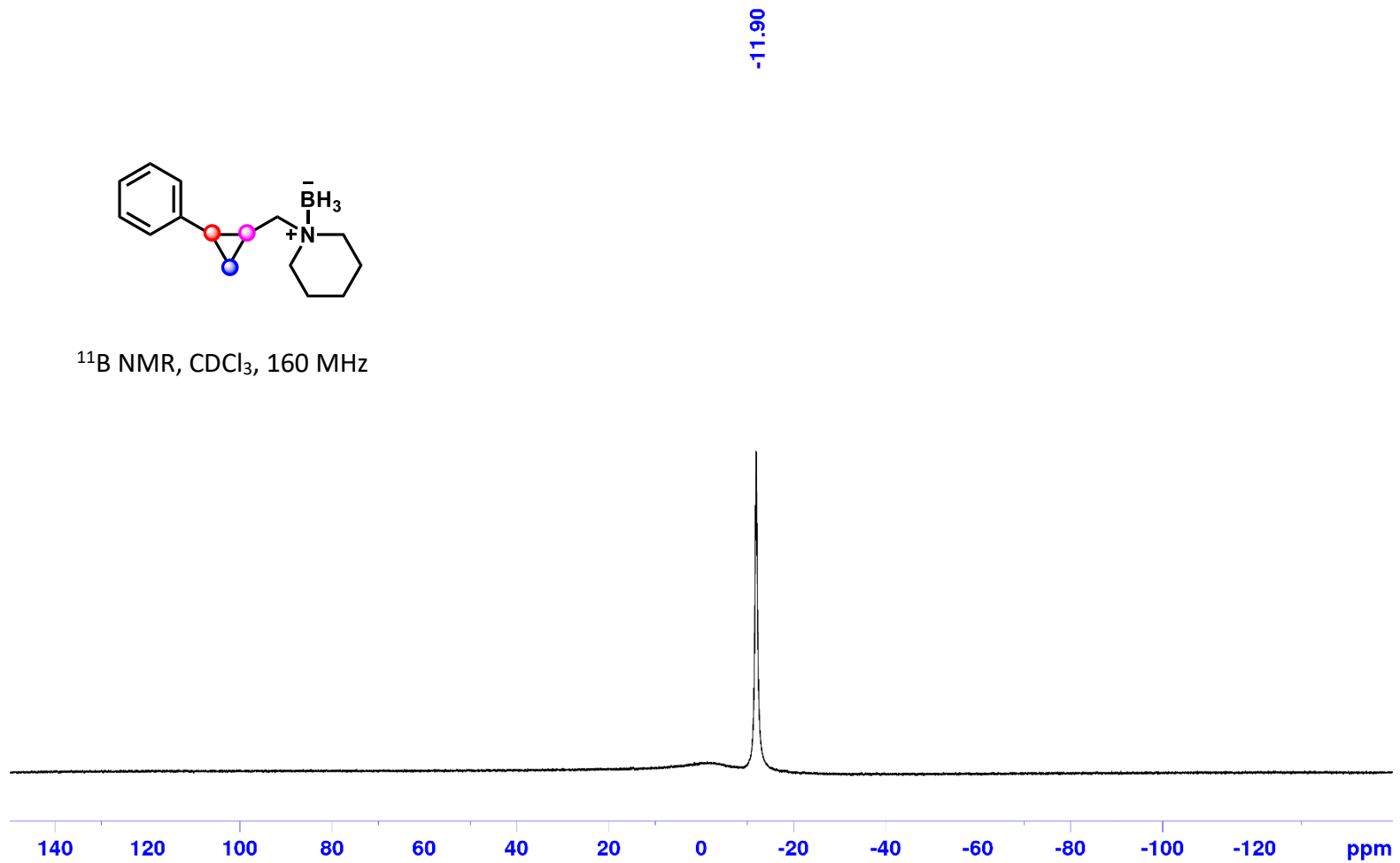
¹¹B NMR, CDCl₃, 160 MHz



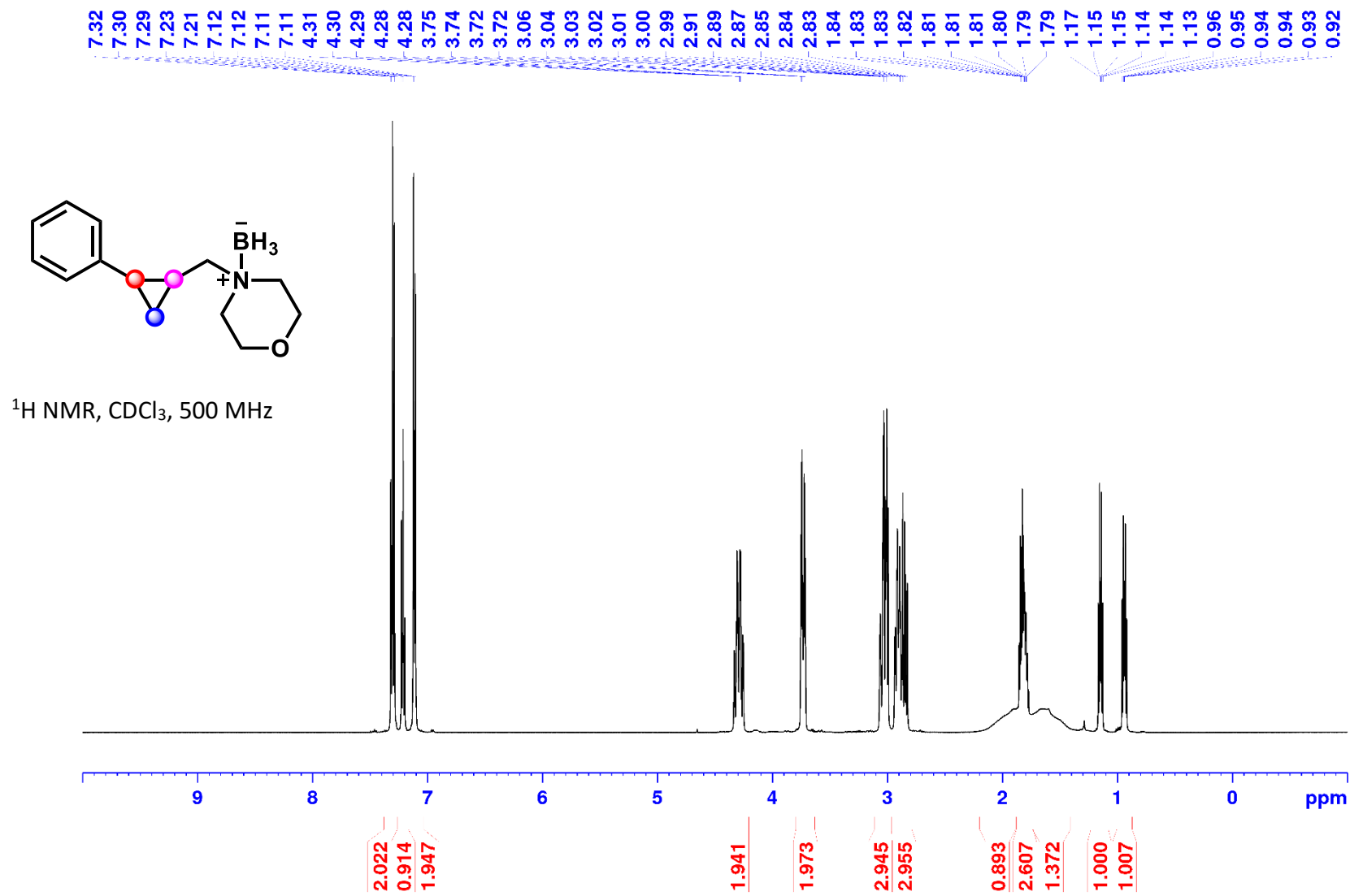
1-((2-Phenylcyclopropyl)methyl)piperidine Borane (1g):



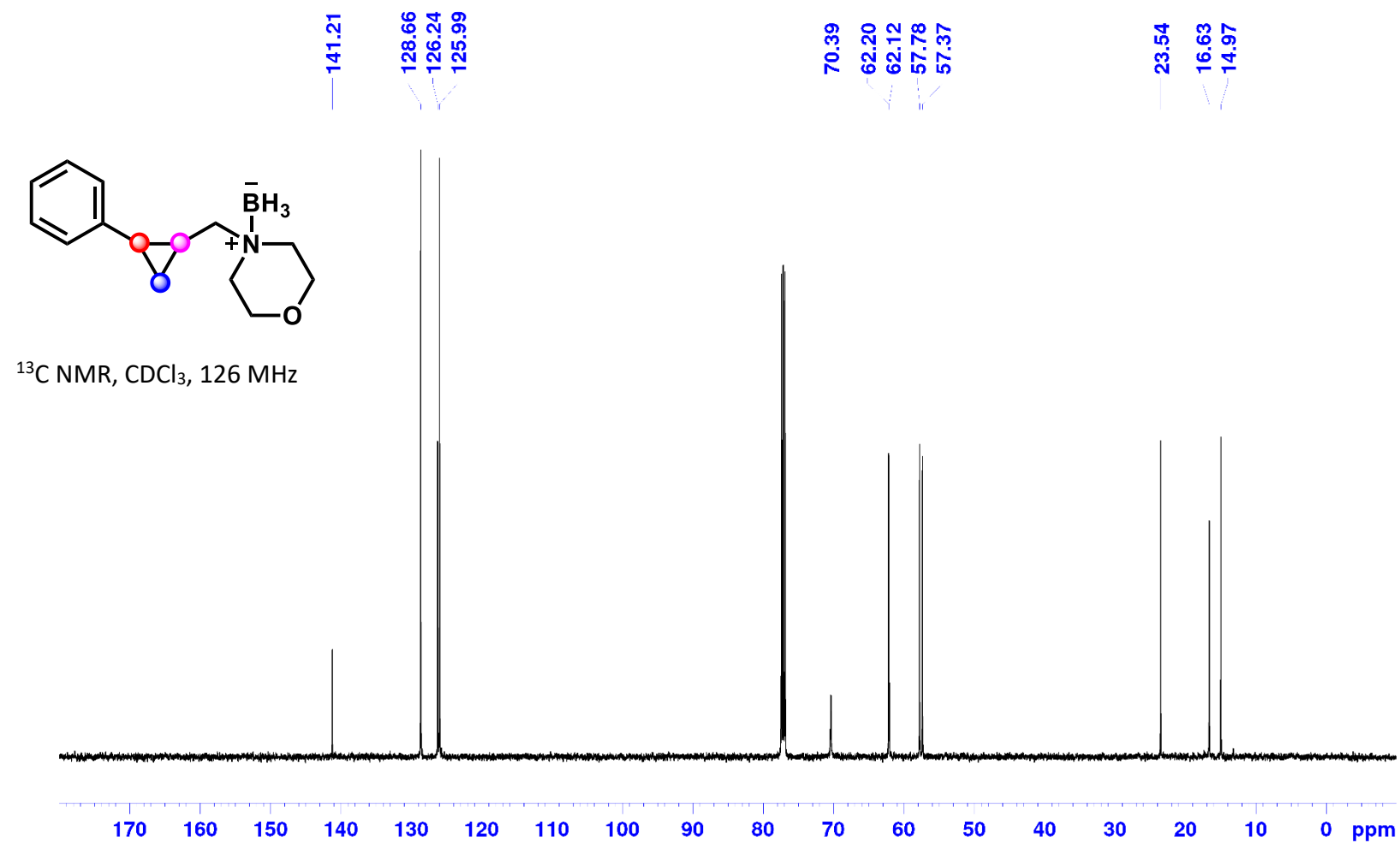
^{11}B NMR, CDCl_3 , 160 MHz



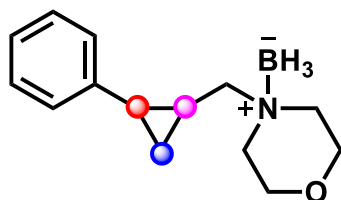
4-((2-Phenylcyclopropyl)methyl)morpholine Borane (1h):



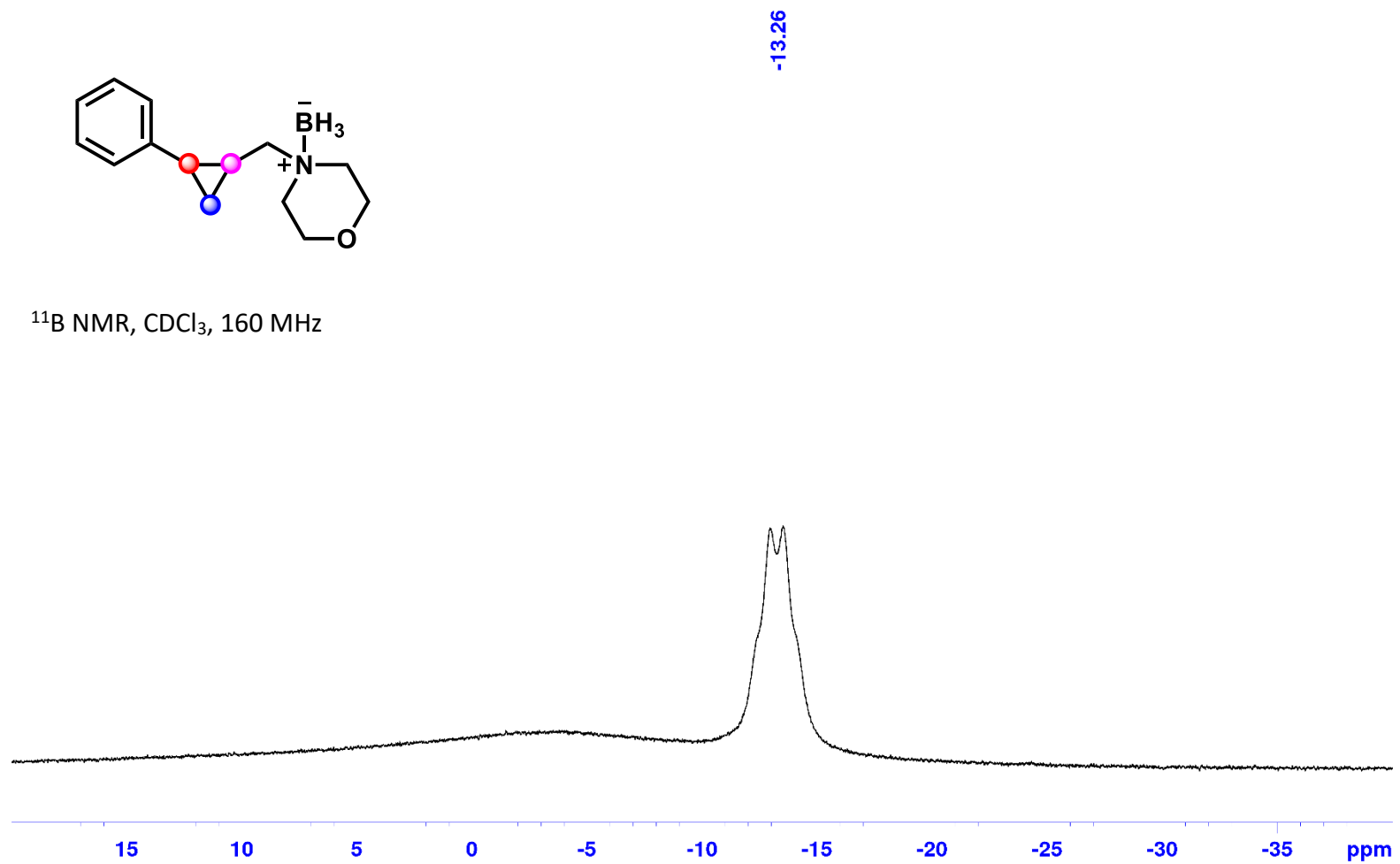
4-((2-Phenylcyclopropyl)methyl)morpholine Borane (1h):



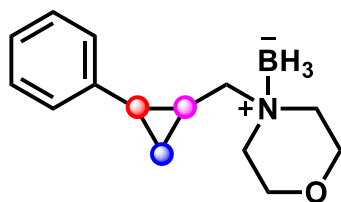
4-((2-Phenylcyclopropyl)methyl)morpholine Borane (1h):



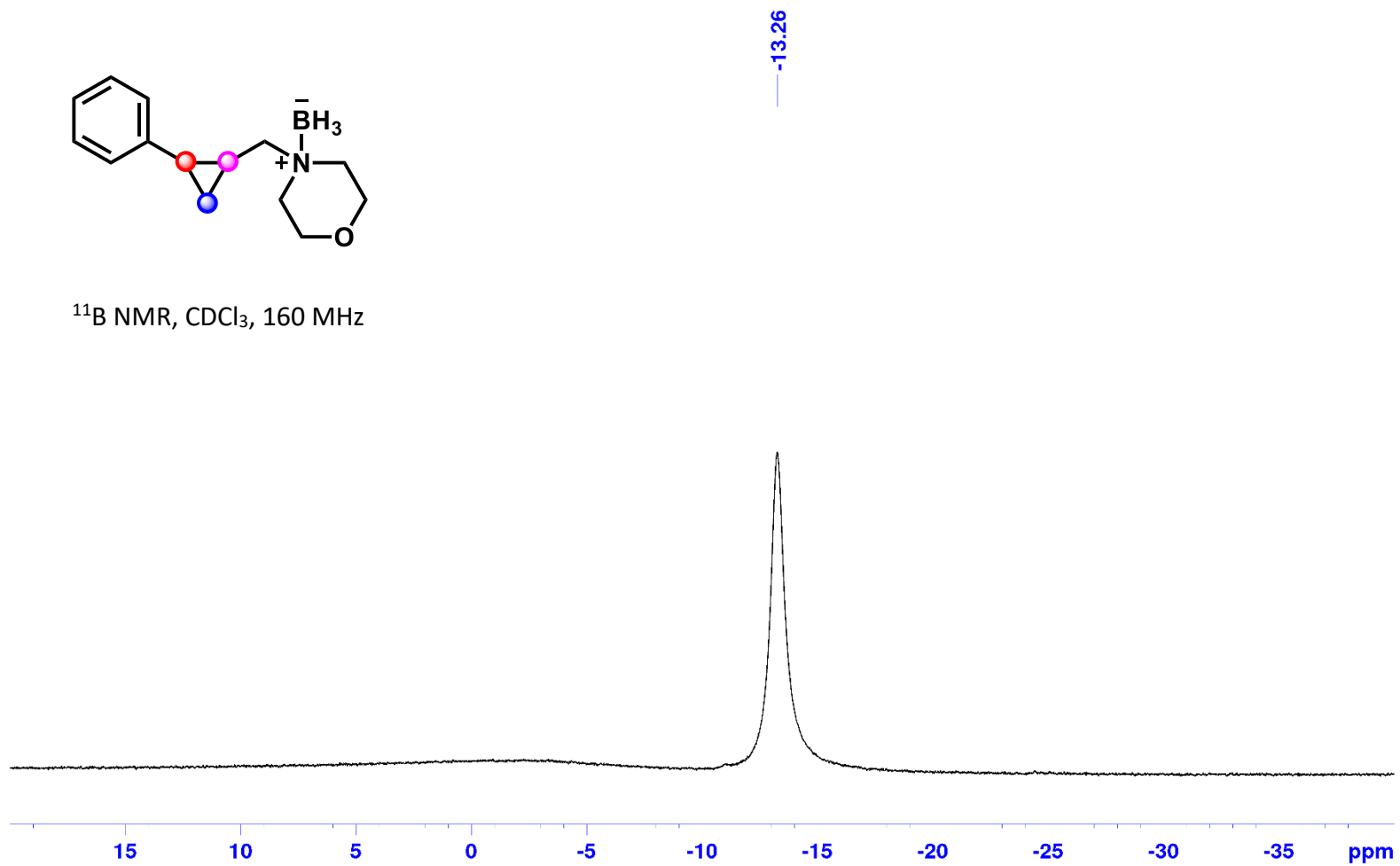
^{11}B NMR, CDCl_3 , 160 MHz



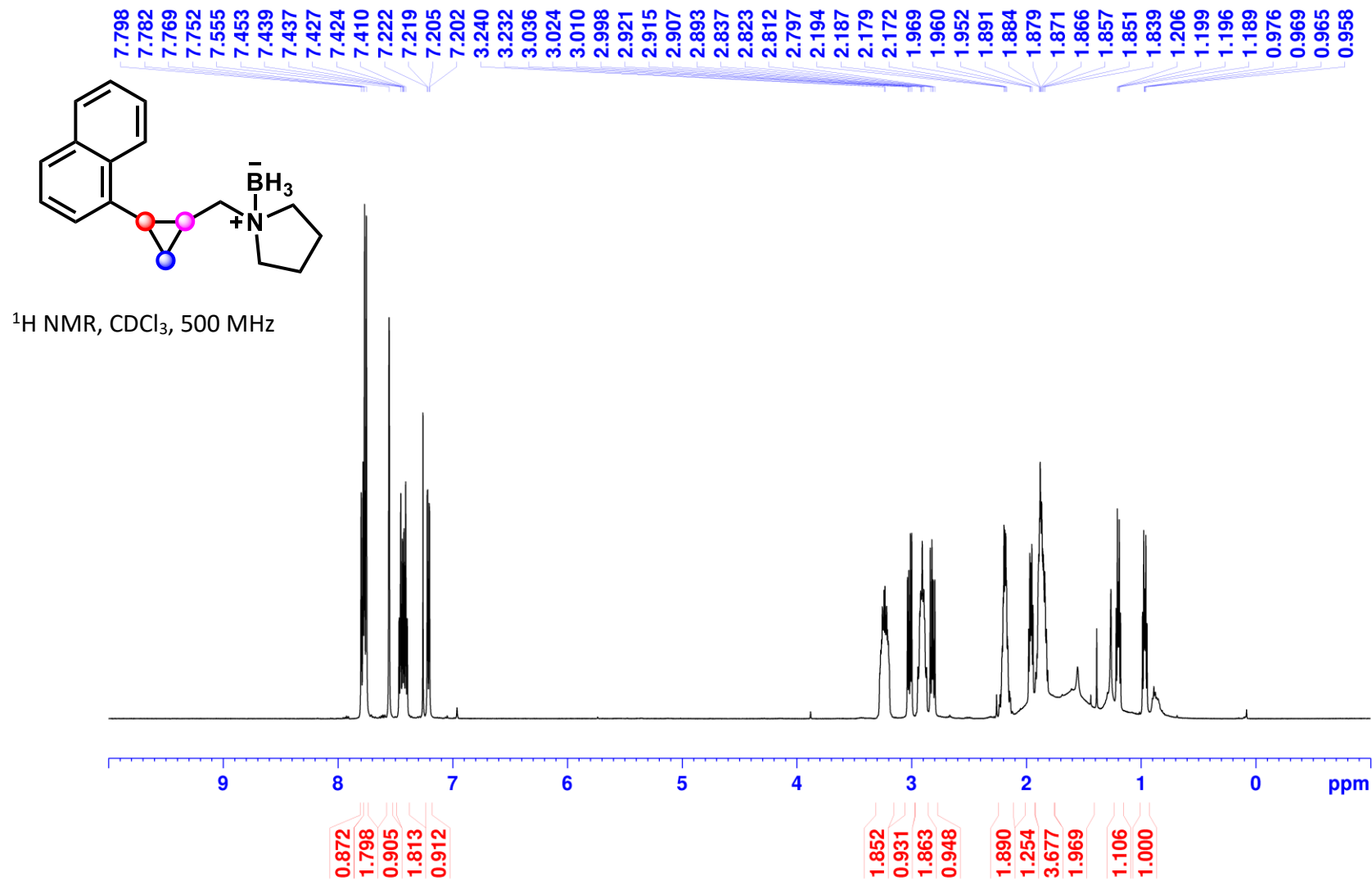
4-((2-Phenylcyclopropyl)methyl)morpholine Borane (1h):



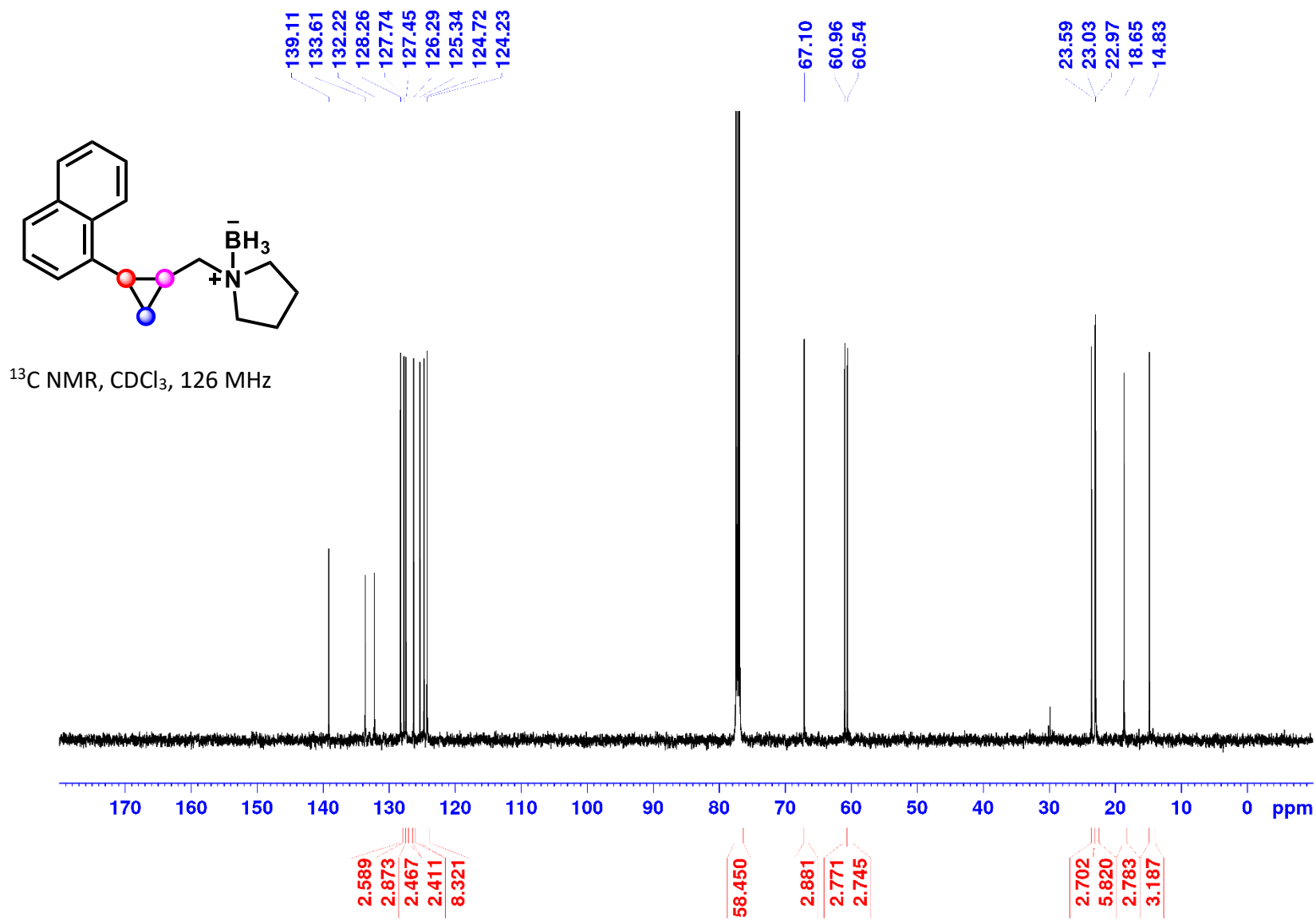
^{11}B NMR, CDCl_3 , 160 MHz



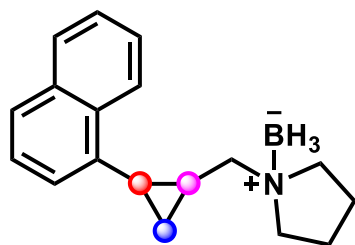
1-((2-(Naphthalen-1-yl)cyclopropyl)methyl)pyrrolidine Borane (1i):



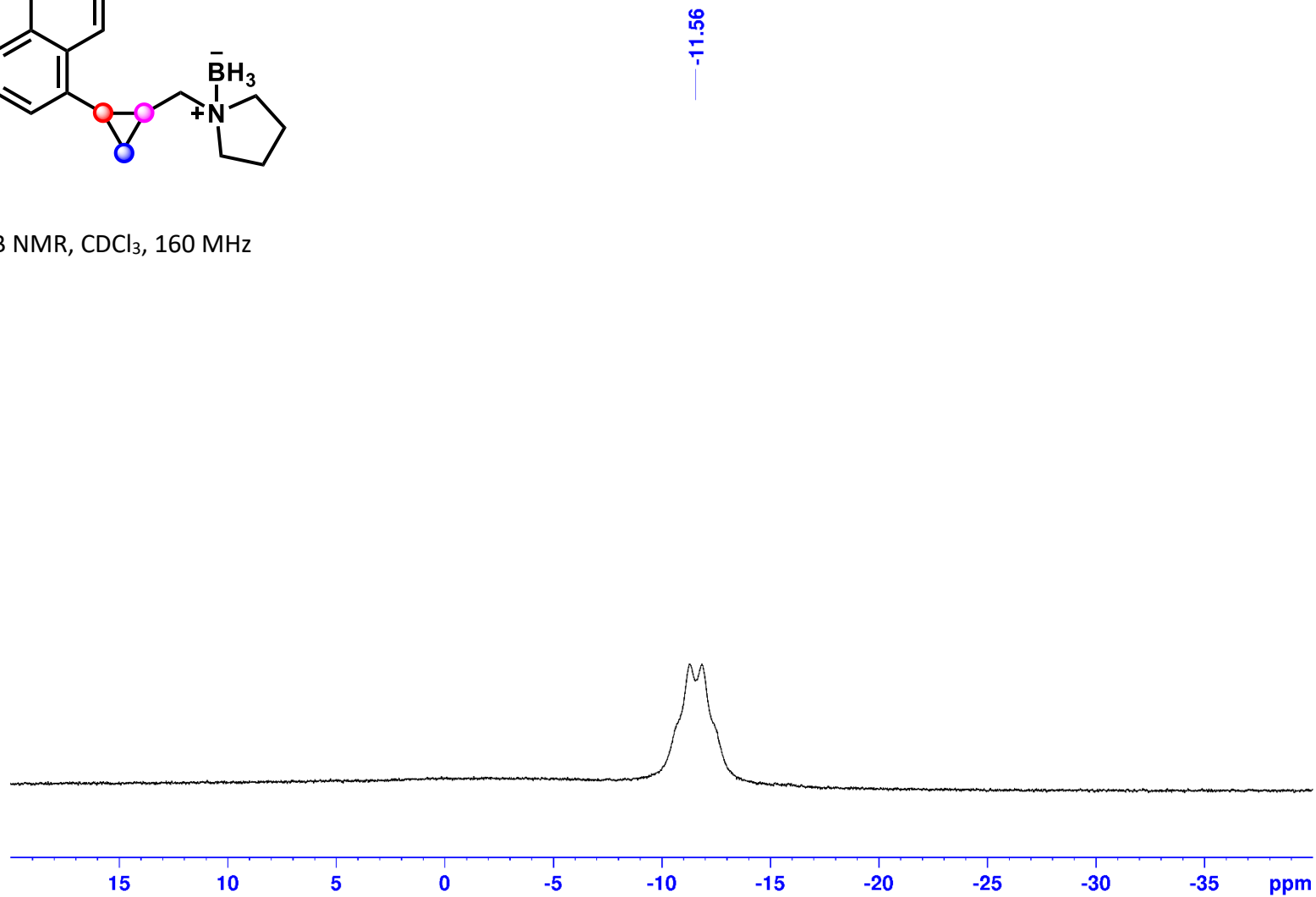
1-((2-(Naphthalen-1-yl)cyclopropyl)methyl)pyrrolidine Borane (1i):



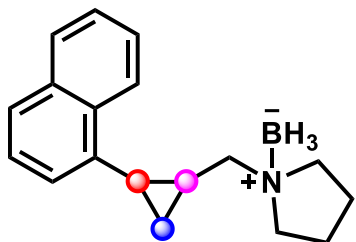
1-((2-(Naphthalen-1-yl)cyclopropyl)methyl)pyrrolidine Borane (1i):



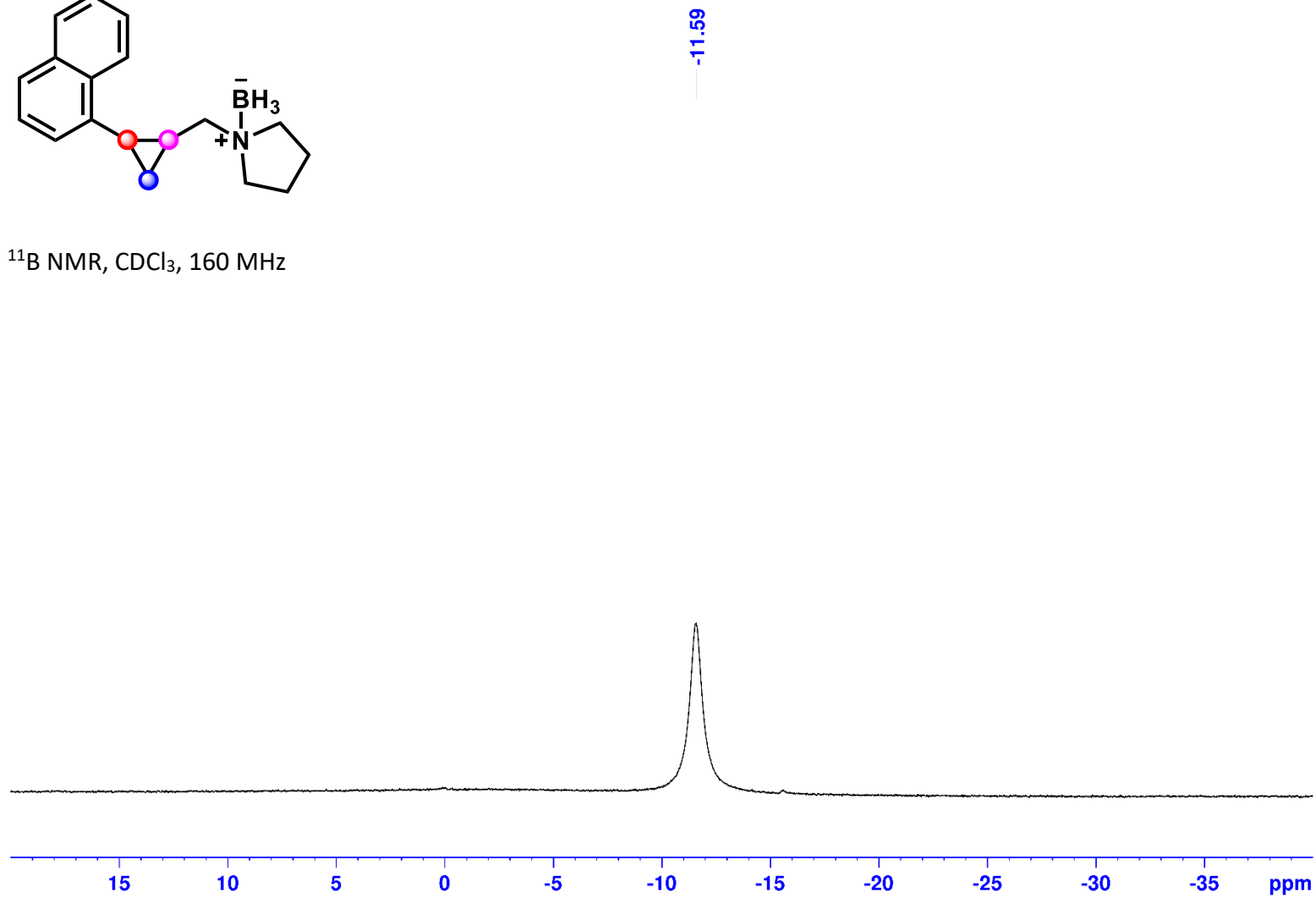
^{11}B NMR, CDCl_3 , 160 MHz



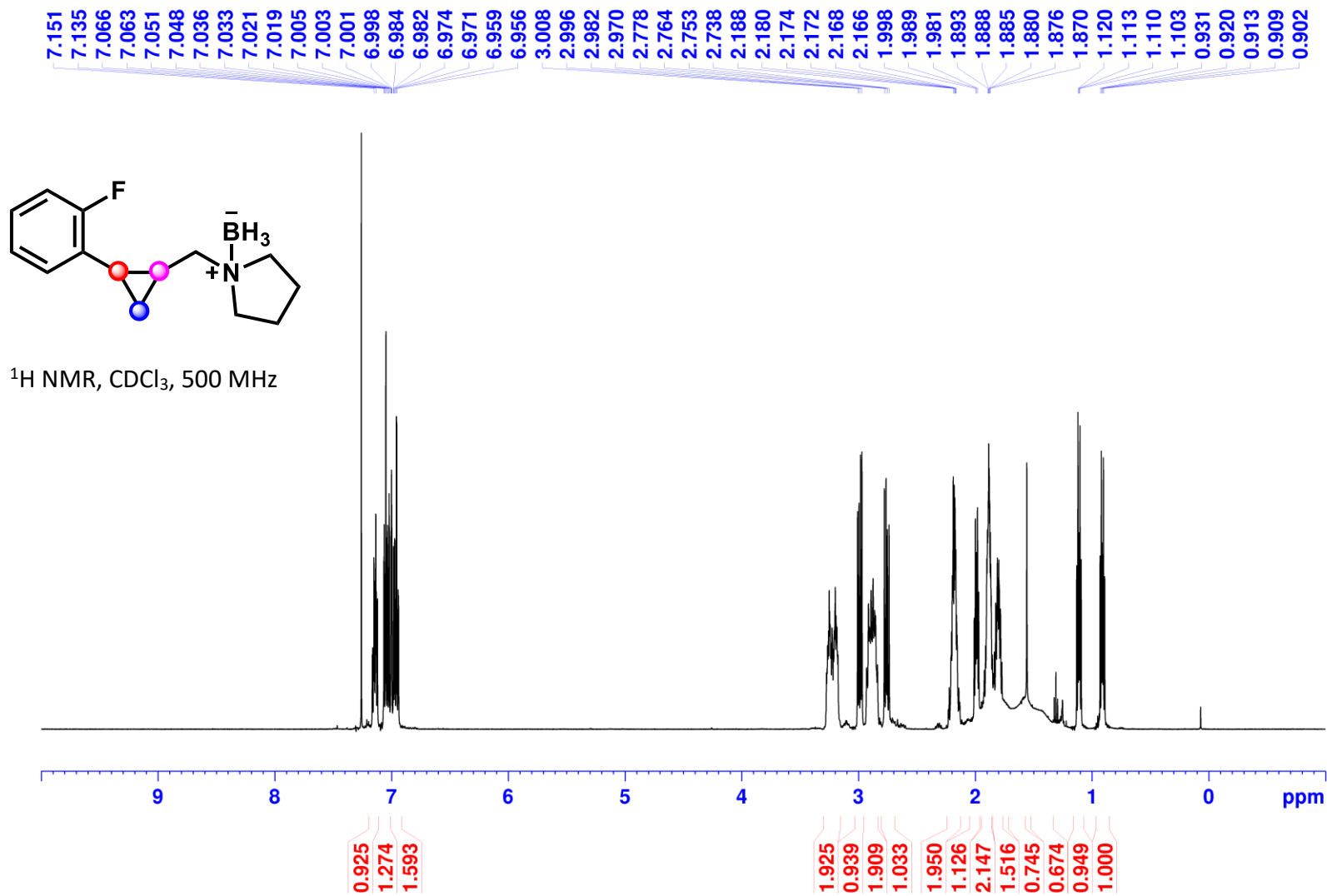
1-((2-(Naphthalen-1-yl)cyclopropyl)methyl)pyrrolidine Borane (1i):



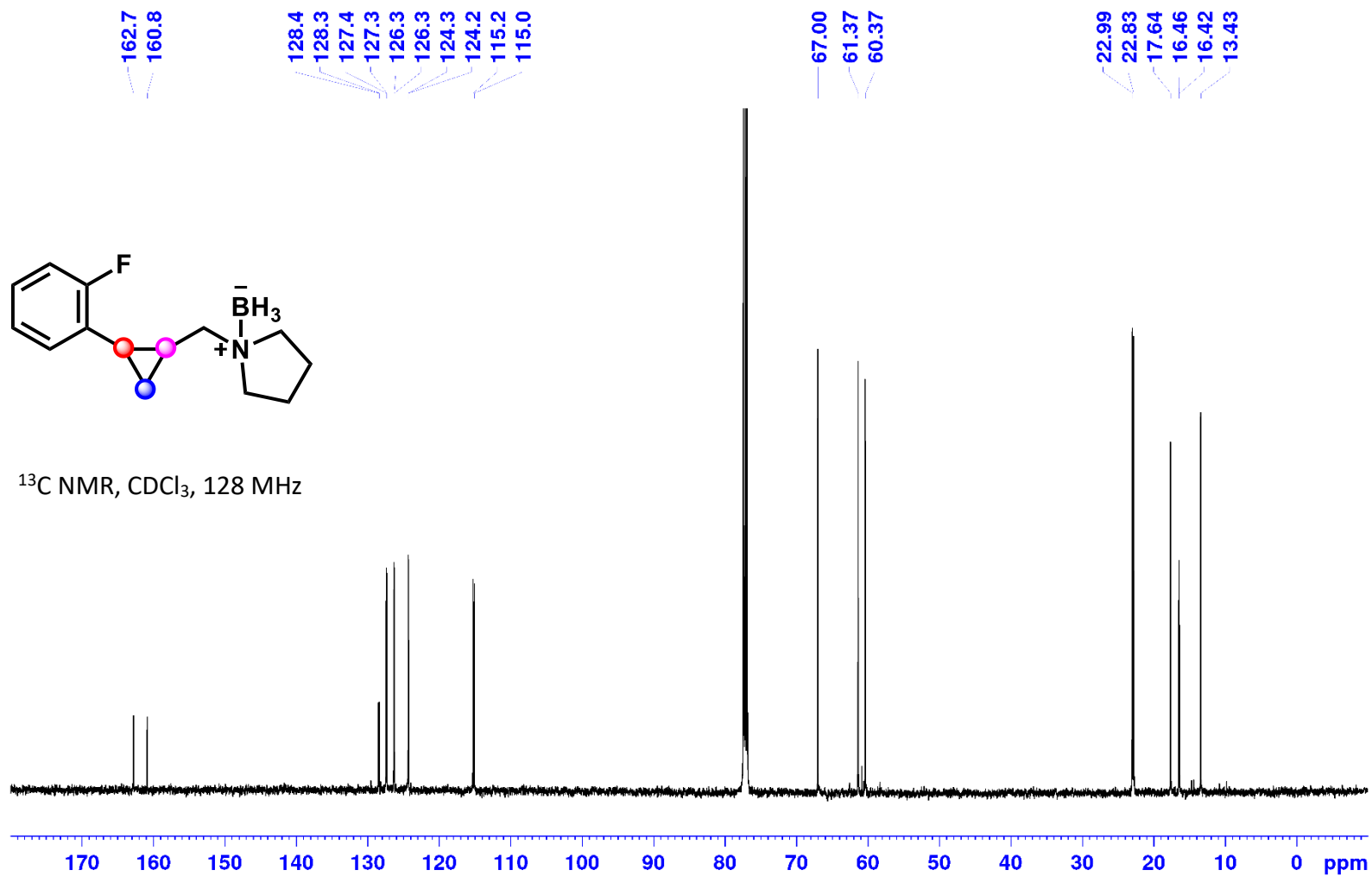
^{11}B NMR, CDCl_3 , 160 MHz



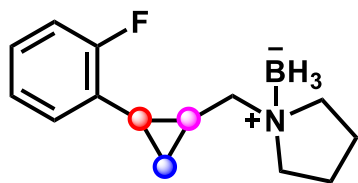
1-((2-(2-Fluorophenyl)cyclopropyl)methyl)pyrrolidine Borane (1j) :



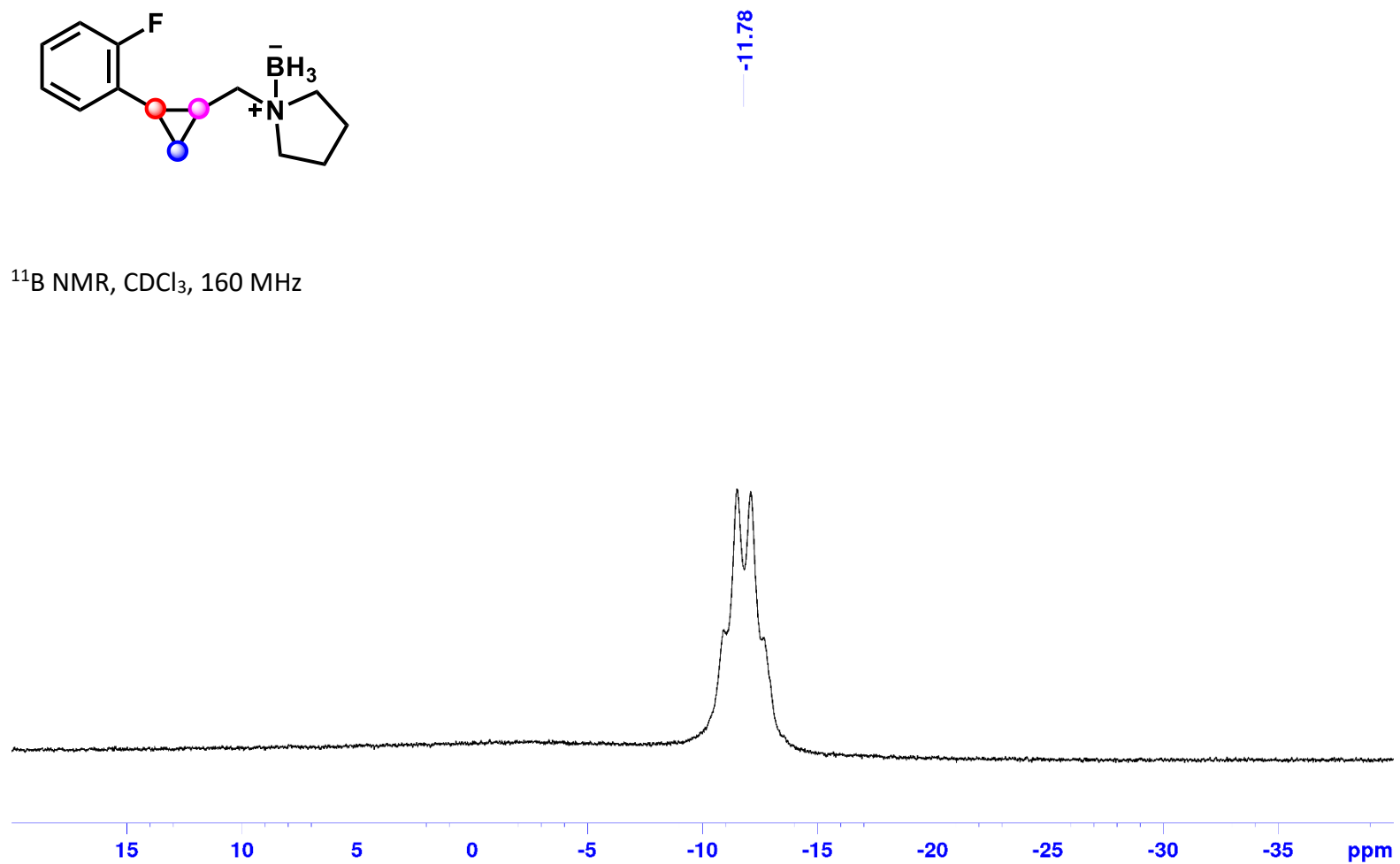
1-((2-(2-Fluorophenyl)cyclopropyl)methyl)pyrrolidine Borane (1j) :



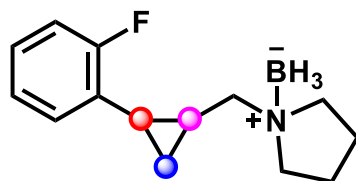
1-((2-(2-Fluorophenyl)cyclopropyl)methyl)pyrrolidine Borane (1j) :



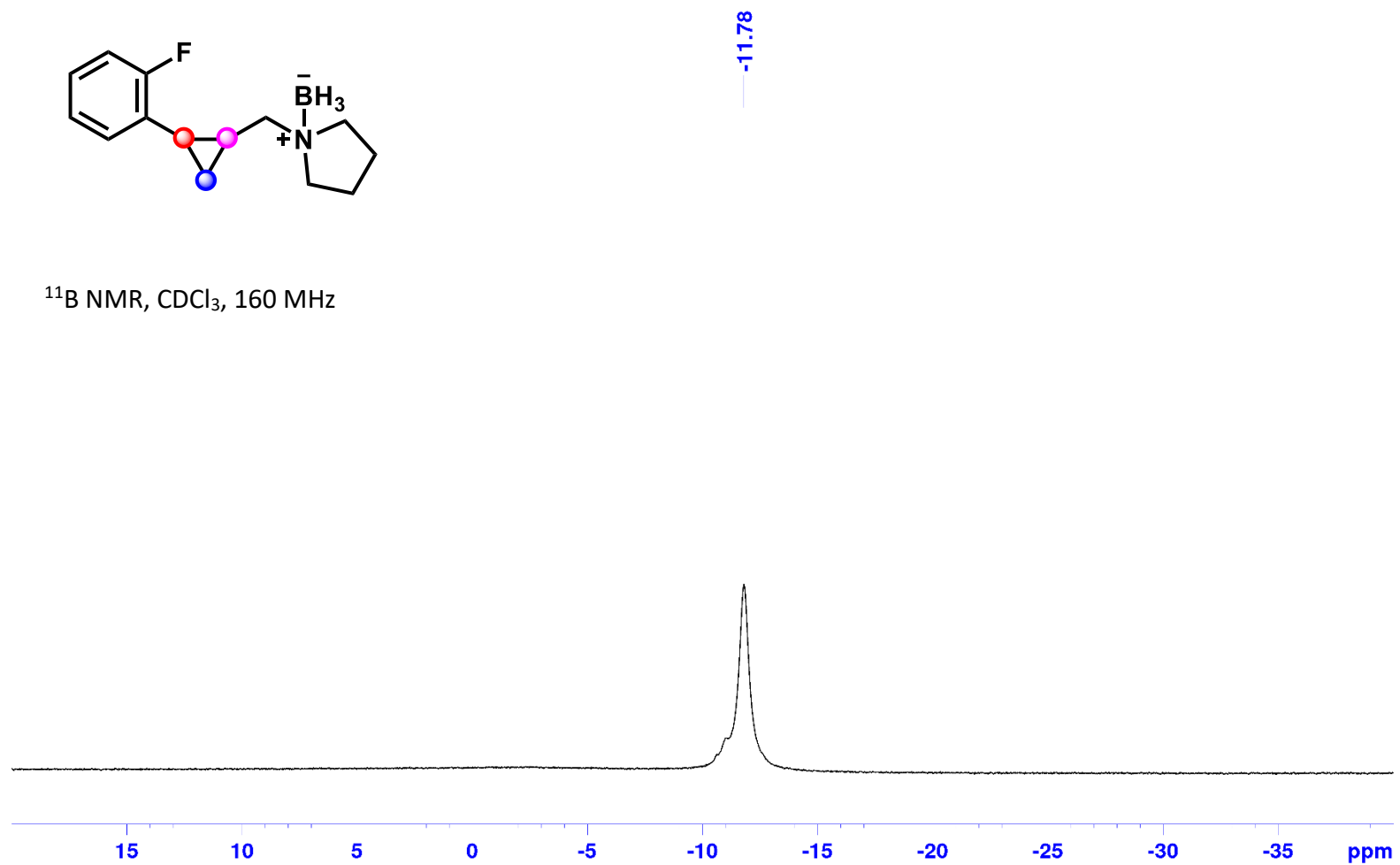
^{11}B NMR, CDCl_3 , 160 MHz



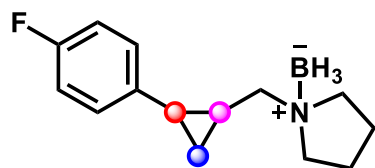
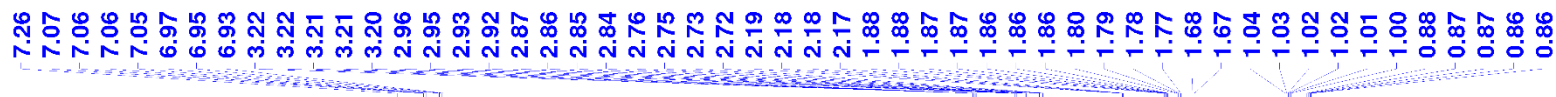
1-((2-(2-Fluorophenyl)cyclopropyl)methyl)pyrrolidine Borane (1j) :



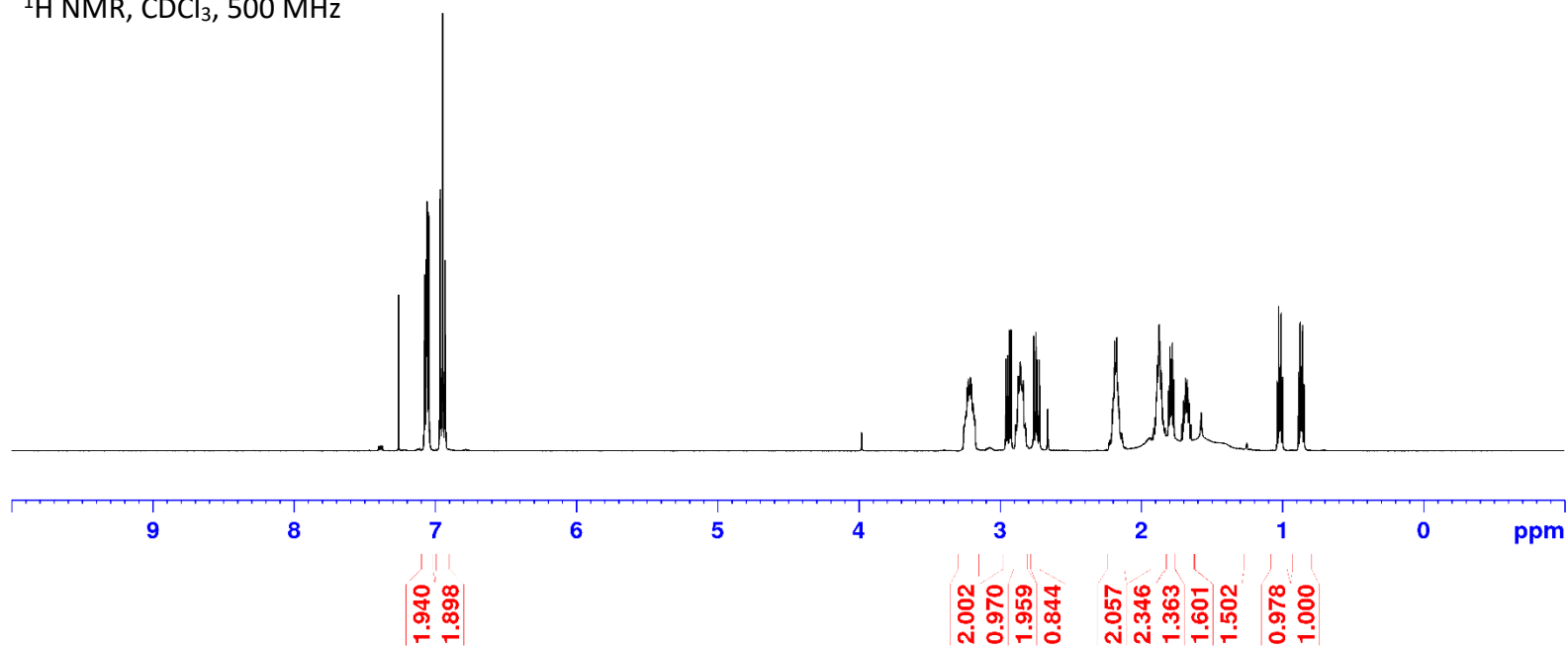
^{11}B NMR, CDCl_3 , 160 MHz



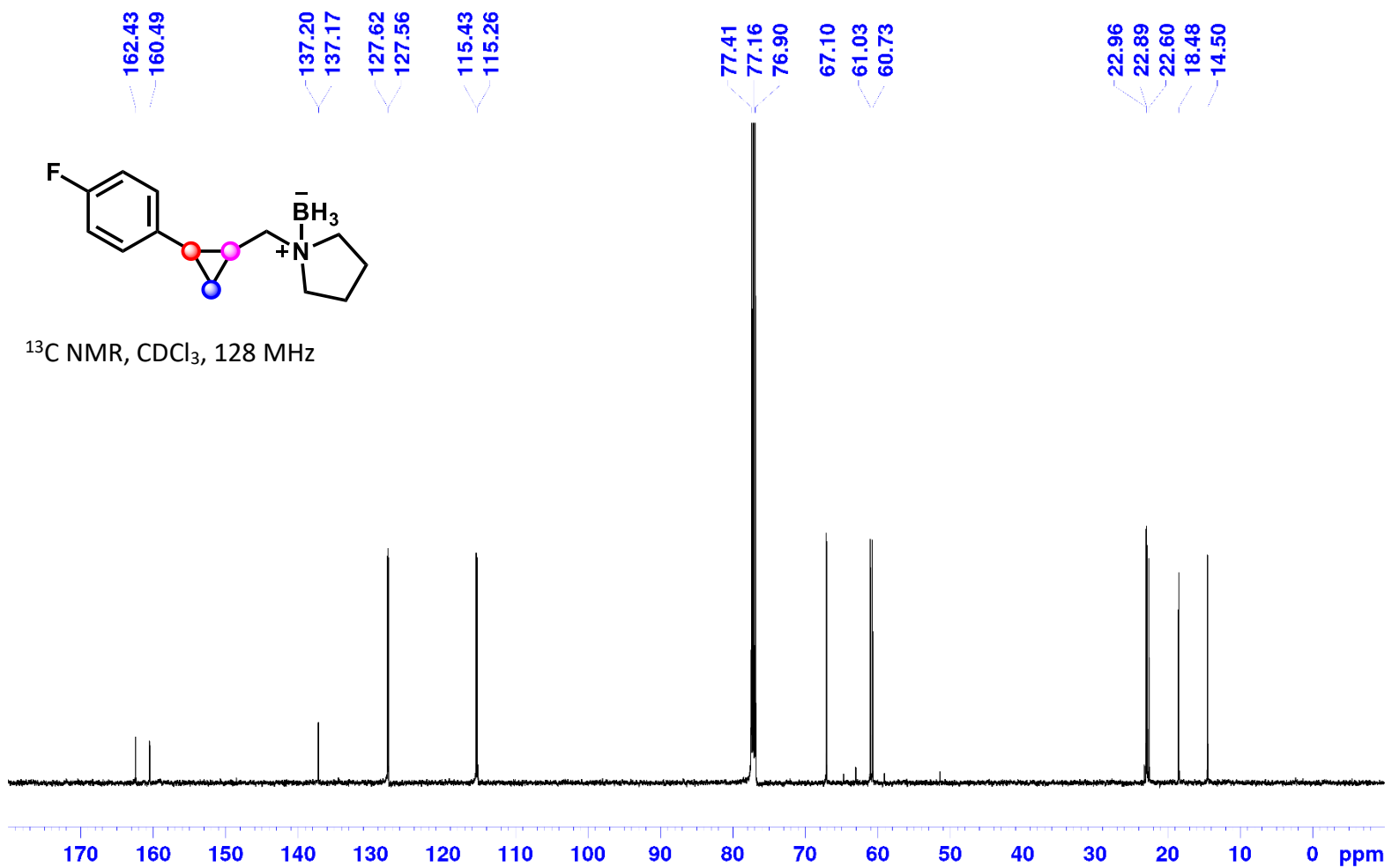
1-((2-(4-Fluorophenyl)cyclopropyl)methyl)pyrrolidine Borane (1k):



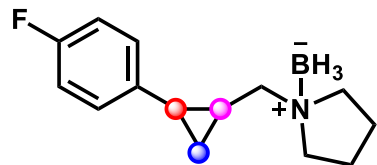
^1H NMR, CDCl_3 , 500 MHz



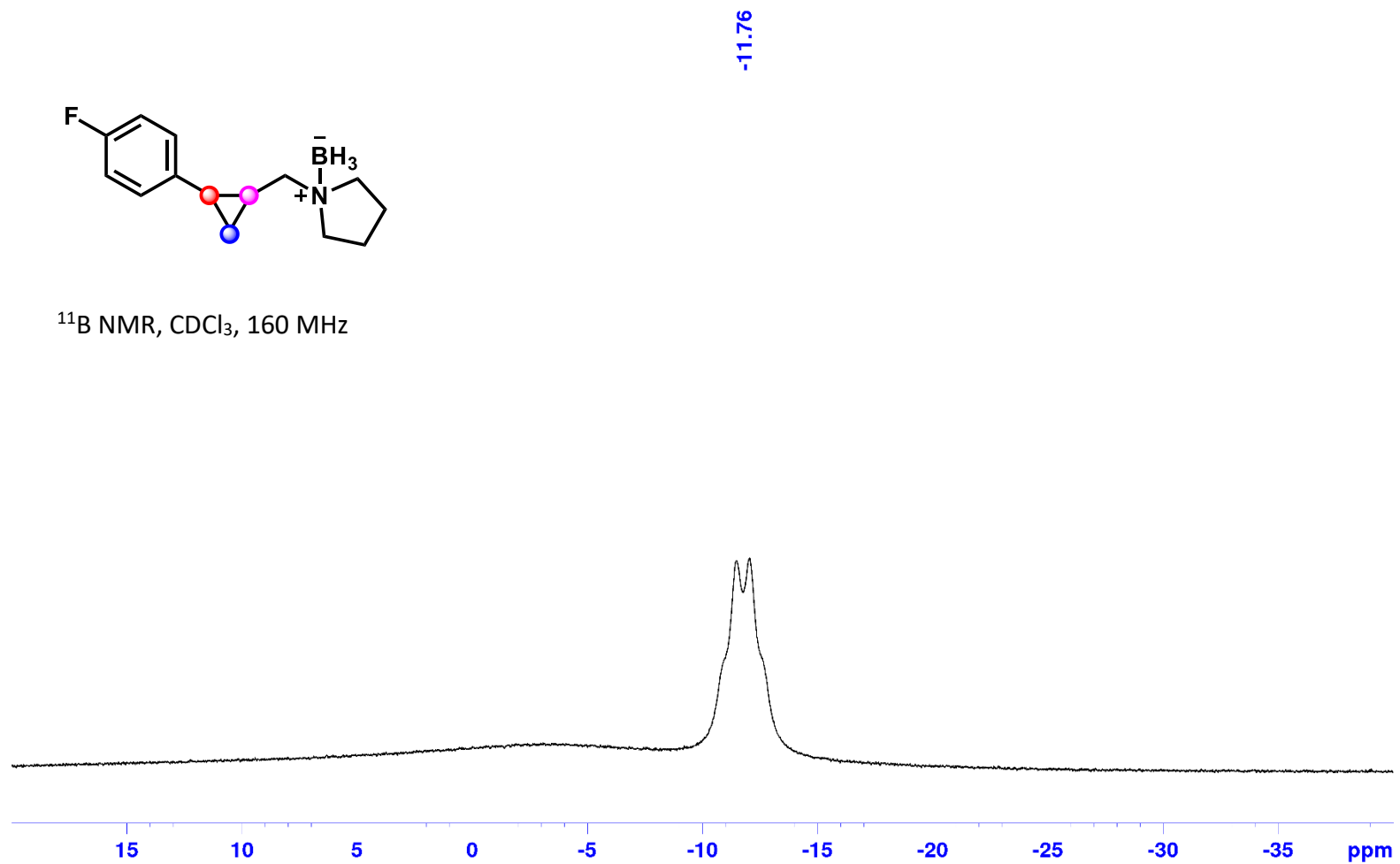
1-((2-(4-Fluorophenyl)cyclopropyl)methyl)pyrrolidine Borane (**1k**):



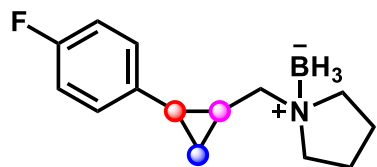
1-((2-(4-Fluorophenyl)cyclopropyl)methyl)pyrrolidine Borane (1k):



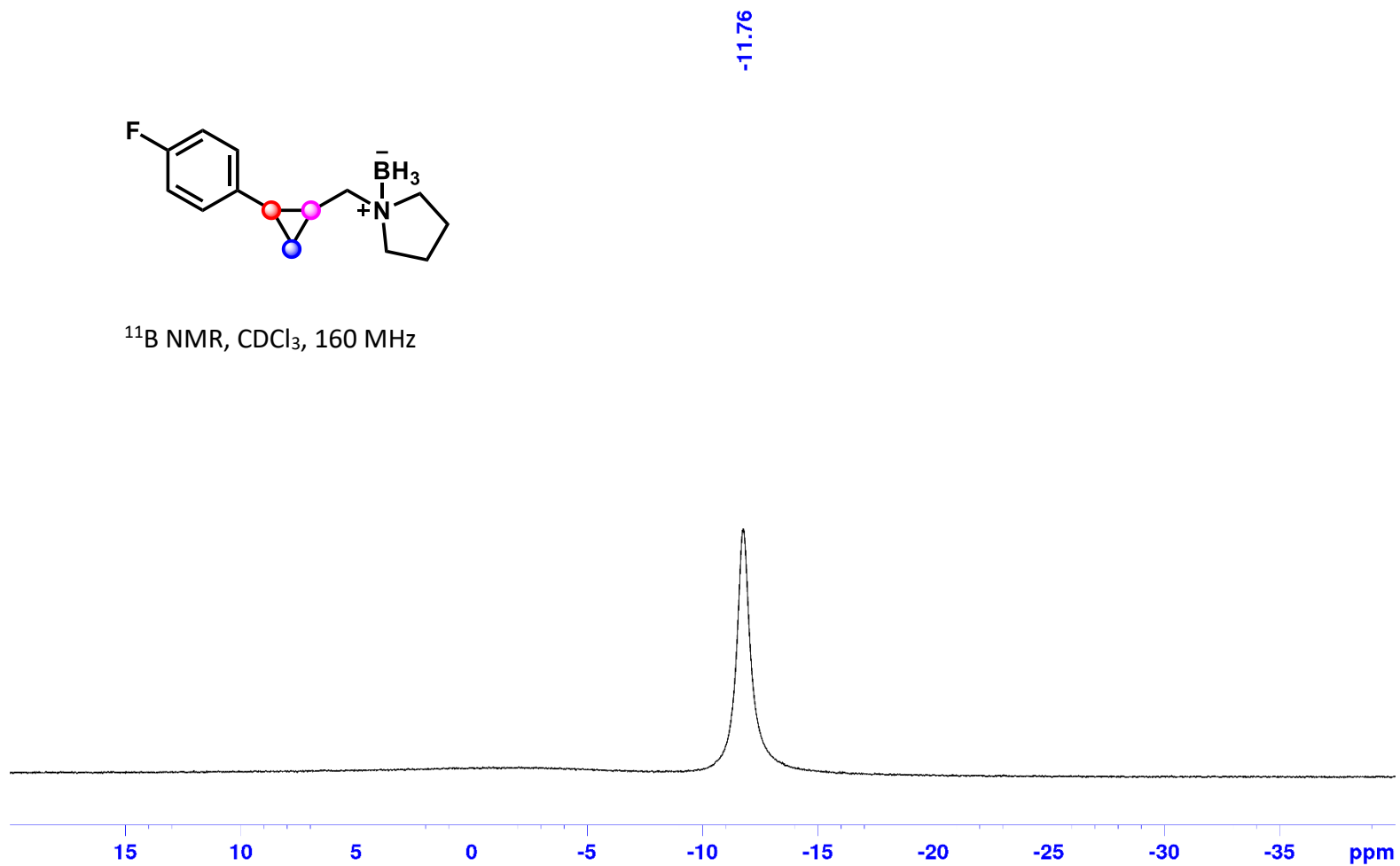
¹¹B NMR, CDCl₃, 160 MHz



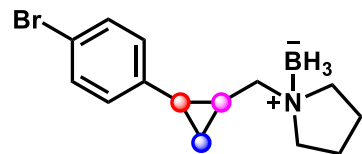
1-((2-(4-Fluorophenyl)cyclopropyl)methyl)pyrrolidine Borane (**1k**):



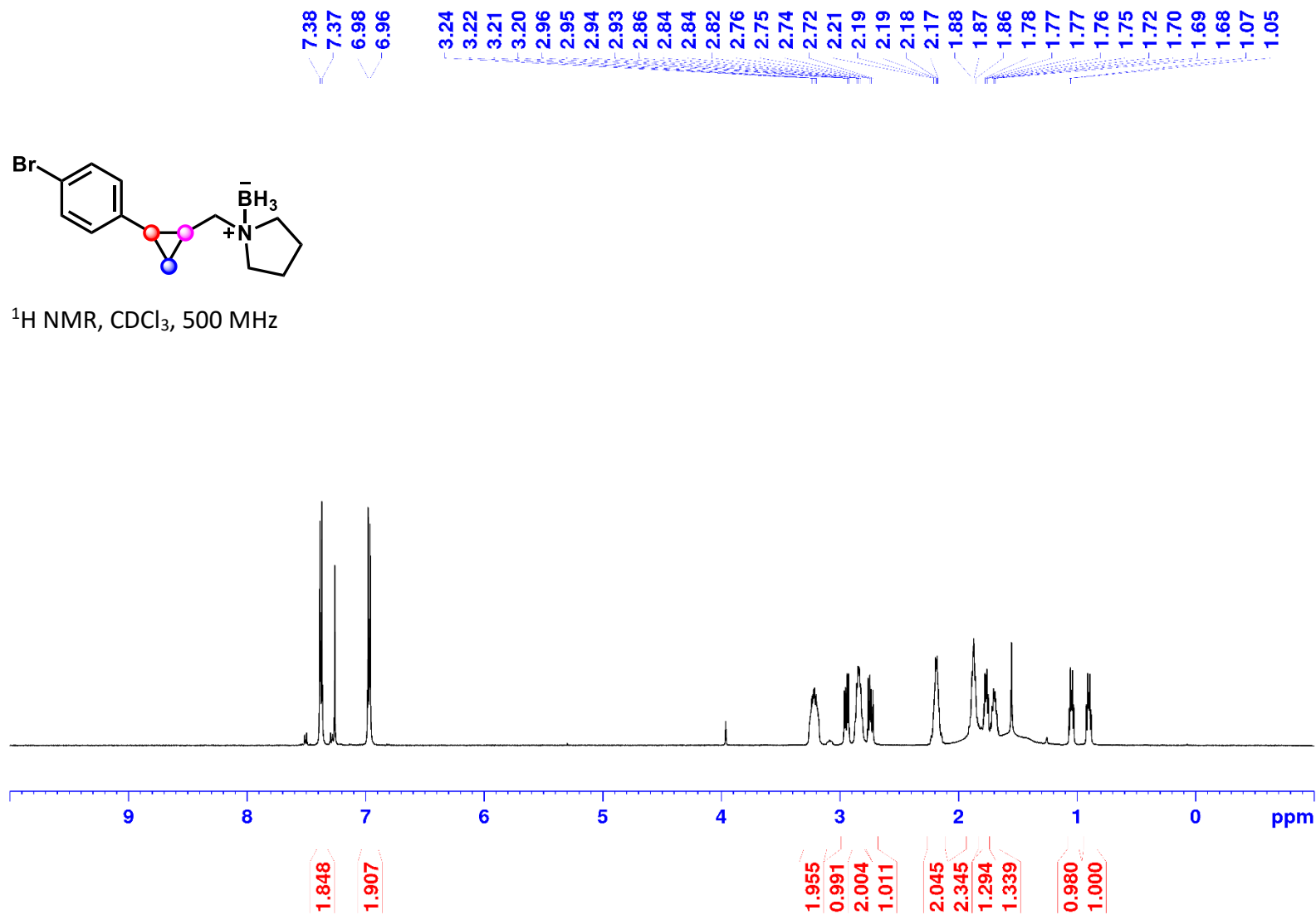
^{11}B NMR, CDCl_3 , 160 MHz



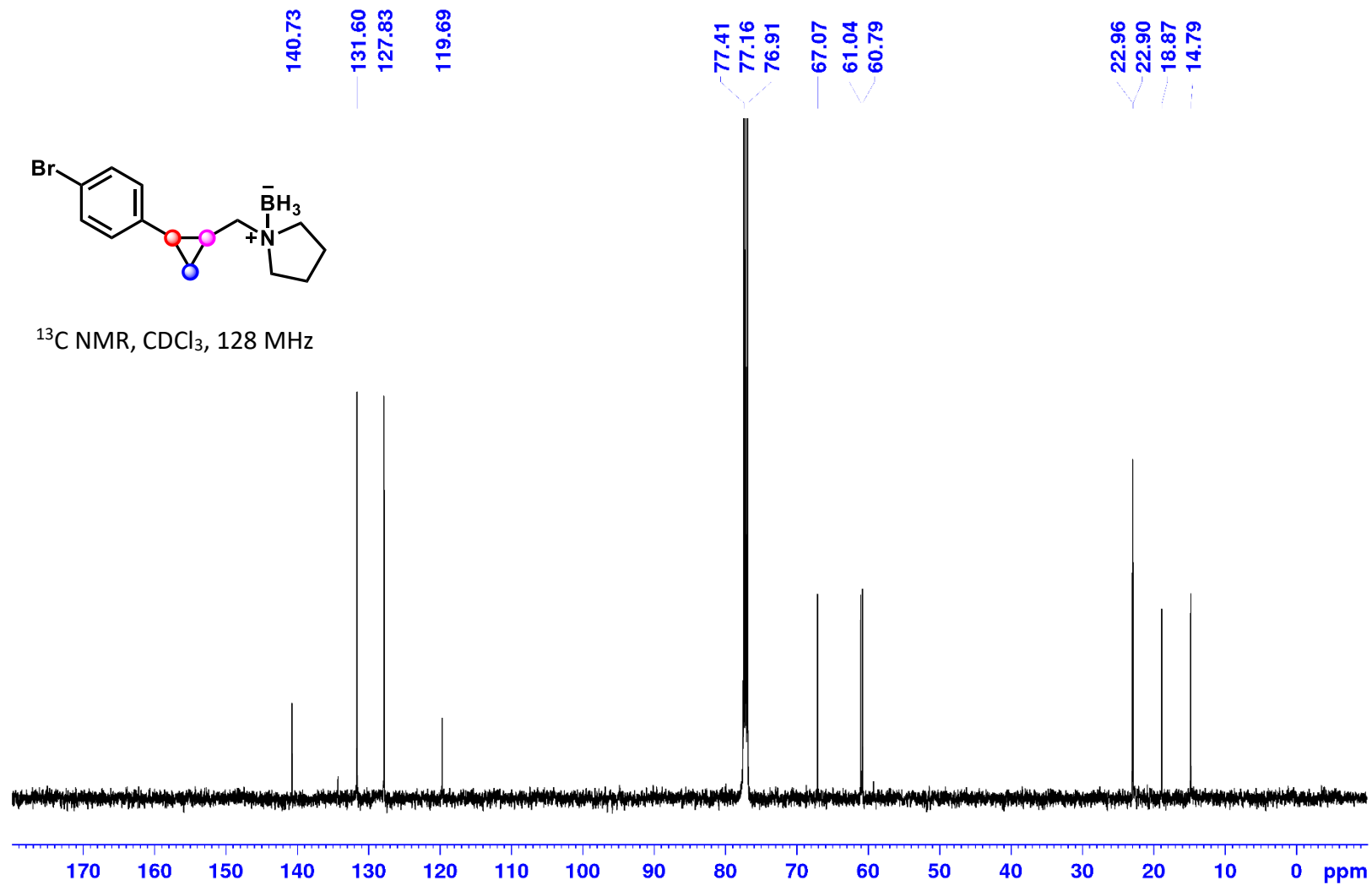
1-((2-(4-Bromophenyl)cyclopropyl)methyl)pyrrolidine Borane (1l):



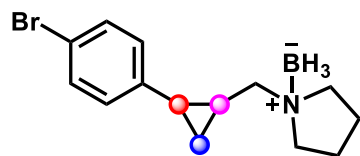
^1H NMR, CDCl_3 , 500 MHz



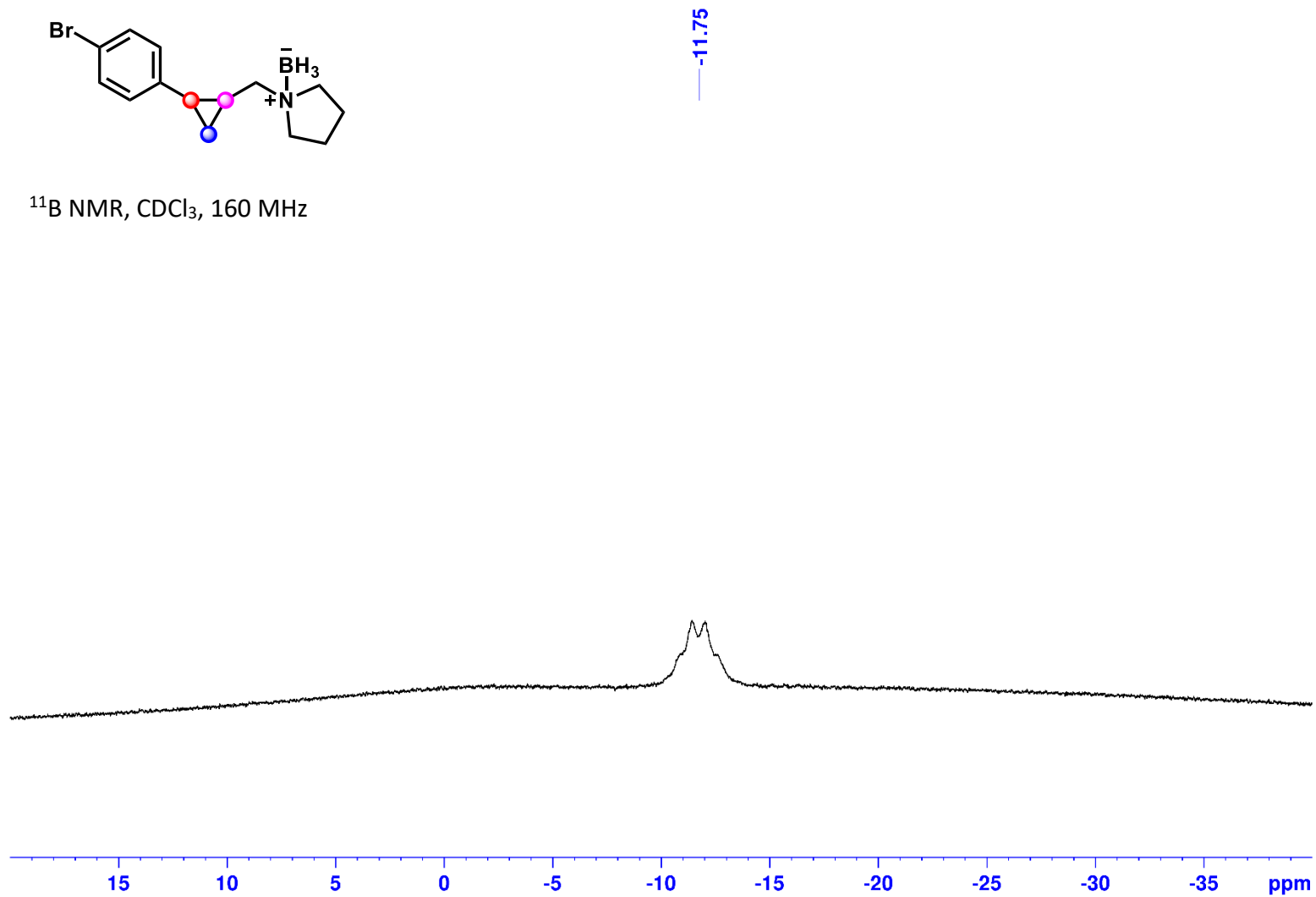
1-((2-(4-Bromophenyl)cyclopropyl)methyl)pyrrolidine Borane (1l):



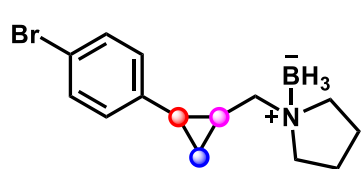
1-((2-(4-Bromophenyl)cyclopropyl)methyl)pyrrolidine Borane (1l):



^{11}B NMR, CDCl_3 , 160 MHz

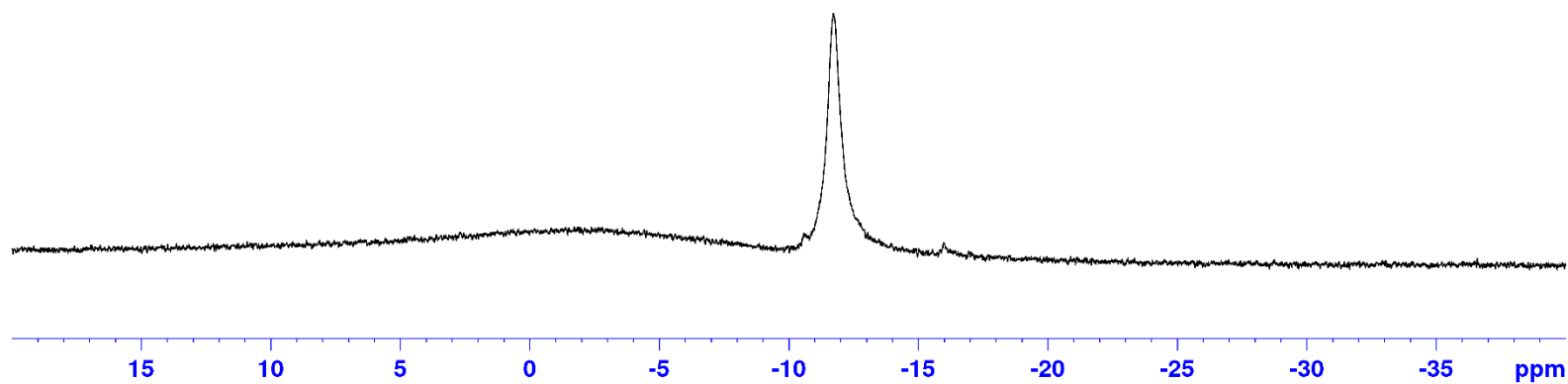


1-((2-(4-Bromophenyl)cyclopropyl)methyl)pyrrolidine Borane (1l):

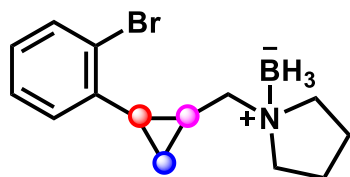


-11.74

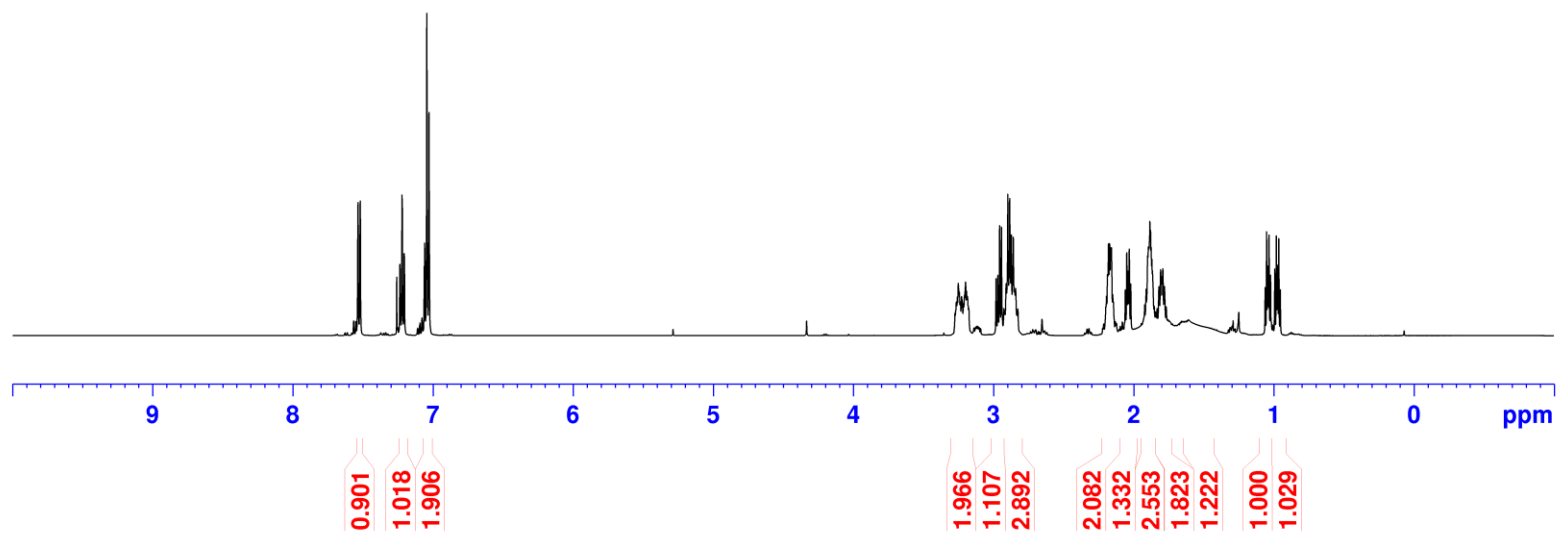
^{11}B NMR, CDCl_3 , 160 MHz



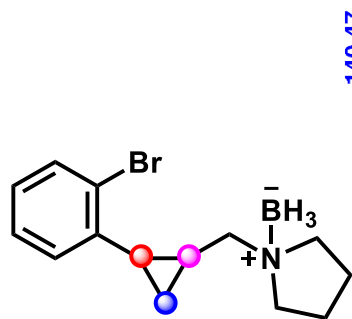
1-((2-(2-Bromophenyl)cyclopropyl)methyl)pyrrolidine Borane (1m):



¹H NMR, CDCl₃, 500 MHz



1-((2-(2-Bromophenyl)cyclopropyl)methyl)pyrrolidine Borane (1m):

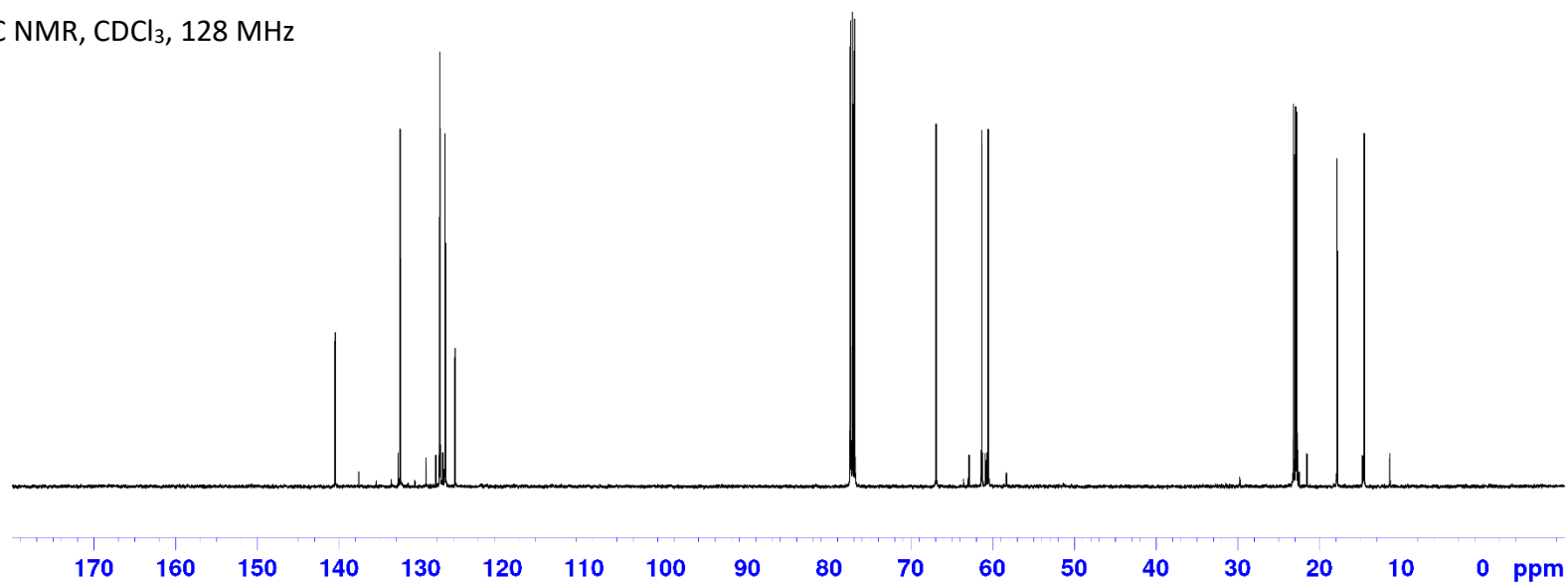


140.47
132.52
127.68
127.67
127.01
125.80

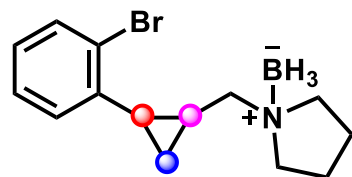
66.92
61.34
60.54

23.17
22.92
22.77
17.84
14.54

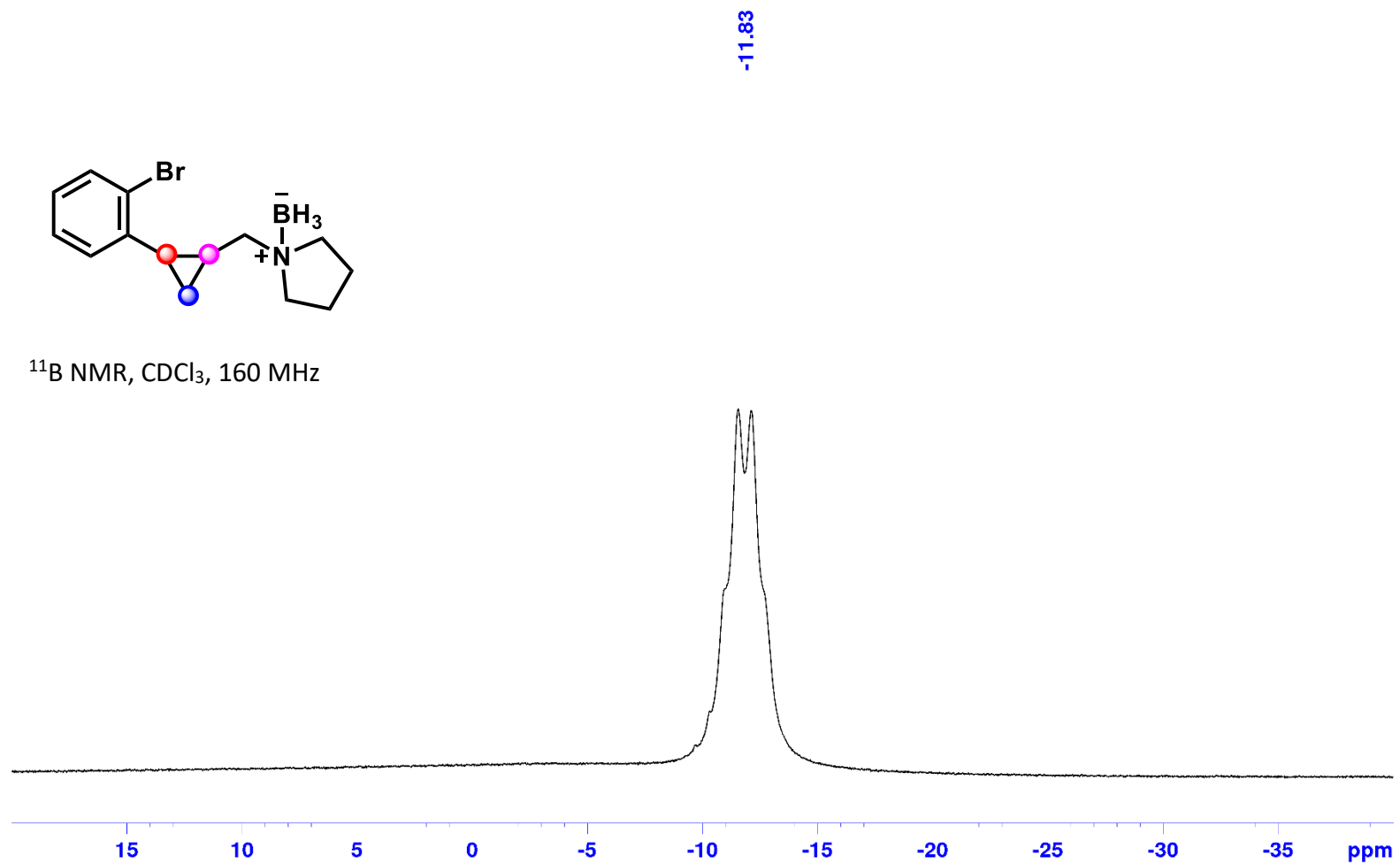
¹³C NMR, CDCl₃, 128 MHz



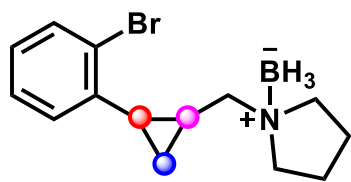
1-((2-(2-Bromophenyl)cyclopropyl)methyl)pyrrolidine Borane (1m):



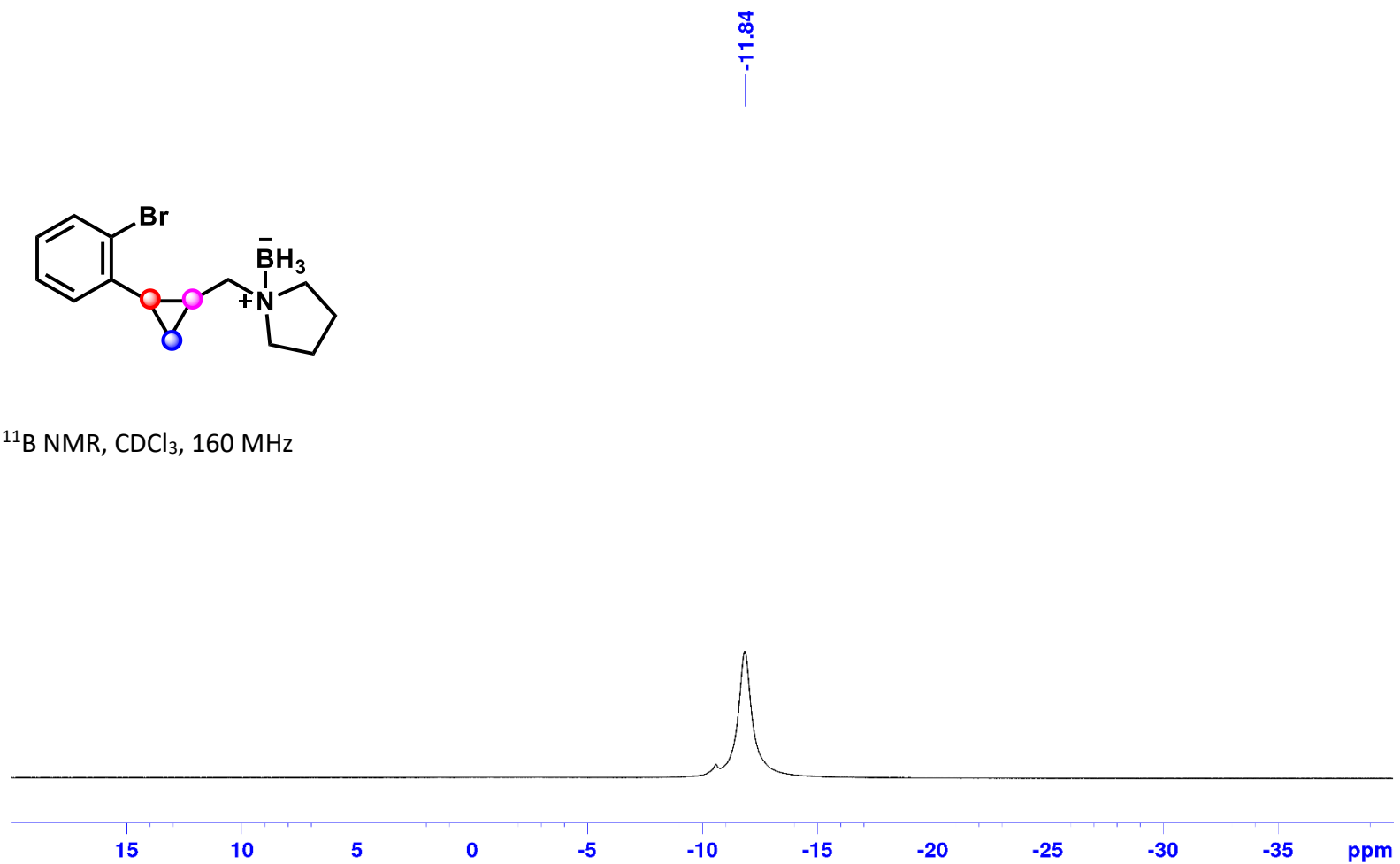
^{11}B NMR, CDCl_3 , 160 MHz



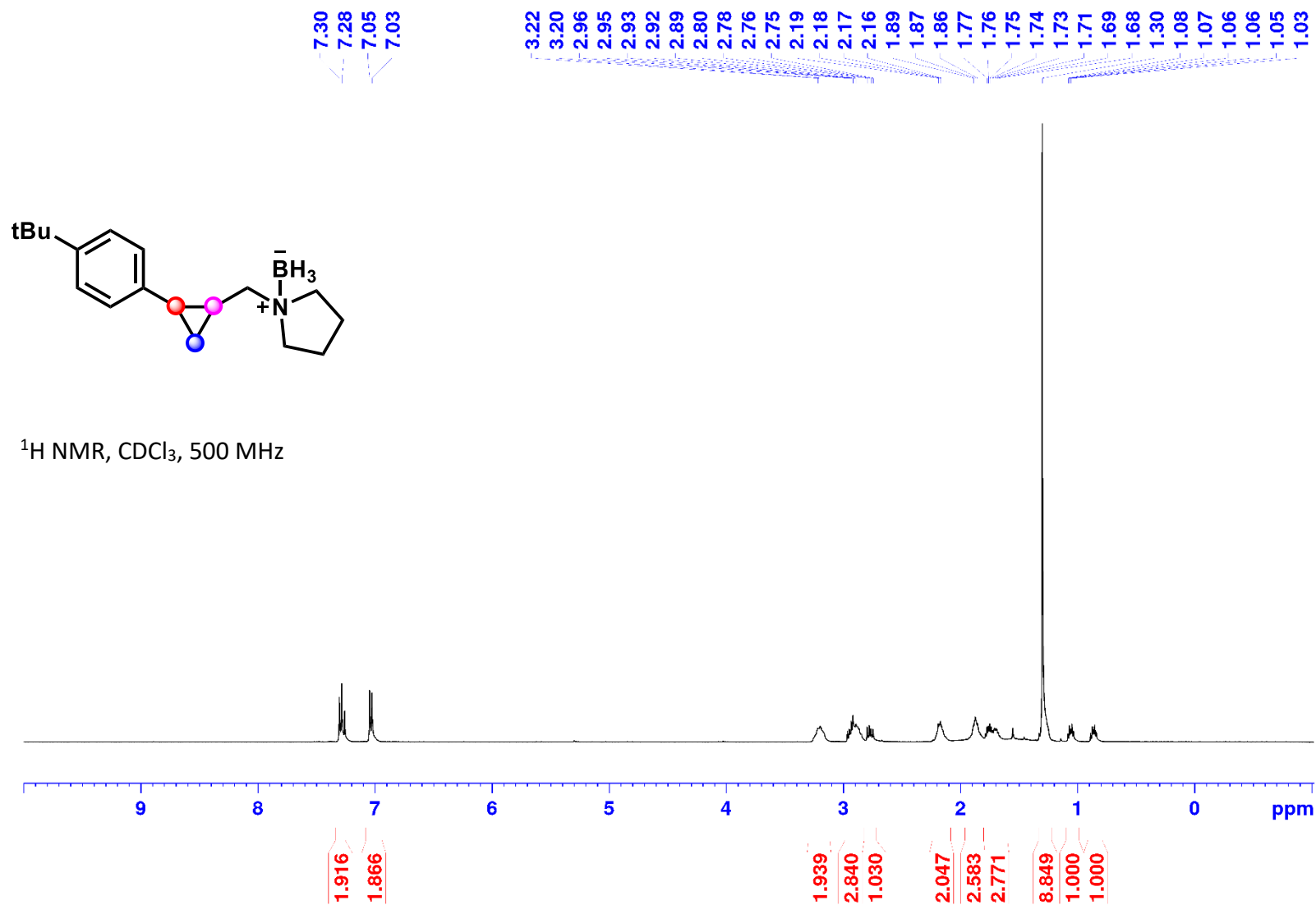
1-((2-(2-Bromophenyl)cyclopropyl)methyl)pyrrolidine Borane (1m):



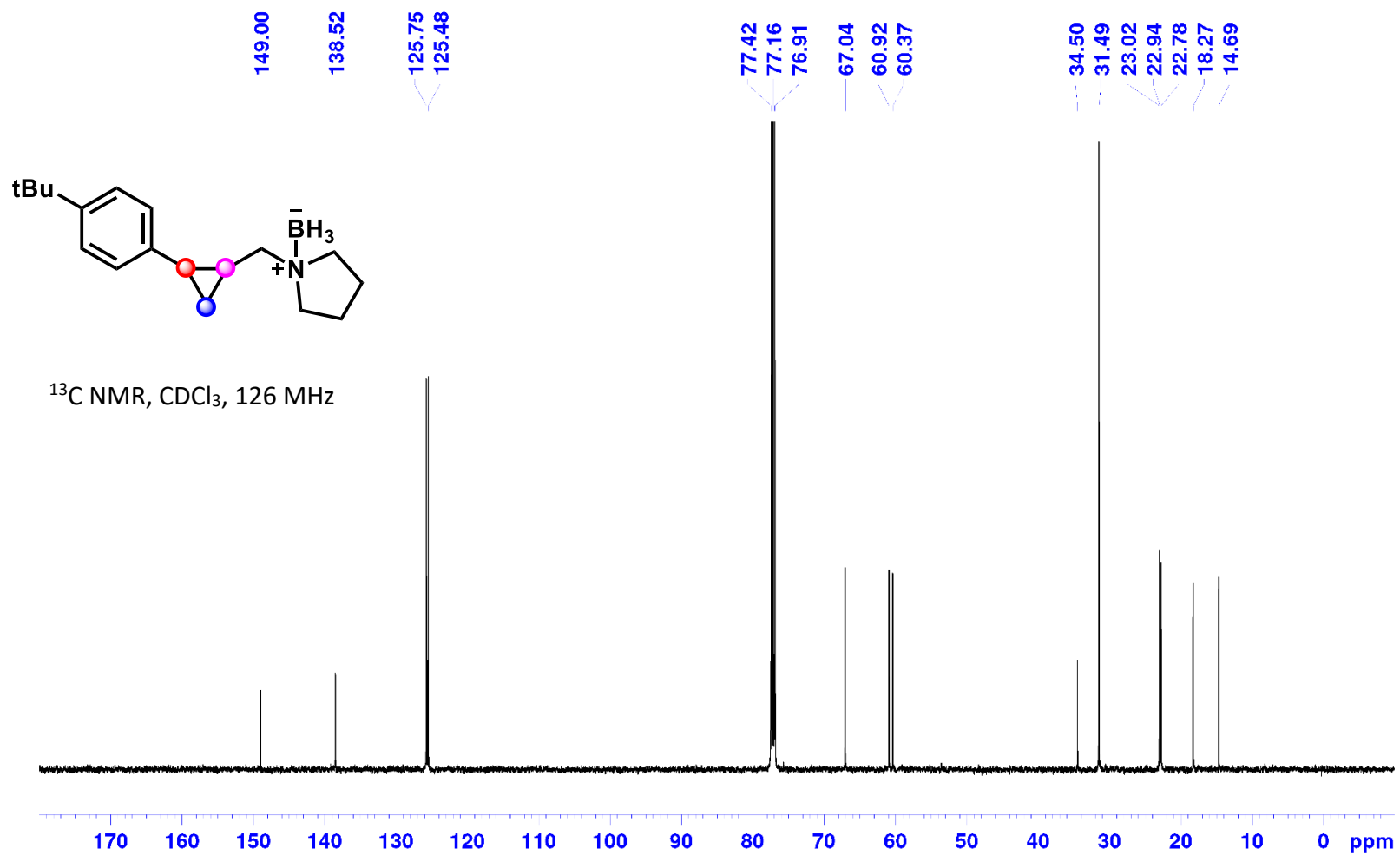
^{11}B NMR, CDCl_3 , 160 MHz



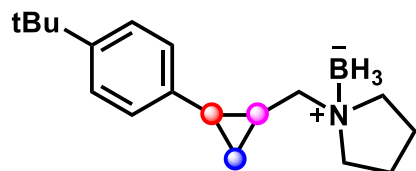
1-((2-(4-(*tert*-Butyl)phenyl)cyclopropyl)methyl)pyrrolidine Borane (1n):



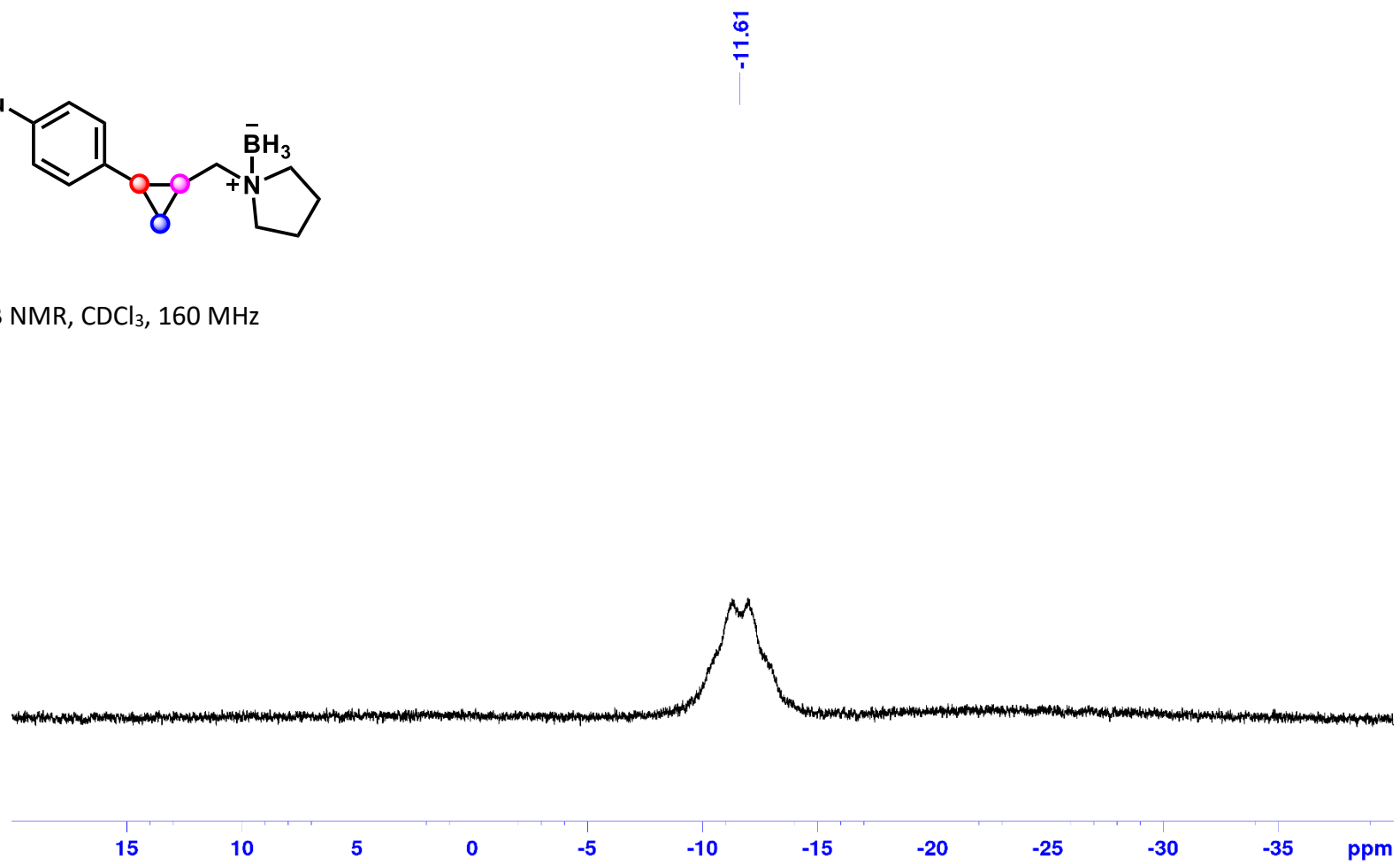
1-((2-(4-(*tert*-Butyl)phenyl)cyclopropyl)methyl)pyrrolidine Borane (1n):



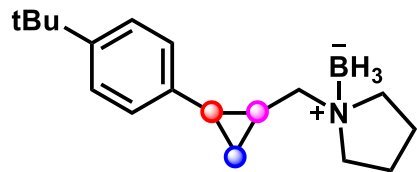
1-((2-(4-(*tert*-Butyl)phenyl)cyclopropyl)methyl)pyrrolidine Borane (1n):



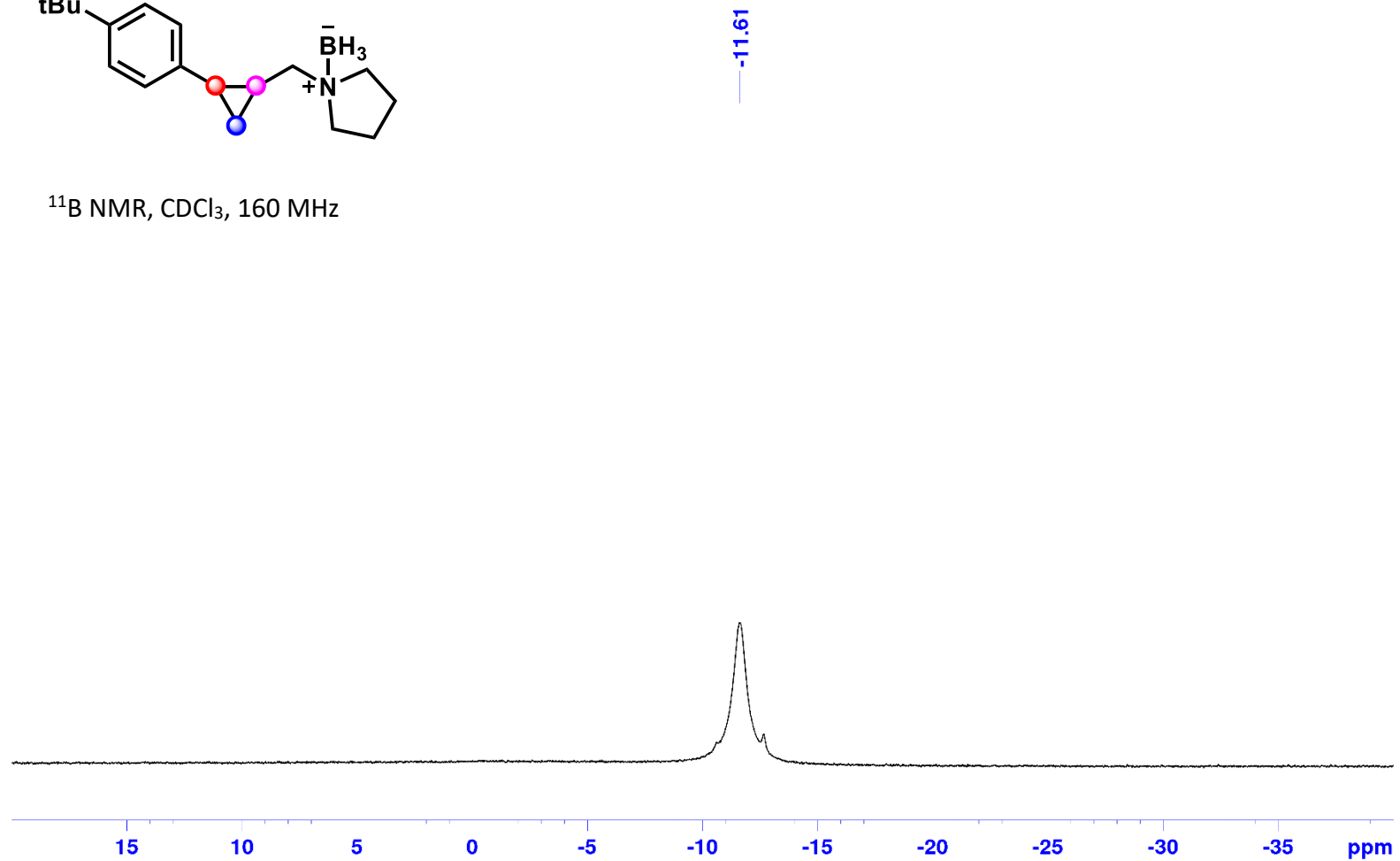
^{11}B NMR, CDCl_3 , 160 MHz



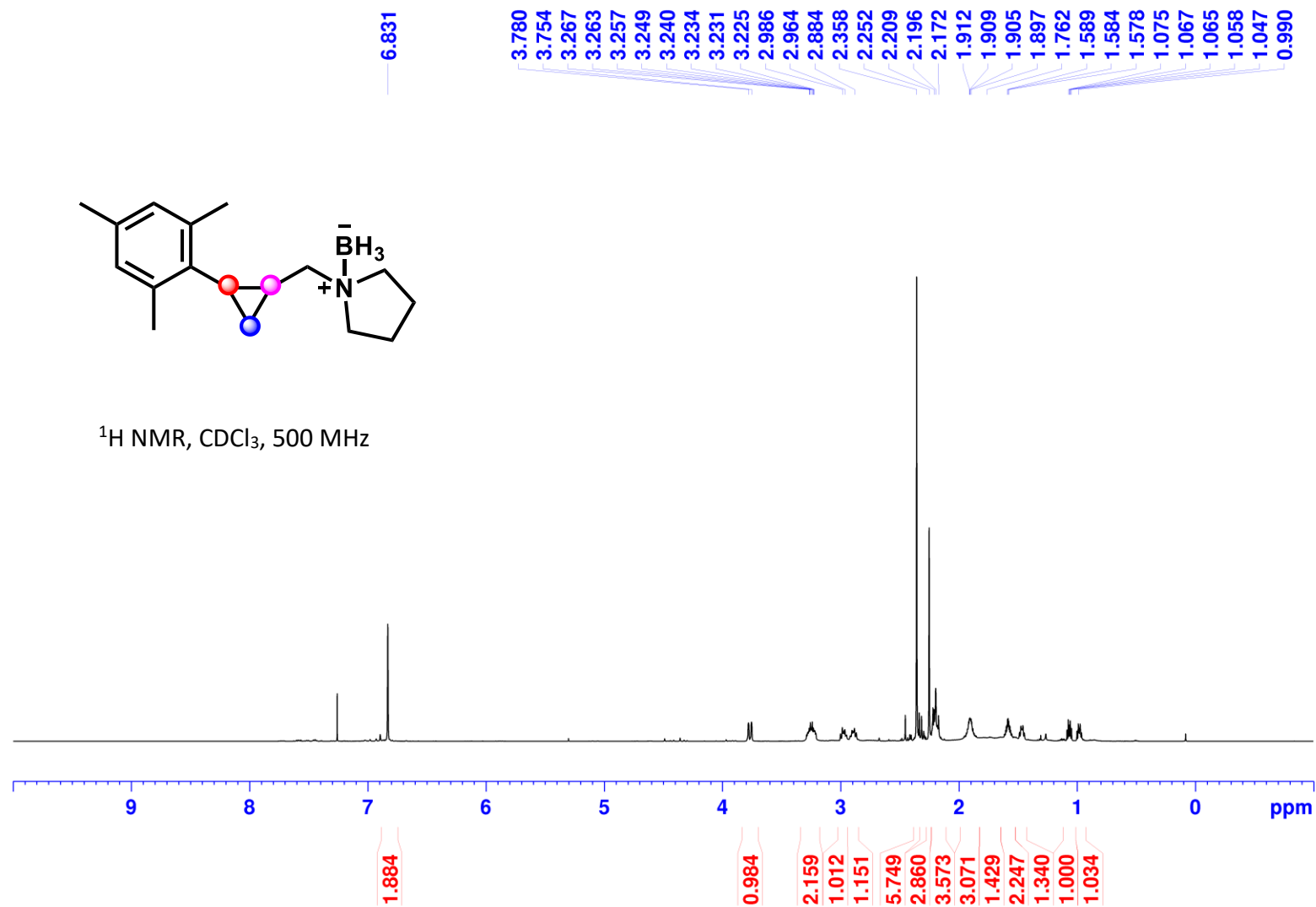
1-((2-(4-(*tert*-Butyl)phenyl)cyclopropyl)methyl)pyrrolidine Borane (1n):



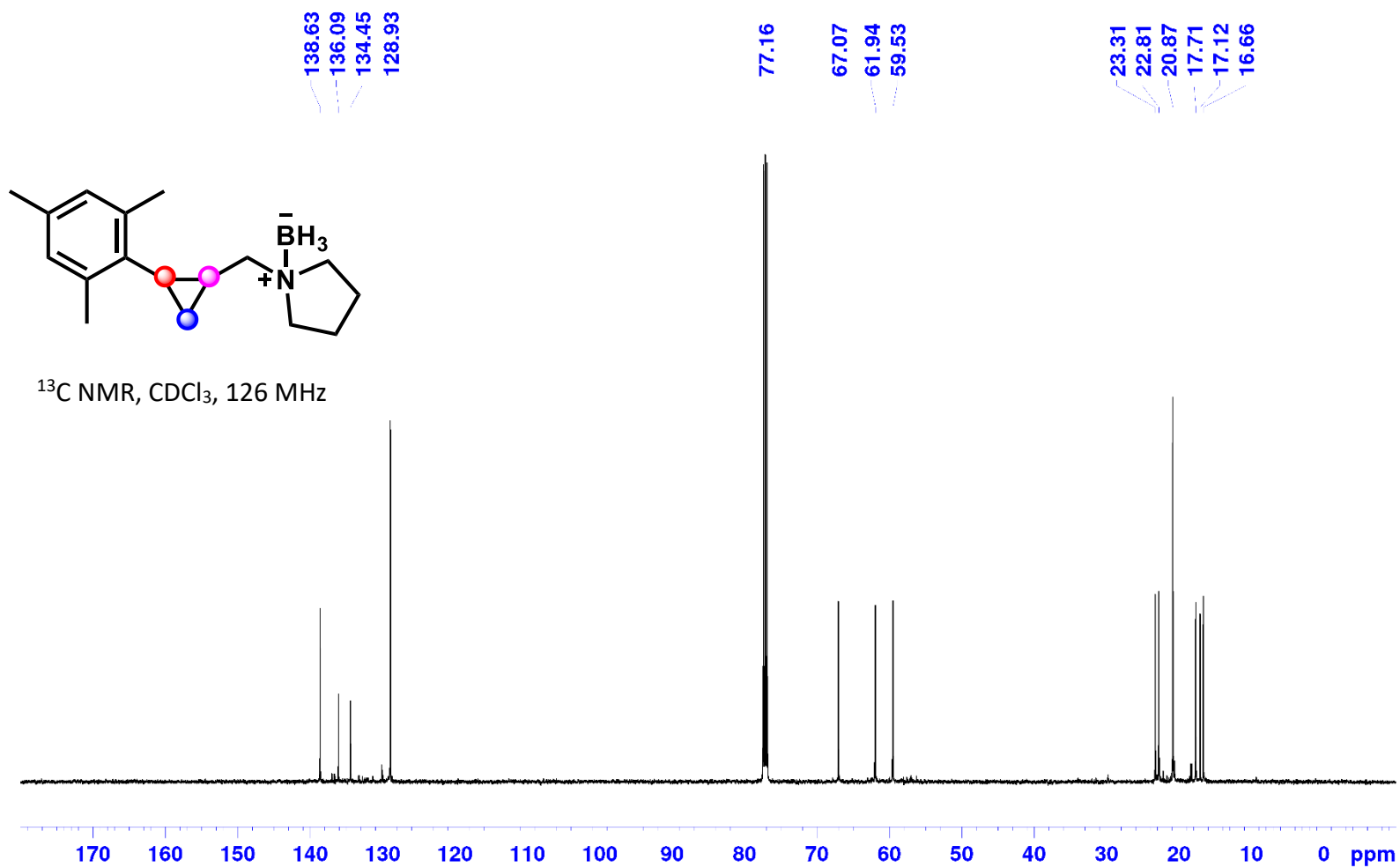
^{11}B NMR, CDCl_3 , 160 MHz



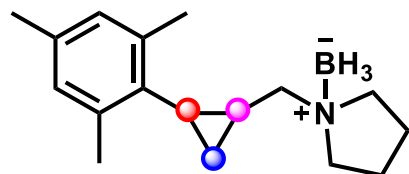
1-((2-Mesitylcyclopropyl)methyl)pyrrolidine Borane (1o):



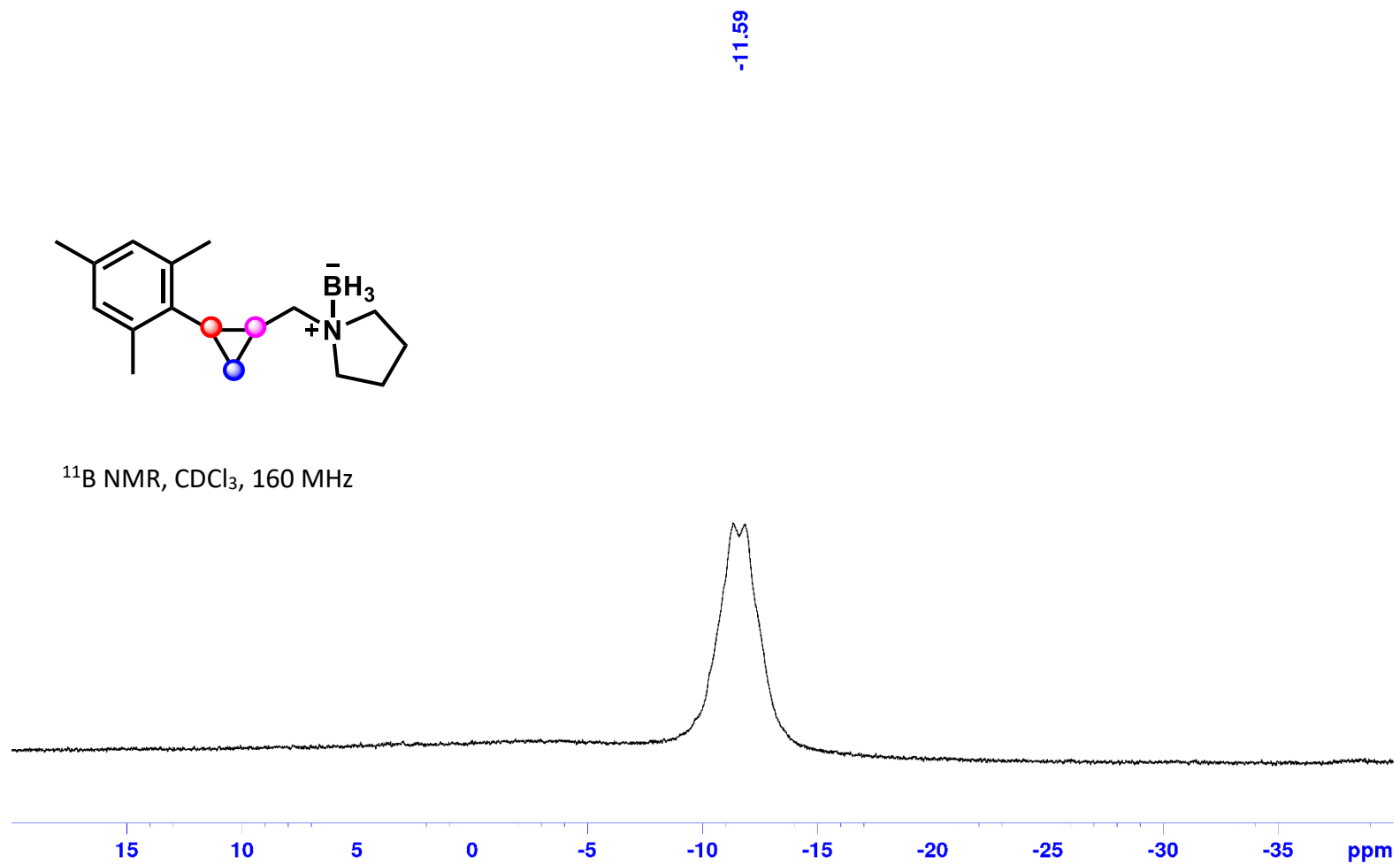
1-((2-Mesitylcyclopropyl)methyl)pyrrolidine Borane (1o):



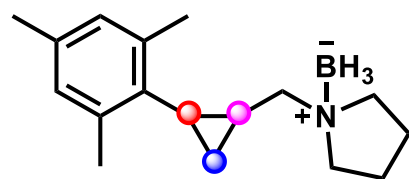
1-((2-Mesitylcyclopropyl)methyl)pyrrolidine Borane (1o):



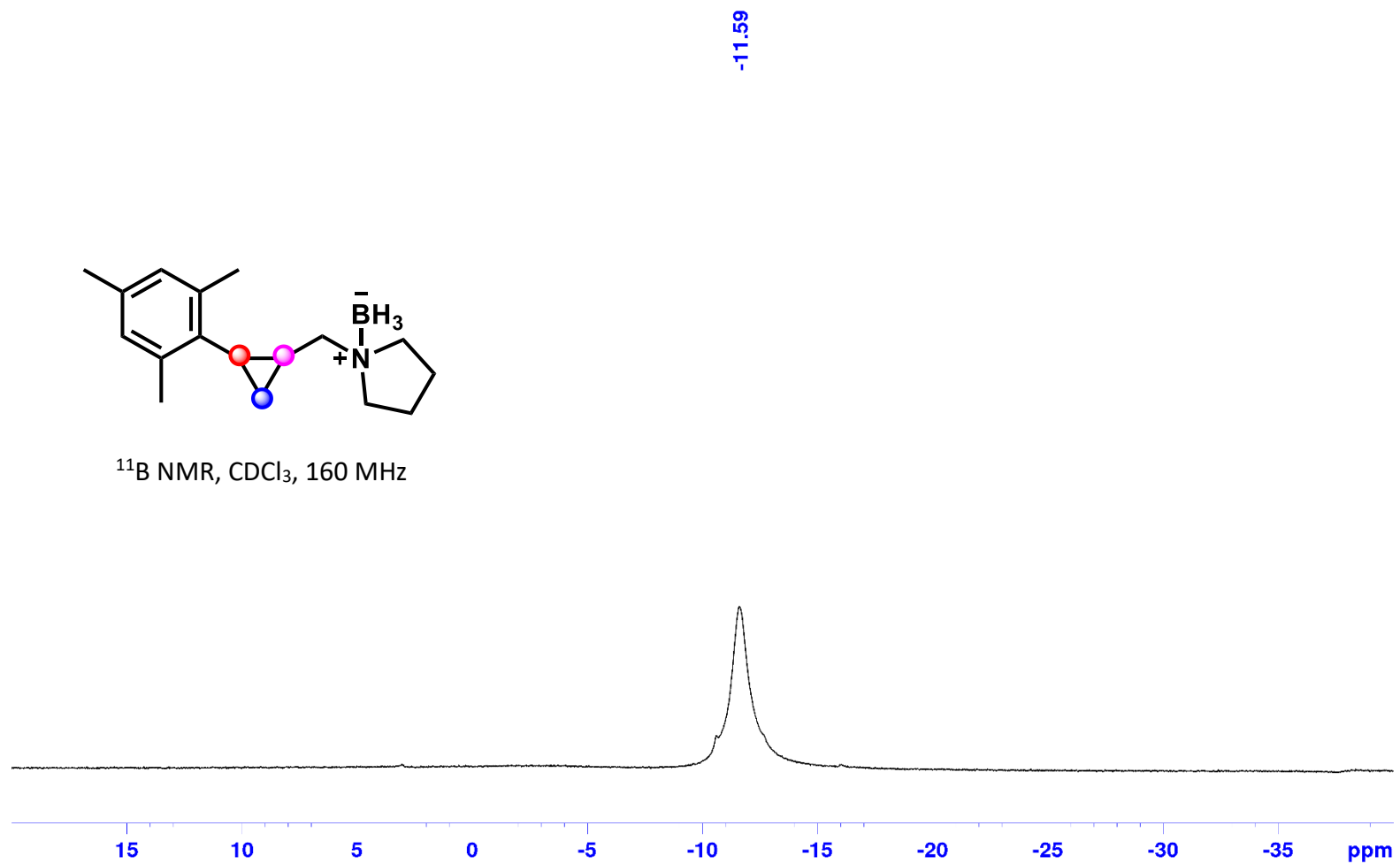
^{11}B NMR, CDCl_3 , 160 MHz



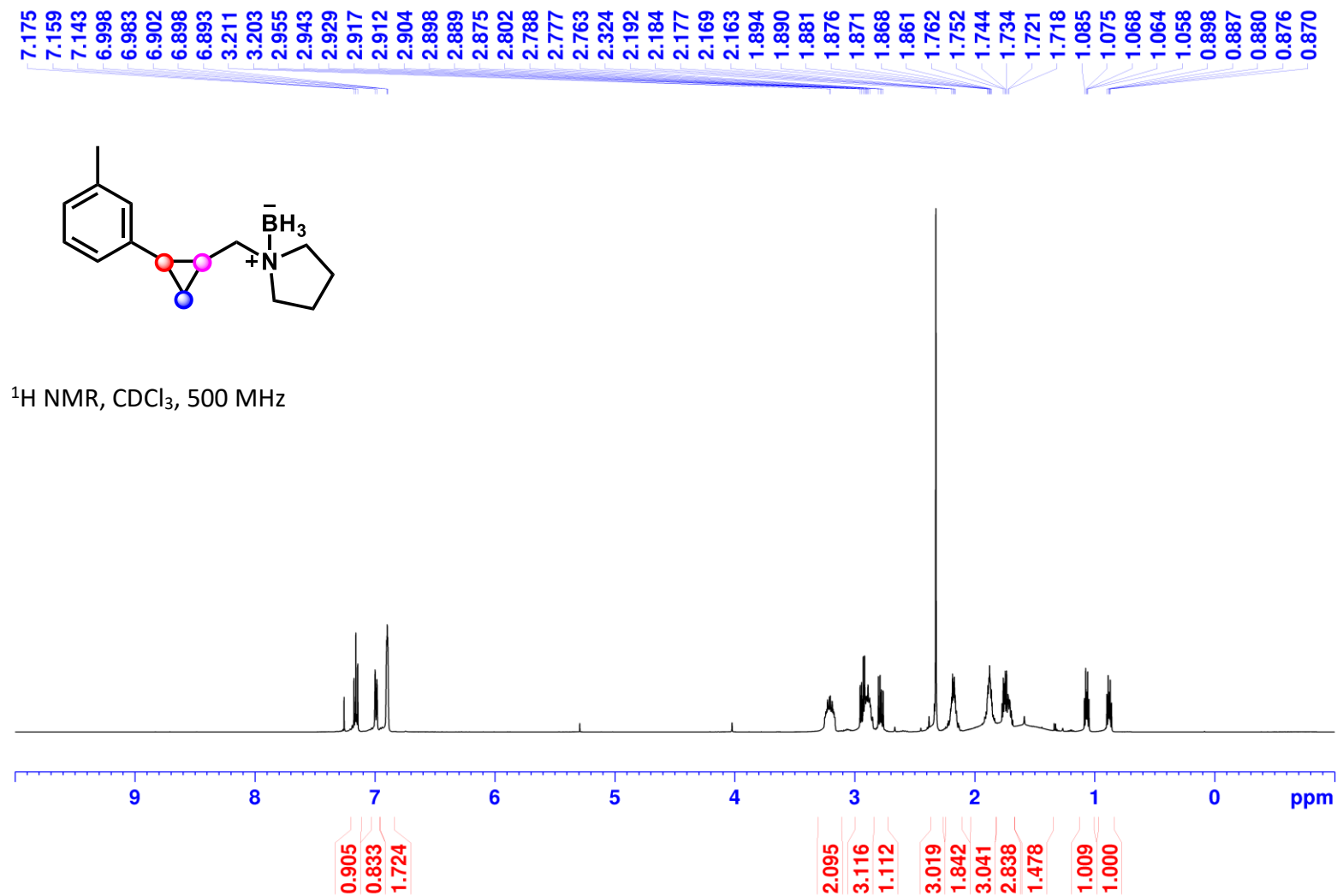
1-((2-Mesitylcyclopropyl)methyl)pyrrolidine Borane (1o):



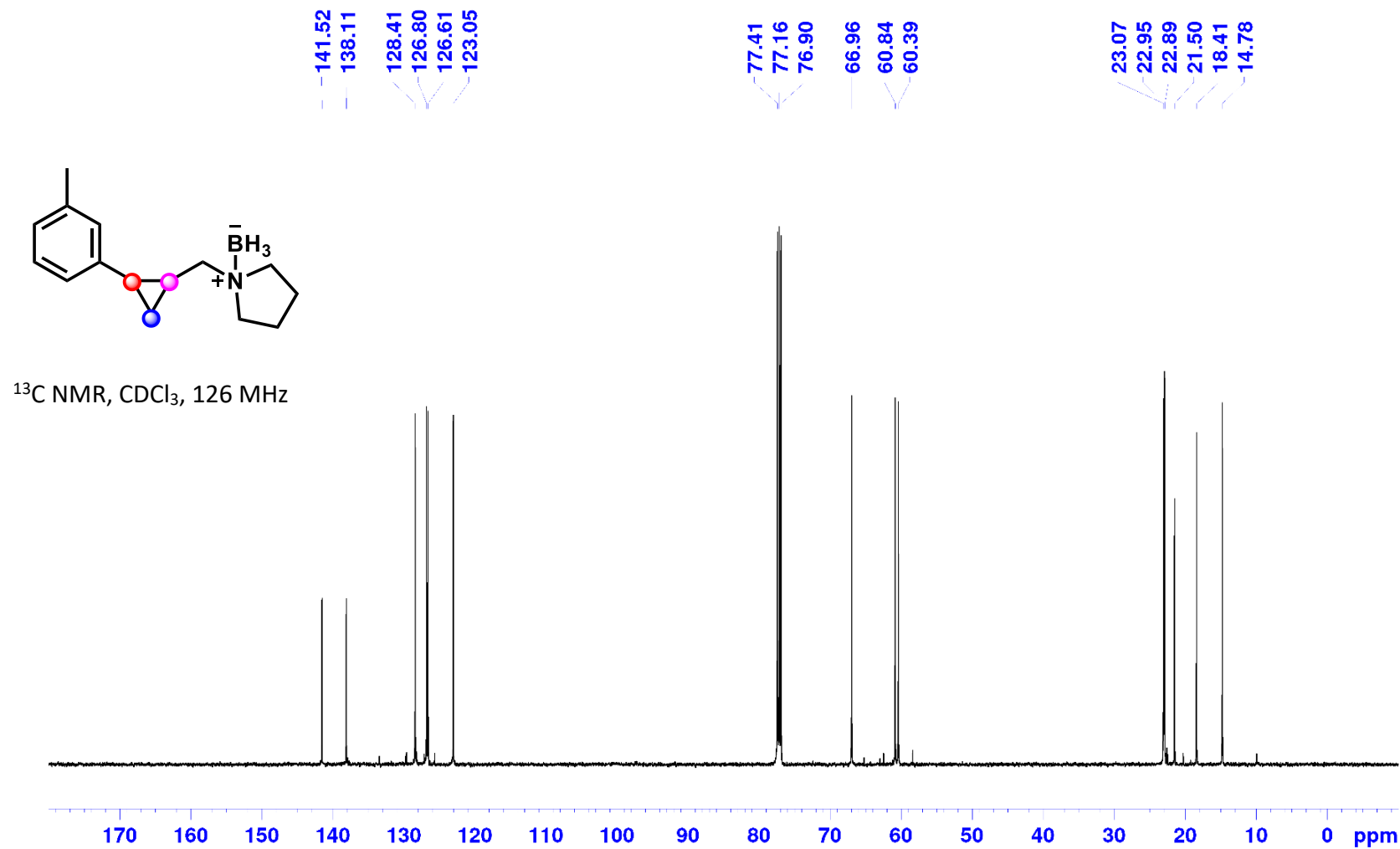
^{11}B NMR, CDCl_3 , 160 MHz



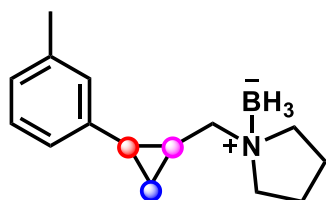
1-((2-(*m*-Tolyl)cyclopropyl)methyl)pyrrolidine Borane (1p):



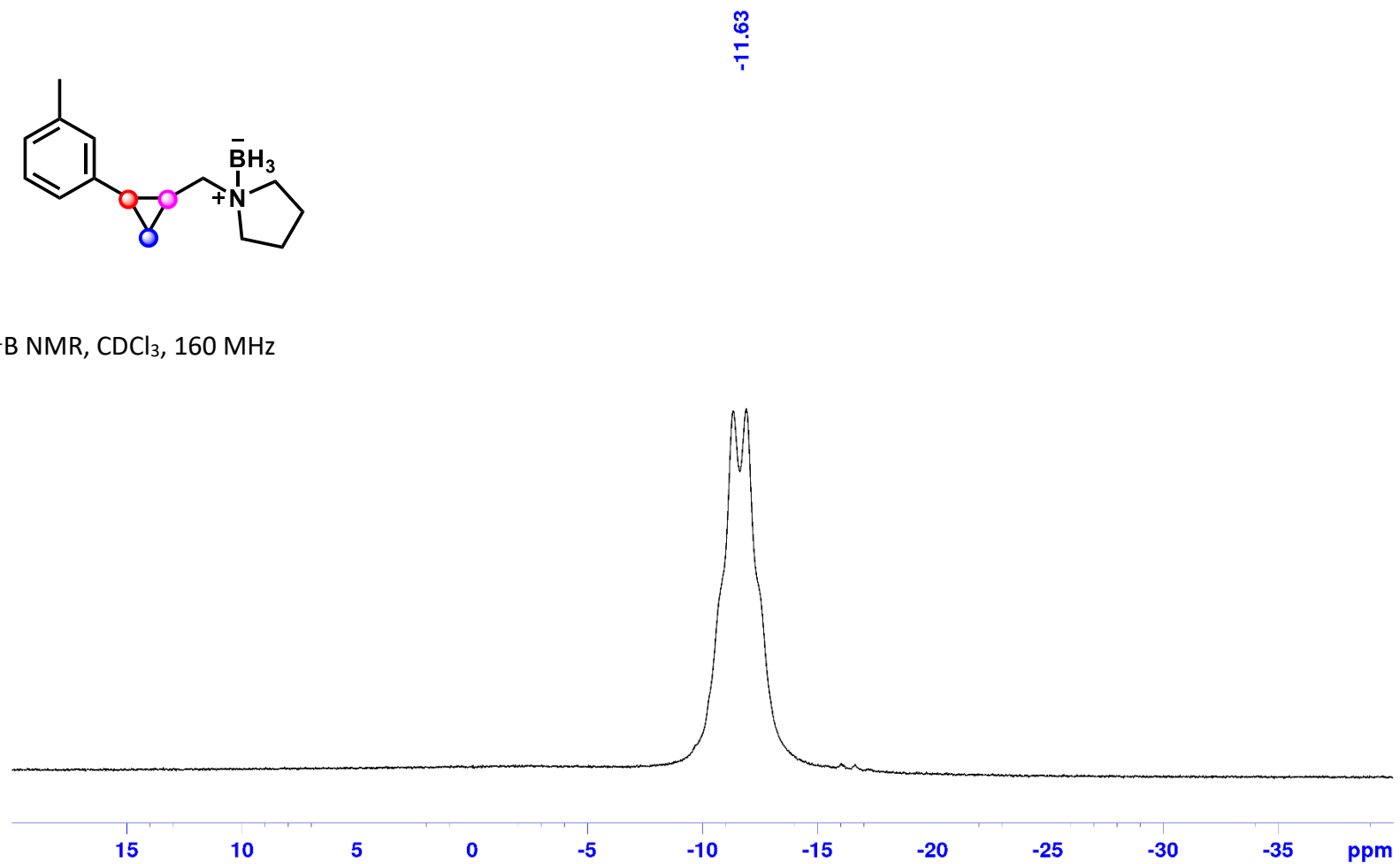
1-((2-(*m*-Tolyl)cyclopropyl)methyl)pyrrolidine Borane (1p):



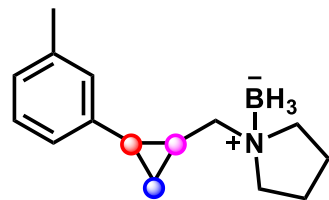
1-((2-(*m*-Tolyl)cyclopropyl)methyl)pyrrolidine Borane (1p):



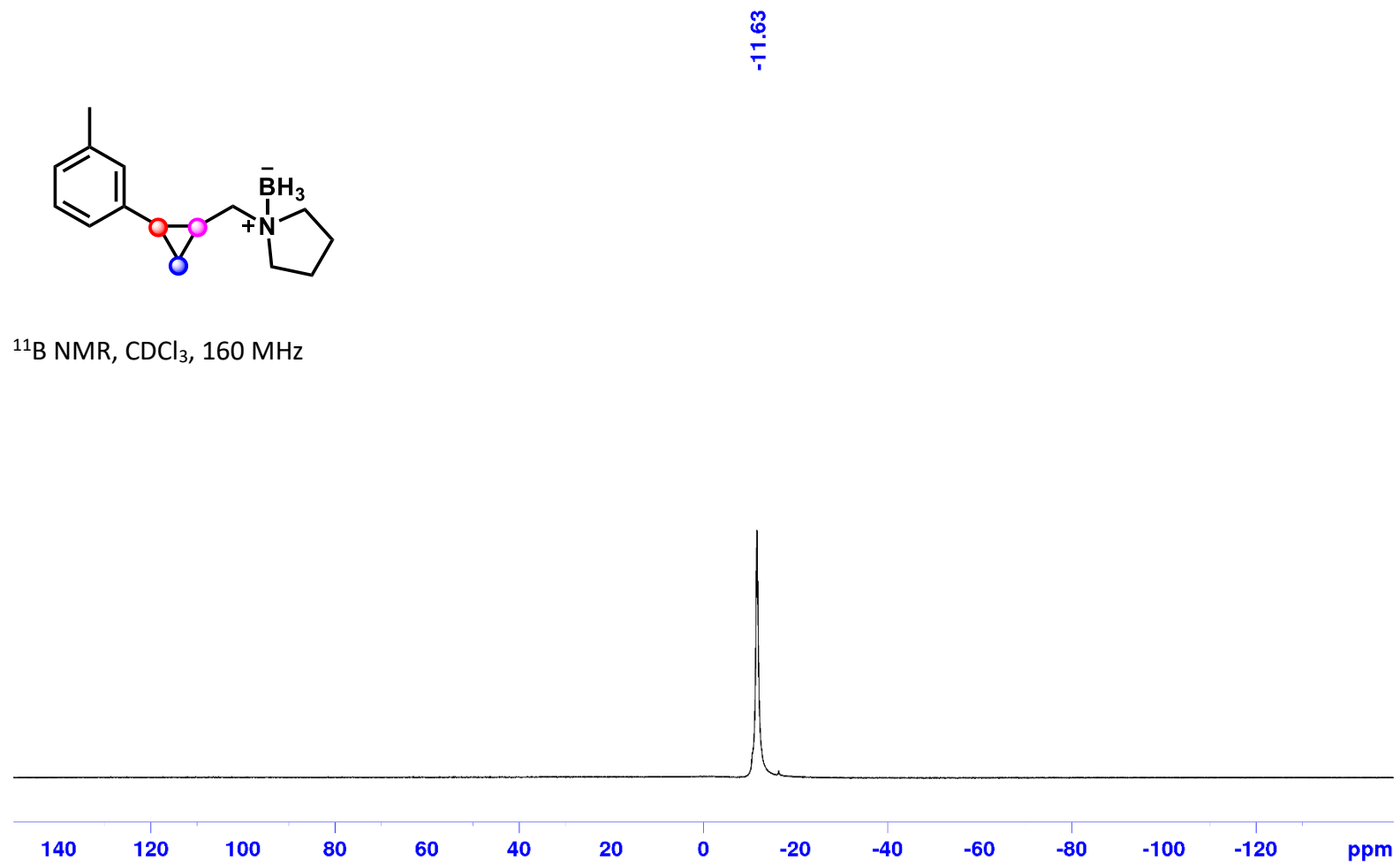
^{11}B NMR, CDCl_3 , 160 MHz



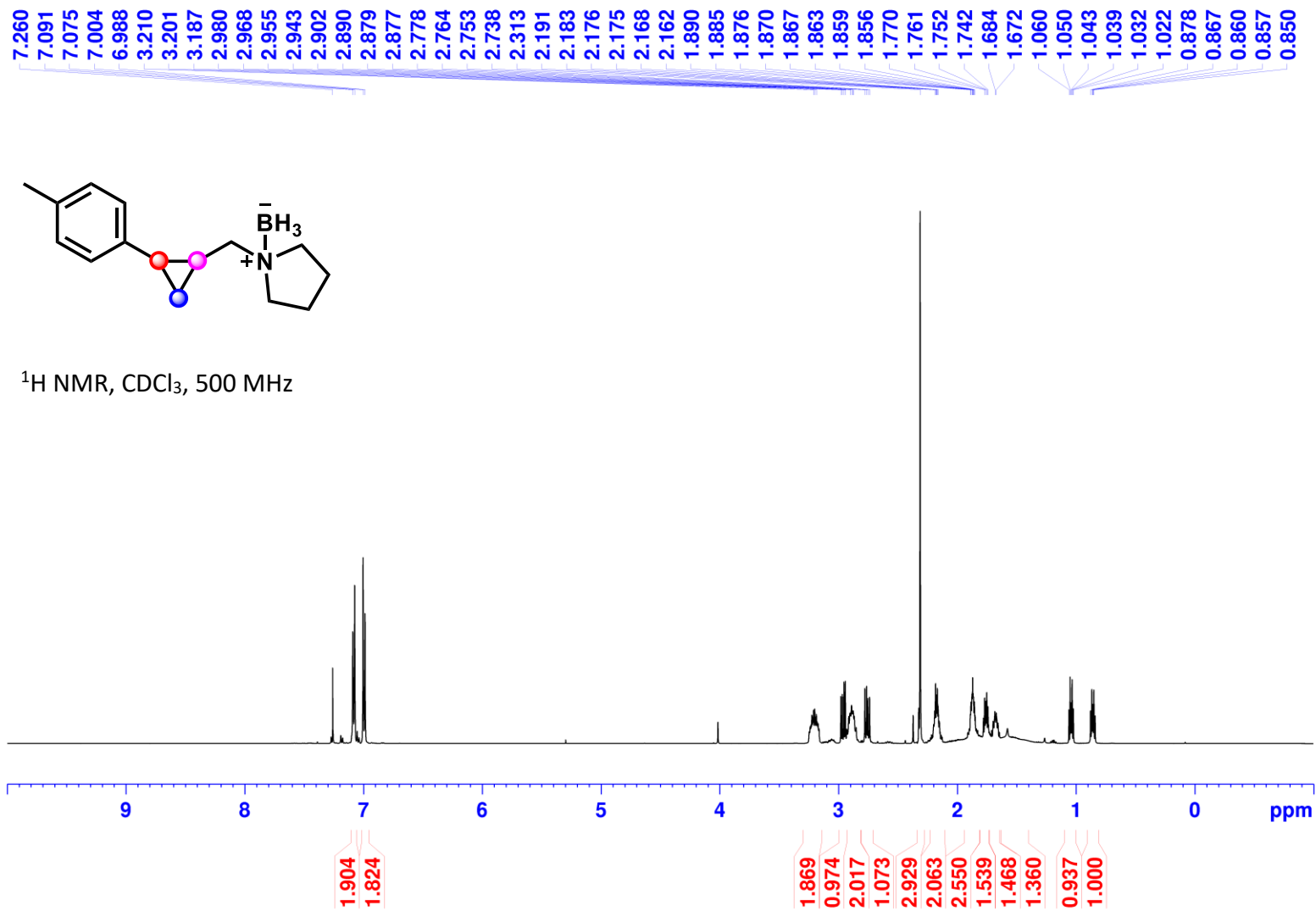
1-((2-(*m*-Tolyl)cyclopropyl)methyl)pyrrolidine Borane (1p):



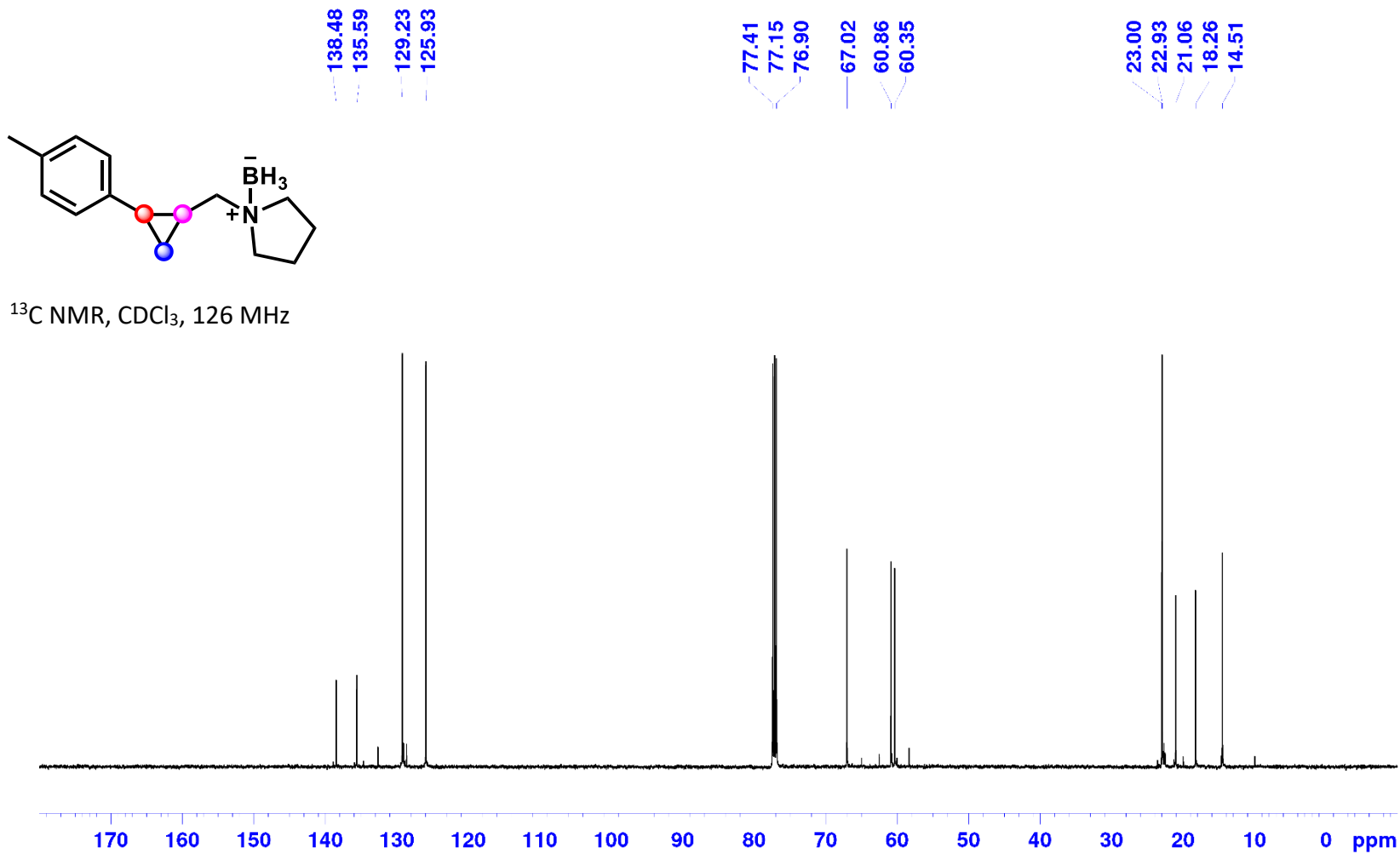
^{11}B NMR, CDCl_3 , 160 MHz



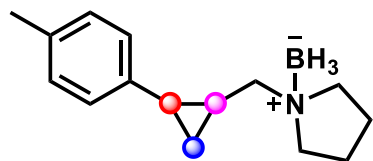
1-((2-(*p*-Tolyl)cyclopropyl)methyl)pyrrolidine Borane (1q):



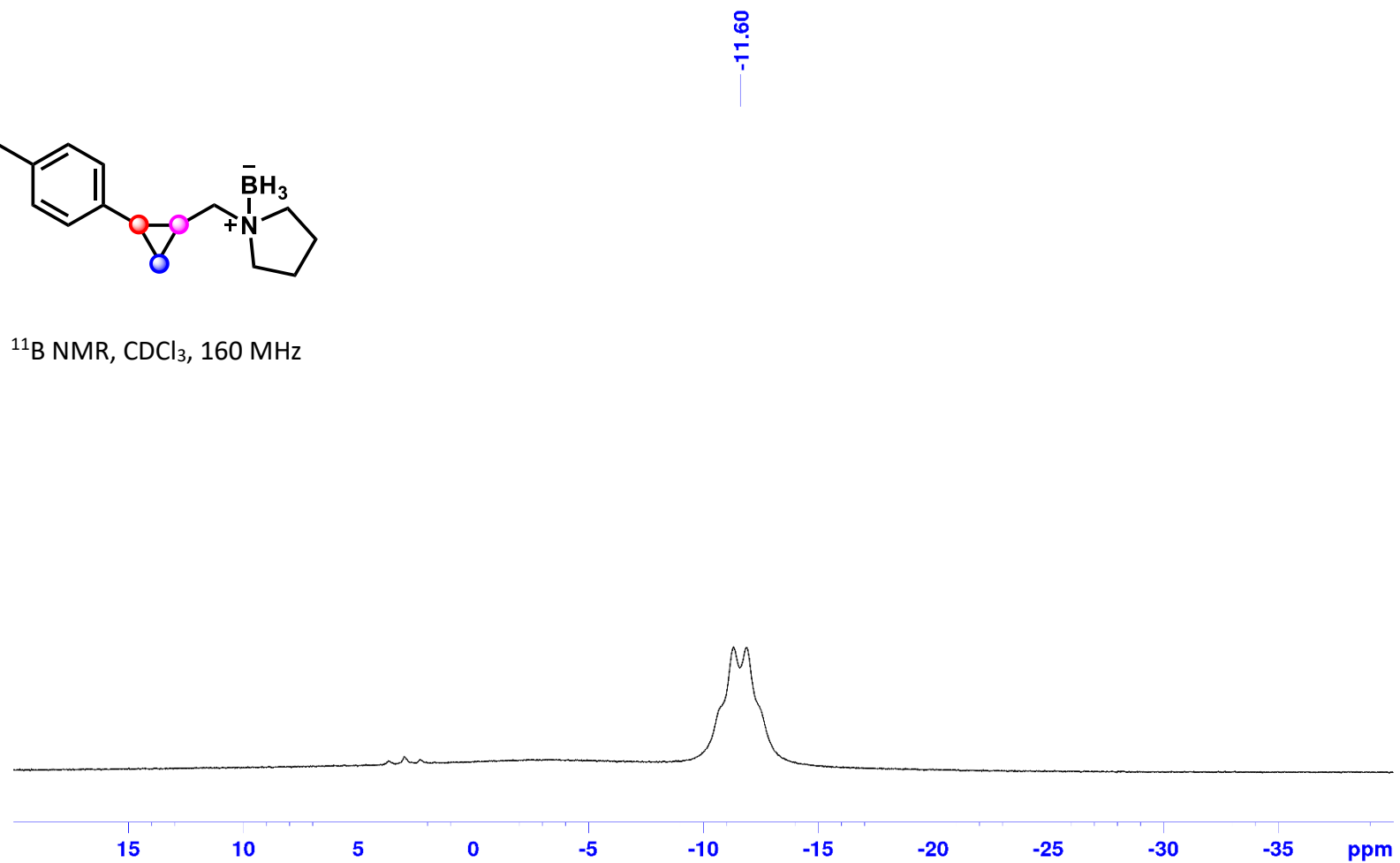
1-((2-(*p*-Tolyl)cyclopropyl)methyl)pyrrolidine Borane (1q):



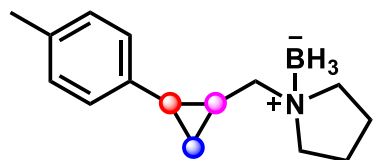
1-((2-(*p*-Tolyl)cyclopropyl)methyl)pyrrolidine Borane (1q):



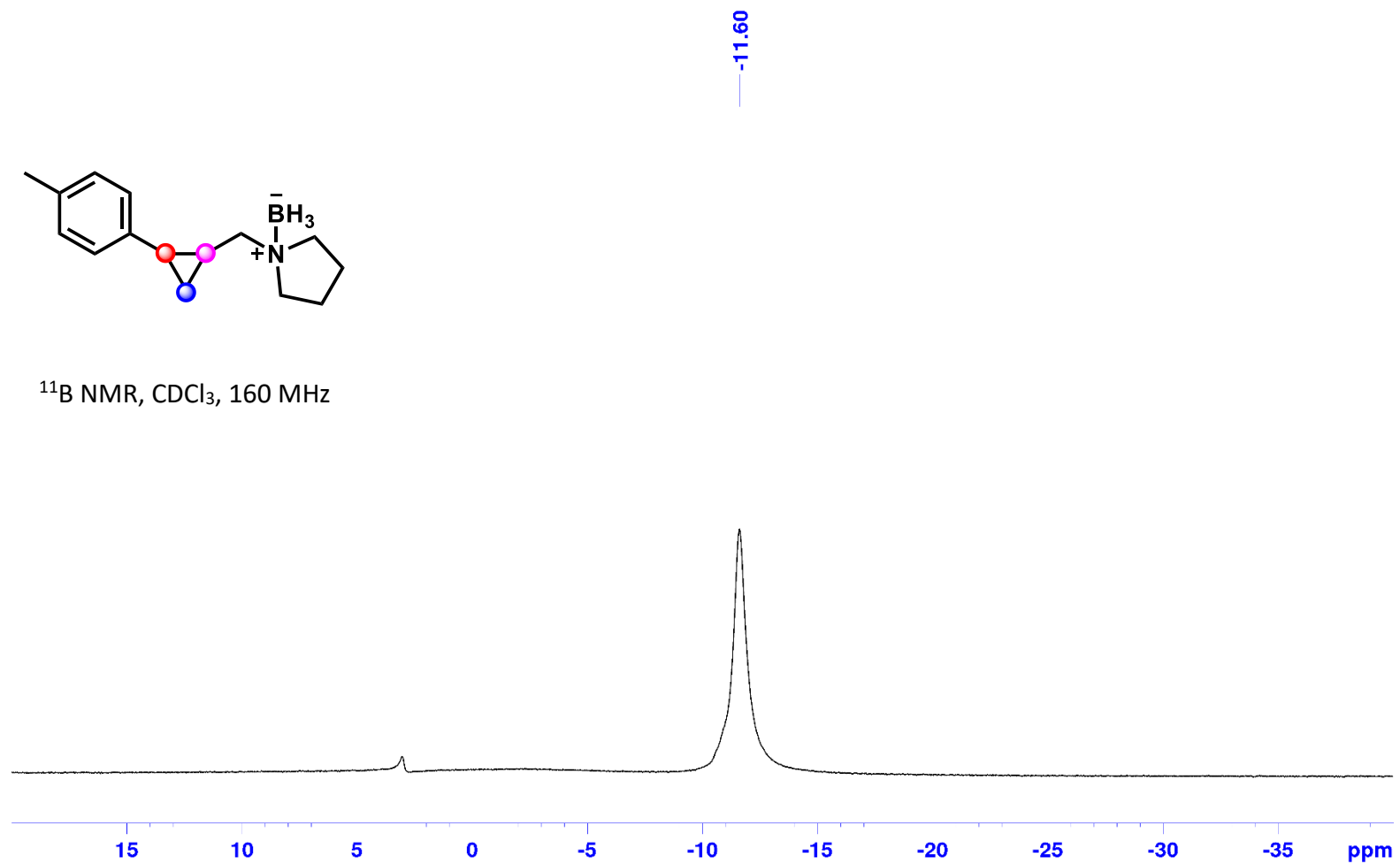
^{11}B NMR, CDCl_3 , 160 MHz



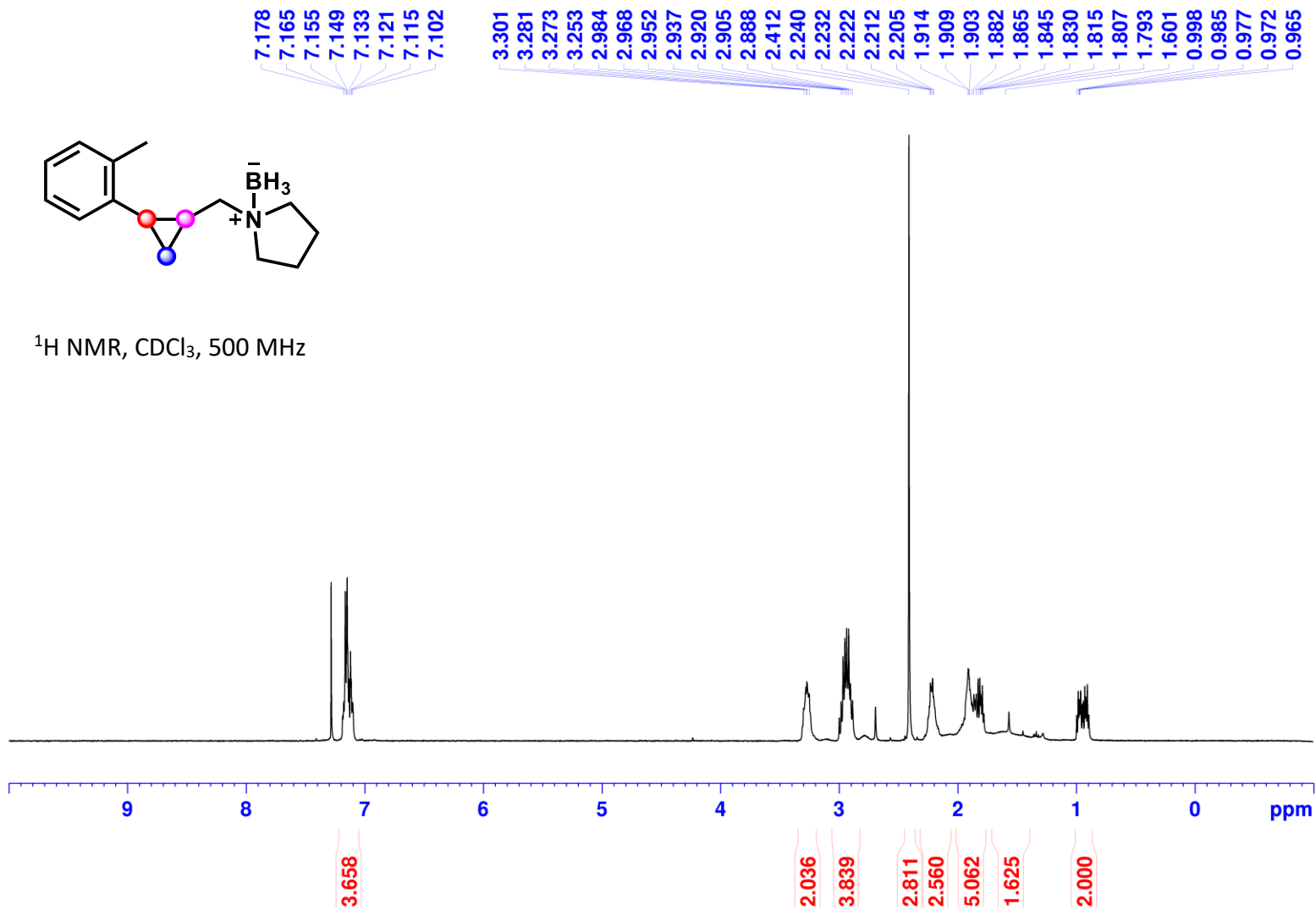
1-((2-(*p*-Tolyl)cyclopropyl)methyl)pyrrolidine Borane (1q):



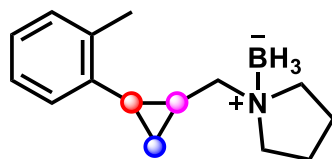
^{11}B NMR, CDCl_3 , 160 MHz



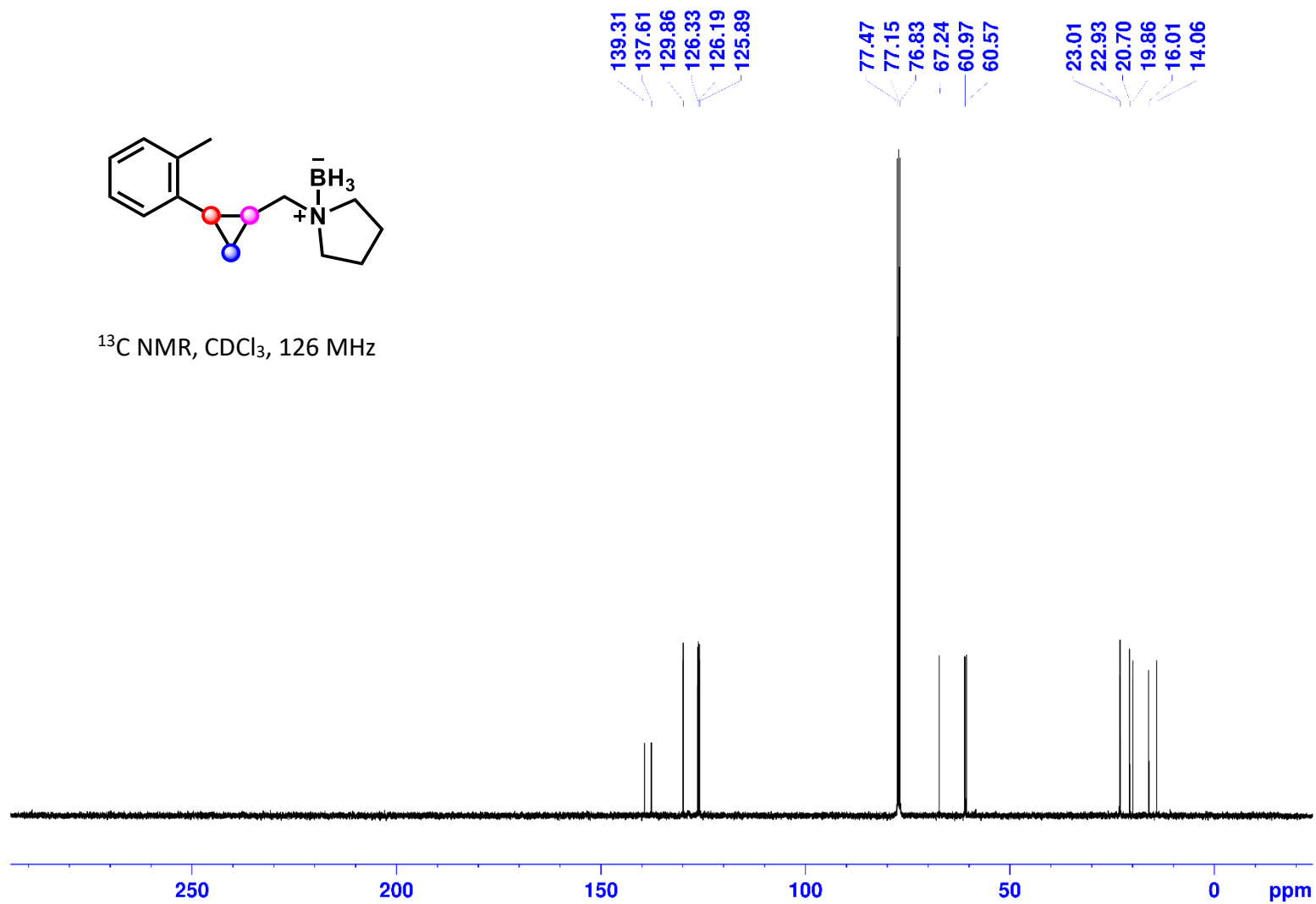
1-((2-(*o*-Tolyl)cyclopropyl)methyl)pyrrolidine Borane (1r):



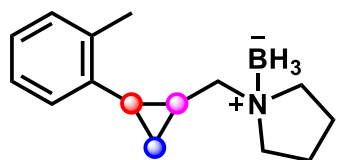
1-((2-(*o*-Tolyl)cyclopropyl)methyl)pyrrolidine Borane (1r):



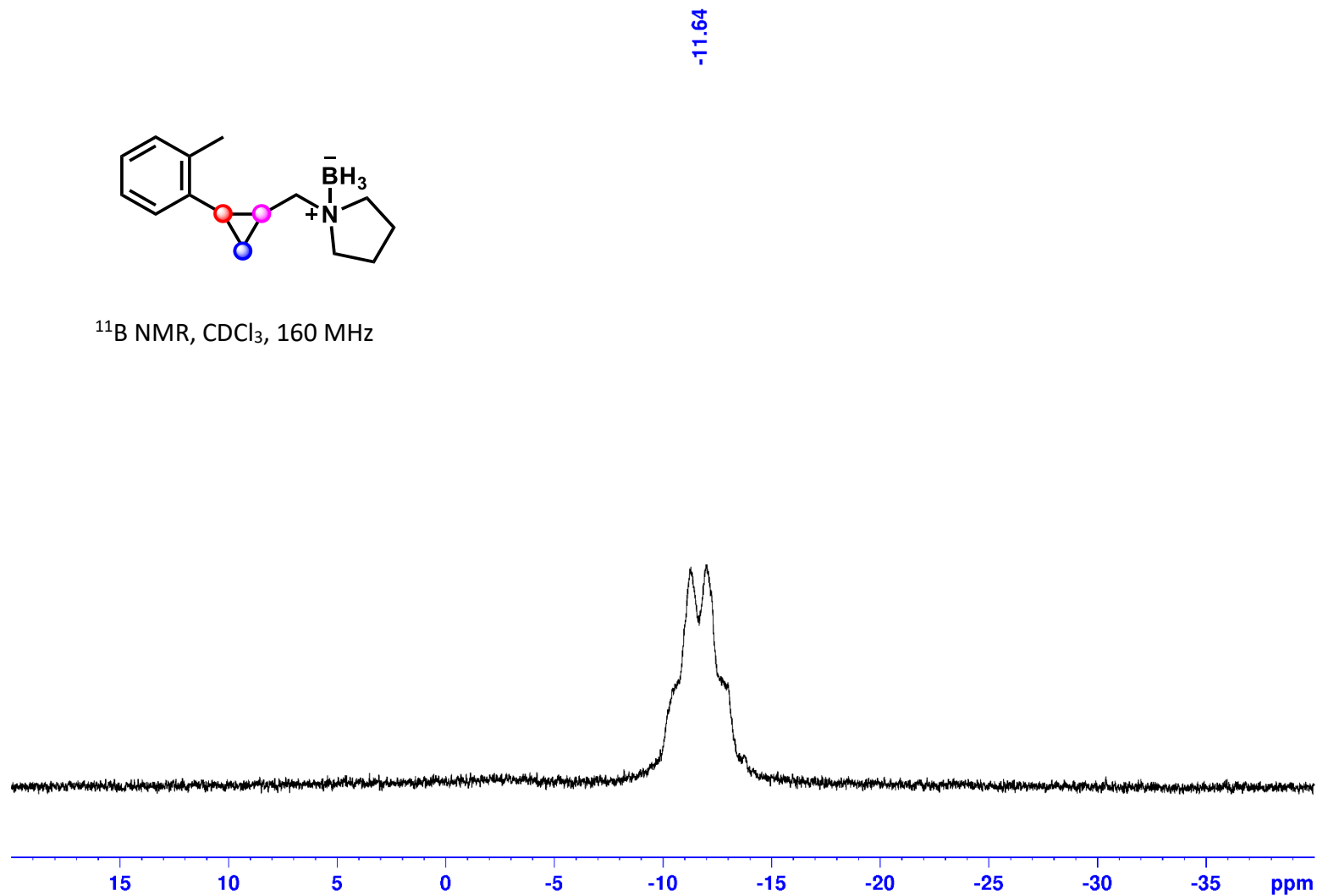
^{13}C NMR, CDCl_3 , 126 MHz



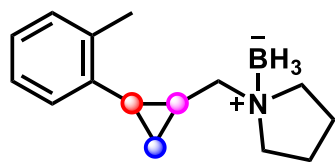
1-((2-(*o*-Tolyl)cyclopropyl)methyl)pyrrolidine Borane (1r):



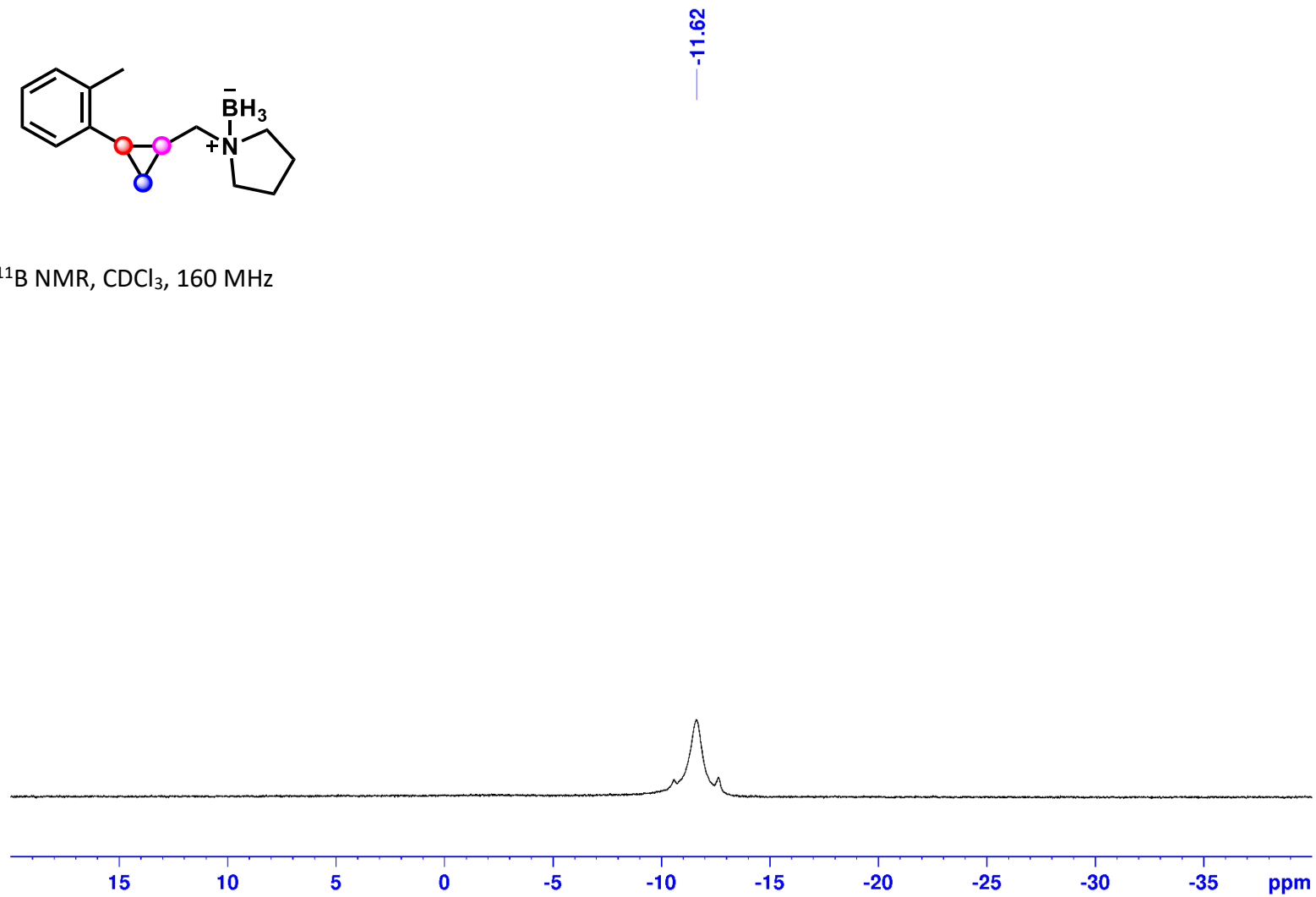
^{11}B NMR, CDCl_3 , 160 MHz



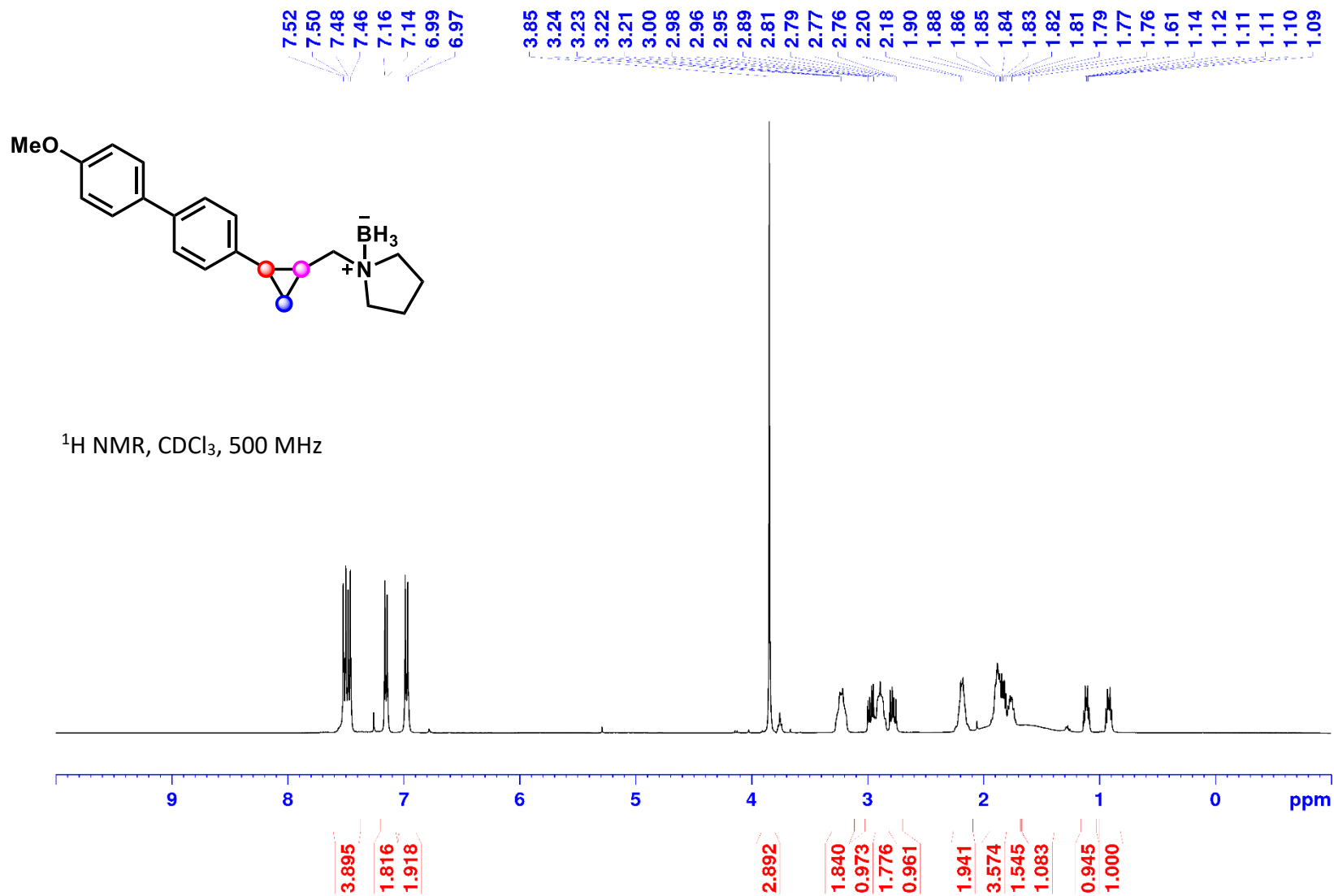
1-((2-(*o*-Tolyl)cyclopropyl)methyl)pyrrolidine Borane (1r):



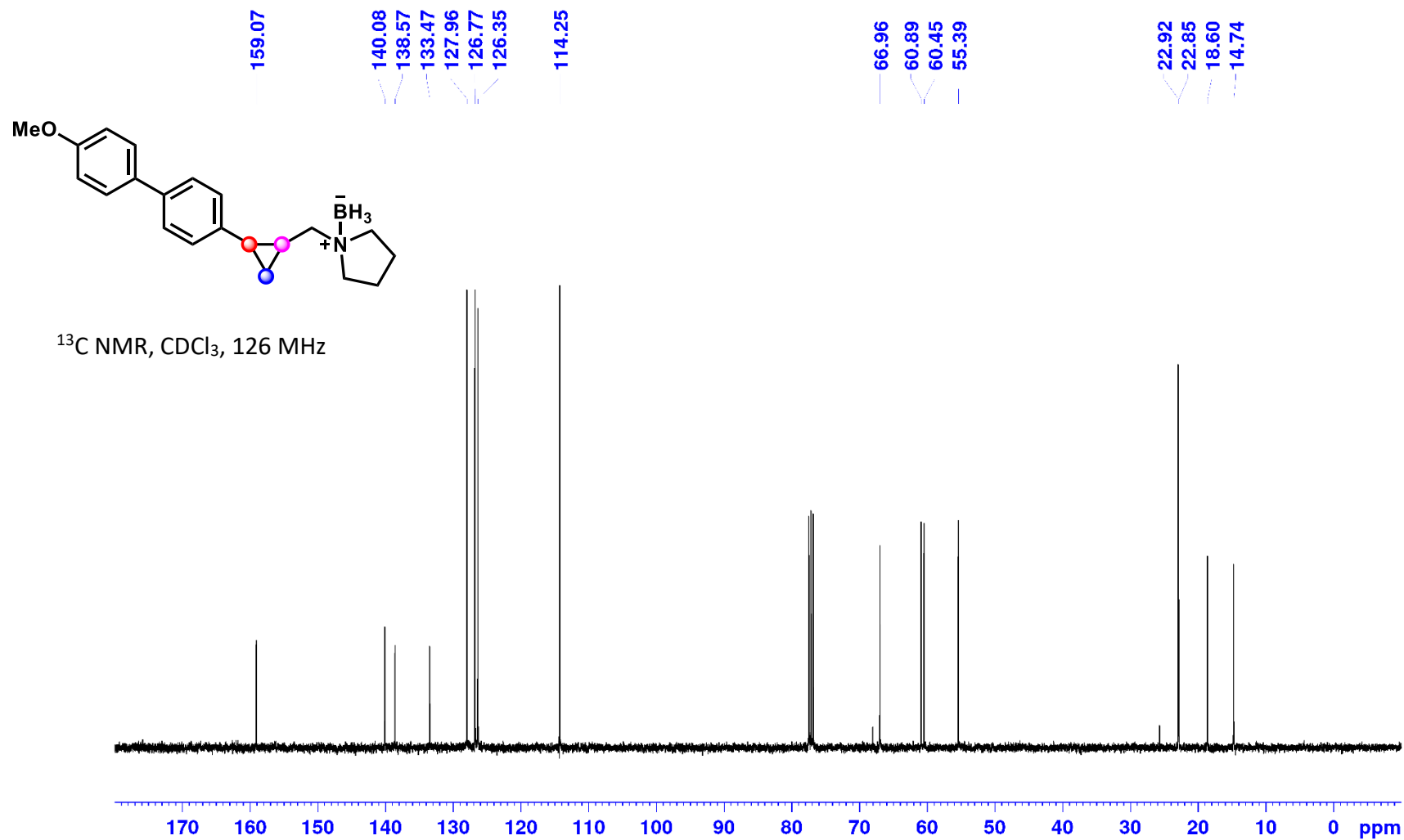
^{11}B NMR, CDCl_3 , 160 MHz



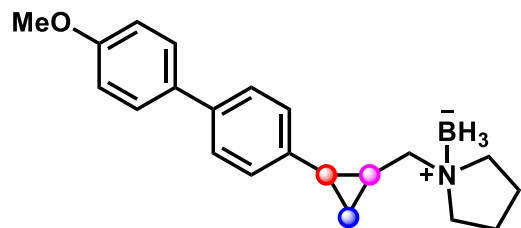
1-((2-(4'-Methoxy-[1,1'-biphenyl]-4-yl)cyclopropyl)methyl)pyrrolidine Borane (1s):



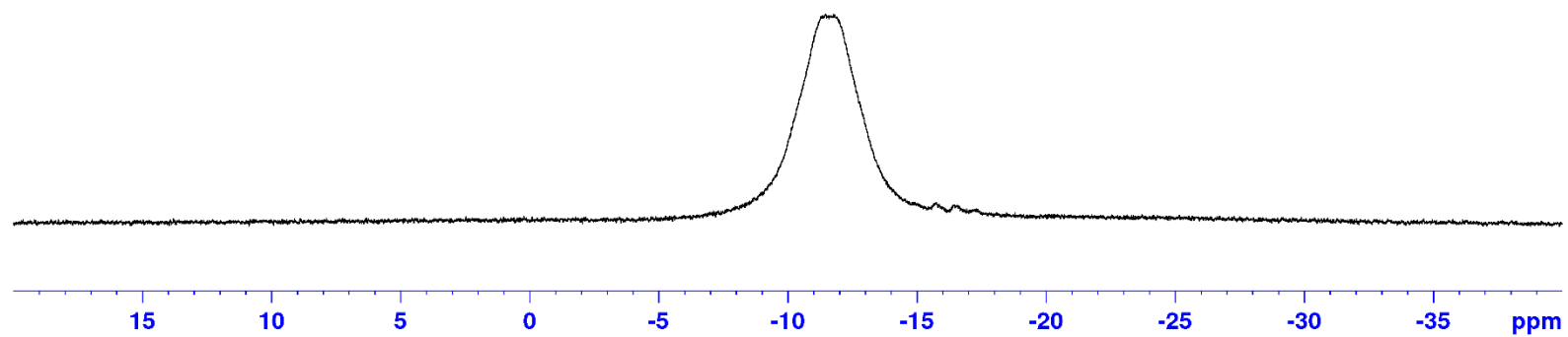
1-((2-(4'-Methoxy-[1,1'-biphenyl]-4-yl)cyclopropyl)methyl)pyrrolidine Borane (1s):



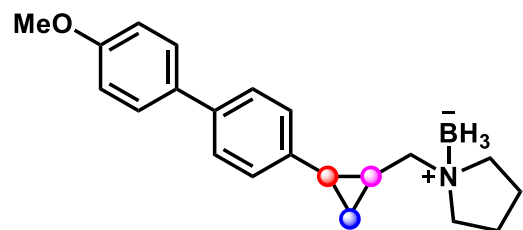
1-((2-(4'-Methoxy-[1,1'-biphenyl]-4-yl)cyclopropyl)methyl)pyrrolidine Borane (1s):



^{11}B NMR, CDCl_3 , 160 MHz

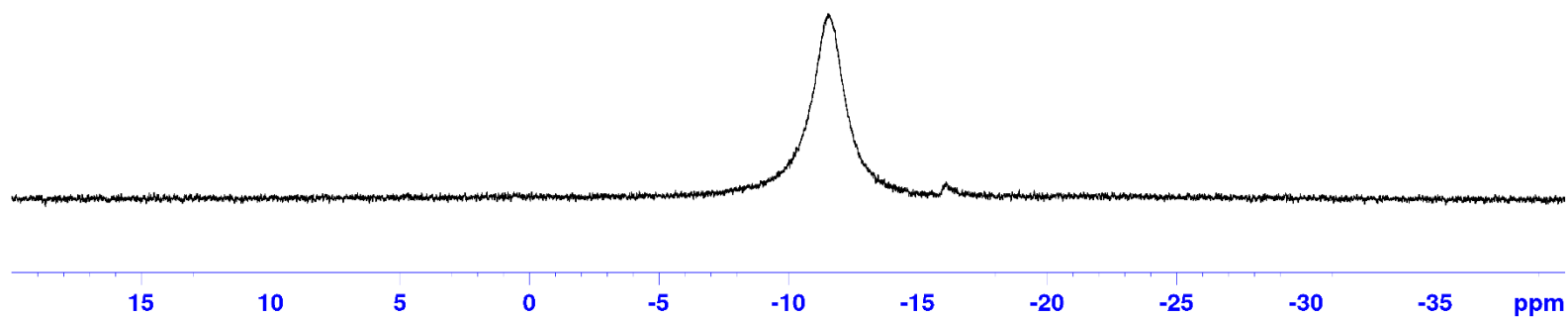


1-((2-(4'-Methoxy-[1,1'-biphenyl]-4-yl)cyclopropyl)methyl)pyrrolidine Borane (1s):

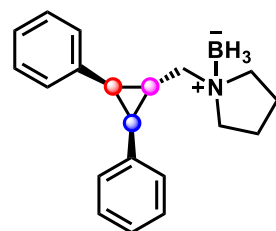


-11.53

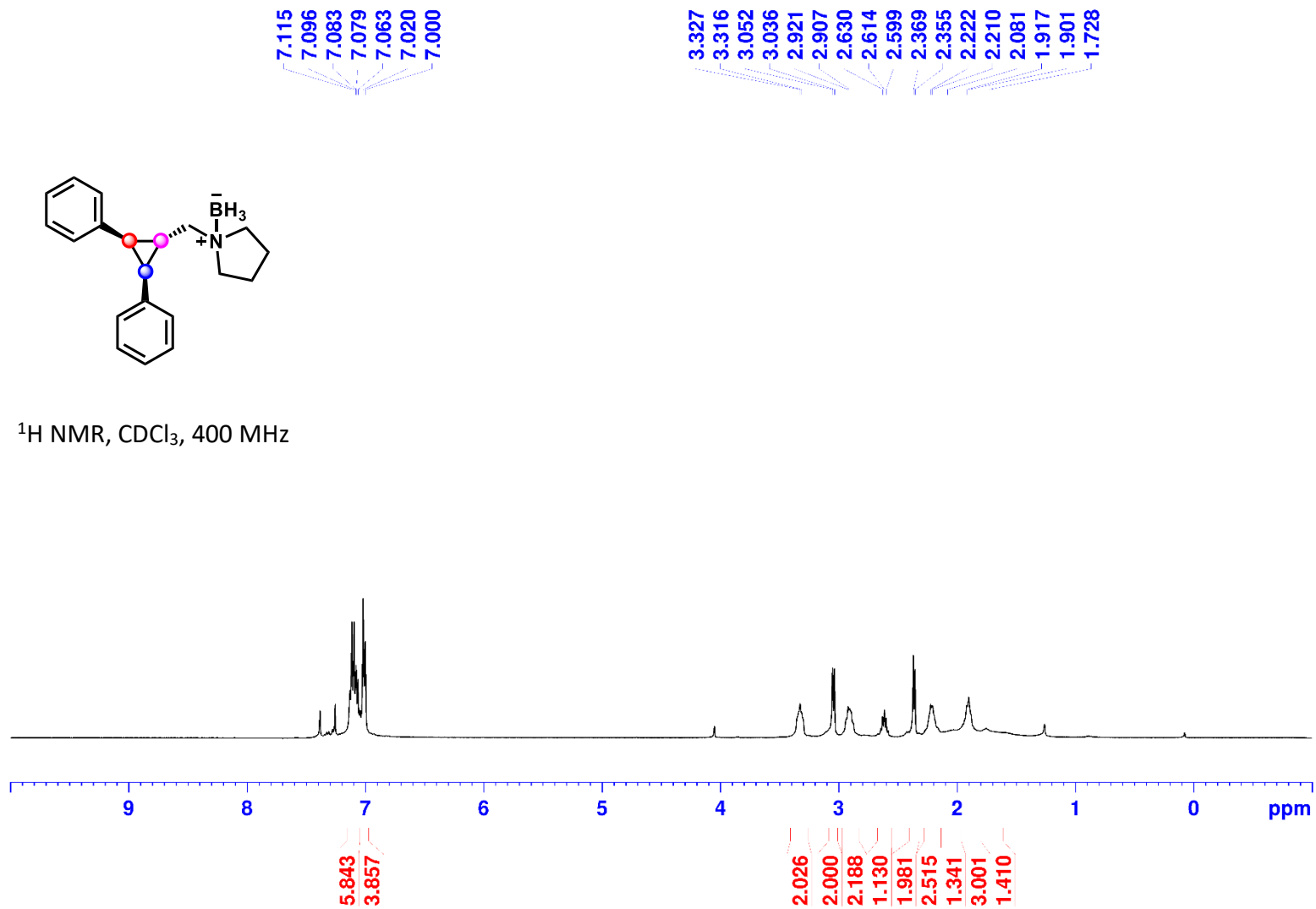
^{11}B NMR, CDCl_3 , 160 MHz



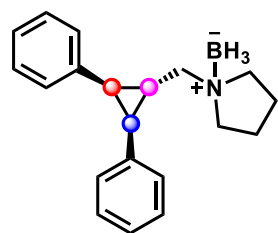
1-(((1*R*,2*R*,3*S*)-2,3-diphenylcyclopropyl)methyl)pyrrolidine Borane (1t):



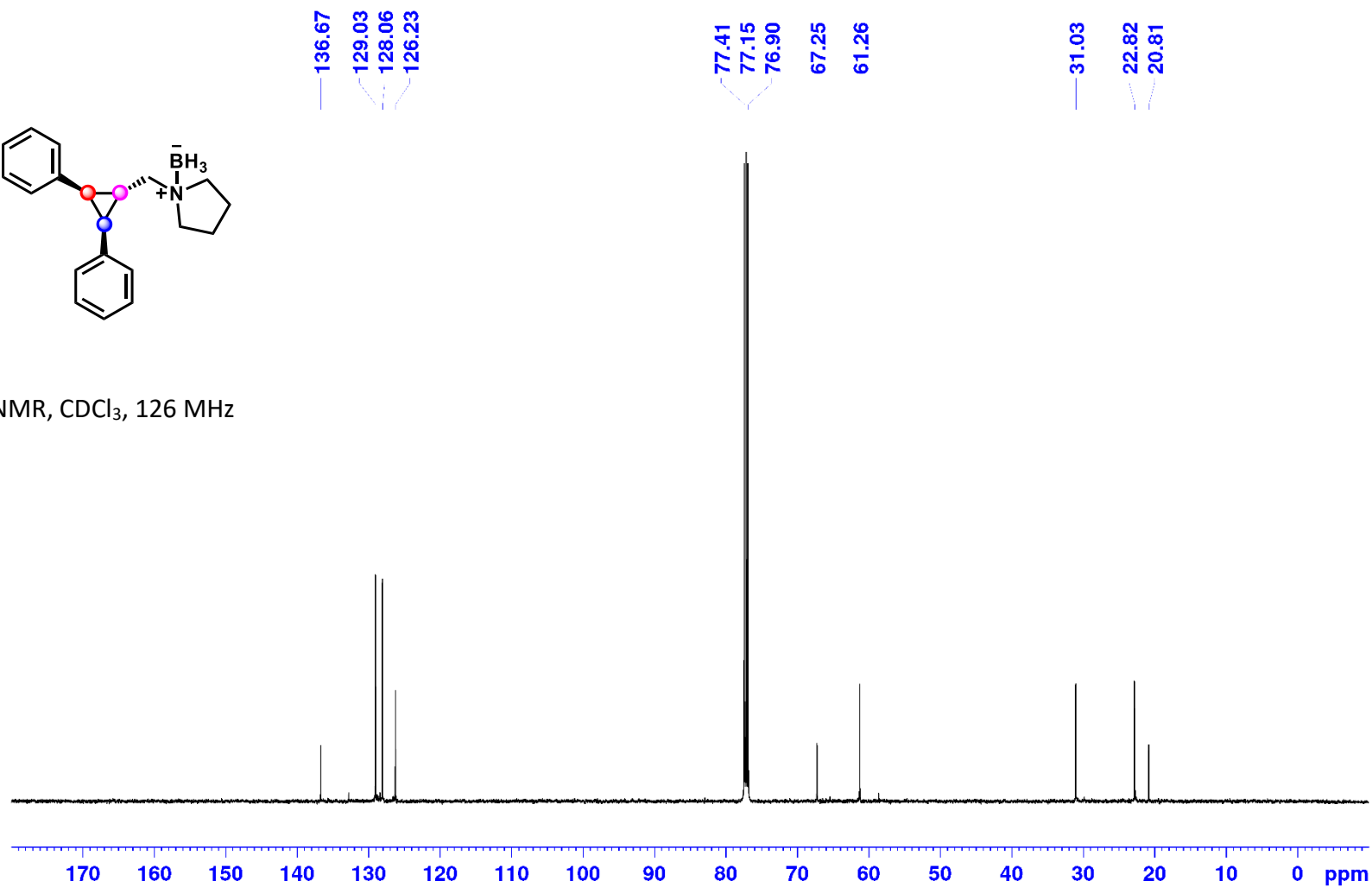
¹H NMR, CDCl₃, 400 MHz



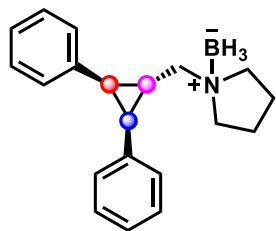
1-(((1*R*,2*R*,3*S*)-2,3-diphenylcyclopropyl)methyl)pyrrolidine Borane (1t):



¹³C NMR, CDCl₃, 126 MHz

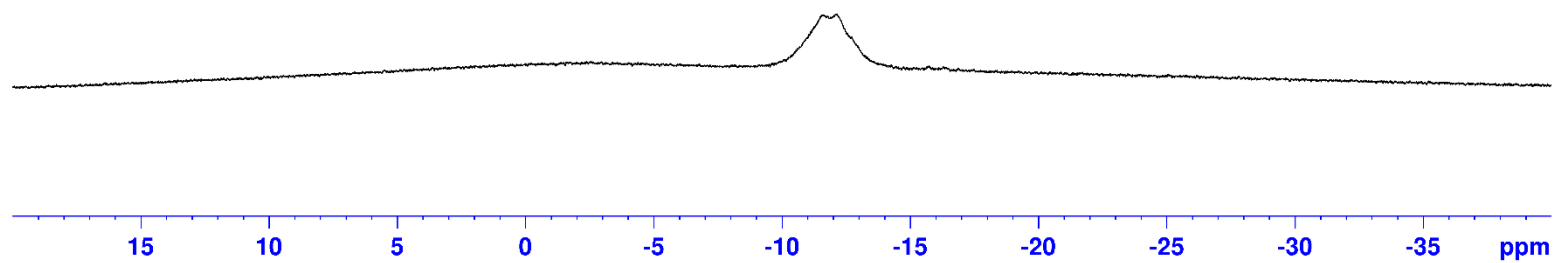


1-(((1*R*,2*R*,3*S*)-2,3-diphenylcyclopropyl)methyl)pyrrolidine Borane (1t):

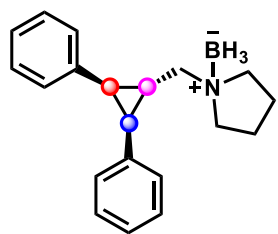


-11.89

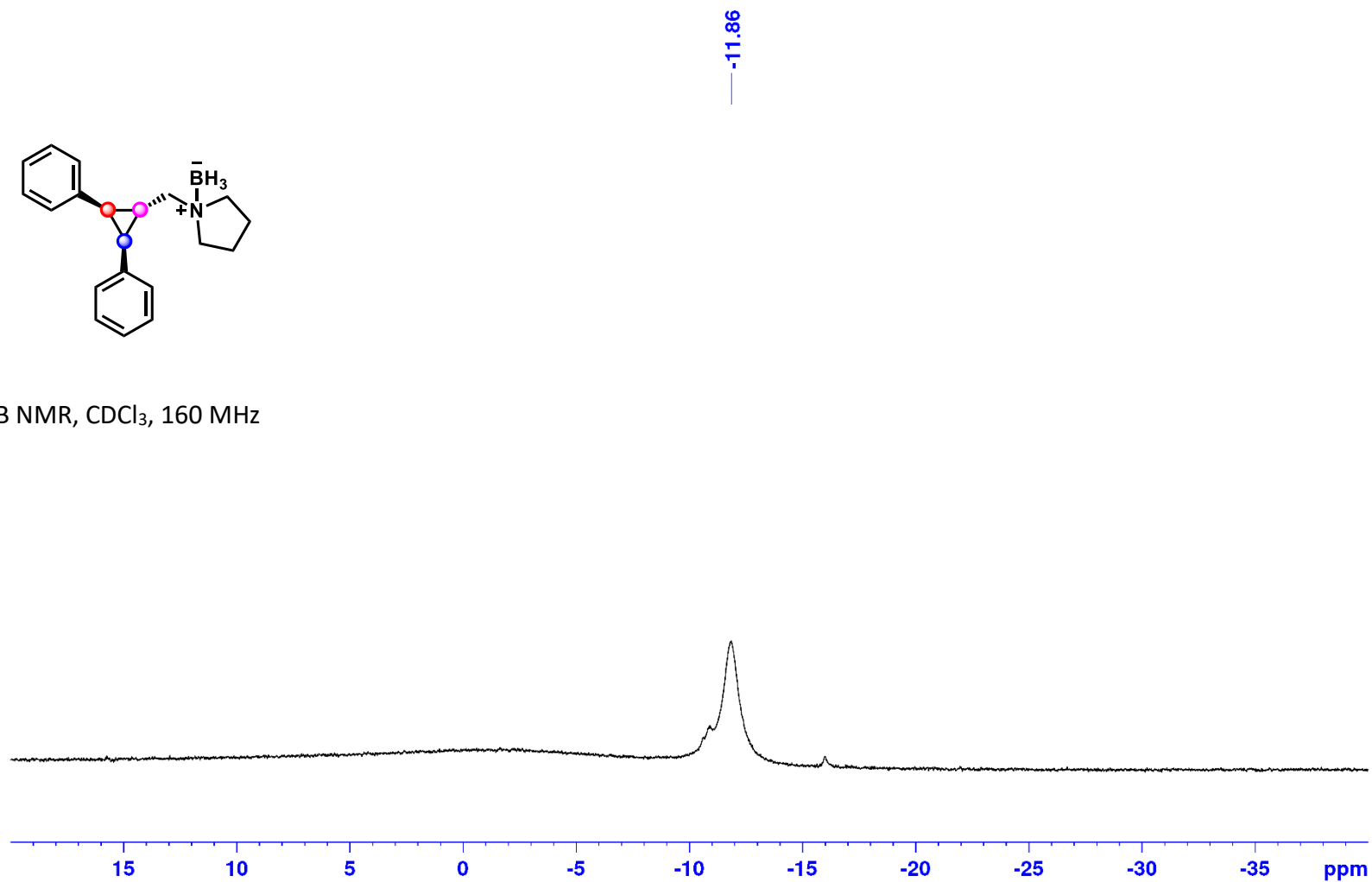
^{11}B NMR, CDCl_3 , 160 MHz



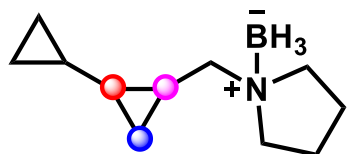
1-(((1*R*,2*R*,3*S*)-2,3-diphenylcyclopropyl)methyl)pyrrolidine Borane (1t):



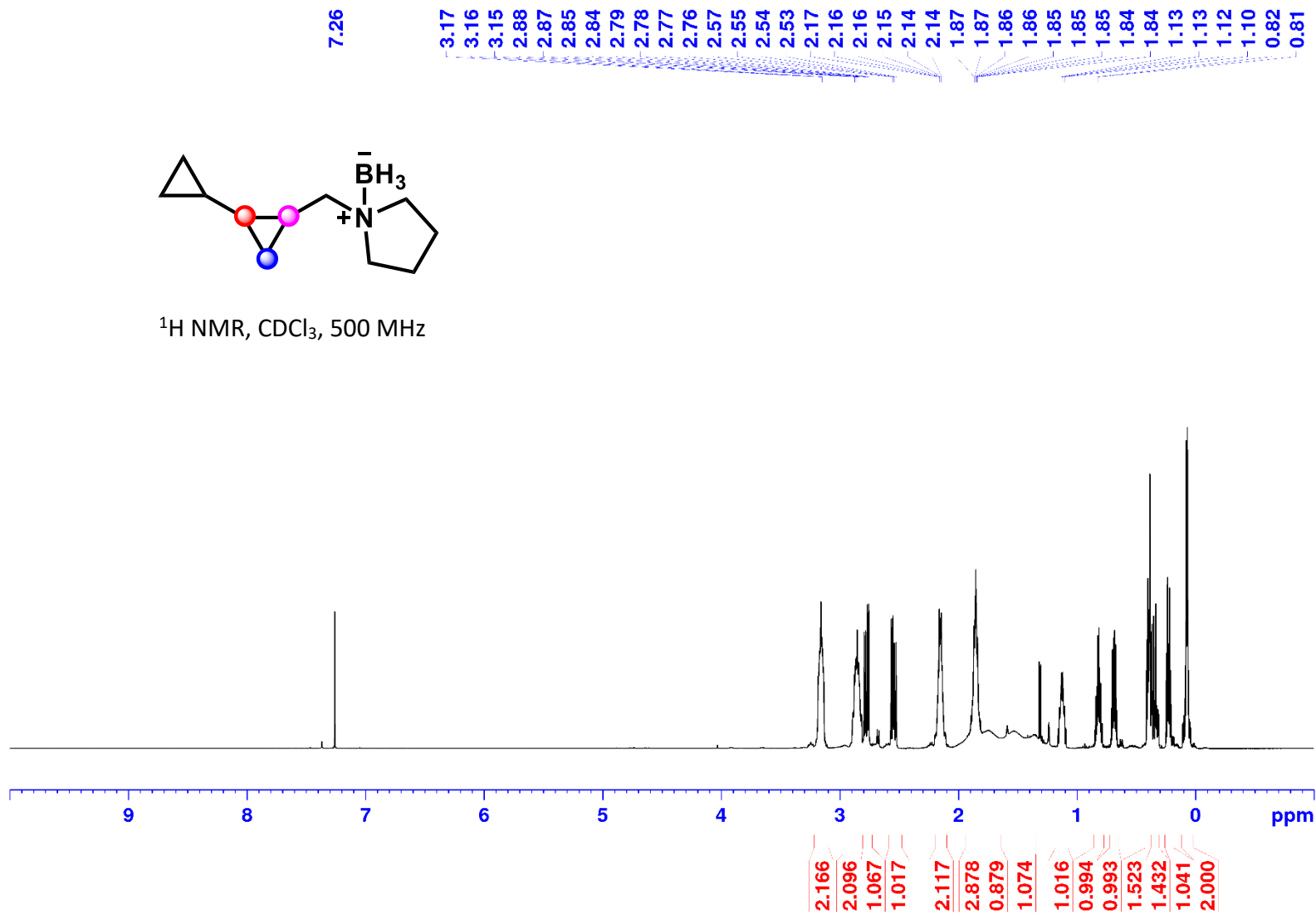
^{11}B NMR, CDCl_3 , 160 MHz



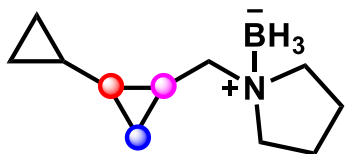
1-([1,1'-bi(Cyclopropan)]-2-ylmethyl)pyrrolidine Borane (1u)



^1H NMR, CDCl_3 , 500 MHz



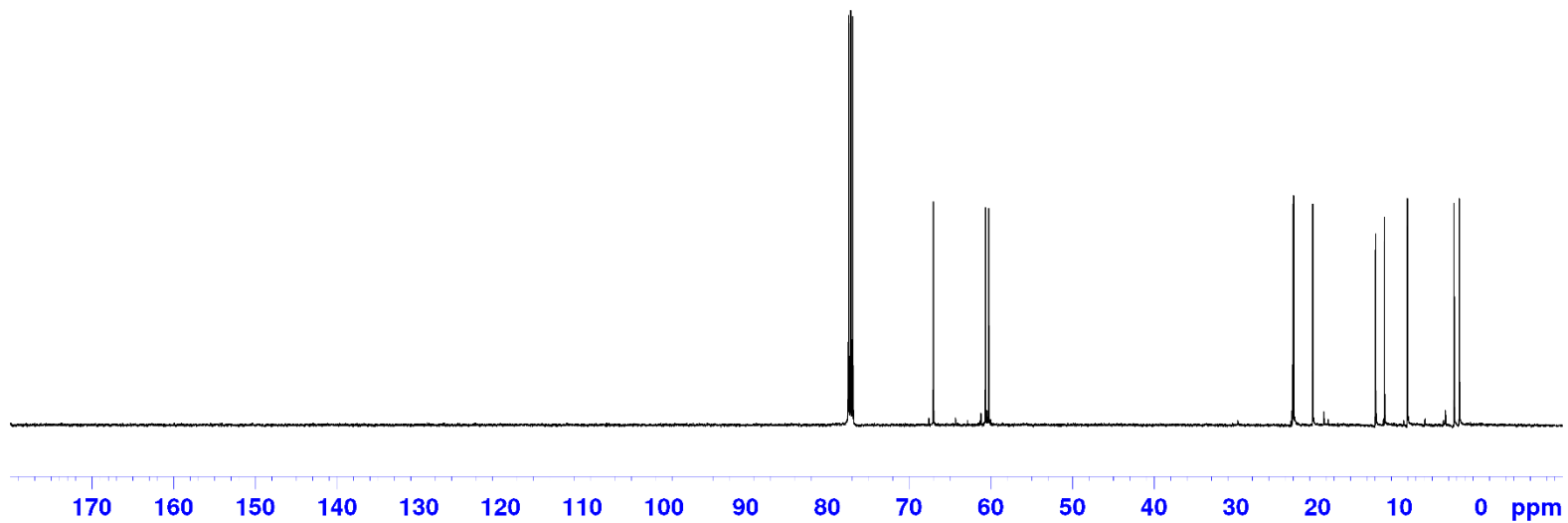
1-([1,1'-bi(Cyclopropan)]-2-ylmethyl)pyrrolidine Borane (1u) :



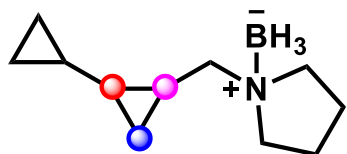
77.41
77.16
76.90
67.03
60.65
60.27

23.03
22.94
20.60
12.92
11.84
9.03
3.33
2.68

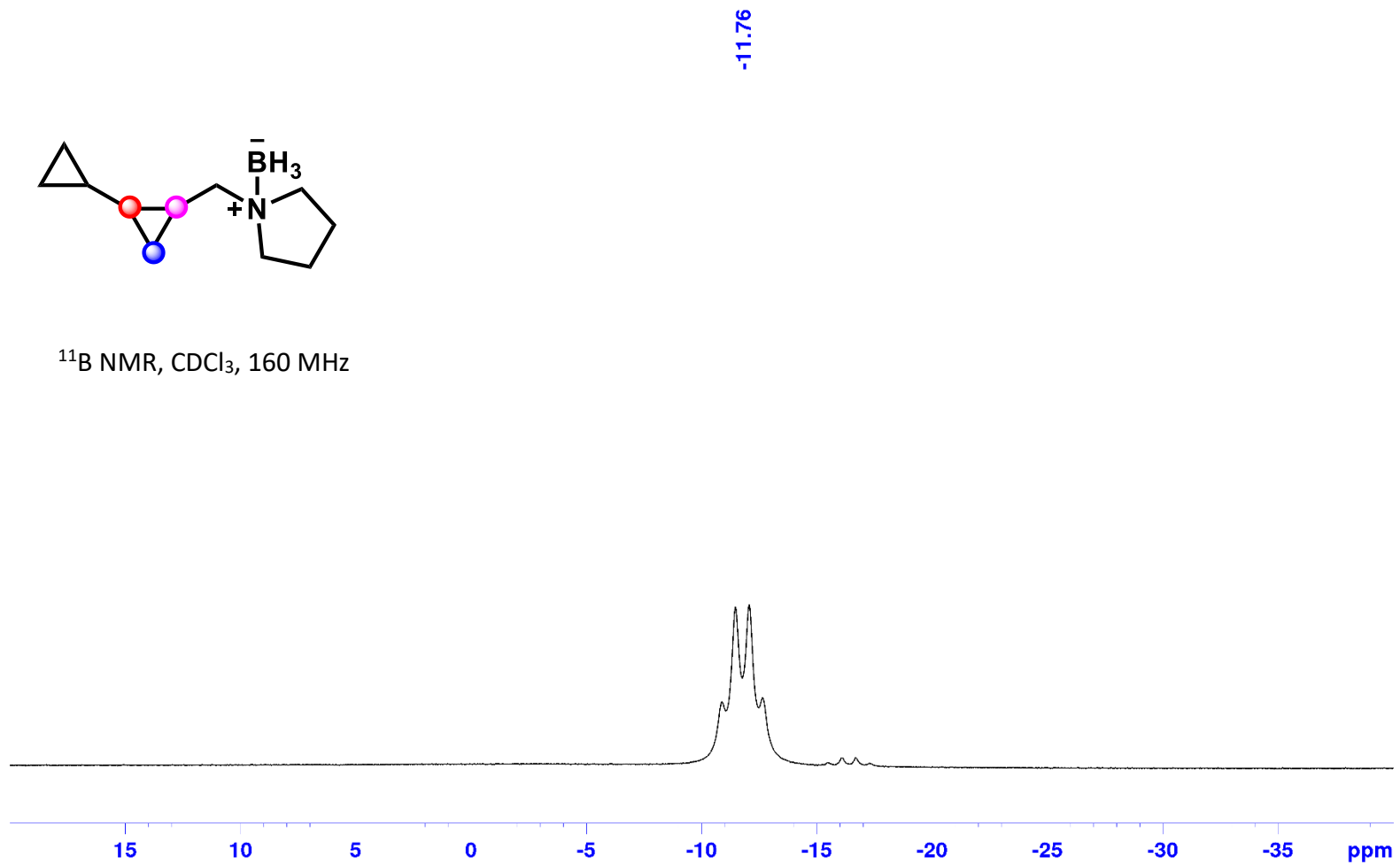
^{13}C NMR, CDCl_3 , 126 MHz



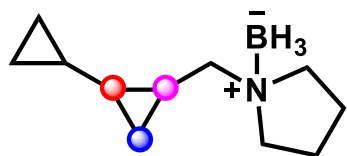
1-([1,1'-bi(Cyclopropan)]-2-ylmethyl)pyrrolidine Borane (1u) :



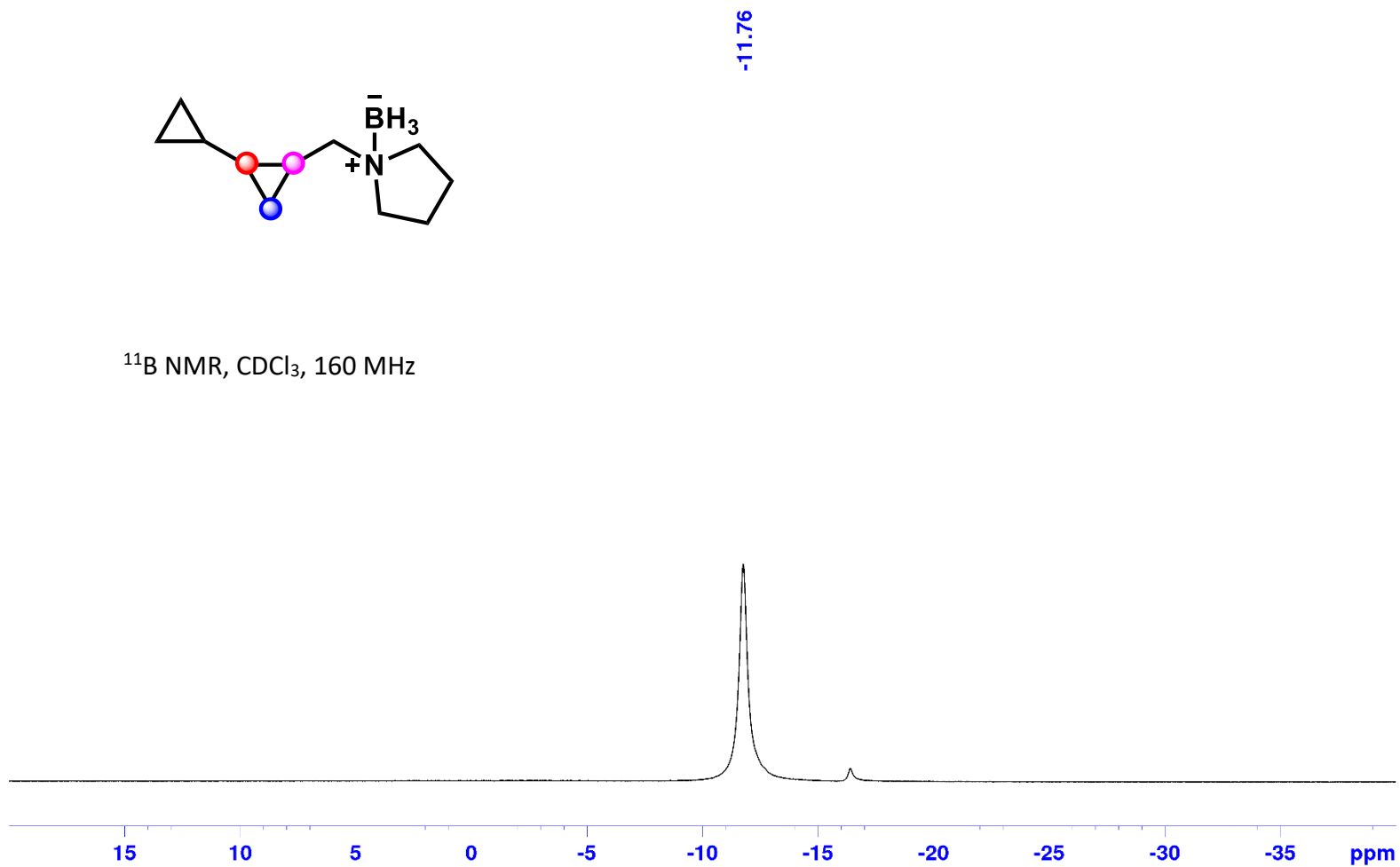
^{11}B NMR, CDCl_3 , 160 MHz



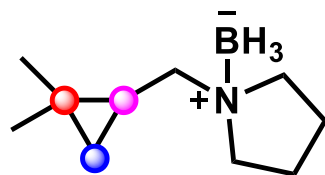
1-([1,1'-bi(Cyclopropan)]-2-ylmethyl)pyrrolidine Borane (1u) :



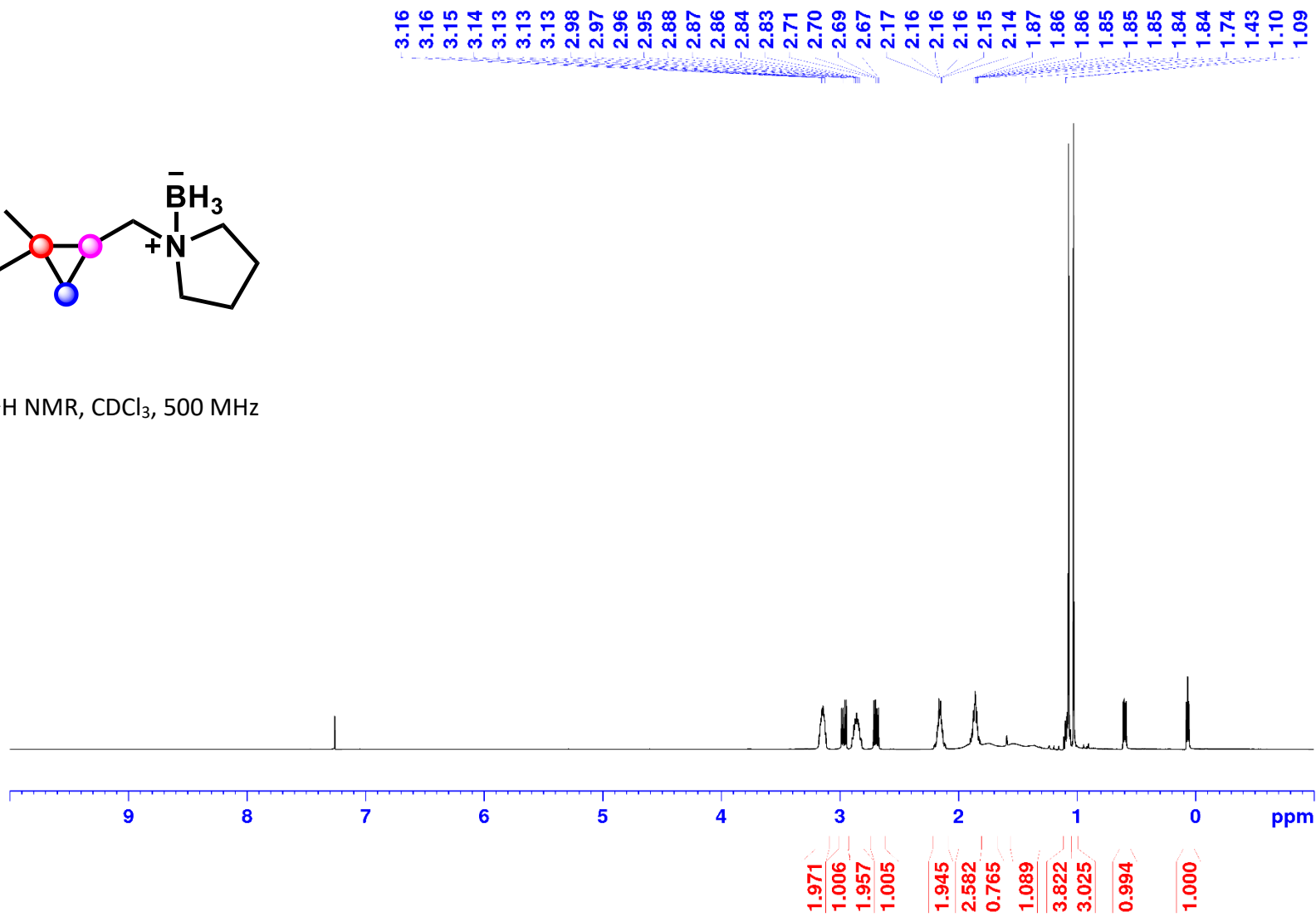
^{11}B NMR, CDCl_3 , 160 MHz



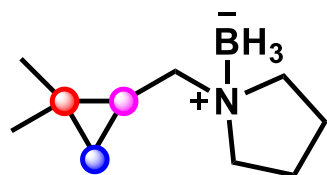
1-((2,2-Dimethylcyclopropyl)methyl)pyrrolidine Borane (1v):



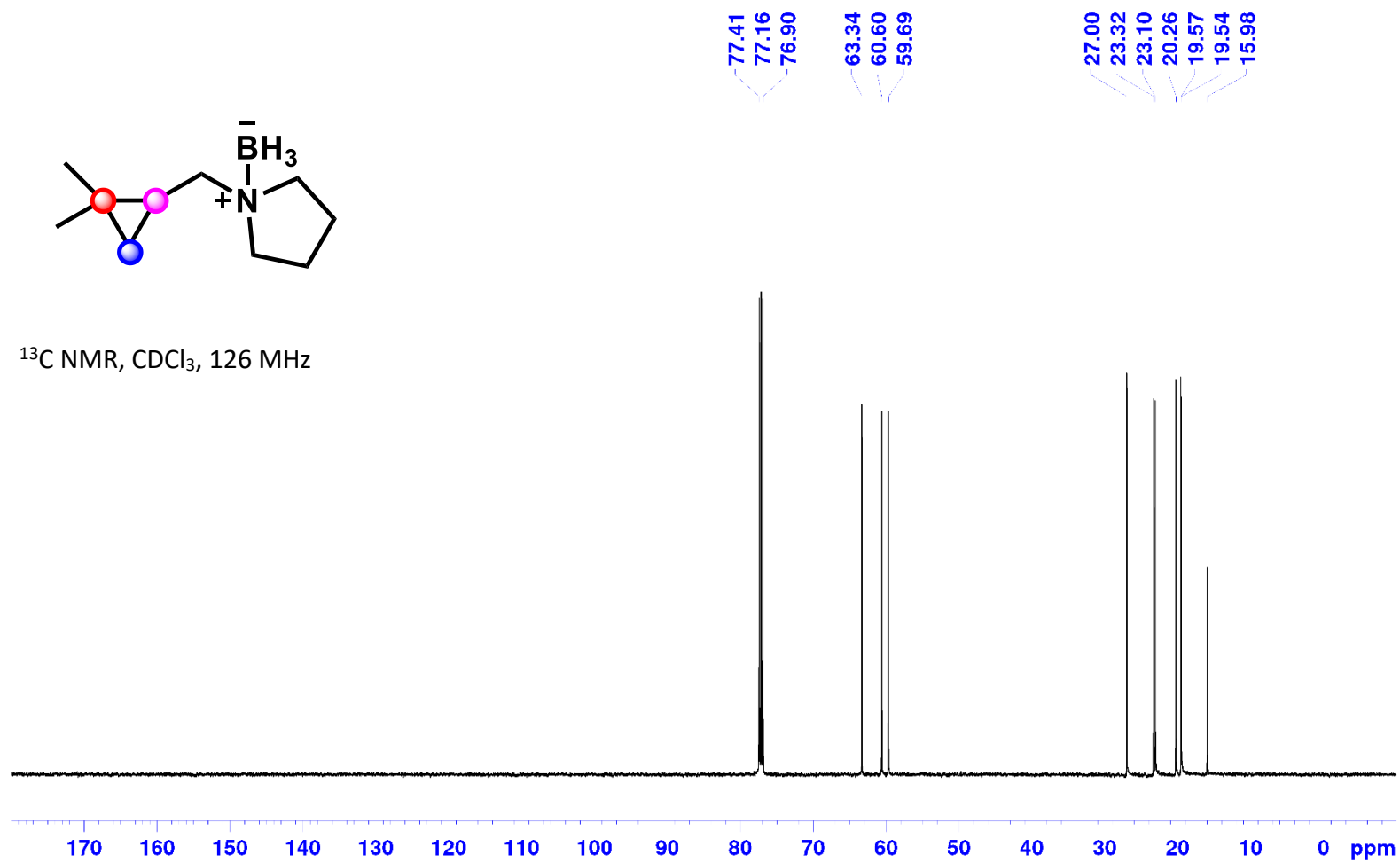
^1H NMR, CDCl_3 , 500 MHz



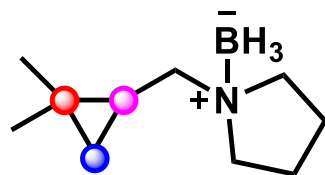
1-((2,2-Dimethylcyclopropyl)methyl)pyrrolidine Borane (1v):



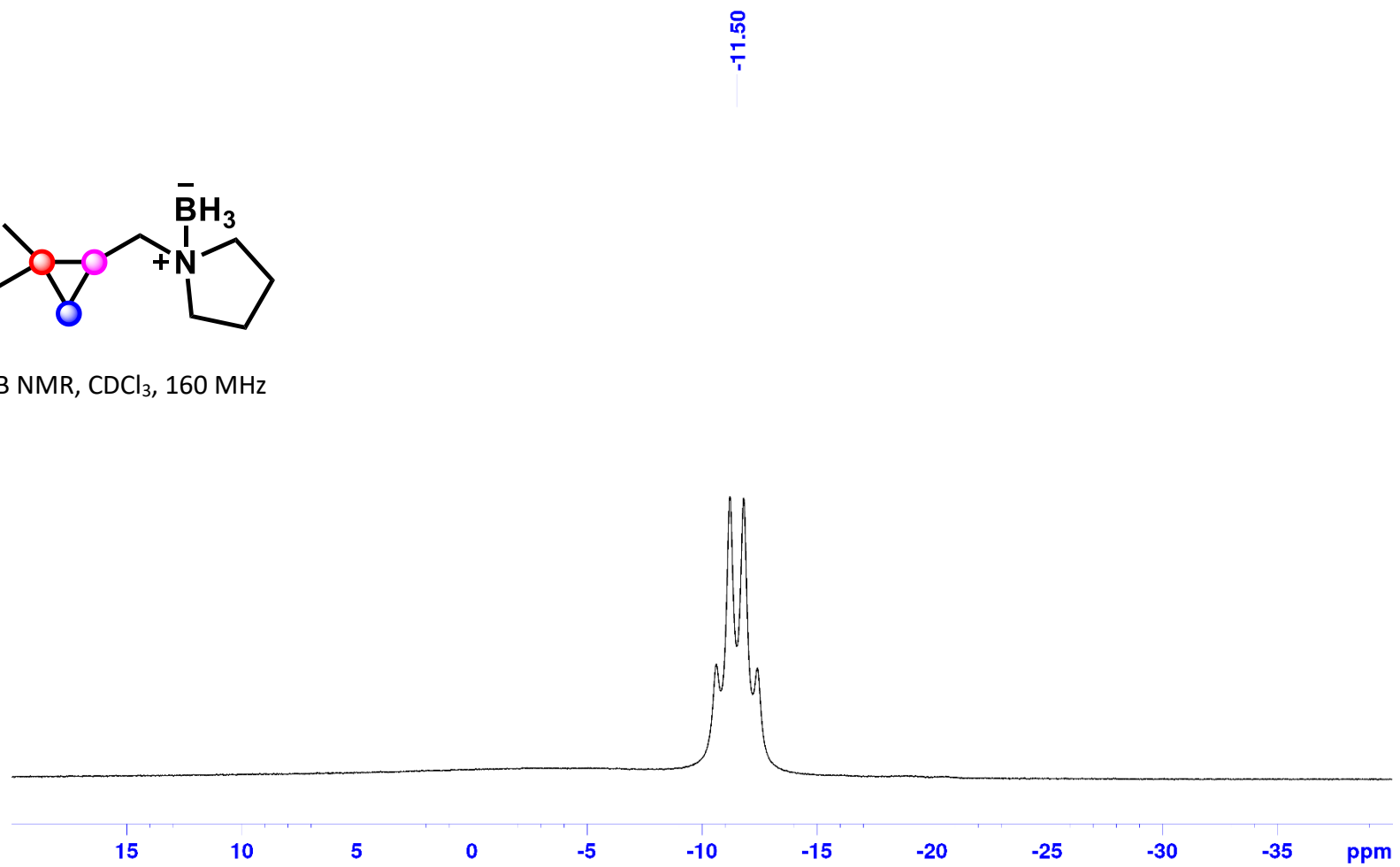
^{13}C NMR, CDCl_3 , 126 MHz



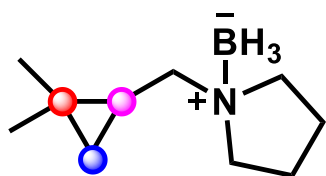
1-((2,2-Dimethylcyclopropyl)methyl)pyrrolidine Borane (1v):



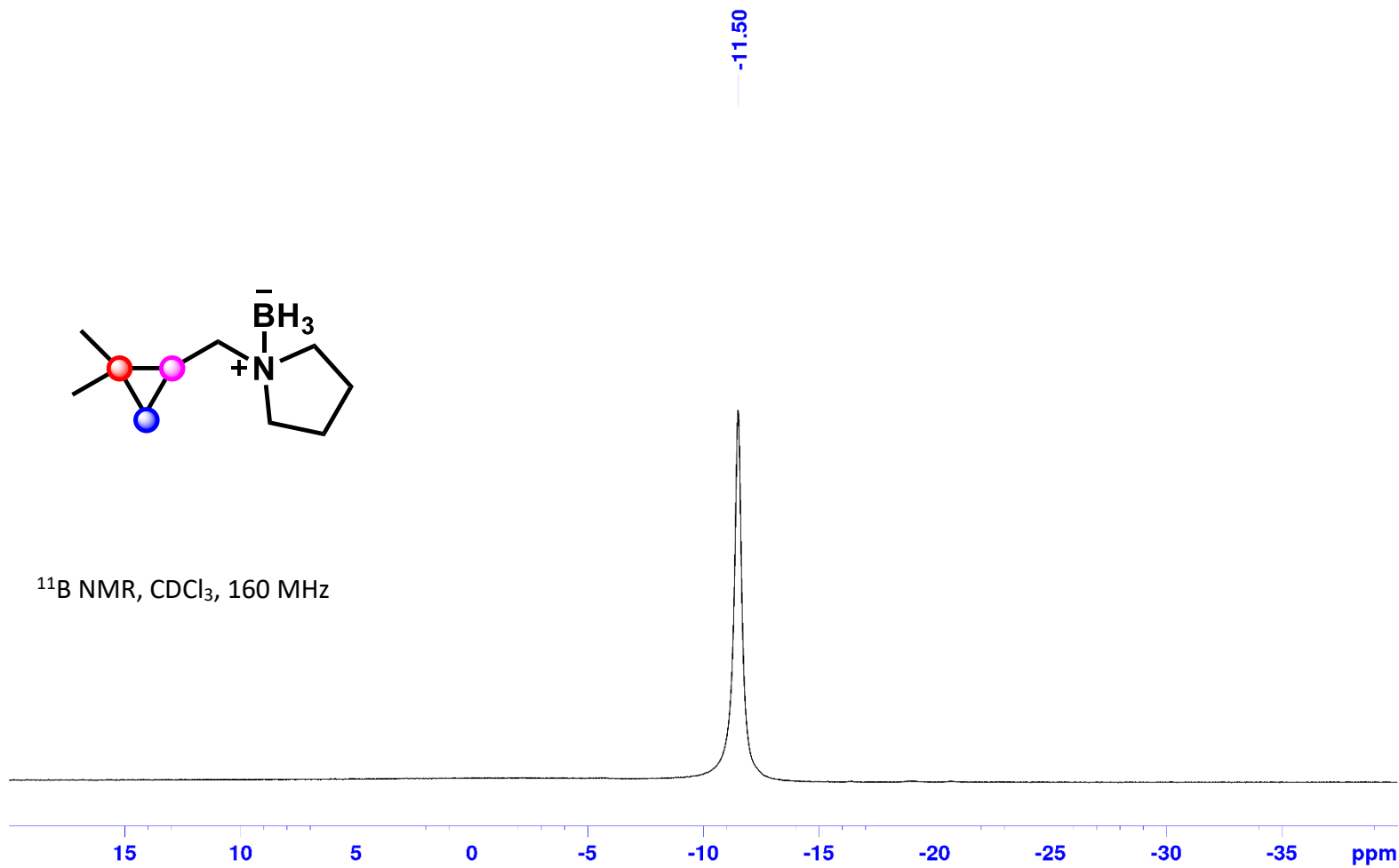
^{11}B NMR, CDCl_3 , 160 MHz



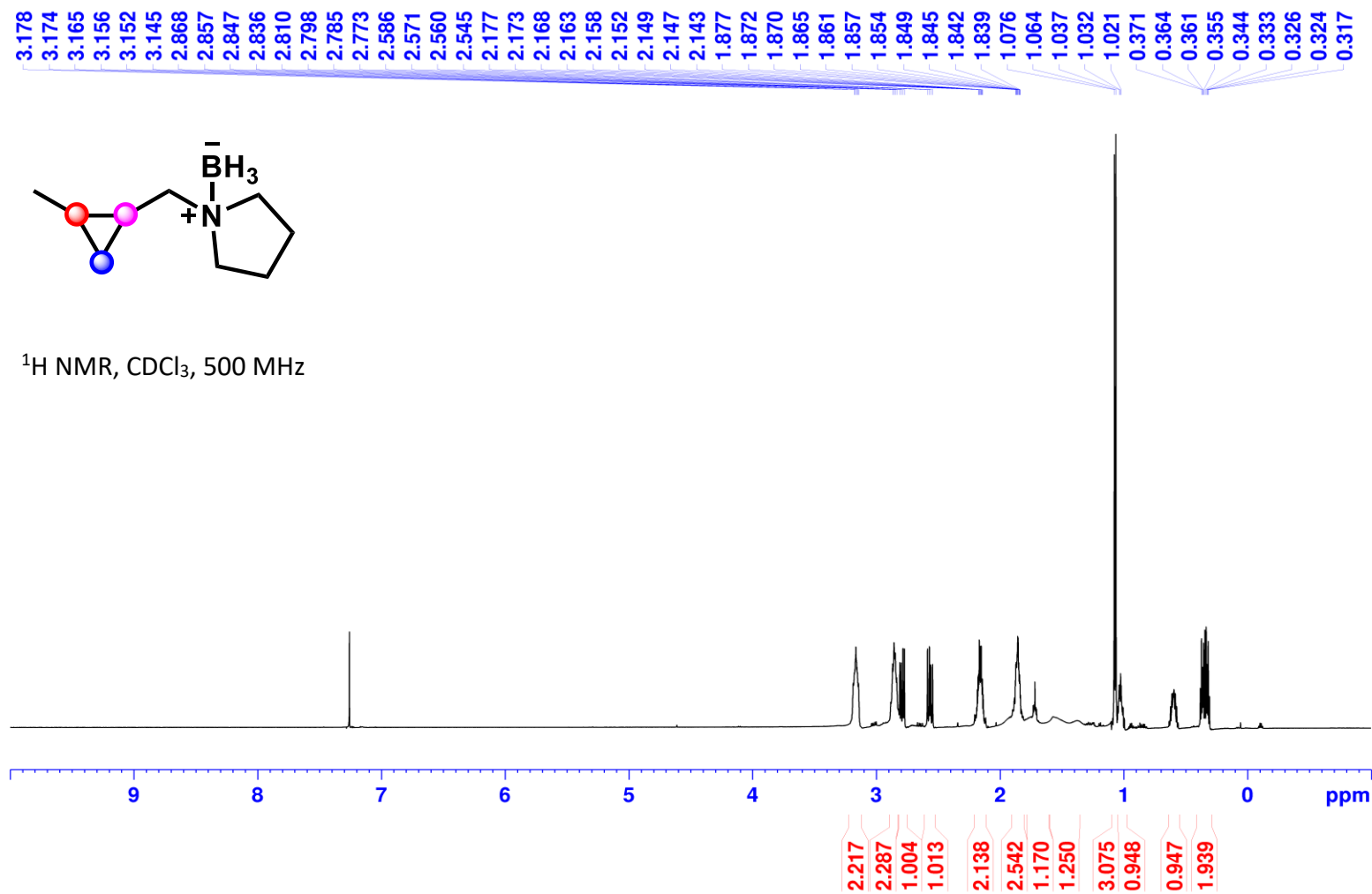
1-((2,2-Dimethylcyclopropyl)methyl)pyrrolidine Borane (1v):



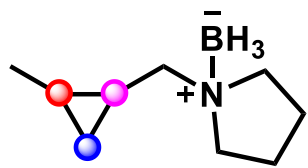
^{11}B NMR, CDCl_3 , 160 MHz



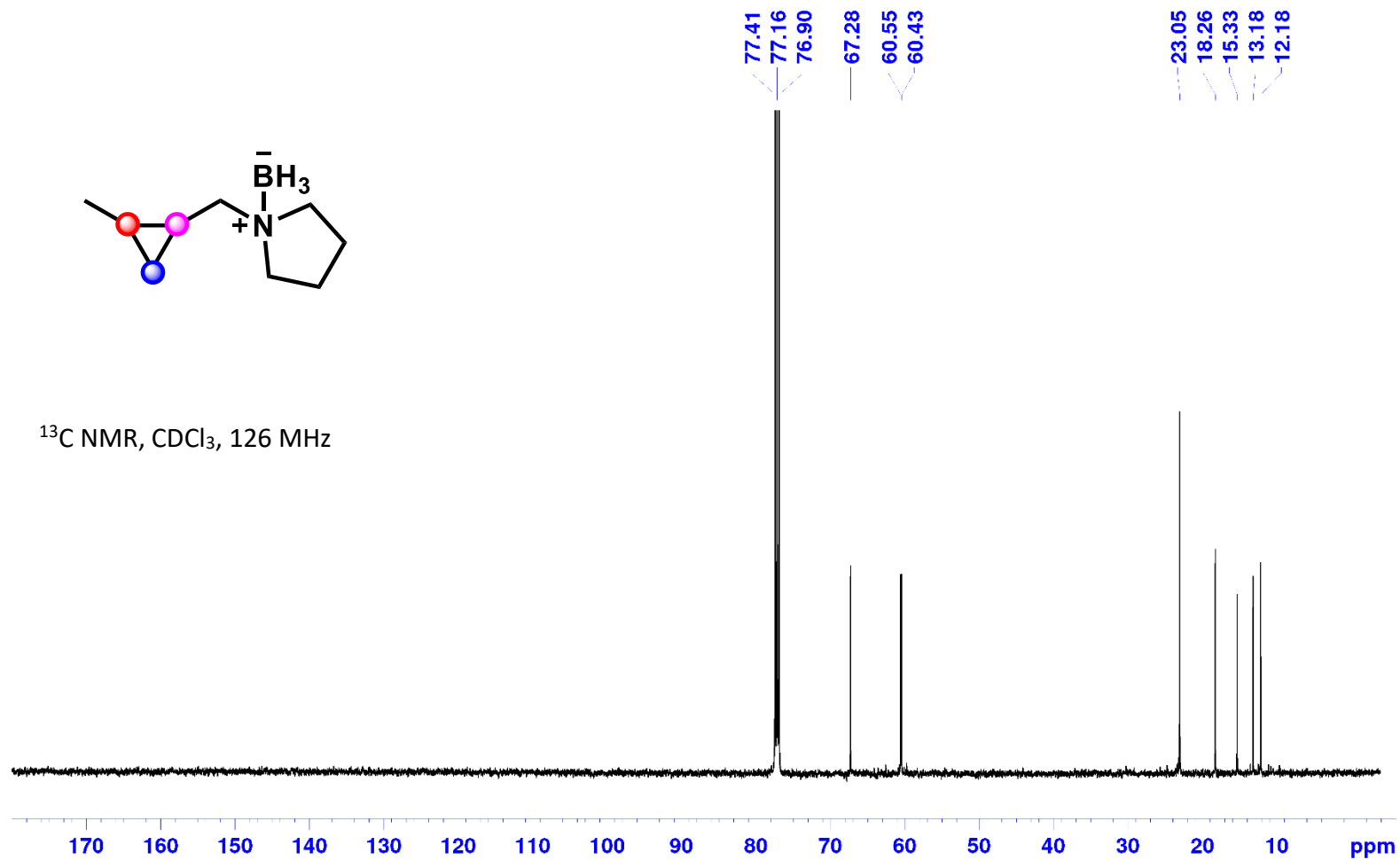
1-((2-Methylcyclopropyl)methyl)pyrrolidine Borane (1w):



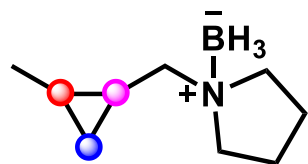
1-((2-Methylcyclopropyl)methyl)pyrrolidine Borane (1w):



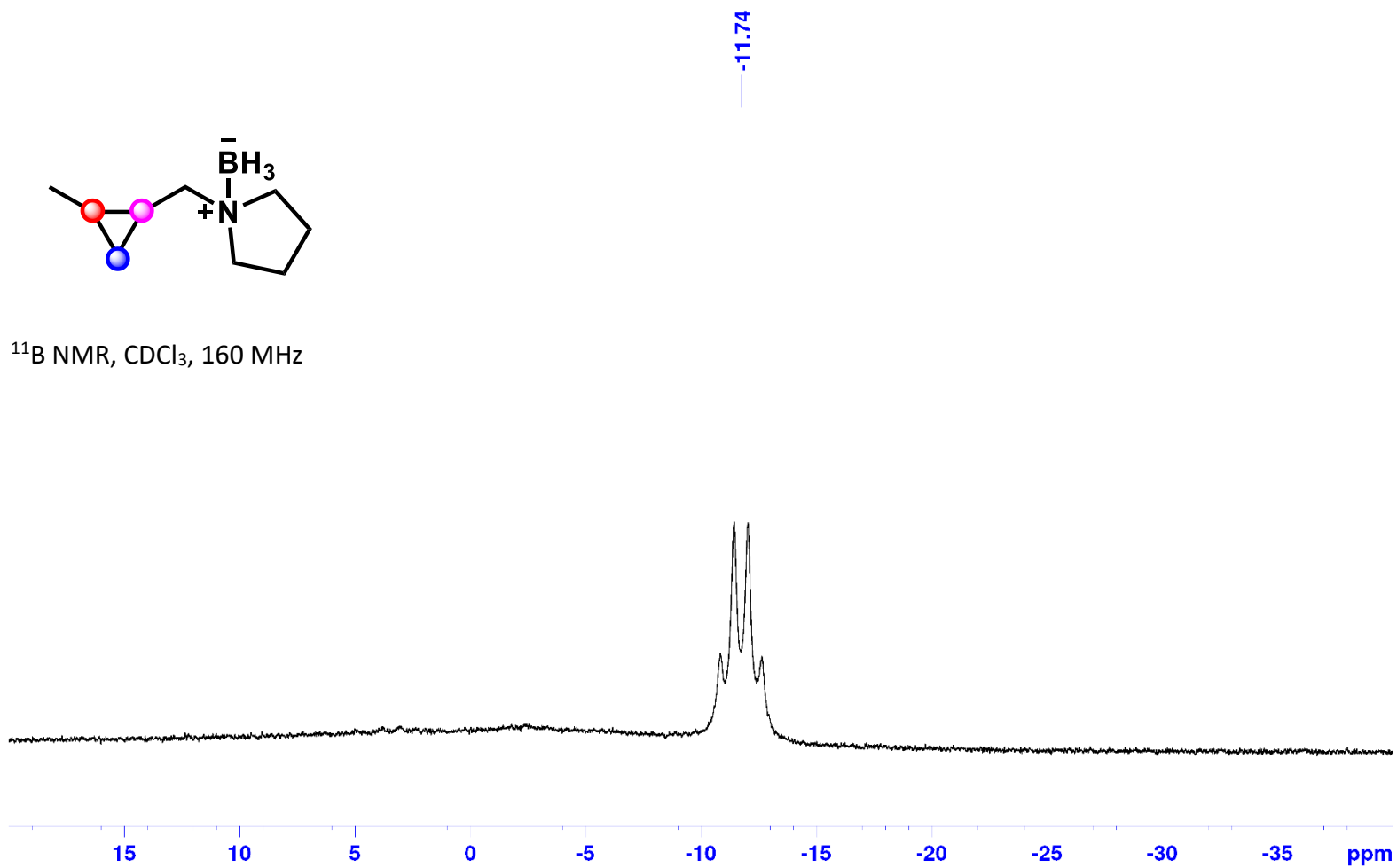
^{13}C NMR, CDCl_3 , 126 MHz



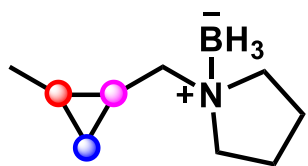
1-((2-Methylcyclopropyl)methyl)pyrrolidine Borane (1w):



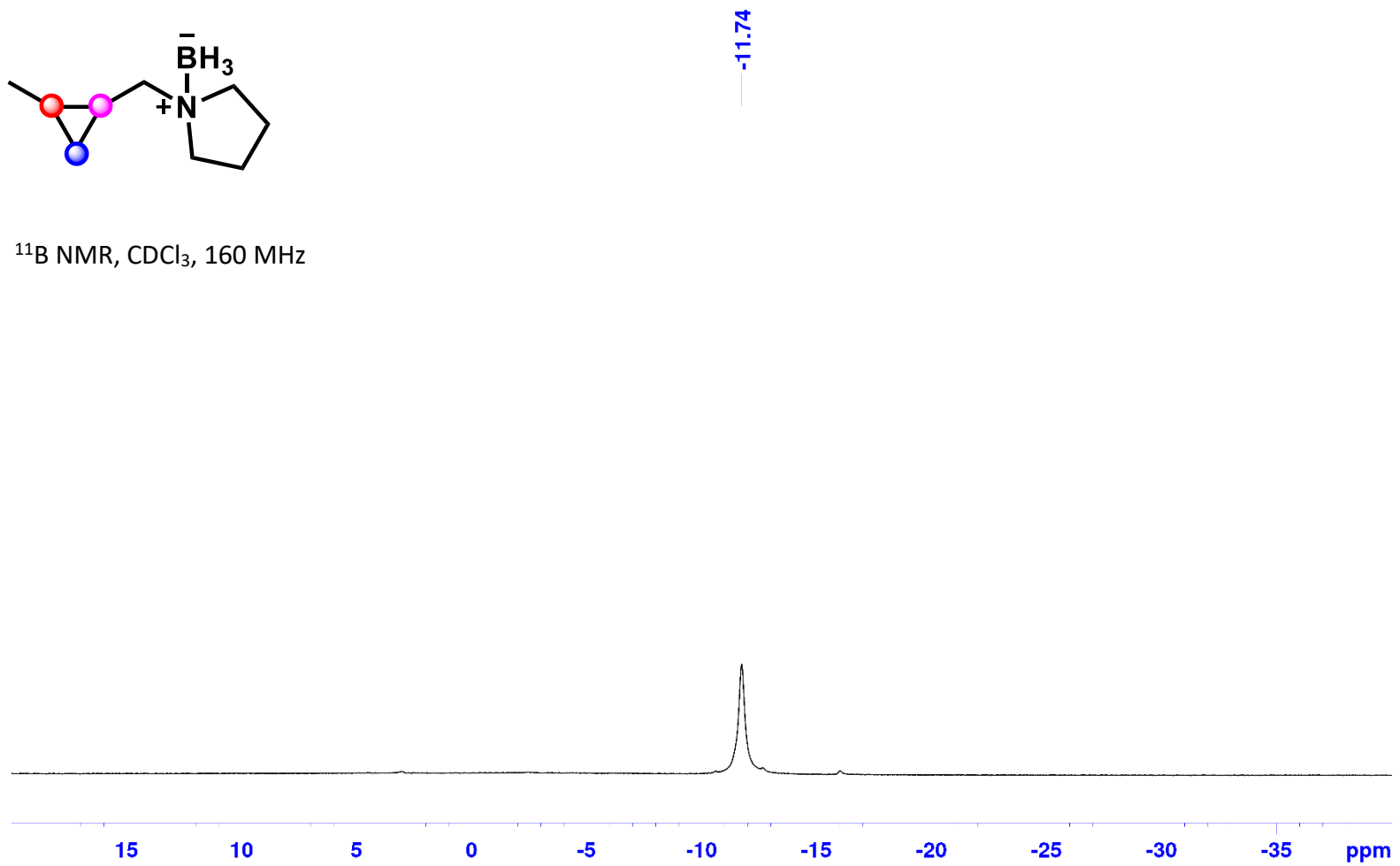
^{11}B NMR, CDCl_3 , 160 MHz



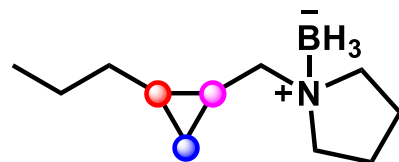
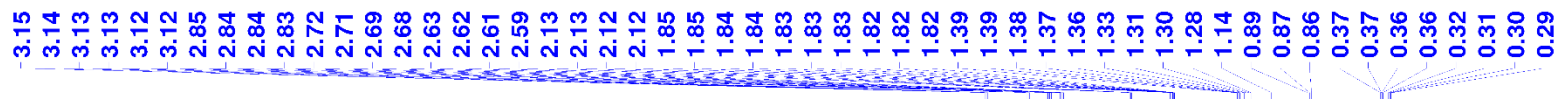
1-((2-Methylcyclopropyl)methyl)pyrrolidine Borane (1w):



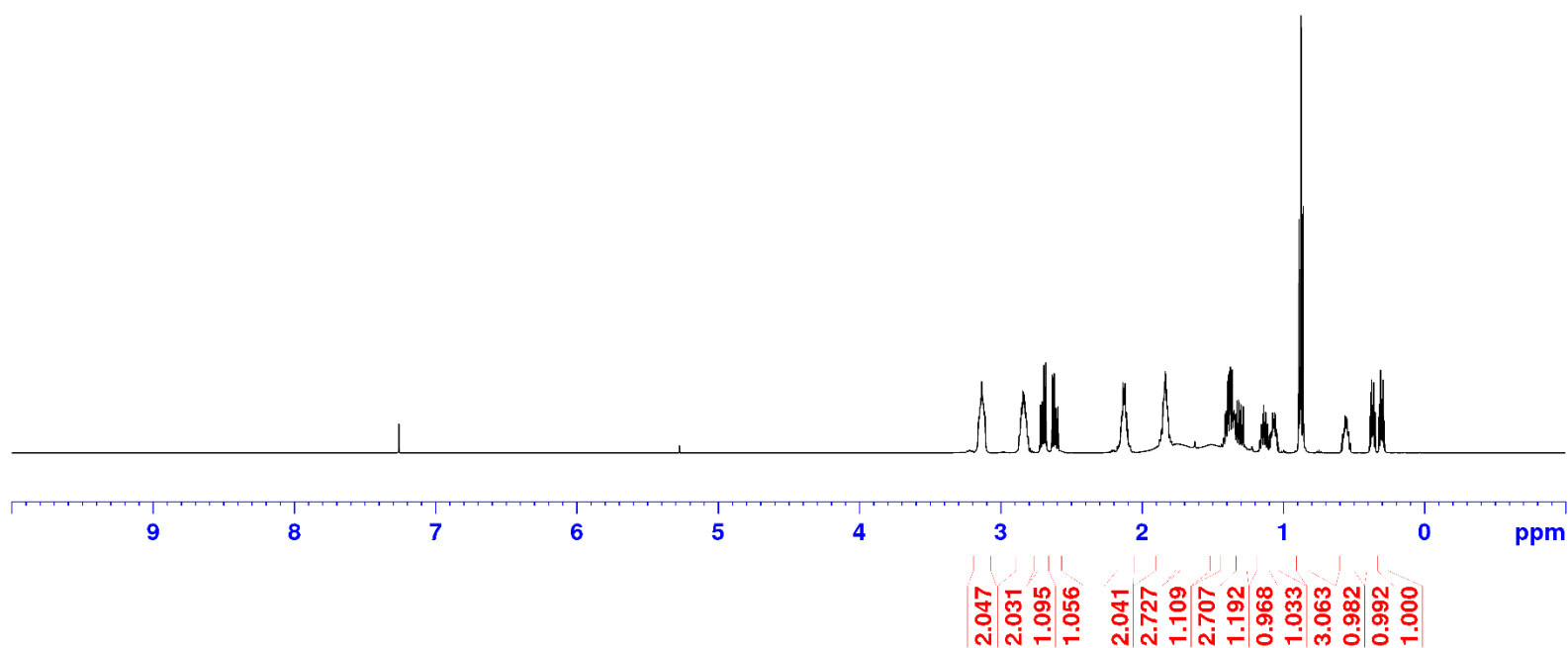
^{11}B NMR, CDCl_3 , 160 MHz



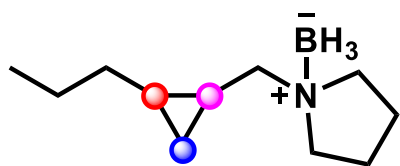
1-((2-Propylcyclopropyl)methyl)pyrrolidine Borane (1x):



¹H NMR, CDCl₃, 500 MHz

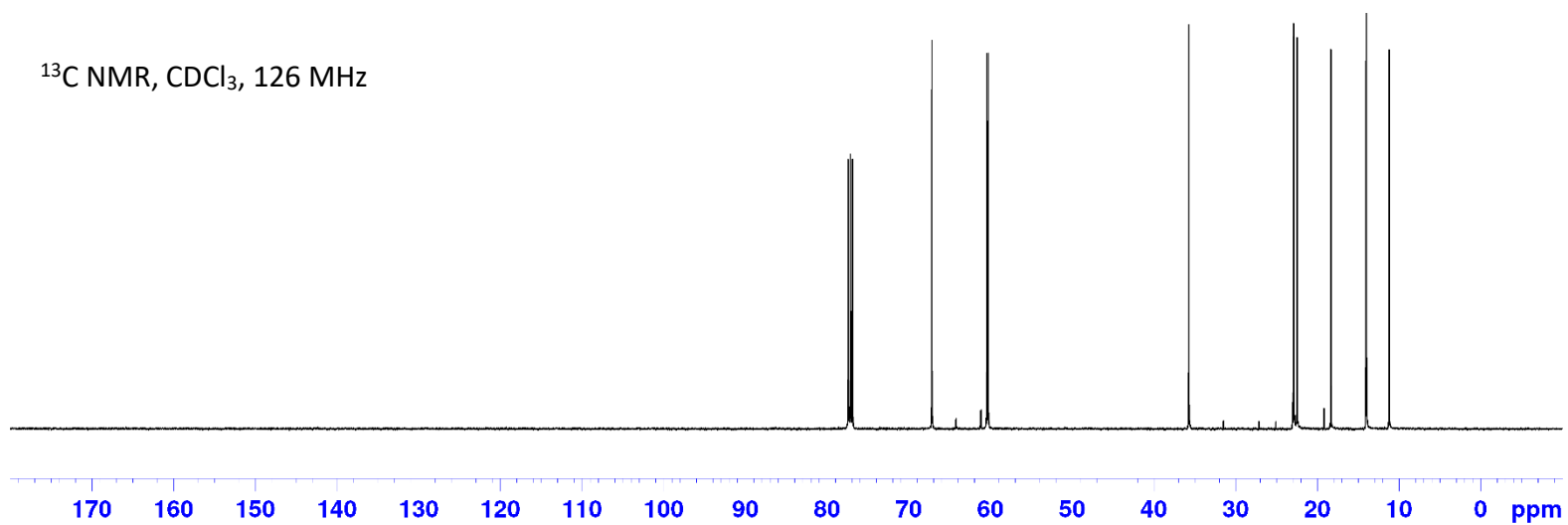


1-((2-Propylcyclopropyl)methyl)pyrrolidine Borane (1x):

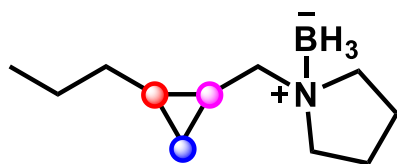


77.41
77.16
76.90
67.19
60.47
60.30
35.73
22.94
22.88
22.49
18.35
14.05
14.01
11.23

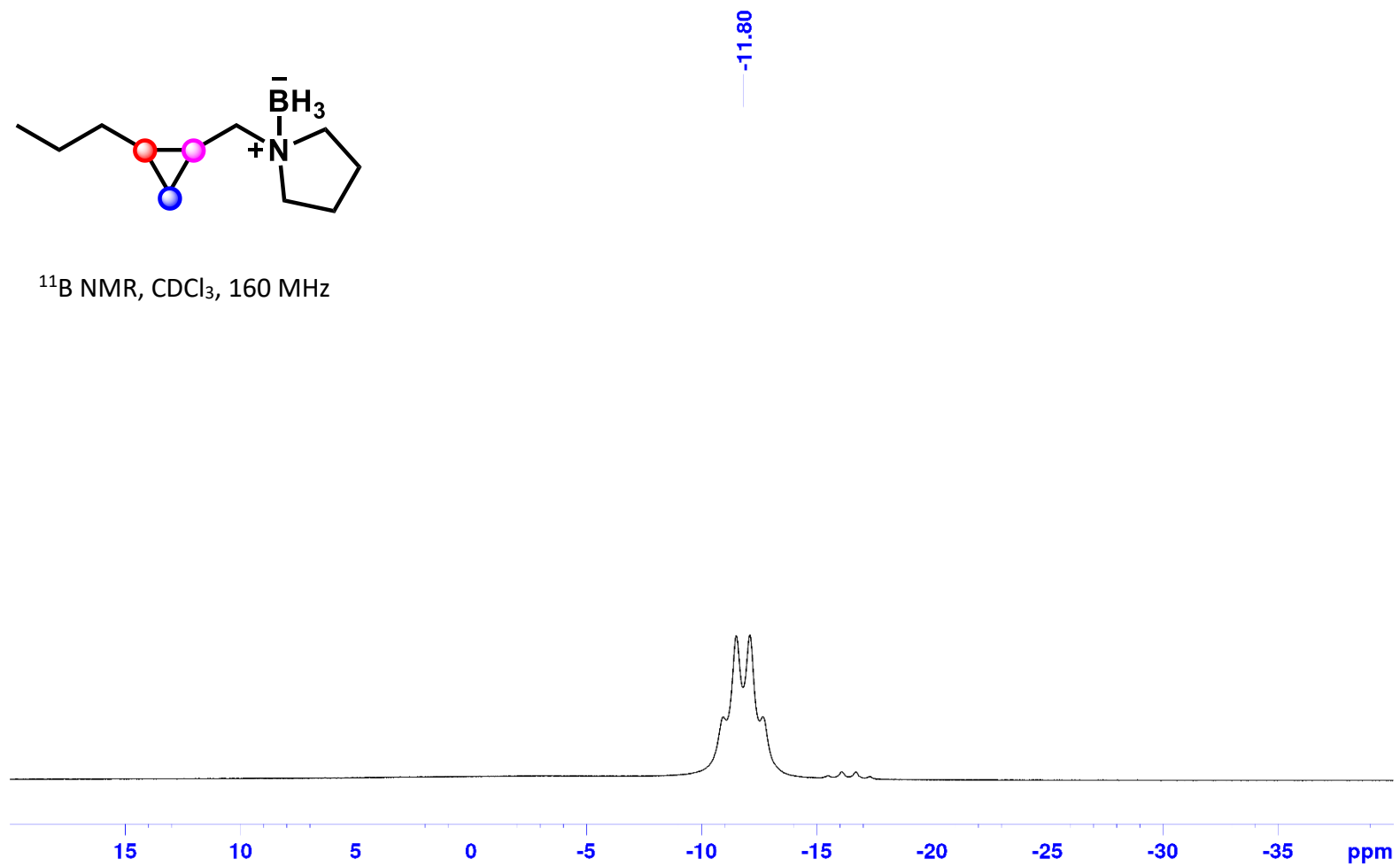
¹³C NMR, CDCl₃, 126 MHz



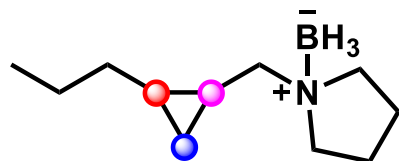
1-((2-Propylcyclopropyl)methyl)pyrrolidine Borane (1x):



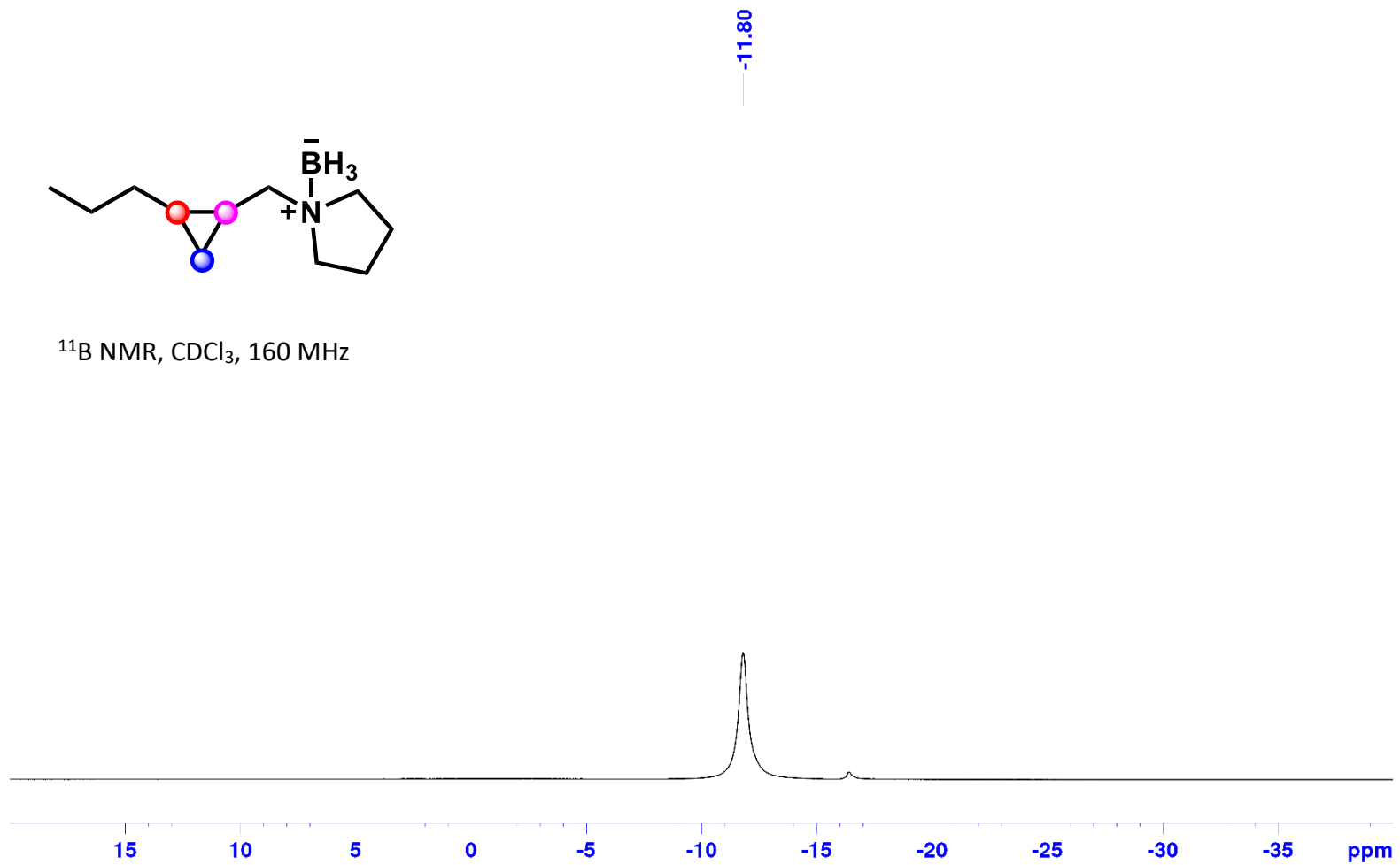
^{11}B NMR, CDCl_3 , 160 MHz



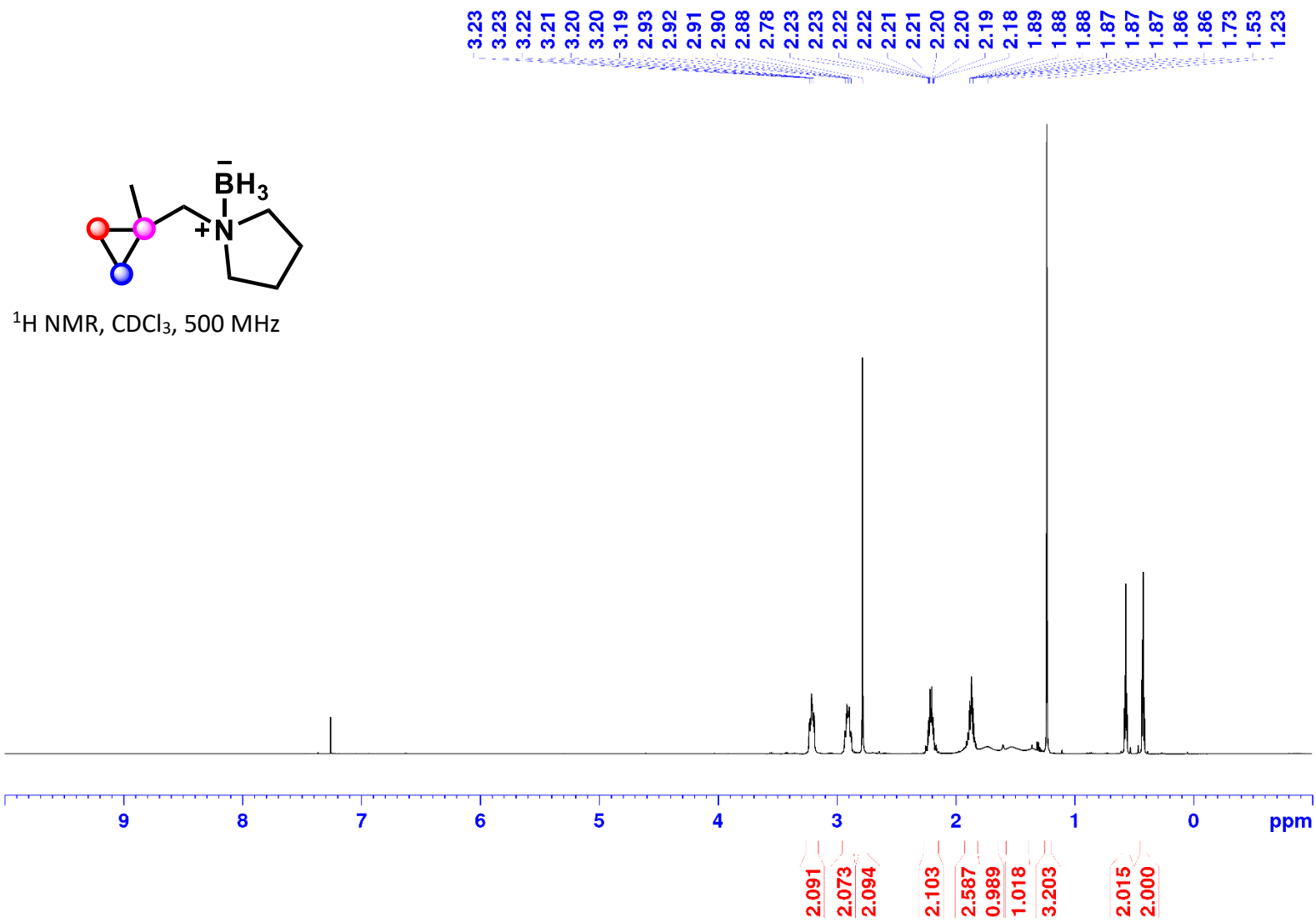
1-((2-Propylcyclopropyl)methyl)pyrrolidine Borane (1x):



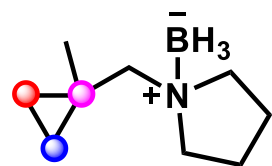
¹¹B NMR, CDCl₃, 160 MHz



1-((1-Methylcyclopropyl)methyl)pyrrolidine Borane (1y):



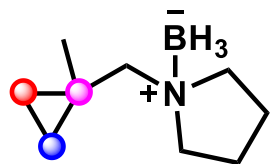
1-((1-Methylcyclopropyl)methyl)pyrrolidine Borane (1y):



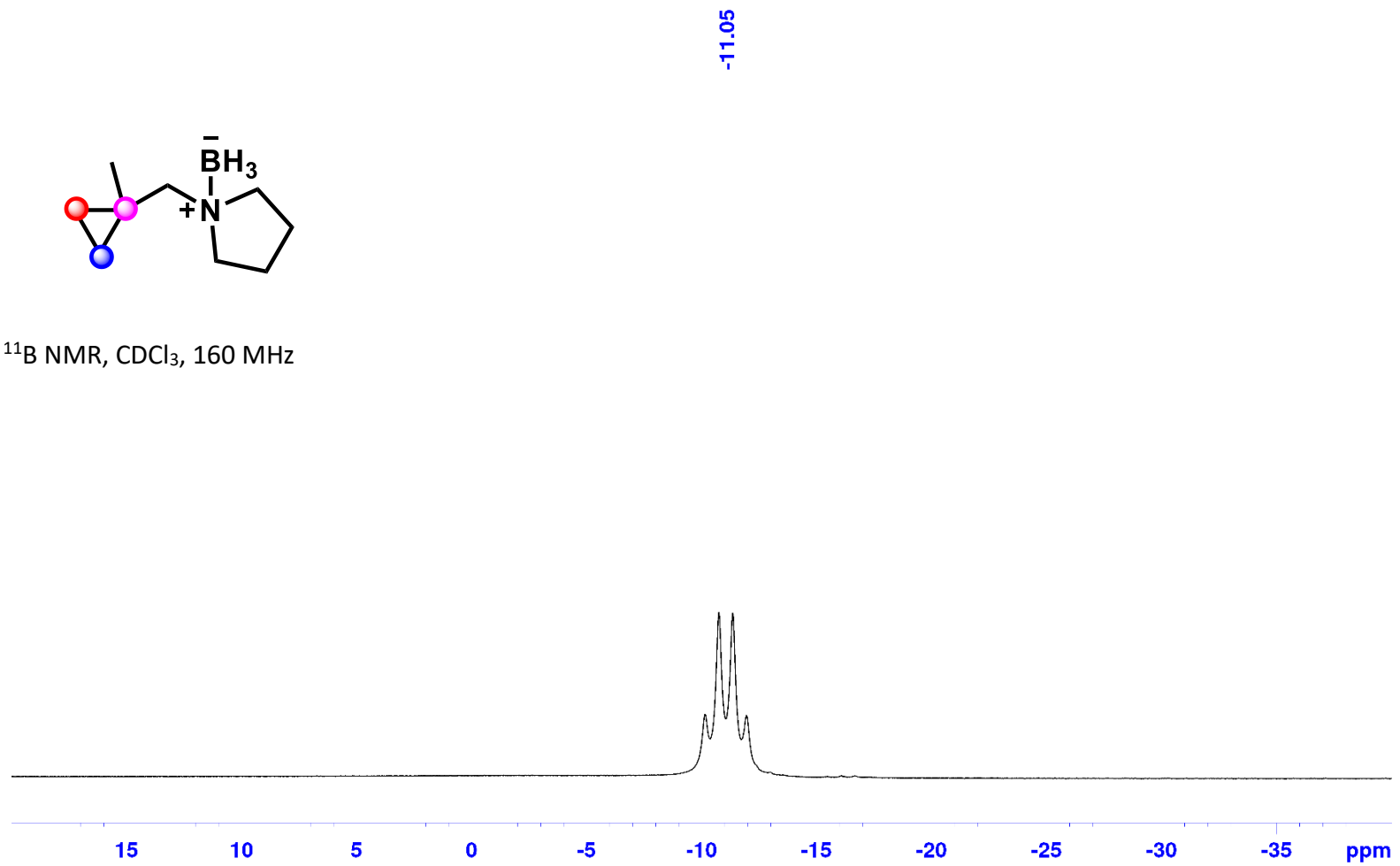
^{13}C NMR, CDCl_3 , 126 MHz



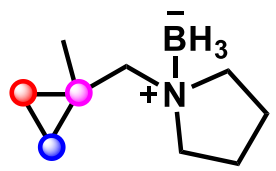
1-((1-Methylcyclopropyl)methyl)pyrrolidine Borane (1y):



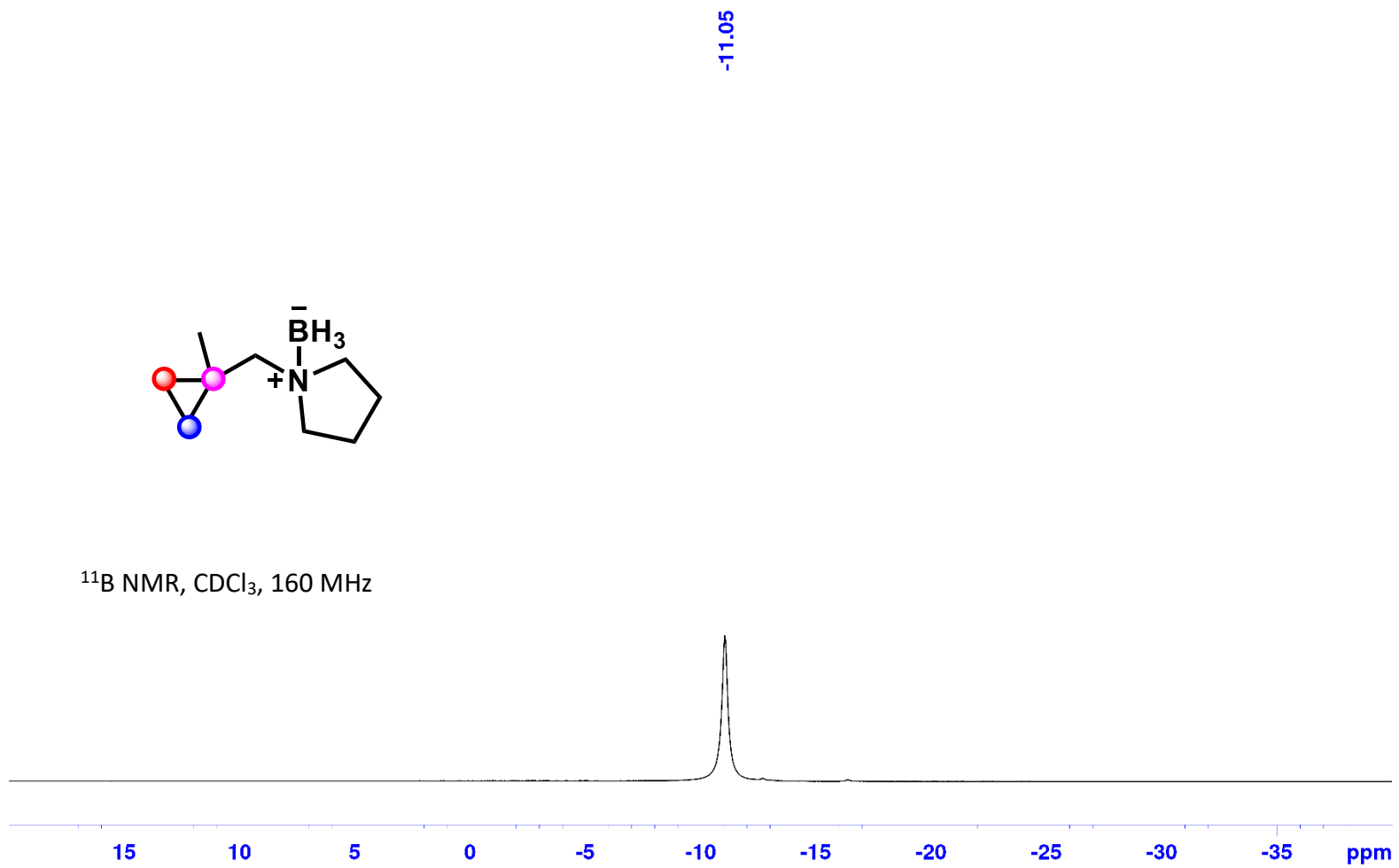
^{11}B NMR, CDCl_3 , 160 MHz



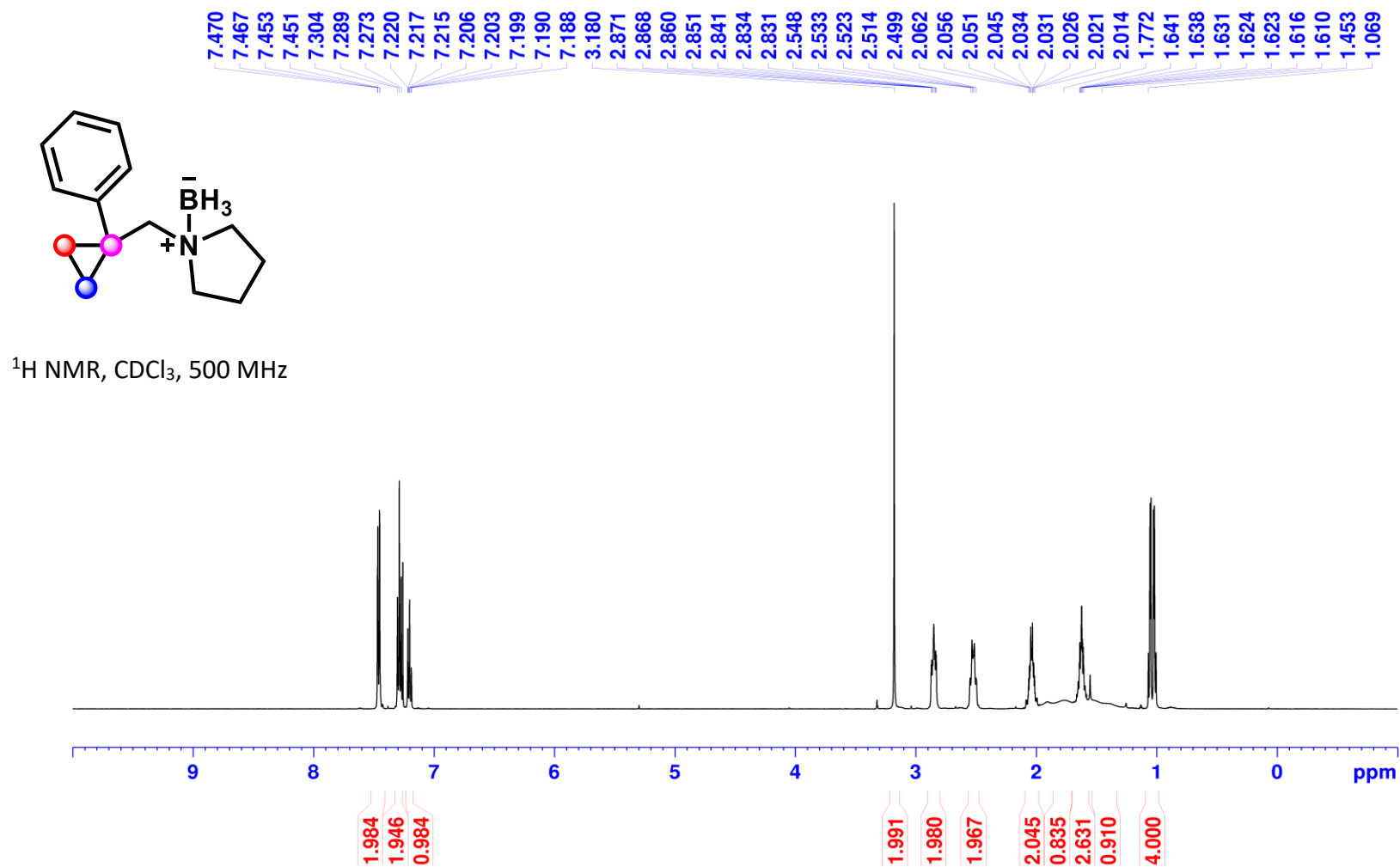
1-((1-Methylcyclopropyl)methyl)pyrrolidine Borane (1y):



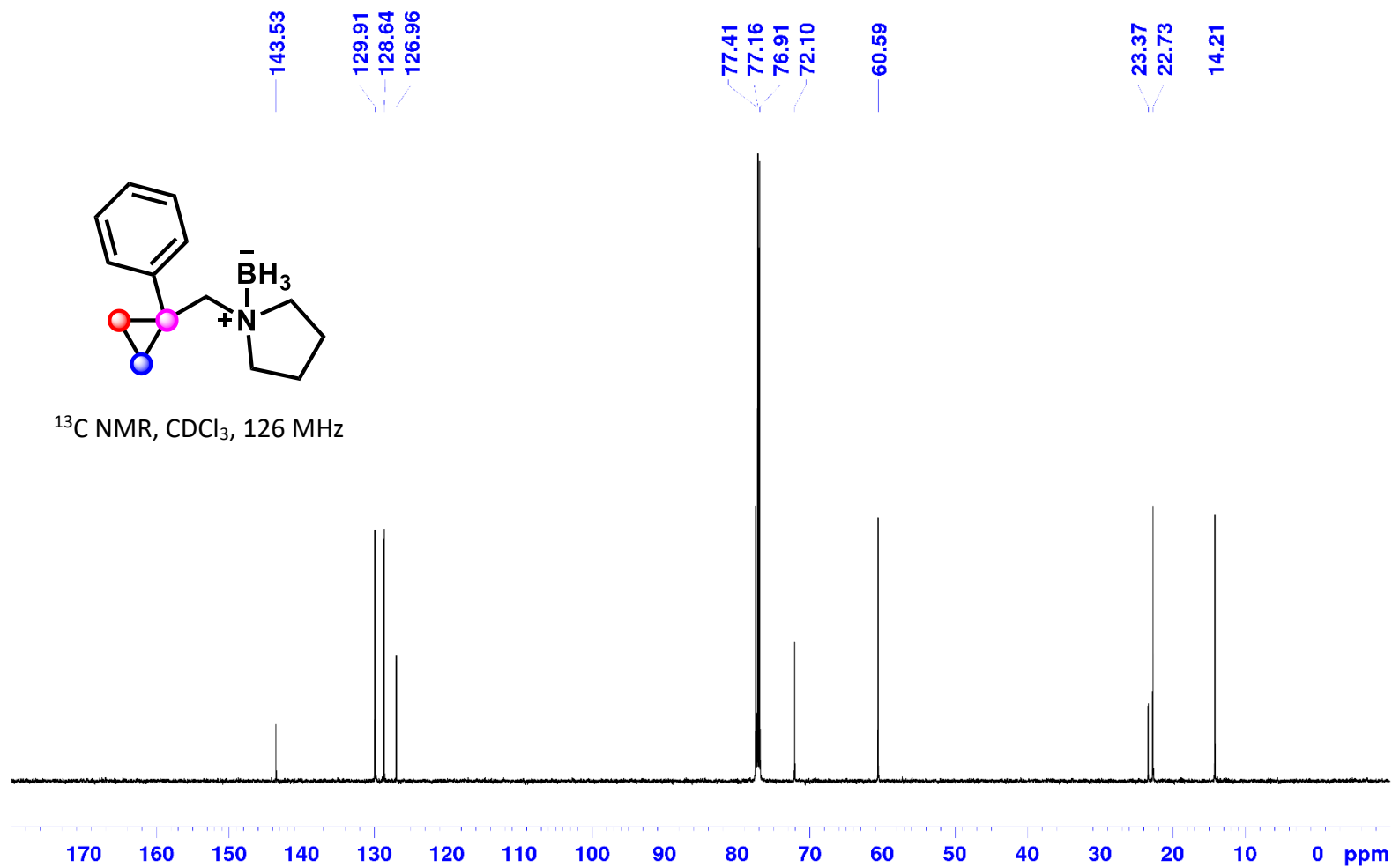
^{11}B NMR, CDCl_3 , 160 MHz



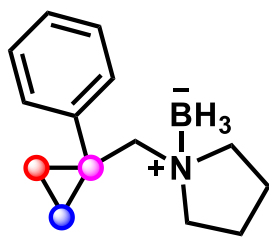
1-((1-Phenylcyclopropyl)methyl)pyrrolidine Borane (1z):



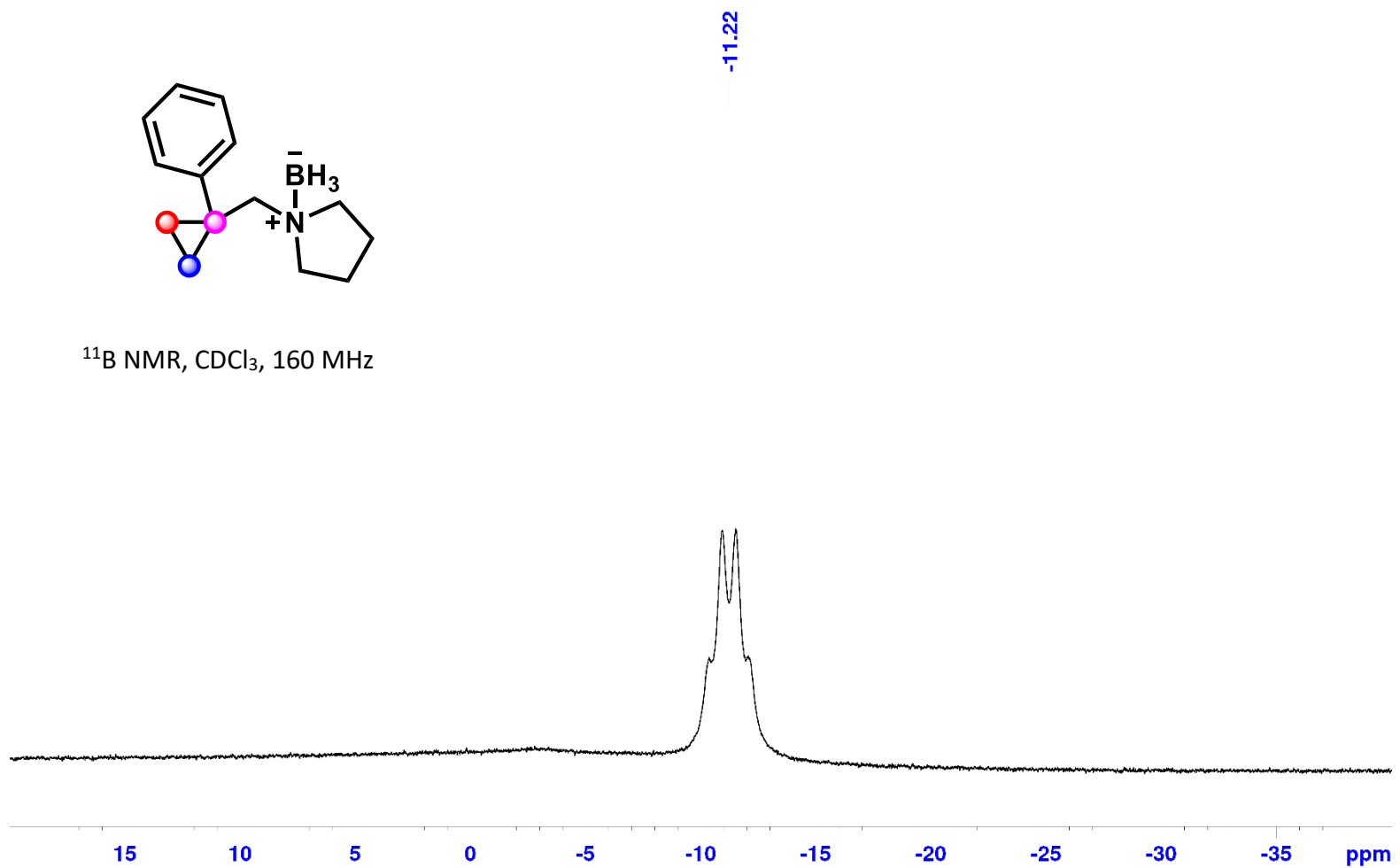
1-((1-Phenylcyclopropyl)methyl)pyrrolidine Borane (1z):



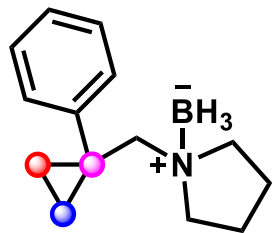
1-((1-Phenylcyclopropyl)methyl)pyrrolidine Borane (1z):



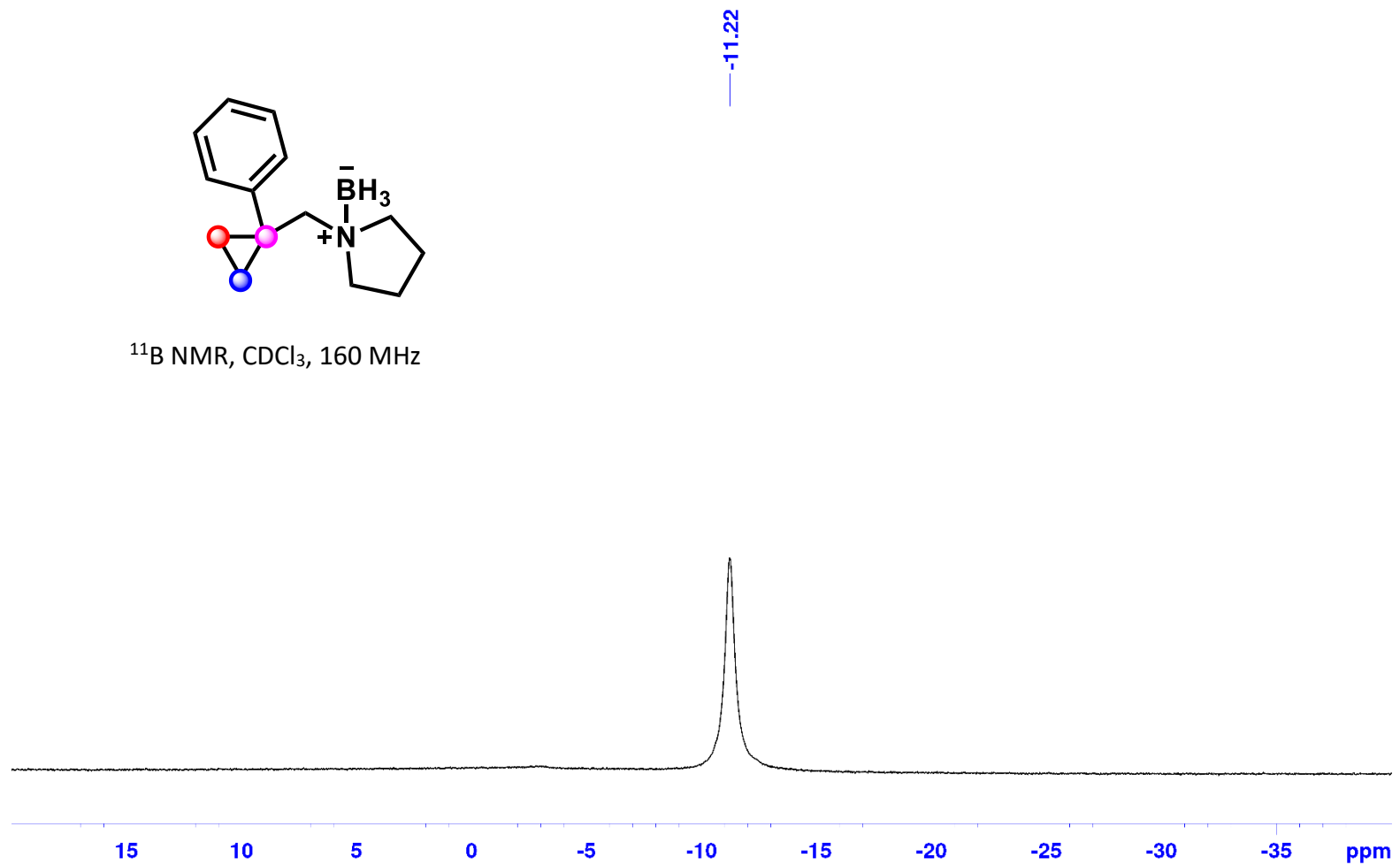
^{11}B NMR, CDCl_3 , 160 MHz



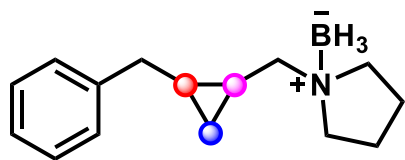
1-((1-Phenylcyclopropyl)methyl)pyrrolidine Borane (1z):



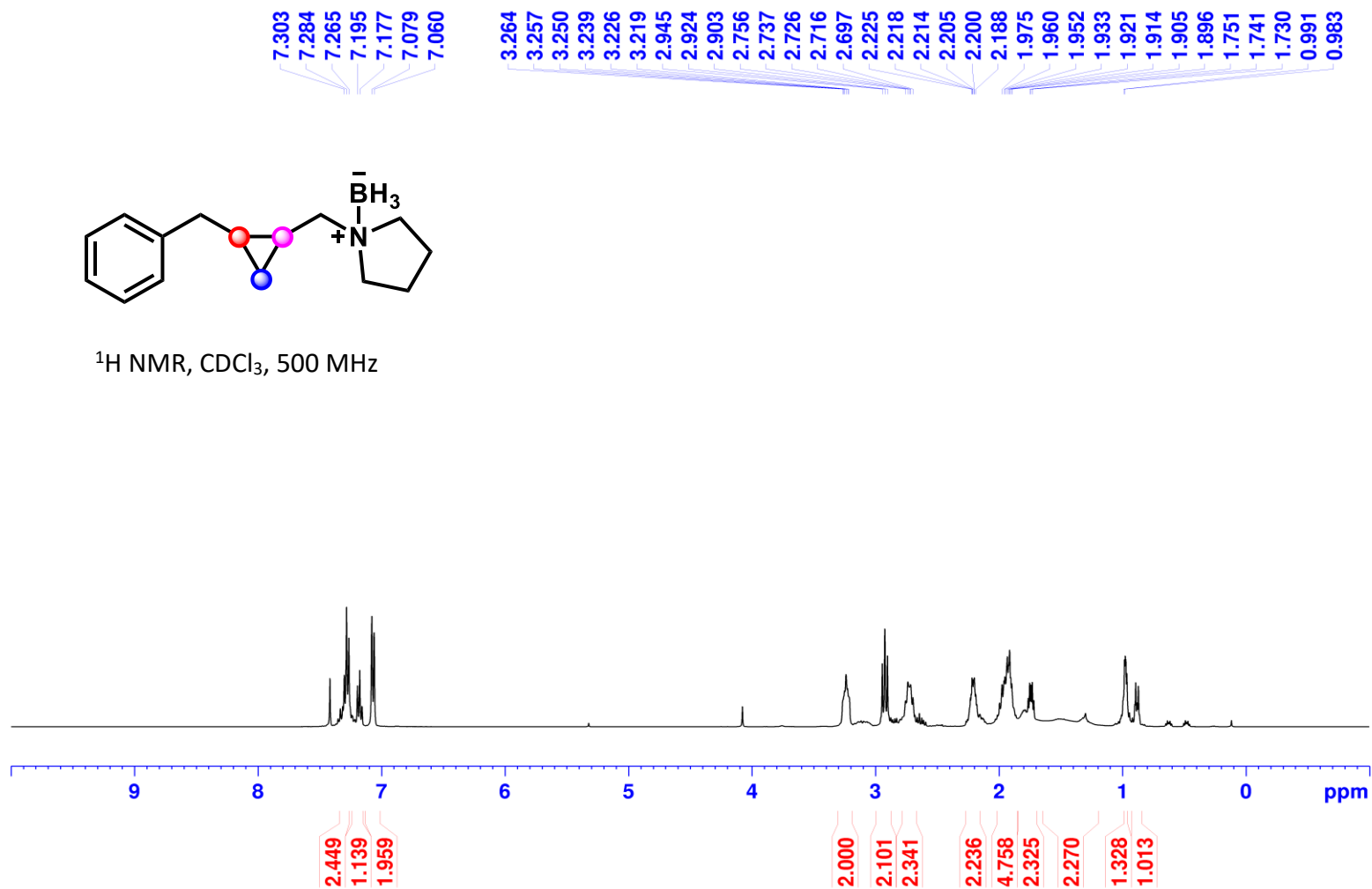
^{11}B NMR, CDCl_3 , 160 MHz



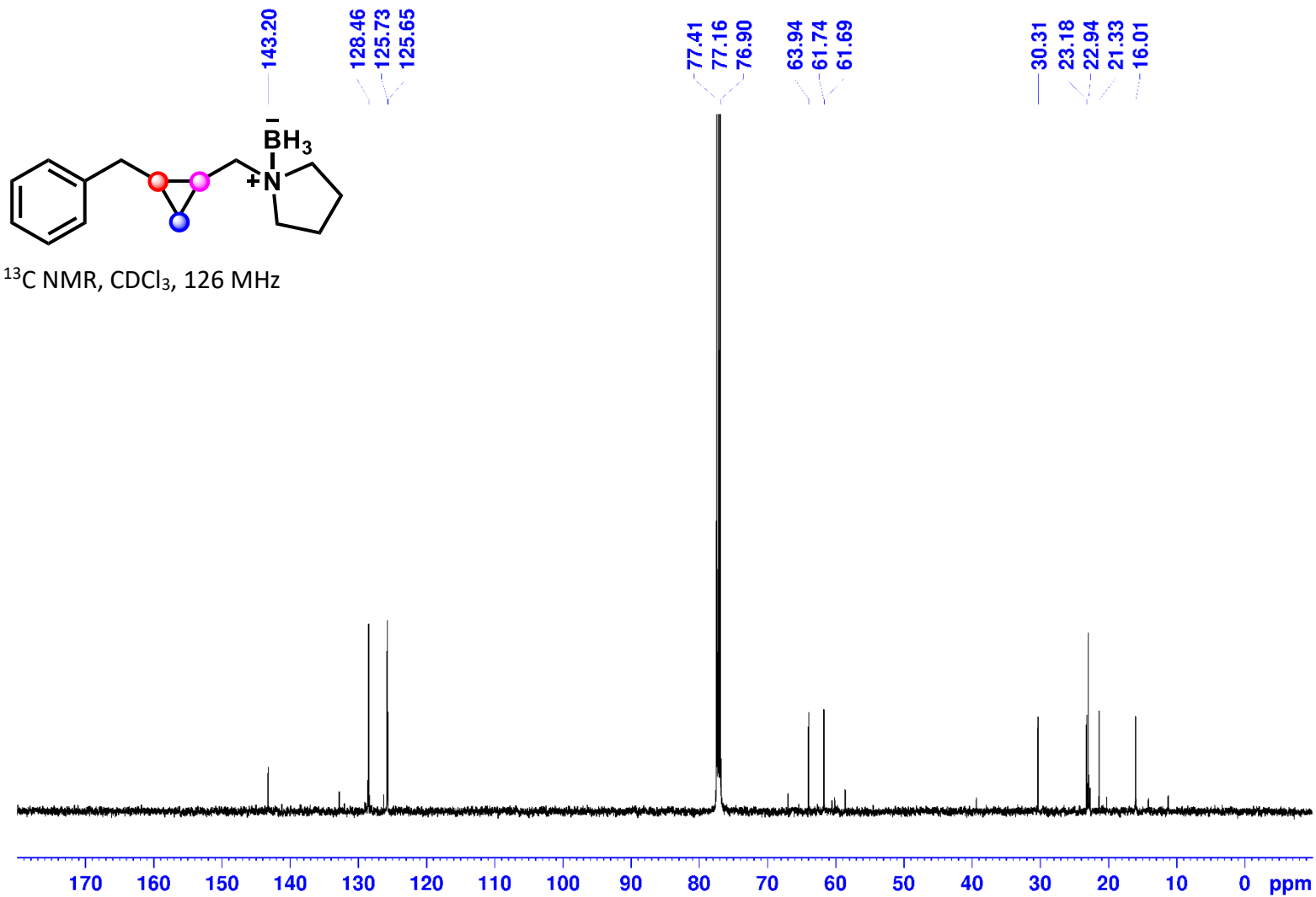
1-((2-Benzylcyclopropyl)methyl)pyrrolidine Borane (1aa):



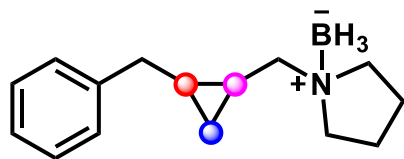
^1H NMR, CDCl_3 , 500 MHz



1-((2-Benzylcyclopropyl)methyl)pyrrolidine Borane (1a):

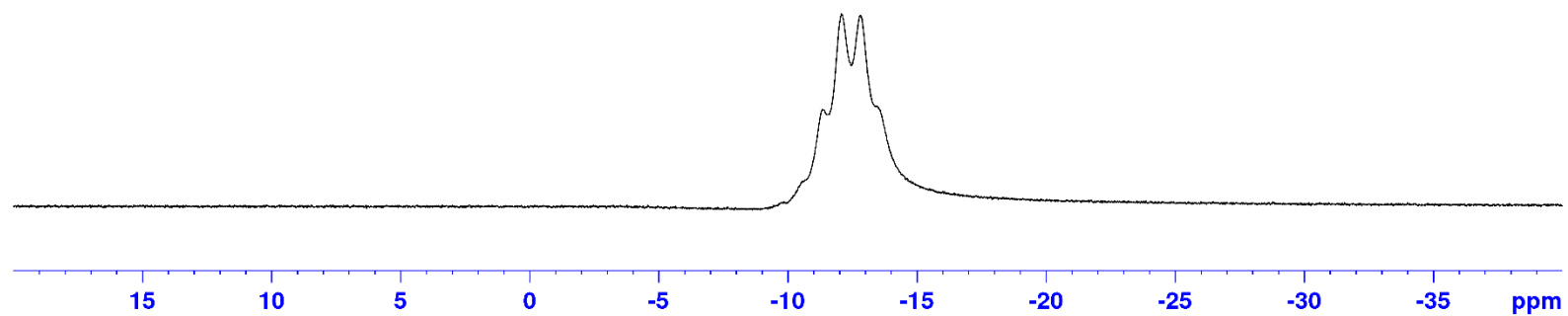


1-((2-Benzylcyclopropyl)methyl)pyrrolidine Borane (1aa):

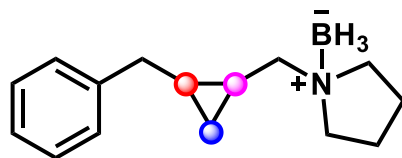


-12.39

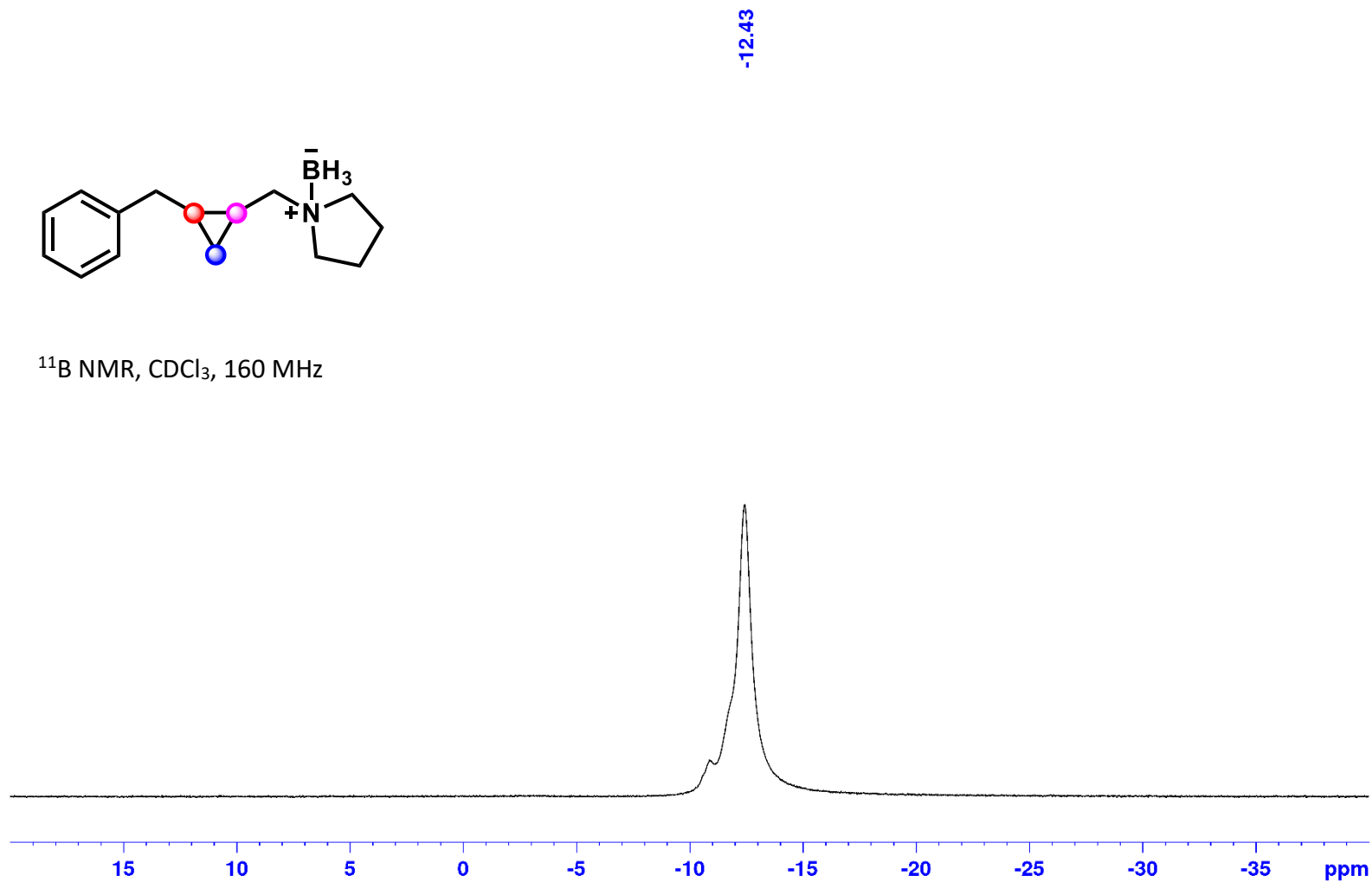
^{11}B NMR, CDCl_3 , 160 MHz



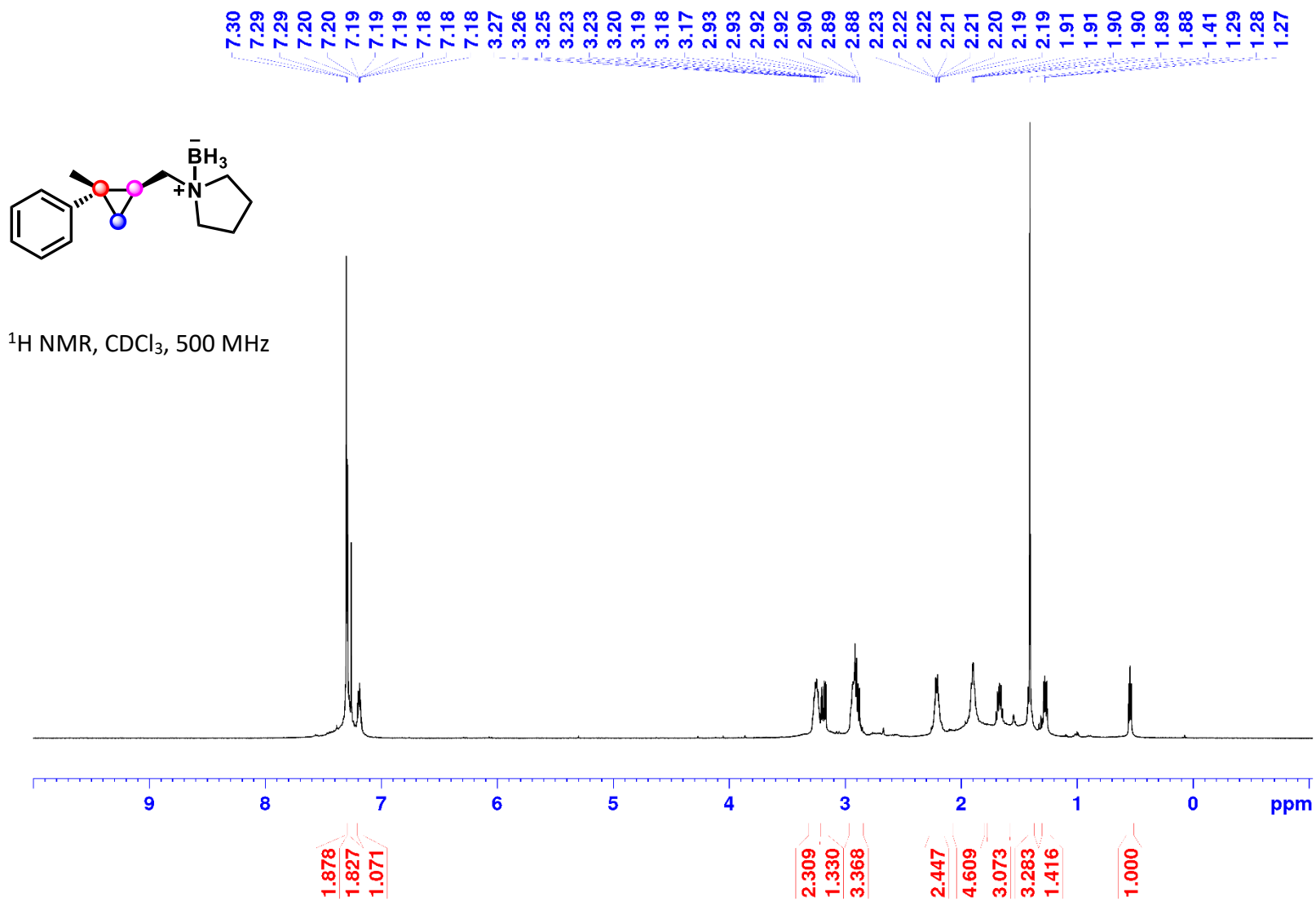
1-((2-Benzylcyclopropyl)methyl)pyrrolidine Borane (1aa):



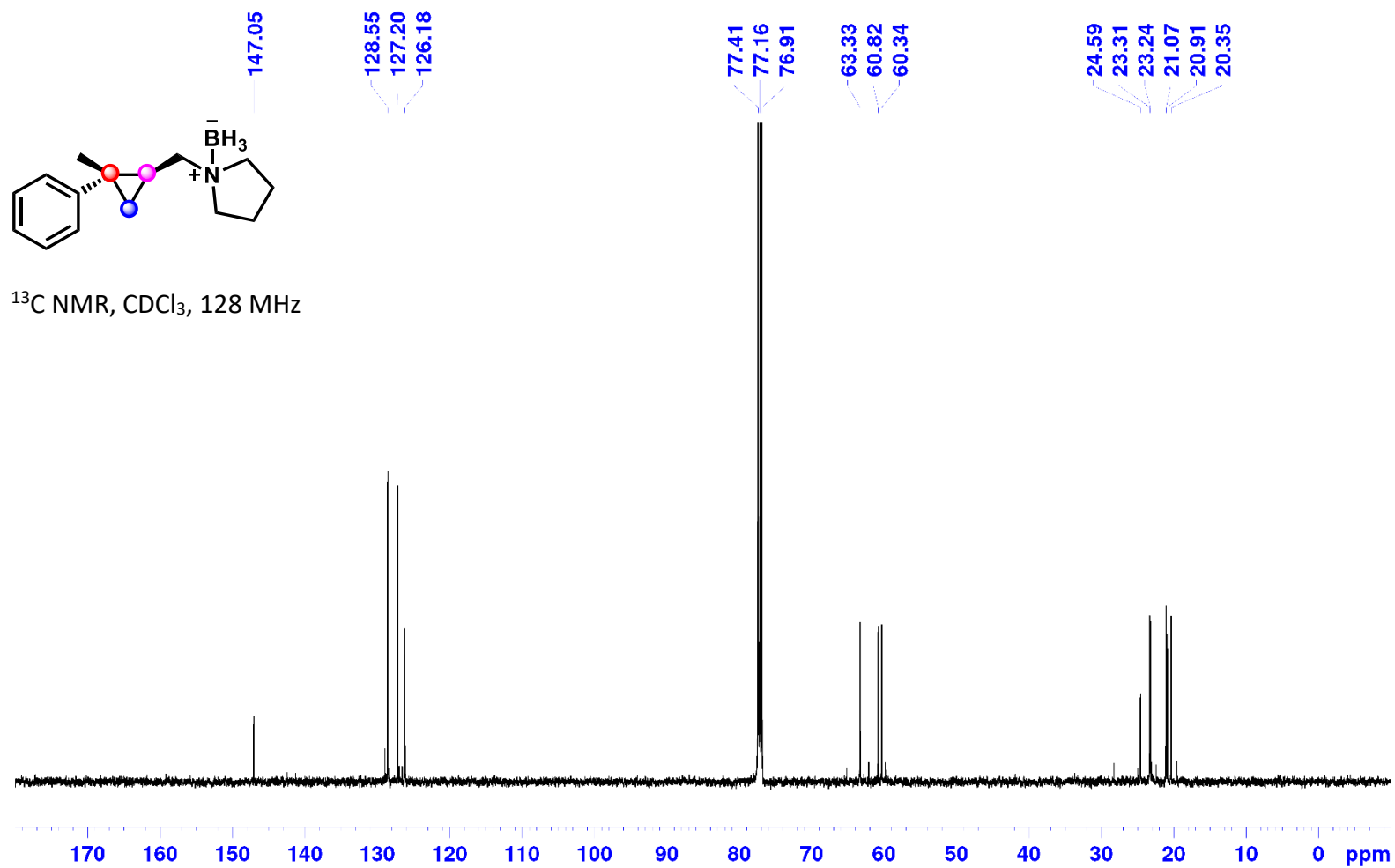
^{11}B NMR, CDCl_3 , 160 MHz



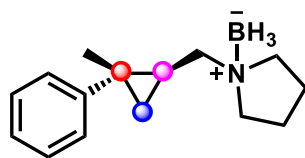
1-(((1S,2S)-2-Methyl-2-phenylcyclopropyl)methyl)pyrrolidine borane (1ab):



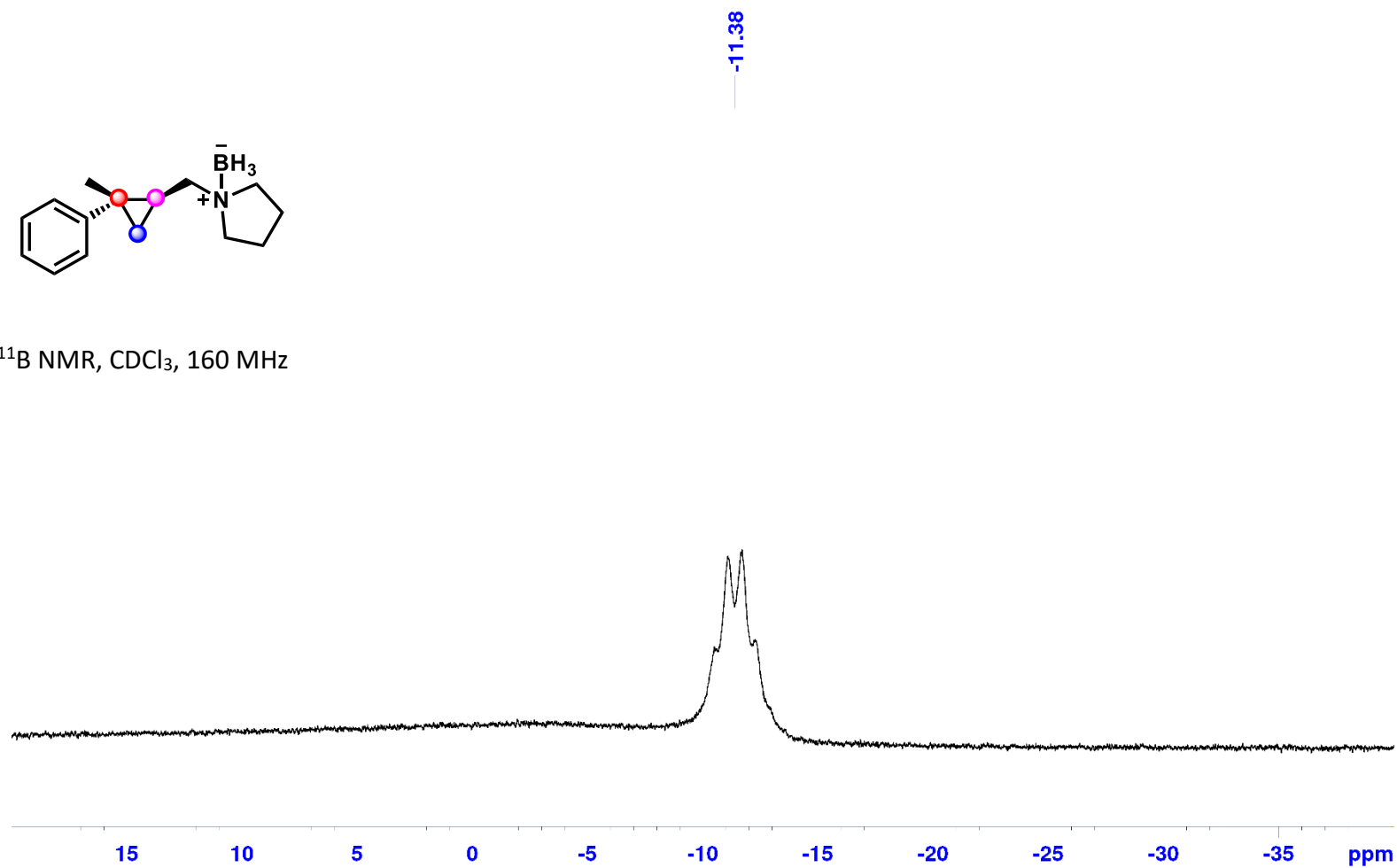
1-(((1*S*,2*S*)-2-Methyl-2-phenylcyclopropyl)methyl)pyrrolidine Borane (**1ab**):



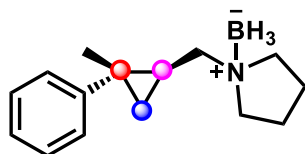
1-(((1S,2S)-2-Methyl-2-phenylcyclopropyl)methyl)pyrrolidine Borane (1ab):



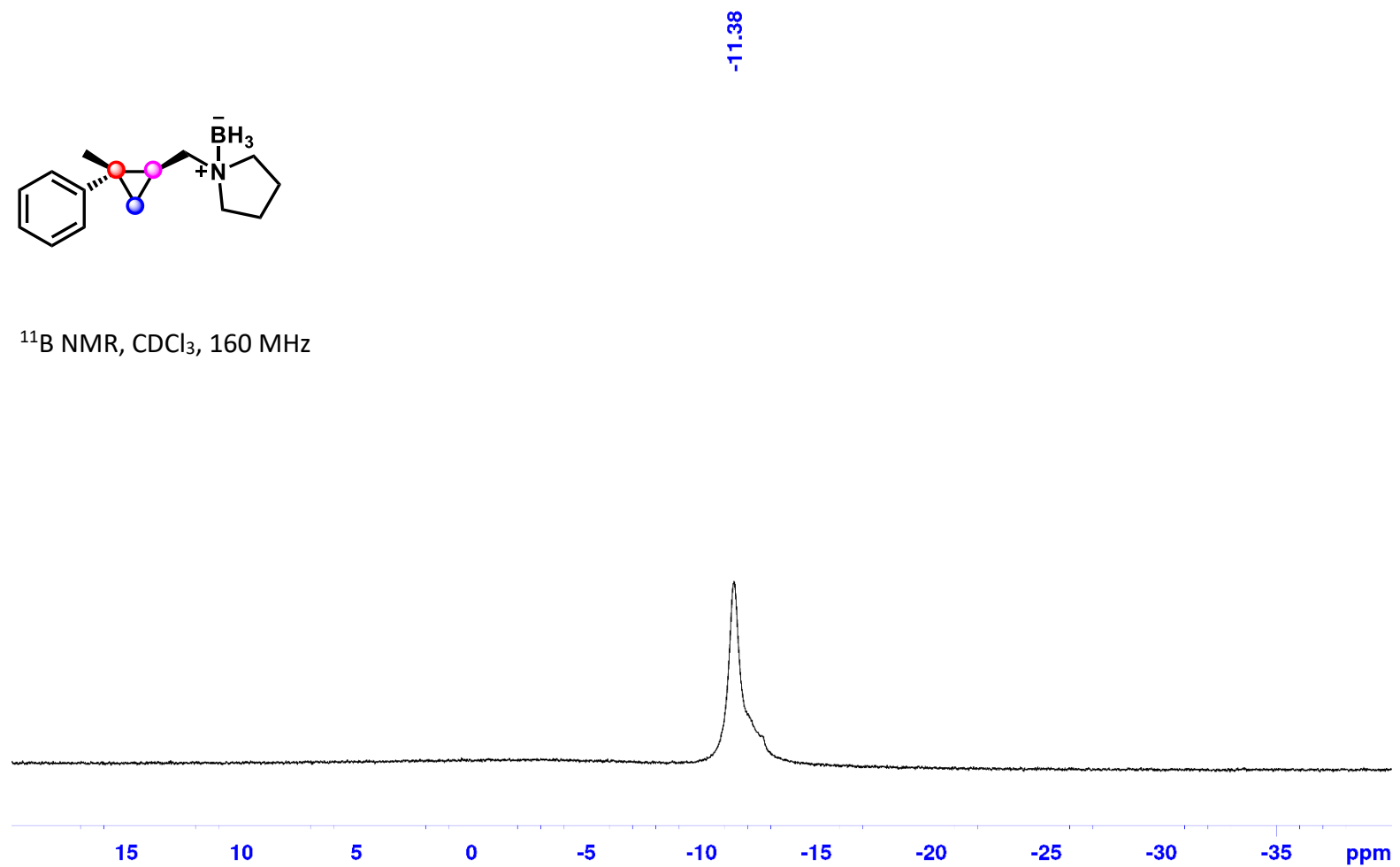
^{11}B NMR, CDCl_3 , 160 MHz



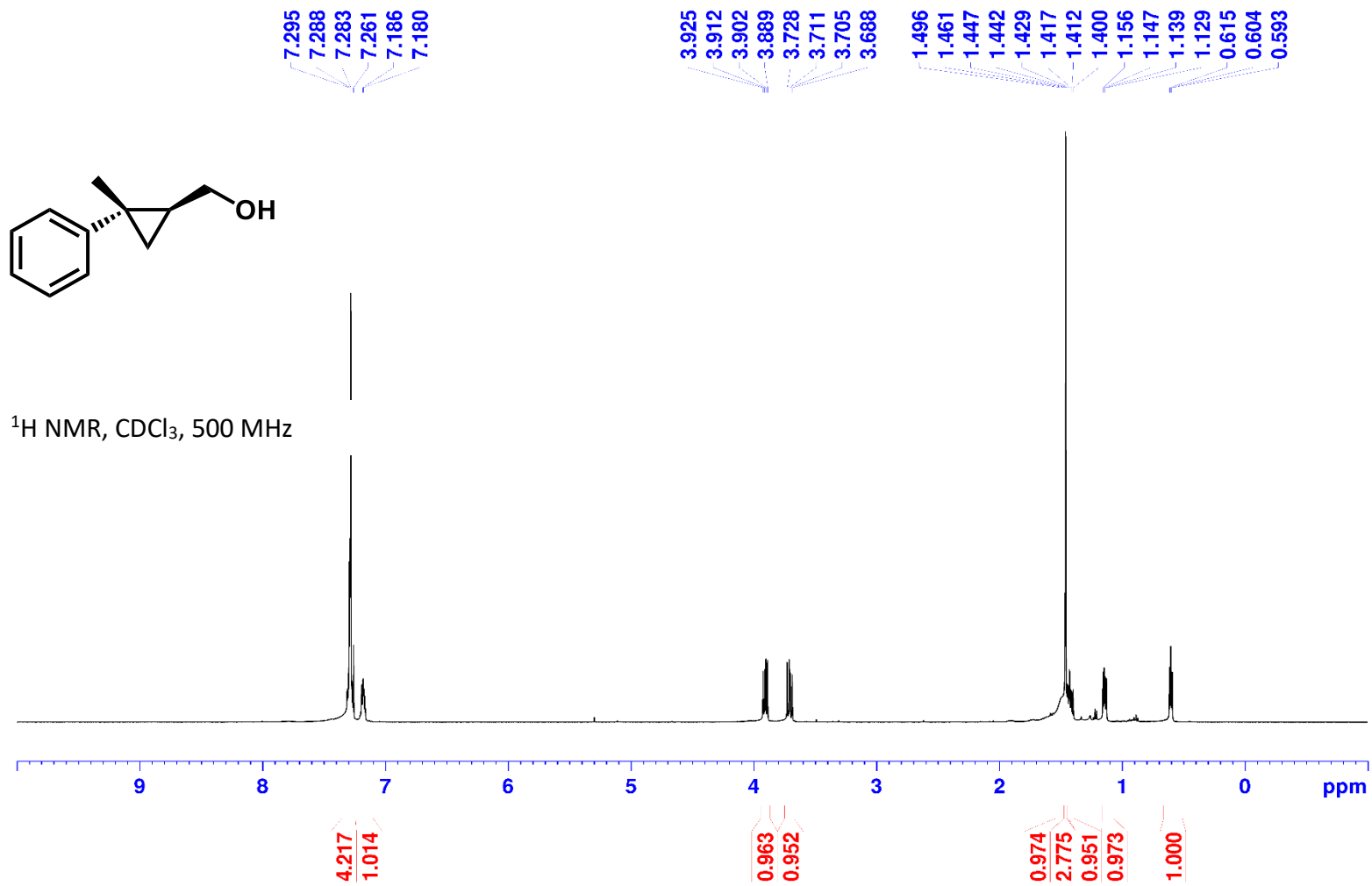
1-(((1S,2S)-2-Methyl-2-phenylcyclopropyl)methyl)pyrrolidine Borane (**1ab**):



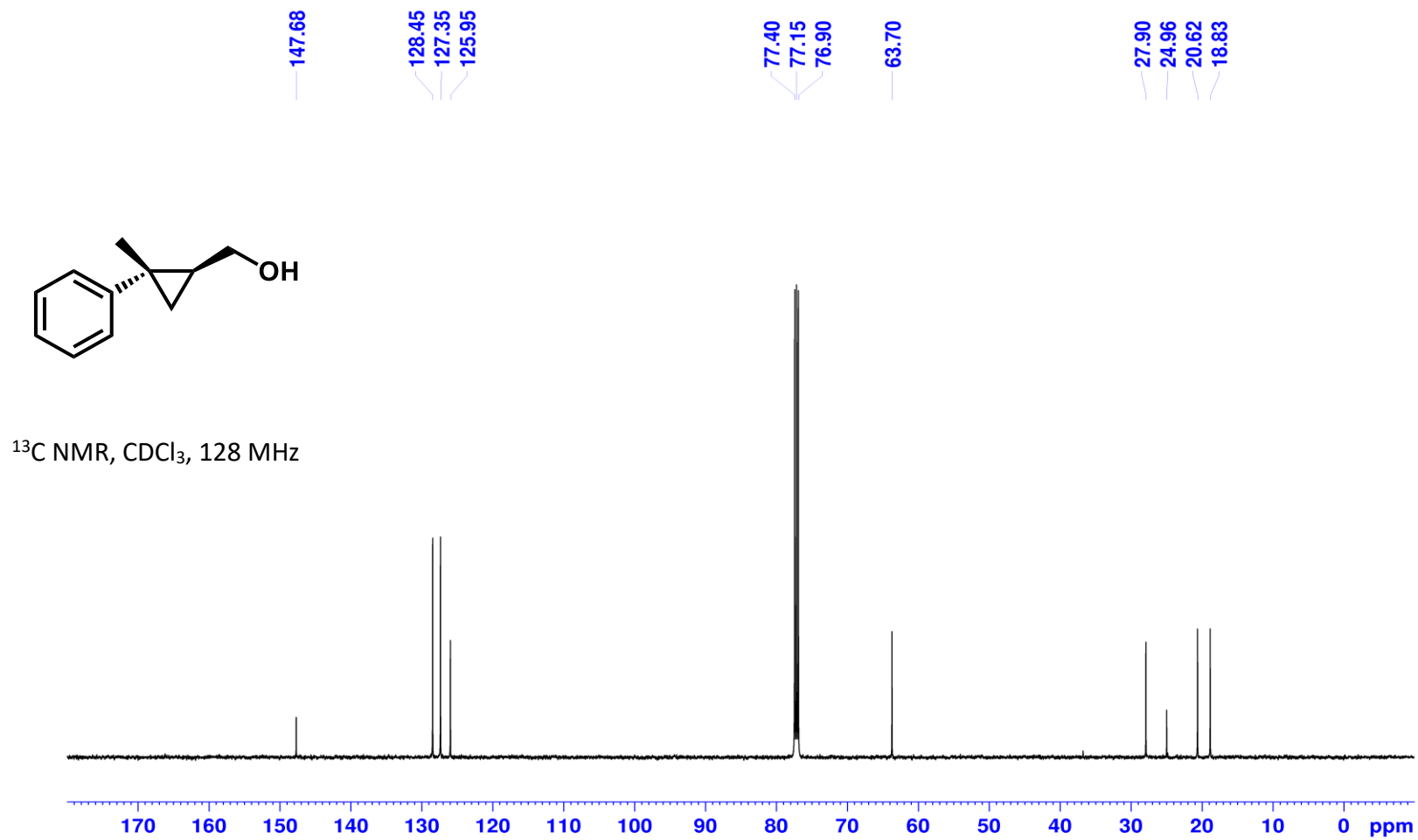
^{11}B NMR, CDCl_3 , 160 MHz



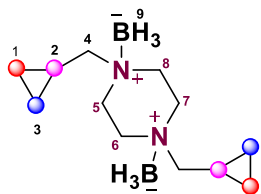
(1*S*,2*S*)-2-Methyl-2-phenylcyclopropylmethanol (S1):



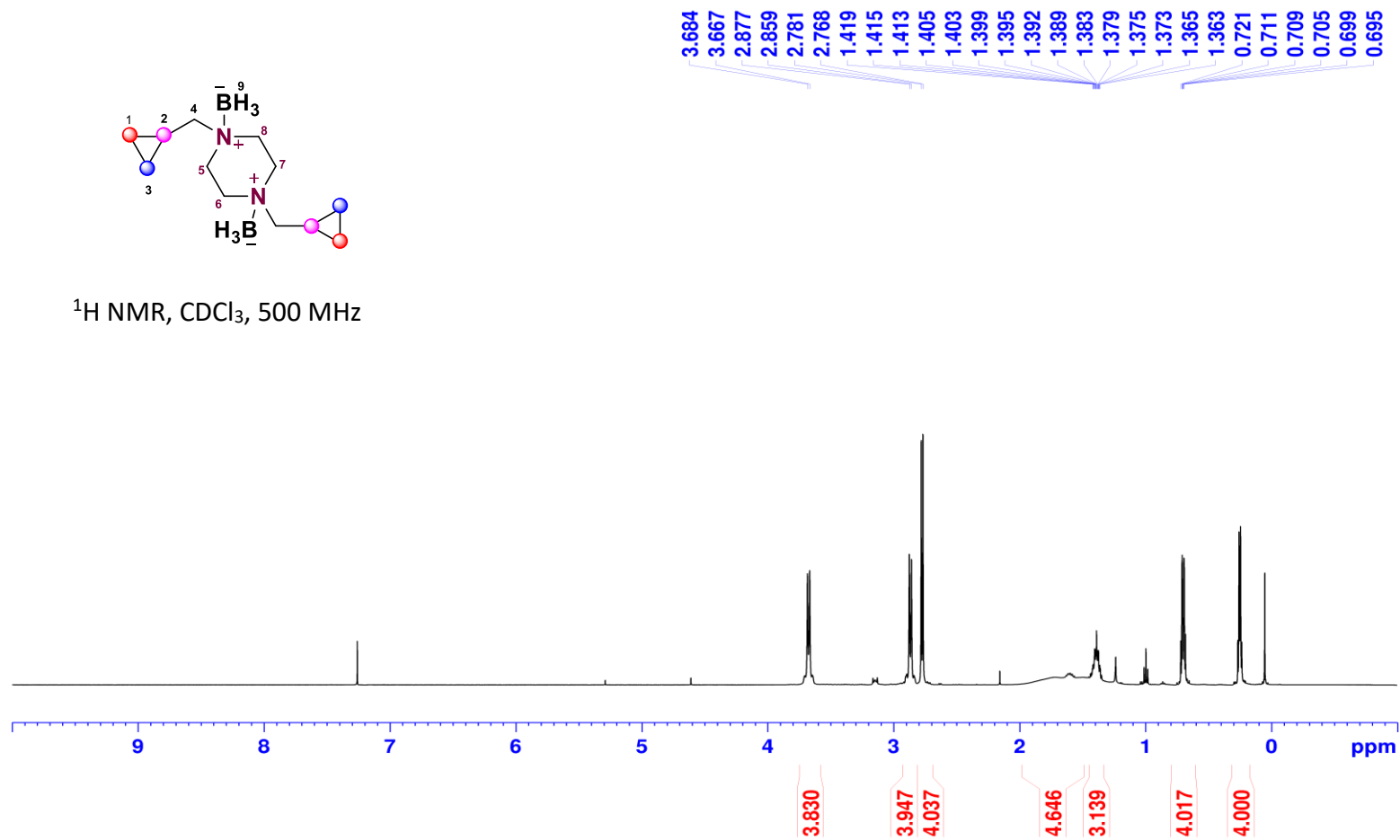
(1*S*,2*S*)-2-Methyl-2-phenylcyclopropylmethanol (S1):



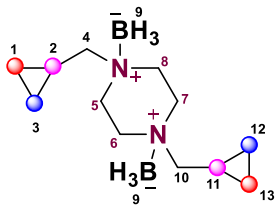
1,4-bis(cyclopropylmethyl)piperazine borane (1ac):



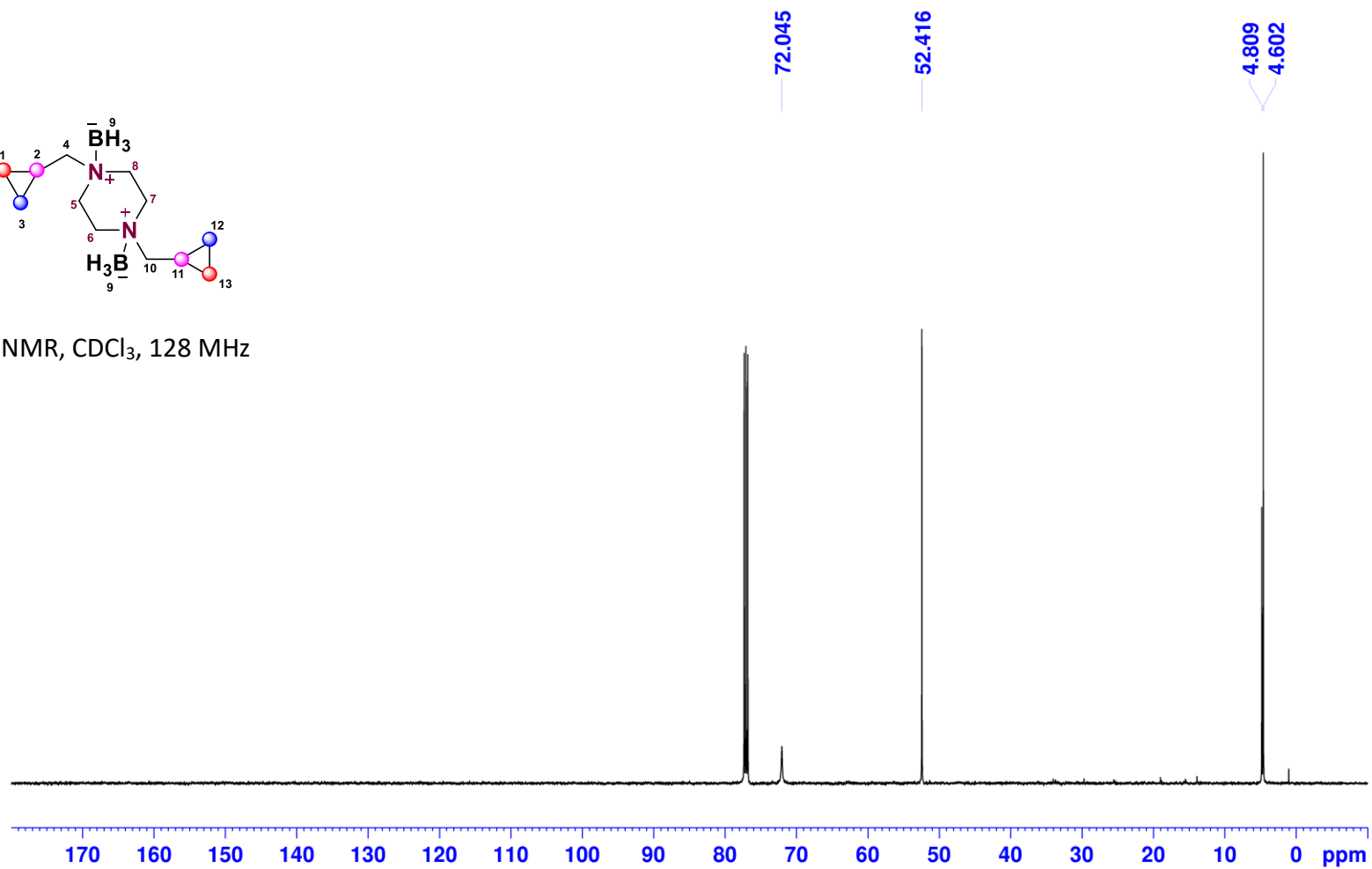
^1H NMR, CDCl_3 , 500 MHz



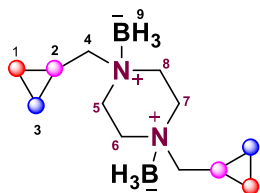
1,4-bis(cyclopropylmethyl)piperazine borane (1ac):



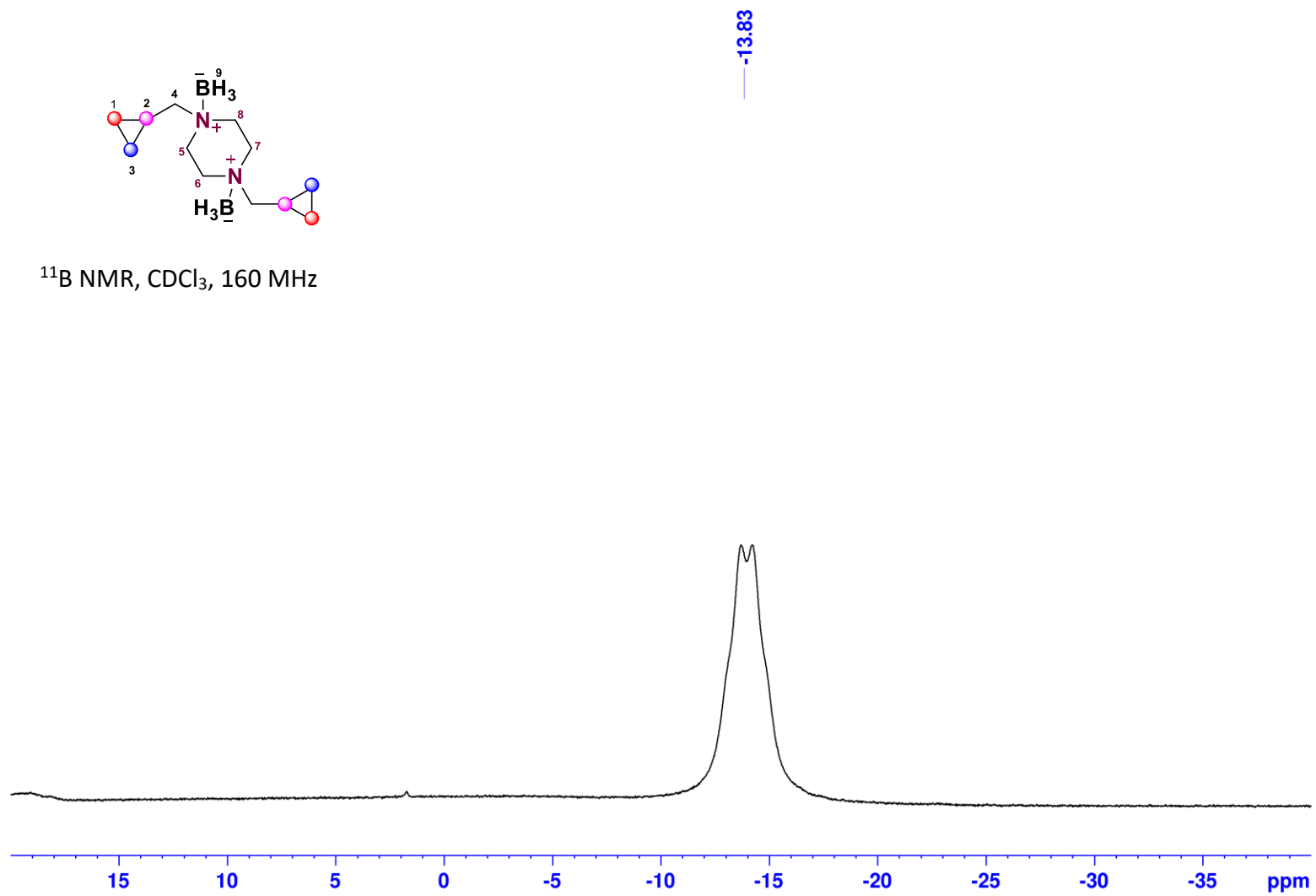
^{13}C NMR, CDCl_3 , 128 MHz



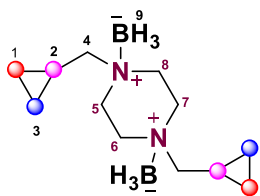
1,4-bis(cyclopropylmethyl)piperazine borane (1ac):



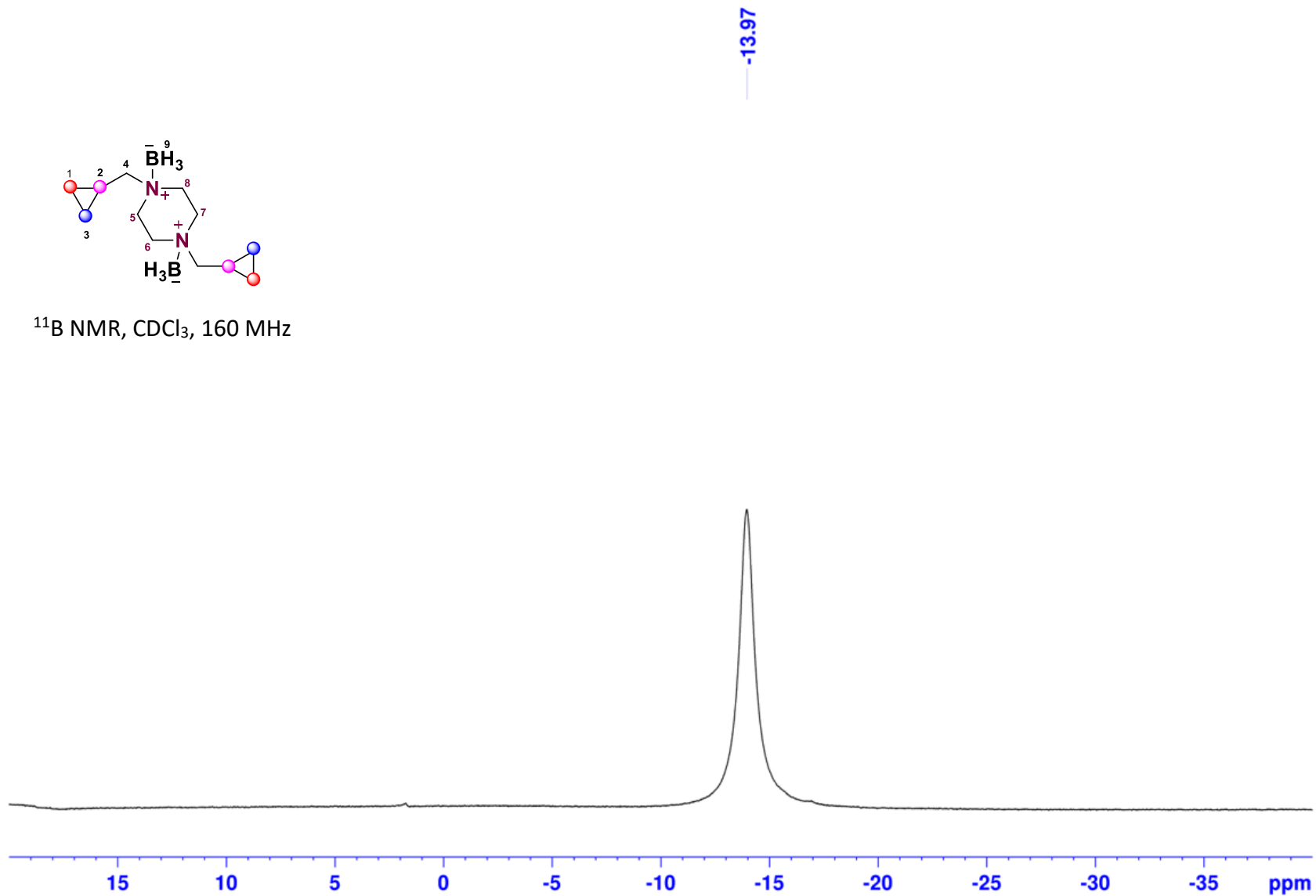
^{11}B NMR, CDCl_3 , 160 MHz



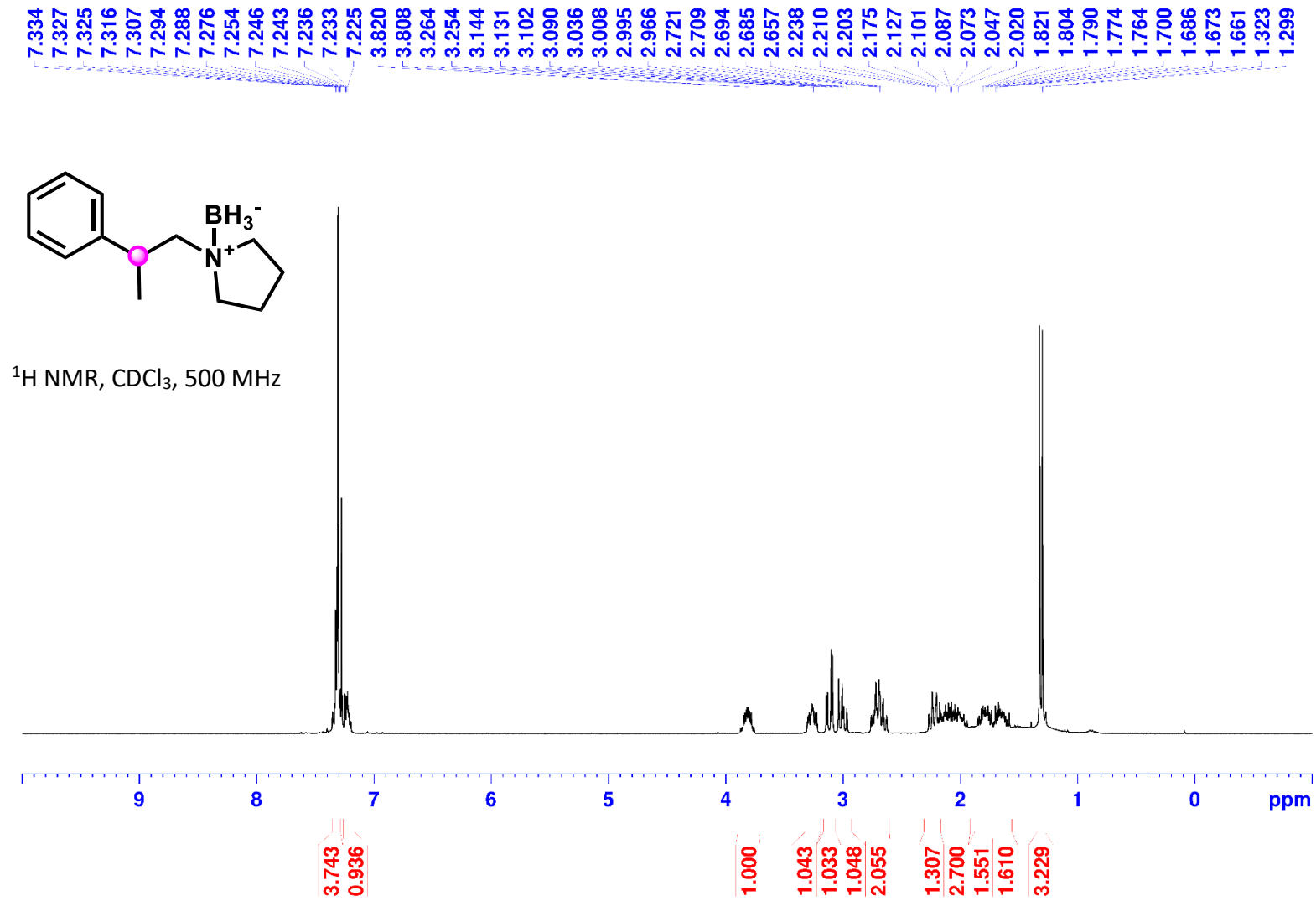
1,4-bis(cyclopropylmethyl)piperazine borane (1ac):



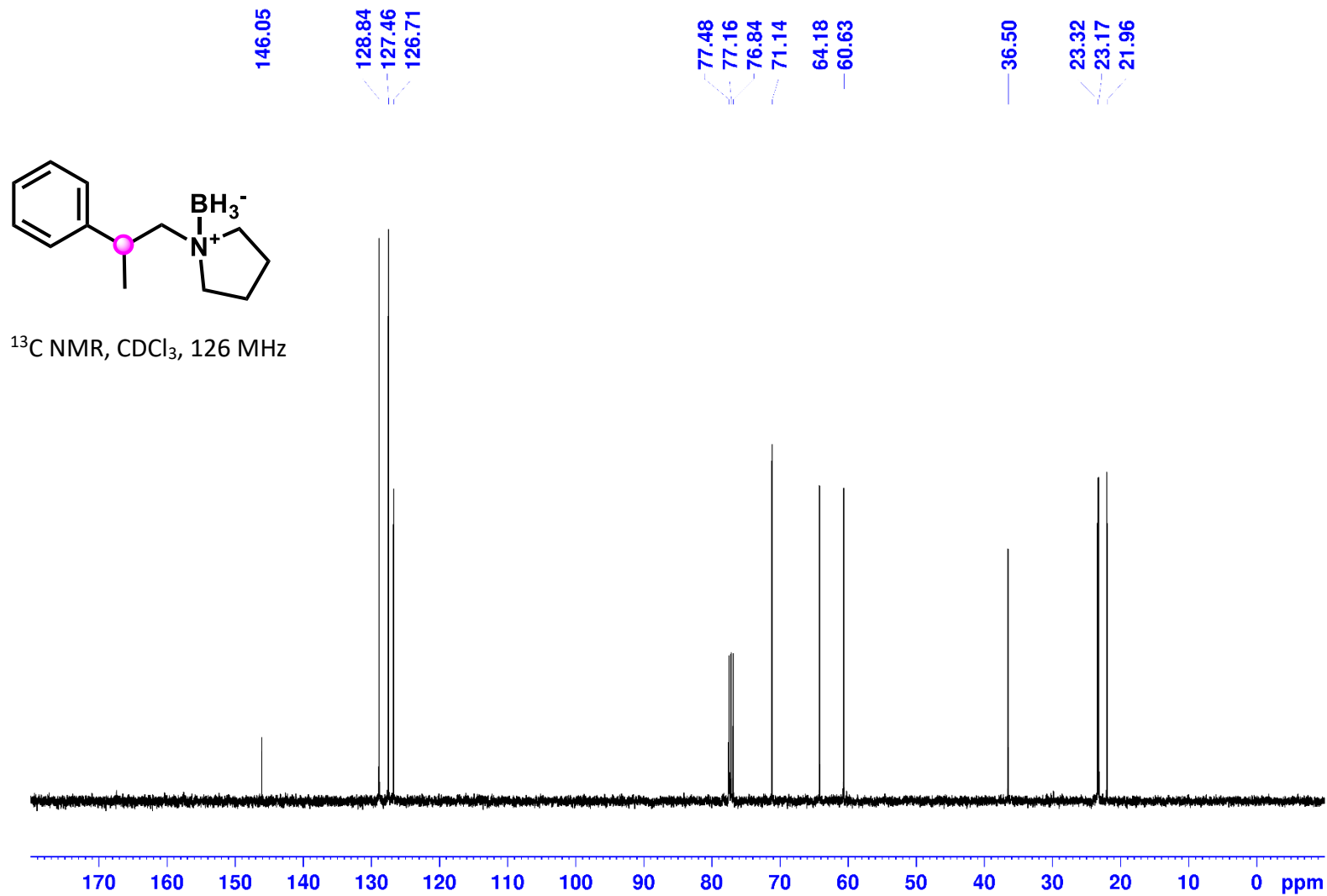
¹¹B NMR, CDCl₃, 160 MHz



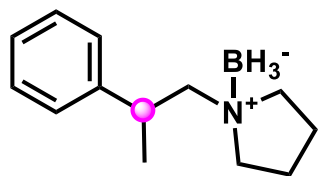
1-(2-Phenylpropyl)pyrrolidine Borane (S2):



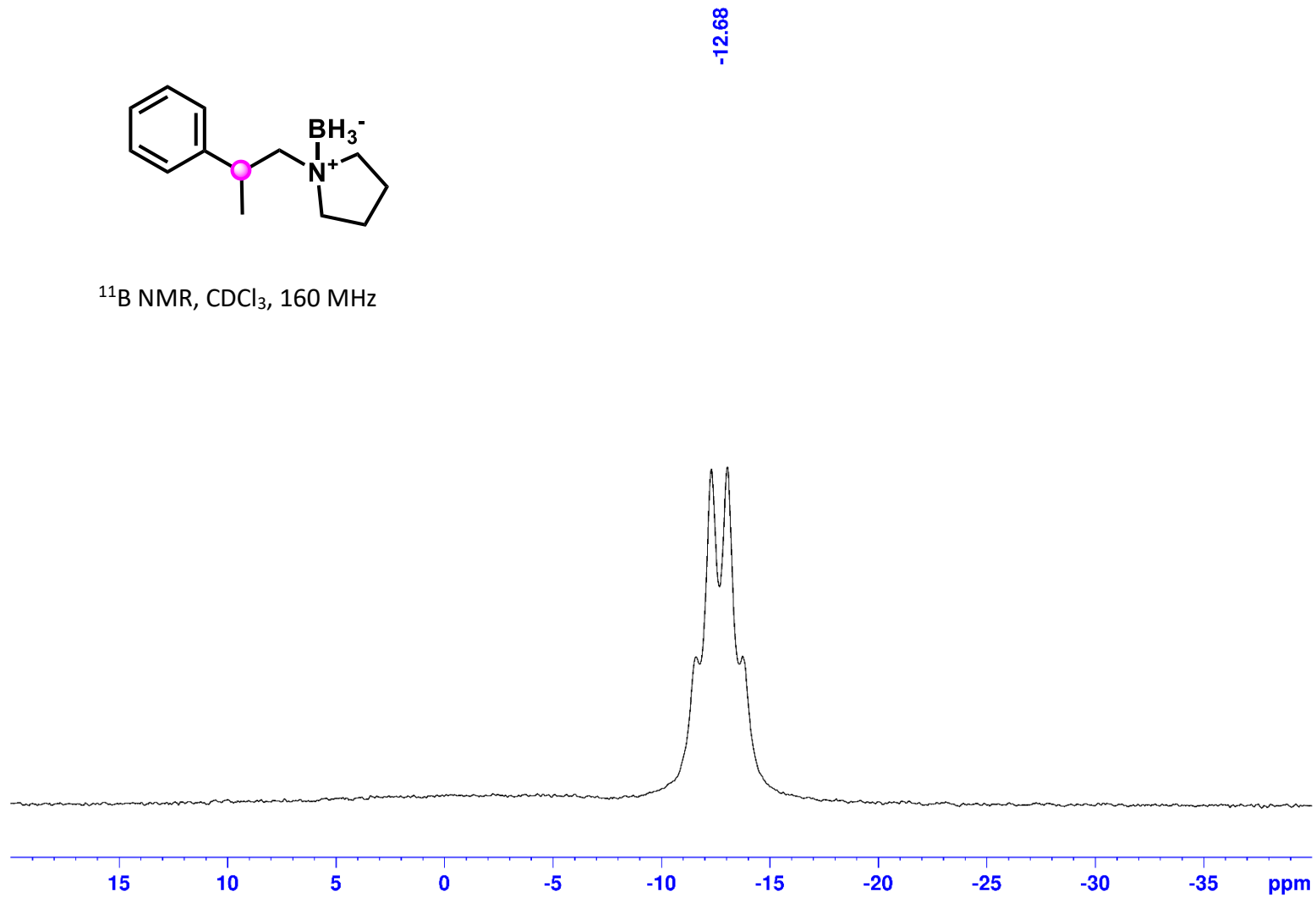
1-(2-Phenylpropyl)pyrrolidine Borane (S2):



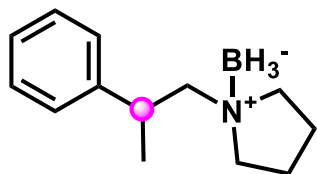
1-(2-Phenylpropyl)pyrrolidine Borane (S2):



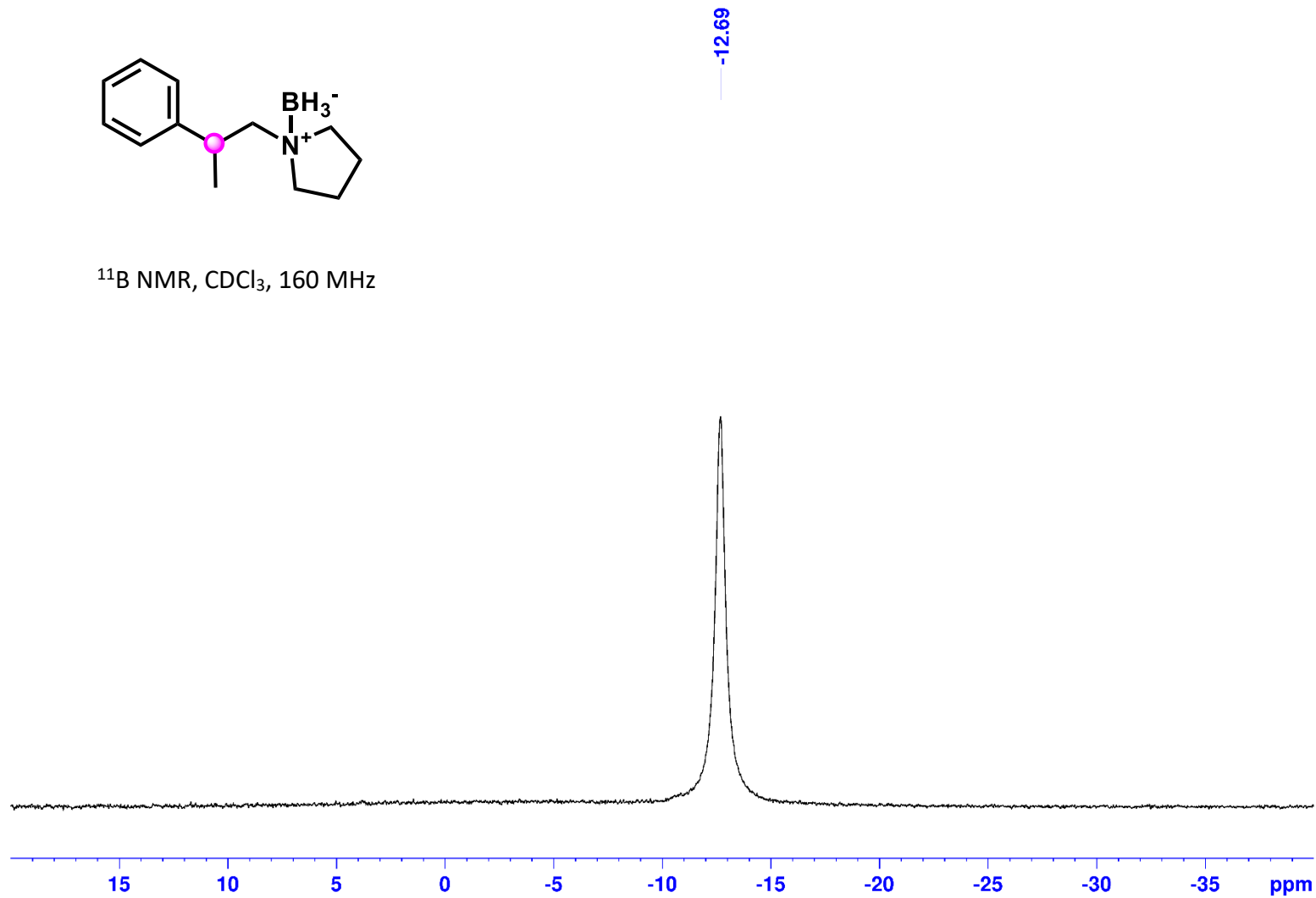
^{11}B NMR, CDCl_3 , 160 MHz



1-(2-Phenylpropyl)pyrrolidine Borane (S2):

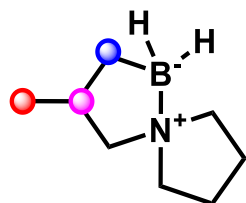


^{11}B NMR, CDCl_3 , 160 MHz

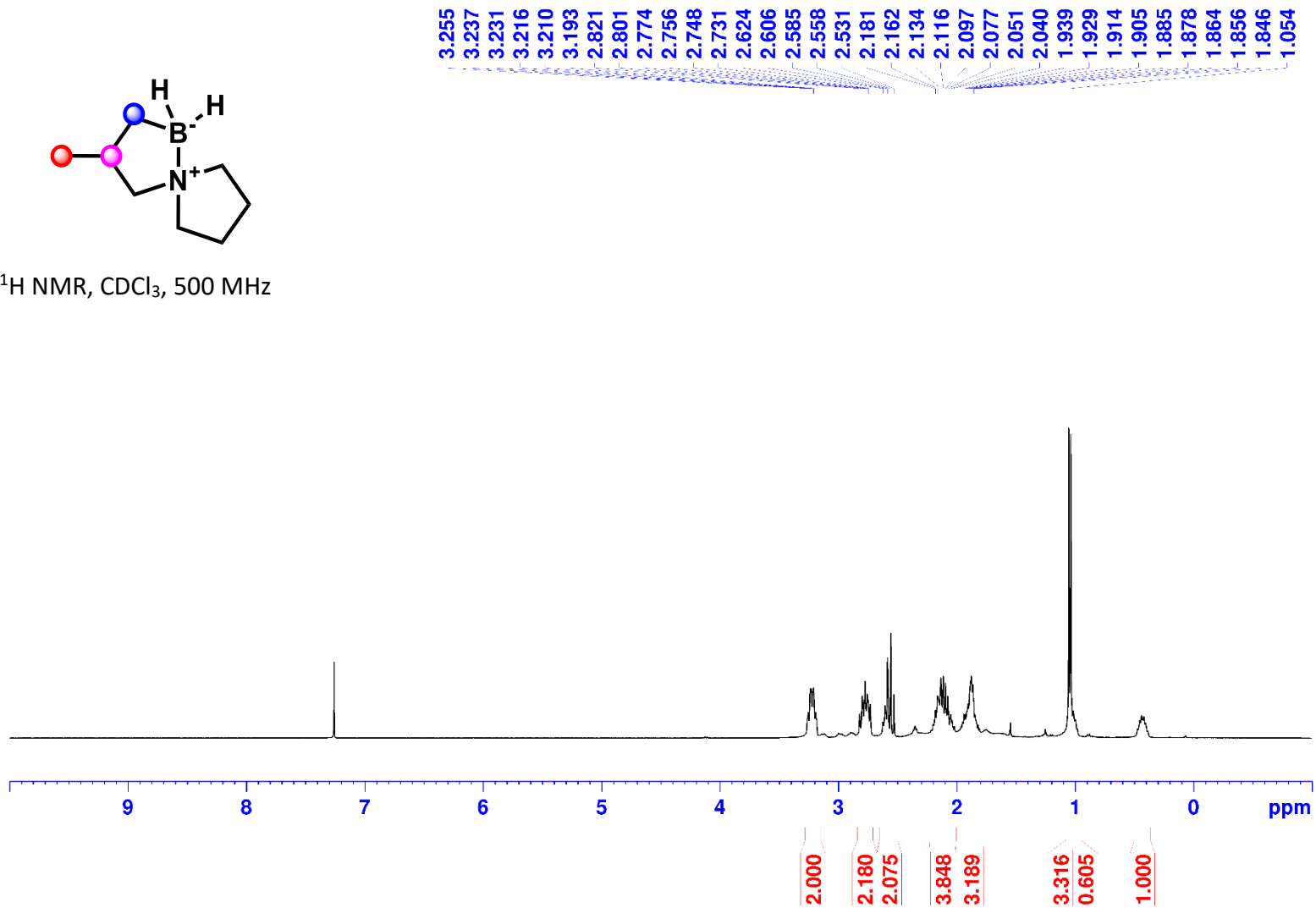


NMR Spectra of SCABs

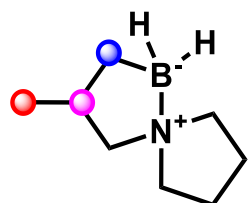
3-Methyl-5-aza-1-borasp[4.4]nonane (2a):



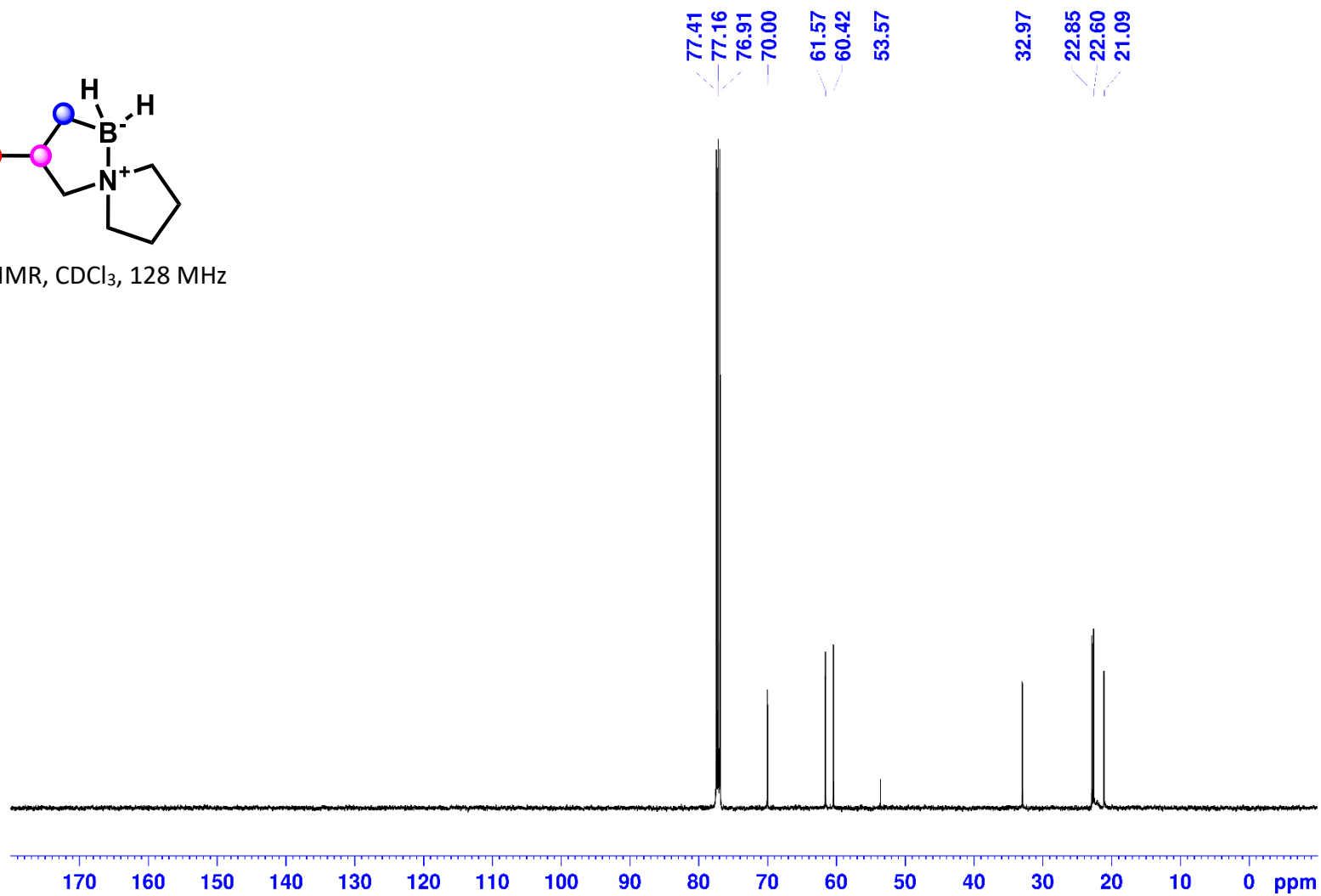
^1H NMR, CDCl_3 , 500 MHz



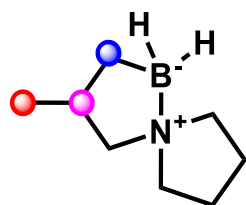
3-Methyl-5-aza-1-borasp[4.4]nonane (2a):



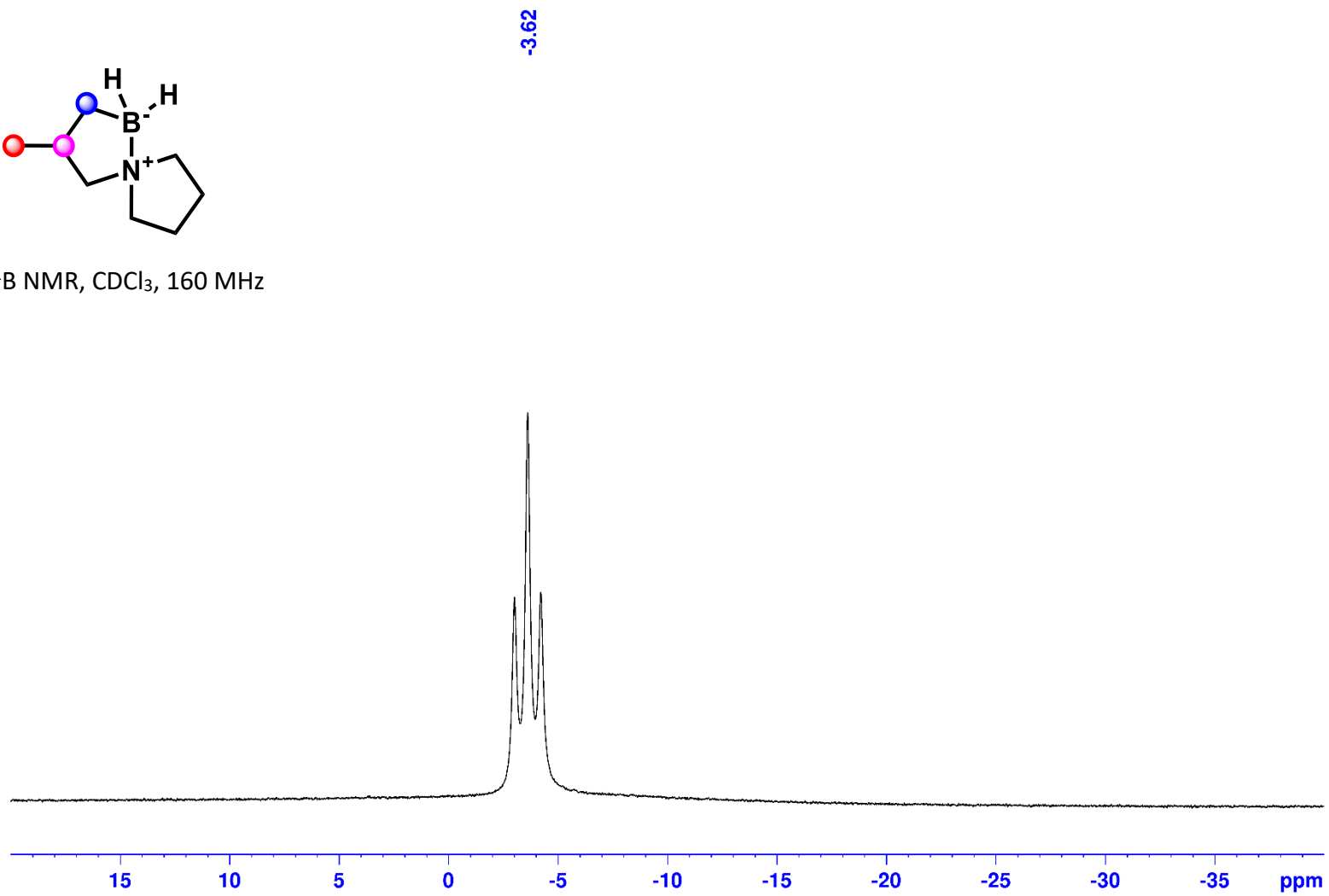
^{13}C NMR, CDCl_3 , 128 MHz



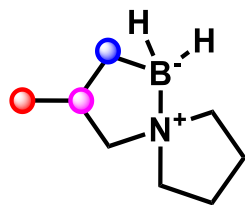
3-Methyl-5-aza-1-borasp[4.4]nonane (2a):



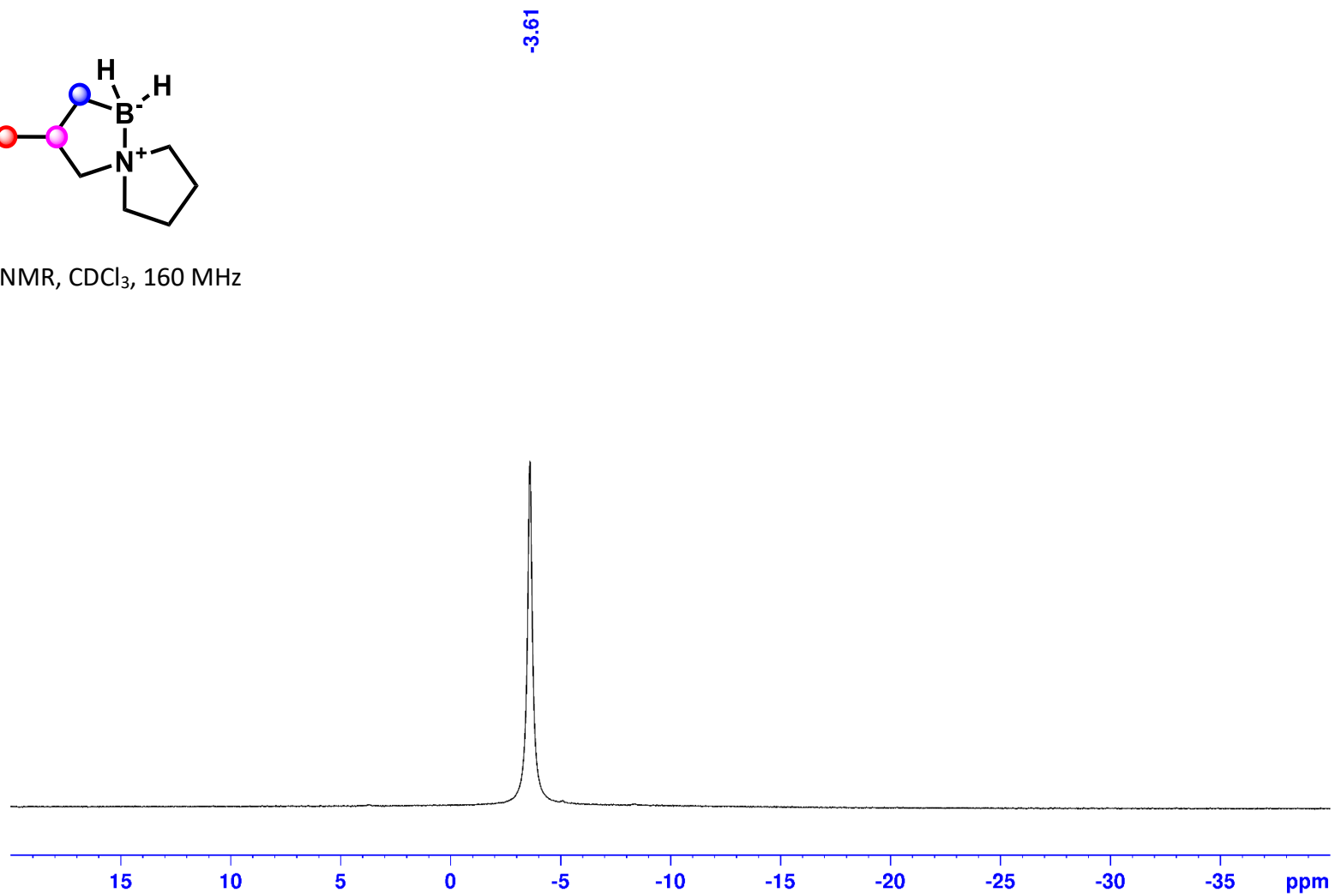
^{11}B NMR, CDCl_3 , 160 MHz



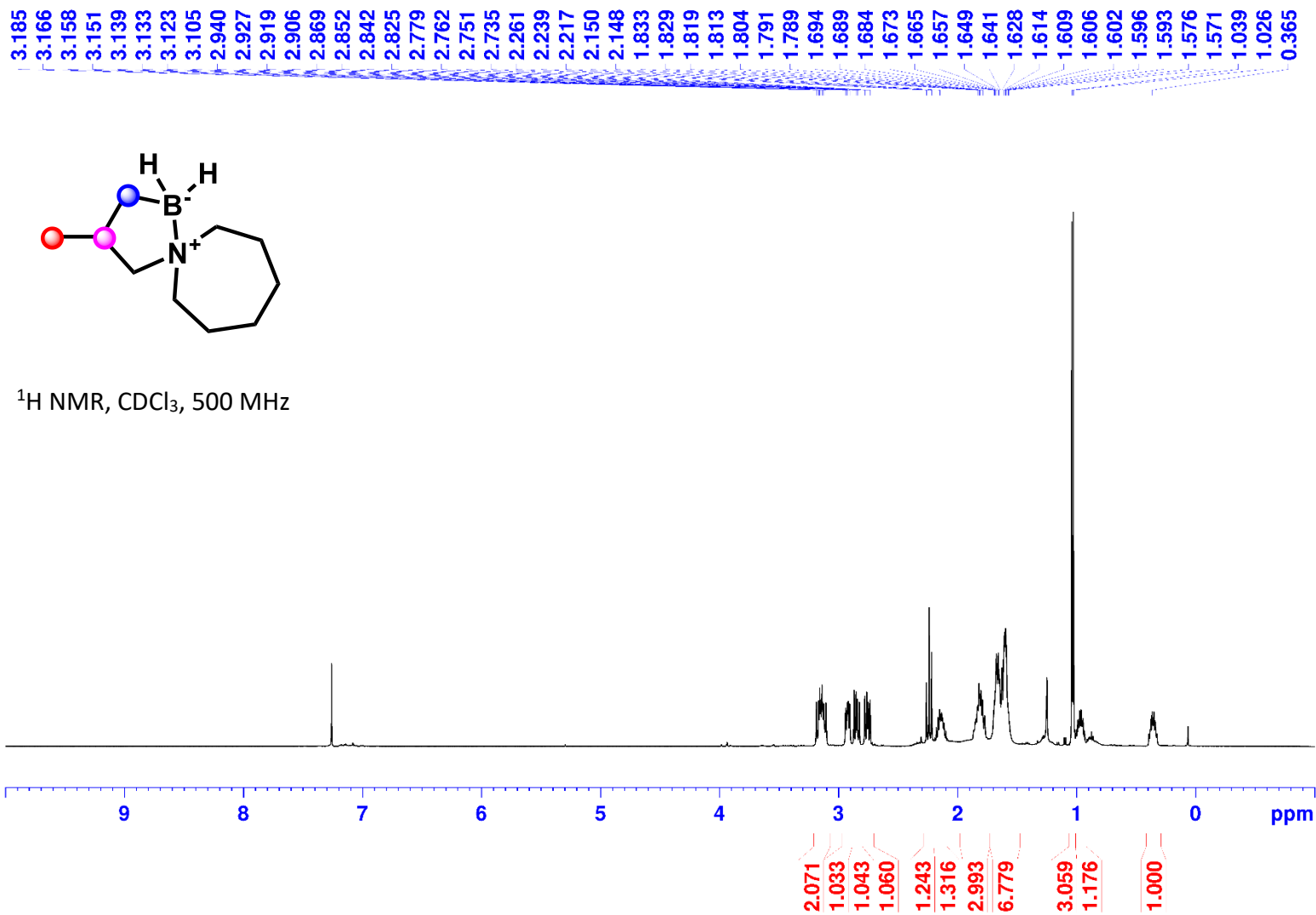
3-Methyl-5-aza-1-borasp[4.4]nonane (2a):



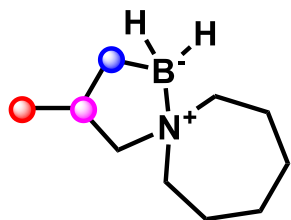
^{11}B NMR, CDCl_3 , 160 MHz



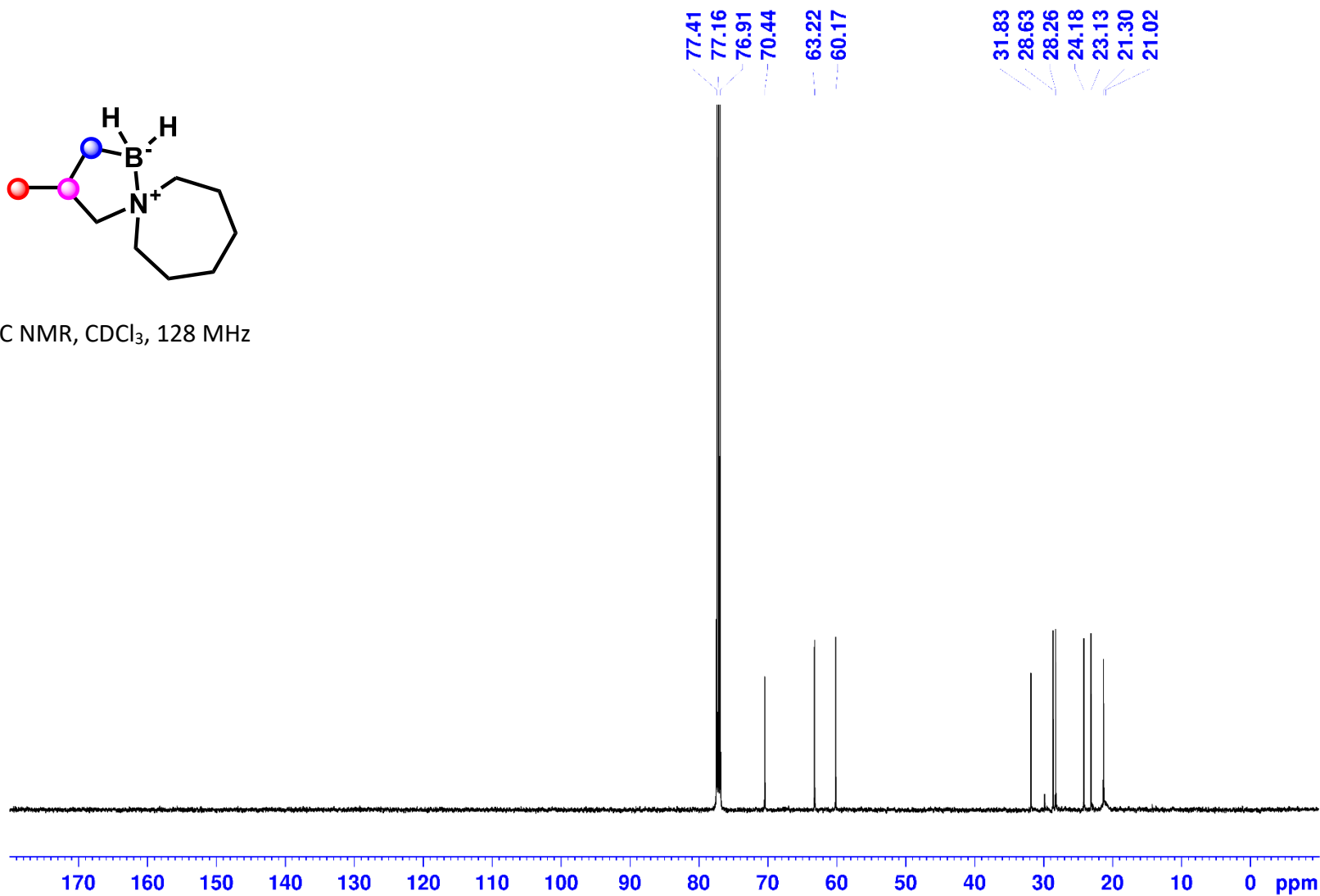
3-Methyl-5-aza-1-borasp[4.6]undecane (2b):



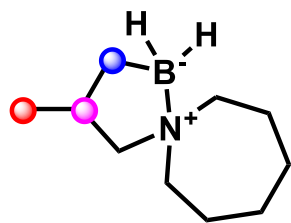
3-Methyl-5-aza-1-borasp[ro[4.6]undecane (2b):



^{13}C NMR, CDCl_3 , 128 MHz

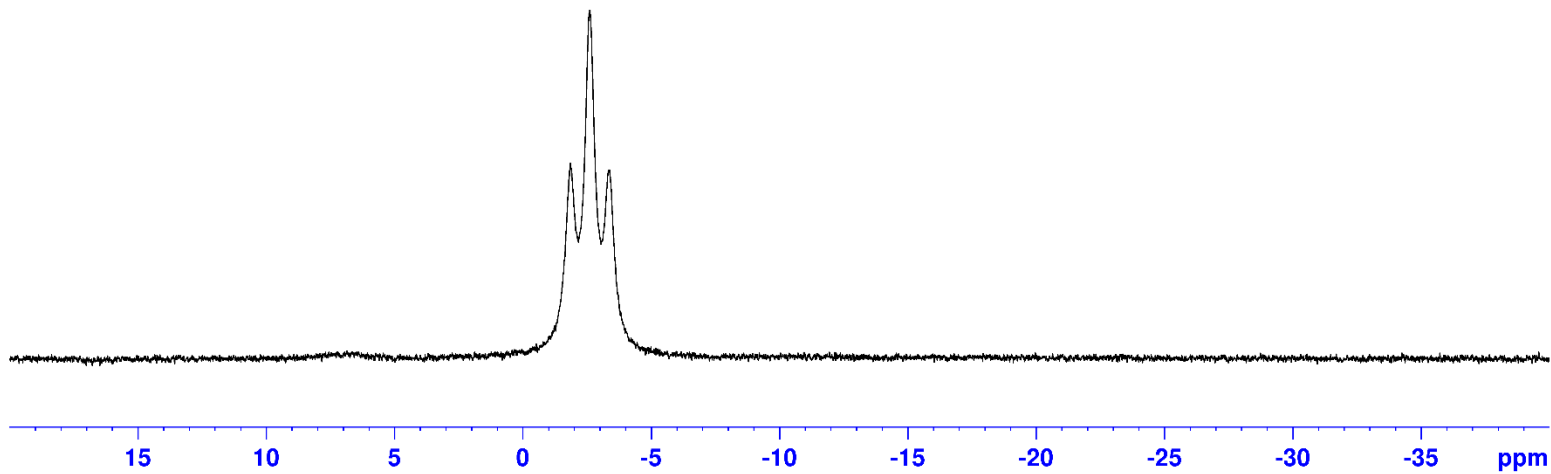


3-Methyl-5-aza-1-borasp[4.6]undecane (2b):

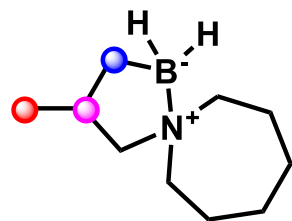


-2.62

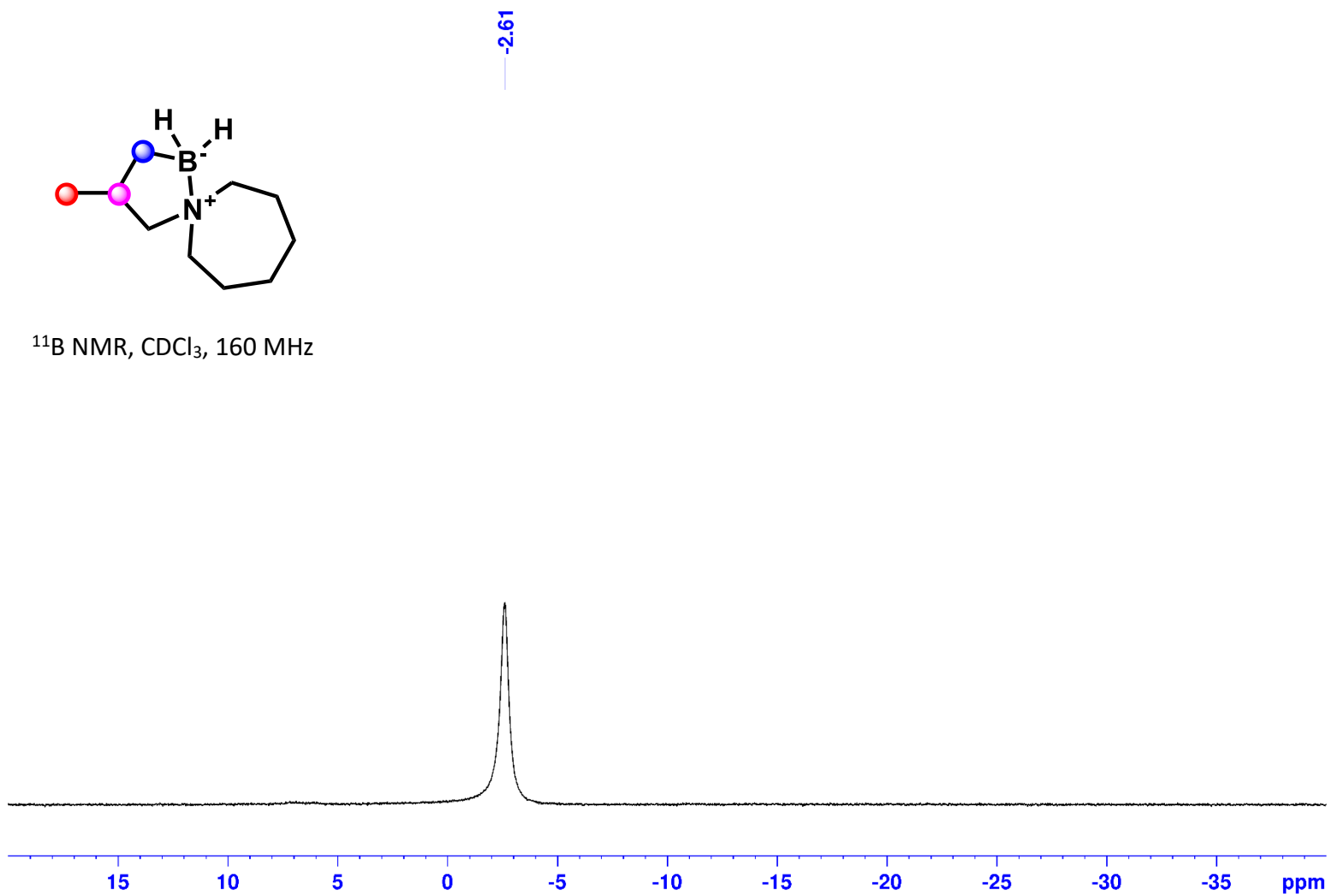
^{11}B NMR, CDCl_3 , 160 MHz



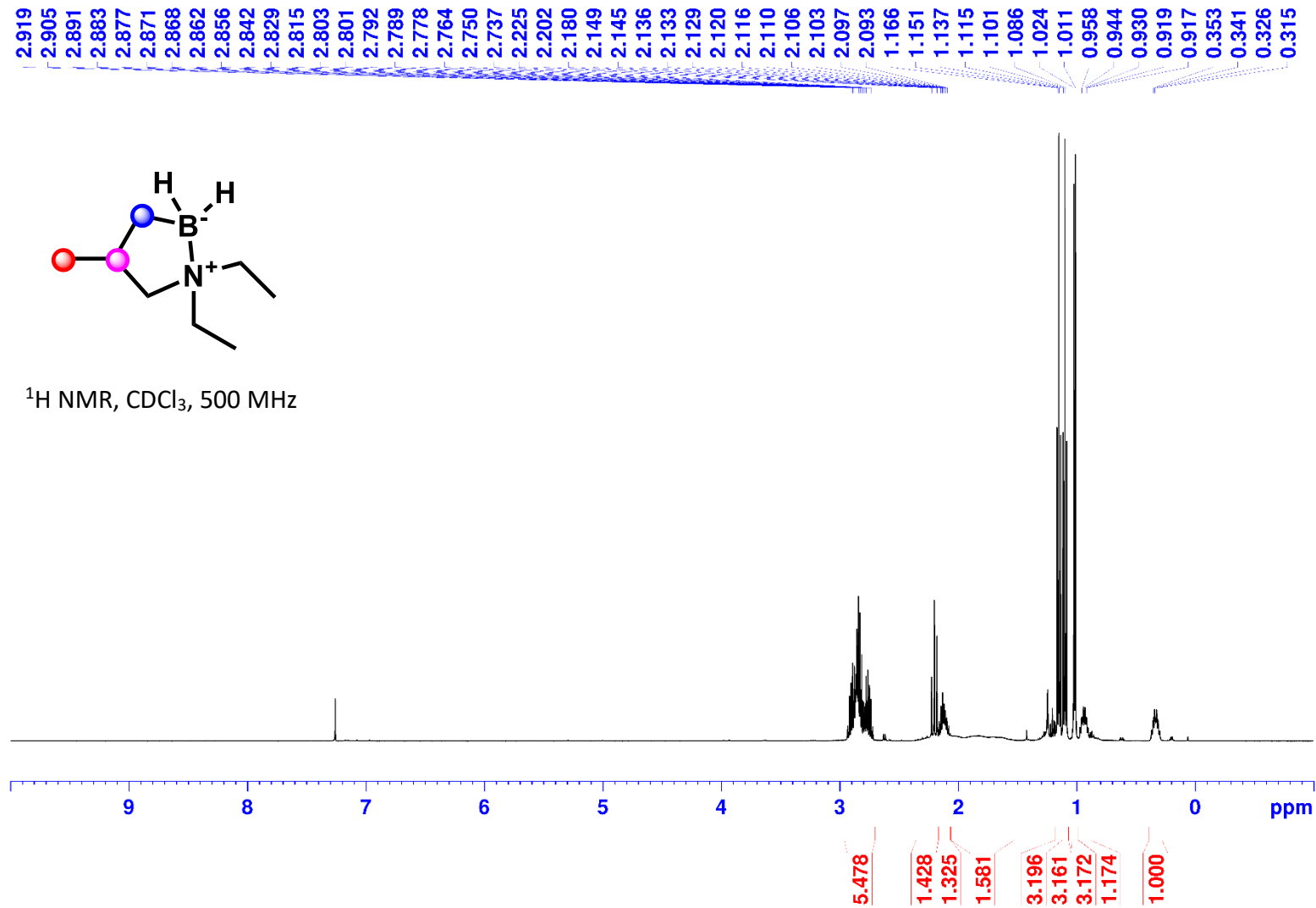
3-Methyl-5-aza-1-borasp[4.6]undecane (2b):



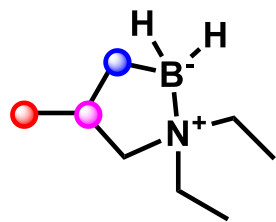
^{11}B NMR, CDCl_3 , 160 MHz



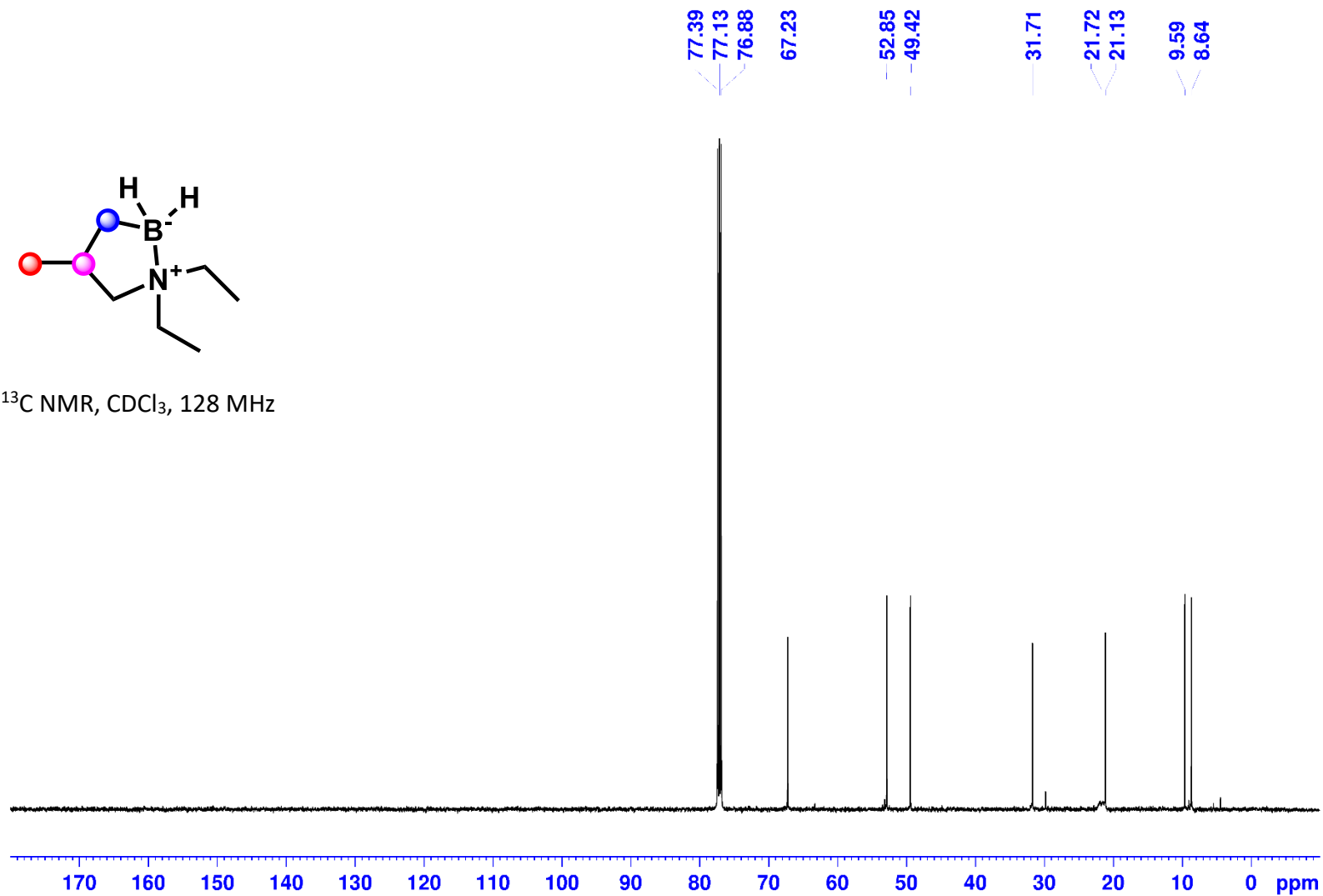
1,1-Diethyl-4-methyl-1,2-azaborolidine (2c):



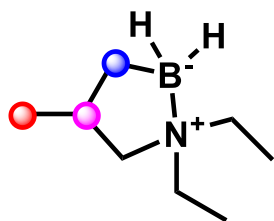
1,1-Diethyl-4-methyl-1,2-azaborolidine (2c):



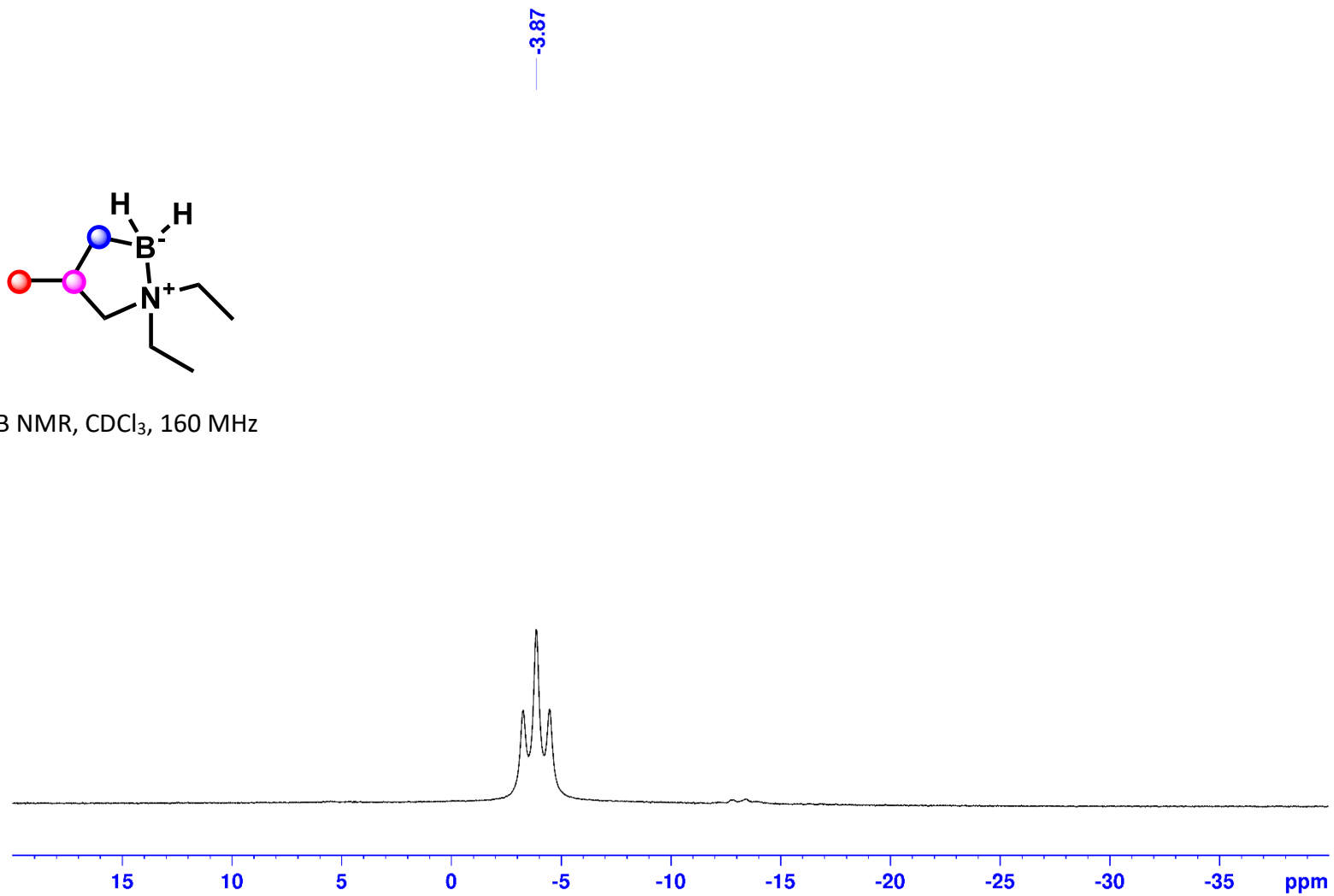
^{13}C NMR, CDCl_3 , 128 MHz



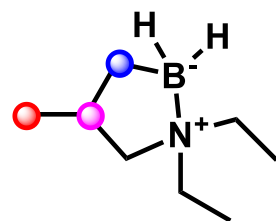
1,1-Diethyl-4-methyl-1,2-azaborolidine (2c):



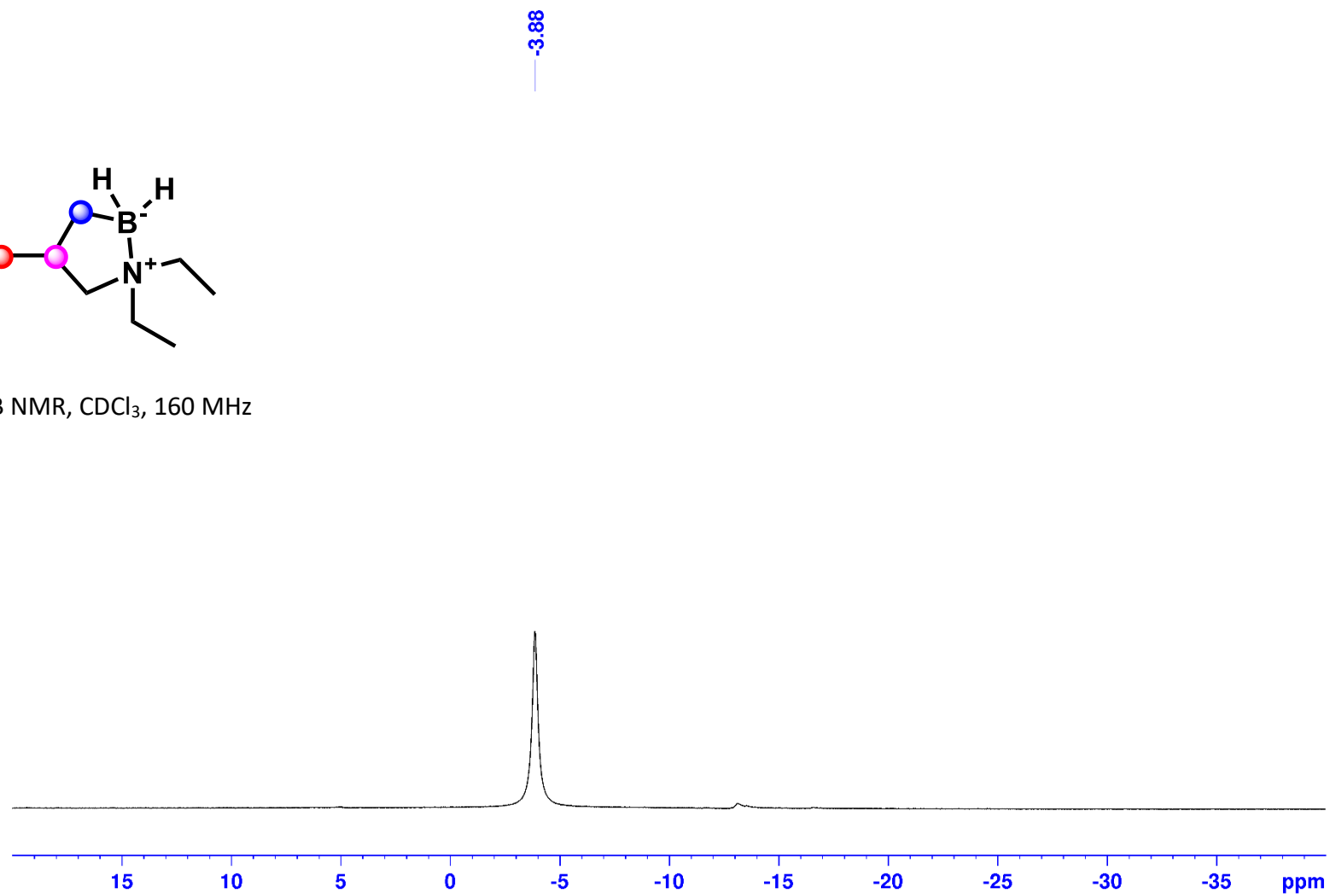
^{11}B NMR, CDCl_3 , 160 MHz



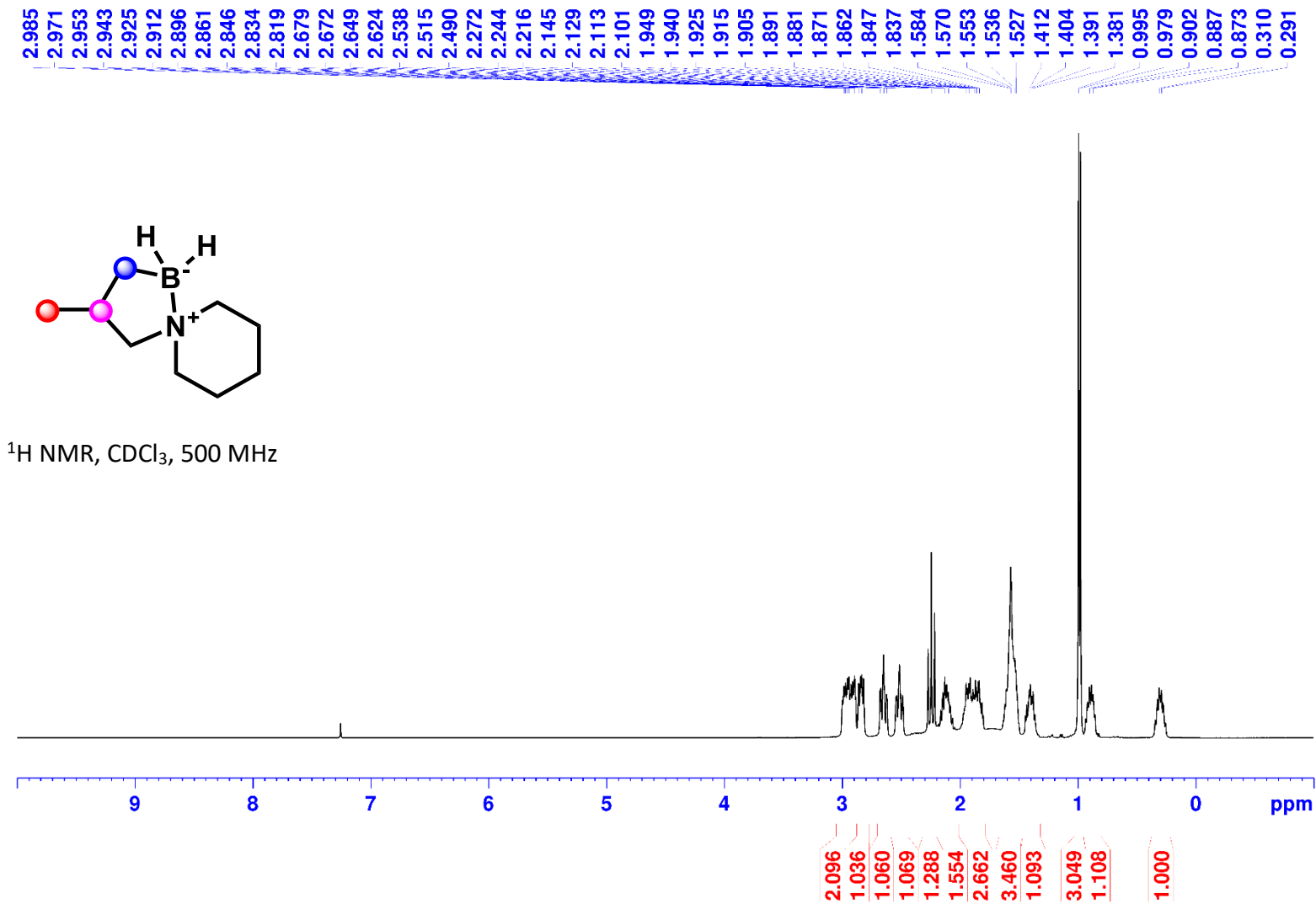
1,1-Diethyl-4-methyl-1,2-azaborolidine (2c):



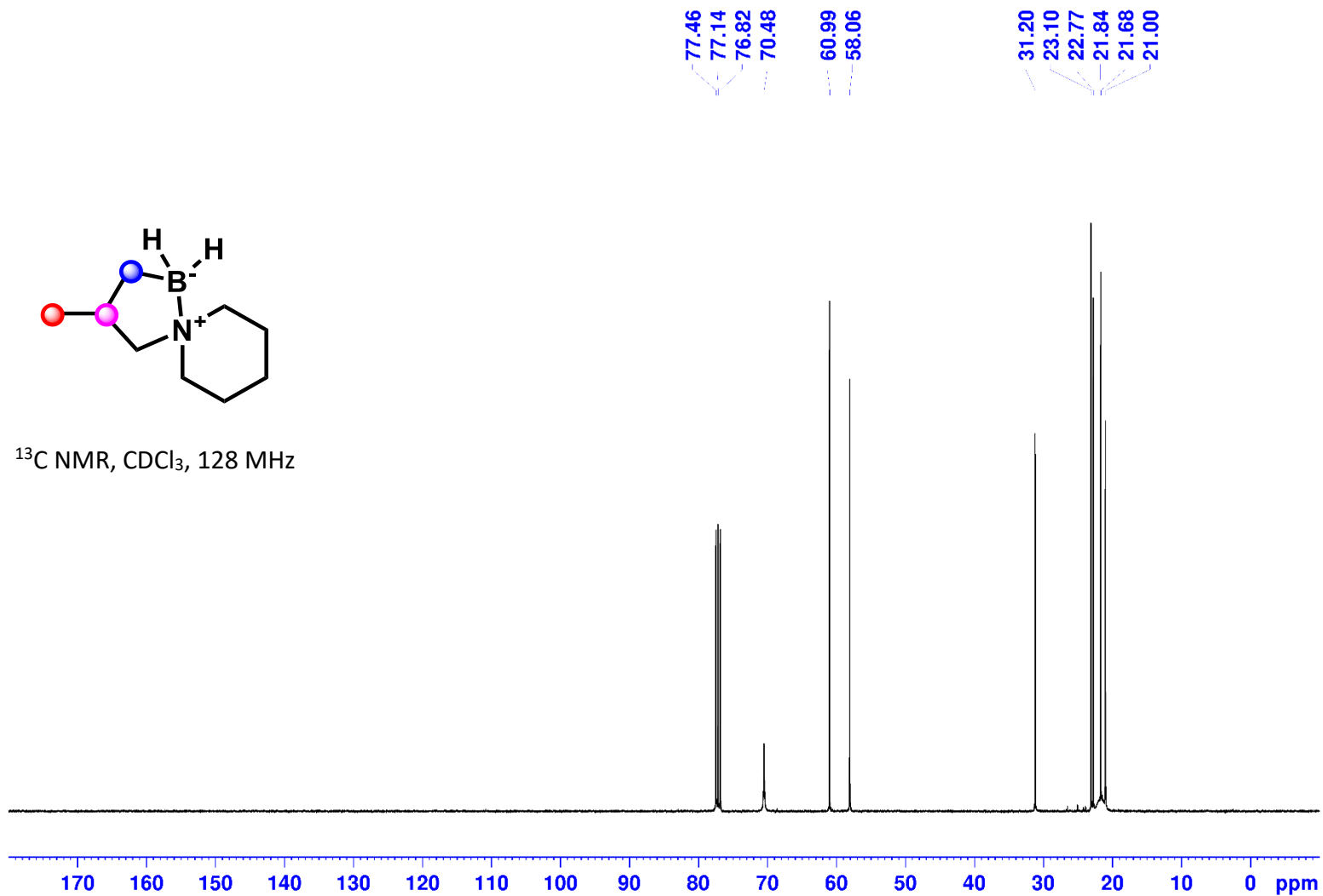
^{11}B NMR, CDCl_3 , 160 MHz



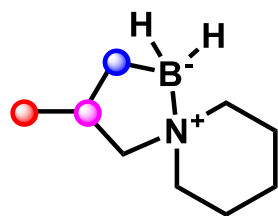
3-Methyl-5-aza-1-borasp[4.5]decane (2d):



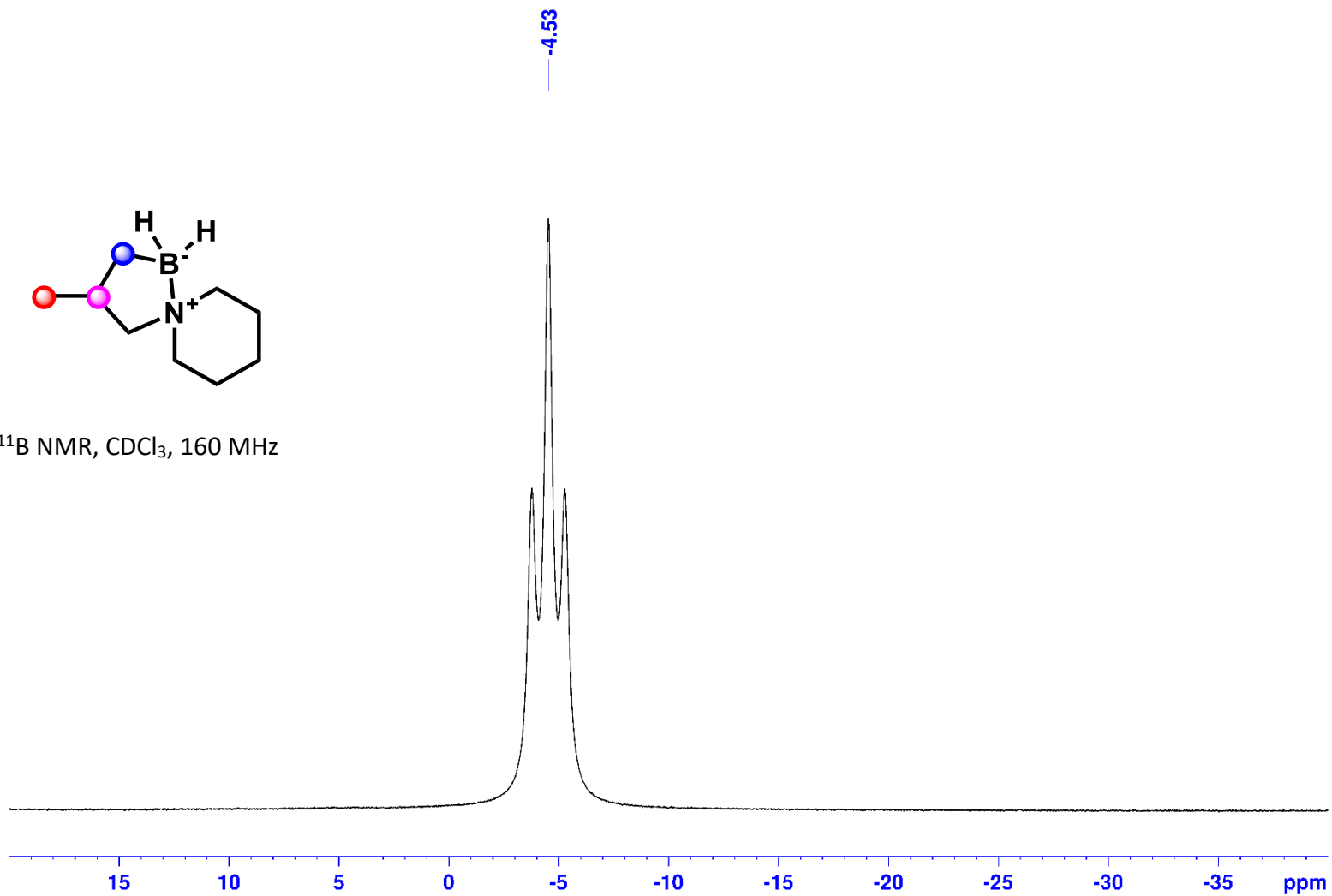
3-Methyl-5-aza-1-borospiro[4.5]decane (2d):



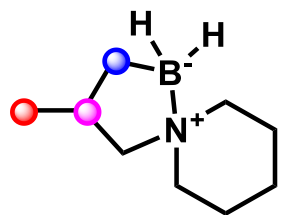
3-Methyl-5-aza-1-borasp[4.5]decane (2d):



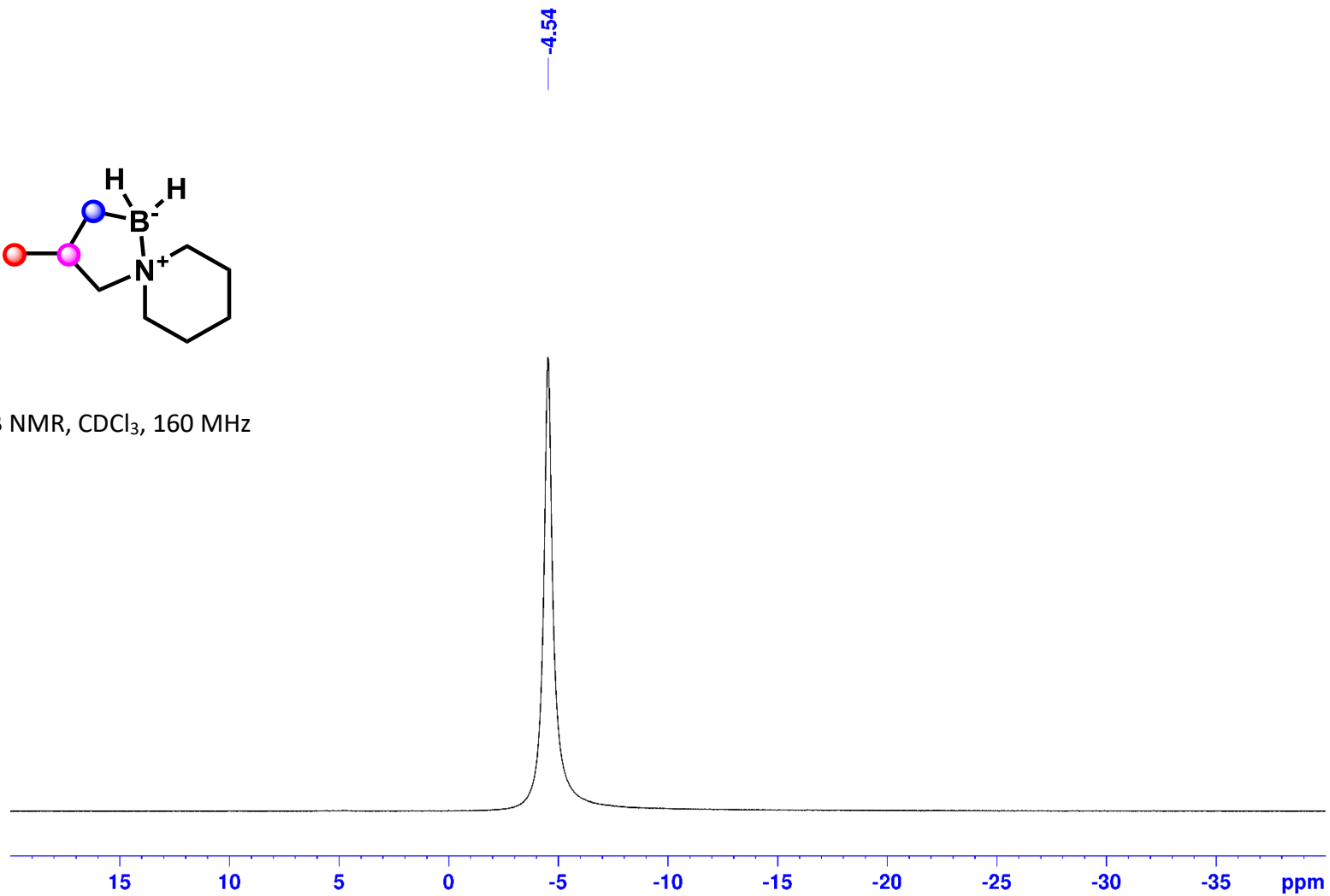
^{11}B NMR, CDCl_3 , 160 MHz



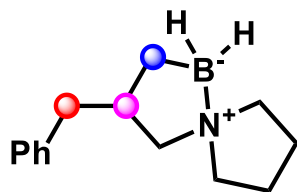
3-Methyl-5-aza-1-borasp[4.5]decane (2d):



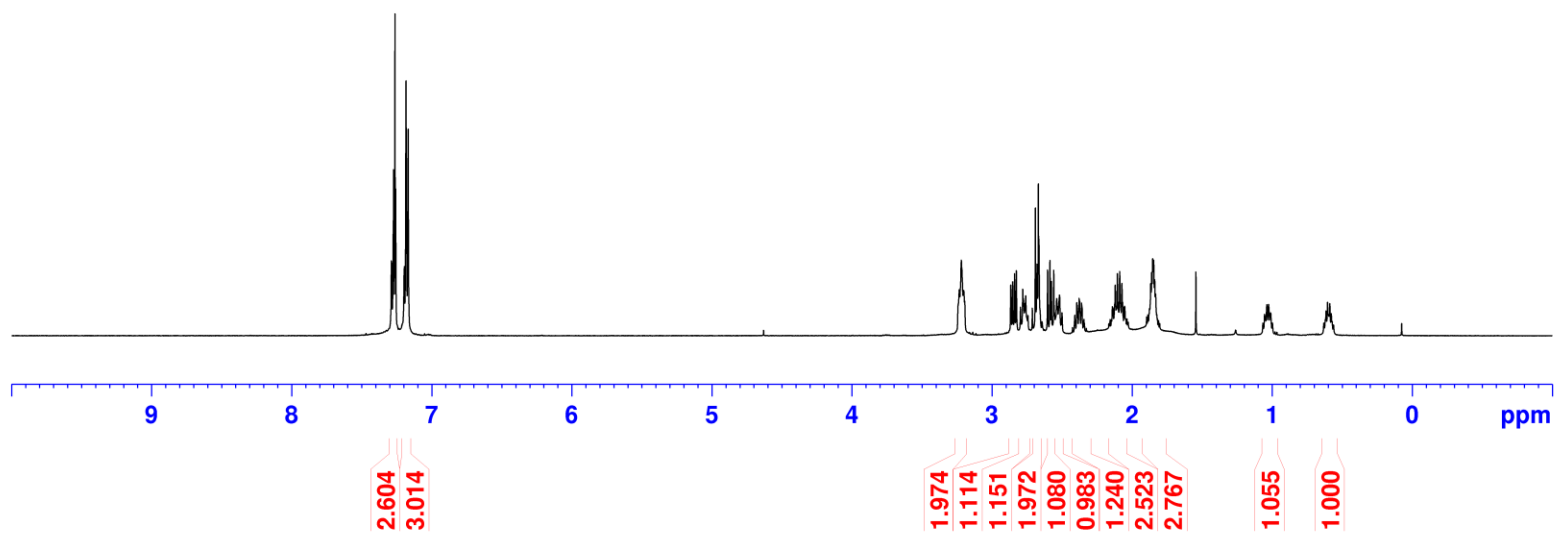
^{11}B NMR, CDCl_3 , 160 MHz



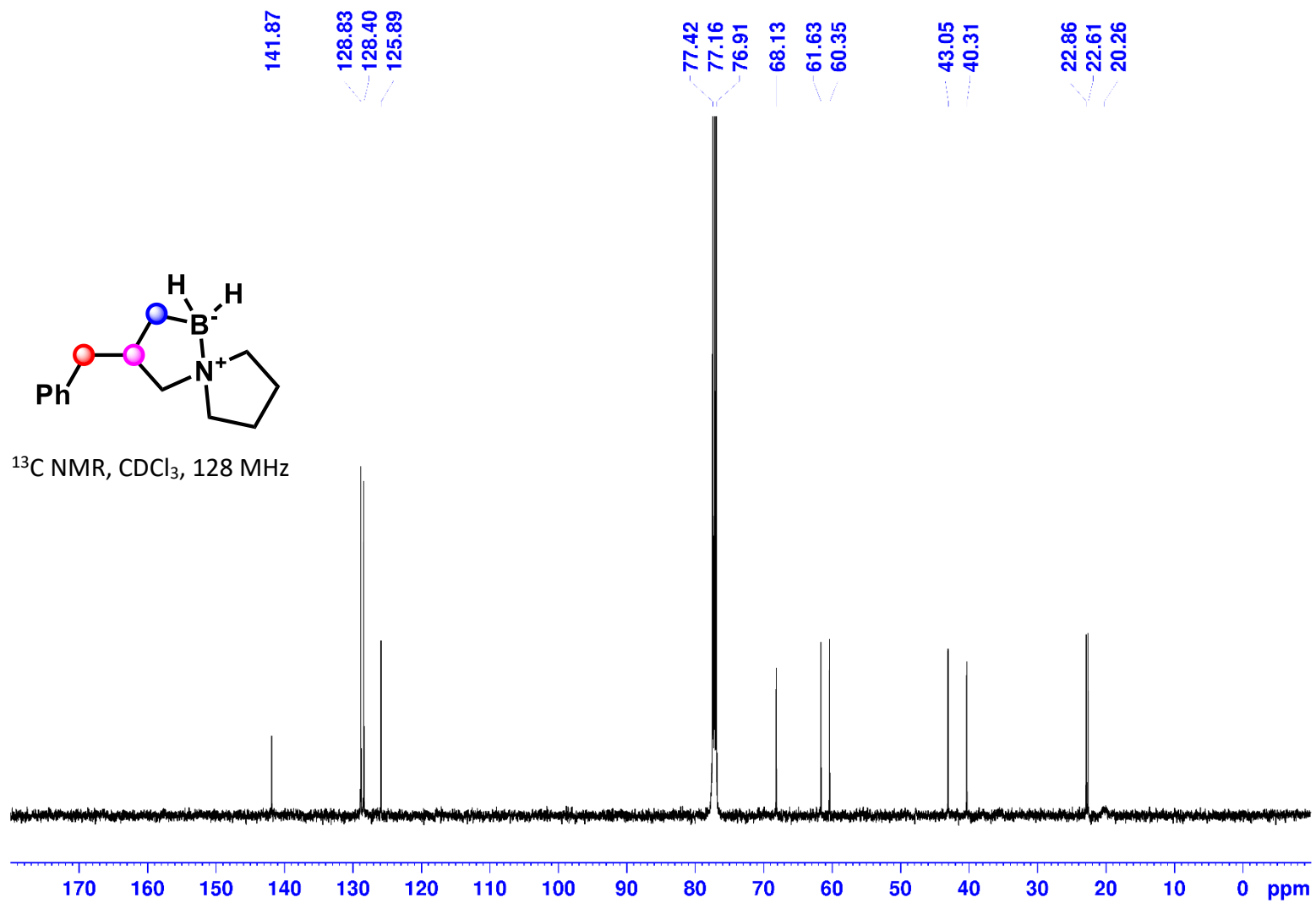
3-Benzyl-5-aza-1-borasp[4.4]nonane (2e):



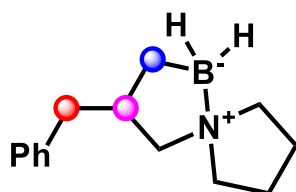
^1H NMR, CDCl_3 , 500 MHz



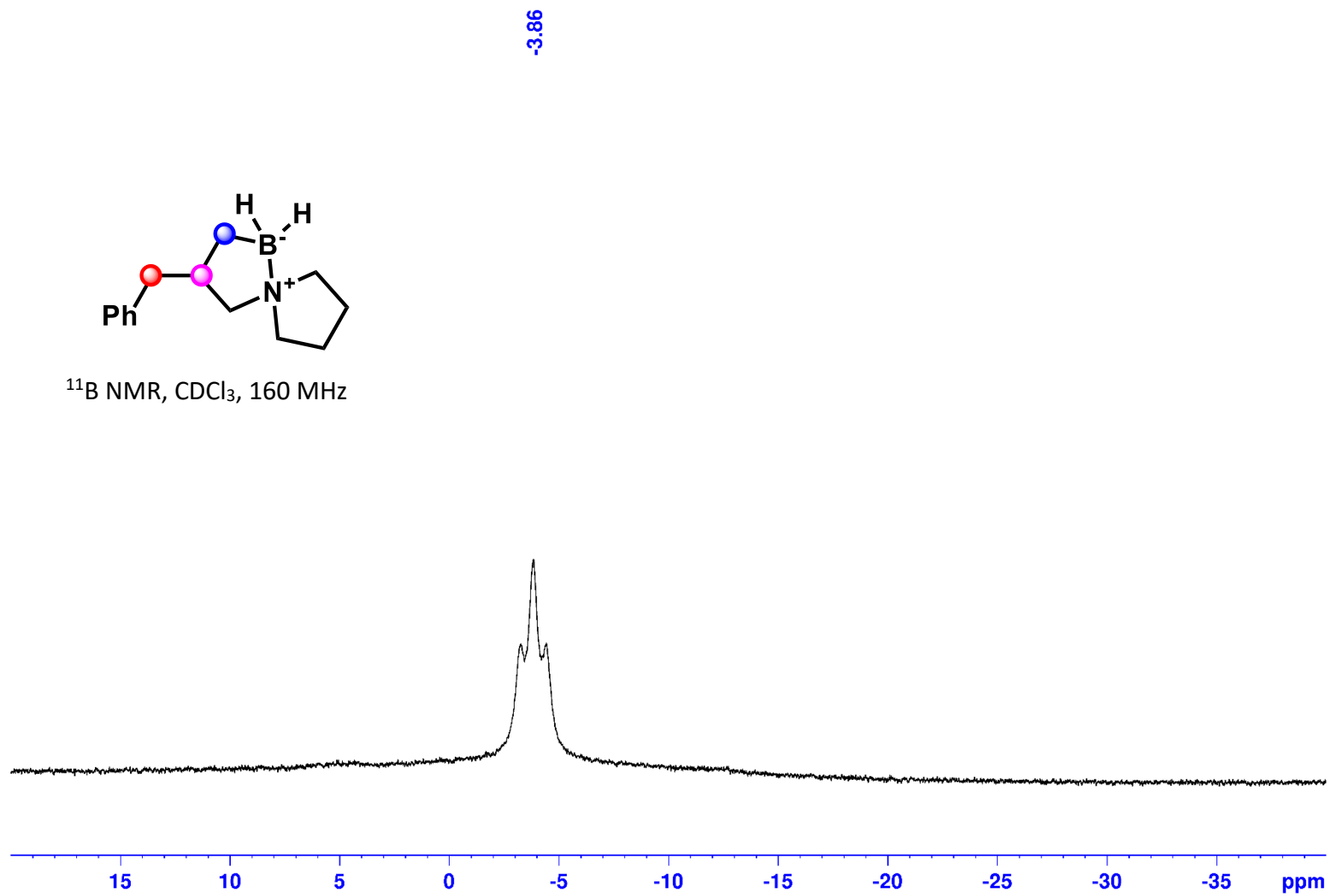
3-Benzyl-5-aza-1-borasp[iro[4.4]nonane (2e):



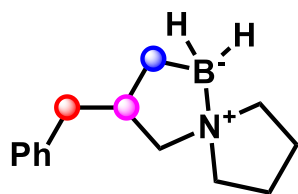
3-Benzyl-5-aza-1-borasp[4.4]nonane (2e):



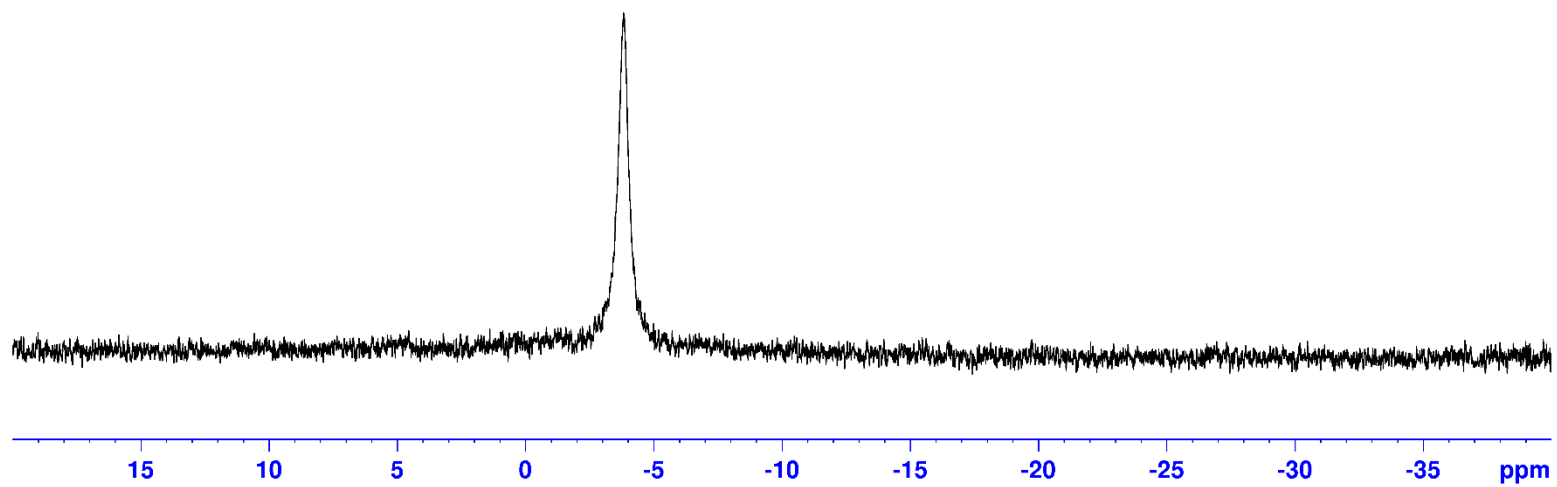
^{11}B NMR, CDCl_3 , 160 MHz



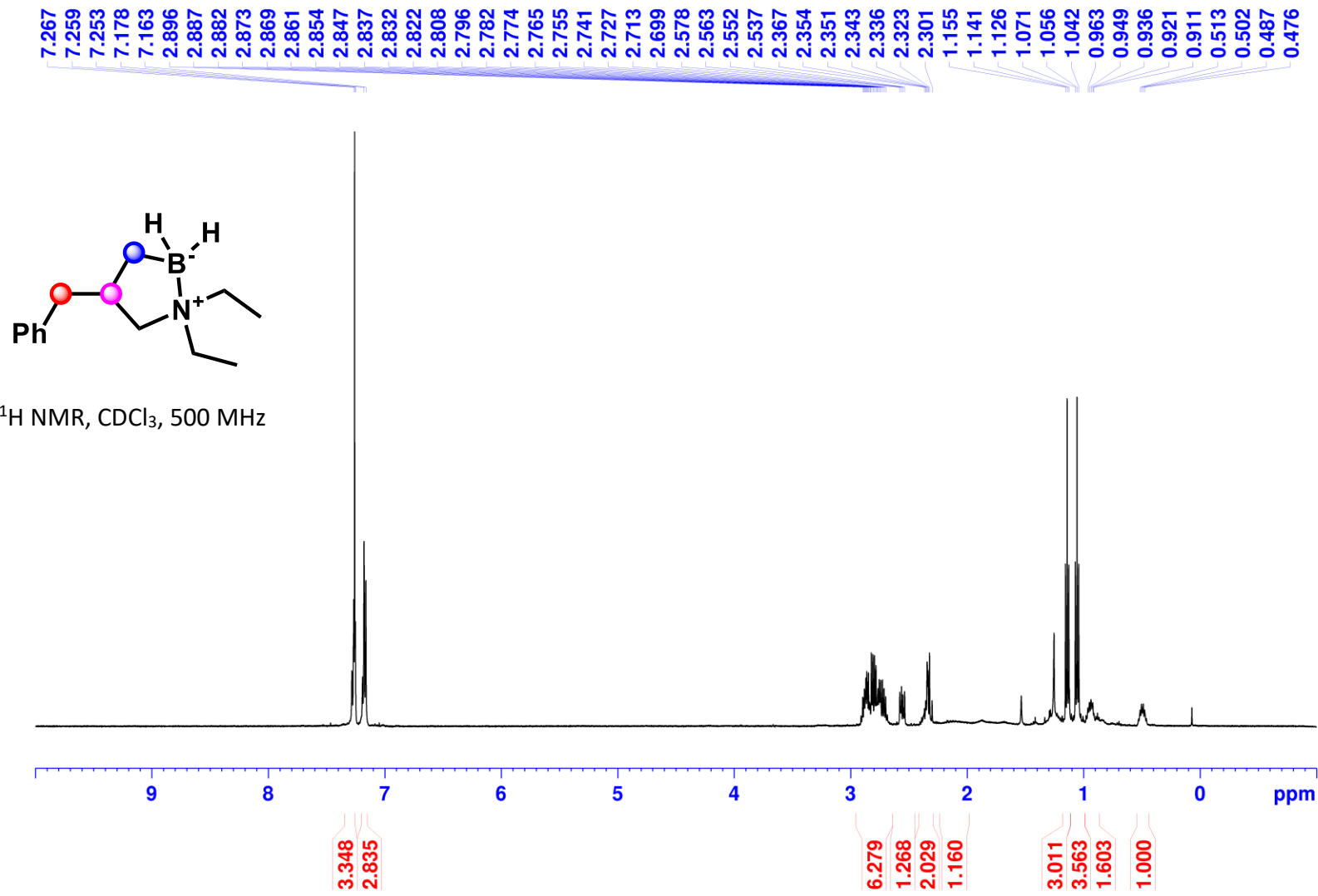
3-Benzyl-5-aza-1-borasp[4.4]nonane (2e):



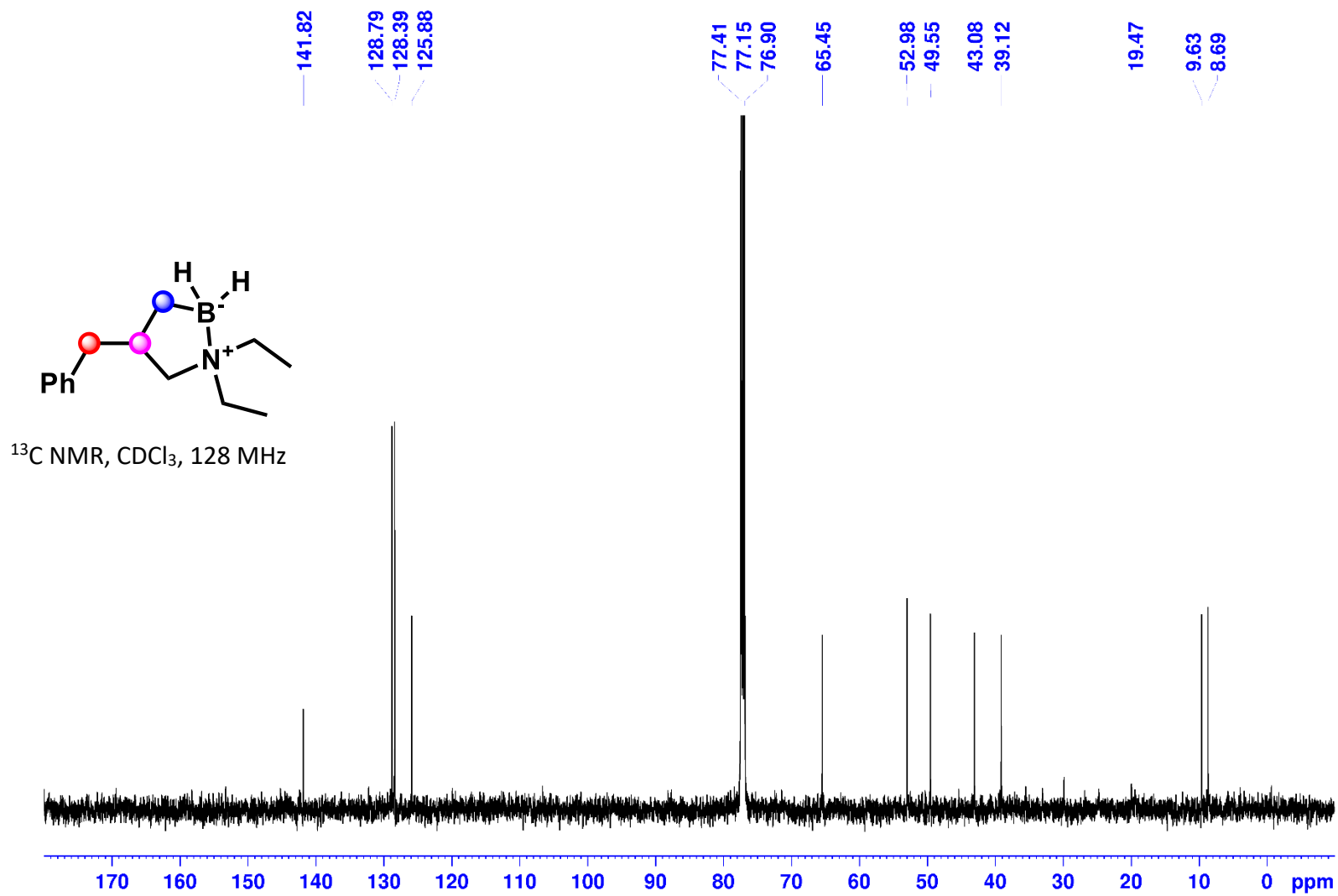
^{11}B NMR, CDCl_3 , 160 MHz



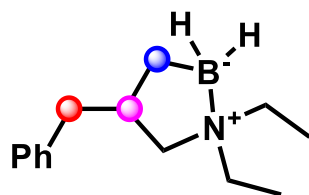
4-Benzyl-1,1-diethyl-1,2-azaborolidine (2f):



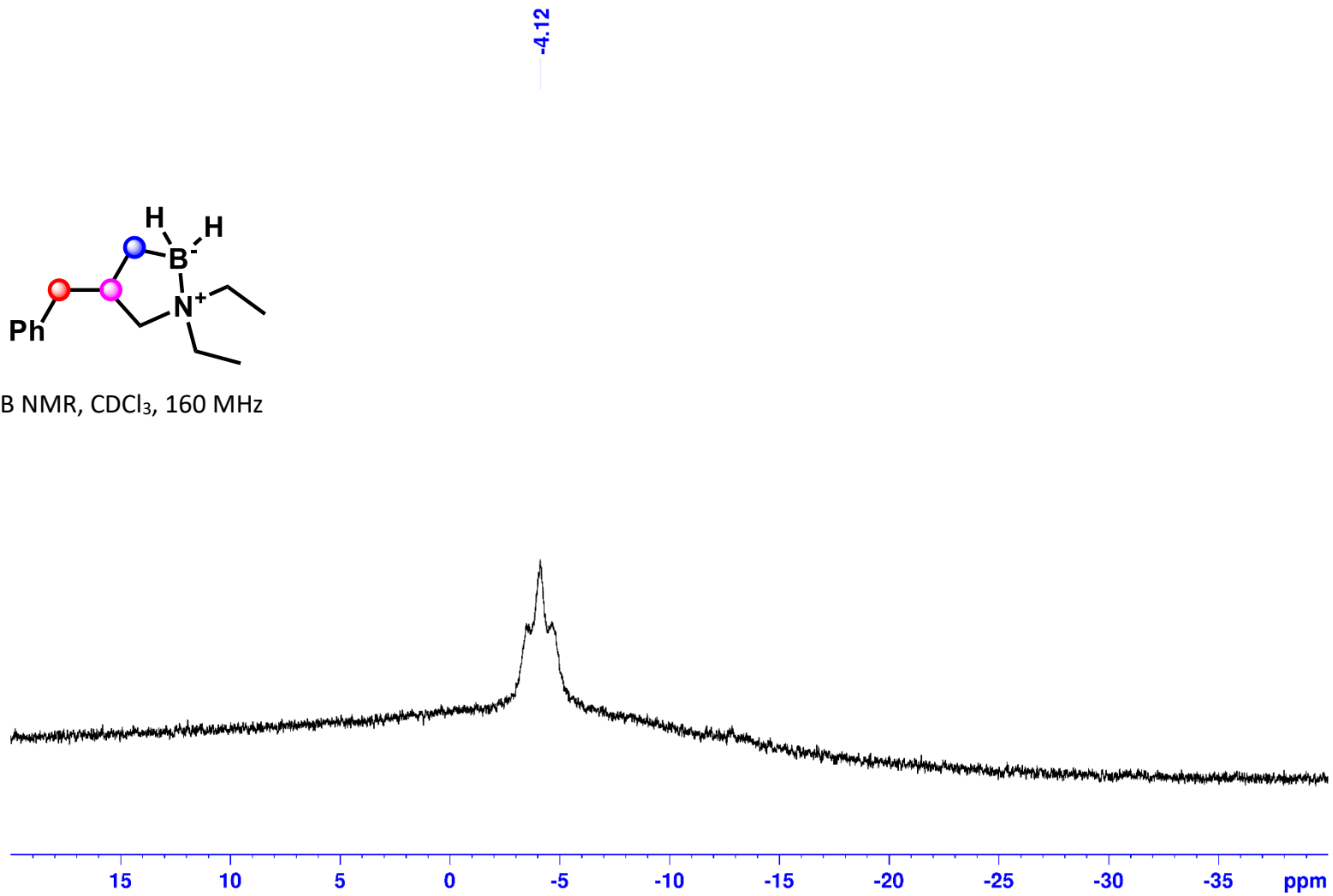
4-Benzyl-1,1-diethyl-1,2-azaborolidine (2f):



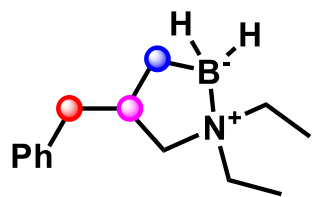
4-Benzyl-1,1-diethyl-1,2-azaborolidine (2f):



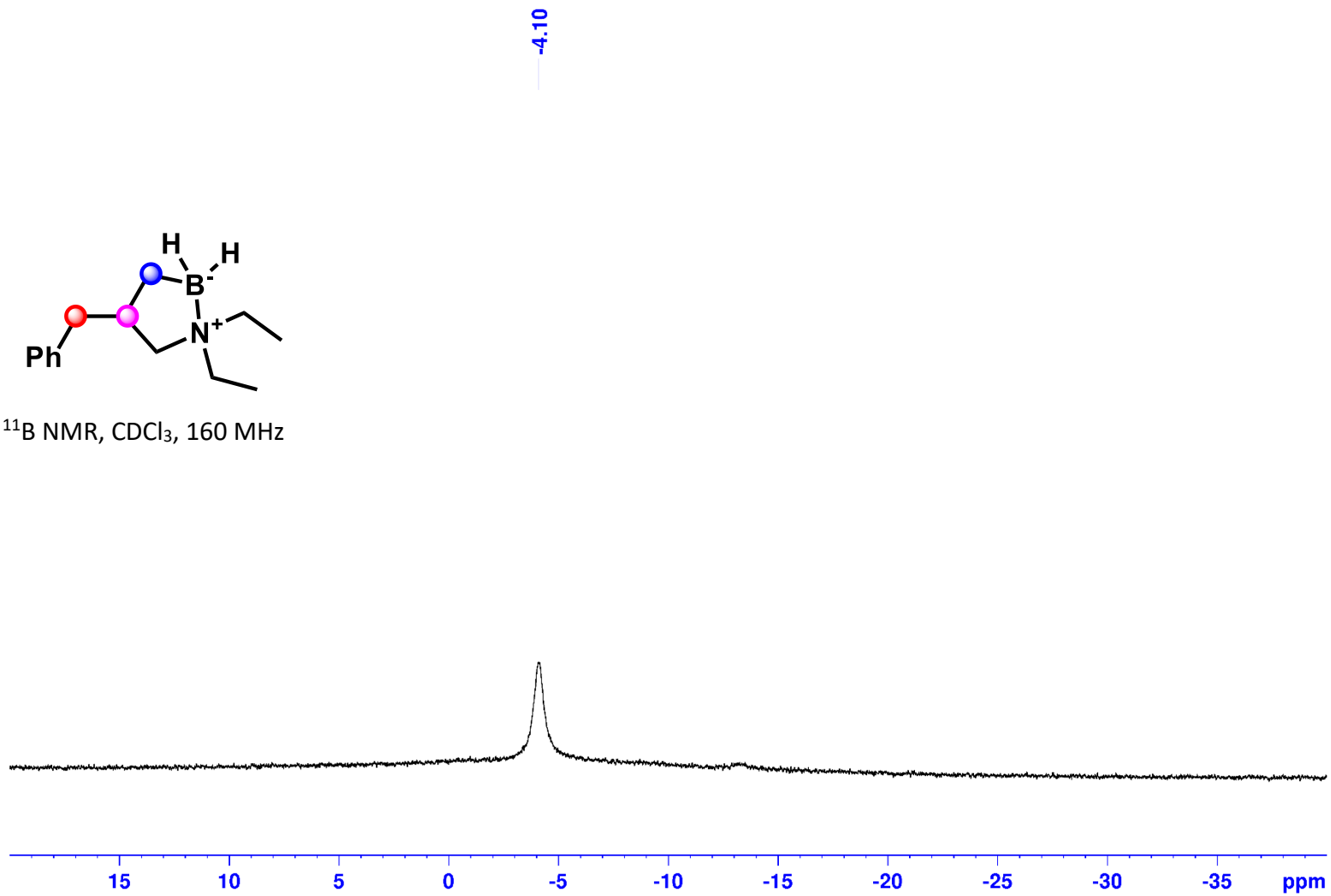
^{11}B NMR, CDCl_3 , 160 MHz



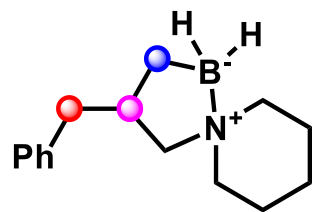
4-Benzyl-1,1-diethyl-1,2-azaborolidine (2f):



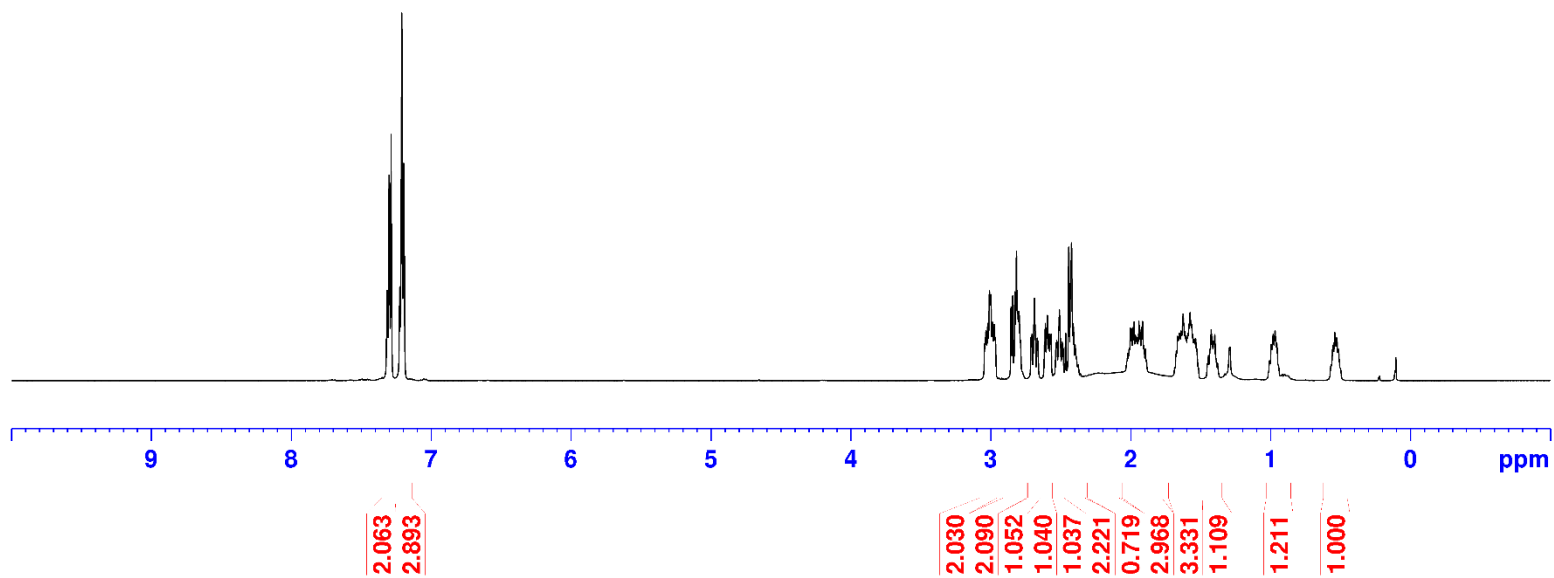
^{11}B NMR, CDCl_3 , 160 MHz



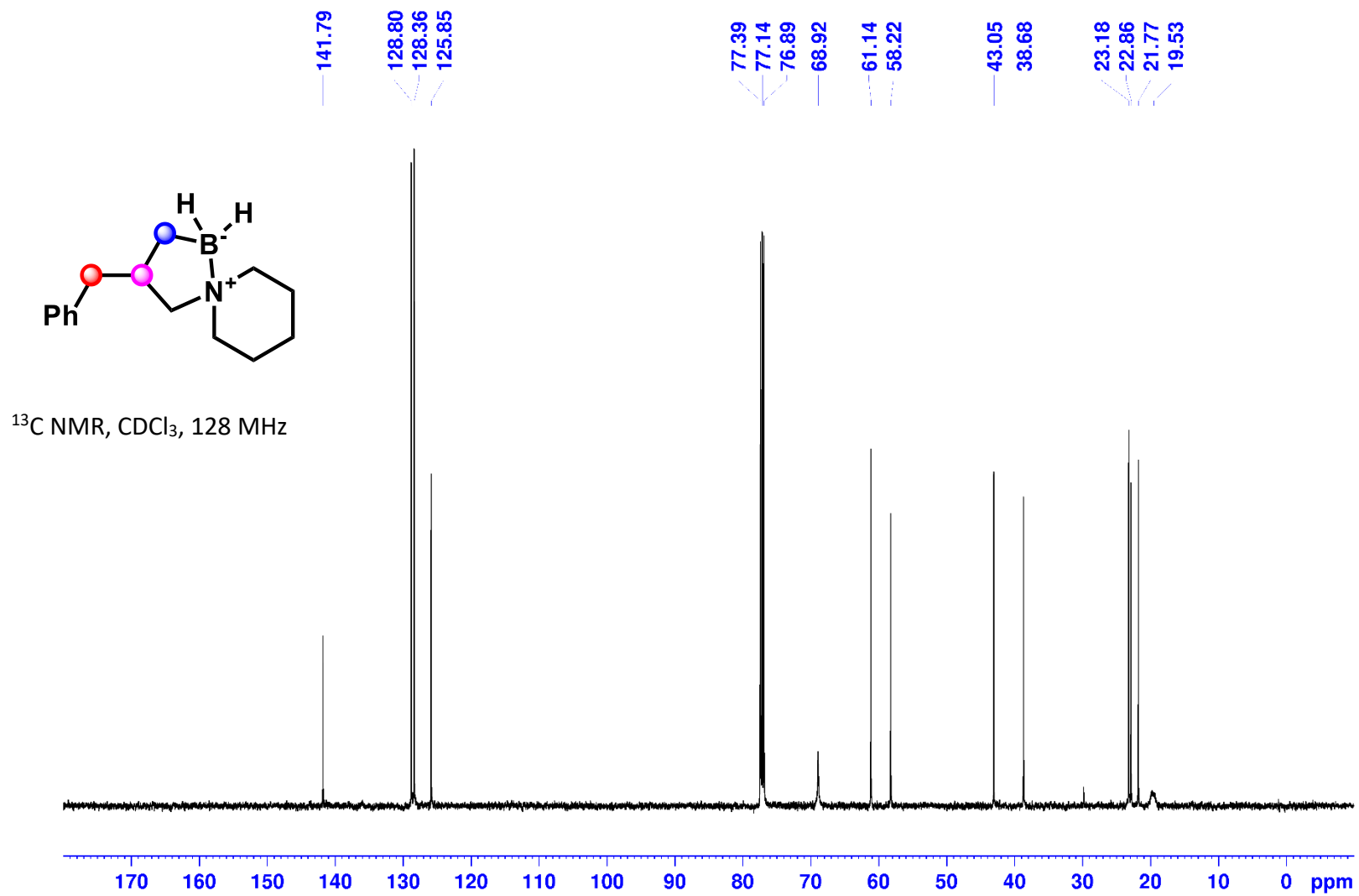
3-Benzyl-5-aza-1-borasp[4.5]decane (2g):



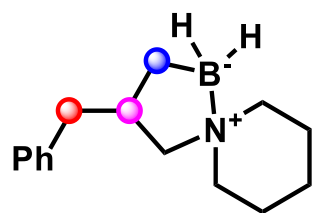
¹H NMR, CDCl₃, 500 MHz



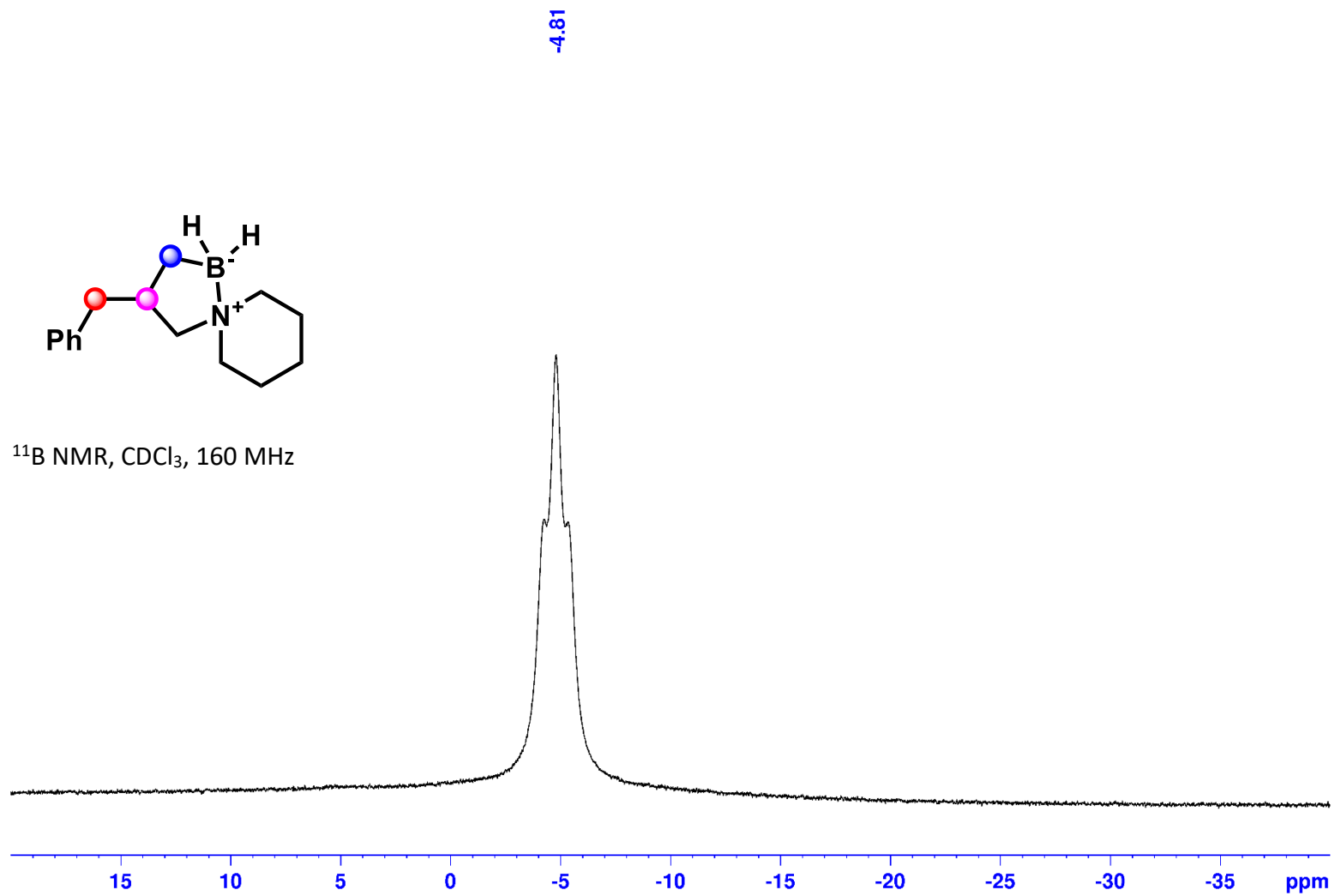
3-Benzyl-5-aza-1-borasp[4.5]decane (2g):



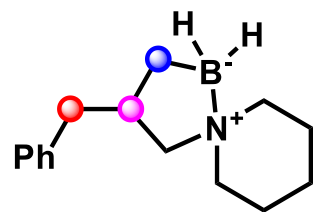
3-Benzyl-5-aza-1-borasp[iro[4.5]decane (2g):



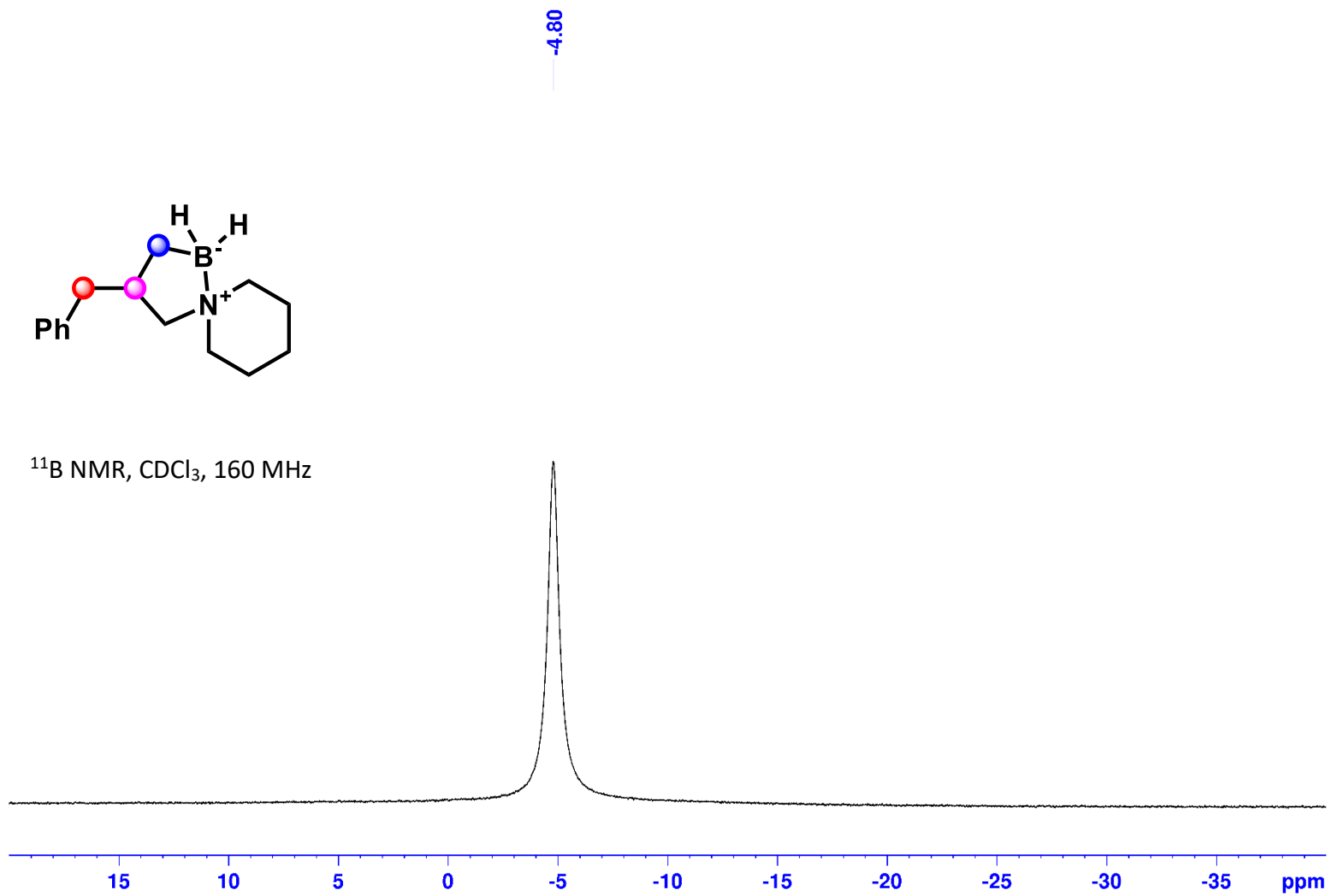
^{11}B NMR, CDCl_3 , 160 MHz



3-Benzyl-5-aza-1-borasp[4.5]decane (2g):

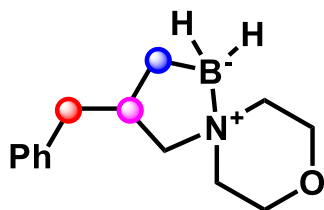


^{11}B NMR, CDCl_3 , 160 MHz

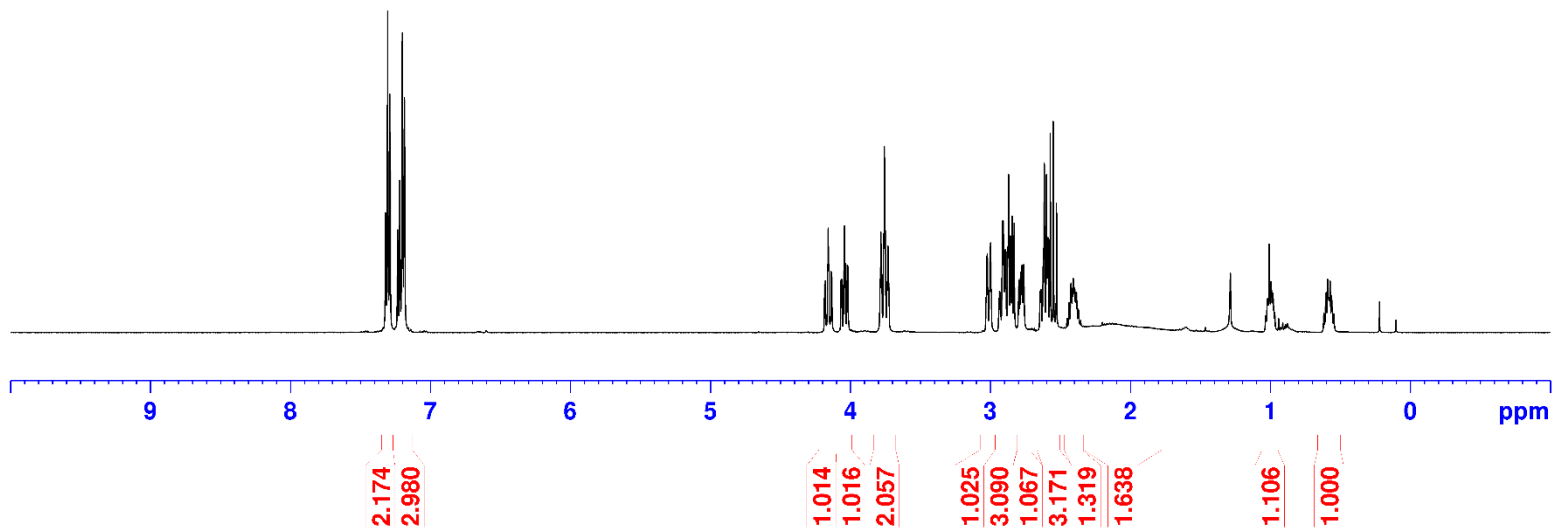


3-Benzyl-8-oxa-5-aza-1-borasp[4.5]decane (2h):

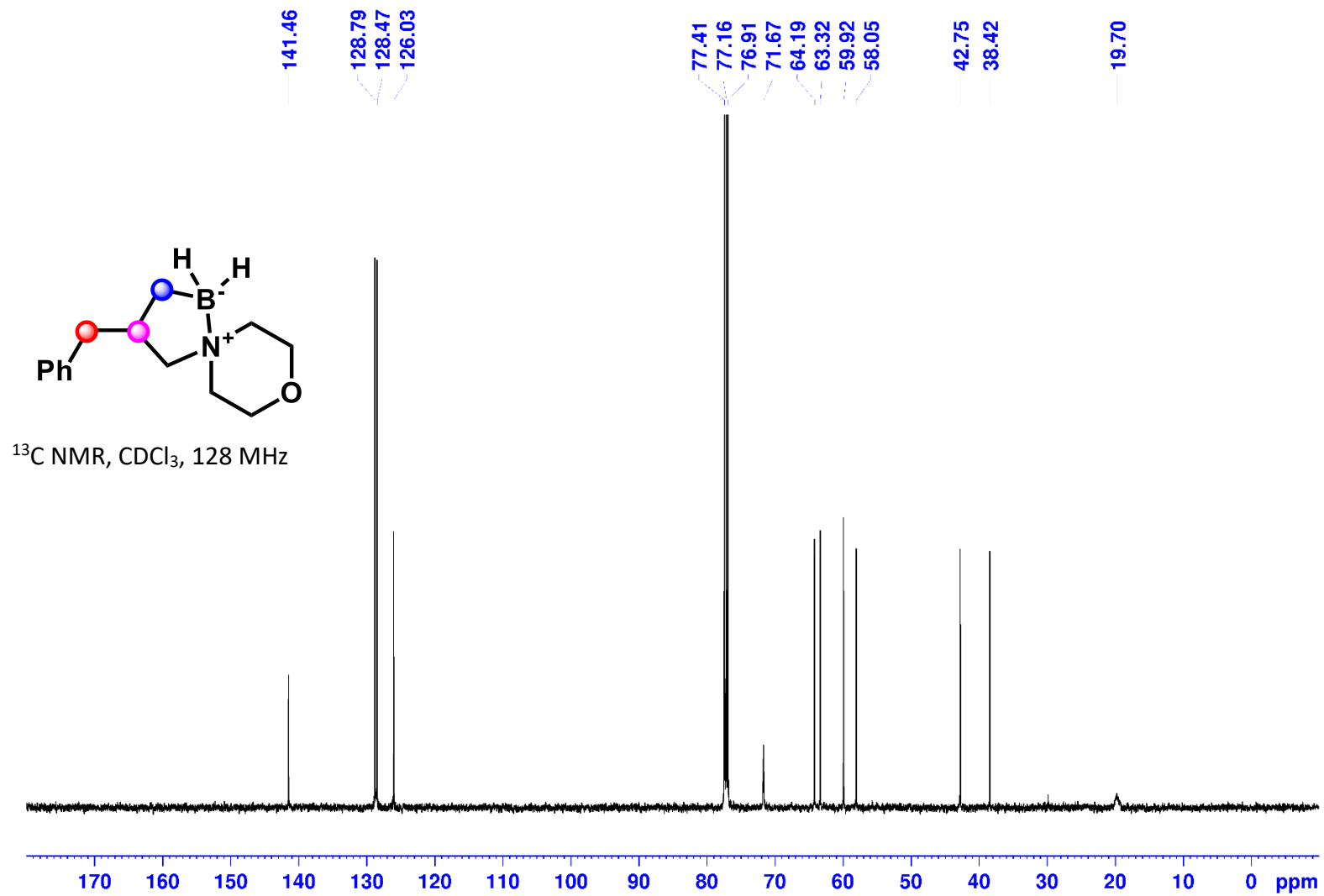
7.321
7.306
7.291
7.287
7.234
7.220
7.202
7.200
7.186
4.162
4.158
4.154
4.138
4.133
4.047
4.042
4.037
4.022
4.017
3.788
3.782
3.776
3.763
3.757
3.751
3.731
3.026
3.022
3.002
2.998
2.911
2.908
2.902
2.896
2.889
2.875
2.869
2.857
2.843
2.830
2.784
2.774
2.762
2.622
2.615
2.598
2.588
2.572
2.550
2.527
2.407
1.008



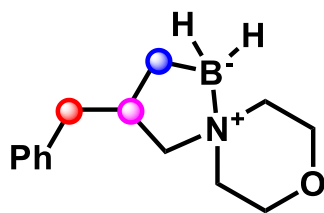
¹H NMR, CDCl₃, 500 MHz



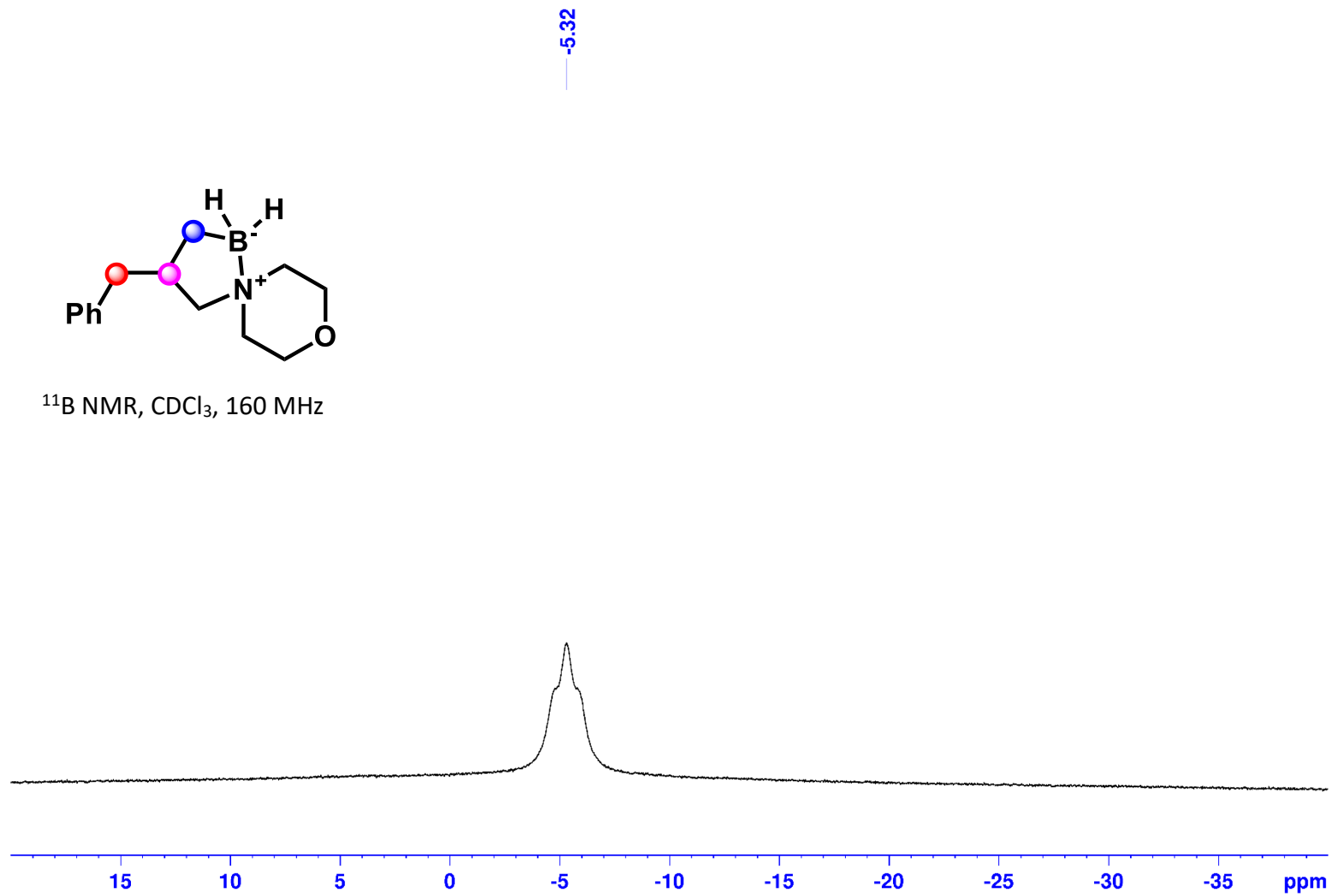
3-Benzyloxy-8-oxa-5-aza-1-borospiro[4.5]decane (2h):



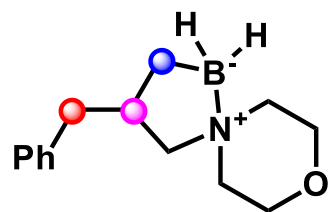
3-Benzyl-8-oxa-5-aza-1-borasp[4.5]decane (2h):



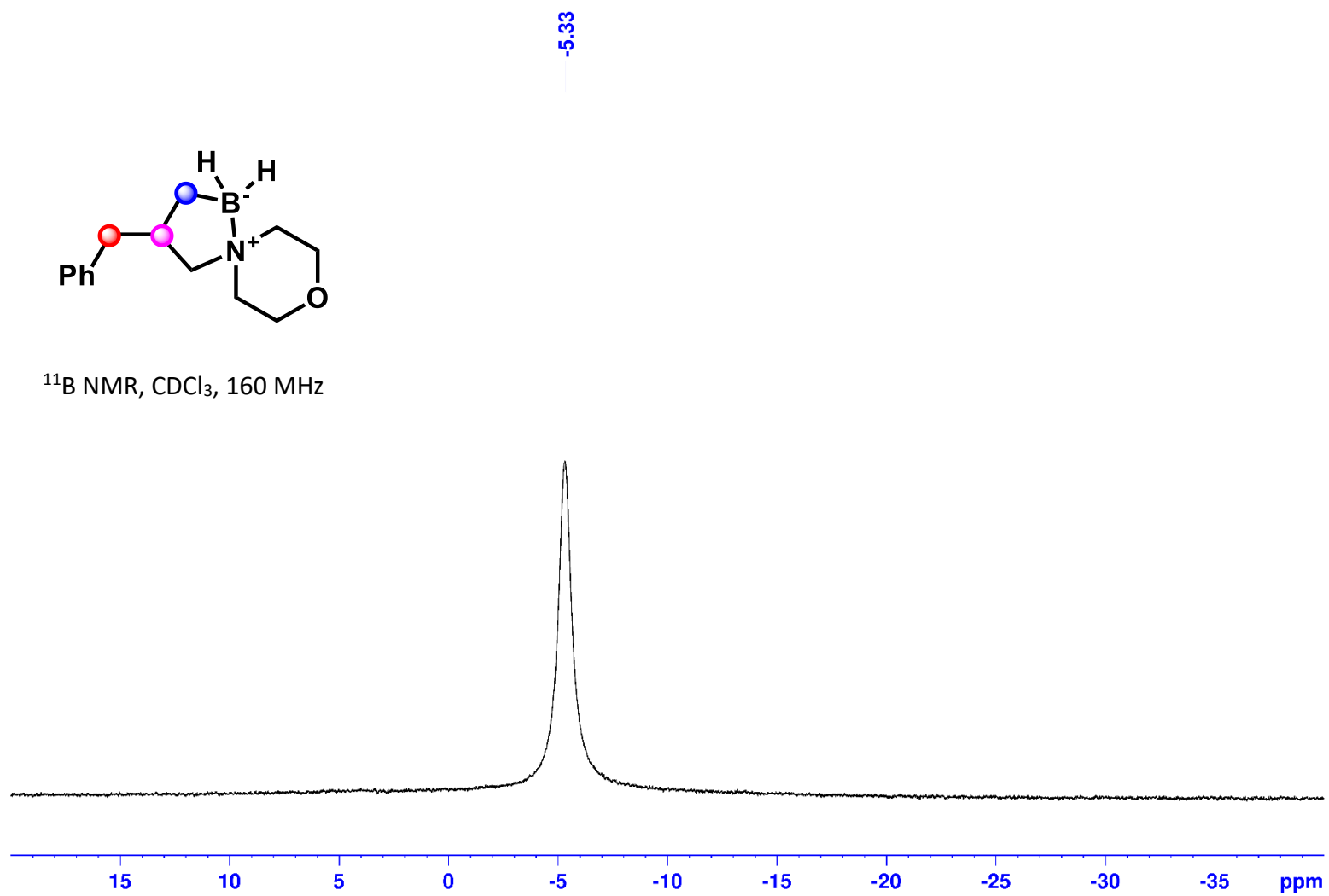
^{11}B NMR, CDCl_3 , 160 MHz



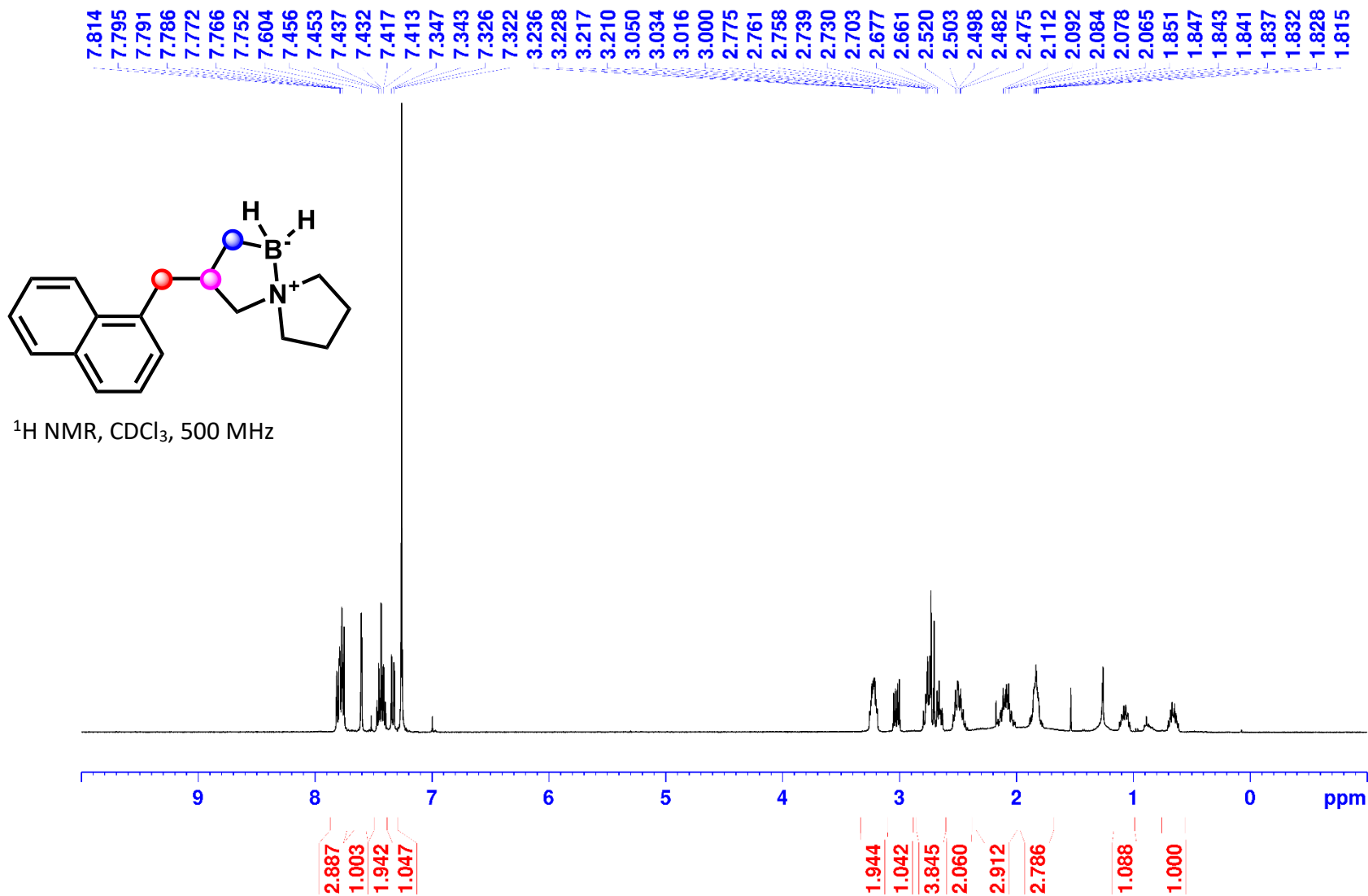
3-Benzyl-8-oxa-5-aza-1-borasp[4.5]decane (2h):



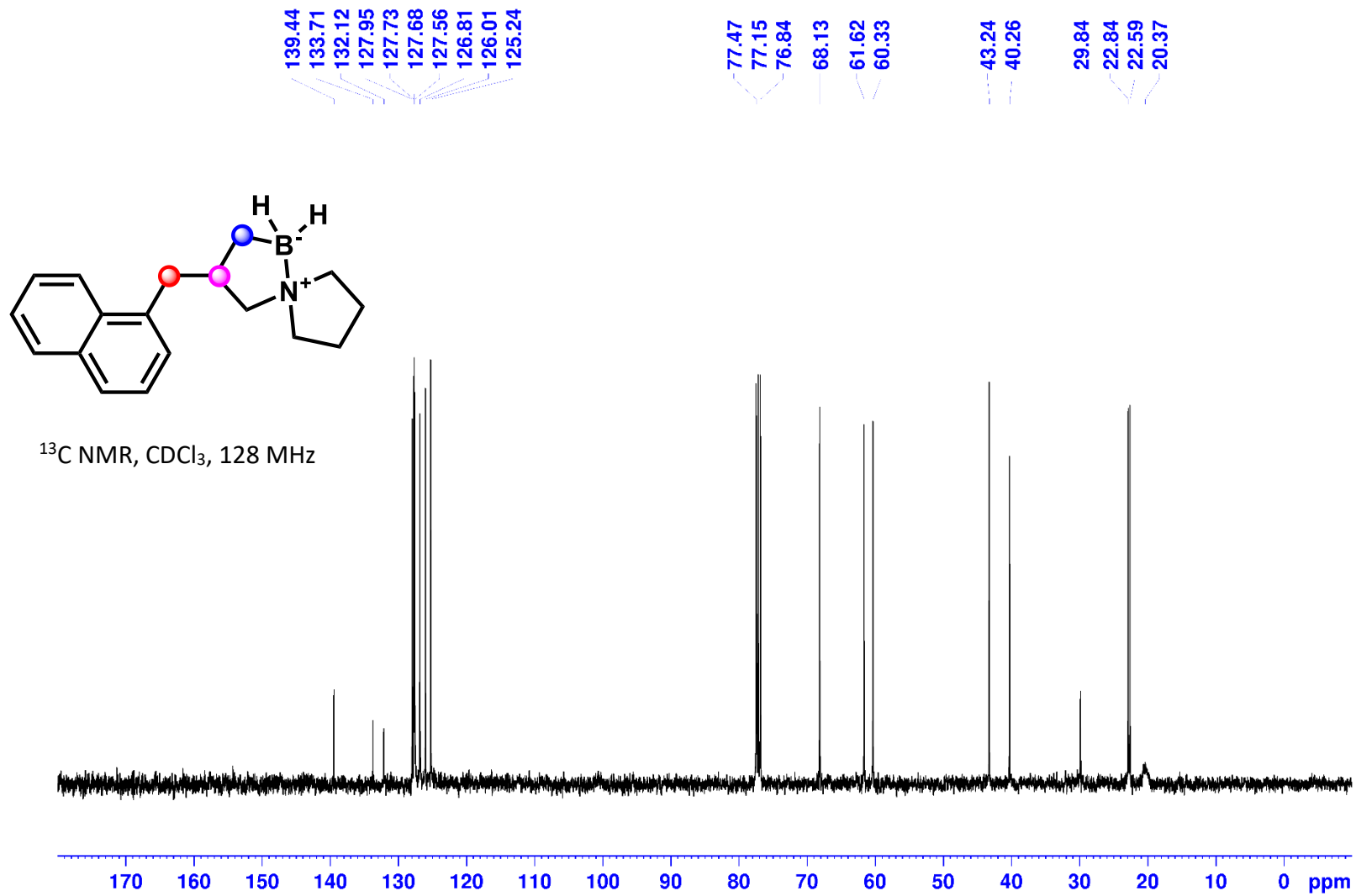
^{11}B NMR, CDCl_3 , 160 MHz



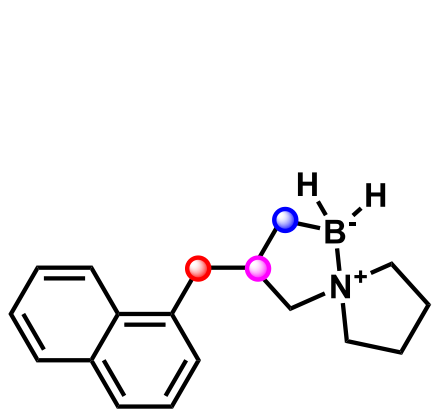
3-(Naphthalen-1-ylmethyl)-5-aza-1-borasp[4.4]nonane (2i):



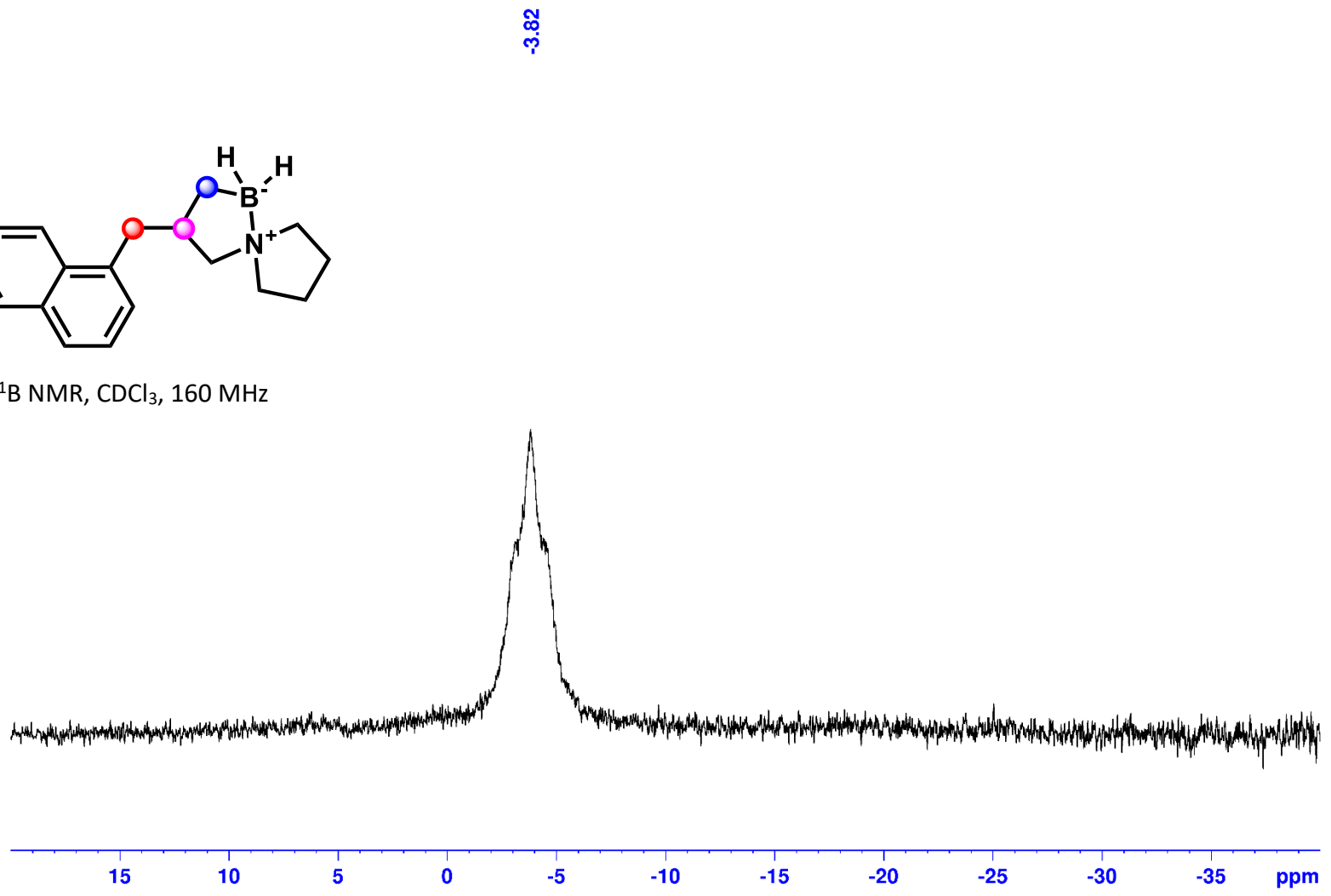
3-(Naphthalen-1-ylmethyl)-5-aza-1-borasp[4.4]nonane (2i):



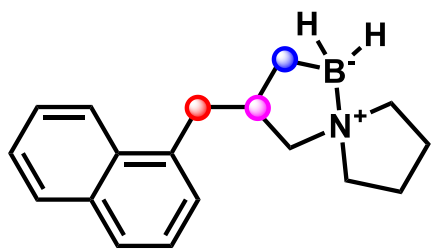
3-(Naphthalen-1-ylmethyl)-5-aza-1-borasp[4.4]nonane (2i):



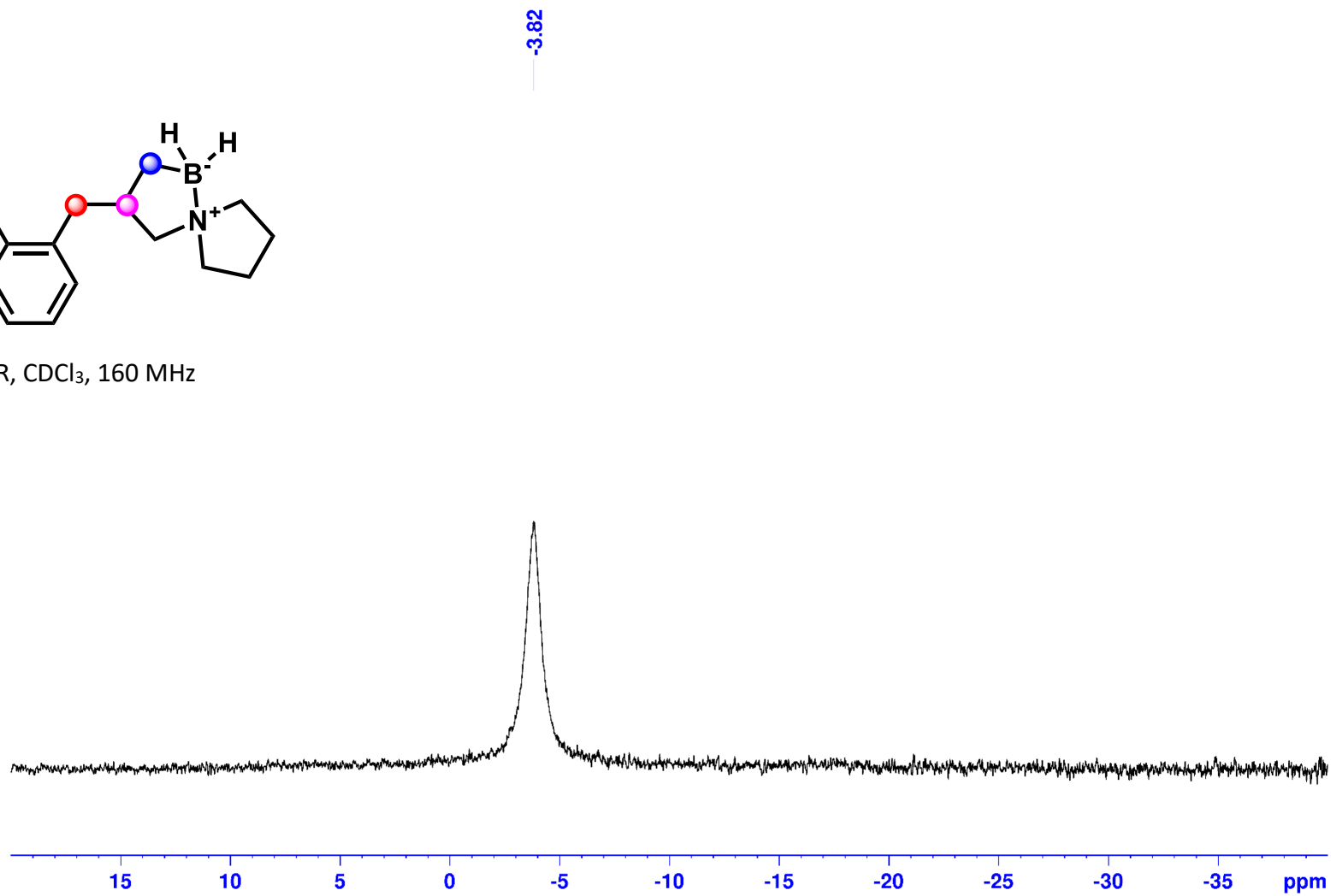
¹¹B NMR, CDCl₃, 160 MHz



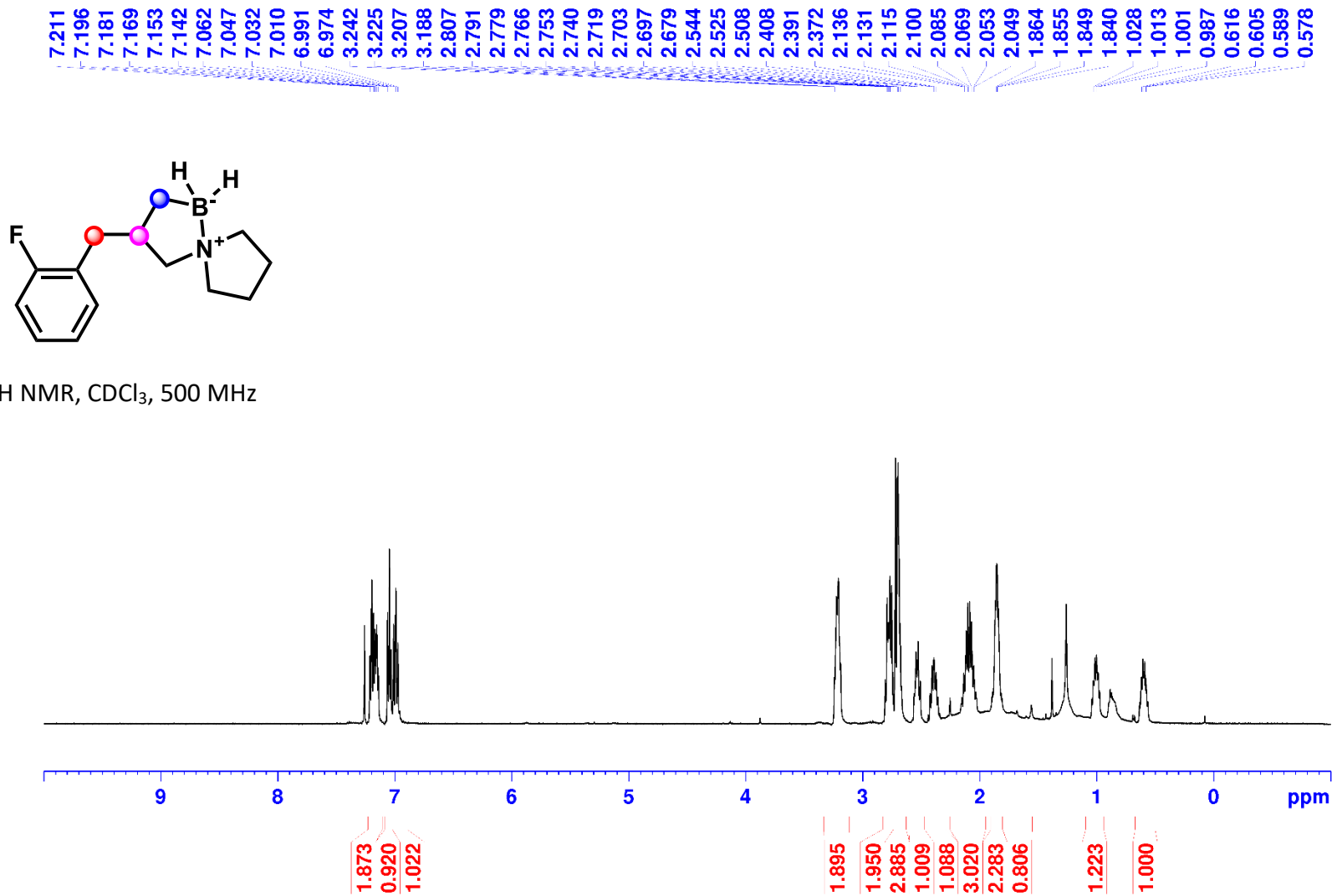
3-(Naphthalen-1-ylmethyl)-5-aza-1-borasp[4.4]nonane (2i):



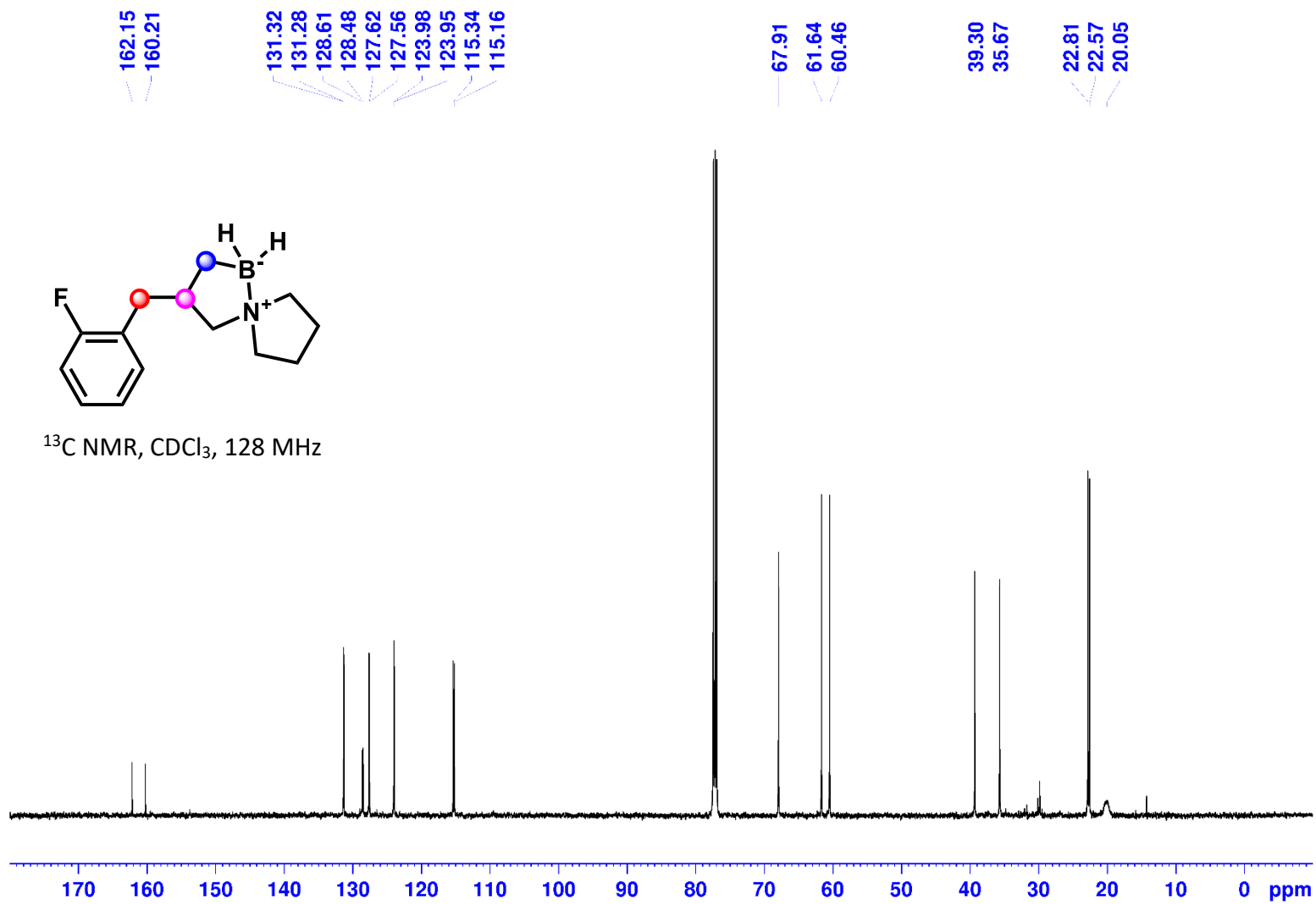
^{11}B NMR, CDCl_3 , 160 MHz



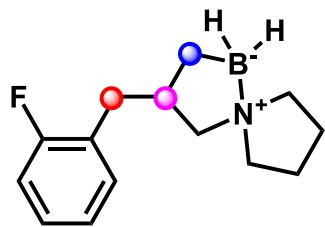
3-(2-Fluorobenzyl)-5-aza-1-borasp[4.4]nonane (2j):



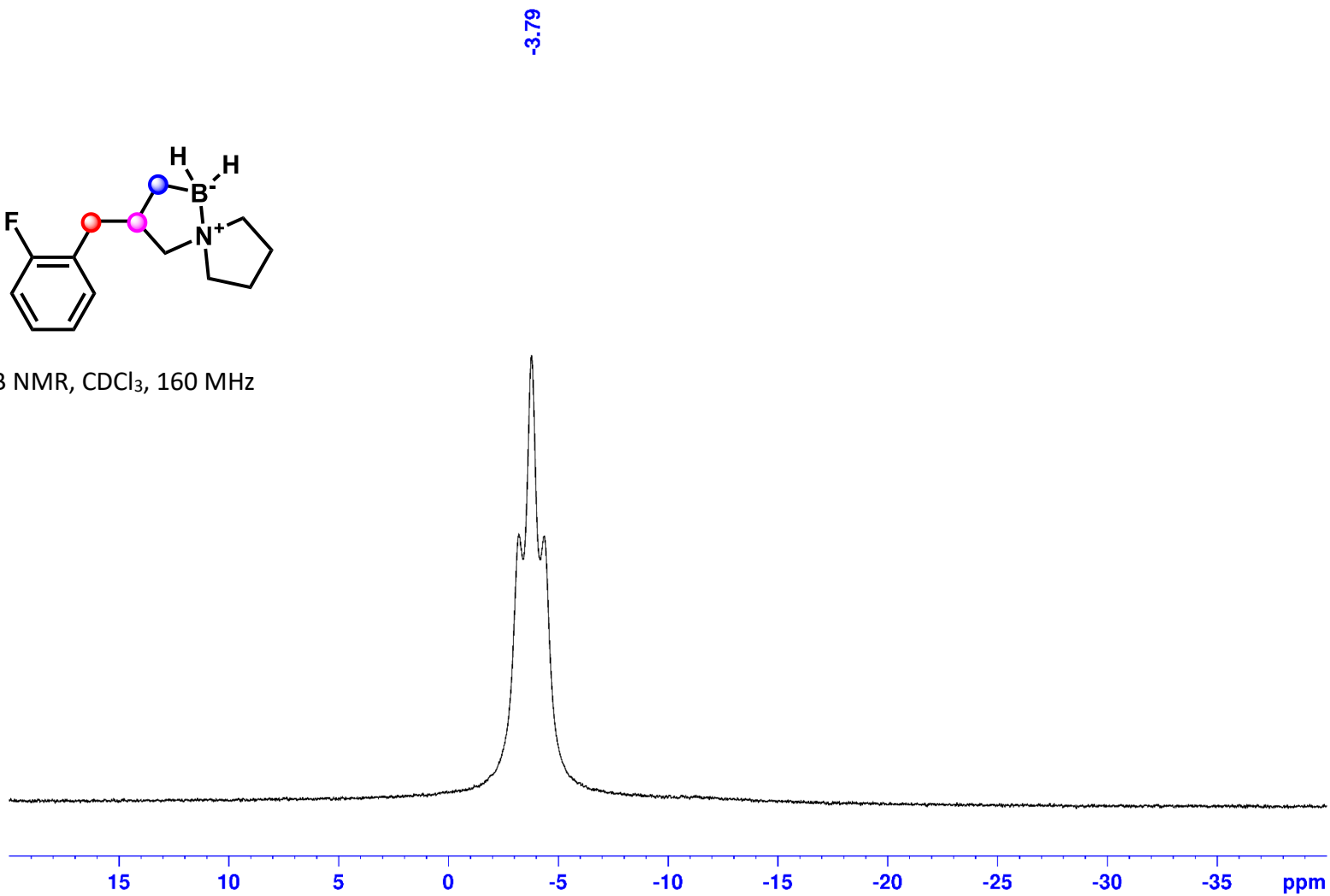
3-(2-Fluorobenzyl)-5-aza-1-borasp[4.4]nonane (2j):



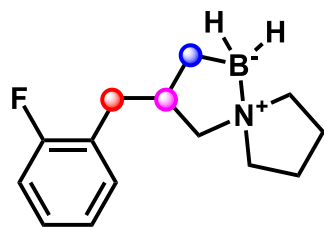
3-(2-Fluorobenzyl)-5-aza-1-borasp[4.4]nonane (2j):



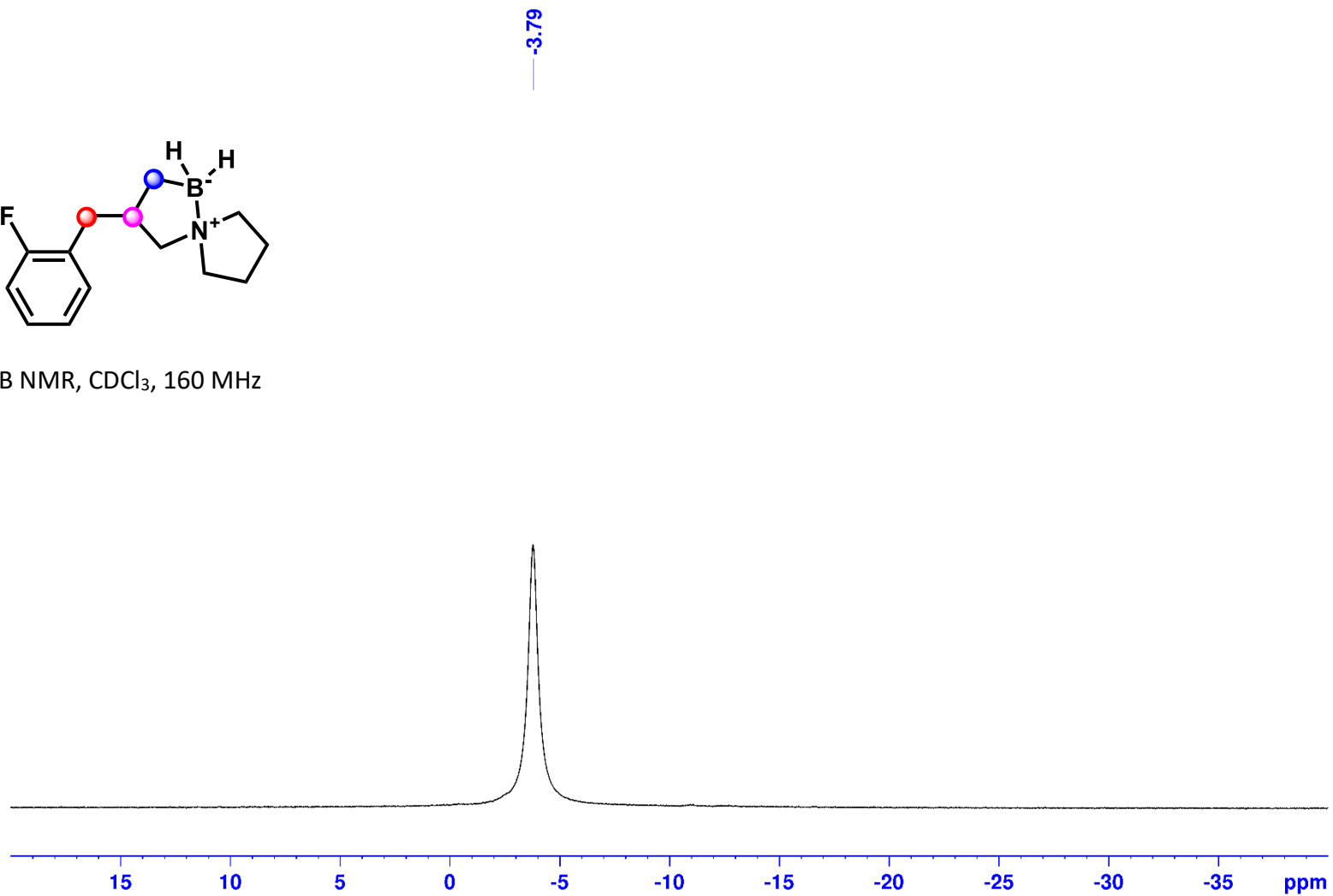
^{11}B NMR, CDCl_3 , 160 MHz



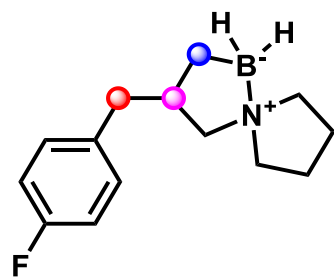
3-(2-Fluorobenzyl)-5-aza-1-borasp[4.4]nonane (2j):



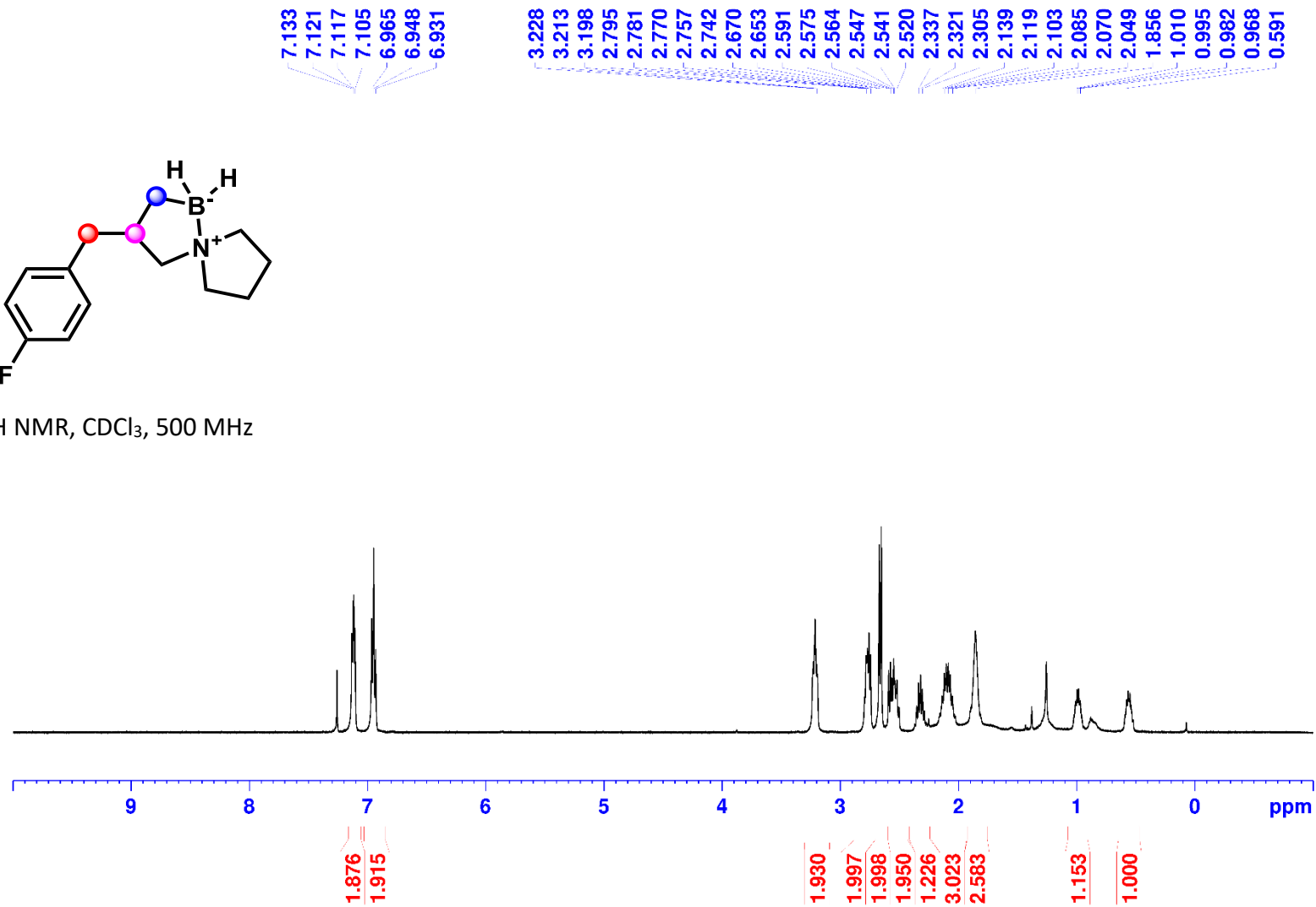
^{11}B NMR, CDCl_3 , 160 MHz



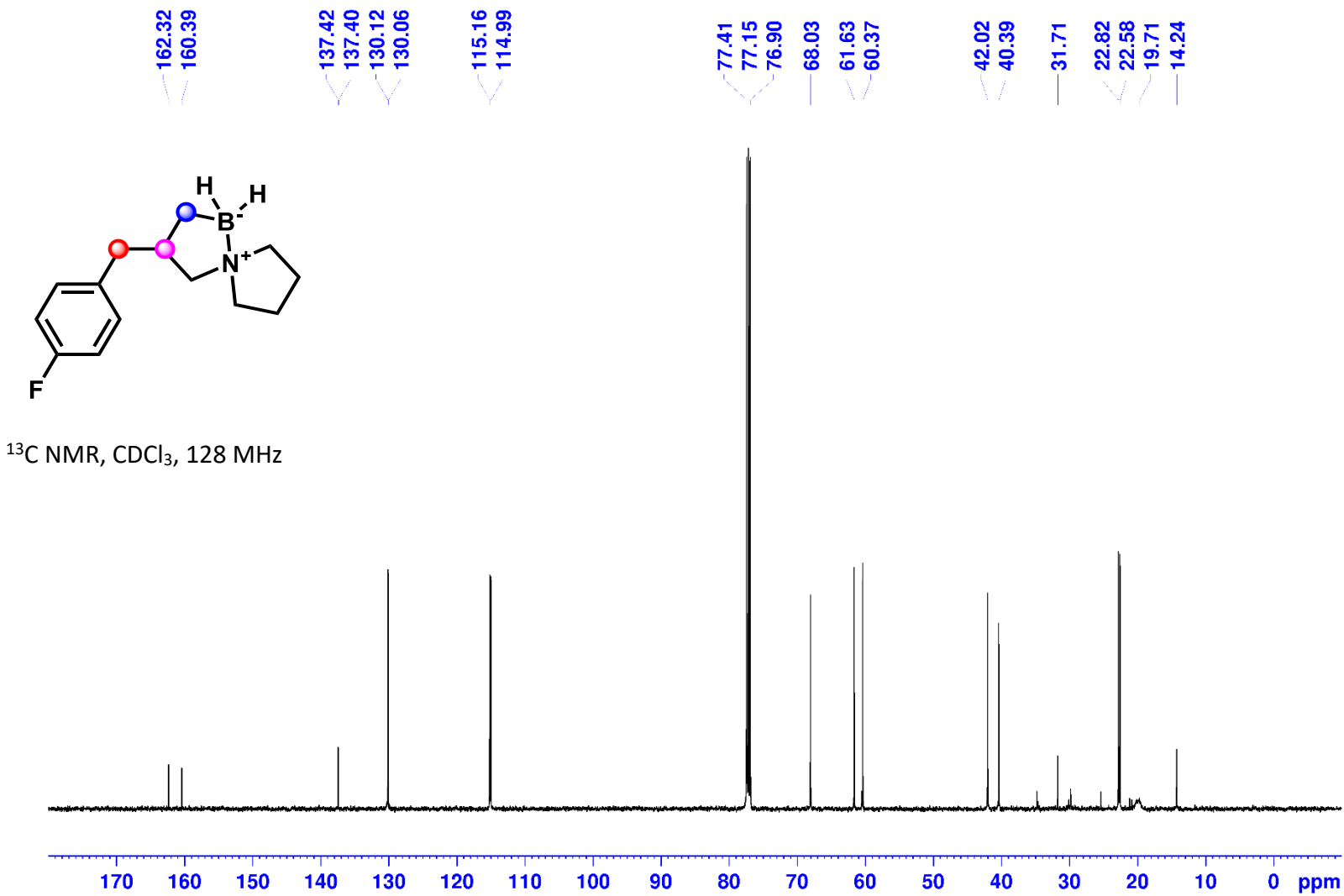
3-(4-Fluorobenzyl)-5-aza-1-borasp[4.4]nonane (2k):



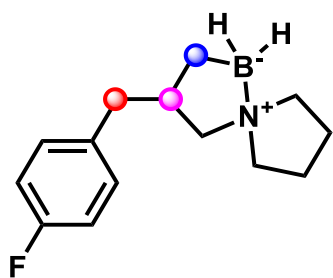
^1H NMR, CDCl_3 , 500 MHz



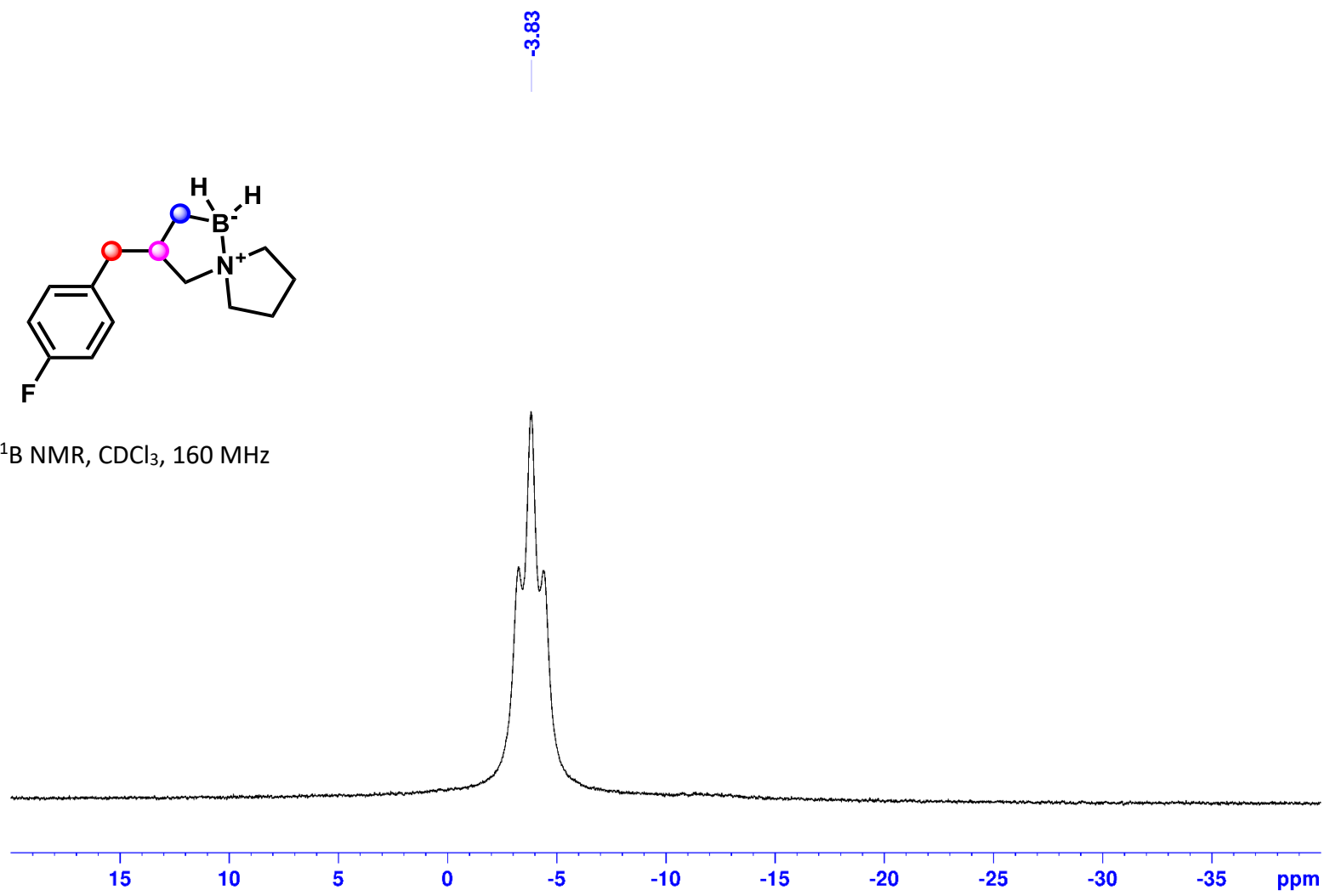
3-(4-Fluorobenzyl)-5-aza-1-borasp[4.4]nonane (2k):



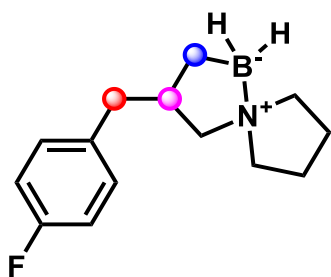
3-(4-Fluorobenzyl)-5-aza-1-borasp[4.4]nonane (2k):



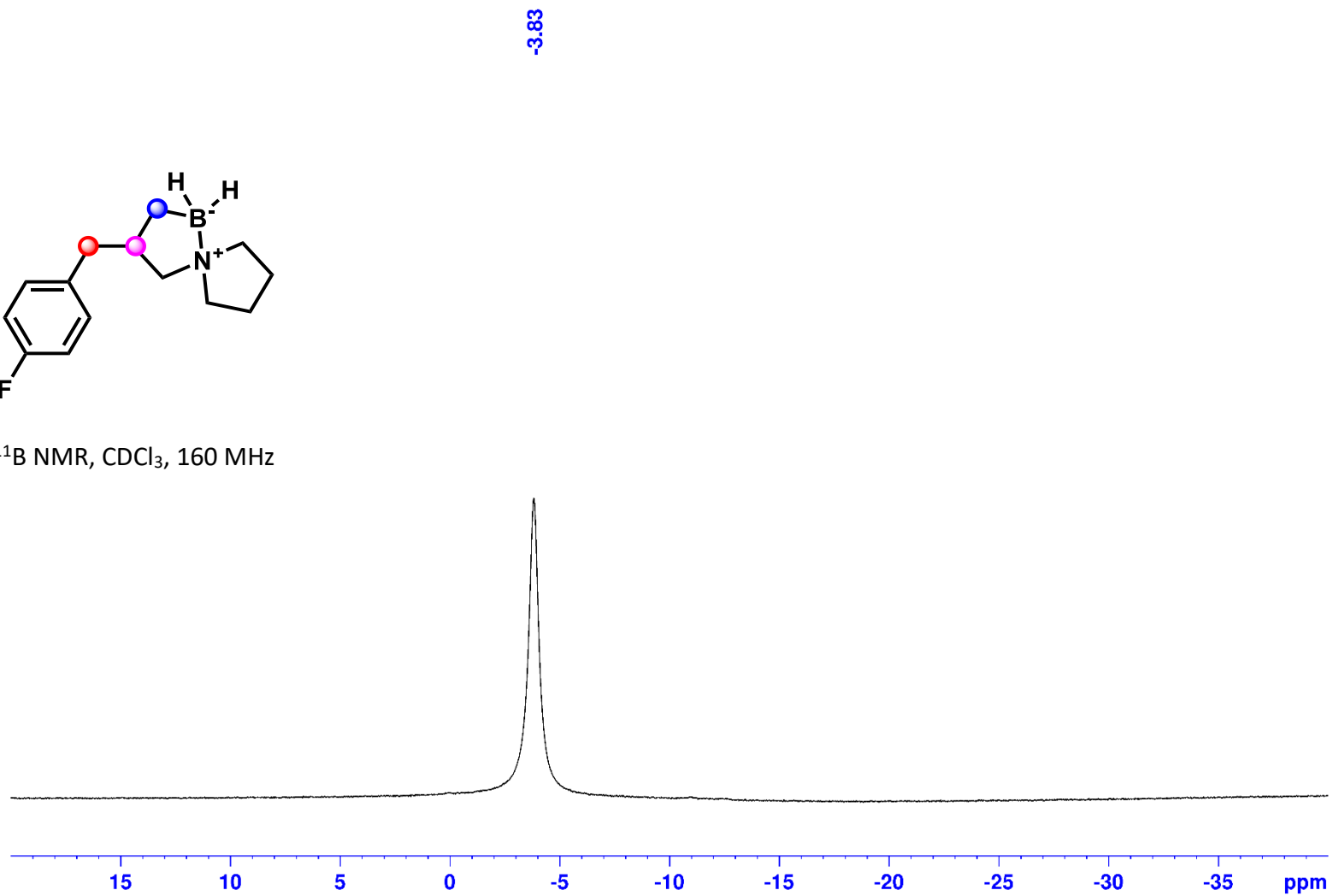
^{11}B NMR, CDCl_3 , 160 MHz



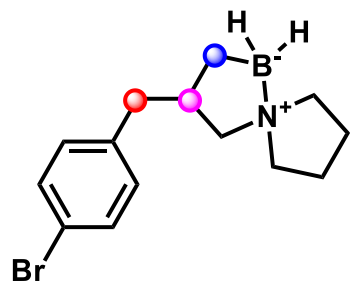
3-(4-Fluorobenzyl)-5-aza-1-borasp[4.4]nonane (2k):



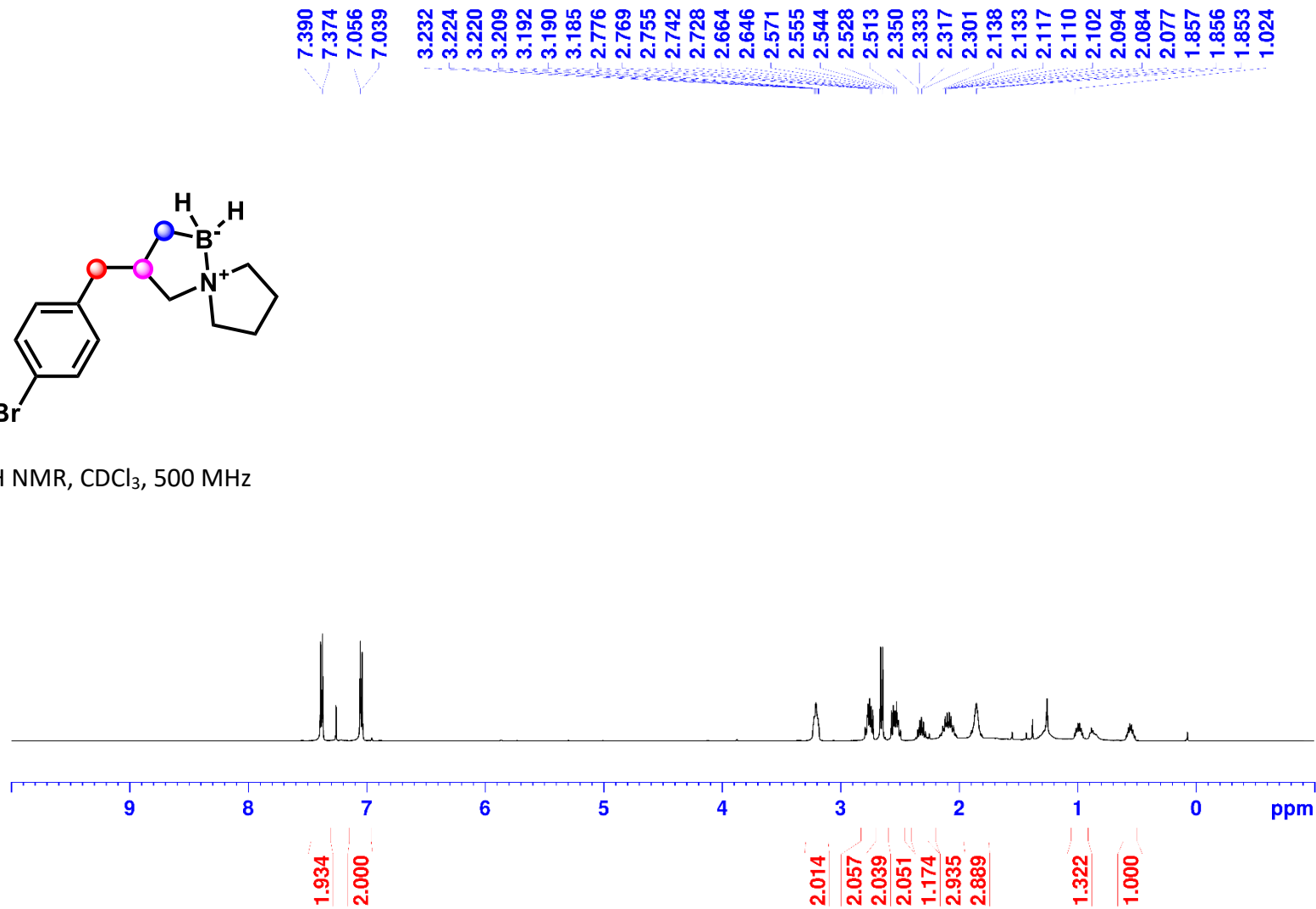
^{11}B NMR, CDCl_3 , 160 MHz



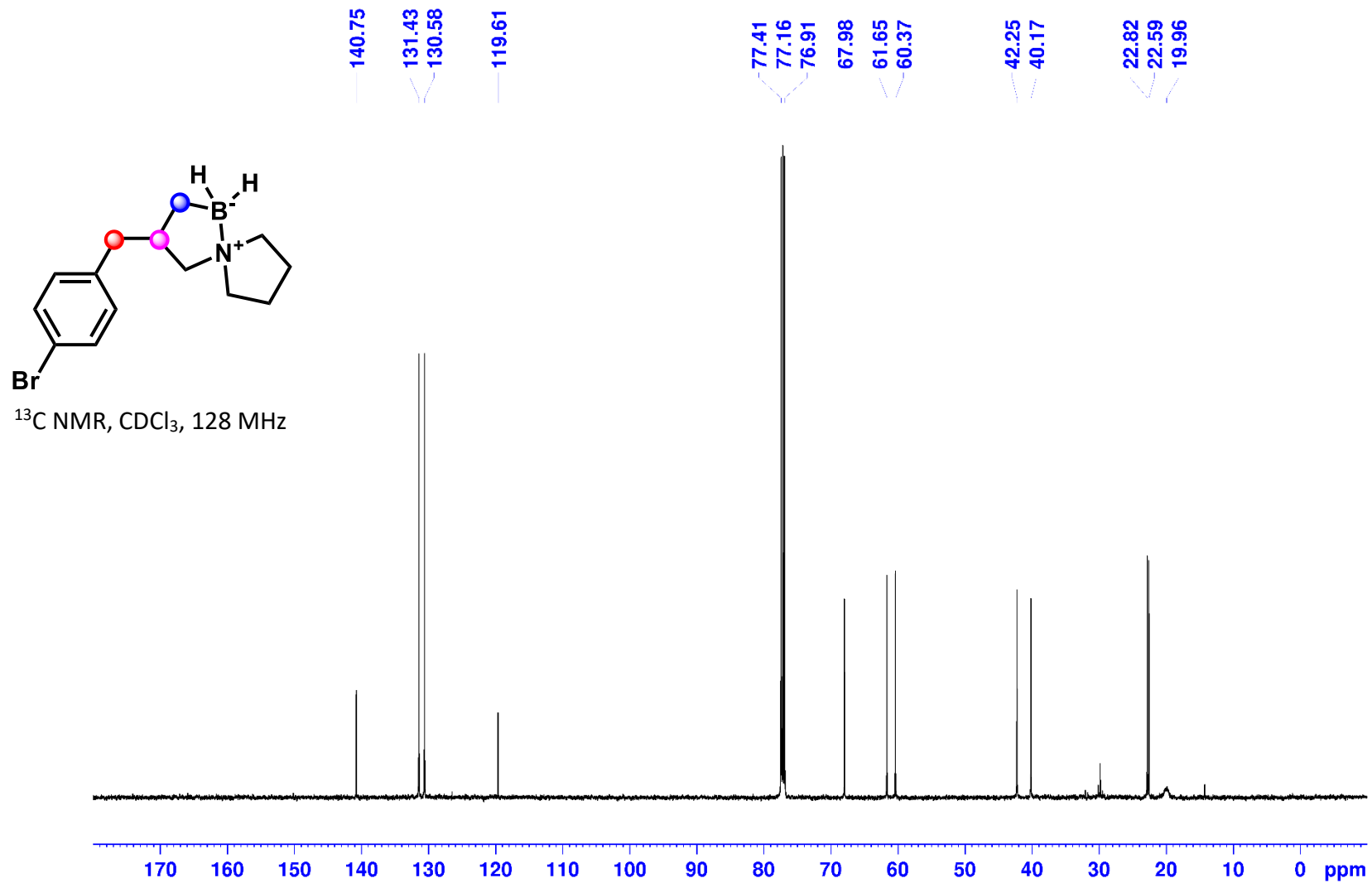
3-(4-Bromobenzyl)-5-aza-1-borasp[4.4]nonane (2l):



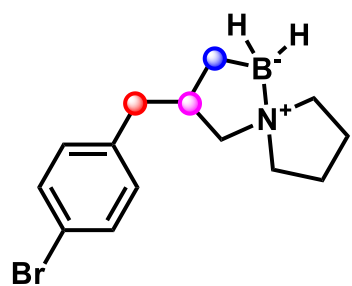
¹H NMR, CDCl₃, 500 MHz



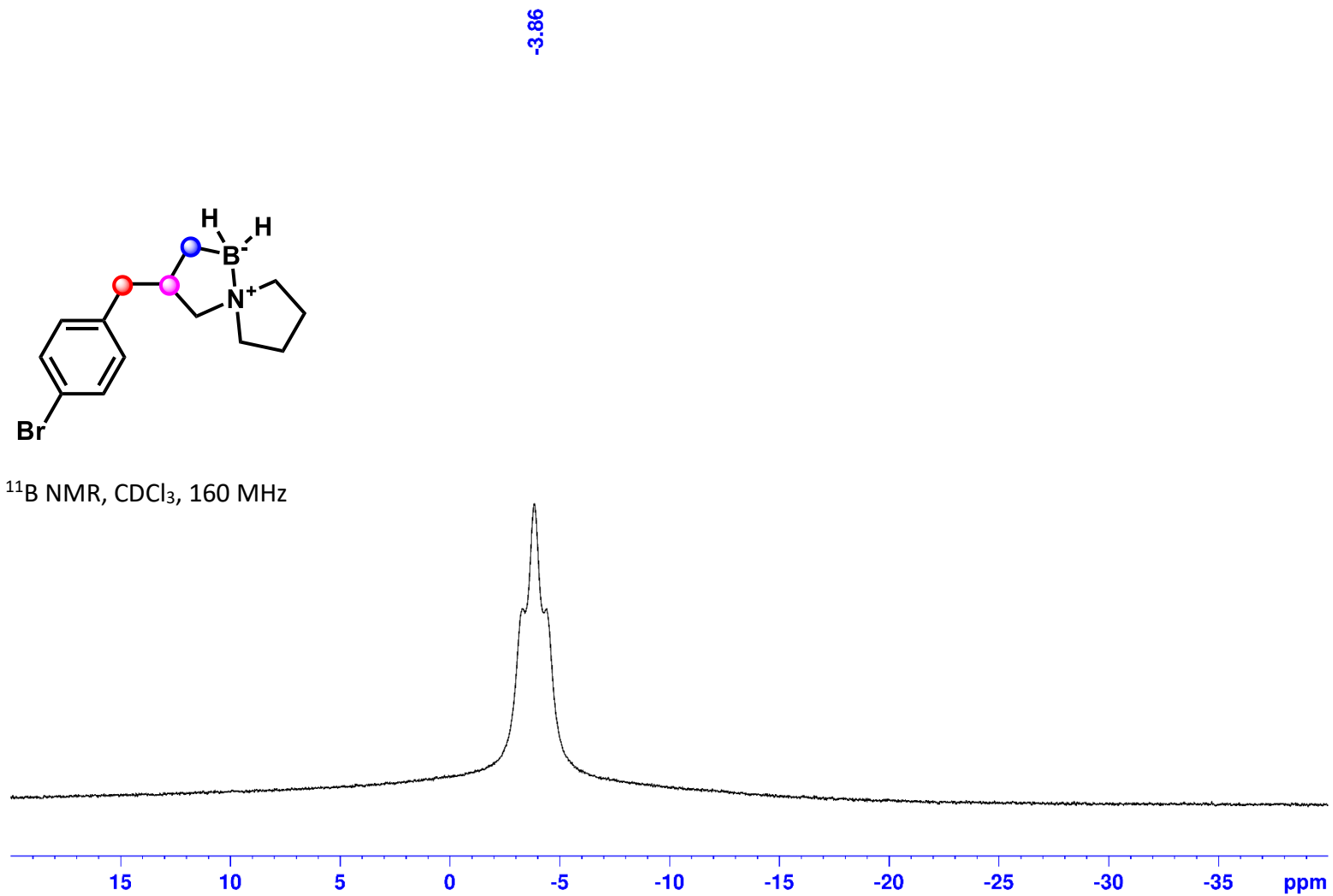
3-(4-Bromobenzyl)-5-aza-1-borasp[4.4]nonane (2l):



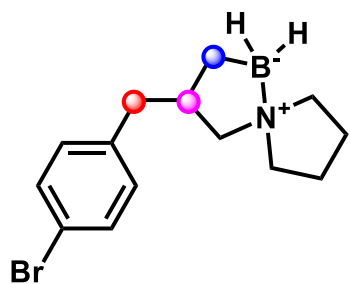
3-(4-Bromobenzyl)-5-aza-1-borasp[4.4]nonane (2l):



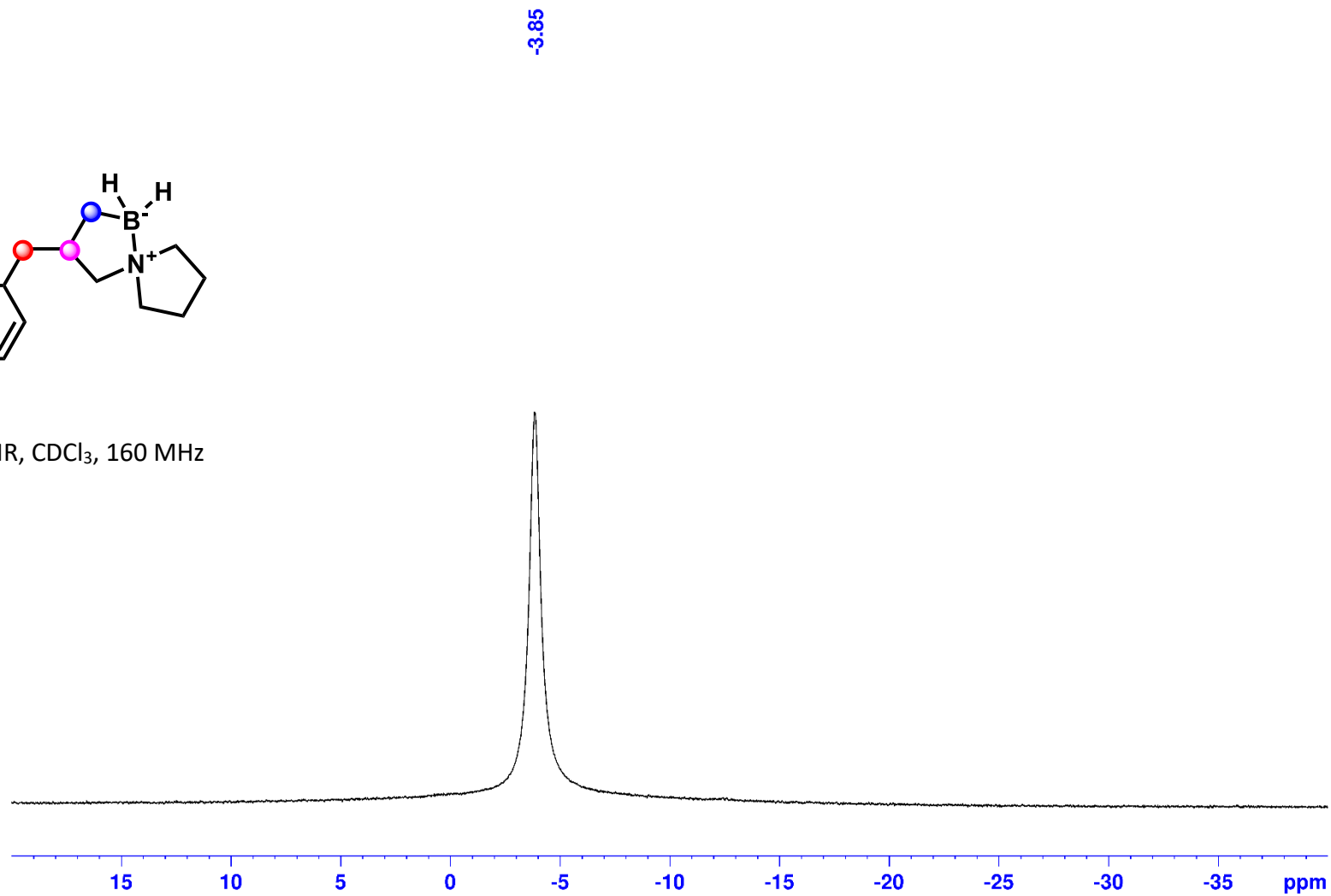
^{11}B NMR, CDCl_3 , 160 MHz



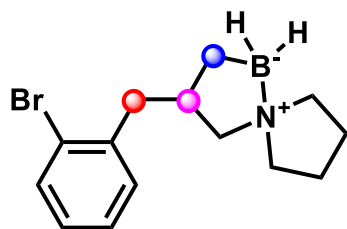
3-(4-Bromobenzyl)-5-aza-1-borasp[4.4]nonane (2l):



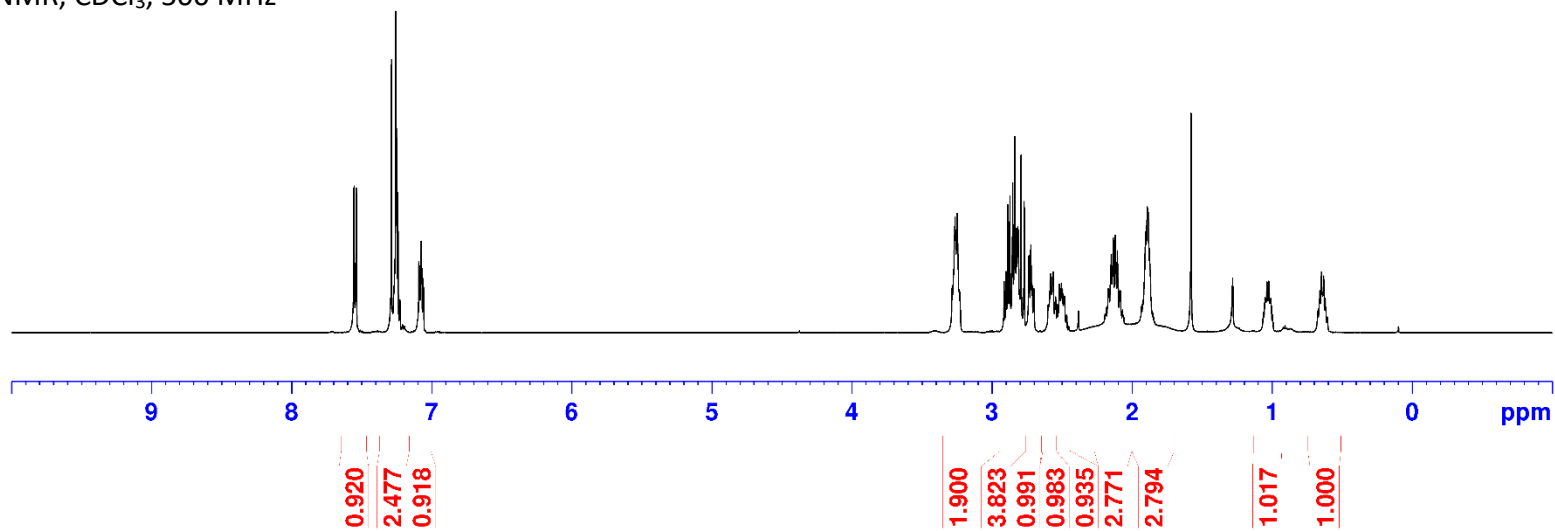
^{11}B NMR, CDCl_3 , 160 MHz



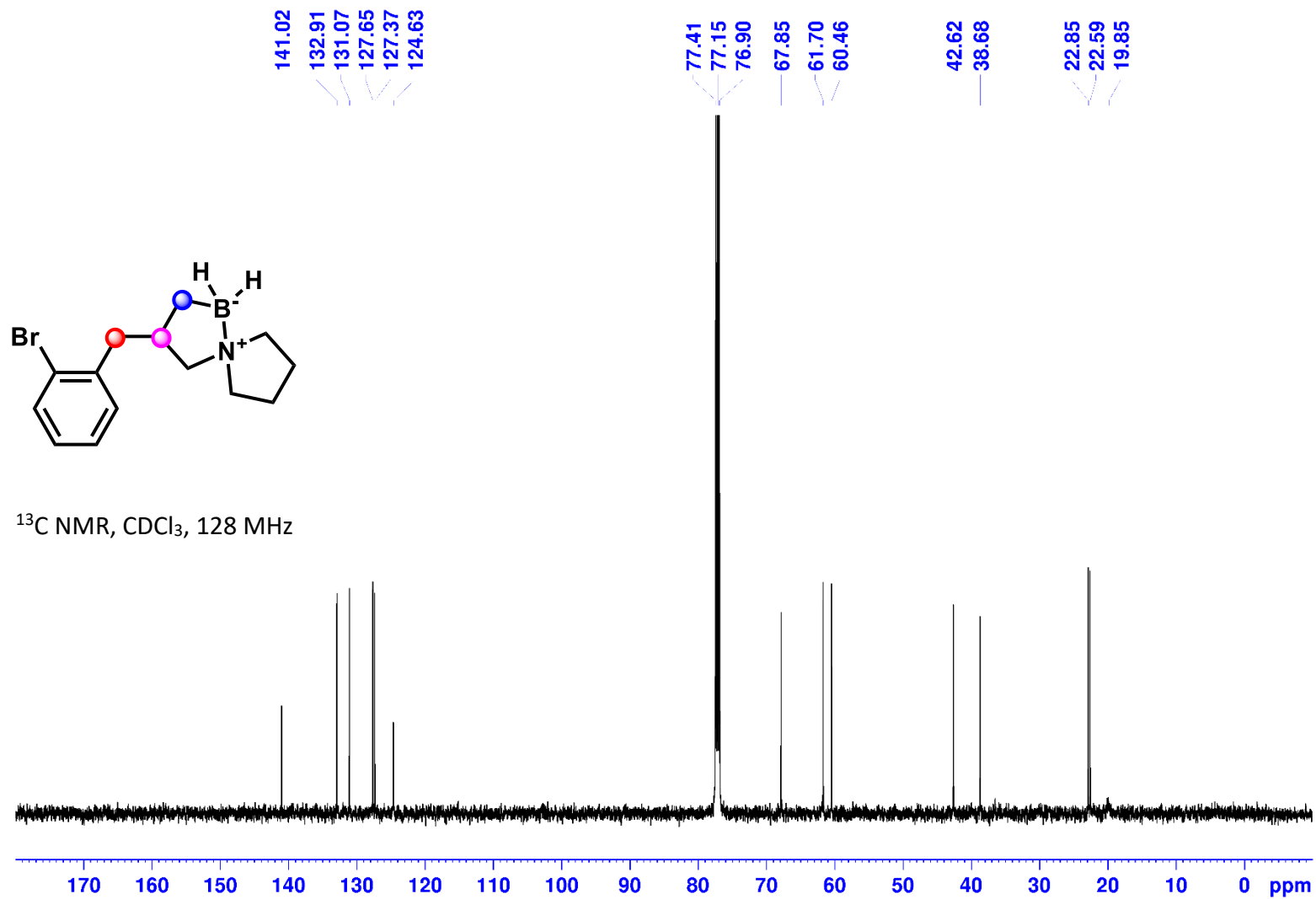
3-(2-Bromobenzyl)-5-aza-1-borasp[4.4]nonane (2m):



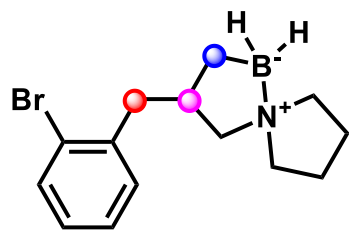
^1H NMR, CDCl_3 , 500 MHz



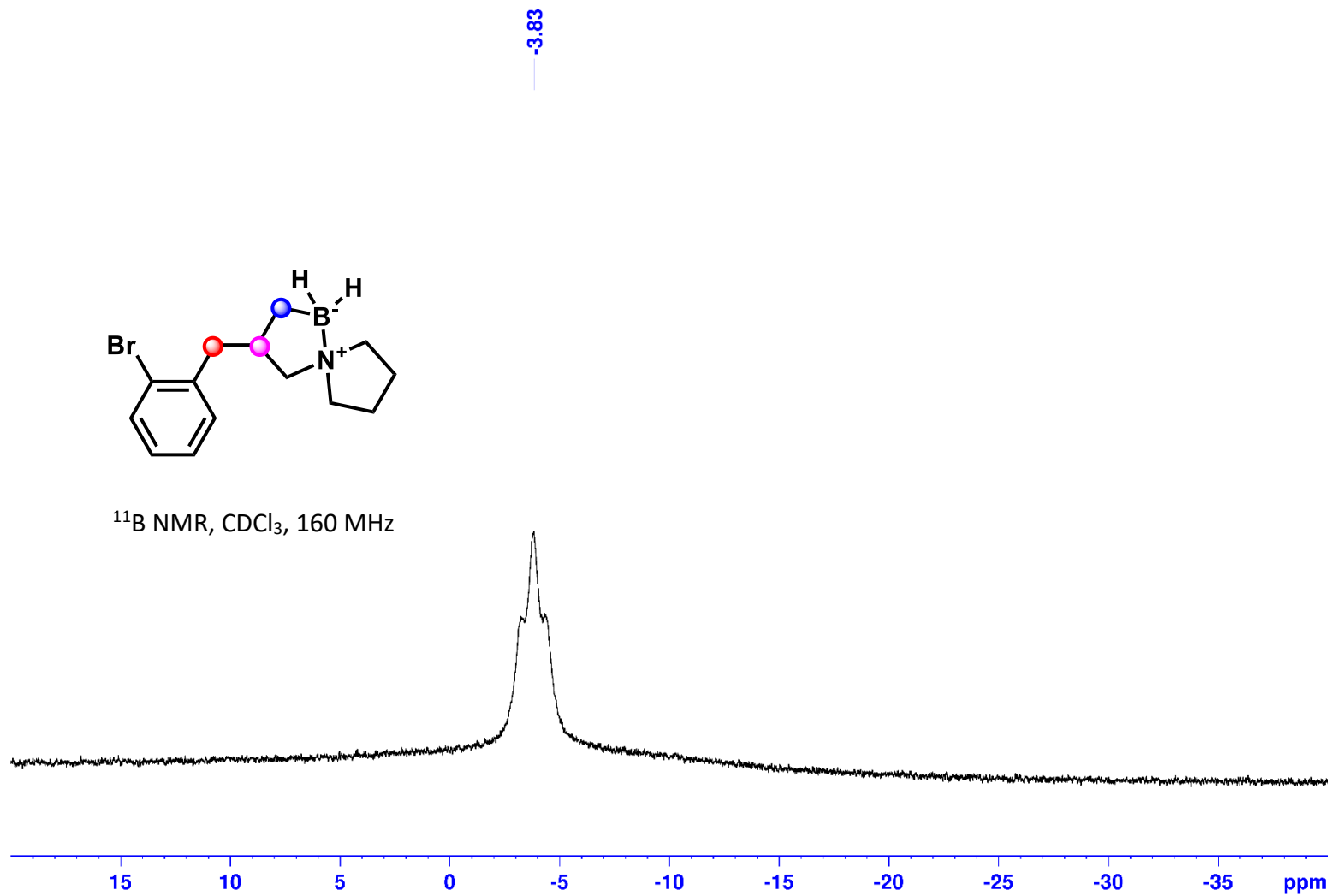
3-(2-Bromobenzyl)-5-aza-1-borasp[4.4]nonane (2m):



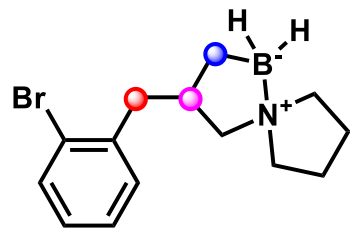
3-(2-Bromobenzyl)-5-aza-1-borasp[4.4]nonane (2m):



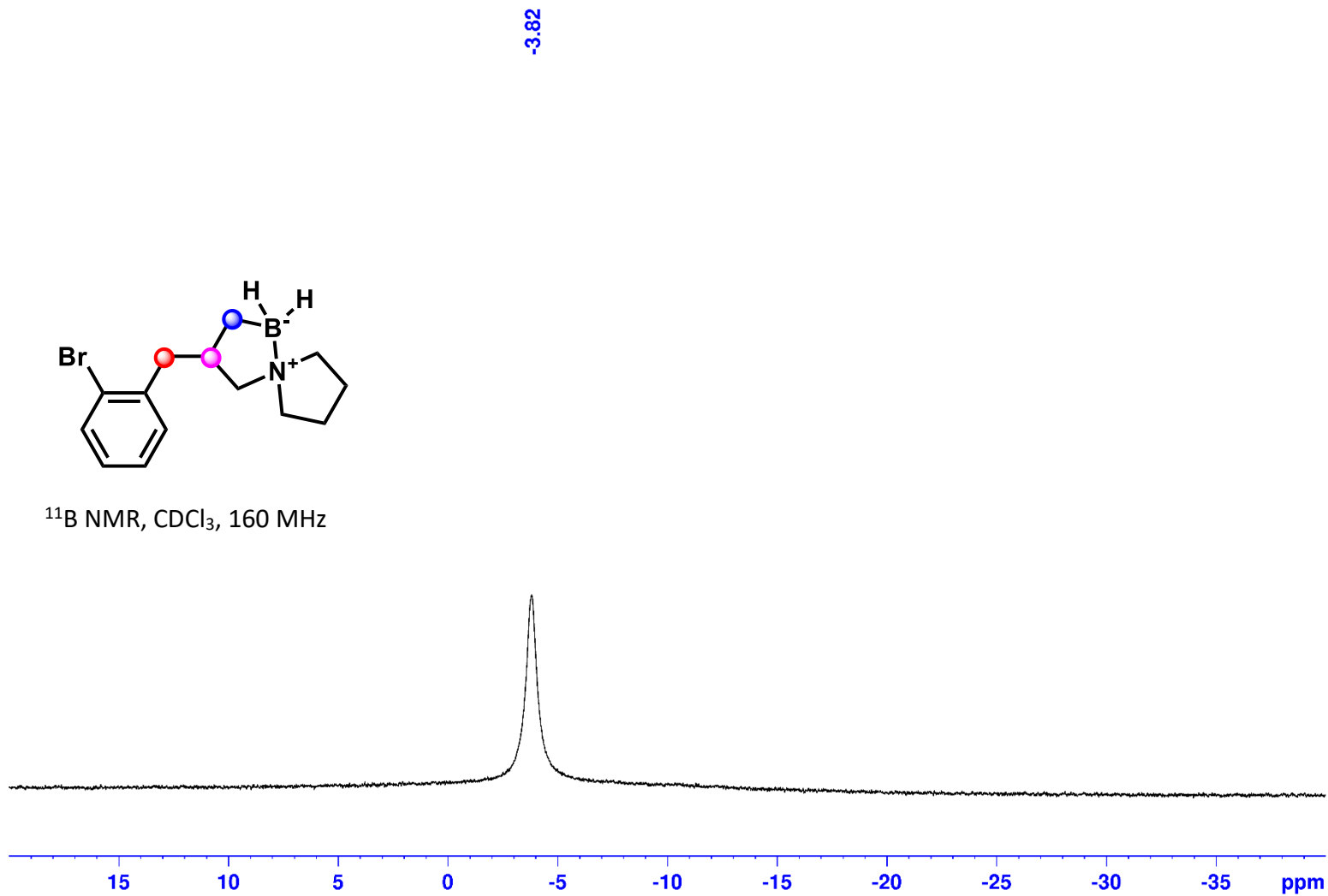
^{11}B NMR, CDCl_3 , 160 MHz



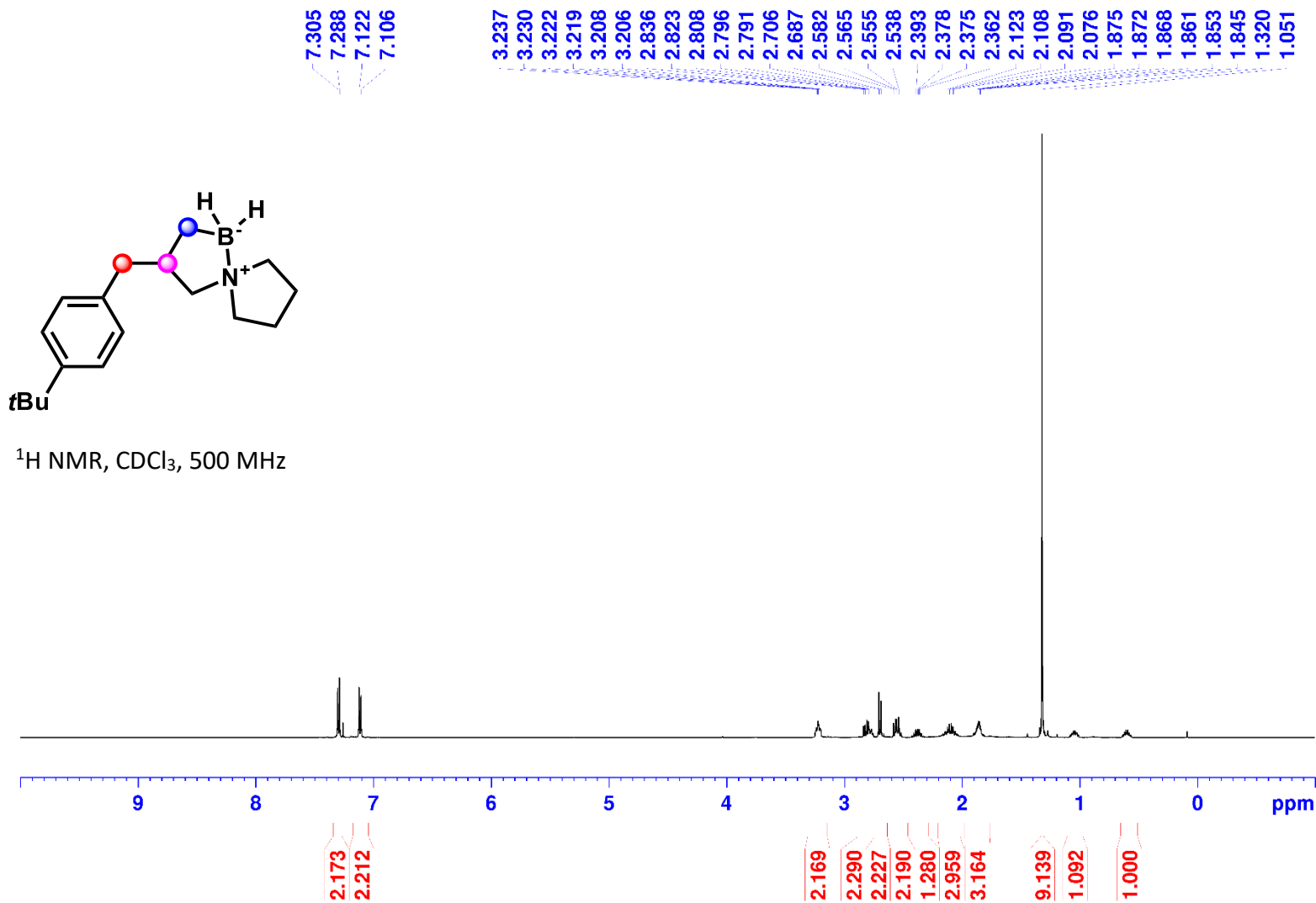
3-(2-Bromobenzyl)-5-aza-1-borasp[4.4]nonane (2m):



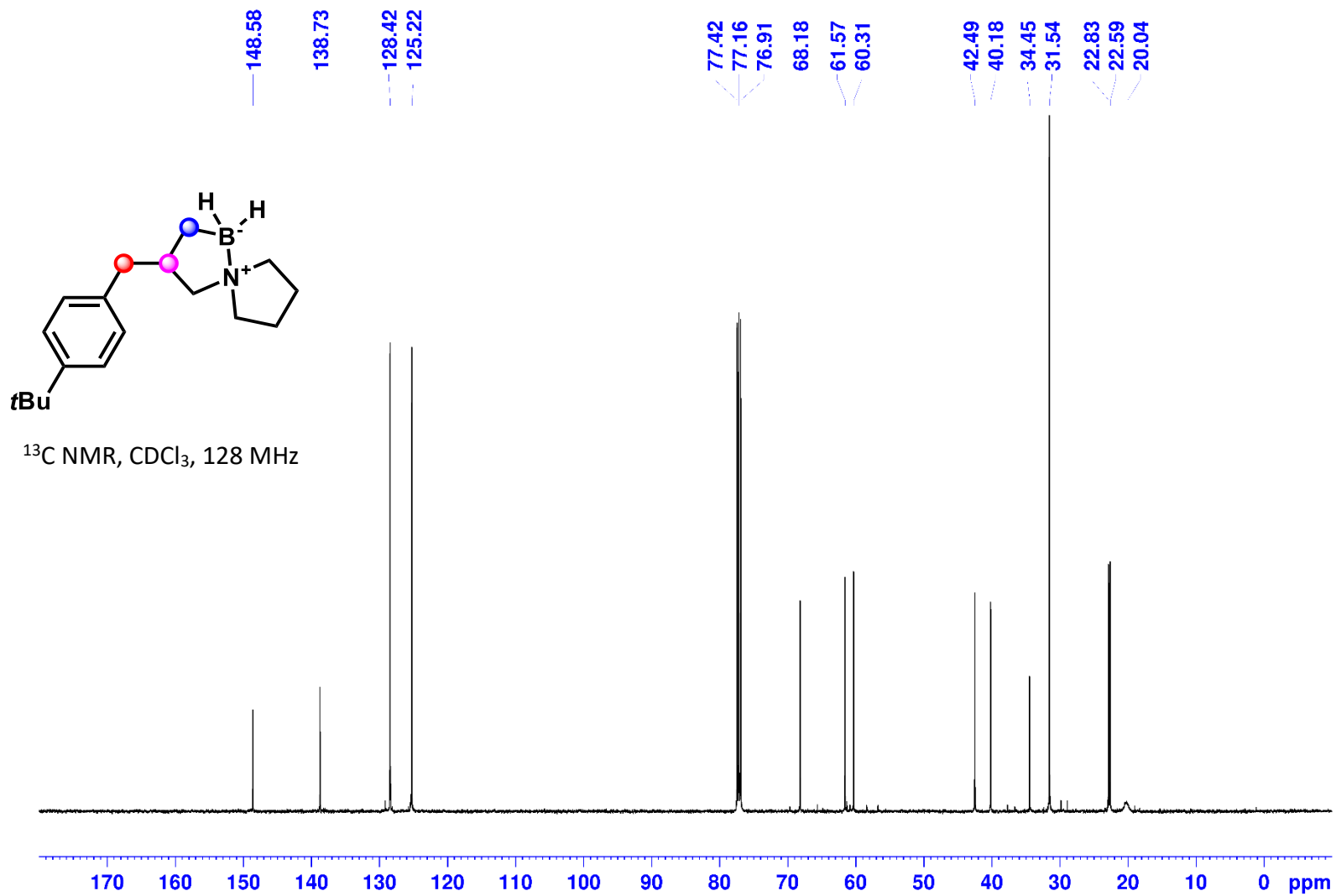
^{11}B NMR, CDCl_3 , 160 MHz



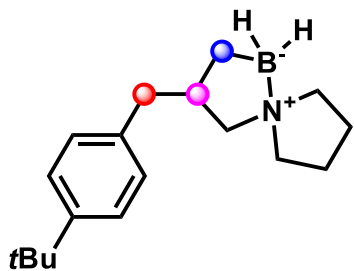
3-(4-(*tert*-Butyl)benzyl)-5-aza-1-borasp[4.4]nonane (2n):



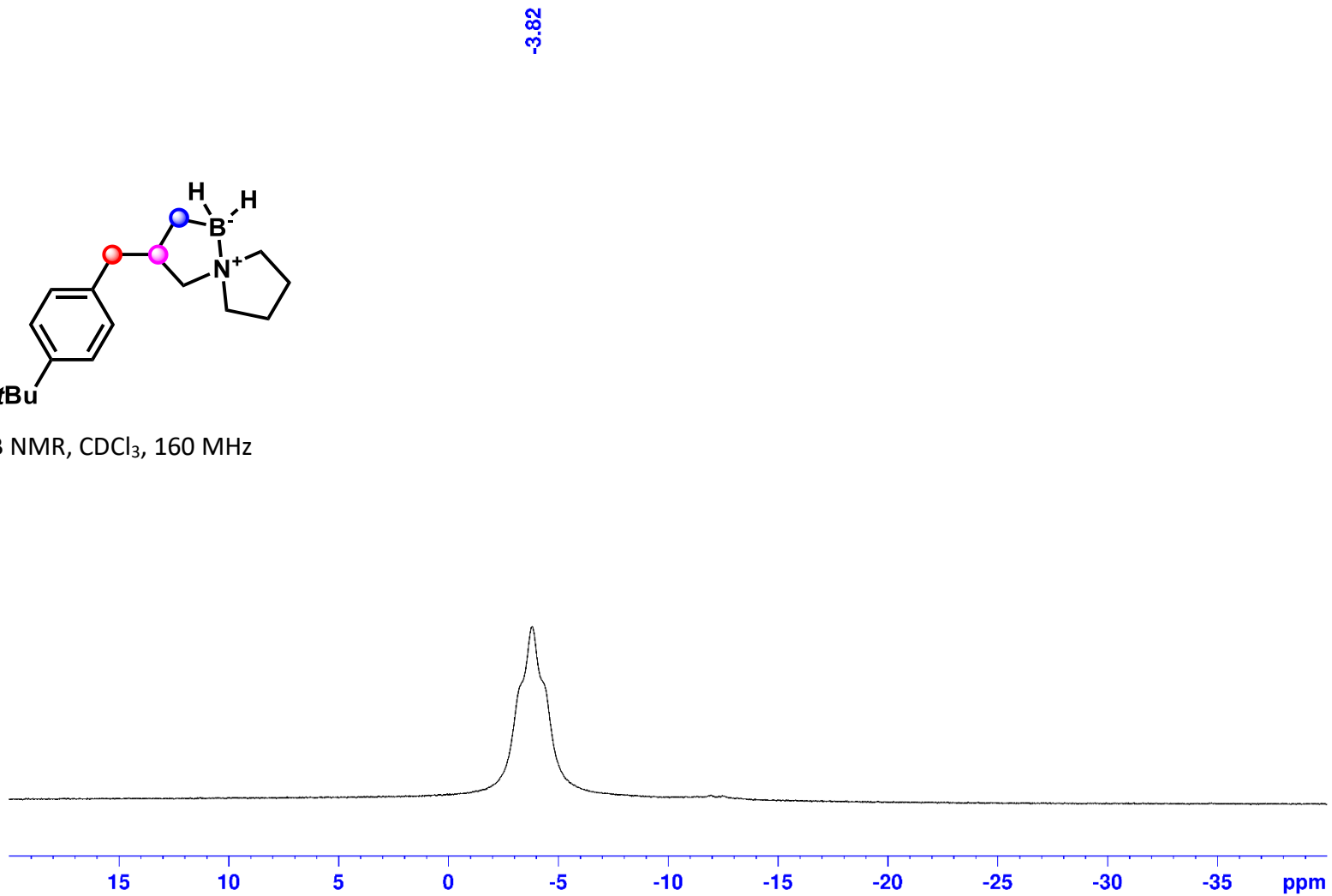
3-(4-(*tert*-Butyl)benzyl)-5-aza-1-borasp[4.4]nonane (2n):



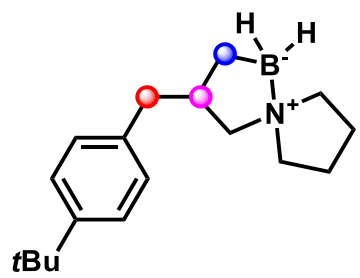
3-(4-(*tert*-Butyl)benzyl)-5-aza-1-borasp[4.4]nonane (2n):



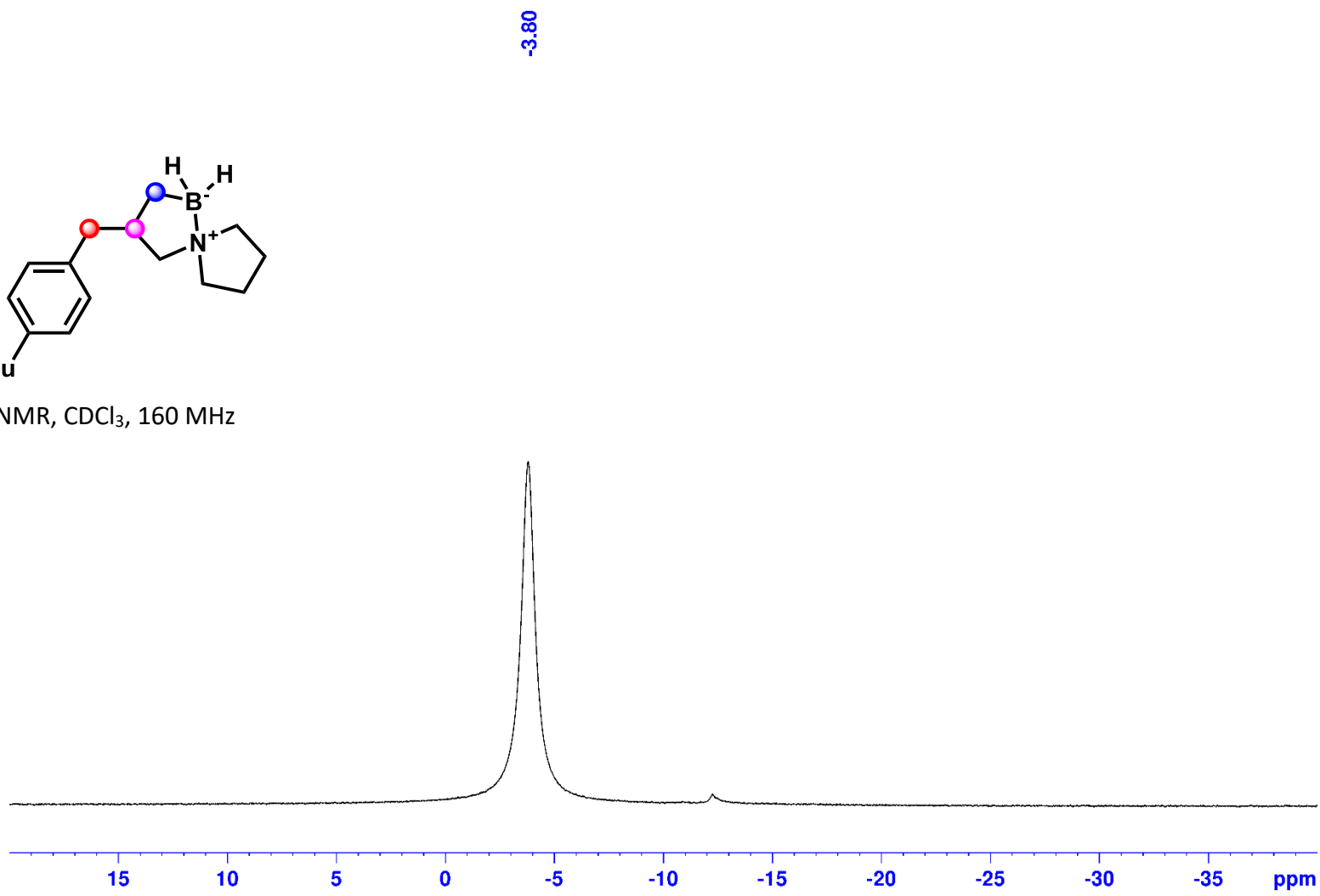
^{11}B NMR, CDCl_3 , 160 MHz



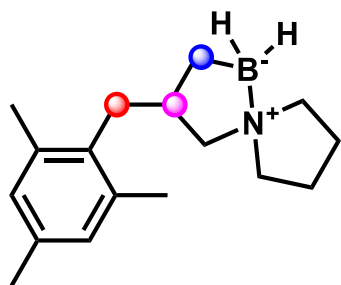
3-(4-(*tert*-Butyl)benzyl)-5-aza-1-borasp[4.4]nonane (2n):



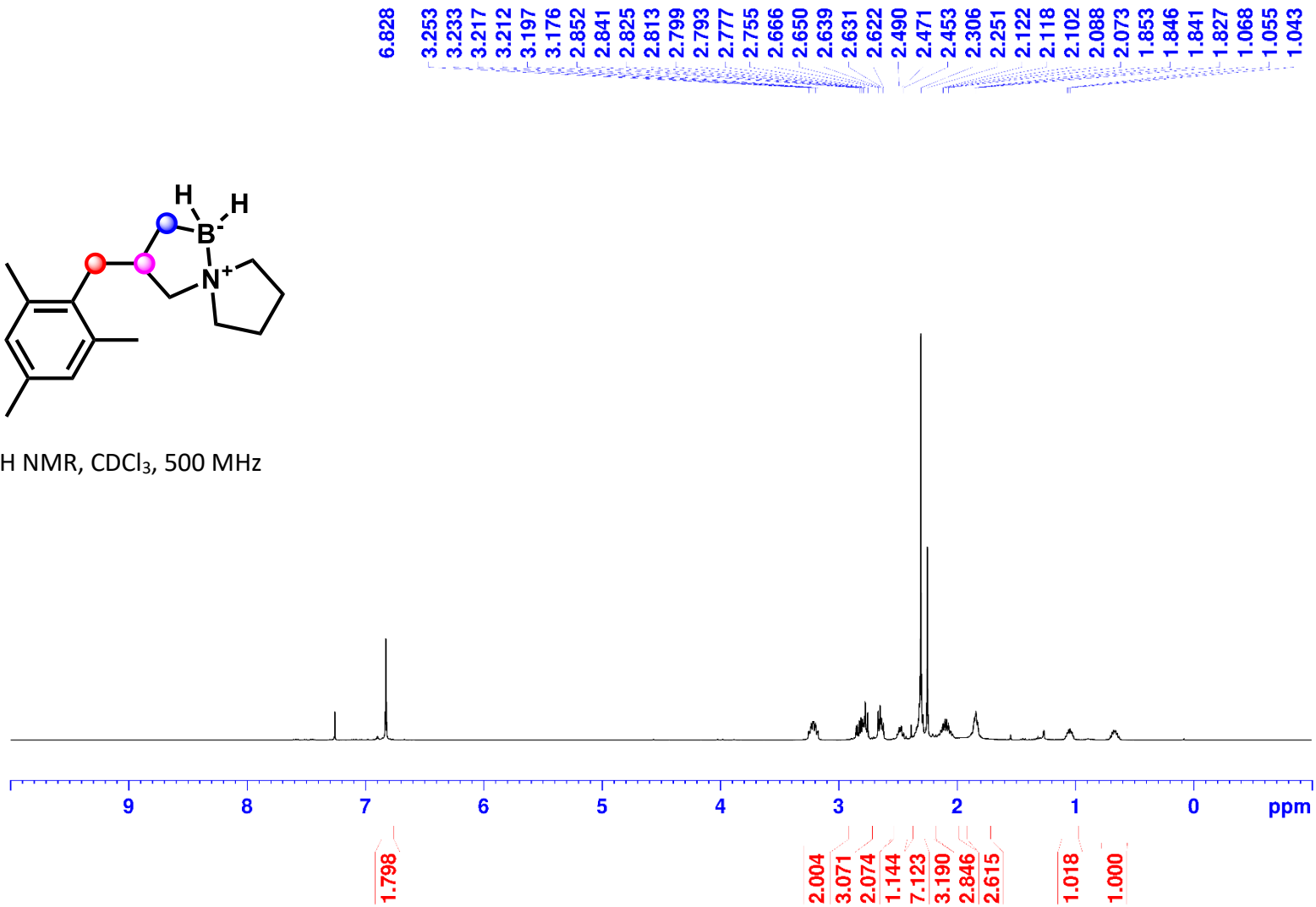
^{11}B NMR, CDCl_3 , 160 MHz



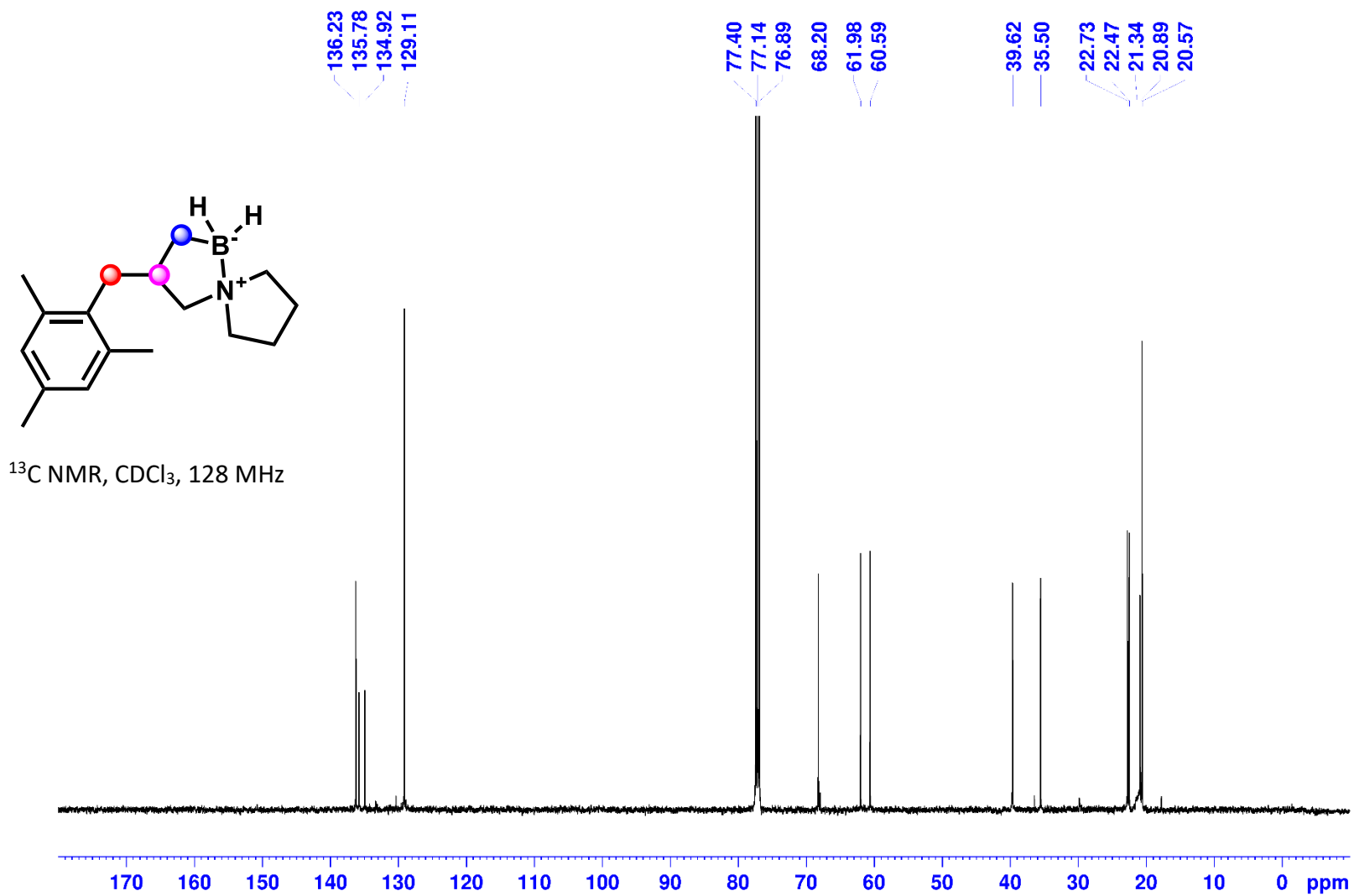
3-(2,4,6-Trimethylbenzyl)-5-aza-1-borasp[4.4]nonane (2o):



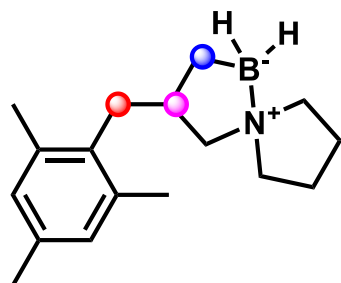
¹H NMR, CDCl₃, 500 MHz



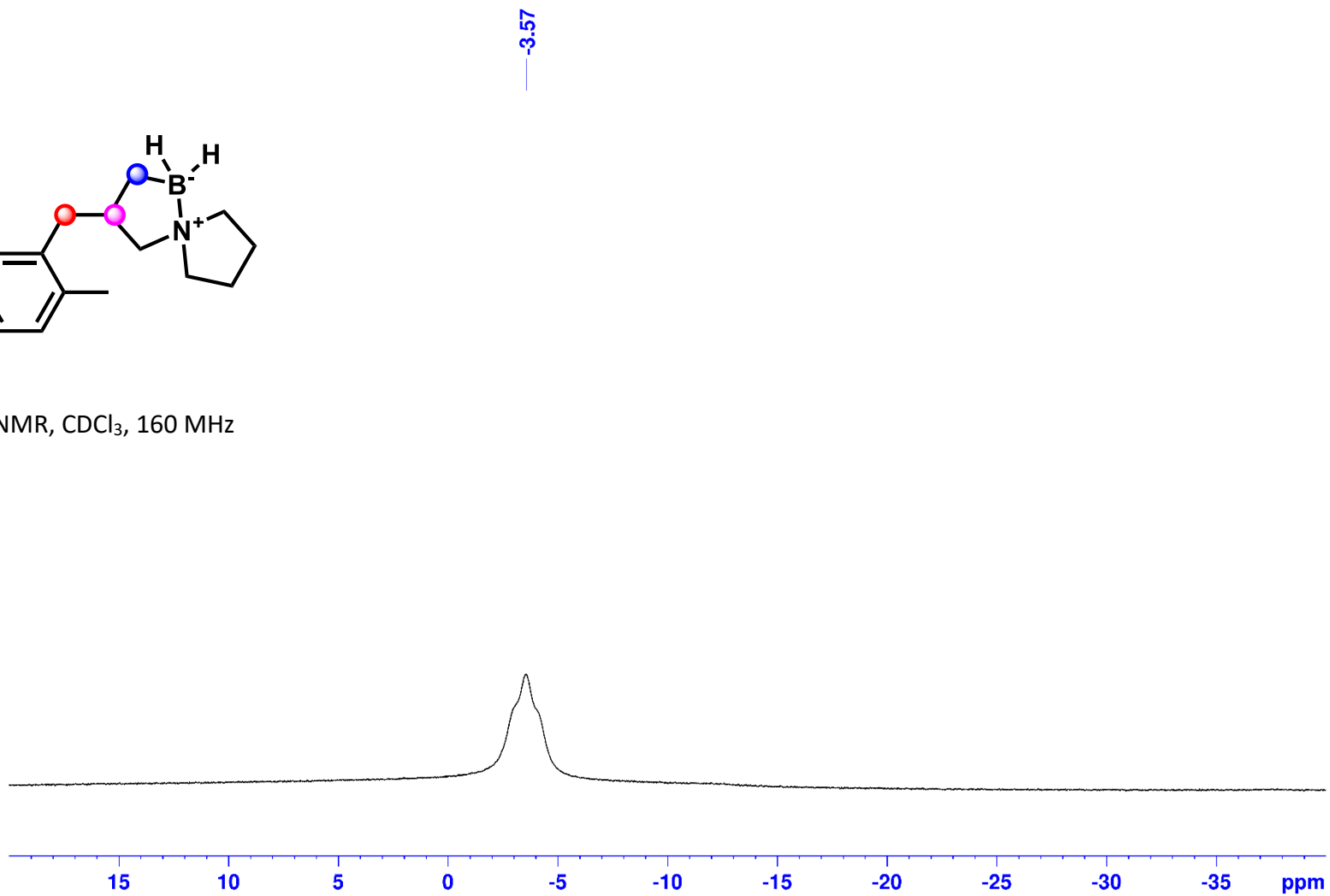
3-(2,4,6-Trimethylbenzyl)-5-aza-1-borasp[4.4]nonane (2o):



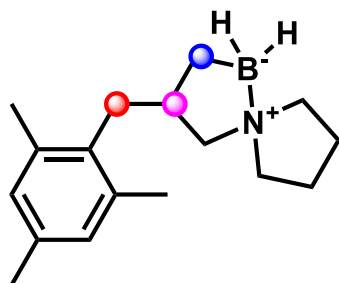
3-(2,4,6-Trimethylbenzyl)-5-aza-1-borasp[4.4]nonane (2o):



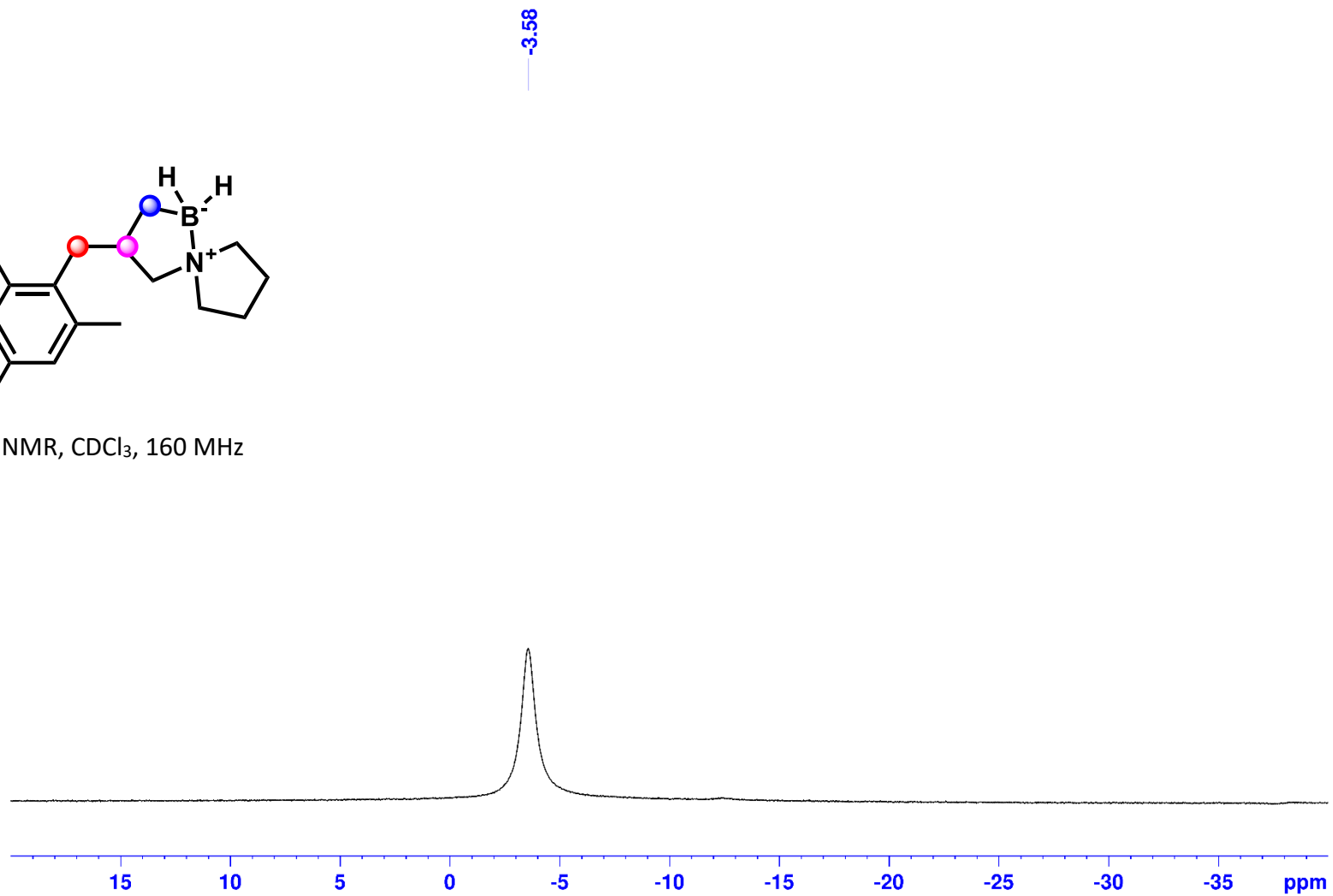
^{11}B NMR, CDCl_3 , 160 MHz



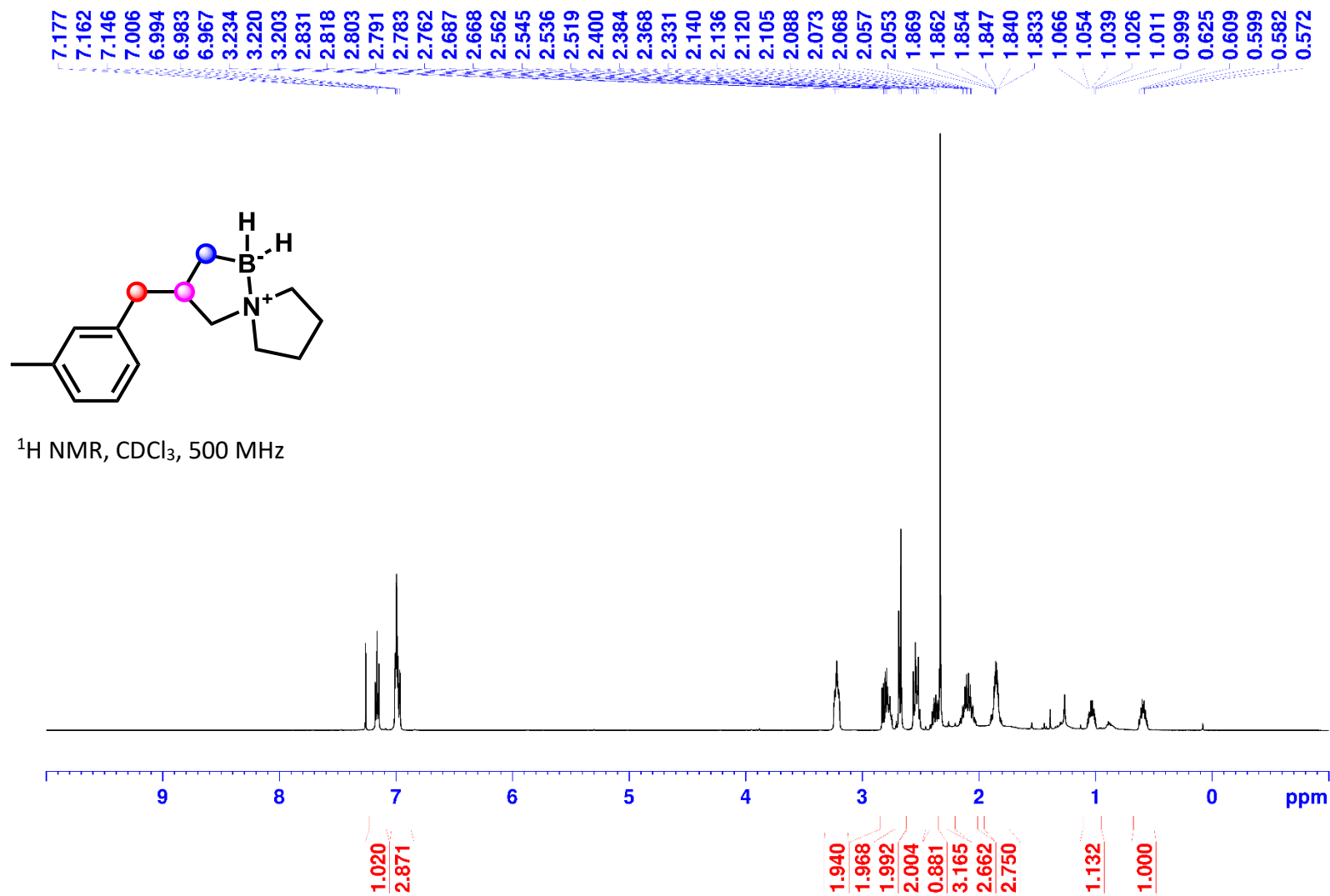
3-(2,4,6-Trimethylbenzyl)-5-aza-1-borasp[4.4]nonane (2o):



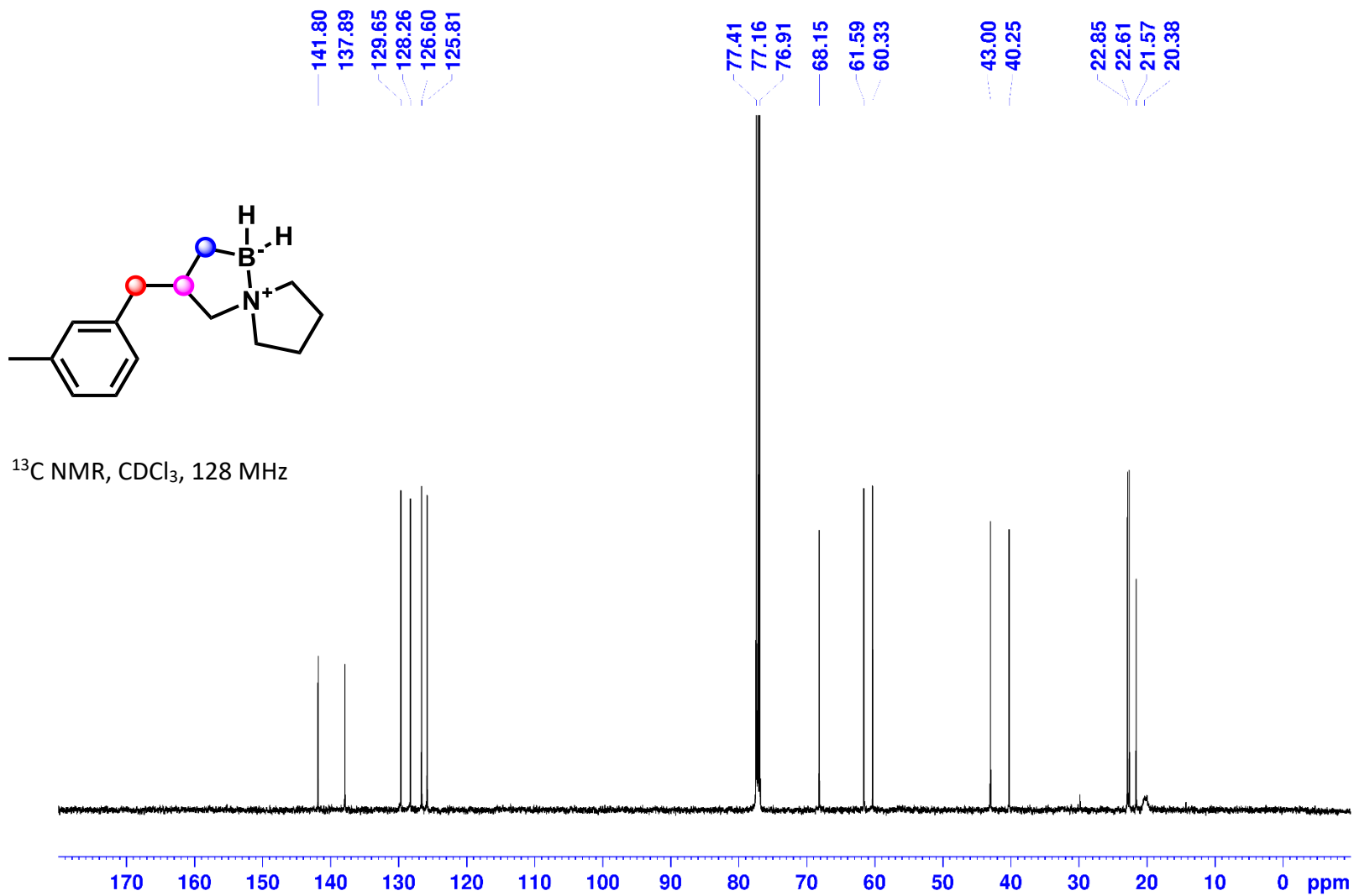
^{11}B NMR, CDCl_3 , 160 MHz



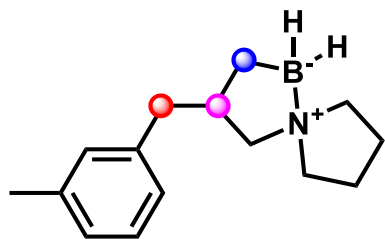
3-(3-Methylbenzyl)-5-aza-1-borasp[4.4]nonane (2p):



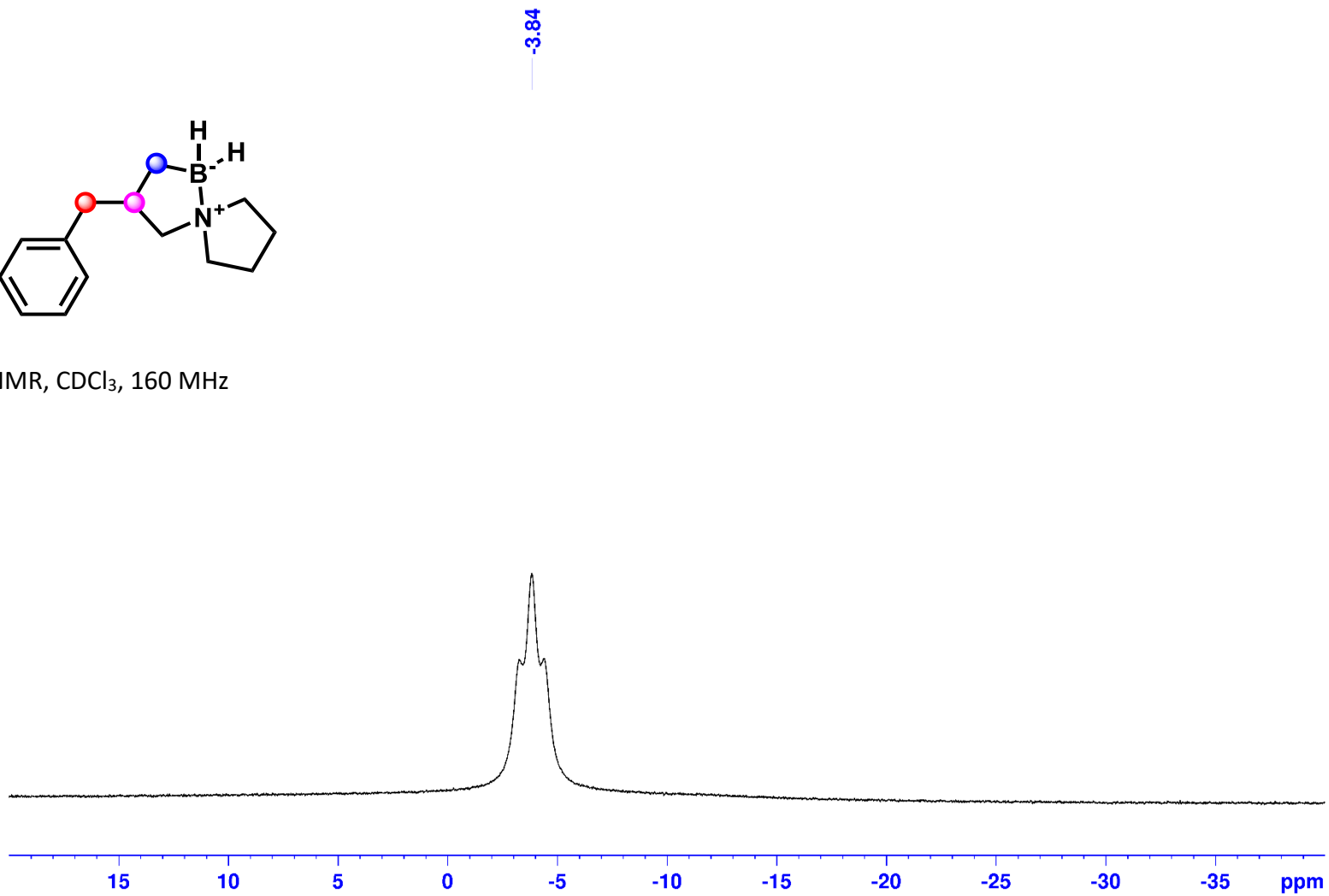
3-(3-Methylbenzyl)-5-aza-1-borasp[4.4]nonane (2p):



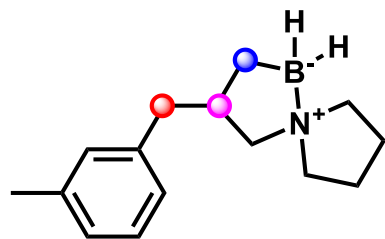
3-(3-Methylbenzyl)-5-aza-1-borasp[4.4]nonane (2p):



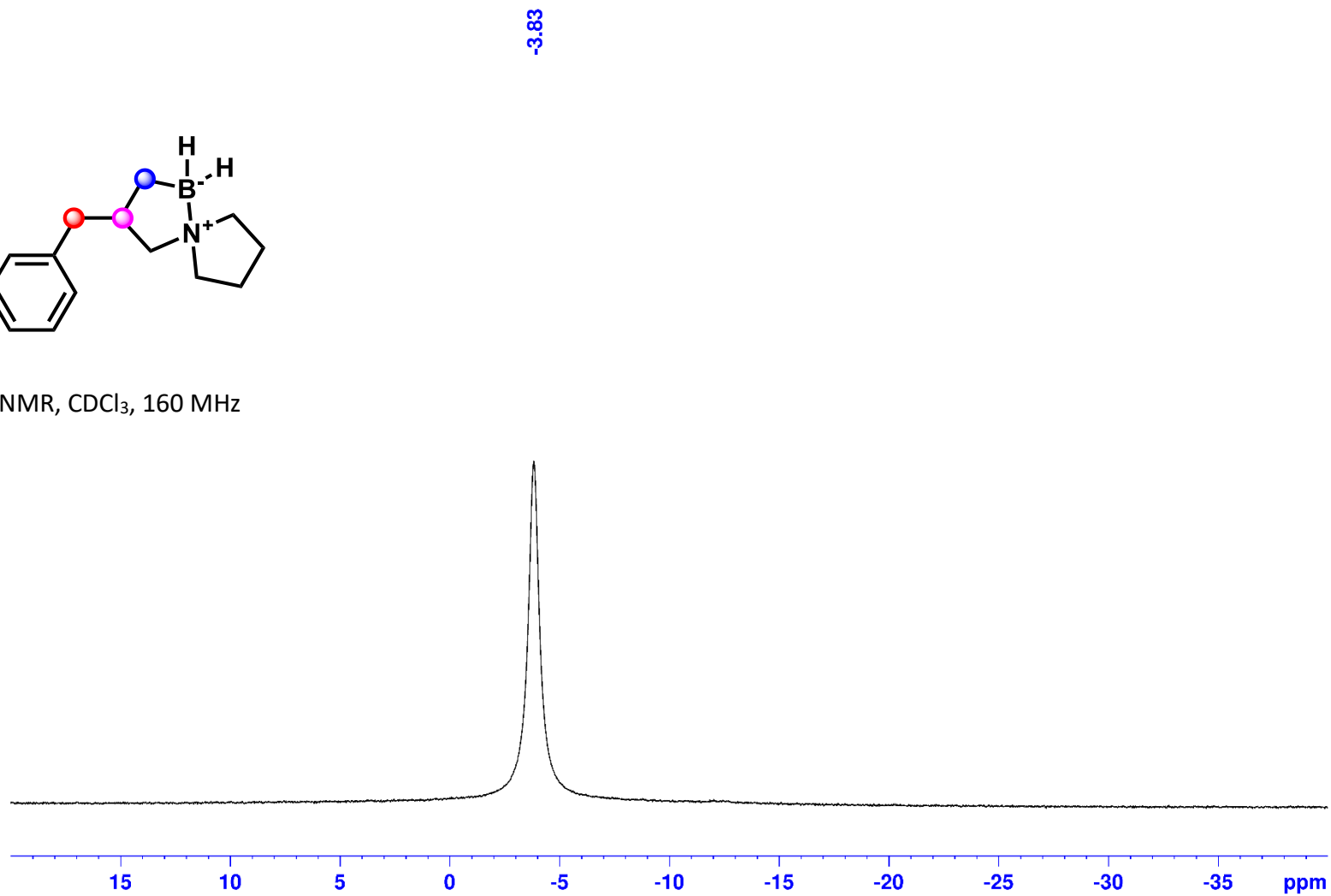
^{11}B NMR, CDCl_3 , 160 MHz



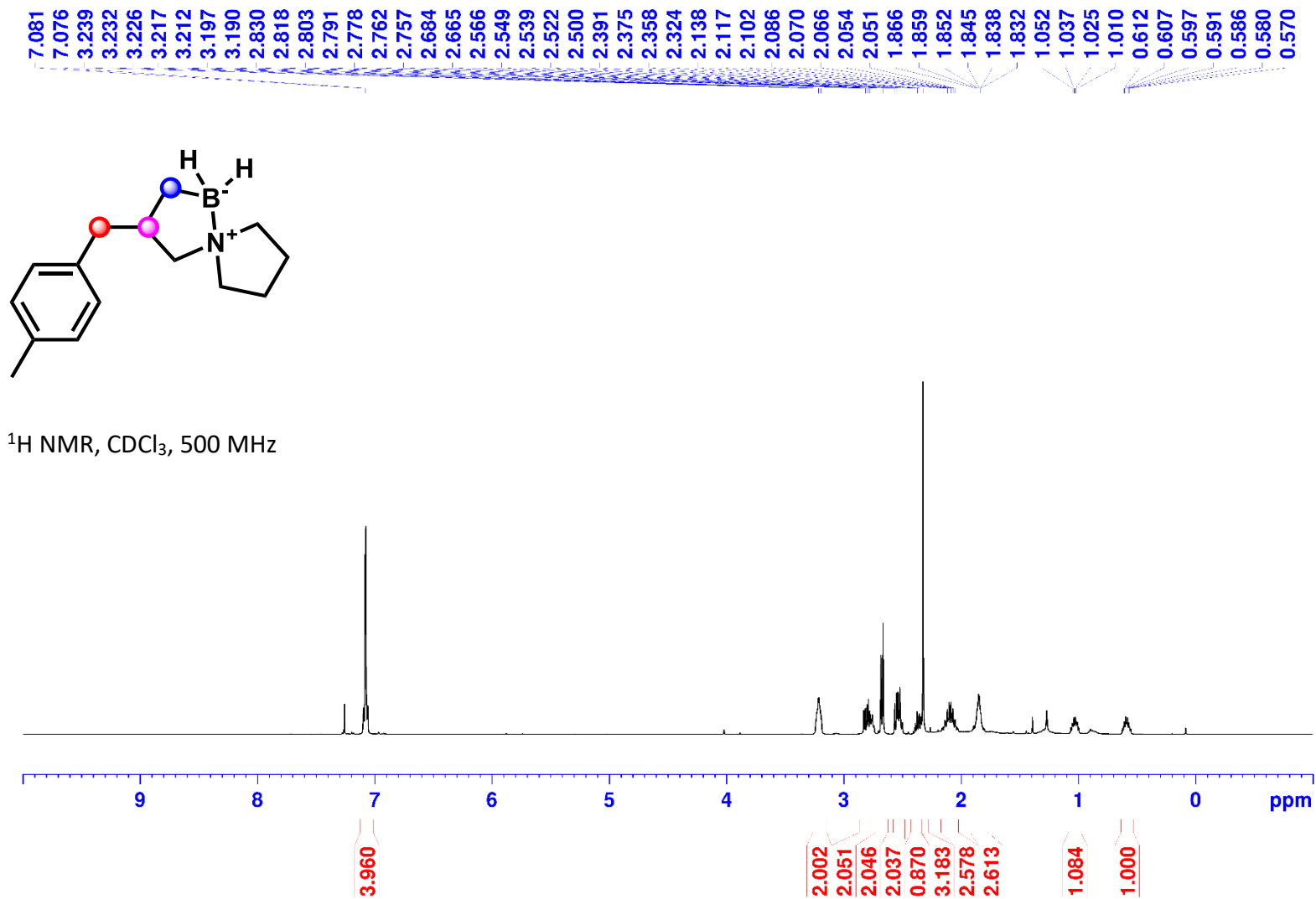
3-(3-Methylbenzyl)-5-aza-1-borasp[4.4]nonane (2p):



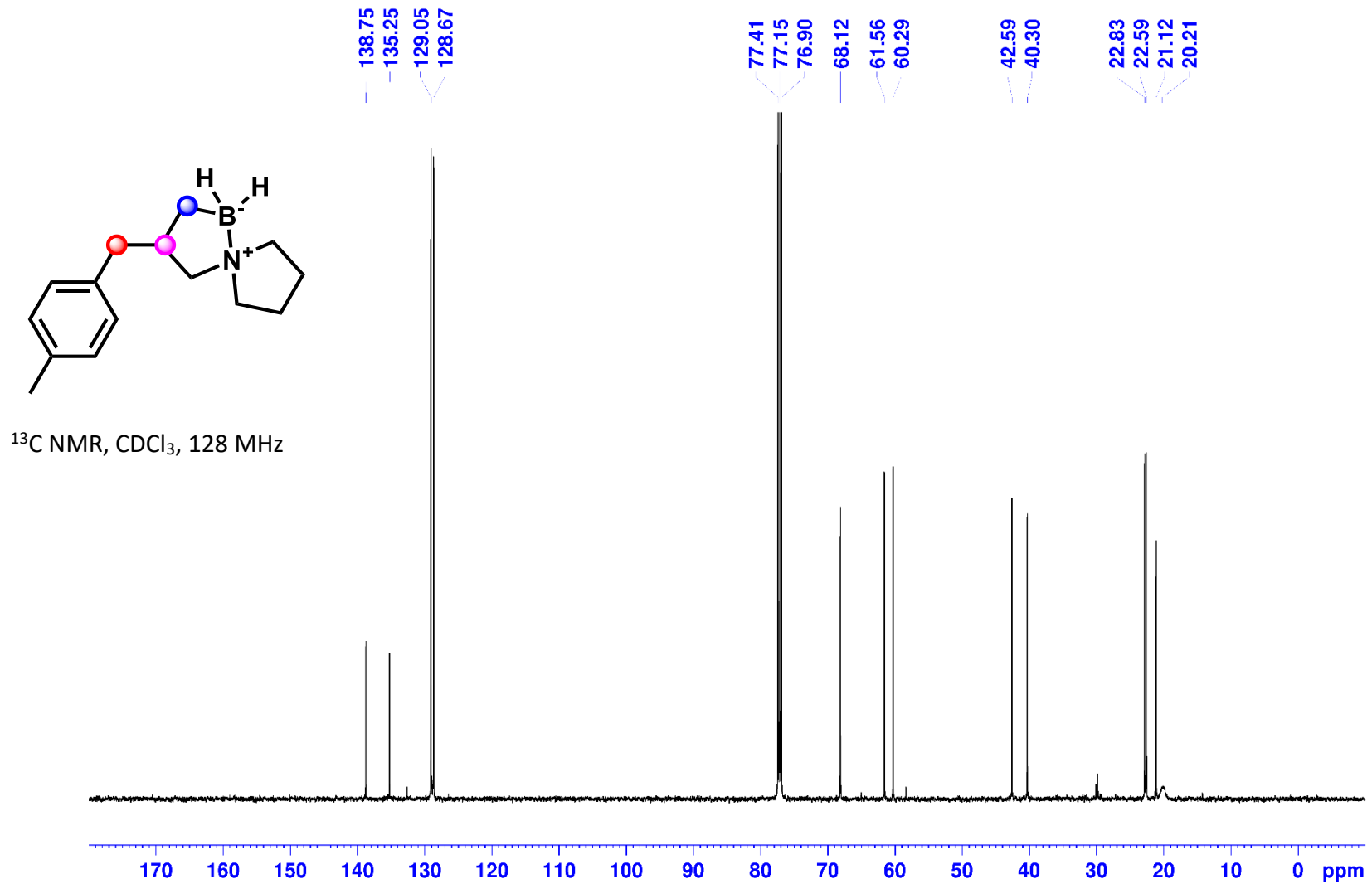
^{11}B NMR, CDCl_3 , 160 MHz



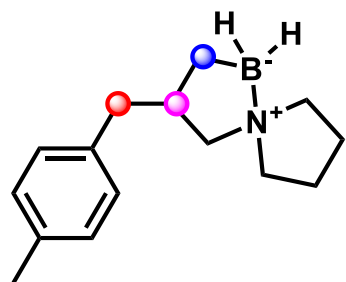
3-(4-Methylbenzyl)-5-aza-1-borasp[4.4]nonane (2q):



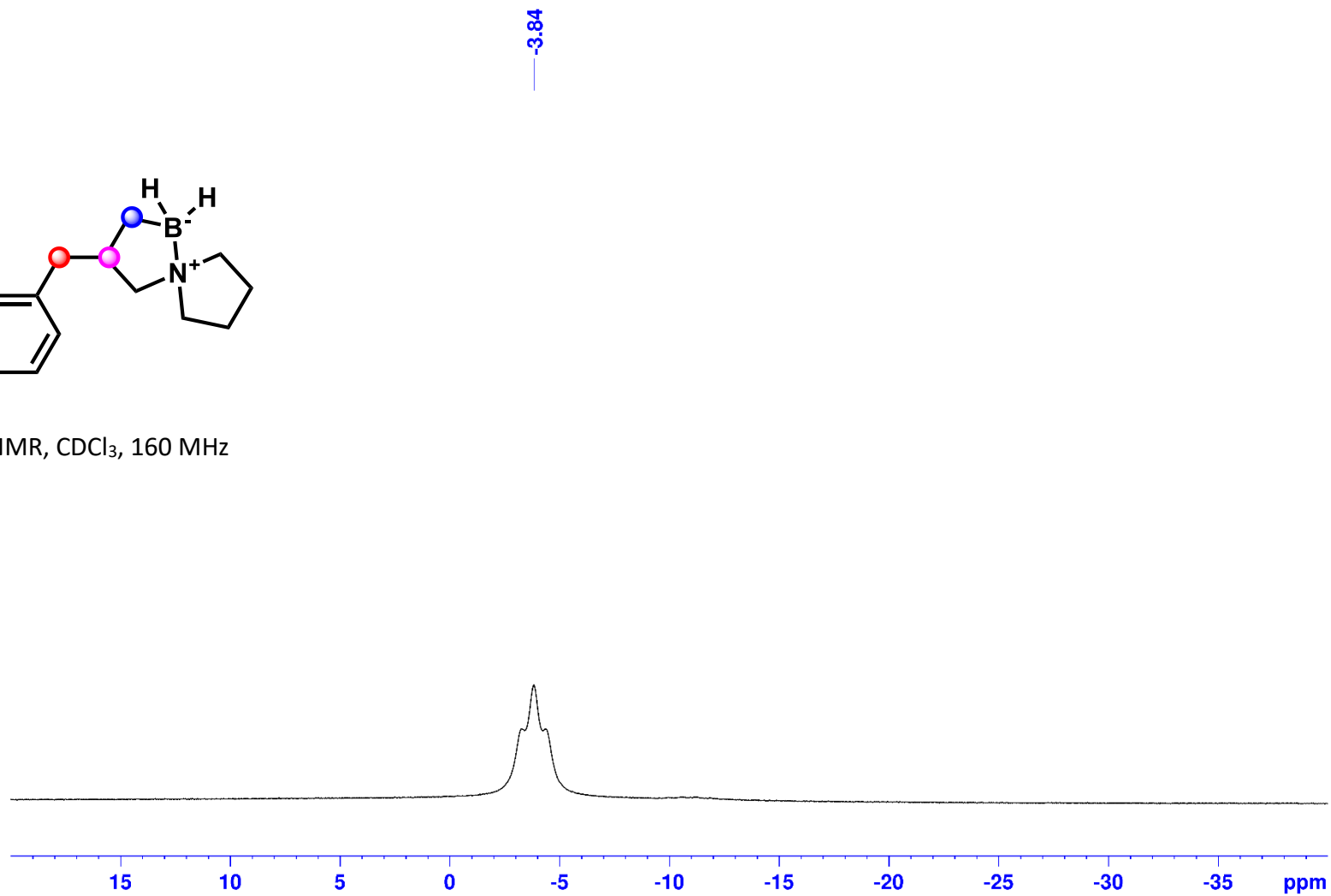
3-(4-Methylbenzyl)-5-aza-1-borasp[4.4]nonane (2q):



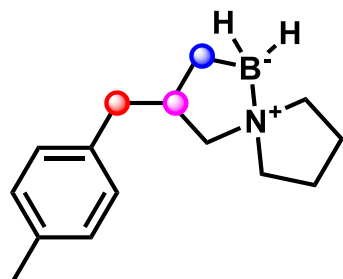
3-(4-Methylbenzyl)-5-aza-1-borasp[4.4]nonane (2q):



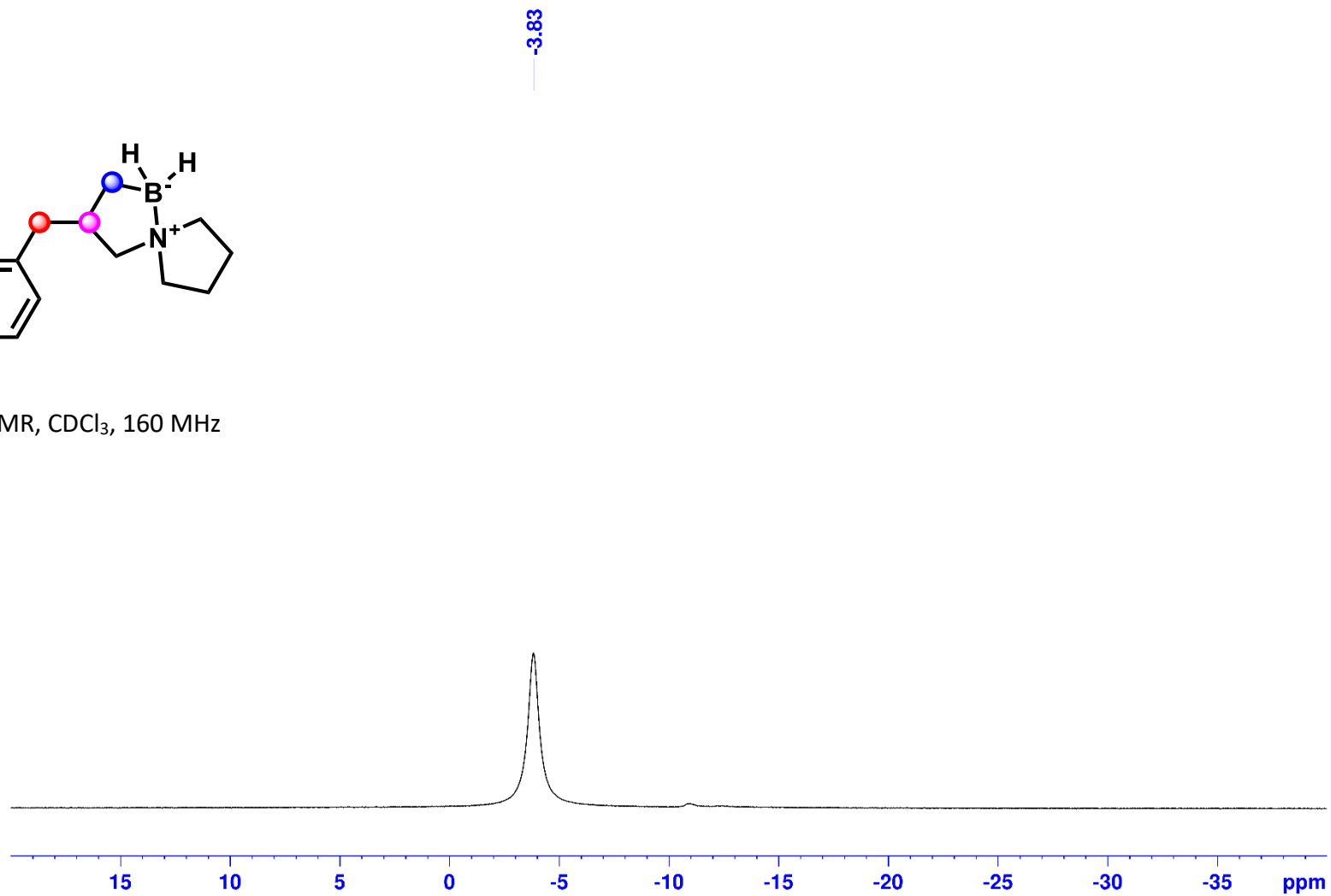
^{11}B NMR, CDCl_3 , 160 MHz



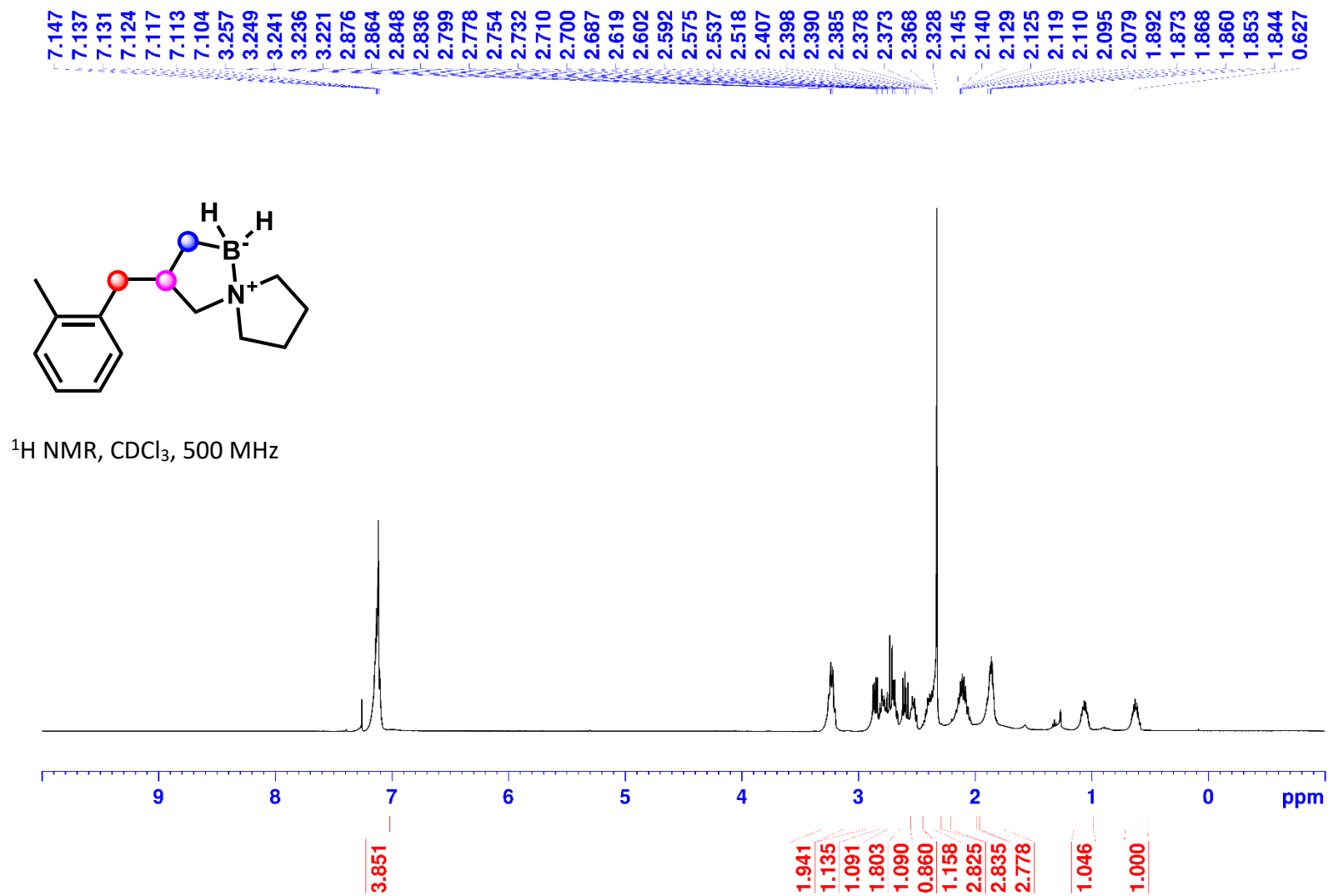
3-(4-Methylbenzyl)-5-aza-1-borasp[4.4]nonane (2q):



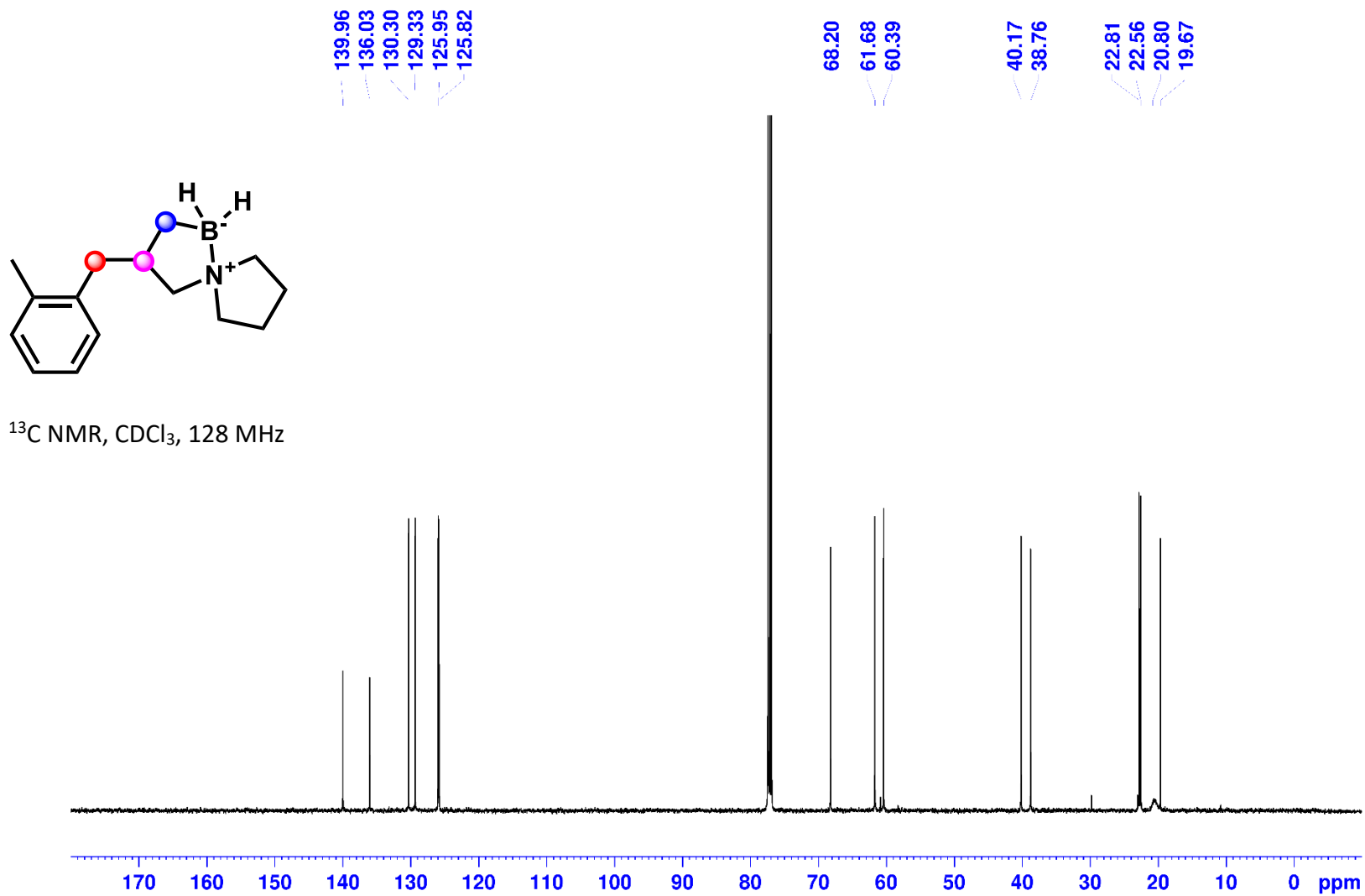
^{11}B NMR, CDCl_3 , 160 MHz



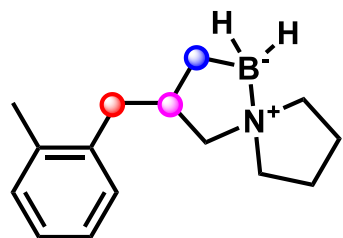
3-(2-Methylbenzyl)-5-aza-1-borasp[4.4]nonane (2r):



3-(2-Methylbenzyl)-5-aza-1-borasp[4.4]nonane (2r):

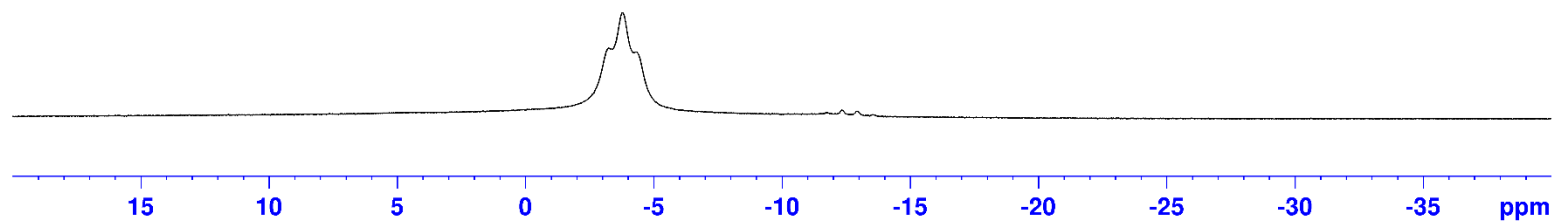


3-(2-Methylbenzyl)-5-aza-1-borasp[4.4]nonane (2r):

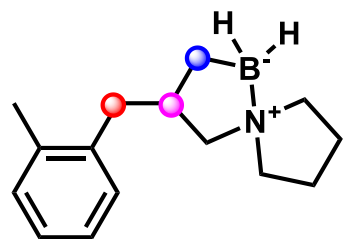


-3.79

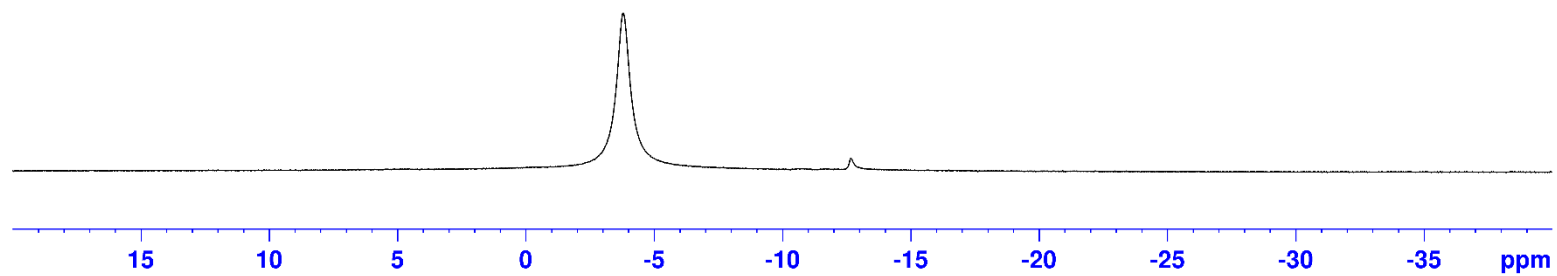
^{11}B NMR, CDCl_3 , 160 MHz



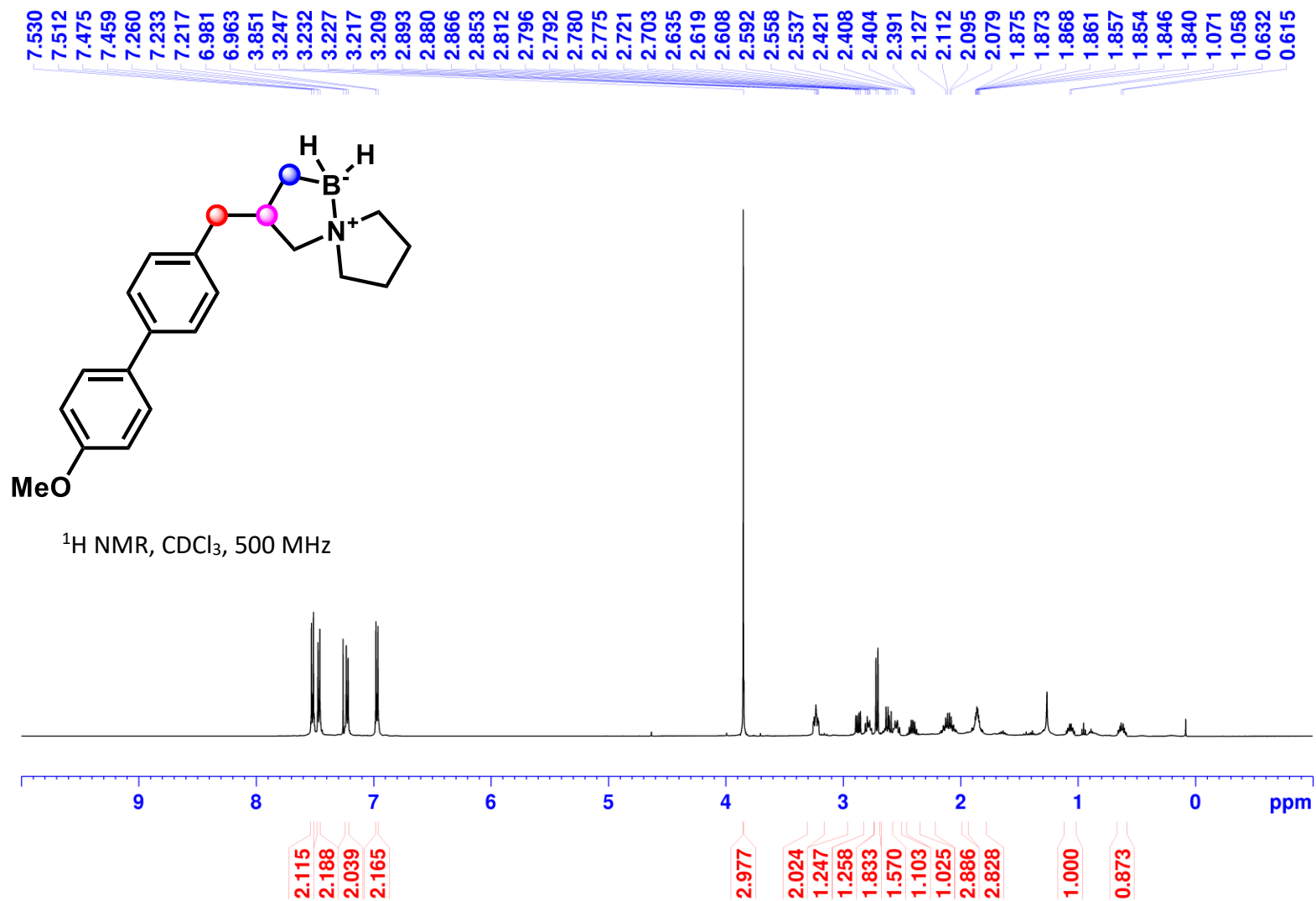
3-(2-Methylbenzyl)-5-aza-1-borasp[4.4]nonane (2r):



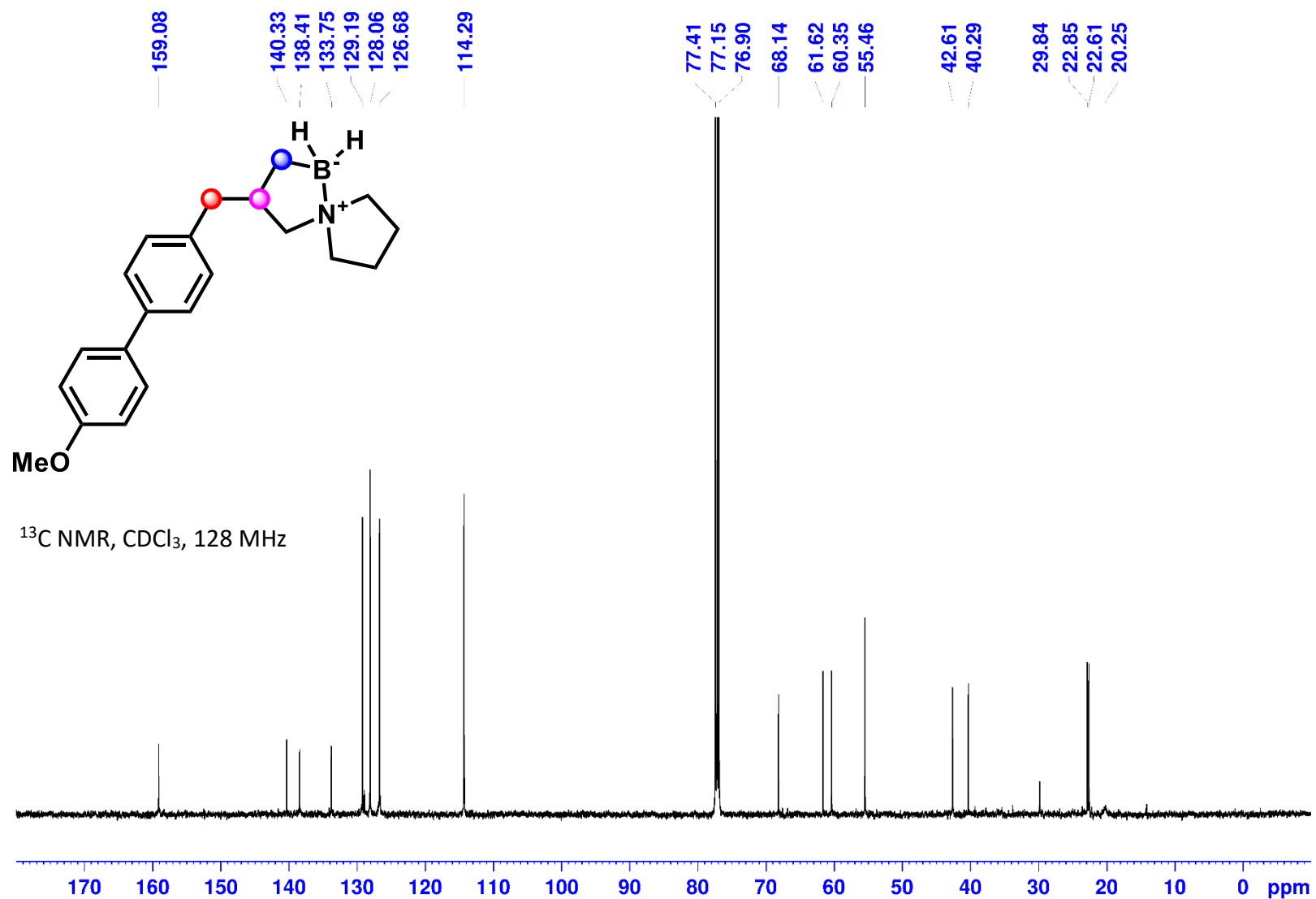
^{11}B NMR, CDCl_3 , 160 MHz



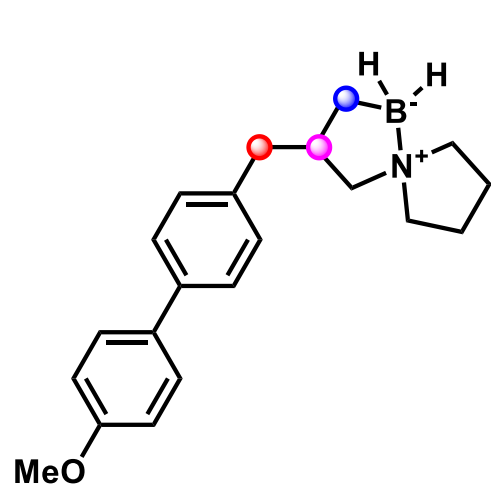
3-((4'-Methoxy-[1,1'-biphenyl]-4-yl)methyl)-5-aza-1-borasp[4.4]nonane (2s):



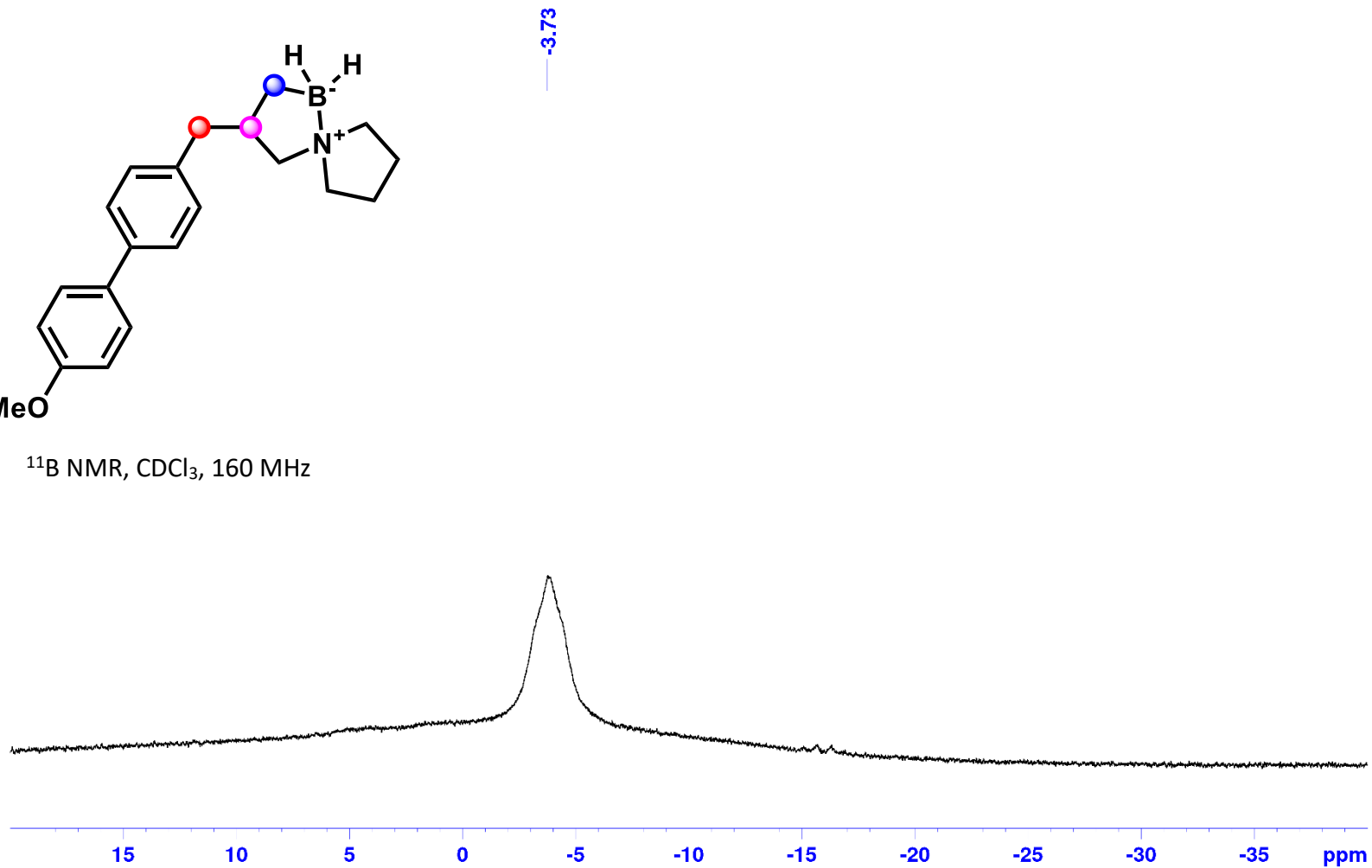
3-((4'-Methoxy-[1,1'-biphenyl]-4-yl)methyl)-5-aza-1-borasp[4.4]nonane (2s):



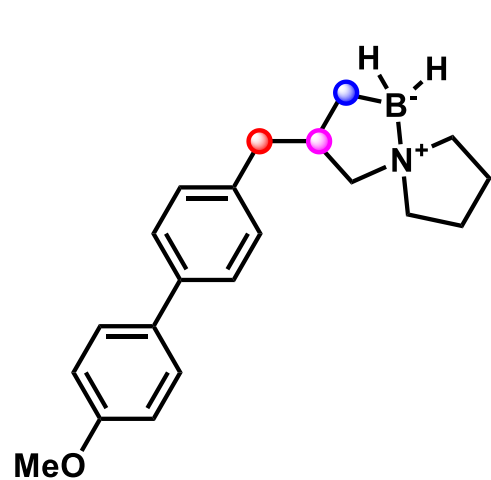
3-((4'-Methoxy-[1,1'-biphenyl]-4-yl)methyl)-5-aza-1-borasp[4.4]nonane (2s):



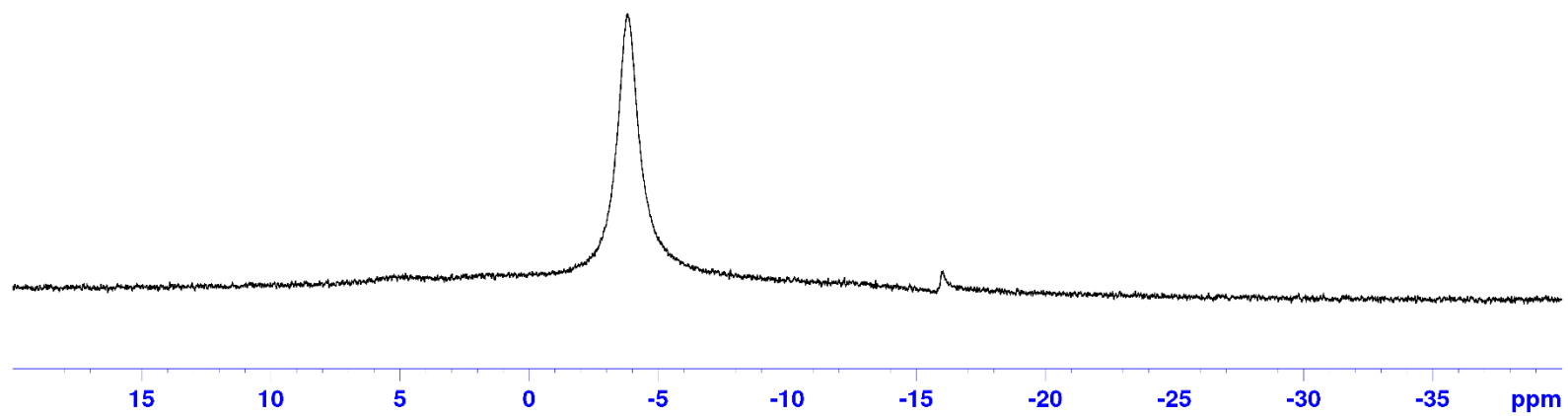
^{11}B NMR, CDCl_3 , 160 MHz



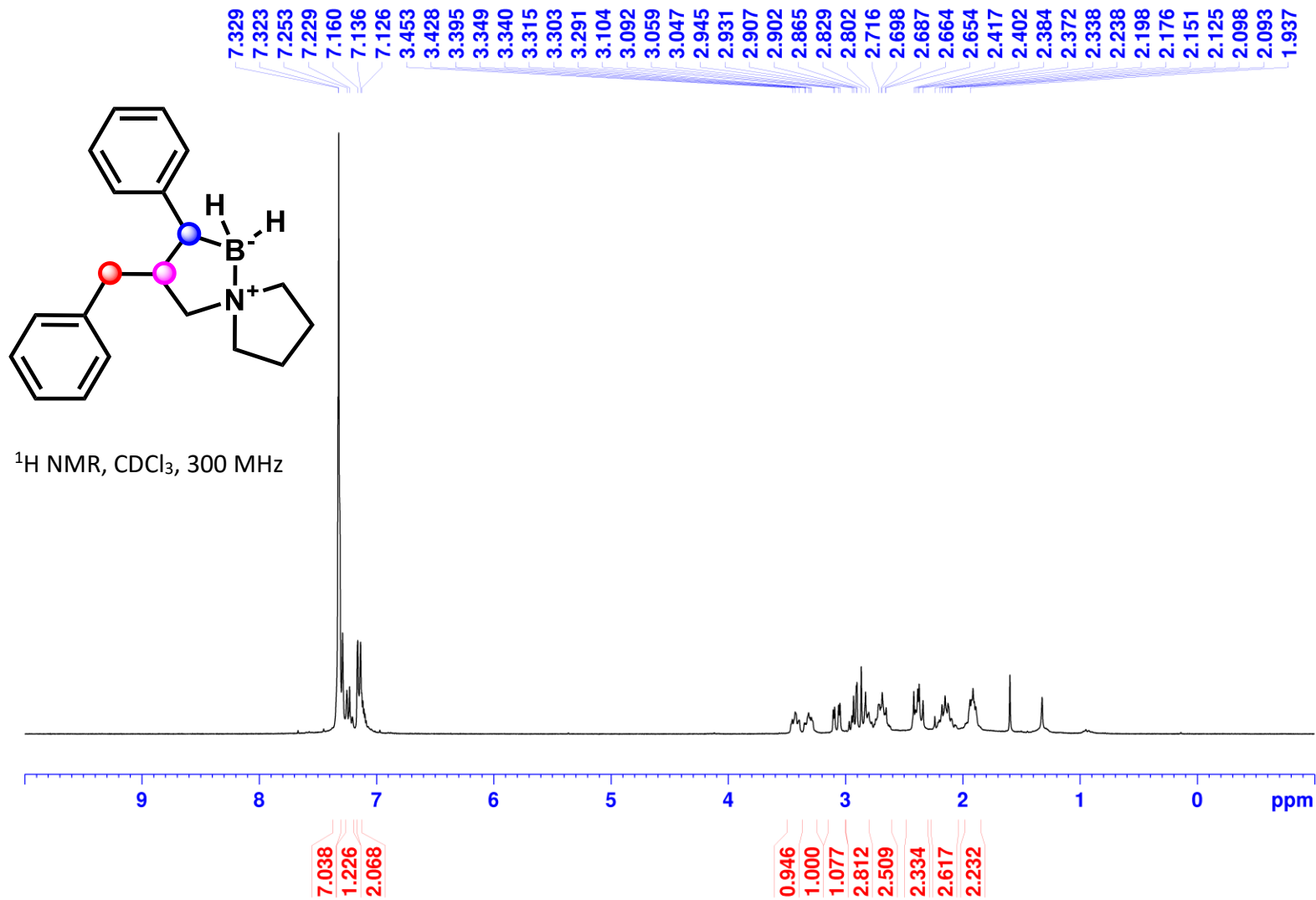
3-((4'-Methoxy-[1,1'-biphenyl]-4-yl)methyl)-5-aza-1-borasp[4.4]nonane (2s):



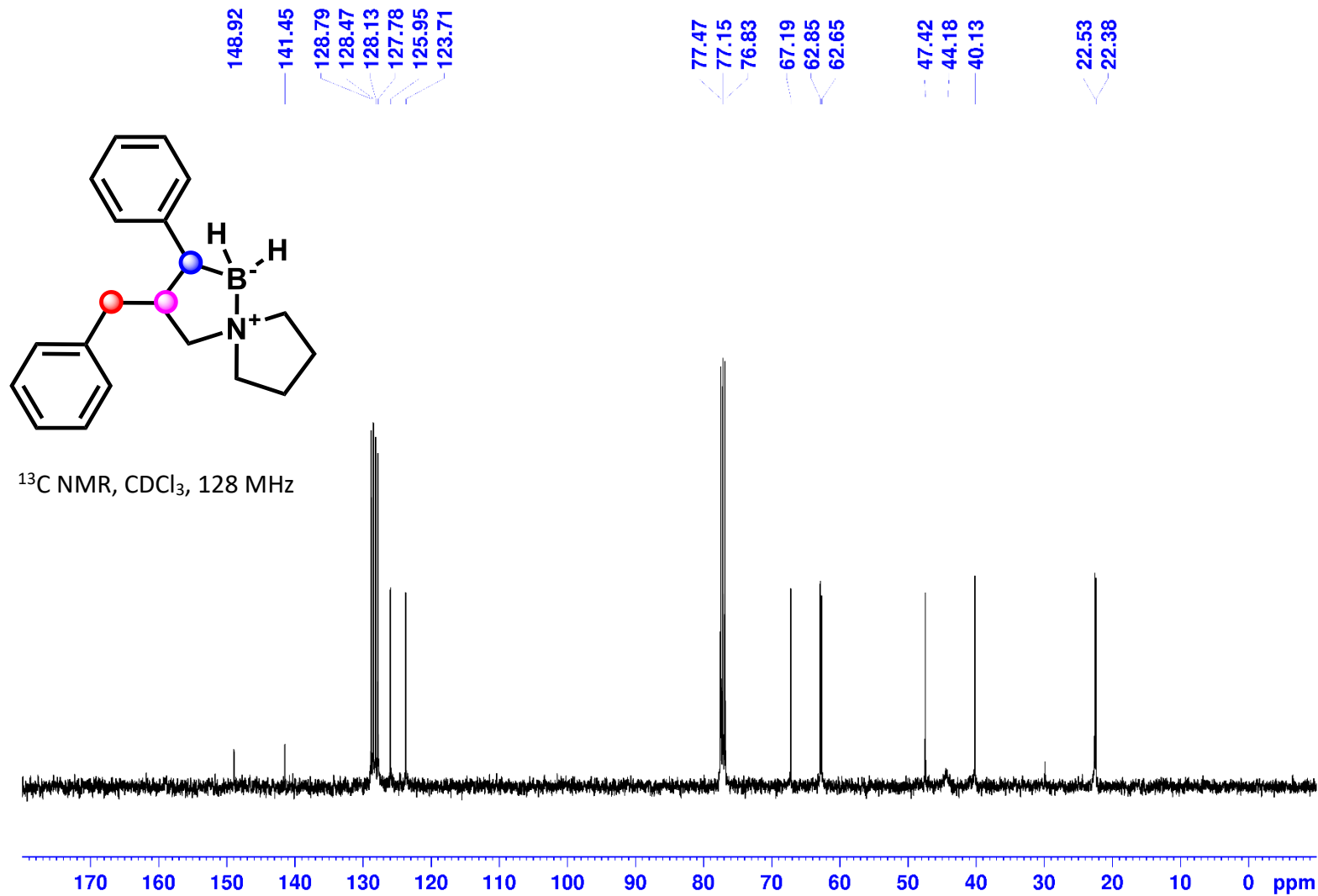
^{11}B NMR, CDCl_3 , 160 MHz



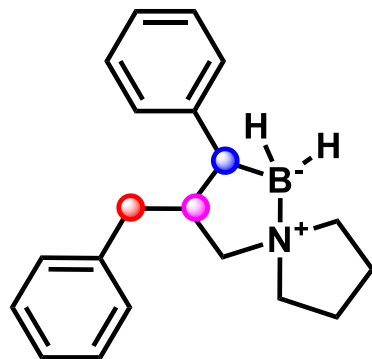
3-Benzyl-2-phenyl-5-aza-1-borasp[4.4]nonane (2t):



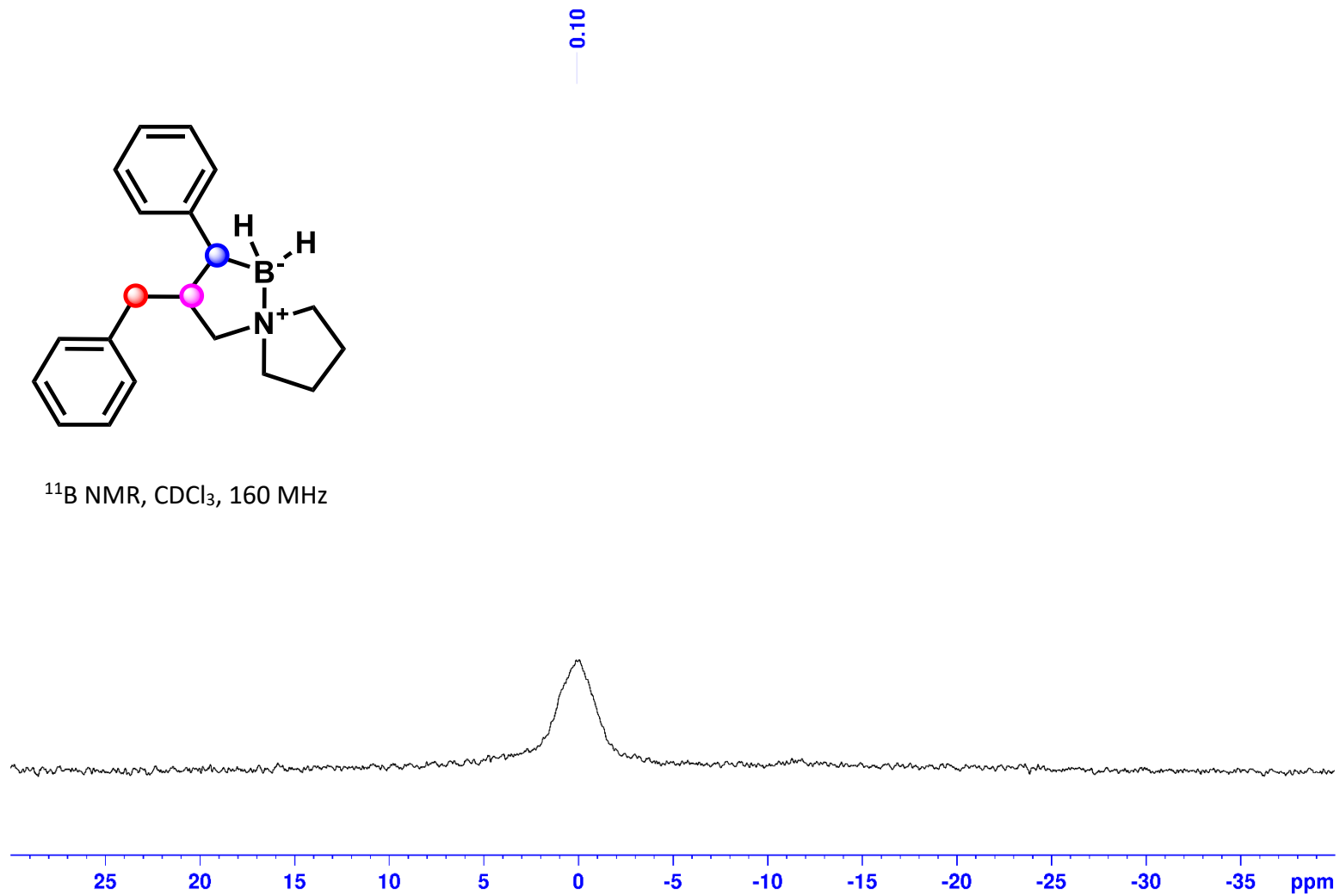
3-Benzyl-2-phenyl-5-aza-1-borasp[4.4]nonane (2t):



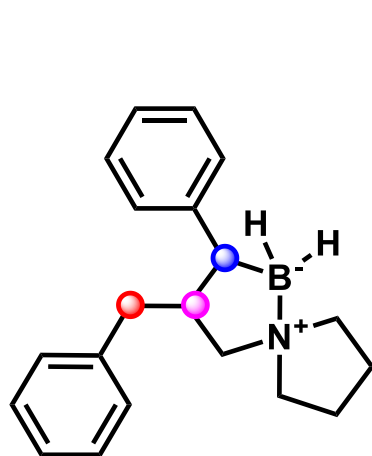
3-Benzyl-2-phenyl-5-aza-1-borospiro[4.4]nonane (2t):



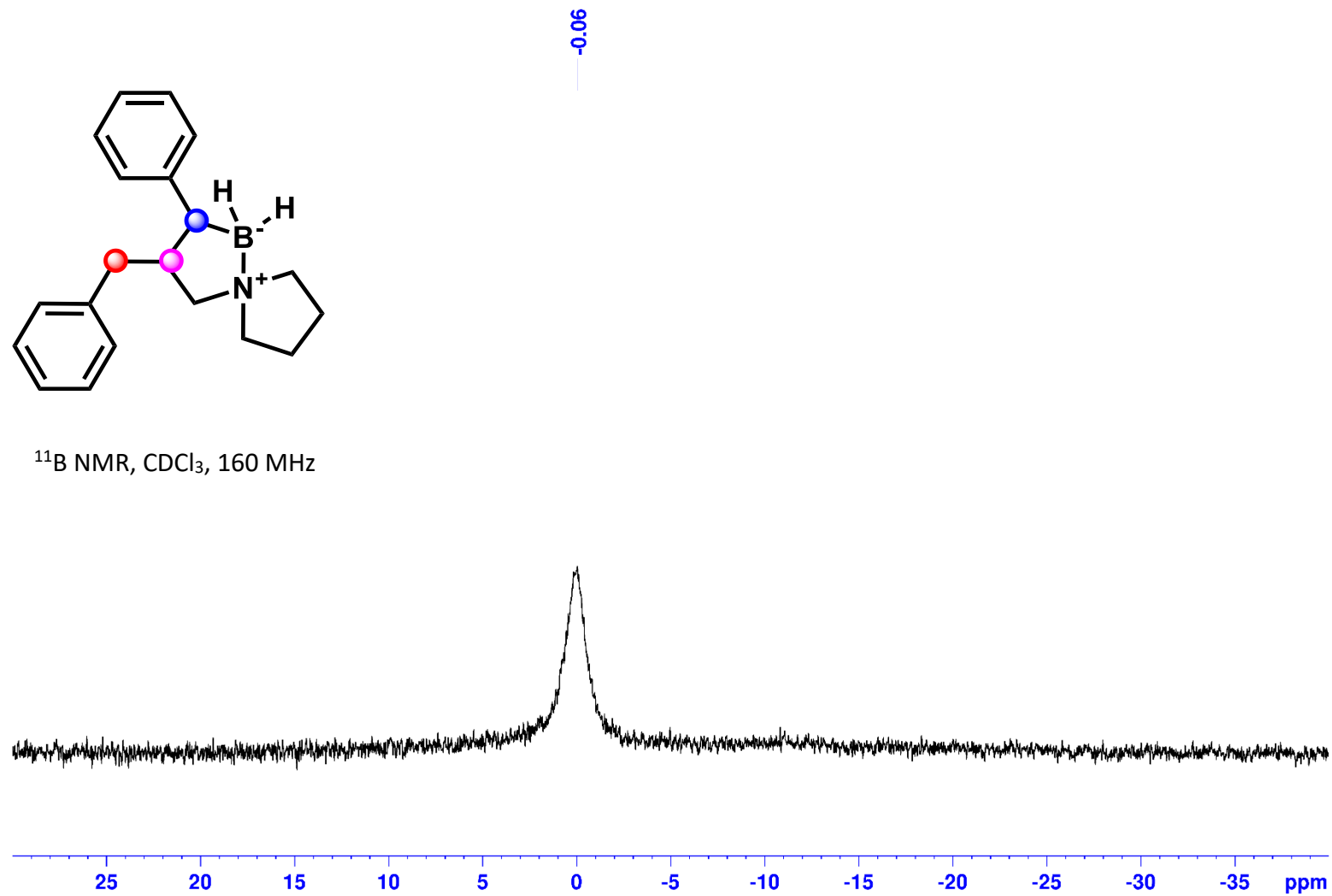
^{11}B NMR, CDCl_3 , 160 MHz



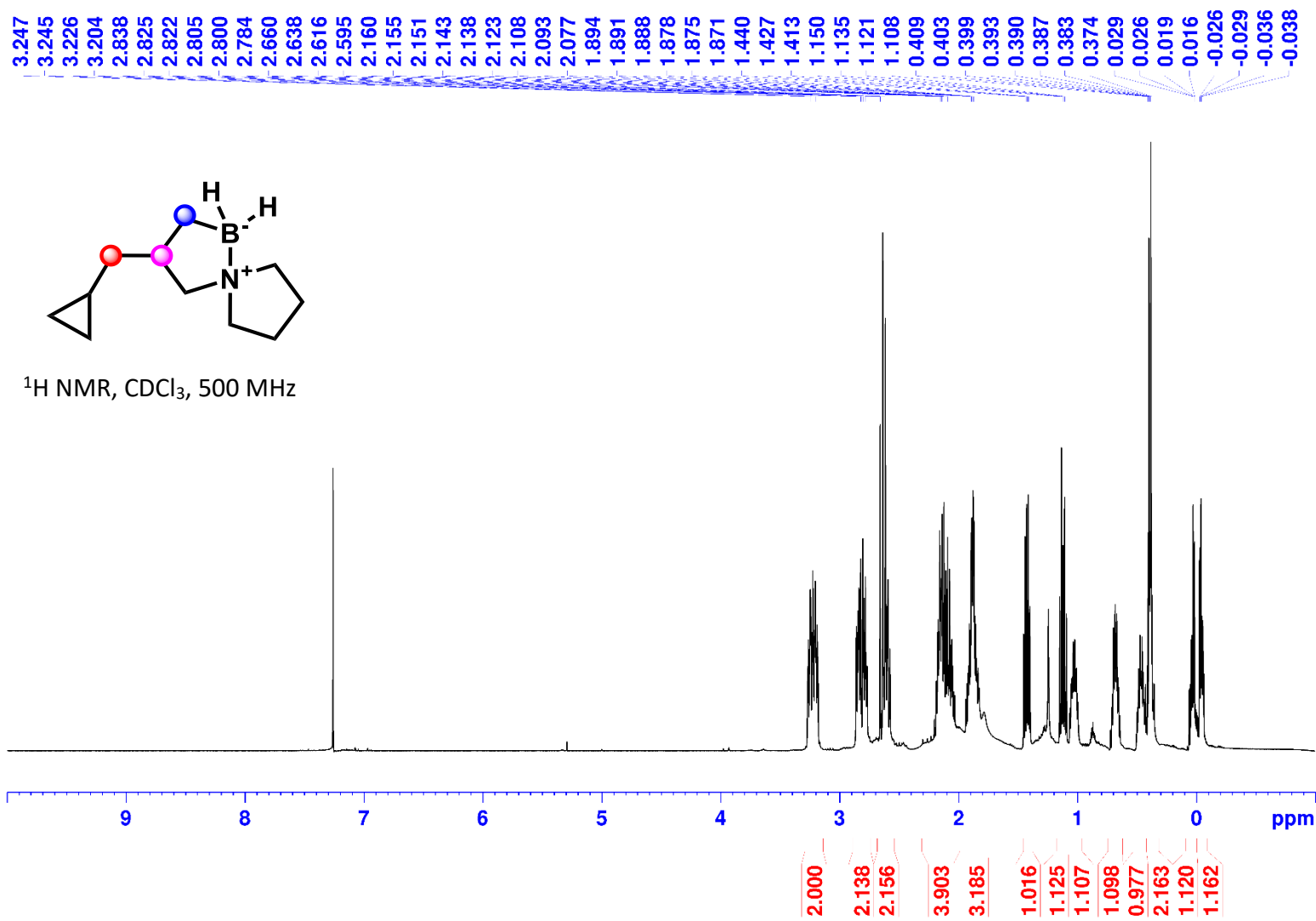
3-Benzyl-2-phenyl-5-aza-1-borasp[4.4]nonane (2t):



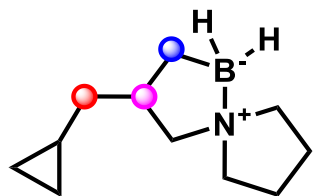
^{11}B NMR, CDCl_3 , 160 MHz



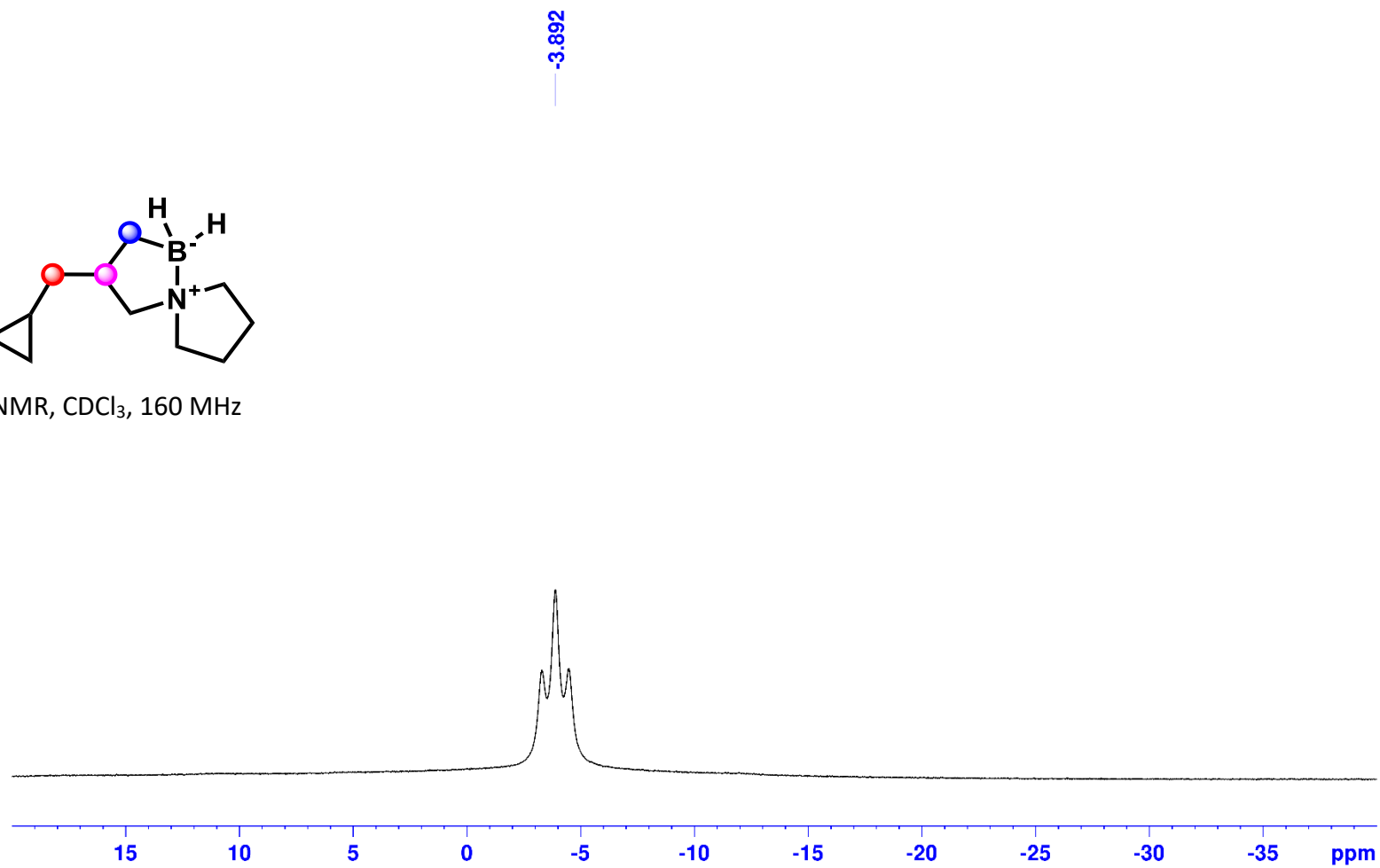
3-(Cyclopropylmethyl)-5-aza-1-boraspiro[4.4]nonane (2u):



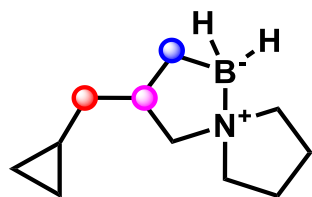
3-(Cyclopropylmethyl)-5-aza-1-borasp[4.4]nonane (2u):



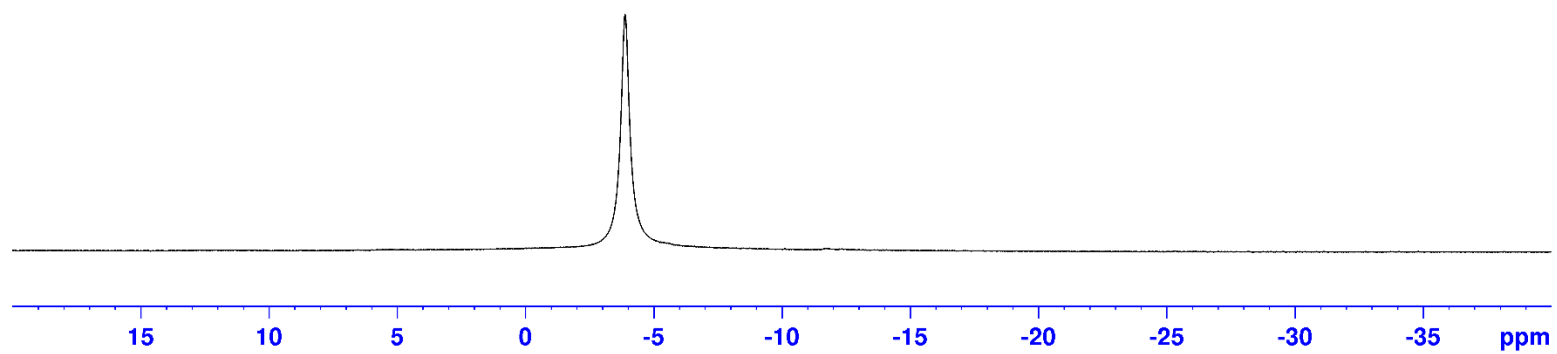
^{11}B NMR, CDCl_3 , 160 MHz



3-(Cyclopropylmethyl)-5-aza-1-borasp[4.4]nonane (2u):



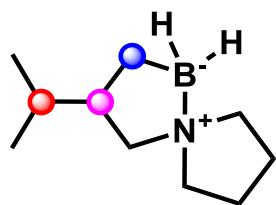
^{11}B NMR, CDCl_3 , 160 MHz



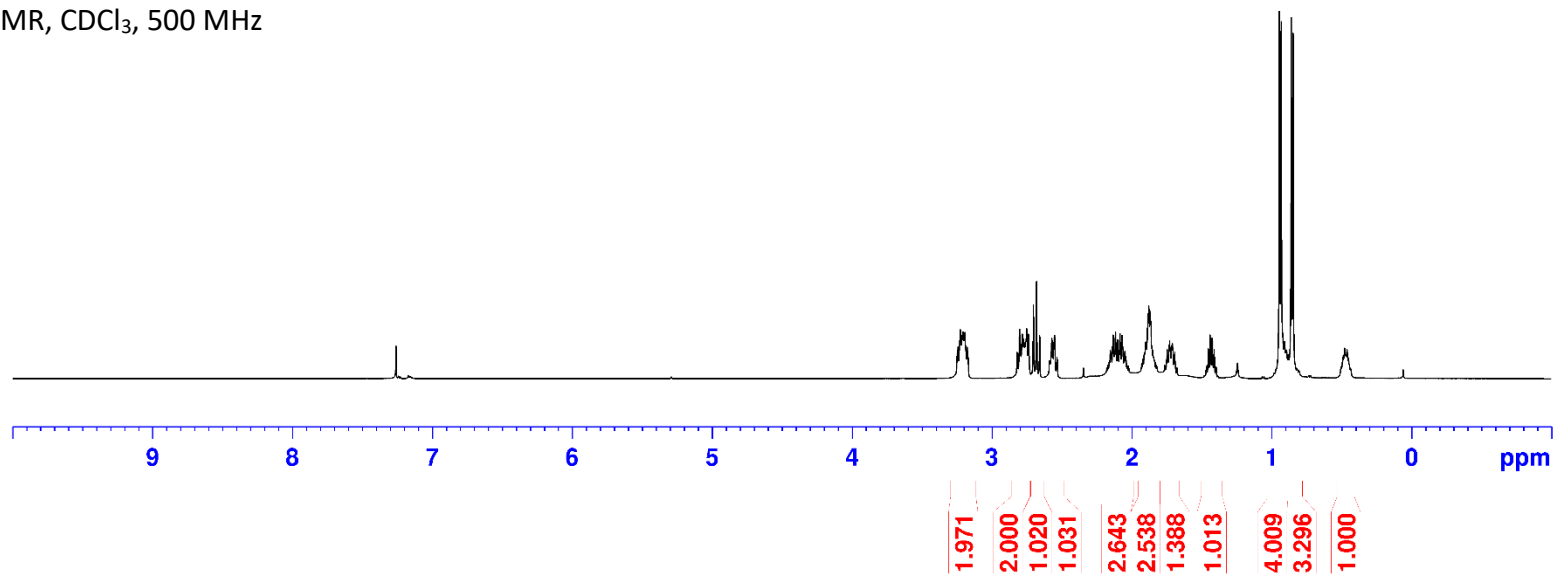
-3.89

3-Isopropyl-5-aza-1-borasp[4.4]nonane (2v):

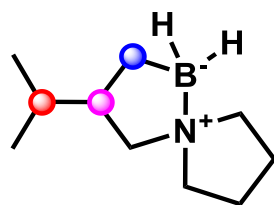
3.242
3.226
3.213
3.205
3.199
3.193
3.178
2.803
2.782
2.773
2.765
2.759
2.752
2.739
2.703
2.681
2.659
2.572
2.553
2.154
2.133
2.117
2.101
2.085
2.070
1.901
1.893
1.885
1.879
1.871
1.865
1.858
1.850
1.747
1.733
1.730
1.724
1.717
1.711
1.707
1.454
1.441
1.427
1.425
1.411
0.945
0.932
0.895
0.860
0.847
0.478
0.461



¹H NMR, CDCl₃, 500 MHz

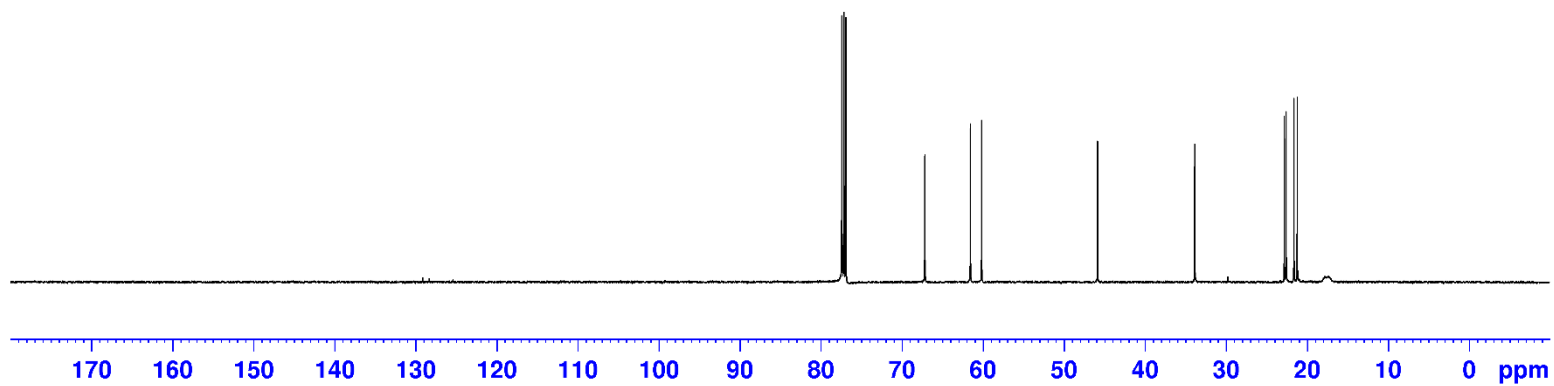


3-Isopropyl-5-aza-1-borasp[4.4]nonane (2v):

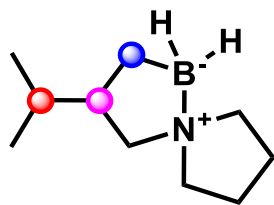


^{13}C NMR, CDCl_3 , 128 MHz

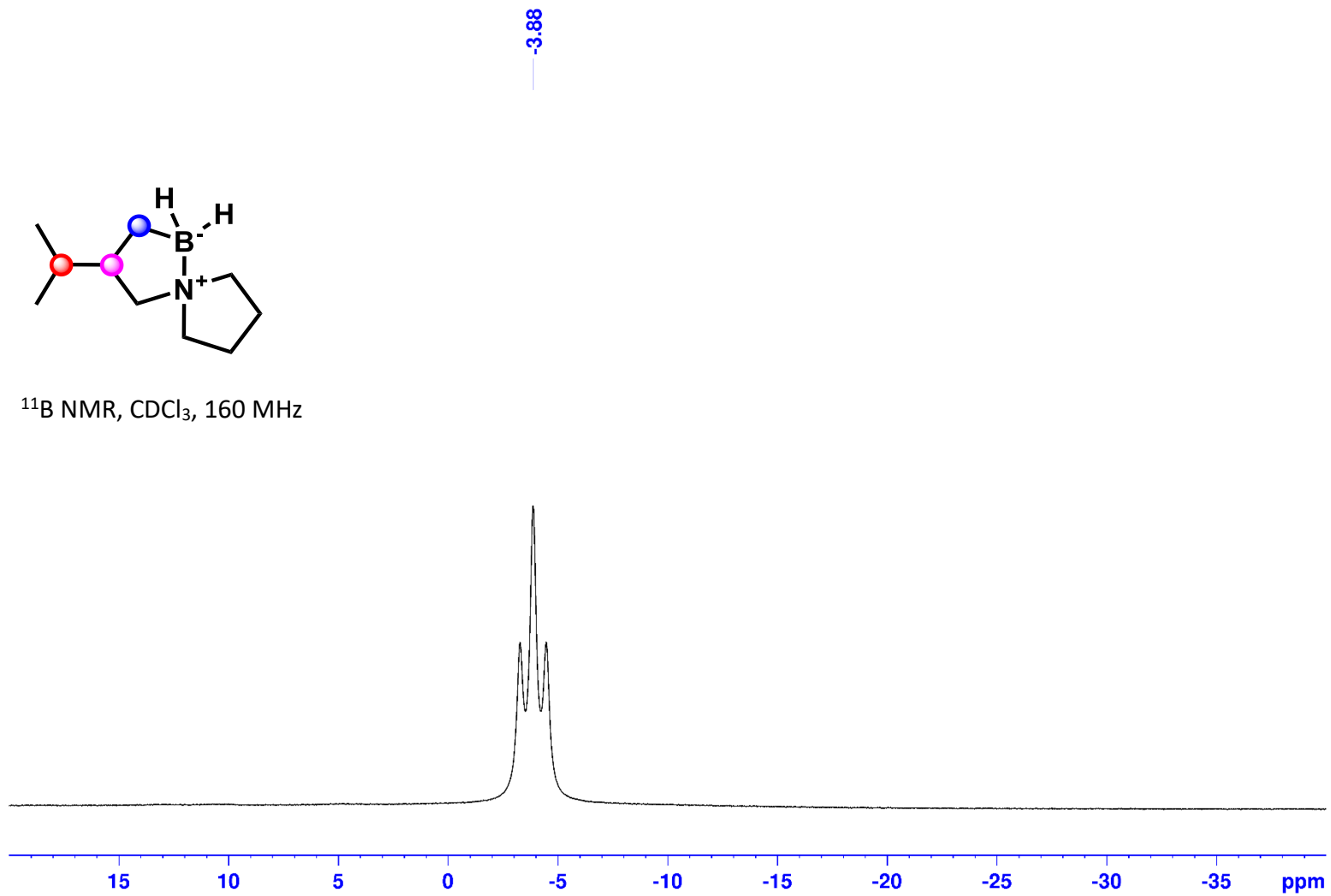
77.41
77.16
76.91
67.17
61.55
60.16
45.87
33.87
22.83
22.61
21.64
21.23
17.62



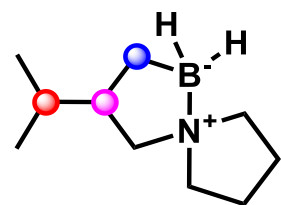
3-Isopropyl-5-aza-1-boraspino[4.4]nonane (2v):



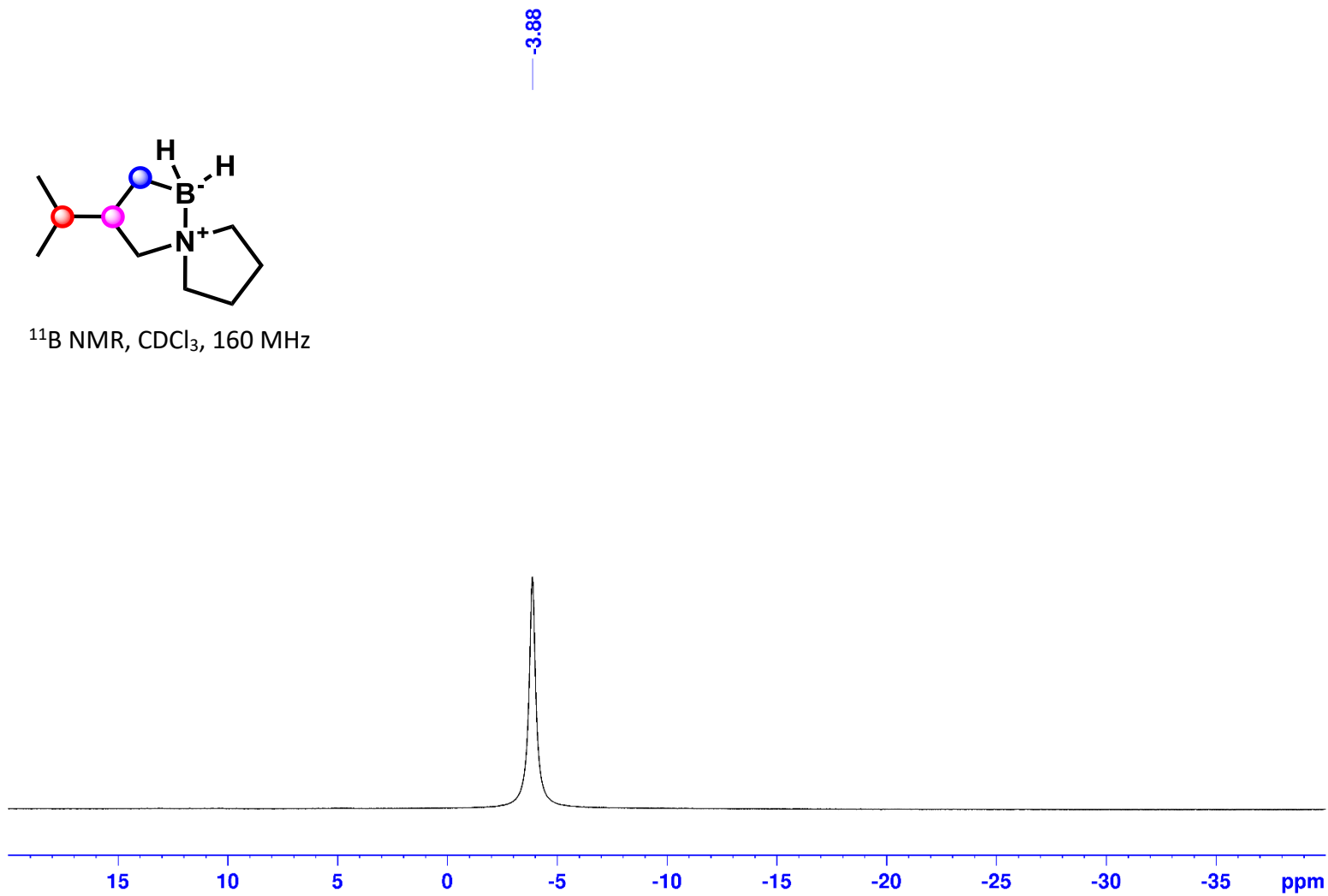
^{11}B NMR, CDCl_3 , 160 MHz



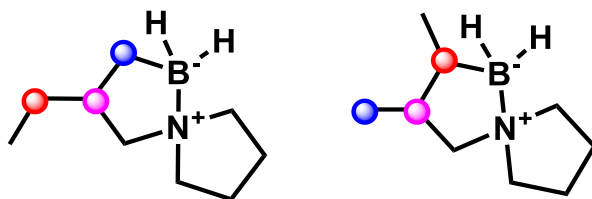
3-Isopropyl-5-aza-1-borasp[4.4]nonane (2v):



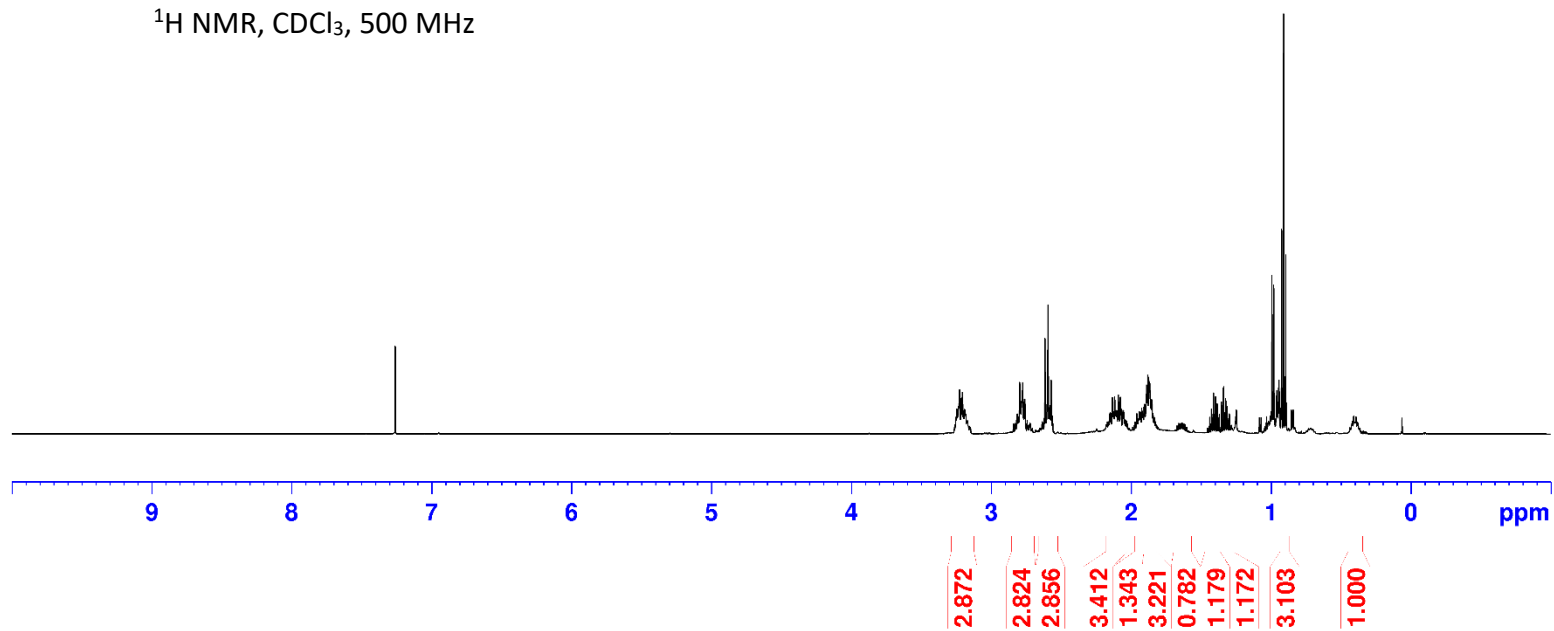
^{11}B NMR, CDCl_3 , 160 MHz



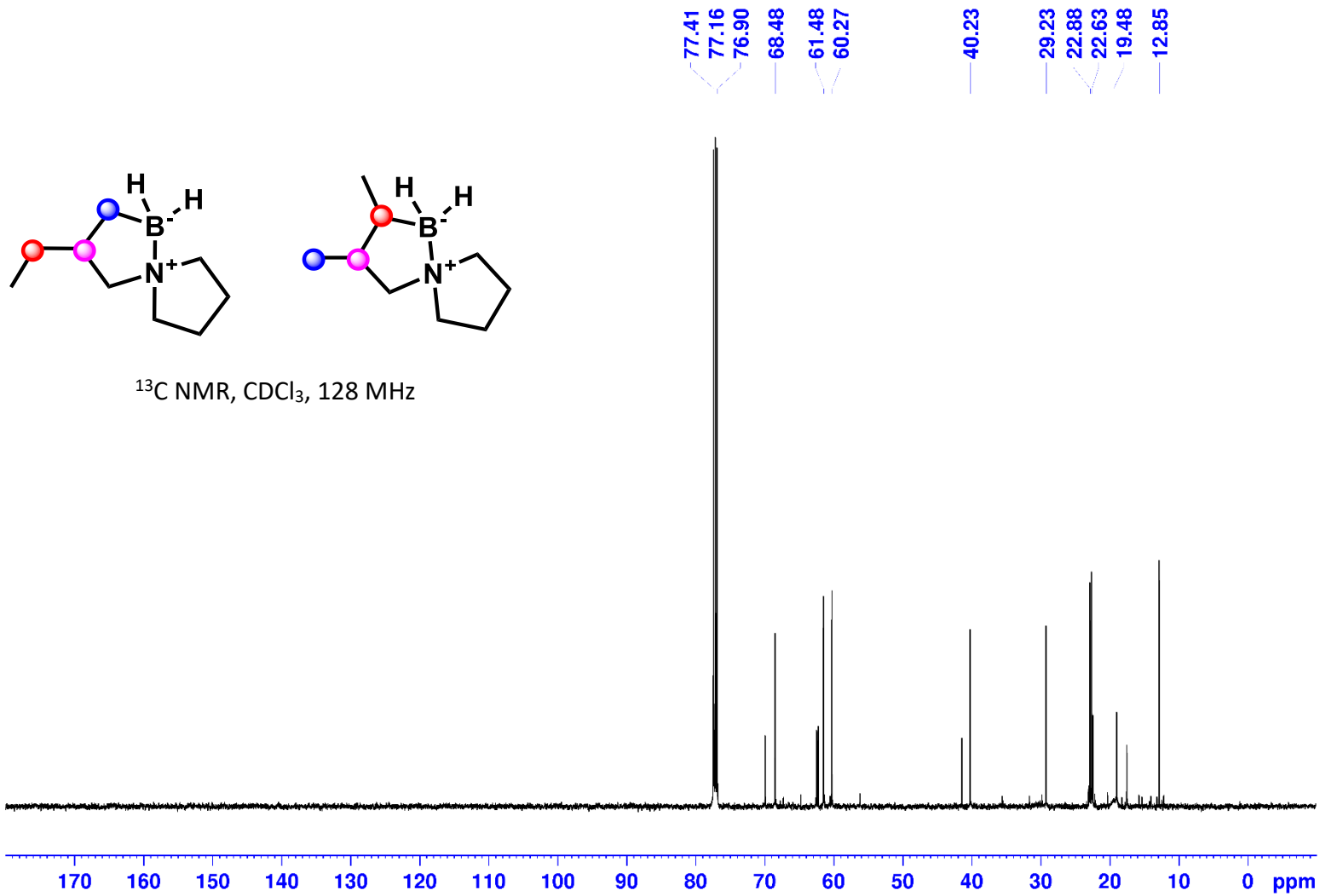
3-ethyl-5-aza-1-borasp[4.4]nonane (2w) and 2,3-dimethyl-5-aza-1-borasp[4.4]nonane (2wa):



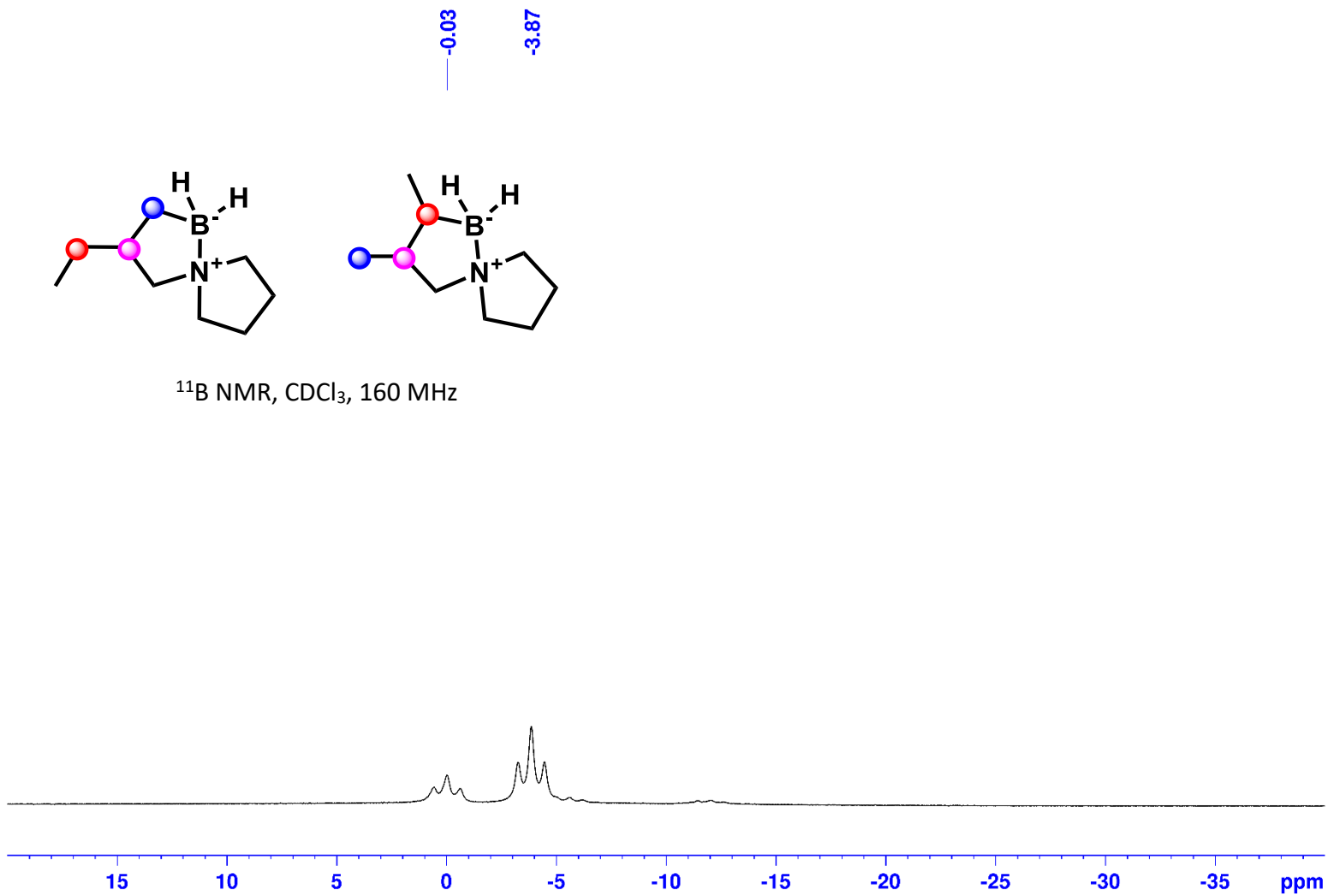
¹H NMR, CDCl₃, 500 MHz



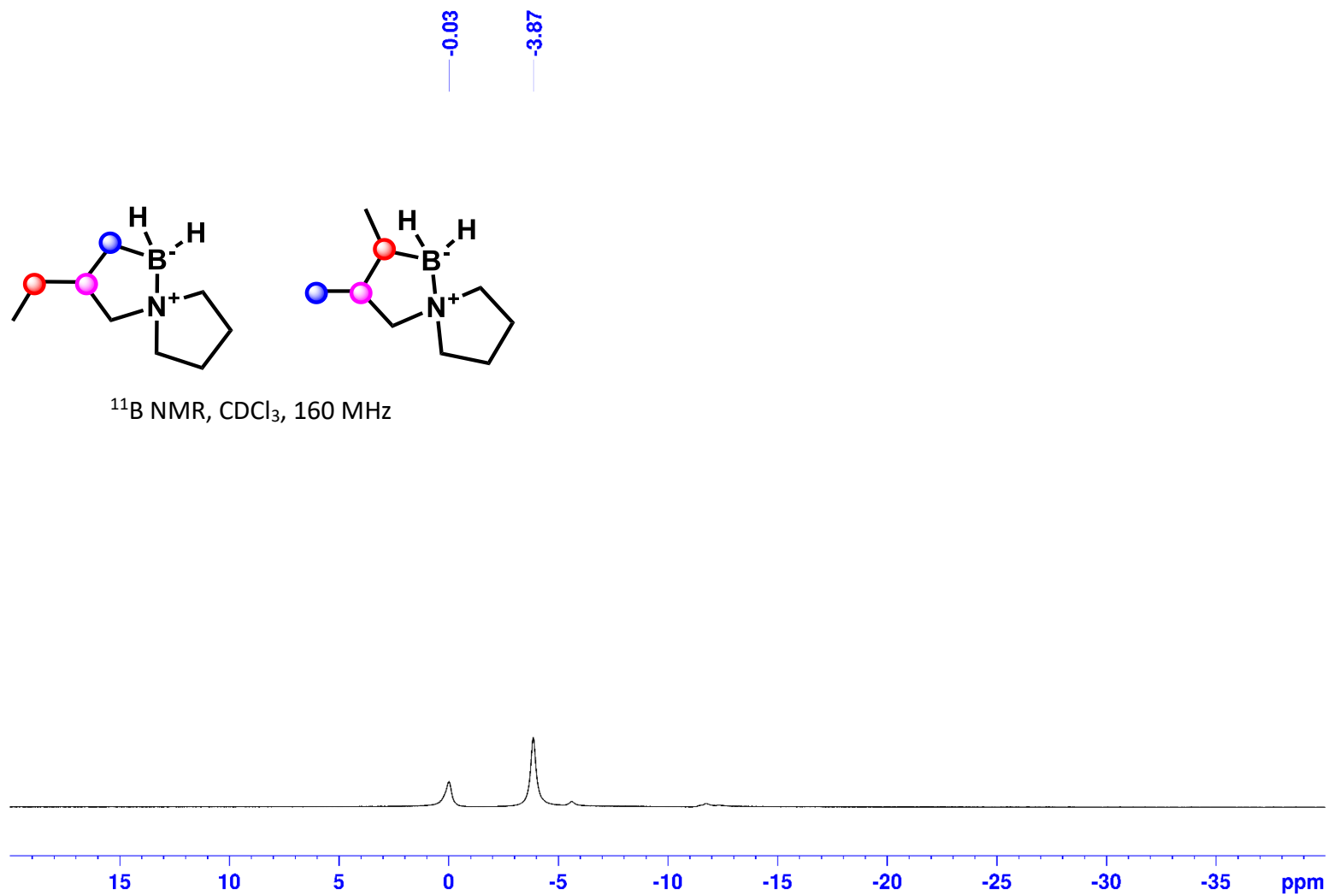
3-ethyl-5-aza-1-borasp[4.4]nonane (2w) and 2,3-dimethyl-5-aza-1-borasp[4.4]nonane (2wa):



3-ethyl-5-aza-1-borasp[4.4]nonane (2w) and 2,3-dimethyl-5-aza-1-borasp[4.4]nonane (2wa):

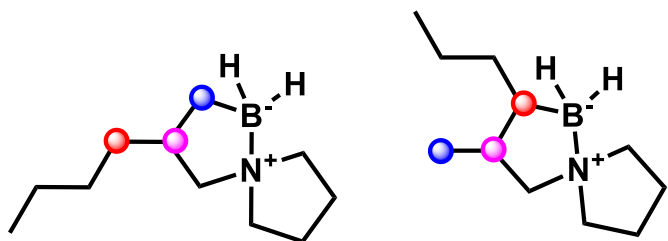


3-ethyl-5-aza-1-borasp[4.4]nonane (2w) and 2,3-dimethyl-5-aza-1-borasp[4.4]nonane (2wa):

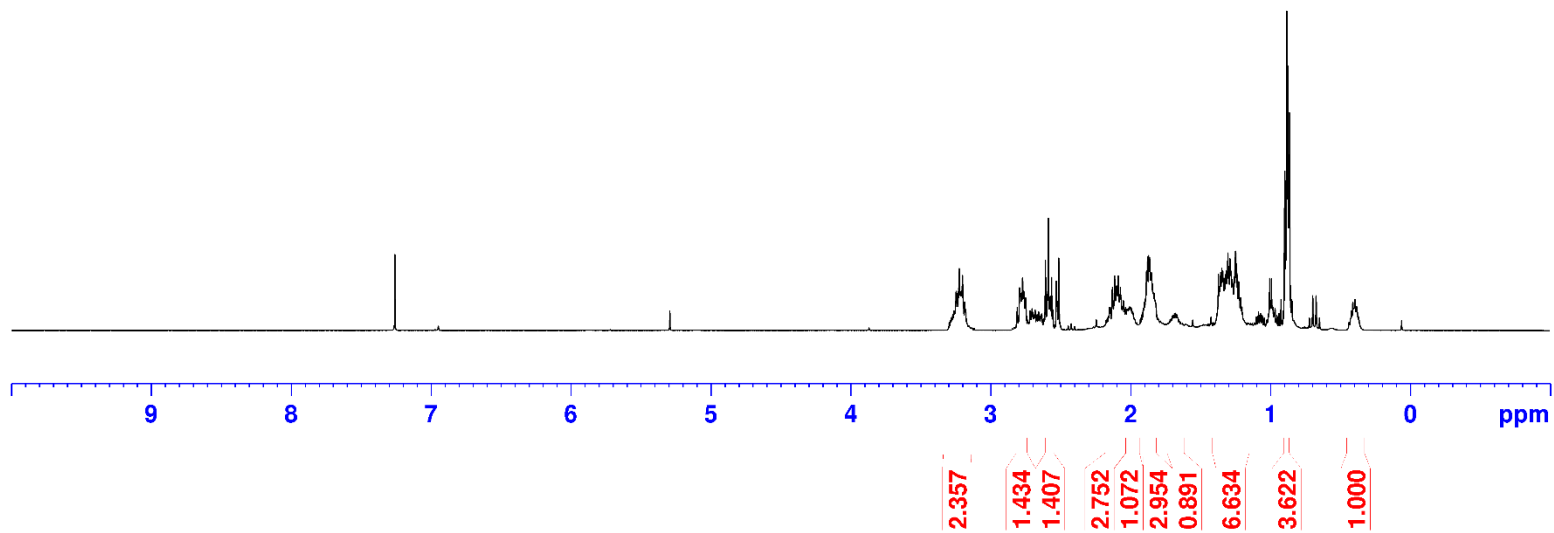


3-Propyl-5-aza-1-borasp[4.4]nonane (2x), 2-ethyl-3-methyl-5-aza-1-borasp[4.4]nonane (2xa):

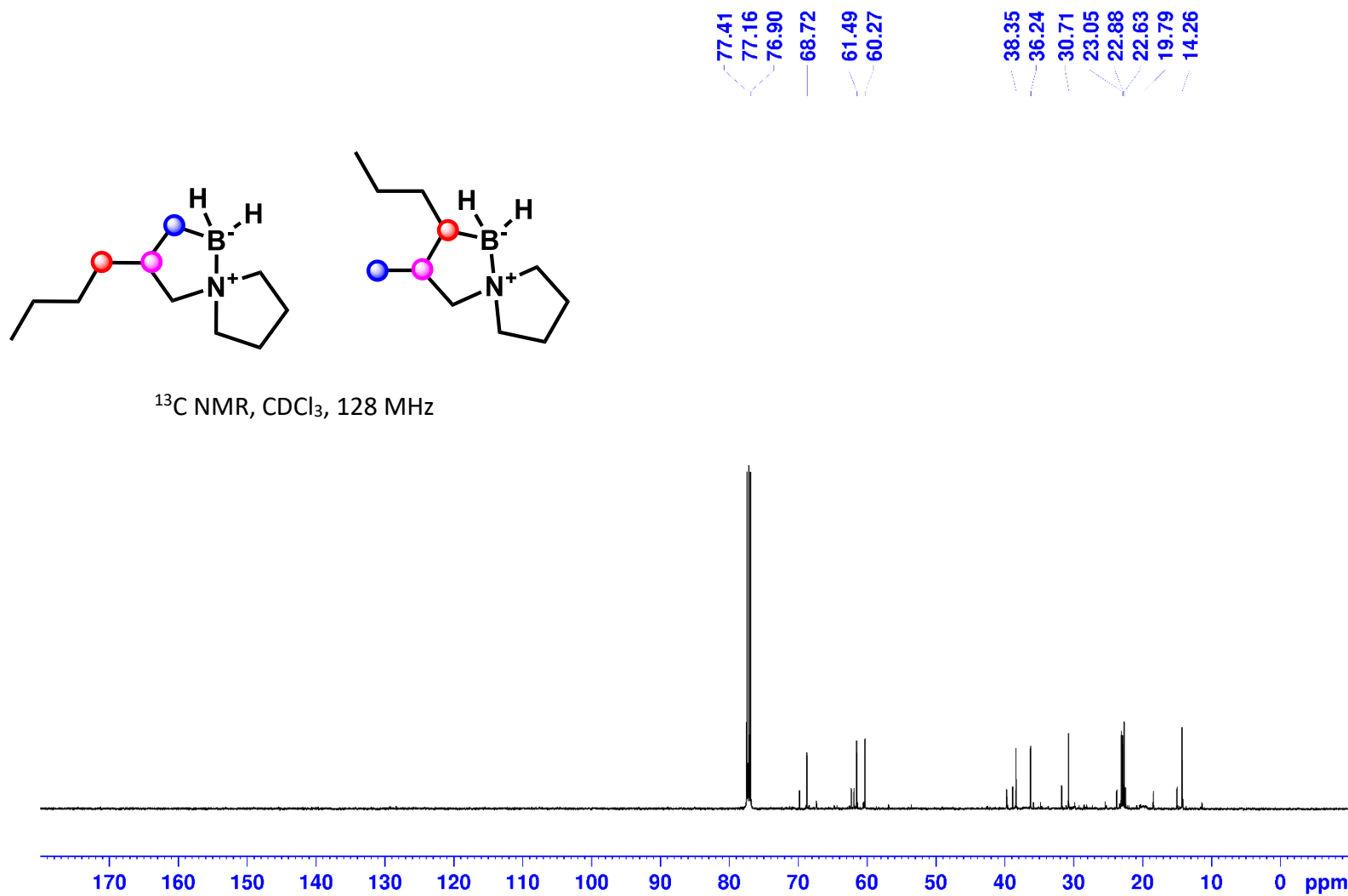
3.247
3.240
3.224
3.215
3.209
3.202
2.794
2.788
2.772
2.763
2.609
2.587
2.573
2.565
2.531
2.513
2.130
2.114
2.100
2.088
2.073
1.886
1.878
1.871
1.864
1.850
1.830
1.372
1.360
1.355
1.348
1.341
1.329
1.319
1.316
1.311
1.305
1.297
1.290
1.283
1.275
1.249
1.240
1.227
1.213
0.897
0.885
0.883
0.876
0.869
0.863
0.395



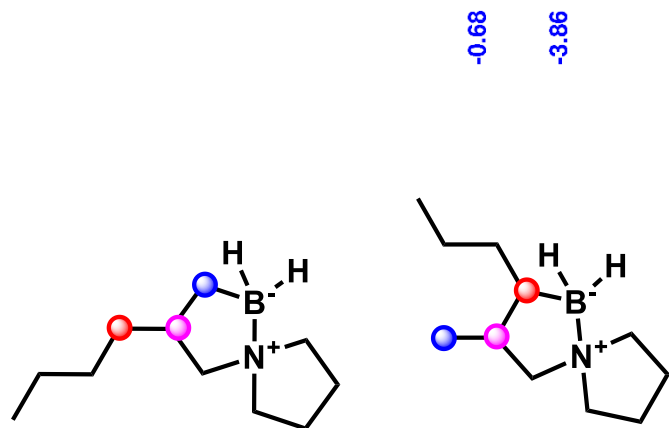
$^1\text{H NMR}$, CDCl_3 , 500 MHz



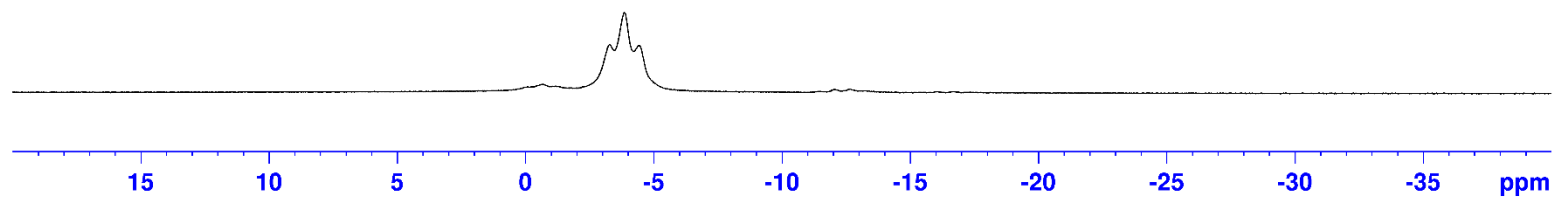
3-Propyl-5-aza-1-borasp[4.4]nonane (2x), 2-ethyl-3-methyl-5-aza-1-borasp[4.4]nonane (2xa):



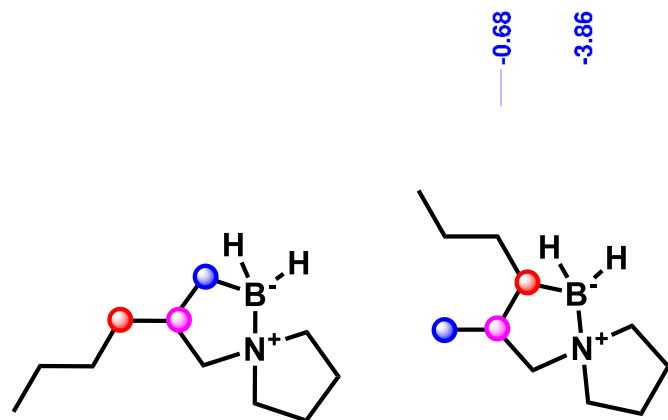
3-Propyl-5-aza-1-borasp[4.4]nonane (2x), 2-ethyl-3-methyl-5-aza-1-borasp[4.4]nonane (2xa):



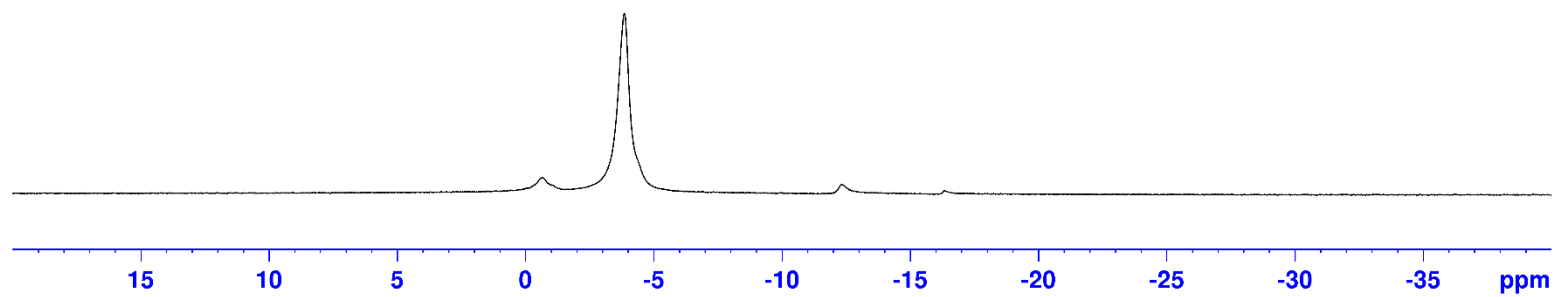
^{11}B NMR, CDCl_3 , 160 MHz



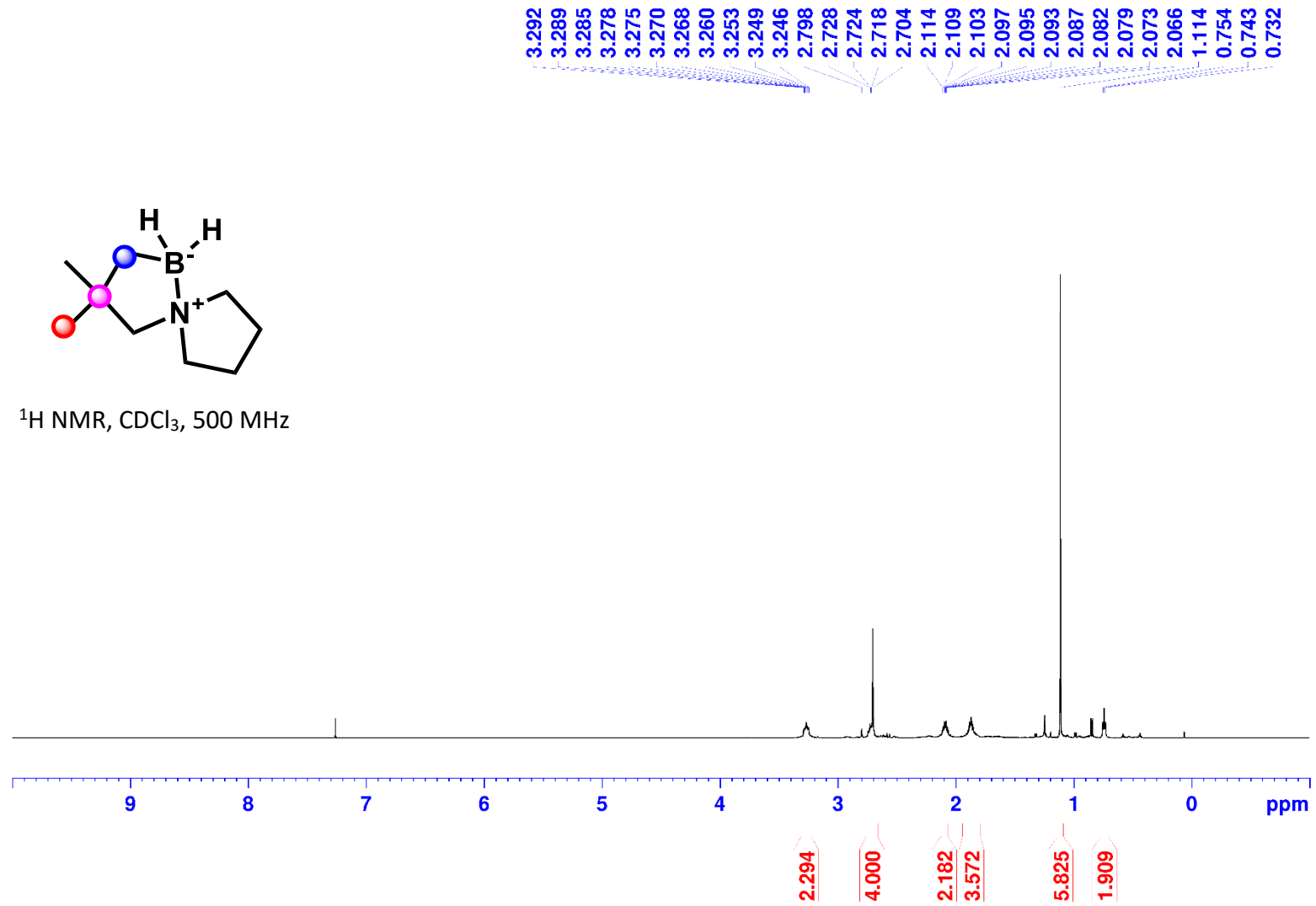
3-Propyl-5-aza-1-borasp[4.4]nonane (2x), 2-ethyl-3-methyl-5-aza-1-borasp[4.4]nonane (2xa):



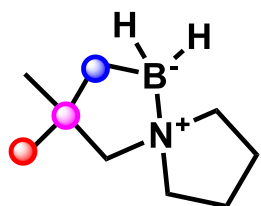
^{11}B NMR, CDCl_3 , 160 MHz



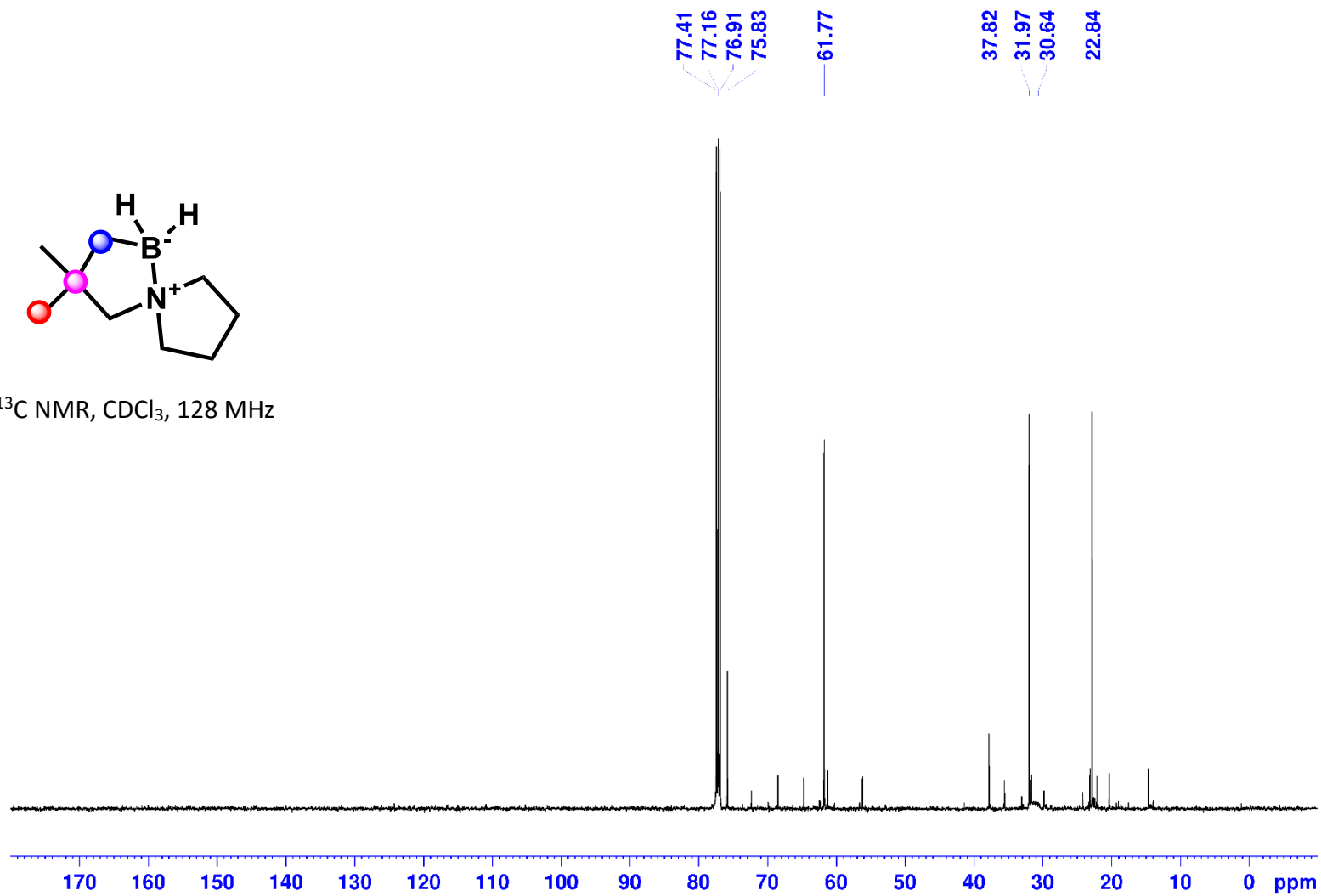
3,3-Dimethyl-5-aza-1-borasp[4.4]nonane (2y):



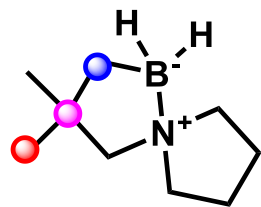
3,3-Dimethyl-5-aza-1-borasp[iro[4.4]nonane (2y):



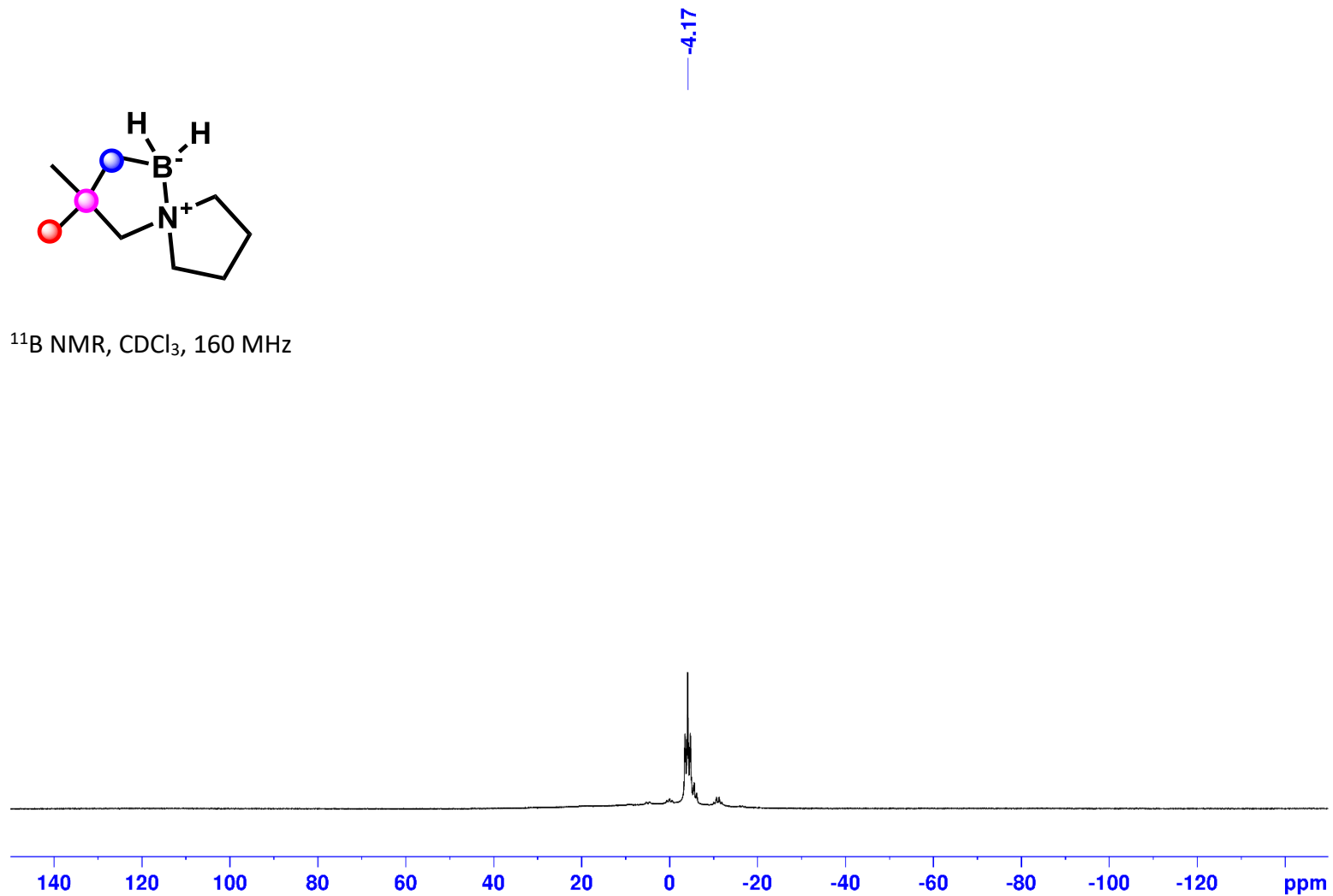
^{13}C NMR, CDCl_3 , 128 MHz



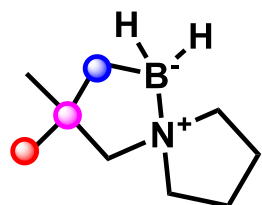
3,3-Dimethyl-5-aza-1-borasp[4.4]nonane (2y):



^{11}B NMR, CDCl_3 , 160 MHz

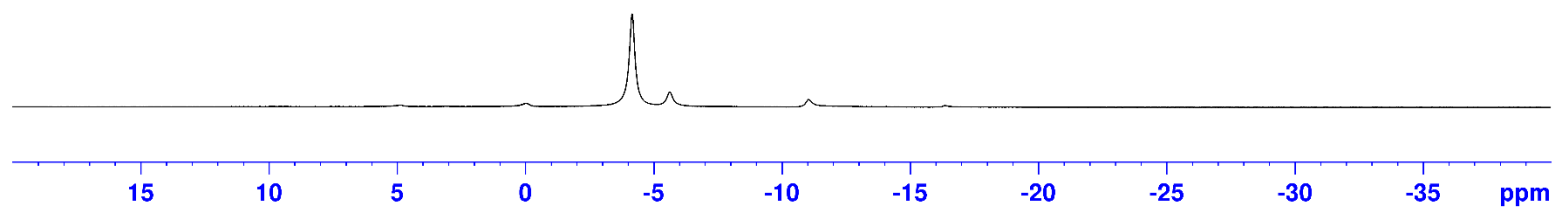


3,3-Dimethyl-5-aza-1-borasp[4.4]nonane (2y):

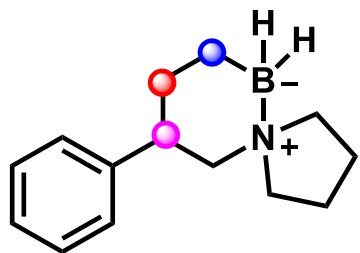


-4.16

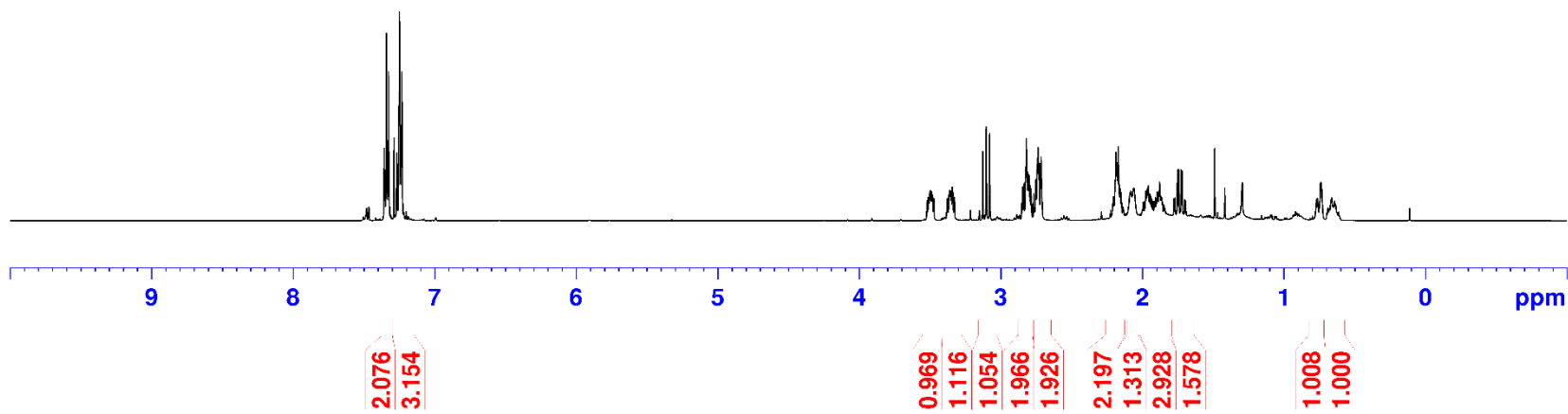
^{11}B NMR, CDCl_3 , 160 MHz



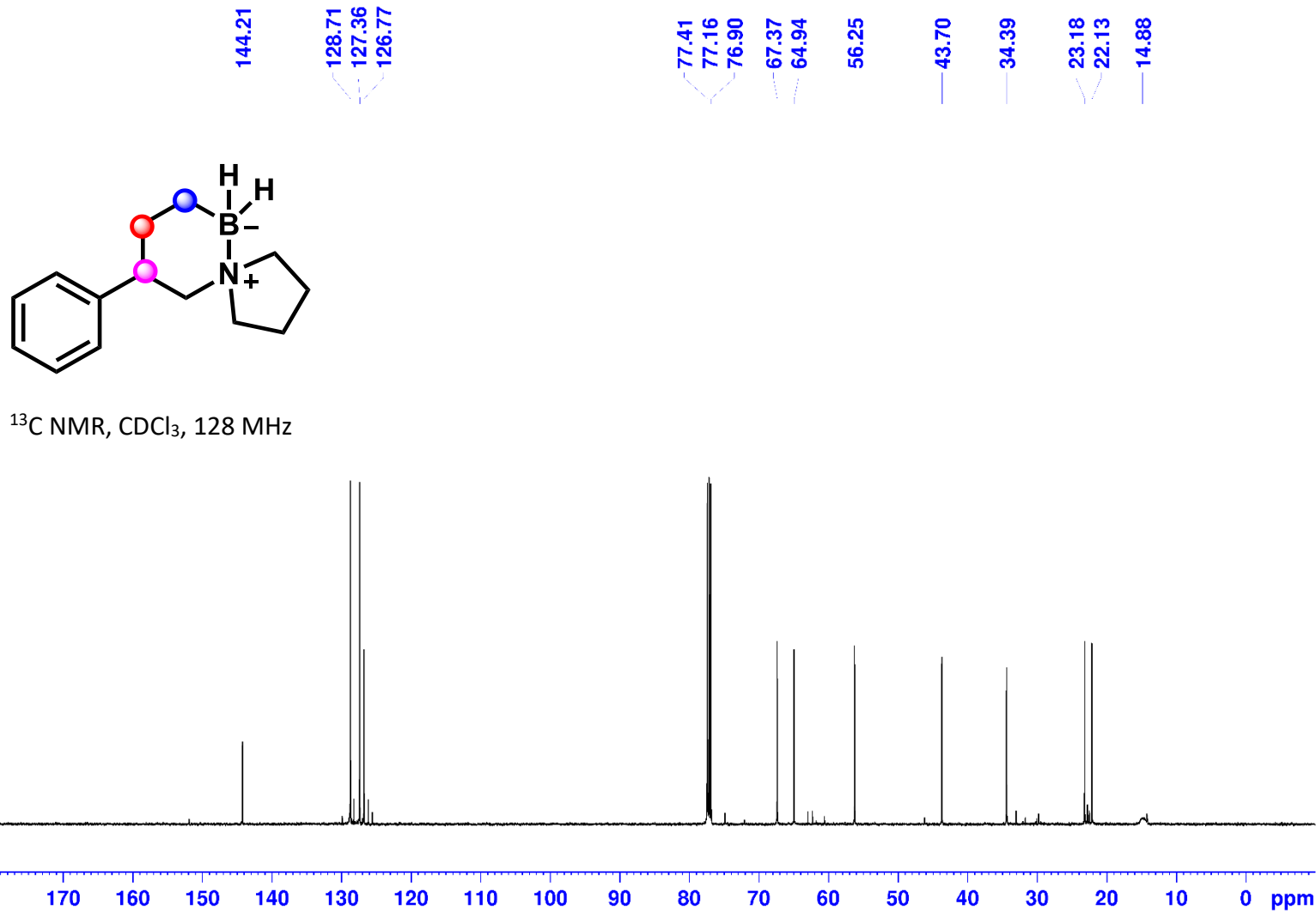
9-Phenyl-5-aza-6-boraspiro[4.5]decane (2z):



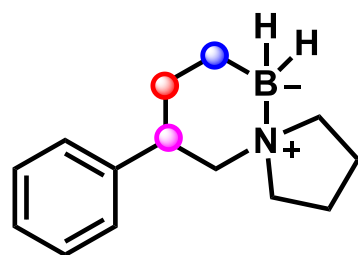
¹H NMR, CDCl₃, 500 MHz



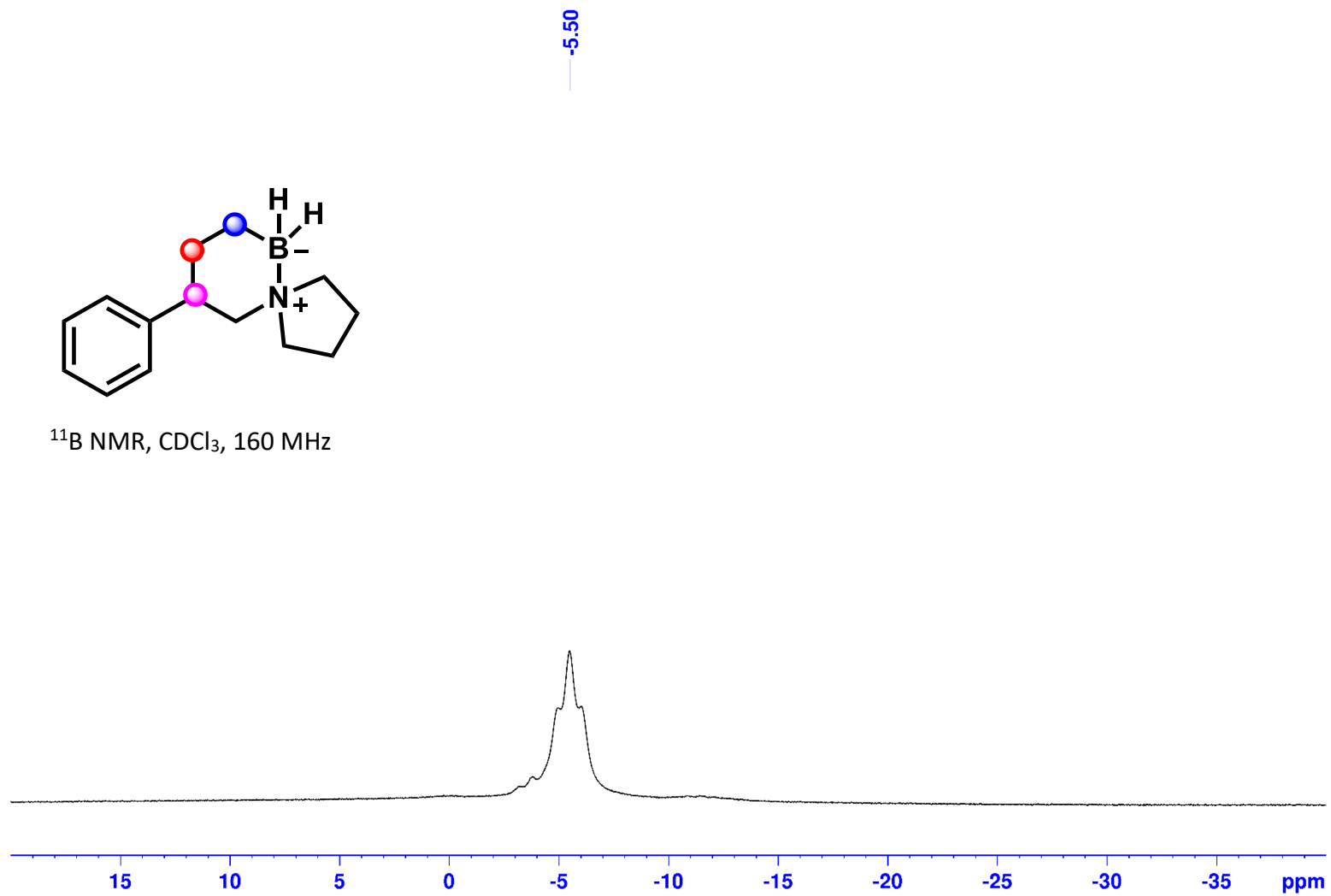
9-Phenyl-5-aza-6-borasp[iro[4.5]decane (2z):



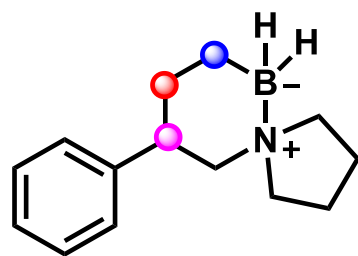
9-Phenyl-5-aza-6-borasp[4.5]decane (2z):



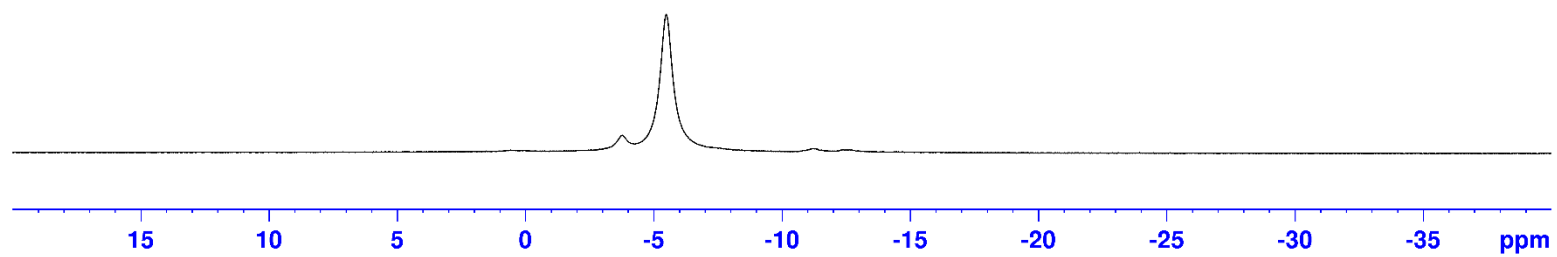
^{11}B NMR, CDCl_3 , 160 MHz



9-Phenyl-5-aza-6-borasp[iro[4.5]decane (2z):

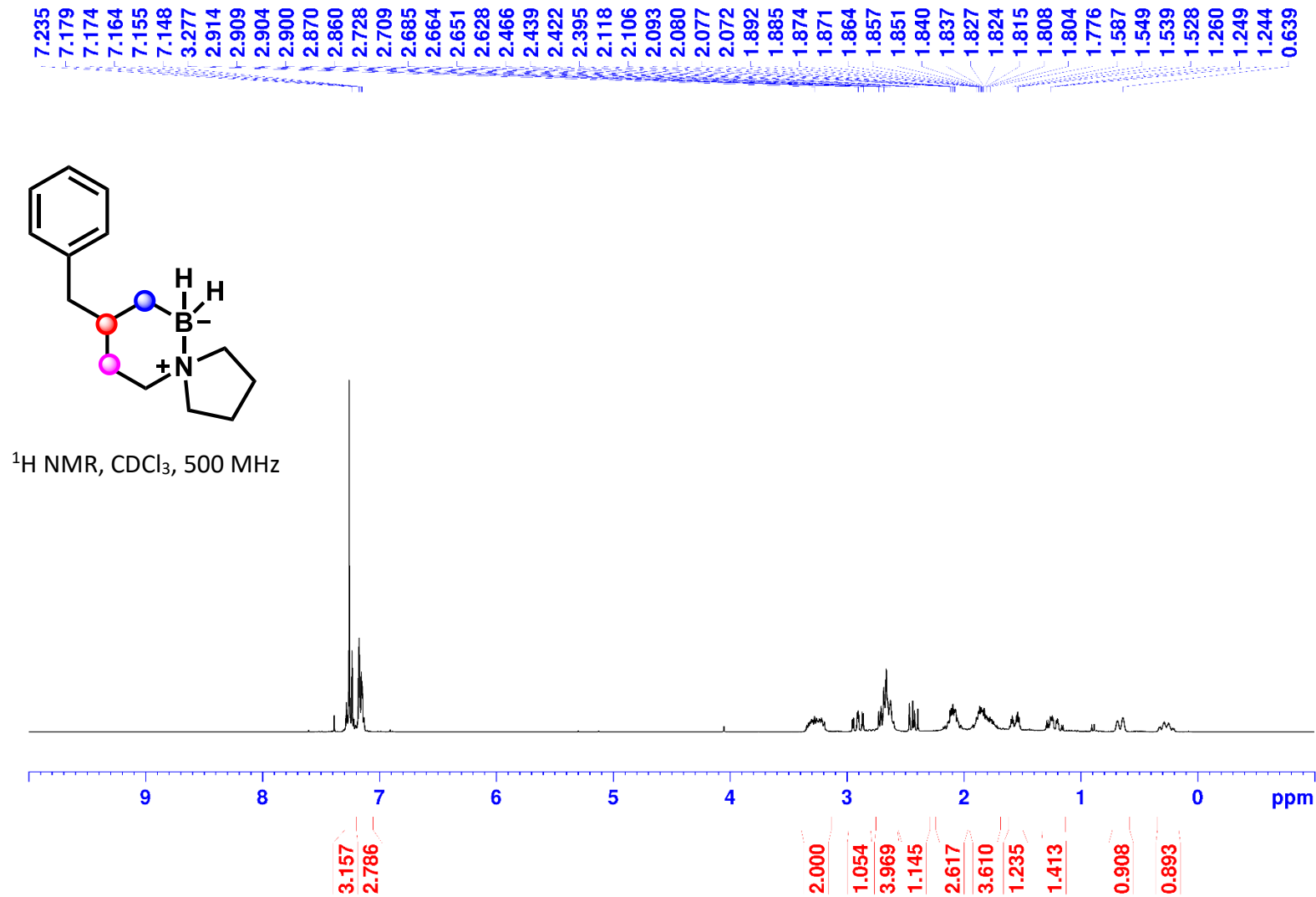


^{11}B NMR, CDCl_3 , 160 MHz

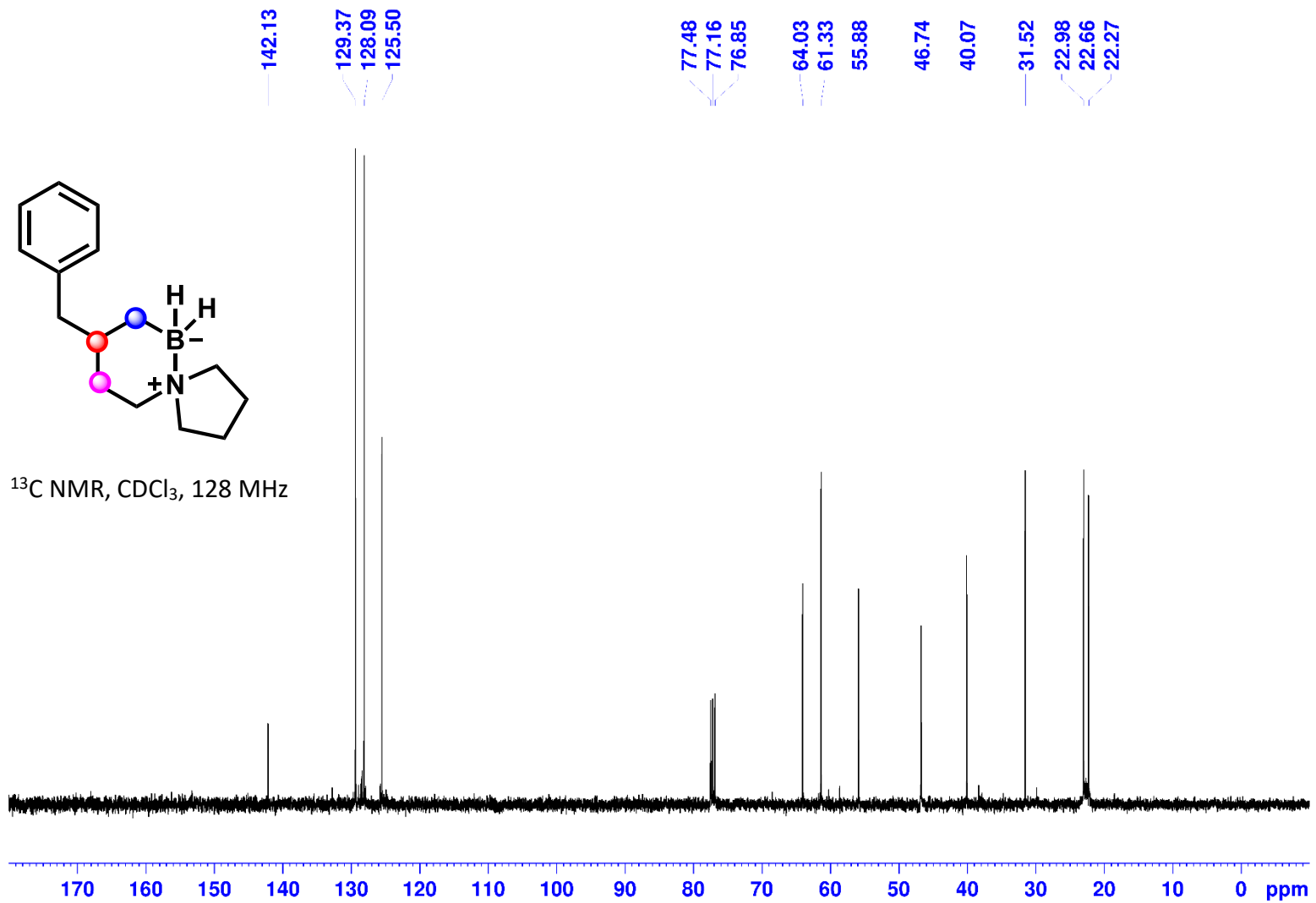


-5.49

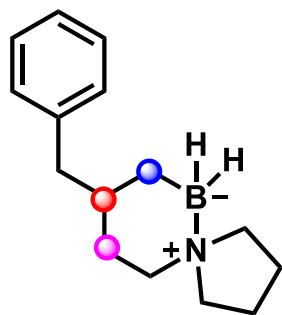
8-Benzyl-5-aza-6-borasp[iro[4.5]decane (2aa):



8-Benzyl-5-aza-6-borasp[4.5]decane (2a):

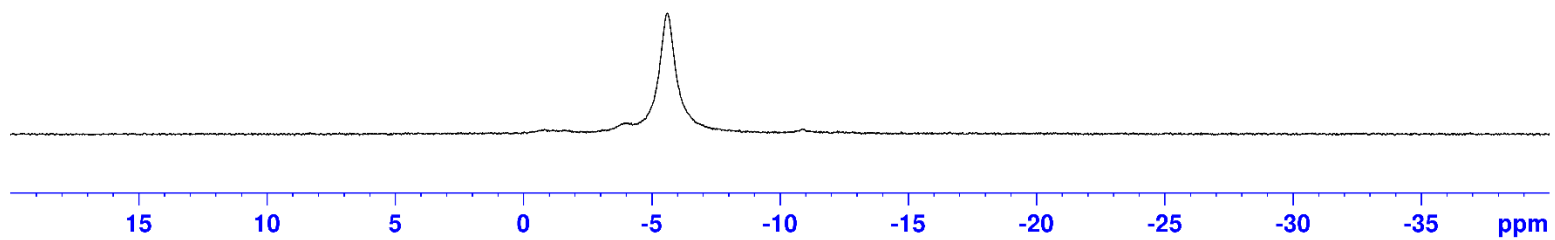


8-Benzyl-5-aza-6-boraspiro[4.5]decane (2aa):

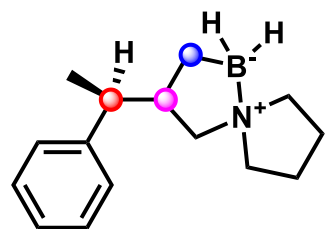


-5.62

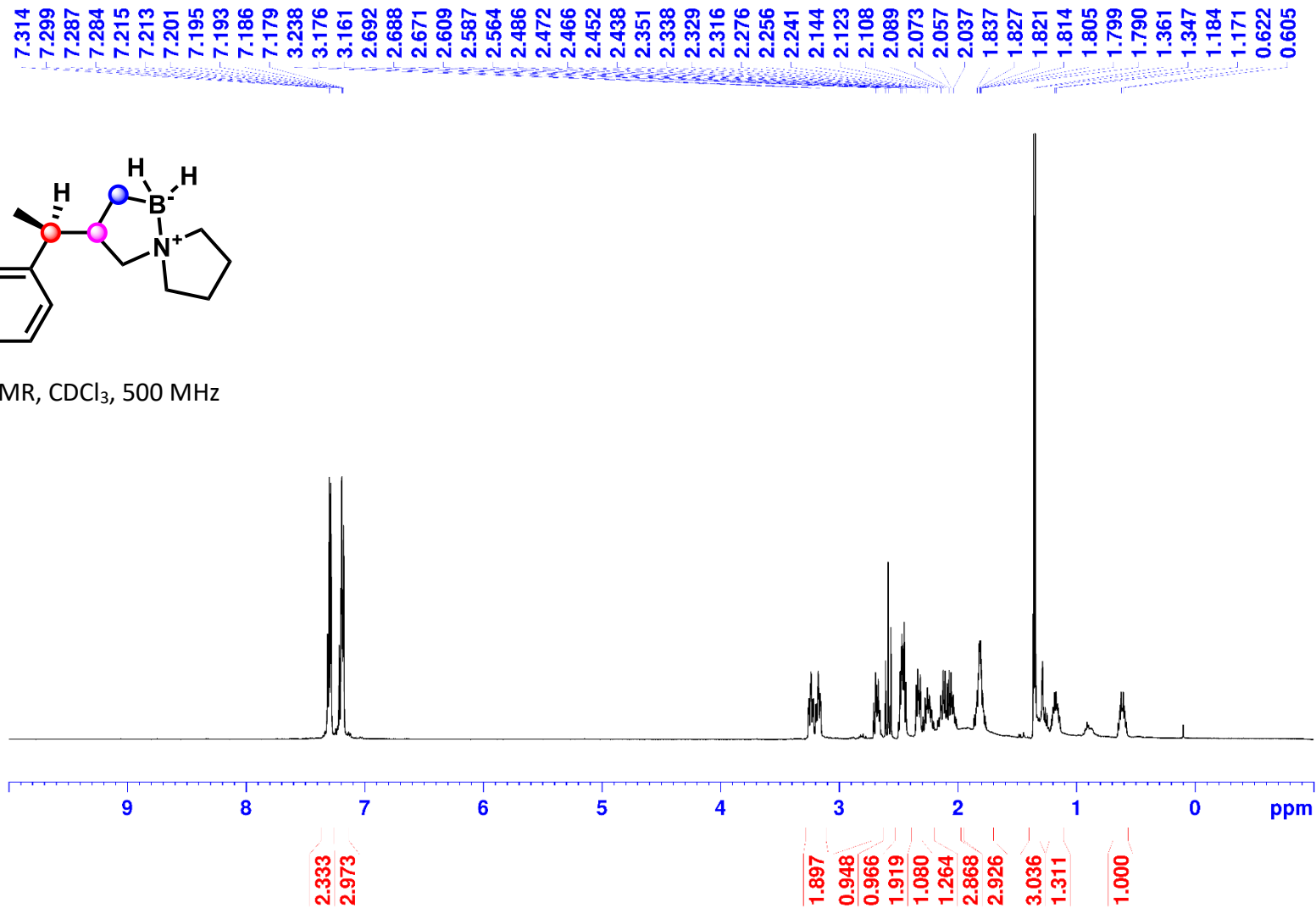
^{11}B NMR, CDCl_3 , 160 MHz



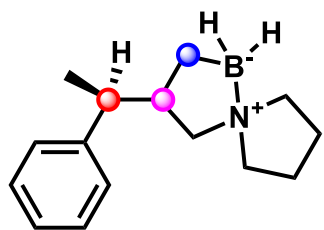
3-((S)-1-Phenylethyl)-5-aza-1-borasp[4.4]nonane (2ab):



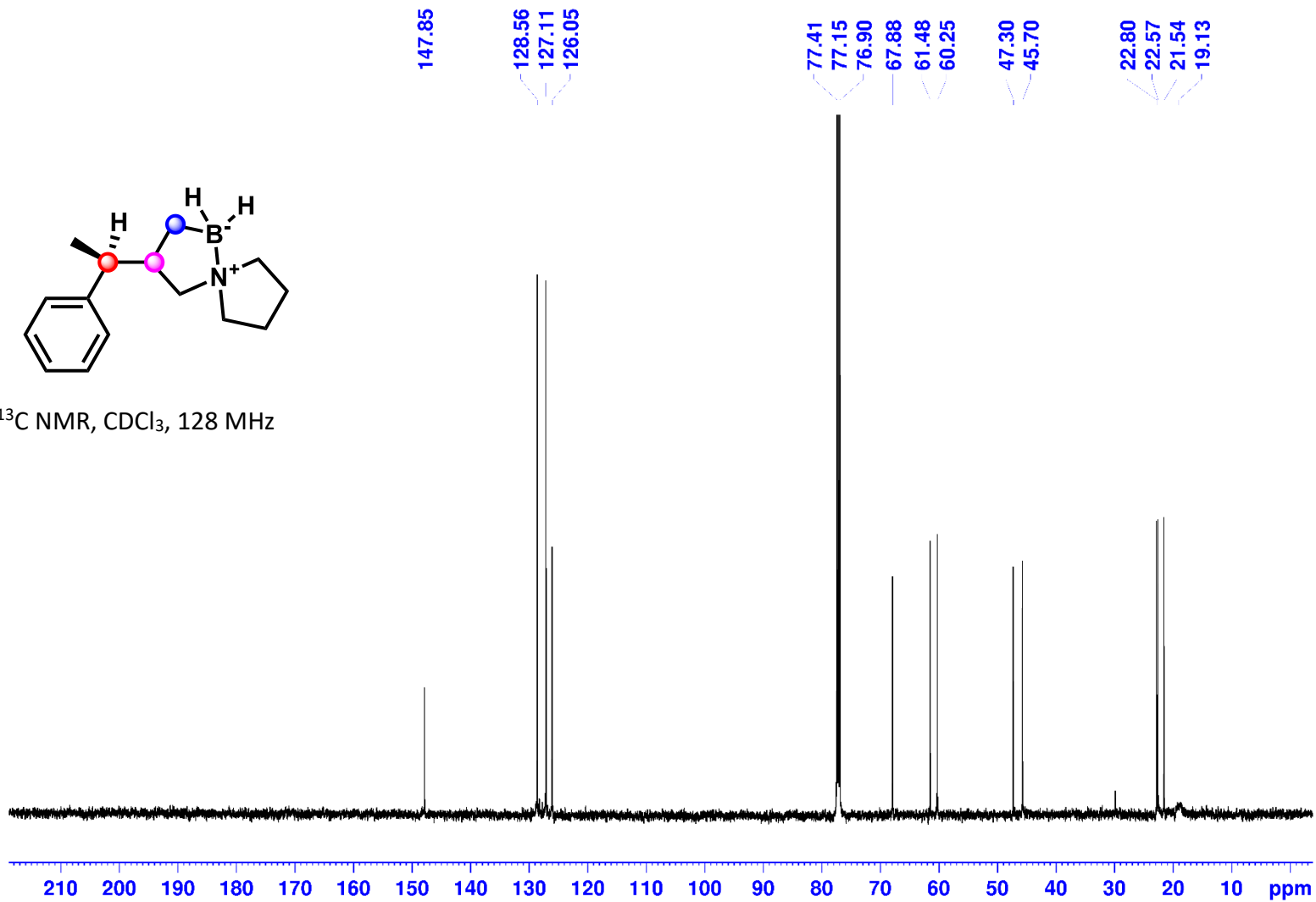
^1H NMR, CDCl_3 , 500 MHz



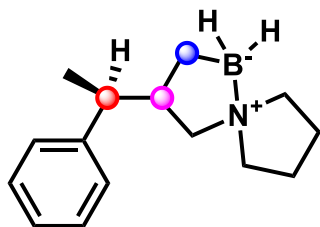
3-((S)-1-Phenylethyl)-5-aza-1-borasp[4.4]nonane (2ab):



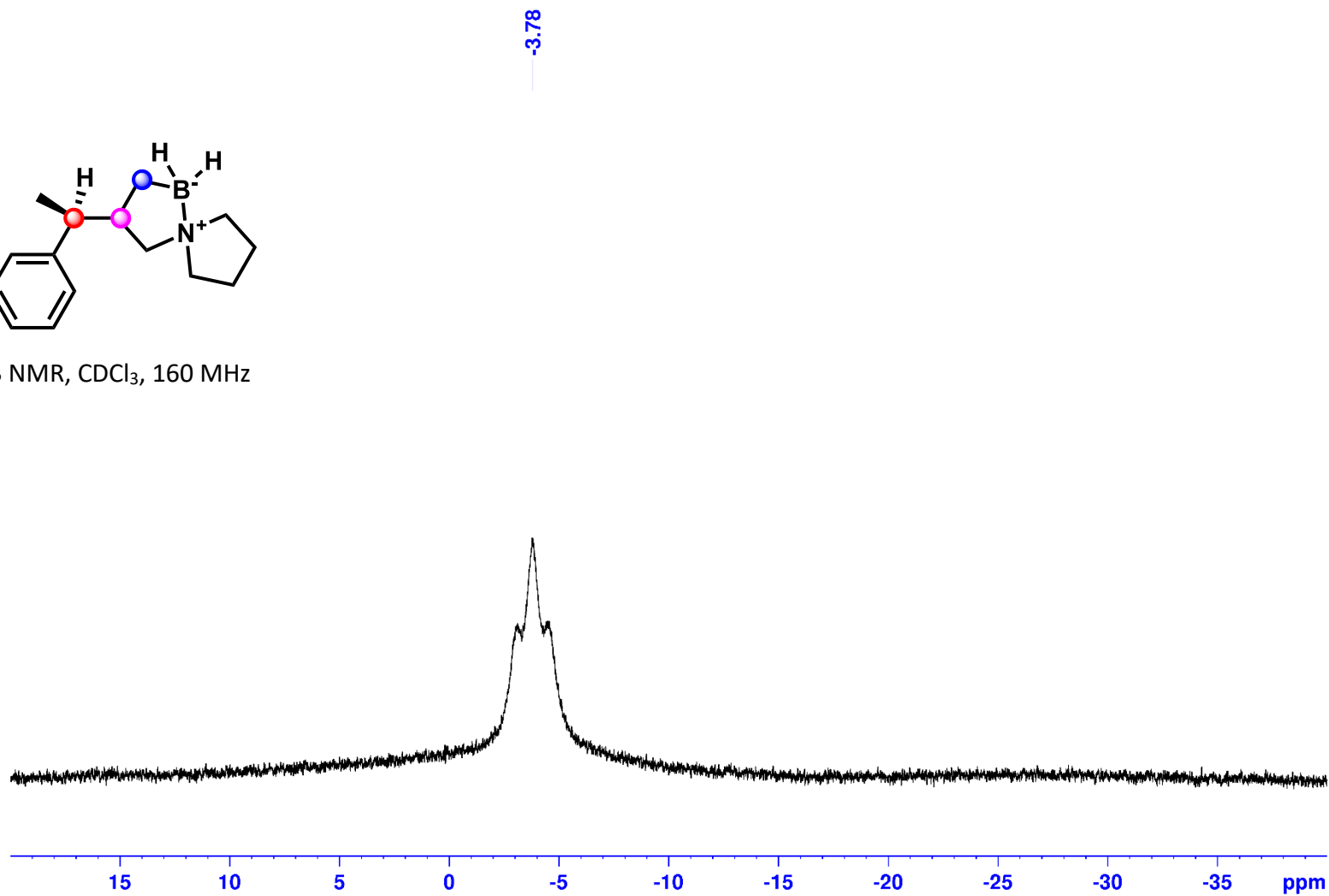
^{13}C NMR, CDCl_3 , 128 MHz



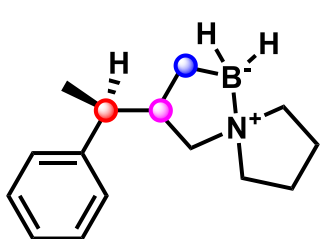
3-((S)-1-Phenylethyl)-5-aza-1-borasp[4.4]nonane (2ab):



^{11}B NMR, CDCl_3 , 160 MHz

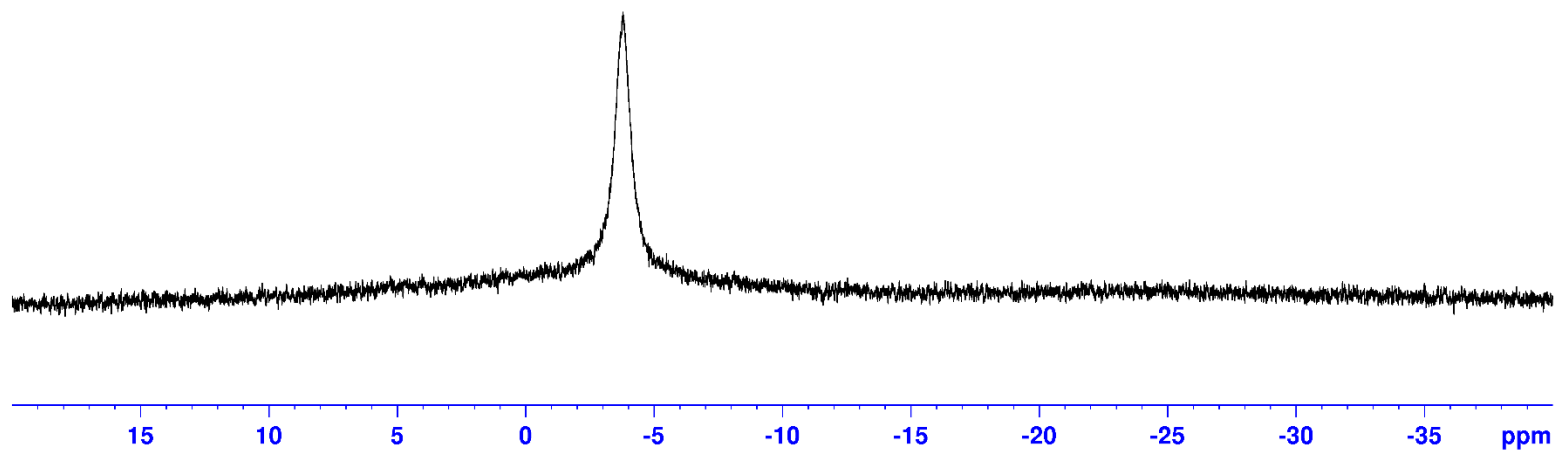


3-((S)-1-Phenylethyl)-5-aza-1-borasp[4.4]nonane (2ab):

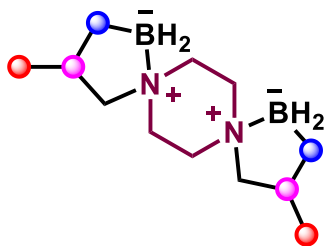


-3.80

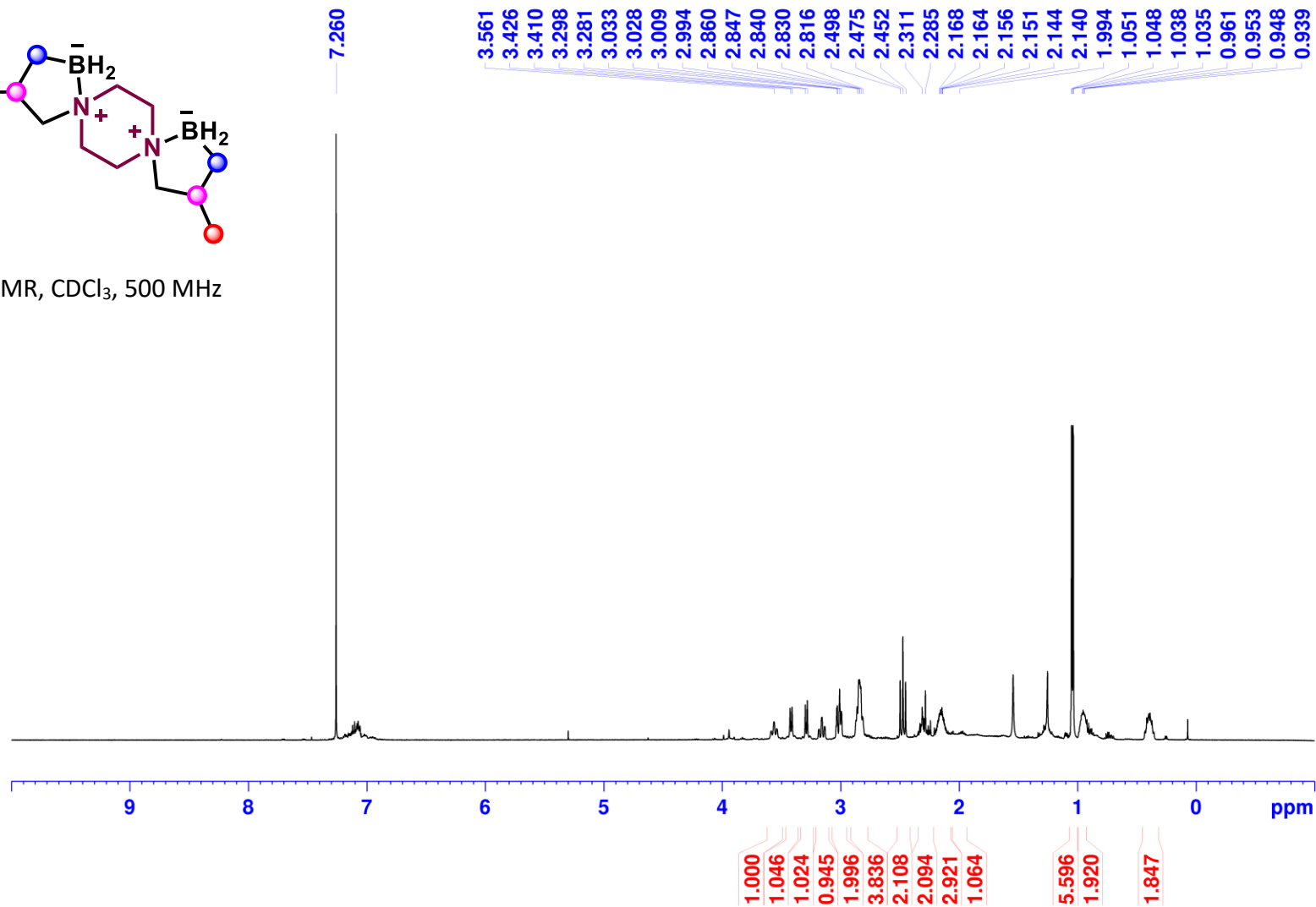
^{11}B NMR, CDCl_3 , 160 MHz



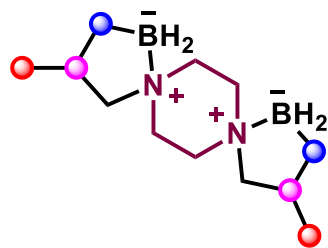
3-Methyl-5-aza-1-borasp[4.4]nonane (2ac):



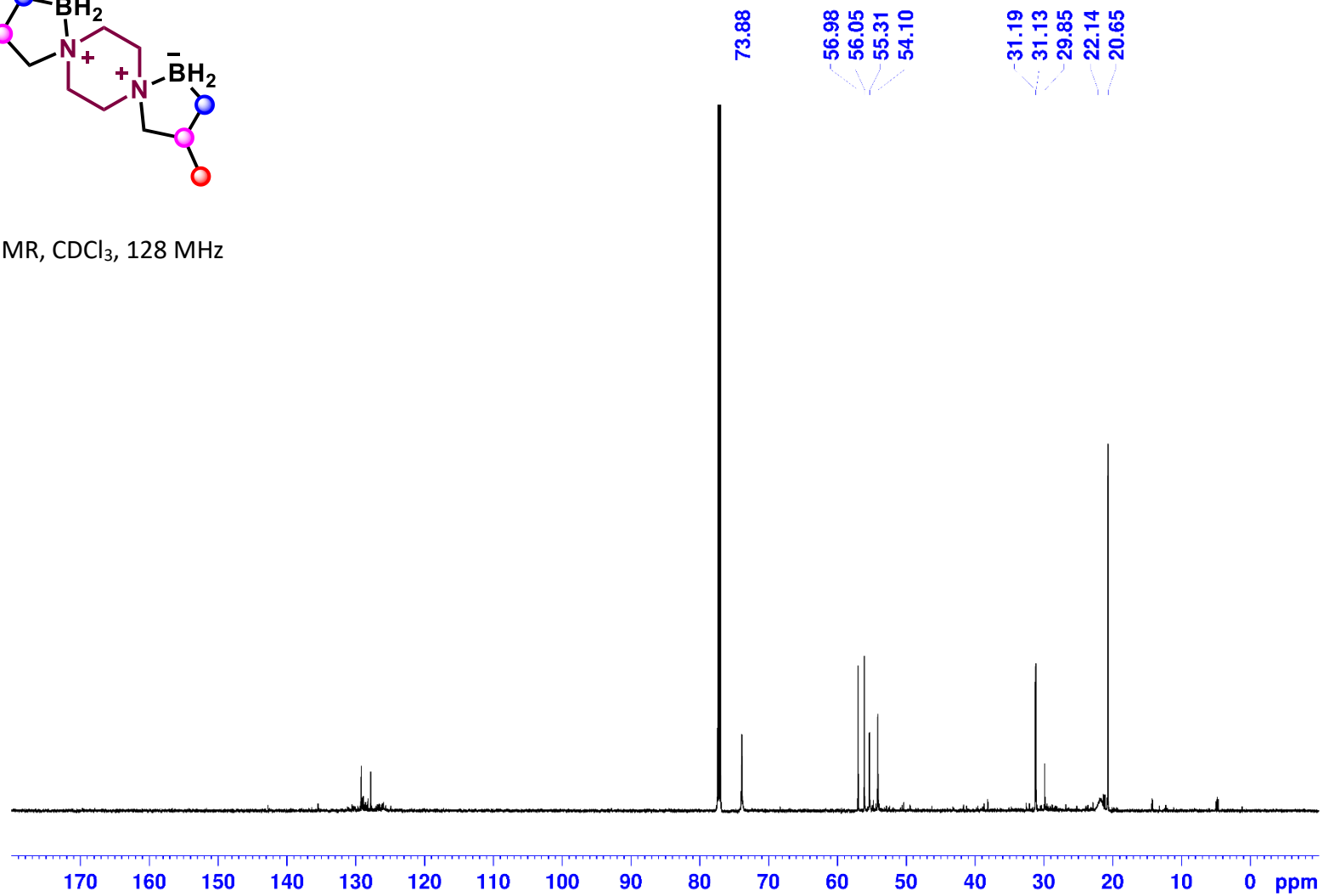
¹H NMR, CDCl₃, 500 MHz



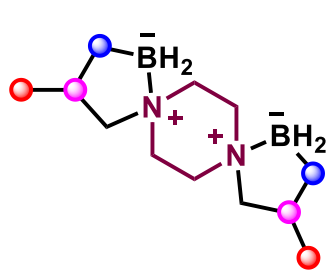
3-Methyl-5-aza-1-boraspino[4.4]nonane (2ac):



^{13}C NMR, CDCl_3 , 128 MHz

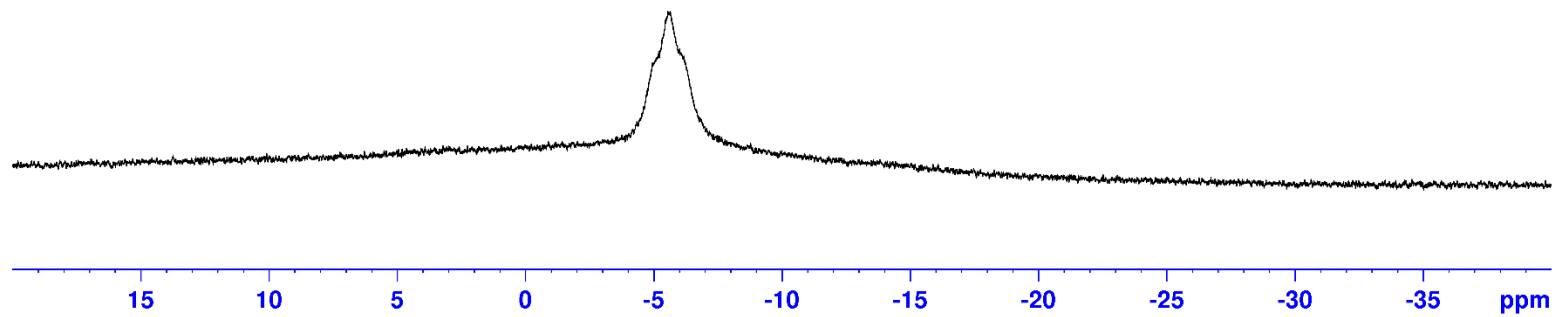


3-Methyl-5-aza-1-borasp[4.4]nonane (2ac):

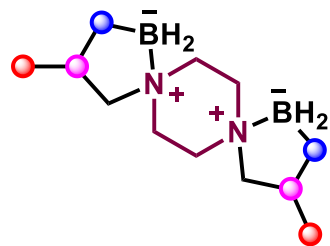


-5.65

^{11}B NMR, CDCl_3 , 160 MHz

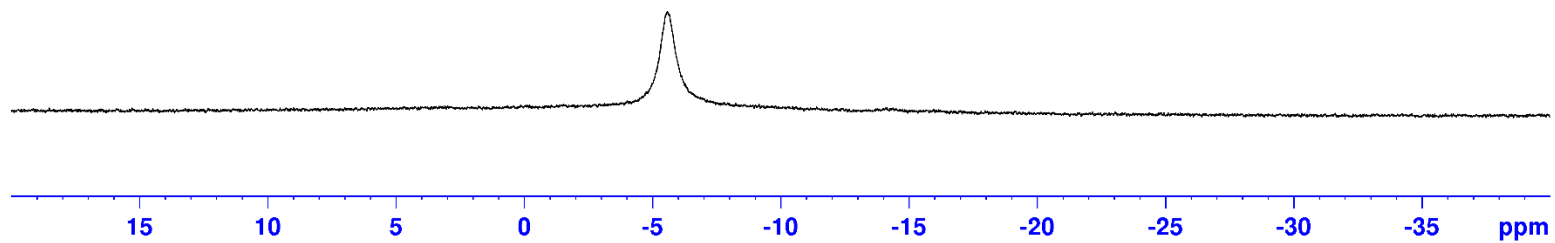


3-Methyl-5-aza-1-borasp[4.4]nonane (2ac):



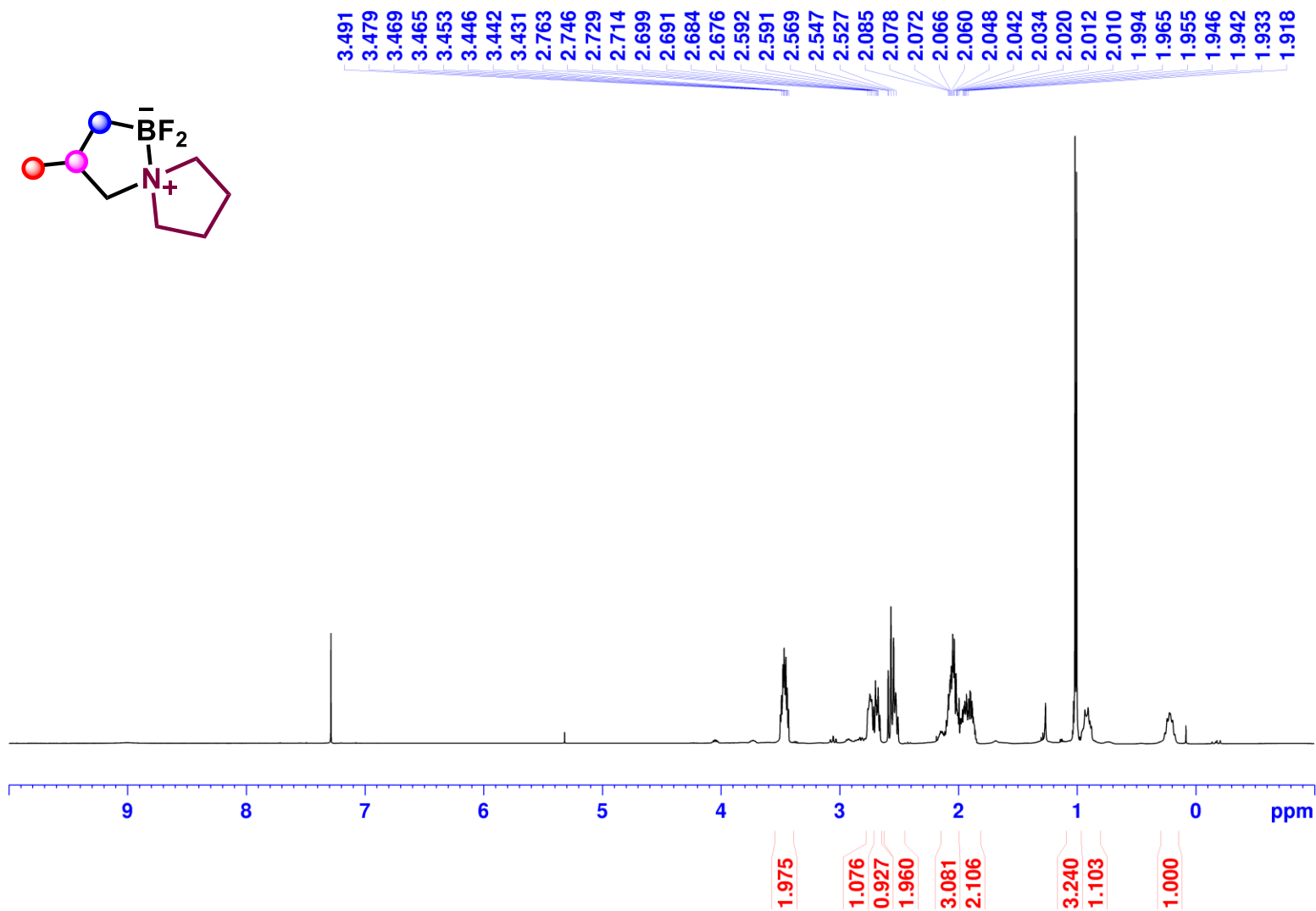
-5.59

^{11}B NMR, CDCl_3 , 160 MHz

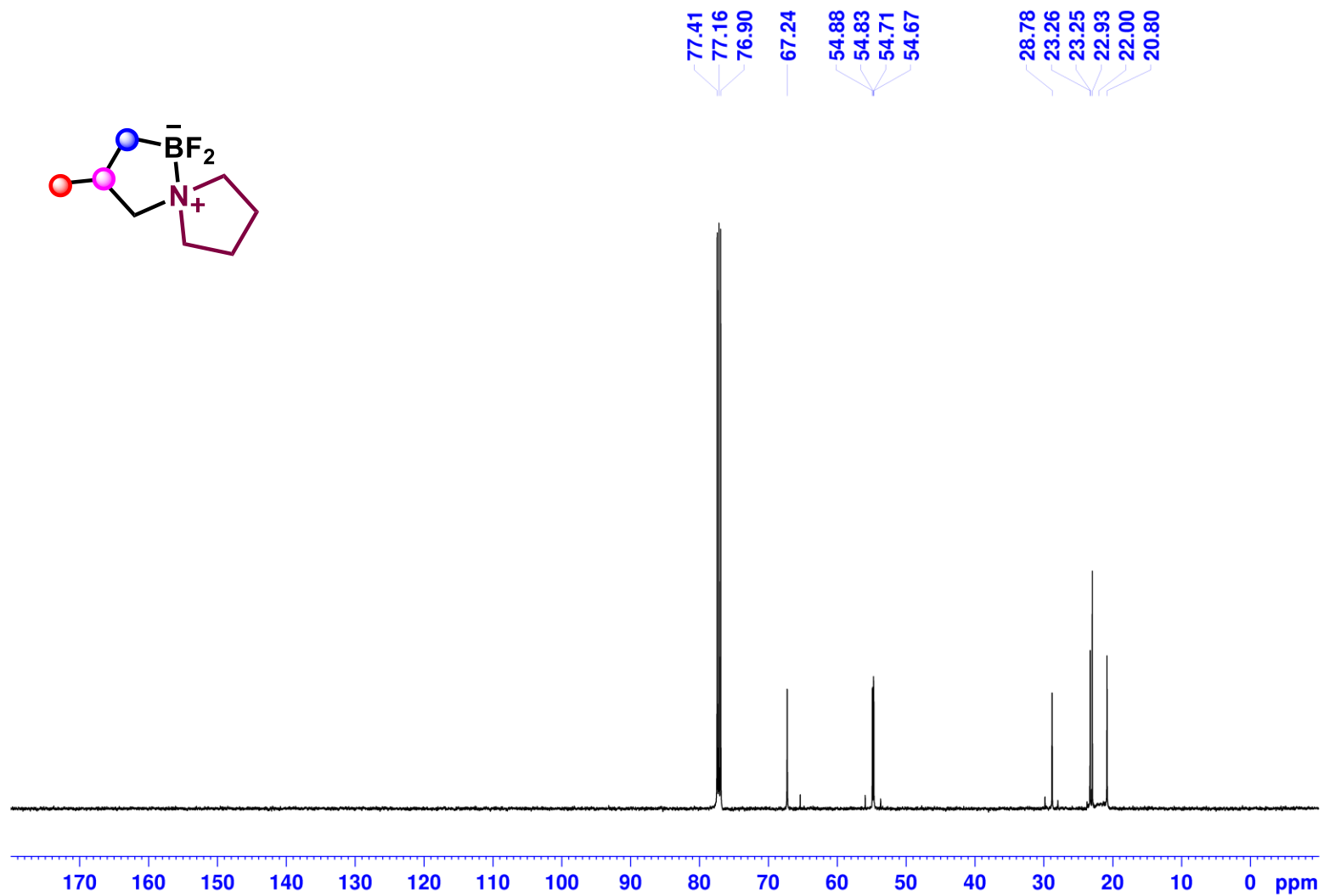


NMR Spectra of Post-Functionalized Products

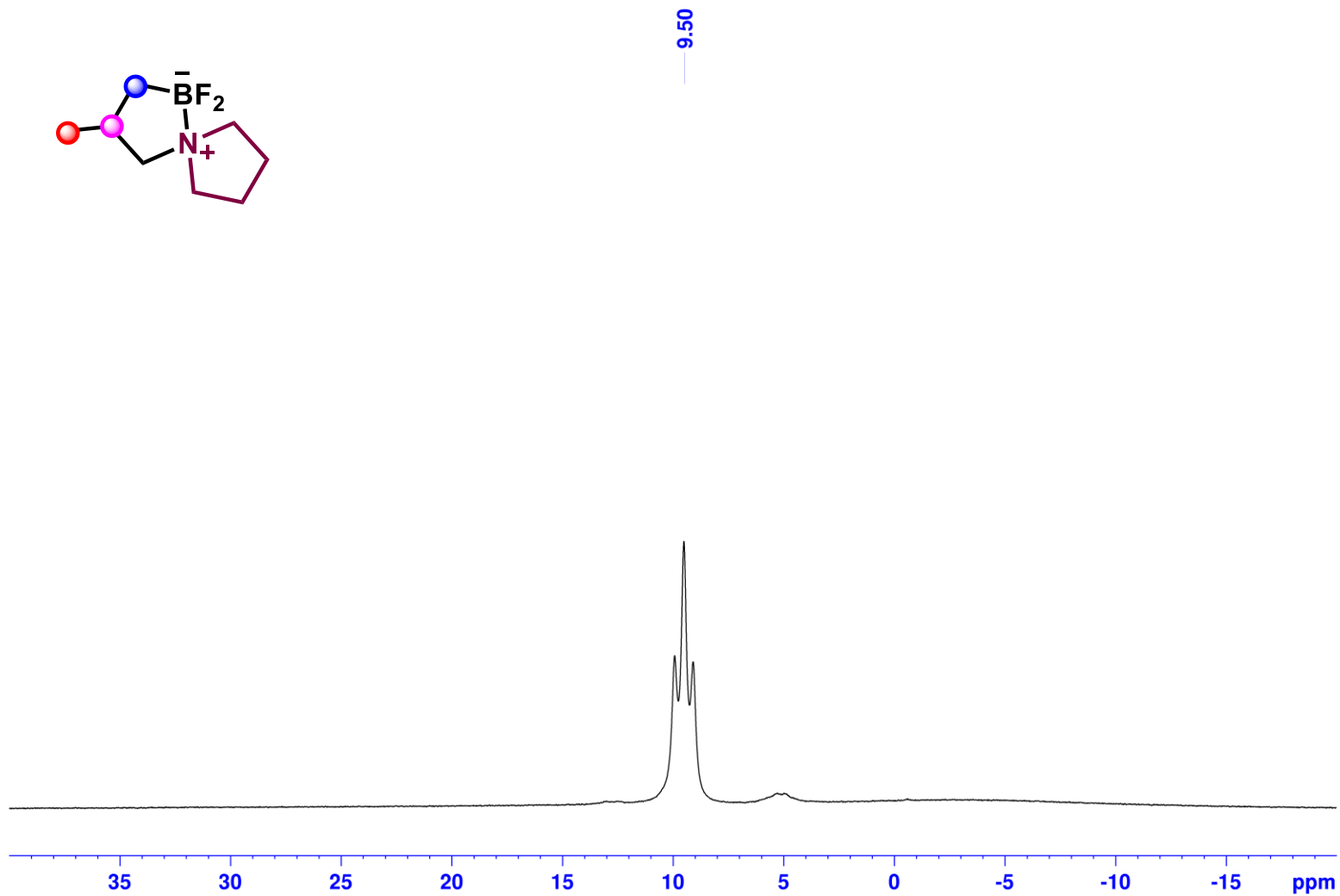
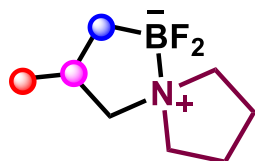
1,1-difluoro-3-methyl-5-aza-1-borasp[4.4]nonane (3a):



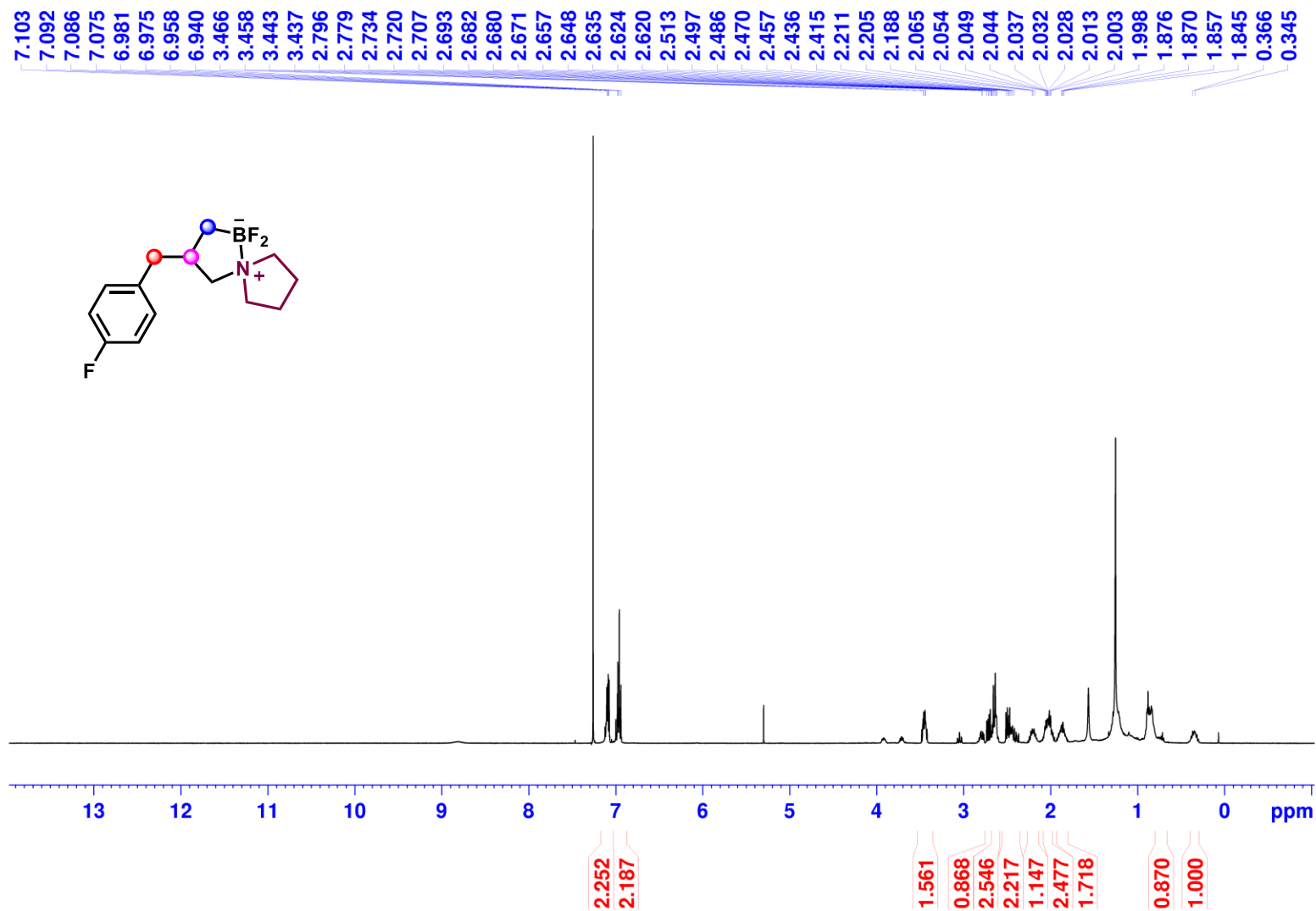
1,1-difluoro-3-methyl-5-aza-1-borasp[4.4]nonane (3a):



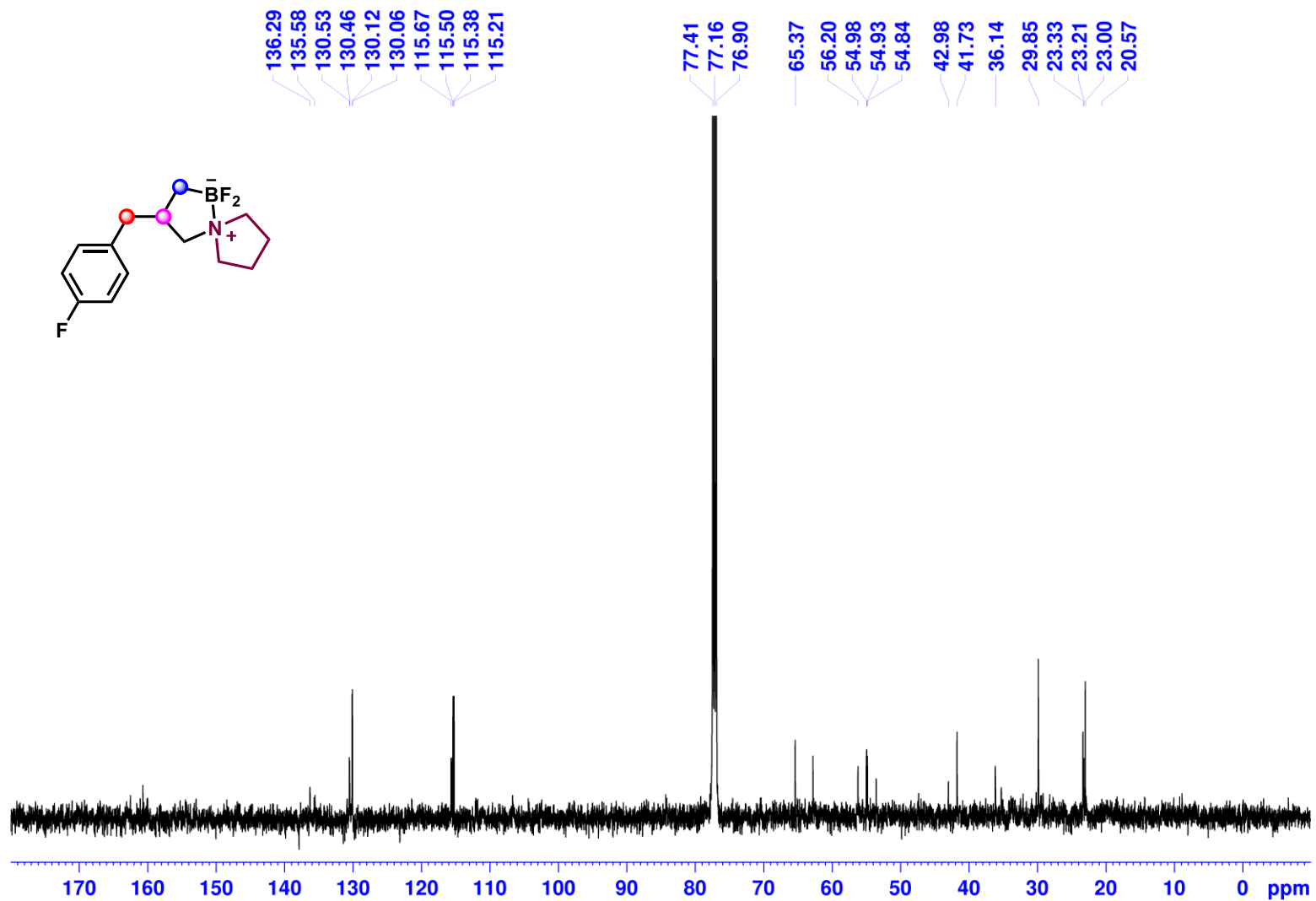
1,1-difluoro-3-methyl-5-aza-1-borasp[4.4]nonane (3a):



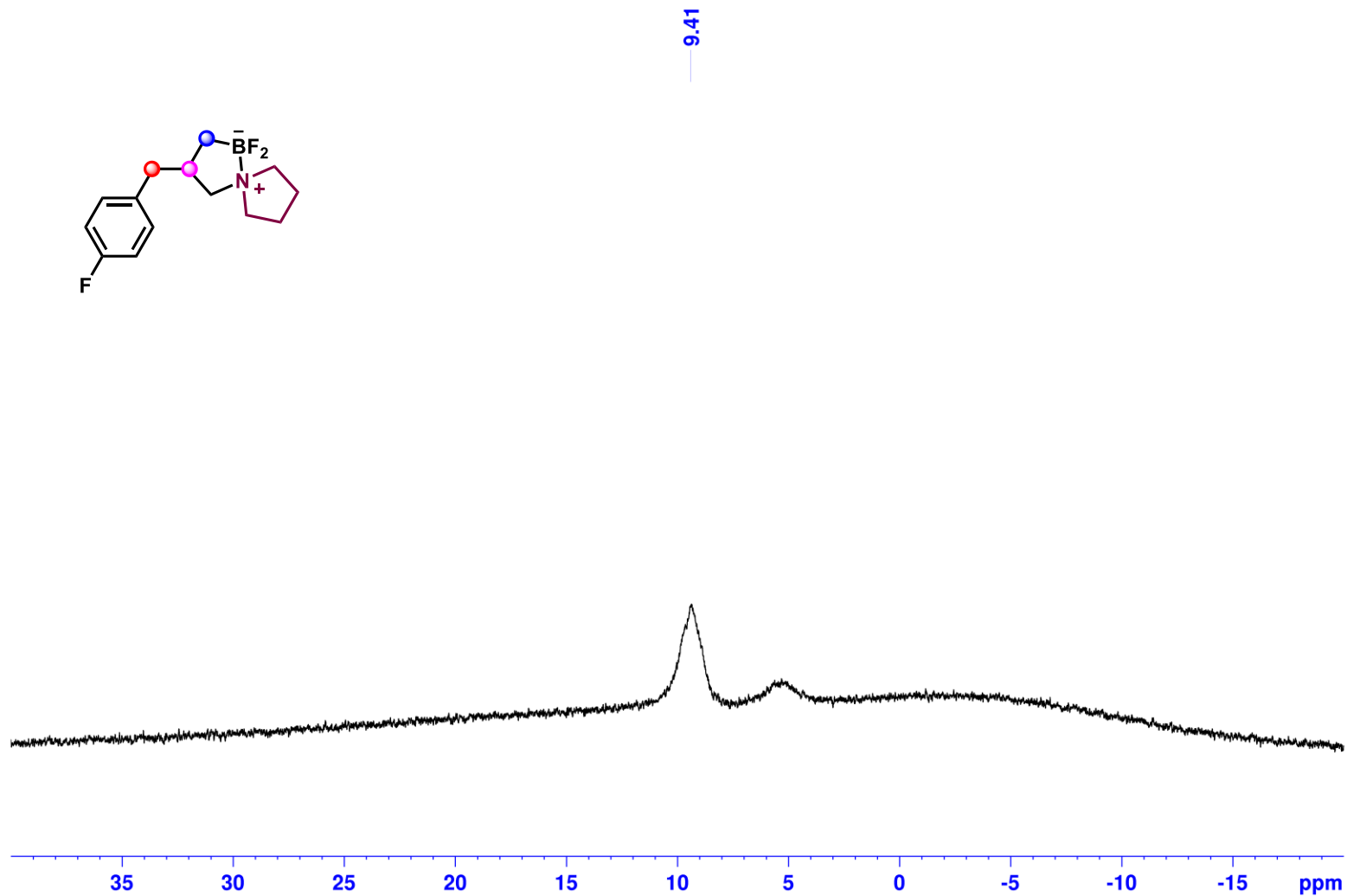
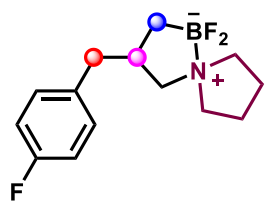
1,1-difluoro-3-(4-fluorobenzyl)-5-aza-1-borasp[4.4]nonane (3b):



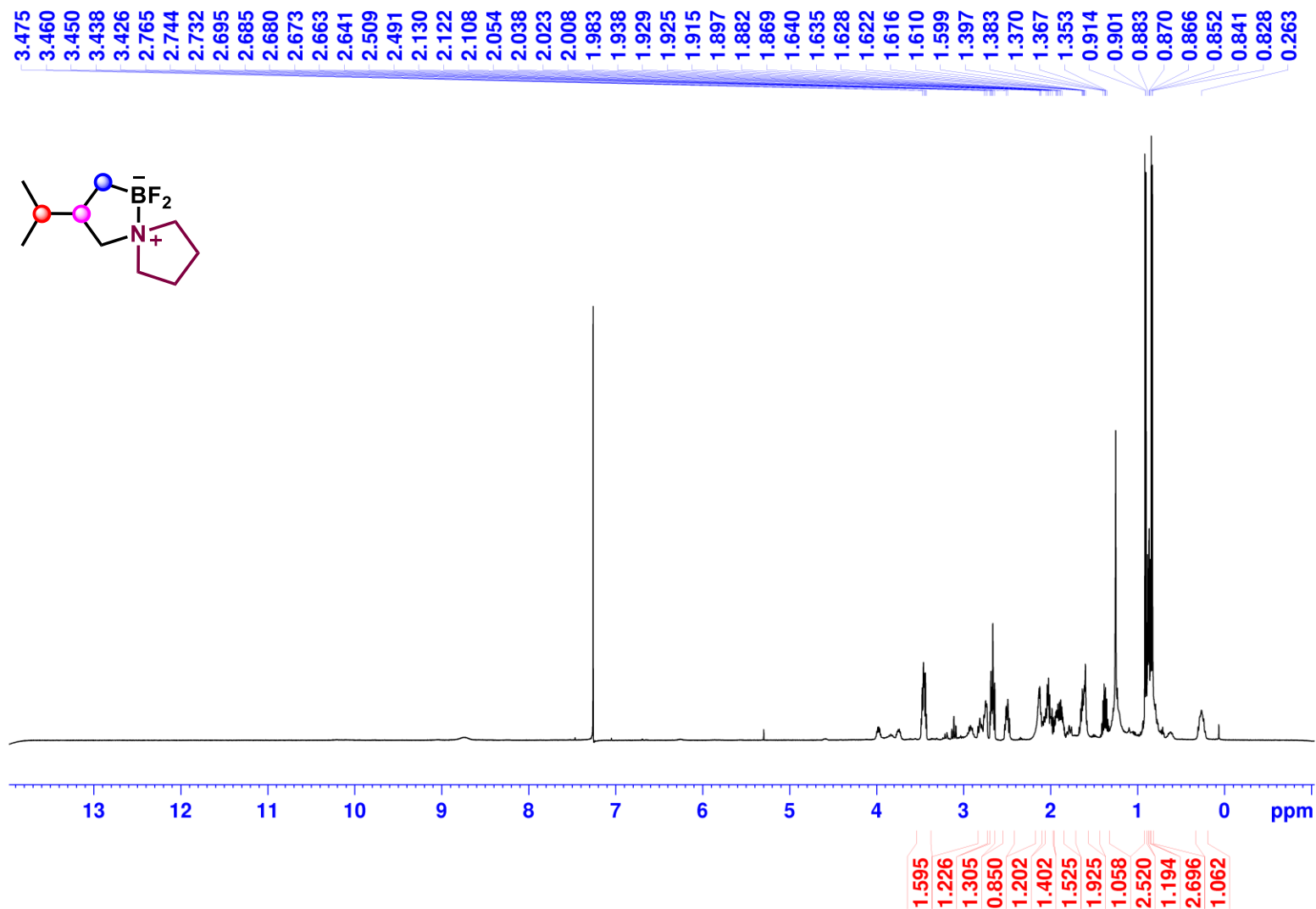
1,1-difluoro-3-(4-fluorobenzyl)-5-aza-1-borasp[4.4]nonane (3b):



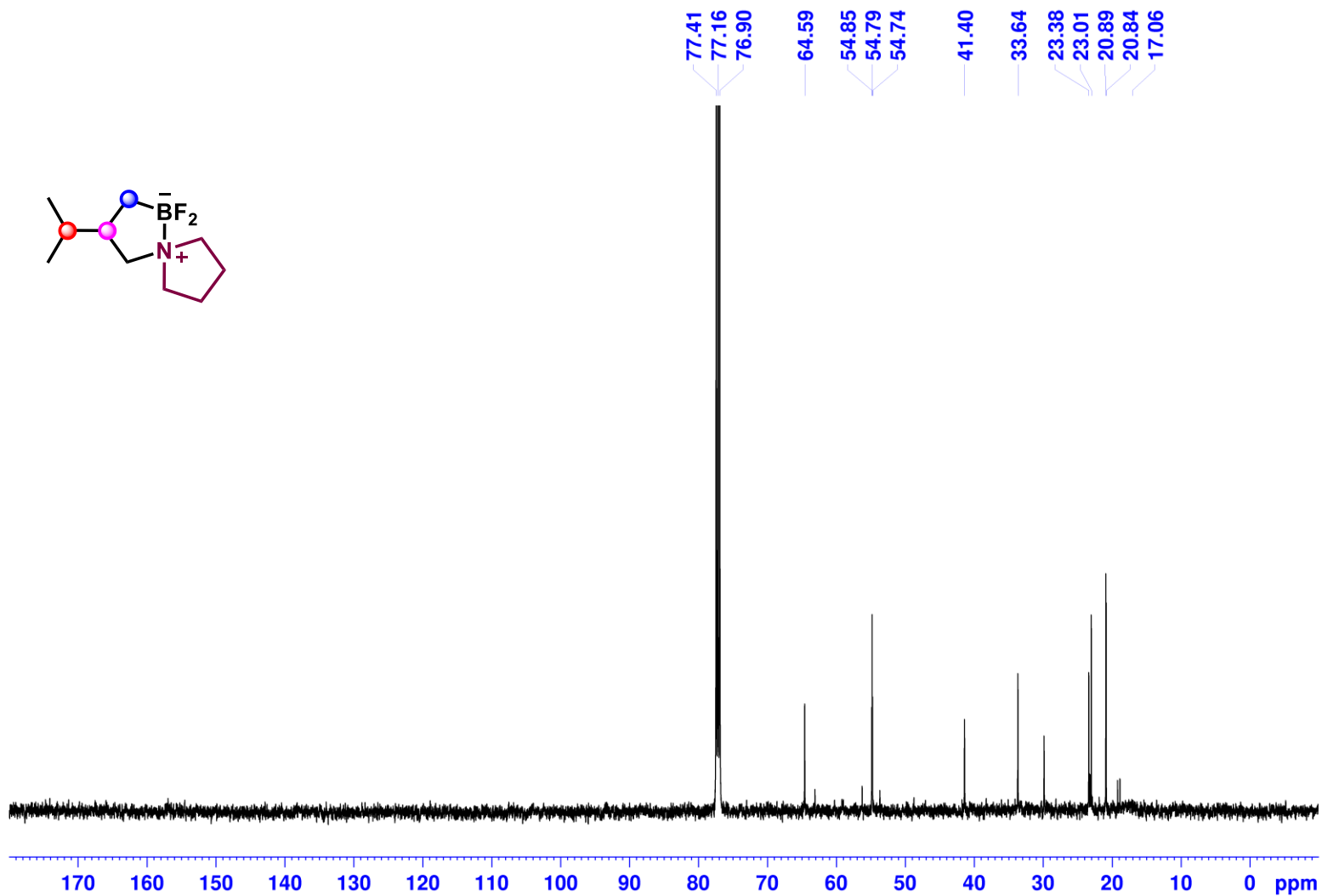
1,1-difluoro-3-(4-fluorobenzyl)-5-aza-1-borasp[4.4]nonane (3b):



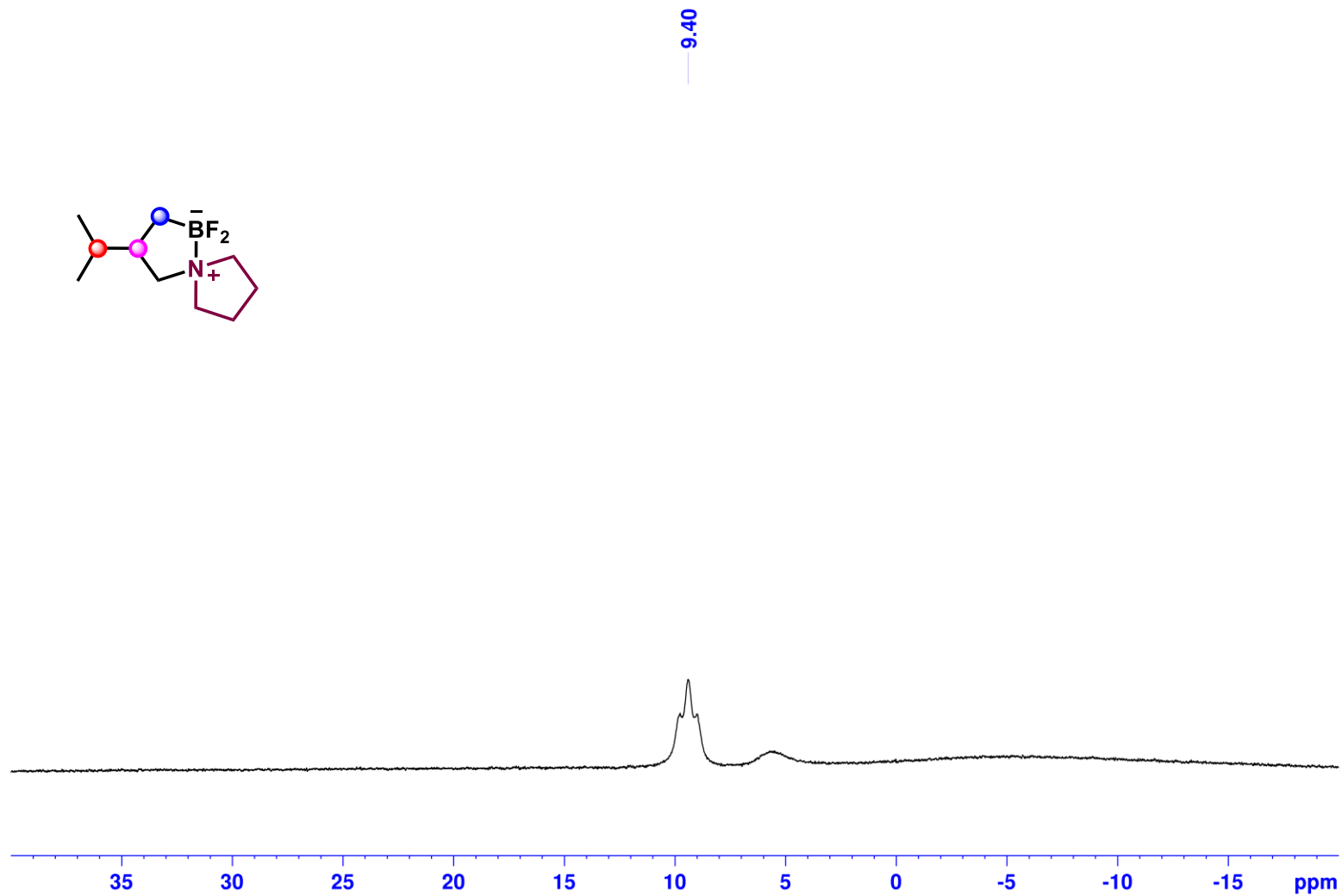
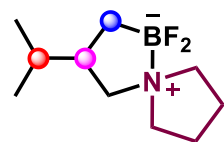
1,1-difluoro-3-isopropyl-5-aza-1-borasp[4.4]nonane (3c)



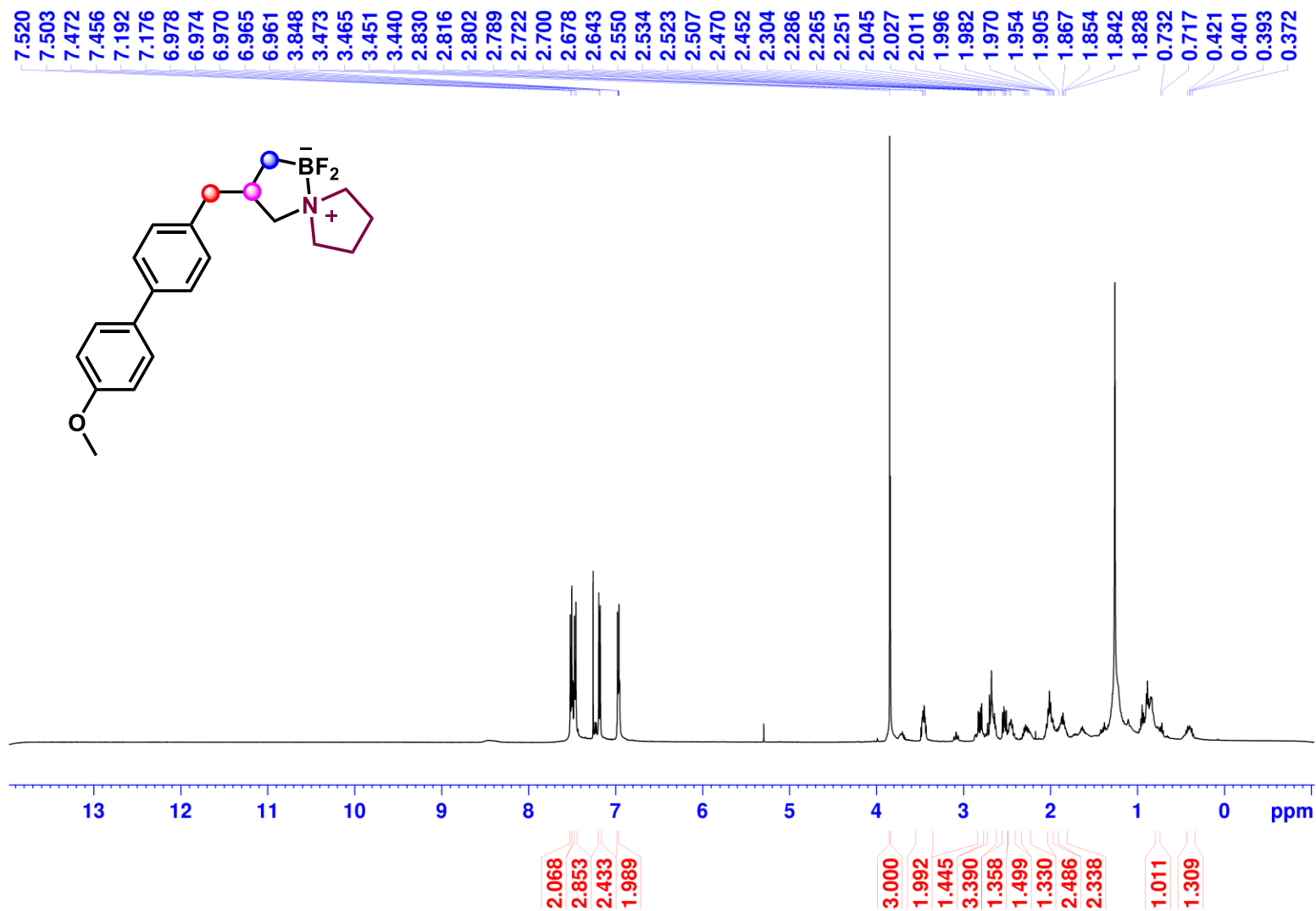
1,1-difluoro-3-isopropyl-5-aza-1-borasp[4.4]nonane (3c)



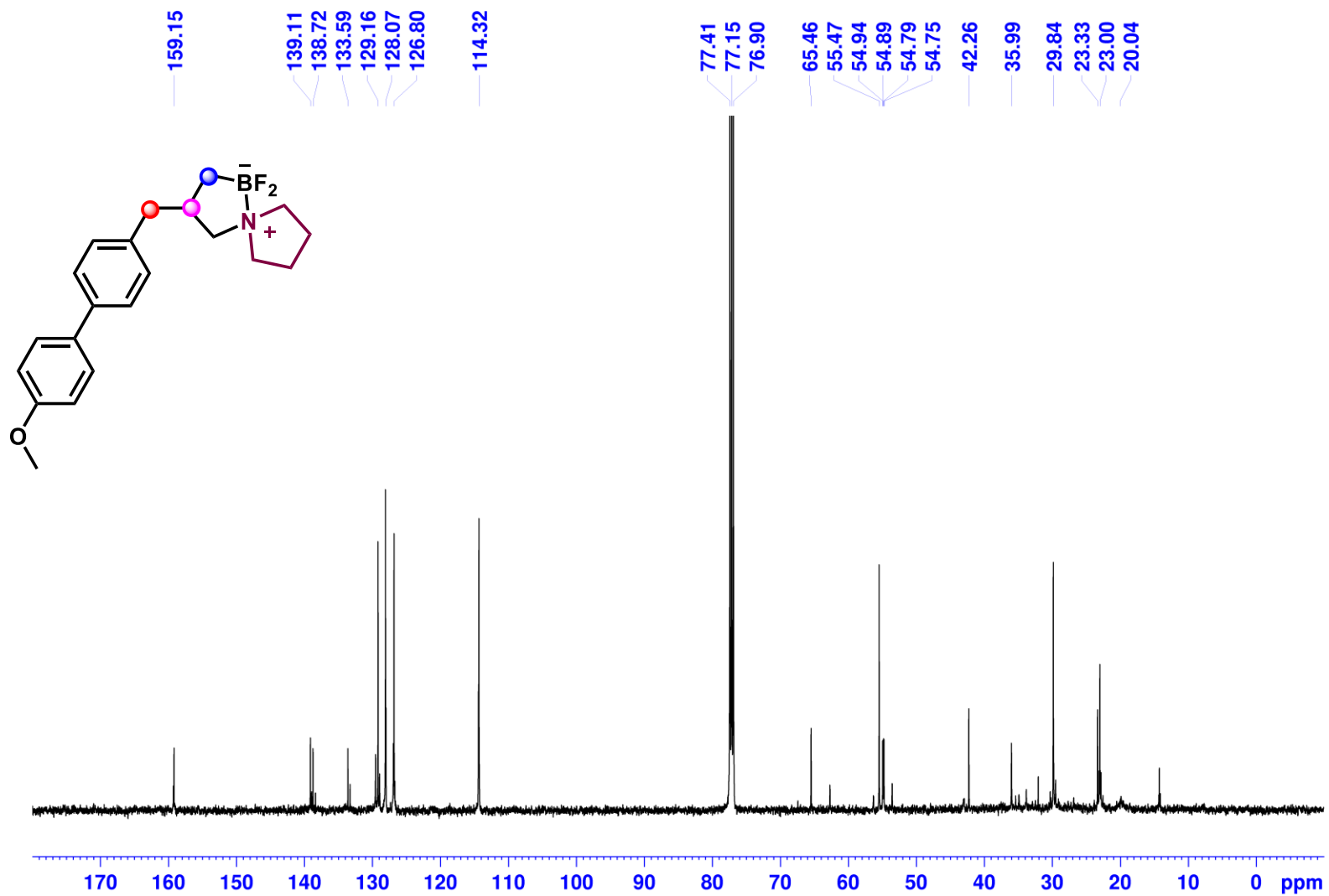
1,1-difluoro-3-isopropyl-5-aza-1-borasp[iro[4.4]nonane (3c)



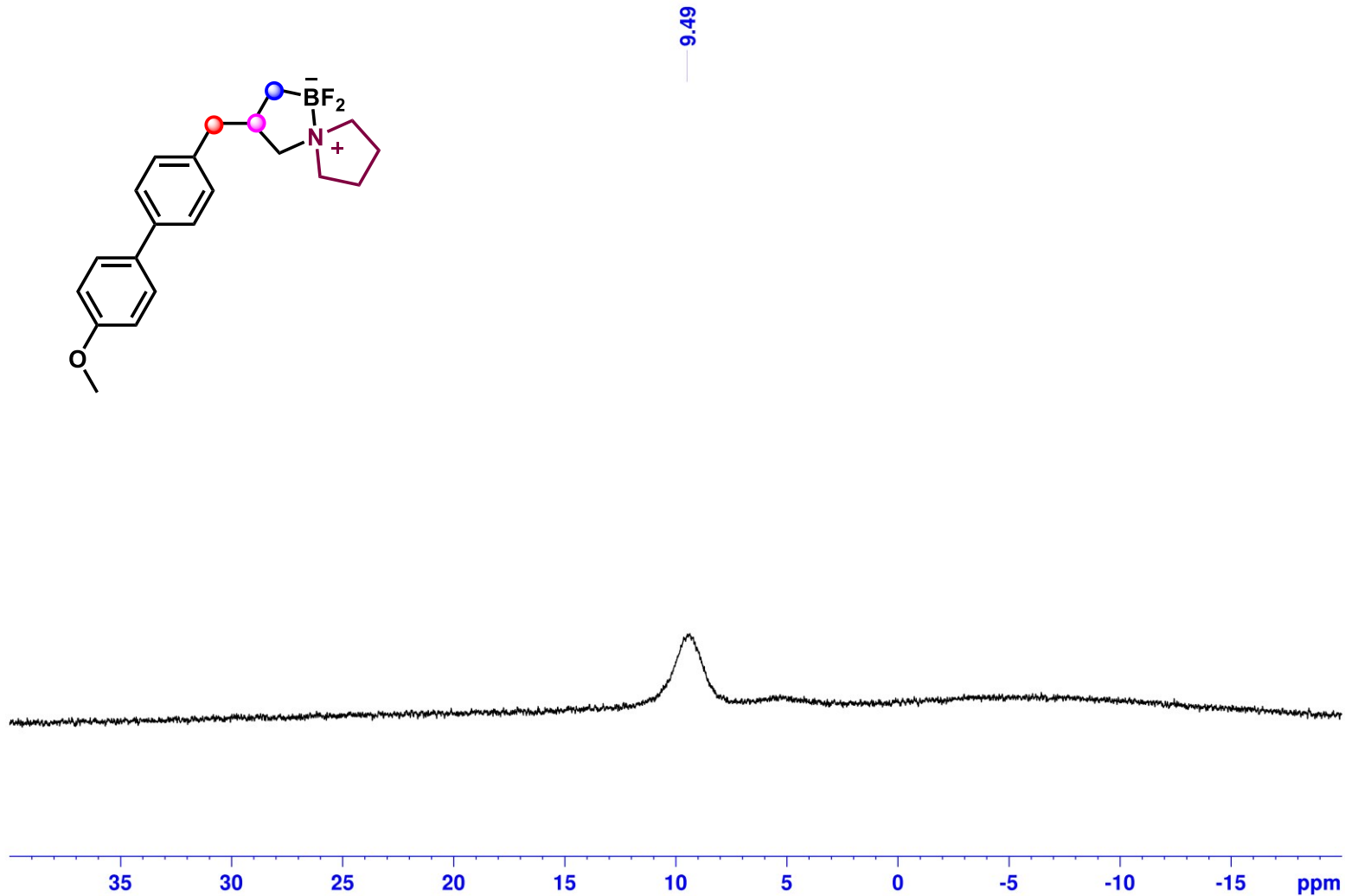
1,1-difluoro-3-((4'-methoxy-[1,1'-biphenyl]-4-yl)methyl)-5-aza-1-borasp[4.4]nonane (3d):



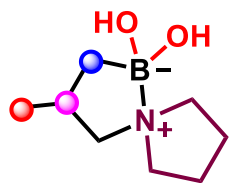
1,1-difluoro-3-((4'-methoxy-[1,1'-biphenyl]-4-yl)methyl)-5-aza-1-boraspino[4.4]nonane (3d):



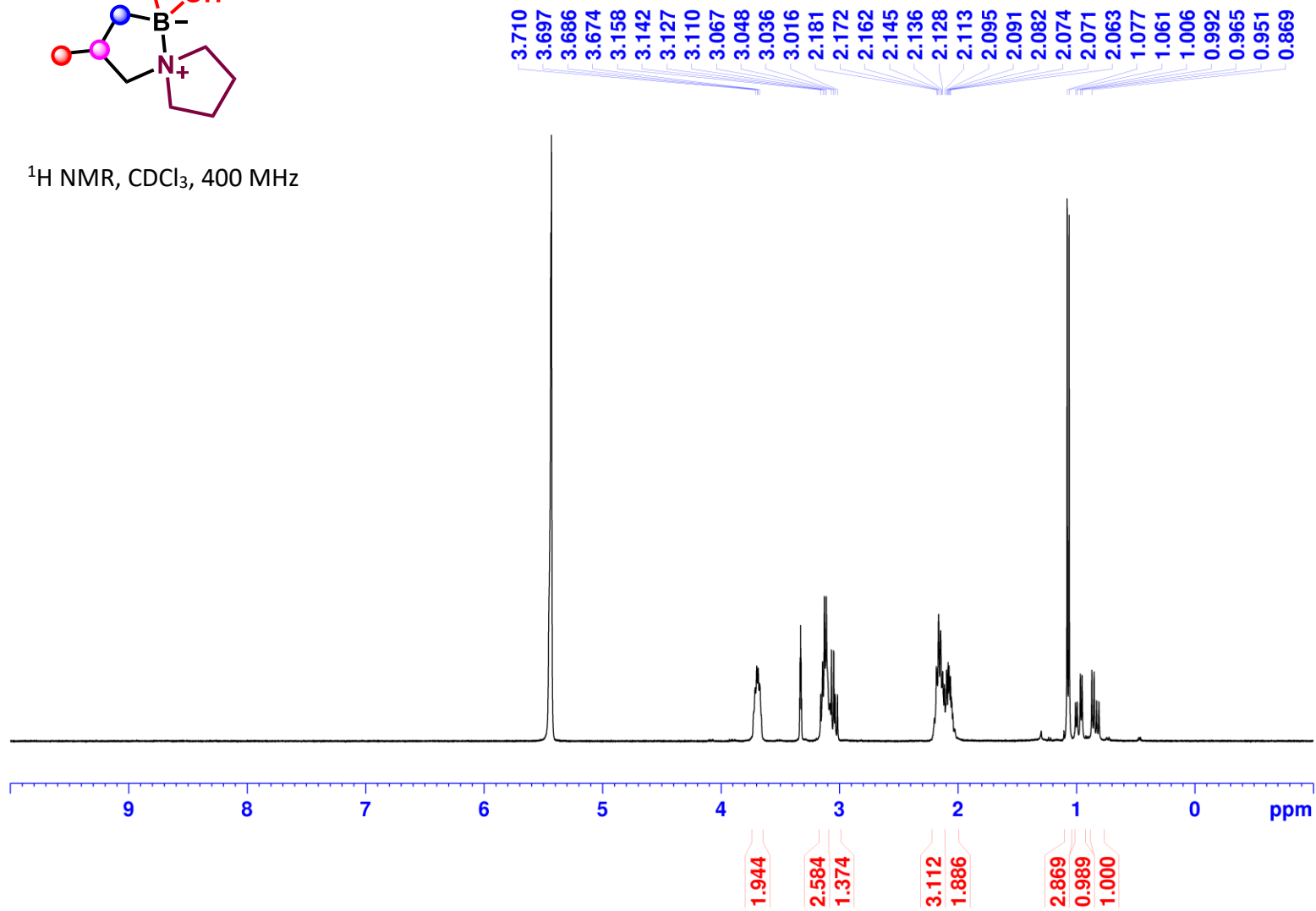
1,1-difluoro-3-((4'-methoxy-[1,1'-biphenyl]-4-yl)methyl)-5-aza-1-boraspino[4.4]nonane (3d):



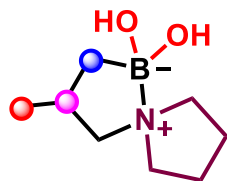
3-methyl-5-aza-1-borasp[4.4]nonane-1,1-diol (3e) :



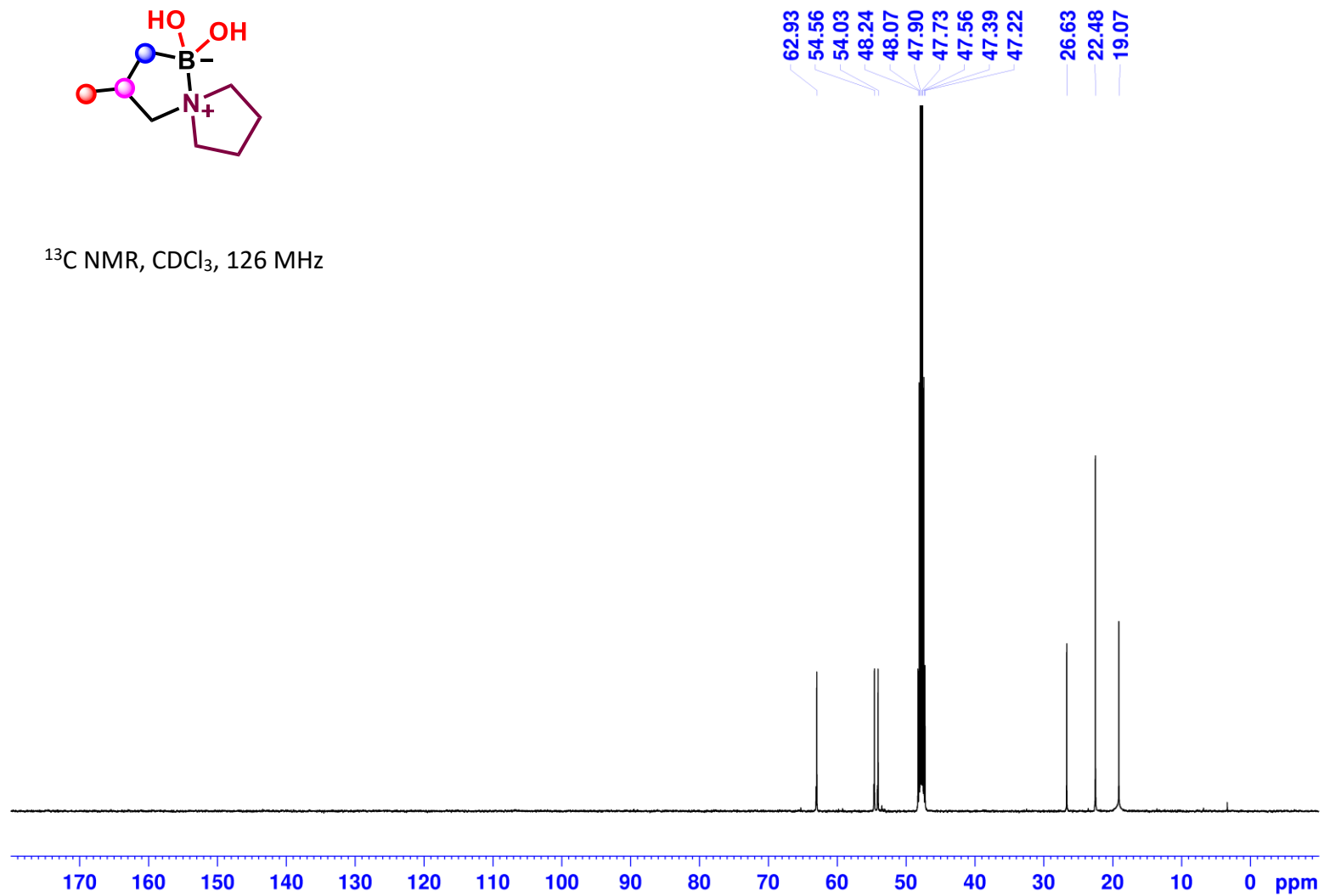
^1H NMR, CDCl_3 , 400 MHz



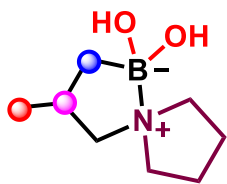
3-methyl-5-aza-1-boraspino[4.4]nonane-1,1-diol (3e) :



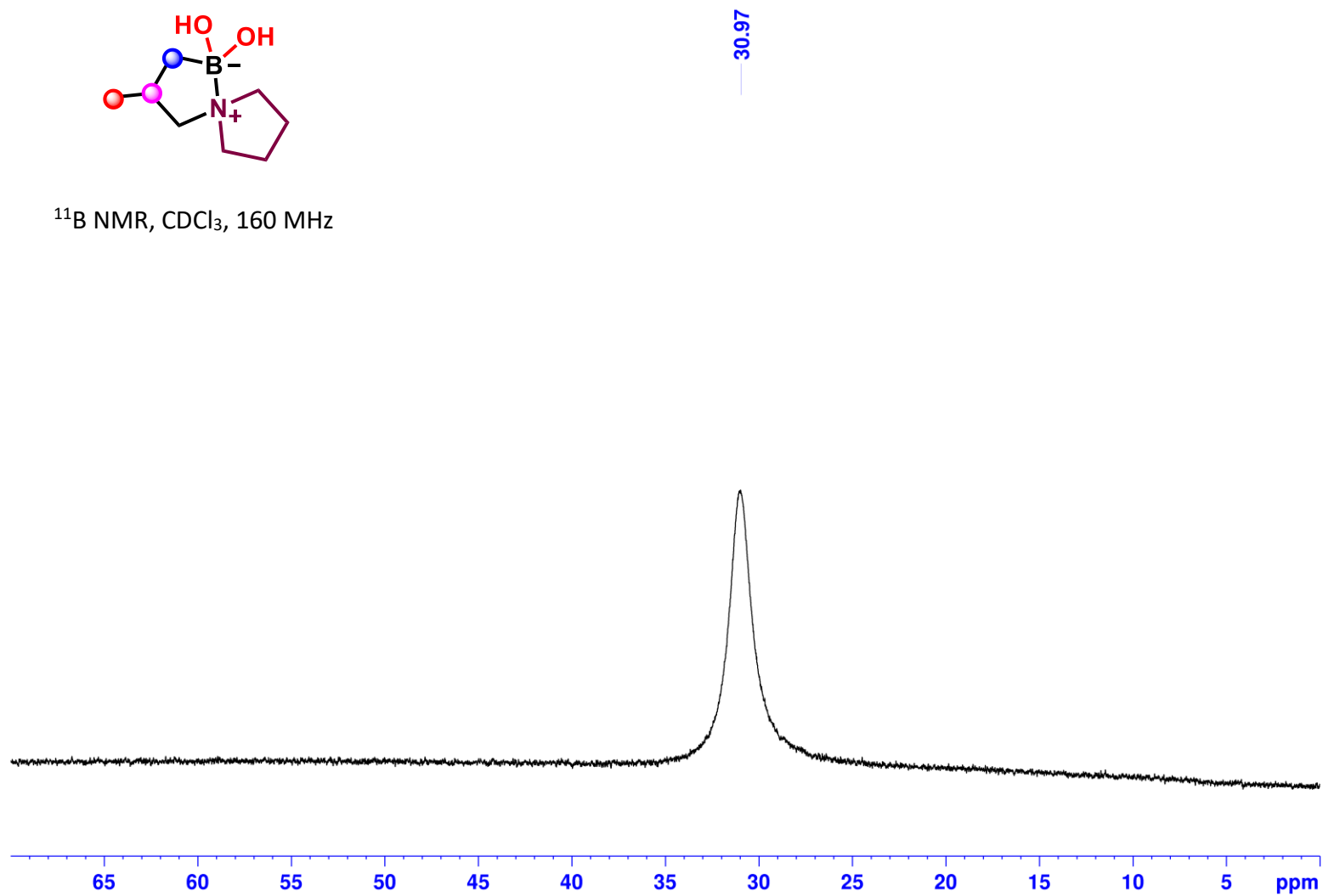
^{13}C NMR, CDCl_3 , 126 MHz



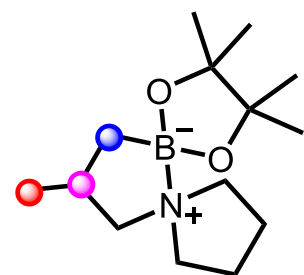
3-methyl-5-aza-1-borospiro[4.4]nonane-1,1-diol (3e) :



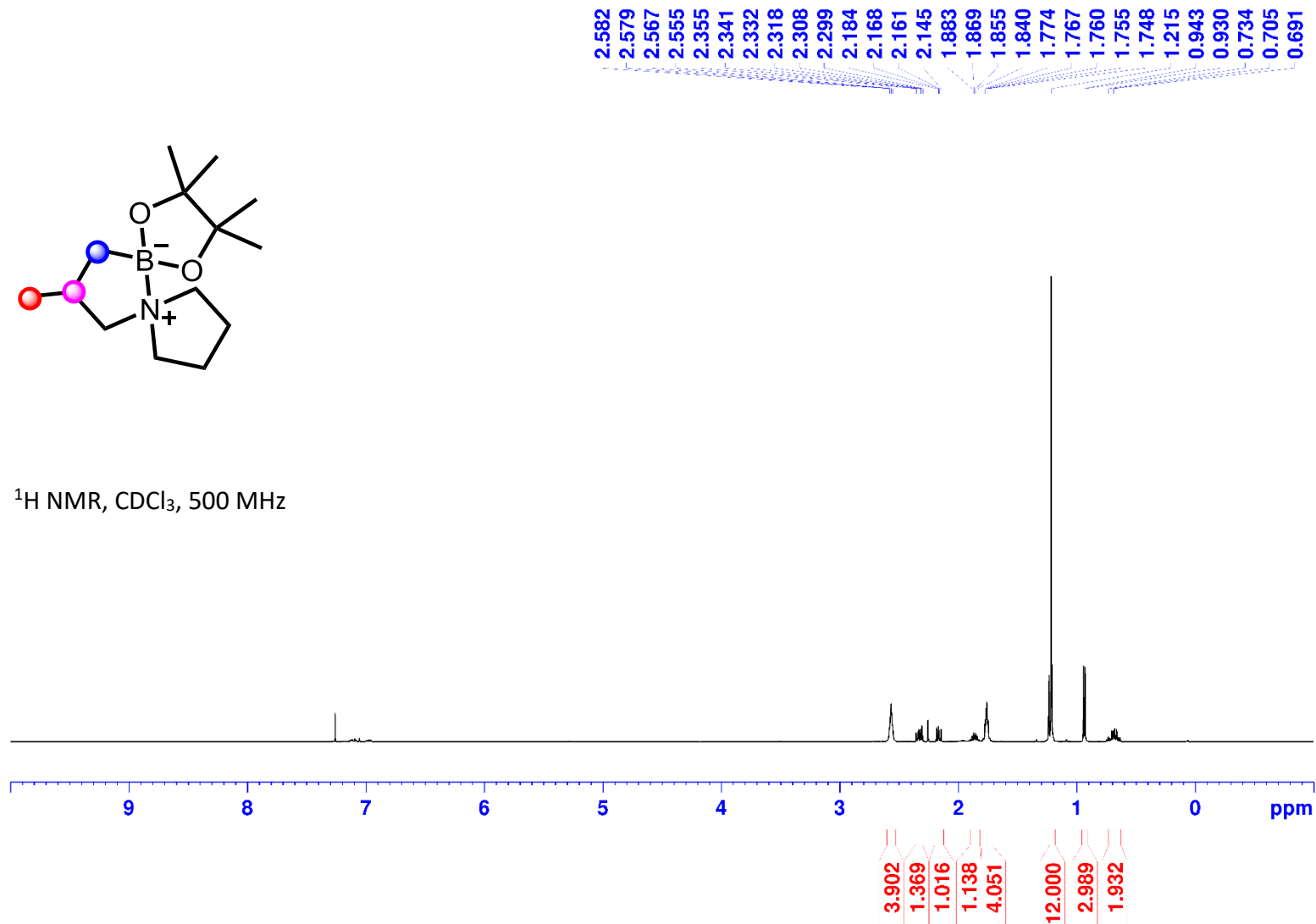
^{11}B NMR, CDCl_3 , 160 MHz



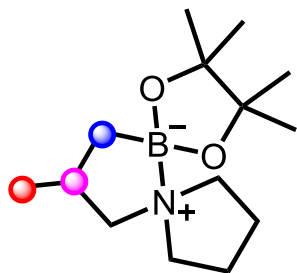
1-(2-Methyl-3-(4,4,5,5-tetramethyl-1,3,2-dioxaborolan-2-yl)propyl)pyrrolidine (3f):



^1H NMR, CDCl_3 , 500 MHz

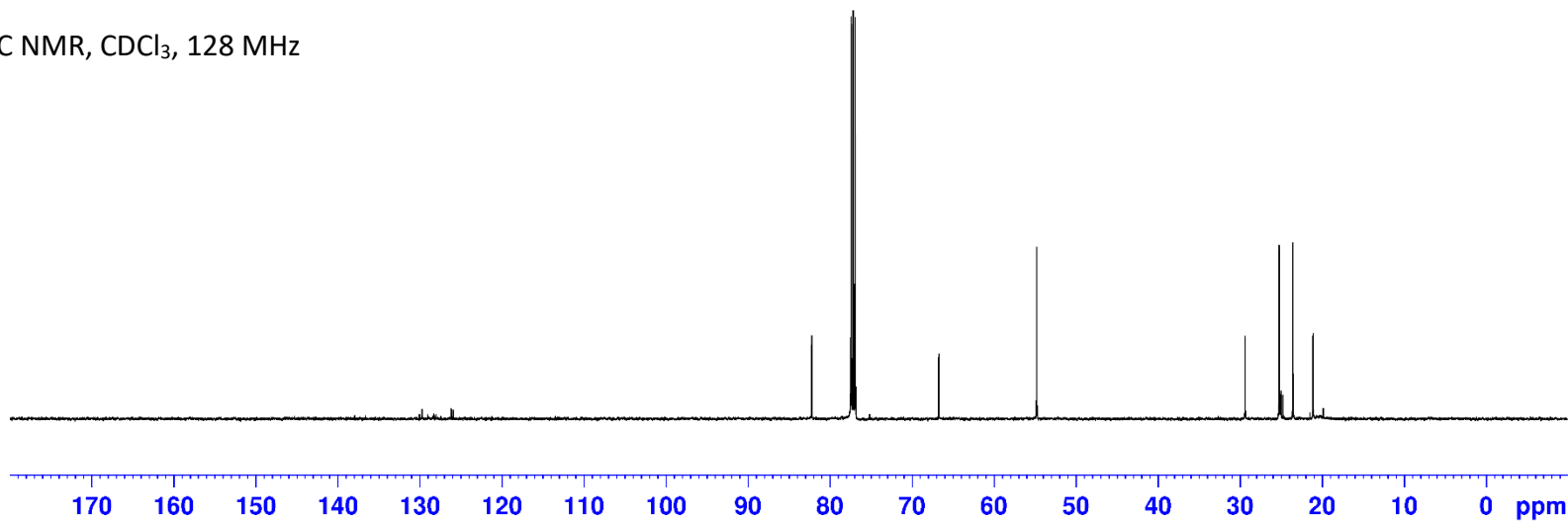


1-(2-Methyl-3-(4,4,5,5-tetramethyl-1,3,2-dioxaborolan-2-yl)propyl)pyrrolidine (3f):



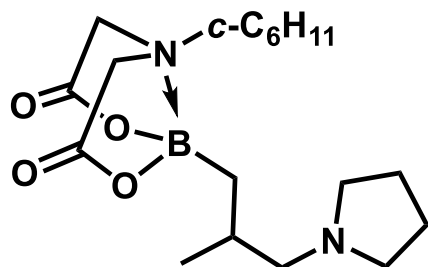
82.20
77.41
77.16
76.90
66.71
54.78
29.38
25.24
25.20
23.56
21.08

^{13}C NMR, CDCl_3 , 128 MHz

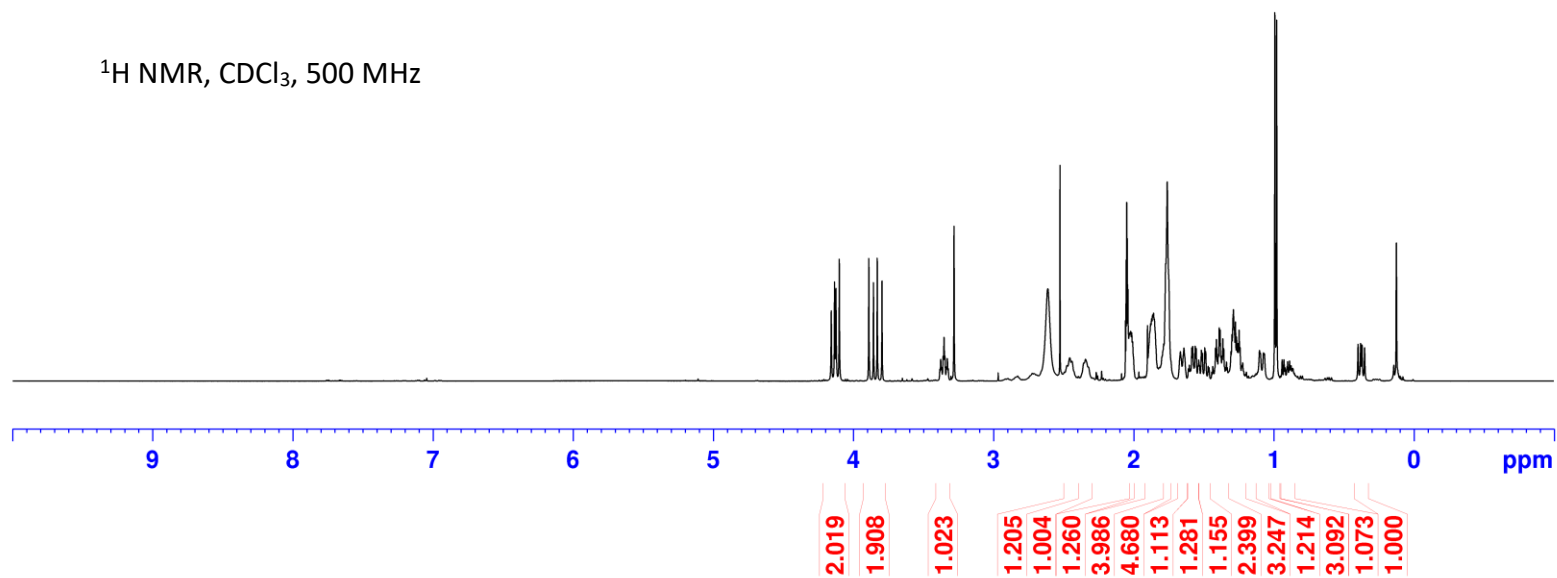


6-cyclohexyl-2-(2-methyl-3-(pyrrolidin-1-yl)propyl)-1,3,6,2-dioxazaborocane-4,8-dione (3g):

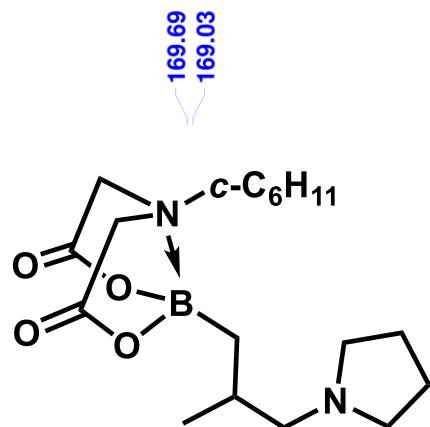
4.158
4.135
4.125
4.101
3.890
3.857
3.830
3.796
3.353
2.027
2.021
2.015
2.008
1.879
1.872
1.866
1.858
1.853
1.772
1.761
1.667
1.641
1.585
1.578
1.561
1.554
1.517
1.493
1.486
1.416
1.409
1.390
1.383
1.364
1.357
1.306
1.299
1.288
1.281
1.274
1.266
1.255
1.248
1.241
1.102
1.074
0.993
0.980
0.399
0.381
0.371
0.352



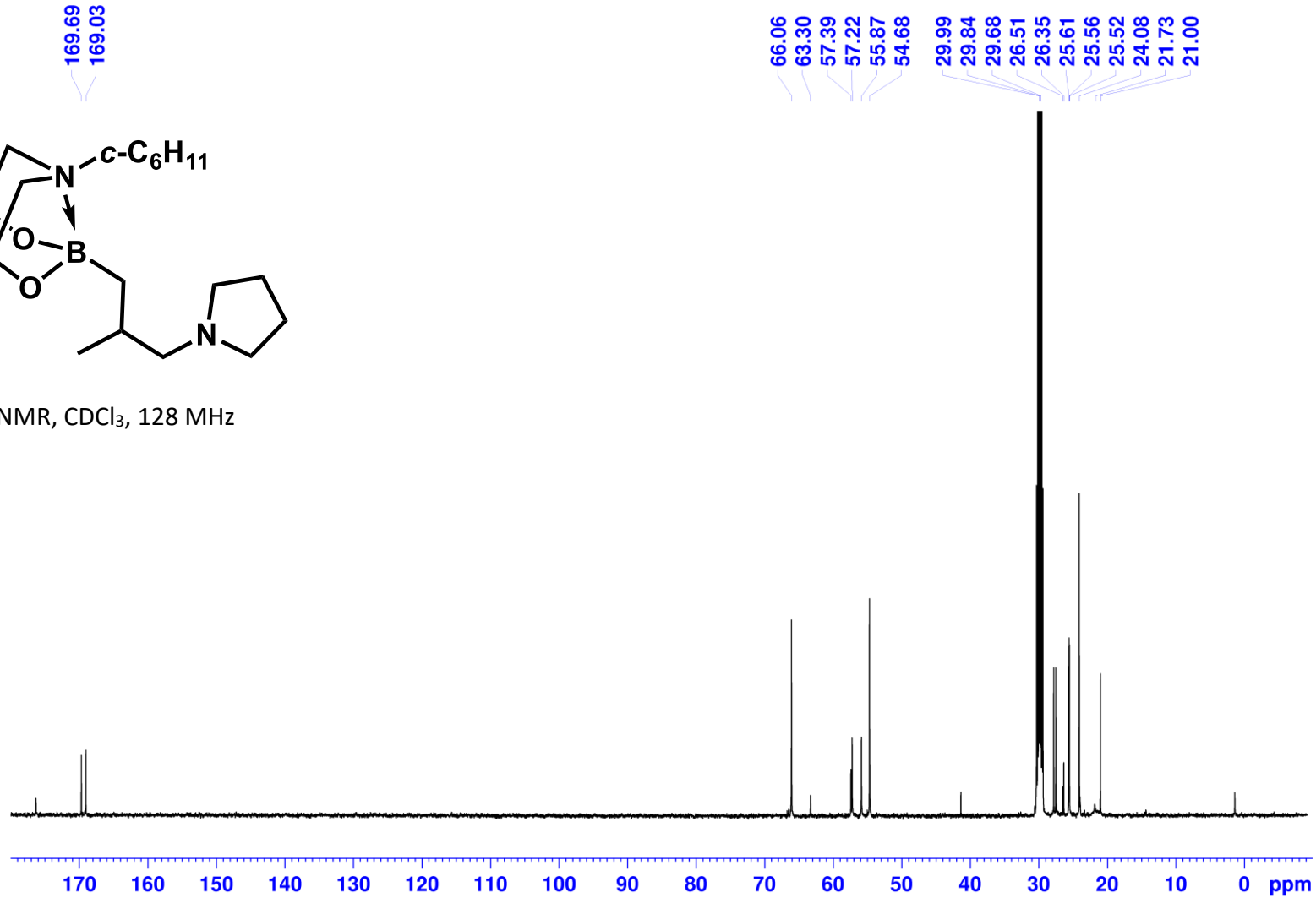
^1H NMR, CDCl_3 , 500 MHz



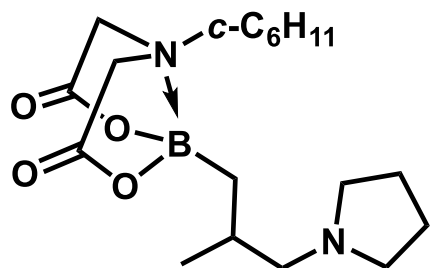
6-cyclohexyl-2-(2-methyl-3-(pyrrolidin-1-yl)propyl)-1,3,6,2-dioxazaborocane-4,8-dione (3g):



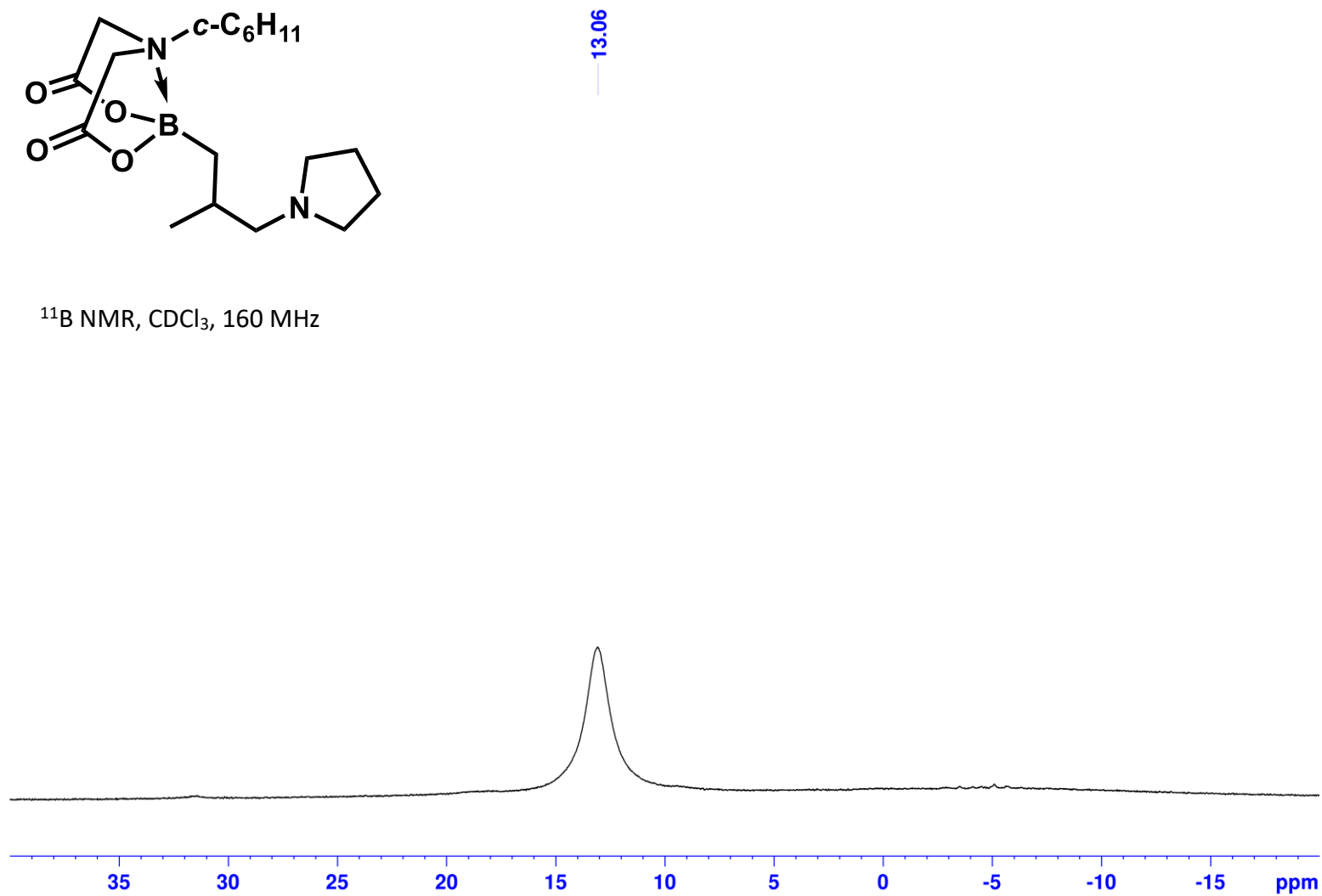
^{13}C NMR, CDCl_3 , 128 MHz



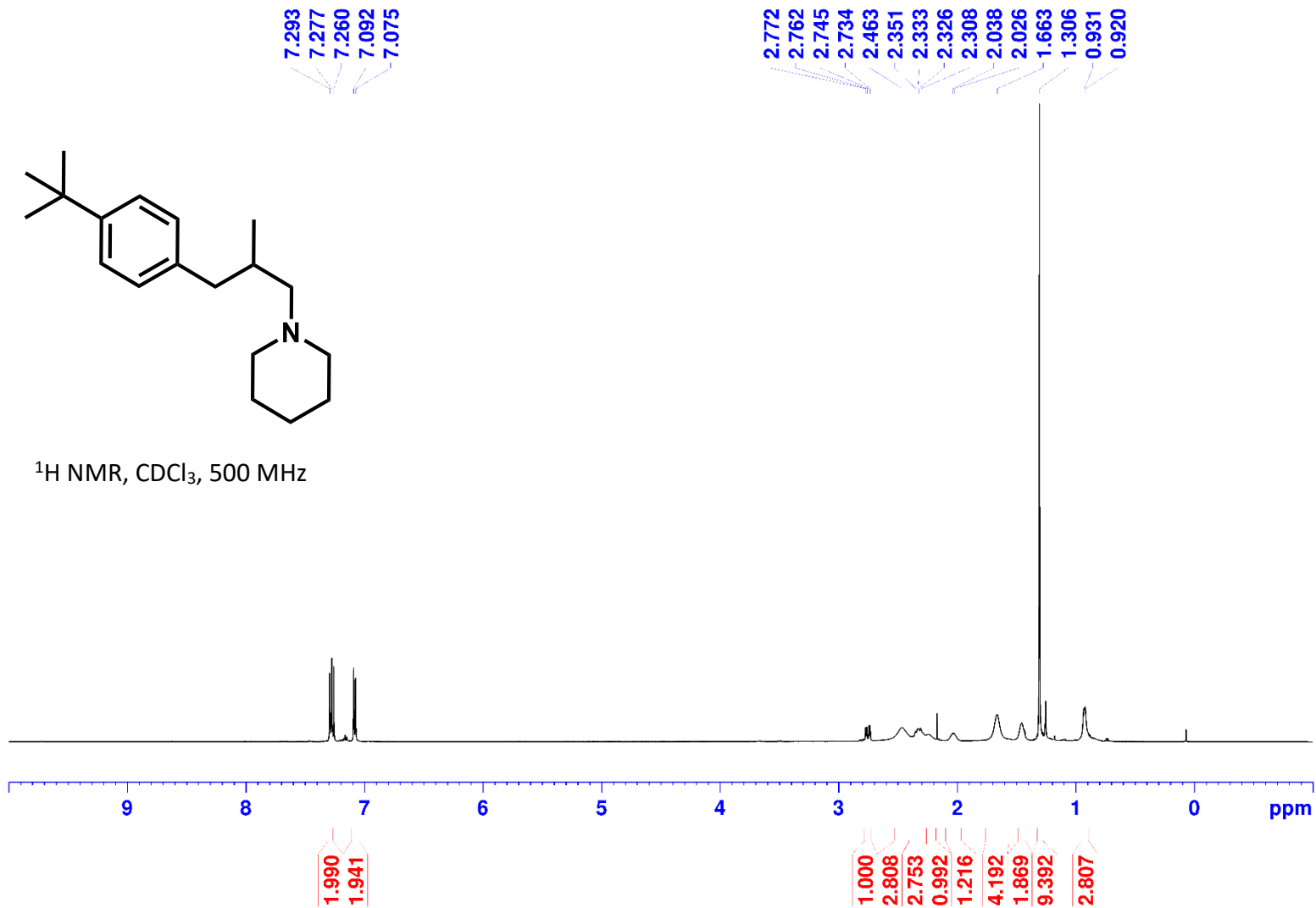
6-cyclohexyl-2-(2-methyl-3-(pyrrolidin-1-yl)propyl)-1,3,6,2-dioxazaborocane-4,8-dione (3g):



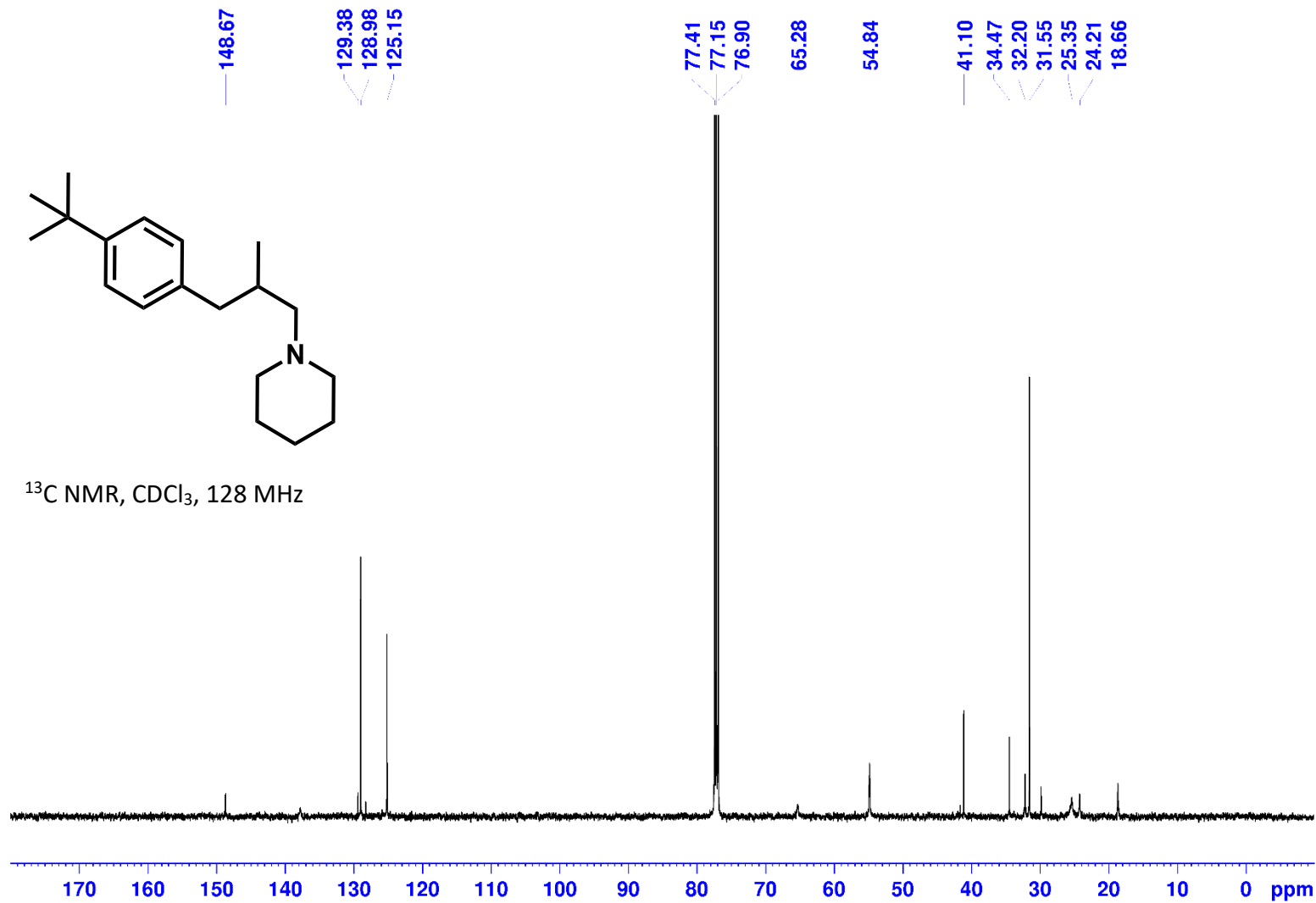
^{11}B NMR, CDCl_3 , 160 MHz



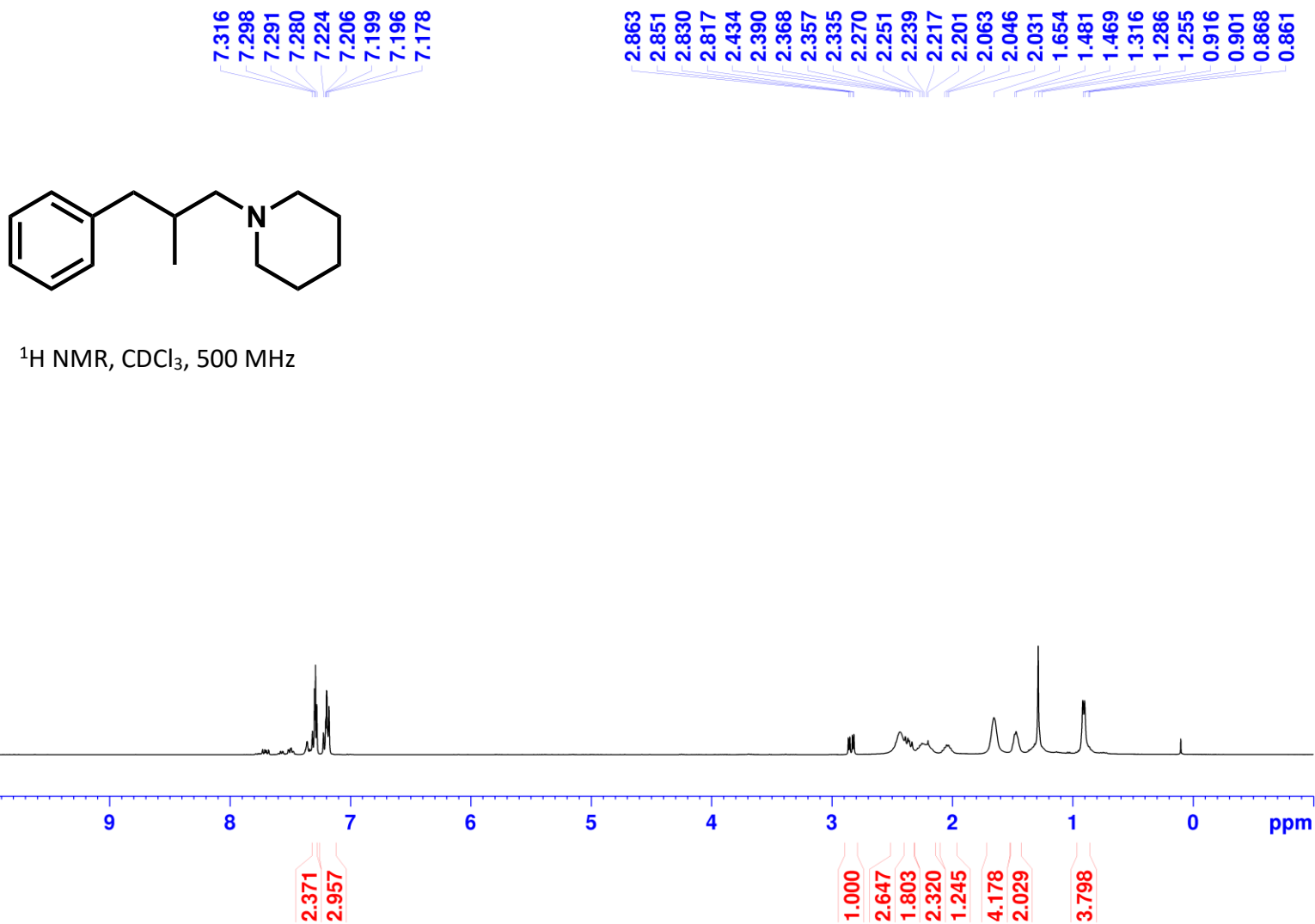
1-(3-(4-(*tert*-Butyl)phenyl)-2-methylpropyl)piperidine 1766 (3h):



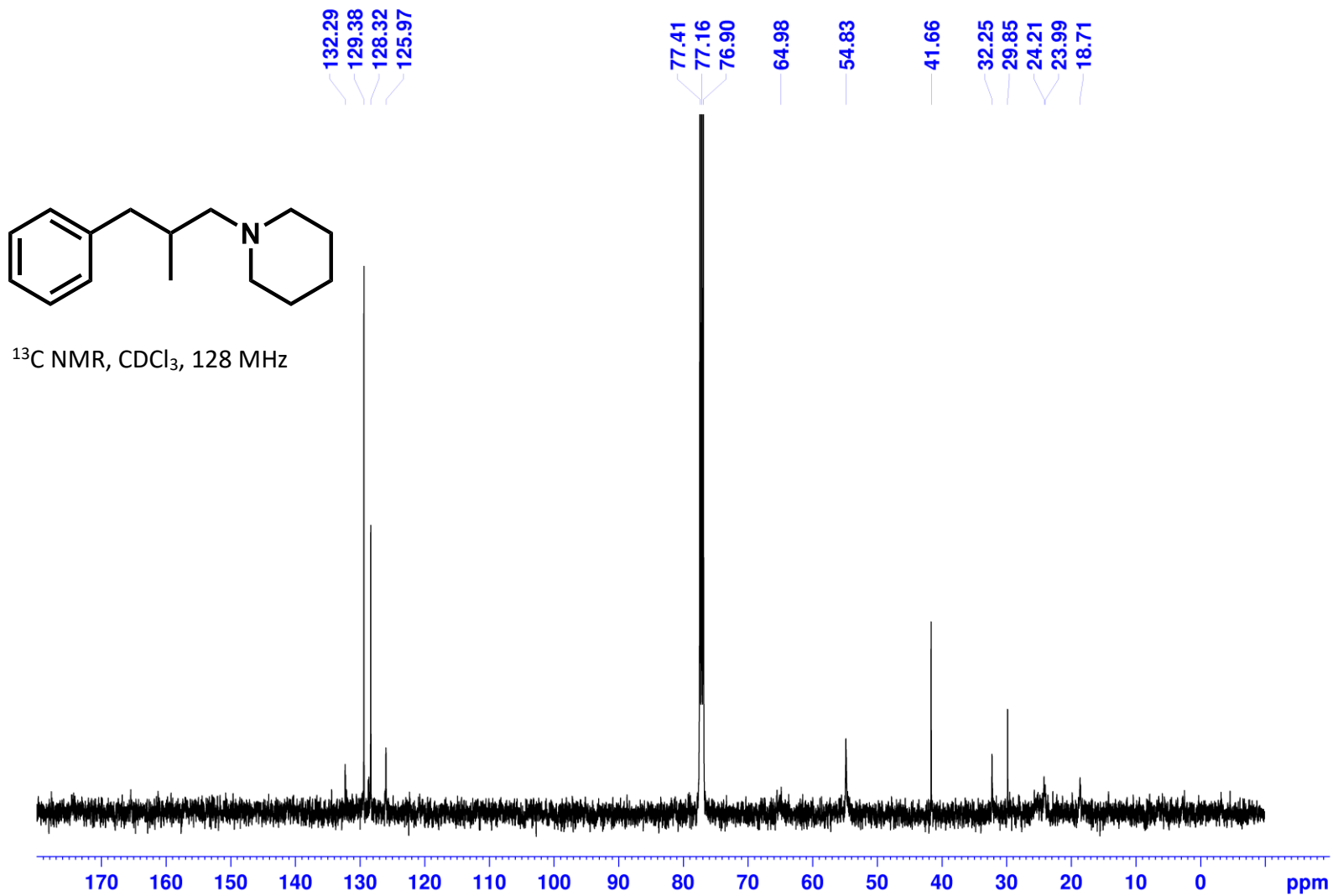
1-(3-(4-(*tert*-Butyl)phenyl)-2-methylpropyl)piperidine 1766 (3h):



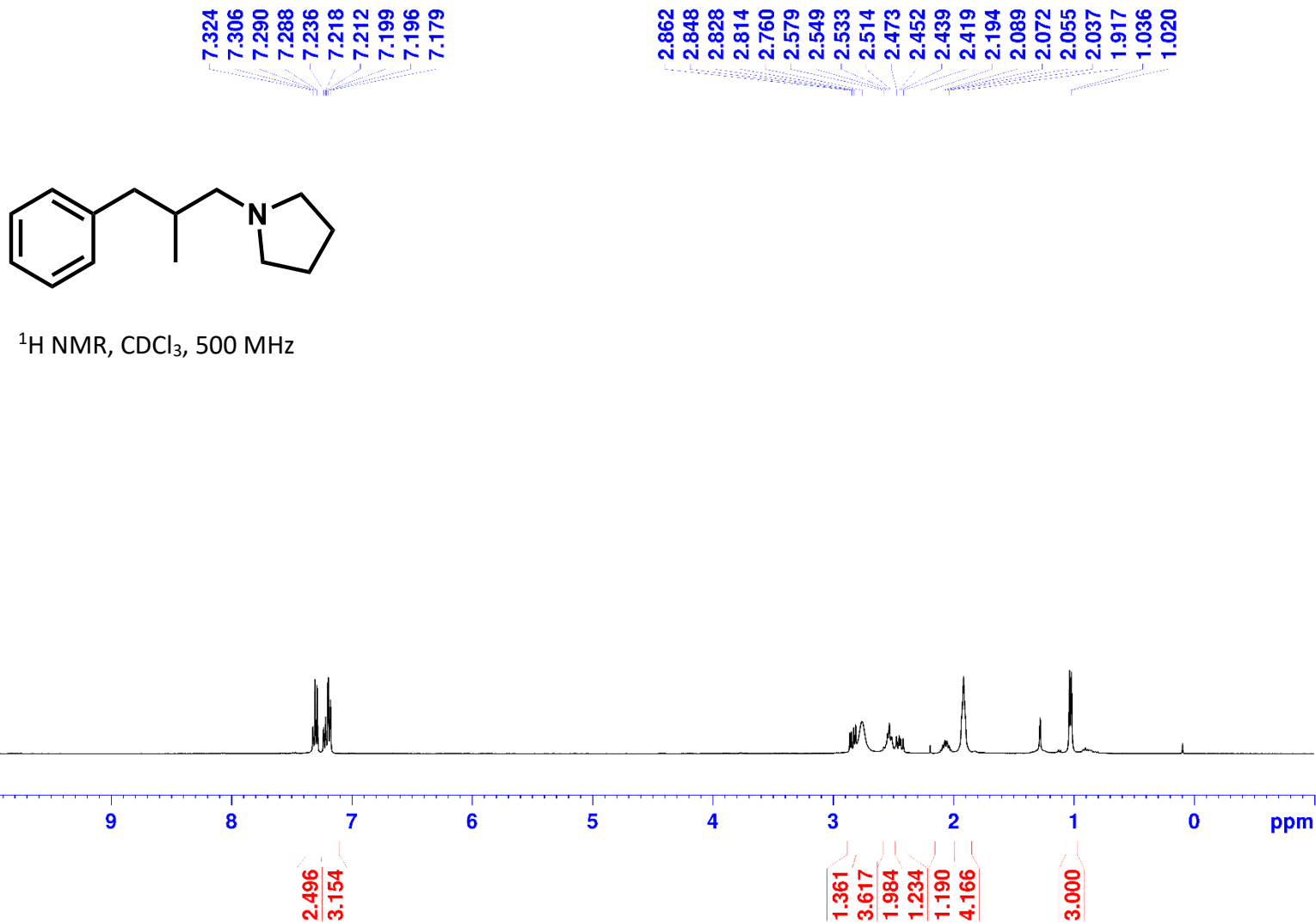
1-(2-Methyl-3-phenylpropyl)piperidine (3i):



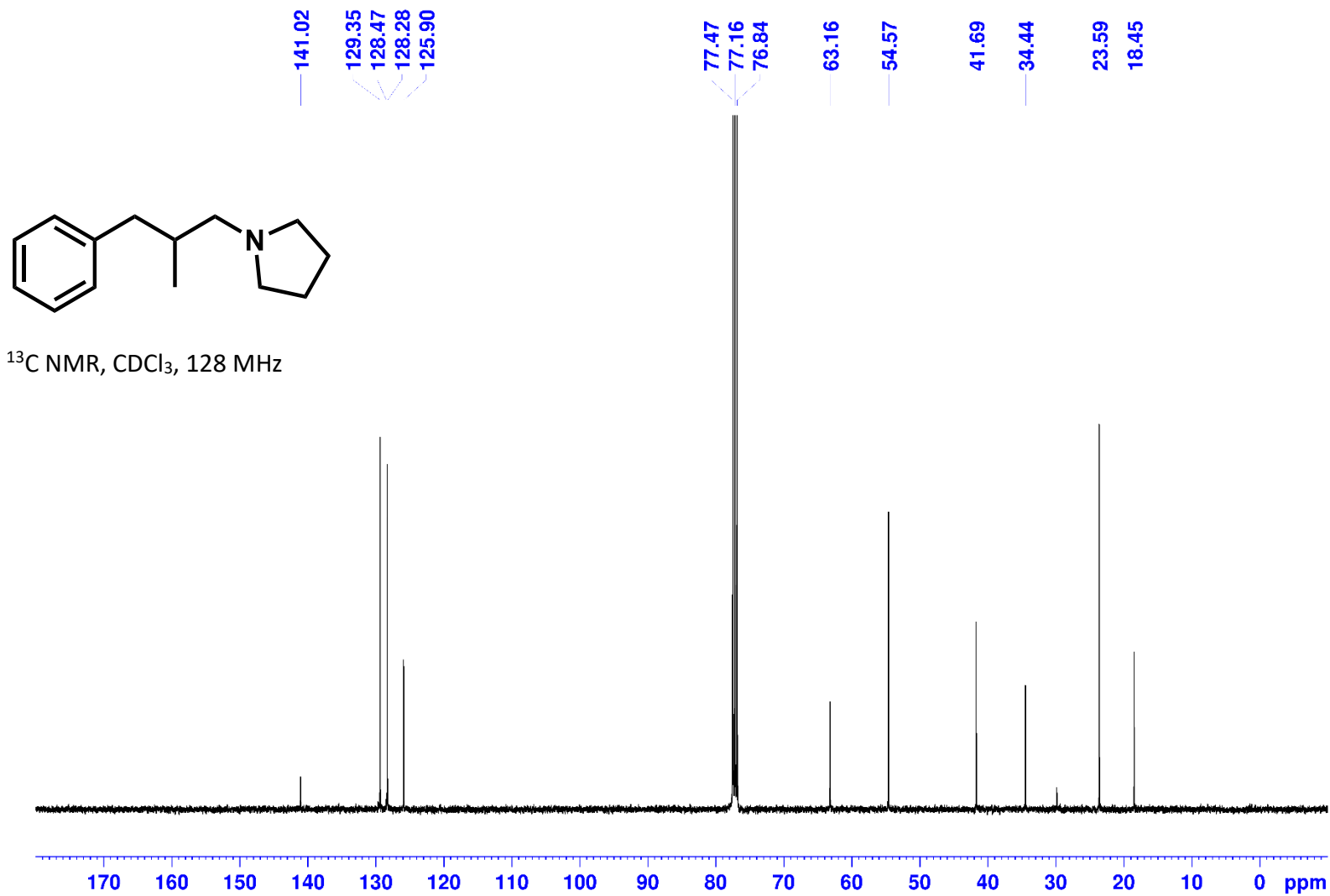
1-(2-Methyl-3-phenylpropyl)piperidine (3i):



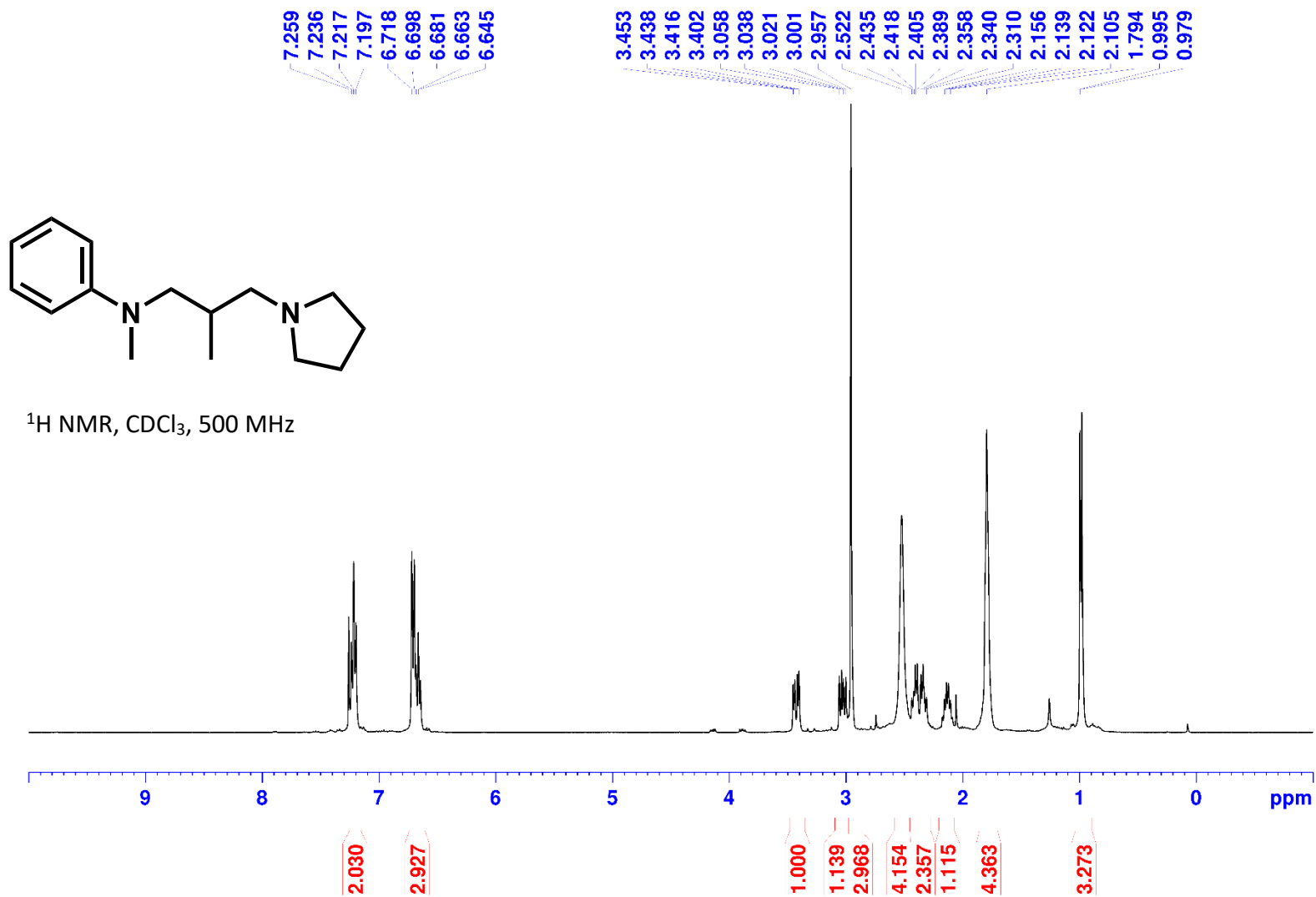
1-(2-Methyl-3-phenylpropyl)pyrrolidine (3j):



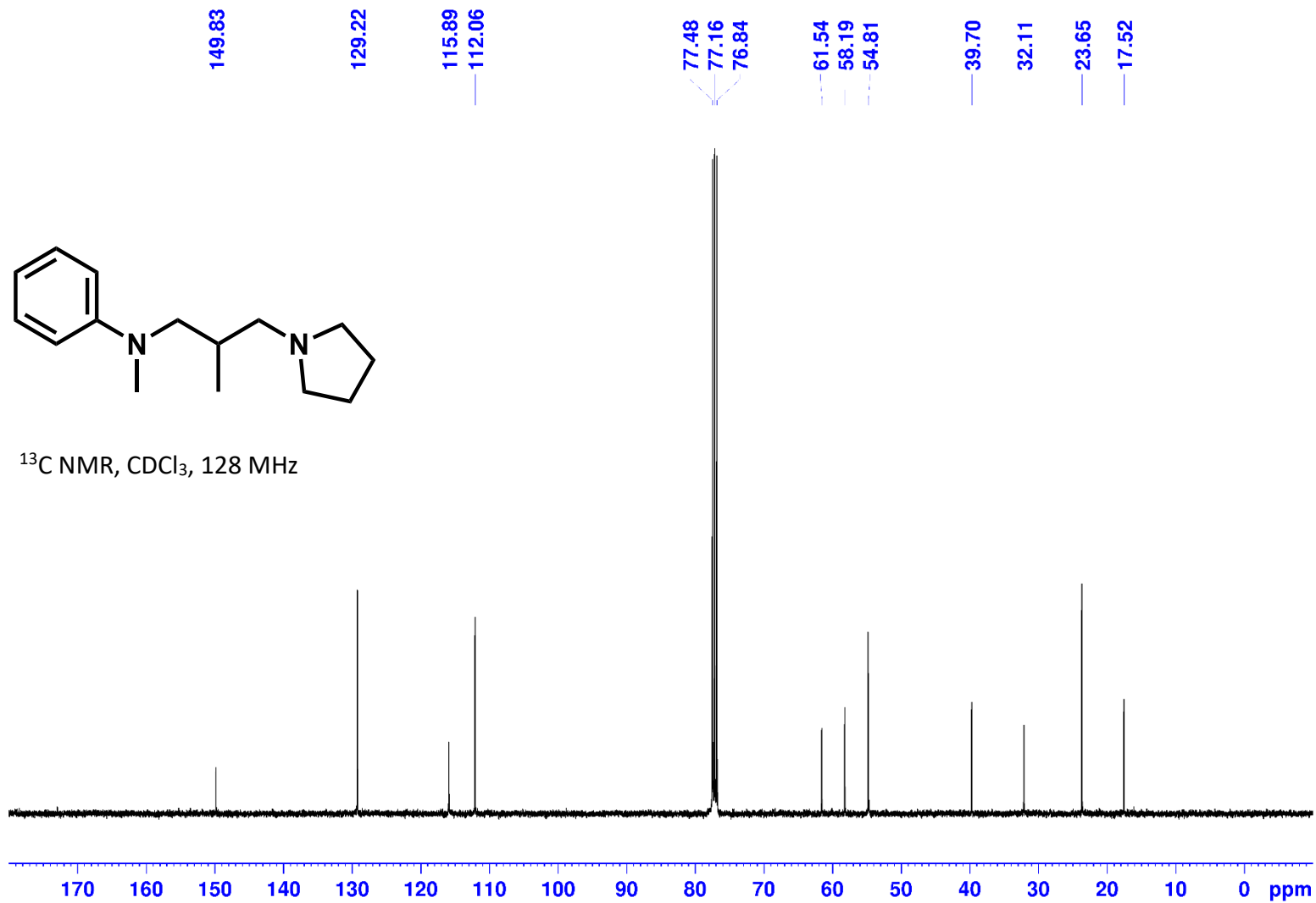
1-(2-Methyl-3-phenylpropyl)pyrrolidine (3j):



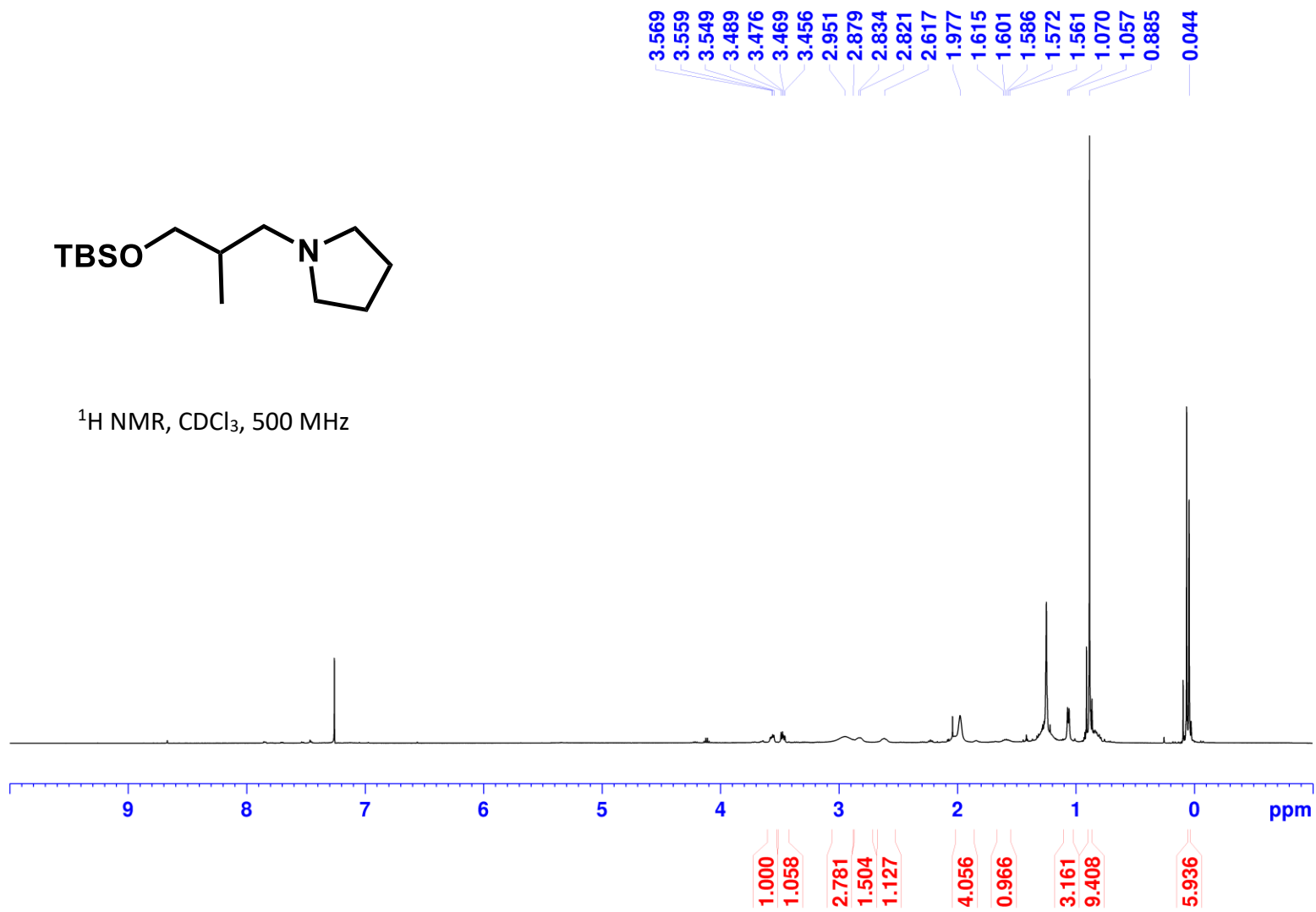
***N*-Methyl-*N*-(2-methyl-3-(pyrrolidin-1-yl)propyl)aniline (3k):**



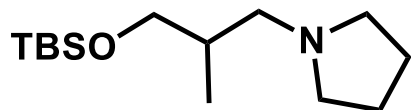
N-Methyl-*N*-(2-methyl-3-(pyrrolidin-1-yl)propyl)aniline (3k):



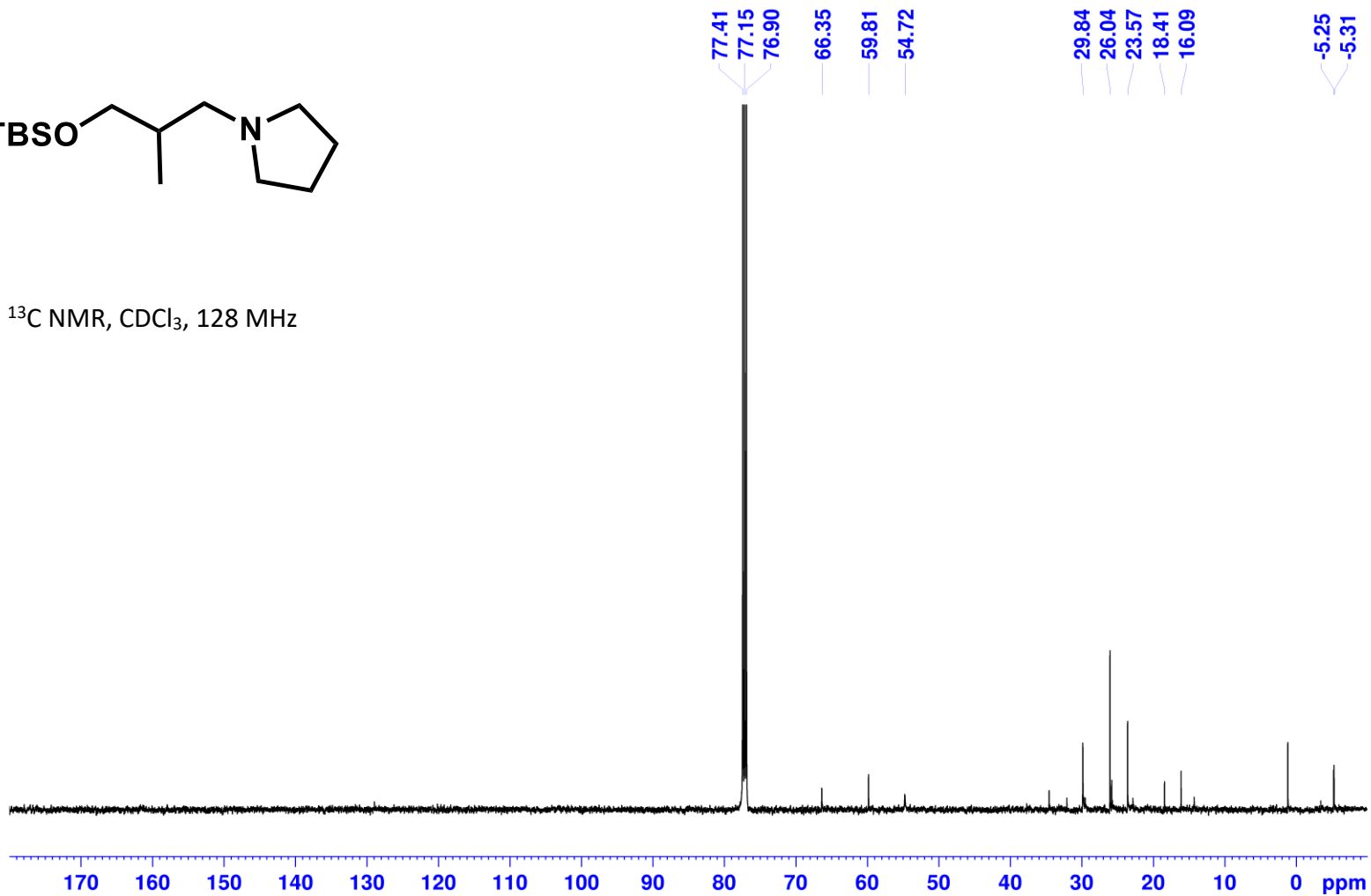
1-(3-((*tert*-Butyldimethylsilyl)oxy)-2-methylpropyl)pyrrolidine (3l):



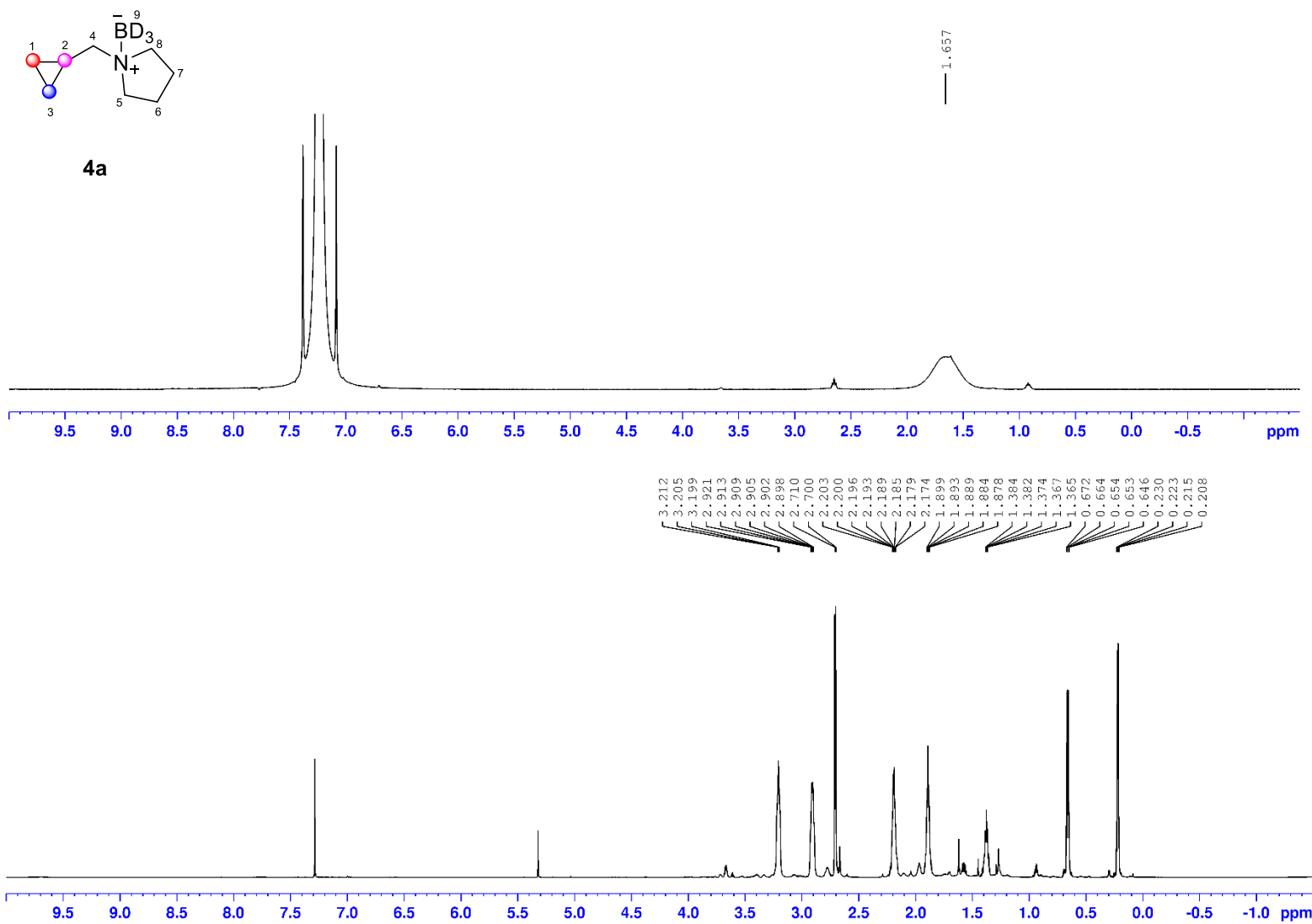
1-(3-((*tert*-Butyldimethylsilyl)oxy)-2-methylpropyl)pyrrolidine (3l):

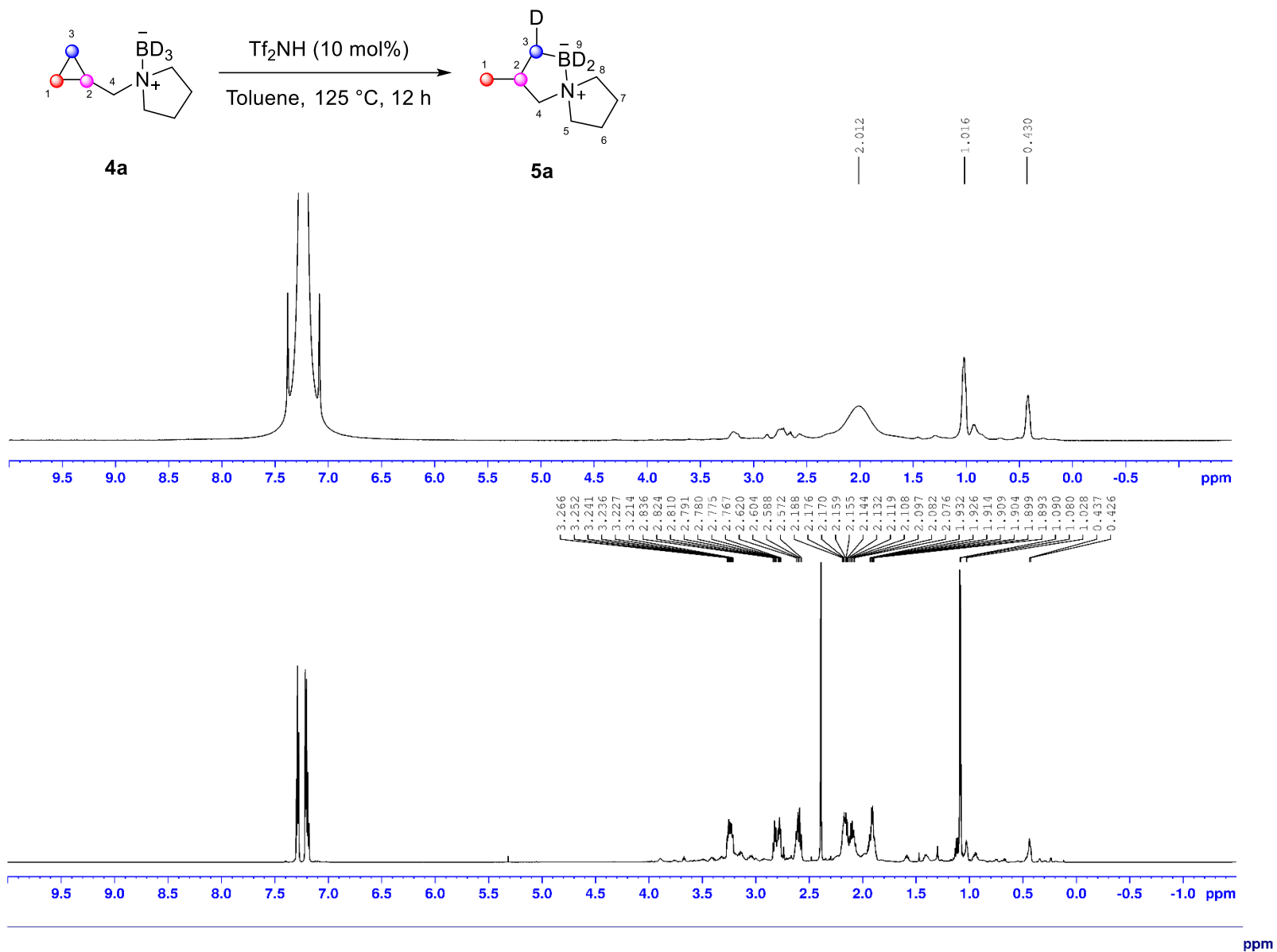


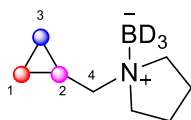
^{13}C NMR, CDCl_3 , 128 MHz



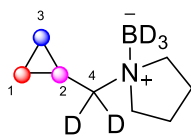
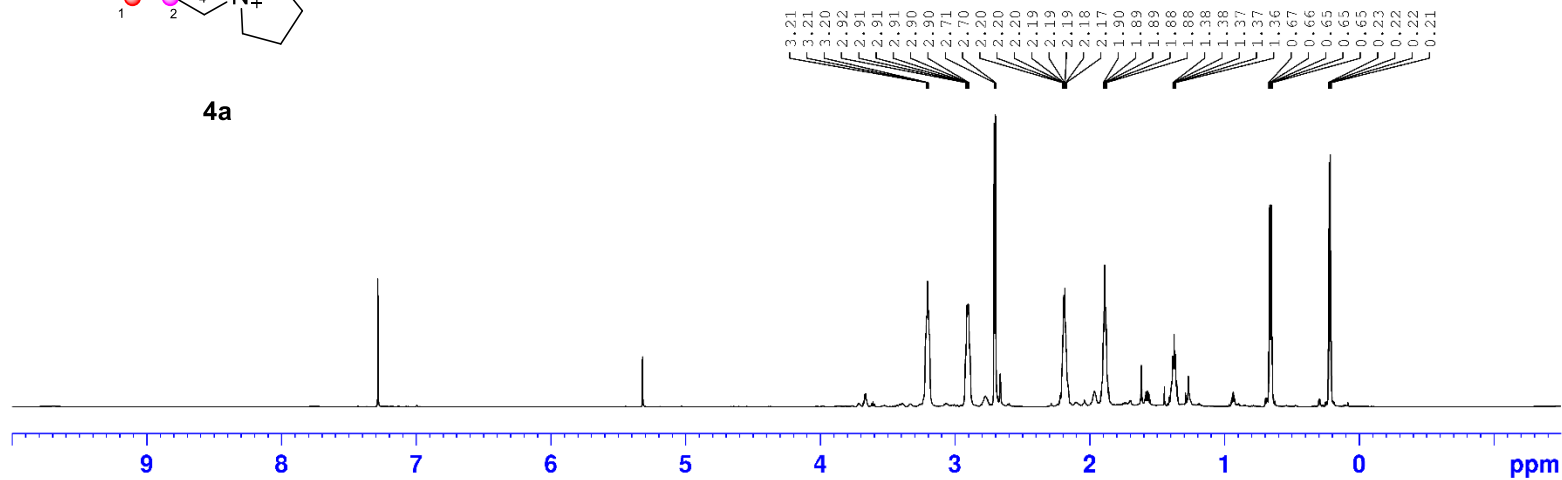
NMR Spectra of Deuterium Experiments



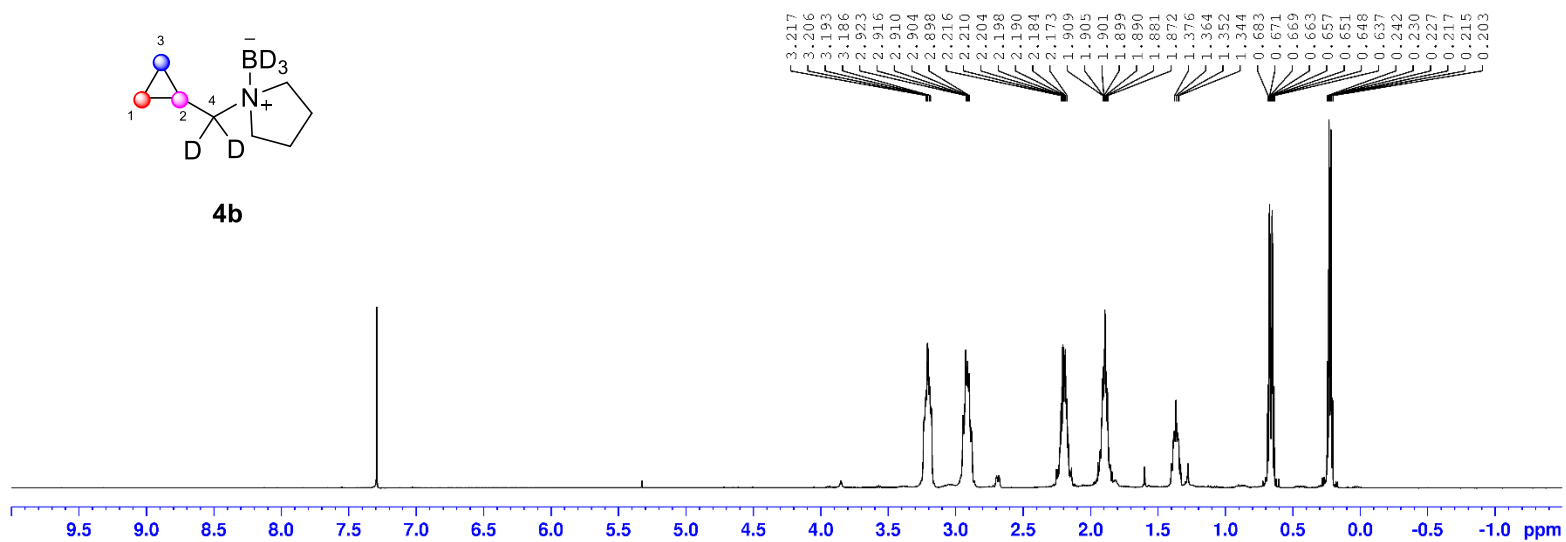


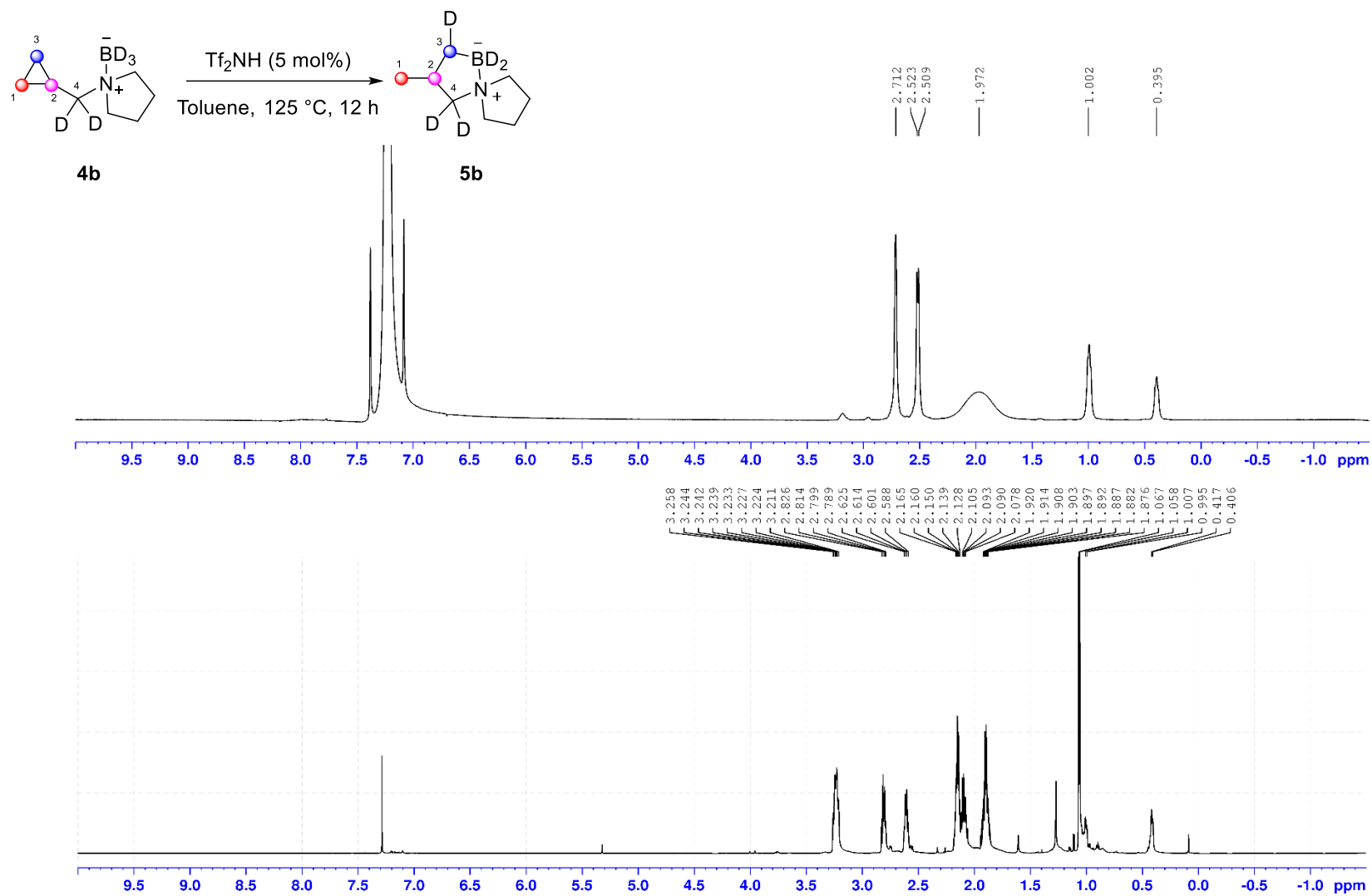


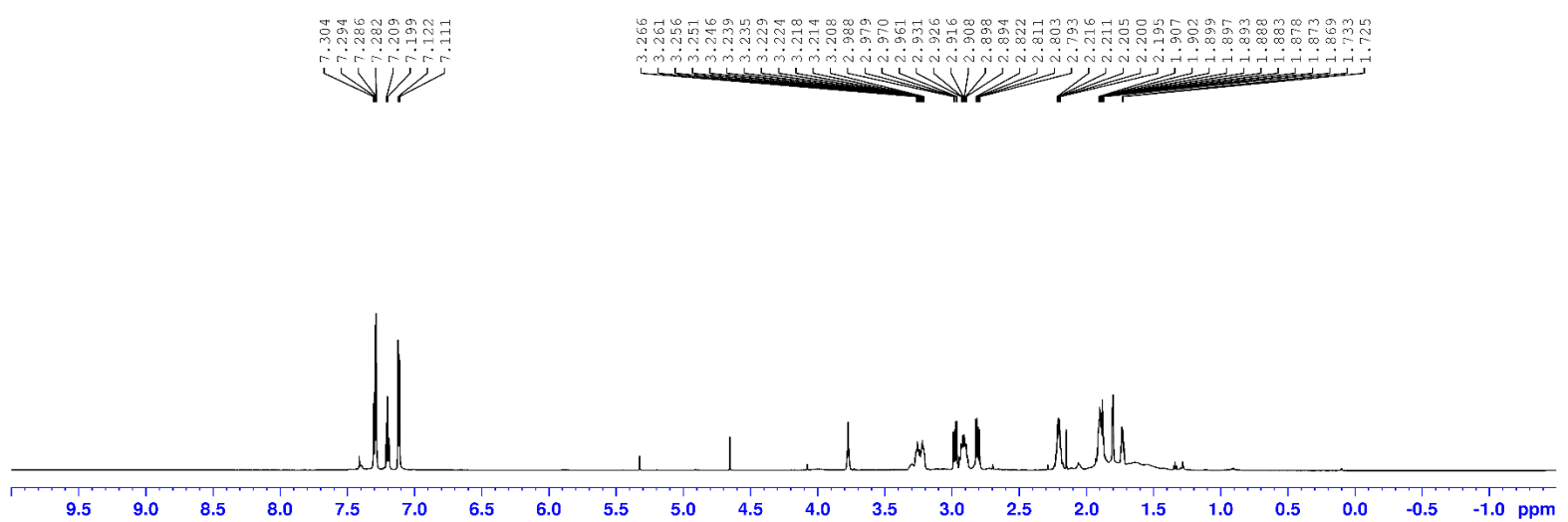
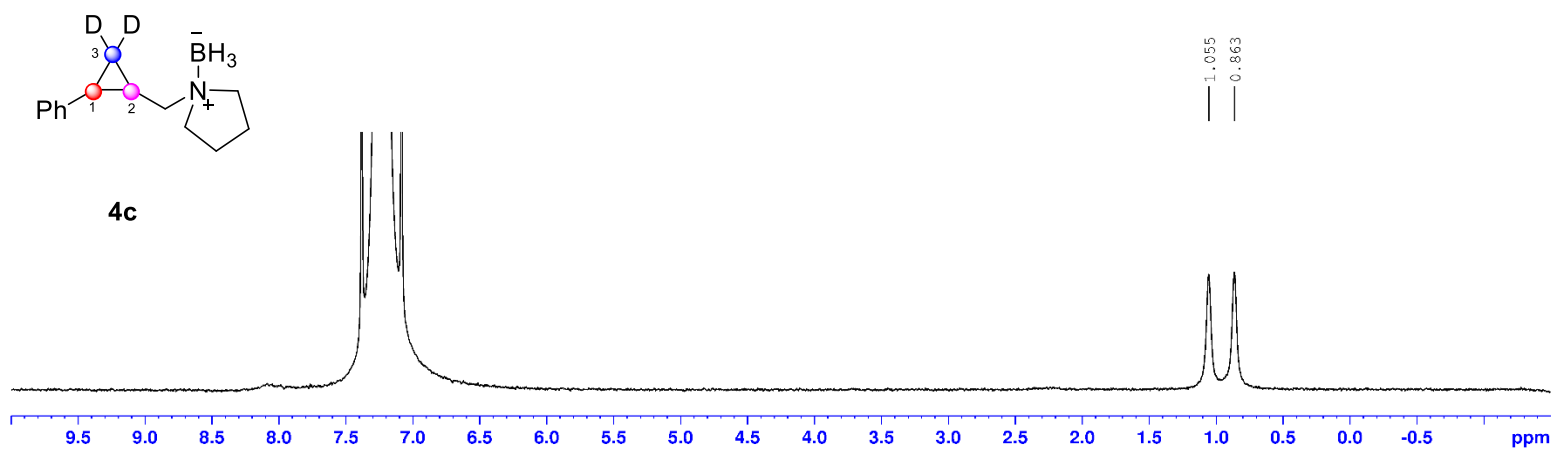
4a

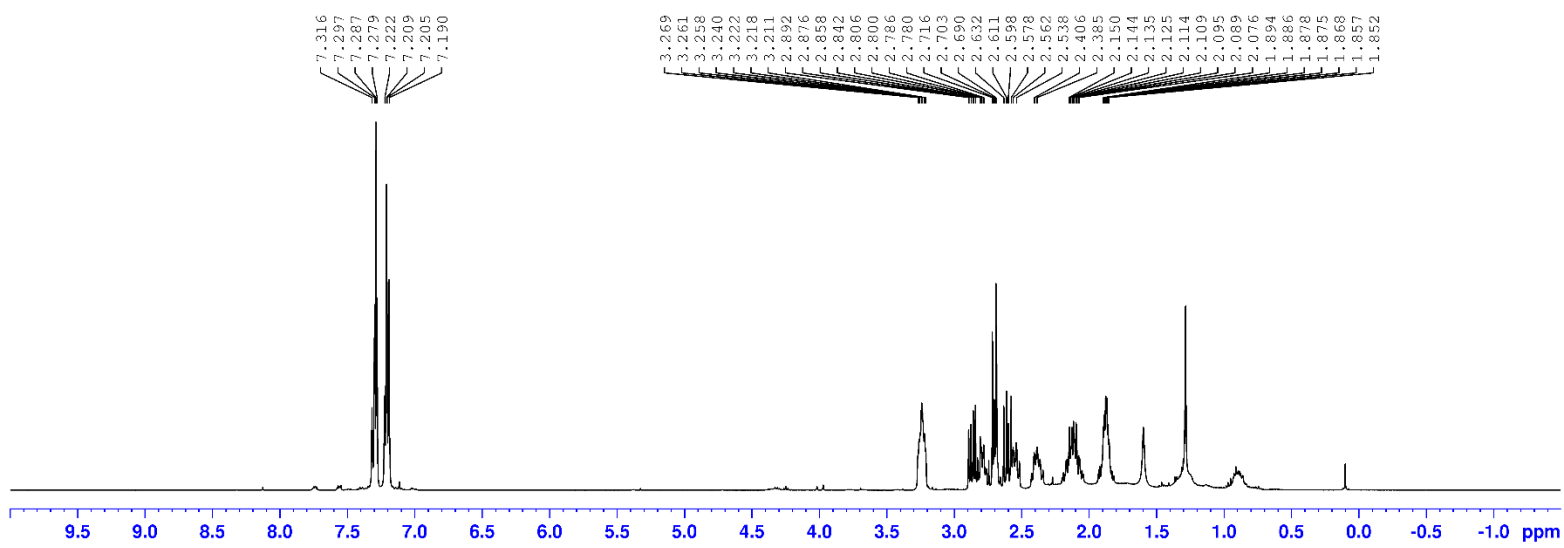
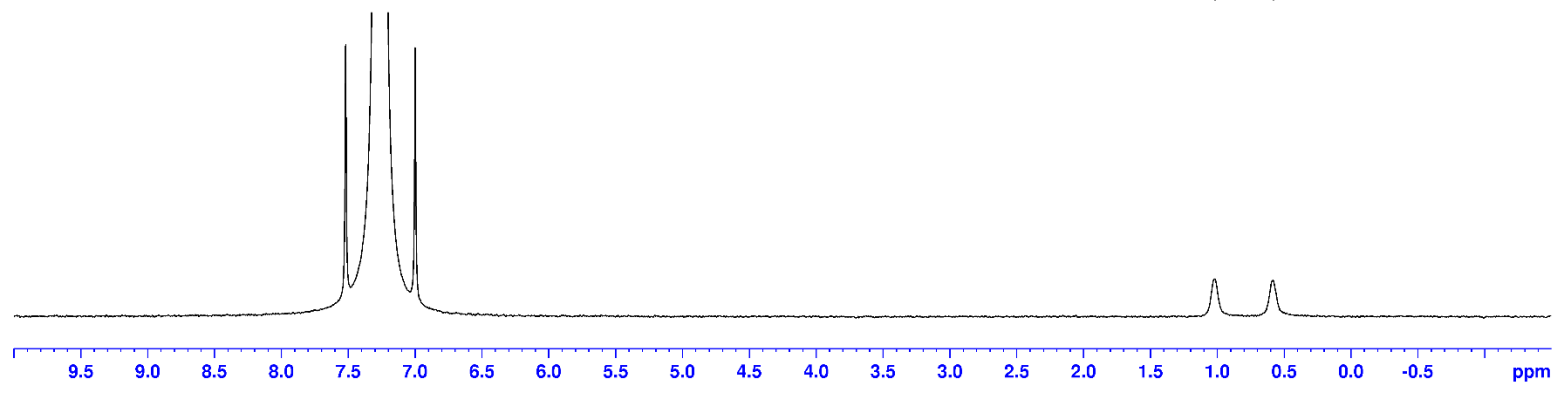
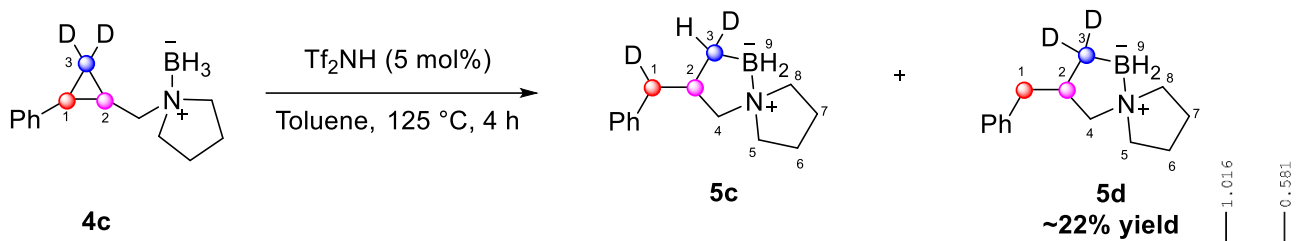


4b

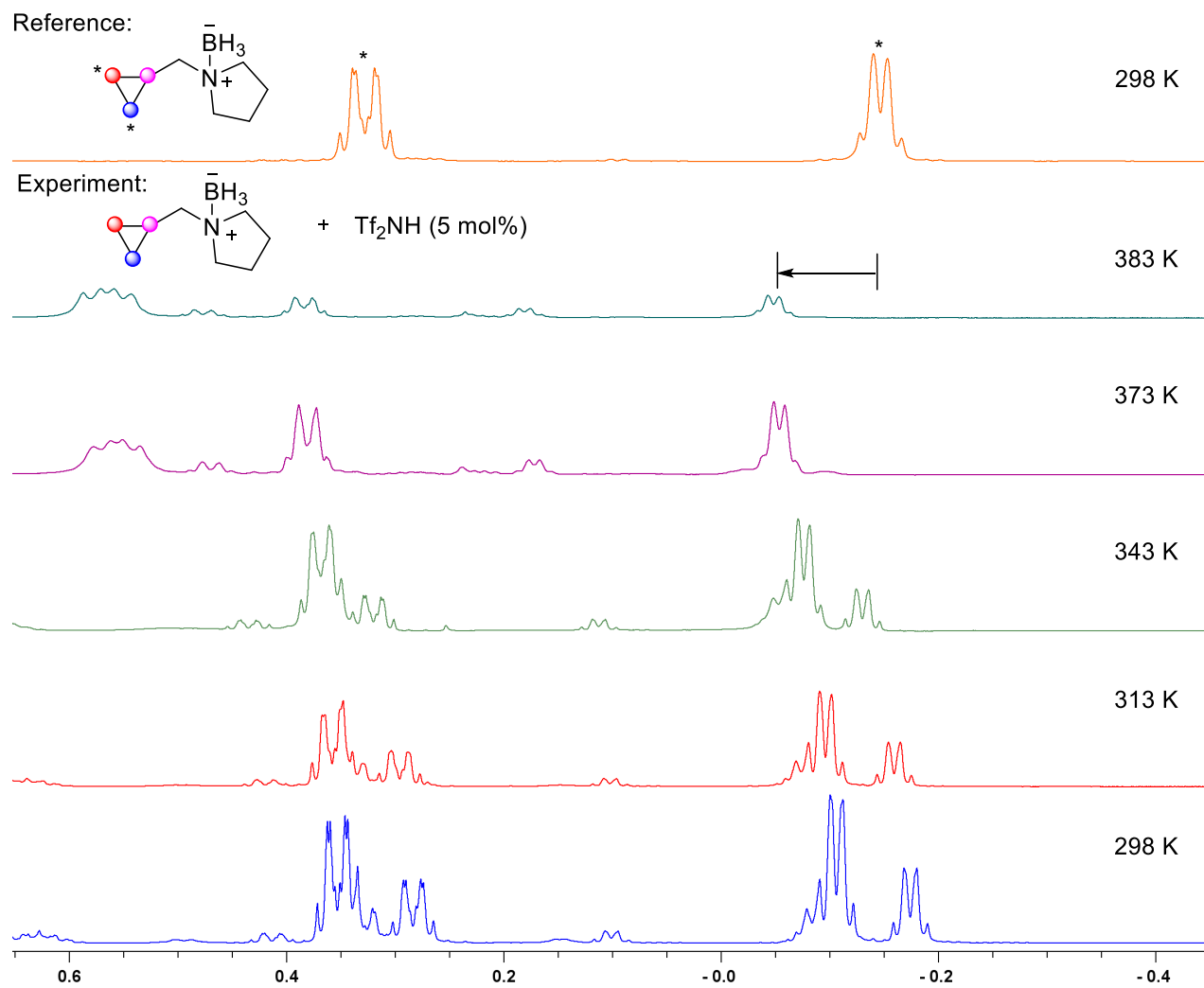








Variable temperature NMR experiment



Annex 3

Experimental Section for Chapter 4

Experimental section

General Methods:

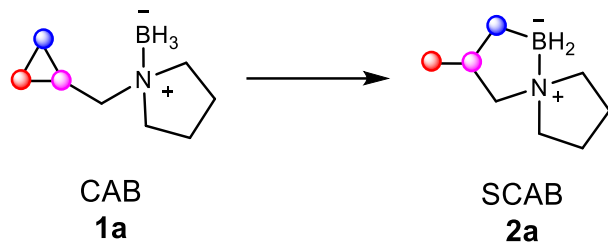
Unless otherwise stated, all glassware was oven dried and/or was flame-dried prior to use. All reactions were set up and carried out under an argon atmosphere.² Anhydrous solvents (dichloromethane, toluene, benzene and tetrahydrofuran) were obtained either by filtration through drying columns on a GlassContour system (Irvine, CA) or by distillation over calcium hydride (dichloromethane). Glacial acetic acid, formic acid, benzoic acid, TFA TfOH, and Tf₂NH were used as is from commercial bottles. Unless otherwise noted, all solutions are aq. solutions. Analytical thin-layer chromatography (TLC) was performed on precoated, glass-backed silica gel (Merck 60 F254). Visualization of the developed chromatogram was performed by UV absorbance (254 nm), UV fluorescence (350 nm) or by staining with aq. potassium permanganate (KMnO₄), *p*-Anisaldehyde, or ninhydrin. Flash column chromatography was performed using silica gel (pore size 60 Å, 230-400 mesh particle size, 40-63 µm particle size) in glass columns for the separation of products. Melting points were obtained on a Buchi melting point B-540 apparatus and are uncorrected. Nuclear magnetic resonance spectra such as ¹H NMR and ¹³C NMR were recorded on Bruker AV400, AV500, and AV700 MHz spectrometers and ¹¹B and ¹⁹F NMR spectra were recorded on AV400 and AV500. The corresponding chemical shifts for ¹H NMR, ¹³C NMR spectra are reported in parts per million relative to the chemical shift of tetramethylsilane and recorded in CDCl₃, using the residual CHCl₃ as a reference (¹H: δ 7.26 ppm, ¹³C: δ 77.2 ppm), (CD₂Cl₂) using the residual solvent as a reference (¹H: δ 5.32 ppm, ¹³C: δ 77.16 ppm), and toluene-*d*₈ (¹H: δ 2.08, 6.97, 7.01, 7.09 ppm, ¹³C: δ 20.43, 125.13, 127.96, 128.87, 137.48 ppm). All ¹³C NMR spectra were obtained with complete proton decoupling. Data is reported as follows: chemical shift, multiplicity (s = singlet, d = doublet, t = triplet, q = quartet, qn = quintet, sx = sextet, h = heptet, m = multiplet and br = broad), coupling constant in Hz and integration. Infrared spectra were taken on a Bruker Vertex Series FTIR (neat) and are reported in reciprocal centimeters (cm⁻¹). High resolution mass spectra (HRMS) were performed on an LC-MSD instrument from Agilent technologies 1200 series in positive electrospray ionization (ESI Pos) and atmospheric-pressure chemical ionization (APCI). Analytical SFC were performed by the Centre de Spectroscopie de Masse de l'Université de Montréal.

Reagents used: All organic extracts were dried over sodium sulfate and concentrated under vacuum. Bis(trifluoromethanesulfonamide), thionyl chloride, pyrrolidine, BH₃-DMS were purchased from Aldrich and were used without further purification. All reagents used were purified using standardized protocols.

²Shriver, D. F. & Drezdson, M. A. The Manipulation of Air-Sensitive Compounds; 2nd Edition; Wiley: New York, 1986.

Synthesis of SCAB•NTf₂ (3):

Synthesis of SCAB:



Into a microwave vial was added cyclopropane amine-borane (CAB) **1a** (14 mmol, 2.0 g) followed by the addition of Tf₂NH (203 mg, 0.7 mmol). Toluene (0.4 M) was added and formation of H₂ was observed. The reaction mixture was stirred for 10 minutes until no bubbles were observed (~10 min). The vial was sealed and heated at 125 °C (oil bath) for 12 h. The reaction mixture was quenched by adding solid nBuNBH₄ (5 mol%). The mixture was then diluted with CH₂Cl₂, filtered through a short plug of silica, and washed with CH₂Cl₂. SCAB was isolated by concentrating the solution and obtained in 96% isolated yield (1.98 g, 13.8 mmol). The spectroscopic data matched that reported in the Annex for chapter 3).

SCAB•NTf₂ (3)

SCAB **2a** (23 mg, 0.2 mmol) was added to an NMR tube followed by the addition of Tf₂NH (47 mg, 0.2 mmol). Tol-*d*₈ (519 μL, 0.3 M) was added to the NMR tube and the solution was shook for 15 min while venting. Both high and low NMR temperature experiments were conducted and ¹H, ¹¹B (¹H coupled and ¹H decoupled), and ¹⁹F NMR spectra were collected.

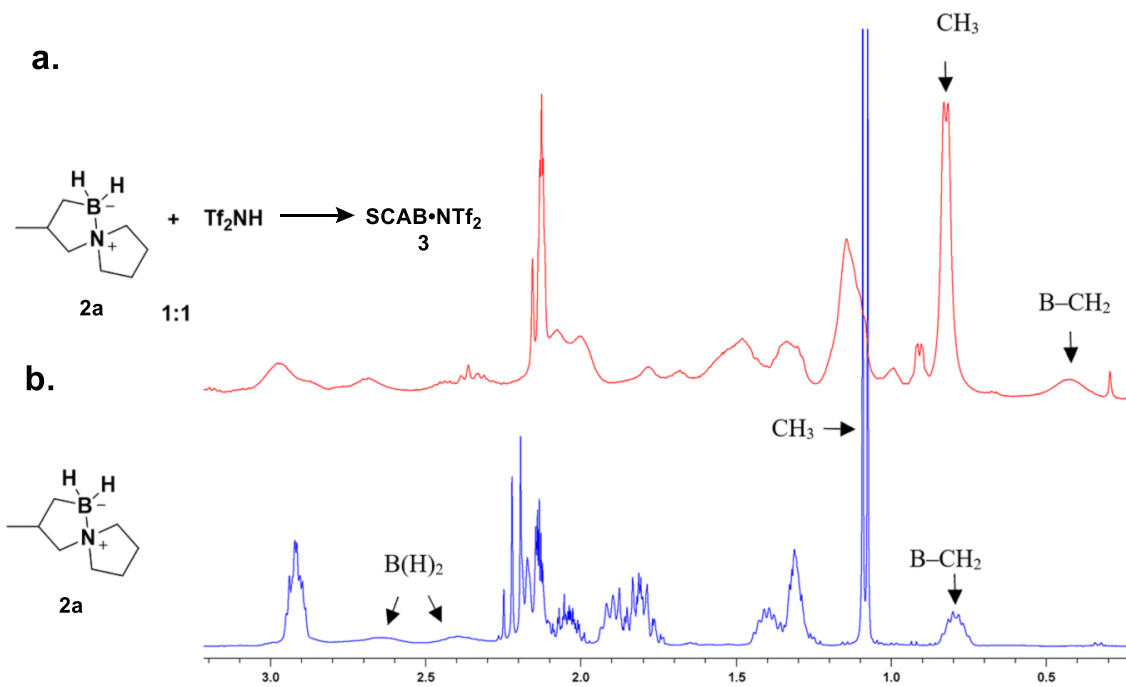


Figure 4A.1 ¹H NMR spectra of a. SCAB•NTf₂ complex **3** vs. b. SCAB **2a**

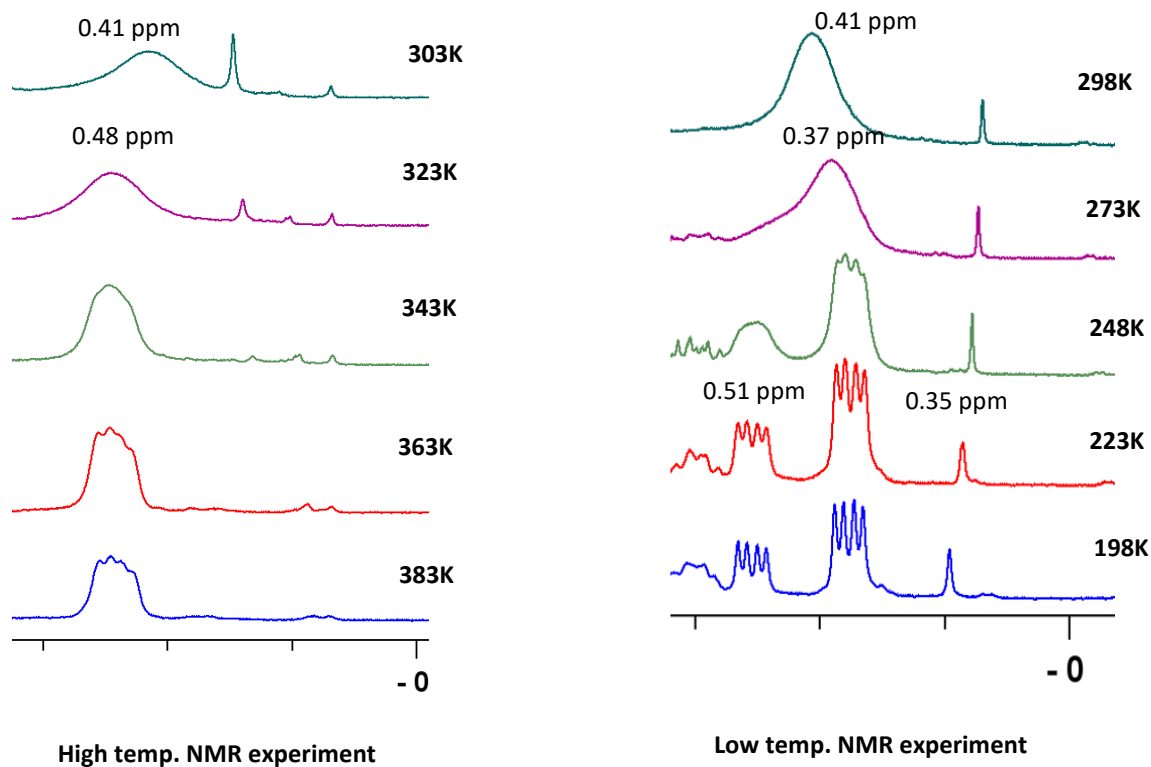


Figure 4A.2: ^1H NMR (toluene- d_8) spectra at variable temperature

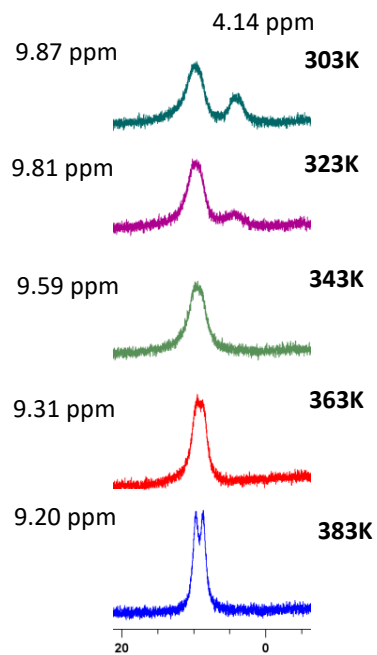


Figure 4A.3: ^{11}B NMR (toluene- d_8) spectra at variable temperatures

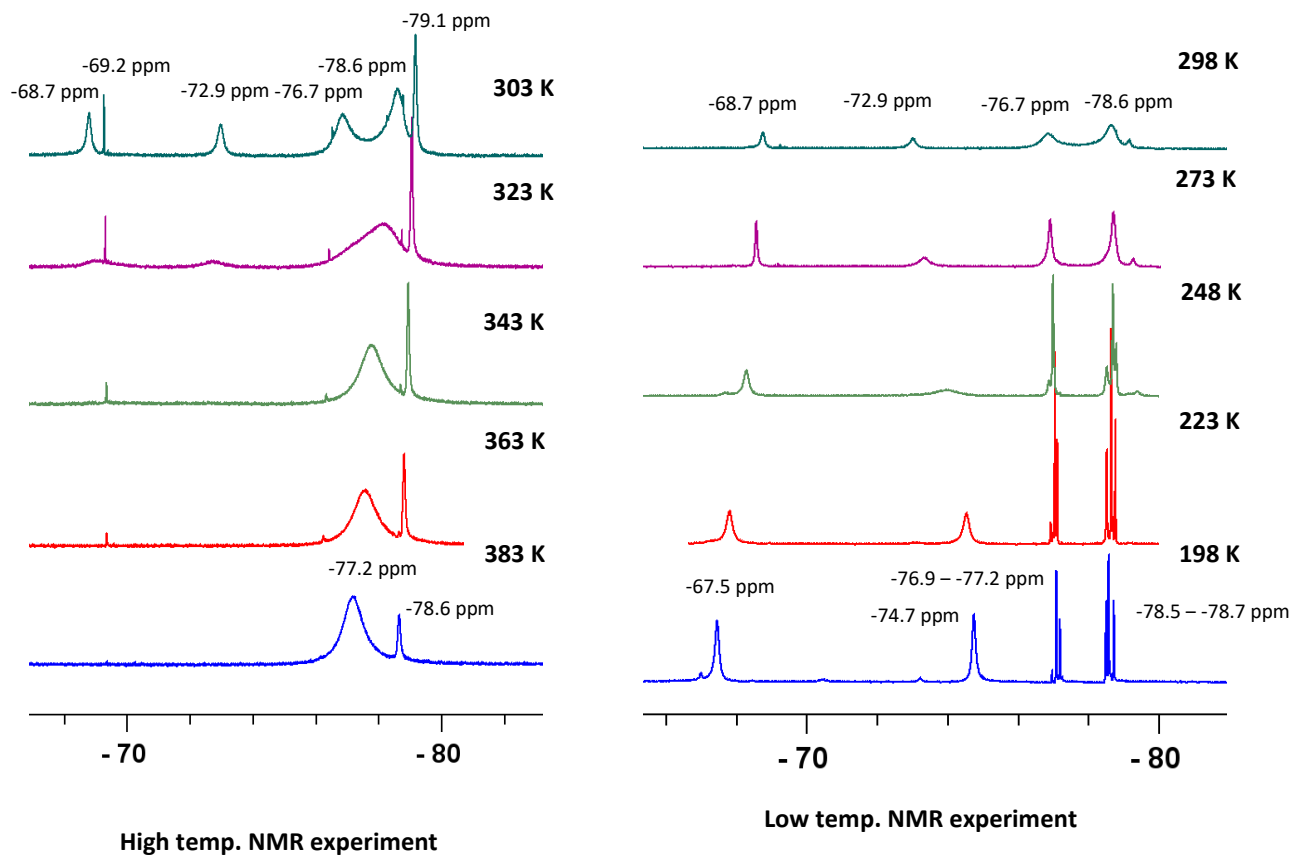


Figure 4A.4 ^{19}F NMR (toluene- d_8) spectra of SCAB•NTf₂ at variable temperatures

IR Spectroscopy

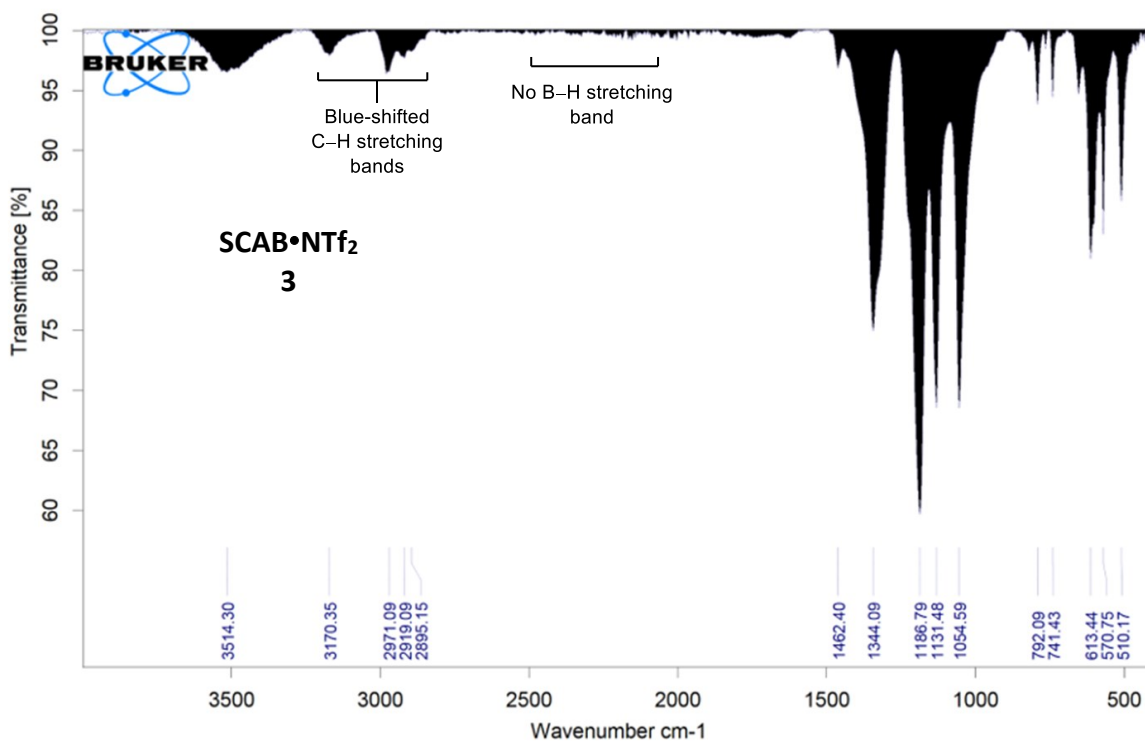
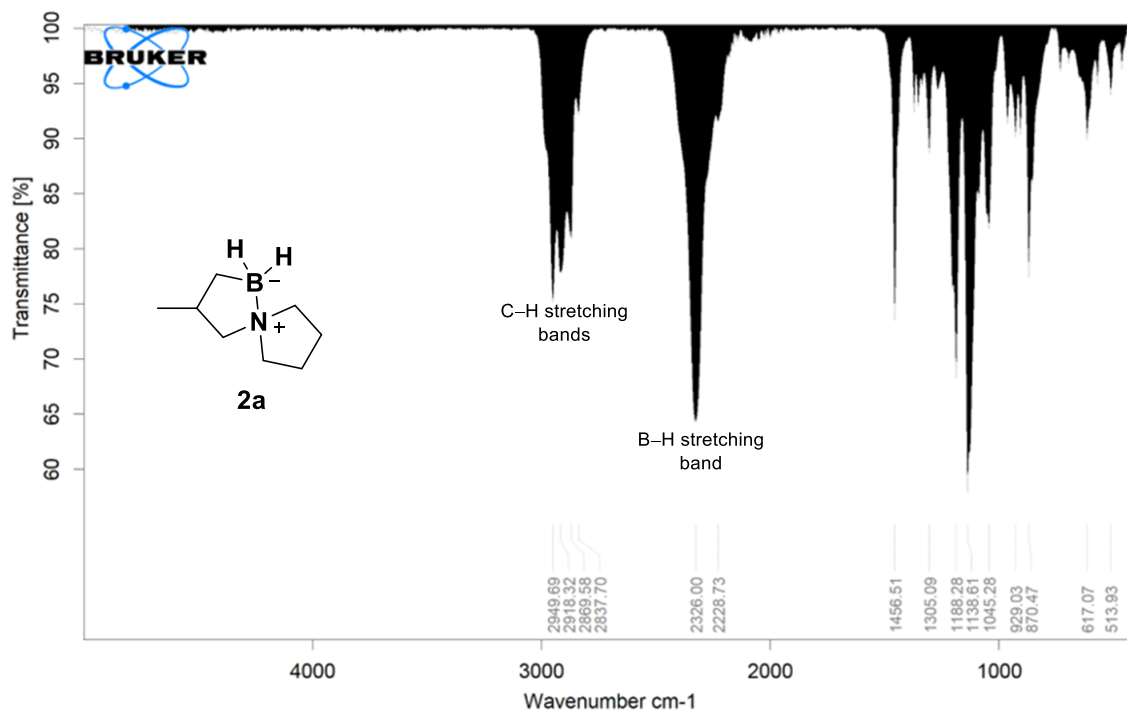


Figure 4A.5 IR spectra of SCAB 2a and SCAB•NTf₂ 3

Raman Spectra

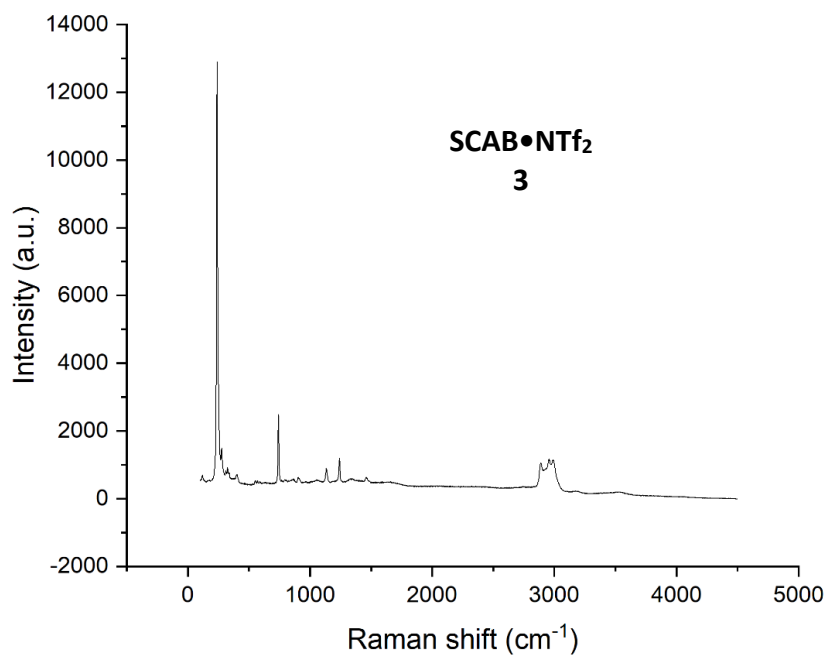
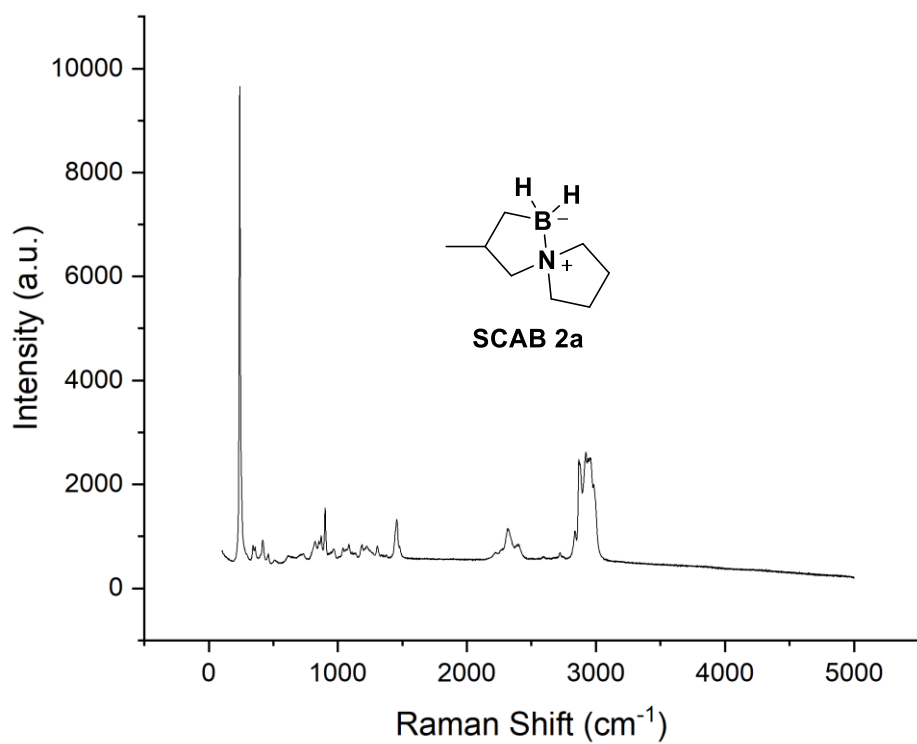
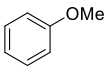
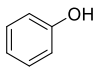
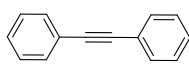
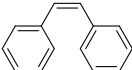
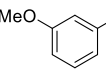
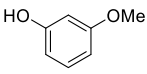
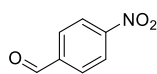
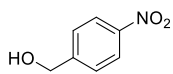
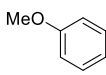
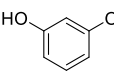
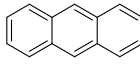
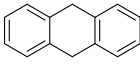
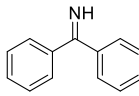
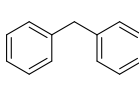
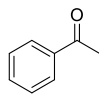
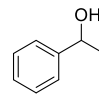
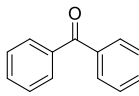
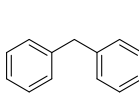
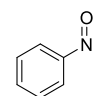
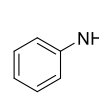
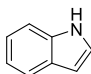
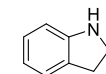
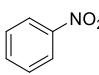
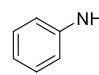


Figure 4A.6 Raman Spectra comparison of SCAB 2a and SCAB NTf₂ 3

Reduction Scope

Table 4A.1 Reaction Scope

SCAB•Tf ₂ N + Substrate		$\xrightarrow[\text{20 min - 72 h, 70 - 160 }^\circ\text{C}]{\text{CH}_2\text{Cl}_2 \text{ or Toluene}}$		Product			
3	4			5			
entry	substrate	product	Yield (%) ^a	entry	substrate	product	Yield (%) ^a
1			92 ^{b, g}	7			53 ⁱ
	4a	5a			4g	5g	
2			89 ^c	8			92 ^j
	4b	5b			4h	5h	
3			86 ^{d, h}	9			42 ^{d, k}
	4c	5c			4i	5i	
4			91 ^e	10			90 ^j
	4d	5d			4j	5j	
5			94 ^f	11			86 ^f
	4e	5e			4k	5k	
6			87 ^e	12			93 ^d
	4f	5f			4l	5l	

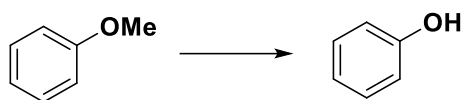
Reactions were run with SCAB•NTf₂ (1 equiv) for 12 h at 100 °C in CH₂Cl₂ unless specified otherwise^a. Yields of isolated product.
^b SCAB•NTf₂ (2 equiv), **2a** (1 equiv) ^c SCAB•NTf₂ (3.5 equiv) ^d SCAB•NTf₂ (4 equiv), **2a** (1 equiv) ^e SCAB•NTf₂ (2 equiv), **2a** (2 equiv) ^f SCAB•NTf₂ (3 equiv), **2a** (1 equiv) ^g 70 °C ^h 160 °C ⁱ 30 min ^j 20 min ^k 72 h ^l Toluene **2a** = SCAB

General Procedure for Reactions:

To a microwave vial was added SCAB **2a** followed by the addition of Tf₂NH (quantity indicated per reduction described below). To the vial was added CH₂Cl₂ was added and stirred for 15 minutes. The substrate was added (for solid compounds the septum was removed, and the solid

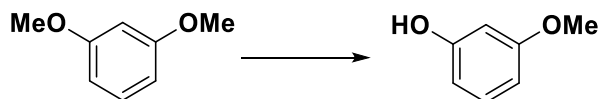
substrate was added) and the vial was sealed and stirred for the indicated time below while heating (100 °C; unless specified otherwise). (*n*Bu)₄NBH₄ (optional) was added to the crude solution and the solution was filtered over a short pad of silica and washed with DCM. The isolated yields (unless specified otherwise) are presented below. *NOTE: SCAB•Tf₂N is capable of a single reduction reaction. (For example: To completely reduce a ketone, 2 equivalents of SCAB•Tf₂N should be used. However, byproducts such as H₂O may react with SCAB•Tf₂N and possibly lead to secondary reactions. We found that the addition of a slight excess of SCAB stabilized SCAB•Tf₂N and prevented secondary interactions with any byproducts formed.*

Anisole (4a) to Phenol (5a)



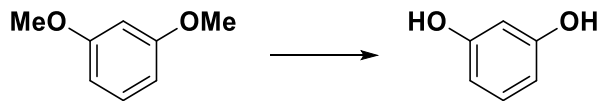
The reaction mixture contained: **2a** (167 mg, 1.2 mmol), Tf₂NH (170 mg, 0.6 mmol), Anisole (32.6 uL, 0.3 mmol). CH₂Cl₂ (1 mL) was used as the solvent. The reaction mixture was stirred at 70 °C for 12 h. The title compound **5a** was obtained in 92% isolated yield (26 mg, 0.28 mmol) and the NMR matched literature.¹ ¹H NMR (400 MHz, CDCl₃) δ 7.35 – 7.20 (m, 2H), 6.97 (t, *J* = 7.4 Hz, 1H), 6.91 – 6.79 (m, 2H), 4.85 (s, 1H). ¹³C NMR (101 MHz, CDCl₃) δ 155.49, 129.69 (2C), 120.81, 115.30 (2C). GCMS +EI: C₆H₆O 94.1000.

1,3-Dimethoxybenzene (4b) to 3-Methoxyphenol (5b)



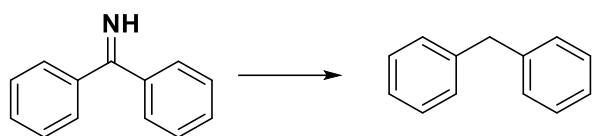
The reaction mixture contained: **2a** (94.7 mg, 0.69 mmol), Tf₂NH (193 mg, 0.69 mmol), 1,3-Dimethoxybenzene (22.3 uL, 0.2 mmol). CH₂Cl₂ (568 uL) was used as the solvent. The reaction mixture was stirred at 100 °C for 12 h. The title compound **5b** was obtained in 89% isolated yield (19 mg, 0.17 mmol) and the NMR matched literature.² ¹H NMR (400 MHz, CDCl₃) δ 7.16 (t, *J* = 8.3 Hz, 1H), 6.58 – 6.49 (m, 1H), 6.45 (m, *J* = 8.3, 1.4 Hz, 2H), 4.87 (s, 1H), 3.81 (s, 3H). ¹³C NMR (101 MHz, CDCl₃) δ 161.00, 156.71, 130.15, 107.74, 106.46, 101.52, 55.29. GCMS +EI: C₇H₈O₂ 124.1000.

1,3-Dimethoxybenzene (4c) to Resorcinol (5c)



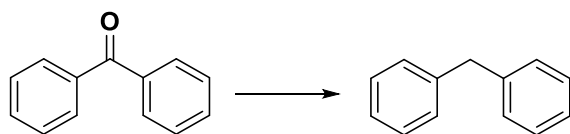
The reaction mixture contained: **2a** (250 mg, 1.8 mmol), Tf₂NH (341 mg, 1.2 mmol), 1,3-Dimethoxybenzene (39.3, 0.3 mmol). Toluene (1 mL) was used as the solvent. The reaction mixture was stirred at 160 °C for 12 h. The title compound **5c** was obtained in 86% isolated yield (28 mg, 0.25 mmol) and the NMR matched literature.³ ¹H NMR (400 MHz, MeOD) δ 6.97 (t, *J* = 7.9 Hz, 1H, ArH), 6.32 – 6.24 (m, 3H, ArH). ¹³C NMR (101 MHz, MeOD) δ 158.19 (2C), 129.42, 106.29 (2C), 102.11. GCMS +EI: C₆H₆O₂ 110.0600.

Benzophenone Imine (4d) to Diphenylmethane (5d)



The reaction mixture contained: **2a** (94.5 mg, 0.68 mmol), Tf₂NH (101 mg, 0.34 mmol), benzophenone imine (30.8, 0.2 mmol). CH₂Cl₂ (566 uL) was used as the solvent. The reaction mixture was stirred at 100 °C for 12 h. The title compound **5d** was obtained in 91% isolated yield (26 mg, 0.15 mmol) and the NMR matched literature.⁴ ¹H NMR (400 MHz, CDCl₃) δ 7.38 – 7.30 (m, 4H, ArH), 7.24 (t, *J* = 6.3 Hz, 6H, ArH), 4.03 (s, 2H, CH₂). ¹³C NMR (101 MHz, CDCl₃) δ 141.14 (2C), 128.96 (4C), 128.48 (4C), 126.08 (2C), 41.96. GCMS +EI: C₁₃H₁₂ 168.100.

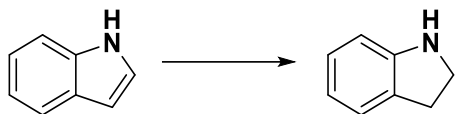
Benzophenone (4e) to Diphenylmethane (5e)



The reaction mixture contained: **2a** (94.5 mg, 0.68 mmol), Tf₂NH (151 mg, 0.51 mmol), benzophenone (31.0, 0.2 mmol). CH₂Cl₂ (566 uL) was used as the solvent. The reaction mixture was stirred at 100 °C for 12 h. The title compound **5e** was obtained in 94% isolated yield (27 mg, 0.16 mmol) and the NMR matched literature.⁴ ¹H NMR (400 MHz, CDCl₃) δ 7.33 (t, *J* = 7.2 Hz, 4H,

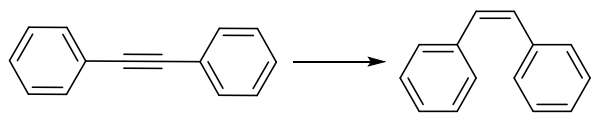
ArH), 7.25 (t, $J = 6.4$ Hz, 6H, ArH), 4.04 (s, 2H, CH₂). ¹³C NMR (101 MHz, CDCl₃) δ 141.14 (2C), 128.96 (4C), 128.47 (4C), 126.08 (2C), 41.97. GCMS +EI: C₁₃H₁₂ 167.1800.

Reduction of Indole (4f) to Indoline (5f)



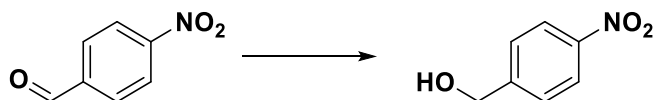
The reaction mixture contained: **2a** (94.3 mg, 0.68 mmol), Tf₂NH (100 mg, 0.34 mmol), indole (20.0, 0.2 mmol). CH₂Cl₂ (565 μ L) was used as the solvent. The reaction mixture was stirred at 100 °C for 12 h. The title compound **5f** was obtained in 87% isolated yield (18 mg, 0.15 mmol) and the NMR matched literature.⁵ ¹H NMR (400 MHz, CDCl₃) δ 7.16 (d, $J = 7.3$ Hz, 1H, ArH), 7.09 – 7.01 (td, 1H, ArH), 6.75 (td, $J = 7.4, 0.8$ Hz, 1H, ArH), 6.69 (d, $J = 7.8$ Hz, 1H, ArH), 3.59 (t, $J = 8.4$ Hz, 2H, CH₂), 3.52 (s, 1H), 3.07 (t, $J = 8.4$ Hz, 2H, CH₂). ¹³C NMR (101 MHz, CDCl₃) δ 151.51, 129.36, 127.23, 124.66, 118.73, 109.51, 47.33, 29.85. HRMS (ESI, m/z): calculated for [M+H]⁺: C₈H₉N requires m/z 120.0808, found m/z 120.0808.

Diphenylacetylene (4g) to *Cis*-Stilbene (5g)



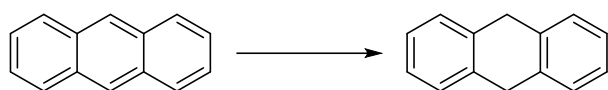
The reaction mixture contained: **2a** (23.7 mg, 0.2 mmol), Tf₂NH (48.3 mg, 0.2 mmol), diphenylacetylene (30.3, 0.2 mmol). CH₂Cl₂ (567 μ L) was used as the solvent. The reaction mixture was stirred at 100 °C for 30 min. The title compound **5g** was obtained in 53% conversion the NMR matched literature.⁶ ¹H NMR (400 MHz, CDCl₃) δ 7.26 (m, $J = 8.2, 4.2$ Hz, 10H, ArH), 6.64 (s, 2H, CH). ¹³C NMR (101 MHz, CDCl₃) δ 137.26 (2C), 130.26 (4C), 128.88 (4C), 128.22 (2C), 127.10 (2C). HRMS (ESI, m/z): calculated for [M]⁺: C₁₄H₁₂ requires m/z 180.0933, found m/z 180.0928.

4-Nitrobenzaldehyde (4h) to (4-Nitrophenyl)Methanol (5h)



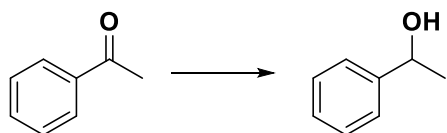
The reaction mixture contained: **2a** (30.7 mg, 0.17 mmol), Tf₂NH (50.3 mg, 0.17 mmol), 4-Nitrobenzaldehyde (25.7, 0.17 mmol). CH₂Cl₂ (567 uL) was used as the solvent. The reaction mixture was stirred at 100 °C for 20 min. The title compound **5h** was obtained in 92% isolated yield (24 mg, 0.15 mmol) and the NMR matched literature.⁷ ¹H NMR (400 MHz, CDCl₃) δ 8.24 (d, *J* = 8.7 Hz, 2H, ArH), 7.56 (d, *J* = 8.7 Hz, 2H, ArH), 4.86 (s, 2H, CH₂), 2.07 (d, *J* = 6.3 Hz, 1H, OH). ¹³C NMR (101 MHz, CDCl₃) δ 148.18, 147.32, 127.01(2C), 123.75 (2C), 64.02. GCMS +EI: C₇H₇NO₃ 153.0600.

Anthracene (**4i**) to 9,10-Dihydroanthracene (**5i**)



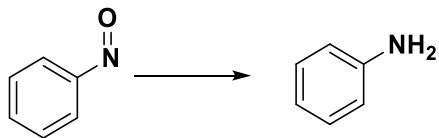
The reaction mixture contained: **2a** (118 mg, 0.9 mmol), Tf₂NH (242 mg, 0.9 mmol), anthracene (30.3, 0.2 mmol). CH₂Cl₂ (666 uL) was used as the solvent. The reaction mixture was stirred at 100 °C for 72 h. The title compound **4i** was obtained in 42% isolated yield (13 mg, 0.07 mmol) and the NMR matched literature.⁸ ¹H NMR (400 MHz, CDCl₃) δ 7.32 (dd, *J* = 5.4, 3.4 Hz, 4H, ArH), 7.22 (dd, *J* = 5.5, 3.3 Hz, 4H, ArH), 3.97 (s, 4H, CH₂). ¹³C NMR (101 MHz, CDCl₃) δ 136.69 (4C), 127.39 (4C), 126.09 (4C), 36.17 (2C). GCMS +EI: C₁₄H₁₂ 179.1000.

Acetophenone (**4j**) to 1-Phenylethan-1-ol (**5j**)



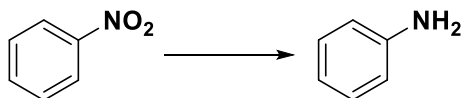
The reaction mixture contained: **2a** (45.2 mg, 0.4 mmol), Tf₂NH (74.0 mg, 0.25 mmol), acetophenone (29.0 uL, 0.25 mmol). CH₂Cl₂ (834 uL) was used as the solvent. The reaction mixture was stirred at 100 °C for 20 min. The title compound **5j** was obtained in 90% isolated yield (28 mg, 0.23 mmol) and the NMR matched literature.⁹ ¹H NMR (400 MHz, CDCl₃) δ 7.39 (d, *J* = 6.7 Hz, 4H, ArH), 7.35 – 7.18 (m, 2H, ArH), 4.93 (q, *J* = 6.4 Hz, 1H, CH), 1.91 (s, 1H, OH), 1.54 (d, *J* = 6.5 Hz, 3H, CH₃). ¹³C NMR (101 MHz, CDCl₃) δ 145.82, 128.52 (2C), 127.50, 125.40 (2C), 70.44, 25.17. GCMS +EI: C₈H₁₀O 122.1000.

Nitrosobenzene (4k) to Aniline (5k)



The reaction mixture contained: **2a** (112 mg, 0.8 mmol), Tf₂NH (119 mg, 0.4 mmol), nitrosobenzene (18.0 uL, 0.20 mmol). CH₂Cl₂ (669 uL) was used as the solvent. The reaction mixture was stirred at 100 °C for 12 h. The title compound **5k** was obtained in 86% isolated yield (16 mg, 0.17 mmol) and the NMR matched literature.¹⁰ ¹H NMR (400 MHz, CDCl₃) δ 7.22 – 7.11 (m, 2H, ArH), 6.79 (t, *J* = 7.4 Hz, 1H, ArH), 6.74 – 6.67 (m, 2H, ArH), 3.65 (br, 2H, NH₂). ¹³C NMR (101 MHz, CDCl₃) δ 146.39, 129.31 (2C), 118.58, 115.13 (2C). **HRMS (ESI, *m/z*)**: calculated for [M+H]⁺: C₆H₇N requires *m/z* 94.0651, found *m/z* 94.0654.

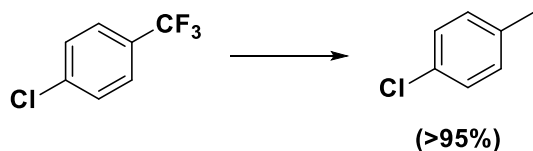
Nitrobenzene (4l) to Aniline (5l)



The reaction mixture contained: **2a** (209 mg, 1.5 mmol), Tf₂NH (266 mg, 0.9 mmol), nitrobenzene (31.0 uL, 0.3 mmol). CH₂Cl₂ (1 mL) was used as the solvent. The reaction mixture was stirred at 100 °C for 12 h. The title compound **5l** was obtained in 93% isolated yield (26 mg, 0.28 mmol) and the NMR matched literature.¹⁰ ¹H NMR (500 MHz, CDCl₃) δ 7.22 – 7.13 (m, 2H, ArH), 6.85 – 6.77 (m, 1H, ArH), 6.75 – 6.66 (m, 2H, ArH), 3.66 (br, 2H, NH₂). ¹³C NMR (126 MHz, CDCl₃) δ 146.37, 129.31 (2C), 118.58, 115.13 (2C). **HRMS (ESI, *m/z*)**: calculated for [M+H]⁺: C₆H₇N requires *m/z* 94.0651, found *m/z* 94.0655.

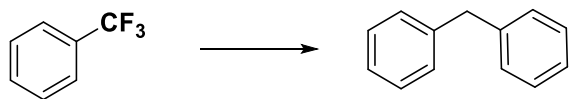
C–F Activation

1-Chloro-4-Methylbenzene (**5m**)



To a microwave vial was added **2a** (94.6 mg, 0.7 mmol) followed by the addition of Tf₂NH (151 mg, 0.5 mmol). The vial was added CH₂Cl₂ (567 μ L) and the mixture was stirred for 15 minutes. 4-chlorobenzotrifluoride (30.7 mg, 0.2 mmol) was added to the vial and the vial was sealed and stirred for 12 h at 65 °C. The solvent was removed under reduced pressure for 4 min at 26 °C (400 mbar). Formation of 4-chlorotoluene was observed in the crude ¹H NMR. The title product **5m** was observed in >95% conversion.¹¹ ¹H NMR (400 MHz, CDCl₃) δ 7.23 (d, J = 8.3 Hz, 2H, ArH), 7.11 (d, J = 8.1 Hz, 2H, ArH), 2.33 (s, 3H, CH₃). ¹³C NMR (101 MHz, CDCl₃) δ 136.31, 131.00, 130.39 (2C), 128.23 (2C), 53.50. GCMS +EI: C₇H₇Cl 126.0700.

Diphenylmethane (**5n**)



To a microwave vial was added **1** (28.5 mg, 0.21 mmol) followed by the addition of Tf₂NH (60.8 mg, 0.21 mmol). CH₂Cl₂ (467 μ L) was added to the vial and the mixture was stirred for 15 minutes. To the vial was then added trifluorotoluene (25.2 μ L, 0.21 mmol) and benzene (55.0 μ L, 0.6 mmol) and the vial was sealed and stirred for 12 h at 60 °C. Remaining Trifluorotoluene was distilled off and the residue was filtered over a short plug of silica and washed with hexanes. The title product **5n** was obtained in 72% isolated yield (25 mg, 0.14 mmol).⁴ ¹H NMR (400 MHz, CDCl₃) δ 7.41 – 7.29 (m, 5H, ArH), 7.23 (dd, J = 7.2, 5.4 Hz, 5H, ArH), 4.02 (s, 2H, CH₂). ¹³C NMR (101 MHz, CDCl₃) δ 141.13, 128.94 (2C), 128.46 (2C), 126.07, 41.95. GCMS +EI: C₁₃H₁₂ 167.1000.

Additional Experiments

Acid Screening

To a microwave vial added SCAB **2a** (20 mg, 0.14 mmol) followed by the addition of the acid (0.14 mmol) and CD₂Cl₂ (479 μL). The vial was sealed, and the mixture was stirred for 15 minutes. The solution was transferred into an NMR tube and an NMR was acquired.

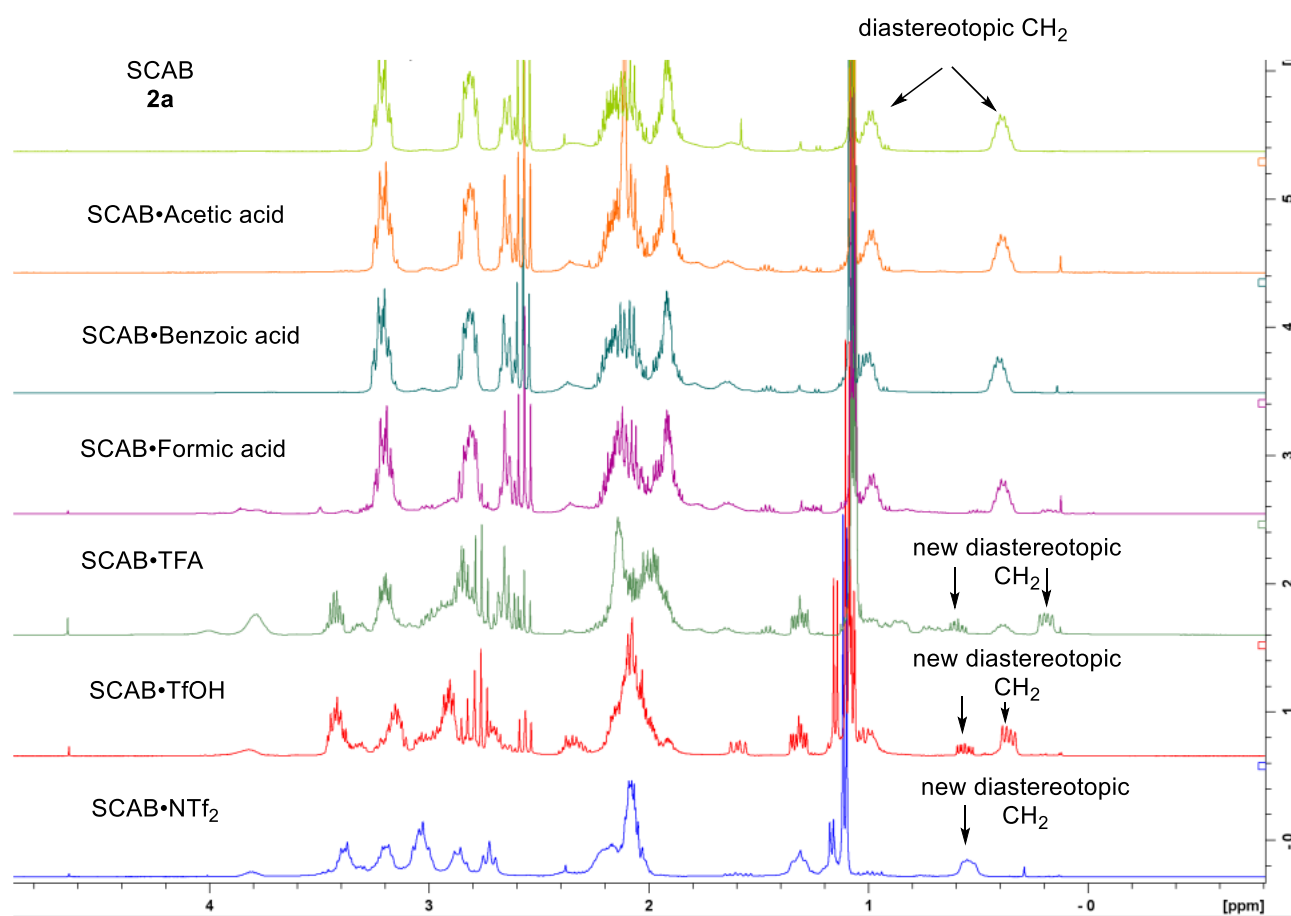


Figure 4A.7 Stacked ¹H NMR spectra of acid screening

"D₂O Shake"

To a microwave vial added SCAB **2a** (23.5 mg, 0.17 mmol) followed by the addition of the Tf₂NH (47.5 mg, 0.17 mmol) and Toluene-*d*₈ (563 μL). The vial was sealed, and the mixture was stirred for 15 minutes. The mixture was transferred into an NMR tube and an NMR was acquired. A drop of D₂O was added and NMR analysis was done.

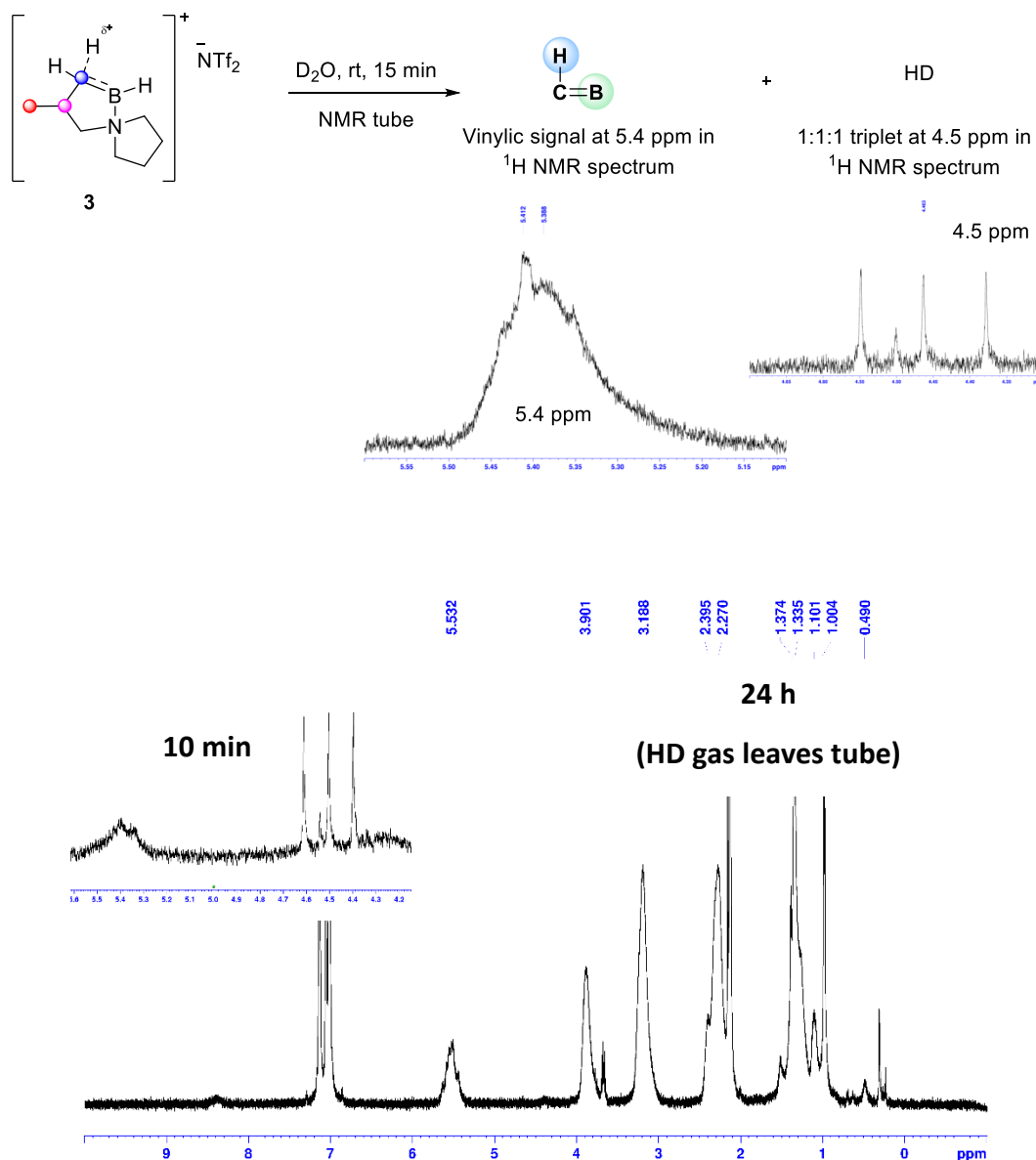


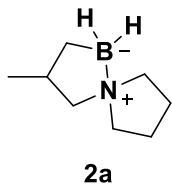
Figure A4.8 "D₂O shake" of SCAB•NTf₂ complex

References

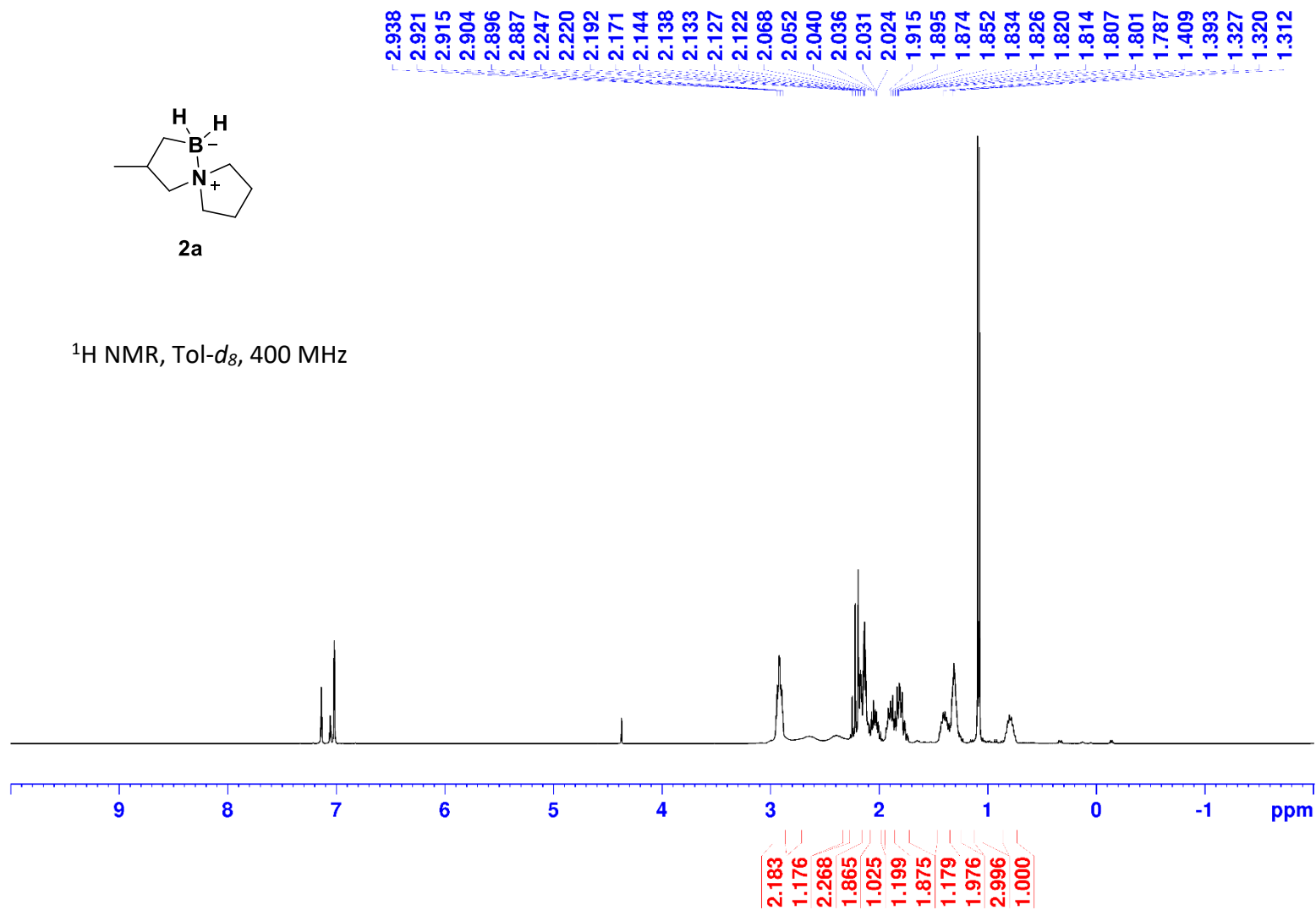
1. Chen, C.; Wu, D.; Liu, P.; Li, J.; Xia, H.; Zhou, M.; Jiang, J., *Green Chem.* **2021**, *23*, 3090-3103.
2. Leow, W. R.; Yu, J.; Li, B.; Hu, B.; Li, W.; Chen, X. E., *Angew. Chem. Int. Ed.* **2018**, *57*, 9780-9784.
3. Xu, Y.-T.; Li, C.-Y.; Huang, X.-B.; Gao, W.-X.; Zhou, Y.-B.; Liu, M.-C.; Wu, H.-Y., *Green Chem.* **2019**, *21*, 4971-4975.
4. Zhou, X.-Y.; Chen, X., *Tetrahedron Lett.* **2020**, *61*, 151447.
5. Points III, G. L.; Stout, K. T.; Beaudry, C. M., *Chem. Eur. J.* **2020**, *26*, 16655-16658.
6. Sugita, K.; Nakano, R.; Yamashita, M., *Chem. Eur. J.* **2020**, *26*, 2174-2177.
7. Nylund, P. V. S.; Segaud, N. C.; Albrecht, M., *Organometallics* **2021**, *40*, 1538-1550.
8. von Grotthuss, E.; Prey, S. E.; Bolte, M.; Lerner, H.-W.; Wagner, M., *J. Am. Chem. Soc.* **2019**, *141*, 6082-6091.
9. Fernandes, J. L. N.; de Souza, M. C.; Brenelli, E. C. S.; Brenelli, J. A., *Synthesis* **2009**, *2009*, 4058-4062.
10. Abraham, R. J.; Reid, M., *J. Chem. Soc., Trans.* **2002**, 1081-1091.
11. Xiao, J.; Ma, Y.; Wu, X.; Gao, J.; Tang, Z.; Han, L.-B., *RSC Adv.* **2019**, *9*, 22343-22347.

NMR Spectra for Chapter 4

SCAB (**2a**) in $\text{tol-}d_8$

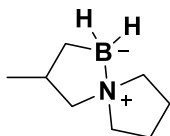


^1H NMR, Tol- d_8 , 400 MHz



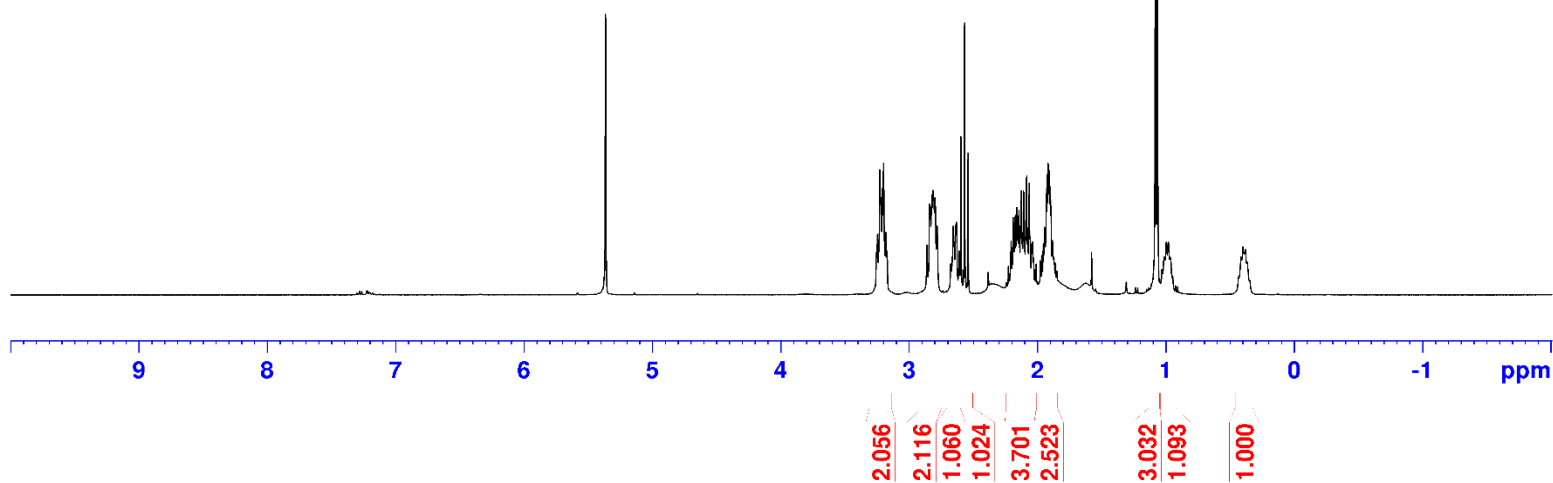
SCAB (**2a**) in CD₂Cl₂

3.246
3.227
3.219
3.207
3.198
3.181
2.841
2.834
2.822
2.814
2.797
2.782
2.656
2.631
2.595
2.568
2.540
2.205
2.188
2.182
2.177
2.172
2.167
2.161
2.155
2.151
2.145
2.140
2.132
2.125
2.119
2.108
2.104
2.088
2.083
2.077
2.064
2.058
2.040
1.944
1.928
1.923
1.918
1.915
1.909
1.903
1.899
1.894
1.883
1.081
1.065
0.980

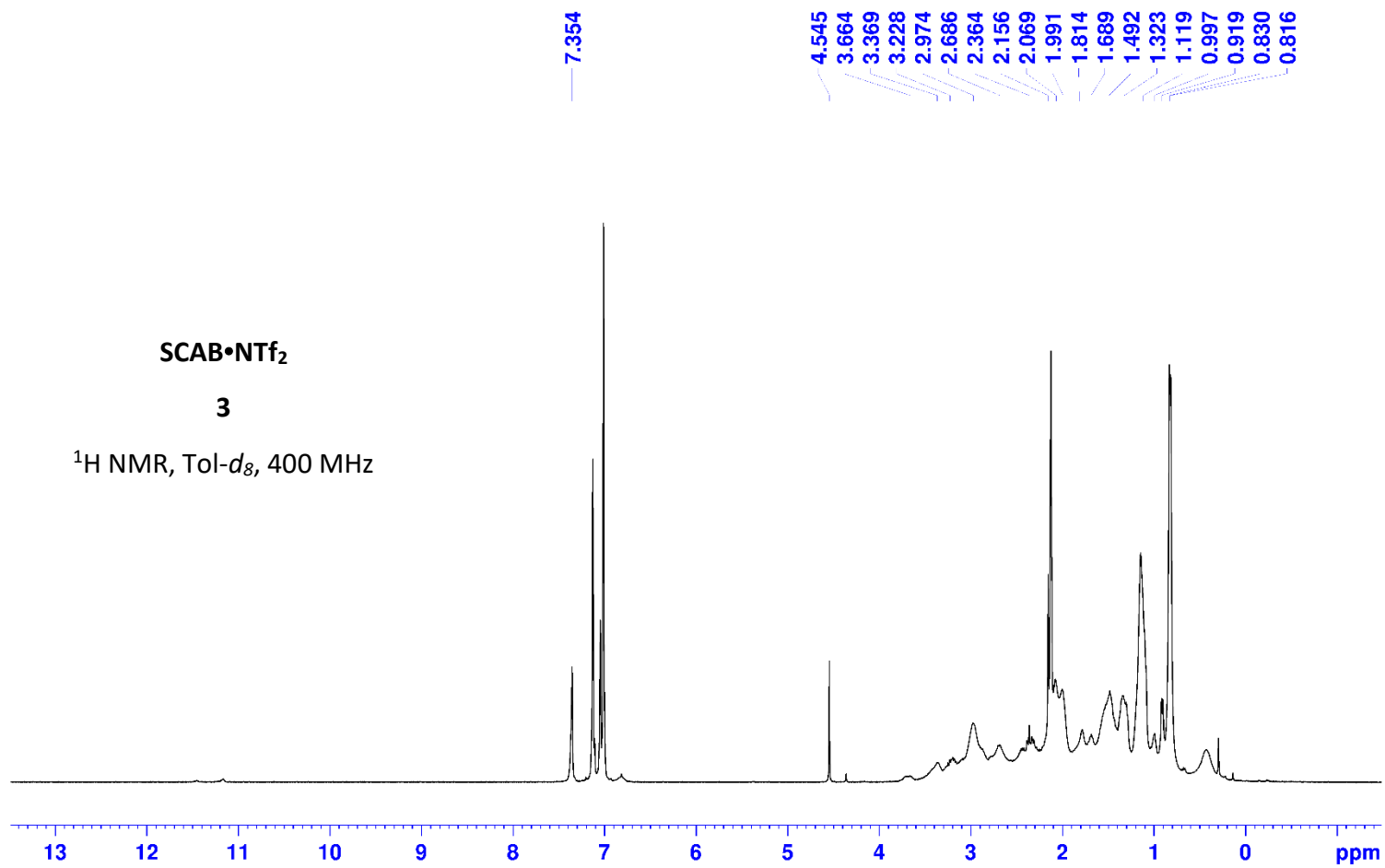


2a

¹H NMR, CD₂Cl₂, 400 MHz



SCAB•NTf₂ (**3**) in tol-*d*₈



SCAB•NTf₂ (3) in CD₂Cl₂

3.801
3.400
3.383
3.371
3.211
3.199
3.183
3.071
3.045
3.027
2.999
2.883
2.856
2.724
2.190
2.171
2.164
2.146
2.125
2.106
2.090
2.082
2.076
2.066
2.059
2.048
2.027
1.308
1.174
1.158
1.114

